DE GRUYTER

STEM

Ralf Steudel

CHEMISTRY OF THE NON-METALS

SYNTHESES – STRUCTURES – BONDING – APPLICATIONS

In cooperation with David Scheschkewitz

2ND EDITION

Ralf Steudel

Chemistry of the Non-Metals

Also of interest

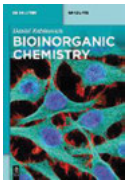

Bioinorganic Chemistry.
Rabinovich, 2020
ISBN 978-3-11-049204-0, e-ISBN 978-3-11-049443-3

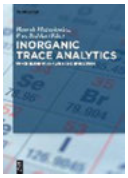

Inorganic Trace Analytics.
Trace Element Analysis and Speciation
Matusiewicz, Bulska (Eds.), 2017
ISBN 978-3-11-037194-9, e-ISBN 978-3-11-036673-0

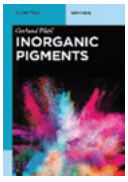

Inorganic Pigments.
Pfaff, 2017
ISBN 978-3-11-048450-2, e-ISBN 978-3-11-048451-9

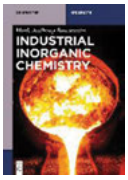

Industrial Inorganic Chemistry.
Benvenuto, 2015
ISBN 978-3-11-033032-8, e-ISBN 978-3-11-033033-5

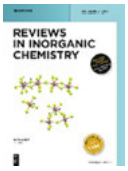

Reviews in Inorganic Chemistry.
Editor-in-Chief: Schulz, Axel
ISSN 0193-4929, e-ISSN 2191-0227

Ralf Steudel

Chemistry of the Non-Metals

Syntheses – Structures – Bonding – Applications

In cooperation with David Scheschkewitz

DE GRUYTER

Authors
Prof. Dr. Ralf Steudel
Grethe-Weiser-Weg 11
D-14055 Berlin, Germany
steudel@sulfur-research.de

Prof. Dr. David Scheschkewitz
Saarland University
Krupp-Chair of General and Inorganic Chemistry
D-66123 Saarbrücken, Germany
scheschkewitz@mx.uni-saarland.de

ISBN 978-3-11-057805-8
e-ISBN (PDF) 978-3-11-057806-5
e-ISBN (EPUB) 978-3-11-057831-7

Library of Congress Control Number: 2019947567

Bibliographic information published by the Deutsche Nationalbibliothek
The Deutsche Nationalbibliothek lists this publication in the Deutsche Nationalbibliografie; detailed bibliographic data are available on the Internet at http://dnb.dnb.de.

Cover image: Philiphotographer / E+ / getty images
Typesetting: Integra Software Services Pvt. Ltd.
Printing and binding: CPI books GmbH, Leck

www.degruyter.com

Preface

How would our planet Earth look like without nonmetals? No water, no air, no life! Not even rocks and sand since oxygen and silicon are responsible for 72.7% of the mass of crustal rocks on the Earth. The human body consists of 96.6% of oxygen, carbon, hydrogen and nitrogen. If all the other nonmetallic elements are added, we end up with 98.0%. Nonmetal compounds play a crucial role in our daily life and in industry as you will see in this book. It is therefore obvious that the chemistry of the nonmetals is a major part of the chemical education at all levels, from high school to university.

The book you are holding in your hands is very special to me. I wrote the first German edition at the very early stage of my academic career, shortly ahead of my one-year sabbatical leave at M.I.T., Cambridge (Massachusetts). It originated from my lectures at the Technical University Berlin, the place known as a hotspot of nonmetal chemistry research. With the years, the book became my lifetime project. I was fortunate enough to share my passion and interest in the chemistry of the nonmetals (and the yellow element in particular) with many friends and colleagues in academia and industry all over the world. Thus, the book was always nourished with the modern developments in fundamental and industrial research.

Five editions of this monograph have been published by de Gruyter, Berlin/Boston, each time completely modernized and extended. This newest international edition is an updated translation of the latest German edition of 2013. I am grateful to my two younger colleagues who share the same passion – Prof. David Scheschkewitz at Saarland University (Germany) who contributed in translating and updating half of the present edition; and Prof. Ingo Krossing at the University of Freiburg (Germany) whose know-how enriched several chapters of a previous German edition.

The book presents an infinite variety and marvelous chemical subtlety of the 22 elements occupying the upper-right section of the Periodic Table and of hydrogen, which was at the origin of the universe when it started 13.8 billion years ago and from which all other elements were formed by nuclear reactions. The work is organized in two parts: Part I explains the basic theoretical concepts needed to understand the structures and reactions of (nonmetallic) molecules and crystals. The larger Part II presents the syntheses, structures and applications of the corresponding compounds and materials. We also address their significance in daily life, chemical industry, environment, material science and farming wherever possible.

Numerous review articles and original publications are cited in footnotes and encourage the readers to study certain topics more extensively. To keep the size of the footnotes with nearly 1000 references under control, however, only one author is given if there are more than three. In addition, well-established handbooks of

https://doi.org/10.1515/9783110578065-202

inorganic chemistry (e.g., GMELIN[1]) and chemical technology (e.g., ULLMANN[2] WINNACKER-KÜCHLER[3] BÜCHEL-MORETTO-WODITSCH[4]and KIRK-OTHMER[5]) may be consulted as a useful source of information. Literature closing date was spring 2019.

In recommending the book to its readers, I like to acknowledge the advice by Profs. Sebastian Hasenstab-Riedel and Christian Müller of the Free University Berlin and the help by Dr. Anja Wiesner who assisted with the graphics. Furthermore, I am most grateful to my wife Dr. Yana Steudel for many years of support and cooperation on the various editions of this book. De Gruyter Publisher in Berlin supported this project from day 1, so that many people who worked with me all these years should be acknowledged.

Many colleagues, coworkers and students contributed to the success of this book with their comments and suggestions and I will be happy to hear from the readers of this edition too.

Berlin-Charlottenburg,
June 2019
Ralf Steudel

1 *Gmelin Handbook of Inorganic and Organometallic Chemistry* – 8th edition, Springer, book series with 185 volumes (partly in English), published in 1936–1995.

2 *Ullmann's Encyclopedia of Industrial Chemistry*, Wiley-VCH, Weinheim, **2006**; many volumes and online edition.

3 Winnacker-Küchler: *Chemische Technik*, Vol. 3: *Anorganische Grundstoffe*, 5th ed., Wiley-VCH, Weinheim, **2005**.

4 K. H. Büchel, H.-H. Moretto, D. Werner (eds.), *Industrial Inorganic Chemistry*, 2nd ed., Wiley-VCH, Weinheim, **2008**.

5 Kirk-Othmer (eds.), *Encyclopedia of Chemical Technology*, 5th ed., Wiley, New York, **2004**; book series with 27 volumes.

Contents

Part II: **Chemistry of the Non-Metals**

Part I: **Chemical Bonds and Properties of Molecules**

1 Introduction

Chemistry is a central science because all life-sustaining processes are based on chemical reactions, and all items that we use in everyday life consist of natural or artificial chemical compounds. "Chemistry is also a fantastic world populated by an unbelievable number of nanometric objects called molecules, the smallest entities that have distinct shapes, sizes and properties. *Molecules are the words of matter*. Indeed, most of the other sciences have been permeated by the concepts of chemistry and the language of molecules. Like words, molecules contain specific pieces of information that are revealed when they interact with one another or when they are stimulated by photons or electrons. In the hand of chemists, molecules, particularly when they are suitably combined or assembled to create supramolecular systems, can play a great variety of functions, even more complex and cleverer than those invented by Nature."[1]

However, chemistry is not only part of the natural sciences but also a *big business* employing millions of people. The global sales of chemical and pharmaceutical industries totaled the enormous amount of 4,751,372,000,000 Euro in 2017, with China contributing the biggest share followed by Europe, the USA and Japan (Table 1.1). In Europe, Germany is by far the biggest producer with BASF at Ludwigshafen (Germany) as the largest chemical site worldwide shown on the cover.

Table 1.1: Sales of the chemical and pharmaceutical industries in 2017 worldwide and in different regions and countries (in billion Euro), ordered by decreasing percentages (other countries: <100 billion Euro each).[2]

World	**4,751**	**100%**
China	1,697	35.7%
Europe	1,015	21.4%
European Union (28)	817	17.2%
USA	723	15.2%
Japan	210	4.4%
Germany	209	4.4%
India	149	3.1%
Republic Korea	137	2.9%
France	113	2.4%

1 M. Venturi, E. Marchi, V. Balzani, *Top. Curr. Chem.* **2012**, *323*, 73.

2 https://www.vci.de/ergaenzende-downloads/chemiemaerkte-weltweit-rankings.pdf.

https://doi.org/10.1515/9783110578065-001

The **nonmetallic elements** and their compounds are the *basis of many classical and modern industrial processes*,[3] resulting in products that enable mankind to live a comfortable and healthy life, at least in the developed countries but increasingly so also in the developing part of the world. For example, fertilizers based on *ammonia* guarantee a sufficient global food production to nourish the 7.7 billion people on the Earth (2019) – and probably even more in the foreseeable future. Without the invention of synthesis of ammonia from the elements, billions of people had probably died from starvation during the last 100 years. Therefore, not less than three NOBEL prizes have been awarded to chemists and engineers for the invention, the industrial development and the mechanistic explanation of the synthesis of ammonia as an archetypical example of heterogeneous *catalysis* (see Chapter 9).

In the following, let us make a short excursion to the main groups of the **Periodic Table** containing 23 nonmetallic elements to demonstrate their importance for modern civilization by selected examples of compounds, products and processes.

Hydrogen gas is not only an important reducing, hydrogenating and desulfurization agent in chemistry but increasingly serves as a fuel and *energy storage* material for environmentally friendly power generation and mobility. Hydrogen-powered fuel cells in cars, trucks and trains have been developed for future transportation in cities plagued by air pollution from the combustion of fossil fuels. Therefore, the cost-efficient production of elemental hydrogen from water using renewable energy sources such as sunlight and wind is presently a research topic of utmost importance, especially the catalytic *water splitting* by solar radiation. Elemental hydrogen is also used to propel rockets to transport heavy cargo into space. As an element, hydrogen is a key component of all organisms, for example, in the form of water, carbohydrates, fats, amino acids, proteins, peptides, enzymes and vitamins. In this context, intermolecular *hydrogen bonds* are of pivotal importance in chemistry, biology and medicine. The three-dimensional structures of virtually all biological molecules such as proteins, enzymes and DNA heavily depend on hydrogen bonds.

Deuterium (^{2}H or D) as the next heavier isotope of hydrogen shows twice the atomic weight, which accounts for unusually pronounced isotopic differences in physical and chemical properties. Heavy water D_2O – first prepared in 1933 by continued electrolysis of water – made the construction of the first nuclear reactor possible in which it served as a neutron moderator and coolant.

Boron compounds are not too visible in daily life, but chemists appreciate every day the chemical and thermal resistance of *borosilicate glassware* in the laboratory. Similarly, *boron nitride* and *boron carbide* are high-performance ceramic materials and serve, inter alia, as neutron absorbers in nuclear reactors. On the other hand, the large absorption cross section of the isotope ^{10}B for neutrons is used for cancer therapy by neutron irradiation. Furthermore, *hydroborates* are important

3 www.essentialchemicalindustry.org.

reducing agents, and *boranes* as well as *boronic acids* are valuable reagents in organic synthesis. Finally, *perborates* are known as powerful bleaching agents in detergents at home.

The inorganic chemistry of **carbon** comprises the allotropes of the element as well as carbon compounds lacking any CH bonds. *Graphite* as the thermodynamically stable modification is most important, but more spectacular are diamonds, graphene, fullerenes and carbon nanotubes. The latter three are *high-tech materials*, which are extensively explored for applications based on their astonishing physical and chemical properties. Graphite is a metallic electrical conductor. Carbon materials of this type are utilized as anodes in lithium-ion batteries, which power mobile phones, laptops and tablets as well as millions of electric cars on the streets. In addition, carbon-based anodes are applied in large-scale industrial processes such as electrolytical production of fluorine, chlorine, sodium, aluminum and many other elements.

Diamonds do not only serve as "girls' best friends," but they make high-performance cutting and drilling tools more durable owing to their unparalleled hardness. The discovery of the new class of carbon allotropes called *fullerenes* resulted in the synthesis of numerous derivatives with amazing structures and properties. *Carbon nanotubes* and *graphene* materials with their unique electronic properties are also investigated with high intensity, and a steadily increasing number of related papers are published each year. The European Union supports this work with 100 million Euros per year. The invention of *carbon fibers* made cars and aircrafts more efficient due to their reduced weight. And composite materials based on carbon nanotubes allow the construction of ever-larger blades for wind generators owing to their enormous tensile strength.

On the dark side, the rising CO_2 concentration in Earth's atmosphere is of great concern since it is held responsible for *global warming* and *climate change* due to the greenhouse effect, together with other "greenhouse gases" such as N_2O, NF_3 and CH_4. Thus, the *decarbonization* or *defossilation* of the world's economy by switching from fossil fuels to renewable energy sources is one of the most important challenges of this century, and chemists are expected to contribute significantly to this energy revolution.

Silicon is the second most abundant element in Earth's crust and has been used in the form of silicates since ancient times to make glass and ceramics. Today, high-purity elemental silicon as a *semiconductor* is a major component in electronic and photovoltaic devices, which changed our civilization dramatically during the last 50 years. The popular expression *Silicon Valley* is an indication for this electronic revolution, which started more than 100 years ago with the first extensive fundamental investigation of the silanes and chlorosilanes by ALFRED STOCK. *Silicones* $(RSiO)_n$ as *inorganic polymers* are another multibillion business owing to their numerous applications in households, construction business and industry. They are based on the first direct synthesis of methyl chlorosilanes independently developed in 1941 by RICHARD MÜLLER in Germany and EUGENE ROCHOW in the USA. Furthermore, *glass fibers*

for optical data transmission with high speed and high volume are made of silicon dioxide. Silicate or silicon carbide fibers form the basis of valuable composite materials.

Nitrogen is one of the most important elements in living organisms in which it occurs in amino acids as components of peptides and proteins. The bases of RNA also contain nitrogen atoms, essential for pairing to DNA via NH···N and NH···O hydrogen bonds. This nitrogen originates from ammonium ions in soil, which are supplemented to some extent through the natural *nitrogen cycle* but in modern agriculture mostly by *fertilizers* containing ammonium salts, urea or nitrates. Artificial nitrogen fertilizers are produced from *ammonia*, which in turn is obtained from dinitrogen from the atmosphere and dihydrogen in the HABER-BOSCH process. Since 1950 the world's production of ammonia has increased faster than the world's population. On the other hand, *nitrogen oxides* (NO_x) are formed from air in all combustion processes including Diesel engines and are blamed for health problems in urban areas. Thus, chemists and engineers work to remove these compounds from exhaust gases by catalytic decomposition. On the other hand, NO functions in tiny concentrations as a signaling molecule in mammals and is responsible for the regulation of blood pressure, blood coagulation and immunity. This discovery has been honored by the NOBEL prize in medicine in 1998. Less well known is the use of *high-energy fuels* such as hydrazine and its derivatives in spacecrafts to propel them into space and to distant planets and comets.

Phosphorus is one of those highly oxophilic elements that occur in Nature exclusively in the form of oxosalts such as phosphates. Animals need calcium phosphate to stabilize their bones and teeth, and adenosine triphosphate (ATP) is the dominating energy storage compound of cells in all organisms including mammals and humans. A resting person converts ca. 40 kg of ATP per day and even 0.5 kg per minute during hard work. The exothermic hydrolysis of ATP to the diphosphate (ADP) and hydrogen monophosphate *under physiological (nonstandard) conditions* (300 K, pH = 7.4) is associated with an enthalpy change of approximately −65 kJ mol^{-1}; the liberated energy is used in muscles and other organs. Therefore, ATP must be permanently re-synthesized by cellular respiration with energy delivered by the oxidation of food components (or by sunlight in plants). Consequently, *phosphates* play a central role as fertilizers and food additives in farming as well as in nutrition. In addition, there are numerous nitrogen- and phosphorus-containing herbicides and insecticides for pest control in the farming business.

Arsenic and its compounds are infamous for their toxicity. This seemingly unpleasant property is in fact applied to good advantage in medicine. For example, arsenic trioxide is used to treat a special form of leukemia, and certain organoarsenic compounds help to treat sleeping sickness. Chemotherapy in medicine was first established by PAUL EHRLICH[4] and coworkers who discovered the beneficial

4 P. Ehrlich (1854–1915), German physician and physiologist (NOBEL prize in medicine in the year 1908).

action of *Salvarsan* and *Neosalvarsan* $(RAs)_n$ (n = 3–5) to treat syphilis in 1910–1912 (both were replaced for this indication by penicillin in the 1940s). Today, arsenic is a valuable *alloying component* in metals; it is also needed to produce *semiconductors* such as gallium and indium arsenides.

Oxygen is the most abundant element in the accessible parts of planet Earth. It occurs as silicates, phosphates, sulfates and oxides in the upper crust, as water in the oceans, lakes, rivers and clouds, as O_2 (and O_3 in minor quantities) in the atmosphere, as well as in numerous organic compounds of what is called *biomass*. While O_2 from *photosynthesis* of green plants is the "elixir of life" for animals and humans, the thin *ozone layer* formed by UV photolysis of O_2 in the stratosphere protects all organisms living on the continents from the destructive hard UV radiation of the Sun. Thus, the formation of the ozone layer was a precondition for life to migrate from the oceans (where it probably originated) to the dry surface of the Earth. On the other hand, reactive oxygen species (ROS) such as radicals and peroxides produced during *respiration* processes are harmful to human health and need to be destroyed by antioxidants such as certain vitamins or possibly also by phenolic components in red wine and chocolate. In industry, huge amounts of O_2 are required to oxidize inorganic and organic compounds in numerous different production processes. Furthermore, O_2 is applied on a large scale to reduce the carbon content of pig iron to turn it into steel.

Sulfur compounds have probably played a crucial role in the *origin of life* nearly 4 billion years ago. Before the atmosphere acquired its high oxygen content of today, it contained substantial concentrations of H_2S and this gas together with FeS and hot water from hydrothermal vents on ocean floors has probably been essential for the synthesis of the first organic molecules by reduction of CO_2 (the biological evolution occurred under anoxic or extremely hypoxic conditions, that is, low in oxygen, most of the time). For all organisms, sulfur is an *essential element*. Therefore, coal and crude oil originating from ancient plants contain up to several percent of sulfur. Today *desulfurization* of crude oil and of sour natural gas yields enormous amounts of H_2S, which is oxidized to elemental sulfur as an essential raw material for large-scale production of *sulfuric acid* and many other chemicals including *fertilizers*. Sulfur and its compounds are also needed for production of tires for cars and trucks as well as other rubber materials by the *vulcanization* process. Future electric cars may even be powered by lithium-sulfur batteries, which have a much higher power capacity than today's lithium-ion batteries and would enable a larger range of operation.

Selenium is a rather rare element on the Earth, but it is essential for life. More than 20 natural *selenoproteins* have been identified as redox regulators in animals. Therefore, fertilizers and animal feed are supplemented with traces of selenium compounds in areas where farmland is Se-deficient. In the electronics industry, selenium and certain selenides such as $CuInSe_2$ serve as *semiconductors* in thin-film photovoltaic cells.

Fluorine is the *most reactive of all chemical elements*. It was first prepared in 1886 by HENRI MOISSAN in France who received the NOBEL prize in chemistry of the year 1906 for this ground-breaking work. Today fluorine-containing groups are present in many *pharmaceutical drugs* and in *agrochemicals* to make them more lipophilic and resisting to metabolic and other degradation reactions for a longer period of time. Fluorine renders high-performance materials such as Teflon and Nafion chemically resistant.

Elemental fluorine is used on a large scale to produce UF_6, which is employed for the enrichment of the uranium isotope ^{235}U from the natural mixture with ^{238}U. Enriched uranium is needed for *nuclear reactors*, which produce energy from the spallation of the ^{235}U nucleus by neutrons. In our daily life, fluorides in toothpaste protect our teeth from caries, while $Li[PF_6]$ serves as an electrolyte in commonplace lithium-ion batteries. Molten $Na_3[AlF_6]$ is most important as electrolyte in *aluminum production* from Al_2O_3 by electrolysis. And even the *theory of chemical bonding* has profited from the high reactivity of elemental fluorine since the first neutral noble gas compounds to be prepared were XeF_2 and XeF_4 (made from the elements), triggering a change of paradigm in chemical thinking beginning in the 1960s.

Chlorine gas is one of the most important reactants in industry although it seldom shows up in the final products for sale. Many organic chemicals are made via reactive *chlorine-containing intermediates*. Cl_2 is produced in huge quantities by electrolysis of aqueous NaCl and the efficiency of this energy-intensive process has recently been improved by 30% using special oxygen-consuming electrodes. Thus, even well-established production processes can still be dramatically modernized to save energy. Chlorine compounds are needed to synthesize pharmaceutical drugs, dyestuffs, fertilizers, insecticides, plastics, fibers and modern functional materials. On the other hand, chlorofluorocarbons (CFCs) are harmful to the protective ozone layer in the stratosphere. For the discovery of this effect, the NOBEL prize in chemistry for the year 1995 has been awarded to PAUL CRUTZEN, MARIO MOLINA and FRANK SHERWOOD ROWLAND. In the meantime, the production of CFCs has been internationally banned and other chemicals have taken their place as refrigerants, propellants and solvents.

The **noble gases**, originally discovered spectroscopically by physicist, are no longer as noble as once thought: the number of molecular and salt-like *xenon compounds* exceeds 100 and is growing from year to year. KrF_2 as a rare example of a krypton compound is also studied extensively. Highly unusual species such as $[Xe_2]^+$ und $[AuXe_4]^{2+}$ have been isolated as salts. The main applications of noble gases, however, are still of a physical nature: Gaseous He is used for cooling of nuclear reactors and to lift balloons and airships. In liquid form, it is employed as *coolant* for superconducting magnets, for example, at the large hadron collider (LHC) in Switzerland and for cooling of man-made satellites orbiting the Earth. Besides, He, Ne, Ar and Kr are used to produce coherent radiation in *gas lasers*; Ne,

Kr and Xe are applied in fluorescent and incandescent *lamps*, and – most importantly for chemists – Ar serves as protective gas in glove boxes in the laboratory as well as in industry.

Very recently, the "oldest molecule of the universe" formed about 100,000 years after the Big Bang was discovered by astrophysicists. At that time the original gas and plasma cloud had cooled down enough that He existed mainly as neutral atoms while hydrogen existed still mostly ionized as free protons. Since He has a high proton affinity, the ion $[HeH]^+$ is thought to be the first molecular entity ever formed in the universe. In 2018 $[HeH]^+$ has been observed by its emission spectrum in the planetary nebula NGC7027 using the high-flying telescope Sofia built into an Airbus aircraft.[5]

In **Part II** of this textbook the preparation, structures, properties and applications of the nonmetallic elements and their most important compounds are described in detail, starting with hydrogen and then following the order of the Periodic Table. The chemical literature up to spring of 2019 has been considered, and many references to recent reviews allow further reading on special topics. To fully understand the structures and reactivities of molecules and materials, however, a good knowledge of the underlying *theory of chemical bonding* is necessary. This theory has originally been developed on the basis of empirical observations, for example, spectroscopic and thermodynamic data. Today theoretical concepts are not only expected to explain well-established facts but to provide reliable *predictions* of the structures and properties of still unknown substances. Only on this basis, new materials with specific functions can be developed for defined high-tech applications.

Therefore, in **Part I** of this book the theoretical concepts necessary for the understanding of nonmetallic systems are discussed. In this context, it is not always necessary to turn to quantum mechanics, since simple *model descriptions* of molecules are often sufficient to rationalize and classify the enormous amount of today's empirical knowledge in chemistry. These model descriptions are also helpful in teaching regardless whether they are true or not. Of course, the limits of the particular model have to be respected and they cannot be used to *explain* Nature. In this sense, the basic concepts of chemical bonding theory are outlined in Chapter 2, the VAN DER WAALS interaction is explained in Chapter 3 and the empirical properties of covalent bonds in molecules such as bond energies, bond lengths, bond polarities and intermolecular interactions are discussed in Chapter 4.

Textbooks are mainly dealing with the present knowledge but only rarely with *still unknown substances*, although they may play an important role in the future. *Chemical Abstract Service* (CAS) in Columbus (Ohio) has already registered more than **$7{\cdot}10^7$ compounds**, but most of the theoretically possible molecules have probably not been synthesized or discovered yet. Combining an increasing number of different chemical elements in one molecule or one material opens the possibility to

5 R. Güsten et al., *Nature* **2019**, *568*, 357.

create completely new functions, for example, for catalysis or medical applications. To predict the physical, chemical and functional properties as well as the potential usefulness of such systems requires a good understanding of the present-day knowledge of atoms, molecules, bond properties and theoretical as well as empirical concepts and relationships. Therefore, the corresponding theoretical fundamentals will be outlined in Part I of this book, followed by the larger Part II covering the synthesis, structures and reactions of the most important inorganic compounds of the nonmetallic elements.

2 The Chemical Bond

The theoretical treatment of chemical bonding in molecules, ions and crystals is among the most challenging problems in chemistry. In particular, if a readily accessible interpretation of experimental observations or of the results of theoretical calculations is sought, the use of appropriate models cannot be avoided. Since the microscopic world is dramatically different from our macroscopic experience, approximations and idealizations are necessary to elucidate the behavior of atoms and molecules. After all, *physics does not describe the real world but only our knowledge of the real world*.

The situation is even less satisfying when having a closer look at the general *properties of electrons*, which are responsible for the bonds between the nuclei of atoms and thus determine most of chemistry. Electrons are practically dimensionless particles (diameter $\leq 10^{-18}$ m) with a certain charge, a certain mass and a spin. The spin is an abstract quantum-mechanical property of electrons and should not be identified with the rotation of a particle, although it has the same dimension as an angular momentum. These particle-like properties follow from spectroscopic observations and from experiments regarding the behavior of electron beams in electric and magnetic fields. On the other hand, electron beams behave as a sequence of small wave packets and thus undergo scattering and interference, which are typical properties of electromagnetic waves (e.g., photons). In other words, in the atomic world there are *complementary properties*. One may ask: How can a seemingly zero-dimensional point have a mass, a charge and a spin? Where does this mass come from? According to quantum field theory all elementary particles are excitations of omnipresent fields, one for each particle.[1]

Despite this ambiguity, theoretical calculations based on the SCHRÖDINGER equation and using *four quantum numbers* for each electron predict the behavior of electrons in atoms and molecules with reasonable accuracy and even provide more or less reliable enthalpies of real and hypothetical chemical reactions. This area of *computational chemistry* has become increasingly popular in recent times. Most chemical publications on inorganic molecules these days contain the results of quantum-chemical calculations to some extent.

A theory is useful if it explains a large body of observations with a minimum of parameters and assumptions. In addition, it should correctly predict the properties, structures and reactions of yet-to-be prepared compounds. We need to keep in mind, however, that any theory exists only in our brain and this also

1 Theoretical physicists believe that the mass of elementary particles is the result of their interaction with a background field first proposed by the British theoretical physicist PETER HIGGS (HIGGS field); he was born in 1929 and received the NOBEL prize in physics for the year 2013.

https://doi.org/10.1515/9783110578065-002

applies to the components of the theory, for example, atomic and molecular orbitals (MOs) as well as bonds. In this sense, *a theory is just a working hypothesis*, which cannot be proven as true, but can always be falsified and replaced by another theory. A good example is the first model of the hydrogen atom published by NIELS BOHR in 1913. At that time, BOHR's theory was considered a revolutionary development in atomic physics and consequently he was awarded the NOBEL prize in physics. Only a few years later the quantum-mechanical model of the hydrogen atom replaced BOHR's theory, and other atomic physicists received the NOBEL prize.[2]

A chemical bond is a result of the accumulation of negative charge density in the region between a pair of (positively charged) nuclei, which is sufficient to balance the forces of electrostatic repulsion. In chemistry, it is common to discuss the phenomenon of chemical bonds at different levels of accuracy, depending on the questions to be answered. A satisfactory *theory of the chemical bond* should be able to provide answers to the following fundamental questions:

Why do atoms combine to form molecules and crystals?
Why do they do so in certain ratios, and often in several ratios, for example, NO, NO_2, N_2O, N_2O_3, N_2O_5?
Why do molecules and crystals have discrete structures?
Why do molecules react with each other the way they do?

To answer these and related questions, it is appropriate to consider distinct bond types:

(a) the ionic bond,
(b) the covalent bond including coordinate or dative bonds and
(c) the VAN DER WAALS interaction.

From the structures of several hundred thousand molecules determined by X-ray crystallography, electron diffraction, vibrational, nuclear magnetic resonance (NMR) and microwave spectroscopy, we have learned that there is a continuous transition between these three fundamental bond types. In most compounds more than one of these idealized types contributes to the overall bonding situation. We begin our discussion with the model of the ionic bond, which is built exclusively on electrostatic forces without any quantum mechanics and therefore most easily understood.

2 NOBEL prizes in physics have been awarded to NIELS BOHR (1922), LOUIS V. DE BROGLIE (1929), WERNER HEISENBERG (1932), ERWIN SCHRÖDINGER (1933), WOLFGANG PAULI (1945) and MAX BORN (1945). WALTER KOHN and JOHN POPLE received the NOBEL prize in 1998 for the development of algorithms and software for quantum-chemical calculations.

2.1 The Ionic Bond

2.1.1 General

A huge number of compounds crystallize in ionic structures consisting of periodic, regular, three-dimensional arrays of cations and anions. The ions may be monoatomic or complex, that is, derived from molecules:

Li^+ and H^- in LiH	$[NO]^+$ and $[HSO_4]^-$ in $[NO][HSO_4]$
Ca^{2+} and F^- in CaF_2	$[H_3O]^+$ and $[ClO_4]^-$ in $[H_3O][ClO_4]$
Al^{3+} and O^{2-} in Al_2O_3	$[NH_4]^+$ and $[BF_4]^-$ in $[NH_4][BF_4]$

Stoichiometric ratios of cations and anions achieve electrical neutrality in the crystal. The crystal type, that is, the geometry and symmetry of the crystal lattice, is determined by the relative sizes of the ions and by the ratio of their charges. Monoatomic anions are generated from neutral atoms by addition of an electron with liberation of an enthalpy called the *electron affinity* E_{ea}. In the case of cations, the removal of an electron requires the *ionization energy* E_i.

2.1.2 The Ionization Energy E_i

The first ionization of a gaseous atom A according to the equation

$$A(g.) \longrightarrow A^+(g.) + e^- \qquad \Delta H° = E_i$$

requires an *enthalpy* $\Delta H°$, which, for historic reasons, is called *ionization energy* E_i and is always positive.[3] For this process it is assumed that the least tightly bound electron is removed from the atom (taken from the highest occupied atomic orbital). The values of E_i depend strongly on the position of the atom A in the Periodic Table. Metal atoms are most easily ionized, while noble gas atoms have the highest E_i values. Ionization energies of neutral atoms range from 4 to 25 eV or 400 to 2400 kJ mol^{-1} (1 eV = 96.49 kJ mol^{-1}).

Figure 2.1 shows the dependence of atomic ionization energies on the corresponding atomic number:

3 In the chemical and physical literature, the symbols *I* and *IE* are also used for the ionization energy and sometimes even the term ionization potential (IP). For data, see: http://webbook.nist.gov/ (website of the National Institute of Science and Technology).

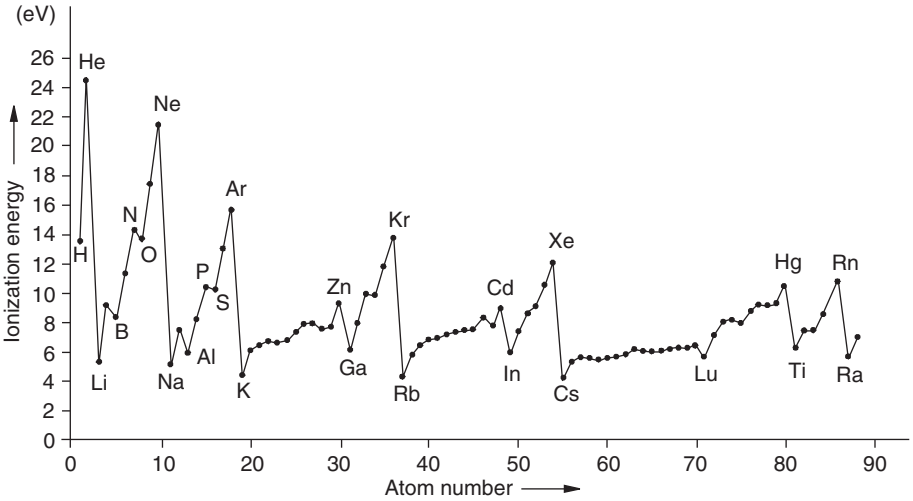

Figure 2.1: Dependence of the first ionization energies $E_i(1)$ of the chemical elements on their atomic number (in eV).

The large ionization energies of the noble gases are of enormous importance; they are caused by the large *effective nuclear charge* Z_{eff} acting on the valence electrons (VEs) of these atoms with their filled *s* and *p* levels. According to empirical rules originally published by JOHN SLATER, the Z_{eff} values can be estimated for each electron configuration taking the partial shielding of the nuclear charge by the other electrons into account. For the elements of the first period, the following data are obtained for the VEs in the highest occupied orbitals:[4]

	Li	Be	B	C	N	O	F	Ne
Z_{eff}:	1.30	1.95	2.60	3.25	3.90	4.55	5.20	5.85
E_i (eV):	5.39	9.32	8.30	11.30	14.53	13.62	17.42	21.56

There is a relationship between the value of the first ionization energy $E_i(1)$ and the absolute energy ε of the orbital from which the electron has been removed.[5] These two energies are often identified with each other, an approximation that is known as KOOPMANS' theorem. For example, E_i of the carbon atom is 11.3 eV, while the energy of the *2p* orbital has been calculated as –10.7 eV. The difference between these two energies, using absolute values, is caused by the simultaneous *rearrangement of*

4 For improved rules to calculate effective nuclear charges, see: E. Clementi, D. L. Raimondi, *J. Chem. Phys.* **1963**, *38*, 2686.

5 The *eigen-values* ε_j of the one-electron SCHRÖDINGER equation are called *orbital energies*.

the remaining electrons during ionization (relaxation) since the effective nuclear charge increases and the interelectron repulsion decreases on ionization. For lithium $E_i(1)$ = 5.39 eV and $\varepsilon(2s)$ = −5.34 eV, while for neon $E_i(1)$ = 21.56 eV and $\varepsilon(2p)$ = −23.14 eV.

As shown above, the ionization energy of oxygen (13.6 eV) is – somewhat unexpectedly – smaller than E_i of nitrogen (14.5 eV). In the N atom and in the cation O^+ there are three electrons of equal spins occupying the 2*p* level resulting in maximal *exchange interaction*, which stabilizes this configuration: the three electrons occupy one orbital each, thus avoiding identical space segments and diminishing the COULOMB repulsion. Their equal spins minimize the PAULI repulsion at the same time.[6] In other words, if the ionization results in a half-filled electronic (sub)shell, the required ionization energy is slightly lower than expected.

Similarly, the lower ionization energy of the boron atom compared to neighboring beryllium is caused by the fact that the removed electron comes from a 2*p* orbital in the case of boron but from the lower 2*s* level in the case of beryllium.

The second ionization energy $E_i(2)$ of an atom according to the equation

$$A^+(g.) \longrightarrow A^{2+}(g.) + e^-$$

is always considerably larger than $E_i(1)$ as the electron must now be removed from a particle bearing a positive charge already. For example, $E_i(2)$ of the carbon atom is 24.4 eV, although the removed electron comes from the same 2*p* level as in the first ionization. This means that the orbital energies of the cation C^+ are much lower than those of the neutral atom, which is readily explained by the higher effective nuclear charge. $E_i(2)$ also varies periodically with the atom number, but the maxima are now observed for the ions with noble gas electron configuration, for example, Na^+ and K^+. The curve in Figure 2.1 would thus be shifted to the right by one atomic number, and in a similar manner for the third ionization energy $E_i(3)$.

2.1.3 The Electron Affinity E_{ea}

Most gaseous nonmetallic atoms B can capture an electron in an exothermic reaction:

$$B(g.) + e^- \longrightarrow B^-(g.) \qquad -\Delta H^\circ = E_{ea}$$

6 According to the PAULI *exclusion principle*, electrons of the same spin behave as if there were a repulsive force acting between them. Consequently, two electrons of equal spin cannot occupy the same space or orbital at the same time. Since only two spin states are possible and since quantum numbers differ by one unit these states are characterized by the *spin quantum numbers* +½ and −½.

The electron affinity E_{ea} is taken as positive if energy is released on electron capture.[7] For stable anions, E_{ea} ranges from 0 to 3.6 eV or 0 to 350 kJ mol^{-1} (Figure 2.2). In contrast to the ionization energies, electron affinities do not show a periodic trend with atomic number. The effect of filled or half-filled electronic (sub)shells, however, is far more pronounced: Noble gases, nitrogen and some metal atoms do not form stable anions and their electron affinities are therefore zero (or even negative).[8]

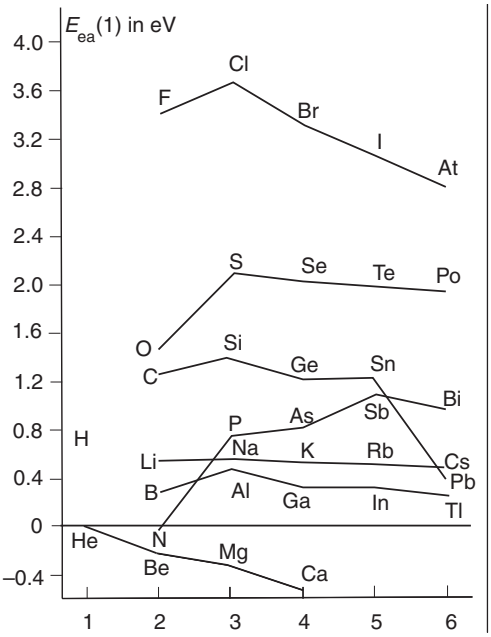

Electron affinity: E_{ea}(1) in eV

H					He
0.75					**0**
B	C	N	**O**	**F**	Ne
0.28	1.27	–0.07	1.46	3.40	0
		(–8.29)	(–8.08)		
Al	Si	P	S	Cl	Ar
0.46	1.38	0.74	2.08	3.61	0
			(–6.11)		
Ga	Ge	As	Se	Br	Kr
0.30	1.24	0.80	2.02	3.36	0
			(–4.35)		
In	Sn	Sb	Te	I	Xe
0.30	1.25	1.05	1.97	3.06	0

Values in parentheses: E_{ea}(2) in eV

Figure 2.2: Electron affinities E_{ea} of main-group elements. E_{ea}(2) denotes the electron affinity for addition of a second electron.

The electron affinity of an atom is identical to the ionization energy of its mono-anion:

$$B^-(g.) \longrightarrow B(g.) + e^- \qquad E_i(B^-) = E_{ea}(B)$$

For example, E_{ea} of the carbon atom is 1.27 eV, and the ionization energy of the anion C^- (1.27 eV) is consequently much smaller than that of the neutral carbon atom (11.3 eV). The formal addition of a second or third electron to an atom is always strongly endothermic, that is, E_{ea}(2) and E_{ea}(3) are always negative and can

7 In the chemical literature the electron affinity is also symbolized by *A* or *EA*; for numerical data see: http://webbook.nist.gov/.

8 J. Furtado, F. De Proft, P. Geerlings, *J. Phys. Chem. A* **2015**, *119*, 1339. K. D. Jordan, V. K. Voora, J. Simons, *Theor. Chem. Acc.* **2014**, *133*, 1.

only be determined by thermochemical cycles (see below) since such ions do not exist except (formally) in crystals. The E_{ea} values in Figure 2.2 demonstrate that ions with noble gas electron configuration are particularly stable. As a consequence, the halogen atoms show the largest electron affinities.

Here it should be stressed that multiple charged anions such as O^{2-} and S^{2-} but also $[CO_3]^{2-}$, $[SO_4]^{2-}$ and $[PO_4]^{3-}$ *do not exist as isolated ions*, for example, in the gas phase. They would immediately lose one or two electrons by a process called *spontaneous electron autodetachment* to form mono-anions. Small complex anions may also dissociate exothermically into mono-anions by what is referred to as COULOMB explosion.[9] Therefore, any experimental observation of such ions in the gas phase is impossible. The negative electron affinities listed in Figure 2.2 have a more formal character and have been derived from thermodynamic cycles, which will be discussed in Section 2.1.6. In condensed phases, on the other hand, all anions are surrounded by cations or polar solvent molecules, which reduce the anionic charges and thus stabilize the multiple charged anions.[10] The real charges of cations and anions in crystals and solutions are known only in a few cases and strongly depend on the volume assigned to these ions.

2.1.4 Ionic Crystals and Ionic Radii

Rock salt (NaCl) will be taken as the standard example of an ionic crystal since the halides of all alkali metals except cesium adopt this structure type.[11] Precise internuclear distances can be determined from X-ray diffraction on a single crystal although the diffraction takes place at the electrons rather than at the nuclei. Since the highest electron density is near the nuclei, their approximate positions can nonetheless be determined.[12] Sodium chloride has a face-centered cubic unit cell. The unit cell is the smallest array containing all the symmetry elements of the crystal, which can formally be constructed by periodic translational repetition of the unit cell in all three dimensions. The infinite set of translational vectors forms the *crystal lattice*. The positions of the ions in the rock salt structure are shown in Figure 2.3.

9 A. I. Boldyrev, J. Simons, *J. Phys. Chem.* **1994**, *98*, 2298. R. Janoschek, *Z. Anorg. Allg. Chem.* **1992**, *616*, 101. Only much larger particles such as the fullerene C_{60} can accommodate more than one additional electron in the gas phase.

10 See for instance: S. Sasaki et al., *Acta Cryst.* A **1980**, *36*, 904.

11 The cesium halides CsX (X=Cl, Br, I) crystallize in cubic body-centered structures with coordination numbers of 8 for all ions (each ion is at the center of a cube of counter-ions).

12 Diffraction of neutrons takes place at the nuclei, and for the exact determination of positions especially of hydrogen atoms with their large vibrational amplitude and low electron density neutron diffraction is the preferred method.

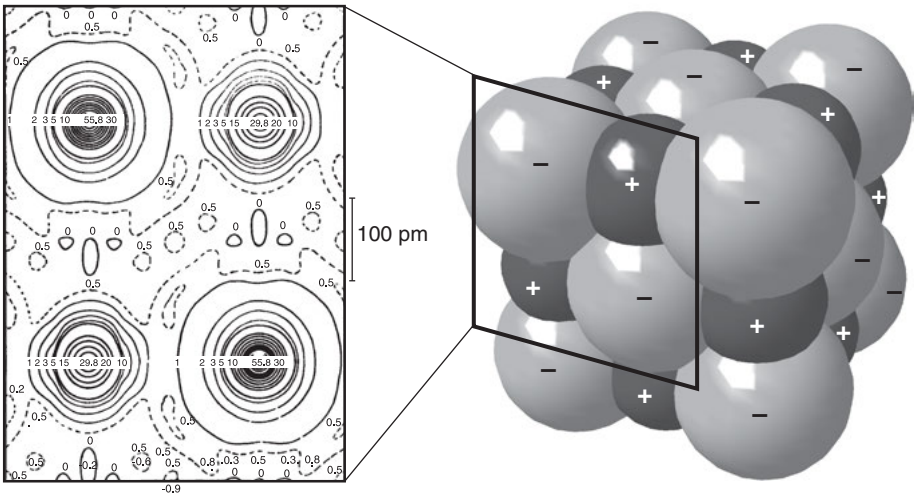

Figure 2.3: Right: Face-centered cubic packing of sodium cations and chloride anions in rock salt. Left: Experimental electron density distribution in the (110) plane of NaCl. The larger Cl^- ions have a maximum charge density of 55.8 and the smaller Na^+ ions of 29.8 e Å^{-3} (1 Å = 100 pm).

From precise X-ray diffraction data, it is possible to calculate, in addition to ion locations, the total electron density distribution in a crystal, measured in $e\ a_0^{-3}$ or e Å^{-3} (1 $e\ a_0^{-3}$ = 6.749 e Å^{-3}). For rock salt, the result is shown in Figure 2.3 in the form of a contour map of isodensities for a segment of the shown (110) plane. The electron densities decrease from the center of the atoms to the outside – strongly at first, then less so. On the shortest connection line between neighboring cations and anions, the density drops to a minimum of 0.2 e Å^{-3} (1 Å = 100 pm). This point of almost zero density can be considered as the boundary of the two contacting ions of opposite charge, with the *ionic radii* defined as the distances from the corresponding nuclei to this point. Integration of the electron density over the spherical volumes limited by the ionic radii yields 10.05 electrons for Na^+ and 17.70 electrons for the Cl^- ion, compared to 10 and 18 for *pseudo*-Ne and *pseudo*-Ar configurations, respectively. The "missing" 0.25 electrons can be expected in the interstices of the spherical packing, which were not considered in the integration (see Figure 2.3). Thus, the structure consists of ions rather than of neutral atoms.

For our future discussions we assume that atomic ions in crystals are approximately spherical and rigid and have a characteristic radius (*crystal radius*). However, the radii derived from electron density maps are not constant but depend on the particular crystal structure and the coordination numbers of the ions.[13] The

13 I. D. Brown, *Encycl. Inorg. Chem.* **2005**, *1*, 446. A. Shannon, *Acta Cryst. A* **1976**, *32*, 751.

variation of ionic radii (in pm) of different ions with the number of electron shells and ionic charges at a constant coordination number of 6 is demonstrated by the following examples (the corresponding *isoelectronic noble gas* is given at the top of each column):

[He]	[Ne]	[Ar]	[Kr]	[Xe]
Li^+: 90	Na^+: 116	K^+: 152	Rb^+: 166	Cs^+: 181
	F^-: 119	Cl^-: 167	Br^-: 182	I^-: 206
	O^{2-}: 126	S^{2-}: 170	Se^{2-}: 184	Te^{2-}: 207

As expected, ionic radii increase with the number of electron shells but decrease with increasing positive charge and increase with increasing negative charge. The latter is the consequence of the varying effective nuclear charge, which attracts the VEs as well as of the varying electron–electron repulsion. In the following series of *isoelectronic ions*, the radii increase from cations to anions:

$$Ca^{2+} < K^+ < Cl^- < S^{2-}$$

The concept of pure ionic bonding is an idealized approximation, which is nearly fullfilled in crystals of two elements with a large electronegativity difference. Since the alkali metals have the lowest and fluorine and oxygen the highest electronegativities (Section 4.6.2), the fluorides and oxides of these metals are probably the best examples for this bond type. As will be seen in the following sections, however, certain covalent contributions by mutual polarization of the ions as well as VAN DER WAALS interactions also contribute to the stability of ionic crystals.

2.1.5 Lattice Energy and Lattice Enthalpy

The stability and properties of ionic compounds are derived from the lattice energy and enthalpy for which the symbols U_o and $\Delta_{lat}H°$ are used, respectively. The lattice enthalpy is defined as the enthalpy liberated when equivalent molar amounts of gaseous cations and anions are combined from infinite distance to form a single crystal:

$$A^+(g.) + B^-(g.) \longrightarrow AB(s.) \qquad \Delta_{lat}H° < 0$$

Since $\Delta_{lat}H°$ is liberated from the system, it always carries a negative sign (a "large lattice energy" means a highly negative value of $\Delta_{lat}H°$). Lattice energy and enthalpy are related by the contribution of the volume change:

$$\Delta_{\text{lat}}H^{\circ} = \Delta_{\text{lat}}U^{\circ} + p\Delta V \tag{2.1}$$

Only at 0 K, $\Delta_{\text{lat}}H°$ and $\Delta_{\text{lat}}U°$ are identical, but nevertheless the term "lattice energy" is often used for either one in the physicochemical literature. This is somehow justified since the absolute values of $\Delta_{\text{lat}}H°$ and $\Delta_{\text{lat}}U°$ differ just slightly at 25 °C. The lattice energy $\Delta_{\text{lat}}U°$ consists of several components, which are summarized for three metal halides in Table 2.1.

Table 2.1: Components of the lattice energy of three metal halides (in kJ mol^{-1}). The decomposition of the total lattice energy into components rests on approximations; therefore, the slight deviations from the accurate enthalpy data in Table 2.2. AgCl crystallizes in the rock-salt structure and CsI in the cubic body-centered CsCl structure.

Salt:	NaCl	AgCl	CsI
COULOMB interaction	−862	−875	−619
Repulsion according to BORN	+100	+146	+63
VAN DER WAALS attraction	−13	−121	−46
Zero-point energy	+8	+4	+29
Sum	−767	−846	−573

The largest contribution arises from the electrostatic attraction between ions of opposite charge and repulsion between ions of equal charge (COULOMB interaction). In addition, VAN DER WAALS attraction works independently of charge (see Chapter 3). Note that this component contains some covalent bonding, the absolute strength of which is inversely proportional to the electronegativity difference $\Delta\chi_P$ between the two elements (PAULING values): $\Delta\chi_P$ = 2.3 (NaCl) > 1.9 (CsI) > 1.3 (AgCl).

At equilibrium, attractive forces are balanced by repulsion arising from mutual interpenetration of the electronic clouds of neighboring ions as well as from the interaction of equally charged next neighbors but one. Like atoms, ions have no fixed boundaries. In the formation of NaCl crystals to reach an internuclear distance of 281.4 pm, the electron clouds of cations and anions mutually penetrate slightly, resulting in some contraction of the ions. This increases the potential energy of the ions and reduces the lattice energy as shown in the second line of Table 2.1 (BORN repulsion).

The fourth component of lattice energy, the zero-point energy, is the vibrational energy of the ions, which remains even at 0 K. This energy can be calculated from the lattice vibration frequencies obtained from infrared (IR) or RAMAN spectra. The zero-point energy has a relatively small effect on the lattice energy; therefore, it is often ignored.

2.1.6 Determination of Lattice Energies and Enthalpies

Unfortunately, lattice energies and enthalpies cannot be measured directly but are obtained by indirect means. If certain thermodynamic data are known, the lattice enthalpy can be calculated from a BORN–HABER cycle[14] as shown in Figure 2.4. Such thermochemical cycles are based on HESS's law,[15] which states that the energy difference between two well defined states 1 and 2 is independent of the route from state 1 to state 2.

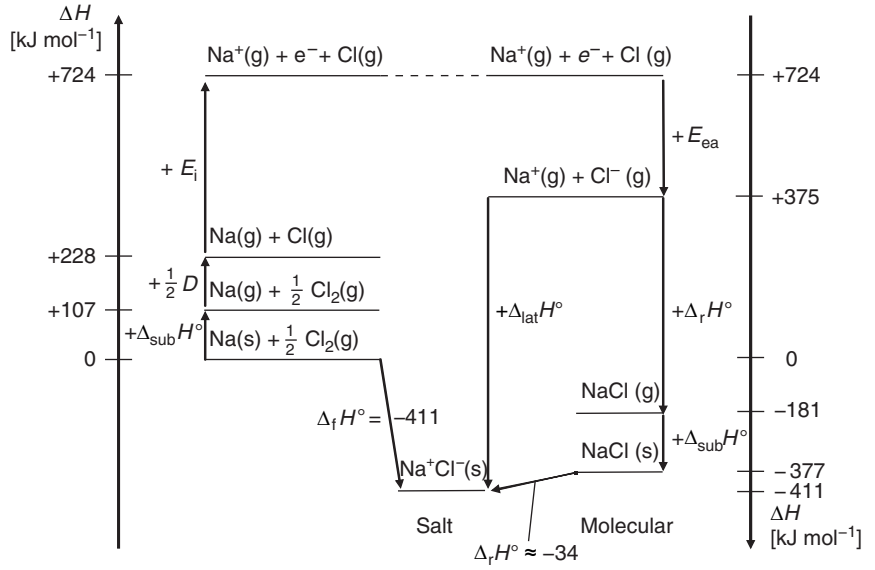

Figure 2.4: Born–Haber cycle for the determination of the lattice enthalpy of the *salt* Na^+Cl^- and, alternatively, for the competing formation of a hypothetical *molecular solid* NaCl.

The single enthalpies of the BORN–HABER cycle for NaCl are as follows:

- $\Delta_{lat}H°$ Lattice enthalpy Na^+Cl^- (–786 kJ mol^{-1}).
- $\Delta_fH°$ Standard enthalpy of formation of crystalline NaCl from the elements (–411 kJ mol^{-1}).
- $\Delta_sH°$ Standard enthalpy of sublimation of sodium metal (+107 kJ mol^{-1}) or of molecular NaCl (+196 kJ mol^{-1}).[16]

14 Published in 1919 by MAX BORN (German physicist; 1882–1970) and FRITZ HABER (German chemist; 1868–1934).

15 Proposed in 1840 by GERMAIN HENRI HESS (Swiss-Russian chemist; 1802–1850).

16 For hypothetical *molecular* NaCl, the enthalpy of sublimation ($\Delta_{sub}H°$) has been estimated as 196 kJ mol^{-1}.

$\Delta_r H°$ Standard enthalpy of formation of gaseous NaCl molecules (–556 kJ mol^{-1}).
E_i First ionization energy of Na atoms (+496 kJ mol^{-1}).
$D°$ Dissociation enthalpy of Cl_2 molecules (+242 kJ mol^{-1}).
E_{ea} Electron affinity of Cl atoms (–349 kJ mol^{-1}).

Starting point of the two competing cycles are the elements in their standard states: solid sodium metal and gaseous chlorine. For this state the overall enthalpy is defined as zero. On the left side of Figure 2.4 endothermic reactions are shown to produce the gaseous ions Na^+ and Cl^- from which either ionic or molecular NaCl can then be theoretically produced (right-hand side). The diagram shows that salt-like NaCl is by just –34 kJ mol^{-1} more favorable than solid molecular NaCl.

This simple example demonstrates that it is not a priori obvious whether a compound such as a phosphorus pentahalide PX_5, for example, exists as a molecular solid or as an ionic salt. In fact, only PF_5 is molecular in the solid state, while solid PCl_5 and PBr_5 form ionic crystals (see Section 10.8.3).

In Figure 2.4, only enthalpy data are given since all reactions are thought to occur at constant pressure (and at 25 °C). Consequently, BORN–HABER cycles yield *lattice enthalpies* that differ from lattice energies by the so-called volume work $p\Delta V$. From Figure 2.4 the relationship between the lattice enthalpy $\Delta_{lat}H°$ and the other thermodynamic data follows as shown in eq. (2.2):

$$\Delta_{lat} H^\circ = \Delta_s H^\circ + E_{ea} - 1/2\, D - E_i - \Delta_{sub} H^\circ \tag{2.2}$$

For NaCl, the volume work is $p\Delta V$ = 5.0 kJ mol^{-1} at 25 °C. Since the accuracy of the thermodynamic data needed to estimate lattice enthalpies is of the same order of magnitude, the volume work is usually neglected, and lattice energies and enthalpies are thought to be practically identical.

Lattice energies U_o of salts can also be calculated from COULOMB's law using *ionic volumes* V_{ion} (rather than ionic radii) as will be shown for a salt of type A^+B^-:

$$V_{ion}(A^+) = \frac{V_{cell}(A^+B^-)}{Z} - V_{ion}(B^-)$$

In this equation, V_{cell} is the volume of the unit cell and Z is the number of formula units in the unit cell. Summation over all ionic volumes V_{ion} yields the molecular volume V_m (in nm^3), which determines the lattice energy:

$$V_m = V_{ion}(A^+) + V_{ion}(B^-)$$

The following equation holds for every salt:

$$U_o = |z_+||z_-| \cdot n \cdot \left(\frac{\alpha}{\sqrt[3]{V_m}} + \beta \right) \tag{2.3}$$

Herein $|z_+|$ and $|z_-|$ are the charge numbers of cations and anions, n is the number of ions (2 for formula AB, 3 for AB_2, etc.); α and β are empirical constants (for A^+B^-: α = 117.3 kJ mol^{-1} nm; β = 51.9 kJ mol^{-1}; for $A^{2+}(B^-)_2$: α = 133.5 kJ mol^{-1} nm; β = 60.9 kJ mol^{-1}).[17] Lattice energies obtained by eq. (2.3) usually agree with those from BORN–HABER cycles within a few kJ mol^{-1}. Larger deviations are observed if covalent contributions play a role, for example, with the heavy copper and silver halides (see Section 2.1.8).

From eq. (2.3) it follows that lattice energies are large if the sum of ionic volumes is small (compare LiF with CsI) or if the ionic charges are large as in Al_2O_3 (see Table 2.2).

Table 2.2: Lattice enthalpies of binary salts at 25 °C (in kJ mol^{-1})[a].

	Hydrides	Fluorides	Chlorides	Bromides	Iodides	Oxides
Li^+	−918	−1049	−864	−820	−764	−2814
Na^+	−807	−930	−790	−754	−705	−2478
K^+	−713	−829	−720	−691	−650	−2232
Rb^+	−684	−795	−695	−668	−632	−2161
Cs^+	−653	−759	−670	−647	−613	−2063
Mg^{2+}	−2718	−2978	−2540	−2451	−2340	−3791
Ca^{2+}	−2406	−2651	−2271	−2131	−2087	−3401
Al^{3+}	–	−6252	−5513	−5360	−5227	−15525
Ag^+	–	−974	−918	−905	−892	−2910

[a] after H. D. B. Jenkins, H. K. Roobottom, *CRC Handbook of Chemistry and Physics*, CRC Press, Boca Raton, 80th ed., 1999–2000, Chapt. 12, p. 22.

2.1.7 Significance of the Lattice Enthalpy

The lattice energy reflects the strength of the bonds between the ions in a crystal. Therefore, the chemical and physical properties of salts are related to their lattice energies. Lattice energies correlate directly with melting and boiling points as well as hardness and indirectly with the coefficients of thermal expansion and compressibility. The very high lattice energy of Al_2O_3 makes the hard corundum a suitable grinding agent, but the high melting point of this oxide (2045 °C) necessitates a eutectic mixture with $Na_3[AlF_6]$ for the smelt electrolysis carried out in the production of aluminum metal.

17 H. D. B. Jenkins, L. Glasser, *Chem. Soc. Rev.* **2005**, *34*, 866. H. D. B. Jenkins, H. K. Roobottom, J. Passmore et al., *Inorg. Chem.* **1999**, *38*, 3609.

The *solubility of salts* is strongly influenced by their lattice energies. The COULOMB attraction *f* of oppositely charged ions in a solvent of dielectric constant ε is decreasing with increasing value of ε. For two singly charged ions we obtain:

$$f = \frac{1}{4\pi\varepsilon_o\,\varepsilon} \cdot \frac{e^2}{d^2} \tag{2.4}$$

d: Internuclear distance of ions

Since ε may have values of up to 100 (see below), the interionic attraction may be reduced to 1% of its vacuum value.

To dissolve a salt, the lattice energy must be overcompensated by a process furnishing the necessary energy. This process is the *solvation of ions*, which is favored by the attraction between the dipole moments of the solvent molecules and the charges of the ions. In addition, hydrogen bonds are often involved. The solvation energy is defined as the energy (or, more precisely, the enthalpy) liberated when 1 mol of gaseous ions is placed in an infinite amount of solvent:

$$A^+(g.) \;+\; \text{solvent (l.)} \longrightarrow A^+(\text{solv.}) \qquad \Delta_{solv}H^\circ << 0$$

As energy liberated by the system, $\Delta_{solv}H^\circ$ is always negative. In practice, solvation enthalpies are derived from thermodynamic cycles or estimated by quantum-chemical calculations. According to MAX BORN, the solvation enthalpy may be calculated approximately by eq. (2.5):

$$\Delta_{solv}H^\circ = -\frac{a^2e^2}{2r}\left(1-\frac{1}{\varepsilon}\right) \tag{2.5}$$

a: ionic charge
r: ionic radius

It follows from eqs. (2.4) and (2.5) that the solubility of a salt is higher, the larger is the dielectric constant ε of the solvent. Water (ε = 80 at 20 °C) and some water-like solvents such as liquid NH_3 (ε = 17 at 20 °C), liquid SO_2 (ε = 16 at 25 °C) and anhydrous HF (ε = 84 at 0 °C) as well as nonaqueous H_2SO_4 and HSO_3F are good solvents for salts, as are strongly polar organic solvents such as dimethyl sulfoxide (DMSO, ε = 47), tetramethylene sulfone (sulfolane), nitromethane (ε = 37), nitrobenzene (ε = 36), acetonitrile (ε = 37), dimethylformamide (ε = 82), hexamethyl phosphoric triamide (HMPA) and tetrahydrofurane (THF; ε = 7.8).[18]

18 For details on the polarity of organic solvents, see: C. Reichardt, *Angew. Chem. Int. Ed.* **1979**, *19*, 98–110; C. Reichardt, *Solvent effects in organic chemistry*, VCH, Weinheim, 1979. Nonpolar solvents are hexane, CCl_4 and CS_2, for example.

Molten salts[19] and ionic liquids (ILs)[20] are also used as solvents and reaction media. ILs are salt-like substances of unusually low melting points (below 100 °C) due to the large size of cations or anions reducing the lattice enthalpy. Examples for suitable cations are shown in Figure 2.5; these ammonium, phosphonium and sulfonium ions are usually combined with anions such as $[BF_4]^-$, $[PF_6]^-$, $[CF_3SO_3]^-$ (triflate), $[Al(OR^F)_4]^-$ and others (R^F = perfluoro alkyl or aryl group). An often used ionic liquid is 1-butyl-3-methyl-imidazolium hexafluorophosphate, abbreviated as [BMIM][PF_6] or [C_4mim][PF_6]. Some ILs are available commercially.

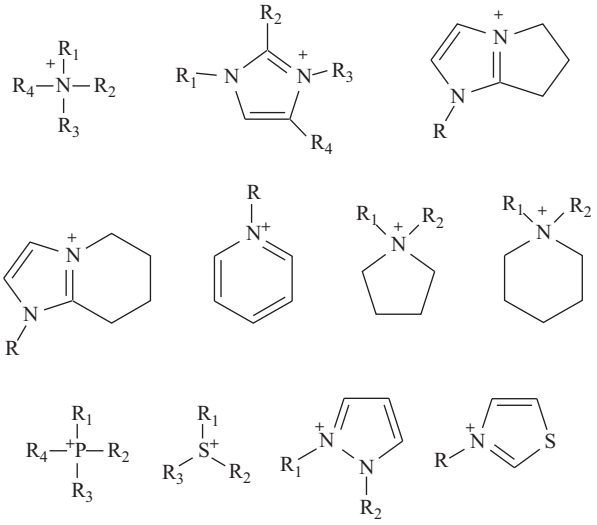

Figure 2.5: Bulky cations used for the preparation of ionic liquids.

According to eq. (2.5) the absolute value of $\Delta_{solv}H°$ increases with decreasing ionic radius and with increasing ionic charge. For soluble salts the sum of solvation enthalpies of cation and anion is larger and for hardly soluble salts smaller than the lattice enthalpy. But in addition to the *solution enthalpy* $\Delta_{sol}H°$ the *entropy of solution* $\Delta_{sol}S°$ is also of importance; the latter is usually positive (excepting salts with fluoride anions). Both parameters are connected by the second law of thermodynamics; see eq. (2.6):

19 T. A. O'Donnell, *Superacids and Acidic Melts as Inorganic Chemical Reaction Media*, VCH, New York, **1993**.

20 See the special issue of *Acc. Chem. Res.* **2007**, *40*, no. 11. P. Wasserscheid, *Chem. unserer Zeit* **2003**, *37*, 52.

$$\Delta_{sol}G^{\circ} = \Delta_{sol}H^{\circ} - T\Delta_{sol}S^{\circ} \tag{2.6}$$

If the GIBBS enthalpy of solution $\Delta_{sol}G°$ is negative, a salt is soluble. In other words, a salt will dissolve in a given solvent if the GIBBS *lattice enthalpy* $\Delta_{lat}G°$ is smaller than the sum of the solvation enthalpies $\Delta_{solv}G°$ of the ions (all enthalpies in absolute values).

2.1.7.1 Complex Formation of Metal Halides

Many metal halides form complexes with halogen compounds Y, the stability of which is a function of the cation size, for example:

$$MF + HF \longrightarrow M[HF_2]$$
$$MCl + ICl_3 \longrightarrow M[ICl_4]$$
$$MF + SF_4 \longrightarrow M[SF_5]$$

Reactions of this type can be analyzed by a thermodynamic cycle:

$$\begin{array}{ccc} M^+(g.) + X^-(g.) + Y & \xrightarrow{II} & M^+(g.) + [XY]^-(g.) \\ \uparrow I & & \downarrow III \\ MX(s.) + Y & \xrightarrow{IV} & M[XY](s.) \end{array}$$

The enthalpy of step IV determines the stability of the solid complex with respect to its components:

$$\begin{aligned} \Delta H(\mathrm{IV}) &= \Delta H(\mathrm{I}) + \Delta H(\mathrm{II}) + \Delta H(\mathrm{III}) \\ &= \Delta_{lat}H^{\circ}(\mathrm{MX}) + \Delta H(\mathrm{II}) - \Delta_{lat}H^{\circ}(\mathrm{M[XY]}) \end{aligned}$$

The dissociation equilibrium IV will tend to shift to the side of the complex salt, the more negative ΔH(IV). Since ΔH(II) is cation independent, ΔH(IV) depends only on the difference in lattice enthalpies $\Delta_{lat}H°$ between the halide MX and the complex salt M[XY] (steps I and III). If Y is a neutral molecule, M[XY] will have a smaller lattice enthalpy than MX, owing to the larger size of the anion. However, the difference in lattice enthalpies also depends on the cation size and is smallest for the largest size cations (see Table 2.2). Hence, complex salts M[XY] containing large cations are most stable with respect to decomposition to the starting materials. For this reason, in preparative chemistry, large cations such as tetraalkylammonium, phosphonium or arsonium ions are often employed to stabilize complex anions in salts. Alkali cations coordinated by cryptand ligands such as $[K(2.2.2.)]^+$ serve the same purpose.

2.1.7.2 Weakly Coordinating Anions

Weakly coordinating anions (WCAs) are used to minimize the interaction between cations and anions.[21] In this way particularly electrophilic cations can be stabilized in salts. Classic examples for relatively weakly coordinating anions are $[BF_4]^-$, $[ClO_4]^-$, $[CF_3SO_3]^-$, $[AsF_6]^-$ and $[SbF_6]^-$. However, in recent times much larger anions with highly electronegative atoms on the outer surface have been synthesized, which allow the isolation of salts with even less stable cations, such as $[P_4H]^+$, $[C_6H_7]^+$, $[C_{60}H]^+$, $[C_{59}N]^+$, $[Me_3C]^+$, $[Ph_3C]^+$ and $[Me_3Si]^+$. Suitable counter-ions are $[B(R^F)_4]^-$, $[Al(OR^F)_4]^-$, $[Al(OTeF_5)_4]^-$, $[CHB_{11}Cl_{11}]^-$ and $[B_{12}Cl_{12}]^{2-}$ (R^F = perfluoro alkyl or aryl group). In these WCAs, the negative charge is delocalized over a large volume resulting in minimum nucleophilicity. At the same time, these anions are chemically robust and of low polarizability, and their large size is favorable for the crystallization with large cations, as discussed in the previous section. As examples, the structures of the two aluminate anions mentioned above[22] are shown in Figure 2.6.

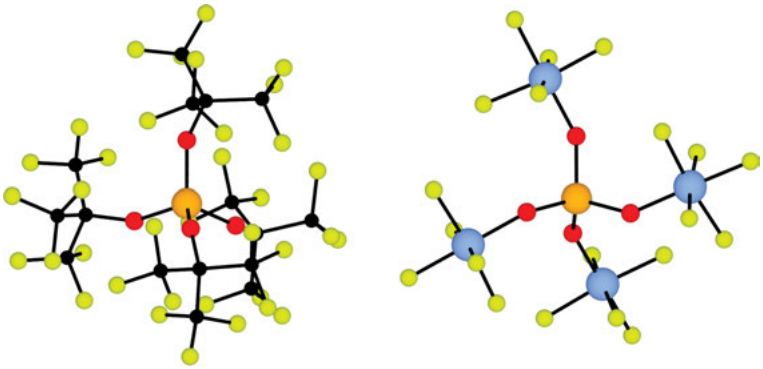

Figure 2.6: Molecular structures of two weakly coordinating aluminate anions with the ligands $OC(CF_3)_3$ (left) and $OTeF_5$ (right); yellow, fluorine; black, carbon; red, oxygen; orange aluminum; blue, tellurium.

2.1.8 Polarization of Anions by Cations

Simple anions such as Br^- and S^{2-} have larger radii than the isoelectronic cations K^+ and Ca^{2+}. Their voluminous electron cloud can therefore be easily deformed when exposed to a strong, unidirectional force. This process is called *polarization*. In salts with coordination numbers of 4 or higher, anion polarization is relatively

21 C. Knapp, *Comprehensive Inorganic Chemistry* II, Chapt. 1.25, Elsevier, Amsterdam, **2013**. C. Reed, *Acc. Chem. Res.* **2010**, *43*, 121. I. Krossing, et al., *Angew. Chem. Int. Ed.* **2018**, *57*, 13982–14024.

22 A. Wiesner, S. Riedel, et al., *Angew. Chem. Int. Ed.* **2017**, *56*, 8263.

moderate since the electrostatic forces act from different directions. In this case, anions may be considered as approximately spherical. If this regular symmetry is reduced as in salt melts or destroyed completely as in solution or in the gas phase, *ion pairs* and similar aggregates may be formed, which are characterized by strongly polar but partly covalent bonds.

The vapor above molten sodium chloride contains diatomic molecules NaCl besides other species. Molecules of this type may be trapped at low temperatures in noble gas matrices, for example, at liquid helium temperature (4 K). With this technique of *matrix isolation* highly reactive species can be studied spectroscopically in detail. The bonding in diatomic *molecules* such as NaCl and AgCl differs considerably from the situation in the corresponding bulk materials of rock salt structure.

For diatomic molecules the electron distribution may be calculated using the so-called spin-free one-electron density function $P(1)$, which is defined for any N-electron wave function $\psi(1, 2 \ldots N)$ as follows:

$$P(1) = N \cdot \int |\psi(1,\ 2\ \ldots\ N)|^2 ds_1\, d\tau_2 \ldots d\tau_N$$

The expression $\int|\psi(1,2 \ldots N)|^2\, ds_1$ means the integration over the spin coordinates of electron 1 and $\int|\psi(1,2 \ldots N)|^2\, d\tau_2 \ldots d\tau_N$ stands for the integration over the space and spin coordinates of all other N–1 electrons. The wave function ψ may be calculated by the HARTREE–FOCK method. The function $P(1)dV_1$ describes the probability to find an electron of any spin in the volume element dV_1, independently from the spins and locations of all other electrons (electron density calculation). This kind of density functions can be visualized by contour plots as shown for the diatomic molecules NaCl, AgCl and Cl_2 in Figure 2.7.

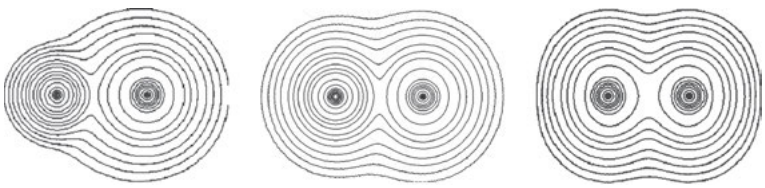

Figure 2.7: Calculated electron densities of the diatomic molecules NaCl, AgCl and Cl_2, demonstrating the effect of the polarization of the chlorine atoms (on the right-hand side). The contour lines, from outside to inside, correspond to electron densities of 0.001, 0.002, 0.004, 0.008, 0.020, 0.040, 0.080, 0.200, ... $e\,a_0^{-3}$ (a_0 = 52.9 pm; 1 e Å^{-3} ≈ 6.75 $e\,a_0^{-3}$). At the saddle points between the atoms the electron densities decrease to 0.23 (NaCl), 0.37 (AgCl) and 1.01 e Å^{-3} (Cl_2), respectively.

If the molecule NaCl ($\Delta\chi_P = 2.3$) were an ideal ion pair with 100% ionic interaction, it should consist of two spherical isoelectronic particles Na^+ and Cl^- attached to each other in one point, which is evidently not the case. Instead, the smaller cation partly penetrates the anionic electron cloud with deformation of the formerly spherical distribution. Some contour lines encompass the whole molecule, which is characteristic for covalent bonds. On the other hand, the minimum electron density between the two atoms is only 0.23 e Å^{-3}, almost the same value as in rock salt and much smaller than in Cl_2 (1.01 e Å^{-3}).

The ions Na^+ and Ag^+ are of almost equal size (ionic radii 113 pm vs 114 pm at coordination number 4) and the electron density distribution in AgCl may be compared with that of NaCl. However, the difference of PAULING electronegativities of Ag and Cl is only 1.3 and a larger covalent contribution to the bonding in the AgCl molecule can be expected. In fact, the minimum electron density between the two atoms is 0.37 e Å^{-3}, which is by a factor of 1.6 larger than that in the NaCl molecule. This is another sign for polarization of the anion by the cation. In the covalent Cl_2 molecule, the minimum density between the atoms is 1.01 e Å^{-3}.

The experimental dipole moments of diatomic molecules AB provide another measure for the ionic or covalent character of the bonds. If the gaseous molecules KCl, KBr and CsCl consisted of spherical ions at internuclear distances d, their dipole moments would be $\mu = e \cdot d$ (e = electron charge). Since the structures of these molecules are known, their theoretical dipole moments have been calculated and range from 13.0 to 14.7 D. However, the experimental dipole moments are in the range 9–11 D, indicating that the atomic charges in these ion pairs are smaller than 1 electrostatic unit due to polarization of B^- by A^+ (see Section 4.6.1).

The relative stability of a gaseous ion pair and the corresponding ionic crystal can be examined on enthalpy grounds. The enthalpy of formation of the *gaseous molecule* NaCl (Δ^{at}_fH) from atoms is the enthalpy of the reaction

$$Na(g.) + Cl(g.) \longrightarrow NaCl(g.)$$

which is $\Delta^{at}_fH = -411$ kJ mol^{-1}. The internuclear distance d_{NaCl} in the molecule is 236 pm; the corresponding value in rock salt is 281 pm. The value lower by 18% in the molecule reflects the polarization of the anion by the cation, which stabilizes the molecule. Nevertheless, NaCl exists as an ionic solid rather than as a molecular gas at 25 °C. The enthalpy of formation of *solid* NaCl (Δ^{at}_sH) from gaseous atoms

$$Na(g.) + Cl(g.) \longrightarrow NaCl(s.)$$

can be calculated from the data discussed in Section 2.1.6 as follows:

$$\Delta^{at}_sH = \Delta_sH^\circ - \Delta_{subl}H^\circ(Na) - {}^1/_2\,D(Cl_2) = -411 - 109 - 121 = -641 \text{ kJ mol}^{-1}$$

This high negative value explains why NaCl exists as a solid salt at 25 °C rather than as a molecular gas. The hypothetical "polymerization" of 1 mol NaCl(g.) to a single crystal of NaCl would liberate an enthalpy of $-641 - (-411) = -230$ kJ mol^{-1}.

Polarization and the concomitant transition from a purely ionic to a polar bond occurs not only in ion pairs but also in crystals, when, for example, a large anion (I^-, S^{2-}) is in contact with a small cation (Li^+, Ag^+) and when polarization is favored by a low coordination number or by a coordination sphere of low symmetry. The proton, owing to its small size, has the greatest field strength, and can penetrate the electron clouds of anions deeply. It has the greatest polarization capability and, therefore, does not form ionic structures even with anions of the most electronegative nonmetals (cf. HF and H_2O).

To conclude the discussion of the ionic bond, it should be mentioned that at very high pressures completely different phases and compositions can be prepared. For example, in the binary system sodium-chlorine the following compositions have been observed and their crystal structures determined by either theoretical calculations or X-ray diffraction: Na_3Cl, Na_2Cl, Na_3Cl_2, $NaCl_3$ and $NaCl_7$.[23] The minimum pressure needed was 20 GPa. Evidently, even-numbered oxidation states cannot be assigned to the atoms in these stoichiometric sodium chlorides. Instead, a band structure calculation is used to explain the properties.

2.2 Molecular Geometry

2.2.1 Structure Determination

The determination of molecular and crystal structures is of utmost importance in modern inorganic chemistry. Depending on the physical properties and the size of the sample, different experimental methods are available. In addition, quantum-mechanical calculations may also be used to predict or confirm the structures of molecules. The following methods are most commonly used:

Structural analysis by X-ray diffraction on single crystals is most often applied and yields structural information within hours or a few days.[24,25] A small crystal is irradiated by monochromatic X-rays and a sophisticated software is used to calculate the crystal and molecular structure from the diffraction pattern. The diffraction of photons takes place at the electrons, but since the maximum electron density is at the center of the atoms, the location of the nuclei can be determined. However,

23 W. Zhang et al., *Science* **2013**, *342*, 1502.

24 P. Luger, *Modern X-Ray Analysis on Single Crystals: A Practical Guide*, de Gruyter, Berlin, **2014**. W. Massa, *Kristallstrukturbestimmung*, 5th ed., Teubner, Wiesbaden, **2007**.

25 D. W. H. Rankin, N. W. Mitzel, C. A. Morrison, *Structural Methods in Molecular Inorganic Chemistry*, Wiley, Hoboken, **2013**. https://www.wiley.com/go/rankin/structural.

atomic nuclei in molecules vibrate even at 0 K; therefore, average atomic locations are obtained (vibrational ellipsoids). With a sample cooling device, even substances can be analyzed, which are liquid or gaseous at standard conditions provided a single crystal can be grown.

Electron diffraction is used to analyze the molecular structures of gaseous or volatile samples, provided the molecules are not too large.[25] The sample is irradiated at low pressure in a vacuum chamber by a beam of monochromatic electrons, that is, which have the same velocity. Unlike X-rays, electrons are negatively charged. The observed diffraction is therefore mostly electrostatic in nature and takes place at both the nuclei and the electrons. This results in much higher signal intensities and short acquisition times. The refinement of atomic positions is typically done with a computational model, except for very small molecules.

Microwave spectroscopy of gaseous samples requires that the molecules possess a permanent dipole moment.[25] The absorption of microwaves initiates rotation of the sample molecules around all three axes, and the required energy depends on the moments of inertia, which in turn are a function of atomic masses, internuclear distances as well as valence and dihedral angles. Since the masses are known, the structures can be calculated. Very accurate geometrical data are obtained for not too large molecules.

Quantum-chemical calculations may be used to support the experimental structure determinations. These methods (ab initio and density functional theory methods) also provide information on isomeric structures, on vibrational frequencies, dipole moments and atomic charges, on transition states between reactants and other valuable data.

Different methods yield slightly differing results since they are based on different physical effects. Only quantum-chemical calculations provide the atomic positions at the minimum of the potential energy surface. Experimental methods yield vibrationally averaged atomic positions. Furthermore, the intermolecular interactions in condensed phases distort the molecular structures in comparison with gaseous samples (so-called *packing effects*; see Chapter 3). Quite often the molecular symmetry in a crystal (so-called *site symmetry*) is lower than in the vapor phase.

The connectivity of atoms in a novel compound can also be determined by indirect methods such as IR, Raman and NMR spectroscopy. For example, a molecule of composition SOF_4 may be either thionyl tetrafluoride $O{=}SF_4$ with the sulfur atom in oxidation state +6 or sulfur trifluoride hypofluorite $FO{-}SF_3$ with sulfur in the oxidation state +4. An IR spectrum would immediately provide the answer: the S=O stretching vibration has the highest frequency and can therefore easily be identified.

Another access to the geometries of small molecules and ions is provided by the model of *valence shell electron pair repulsion* (VSEPR), which assumes that the molecular geometry results from the repulsion between bonding and nonbonding electrons at neighboring atoms. This model – also known as the GILLESPIE-NYHOLM rules – has

for many years provided a useful basis for understanding and rationalizing molecular geometry, and because of its simplicity it has gained widespread acceptance as a pedagogical tool. This empirical method will be discussed in the following section.

2.2.2 The VSEPR Model for Estimation of Molecular Geometries

More than 100 years ago, the American physical-chemist GILBERT NEWTON LEWIS (1875–1946) laid the foundations for modern views on covalent bonds by suggesting the pairing and sharing of VEs between atoms to reach a noble gas electron configuration for each of them as the driving force.[26] In the case of two hydrogen atoms, the *common electron pair* corresponds formally to a He configuration *for each atom*:

$$H\cdot + \cdot H \longrightarrow H{-}H$$

Normally a covalent bond is symbolized by a line (e.g., H–H)[27] but often bonding electron pairs are indicated by double dots (H:H). By now we know that a "covalent bond" and an "electron pair between two atoms" are not necessarily the same thing as will be shown in the case of the oxygen molecule. Oxygen atoms possess two unpaired electrons in the valence shell and if these are paired as in O_2 a "double bond" could result with eight VEs for each atom (Ne configuration). The remaining electron pairs would form "nonbonding" or "lone" pairs since they seemingly do not take part in the molecule formation:

$$:\dot{\underset{\cdot\cdot}{O}}\cdot + \cdot\dot{\underset{\cdot\cdot}{O}}: \longrightarrow :\overset{\cdot\cdot}{O}{=}\overset{\cdot\cdot}{O}:$$

In Section 2.4.3 we will show, however, that this picture is not correct as O_2 turns out to be a paramagnetic molecule with two unpaired electrons of equal spin.

In a similar manner, the LEWIS concept proposes a "triple bond" for the nitrogen molecule:

$$:\dot{N}\cdot + \cdot\dot{N}: \longrightarrow :N{\equiv}N:$$

In this case, the simple LEWIS formula concurs with more sophisticated tools of bonding analysis. The extremely high bond strength of N_2 is in accordance with this description.

If a nitrogen atom is combined with three hydrogen atoms, ammonia results that shows a pyramidal geometry:

26 G. N. Lewis, *J. Am. Chem. Soc.* **1916**, *38*, 762.

27 The line connecting atoms linked to each other has been introduced by ARCHIBALD SCOTT COUPER in 1858 and by CRUM BROWN in 1864, both in the case of the acetic acid molecule.

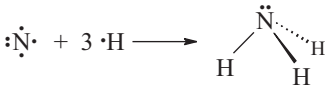

In these examples the atoms reach a noble gas configuration if the bonding electrons are counted on each side of the bond. For the N and O atoms in these examples an *octet configuration* is thus reached, which all noble gases have in their valence shell except helium. The VSEPR model proposes that the *repulsion* between the four bonding and nonbonding *electron pairs* determines the geometry of molecules.[28]

The interaction of electrons in a molecule is determined by the COULOMB repulsion owing to their equal charge and by PAULI's principle, which does not allow two electrons of like spin to occupy the same space segment at the same time. On the other hand, the attraction by the nuclei or atomic cores tends to pull the electrons into the regions of highest effective positive charge. The PAULI principle places no restrictions on electrons of opposite spin, however, which may indeed be relatively close together and thus in the same orbital.

Consider some simple molecules of type AX_n with univalent substituents X and n identical covalent bonds A–X. Examples are H_2O, NH_3 and CH_4 with eight electrons each in the valence shells of the central atoms. In the absence of a bonding partner as in neon, these electrons will arrange themselves about the core of the central atom such that COULOMB attraction is maximized, COULOMB repulsion is minimized and the PAULI principle is obeyed. The maximum distance between electrons with spin α ($s = +½$) for the isolated Ne atom is achieved for a tetrahedral arrangement and the same holds for the electrons with spin β ($s = -½$). As the two resulting tetrahedra repel each other, they will be oriented such that the one is related to the other by inversion as shown in Figure 2.8.

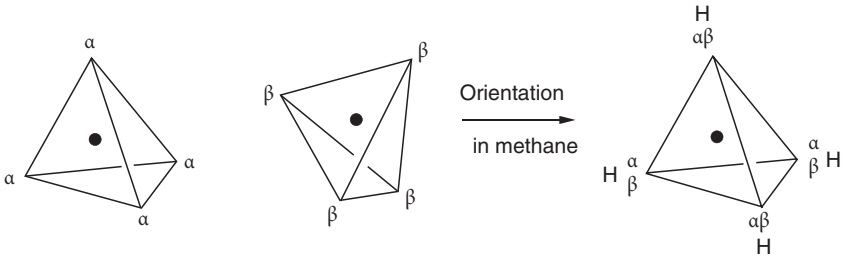

Figure 2.8: Most probable arrangement of four valence shell electrons with spins α and β, respectively, of the Ne atom (left and center), and of eight valence shell electrons in the methane molecule in which the hydrogen nuclei pull the electrons in the regions between the five atoms (right).

28 R. J. Gillespie, E. A. Robinson. *Angew. Chem. Int. Ed.* **1996**, *35*, 495–514. R. J. Gillespie, P. L. A. Popelier, *Chemical Bonding and Molecular Geometry*, Oxford Univ. Press, New York, **2001**.

Conversely, in methane, the attraction by the hydrogen nuclei pulls the electrons in the regions between the atoms forming electron pairs or so-called electron domains (Figure 2.8, right). With this tetrahedral geometry the repulsion between the hydrogen nuclei is also minimal. The resulting bond angles are approximately 109.47° (*tetrahedral angle*).

The electron domains of one or two electrons are assumed not to overlap and thus determine the geometry of the molecule on the surface of a spherical core. For nonmetal compounds the latter assumption is usually fulfilled. To extend this model to other molecules of type AX_n, we need to maximize the distances between n points (electron domains) on the surface of a sphere (atomic core). The mathematical solutions are shown in Figure 2.9. For $n = 2$ a linear arrangement, for $n = 3$ an equilateral triangle and for $n = 4$ a tetrahedron are obtained. For $n = 5$ a trigonal bipyramidal arrangement with two axial and three equatorial positions is slightly favored over a square pyramid with a unique apical position and four base positions. In fact, most nonmetallic compounds of type AX_5 prefer the trigonal bipyramid. Exceptions exist mostly for transition metal species.

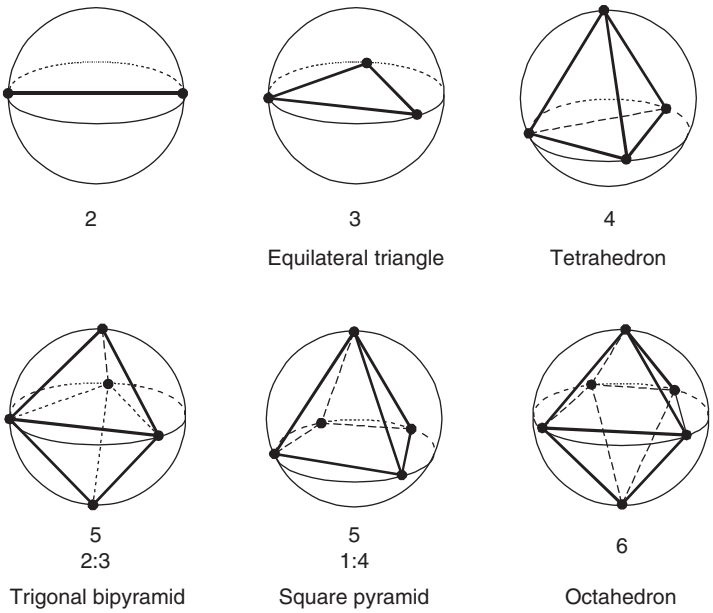

Figure 2.9: Mathematical solutions to position n points on the surface of a sphere with maximum distances between all points; for $n = 5$, two possibilities result (a trigonal bipyramid and a square pyramid).

The solutions shown in Figure 2.9 are used to predict the overall geometries (symmetries) of simple molecules and ions of type AX_n without nonbonding electron

Table 2.3: Geometries of molecules and ions according to the VSEPR model (X: halogen, E: lone pair).

Number of electron pairs	Symmetry	Type	Geometry	Examples
2	Linear	AX_2	Linear	BeF_2 (g.)
3	Triangular	AX_3	Triangle	BX_3, $[CO_3]^{2-}$
		AX_2E	V-shaped	CF_2, $SiCl_2$
4	Tetrahedral	AX_4	Tetrahedral	$[BeX_4]^{2-}$, $[BX_4]^-$, CX_4, $[NX_4]^+$ SiX_4, GeX_4, $[PX_4]^+$, $[AsX_4]^+$
		AX_3E	Trigonal pyramid	NX_3, $[OH_3]^+$, PX_3, AsX_3, SbX_3, P_4O_6, As_2O_3, Sb_2O_3
		AX_2E_2	V-shaped	OX_2, SX_2, SeX_2, TeX_2
5	Trigonal-bipyramidal	AX_5	Trigonal bipyramid	PCl_5, PF_5, PF_3Cl_2, $SbCl_5$, $Sb(CH_3)_3Cl_2$
		AX_4E	C_{2v} symmetry	SF_4, SeF_4, R_2SeCl_2, R_2SeBr_2, R_2TeCl_2, R_2TeBr_2
		AX_3E_2	T-shaped	ClF_3, BrF_3, $C_6H_5ICl_2$
		AX_2E_3	Linear	$[ICl_2]^-$, $[I_3]^-$, XeF_2
6	Octahedral	AX_6	Octahedral	SF_6, SeF_6, TeF_6, S_2F_{10}, $Te(OH)_6$, $[PCl_6]^-$, $[PF_6]^-$, $[Sb(OH)_6]^-$, $[SbF_6]^-$, $[SiF_6]^{2-}$
		AX_5E	Square pyramid	ClF_5, BrF_5, IF_5
		AX_4E_2	Square	XeF_4, $[ICl_4]^-$, I_2Cl_6, $[BrF_4]^-$

pairs (A: central atom, X: univalent substituent, *n*: number of electron domains); see Figure 2.8 and Table 2.3.

More examples of species with between two and six electron domains at the central atom are shown in Figure 2.10. If only two electron pairs are present as in gaseous BeF_2 the molecule is linear. For three electron pair domains as in BF_3 a planar, star-like structure with the substituents at the apexes of an equilateral triangle is obtained. Five and six domains yield trigonal-bipyramidal and octahedral structures, respectively.

Molecules with *lone pairs at the central atom* are of type AX_nE_m. In this case, the total number of electron pair domains at the central atom is $n + m$. Within the VSEPR model, these lone pairs are treated as stereochemically active *pseudo-substituents*. For example, in H_2O (type AX_2E_2) the four electron domains occupy

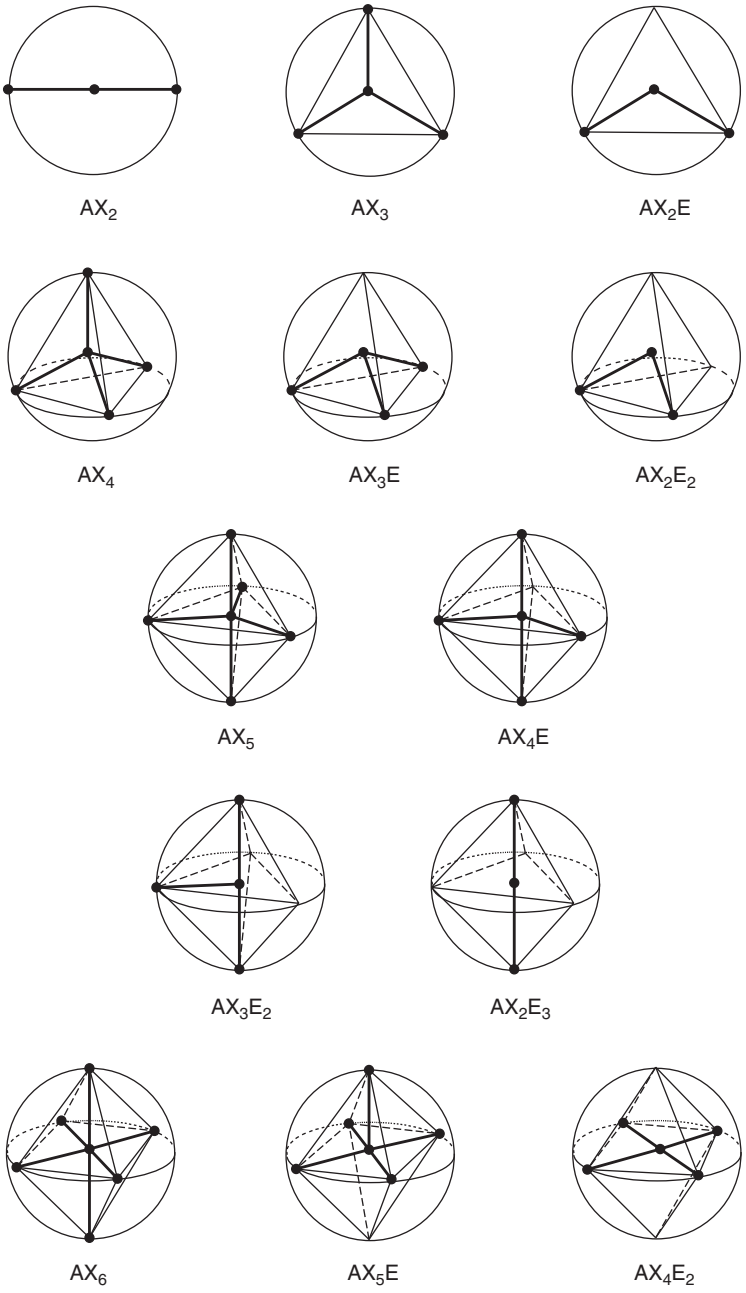

Figure 2.10: Schematic representation of the geometries of molecules with up to six electron domains in the valence shell (X: univalent substituent, E: lone pair of electrons).

the apexes of a tetrahedron and the molecule is bent. For NH_3 (type AX_3E) with only one lone pair a trigonal pyramid results.

The bond angles in H_2O (104.5°) and NH_3 (107.3°), however, do not agree with the ideal tetrahedral angle of 109.5°. Evidently, the electron domains of bonding pairs and of lone pairs are of different size, with the lone pairs requiring more space since they are attracted by the positive electric field of only *one* nucleus. The same holds for other molecules and ions with lone pairs at the central atom (see Tables 2.4 and 2.5).

Table 2.4: Bond angles α of molecules and ions of type AX_2E_2 (E: lone pair).

Molecule	α (°)	Molecule	α (°)
OH_2	104.5	$[Cl_3]^+$	96
SH_2	92.1	$[BrF_2]^+$	92
SeH_2	90.9	$[ICl_2]^+$	93
TeH_2	90.3	HOF	97.3
OF_2	103.1	HOCl	102.5
SF_2	98.2	HOBr	110
SeF_2	94	$[ClO_2]^-$	108.6
OCl_2	111.2	$[NH_2]^-$	99.4
SCl_2	102.8	$[NF_2]^-$	96.7
$SeCl_2$	99.6	$[ClF_2]^+$	96
$SeBr_2$	101.6		
$TeCl_2$	97.0		

Table 2.5: Bond angles α of molecules and ions of type AX_3E (E: lone pair).

Molecule	α (°)	Molecule	α (°)
NH_3	107.3	PBr_3	101.1
PH_3	93.8	$AsBr_3$	99.8
AsH_3	91.8	$SbBr_3$	98.2
SbH_3	91.7	PI_3	102
NF_3	102.2	AsI_3	100.2
PF_3	97.8	SbI_3	99.3
AsF_3	96.1	$[SF_3]^+$	97.5
SbF_3	87.3	$[SeF_3]^+$	94.5
NCl_3	107.1	$[TeF_3]^+$	90(2)
PCl_3	100.3	$[SCl_3]^+$	103.3
$AsCl_3$	98.6		
$SbCl_3$	97.2		

It is remarkable that the experimental gas phase structures of most nonmetallic compounds and ions agree with the predictions by the VSEPR model. Deviations are observed for some species with formally more than six electron pair domains at the central atom.[29] These species will be discussed in later chapters. It should be noted in passing that some heavier alkaline earth metal halides of type MX_2 adopt bent structures in the gas phase due to admixture of vacant *d* orbitals to filled orbitals.[30]

The regular structures shown in Figure 2.10 only apply to molecules of type AX_n with identical substituents. Different substituents, lone pairs and multiple bonds result in distortions (symmetry reductions) according to rules discussed in the following sections. It should be kept in mind that although the reasoning of these rules is plausible, it does not provide any scientifically rigorous explanations.

2.2.2.1 Lone Electron Pairs

The lone electron pairs (E) in a molecule of type AX_nE_m, unlike the bonding pairs, are influenced by the electric field of only one nucleus; consequently, their domains are larger and take up more space. For example, if a bonding domain in a regular octahedron such as SF_6 is replaced by a lone pair as in ClF_5 the bond angles between the axial and equatorial bonds of the square pyramid decrease slightly from 90°. In addition, the axial bond is now shorter than the bonds at the base of the pyramid. For more examples, see Table 2.6.

Table 2.6: Internuclear distances *d* (pm) and bond angles α (°) of molecules and ions of type AX_5E (E: lone pair; standard deviations in parentheses).

Compound	d_{ax}	d_{eq}	α
$[XeF_5][RuF_6]$	179.3(9)	184.5(8)	–
$[XeF_5][AgF_4]$	182.6(9)	185.2(19)	77.7(3)
$[XeF_5][PtF_6]$	181.0	184.3	79
ClF_5	157(1)	167(2)	86(2)
BrF_5	168.9(8)	177.4(3)	84.8(1)
IF_5	184.4(25)	186.9(5)	81.9(5)
$Na[TeF_5]$	186.2(4)	195.2(4)	87.8
$[NH_4]_2[Sb^{III}F_5]$	191.6(4)	207.5(2)	88.0
$[NH_4]_2[Sb^{III}Cl_5]$	236	258–269	85

29 For hepta-coordinate molecules such as IF_7, see: R. Minkwitz, *Angew. Chem. Int. Ed.* **1994**, *33*, 1941.
30 P. v. R. Schleyer et al., *J. Am. Chem. Soc.* **1991**, *113*, 6012.

Since lone pair domains are larger than bonding electron pair domains, the former tend to occupy positions as far away from each other as possible. In a molecule or ion of type AX_4E_2 the lone pairs will therefore occupy *trans* positions of the pseudo-octahedron and the molecule will have a square planar geometry (e.g., XeF_4).

The axial and equatorial positions of a regular trigonal bipyramid are not equivalent. The bond angles within the trigonal plane are larger (120°) than those between the plane and the axial bonds (90°). Therefore, lone pairs always occupy the equatorial position(s) of the pseudo-bipyramid, as the following examples for molecules of type AX_nE_m ($m + n = 5$) illustrate:

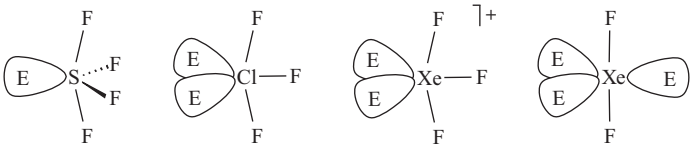

Due to the larger space requirements of lone pairs, the bond angles in molecules and ions of types AX_4E and AX_3E_2 are smaller than the ideal values of a regular trigonal bipyramid (90°, 120° and 180°). For example, the bond angles of SF_4 are 101.6° (F_{eq}–S–F_{eq}) and 173.1° (F_{ax}–S–F_{ax}), and of ClF_3 87.5° (F_{ax}–Cl–F_{eq}) and 175° (F_{ax}–Cl–F_{ax}). XeF_2 is a linear molecule. Owing to the difference of the equatorial and axial positions, AX_5, AX_4E and AX_3E_2 molecules also have two different A–X bond lengths with d_{AX}(eq) by 5–15% shorter than d_{AX}(ax); see Table 2.7.

Table 2.7: Internuclear distances *d* (pm) and bond angles α (°) of disphenoidal AX_4E and of T-shaped AX_3E_2 molecules and ions (E: lone pair).

Molecule/Ion	d_{ax}	d_{eq}	α (ax-ax/eq-eq)
AX_4E:			
$[PF_4]^-$	174	160	168.3/99.9
SF_4	164.6	154.5	173.1/101.6
$FS–SF_3$	167.3	156.9	167.0/104.9
SeF_4	177.1	168.2	169.2/100.6
Ph_2TeF_2	200.6	211.5	175.3/96.9
Me_2TeCl_2	251	210	172.3/98.2
$[BrF_4]^+[Sb_2F_{11}]^-$	186	177	173.5/92.4
$[IF_4]^+$	184	177	160/92
$ClOF_3$	171.3	160.3	170.5 (ax)
$[IO_2F]^-$	200	193	180 (ax)
XeO_2F_2	189.9	171.4	183.2 (ax)

Table 2.7 (continued)

Molecule/Ion	d_{ax}	d_{eq}	α (ax-ax/eq-eq)
AX_3E_2:			
ClF_3	169.8	159.8	175.4 (ax)
BrF_3	181.0	172.1	172.4 (ax)
$[XeF_3]^+[SbF_6]^-$	190.5	183.5	160.9 (ax)

2.2.2.2 Single Electron Domains

In some free radicals the unpaired electron is located mainly on a single atom. A single electron can be considered to occupy a single electron domain that is expected to be smaller than an electron pair domain, so it affects the geometry of a molecule less than a lone pair as exemplified by the three species $[NO_2]^+$ (type AX_2), $[NO_2]^\bullet$ (free radical) and $[:NO_2]^-$ (type AX_2E), which have bond angles of 180°, 134° and 115°, respectively.

2.2.2.3 Substituents of Differing Electronegativity

The electronegativity of an atom or a group is defined as its ability to attract the electrons of a bond. The electronegativity χ increases in the Periodic Table from the lower left to the upper right; see Section 4.6.2. Bonding electron domains contract under the influence of highly electronegative substituents such as fluorine or oxygen, and their reduced spatial requirements allow other bonding and lone pairs to expand. Bond angles of molecules of type AX_n therefore decrease with increasing electronegativity of the substituents X, as the following examples illustrate:

$$H_2O\colon 104.5^\circ / OF_2\colon 103.1^\circ, \text{since } \chi(F) > \chi(H)$$

$$PBr_3\colon 101.1^\circ / PCl_3\colon 100.3^\circ / PF_3\colon 97.8^\circ, \text{since } \chi(F) > \chi(Cl) > \chi(Br)$$

More examples are given in Tables 2.4–2.7. With decreasing electronegativity of the central atom, the lone pairs on its surface expand and the bond angles decrease as in the series $H_2O > H_2S > H_2Se > H_2Te$ (Table 2.4). In molecules with substituents of differing electronegativity, the angles between the more electronegative ones are smaller. Obviously, if substituents are very bulky their steric requirements will influence the bond angles as well.

In a trigonal bipyramid with its nonequivalent positions, the most electronegative substituents always occupy the axial positions first, as do the fluorine atoms in

PCl_4F and PCl_3F_3. There are no stable isomers for these two compounds with F atoms in equatorial positions. In CH_3PF_4 and $(CH_3)_2PF_3$, the less electronegative methyl groups are equatorial, as expected.

2.2.2.4 Multiple Bonds

The VSEPR model of chemical structures assumes that the higher number of electrons of a multiple bond reside in *one domain*, which is assumed to require more space than electron pair domains of single bonds. For example, the linear geometry of carbon dioxide is explained by the repulsion of the *two domains* in O=C=O. Thus, in AX_3Y molecules with a double bond A=Y, the angles X–A–X are smaller than the angles X–A=Y. Molecules with both double bonds and lone pairs at the central atom show particularly large deviations from regular shapes, as the following examples demonstrate:

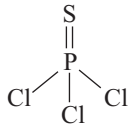

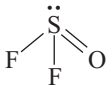

angle: FPF: 101.1° ClPCl: 101.8° OSF: 106.8°
FSF: 92.8°

In tetrahedral molecules with several double bonds, the angle between these bonds is the largest of all:

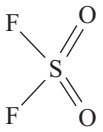

OSO: 124.0°
FSF: 96.1°

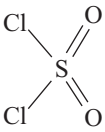

OSO: 123.5°
ClSCl: 100.3°

In trigonal-bipyramidal molecules, the multiply bonded substituents always occupy equatorial positions where more space is available. Examples are thionyl tetrafluoride SOF_4 and xenon dioxide difluoride XeO_2F_2. In Figure 2.11 an overview on the geometries of molecules with formal double bonds is given.

2.2.2.5 Final Remarks on the VSEPR Model

The VSEPR model, particularly when formulated in terms of electron pair domains, continues to be the most useful and most easily used model for the *qualitative prediction of molecular shapes*. It enables us to understand in a qualitative way many features of the structures of molecules that are not readily accounted for in other ways, and it continues to form the basis for the discussion and

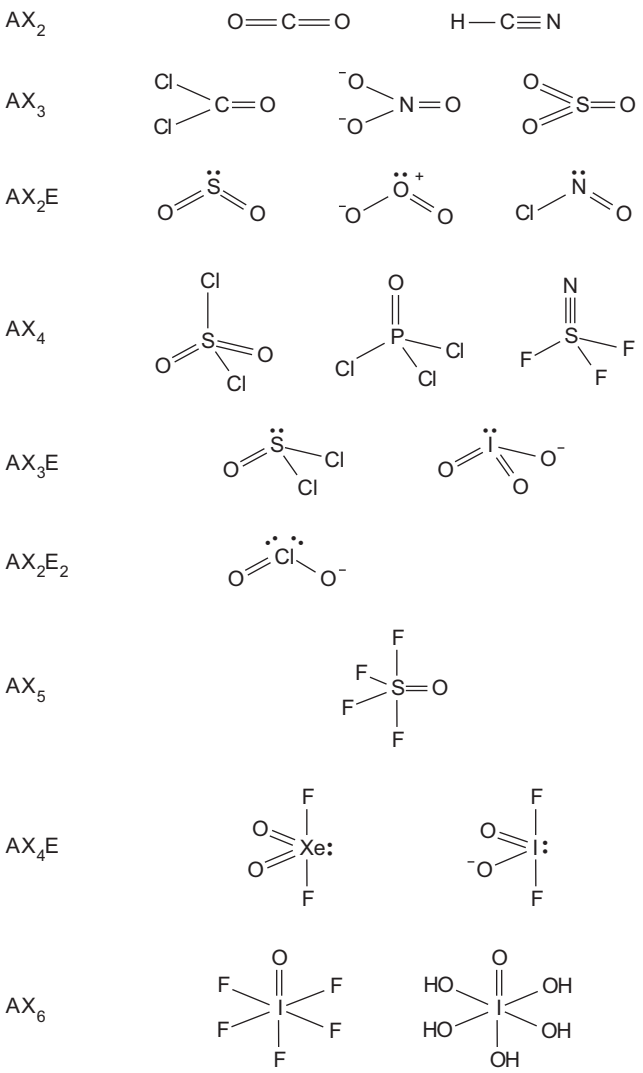

Figure 2.11: Geometries of molecules with multiple bond(s).

understanding of the structures of many new molecules. Its physical basis rests on the PAULI principle, and it is independent of any orbital model. Although the model has originally been derived empirically, it also has received some theoretical justification.[31]

31 R. F. Bader, R. J. Gillespie, P. J. MacDougall, *J. Am. Chem. Soc.* **1988**, *110*, 7329. P. J. MacDougall et al., *Can. J. Chem.* **1989**, *67*, 1842.

Nonetheless, for certain ions with high coordination numbers, the model predicts wrong structures. For example, the anions $[BrF_6]^-$, $[SeX_6]^{2-}$ and $[TeX_6]^{2-}$ with X=Cl, Br or I are of type AX_6E and should form distorted octahedrons. In contrast, they are all regular octahedrons, that is, the lone pair E is stereochemically inactive. For the bromides and iodides, the regular structures are probably the result of repulsion between the bulky substituents (steric effects), but the increased *s* character of the lone pair due to *d*- and *f*-block contraction contribute as well to the stereochemical inactivity. Similarly, in the chemistry of the transition metals itself the VSEPR model is of little predictive use.

It should also be pointed out that the model does not describe the actual electron density distribution in molecules and ions. A covalent bond can be established not only by electron pairs but also by a single electron as in the ion $[H_2]^+$. And bond strengths can vary *continuously* from partial bonds via single and double bonds up to triple bonds. Later we will see that most of the molecules discussed in this section contain *multicenter bonds*, which are characterized by bonding electrons delocalized over more than two centers as in CO_2, XeF_2 and SF_6, for example.

The simplest carbene CH_2 is an example of an important molecule, which deviates from the predictions of the VSEPR model. The bent structure of CH_2 is correctly predicted by the VSEPR model, but CH_2 is a paramagnetic species with a triplet ground state and its bond angle of 131.5° is in sharp contrast to the VSEPR predicted value of <120°.

Therefore, the VSEPR model should always be used with caution, since exact solutions for geometrical problems can only be provided by a theory based on quantum-mechanics, as will be discussed in Section 2.4.

2.3 Molecular Symmetry and Point Group Symbols

Chemists often need to know not only the approximate molecular geometry but also the precise symmetry of a molecule, for example, for the interpretation of IR and Raman spectra as well as for the elucidation of the orbital overlap in polyatomic molecules. The symmetry of a molecule is also an aesthetic issue since a high symmetry and harmonic proportions generally determine the beauty of a molecular structure, of a crystal, a flower, a house door, a building, a human face and so on.[32] In a way, chemists are artist because they create novel molecular objects for

32 L. Fabbrizzi (ed.), *Beauty in chemistry: artistry in the creation of new molecules, Top. Curr. Chem.* **2012**, Vol. 323.

displaying a practical function, but their structure may also cause emotion, pleasure and ultimately a sense of beauty.

The symmetry of a molecule is obtained from its behavior in certain *symmetry operations*. Consider the bent molecules H_2O and HOCl:

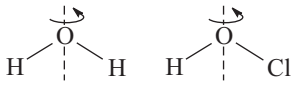

If the water molecule is rotated about the bisector of the bond angle by 180°, it is indistinguishable from the initial configuration, and after another rotation by an additional 180° it is back at the starting position. Such a rotation is called a *symmetry operation*, and the rotational axis (symbol: *C*) is termed a *symmetry element* of the molecule. The order *n* of the rotational axis is written as a subscript (C_n). After *n*-fold rotation about an angle $\varphi = 360°/n$, the molecule is back at the starting configuration. In other words, in H_2O there is the symmetry element C_2. The HOCl molecule, however, possesses only a C_1 rotational axis (rotation about 360°), which is trivial since present in all molecules; in *group theory* this symmetry element is also called *identity* (symbol: *E*). Examples for various rotational axes are:

C_2: $\varphi = 180°$	H_2O
C_3: $\varphi = 120°$	BF_3
C_4: $\varphi = 90°$	XeF_4
C_5: $\varphi = 72°$	$[C_5H_5]^-$
C_6: $\varphi = 60°$	C_6H_6
C_∞: φ arbitrary	all linear molecules

The ∞-fold rotational axis C_∞ exists in linear molecules only (molecular axis); it means that rotation about any angle is possible without changing the arrangement of the atoms. The rotational axis of highest order is the *principal axis* and is usually identified with the Cartesian *z*-axis of the molecule.

An additional symmetry element of the H_2O molecule is a *mirror plane* (symbol: σ), which bisects the bond angle and is perpendicular to the molecular plane. Reflection of the atoms in this plane exchanges the hydrogen atoms, but the initial and final arrangements are indistinguishable. This mirror plane is not present in the HOCl molecule. However, both H_2O and HOCl have a mirror plane that coincides with the molecular plane. This symmetry element is *common to all planar molecules*. Obviously, H_2O is of higher symmetry than that of HOCl since it has more symmetry elements (C_2 and two σ versus just one σ).

A special symmetry operation is the *improper rotation* S_n consisting of an *n*-fold rotation about an axis C_n followed by reflection in a plane perpendicular to this axis (second-order symmetry operation) or vice versa. Neither the axis of rotation nor the mirror plane needs to be a true symmetry element that can stand alone. Molecules

with S_n axes are, for example, tetrahedral $SiCl_4$ (S_4 bisects the angle Cl–Si–Cl) and planar *trans*-dichloroethene ClHC=CHCl (S_2 along the carbon–carbon axis):

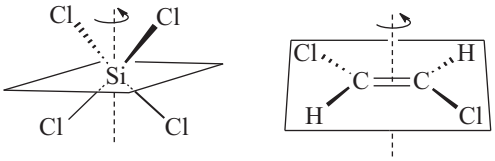

$SiCl_4$ (S_4) $1,2\text{-}C_2H_2Cl_2$ (S_2)

A fourth type of symmetry operation is the *inversion*, that is, the reflection of all atoms through a point that is called *center of symmetry* or *inversion center* (symbol: *i*). In other words, a molecule has a center of symmetry if it is possible to move in a straight line from every part of the molecule through a single point (*i*) to an identical part at the same distance on the other side of the center. Inversion centers are present in CO_2 (linear), XeF_4 (square), SF_6 (octahedron) and C_6H_6 (regular hexagon), but not in SiF_4 (tetrahedron). A part of an atom or a molecule (e.g., an orbital) that is symmetric to *i* is called *gerade* (g), and if it is antisymmetric it is termed *ungerade* (u).[33] Atomic *s* and *d* orbitals are *gerade*, while *p* orbitals are *ungerade* since the sign of the wave function changes on reflection on *i*. The electron density ψ^2 in these orbitals is always *gerade*.

In vibrational spectroscopy the *rule of mutual exclusion* applies to molecules and ions with inversion centers, which means that fundamental vibrations can be observed only in either IR or Raman spectra (or not at all) and not in both. For example, of the three vibrational degrees of freedom of CS_2 the asymmetric stretching and the bending vibrations are IR active while the symmetric stretching mode is Raman active. In other words, the IR spectrum shows two signals, and the Raman spectrum only one line. But in addition, there may be weaker signals caused by overtones and combination vibrations at higher wavenumbers.

Another symmetry operation, albeit trivial, is the aforementioned identity with symbol *E*; only the systematics of group theory require this operation. The four nontrivial symmetry operations and related symmetry elements are summarized in Table 2.8.

To characterize the symmetry of a molecule it is not necessary to mention all its symmetry elements. Instead the corresponding *point group* is used, which is represented by certain symbols that differ for the various symmetry classes. To derive these symbols the flowchart in Figure 2.12 may be used as detailed further on.

Point group symbols consist of a capital letter and a lower-case subscript, which can be a number, a lower-case letter or a combination of both. Certain very high symmetries have their own symbols: T_d stands for tetrahedron (e.g,. CH_4, P_4), O_h for octahedron (e.g., $[SiF_6]^{2-}$, $[PCl_6]^-$) and I_h for icosahedron (e.g., $[B_{12}H_{12}]^{2-}$). In

33 These two German words mean *even* and *uneven*.

Table 2.8: Symmetry operations and symmetry elements (v: vertical, h: horizontal, d: dihedral).

Symmetry operation	Symmetry element	Symbol	Important types
Rotation	Rotational axis	C	C_2, C_3, C_4, C_5, C_6, C_∞
Reflection	Mirror plane	σ	σ_v, σ_h, σ_d
Improper rotation	Improper rotation axis	S	S_2, S_4
Inversion	Inversion center	i	

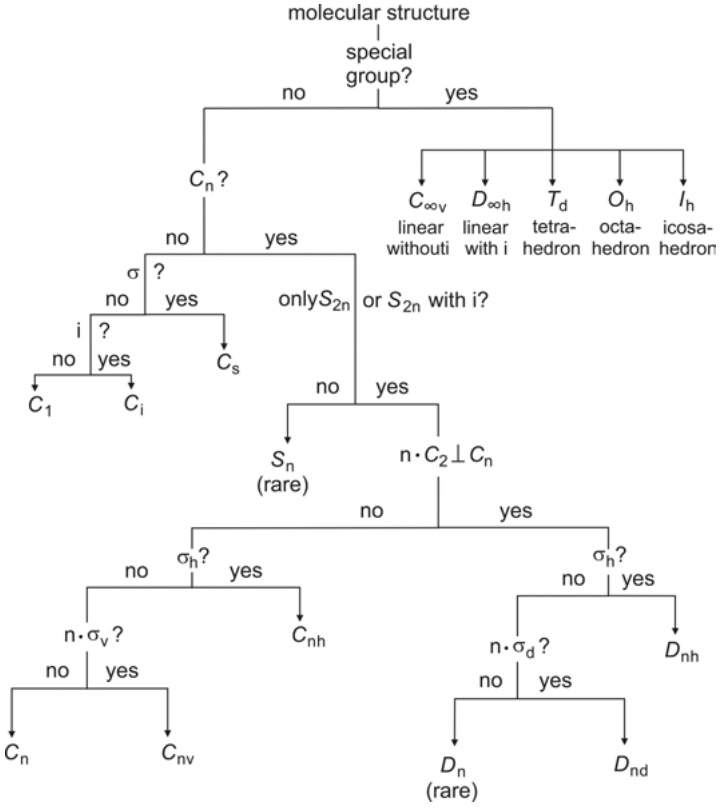

Figure 2.12: Flowchart to derive point symmetries and point group symbols of molecules and ions.

these polyhedrons all atoms at the apexes are equivalent and the "surfaces" are formed by equilateral triangles; see Figure 2.13.

Linear molecules and ions without a center of symmetry such as CO, N_2O, ClCN, OCS and $[SCN]^-$ are given the symbol $C_{\infty v}$. These species have a ∞-fold rotational axis (C_∞). The axis with the highest rotation number is chosen as the *vertical axis*

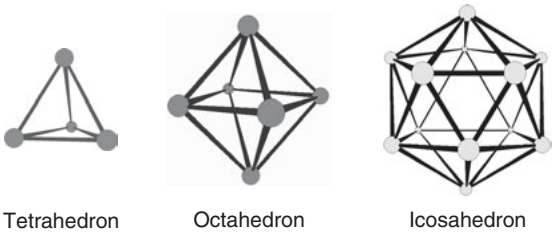

Figure 2.13: Polyhedrons of particularly high symmetry (PLATONic solids): *tetrahedron* with 24 symmetry operations ($8C_3$, $3C_2$, $6S_4$, $6\sigma_d$, E); *octahedron* with 48 symmetry operations ($6C_4$, $8C_3$, $6C_2$, i, $8S_6$, $6S_4$, $3\sigma_h$, $6\sigma_d$, E); *icosahedron* with 120 symmetry operations (e.g., $12C_5$, $10C_3$, $15C_2$, i, ...). A *cube* also belongs to point group O_h.

with the subscript "v" as in $C_{\infty v}$. Such molecules have an infinite number of mirror planes, which contain the molecular axis and are referred to as vertical (σ_v), as well as innumerable improper rotational axes perpendicular to the molecular axes. There are no other symmetry elements.

Linear species with inversion center are given the point group symbol $D_{\infty h}$. Examples are the molecules N_2, CO_2, CS_2, XeF_2, C_3O_2 and the ions $[NO_2]^+$, $[N_3]^-$, $[HF_2]^-$. Perpendicular to the $C_{\infty v}$ axis there are ∞C_2 axes, and the molecule is of *dihedral symmetry* (symbol: D), a high symmetry found if n twofold axes exist perpendicular to the highest-fold C_n axis: $nC_2 \perp C_n$. Other dihedral molecules are, for example, BF_3, XeF_4, PF_5 and IF_7. The subscript "h" for horizontal in a point group symbol denotes a mirror plane (σ_h) perpendicular to the highest-fold axis as in CO_2.

Point group symbols for any molecule may be derived using the flow scheme in Figure 2.12. After identifying special groups, a rotation axis C_n of at least twofold order is sought. If C_n axes are absent, then σ or i may be symmetry elements. A molecule without any symmetry is given the symbol C_1 (e.g., the methane derivative CFClBrI, which has in fact been prepared). If the molecule has a C_n axis ($n > 1$), then an even-fold improper rotation axis S_{2n} and possibly an inversion center i may be the only additional symmetry elements to give the rare group S_n. In most cases, there are additional rotational axes (e.g., C_2) or mirror planes (σ_v, σ_h, σ_d). The symbol σ_d denotes a diagonal mirror plane, that is, a vertical mirror plane lying between two C_2 axes in a dihedral molecule. For example, the trigonal-planar molecule BF_3 has the following symmetry elements: C_3, $3C_2 \perp C_3$, σ_h and $3\sigma_d$ to give the symbol D_{3h}. Further examples of symmetric molecules are given in Table 2.9.

All point groups with more than twofold rotational axes (C_3, C_4, ...) or improper axes (S_3, ...) are called *degenerate*. Many highly symmetric molecules belong to degenerate groups, including linear, trigonal-planar, tetrahedral, trigonal-bipyramidal, octahedral and icosahedral species. In such cases there are degenerate MOs and

Table 2.9: Point group symbols of familiar molecules and ions.

Type	Geometry	Examples	Point group
AB_2	Linear	CO_2, XeF_2, C_3O_2	$D_{\infty h}$
	Bent	SO_2, $[NO_2]^-$	C_{2v}
ABC	Linear	COS, N_2O	$C_{\infty v}$
	Bent	HOCl, ClNO	C_S
AB_3	Trigonal-planar	BCl_3, $[NO_3]^-$	D_{3h}
	Trigonal-pyramidal	PH_3, XeO_3	C_{3v}
AB_2C	Planar	$BClF_2$, $ClNO_2$	C_{2v}
	Pyramidal	$ClNH_2$, $OSCl_2$	C_S
AB_4	Tetrahedral	$[ClO_4]^-$, $[BF_4]^-$	T_d
	Square	XeF_4	D_{4h}
AB_3C	Tetrahedral	$OPCl_3$, $[S_2O_3]^{2-}$	C_{3v}
AB_5	Trigonal-bipyramidal	PF_5	D_{3h}
AB_6	Octahedral	SF_6	O_h
AB_5C	Octahedral	$SClF_5$	C_{4v}

degenerate fundamental vibrational modes, that is, orbitals and vibrations of *identical energy*. This important issue will be discussed later in this chapter.

The *local symmetry* of a molecule or ion describes the symmetry of a part of the molecule, which is under discussion. For example, the methyl group of CH_3–NF_2 is of approximate C_{3v} symmetry and the difluoroamino group is of approximate C_{2v} symmetry, while the whole molecule is only of C_s symmetry.

2.4 The Covalent Bond

In molecules, atoms are linked by covalent bonds and accordingly lose their identity to some degree in favor of something new. But chemists tend to rationalize the chemical bond in such a way that the original atoms can still be recognized in molecules. The most prominent example for this kind of treatment is RICHARD BADER's theory of *atoms in molecules* (AIM), which will be discussed below.[34] But the

34 R. F. W. BADER (1931–2012), Canadian theoretician. For an introduction to AIM theory, see: http://www.chemistry.mcmaster.ca/bader/aim/ and P. L. A. Popelier, *An Introduction to the Theory of Atoms in Molecules*, Pearson Education, Harlow, U.K., **2000**.

strictest theoretical treatment of covalent bonding using the principles of quantum-mechanics has been developed early last century by WALTER H. HEITLER, FRITZ W. LONDON and LINUS PAULING, who established the valence bond (VB) theory, and independently by FRIEDRICH HUND and ROBERT S. MULLIKEN, who are the founders of MO theory. In inorganic chemistry, **MO theory** is most widely used[35] and will therefore be discussed in this section exclusively.

All theories of covalent bonding rest on three fundamental concepts: COULOMB's law of electrostatic interaction (Section 2.1.7), PAULI's exclusion principle (Section 2.2.2) and HEISENBERG's uncertainty principle, which all are needed to understand the electronic structure and behavior of atoms. WERNER HEISENBERG[36] published in 1927 the fundamental idea that in atomic dimensions the location (x) and the momentum or impulse (p) of a particle cannot be determined at any level of accuracy at the same time because the following relationship holds: $\Delta x \cdot \Delta p \geq h/2\pi$ (h: PLANCK's constant). This relationship has become known as uncertainty principle. A sharp definition of the energy of a particle (e.g., an electron in an atom) requires its spatial delocalization, described by a wave function. In MO theory, it is postulated that in molecules the VEs cannot longer be assigned to specific atoms but are delocalized over a certain section of the molecule, that is, atomic orbitals are replaced by multicenter MOs extending over the whole atomic framework. All electrons are indistinguishable, of course.

In the following we use the simplest molecule with a covalent bond, the molecular ion $[H_2]^+$ (it consists of just two protons and one electron), to develop the principles of MO theory. Subsequently, the model will be extended to multielectron systems in a similar manner, as the hydrogen atom is used as a model in atomic theory to describe and understand the structure of atoms with more than one electron.

2.4.1 The Molecular Ion $[H_2]^+$

The ion $[H_2]^+$ is formed on ionization of H_2 molecules in an electric discharge or in the ion source of a mass spectrometer by collision with fast electrons with a kinetic energy exceeding the ionization energy of H_2 (15.4 eV):

$$H_2 \longrightarrow [H_2]^+ + e^- \qquad \Delta H° = 1.49 \text{ MJ mol}^{-1}$$

35 T. A. Albright, J. K. Burdett, M.-H. Whangbo, *Orbital Interactions in Chemistry*, 2nd ed., Wiley, New York, **2013**. J. Reinhold, *Quantentheorie der Moleküle*, 5th ed., Springer, Heidelberg, **2015**. B. M. Gimarc, *Molecular Structure and Bonding – The Qualitative Molecular Orbital Approach*, Academic, New York, **1979**.

36 German physicist (1901–1976); NOBEL prize in physics 1932.

The spectroscopically determined internuclear distance d_{HH} of $[H_2]^+$ is 106 pm or 2.00 a_0 (atomic units; 1 a_0 = 52.9 pm). The bond enthalpy of 269 kJ mol^{-1} at 25 °C is markedly smaller than for H_2 (457 kJ mol^{-1}). The molecular symmetry of $[H_2]^+$ is $D_{\infty h}$.

The electron in $[H_2]^+$ moves in the field of two nuclei, and the MOs are two-centered. The mathematical problem in MO theory is finding a wave function ψ that describes such an electronic state. But even if such a function can be found, the SCHRÖDINGER equation cannot be solved analytically. The potential energy of an electron in the field of two vibrating nuclei[37] constitutes the simplest three-body problem in chemistry and as such can only be approximated. A suitable solution to this problem is provided by the BORN–OPPENHEIMER approximation, which is based on the fact that electrons move orders of magnitude faster than the heavier nuclei. The movement of the latter can therefore be considered as irrelevant and thus neglected. MO theory depends on approximations even in the case of the smallest molecule!

Suitable polycentered wave functions ψ (MOs) are then constructed on a trial basis by combinations of single-centered hydrogen-like atomic functions ϕ (AOs), called LCAO approximation (*linear combination of atomic orbitals*). In the following, we use the symbol ψ for the polycentered wave functions of molecules and ϕ for hydrogen-like atomic orbitals. In an iterative process, these "guessed" wavefunctions are optimized against the total energy of the system.

2.4.1.1 The LCAO Approximation

The nuclei in the hydrogen molecular ion, designated as A and B, are placed at the experimental distance. At each nucleus, there is a spherical 1*s* atomic orbital. These orbitals overlap in the region between the two nuclei as shown in Figure 2.14.

The electron of $[H_2]^+$ moves near the nuclei with largest probability, and when close to nucleus A will be little influenced by nucleus B and vice versa. In the absence of nucleus B, the electron would be in the 1*s* AO of atom A. Thus, it can be assumed that the MO near A is similar to 1*s* AO of A, and similar considerations hold for atom B. Therefore, if we neglect the influence of B on A and vice versa, we can write the following linear combination to construct a wave function for the MO of $[H_2]^+$ in its ground state:

$$\psi = c_1 \cdot \phi_A(1s) + c_2 \cdot \phi_B(1s)$$

By varying the two coefficients c_i any mixing ratio of the two atomic functions can in principle be achieved. However, this equation is generally used in the form:

37 All nuclei of a molecule vibrate against each other even at 0 K (zero-point vibration) to obey the HEISENBERG uncertainty principle (see Chapter 4.2.1).

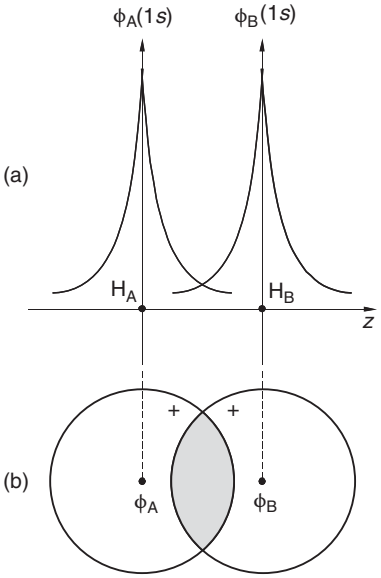

Figure 2.14: Overlap of the two 1s orbitals of the atoms in the ion $[H_2]^+$. (a) Profiles of the two wave functions ϕ_A and ϕ_B; (b) Projections of the surfaces of the spherical orbitals onto the molecular plane.

$$\psi = N\,[\phi_A(1s) + \lambda \cdot \phi_B(1s)] \tag{2.7}$$

N: Normalizing factor and
λ: mixing coefficient.

The normalizing factor is needed to guarantee the correct number of electrons after raising ψ to the power of two and integration over the whole volume of the ion. The mixing coefficient λ assigns the relative weight to the two AOs and reflects the polarity of the MO in a heteronuclear molecule. In general, this coefficient can assume values between $-\infty$ and $+\infty$. However, the electron density of $[H_2]^+$ is of $D_{\infty h}$ symmetry; this density is proportional to the *squares* of the wave functions $(c_1\phi_A)^2$ and $(c_2\phi_B)^2$. For A identical to B it follows $c_1^2 = c_2^2$ resulting in the two solutions $c_1 = c_2$ and $c_1 = -c_2$ or $\lambda = \pm 1$. Evidently, the linear combination in eq. (2.7) describes *two* MOs (ψ^+ and ψ^-):

$$\psi^+ = N^+ (\phi_A + \phi_B) \quad \text{with } N^+ = \frac{1}{\sqrt{2\,(1+S)}} \tag{2.8}$$

$$\psi^- = N^- (\phi_A - \phi_B) \quad \text{with } N^- = \frac{1}{\sqrt{2\,(1-S)}} \tag{2.9}$$

The normalizing factors N contain the overlap integral S,

$$S = \int \phi_A^* \, \phi_B \, d\tau$$

which, after integration on all volume increments dτ, will be positive if the two atomic wave functions have the same sign in the overlap region (between the nuclei); otherwise S will be negative. $S > 0$ results in attraction (bonding), and $S < 0$ is equivalent to repulsion or "antibonding." The two-center wave functions in eqs. (2.8) and (2.9) may now be used to calculate the total electronic energy $E_e = E_{pot} + E_{kin}$ of the molecular ion $[H_2]^+$ as a function of the internuclear distance R by inserting ψ^+ and ψ^- into the SCHRÖDINGER equation:

$$\boldsymbol{H}\,\psi = E_e \cdot \psi$$

The Hamiltonian operator $\boldsymbol{H}$ acts on the molecular wavefunction ψ to yield the permitted energy levels E_e (the *eigenvalues*) of the molecule from which one can calculate many molecular properties. The potential energy of the electron E_{pot} is calculated by COULOMB's law from the electrostatic interactions between the three particles:

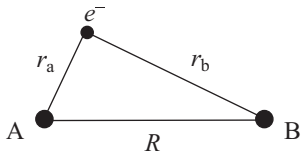

$$E_{pot} = -\frac{e^2}{r_a} - \frac{e^2}{r_b}$$

The *total energy* E of the ion $[H_2]^+$ with respect to its dissociation products H und H^+ (i.e., the bond energy) is the sum of the (negative) electronic energy E_e and the (positive) internuclear repulsion e^2/R diminished by the (negative) electronic energy of a hydrogen atom (E_H):

$$E = E_e + \frac{e^2}{R} - E_H \qquad E_H = -13.6\ \text{eV}$$

The energies of the ion $[H_2]^+$ calculated from the wave functions ψ^+ and ψ^- as a function of internuclear distance R are shown in Figure 2.15. The combined energies of the separate particles H and H^+ have been set to zero. Only the function ψ^+ describes a bonding interaction with a well-defined energy minimum (bond energy maximum), that is, a stable molecular "state." The symmetry of the corresponding MO is *gerade* and the MO is numbered as $1\sigma_g$. On the other hand, the function ψ^- yields positive energies for all values of R, which is termed as antibonding or repulsive interaction. This MO is *ungerade*, and $1\sigma_u$, when occupied by one electron, does not describe a "state" of the ion since spontaneous dissociation would occur at all values of R. Antibonding orbitals are often symbolized by a star added to the term symbol of the wave function (ψ^*). For σ orbitals the internuclear axis is a rotational axis.

In Figure 2.16 the electron densities (ψ^2) of the ion $[H_2]^+$ are shown, calculated from the wave functions ψ^+ and ψ^-, respectively, and for a *fixed distance* R, which corresponds to the energy minimum shown in Figure 2.15. It is assumed that the

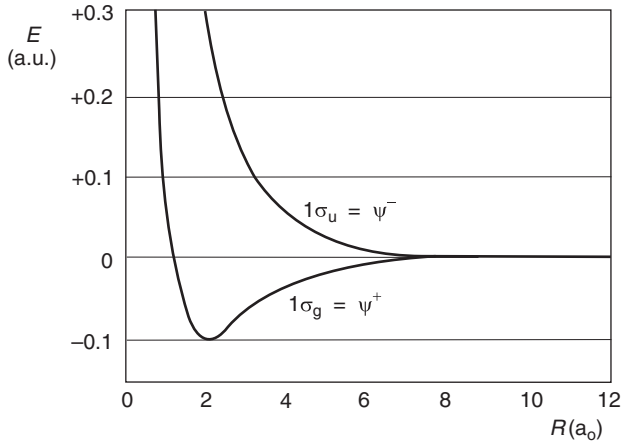

Figure 2.15: Bond energy of the ion $[H_2]^+$ as a function of internuclear distance R with inclusion of the internuclear repulsion (1 a.u. = 1 Hartree = 27.2 eV = 2625.5 kJ mol^{-1}). The wave function ψ^+ describes the bonding, and ψ^- the antibonding interaction of the two atomic orbitals.

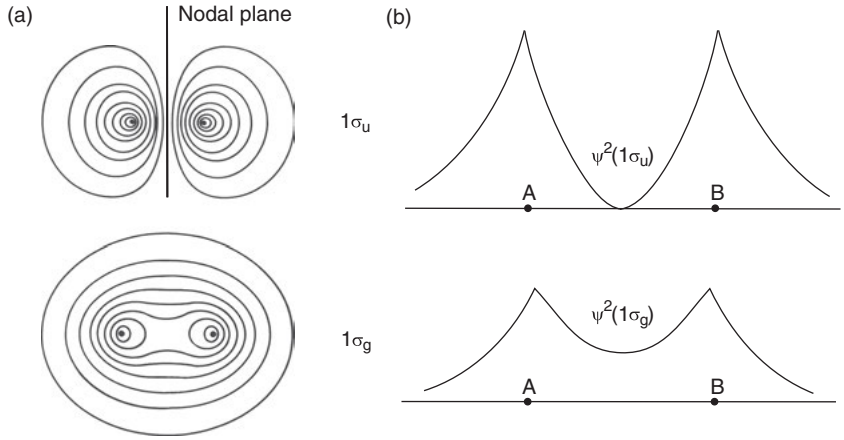

Figure 2.16: (a) Contour plots of the calculated electron densities for the molecular orbitals $1\sigma_g$ and $1\sigma_u$ of the ion $[H_2]^+$ if either one is occupied by one electron (isodensity contours). (b) Electron density variation along the internuclear axis of $[H_2]^+$ for the two singly occupied molecular orbitals $1\sigma_g$ and $1\sigma_u$.

single electron occupies either orbital $1\sigma_g$ or $1\sigma_u$. In Figure 2.16a, the two nuclei are in the projection plane. As shown in Figure 2.16b, the function $1\sigma_g$ results in a substantial electron density accumulation between the two nuclei. This constitutes the bonding interaction. On the other hand, function $1\sigma_u$ with a nodal plane between the nuclei yields an electron density of zero in the middle between the two protons and hence repulsion occurs due to their positive charge. The line of maximum

electron density between atoms A and B is called *bond path*, and the point of minimum electron density along this path is termed *bond critical point (BCP)*. At this "point" the two atoms "touch" each other, so to speak. According to the AIM theory, a covalent bond is identified if there is a significant electron density at the bond critical point (in contrast to a purely ionic bond or no bond at all).[38]

With the wave function ψ^+ from eq. (2.7) and $\lambda = 1$, the maximum bond energy of $[H_2]^+$ is calculated from the SCHRÖDINGER equation as 165 kJ mol^{-1} at a bond length of R = 130 pm. The experimental values (269 kJ mol^{-1} and 105.2 pm) are quite different. Therefore, the wave functions ϕ_A and ϕ_B need to be modified, for example, by taking into account that the electron of $[H_2]^+$ moves in the electric field of *two* protons. The effective nuclear charge Z_{eff} the electron feels must be between 1 (at $R = \infty$) and 2 (at $R = 0$). By varying Z_{eff} to find the maximum bond energy the optimum bond length is obtained as $R = 2a_o$ (105.8 pm) at $Z_{eff} = 1.25$. This nuclear charge is equivalent to a *contraction of the 1s AOs* since the nuclear charge is part of the negative exponent in the general formula for the 1*s* wave function:

$$\phi(1s) = \mathrm{N}\cdot\mathrm{e}^{-\frac{Zr}{a_o}}$$

With this effective nuclear charge, the maximum bond energy is calculated as 236 kJ mol^{-1} corresponding to 88% of the experimental value. Another improvement of the LCAO approximation is achieved by polarization of the modified 1*s* AOs due to the molecular $D_{\infty h}$ symmetry. The 1*s* AOs cannot longer be spherical since the valence electron is attracted by the second nucleus also. This kind of deformation in the direction of the *z* axis is mathematically expressed by a *polarization function* added to the wave function as follows:

$$\phi'(1s) = \mathrm{N}\cdot\mathrm{e}^{-\frac{Zr}{a_o}}\ [1 + \lambda z]$$

Optimization of the bond energy by variation of the novel coefficient λ shows that it assumes relatively small values (0.01–0.03). The polarized atomic orbitals are elongated toward the neighboring atom but shrunk in the opposite direction. This polarization can be understood as the admixing of some $2p_z$ character to the originally spherical 1*s* AOs of the hydrogen atoms:[39]

38 In the case of weak bonds or unusual geometrical arrangements this criterium may be difficult to interpret. For electron-rich molecules such as SCl_2 the electron density at the bond critical point (in this case 0.133 $e\ a_0^{-3}$) is by several orders of magnitude smaller than at the centers of the atoms. Therefore, the Laplacian (the 2nd derivative) of the electron density is typically used instead.

39 In a similar fashion the base functions of many-electron atoms are modified by mixing in some *d*-, *f*- or even *g*-contributions to achieve optimal polarization; see: J. Simons, *J. Phys. Chem.* **1991**, *95*, 1017.

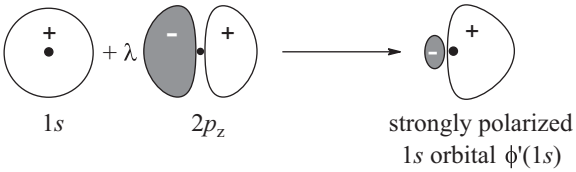

With this polarized *basis function* ϕ' the bond energy of $[H_2]^+$ is calculated as 263 kJ mol^{-1}, which deviates only marginally from the experimental value.[40]

In all future discussion *modified wave functions* will be used to describe atomic orbitals even if this is not mentioned explicitly. Since the true wave functions remain unknown the mathematical modifications of the hydrogen-like atomic orbitals are a suitable approximation. It is interesting to compare the potential and kinetic energies of the ion $[H_2]^+$ with those of the isolated hydrogen atom to identify *the reason for bond formation*. Since the total energy E decreases on bond formation, either E_{kin} or E_{pot} of the hydrogen electron must decrease (H^+ does not have any electronic energy). Calculations showed that E_{kin} of the H atom is 0.5 Hartree and of $[H_2]^+$ at the equilibrium distance it is 0.6 Hartree. In other words, the contraction of the 1*s* AOs increases the kinetic energy of the electron. Therefore, it must be the *decrease of the potential energy of the electron* in the field of *two* nuclei, which leads to a covalent bond. Both "atoms" in $[H_2]^+$ bear a partial charge of +0.5 *e*.

The formation of molecules from atoms can be elucidated in *energy level diagrams*, or short MO diagrams, which compare the orbital energies of the isolated atoms with the energy levels of the electrons in a molecule. Stable states have negative energies. The 1*s* orbital energy of hydrogen atoms is −13.6 eV (−0.5 Hartree), which is equivalent to the negative ionization energy. For H^+ an orbital energy cannot be defined since the (virtual) 1*s* AO is empty; in Figure 2.17 its energy is set equal to that of the H atom. The energies of the MOs $1\sigma_g$ and $1\sigma_u$ have been calculated for the equilibrium internuclear distance $2a_o$ with the electron occupying either one of the two MOs. The spin quantum number of the electron is symbolized by an arrow, which points either up or down corresponding to spin α resp. β. In isolated hydrogen atoms the spin of the electron can have any of the two values. Figure 2.17 demonstrates that occupation of the bonding MO with just one electron results in a stable state, which is by 269 kJ mol^{-1} (2.7 eV) lower than the separated particles H and H^+. This configuration is called a *one-electron bond*.

If the bonding electron would be promoted to the antibonding level, the $[H_2]^+$ ion would spontaneously dissociate, since the energetic splitting of two MOs is *asymmetric* with respect to the 1*s* AO of hydrogen (see below). The antibonding

40 A near-perfect agreement between calculated and experimental values is achieved with further modifications of the basis function; see: W. Kolos, L. Wolniewicz, *J. Chem. Phys.* **1964**, *41*, 3663 and 3674.

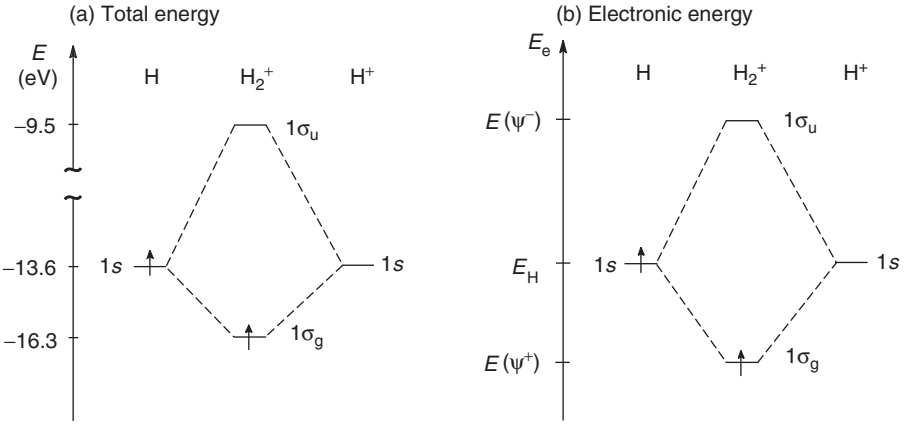

Figure 2.17: Energy level diagram for the molecular ion $[H_2]^+$. In (a) the ordinate shows the total energy consisting of electronic energy as well as the nuclear repulsion. In (b) the ordinate shows just the electronic energy.

level is more destabilized than the bonding level is stabilized. The energy zero for the electron is defined by the complete separation of the particles equivalent to ionization of $[H_2]^+$ (*ionization limit*). In the following sections, diagrams as in Figure 2.17b will be used to discuss the covalent bonds of similar molecules.

The orbital energies for the MOs $1\sigma_g$ and $1\sigma_u$ can be calculated using the LCAO approximation if the *overlap integral S* as well as the resonance integral β are known. For $[H_2]^+$ the following relationships apply approximately:[41]

$$E(\psi^+) = E(\phi_A) + \frac{\beta}{(1+S)}$$
$$E(\psi^-) = E(\phi_A) - \frac{\beta}{(1-S)}$$

For $[H_2]^+$, the integral *S* is about 0.6 and β is approximately –0.16 at the energy minimum (β is always negative). Therefore, the orbital energies of the MOs $1\sigma_g$ and $1\sigma_u$ differ from the atomic H(1*s*) level as shown in Figure 2.17: the splitting is asymmetric.[42] The valence electron occupies the $1\sigma_g$ MO, which is considerably more stable than the 1*s* AO of a hydrogen atom. Would a second electron be placed into the $1\sigma_u$ MO of $[H_2]^+$ the resulting neutral but electronically excited molecule $[H_2]^*$ would

41 In both equations, $E(\phi_A)$ is the quasi-classical energy of the molecular ion, i.e. the electronic energy of a hydrogen atom at distance $2a_0$ to an additional proton; for an exact calculation, see: W. Kutzelnigg, *Einführung in die Theoretische Chemie*, Vol. 2, VCH, Weinheim, **1978**.

42 In some publications the splitting is shown to be symmetric assuming $S \approx 0$. However, for larger molecules, *S* has values of between 0.2 and 0.3; inorganic chemistry cannot be understood neglecting overlap since it is an oversimplification.

immediately dissociate since the destabilization by this additional electron would be stronger than the stabilization by the electron in the bonding MO. On the other hand, $[H_2]^*$ could emit a photon when the electron jumped from the $1\sigma_u$ MO to the lower $1\sigma_g$ MO forming a normal H_2 molecule; however, such an electronic transition between MOs of differing symmetry is forbidden by quantum-mechanical laws.

2.4.2 The Molecule H_2

The covalent bond in the molecule H_2 can be understood using the diagrams in Figure 2.17. The additional electron occupies the bonding orbital $1\sigma_g$ resulting in a much higher bond enthalpy (457 kJ mol^{-1} at 25 °C) and a much shorter internuclear distance d_{HH} of 74.1 pm ($1.40a_0$) compared to the one-electron bond in $[H_2]^+$. An added complication, however, is the interelectronic repulsion of the two electrons (1) and (2). These electrons no longer move in the electric field of just two fixed protons A and B but also in the repulsive field of the neighboring electron in the same MO:

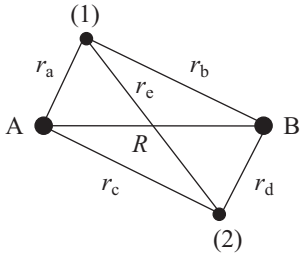

$$E_{pot} = -\frac{e^2}{r_a} - \frac{e^2}{r_b} - \frac{e^2}{r_c} - \frac{e^2}{r_d} + \frac{e^2}{r_e} + \frac{e^2}{R}$$

Since the two electrons move in an undetermined manner, the potential energy E_{pot} cannot be calculated accurately. Fortunately, there are excellent mathematical approximations to this problem. If the one-electron wave functions ψ from eq. (2.7) and an effective nuclear charge of $Z_{eff} = 1.19$ are used together with the polarization of the atomic 1*s* orbitals as described in Section 2.4.1, the internuclear distance of H_2 is correctly predicted as $1.40a_0$. For the bond energy, however, only 77% of the experimental value is obtained; below we will show how a better agreement between theory and observation can be achieved.

In the lower part of Figure 2.18a, the MO diagram for H_2 in its ground state $^1\sum_g^+$ is shown. In order to satisfy the PAULI principle, the spins of the two electrons must be antiparallel (α and β). The term symbol $^1\sum_g^+$ contains elements of the orbital symmetry (σ_g) and describes a *singlet state* as the total spin quantum number $S = 0$ corresponds to a *multiplicity* of $2S + 1 = 1$. If the orbitals $1\sigma_g$ and $1\sigma_u$ were occupied by one electron each as shown in the upper part of Figure 2.18a, their spins could both be +½ and the multiplicity would be 3 (*triplet state*). A molecule of this type cannot exist since its energy would be positive at all internuclear distances $R < \infty$, as

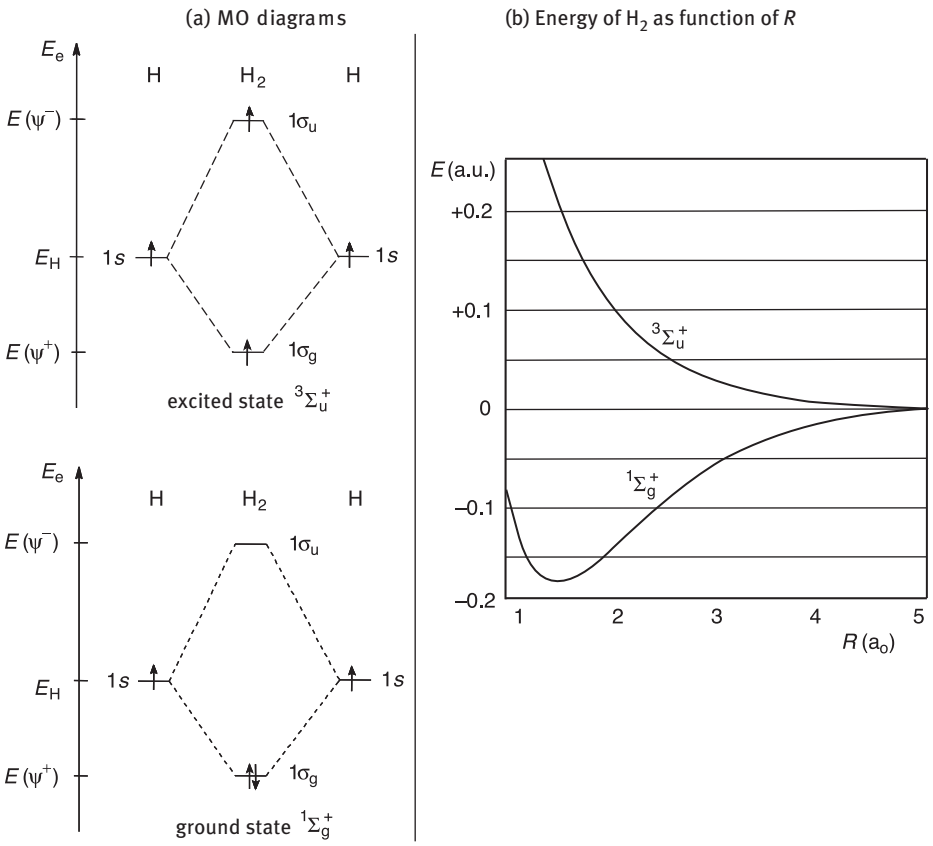

Figure 2.18: (a) MO diagram of the molecule H_2 in the $^1\sum_g^+$ ground state (below) and in its first excited state $^3\sum_u^+$ (above). Depicted are the electronic energies of H atoms and the H_2 molecule. The spins of the isolated atoms are arbitrary. (b) Energies of H_2 in the states $^1\sum_g^+$ and $^3\sum_u^+$ as functions of internuclear distance *R*. The energy of the separated hydrogen atoms has been set zero.

shown in Figure 2.18b. In other words, if one of the two VEs of ground state H_2 is promoted to the $1\sigma_u$ MO spontaneous dissociation must occur.

To reach a better agreement between calculated and observed bond energy, the *electron correlation* needs to be taken into account, which is important for all many-electron systems. Obviously, the two electrons cannot move independently but they will rather try to avoid being in the same space element at the same time due to their equal charges (COULOMB repulsion). For the H_2 molecule, this effect can be allowed for by adding a few more terms to the linear combination of the atomic orbitals.[43] With 10 additional terms, the calculated bond energy deviates by less than

43 J. Simmons, *J. Phys. Chem.* **1991**, *95*, 1017.

4 kJ mol^{-1} from the experimental value. Electron correlation is also responsible for the bond energy of H_2 being less than twice that of $[H_2]^+$. In addition, the repulsion of the nuclei is stronger in H_2 than in $[H_2]^+$ since the internuclear distance is much shorter. The ionization energy of H_2 is 15.4 eV.

2.4.2.1 The Cation $[He_2]^+$

The discussion of the bonding situations of $[H_2]^+$ and H_2 can be extended to the cation $[He_2]^+$, which is produced if helium gas is exposed to an electrical discharge in which He atoms are ionized. The resulting He^+ cations combine exothermically with He atoms to give $[He_2]^+$ with a bond energy of 228 kJ mol^{-1} and an internuclear distance d_{HeHe} of 108.1 pm. Since the electrons of helium atoms occupy the 1*s* AO the linear combination of these orbitals can produce the same type of MOs as has been shown for dihydrogen. However, when the diagrams in Figures 2.17 and 2.18 are used, the much lower orbital energy of the 1*s* AO of He (−24.5 eV) has to be taken into account, which is the consequence of the higher nuclear charge. The *three-electron bond* of $[He_2]^+$ originates from two bonding electrons in the $1\sigma_g$ MO and just one antibonding electron at the $1\sigma_u$ level.

The life-time of cations such as $[He_2]^+$ in a gas discharge is short since they rapidly capture an electron and dissociate into two neutral atoms. The caught electron would enter the $1\sigma_u$ MO and due to the asymmetric splitting between bonding and antibonding MOs the repulsion is stronger than the attraction by two electrons each and the particle dissociates. However, there exist weakly bonded so-called VAN DER WAALS molecules He_2 with a rather large "bond length"; see Section 3.5.

In the chemical literature, so-called MO bond orders have been proposed that are calculated in a first approximation by subtracting the number of antibonding electrons from the number of bonding electrons. These bond orders are qualitative in nature since we have seen that the repulsive action of an antibonding electron is stronger than the attraction by a bonding electron. In addition, the strength of a covalent bond depends on the overlap and resonance integrals, which determine the splitting of the MOs into bonding and antibonding levels. More realistic values for bond orders can therefore be obtained from quantum chemical calculations (e.g., the Mayer bond order).[44] In any case, *observable quantities* such as dissociation enthalpy, bond length and force constant are quantifiable measures to characterize a covalent bond and its strength (see Chapter 4).

2.4.2.2 The Role of Antibonding Molecular Orbitals

For the understanding of the structures and reactivities of molecules the antibonding MOs are as important as the bonding MOs. Two simple examples will be used to

44 A. J. Bridgeman et al., *J. Chem. Soc., Dalton Trans.* **2001**, 2095.

illustrate this. First, if hydrogen gas is reacted with liquid sodium metal the salt-like hydride NaH is formed in an exothermic reaction (see Section 5.7.4). This reaction can be explained as follows. The ionization energy of sodium atoms is only 5.1 eV and liquid sodium can be ionized even easier. On the other hand, the lowest unoccupied MO (LUMO) of H_2 has an orbital energy of ca. –11 eV (Figure 2.16). Therefore, the transfer of an electron from the 3*s* AO of Na to the $1\sigma_u$ MO of H_2 is an exothermic process. Occupation of the antibonding $1\sigma_u$ MO of H_2 by two electrons from sodium metal initiates dissociation of the hydrogen molecule with the formation of two hydride anions H^-, which combine with the sodium cations to form solid NaH.

A second simple example is the isotope exchange reaction between H_2 and D_2 to give two HD molecules:

$$H_2 + D_2 \rightleftharpoons 2\,HD$$

This seemingly simple reaction requires a rather high activation energy, although one might be tempted to think that a four-center reaction (a) with simultaneous dissolution of the bonds in H_2 and D_2 and formation of the new bonds in two molecules H–D should be possible:

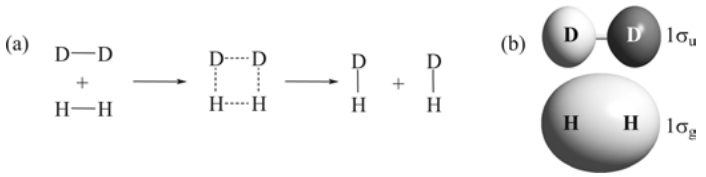

As shown in (b), however, such a reaction is *symmetry forbidden* since the overall overlap integral between the $1\sigma_g$ MO of H_2 and the $1\sigma_u$ MO of D_2 (or *vice versa*) is zero (the two MOs are orthogonal). Any interaction of the two $1\sigma_g$ MOs of H_2 and D_2 can be excluded either since they are both doubly occupied and repel each other. Finally, the interaction of the two antibonding $1\sigma_u$ MOs is also without effect due to lack of electrons. Therefore, in reality the reaction proceeds via hydrogen atoms in a chain-reaction after the energetically costly homolytic dissociation of either H_2 or D_2:

$$H_2 \longrightarrow 2\,H$$
$$H + D_2 \longrightarrow HD + D \quad \text{etc.}$$

Another example for the role of symmetry and the importance of antibonding orbitals in reactivity is the function of dihydrogen molecules as ligands in metal complexes, which will be discussed in Section 5.7.3.

2.4.3 Homonuclear Diatomic Molecules

In order to explain the covalent bonds in the homoatomic diatomic molecules of the elements in the first row of eight of the Periodic Table (Li_2 to F_2), the interaction

of the 2*s* and 2*p* AOs must be analyzed. MOs are formed when the overlap integral *S* is either positive (bonding MOs) or negative (antibonding MOs). Nonbonding MOs have $S = 0$. The 1*s* AOs of these elements do not take part in bonding since their overlap integral with all other orbitals is close to zero due to their small size as the result of the high nuclear charge. However, the overlap integral of any two other orbitals can also be zero for reasons of symmetry as shown in Figure 2.19; orbitals of this type are called "orthogonal".

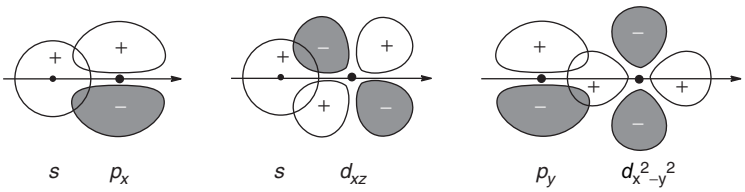

Figure 2.19: Overlap of atomic orbitals of differing symmetry (orthogonal orbitals); the overlap integral is zero in all cases although overlap takes place.

As a general rule, only orbitals of the same symmetry give a nonzero overlap integral. In other words, two AOs of σ symmetry give σ and σ* MOs while two π AOs yield π and π* MOs (σ MOs are rotationally symmetric to the internuclear *z* axis, while for π MOs this axis is part of a nodal plane). The combination of σ with π AOs is unproductive, although overlap takes place.

In Figure 2.20 various linear combinations of 2σ and 2π AOs with a nonzero overlap integral are shown. The calculated surfaces of the obtained MOs are shown on the right-hand side, defined by a formal residual electron density of 0.05 e Å^{-3}.[45] All *s* and p_z AOs are of σ symmetry and can mutually be combined with each other, while the AOs p_x as well as p_y are of π symmetry. The molecular symmetry of a homonuclear diatomic molecule is $D_{\infty h}$, which is a degenerate point group containing a center of symmetry. Therefore, all MOs are classified as either *gerade* (g) or *ungerade* (u). The p_x and p_y AOs are degenerate and can only be combined with AOs of exactly the same type since p_x and p_y are orthogonal to each other.[46]

The energetic splitting of two overlapping atomic orbitals into bonding and antibonding MOs is the larger, the better the net overlap as the resonance integral β at the equilibrium bond length is proportional to the overlap integral *S*. For reasons of symmetry, the overlap of two σ orbitals is always stronger than for two π orbitals, provided the internuclear distance and the orbital energies are the same. This orbital energy is

45 Such a formal density as the square of the wave function can even be calculated for unoccupied MOs (all corresponding Figures are courtesy of Prof. Ingo Krossing).

46 Later, we will see that the valence shell of principal quantum number 3 comprises five *d* orbitals, which – in a linear molecule – are either of σ (d_{z^2}), or π (d_{xz}, d_{yz}) or δ symmetry (d_{xy}, $d_{x^2-y^2}$).

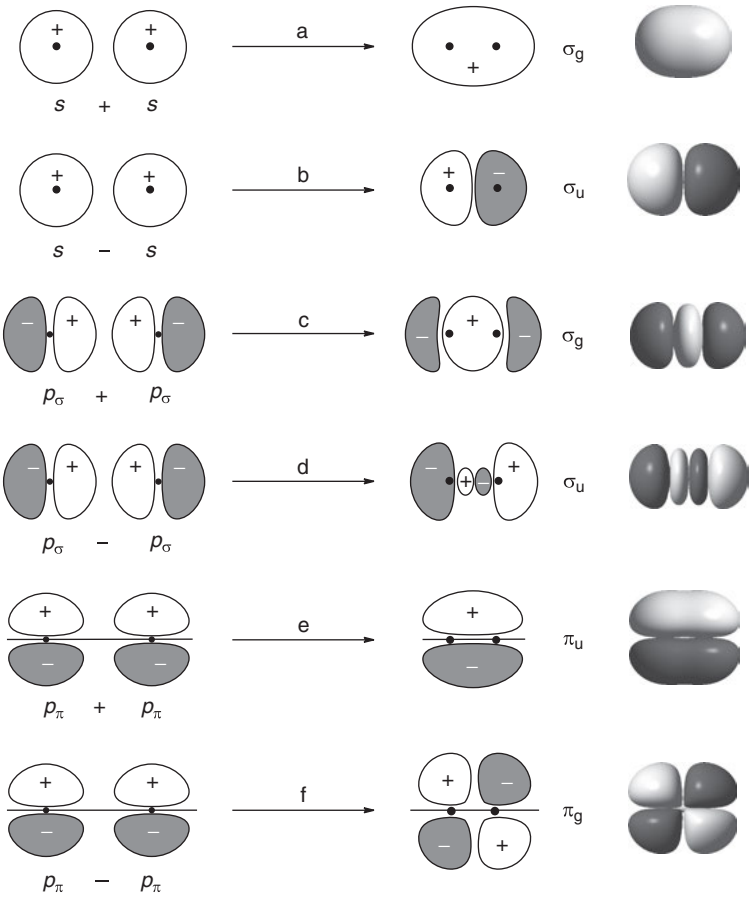

Figure 2.20: Linear combinations of 2*s* and 2*p* AOs (left side) to give bonding and antibonding MOs (center) of either σ or π symmetry. On the right-hand side, the calculated molecular orbitals of the F_2 molecule are shown as isodensity surfaces with a residual electron density of 0.05 *e* Å^{-3} ("isosurface").

decisive since the quantum-mechanical interaction between two AOs is better when their orbital energies are closer. If these AO energies differ by more than 15 eV or 1550 kJ mol^{-1}, the interaction can be neglected even if the symmetries are the same.

For the elements of the first row the orbital energies of the 2*s* and 2*p* levels are shown in Figure 2.21. For lithium the difference is very small, but it steadily increases to the right and exceeds 15 eV for oxygen atoms. For this reason, the MO treatments of F_2 and O_2 are somewhat simpler than those of the other diatomic species of the first-row elements. Therefore, we begin our discussion with **F_2**.

In the fluorine atom the electrons occupy the orbitals 1*s*, 2*s*, 2p_x, p_y and p_z. If two F atoms approach each other, these AOs interact, and MOs can be constructed

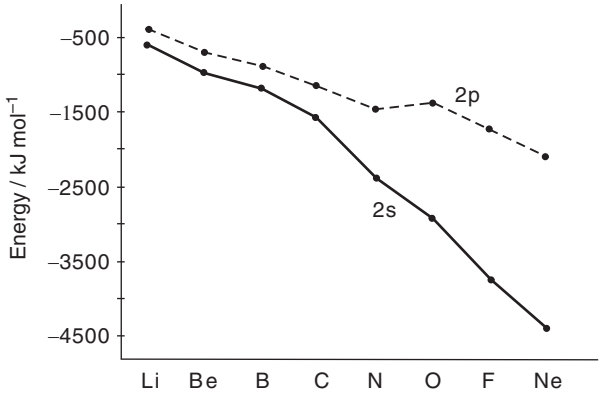

Figure 2.21: Orbital energies of levels 2*s* and 2*p* for the eight elements of the first row of the Periodic Table.

by the LCAO approximation, provided the symmetries and energies of the AOs are compatible. The resulting MO diagram of $\mathbf{F_2}$ is shown in Figure 2.22.

From Figure 2.22 it can be seen that some MOs originating from either 2*s* or 2*p* AOs approach each other energetically (e.g., $2\sigma_u$ and $3\sigma_g$) but, since their symmetries

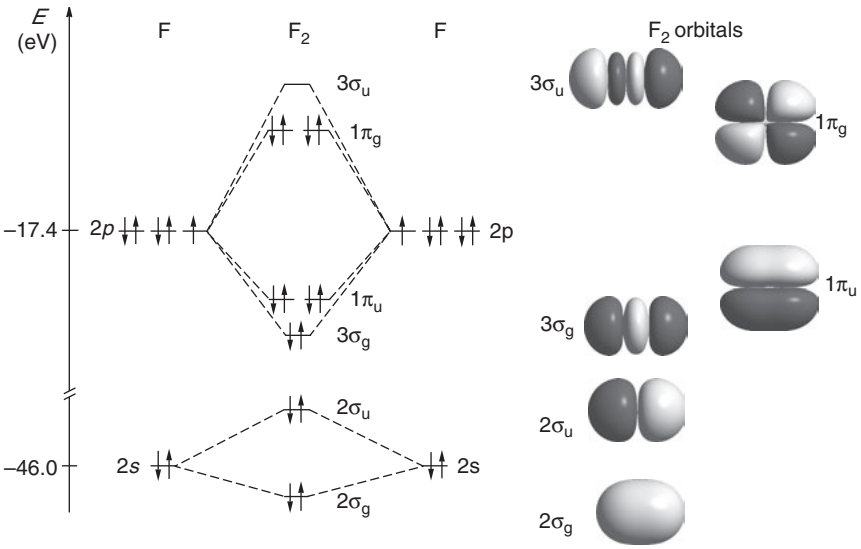

Figure 2.22: MO diagram for the formation of an F_2 molecule from two fluorine atoms. Any interaction between *s* and *p* orbitals can be neglected since their energies are too different. The 14 valence electrons occupy four bonding and three antibonding MOs. On the right-hand side the calculated isodensity surfaces of the MOs are shown with a residual electron density of 0.05 *e* Å^{-3}.

are different, they cannot interact. The 1*s* orbitals have been omitted from Figure 2.22 as their energies are so low that any interaction between them or with the 2*s* AOs can be neglected. For formal reasons, however, the MOs resulting from the combinations $\phi_{1s}+\phi_{1s}$ and $\phi_{1s}-\phi_{1s}$ are counted as $1\sigma_g$ and $1\sigma_u$. The 2*s* AOs form the new levels $2\sigma_g$ and $2\sigma_u$ and the $2p_z$ AOs the levels $3\sigma_g$ and $3\sigma_u$. The latter MO is the *lowest unoccupied molecular orbital* (LUMO) of the molecule.

The π AOs can interact only pairwise, that is, p_x with p_x and p_y with p_y, since other combinations would be orthogonal with zero overlap integrals. These pairs of MOs are twofold degenerate and therefore their numbering is just $1\pi_u$ and $1\pi_g$. Notice that in contrast to the σ MOs it is now the *ungerade* combination, which is bonding. The MO $1\pi_g$ constitutes the *highest occupied molecular orbital* (HOMO) of this molecule.

The qualitative picture in Figure 2.22 agrees with experimental properties of the F_2 molecule. For example, the ionization energy of F_2 (15.7 eV) is smaller than that of F atoms (17.4 eV) because an antibonding electron is removed from the $1\pi_g$ level. The resulting cation $[F_2]^+$ has a stronger bond than F_2, which is apparent from its internuclear distance of d_{FF} = 132 pm. The bond length of F_2 (d_{FF} = 142 pm) and its dissociation enthalpy of 159 kJ mol^{-1} correspond to a single bond, although this bond is much weaker than, for example, the CC bond in ethane with a mean bond enthalpy of 362 kJ mol^{-1} (see Table 4.7). The main reasons for the weakness of the FF bond are as follows: (1) The high effective nuclear charge of fluorine (Z = 9) contracts the orbitals so much that overlap integrals are small.[47] (2) The many electrons in the region between the two atoms repel each other (COULOMB repulsion). (3) There are no nonbonding MOs that would shift electron density to the outer regions of the molecule. The resulting weak "single" bond of F_2 is one of the reasons for the extremely high reactivity of elemental fluorine (see Chapter 13).

A hypothetical molecule **Ne_2**, according to the scheme in Figure 2.22, but with two more VEs would have all bonding and antibonding MOs doubly occupied and the net interaction would be repulsive. Therefore, such a molecule does not exist (except as a loosely bonded VAN DER WAALS molecule; see Chapter 3). When Ne gas is ionized in a glow discharge, however, the Ne^+ ions combine with Ne atoms to form stable cations $[Ne_2]^+$ with a dissociation enthalpy of 131 kJ mol^{-1}, quite similar to that of F_2 (159 kJ mol^{-1}). The positive charge of such cations stabilizes all orbitals (or electrons) by the increased effective nuclear charge.

The dioxygen molecule **O_2** has 12 VEs occupying the MOs $2\sigma_g$, $2\sigma_u$, $3\sigma_g$ and $1\pi_u$ in Figure 2.23 by electron pairs and leaving two unpaired electrons for the degenerate $1\pi_g$ level. COULOMB repulsion, exchange interaction and PAULI principle require that these two electrons occupy the two orthogonal MOs of this level with equal spins making O_2 a *paramagnetic molecule*. The term symbol for such a triplet

47 The atomic radii of the second-row atoms decrease from left to right in the Periodic Table (see Table 4.3).

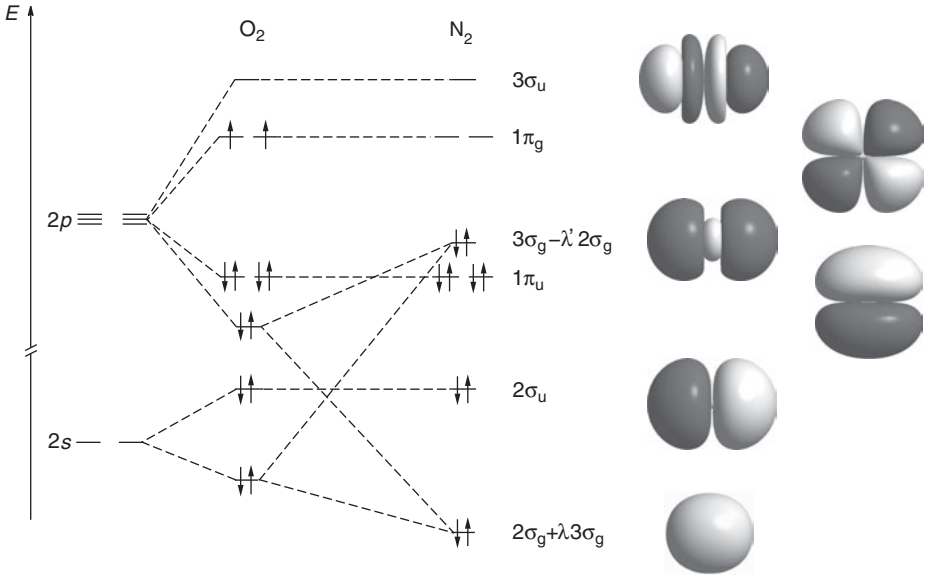

Figure 2.23: Energy level diagrams for the molecules O_2 (left) and N_2 (center). On the right the isosurfaces for the MOs of N_2 are shown, calculated with a residual electron density of 0.05 e Å^{-3}. The interaction of energy levels $2\sigma_g$ and $3\sigma_g$ in the case of N_2 due to the lower $2s/2p$ energy gap yields a different energetic order of the molecular orbitals. Note that the MOs of N_2 are slightly higher than those of O_2 due to the lower effective nuclear charge of nitrogen atoms.

molecule is $^3\sum_g^-$. Since the orbital energy of the $1\pi_g$ MO is higher than that of the atomic $2p$ level the ionization energy of O_2 is smaller (12.1 eV) than that of oxygen atoms (13.6 eV). Other properties of O_2 are listed in Table 2.10, and in Section 11.1.1 we will show that O_2 can also exist in two singlet states.

Table 2.10: Bond properties of various homonuclear diatomic molecules in the gas phase.

Molecule	Number of valence electrons	Dissociation enthalpy at 298 K (kJ mol^{-1})	Internuclear distance (pm)	Spin state
$[Ne_2]^+$	15	131	175	doublet
F_2	14	159	142	singlet
O_2	12	495	121	triplet
N_2	10	945	109	singlet
C_2	8	608	125	singlet
B_2	6	300	159	triplet
Be_2	4	11[a]	245[a]	singlet
Li_2	2	103	267	singlet

[a] Equilibrium values of D_e and r_e; see: J. M. Merritt, V. E. Bondybey, M. C. Heaven, *Science* **2009**, *324*, 1548.

In order to illustrate the geometry of the valence orbitals of O_2, a graphical representation of the calculated electron densities ρ in the occupied MOs can be used; the electron density is proportional to the square of the wave function ψ. In Figure 2.24 contour plots of these densities for the levels $2\sigma_g$, $2\sigma_u$, $3\sigma_g$, $1\pi_u$ and $1\pi_g$ of O_2 are shown. In contrast to the MOs, the density plots need to be symmetric to

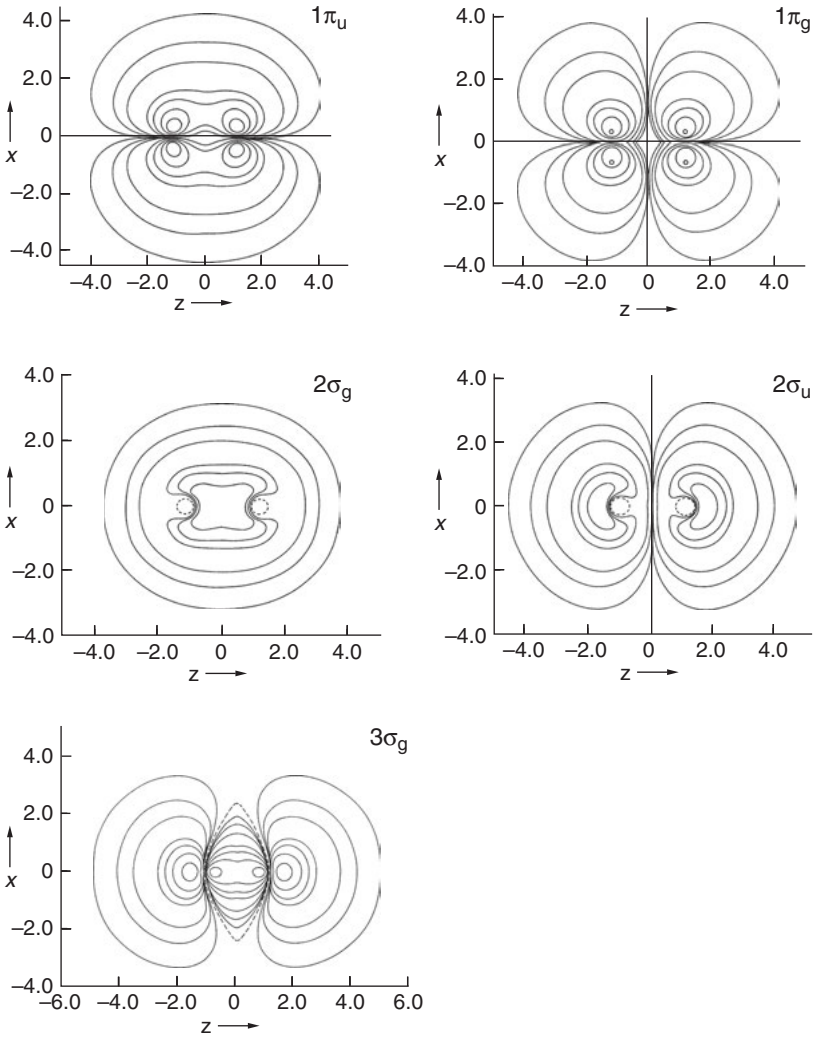

Figure 2.24: Contour plots of the electron densities for the five highest occupied molecular orbitals of the O_2 molecule (see Figure 2.23). The isodensity lines from outside to the center are drawn at 0.0001, 0.001, 0.005, 0.05, 0.1, 0.25 and 0.5 $e\,a_0^{-3}$ (a_0 = 52.9 pm); the distances are given in units of a_0. Shown are cuts through the orbitals with the nuclei in the *xz* plane.

all symmetry elements of the molecule (they are *totally symmetric* as is the total electron density of O_2).

The energy difference between 2*s* and 2*p* levels decreases markedly in the series Ne > F > O > N > C > B, from more than 25 eV for Ne to ca. 3 eV for B (see Figure 2.21). The smaller this difference, the more likely is the interaction of the 2*s* and 2*p* levels leading to mixing and resulting in a different sequence of the MOs in the energy level diagram. For the diatomic molecules N_2, C_2 and B_2, the left part of Figure 2.23 should no longer be used. The correct diagram for these molecules is shown on the right-hand side of this figure in which the mixing of MOs of equal symmetry and similar energy ($2\sigma_g$ and $3\sigma_g$) is introduced by the linear combinations $2\sigma_g+\lambda 3\sigma_g$ and $3\sigma_g-\lambda' 2\sigma_g$ (λ and λ' are mixing coefficients and both are smaller than 1). Consequently, the level $3\sigma_g-\lambda' 2\sigma_g$ is now higher in energy than the $1\pi_u$ level and the HOMO of N_2 is of σ rather than of π symmetry; this HOMO is no longer a pure *p* orbital but an *s*-*p* hybrid MO.

The diagram in the center of Figure 2.23 can now be used to explain the electronic and bond properties of the diatomic molecules N_2, C_2, B_2 and Li_2. Dinitrogen **N_2** has 10 VEs, which occupy the levels $2\sigma_g+\lambda 3\sigma_g$, $2\sigma_u$, $1\pi_u$ and $3\sigma_g-\lambda' 2\sigma_g$. Since the number of bonding electrons exceeds the number of antibonding electrons considerably, a very strong and short bond is established (see Table 2.10). The HOMO of N_2 is slightly bonding and therefore the ionization energy of the molecule (15.6 eV) is higher than that of the isolated nitrogen atoms (14.5 eV). In the lithium diazenides $Li[N_2]$ and $Li_2[N_2]$, which are stable in the pressure range 11–70 GPa, the NN bond lengths are 119.7 and 132.0 pm, respectively, in agreement with the partial occupation of the $1\pi^\star$ level of the N_2 unit by one or two electrons in the anions $[N_2]^-$ and $[N_2]^{2-}$, respectively.

The molecule **C_2** has been observed in hydrocarbon flames and in the vapor above hot graphite. Its electronic properties can only be understood with the diagram at the center of Figure 2.23. The eight VEs occupy the levels $2\sigma_g+\lambda 3\sigma_g$, $2\sigma_u$, $3\sigma_g-\lambda' 2\sigma_g$ and $1\pi_u$, and the molecule exists in a singlet ground state with a strong bond. The ionization energy of C_2 is 11.4 eV compared to 11.26 eV for the isolated carbon atom. The B_2 molecule, on the other hand, has a triplet ground state since the six VEs do not allow for a closed shell configuration. Instead, the $1\pi_u$ level holds two unpaired electrons of equal spin (Table 2.10).

Beryllium atoms have the VE configuration $2s^2$ and the interaction of two of these atomic orbitals in a **Be_2** molecule yields a strongly bonding $2\sigma_g+\lambda 3\sigma_g$ MO and a less strongly antibonding $2\sigma_u$ MO, occupied by two of the four VEs each. Since the effects of the attractive and repulsive interactions almost cancel each other, the covalent bond of Be_2 is extremely weak with a dissociation enthalpy of just 11 kJ mol^{-1}. It is the interaction of the two σ_g levels that makes the $2\sigma_g+\lambda 3\sigma_g$ MO so strongly bonding to allow for this molecule to exist at all; the diagram on the left-hand side of Figure 2.23 could not explain its existence.

The vapor above liquid lithium metal contains **Li_2** molecules together with isolated atoms. Analogous observations have been made for the other alkali metals. Compared to Be_2 the covalent bond of Li_2 is quite strong, but compared to the bond of H_2 it is extremely weak. Since the effective nuclear charge to which the VEs of lithium atoms are exposed is rather low, the 2*s* AO is voluminous and diffuse and the resulting overlap integral for the linear combination 2*s* + 2*s* of Li_2 is small. Therefore, the dissociation enthalpy of Li_2 is only 103 kJ mol^{-1}; the internuclear distance is 267 pm, more than three times that of H_2 (74 pm).

2.4.4 Photoelectron Spectroscopy of Small Molecules

The construction of energy level diagrams for small molecules as in Figure 2.23 requires the knowledge of the orbital energies. By photoelectron spectroscopy (PES) these energies can be measured or estimated.[48] The underlying approximation is to identify the orbital energy with the ionization energy of an electron from the corresponding level. This postulate is known as KOOPMANS' theorem (Section 2.1.2). On ionization of a molecule, however, all occupied orbitals are stabilized since the effective nuclear charge increases and the electron–electron repulsion decreases. Therefore, a *relaxation of the cation* takes place, which is neglected by KOOPMANS' theorem.

To ionize a small gaseous molecule, it is irradiated with monochromatic ultraviolet radiation to remove an electron from any valence MO (UV-PES or UPS). If the photon energy is sufficiently high even electrons from the atomic core can be split off, for example, by X-rays (XPS). The photon energy $h \cdot \nu$ is partly consumed by the ionization energy E_i of the molecule M and the excess of energy is exclusively converted to kinetic energy of the removed electron:

$$h \cdot \nu = E_i(\mathrm{M}) + E_{kin}(e)$$

Since the photon energy $h \cdot \nu$ is known, the determination of the kinetic energy of the photoelectrons directly gives E_i(M).[49] UPS spectrometers are usually equipped with a helium discharge lamp that emits a monochromatic line of energy 21.22 eV (α-line of He-I). In the discharge helium atoms are excited to the electron configuration $1s^1 2p^1$. When they spontaneously return to the ground state, the energy difference is emitted as α-line. The energy of 21.22 eV is sufficient to ionize both *s* and *p* electrons from the valence shells of small molecules.

48 J. H. D. Eland, *Photoelectron Spectroscopy: An Introduction to Ultraviolet Photoelectron Spectroscopy in the Gas Phase*, Butterworths, London, **2013**. S. Hüfner, *Photoelectron Spectroscopy*, 3rd ed., Springer, Berlin, **2003**.

49 ALBERT EINSTEIN (1879–1955) was awarded the NOBEL prize in physics of the year 1921 for the first correct interpretation of the *photoelectric effect* as a quantized phenomenon in 1905.

In principle, a PES spectrometer functions similar to a mass spectrometer. A gaseous sample is ionized by UV irradiation in an ion source at low pressure. While the cations are absorbed by the walls of the chamber, the electrons pass through a small hole in the wall of the chamber after which they enter an electric capacitor field. The kinetic energy and therefore the speed of the electrons differs depending on which MO they originated from. Faster electrons spend less time in the electric field and are less deflected than slower electrons. By variation of the field strength, electrons of all speeds are made to arrive one after another at the detector (multiplier) that measures the intensity I (number of electrons per second), which is plotted as a function of the ionization energy $E_i(M)$.

Each occupied MO results in a signal in the PE spectrum, provided the photon energy is sufficient for ionization. This signal may be a single line or a group of *equally spaced lines*. As an example, the PES spectrum of N_2 gas, ionized with He-I radiation, is shown in Figure 2.25. The signals in the range from 15.6 to 19.1 eV correspond to the ionization of N_2 by removal of an electron from one of the three highest occupied MOs.

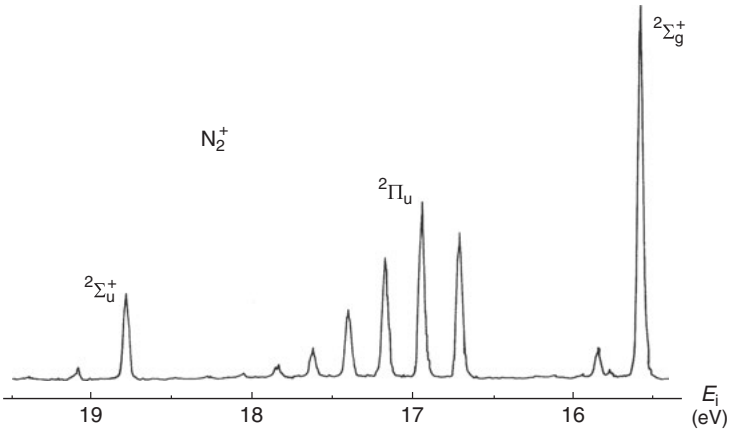

Figure 2.25: Photoelectron spectrum of gaseous N_2 in the range of the valence electrons. The three groups of lines correspond to the ionization from either one of the three highest occupied molecular orbitals.

The intense line at the lowest ionization energy of 15.6 eV originates from the removal of an electron from the HOMO of the molecule in its vibrational ground state, and the $[N_2]^+$ cation formed is also in its electronic and vibrational ground state. The term symbol of this cation is $^2\sum_g^+$, representing a doublet state with one unpaired electron in a σ_g MO (see Figure 2.23). Since the photon energy is much higher than the ionization energy and the bond strength of the cation is lower than that of the neutral molecule after removal of a bonding electron, the ionization may be

accompanied by a *vibrational excitation of the cation*. Therefore, the line at 15.6 eV has a weak *satellite line at a slightly higher energy* due to the additional *vibrational energy h·ν of the cation*. This is a very important information since it provides the vibrational wavenumber of the $[N_2]^+$ cation in its $^2\sum_g^+$ ground state as 2190 cm^{-1}. Comparison of this wavenumber with that of the neutral N_2 molecule, determined by RAMAN spectroscopy as 2345 cm^{-1}, shows that the removed *electron has come from a bonding MO* since the wavenumber is directly related to the bond strength (see Section 4.4.1).

The equidistant lines in the range 16.7–18.2 eV of Figure 2.25 correspond to the removal of an electron from the $1\pi_u$ MO of N_2, which leads to a cation with term symbol $^2\Pi_u$. This cation is produced not only in its vibrational ground state but also in at least six vibrationally excited states. The model of the harmonic two-atomic oscillator discussed in Section 4.4.1 explains the equal spacing of these lines by the equal spacing of the vibrational energy levels in the potential diagram (Figure 4.1). The large number of the vibrational satellites is typical for the removal of an electron from a strongly bonding orbital, and in fact the vibrational wavenumber of $[N_2]^+$ ($^2\Pi_u$) has been determined as only 1850 cm^{-1}. Thus, the NN bond in this cation is much weaker than that of the neutral dinitrogen molecule.

The lines at 18.8 and 19.1 eV in the PE spectrum of N_2 (Figure 2.25) indicate ionization by removal of an electron from the antibonding $2\sigma_u$ MO yielding a cation with the term symbol $^2\sum_u^+$ for its electron configuration. The energy difference of these two lines yields a vibrational wavenumber of 2397 cm^{-1} for this cation, which is *larger* than for the N_2 molecule (2345 cm^{-1}). Thus, the covalent bond in $[N_2]^+$ ($^2\sum_u^+$) is *stronger* than the triple bond of N_2!

In summary, we state that PE spectra of small molecules yield information on (1) the number of occupied energy levels in the molecule, (2) the approximate orbital energies, (3) the bonding, nonbonding and antibonding character of the MOs and (4) the bond strength and vibrational wavenumbers of the cations produced.

2.4.5 Heteronuclear Diatomic Molecules

To analyze the bonding situation in heteronuclear molecules by MO theory, we need to know the energies and symmetries of all valence orbitals to find out which AOs are suitable for a linear combination (LCAO) and whether the overlap integrals and hence the energetic splitting between bonding and antibonding MOs will be large or small. The orbital energies of the AOs can be estimated from the negative ionization energies determined by PES.

The molecules HF and CO may be used to illustrate the situation. The construction of the energy level diagram for **HF** requires the ionization energies $E_i(H)$ = 13.6 eV and $E_i(F)$ = 17.4 eV. For linear molecules, the molecular axis is defined as z axis and the atomic orbitals are classified as either σ or π AOs. The MO diagram of HF is shown in

Figure 2.26. The two σ orbitals 1*s*(H) and 2p_z(F) have comparable orbital energies and their combination yields a bonding and an antibonding MO. All other orbitals of the fluorine atom remain nonbonding since hydrogen has no π AOs and since the orbital energy of 2*s*(F) is much too low (–46.4 eV) for any substantial interaction with the 1*s* AO of hydrogen (–13.6 eV). In other words, there are three nonbonding electron pairs at fluorine albeit on two different energy levels. They correspond to the three nonbonding pairs in the LEWIS formula of HF.

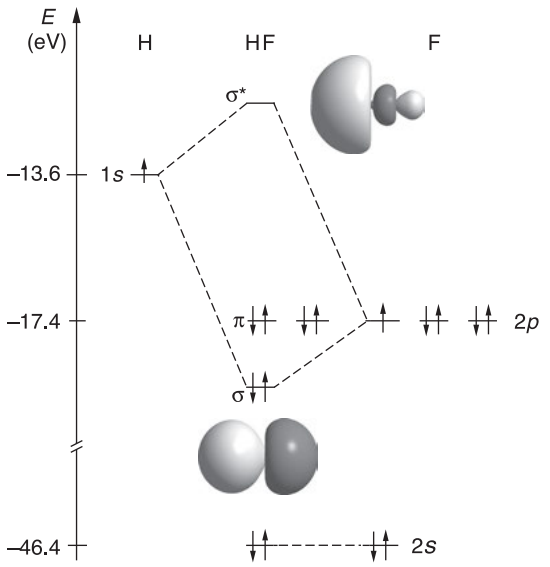

Figure 2.26: MO diagram for the molecule HF. The two π orbitals of the fluorine atom are nonbonding and form the HOMO of the molecule. The calculated isodensity surfaces of the σ and σ* MOs are shown using a residual electron density of 0.05 *e* Å^{-3}.

The bonding σ MO of HF has a high fluorine contribution since its energy is close to the 2*p* level of fluorine. In the linear combination 2p_z(F) + λ1*s*(H), the mixing coefficient λ is smaller than 1 and therefore the bonding electron pair is concentrated near the fluorine atom, which in this way acquires a partial charge of –0.55 *e*. The polar character of the bond resulting from the difference in electronegativities of H and F is evident from this analysis. On the other hand, the σ* MO obtained by the linear combination 1*s*(H)–λ′2p_z(F) has a high hydrogen contribution (λ′ < 1) since its orbital energy is close to that of 1*s*(H).[50] The photoelectron spectrum of HF is in line

50 For a detailed discussion of the bonding in HF, see: F. Weinhold, C. R. Landis, *Discovering Chemistry with Natural Bond Orbitals*, Wiley, Hoboken, **2012**. The 2*s* AO of fluorine is no longer spherical but slightly deformed due to repulsion by the bonding pair.

with this analysis showing that the eight VEs occupy three distinct energy levels. The ionization energy of HF is 16.0 eV, slightly smaller than that of F atoms (17.4 eV), which arises from the negative partial charge of the F atom in HF. In Figure 2.26 the HOMO of HF should therefore be drawn slightly higher in energy than at –17.4 eV (although the ionization energy is only an approximate measure of the orbital energy due to relaxation of all electrons in the cation $[HF]^+$).

The large bond enthalpy of HF (565 kJ mol^{-1}) can be understood by the considerable energy gain on transferring the hydrogen electron from the 1*s* level to the much lower σ MO; in addition, the unpaired fluorine electron is also slightly stabilized. There is also a considerable ionic contribution from the COULOMB attraction between the partial charges. Consequently, HF has one of the strongest known single bonds (see Table 4.1).

The molecules **CO** and N_2 are *isosteric* since they agree in (a) number of atoms, (b) number of electrons, (c) configuration of electrons and (d) sum of nuclear charges. Therefore, the MO energy level diagram of N_2 in Figure 2.23 can be used as an approximation for CO, which can be considered as a distorted N_2 molecule. The differing electronegativities of carbon and oxygen (Table 4.8) are related to the fact that their ionization energies E_i are different (Figure 2.1). According to ALLEN the electronegativity χ of an atom follows from the ionization energies of all its VEs (Section 4.6.2). Therefore, the ionization energies of carbon (11.3 eV) and oxygen (13.6 eV) can be estimated from their electronegativities (which are easier to remember). All AOs of oxygen are energetically lower than the corresponding carbon orbitals, and the MO diagram of CO is somewhat asymmetric compared to that of N_2. The HOMO of CO is slightly antibonding and mainly located at the carbon atom, which is important for the reactivity of CO as a ligand in metal complexes. As expected, the carbon atom of CO bears a positive partial charge.[51]

In a similar manner, the properties of other molecules and ions isoelectronic with N_2 can be explained using the diagram in Figure 2.23, for example, $[CN]^-$ and $[NO]^+$. *Isoelectronic species* agree only in the above criteria (a)–(c).[52]

2.4.5.1 General Rules for the construction of MOs

The MO level diagrams discussed in this book are based on several simplifications and approximations, and hence are only useful in qualitative and comparative discussions. Their construction is based on the following rules:

51 G. Frenking et al, *J. Comput. Chem.* **2007**, *28*, 117.

52 Sometimes even molecules and ions are called isoelectronic if they agree only in the number and configuration of the *valence electrons*, e.g. HF versus HCl and $[SO_4]^{2-}$ versus $[BrO_4]^-$. More correctly, they should be referred to as iso-valence electronic.

(a) The linear combination of n AOs gives n MOs.
(b) Only AOs of same symmetries can be combined (σ with σ; π with π).
(c) The orbital energies of the combined AOs should not be too different ($\Delta E < 15$eV).
(d) The combined AOs must overlap to give MOs.
(e) The resulting MOs must be orthogonal to each other (zero overlap integral).
(f) Nondegenerate MOs must be either symmetric or antisymmetric (and not asymmetric) to the symmetry elements of the molecular point group.
(g) Antibonding MOs are more destabilized than the corresponding bonding MOs are stabilized compared to the AOs from which they originate.

In Section 2.4.8 we will learn that degenerate point groups with an odd-numbered highest rotational axis require another rule.

2.4.6 Three-Atomic Molecules of $D_{\infty h}$ Symmetry

Linear molecules with center of inversion belong to point group $D_{\infty h}$. Well-known examples are XeF_2, $[HF_2]^-$ and $[I_3]^-$, which have only σ bonds. Multiple bonds are present in CO_2, CS_2, $[NO_2]^+$ and $[N_3]^-$. From a theoretical point of view, the bonding situation in $[HF_2]^-$ is the simplest case and will therefore be discussed first, followed by the MO analysis of CO_2. The dihalides of the noble gases are also linear and are explained in Section 14.6.2.

Salts with the anion $[HF_2]^-$ are of enormous industrial importance since $K[HF_2]$ dissolved in anhydrous HF (aHF) is used as electrolyte in the production of elemental fluorine by electrolysis (Sections 5.6.4 and 13.4). Hydrogen difluorides $M[HF_2]$ are prepared from metal fluorides MF by dissolution in aHF or by reaction with gaseous HF. This exothermic reaction is reversible, and the equilibrium can be shifted to the left by heating:

$$KF + HF \rightleftharpoons K[HF_2]$$

As the three atoms FHF define the z axis of the ion, the orbitals 1s(H) and 2p_z(F) are of σ symmetry. And since there are no p orbitals at hydrogen, other fluorine AOs can be neglected. The bonding situation resembles the one of HF (see Figure 2.26). Consequently, only three AOs need to be combined to construct the MOs by LCAO; their overlap is shown in Figure 2.27.

The equations for the three linear combinations to construct the MOs of $[HF_2]^-$ are (N_i: normalizing factors):

$$\psi_1(\sigma_g) = N_1[\phi^{F1}_{2p} + \lambda\phi^{H}_{1s} + \phi^{F2}_{2p}]$$
$$\psi_2(\sigma_u) = N_2[\phi^{F1}_{2p} - \phi^{F2}_{2p}]$$
$$\psi_3(\sigma^*_g) = N_3[\phi^{F1}_{2p} - \lambda'\phi^{H}_{1s} + \phi^{F2}_{2p}]$$

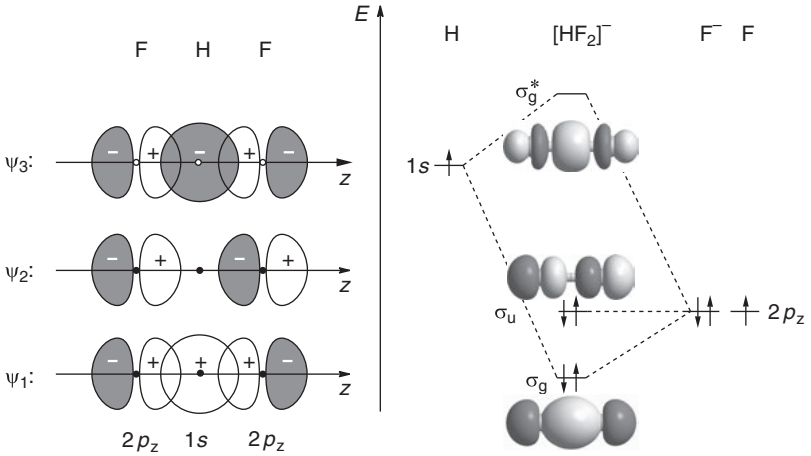

Figure 2.27: The overlap of orbitals to form the three-center four-electron bond of the linear anion $[HF_2]^-$. Left: Linear combinations of the three σ AOs (different shading indicates differing signs of the wave functions). Right: Energy level diagram of the MOs. The isodensity surfaces have been calculated with a residual electron density of 0.05 e Å^{-3} to show the approximate shape of the MOs.

The wave function $\psi_1(\sigma_g)$ represents a bonding MO since the overlap integral is positive in all regions between the nuclei (no nodal plane between nuclei).[53] The function $\psi_2(\sigma_u)$ has one node between the nuclei bisecting the molecule at the hydrogen atom, which does not take part in this particular linear combination. Since the overlap between the two $2p_z$ AOs is very weak, this MO is nonbonding or very weakly antibonding. The *gerade* function $\psi_3(\sigma^\star)$ with two nodes between the fluorine nuclei is antibonding and represents the LUMO of the ion. All three linear combinations are orthogonal to each other.

The σ system of $[HF_2]^-$ comprises four VEs, which occupy the levels σ_g and σ_u forming a three-center four-electron bond, which is established by just one bonding pair of electrons. This bonding pair is symmetrically delocalized over the three atoms meaning that one electron each will preferentially reside in the left and the right bonding region, respectively. Note that hydrogen can bind several partner atoms using just *one* orbital.[54] The resulting three-center bond is much weaker and longer than the bond of HF as the following comparison demonstrates (d_{HF}: internuclear distance H–F; f_r: valence force constant):

	HF	**$[HF_2]^-$**
d_{HF}(pm)	93	113
f_r (N cm^{-1})	97	23

53 Remember the model of *electron in a linear box*: the state of lowest energy does not have a node, while higher states have 1, 2, . . . nodes *between the walls* of the box.

54 The maximum coordination number of hydrogen atoms in hydrides is 6 (see Chapter 5).

The linear geometry of the hydrogen difluoride anion follows mainly from the repulsion of the many nonbonding electrons in the fluorine orbitals 2*s*, $2p_x$ and $2p_y$ as well as from the repulsion of the negatively charged F atoms. Sometimes the bonding in $[HF_2]^-$ is considered a special case of hydrogen bonding since H forms a bridge between two electron-rich partner atoms. Hydrogen bonding in general is discussed in Section 5.6.

2.4.6.1 The Molecule BeH_2

Beryllium dihydride is a polymeric substance and cannot be vaporized without decomposition. Nevertheless, the hypothetical linear molecule BeH_2 can serve as a model for a three-atomic species with a central atom having *s and p orbitals* in the valence shell but still can only form σ bonds to hydrogen atoms. The MO treatment of BeH_2 will later be needed for understanding the bonding in CO_2, which is discussed in the next section. The electron configuration of Be is $2s^2$ but as we have seen in Figure 2.21 the orbital energies of 2*s* and 2*p* of beryllium differ only very slightly. Therefore, the empty $2p_z$ AO of Be takes part in the bonding of BeH_2.

Gaseous BeF_2 is of $D_{\infty h}$ symmetry and the same is predicted for BeH_2 by quantum-chemical calculations. The ionization energy of Be atoms is 9.2 eV, not too far from that of hydrogen (13.6 eV). Therefore, the 1*s* AOs of the hydrogen atoms can be combined with the 2*s* and $2p_z$ AOs of Be to construct four linear combinations of atomic σ orbitals resulting in four MOs, two of which are bonding and two are antibonding. These combinations are shown on the left-hand side of Figure 2.28, and it can easily be demonstrated that they are all orthogonal (if the mixing coefficients λ are chosen correctly). The corresponding energy level diagram of BeH_2 on the right-hand side of this figure indicates that the four VEs occupy the two bonding MOs while all nonbonding and antibonding MOs remain empty.

This analysis shows that the covalent bonds of BeH_2 can be constructed without unpaired electrons at the Be atom and without any hybridization of atomic orbitals as in VB theory. All four σ MOs are of either pure *s* or *p* character as far as the central atom is concerned; their differing symmetries prevent any further interaction. The linear geometry of BeH_2 simply follows from maximizing the overlap for the two bonding MOs under this geometry, especially for the σ_u MO. Any additional VEs would have to occupy the nonbonding π level. Thus, BeH_2 is *a stable molecule but not a stable compound* since its (hypothetical) polymerization to $(BeH_2)_x$ with four-coordinate Be atoms would be exothermic ($\Delta H < 0$) and exergonic ($\Delta G < 0$).[55]

55 It is important to differentiate between the *stability of a single molecule* and the *stability of a compound*, i.e. a collection of identical molecules which may react with each other. For example, single (isolated) hydrogen atoms are perfectly stable, but in a cohort, H atoms react with each other exothermically to H_2.

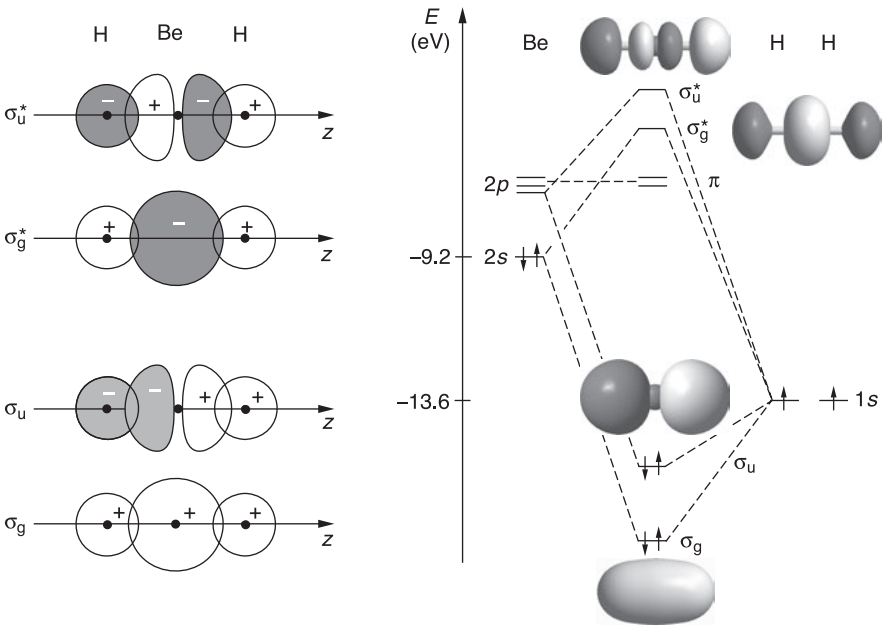

Figure 2.28: Energy level diagram of the linear molecule BeH_2. The four valence electrons occupy the two three-center MOs σ_g and σ_u. The isodensity surfaces of the four molecular orbitals have been calculated with a residual electron density of 0.05 e Å^{-3}. Differing shadings indicate different signs of the wave function.

2.4.6.2 The Molecule CO_2

The σ bonding system of carbon dioxide resembles that of BeH_2, which may be used as a model. As in BeH_2, the central atom contributes the σ AOs 2*s* and $2p_z$ and the oxygen atoms only the $2p_z$ AOs. The 2*s* AOs of the oxygen atoms are too low in energy and do not interact with the carbon orbitals (see Figure 2.21). Therefore, the linear combinations of the four AOs yield two bonding and two antibonding σ MOs. The energy level diagram of CO_2 is shown in Figure 2.29a; it also contains the π orbitals in addition to the σ system.

As in the molecules O_2 and N_2 (Section 2.4.3) the two orthogonal π bond systems of CO_2 are oriented in two perpendicular planes (*xz* and *yz* planes). For reasons of symmetry, these MOs are doubly degenerate. The overlap of the three $2p_x$ AOs is schematically shown in Figure 2.29b. The $1\pi_u$ MO is bonding since it has no nodal plane *between the oxygen atoms*; it is antisymmetric to the center of inversion of the molecule. The $1\pi_g$ MO with one node between the oxygen atoms is slightly antibonding but the overlap integral is very small, and the character is almost nonbonding. The $2\pi_u$ MO is strongly antibonding with two nodal planes between the oxygen atoms.

In *linear molecules* the combination of three atomic orbitals always gives one bonding, one nonbonding and one antibonding MO, regardless whether the AOs

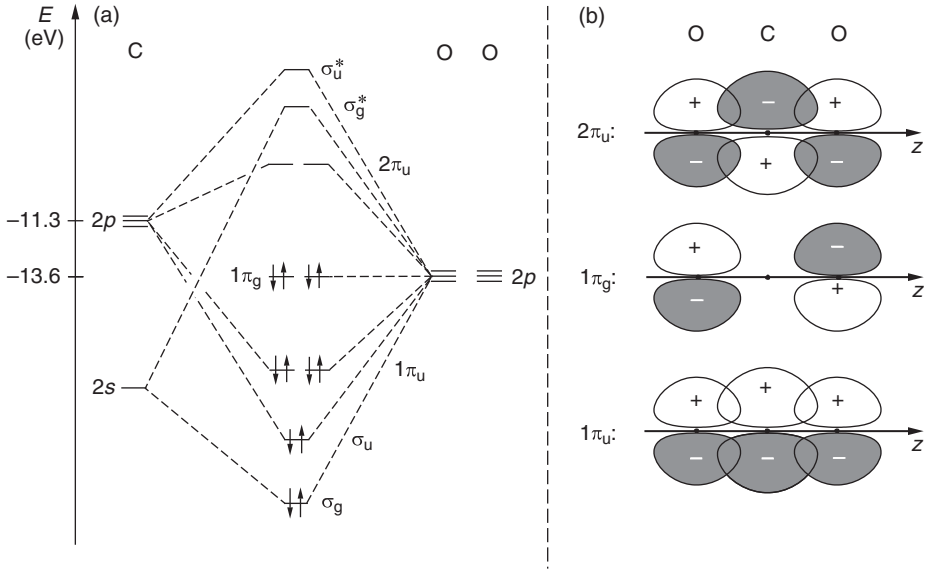

Figure 2.29: (a) MO diagram for the σ and π MOs of CO_2 ($D_{\infty h}$ symmetry). All energetically favorable molecular orbitals are occupied by electron pairs giving very strong bonds. The four bonding pairs are delocalized over the three atoms (three-center bonds). (b) Schematic representation of the overlap of the three π orbitals in the *yz* plane; a second and orthogonal set of π MOs can be constructed in the *xz* plane. Only the degenerate levels $1\pi_g$ und $1\pi_u$ are occupied by electron pairs (the $1\pi_g$ MO is weakly antibonding). The 2*s* electrons of the oxygen atoms form two additional nonbonding pairs at low energy.

are of σ or π symmetry. The rotational symmetry of the molecules requires that the orbitals $1\pi_u$, $1\pi_g$ and $2\pi_u$ are doubly degenerate. Since the three atoms of CO_2 contribute four VEs each (we neglect the 2*s* level of oxygen for reasons of energy), all bonding and nonbonding MOs are occupied by electron pairs and the four antibonding MOs remain empty. The polarity of the CO bonds results from the larger mixing coefficient λ of the oxygen orbitals to the bonding MOs to which they are relatively close in energy. While the four bonding pairs are delocalized, the nonbonding electrons at the HOMO level $1\pi_g$ are localized at the oxygen atoms.

In a similar manner, the bonds in the isoelectronic species azide anion $[N_3]^-$, nitronium cation $[NO_2]^+$ and carbon disulfide CS_2 can be explained.

2.4.7 Three-Atomic Molecules of C_{2v} Symmetry

The point group C_{2v} is a nondegenerate group to which many three-atomic molecules and ions belong, for example, H_2O, H_2S, OF_2, SCl_2, CF_2, SiF_2 and $[ClF_2]^+$ all of which contain only σ bonds. Bent species with σ and π bonds are NO_2, $[NO_2]^-$, O_3,

SO_2 and ClO_2, for example. Neither contains degenerate MOs. As a representative example for an AB_2 molecule without π bond the water molecule will be discussed in detail; for a typical bent molecule with σ and π bonds, see O_3 in Section 11.1.3.

The principal symmetry element of the H_2O molecule (bond angle 104.5°) is the C_2 rotational axis that is defined as the z axis. If the y axis is perpendicular to the molecular plane, the $2p_y$ AO of the oxygen atom has π symmetry and remains nonbonding since hydrogen atoms have no accessible π orbitals in the valence shell. Consequently, the oxygen orbitals $2s$, $2p_x$ and $2p_z$ can in principle be combined with the $1s$ AOs of the two hydrogen atoms. As a first approximation, the $2s$ AO may be considered as nonbonding due to its low energy (the difference of orbital energies between $2s$(O) and $1s$(H) is 18 eV). The linear combinations of the remaining AOs are shown in Figure 2.30.

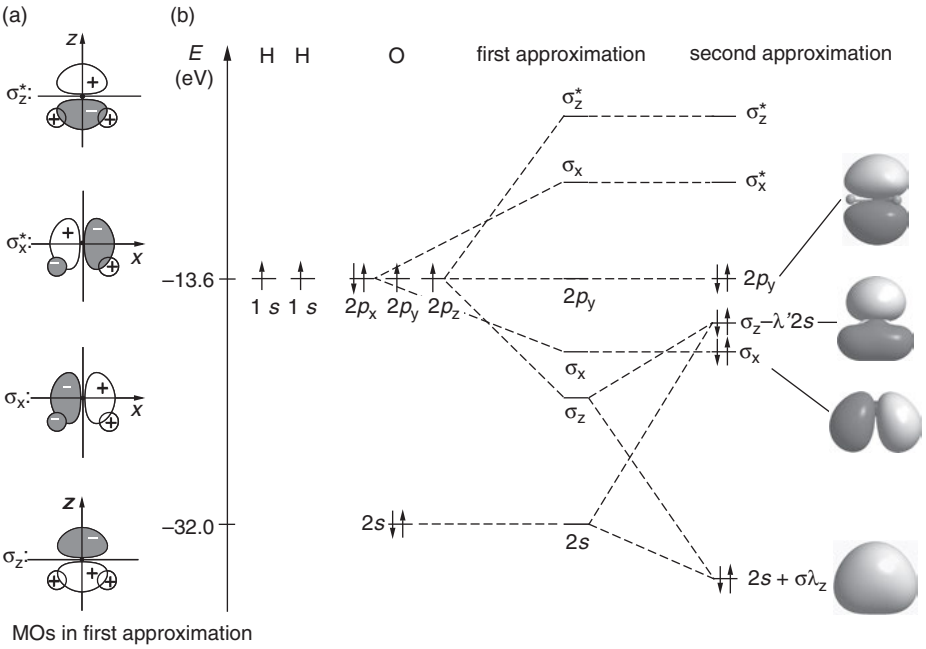

Figure 2.30: (a) Linear combinations of AOs of the water molecule to construct the four σ MOs in a first approximation by neglecting the $2s$(O) orbital. (b) Energy level diagram of the MOs. The highest occupied AOs of hydrogen and oxygen incidentally have the same orbital energies. The diagram on the right-hand side (second approximation) takes the interaction of the orbitals $2s$(O) and σ_z into account yielding two novel MOs of types $2s(O)+\lambda\sigma_z$ and $\sigma_z-\lambda' 2s(O)$. This diagram should be used only for H_2O. Of the eight valence electrons six occupy bonding MOs and one the nonbonding MO $2p_y$, which is the HOMO of the molecule. These nonbonding electrons are localized at the oxygen atom while all others are delocalized in three-center bonds. The isodensity surfaces of the MOs on the far right have been calculated with a residual electron density of 0.05 e Å^{-3}.

The MOs σ_z and σ_x are bonding but of different energy; quantum chemical calculations show that σ_z is lower than σ_x. The σ_z MO and the 2*s* AO of oxygen are both *totally symmetric* (i.e., to all symmetry elements of the point group) and close in energy. Therefore, these two energy levels interact and produce two new levels by the linear combinations $2s(O)+\lambda\sigma_z$ and $\sigma_z-\lambda' 2s(O)$. The latter MO is now higher in energy than the σ_x MO. The eight VEs of H_2O occupy four MOs of different energy. This analysis is supported by the photoelectron spectrum of water vapor, which shows four groups of lines in the region <20 eV.[56] The ionization energy of H_2O is 12.6 eV; the difference to the ionization energy of oxygen atoms (13.6 eV) can be explained by the negative partial charge of the oxygen atom in H_2O and by the stabilization of all levels in the cation $[H_2O]^+$ due to the reduced electron repulsion and the increased effective nuclear charge (relaxation).

The LEWIS formula of H_2O is written with *two* lone pairs. However, our MO analysis shows that only *one* truly nonbonding pair is present in the water molecule (in the HOMO $2p_y$), while the electrons in HOMO–1 are by 1.5 eV lower in energy. The electron density in the latter orbital ($\sigma_z-\lambda' 2s$) is somewhat elongated in the *z* direction. But the total electron density distribution in the molecular *xz* plane shown in Figure 2.31 is almost circular and the same holds for the *yz* plane.

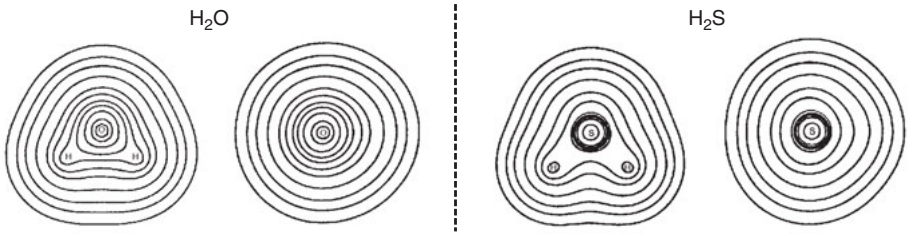

Figure 2.31: Calculated total electron density of H_2O and H_2S both in the molecular *xz* plane (left diagrams) and in the *yz* plane (right diagrams; H atoms are on the right).

Why is the water molecule bent and not linear like BeH_2? The energy level diagram of BeH_2 in Figure 2.28 shows that in linear H_2O with eight VEs two lone pairs would occupy the degenerate π level and only two pairs would be bonding. According to quantum-chemical calculations, linear H_2O is by 133 kJ mol^{-1} less stable than the bent ground state. It is the number of VEs that determines the geometry. The bonds in H_2S can be treated in an analogous manner taking the lower ionization energy of the sulfur atom (10.36 eV) into account; the ionization energy of H_2S is 10.5 eV.

The MO diagram in Figure 2.30 can also be used to explain the violent reaction of water with elemental sodium. Sodium metal has an ionization energy of only

56 H. Bock, *Angew. Chem. Int. Ed.* **1977**, *16*, 613–637.

5 eV (FERMI energy), while the LUMO of the water molecule (σ_x*) has a much lower orbital energy. Therefore, transfer of an electron from Na to H_2O is an exothermic process resulting in Na^+ and $[OH]^-$ together with H_2.[57]

2.4.8 Four-Atomic Molecules of D_{3h} Symmetry

A trigonal-planar star is of D_{3h} symmetry, with the threefold rotational axis as the principal symmetry element, which is defined as the *z* axis. Molecular examples are BF_3, BCl_3, SO_3, $[CO_3]^{2-}$ and $[NO_3]^-$, all containing both σ and π bonds. We will use BF_3 to demonstrate how the MOs of such species can be derived using the LCAO method. The orientation of the BF_3 molecule is defined so that one B–F bond points in the direction of the *x* axis.

The point group D_{3h} is a *degenerate group* and therefore degenerate σ and π MOs are to be expected. As a *general rule*, however, degenerate MOs in point groups with an odd-numbered principal rotational axis cannot be all symmetric or antisymmetric to the C_3 axis (and some other symmetry elements), but some are asymmetric.

As shown in Figure 2.32, the σ bonds of BF_3 are constructed from the boron orbitals 2*s*, $2p_x$ and $2p_y$ and those $2p_\sigma$ AOs of the three fluorine atoms oriented toward the boron atom (their orbital energies differ by less than 15 eV). The 2*s* AOs of fluorine are neglected because of their low orbital energy.

Combination of 2*s*(B) with three $2p_\sigma$(F) yields the totally symmetric MOs σ_s and σ_s*. The molecular symmetry requires that the overlap integral with all fluorine orbitals be identical (four-center bond). The $2p_x$ AO of boron is combined with the three fluorine σ orbitals to give two MOs, which are asymmetric to the C_3 rotational axis of the molecule since the overlap along the *x* axis is stronger than with the other two fluorine orbitals (shown on the right-hand side of Figure 2.32). This asymmetry is balanced by the other linear combinations with the same fluorine orbitals: the overlap of the orbital $2p_y$(B) with the same three fluorine σ orbitals is also asymmetric to C_3 but now the fluorine orbital on the *x* axis is orthogonal and therefore does not take part in the linear combination (lower left-hand side of Figure 2.32). These two sets of bonding and antibonding MOs (σ_x/σ_y and σ_x*/σ_y*) are pairwise degenerate and *together they reflect the D_{3h} symmetry of the molecule* (the mixing coefficients λ in the linear combination are chosen to fit the symmetry). The total electron density in both orbitals is again of D_{3h} symmetry.

The complete energy level diagram of BF_3 shown in Figure 2.32 also contains the four π MOs that originate from the overlap of the orbital $2p_z$(B) with three $2p_z$(F). The corresponding linear combinations are shown in Figure 2.33 as projections of

57 S. Bauerecker, P. Jungwirth et al., *Nature Chem.* **2015**, *7*, 250 and *Angew. Chem. Int. Ed.* **2016**, *55*, 13019.

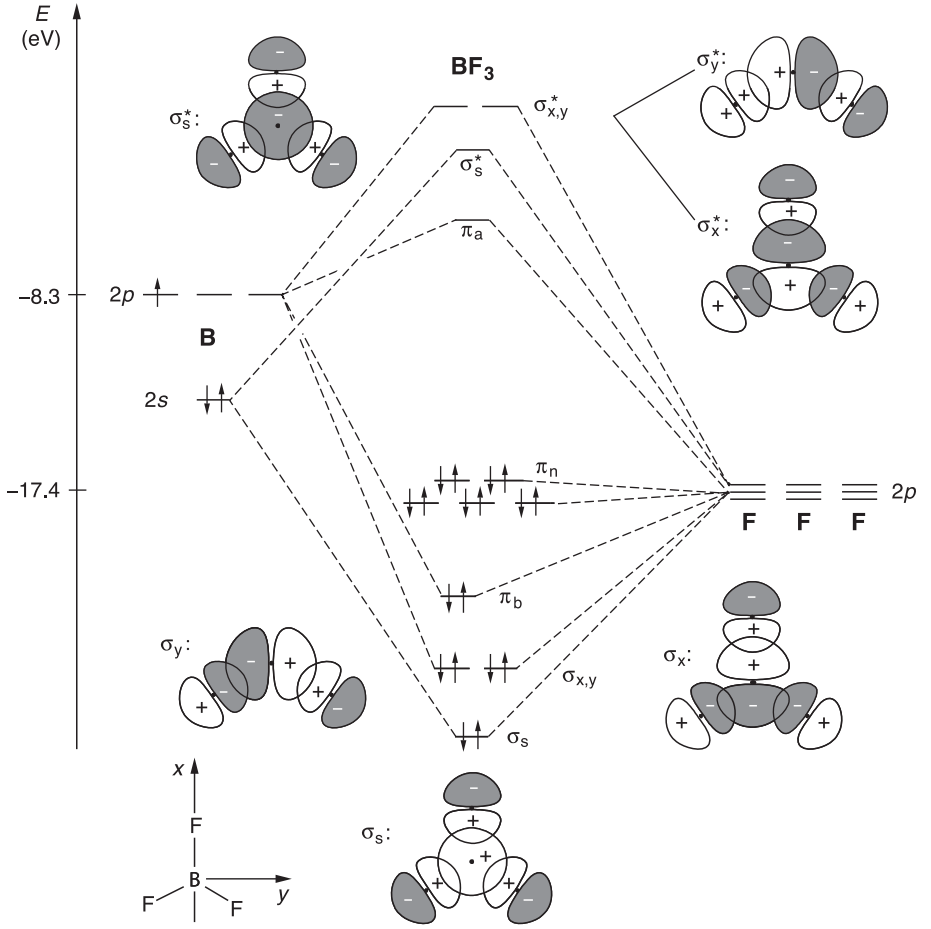

Figure 2.32: Schematic diagrams of the σ and π molecular orbitals of BF_3 (D_{3h}) as projections into the molecular *xy* plane as well as energy level diagram. The 2*s* AOs of fluorine have been omitted due to their low orbital energy. There are 18 valence electrons that occupy the four bonding MOs σ_s, σ_x, σ_y, π_b as well as the five nonbonding orbitals three of which are in the molecular plane and localized at the fluorine atoms. The latter are considered as approximately nonbonding (although they are part of the σ system). Overlap of the π orbitals perpendicular to the molecular plane is shown in Figure 2.33.

the overlapping AOs into the molecular plane. There are one bonding (π_b), two asymmetric degenerate nonbonding (π_n) and one antibonding (π_a) linear combinations. The nonbonding MOs are constructed without any boron contribution, that is, the corresponding electrons form lone pairs at the fluorine atoms. Together, the four MOs reflect the molecular symmetry, that is, all fluorine π orbitals contribute equally to the four wavefunctions. Finally, there are three fluorine AOs left with rotational axes oriented in the molecular plane but perpendicular to the B–F bonds.

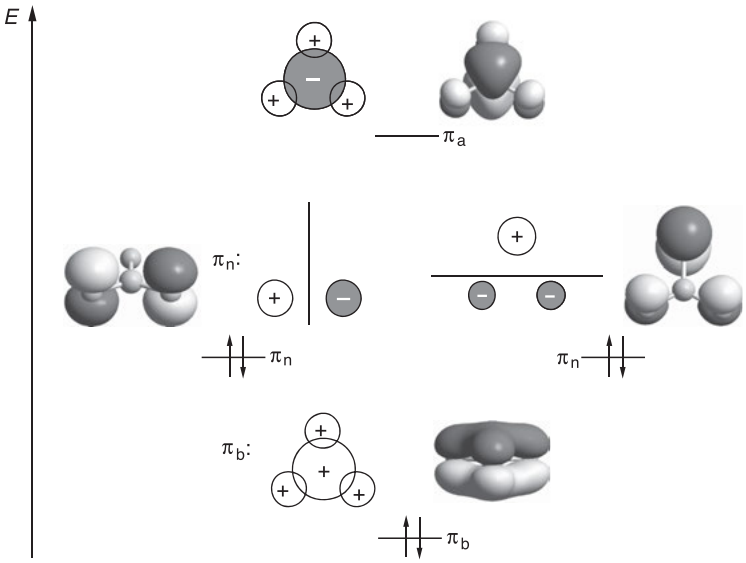

Figure 2.33: Molecular orbitals of BF_3 with π symmetry (perpendicular to the molecular *xy* plane). Linear combinations of the boron $2p_z$ AO with the $2p_z$ AOs of the three fluorine atoms yield one bonding, two degenerate nonbonding and one antibonding MO. The projections of the MOs into the molecular plane are shown schematically together with isodensity surfaces of the MOs calculated with a residual electron density of 0.05 e Å^{-3}.

These AOs are considered as approximately nonbonding orbitals, although they are part of the σ system; the corresponding electron pairs are therefore lone pairs at the F atoms. The nonbonding level forms the HOMO of the molecule; the ionization energy of BF_3 is 15.7 eV.

In summary, four of the 13 obtained MOs of BF_3 are bonding, five nonbonding and four antibonding. The 18 VEs occupy all bonding and nonbonding orbitals (Figure 2.32). The four bonding pairs are particularly of interest as they are responsible for the stability of the molecule. The three electron pairs in the σ MOs contribute most to the overall bond energy. Since the orbital energy of the fluorine 2*p* level is much lower than that of the boron orbitals, the electron density in the σ MOs is polarized toward the fluorine atoms, which results in a positive partial charge at the boron atom and corresponding negative partial charges at the fluorine atoms. In fact, BF_3 is a strong LEWIS acid reacting with LEWIS bases X with the formation of dative B←X bonds.

The π bond of BF_3 is a four-center six-electron (4c,6e) system in which the electron density is also polarized toward the fluorine atoms. The bonding pair in the π_b MO is completely delocalized over the four atoms. This analysis can be extended to the isoelectronic ions $[CO_3]^{2-}$ and $[NO_3]^-$, which are also of D_{3h} symmetry. According to HÜCKEL's MO theory, planar molecules with $4n + 2$ π electrons are

termed as *aromatic* (n = 0, 1, 2, ...), that is, species of enhanced stability. Although HÜCKEL originally applied his concept to homocyclic rings such as benzene (C_6H_6) with six and naphthalene ($C_{10}H_8$) with 10 π electrons, it has become custom to extend his concept to other planar systems and even noncyclic species such as BF_3. Since this molecule is somehow Y-shaped, its π system is considered as an example of *Y aromaticity*.

The molecules BF_3 and BCl_3 are strong LEWIS acids (Sections 2.5 and 6.2). For example, BF_3 adds fluoride anions F^- with the formation of the tetrahedral anion $[BF_4]^-$. In this reaction, an electron pair of the fluoride ion is partly delocalized into the π_a MO of BF_3 (the LUMO); this level is only slightly less stable than the 2*p* level of the isolated boron atom (Figure 2.32). Simultaneously, the geometry of BF_3 changes from D_{3h} initially to C_{3v}. In the resulting ion $[BF_4]^-$, however, all four bonds are equal, and the molecular symmetry is T_d. Molecules of this symmetry are discussed in Section 2.4.10.

Why is the molecule BF_3 trigonal-planar and not pyramidal like NF_3? Only the planar geometry allows a π bond to be formed that contributes to the overall bond energy. Furthermore, the negatively charged fluorine atoms repel each other and have the largest interatomic distance at a planar configuration. On the other hand, NF_3 has two more VEs that need to be accommodated on the surface of the central atom, and therefore the molecule is pyramidal as explained in the next section.

2.4.9 Four-Atomic Molecules of C_{3v} Symmetry

Ammonia is a typical example for molecules of C_{3v} symmetry and at the same time an interesting case since NH_3 is undergoing *pyramidal inversion* at room temperature, an aspect that will be discussed in Section 9.3. In pyramidal molecules it is no longer possible to strictly separate the bond system into MOs of either σ or π symmetry. But on a local basis π bonds are still possible as will be shown later for the oxo-anions sulfite $[SO_3]^{2-}$ and chlorate $[ClO_3]^-$.

The principal symmetry element under point group C_{3v} is the C_3 axis, which we define as the *z* axis of the molecule as per convention. The *x* axis is assumed to lie in one of the mirror planes. The four valence orbitals 2*s* and $2p_xp_yp_z$ of the nitrogen atom are combined with the three 1*s* AOs of the hydrogen atoms to give seven MOs of σ symmetry, which can be constructed in a similar manner as has been shown above for H_2O and BF_3. In a first approximation, we consider the 2*s* AO of nitrogen as nonbonding due to its low orbital energy, 12 eV lower than that of the 1*s* AO of hydrogen. The overlap of the remaining six AOs is shown on the left-hand side of Figure 2.34. From each nitrogen orbital originates one bonding and one antibonding MO. A quantum-chemical calculation shows that the asymmetric bonding MOs σ_x and σ_y as well as the antibonding MOs σ_x^* and σ_y^* are pairwise degenerate for which the symmetry symbol *e* is used in group theory.

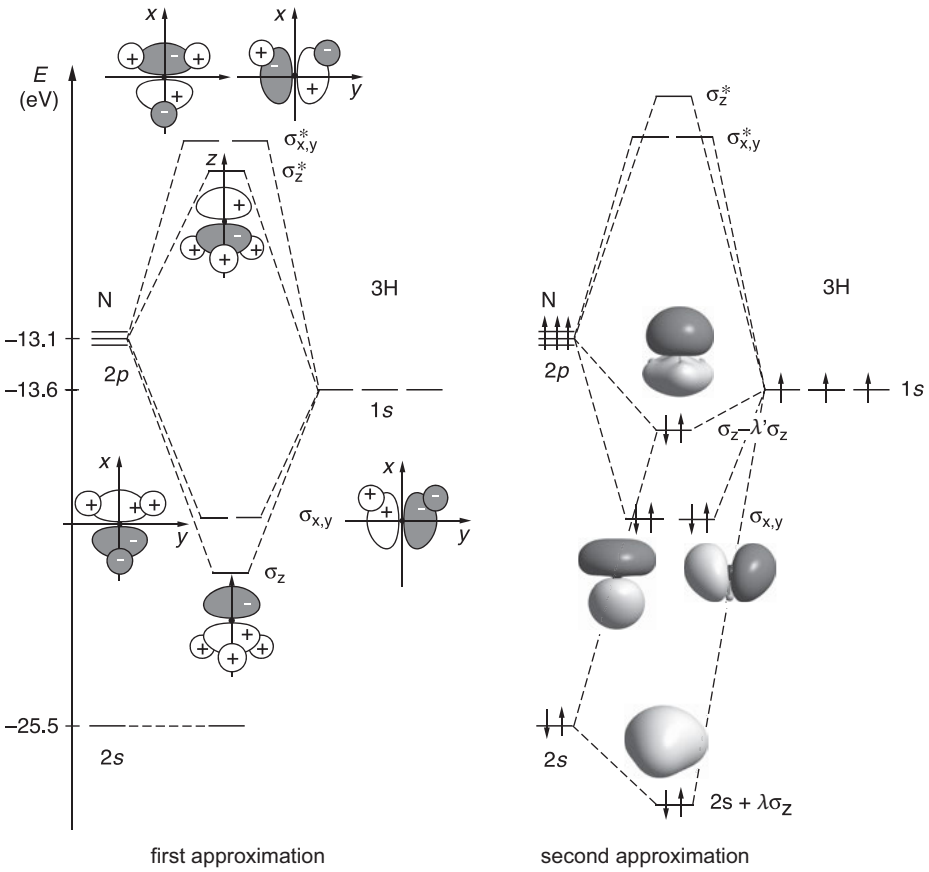

Figure 2.34: Energy level diagram for the molecule NH_3. Left: first approximation by neglecting the interaction between the orbitals 2*s*(N) and σ_z, which differ in energy by about 10 eV. Right: second approximation taking the interaction between the totally symmetric orbitals 2*s*(N) and σ_z into account. The asymmetric linear combinations σ_x/σ_y and σ_x^*/σ_y^* are pairwise degenerate. The corresponding isodensity surfaces of the electron density shown in the right diagram have been calculated with a residual density of 0.05 *e* Å^{-3}. All eight valence electrons occupy bonding MOs.

The energy levels in Figure 2.34 reveal that the orbital energies of 2*s*(N) and σ_x MO are now rather close (ΔE < 12eV), and since both are of the same symmetry (totally symmetric) they interact as shown on the right-hand side of this figure as a second approximation. The novel linear combinations are 2*s*+λσ_z and σ_z–λ′2*s*. In the end, there are three strongly bonding, one weakly bonding and three strongly antibonding MOs. All bonding orbitals are occupied by electron pairs; the ionization energy of NH_3 is 10.07 eV. The HOMO of the molecule is the totally symmetric and weakly bonding σ_z–λ′2*s* orbital (a_1 symmetry):

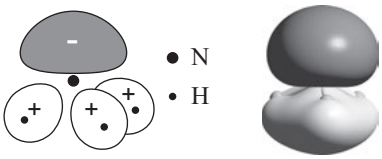

The electron pair in the HOMO of the ammonia molecule is responsible for its atomic dipole moment, which comes in addition to the bonding moments (see Section 4.6.3). The overall dipole moment of 1.5 D influences many reactions of ammonia, for example, its ligand properties. The bond angle of 107° is larger than for the analogous hydrides PH_3 (94°) and AsH_3 (92°), which can be explained by the larger bond lengths and smaller partial charges of the higher hydrides of Group 15; see Table 2.5. The oxonium ion $[H_3O]^+$ and the sulfonium ion $[H_3S]^+$ are isoelectronic with NH_3 and also of C_{3v} symmetry.

The tetrahedral **molecule P_4** represents a special case for a trigonal-pyramidal coordination with local C_{3v} symmetry at the atoms. P_4 is the constituent of white phosphorus (Section 10.3.2). Since its overall symmetry is T_d the bond angles of P_4 are only 60° (Figure 2.35). In the past, it has sometimes been assumed that this bonding situation is the reason for the high reactivity of white phosphorus, but this is no longer the case. In fact, P_4 is a thermally rather robust *cluster molecule* since the overlap of the atomic orbitals at the interior of the cluster is very strong. Therefore, the bond length of 220 pm and the bond energy are close to those of the other (polymeric) phosphorus allotropes with larger bond angles (see Section 10.3.2).

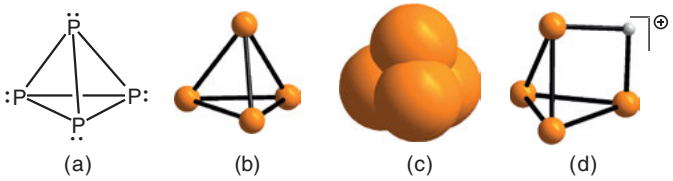

Figure 2.35: (a) Classical Lewis formula of P_4; (b) structure of the P_4 molecule as ball-and-stick model, and (c) as space-filling model and (d) experimental geometry of the cation $[P_4H]^+$ with a three-center two-electron P–H–P bridge bond.

Under the high symmetry T_d, some of the MOs of P_4 are doubly (*e*) and others triply (*t*) degenerate as the calculated energy level diagram in Figure 2.36 illustrates. The ionization energy of P_4 as determined by PES is only 9.52 eV,[58] while the ionization energy of phosphorus atoms is 10.48 eV. This difference is due to strong relaxation during the formation of the cation $[P_4]^+$, which is no longer tetrahedral. A considerable

58 C. C. Cummins, N. W. Mitzel, G. Wu et al., *J. Am. Chem. Soc.* **2010**, *132*, 8459.

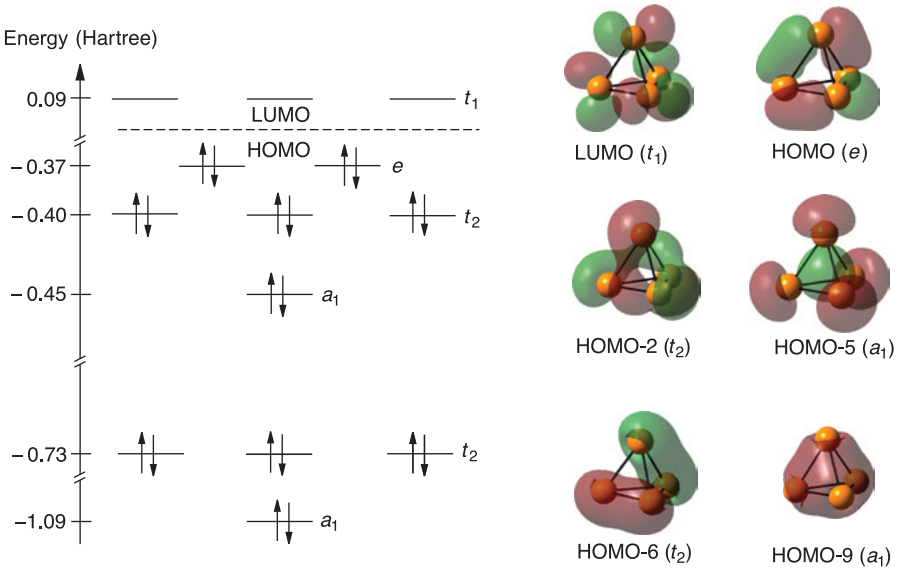

Figure 2.36: Left: Energy level diagram of the molecule P_4 (1 Hartree = 27.2 eV). Right: Isodensity surfaces of the molecular orbitals calculated with a residual electron density of 0.05 e Å^{-3}. For the degenerate MOs only one version of the two (e) or three (t) symmetry-equivalent linear combinations is shown.

amount of energy is gained by reduction of the total symmetry to C_{3v}, which results in a splitting of the former e level into two nondegenerate levels (JAHN–TELLER effect). In other words, the calculated orbital energy of the e level in Figure 2.36 and the ionization energy of P_4 deviate slightly.

From the orbital pictures in Figure 2.36 it can be seen that P_4 is a *strain-free cluster molecule* with 20 delocalized VEs and strong bonding interactions. The lower set of four MOs of a_1 and t_2 symmetry originates exclusively from the interaction of the four 3*s* AOs; these MOs are partly bonding and partly antibonding with the result that they do not contribute to the overall bond energy. In a way, the electrons in these MOs represent the four lone pairs at the phosphorus atoms of the LEWIS-type structure in Figure 2.35. The upper set of six orbitals of a_1, t_2 and e symmetry originates exclusively from the 3*p* AOs and this set is responsible for the six PP bonds. In other words, there is no mixing of *s* and *p* orbitals. These six occupied MOs are all bonding and give rise to a thermally very stable although chemically highly reactive molecule.

Since the mentioned lone pairs in the 3*s* AOs are localized at the atomic cores, they do not give rise to much LEWIS base character of P_4. Therefore, protonation of P_4 by the superacid $H[Al(OTeF_5)_4]$ produces a cation $[P_4H]^+$ with the proton occupying an *edge* rather than an *apex* of the P_4 tetrahedron (Figure 2.35d). The edge represents the location of the HOMO of *e* symmetry as shown in Figure 2.36. The cation

structure of C_{2v} symmetry follows convincingly from the triplets observed both in the $^{1}H-$ and $^{31}P-$NMR spectra of dissolved $[P_4H][Al(OTeF_5)_4]$. Quantum-chemical calculations revealed that the (gaseous) isomer with the proton attached to an apex atom of the P_4 tetrahedron is by 61.4 kJ mol^{-1} less stable.[59]

2.4.10 Five-Atomic Molecules

The isoelectronic species $[BH_4]^-$, CH_4 and $[NH_4]^+$ as well as $[AlH_4]^-$, SiH_4 and $[PH_4]^+$ are well-known examples of tetrahedral molecules and ions of type AB_4. Due to their high (cubic) symmetry, the construction of MOs is rather straightforward as will be shown for methane. The hydrogen atoms can be thought to be located at opposite apexes of a cube (Figure 2.37). The point group T_d contains eight principal C_3 rotational axes along the C–H bonds as well as three C_2 axes bisecting the H–C–H bond angles (Section 2.3). These twofold rotational axes are parallel to the edges of the cube and are used to define the Cartesian coordinates *x*, *y* and *z*.

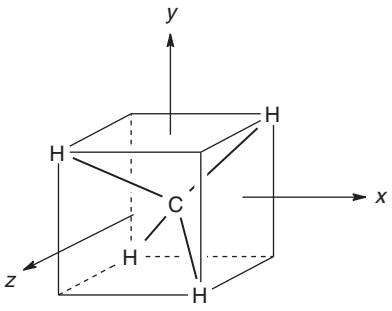

Figure 2.37: Definition of Cartesian coordinates for tetrahedral molecules AB_4 like methane using a cube for illustration.

The four valence orbitals of carbon together with the 1*s* orbitals of four hydrogen atoms yield eight MOs, some of which are asymmetric and degenerate due to the principal C_3 axis of the molecule. The results are shown in Figure 2.38. The linear combination of the five *s* orbitals yields the totally symmetric five-center MOs σ_s and $\sigma_s^\star$ of a_1 symmetry. The 2*p* AOs of carbon overlap equally with the four hydrogen orbitals, but the resulting MOs are asymmetric with regard to the C_3 axis. As usual for degenerate orbital terms, the sum of the t_2 MOs σ_x, σ_y, σ_z and $\sigma_x^\star$, $\sigma_y^\star$, $\sigma_z^\star$ yield the correct symmetry of the molecular electron density. The eight VEs occupy the four five-center bonding MOs to form a very stable molecule. There are no nonbonding levels, and the antibonding MOs remain empty.

59 A. Wiesner, S. Steinhauer, H. Beckers, C. Müller, S. Riedel, *Chem. Sci.* **2018**, *9*, 7169.

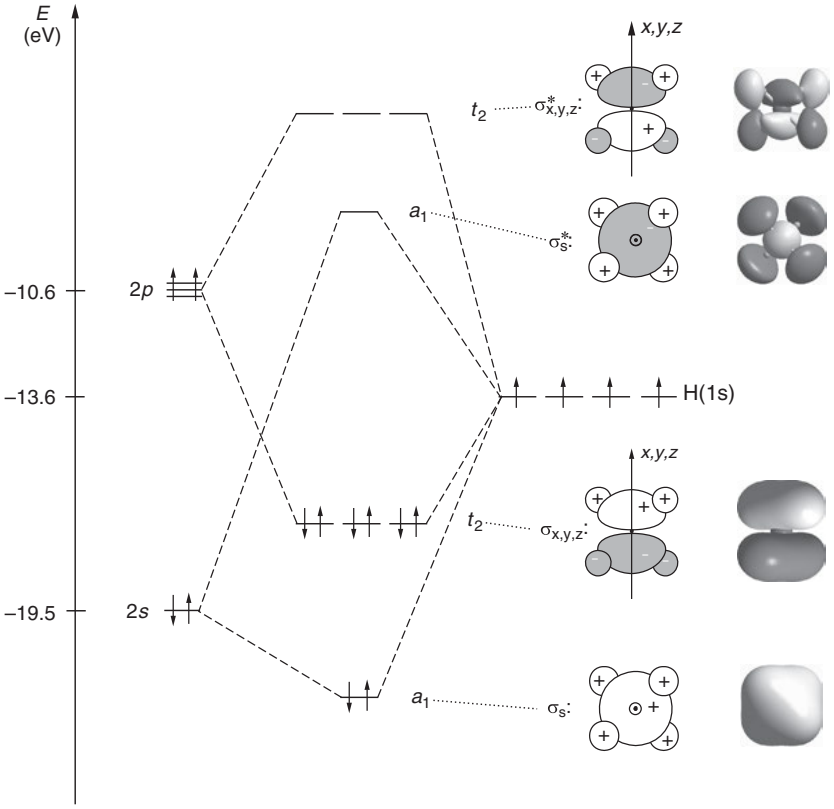

Figure 2.38: Energy level diagram and molecular orbitals for methane. Left: The two MOs of a_1 symmetry are totally symmetric while the t_2 MOs are triply degenerate. This follows from the fact that the three 2*p* AOs of carbon are degenerate under cubic symmetry and consequently also the MOs σ_x, σ_y, σ_z as well as σ_x*, σ_y*, σ_z*. Mixing of *s* and *p* type orbitals is prevented by the differing symmetries of the corresponding MOs. Right: Linear combinations of the four 1*s* AOs of the hydrogen atoms with the carbon 2*s* and 2*p* orbitals to give eight molecular orbitals. The isodensity surfaces of the MOs have been calculated with a residual electron density of 0.05 *e* Å^{-3}.

The photoelectron spectrum of methane shown in Figure 2.39 is in full agreement with the MO diagram derived from first principles in Figure 2.38. There are two groups of signals corresponding to the removal of an electron from either the a_1 or the t_2 level. The ionization energy of methane is only 12.6 eV due to strong relaxation of the cation $[CH_4]^+$, which is no longer tetrahedral since energy is gained by reduction of the symmetry to C_{3v} resulting in a splitting of the former t_2 level into a doubly degenerate level with four electrons and a singly occupied orbital (JAHN–TELLER

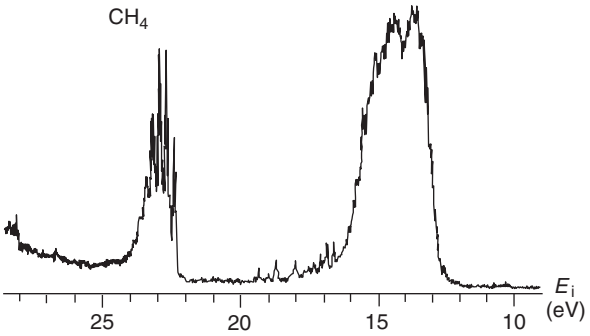

Figure 2.39: Photoelectron spectrum of methane for the region of the valence electrons. The signals in the range 12.6–17 eV correspond to the removal of an electron from the t_2 level which is the HOMO of the molecule. Spin-orbit coupling, vibrational excitation of the cation as well as a Jahn-Teller effect in the cation result in splitting and broadening of the lines. The signals in the range 22–24 eV indicate the removal of an electron from the strongly bonding a_1 level, which is also accompanied by vibrational excitation of the tetrahedral cation.

effect). In other words, the calculated orbital energy of the t_2 level and the ionization energy of methane deviate considerably in this case. The ionization energy of the isolated C atom is 11.30 eV.

The strong bonds originating from the tetrahedrally coordinate carbon atom are also responsible for the extreme hardness of diamond (Section 7.3.2). Unlike in the case of VB theory, these bonds are constructed directly from the ground state of the carbon atom without any hybridization of atomic orbitals or promotion of an electron to a higher level. All electrons of methane reside in strongly bonding MOs and are delocalized over the five atoms (five-center bonds).

Tetrahedral molecules and ions with σ as well as π bonds are also known, for example, oxo-anions like phosphate, sulfate and perchlorate. These species are discussed in Section 2.6.

2.5 The Coordinate Bond

If two atoms or molecules form a bond by the overlap of two orbitals, the bonding electron pair may originate from one single electron from each of the *two* bonding partners (as in the covalent cases discussed in previous sections) or it may be provided by just *one* of the partners:

$$A\cdot + \cdot B \longrightarrow A{-}B \qquad A + :D \longrightarrow \overset{\ominus}{A}{-}\overset{\oplus}{D}$$

The second scheme describes the formation of a *dative or coordinate bond* between an acceptor A and a donor D resulting in *formal charges* ⊕ and ⊖.[60] It should be noted, however, that these charges are formal in nature only and do not always agree with the actual partial charges of the corresponding atoms. Electron density from the donor orbital is only transferred toward the acceptor atom to a certain extent, that is, the mixing coefficient λ in the linear combination is such that the donor orbital is weighted much higher than 50%. In the end, the two partners bear *partial charges* δe^+ and δe^- as indicated by formulas such as $A^{\delta-}$–$B^{\delta+}$. Since partial charges are common to covalently bonded atoms of different electronegativities as well, the dative bonds do not differ in this respect (see Section 4.6.3).

In some dative bonds the actual atomic charges are opposite to the formal charges (⊕ and ⊖), for example, in the adduct $F_3B{\leftarrow}NH_3$ in which some electron density from the HOMO of ammonia is transferred to the LUMO of boron trifluoride. The following molecular structures show the formal charges on the left-hand side and the calculated partial atomic charges on the right-hand side:

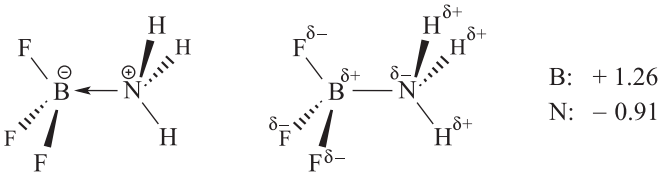

The arrow in the left structure indicates the direction of electron density transfer. The actual charges are in line with the electronegativities χ of the atoms involved (B: 2.0; N: 3.1; H: 2.2; F: 4.1; see Table 4.8). The calculated atomic charges of the separate molecules F_3B and NH_3 are: B = +1.43, N = –1.07. As expected, these values are diminished by the formation of the coordinate bond.

According to a theory proposed by GILBERT NEWTON LEWIS in 1923, the formation of a coordinate bond can be considered as a reaction between a LEWIS acid (electron acceptor) and a LEWIS base (electron donor). Well-known LEWIS acids are: BH_3, BF_3, BCl_3, $AlCl_3$, SiF_4, $SiCl_4$, PF_5, AsF_5, SbF_5, BrF_3, XeF_6 and SO_3. The proton H^+ may be considered the strongest LEWIS acid of all. These molecules are characterized by a low-lying molecular orbital (LUMO), which may accept electron density from a suitable electron donor.

LEWIS bases are compounds with an occupied nonbonding or weakly bonding molecular orbital (HOMO), for example, R_3N (amines, R = organic group), R_3P (phosphanes), R_3PO (phosphane oxides), H_2O, R_2O (ethers), R_2S (sulfanes), R_2SO (sulfoxides) as well as anions X^- (X = F, Cl, Br, I, OH, CN, etc.).

60 A. Haaland, *Angew. Chem. Int. Ed.* **1989**, *28*, 992–1007. G. Frenking, *Angew. Chem. Int. Ed.* **2014**, *53*, 6040.

The concept of *hard and soft acids and bases*[61] can help to understand the different types of coordinate bonds. The so-called hard and strongly polarizing acids preferentially bind hard bases, which themselves are defined as difficult to polarize.[62] In this case, the orbital energies of donor and acceptor are quite different as shown at the center of Figure 2.40. The resulting dative bond is partly covalent and partly ionic as in the octahedral ion $[SiF_6]^{2-}$, which is spontaneously formed from SiF_4 and sodium fluoride.

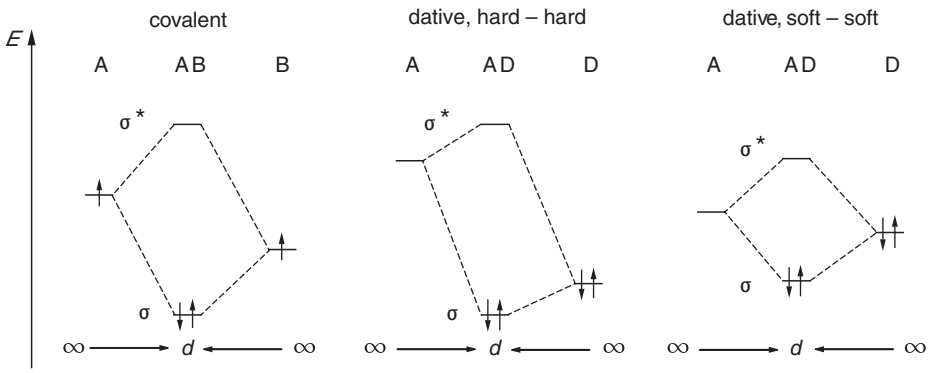

Figure 2.40: Energy level diagrams for the formation of covalent bonds between two atoms A and B with unpaired electrons (left), between an acceptor A and a donor D of strongly different orbital energies (center) and between two partners A and D with similar orbital energies (right). The horizontal arrows indicate the approach of the two fragments to the equilibrium internuclear distance *d*.

On the other hand, a dative bond between soft (polarizable) donors and acceptors is mainly covalent with little ionic contributions. In this case, the bond energy results mainly from the stabilization of the common σ MO compared to the energies of the starting orbitals of A and D (Figure 2.40, right). In this case, however, the total bond energy is lower compared to the more ionic bond between hard partners.

The *adduct* formed from acceptor A and donor D is sometimes written with a point between the bonding partners as in $BF_3{\cdot}NR_3$. Whether a molecule contains a classical covalent or a dative bond is not always easy to answer, although coordinate bonds are typically strongly polarized as can be seen from the molecular dipole moment. A drastic example is the ammonia–borane adduct $H_3B{\leftarrow}NH_3$, which is *isoelectronic* and even *isosteric* with the ethane molecule (not only the number of atoms and VEs but also the number of nuclear charges agree in both compounds). However, the properties of their central bonds differ considerably as the data in Table 2.11 illustrate.

61 R. G. Pearson (ed.), *Chemical Hardness*, Wiley-VCH, Weinheim, Germany, **1997**.

62 The polarizability of atoms and molecules is discussed in Chapter 3.

Table 2.11: Comparison of the bond properties of the isoelectronic species ethane C_2H_6 and the adduct ammonia–borane $H_3B{\leftarrow}NH_3$ ($\Delta_rH°$: dissociation enthalpy; *d*: internuclear distance of the central bond; μ: molecular dipole moment).

	$H_3C–CH_3$	$H_3B{\leftarrow}NH_3$
$\Delta_rH°$ (kJ mol^{-1})	377	130
d (pm)	153	166
μ (D)	0	5.2

While the dipole moment of ethane is zero for reasons of symmetry, ammonia–borane is a highly polar adduct. The melting points of ethane (–183 °C) and of $H_3B{\leftarrow}NH_3$ (+124 °C) reflect the extremely differing polarities: the interaction between the nonpolar hydrocarbon molecules is mainly due to weak dispersion forces while the crystals of the adduct $H_3B{\leftarrow}NH_3$ are dominated by strong intermolecular dipole forces and dihydrogen bonds (see Chapters 3 and 6). Since the electronegativity of nitrogen is much higher than that of boron, the dipole vector of $H_3B{\leftarrow}NH_3$ is pointing from the (negative) nitrogen to the (positive) boron center. The thermal dissociation of $H_3B{\leftarrow}NH_3$ results in the molecules BH_3 and NH_3 in sharp contrast to the dissociation of ethane which yields two methyl radicals.

If a molecule contains both acceptor and donor sites in suitable proximity, an *intramolecular coordinate bond* may be established, either of σ or π type. Many examples of such bonds are encountered in the chemistry of boron–nitrogen compounds (Section 6.10). The molecule BF_3 contains an intramolecular π bond as already discussed in Section 2.4.8. Another interesting case is the molecule (dimethylamino)(chloro)silane $Me_2N–SiH_2Cl$, which is monomeric in the gas phase but dimeric in the solid state:

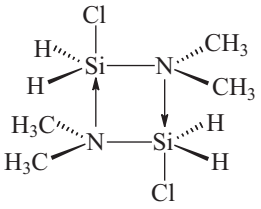

$d(\mathrm{Si—N_{eq}}) = 181$ pm

$d(\mathrm{Si{\leftarrow}N_{ax}}) = 206$ pm

The geometry at the silicon atoms of the dimer is approximately trigonal-bipyramidal. The dative Si–N bonds are longer than regular covalent bonds between silicon and nitrogen, even if this is by no means always the case. In the ions $[NH_4]^+$ (tetrahedron) and $[SiF_6]^{2-}$ (octahedron), for instance, all bonds are identical, although they are formed from NH_3 and SiF_4 by coordination of H^+ and 2 F^-, respectively. The coordination of an additional donor to the acceptor atom always changes the overall coordination geometry.

The strength of dative bonds can be influenced by inductive effects (Section 4.6). For example, Me_3N is a stronger LEWIS base than NH_3 since the methyl groups donate electron density to the nitrogen atom. Therefore, the dissociation enthalpy of the adduct $H_3B{\leftarrow}NMe_3$ is by 15 kJ mol^{-1} larger than that of $H_3B{\leftarrow}NH_3$. In addition to inductive effects, the steric requirements play a role as well: While the LEWIS acidity of BH_3 can be considerably enhanced by substituting the hydrogen atoms by electron-withdrawing C_6F_5 groups and the LEWIS basicity of PH_3 can be increased by *tert*-butyl substitution, $B(C_6F_5)_3$ and $^tBu_3P$ are unable to form an adduct due to the severe steric repulsion of the bulky substituents (*steric crowding*). Such sterically hindered acid–base pairs are called *frustrated LEWIS pairs*.[63] Systems of this type are important metal-free catalysts; they activate small molecules such as H_2 even under mild conditions (25 °C, 1 bar). Initially, the H_2 molecule forms a bridge between the acidic (B) and the basic (P) centers before being heterolytically cleaved (see Section 5.7.2).

2.6 Hypercoordinate Molecules

There are many nonmetallic compounds in which the number of electrons in the valence shell of the central atom is seemingly larger than eight, which would be a *violation of the octet rule* discussed in Section 2.2.2. Historically, such compounds are therefore referred to as hypervalent. Examples are given in Table 2.12 together with the experimental geometries, which in most cases agree with the predictions by the VSEPR model (see Section 2.2.2). For the determination of the number of VE at the central atom, it is *postulated* by this model that singly bonded substituents such as fluorine require *two* bonding electrons and that doubly bonded substituents such as oxygen atoms (of coordination number 1) require *four* bonding electrons. In the following, however, it will be shown that this postulate is in error and multicenter bonds are at work in such compounds instead, which therefore should be termed *hypercoordinate* rather than *hypervalent molecules*.[64]

We use the well-studied molecule SF_6 as an example to analyze the bonding situation in such hypercoordinate species by MO theory. SF_6 is a colorless and thermally very stable gas of low reactivity, which is industrially produced from the elements in a highly exothermic reaction suggesting its bonds to be very strong. The geometry is octahedral and the linear axes F–S–F may be used to define the Cartesian coordinates x, y and z, which are all equivalent under the point group O_h. The principal symmetry elements of an octahedron are the center of symmetry (i) and the fourfold rotational axes (C_4), which have the highest order. Therefore, degenerate and asymmetric MOs are to be expected. The six VEs of a sulfur atom occupy the orbitals 3s and the triply degenerate level $3p_xp_yp_z$. In contrast, the

63 D. W. Stephan, G. Erker, *Angew. Chem. Int. Ed.* **2010**, *49*, 46–76.
64 G. S. McGrady, J. W. Steed, *Encycl. Inorg. Chem.* **2005**, *3*, 1938.

Table 2.12: Hypercoordinate (hypervalent) compounds of nonmetals (VE: formal number of valence electrons at the central atom).

Coordination number	VE at central atom	Molecule/Ion	Approximate geometry at central atom
2	10	$[I_3]^-$, XeF_2	Linear
	10	SO_2	Bent
3	12	SO_3, $S(NR)_3$	Trigonal-planar
	10	$OSCl_2$, $OSeF_2$, $[SO_3]^{2-}$	Trigonal-pyramidal
	14	XeO_3	Trigonal-pyramidal
4	10	$OPCl_3$	Tetrahedral
	12	Cl_2SO_2, $[SO_4]^{2-}$	Tetrahedral
	14	$[ClO_4]^-$	Tetrahedral
	12	XeF_4	Square-planar
5	10	PF_5	Trigonal-bipyramidal
	12	SOF_4	Trigonal-bipyramidal
	12	$[SF_5]^-$	Square-pyramidal
	14	$[XeF_5]^-$	Pentagonal-planar
6	12	SF_6, SeF_6, TeF_6, $[ClF_6]^+$,	Octahedral
	14	$[BrF_6]^+$, $[PF_6]^-$, $[SiF_6]^{2-}$	Distorted octahedral
		$[SeCl_6]^{2-}$, XeF_6	
7	14	IF_7, $[TeF_7]^-$, $[SbF_7]^{2-}$	Pentagonal-bipyramidal
8	16	$[TeF_8]^{2-}$	Square-antiprismatic

calculated orbital energy of the 3*d* level is so high that these orbitals can be neglected in a first approximation (the same holds for other third-row nonmetals such as Si, P and Cl).[65] In other words, we have four valence orbitals on sulfur to create six equivalent bonds to the fluorine atoms in SF_6. This can be achieved by the use of *multicenter bonds*.

The energy level diagram in Figure 2.41 shows that the 2*p* orbital energy of fluorine is compatible with both the energies of the S(3*s*) and S($3p_xp_yp_z$) levels ($\Delta E < 15$ eV). Therefore, 10 MOs may be constructed by the LCAO method, which is a rather easy task in this case due to the high molecular symmetry.

The spherical 3*s* AO and the octahedrally oriented $2p_\sigma$ AOs of the six fluorine atoms yield one strongly bonding and one antibonding MO of a_{1g} symmetry; the term symbol a_{1g} indicates totally symmetric properties, that is, with respect to the

65 A. E. Reed, F. Weinhold, *J. Am. Chem. Soc.* **1986**, *108*, 3586. C. S. Ewig, J. R. van Wazer, *J. Am. Chem. Soc.* **1989**, *111*, 1552. A. E. Reed, P. von Ragué Schleyer, *J. Am. Chem. Soc.* **1990**, *112*, 1434. E. Magnusson, *J. Am. Chem. Soc.* **1993**, *115*, 1051. J. M. Galbraith, *J. Chem. Educ.* **2007**, *84*, 783.

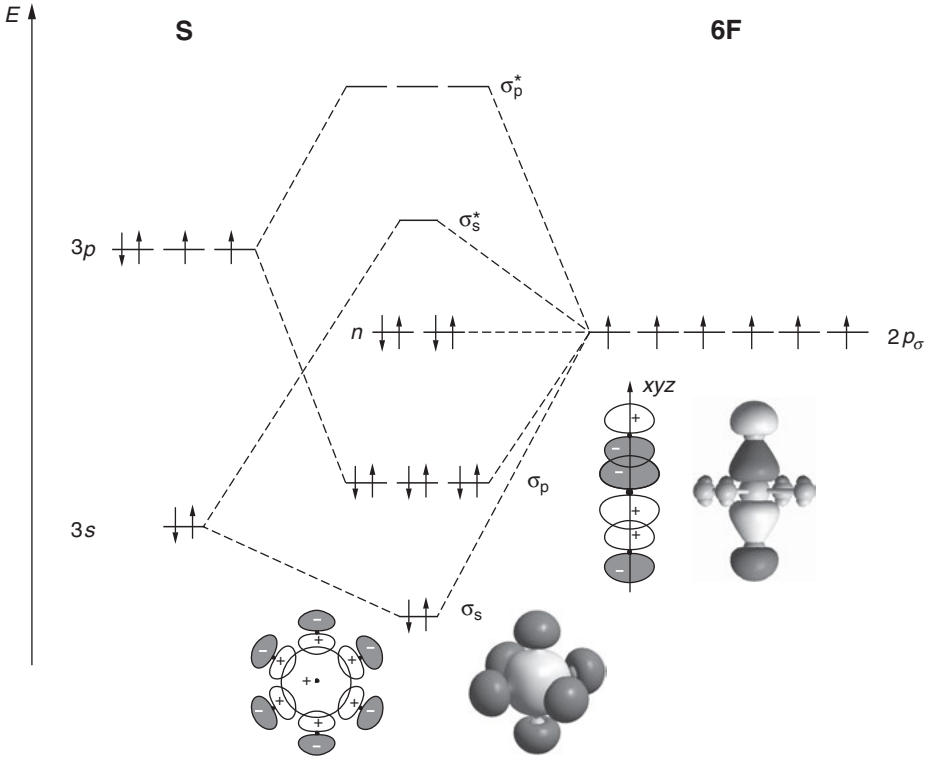

Figure 2.41: Energy level diagram (simplified) and bonding molecular orbitals of SF_6 constructed from the 3*s* and 3*p* AOs of sulfur and the $2p_\sigma$ AOs of six fluorine atoms. In the lower part of the figure the overlap between the 3*s* AO and the six $2p_\sigma$ AOs is shown together with the calculated isodensity surface of the resulting bonding σ_s MO calculated with a residual electron density of 0.05 *e* Å^{-3}. This seven-center MO is totally symmetric as is the corresponding σ_s* MO. On the right-hand side one of the linear combinations between a 3*p* AO of sulfur and the $2p_\sigma$ AOs of two fluorine atoms is shown. This three-center MO is part of the triply degenerate $\sigma_p(t_{1u})$ level since identical MOs can be constructed in the *x, y* and *z* directions. The corresponding isodensity surface has been calculated with a residual electron density of 0.08 *e* Å^{-3}.

C_3 axis (*a*), to the mirror planes (1), and to the center of inversion (g). Since the symmetry-equivalent fluorine atoms have identical distances to the sulfur atom, all their orbitals overlap with the same weight yielding a seven-center σ bond. The 3*p* AOs of sulfur, on the other hand, interact only with those fluorine orbitals that are oriented along the corresponding Cartesian axis since all other F orbitals are orthogonal to the sulfur AO. The linear combination of the AOs $3p_xp_yp_z$ with the corresponding fluorine orbitals provides another set of bonding and antibonding triply degenerate MOs (*t*) corresponding in symmetry to the sulfur 3*p* orbitals. The resulting level is of t_{1u} symmetry, that is, *ungerade* (u) with regard to the center of symmetry. Due to their differing symmetries the levels σ_s and σ_p cannot interact with each other.

Besides these eight bonding and antibonding MOs, there are only two possible nonbonding linear combinations according to the rules for construction of MOs from AOs, especially the principle of mutual orthogonality of all MOs (see Section 2.4.5). The nonbonding doubly degenerate set of MOs is constructed from four F($2p_\sigma$) AOs each yielding an e_g symmetric term. The eventually resulting 10 MOs are occupied by the 12 VEs as shown in Figure 2.41. Four bonding pairs bind all six F atoms equally, and there are only eight electrons in the valence shell of the sulfur atom as the nonbonding electrons on the e_g level are exclusively delocalized across the fluorine atoms. In other words, the octetrule for the central atom is formally obeyed. In addition, there are six nonbonding electron pairs in fluorine orbitals perpendicular to the S–F bonds (not shown in Figure 2.41).

The electronegativities of sulfur and fluorine atoms differ by 1.5 units with the consequence that the SF bonds of SF_6 are highly polar. The fluorine atoms are negatively charged, while the positive charge at the sulfur atom exceeds two electrostatic units. Therefore, *backbonding* can be expected by which electron density is delocalized back from nonbonding $2p_\pi$ AOs of fluorine to the empty antibonding σ_p* MO, which is mainly localized at the sulfur atom and shows 3*p* character predominantly (interaction of the F lone-pairs with the 3*s* AO of sulfur is symmetry forbidden).

In this manner, a weak dative π bond between the fluorine atoms and the sulfur atom is established, which reduces the negative charge at the ligand atoms. Due to the bond angles of 90° the intramolecular F ⋯ F distance is smaller than the sum of VAN DER WAALS radii and strong COULOMB repulsion occurs. In addition, the nonbonding electrons at the e_g level may be partly delocalized into the empty $3d_{xy}$, d_{xz} and d_{yz} orbitals of sulfur to establish a second type of backbonding (these AOs are also *gerade*). However, the high energy of the sulfur 3*d* orbitals results in only a very small overlap integral. In summary, we can state that several multicenter σ and π bonds stabilize the SF_6 molecule as an archetype of octahedral species in nonmetal chemistry.

In addition to SF_6, the higher homologues SeF_6 and TeF_6 have been prepared and are very stable molecules as well. The corresponding oxygen species **OF_6**, however, does *not* exist. Several reasons can be put forward why oxygen and fluorine only form the binary compounds OF_2 and O_2F_2 at standard conditions (Section 11.4). First, the oxygen atom is considerably smaller than sulfur and there is simply not enough room on its surface for six ligand atoms. Secondly, the bonds OF (e.g., in OF_2) are shorter than SF bonds and the fluorine atoms of hypothetical OF_6 would be very close to each other, that is, the repulsion probably stronger than the bond enthalpy. Thirdly, the OF bond enthalpy (e.g., in OF_2) is much smaller (190 kJ mol^{-1}) than the SF bond enthalpy (360 kJ mol^{-1}; Table 4.1), partly because the ionic contribution is smaller owing to the smaller electronegativity difference. Finally, the 2*s* AO of oxygen is so low in energy (–31.1 eV) that it would hardly interact with the 2*p* AOs of the six fluorine atoms (–17.4 eV). As a consequence, in an energy level

diagram for OF_6 in analogy to Figure 2.41 *only three bonding MOs* would be obtained for the six bonds. Thus, OF_6 is likely to remain a member of large collection of interesting but *nonexisting molecules*.

But why does the hypothetical "super hydrogen sulfide" **H_6S** not exist, although the hydrogen atoms are very small and the SH bond enthalpy (e.g., in H_2S) is quite large (363 kJ mol^{-1}). While the dissociation of SF_6 into either $SF_4 + F_2$ or $SF_2 + 2F_2$ is endothermic, quantum-chemical calculations have shown that the dissociation of H_6S into $H_2S + 2H_2$ would be exothermic. The main reason for this difference is the extraordinarily high bond enthalpy of dihydrogen H_2 (D_{298} = 436 kJ mol^{-1}), which is more than three times as large as the dissociation enthalpy of F_2 (D_{298} = 159 kJ mol^{-1}).

Under special conditions, however, *endothermic compounds* can be prepared if the activation energy for their decomposition is high enough to stabilize the molecules. For example, **Me_6Te** is a well-known hypercoordinate species (Section 12.12.4), although the dissociation into either $Me_4Te + Me_2$ or $Me_2Te + 2Me_2$ is exothermic, that is, the compound is metastable. The high CC bond energy of ethane C_2H_6 (i.e., Me_2: 331 kJ mol^{-1}) is responsible for these thermodynamic relationships. These data make it plausible why PH_5, ClH_5 and H_2Xe do not exist, although PF_5, ClF_5 and XeF_2 are well-known thermodynamically stable molecules: The relatively low dissociation enthalpy of F_2 accounts for the difference. Many more examples for hypercoordinate molecules are presented in the following chapters.

The theoretical analysis of the bonds in SF_6 by MO theory has model character and can be used to discuss the stability of analogous hypercoordinate compounds of other nonmetals such as phosphoranes PX_5, sulfuranes SX_4, as well as interhalogen and noble gas compounds. Such species can be understood using both the concept of *negative hyperconjugation* (see below and Section 14.6.2) and that of *multicenter bonds*.[66] As in SF_6, the participation of the valence shell *d* orbitals of the central atoms is small in all cases since their orbital energies are far too high. The promotion of a 3*p* electron of chlorine to the 3*d* level requires an energy of 11.2 eV, and in the case of phosphorus even 16 eV are needed to promote a 3*s* electron to the 3*d* level. For comparison, bond enthalpies are only in the range of 1–5 eV and thus cannot compensate these enormous promotion energies. Consequently, *we must give up the original idea used in PAULING's VB theory that n singly occupied orbitals are needed at the central atom to establish n covalent bonds in a molecule of type* AB_n.

The tetrahedral sulfate ion $[SO_4]^{2-}$ is the second most abundant anion in the oceans, after chloride. It is isoelectronic with the species $[SiO_4]^{4-}$, $[PO_4]^{3-}$, $[SO_3F]^-$, SO_2F_2 and $[ClO_4]^-$. These ions all show a certain degree of π backbonding of lone pairs at the ligand atoms into σ* orbitals at the central atom in addition to the

66 J. Cioslowski, S. T. Mixon, *Inorg. Chem.* **1993**, *32*, 3209. D. L. Cooper et al., *J. Am. Chem. Soc.* **1994**, *116*, 4414. G. S. McGrady, J. W. Steed, *Encycl. Inorg. Chem.* **2005**, *3*, 1938. J. M. Galbraith, *J. Chem. Educ.* **2007**, *84*, 783.

σ-bonded molecular skeleton. The σ bonds of sulfate can be constructed in a similar manner as for the methane molecule (see above) using the orbitals 3*s*, $3p_x$, $3p_y$ and $3p_z$ of the sulfur atom and four $2p_\sigma$ AOs of the oxygen atoms:

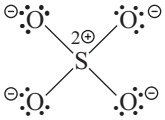

In this LEWIS-type formula the octet rule for the central atom is obeyed and the negative charges are evenly distributed over the four oxygen atoms. The corresponding energy level diagram is shown in Figure 2.42. There are four occupied MOs of a_1 and t_2 symmetry originating from the 2*s* AOs of the oxygen atoms, although these doubly occupied orbitals do not contribute significantly to the bond energy. The linear

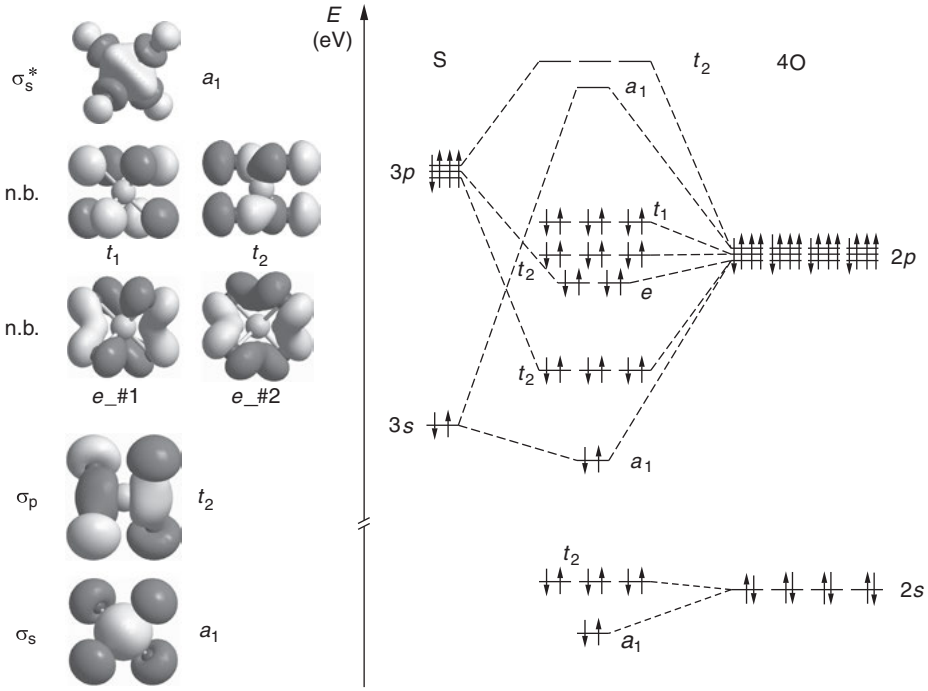

Figure 2.42: Molecular orbitals and energy level diagram for the sulfate ion. The lowest four MOs originating from the O(2*s*) orbitals are essentially nonbonding. The σ bonds are formed by the electrons in the σ_s and the three σ_p MOs, the calculated isodensity surfaces of which are shown on the left-hand side (calculated with a residual electron density of 0.05 *e* Å^{-3}). The totally symmetric σ_s MO represents the linear combination of the sulfur 3s AO with four oxygen 2*p* AOs. Linear combination of the three sulfur $3p_{x,y,z}$ orbitals with the 2*p* AOs of four oxygen atoms yields the three degenerate σ_p MOs. As a result, there are four 5-center bonds. The nonbonding electrons at the levels of *e*, t_2 and t_1 symmetry represent the lone-pairs at the oxygen atoms.

combination of the 3*s* AO of sulfur with suitable oxygen orbitals yields the totally symmetric bonding and antibonding MOs of a_1 symmetry, while the degenerate sulfur 3*p* orbitals give rise to eight MOs of *e* and t_2 symmetry. In addition, occupied nonbonding 2*s* and 2*p* orbitals at the oxygen atoms represent the lone-pairs of the LEWIS structure.

Due to the electronegativity difference of more than one unit between sulfur and oxygen, the bonds of the sulfate ion are strongly polar, and the sulfur atom is highly charged. Therefore, the lone-pair electrons at the oxygen atoms are attracted by the sulfur atom and partial delocalization of electron density from the oxygen $2p_\pi$ AOs into the empty $\sigma_p^\star$ MOs of t_2 symmetry takes place. This effect is called *negative hyperconjugation*[67] or *backbonding* and is a phenomenon widespread in polar molecules. As shown in Figure 2.40 there is always a gain in energy if an occupied orbital interacts with an empty orbital of suitable symmetry, although this energy gain decreases with increasing energy difference between the involved orbitals. The overall interaction may then be expressed by the classical structural formulae for sulfate ions as follows:

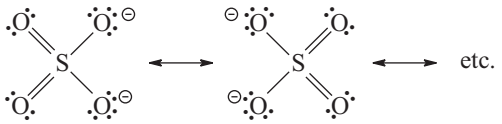

In these resonance structures the σ bonds are much stronger than the π bonds, but in addition there are strong ionic contributions to the bond enthalpy due to the considerable atomic charges (COULOMB attraction). Therefore, the internuclear SO distances of the sulfate ion (typically d_{SO} = 149 pm) are much shorter than for typical SO single bonds as in sulfoxylates R–O–S–O–R (for R = Me: d_{SO} = 162 pm).

The bonding situation in the sulfur oxides SO_2 (C_{2v} symmetry) and SO_3 (D_{3h} symmetry) can be described in a similar manner.[68] The σ bonds of SO_2 can be derived in analogy to those of H_2O (Figure 2.30), and the σ bonds of SO_3 in a similar manner as shown for BF_3 (Figure 2.32):

Ab initio MO calculations have shown that the atomic charges in these molecules approximately amount to the values shown in these LEWIS structures. In both molecules,

67 A. E. Reed, P. v. R. Schleyer, *J. Am. Chem. Soc.* **1990**, *112*, 1434.
68 T. P. Cunningham et al., *J. Chem. Soc. Faraday Trans.* **1997**, *93*, 2247. S. Grabowski et al., *Angew. Chem. Int. Ed.* **2012**, *51*, 6776.

however, there is an empty $3p_\pi$ orbital at the sulfur atom, which may accept electron density from the lone pairs at the oxygen atoms (dative *p-p* π backbonding). These multicenter π bonds resemble those of O_3 (Section 11.1.3) and of BF_3 (Section 2.4.8), respectively. Consequently, the *strength of the SO bonds* in the sulfur oxides is often described using the following modified formulae with multiple bonds:

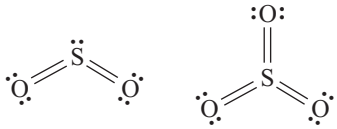

The bond lengths of SO_2 (143 pm) and SO_3 (142 pm) agree with the notion of a certain double bond character as illustrated by these LEWIS structures. The use of double lines ("="), however, does not imply the presence of double bonds such as those in ethene. Instead, they symbolize the bonding interactions in addition to the σ bonds (please note once again that – contrary to earlier concepts of the VB theory – 3*d* orbitals at the sulfur center are not significantly involved in the bonding). The analogous selenium and tellurium oxides are polymeric at 25 °C, which indicates a decreasing tendency in Group 16 (as well as in the other main-groups) to form π bonds when going down from oxygen to tellurium (see Chapter 12). Evidently, the overlap integral becomes too small if the size difference of the atoms becomes too large.

3 VAN DER WAALS Interaction

Atomic and molecular gases (Ar, Xe, HCl, SiH_4, etc.) can be liquefied and eventually solidified at ambient pressure by cooling to sufficiently low temperatures (only the solidification of He requires a pressure of 26 bar). This is evidence for the presence of attractive forces between atoms and molecules that do not engage in intermolecular (or interatomic) covalent, ionic or metallic bonding. These forces are called VAN DER WAALS forces.[1] They lead to relatively weak bonds with bond energies of less than 20 kJ mol^{-1}. This energy is manifest as enthalpy of sublimation of atomic or molecular solids and as enthalpy of vaporization of liquids. VAN DER WAALS forces exist between all atoms, ions and molecules, and further contribute to the energy of covalent bonds and to the lattice energy of crystals (salts and metals).[2]

VAN DER WAALS forces may be divided into three components: dispersion effects (which are always present) and – between polar molecules – additional dipole and induction effects. The dipole effect is most easily understood and will be discussed first.

3.1 The Dipole Effect

An atom, a molecule or a part of a molecule has a dipole moment μ if the centers of positive and negative charges do not coincide, but are separated by the distance l. The dipole moment is defined as $\mu = e \cdot l$ (e represents electron charge) in which μ is a vector with the unit Debye (D)[3] that can be determined directly by microwave spectroscopy of gaseous samples or from the orientation polarization of dissolved molecules in an electric field. Two charges e^+ and e^- separated by 100 pm create a dipole moment of 4.8 D. The S.I. unit of μ is Coulomb·meter with $1\ D = 3.336 \cdot 10^{-30}$ C m.

Molecules can have a dipole moment only if they belong to one of the point groups C_n or C_{nv} (n = 1, 2, 3...; $C_{1v} \equiv C_s$). In all other cases, the centers of positive

1 The Dutch physicist JOHANNES VAN DER WAALS (1837–1923) published the first equation of state for real gases in 1873, taking the volume and the interaction of particles in the gas phase into account. He received the NOBEL prize in physics of the year 1910; for a recognition of his life and work, see K.-T. Tang, J. P. Toennies, *Angew. Chem. Int. Ed.* **2010**, *49*, 9574.

2 J. N. Israelachvilli, *Intermolecular and Surface Forces*, 3rd ed., Academic Press, Waltham, USA, **2011**. I. G. Kaplan, *Intermolecular Interactions*, Wiley, Chichester, **2006**. A. J. Stone, *The Theory of Intermolecular Forces*, Oxford University Press, Oxford, **1997**. G. C. Maitland, M. Rigby, E. B. Smith, W. A. Wakeham, *Intermolecular Forces – Their Origin and Determination*, Oxford, **1987**. An extensive and still valuable discussion is given by H. A. Stuart, *Molekülstruktur*, 3rd ed., Springer, Berlin, **1967**.

3 In honor of the physicist PETER DEBYE (1884–1966; NOBEL prize in chemistry for the year 1936).

https://doi.org/10.1515/9783110578065-003

and negative charges coincide, and the bond moments cancel each other out. Dipole moment data of some nonmetallic molecules are given in Table 3.1.

Table 3.1: Dipole moments μ of simple molecules in the gas phase (in Debye; data after Landolt-Börnstein, Springer, Berlin, 1982/3).

	μ		μ		μ		μ
CO	0.11	H_2O	1.86	O_3	0.53	CH_3F	1.86
NO	0.14	H_2S	0.94	H_2O_2	1.57	CH_3CN	3.92
HF	1.87	NH_3	1.47	SO_2	1.63	pyridine	2.22
HCl	1.11	PH_3	0.57	SCl_2	0.36	THF[a]	1.63
HBr	0.83	N_2O	0.16	H_2SO_4	2.73	HCN	2.98
HI	0.45	NF_3	0.23	OPF_3	1.87	CH_3OH	1.70
IF	1.95	NCl_3	0.39	HN_3	1.70	Me_2NH	1.01
IBr	0.73	SF_4	1.78	$(H_2O)_2$	2.64	B_6H_{10}	2.50

[a]THF, tetrahydrofuran.

The dipole moment of a *diatomic molecule* can also be defined using the partial atomic charges δe together with the internuclear distance d: $\mu = \delta e \cdot d$ (for atomic charges see Section 4.6). At moderate temperatures, molecular dipoles adopt one of the following arrangements to minimize the energy of the system by maximizing the distance between equal charges and simultaneously minimizing the distance between opposite charges:

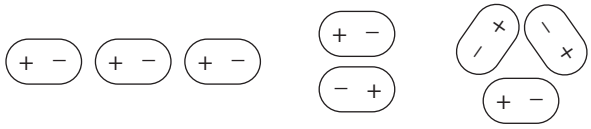

The energy in the first two arrangements is proportional to μ^2/r^3 as long as the distance r between the dipole centers is large compared to l and as long as μ^2/r^3 is large compared to the product $k{\cdot}T$ (rigid orientation: k, BOLTZMANN constant; T, absolute temperature). At higher temperatures the favorable dipole orientations are disturbed and partially destroyed by thermal motion and the energy becomes temperature dependent and proportional to μ^4/kTr^6. Obviously, the dipole effect is large for small molecules with large dipole moments resulting in higher boiling points compared to molecules of similar mass but smaller or no dipole moment. For example, the boiling point of SF_4 (symmetry C_{2v}) is −40°C, but for the larger SF_6 (symmetry O_h) it is −64 °C.

Of course, dipole molecules can also repel each other, but such arrangements are obviously higher in energy and hence less probable. Therefore, the association of molecules in liquids is typically only incompletely disrupted by thermal motion unless the temperature is very high. The effective range of a dipole is about 500 pm. Beyond this distance, the interaction energy U decreases to an amount equal to the product $k{\cdot}T$ (2.5 kJ mol^{-1} at 25 °C), which is the energy stored in one vibrational degree of freedom. If $k{\cdot}T$ is larger than U, a *single* vibration leads to dissociation of the bonding interaction. Cation–anion interactions have an effective range of ca. 50000 pm (in vacuo), and for ion–dipole interactions, the range is about 1400 pm. In other words, the dipole–dipole interactions have the smallest effective range because of the high power of r in the denominator of the energy–distance law given above.

Molecules without dipole moment may have a multipole moment, that is, several internal dipoles that cancel each other for reasons of symmetry. For example, the linear molecule XeF_2 of $D_{\infty h}$ symmetry contains two highly polar XeF bonds with corresponding local dipole moments, albeit in opposite directions and thus canceling each other. Nevertheless, quadrupole moments may result in attractive intermolecular interactions as can be seen in the crystal structure of XeF_2 shown in Figure 3.1. While the positively charged Xe atoms are separated by 431.5 pm, which is more than the interatomic distance in solid xenon, the shortest intermolecular

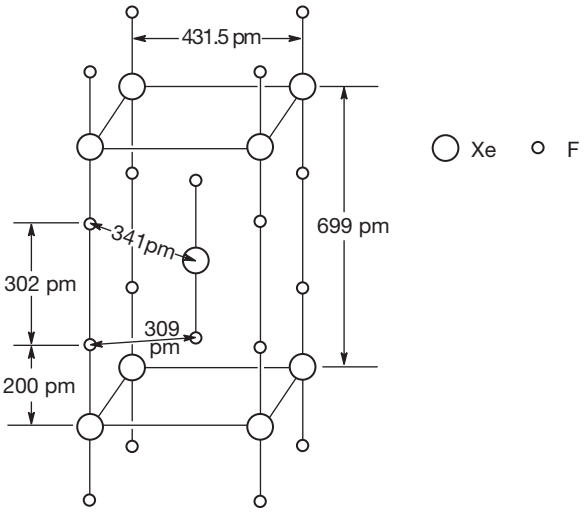

Figure 3.1: Tetragonal crystal structure of xenon difluoride, XeF_2. The intramolecular Xe–F distance d_{XeF} is 200 pm. In addition, there are eight intermolecular shortest Xe···F distances of 341 pm indicating attractive quadrupole interactions (coordination number of Xe: 2 + 8).

distances Xe···F are 341 pm, that is considerably less than the sum of the VAN DER WAALS radii (365 pm; see Table 3.3). One of the consequences is the higher melting point of XeF_2 compared to XeF_4 and XeF_6 (Table 14.1 in Chapter 14 on noble gases).

Since the interaction of quadrupole molecules decreases rapidly with their distance the effect is only noticeable for molecules in close vicinity to each other.

3.2 Induced Dipole Effect

A molecule with a permanent dipole moment μ induces a dipole moment μ_{ind} in any neighboring molecule, regardless of whether the neighboring molecule is a permanent dipole or not. Both dipoles are always oriented in such a manner that attraction results. This induction is *independent* of temperature and is always superimposed onto an existing dipole effect but is generally much weaker than the dipole and dispersion effects and consequently often neglected. The interaction energy is proportional to $\alpha\mu^2/r^6$ (α: polarizability). A stronger interaction between particles results from the dipole moment induced in a neighboring molecule by a charge q, with the power law: $E \sim \alpha q^2/r^4$.

3.3 The Dispersion Effect

A gecko can walk up a smooth glass window because of the adhesion of the millions of hydrophobic setae (bristles) on its toes due to VAN DER WAALS interactions with the glass surface. This basic scientific discovery rapidly led to a commercial product, the gecko tape. The attractive part of such interactions is an electron correlation (quantum mechanical many-body) effect normally referred to as LONDON dispersion. Its overwhelming role in the formation of condensed matter has been known since the pioneering contributions of JOHANNES VAN DER WAALS and FRITZ LONDON.[4] These effects will now be discussed in detail since the dispersion contribution to the VAN DER WAALS interactions in molecules with small dipole moments (<1 D) is larger than the dipole and induction effects combined.[5]

The noble gases crystallize at low temperatures in cubic closest packed arrays with coordination number 12, solely due to the dispersion effect. Similarly, for molecules without dipole moment such as Cl_2, CH_4 and SF_6, the dispersion effect is the main contribution to the lattice energy in the solid state and mainly responsible for the energies of sublimation and vaporization.

4 FRITZ WOLFGANG LONDON, German-American physicist (1900–1954).

5 J. P. Wagner, P. R. Schreiner, *Angew. Chem. Int. Ed.* **2015**, *54*, 12274–12296.

As all isolated atoms, noble gas atoms are spherical to a first approximation disregarding the multipole of the nucleus. Even with this boundary condition, however, this assumption only holds in the time average. At any special moment in time, the atoms have a nonzero dipole moment due to the asymmetrical positions of their electrons and the nucleus resulting in an *atomic dipole moment* μ_{at}. For example, the two electrons of a helium atom are most probably found on opposite sides of the nucleus and with different distances and an angle of less than 180°. The resulting atomic dipole moment now induces a dipole moment μ_{ind} of same direction in any neighboring atom so that an overall attractive force results:

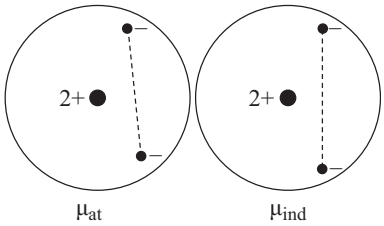

According to LONDON, the binding energy U for two identical atoms is expressed as:

$$U = -\frac{3}{4} \cdot \frac{1}{(4\pi\varepsilon_o)^2} \cdot \frac{\alpha^2}{r^6} \cdot E_i$$

E_i: Ionization energy (eV)
α: Polarizability
r: Internuclear distance

This equation holds only if r is large compared to the atomic diameters. Dispersion is effective up to about 400 pm and is important in atoms and molecules with high *polarizability* α such as the "soft" atoms of the heavy nonmetals Se, Br, I and Xe; "hard" atoms with little polarizability (C, N, O, F and Ne) are found in the first row of the Periodic Table. This explains why F_2 and Cl_2 are gases under standard condition while Br_2 is a liquid and I_2 a solid material.[6] The *hardness* η of an atom is defined as half the difference between the ionization energy and the electron affinity: $\eta = {}^1/_2(E_i - E_{ea})$.

If two noble gas atoms approach each other, the attraction due to the dispersion effect dominates and the energy of the system is lowered. However, at a certain internuclear distance the energy increases again since repulsive forces between the

6 A more elaborate explanation based on molecular orbitals is given in Sections 13.3 and 13.5.3 (halogen bond and σ holes).

valence electrons of both atoms become dominant. Consequently, the total interaction energy E must contain both attractive and repulsive terms:

$$E = -\frac{a}{r^6} + \frac{b}{r^{12}}$$

This so-called LENNARD-JONES potential is valid for nonpolar and neutral particles. The two atomic constants a and b have characteristic values for each particle and are derived from experimentally accessible parameters such as the polarizability α and the ionization energy E_i. Potential energy curves for the noble gases according to the above equation are shown in Figure 3.2. Obviously, the binding energy and the internuclear distance at the potential minimum increase with atomic mass and number of electrons.

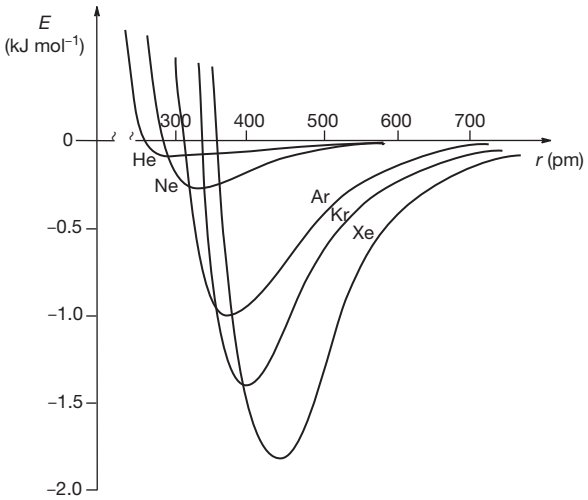

Figure 3.2: Dependence of the potential energy E of two identical noble gas atoms as a function of their internuclear distance r. For very large values of r, the energy is defined as zero. The internuclear distance at the energy minimum is the equilibrium distance d at 0 K.

Therefore, melting and boiling point temperatures as well as enthalpies of melting and vaporization increase from He to Rn (see Table 3.2).

In summary, we can state that the dispersion effect dominates if the atoms or molecules are close to each other. Only for small and "hard" molecules with large dipole moments such as H_2O and HCN the dipole effect is the more important type of interaction. Of course, dispersion effects also occur *intramolecularly*. They are, for instance, responsible for the higher stability of branched alkanes C_nH_{2n+2} compared to their chain-like isomers. Even *within* the chlorine molecule Cl_2, the

Table 3.2: Melting and boiling points (in Kelvin) as well as enthalpies (kJ mol^{-1}) of melting and of vaporization of the rare gases at ambient pressure.

	Melting point	Boiling point	ΔH^0 (melt.)	ΔH^0 (vap.)
Helium	0.95[a]	4.2	0.021	0.082
Neon	24	27	0.324	1.736
Argon	84	87	1.21	6.53
Krypton	117	121	1.64	9.1
Xenon	161	166	3.10	12.7
Radon	202	211	–	18.1

[a] Solidification of helium at 0.95 K requires a pressure of 2.6 MPa.

dispersion attraction between the two atoms is stronger than in the fluorine molecule F_2 and contributes to the total dissociation enthalpy.[5]

3.4 VAN DER WAALS Radii

In crystalline xenon at 5 K and ambient pressure, the atoms occupy positions that approximately correspond to the energy minimum shown in Figure 3.2 with an internuclear distance of 432 pm at which attractive and repulsive forces are balanced. The smallest internuclear distance in the cubic closest packed lattice is the VAN DER WAALS distance and half of this distance is defined as VAN DER WAALS radius. The other noble gases also crystallize in cubic closest packed structures with closest internuclear distances extrapolated to a temperature of 0 K as follows (in pm): Ne 315.5, Ar 375.5, Kr 399.1 and Xe 433.6.[7] With increasing temperature, these distances get larger due to anharmonic thermal vibrations. On the other hand, noble gases (E) form weakly bonded dimers E_2 and complexes EX (X = halogen) in the gas phase, which have also been used to derive atomic VAN DER WAALS radii (see Table 3.3). In this context, it should be kept in mind, however, that atoms are not hard spheres with rigid boundaries but do penetrate each other to some degree. Therefore, slightly varying data for atomic radii have been derived.

In case of molecular crystals, the shortest internuclear distances between neighboring atoms are used to derive the VAN DER WAALS radii. For example, the very compact crystal structure of *cyclo*-hexasulfur (S_6) yields 175 pm for the radius

7 J. Donohue, *The Structures of the Elements*, Wiley, New York, **1974**.

Table 3.3: Van der Waals radii derived from internuclear distances (in pm).[a]

H: 110					He: 143
B: 192	C: 170	N: 155	O: 152	F: 147	Ne: 158
	Si: 210	P: 180	S: 180	Cl: 175	Ar: 194
	Ge: 211	As: 185	Se: 190	Br: 183	Kr: 207
	Sn: 217	Sb: 206	Te: 206	I: 198	Xe: 228

[a] After D. G. Truhlar et al., *J. Phys.Chem. A* **2009**, *113*, 5806, and J. Vogt, S. Alvarez, *Inorg. Chem*. **2014**, *53*, 9260 (noble gases).

of the sulfur atom, while 180 pm are obtained from the structure of orthorhombic α-sulfur (S_8). Therefore, the data in Table 3.3 should be used with caution. Two like atoms may have slightly different distances and still be in contact. In addition, atoms in molecules deviate substantially from the spherical shape (see below) and different radii may apply in different directions. Covalent and VAN DER WAALS radii also depend on the oxidation state as well as on the coordination number (see Chapter 4.3).[8] Finally, crystal structures are determined at different sample temperatures and the molecular vibrations influence the average internuclear distances due to the anharmonicity of the potential energy curves.

VAN DER WAALS radii are used to construct *space-filling models* of molecules as shown in Figure 3.3. In this figure, r_1 and r_2 are VAN DER WAALS radii and r_3 and r_4 are covalent radii of which the latter two combined give the internuclear distance d (assuming additivity; see Section 4.3). Such geometrical models provide a nearly realistic picture of the shape of molecules.

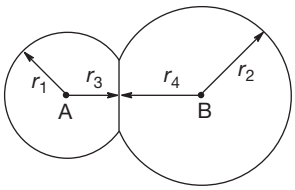

Figure 3.3: Space-filling model of a two-atomic molecule AB (r_1, r_2: van der Waals radii; r_3, r_4: covalent radii).

Distances between nonbonded atoms in a molecule or crystal that are substantially smaller than the sum of the VAN DER WAALS radii may imply weak covalent

8 For a discussion of the factors influencing VAN DER WAALS radii, see S. C. Nyburg, C. H. Faerman, *Acta Cryst*. **1985**, *341*, 274, and S. S. Batsanov, *J. Chem. Soc., Dalton Trans*. **1998**, 1541.

bonds, provided both atoms have suitable orbitals for either σ or π bonding. Examples are the molecules S_4N_4 and $[S_8]^{2+}$ with their weak *trans*-annular bonds (Sections 12.5 and 12.13).

On the other hand, geminal atoms are sometimes forced up to 80 pm closer than their VAN DER WAALS distances without any bonding interaction. For example, the chlorine atoms in the bent molecule Cl_2O are only 280 pm and in SCl_2 only 310 pm apart (VAN DER WAALS distance 350 pm; see Table 3.3). The fluorine atoms in SF_6 are only about 221 pm apart, although the VAN DER WAALS distance is 294 pm. Such close FF contacts are the main reason that OF_6 does not exist. Its nonbonding FF distances would have to be even smaller due to the reduced size of the oxygen atom. Likewise, the 1,3-distance between the oxygen atoms in SO_2, SO_3, NO_2, $[NO_2]^-$, $[ClO_2]^-$, $[SO_4]^{2-}$ and $[ClO_4]^-$ is about 40–90 pm less than the VAN DER WAALS distance. A similar situation applies to the iodine atoms in I_2O_5. In conclusion, nonbonded atoms can interpenetrate to some degree thereby generating repulsive forces, balancing the attractive bonding forces to give a stable molecular structure.

At very high pressures, the atoms in solid noble gases and other molecular crystals are forced to smaller internuclear distances resulting in novel physical properties. For example, solid xenon changes to a metallic state at pressures above 150 GPa. Under these conditions, the valence orbitals of neighboring atoms overlap and form an electronic band structure as in metals.

3.5 VAN DER WAALS Molecules

VAN DER WAALS interactions have been observed not only in condensed phases but also in the gas phase, despite the low bond energy (which has to be higher than the thermal energy for the interactions to persist). Sophisticated spectroscopic techniques have revealed that even noble gas atoms and nonpolar molecules form dimers in the gas phase. Such aggregates are termed VAN DER WAALS molecules or complexes.[9] The properties of such species have also been investigated by theoretical methods.[10] With rising pressure and decreasing temperatures even larger VAN DER WAALS clusters have been observed, which may be considered as intermediates between monomeric gaseous molecules and condensed phases as in liquids and crystals.

For example, gaseous argon contains 0.5% dimers (Ar_2) at 120 K and a pressure of 445 hPa. If compressed argon is expanded into a vacuum by a nozzle, the

9 J. S. Winn, *Acc. Chem. Res.* **1981**, *14*, 341. P. Schuster, *Angew. Chem. Int. Ed.* **1981**, *20*, 546–568. Special issues: *Chem. Rev.* **1994**, *94* and **2000**, *100*.

10 G. Chalasinski, M. M. Szczesniak, *Chem. Rev.* **1994**, *94*, 1723 and **2000**, *100*, 4227.

temperature drops drastically and clusters of up to 20 atoms are formed, which have been detected in such *molecular beams* by mass spectrometry. The bond energy of Ar_2 in the vibrational ground state is only 1.2 kJ $mol^{-1,}$ and the internuclear distance is 375.7 pm.[11] However, at room temperature many dimers of this type are already vibrationally excited. In case of hydrogen, the dimers $(H_2)_2$ show a still lower bond energy since the polarizability of hydrogen atoms is much lower compared to Ar. On the other hand, the species Ar·HCl and $Ar{\cdot}H_2O$ have been detected spectroscopically in mixtures of Ar and the corresponding hydrogen species. Similar *pre-reactive complexes* between molecules such as F_2 + H_2O may serve as precursors in chemical reactions and their geometry may influence reaction mechanisms.[12]

The complex between dimethyl sulfide and sulfur dioxide, $Me_2S{\cdot}SO_2$, shown in Figure 3.4 is a VAN DER WAALS molecule in which dispersion, induction and dipole effects play a role. Its gas phase structure has been determined by rotational spectroscopy as well as by quantum-chemical calculations and revealed a long sulfur–sulfur "bond" of 295 pm between the two molecules, which are oriented in such a way that their C_2 axes are almost parallel. The atomic charges of the two sulfur atoms differ by about 1.5 electrostatic units – very slightly positive in Me_2S and strongly positive in SO_2 – and therefore the interaction energy of −31 kJ mol^{-1} is mainly of electrostatic origin with some electron density transferred from the sulfur lone pair of Me_2S (HOMO) to the OSO antibonding MO (LUMO) of SO_2. In addition, the dipole vectors are antiparallel and the two O···H contacts also stabilize the molecule owing to the opposite charges of these atoms.[13]

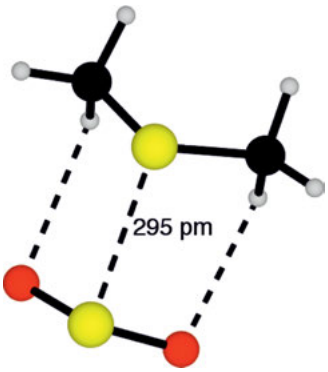

Figure 3.4: Molecular structure of the gaseous VAN DER WAALS molecule $Me_2S{\cdot}SO_2$.

11 The internuclear distances of He_2 and Ne_2 are 297.0 and 309.9 pm, respectively.
12 H. Bürger, *Angew. Chem. Int. Ed.* **1997**, *36*, 718.
13 U. Grabow, V. Barone et al., *Angew. Chem. Int. Ed.* **2018**, *57*, 15822.

Theoretical methods have revealed that *atoms in molecules* are no longer spherical, and that negatively or positively charged atoms in polar molecules may show regions of differing electrostatic potential on their surfaces. These potentials are the origin for a special type of intermolecular interaction, which has first been observed for halogen compounds and therefore is called **halogen bonding**. Later, it has been observed with chalcogens too; this important effect will be discussed in Section 4.7.

4 Bond Properties

4.1 Introduction

The theories of different types of chemical bonding have been discussed in previous chapters, but we did not yet define what *a chemical bond* is and whether and how it can be treated separately from the rest of the molecule. According to IUPAC,[1] the definition is as follows:

There is a chemical bond between two atoms or groups of atoms in the case that the forces acting between them are such as to lead to the formation of an aggregation with sufficient stability to make it convenient for the chemists to consider it as an independent molecular species.

Then we may ask more questions:

(a) Do all covalent bonds have similar properties?
(b) How can covalent bonds be characterized experimentally?
(c) Which measurable differences are there between various types of σ bonds on the one hand and between σ and π bonds on the other hand?
(d) How can we explain the different reactivities of covalent bonds?

It turns out that a covalent bond is a part of a molecule that in principle cannot be treated separately from the rest of the molecule since the valence electrons are partially delocalized and any change in one part of a molecule has an impact on the other parts. Experimentally accessible bond properties are the bond enthalpy (B.E.), the dissociation enthalpy (D), the internuclear distance (d) and the valence force constant (f_r). Most of these parameters can also be approximated using quantum-chemical theory.

Often the term "bond order" is used in context with covalent bonds although it is not an observable parameter and has no real physical meaning. Nevertheless, *single bonds* as in ethane $H_3C–CH_3$, *double bonds* as the central bond in ethene $H_2C=CH_2$ and *triple bonds* as in acetylene $HC\equiv CH$ are standard terms in organic chemistry while in inorganic chemistry they are less meaningful. In this chapter, we will elaborate that the strength or "order" of covalent bonds between main group elements can adopt any value between 0 and 3.[2] In addition, a covalent bond may consist of several components as, for example, in thionyl chloride where the

1 IUPAC: International Union of Pure and Applied Chemistry.

2 Bonds of higher order are possible between transition metals through involvement of d orbitals resulting in bonds of δ symmetry.

https://doi.org/10.1515/9783110578065-004

covalent interaction between sulfur and oxygen is superimposed by an ionic interaction as illustrated by the following structures:

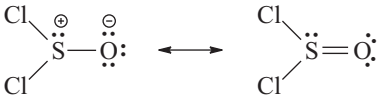

In other words, the SO bond is neither "single" nor "double" but rather of intermediate strength ("multiple bond").[3] The double arrow ↔ is borrowed from valence bond (VB) theory and describes this bonding situation as a "resonance" between two hypothetical structures of different electron distribution but identical nuclear positions ("canonical structures"). Lacking an alternative description of polar covalent bonds, we will use this kind of symbols quite often to visualize the bonds in molecules.

4.2 Bond Enthalpy and Dissociation Enthalpy

4.2.1 Diatomic Molecules

Let us consider the formation of a diatomic molecule AB from the gaseous atoms A and B, both having a singly occupied low-lying atomic orbital available to form a covalent bond:

$$A(g.) + B(g.) \longrightarrow AB(g.)$$

As atom A approaches B, the energy of the system changes according to the curve shown in Figure 4.1. This function results from a complex superposition of attractive and repulsive COULOMB forces. The attractive forces originate from the quantum-chemical interaction of the two atomic orbitals and the stabilization of the formerly unpaired valence electrons in a bonding molecular orbital of lower energy. At the same time the kinetic energy of the valence electrons changes due to the larger space in the molecular orbital but also due to the contraction and polarization of the formerly spherical atomic orbitals (see Section 2.4.1). On the other hand, at very small distances R the repulsion between the two nuclei becomes dominant. In other words, the *potential curve* in Figure 4.1 describes the total energy E of the system (A,B) as a function of R and not the potential energy alone.

At very large distances R, the energy E is defined as zero. At the equilibrium position of the molecule, that is, at the energy minimum of the potential curve, the internuclear distance equals R_e and the bond energy B.E. is at its maximum (although the total energy is negative). In spectroscopy, this energy is normally symbolized as

3 I. Love, *J. Phys. Chem. A* **2009**, *113*, 2640.

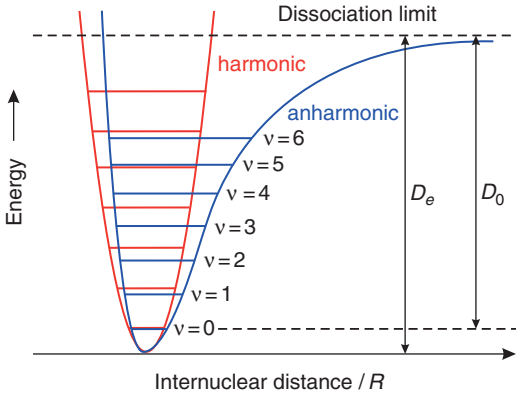

Figure 4.1: Total energy of a covalent molecule AB as a function of the internuclear distance R (D_0: dissociation energy at 0 K; D_e: bond energy (B.E.). The curvature at energy minimum is equivalent to the valence force constant f_r. The red curve represents the parabolic potential according to HOOKE's law, while the more realistic anharmonic MORSE potential is shown in blue. The vibrational spacings of the energy levels ν = 1–6 have been exaggerated for clarity.

D_e (the index e means *equilibrium*).[4] Since spectroscopic experiments are usually carried out at constant pressure rather than at constant volume, the above-mentioned "energies" are in fact *enthalpies*, which become identical to the energies only at 0 K. Therefore, the term enthalpy is to be preferred and will exclusively been used in the following sections (the two terms are often mixed up in the scientific literature).

When atoms A and B are combined to a molecule AB only the *dissociation enthalpy* D_0 is liberated, which is smaller than the total bond enthalpy D_e (the subscript "0" indicates the temperature of the experiment). The difference D_e–D_0 defines the zero-point energy (ZPE). This is the vibrational energy retained by the molecule even at 0 K when all degrees of freedom of translation and rotation are frozen.[5] The ZPE is a consequence of the requirements of HEISENBERG's uncertainty principle. Thus, for a diatomic molecule, ZPE = $^1/_2\ h\nu$ (h is PLANCK's constant; ν the frequency of the ground state vibration of molecule AB). This frequency may be obtained from vibrational spectra (see Section 4.4). For 1 mol H_2, it is given as follows (N_A = AVOGADRO's constant):

4 Physicists often use the symbols R_e or r_e for the internuclear distance at the potential minimum, but chemists usually prefer d for the internuclear separation.

5 Vibrational excitation does not change the volume, and energy and enthalpy are identical. Therefore, we use the traditional terms vibrational *energy* and ZPE rather than *enthalpy*. For the question whether bonds should be characterized by their energy or enthalpy, see R. S. Treptow, *J. Chem. Educ.* **1995**, *72*, 497.

$$\frac{1}{2} h \nu N_A = 0.5 \cdot (6.626 \cdot 10^{-34}) \cdot (1.25 \cdot 10^{14}) \cdot (6.023 \cdot 10^{23}) = 25 \text{ kJ mol}^{-1}$$

The B.E. results as follows:

$$\text{B.E.} = D_0 + \frac{1}{2} h \nu N_A = 432 + 25 = 457 \text{ kJ mol}^{-1} \text{ (at 0 K)}$$

For diatomic molecules the value of $^1/_2\ h\nu$ is largest for H_2 since the frequency ν rapidly decreases with increasing mass of the atoms (H_2: $\nu = 1.25 \cdot 10^{14}$, O_2: $\nu = 0.47 \cdot 10^{14}$, Cl_2: $0.17 \cdot 10^{14}$ s^{-1}). For example, the ZPE of O_2 is only 9 kJ mol^{-1} and of Cl_2 it is 3 kJ mol^{-1}. Since these data are of the same order of magnitude as the experimental errors of D, the difference between B.E. and D_0 is often neglected. In case of polyatomic molecules with many vibrational degrees of freedom, however, the ZPE can be substantially higher (see Section 4.4.3).

Since the energy of the molecule AB does not correspond to the minimum of the potential energy curve but rather to the lowest vibrational level, the internuclear distance permanently changes in a vibrational motion between the two extreme values at the intersections of this level and the curve shown in Figure 4.1. In experimental structure determinations, the *average value* of these two extremes is defined as *bond length d*. This average length at 0 K (d_0) is not identical to the internuclear distance at the minimum (R_e or r_e) but is slightly larger due to the *anharmonicity* (asymmetry) of the potential curve. The higher the temperature, the larger the difference between d and R_e.

Dissociation enthalpies D may be calculated from thermodynamic data[6] or derived from UV band spectra of gaseous molecules. From D_0 and vibrational spectra, the bond energy B.E. can be calculated. For diatomic molecules D_0 is equivalent to the *atomic enthalpy of formation* at 0 K, that is, the enthalpy liberated during molecule formation from gaseous atoms. For reasons explained below, D depends on the temperature: $D_0(H_2)$ = 432.1 kJ mol^{-1} and $D_{300}(H_2)$ = 436.0 kJ mol^{-1}; this small difference, however, is often neglected. In case of H_2 all vibrations except for the zero-point vibration are practically frozen at 300 K. The remaining three translational degrees of freedom require an energy of 3/2 RT and the two rotational degrees of freedom another RT (R: universal gas constant = 8.314 J K^{-1} mol^{-1}). In other words, the *thermal energy* of H_2 at 300 K is by 5/2 RT larger than at 0 K. Two separated H atoms, on the other hand, possess just six translational degrees of freedom and their thermal energy is 6/2 RT or 3RT. Therefore, on dissociation of H_2 into atoms the thermal

6 I. Barin, *Thermochemical Data of Pure Substances*, Parts I and II, 2nd ed., VCH, Weinheim, **1993**. M. W. Chase et al., *NIST-JANAF Thermochemical Tables*, 4th ed., *J. Phys. Chem. Ref. Data Monograph* 9, Woodbury, NY, **1998**, Suppl. 1. P. J. Linstrom, W. G. Mallard (eds.), *NIST Chemistry Webbook*, NIST Standard Reference Data Base no. 69, June **2005**, National Institute of Standards and Technology (http://webbook.nist.gov/chemistry/). T.-R. Luo, *Comprehensive Handbook of Chemical Bond Energies*, CRC Press, Boca Raton, FL, **2007**.

energy of the system increases by 1/2 RT (1.247 kJ mol^{-1} at 300 K), which is the amount that needs to be provided in addition to the dissociation energy. But the increase in volume upon dissociation requires another energy given by $p\Delta V = RT$. Consequently, the difference between D_{300} and D_0 is at least 3/2 RT or 3.74 kJ mol^{-1}. For heavy dihydrogen (D_2), the dissociation energy is D_0 = 439.6 kJ mol^{-1}, since the higher mass of the atoms leads to a lower vibrational frequency and thus to a smaller ZPE.[7] At high temperatures, the additional vibrational excitation energy must be taken into account.

As shown here and in previous chapters, an energy minimum of the potential curve of the molecule AB is the condition for the formation of a covalent bond. Normally, this minimum corresponds to a negative total energy (stable molecule). But there are few cases in which the energy minimum is at a positive value. For example, the cation $[He_2]^{2+}$, isoelectronic with H_2, is higher in energy than 2 He^+ by approximately 835 kJ mol^{-1} due to strong nuclear repulsion. For the bond dissociation, however, a barrier of approximately 135 kJ mol^{-1} needs to be overcome; thus, the molecule is metastable. Its energy corresponds to a *local minimum* of the potential energy curve. The internuclear distance of $[He_2]^{2+}$ is 70.25 pm, slightly smaller than in H_2 (74.14 pm). Interestingly, the electronically excited helium molecule He_2^* with the electron configuration $(1\sigma_g)^2(1\sigma_u)^1(2\sigma_g)^1$ is also a bound state since there are three bonding electrons and only one antibonding electron (compare Figures 2.18 and 2.22).

4.2.2 Polyatomic Molecules

In polyatomic molecules such as SO_2, H_2O or BF_3, which contain only like bonds, the B.E.s of the symmetry-related bonds are identical. During a *stepwise dissociation*, however, the required enthalpies are unequal as the following examples demonstrate:

$$\begin{array}{lll} SO_2 \longrightarrow SO + O & & D_1 = 546 \text{ kJ mol}^{-1} \\ SO \longrightarrow S + O & & D_2 = 517 \text{ kJ mol}^{-1} \\ \hline SO_2 \longrightarrow S + 2\,O & & \Delta H^\circ = 1063 \text{ kJ mol}^{-1} \end{array}$$

These data apply to the species in their electronic ground states. In case of SO_2, $D_1 > D_2$, since dissociation of the first SO bond generates sulfur monoxide containing a longer (weaker) SO bond (148 pm) compared to that of SO_2 (143 pm). Consequently, dissociation of SO into atoms requires a lower enthalpy. Sulfur monoxide is a highly reactive molecule with a triplet ground state in analogy to O_2. The rearrangement of valence electrons during dissociation of bonds in polyatomic molecules is a common phenomenon.

7 B. Jeziorski et al., *J. Chem. Theory Comput.* **2009**, *5*, 3039.

For the stepwise dissociation of carbon dioxide, one obtains $D_1 < D_2$ since the first dissociation step generates a very stable carbon monoxide molecule with an internuclear distance of 113 pm compared to 116 pm in CO_2:

$$\begin{array}{lll} CO_2 \longrightarrow CO + O & & D_1 = 532 \text{ kJ mol}^{-1} \\ CO \longrightarrow C + O & & D_2 = 1076 \text{ kJ mol}^{-1} \\ \hline CO_2 \longrightarrow C + 2\,O & & \Delta H^\circ_{298} = 1608 \text{ kJ mol}^{-1} \end{array}$$

The stabilization of the remaining bond during CO_2 dissociation results in a lower dissociation enthalpy for the first step but at the expense of a much larger amount of energy for the second.

For symmetrical binary molecules AB_n, containing only identical bonds, a *mean bond enthalpy* (m.B.E.) is defined as arithmetic mean of the single dissociation enthalpies. For SO_2 we obtain:

$$\text{m.B.E.} = \frac{1}{2}(D_1 + D_2) = \frac{1}{2} \cdot 1063 = 531.5 \text{ kJ mol}^{-1}$$

Electron reorganization during dissociation processes may change not only internuclear distances but also valence angles. For example, the homolytic dissociation of one bond of the tetrahedral CCl_4 molecule to generate CCl_3 and a Cl atom takes place at 1000 °C. The pyramidal fragment CCl_3 rearranges simultaneously to the trigonal-planar $CCl_3^\bullet$ radical, which has been trapped in a cold matrix and characterized by low-temperature IR and ESR spectra:

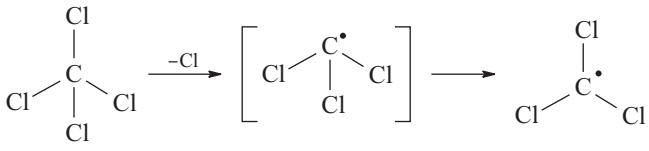

T_d C_{3v} D_{3h}

In other words, the bond angles change during this dissociation from 109.5° in CCl_4 to 120° in $CCl_3^\bullet$. The same holds for the thermal dissociation of CCl_3Br and CCl_3I into $CCl_3^\bullet$ and a bromine or iodine atom, respectively, which require considerably lower temperatures.

If a molecule contains different bonds, m.B.E.s cannot be calculated from experimental dissociation enthalpies. In this case, binary compounds may serve as models in a first approximation, possibly with some adjustments based on a comparison of bond distances and force constants with binary compounds. For example, the bonds in BCl_2F could be compared to those in BCl_3 and BF_3, respectively. The sum of all bond dissociation enthalpies of BCl_2F must be identical to its negative enthalpy of formation from atoms.

The m.B.E.s of typical "single," "double" and "triple" bonds between two nonmetallic elements E are usually found in the following ranges:

E–E: 100–565 kJ mol^{-1}
E=E: 420–810 kJ mol^{-1}
E≡E: 800–1090 kJ mol^{-1}

As mentioned earlier, "bond orders" cannot be measured but are always derived from experimentally determined parameters. As they are based on various *particular definitions*, the published bond orders of covalent bonds in molecules can vary widely.

Table 4.1 contains m.B.E.s that are frequently used in the chemical literature. The highest single bond values are obtained for strongly polar bonds such as BF, SiF, HF, PF, CF, AsF, OH and GeF with B.E.s above 450 kJ mol^{-1}. In fact, there is a linear correlation between the bond enthalpy D_{AB} of diatomic main-group molecules AB and the difference in electronegativities ($\Delta\chi$) of atoms A and B.[8] $D_{AA,}$ respectively, D_{BB} are the B.E.s of the homonuclear diatomic molecules A_2 and B_2 (in kJ mol^{-1}):

$$D_{AB} = \sqrt{D_{AA} \cdot D_{BB}} + 32.06 \cdot \Delta\chi$$

The m.B.E. of *homonuclear single bonds* of the main group elements systematically depend on the atomic number *Z* as shown in Figure 4.2. A systematic decrease of *D* is observed within each group of the Periodic Table but there are some interesting exceptions. Diatomic molecules of the alkali metals are present in the vapors of these elements. Their B.E.s decrease from approximately 100 kJ mol^{-1} for Li_2 to approximately 38 kJ mol^{-1} for Cs_2. As in the H_2 molecule, the covalent bonds in these molecules are formed from the singly occupied *s* orbitals. But the overlap integral between larger *s* orbitals decreases sharply with increasing principal quantum number; the electron density is distributed in a more and more diffuse cloud with the increasing size of the corresponding orbitals. In addition, the increasing nuclear charge and rising number of inner electrons result in an increasing repulsion between the "cores" of the heavier atoms. Therefore, H_2 has the strongest homonuclear single bond known, while the molecule Cs_2 has one of the weakest covalent bonds with an internuclear distance of 465.1 pm. In general, the weakest homonuclear single bonds are formed between the heaviest atoms.

A similar trend can be observed in Group 13 of the Periodic Table. The diatomic molecules B_2 to In_2 have single bonds; their dissociation enthalpies have been used as B.E.s (for B_2, see Table 2.10 in Section 2.4.3). For Group 14 elements, the single B.E.s of diamond, silicon, germanium and α-tin have been used,

8 R. R. Reddy, T. V. R. Rao, R. Visvanath, *J. Am. Chem. Soc.* **1989**, *111*, 2914.

Table 4.1: Mean bond enthalpies, m.B.E. (25 °C; kJ mol^{-1}), with neglection of zero-point energies (data partly from *Encycl. Inorg. Chem.* 2005, Vol. 1, p. 442; see also ref. 6).

Single bond enthalpies:	**H**	**B**	**C**	**N**	**O**	**F**	**Si**	**P**	**S**	**Cl**	**Ge**	**As**	**Se**	**Br**	**Sb**	**Te**	**I**
H	432																
B	390	293															
C	411	369	362														
N	386	–	305	159													
O	459	536	358	201	138												
F	565	643	485	283	190	155											
Si	326	–	301	–	452	582	226										
P	322	–	264	300	352	490	214	201									
S	363	–	272	247	–	360	226	230	264								
Cl	428	444	327	201	218	251	391	326	255	240							
Ge	289	–	243	–	–	452	–	–	–	349	188						
As	247	–	–	–	301	484	–	–	–	322	–	146					
Se	276	–	234	–	–	285	–	–	–	200	–	–	193				
Br	362	365	285	243	201	249	310	264	217	216	276	258	226	190			
Sb	–	–	–	–	–	440	–	–	–	314	–	–	–	260	126		
Te	238	–	≈200	–	–	330	–	–	–	311	–	–	–	176	–	149	
I	295	336	213	201	201	281	234	184	–	211	212	200	–	175	195	121	151

Enthalpies of multiple bonds:							
C=C 582	C=N 615	C=O 699	N=N 418	P=P 290	O=O 494	S=O 420	C=S 573
C≡C 759	C≡N 887	C≡O 1072	N≡N 941	P≡P 481	S=S 423	Se=O 425	C=Se 456

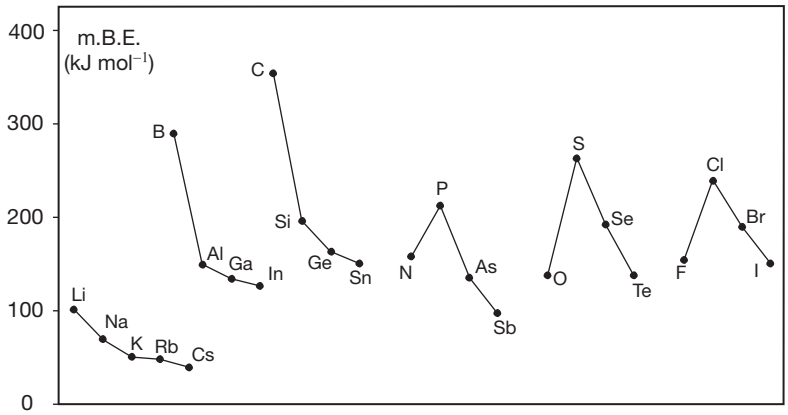

Figure 4.2: Dependence of the mean bond enthalpies (25 °C; kJ mol^{-1}) of homonuclear single bonds between two main group elements of the Periodic Table on the period and the atomic number. For alkali metals, the Group 13 elements, and for halogens the dissociation enthalpies of the diatomic molecules E_2 have been used. For the other groups, the data in Table 4.1 were employed.

which all crystallize in cubic structures with tetrahedrally coordinated atoms. Again, these enthalpies decrease with increasing size of the atoms (Figure 4.2).

However, in Groups 15 through 17, the first elements (N, O and F) do not follow the trend of their heavier congeners. The single bonds NN, OO and FF are surprisingly weak, which led to extensive discussions in the chemical literature.[9] These weak bonds are responsible for the high reactivity of hydrazine N_2H_4, hydrogen peroxide H_2O_2 and elemental fluorine F_2. The origin of these weaker bonds is complex. On the one hand, the PAULI repulsion between the lone pairs in these relatively small atoms lowers the homonuclear dissociation enthalpy. On the other hand, atoms N, O and F are quite compact due to their high effective nuclear charge. The corresponding overlap integrals are consequently small, and because of the high local electron density even the repulsion between lone pairs and bonding electrons becomes significant.[10]

The weakening effects discussed above are not present in the carbon–carbon single bond, which is one of the strongest homonuclear bonds. In case of PP, SS and ClCl bonds, the local electron density is much smaller and the larger internuclear distances reduce the repulsion between the lone pairs of adjacent atoms. The heteronuclear single bonds NO, NF, OF and ClO, however, are also relatively weak, with the consequence that most oxides of nitrogen and chlorine are endothermic

9 A. Kovacs, C. Esterhuysen, G. Frenking, *Chem. Eur. J.* **2005**, *11*, 1813.
10 D. Lauvergnat, P. C. Hiberty, *J. Mol. Struct. (Theochem)* **1995**, *338*, 283.

substances. The low B.E.s of NN and OO single bonds are also responsible for the fact that elemental nitrogen and oxygen are gases while phosphorus and sulfur are solids at ambient conditions (e.g., P_4 and S_8). In the following section, the thermodynamic basis for these observations will be outlined in detail.

4.2.3 Why Is Oxygen a Gas and Sulfur a Solid?

The strongly differing molecular structures of elemental oxygen (O_2) and sulfur (S_8) at standard conditions can be explained by a simple thermodynamic calculation using the data in Table 4.1. We first assume that oxygen formed a cyclic crown-shaped molecule O_8 of D_{4d} symmetry in analogy to *cyclo*-S_8, and then calculate the reaction enthalpy of a hypothetical gas phase equilibrium between four O_2 and O_8:

$$4\ O_2(g.) \rightleftharpoons O_8(g.) \qquad (1)$$

Equilibrium (1) would be on the left-hand side if the GIBBS energy $\Delta G°(1)$ of this reaction were positive. Such reactions are called *endergonic*. The value of $\Delta G°(1)$ can be estimated from the reaction enthalpy $\Delta H°$ if the temperature is sufficiently low (e.g., 300 K). According to the second law of thermodynamics:

$$\Delta G^\circ = \Delta H^\circ - T \cdot \Delta S^\circ$$

It follows that $\Delta G° > 0$ for $\Delta H° >> 0$ and $\Delta G° < 0$ for $\Delta H° << 0$ if $T{\cdot}\Delta S°$ is small (e.g., at room temperature or lower).

In the hypothetical oligomerization of four O_2 molecules to cyclic O_8, four O=O double bonds of 498 kJ mol^{-1} each would be cleaved and eight O–O single bonds of B.E. 138 kJ mol^{-1} would be formed. Using the data in Table 4.1, the resulting enthalpy balance would then be

$$\Delta H^\circ_{300} = 4 \cdot 498 - 8 \cdot 138 = +887\,\mathrm{kJmol^{-1}}\ (O_8)$$

Thus, O_2 is more stable at 300 K than O_8 since $\Delta H° >> 0$ and therefore $\Delta G° > 0$.

The analogous equilibrium between S_2 molecules and gaseous S_8 has been observed in sulfur vapor at high temperatures (see Section 12.4.1):

$$4\ S_2(g.) \rightleftharpoons S_8(g.) \qquad (2)$$

In this case, the reaction is highly exothermic due to the much larger S–S single B.E.:

$$\Delta H^\circ_{300} = 4 \cdot 425 - 8 \cdot 264 = -410\,\mathrm{kJmol^{-1}}\ (S_8)$$

Since $\Delta H° << 0$, we expect $\Delta G° < 0$, that is, the reaction should be *exergonic*, and the equilibrium (2) should be on the right side at 300 K.

The above calculations are just first approximations. To obtain the correct values of $\Delta G°$ for reactions (1) and (2), the contribution of the entropy $S°$ must be taken into account.[11] For the two sulfur molecules, the following values apply:

$$S°_{300}(S_2)\text{: } 0.228 \text{ kJ mol}^{-1}\text{ K}^{-1} \quad S°_{300}(S_8)\text{: } 0.424 \text{ kJ mol}^{-1}\text{ K}^{-1}$$

Thus, the entropy change $\Delta S°_{300}$ for reaction (2) is -0.488 kJ mol^{-1} and the product $T{\cdot}\Delta S°_{300}$ is equal to -145 kJ mol^{-1}. From these data it follows that $\Delta G°_{300}$ (2) = -265 kJ mol^{-1}. For the chemical equilibrium of gaseous species, the law of mass action is (p_i: partial pressure of species i):

$$K_p = \frac{p\,(S_8)}{p^4(S_2)}$$

Since $\ln K_p = -\Delta G°/RT$, the equilibrium constant K_p of reaction (2) can be calculated as $6{\cdot}10^{45}$ at 300 K. In other words, the concentration of S_2 is negligible at this temperature.

However, sulfur vapor heated well above 500 K contains all molecules from S_2 to S_7 formed by thermal degradation of S_8, and above 1000 K S_2 is the dominating species (Section 12.4.1). The calculation of the GIBBS energy change ($\Delta G°$) of reaction (2) at 1000 K requires the following entropy data that strongly depend on temperature:

$$S°_{1000}(S_2)\text{: } 0.270 \text{ kJmol}^{-1}\text{ K}^{-1}$$

$$S°_{1000}(S_8)\text{: } 0.631 \text{ kJmol}^{-1}\text{ K}^{-1}$$

$$\Delta S°_{1000} = \ -0.449 \text{ kJmol}^{-1}\text{ K}^{-1}$$

From these data we obtain $T{\cdot}\Delta S°_{1000} = -449$ kJ mol^{-1} and $\Delta G°_{1000}(2) = +39$ kJ mol^{-1}. In other words, at 1000 K, equilibrium (2) is completely on the left-hand side!

The molecule S_2 has a triplet ground state as does O_2. Their high B.E.s and short internuclear distances suggest that both molecules contain "double bonds." This shows that elements of higher periods can also form molecules with stable double bonds. Thiothionyl fluoride $S{=}SF_2$ is another example for a molecule with an SS double bond of almost the same bond length (Section 12.12.2). The fact that S_2 does not exist at room temperature like O_2 does is not the consequence of its weak covalent bond but is the result of the strong single bonds in S_8, which are much stronger than OO single bonds. Therefore, the polymerization of S_2 is strongly

11 The entropy of a gaseous molecule is a function of state and depends only on its mass, geometry, fundamental vibrations and the temperature and can thus be calculated by methods of statistical thermodynamics, assuming an ideal gas.

exothermic and exergonic at 300 K. At high temperatures, the *entropy increase* $\Delta S°$ is responsible for the disintegration of S_8 to smaller sulfur species.

Mean B.E. values are well suitable for thermodynamic considerations of this kind. With the data in Table 4.1, it can also be shown why *elemental nitrogen* is a gas while phosphorus exists as solid allotropes at 25 °C and ambient pressure. The dimerization of P_2 to the tetrahedral P_4 is exothermic while the hypothetical reaction of N_2 to the analogous N_4 would be strongly endothermic. Again, it is the weakness of the NN single bonds keeping N_2 from polymerization. Only under extreme conditions (2000 K, 110 GPa), nitrogen forms a solid phase with NN "single bonds" and trigonal-pyramidal coordination of the atoms, in analogy to the structure of black phosphorus, which is the thermodynamically stable form of this element. The data in Table 4.1 should, however, not be applied to such high-pressure phases exhibiting totally different bond lengths. Phosphorus compounds with PP double bonds (diphosphenes) are discussed in Section 10.7.

Reaction mechanisms deal with the homolytic cleavage of *individual bonds*. In this case, *bond dissociation enthalpies* rather than m.B.E.s should be used. The values of these two quantities can be quite different. For example, the m.B.E. of the S_8 ring is 264 kJ mol^{-1}, which is the arithmetic mean of all eight bond dissociation enthalpies. But for the homolytic cleavage of just the first bond of S_8 (ring opening reaction with formation of a chain-like diradical) only 154 kJ mol^{-1} are needed at 25 °C since some of the remaining bonds are stabilized by electron rearrangement.[12]

4.3 The Internuclear Distance

The internuclear distance d of a covalent bond is a characteristic bond property, as the B.E. is. For example, in various chlorosilanes the values of d_{SiCl} range from 199 to 205 pm, provided the coordination numbers of the silicon atoms are identical (Table 4.2).

As a first approximation, internuclear distances of covalent bonds consist of independent contributions from both atoms called covalent atomic radii r. In some cases, these radii can be obtained from *homonuclear single bonds* assuming additivity. For example, in diamond the internuclear distance of the CC bonds is 154.5 pm, which must be equal to $2r$. Consequently, the single bond radius of the tetrahedrally coordinated carbon atom results in $r_1(C) = 77.3$ pm. In a similar fashion, the bond length of the chlorine molecule (198.8 pm) yields $r_1(Cl) = 99.4$ pm. It is then possible to predict the internuclear distance of the four equivalent CCl bonds in the tetrahedral CCl_4 molecule as

$$d_{CCl} = r_1(C) + r_1(Cl) = 77.3 + 99.4 = 176.7 \text{ pm}$$

12 M. W. Wong, Y. Steudel, R. Steudel, *Chem. Phys. Lett.* **2002**, *364*, 387.

Table 4.2: Internuclear distances d_{SiCl} of various chlorosilanes (Ph: phenyl).

Compound	d_{SiCl} (pm)
$SiClF_3$	199
$PhSiCl_3$	200
CCl_3SiCl_3	201
Si_2Cl_6	201
$SiCl_4$	202
$(SiCl_3)_2O$	202
$SiCl_3SH$	202
$HSiCl_3$	202
H_2SiCl_2	202
H_3SiCl	205

The predicted value is almost identical to the experimental bond length of 176.6 pm. For the hydrogen atom, however, r_1 is not derived from the H_2 molecule but rather from the internuclear distances of several heteronuclear EH bonds (E represents nonmetal).

If the *additivity theorem* of atomic radii is applied to elemental silicon (diamond structure; d_{SiSi} = 235.2 pm), the single bond radius of the silicon atom is obtained as 117.6 pm. Using r_1(Cl) = 77.3 pm, the SiCl single bond distance in chlorosilanes is then predicted as 217.0 pm. The data in Table 4.2 demonstrate, however, that corresponding compounds have shorter than predicted SiCl bonds. The electronegativities of Si (2.1) and Cl (3.2) differ substantially and the polarity of the SiCl bond obviously causes a bond contraction due to the additional COULOMB attraction (compare, e.g., SiH_3Cl with $SiClF_3$).

An alternative interpretation of the bond shortening proposes a partial delocalization of the lone pairs of the chlorine atoms into empty antibonding molecular orbitals of t_2 symmetry at silicon in a similar fashion as in the sulfate anion (Section 2.4.10). This *hyperconjugation* leads to the formation of a dative bond of approximate π symmetry (Section 2.6), as in many other molecules and ions. Summing up, the definition of covalent atomic radii is not trivial; therefore, the structures of hundreds of molecules were required to obtain the data in Table 4.3, calculated by a least-squares fit.[13]

Covalent double and triple bonds are shorter than single bonds; therefore, the corresponding atomic radii are smaller. Such radii have been derived from suitable bond length data assuming additivity.[14] For example, the triple bonds in N_2 and acetylene (C_2H_2) yield the respective radii of nitrogen (r_3 = 55 pm) and carbon (r_3 = 60 pm).

13 Slightly different values have been published by P. Pyykkö, M. Atsumi, *Chem. Eur. J.* **2009**, *15*, 186.
14 P. Pyykkö et al., *Chem. Eur. J.* **2005**, *11*, 3511 and **2009**, *15*, 12770.

Table 4.3: Covalent single bond radii (r_1) of main group elements (in pm; estimated standard deviations in parentheses; after S. Alvarez et al., *Dalton Trans.* **2008**, 2832).

H	31(5)	C[a]	76(1)	N	71(1)	O	66(2)	F[b]	57(3)
B	84(3)	Si	111(2)	P	107(3)	S	105(3)	Cl	102(4)
		Ge	120(4)	As	119(4)	Se	120(4)	Br	120(3)
		Sn	139(4)	Sb	139(5)	Te	138(4)	I	139(3)

[a]For coordination number (C.N.) = 4; for C.N. = 3: 73(1) and for C.N. = 2: 69(1) pm.
[b]For fluorine, other values have also been proposed: R. J. Gillespie, E. A. Robinson, *Inorg. Chem.* **1992**, *31*, 1960.

Accordingly, the bond length in nitriles can be estimated as 115 pm, which is in good agreement with experimental data.

The strength of covalent bonds varies *continuously* and the same holds for internuclear distances. The weakest interaction is of VAN DER WAALS type while the strongest bonds possible for nonmetallic elements are triple bonds. In Table 4.4, internuclear distances of various nitrogen–oxygen bonds of differing strengths are listed with bond lengths ranging from 106 to 151.5 pm. Obviously, there is no correlation between the nitrogen oxidation state and the NO bond length. In addition, it is clear that the "bond orders" are not always integer numbers.

Table 4.4: Internuclear distances (pm) of NO bonds in nitrogen compounds of formal oxidation states –1 to +5 (term.: terminal bond).

$[NO]^+$	106	NO_2	119.7
ClNO	109	N_2O_4	121
ONONO (term.)	112	ON–O–NO	121
FNO	113.6	$HONO_2$ (term.)	121.0
NO	115	$[NO_3]^-$	122.2
$[NO_2]^+$	115.0	FNO_2	123
ONF_3	115.8	$[NO_2]^-$	123.6
cis-N_2O_2	116	$[cis\text{-}N_2O_2]^{2-}$	140
HONO (term.)	117.7	$HO–NO_2$	140.6
N_2O	118.4	HO–NO	143.3
FNO_2	118	$H_2N–OH$	147
$FONO_2$ (term.)	118.8	$ClO–NO_2$	147
$ClNO_2$	119	$FO–NO_2$	151.5
$ClONO_2$ (term.)	119		

Compounds of types AB_5, AB_4E and AB_3E_2 are special cases since apical bonds in trigonal–pyramidal molecules are longer than equatorial ones. For example, for PF_5: $d(PF_{ap})$ = 157.7 pm and $d(PF_{eq})$ = 153.4 pm. If the radius of the fluorine atom is assumed to be constant, it follows that the phosphorus atom has an apical single bond radius of 101 pm and of 96 pm in the equatorial direction. Similarly, sulfur in SF_4 (type AB_4E) and chlorine in ClF_3 (type AB_3E_2) have two differing covalent single bond radii each.

4.4 The Valence Force Constant

4.4.1 Diatomic Molecules

Two covalently bonded atoms form a *diatomic oscillator*. If some external force changes the internuclear distance, a counterforce F is created, as can be seen from the potential curve in Figure 4.1. In most molecules, F is approximately proportional to the change in internuclear distance Δr:

$$F = f_r \cdot \Delta r$$

This relationship is known as HOOKE's law. The factor f_r is the *valence force constant* in Newton per centimeter (N cm^{-1}).[15] The force constant describes the strength of a covalent bond by defining the *curvature of the potential curve at the minimum*; typical values of f_r in common molecules range from 1 to 25 N cm^{-1}.

Application of HOOKE's law implies that the potential curve at and near the minimum is parabolic:

$$E_{\text{pot}} = \int F \mathrm{d}r = \int f_r \cdot \Delta r \cdot \mathrm{d}(\Delta r) = \tfrac{1}{2} f_r (\Delta r)^2$$

However, this assumption is only true for small vibrational amplitudes Δr. Hydrogen atoms, owing to their small mass, have relatively large amplitudes and require corrections according to the MORSE potential shown in Figure 4.1.[16] Systems that can be described by HOOKE's law are called *harmonic oscillators*.

The frequency ν of such an oscillator depends only on the atomic masses m_1 and m_2 and on the valence force constant f_r:

$$\nu(\mathrm{s}^{-1}) = \frac{1}{2\pi} \cdot \sqrt{\frac{f_r \cdot (m_1 + m_2)}{m_1 \cdot m_2}}$$

In vibrational spectroscopy wavenumbers $\tilde{\nu}$ (or ω) are normally preferred over frequencies ν, defined as follows:[17]

$$\tilde{\nu} = \frac{1}{\lambda} = \frac{\nu(\text{frequency})}{c}$$

$\tilde{\nu}$: wavenumber (cm^{-1})
λ: wavelength (cm)
c: speed of light (cm s^{-1})

15 In the older literature, the following units are often used: 1 mdyn/Å = 1 N cm^{-1} and 1 dyn cm^{-1} = 10^{-5} N cm^{-1}. Thus, the force constant gives the force needed to stretch the bond by the unit length (or a tiny fraction of it) without any electron rearrangement.

16 The MORSE potential is given by $E(R) = D_e \cdot \{1 - \exp[-a(R - R_e)]\}^2$ with "a" being a constant.

17 K. Nakamoto, *Infrared and Raman Spectra of Inorganic and Coordination Compounds*, 6th ed., Part A, Wiley, New York, **2008**. J. Weidlein, U. Müller, K. Dehnicke, *Schwingungsspektroskopie*, 2nd ed., Thieme, Stuttgart, **1988**.

Unfortunately, wavenumbers are quite often also called "frequencies." In *stretching vibrations,* the internuclear distance changes periodically. Depending on the atomic masses and the force constant(s), stretching vibrations are observed in the range 150–4200 cm^{-1}. If relative masses M_1, M_2 and f_r in N cm^{-1} are used, then:

$$\tilde{\nu}(\mathrm{cm}^{-1}) = 1303 \cdot \sqrt{\frac{f_\mathrm{r} \cdot (M_1 + M_2)}{M_1 \cdot M_2}}$$

or

$$f_\mathrm{r}(\mathrm{N\ cm}^{-1}) = 0.589 \cdot 10^{-6} \cdot \tilde{\nu}^2 \cdot \frac{M_1 \cdot M_2}{M_1 + M_2}$$

In order to calculate f_r for a diatomic molecule, the wavenumber $\tilde{\nu}$ of the stretching vibration is determined by infrared or RAMAN spectroscopy or is derived from a band analysis of the UV spectra. Examples for $\tilde{\nu}$ and f_r are given in Table 4.5. Only the wavenumbers are proportional to the vibrational energy (1 cm^{-1} = 11.96 J mol^{-1}).

Table 4.5: Experimental wavenumbers $\tilde{\nu}$ of stretching vibrations and corresponding valence force constants f_r of diatomic molecules.

	$\tilde{\nu}$ (cm^{-1})	f_r (N cm^{-1})
H_2	4161	5.14
F_2	892	4.45
O_2	1556	11.4
N_2	2330	22.4
Cl_2	558	3.20
Br_2	317	2.37
I_2	207	1.60

4.4.2 Diatomic Groups

The model of the diatomic harmonic oscillator can sometimes be applied to larger molecules as well, if there is a diatomic group the stretching vibration of which is nearly independent of the vibrations of the rest of the molecule. For example, the SO group in thionyl compounds $X_2S{=}O$ and the PO group in phosphoryl compounds $X_3P{=}O$ may be treated as diatomic oscillators if the substituents X are halogen atoms. All 10 phosphoryl halides POX_3 with X = F, Cl, Br have been prepared and studied by IR spectroscopy. The wavenumbers of their PO stretching vibrations are shown in Figure 4.3 as a function of the PAULING electronegativities of the substituents X (taken from Table 4.8).

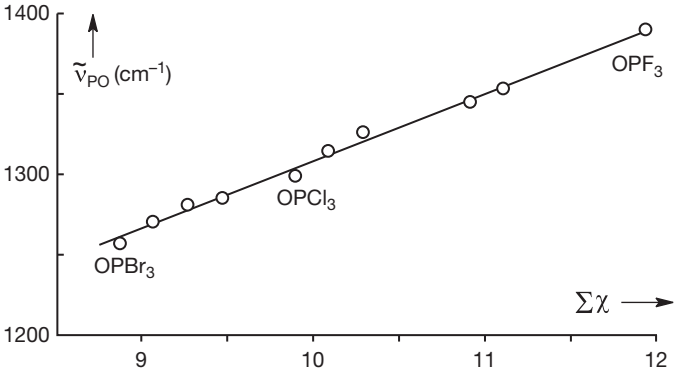

Figure 4.3: Wavenumbers $\tilde{\nu}$ of the PO stretching vibration in 10 phosphoryl halides POX_3 (X = F, Cl, Br) as a function of the sum of the PAULING electronegativities χ of the halogen atoms (including mixed halides).

Due to the partial double bond character of the PO bond, its stretching vibration is found at much higher wavenumbers than the PX stretching vibrations and can therefore be considered as decoupled from the rest of the molecule. The linear relationship shown in Figure 4.3 reflects the *inductive effect of the halogen atoms*, which can be explained by a resonance between the following LEWIS structures:

The higher the electronegativities of substituents X, the higher the positive charge at the phosphorus atom, which attracts the nonbonding lone pairs of oxygen. Therefore, the structure on the left-hand side is favored and corresponds to a higher PO bond strength. The resulting PO π bond can be rationalized by *hyperconjugation* between the $2p_\pi$ AOs of oxygen and the antibonding t_2 MO at phosphorus. The force constant f_r(PO) can then be calculated using the diatomic oscillator model.

4.4.3 Three-Atomic Molecules

Polyatomic molecules consisting of n atoms have $3n-6$ vibrational degrees of freedom. To calculate force constants, the geometry of the molecule must be known as well as all fundamental vibrations, possibly even for several isotopomers. However, the number of force constants increases rapidly with n, and even for a symmetrical three-atomic molecule AB_2 four force constants are needed to describe the molecular

vibrations since the potential energy E_{pot} depends on the *internal coordinates* r_i (internuclear distances) and α (bond angle) as follows:

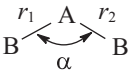

$$E_{pot} = f_r(\Delta r)^2 + \frac{1}{2} f_\alpha(\Delta\alpha)^2 + f_{rr}(\Delta r_1)(\Delta r_2) + f_{r\alpha}(\Delta r)(\Delta\alpha)$$

The vibrational energy is calculated as the sum of contributions from bond length and bond angle changes (Δ). As with the diatomic harmonic oscillator, each bond contributes $1/2\, f_r \cdot (\Delta r)^2$; thus, for two identical bonds: $f_r \cdot (\Delta r)^2$. The deformation of the angle by $\Delta\alpha$ contributes $1/2\, f_\alpha \cdot (\Delta\alpha)^2$ to the potential energy; f_α is called bending force constant. However, these contributions are not independent from each other since the change in bond length Δr_1 results in an reorganization of the valence electrons and consequently in a change of the other bond length (Δr_2) and possibly even of the bond angle. These contributions are being taken care of by *interaction force constants* between the two bonds (f_{rr}) and between the bonds and the angle ($f_{r\alpha}$). With this set of force constants, the harmonic vibrations of a three-atomic molecule of C_{2v} symmetry can be calculated exactly.

A molecule of this type (e.g., SO_2) has three vibrational degrees of freedom usually depicted by *normal coordinates*:

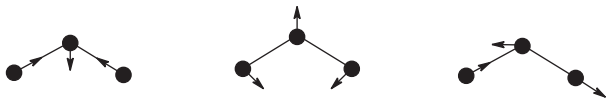

$\tilde{\nu}_s$ symmetric stretching vibration — δ deformation vibration — $\tilde{\nu}_{as}$ asymmetric stretching vibration

Since four force constants cannot be calculated from three vibrational wavenumbers additional experimental data are needed, for instance, from the spectra of isotopically substituted derivatives. In this case, it is assumed that the geometry is independent of the mass of the atoms and that the force constants are identical for all isotopomers. For harmonic vibrations this is indeed the case. If the oxygen atoms ^{16}O in SO_2 are partially or totally replaced by ^{18}O, six novel vibrational wavenumbers can be determined (Table 4.6).

Table 4.6: Fundamental vibrations of various gaseous isotopomers of sulfur dioxide (wavenumbers in cm^{-1}).

Isotopomer	$\tilde{\nu}_{sym}$	δ_{sym}	$\tilde{\nu}_{asym}$
$^{32}S^{16}O_2$	1151.4	517.8	1360.5
$^{32}S^{16}O^{18}O$	1122.5	507.3	1341.1
$^{32}S^{18}O_2$	1099.0	496.8	1316.3

From the data in Table 4.6 the following force constants of SO_2 (in N cm^{-1}) have been calculated:

$$f_r\text{: } 10.08 \quad f_\alpha\text{: } 0.79 \quad f_{rr}\text{: } 0.10 \quad f_{r\alpha}\text{: } 0.30$$

It is evident that changing the bond distance requires a much stronger force (higher energy) than bending the molecule ($f_r > f_\alpha$), and that the interaction constants are the smallest. Therefore, the wavenumbers of stretching vibrations are usually much higher than those of bending modes. In addition, we notice that a molecule is not as rigid as indicated by the popular ball-and-stick models used in chemical education.

The ZPE of a polyatomic molecule is given by the following sum over all fundamental vibrations (N_A: AVOGADRO's number; ν in s^{-1}, $\tilde{\nu}$ in cm^{-1}):

$$\text{ZPE (J mol}^{-1}) = 0.5 \cdot N_A \cdot \sum_i (h \cdot \nu_i) = 6.05 \sum_i \tilde{\nu}_i$$

For SO_2, the ZPE is 18 kJ mol^{-1} while for H_2O it is 55 kJ mol^{-1} since the OH stretching modes occur at much larger wavenumbers (>3000 cm^{-1}) than the SO stretching vibrations. At ambient temperature, the total vibrational energy of these molecules is even higher.

The absorption of infrared radiation by small molecules in the Earth's atmosphere is responsible for the **greenhouse effect**. At daytime, the Sun with its entire spectral width heats the solid surface of our planet, which in turn emits radiation in the infrared spectral region exclusively. A good fraction of this radiation is leaving the Earth through the atmosphere toward outer space. Certain infrared-active compounds with polar bonds in the atmosphere such as H_2O and CO_2, however, absorb infrared radiation resulting in a higher temperature of the atmosphere compared to that of a pure nitrogen–oxygen mixture (which does not absorb IR radiation). During previous centuries, a thermal equilibrium has been established between the surface temperature of the Earth and the temperature of its lower atmosphere, and present-day's life is well adjusted to this situation. In fact, the greenhouse effect is largely responsible for the benign temperature range on planet Earth as well as for the relatively small temperature changes between day and night, which are necessary prerequisites for life as we know it. But due to the progressive industrialization and the ensuing dramatic population growth, the concentration of CO_2 steadily increases and the same holds for other IR-active atmospheric pollutants such as N_2O and CH_4. Consequently, the global average surface temperature of the Earth rises steadily (atmosphere and oceans).

The *greenhouse potential* of a compound depends not only on its IR spectrum (number and intensity of absorptions) but also on its half-life in the atmosphere. Water-soluble species will be washed out with the rain but hydrophobic molecules such as CFCs (see Section 7.6) and SF_6 remain for long periods of time. To be greenhouse active, the absorptions of the novel pollutants must not be in the same regions where the dominating compounds H_2O and CO_2 already absorb most of the IR photons.

This holds for methane and nitrous oxide or "laughing gas," the greenhouse potentials of which are by factors of 21 (CH_4) and 300 (N_2O) larger than that of CO_2. For CFCs, these factors are even in the range of 10^3 to $2{\cdot}10^4$. Nevertheless, water vapor and carbon dioxide still contribute most (84%) to the present greenhouse warming effect.[18]

Most man-made greenhouse gases are emitted by the People's Republic of China and by the United States of America, in part due to their large populations. But it should be mentioned that the many active volcanoes are also substantial sources of CO_2 and SO_2 and these gases influence the global temperature markedly after major eruptions have occurred. Despite these additional amounts of IR active gases, however, volcanic activity normally has a net cooling effect in the short term due to the huge amounts of aerosols ejected into the higher atmosphere, which reflect the inbound solar radiation back into space for 1 or 2 years. However, the residence time of CO_2 in the atmosphere is larger than 100 years and, therefore, the emitted CO_2 results in a warming effect in the long term.

4.5 Relationships Between Different Bond Properties

In previous sections of this chapter, various bond properties of covalent molecules have been discussed, especially the internuclear distance *d*, often called bond length, the valence force constant f_r and the B.E. Figure 4.4 illustrates these properties for

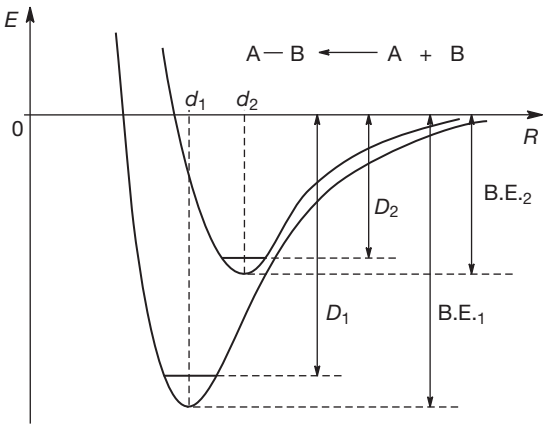

Figure 4.4: Potential energy curves for two molecules AB with covalent bonds of different strength (*R*, variable internuclear distance; *d*, distance at energy minimum; f_r, valence force constant ≡ curvature at minimum; *D*, dissociation enthalpy at 0 K; B.E., bond enthalpy at potential minimum).

18 D. Möller, *Chemistry of the Climate System*, de Gruyter, Berlin, **2010**. M. E. Elrod, *J. Chem. Educ.* **1999**, *76*, 1702. See also the special issue of *Chem. unserer Zeit* **2007**, *41*, issue 4.

two molecules with covalent bonds of different strength. It is obvious that d is small if B.E. is large and at the same time the curvature at the minimum (f_r) is also large.

Numerous empirical correlations between these bond properties have been established. The carbon–carbon bonds in well-known compounds may serve to illustrate these relationships. The corresponding data are given in Table 4.7. The CC bonds in diamond and ethane with sp^3 hybridization of the carbon atoms are usually considered as single bonds, while ethene contains a CC double bond and ethine (acetylene) a CC triple bond. As can be seen, increasing bond strength results in decreasing bond lengths and increasing force constants as well as increasing m.B.Es. While the internuclear distances change relatively little with bond strength, the valence force constants vary dramatically as do the B.Es.

Table 4.7: Properties of carbon–carbon bonds in well-known compounds (d, internuclear distance; f_r, valence force constant; m.B.E., mean bond enthalpy; for bonding details, see D. Yoshida et al, *Angew. Chem. Int. Ed.* **2018**, *57*, 7012).

Compound	Formula	d(CC) (pm)	f_r(CC) (N cm^{-1})	m.B.E. (kJ mol^{-1})
Diamond	C_n	154.5	–	357
Ethane	C_2H_6	153.4	4.4	362
Graphite	C_n	141.5	–	478
Benzene	C_6H_6	139.8	6.7	504
Ethene	C_2H_4	133.9	9.2	582
Dicarbon	C_2	124.5	12.2	608
Ethine	C_2H_2	120.4	15.8	759

In Figure 4.5, correlations between the experimental properties of carbon–carbon bonds of differing strength are shown. These functions may be used to estimate the corresponding parameters for bonds of intermediate strength as in graphite. It can also be seen that the properties of the CC bonds in benzene are intermediate between those of single and double bonds.

Similar correlations have been published for many other combinations of nonmetallic elements, but there are also exceptions, especially for fluorine-containing molecules.

Homonuclear single, double and triple bonds can also be characterized by the *electron density at the bond critical point*, which has been defined in Section 2.4. This density increases with bond order as can be demonstrated for the CC bonds in ethane, ethene and ethine as well as for the NN bonds in hydrazine, diimine and dinitrogen by the following data (values in e Å^{-3}):

C_2H_6: 1.6	C_2H_4: 2.4	C_2H_2: 2.9
N_2H_4: 1.0	N_2H_2: 3.1	N_2: 4.8

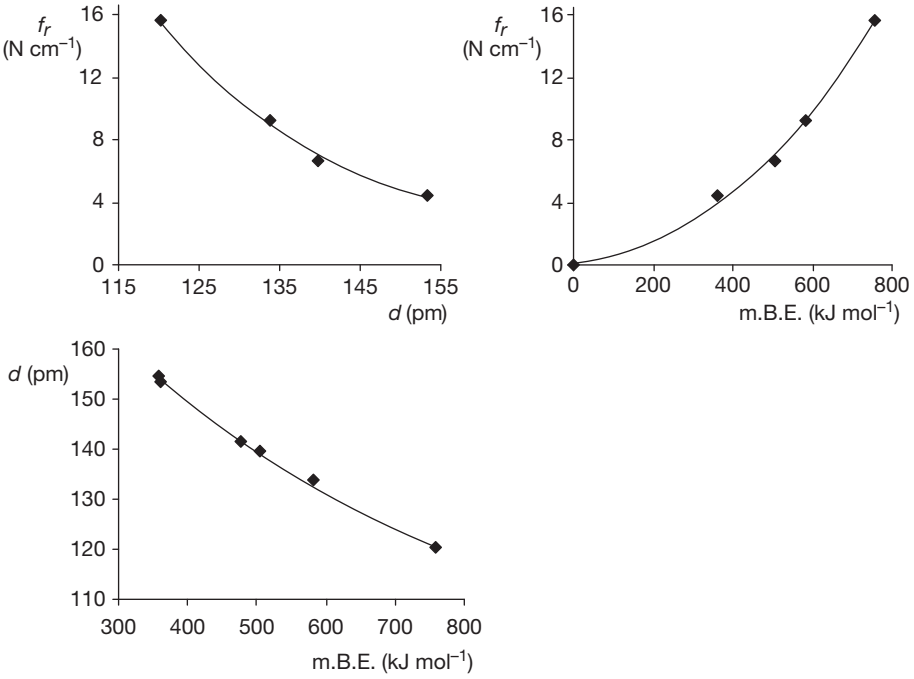

Figure 4.5: Correlations between experimental properties of carbon–carbon bonds in diamond, graphite and four hydrocarbons based on the data in Table 4.7 (*d*, internuclear distance; f_r, valence force constant; m.B.E., mean bond enthalpy).

4.6 Polarity of Covalent Bonds and Electronegativity

4.6.1 Introduction

A covalent bond is polar if the distribution of electrons is unsymmetrical, so that the centers of electronic and nuclear charges do not coincide. All bonds between dissimilar atoms are polar, just as are bonds between like but not equivalent atoms as the SS bond in the thiosulfate ion $[SSO_3]^{2-}$, which contains sulfur atoms in the formal oxidation states of −2 and +6. Nonpolar bonds exist only between identical atoms in identical environments, as in homonuclear molecules such as O_2, S_8 and Cl_2 or the CC bonds listed in Table 4.7.

The polarity of bonds can be demonstrated experimentally by the ESCA method (*electron spectroscopy for chemical analysis*), which is a variant of *photoelectron spectroscopy* (PES) using very hard monochromatic radiation, for example, X-rays (X-ray photoelectron spectroscopy, XPS), to ionize the sample molecules. Solid, liquid and gaseous compounds may be investigated (see Section 2.4.4 for the basics of PES). The kinetic energy of the emitted electrons is determined, and the ionization

energy of the atom and thus the *binding energy* of these electrons can be calculated. The high energy of X-rays allows even the removal of one of the core electrons of the molecule. To a first approximation, these inner electrons do not take part in the bonding to neighboring atoms, but their binding energy depends on the partial charge of the particular atom. A negative atomic charge lowers, and a positive charge increases the ionization energy.

For example, in case of sulfur with its valence electrons occupying the levels 3*s* and 3*p* the ionization energy of the 2*p* electrons can be used to estimate the atomic charge. Elemental sulfur (S_8) may be used as a reference sample for uncharged atoms to be compared with the ESCA spectrum of sodium thiosulfate shown in Figure 4.6. This spectrum demonstrates that the thiosulfate anion contains sulfur atoms of different charges with binding energies that are by 3.7 eV higher and by 2.3 eV lower, respectively, than the binding energy of uncharged sulfur atoms of 164.2 eV. These ionization energies E_i can be used to estimate the atomic charges by a simple electrostatic calculation using COULOMB's law. By comparison with the spectra of other sulfur compounds such as sulfide, sulfite and sulfate, the oxidation states of the S atoms in $Na_2[S_2O_3]$ follow as −2 and +6.[19]

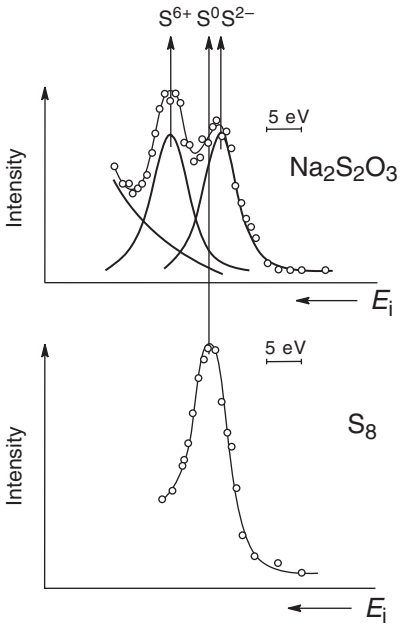

Figure 4.6: Photoelectron spectra (XPS) of sodium thiosulfate (above) and of α-S_8 (below). The ionization energy (E_i) of the 2*p* electrons of the sulfur atoms is shown on the abscissa (increasing values from right to left). The thiosulfate spectrum has been deconvoluted into components to demonstrate the differing atomic charges.

19 B. J. Lindberg et al., *Physica Scripta* **1970**, *1*, 286.

The concept of bond polarity is of outstanding importance in the understanding of properties and reactions of chemical bonds and compounds. There are various empirical methods to estimate the size and direction of polarities of covalent bonds. The most important of these is the concept of electronegativity, which will be discussed in the following sections. However, bond polarities, atomic charges and charge distribution in molecules can also be calculated by quantum-chemical methods. Furthermore, the charge distribution in crystals can be determined by sophisticated X-ray diffraction methods.

4.6.2 Electronegativities (χ)

The electronegativity of atoms was introduced by LINUS PAULING[20] in 1932 as a force of an atom in a molecule to attract the valence electrons it formally shares with its bonding partner(s). Although it is not possible to measure this force directly, the concept of electronegativity has had an enormous impact on chemistry. Pauling used bond energies to estimate χ values, but later A. L. ALLRED and E. G. ROCHOW proposed a method based on effective nuclear charges and radii of atoms in molecules. L. C. ALLEN suggested another procedure based on the orbital energies of isolated atoms. These most popular methods to define and calculate electronegativities are now discussed in detail.[21]

4.6.2.1 Thermodynamic Electronegativities by PAULING

The following binary fluorides demonstrate that there is a continuous change from nonpolar bonds as in elemental fluorine F_2 via moderately polar bonds as in NF_3 to the mainly ionic bond in the gaseous molecule LiF:

$$F_2 - OF_2 - NF_3 - CF_4 - BF_3 - BeF_2 - LiF$$

In the following series of molecules, the bond polarity changes almost continuously from the molecule HF containing a strongly polar bond with positively charged hydrogen via CH_4 with almost nonpolar bonds to LiH with a negatively charged hydrogen atom:

$$HF - H_2O - NH_3 - CH_4 - BH_3 - LiH$$

Under standard conditions both LiF and LiH form ionic crystals. In the other cases, the bond polarities follow from chemical reactivity, spectroscopic observations and quantum-chemical calculations.

---

20 L. PAULING, US chemist (1901–1994); NOBEL prize in chemistry for the year 1954.

21 For other methods, see K. D. Sen, C. K. Jørgensen (eds.), *Electronegativity*, in: *Struct. Bonding (Berlin)* **1987**, *66*, 1–190.

PAULING had observed that the *m.B.E.s* of polar covalent bonds are much higher than that of comparable nonpolar bonds, as the following examples show (values in kJ mol^{-1}):

HF: 565 H_2O: 465 NH_3: 389 CH_4: 415

The dissociation enthalpies and valence force constants of related diatomic molecules and radicals AB demonstrate this effect even more clearly:

AB	HF	OH	NH	CH
D_0^0 (kJ mol^{-1}):	566	424	335	334
f_r (N cm^{-1}):	9.7	7.8	6.0	4.5

Consequently, PAULING proposed that the B.E. of a molecule AB should be equal to the arithmetic mean between the B.E.s of the corresponding homonuclear molecules A_2 and B_2 if the polarity of the bond were neglected. Using the dissociation enthalpies rather than B.E.s and neglecting zero-point energies as an approximation, we obtain:

$$D_{AB} = \frac{1}{2}\,(D_{A_2} + D_{B_2})$$

For example, in case of hydrogen chloride:

$$D_{HCl} = \frac{1}{2}\,(D_{H_2} + D_{Cl_2}) = \frac{1}{2}\,(436 + 240) = 338 \text{ kJ mol}^{-1}$$

The experimental dissociation energy of HCl, however, is 432 kJ mol^{-1}. PAULING ascribed the difference of Δ = 432–338 = 94 kJ mol^{-1} to the polarity of the bond in HCl and termed Δ as the *ionic resonance energy* or *ion-covalence resonance energy*:

$$D_{HCl} = \frac{1}{2}(D_{H_2} + D_{Cl_2}) + \Delta$$

In general:

$$D_{AB} = \frac{1}{2}\,(D_{A_2} + D_{B_2}) + \Delta$$

PAULING postulated Δ to be proportional to the square of the electronegativity difference between atoms A and B:

$$\Delta = 96.5\,|\chi(B) - \chi(A)|^2 = 96.5\,|\Delta\chi|^2$$

The proportionality factor 96.5 results from the unit electron volt (eV) used by PAULING, while today dissociation enthalpies are typically given in kJ mol^{-1} (1 eV = 96.5 kJ mol^{-1}). The difference Δχ is given as follows:

$$\Delta\chi = 0.102 \cdot \sqrt{\Delta}$$

After χ has been arbitrarily defined for one element, all other electronegativities can be calculated. PAULING used the hydrogen atom as a standard with $\chi_P = 2.2$, and consequently:

$$\chi_P(\mathrm{Cl}) = 0.102 \cdot \sqrt{92} + \chi_P(\mathrm{H}) = 0.102 \cdot 9.59 + 2.2 = 3.2$$

The PAULING electronegativities χ_P of the main group elements are listed in Table 4.8, based on published m.B.E. data of many molecules.[22] Electronegativities of the main group elements increase from the left lower corner of the Periodic Table (cesium) to the right upper corner (fluorine) with values ranging from 0.8 to 3.98. The χ_P values of transition metals are in the region 1.2–2.5.

PAULING's electronegativities have been used very successfully to estimate bond polarities, inductive effects, and to correct internuclear distances. However, the accuracy of the χ_P values should not be overestimated. They depend on the accuracy of the thermochemical input data. Furthermore, the coordination numbers of atoms are of significance,[23] and sometimes apparent single bonds are strengthened by additional π bonding effects as in BF_3, SiF_4 and PF_3 (hyperconjugation). In other words, only pure single bond data should be used to derive χ_P values and all atoms should have a noble gas configuration.

4.6.2.2 Electronegativities according to ALLRED and ROCHOW

In 1958, the US-American chemists A. LOUIS ALLRED and EUGENE GEORGE ROCHOW proposed another method to determine electronegativities using the effective nuclear charge at the surface of an atom together with its covalent radius.[24] This concept has become quite popular. In a covalent bond between atoms A and B, the atomic cores compete for the valence electrons. The attractive force *F* of an atomic core on the bonding electrons can be expressed by COULOMB's law:

22 A. L. Allred, *J. Inorg. Nucl. Chem.* **1961**, *17*, 215. For silicon and germanium, see D. Quane, *ibid.* **1971**, *33*, 2722.

23 For example, the CH bonds in methane are almost nonpolar, but in acetylene (ethine) they are highly polar, and acetylene is in fact an acid in water.

24 A. L. Allred, E. G. Rochow, *J. Inorg. Nucl. Chem.* **1958**, *5*, 264. See also: D. Ch. Ghosh, T. Chakraborty, B. Mandal, *Theor. Chem. Acc.* **2009**, *124*, 295.

Table 4.8: Electronegativities of the main group elements of the Periodic Table[a].

Atom	χ_P(Pauling)	χ_{AR}(Allred/Rochow)	χ_{spec}(Allen)
H	2.20	2.20	2.30
Li	0.98	0.97	0.91
Be	1.57	1.47	1.58
B	2.04	2.01	2.05
C	2.55	2.50	2.54
N	3.04	3.07	3.07
O	3.44	3.50	3.61
F	3.98	4.10	4.19
Ne		4.77	4.79
Na	0.93	1.01	0.87
Mg	1.31	1.23	1.29
Al	1.61	1.47	1.61
Si	1.90	1.74	1.92
P	2.19	2.06	2.25
S	2.58	2.44	2.59
Cl	3.16	2.83	2.87
Ar	–	3.29	3.24
K	0.82	0.91	0.73
Ca	1.00	1.04	1.03
Ga	1.81	1.82	1.76
Ge	2.01	2.02	1.99
As	2.18	2.20	2.21
Se	2.55	2.48	2.42
Br	2.96	2.74	2.69
Kr	–	3.00	2.97
Rb	0.82	0.89	0.71
Sr	0.95	0.99	0.96
In	1.78	1.49	1.66
Sn	1.96	1.72	1.82
Sb	2.05	1.82	1.98
Te	2.10	2.01	2.16
I	2.66	2.21	2.36
Xe	–	2.45	2.58

[a]For noble gas data, see T. L. Meek, *J. Chem. Educ*. **1995**, *72*, 17, and J. Futado, F. De Proft, P. Geerlings, *J. Phys. Chem. A* **2015**, *119*, 1339.

$$F = \frac{1}{4\pi\varepsilon_o} \cdot \frac{Z_{\text{eff}} \cdot e^2}{r^2} \qquad \begin{array}{l} Z_{\text{eff}}\text{: effective nuclear charge} \\ r\text{: covalent radius} \end{array}$$

The bonding electrons are assumed to reside at a distance from the nucleus that is equivalent to the covalent radius of the atom (Section 4.3), and Z_{eff} is calculated by empirical rules of atomic physics.[25] It follows that the electronegativity of an atom should be proportional to Z_{eff}/r^2:

$$\chi \sim \frac{Z_{\text{eff}}}{r^2}$$

The calculation of numerical χ_{AR} values requires a proportionality factor and the addition of a corrective value, which are selected so that an optimal correlation with PAULING's values results (r in Å):

$$\chi_{\text{AR}} = 0.359 \cdot \frac{Z_{\text{eff}}}{r^2} + 0.744$$

There is a linear correlation between ALLRED-ROCHOW'S and PAULING'S electronegativities, implying that both systems are equivalent. The χ_{AR} values are listed in Table 4.8 and are shown in Figure 4.7. It is obvious that the values decrease in each

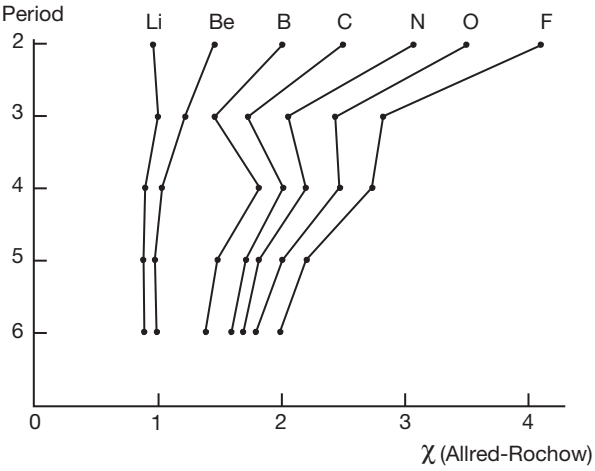

Figure 4.7: Electronegativities of the main group elements in single bonds according to Allred and Rochow. Note the irregularity caused by the transition metal elements and the occupation of 3*d* orbitals in period 4.

25 G. Burns, *J. Chem. Phys.* **1964**, *41*, 1521, and references cited therein.

group from top to bottom, but the change is not smooth due to insertion of the transition metal elements with occupation of the 3*d* orbitals after calcium. The ALLRED-ROCHOW electronegativities of the nonmetals are larger than 1.8, those of the metals are smaller than 1.5 and in the range 1.2–1.8 elements are found that exist as metallic and nonmetallic allotropes (*metalloids*).

It should be noted, however, that covalent radii depend on the bond strength, and the data in Table 4.8 have been derived for single bonds only. Multiple bonds are shorter, and the corresponding radii are smaller. Therefore, the electronegativity of an atom in such a bonding situation is larger, and the polarities of the corresponding bonds change accordingly.

4.6.2.3 Spectroscopic Electronegativities according to ALLEN

The concepts of PAULING and ALLRED-ROCHOW to derive electronegativities of atoms are based on molecular properties, some of which are not easy to determine accurately. In contrast, the method by LELAND C. ALLEN published in 1989 uses the one-electron energy of the valence shell electrons of free atoms in their ground state to determine *spectroscopic electronegativities* (χ_{spec}).

According to modern theoretical results the main group elements form bonds using only *s* and *p* electrons. Consequently, the orbital energies ε_i of these electrons should be a measure for the attractive force of an atomic core with respect to its valence electrons, and χ_{spec} can be defined as follows:

$$\chi_{spec} = \frac{m \cdot \varepsilon_p + n \cdot \varepsilon_s}{m + n}$$

where *m* and *n* are the numbers of *p*, respectively, *s* electrons, and their absolute orbital energies ε_i are approximated by the corresponding experimental ionization energies (in eV).[26] An average energy is used in case of multiplet states. The obtained spectroscopic electronegativities agree well with the PAULING data if scaled by a factor of 0.169; the results are shown in Table 4.8. Again, it is observed that χ_{spec}(Ge) is larger than χ_{spec}(Si).

The method by ALLEN provides a possibility to calculate electronegativities of noble gases, and in agreement with the general trend in the Periodic Table their χ_{spec} values are larger than those of the preceding halogen atoms (see Figure 4.8 and Section 14.5).

Spectroscopic electronegativities can also be determined for charged atoms. The ionization energy E_i of the neutral carbon atom is 11.3 eV but for the cation C^+

26 L. C. Allen, *J. Am. Chem. Soc.* **1989**, *111*, 9003.

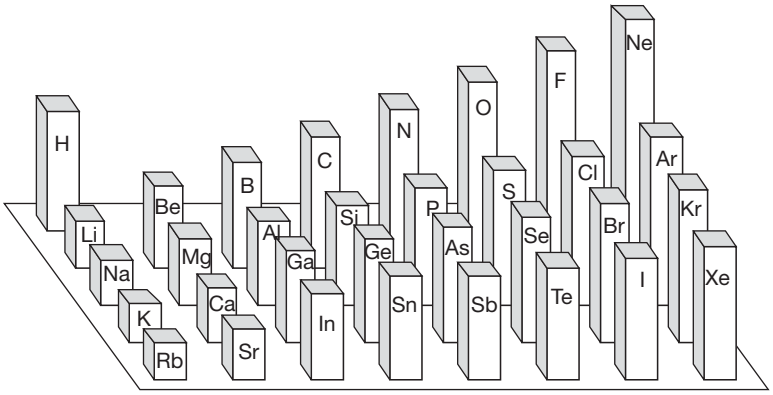

Figure 4.8: Spectroscopic electronegativities for the main group elements after ALLEN as "Third dimension of the Periodic Table." The heights of the columns correspond to the values of $\chi_{spec.}$ Note the special situation of hydrogen.

one obtains E_i = 24.4 eV and for the singly charged anion C^-, E_i = 1.6 eV. Consequently, a positive partial charge increases the electronegativity of an atom and a negative charge decreases it. This result is important for the estimation of group electronegativities discussed in the following section.

4.6.2.4 Group Electronegativities

Electronegativities may also be defined for polyatomic groups and substituents R. Corresponding numerical data can be calculated[27] as well as derived from spectroscopic observations. For example, the chemical shifts in NMR spectra and the vibrational frequencies in infrared or Raman spectra have been correlated with the electronegativity of group R (see Section 4.4.2). The results obtained depend somewhat on the method, and the influence of neighboring groups needs to be taken into account occasionally, but inductive effects are always well reproduced. For example, the group electronegativities of the series $-CH_3$ (χ = 2.5), $-CCl_3$ (2.8), $-CF_3$ (3.2) increase since the halogen atoms withdraw electron density from the carbon atoms resulting in positive partial charges that in turn increase the group electronegativity. The electron withdrawing ability of perfluorinated alkyl groups (R^F) increases in the order: CF_3, C_2F_5, *n*-C_3F_7, *n*-C_4F_9.

27 S. G. Bratsch, *J. Chem. Educ.* **1988**, *65*, 223. D. Bergmann, J. Hinze, *Struct. Bonding (Berlin)* **1985**, *66*, 145.

4.6.3 The Dipole Moment

Many molecules with polar bonds show a permanent dipole moment μ that can be separated into four components:[28]

$$\mu = \mu_e + \mu_{at} + \mu_{hom} + \mu_{pol}$$

The first component (μ_e) arises from the transfer of the charge δe between the two atoms due to their *electronegativity difference*. This charge transfer leads to a positive partial charge at the atom of lower electronegativity and a negative charge of equal size at the other atom:

$$\overset{\delta+}{A}—\overset{\delta-}{B}$$

If the internuclear distance is d, then $\mu_e = \delta e \cdot d$. Owing to the partial charges, the electronegativity of atom A increases and that of atom B decreases. According to the *principle of electronegativity equalization* the charge transfer only occurs to such an extent that the electronegativities of A and B *within the molecule* AB become equal because of their partial atomic charges:

$$\text{isolated atoms:} \quad \chi(A) < \chi(B)$$

$$\text{atoms in molecule AB:} \quad \chi(A^{\delta+}) = \chi(B^{\delta-})$$

In other words, in (small) molecules the atoms are of intermediate electronegativities, which can be estimated by the geometrical mean of the free atom electronegativities of (uncharged) atoms A and B.[29]

Two point charges e^+ and e^- separated by 100 pm generate a dipole moment of 4.8 D. For example, if the gaseous molecule KCl (d = 266.7 pm) consisted of spherical ions K^+ and Cl^- (without any charge transfer or polarization) the dipole moment would be 12.80 D (2.667 × 4.8). The experimental dipole moment of this molecule, however, has been determined as 10.27 D. Therefore, the ionic charges in the KCl molecule are only 80% of the elementary charge (δ = 0.8).[30] It should be noted, however, that this calculation is oversimplified since the atoms in a molecule are no longer spherical as will be discussed below. Dipole moments are *vectors*, and usually the negative end of the dipole is taken as origin of the vector.

28 M. Klessinger, *Angew. Chem. Int. Ed.* **1970**, *9*, 500.

29 R. T. Sanderson, *J. Chem. Educ.* **1988**, *65*, 112 and 227. The geometric mean is the square root of the product of the two electronegativities. For larger molecules, the connectivity of the atoms also influences the charge distribution.

30 In crystalline KCl the atomic (ionic) charges are even lower than in the gaseous molecule.

The atomic charges in molecules can be approximately determined by XPS. For example, the atomic charges of the carbon atoms of the molecules listed in Table 4.9 can be estimated from the ionization energies E_i of the 1*s* electrons, which increase from ethane to tetrafluoromethane due to the inductive effect of the electronegative substituent atoms.[31] The ionization energies of the methane derivatives CH_mF_n increase with each additional fluorine atom by circa 2.75 eV. Therefore, the carbon atom in CF_4 must be highly positively charged since $E_i(1s)$ is by 11 eV larger than for CH_4.

Table 4.9: Difference in the ionization energies ΔE_i of the 1*s* electrons of carbon in various molecules compared to the $E_i(1s)$ of methane (determined by XPS).

Molecule	ΔE_i (eV)
Ethane, C_2H_6	−0.20
Ethene, C_2H_4	−0.10
Methane, CH_4	0.00
Acetone, $CH_3\mathbf{C}OCH_3$	1.40
Methanol, CH_3OH	1.60
Fluoromethane, CH_3F	2.80
Formaldehyde, CH_2O	3.30
Tetrafluoroethene, C_2F_4	5.58
Difluoromethane, CH_2F_2	5.60
Trifluoromethane, CHF_3	8.28
Tetrafluoromethane, CF_4	11.00

In acetone the central atom is chosen.

It should be noted, however, that the charge distribution of an atom participating in a covalent bond is anisotropic, which will be discussed in detail in Section 4.7. In addition, atoms do not have strict boundaries, and summing up the electron density over a certain volume in order to determine the atomic charge is subject to definition. Therefore, different atomic charges have been published for certain molecules, based on various types of quantum-chemical calculations. The trends, however, are always similar.

The second contribution to the dipole moment of a molecule, the *atomic dipole moment* (μ_{at}), results from the asymmetry of the charge distribution in certain molecular orbitals. For example, the HOMO of NH_3 is quite asymmetric and the center of the electron charges in this orbital does not agree with the atomic nucleus of

31 Data after D. Bergmann, J. Hinze, *Angew. Chem. Int. Ed.* **1996**, *35*, 150.

nitrogen (see Figure 4.9). The resulting dipole moment is called "atomic moment" since it is seemingly located at just one atom ("lone pair moment"). This moment explains the large overall dipole moment of ammonia (1.468 D) despite the relatively small difference of electronegativities χ between nitrogen and hydrogen ($\Delta\chi_{AR}$ = 0.9). The hydrogen atoms carry a partial positive charge, and the three bond moments add to a resulting electrostatic moment μ_e in the direction of the threefold rotation axis of the molecule (C_{3v} symmetry; Figure 4.9). Since the atomic moment μ_{at} has the same direction as μ_e the two components add to the total moment μ_{tot}, which makes NH_3 such a good LEWIS base and in liquid form a good solvent for salts.

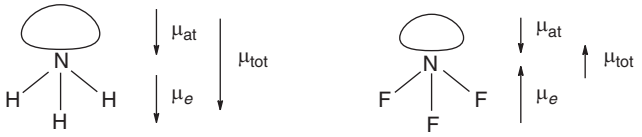

Figure 4.9: Vector addition of the dipole moments μ_e und μ_{at} of the molecules NH_3 and NF_3 to give the total moment μ_{tot} (molecular symmetry C_{3v}).

The dipole moment of the analogous NF_3 is much smaller (0.235 D) than that of ammonia although the electronegativity difference between N and F is slightly larger ($\Delta\chi_{AR}$ = 1.0). This is explained by the different directions of μ_e and μ_{at} in both molecules. While these two vectors are pointing in the same direction in NH_3, they are of opposite directions in NF_3 resulting in partial compensation, and nitrogen is now the positively charged atom (Figure 4.9). This positive charge causes a contraction of the HOMO at nitrogen, and the *total moment* has even the opposite direction compared to ammonia. Therefore, NF_3 is a very weak LEWIS base. Its *pyramidal inversion* requires an enthalpy of 250 kJ mol^{-1} compared to only 24 kJ mol^{-1} for NH_3 (see Section 9.3).

Atomic dipole moments may be quite large and atomic charges calculated without taking them into account may be considerably in error. For example, the experimental dipole moment of CO is only 0.11 D, and its internuclear distance is 113 pm, which, if we ignored the atomic dipoles, gave very small partial charges despite the large electronegativity difference between carbon and oxygen ($\Delta\chi_{AR}$ = 1.0). Evidently, the large atomic dipoles at carbon and oxygen compensate the ionic bond moment to some extent.

The third contribution to the total dipole moment of molecules is the *homopolar moment* μ_{hom} resulting from the unequal size of the atomic orbitals forming a covalent bond. This moment is directed toward the larger atom since electron charge accumulates in the bonding region near the smaller atom (Figure 4.10). In the HCl molecule, for example, μ_{hom} is directed opposite to the electrostatic moment μ_e (H←Cl).

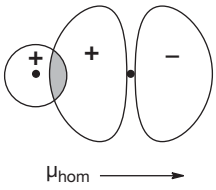

Figure 4.10: The homopolar dipole moment μ_{hom} of a covalent bond between two atoms A and B resulting from the unequal size of their atomic orbitals. Negative charge accumulates in the cross-hatched region of the overlap. The direction of μ_{hom} is toward the larger atom.

The three moments μ_e, μ_{at} and μ_{hom} are not completely independent, but mutual polarization requires a fourth term μ_{pol}. These four components of the total dipole moment of a molecule may have different directions and may partially compensate each other. Therefore, the dipole moment of a molecule is a complex issue, especially when the electronegativity differences of the atoms are small. For large differences $\Delta\chi$, the electrostatic moment μ_e usually dominates the total dipole moment. Strongly polar bonds with electronegativity differences of >1 are, for example, E–F (E: H, B, C, N, Si, P, S), E–O (E: H, B, C, Si, P, S) and E–Cl (E: B, Si).

In this context, the *charge capacity* κ of an atom is an important property, which is defined as the reciprocal of the first derivative of the electronegativity to the charge Q of an atom[32]:

$$\frac{1}{\kappa} = \left(\frac{\delta\chi}{\delta Q}\right)_{Q=0}$$

Small electronegative atoms such as F, O and N have small charge capacities. As neutral atoms they strongly attract electron density, but they are rapidly saturated since the electronegativity rapidly decreases with increasing negative partial charge δQ. This can be demonstrated by the following example. The electron affinity of the fluorine atom is 3.45 eV, that is, the fluoride ion F^- (charge −1 *e*) is by this energy more stable than the neutral atom and an infinitely separated electron. However, a fluorine atom with a partial charge of only −0.65 *e* is by 4.2 eV more stable than a neutral F atom. In other words, the increase in atomic charge from −0.65 to −1.00 leads to an *increase* in energy by 0.75 eV!

The lacking charge capacity of relatively small molecular clusters is the reason that dianions such as $[CO_3]^{2-}$ and $[SO_4]^{2-}$ do not exist in the gas phase (see Section 2.1.3).

Whether a molecule has a dipole moment depends solely on its symmetry. Only molecules belonging to the point groups C_n, C_s and C_{nv} (n = 1, 2,...) can have a dipole moment. In all other cases, the bond moments compensate each other. The molecule SiF_4, for example, contains highly polar bonds, but its total dipole moment is zero since the vector sum of the individual bond moments is zero.

32 P. Politzer et al., *J. Mol. Struct. (Theochem)* **1992**, *259*, 99.

Dipole moments of molecules determine intermolecular association, including hydrogen bonding, chemical reactivity, absorption intensity of infrared radiation and formation of coordination compounds, to name just a few. For dipole moments of small molecules, see Table 3.1.

4.7 Electron Density Distribution in Molecules and Crystals

4.7.1 Promolecule and Deformation Density

The electron density distribution in molecules can be obtained from quantum-chemical calculations as well as by X-ray diffraction on single crystals.[33] Details of the electron density of H_2O and H_2S have already been discussed (Figure 2.31), and in Figure 2.24 it was shown that the electron density of the O_2 molecule can be calculated even for individual molecular orbitals. However, the *charge redistribution during bond formation* is much more interesting for the understanding of molecules. In this case, the densities of the separated atoms at the positions in the molecule of interest are calculated first. This hypothetical configuration without covalent bonds is called a *promolecule*. Next, the density of the molecule is calculated in its equilibrium configuration, and by subtraction of the density of the promolecule the *density difference* is obtained, which describes the rearrangement of electrons on bond formation. This density difference is also called *deformation density*.

In Figure 4.11a the deformation density of the F_2 molecule is shown. It is evident that on bond formation the overall electron density between the two nuclei increases, while it decreases close to the nuclei. Note that the increase in the bonding region is higher than the added densities of the two separated atoms in the promolecule. In this way, the repulsion of the two nuclei is overcompensated. Somewhat surprisingly, the density increases also in the outer regions of the molecular axis, which is caused by the shape of the highest bonding molecular orbital $3\sigma_g$, obtained by linear combination of the two $2p_z$ AOs of the fluorine atoms (see Figure 2.22).[34]

If a similar calculation is carried out for a hypothetical Ne_2 molecule with the same internuclear distance as in F_2, the density at the center of the molecule decreases while it increases near the nuclei due to PAULI repulsion. Consequently, such a "molecule" would not be stable and, therefore, does not exist. Only at a much larger internuclear distance there is some attraction between two noble gas atoms caused by dispersion forces (see VAN DER WAALS molecules in Section 3.5).

33 The common units of electron density are e Å^{-3} (1 Å = 100 pm) and $e\ a_0^{-3}$ (a_0: atomic unit of length, 52.9 pm; 1 $e\ a_0^{-3}$ = 6.749 e Å^{-3}).

34 L. G. Vanquickenborne, in P. L. Huyskens, W. A. P. Luck, T. Zeegers-Huyskens (eds.), *Intermolecular Forces*, Chapter II, Springer, Berlin, **1991**, p. 31. See also: K. L. Kunze, M. B. Hall, *J. Am. Chem. Soc*. **1986**, *108*, 5122.

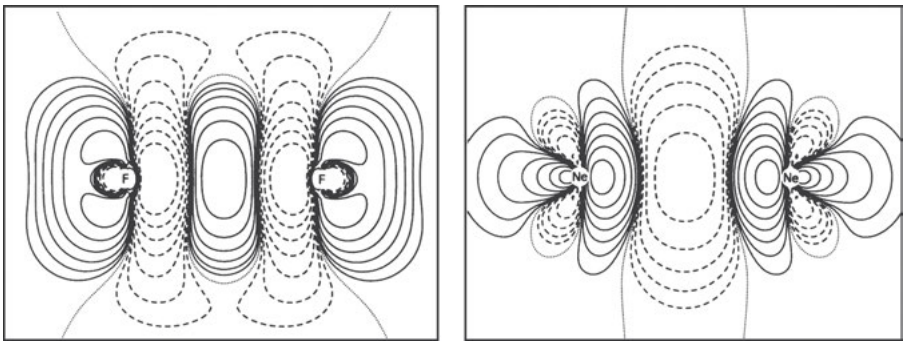

Figure 4.11: Calculated electron density difference maps for the molecule F_2 (left) and for the hypothetical species Ne_2 (at an internuclear distance of 159 pm as in F_2; right). The contour lines connect points of equal charge increase (solid lines) or decrease (broken lines); dotted lines indicate nodes.

In recent years, the electron density of molecules has also been determined by X-ray diffraction on single crystals at low temperatures (to minimize atomic vibrations). Many reflections need to be measured to very high diffraction angles θ and a complex mathematical analysis is necessary. In this way, the electron density can also be determined under the polarizing influence of neighboring molecules as in condensed phases.[35] The results show that a complex anisotropic charge redistribution occurs on formation of a covalent bond and that atoms in molecules are not spherical. Therefore, the atomic charges discussed earlier in this chapter are only crude measures of the real charges. This can most impressively be demonstrated by the **electrostatic potential** on the surface of atoms in molecules. This potential $V(r)$ at position r from the nucleus results from the superposition of the effective nuclear charge Z_{eff} and the electron density ρ. The significance of $V(r)$ is that it gives the interaction energy E between a negative point charge q placed at r and the rest of the molecule, in other words, the interaction of q with all other charged components of a molecule:

$$E = V(r) \cdot q$$

This equation is in atomic units with distances in Bohr (1 Bohr or a_0 = 52.9 pm) and energies in Hartree (1 Hartree = 2625.5 kJ mol^{-1}). If E is negative, the interaction is attractive ($V > 0$); if positive, it is repulsive ($V < 0$). The potential $V(r)$ is a real physical property, that is, an observable that can be obtained experimentally by diffraction methods as well as by theoretical calculations. It represents the complete

35 P. Coppens, *Angew. Chem. Int. Ed.* **2005**, *44*, 6792–6802 and 6810. T. S. Koritsánszky, P. Coppens, *Chem. Rev.* **2001**, *101*, 1583.

charge distribution, whereas the electronic density explicitly reflects only the electronic component. The potential is also more meaningful than atomic charges, which are arbitrarily defined quantities with no rigorous physical basis. The "surface" of a molecule is usually defined by $V(r) = 0.001\ e\ a_0^{-3}$ and the values of $V(r)$ are shown in differing colors as for the two examples in Figure 4.12.

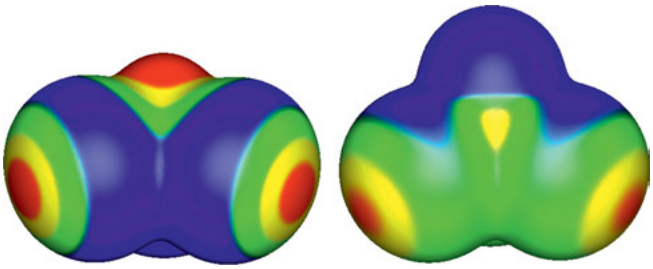

Figure 4.12: Representation of the electrostatic potentials $V(r)$ on the surfaces of CHI_3 (left) and $OPBr_3$ (right); the red colored (positive) regions are called σ holes of the molecules. Figure courtesy of Peter Politzer and Jane Murray.

The usefulness of $V(r)$ can be demonstrated by analyzing a special noncovalent intermolecular interaction called *halogen bonding* which will be discussed in the next section.

4.7.2 Halogen Bonding

Halogen bonding[36] (also see Section 13.3) and the related chalcogen bonding have received enormous attention in recent years because of their significance for synthesis, structural chemistry, crystal engineering, materials chemistry, catalysis and even medicinal chemistry (drug design).[37]

Halogen atoms are among the most electronegative in the Periodic Table (Section 4.6.2). They typically carry a partial negative charge when covalently bonded to other atoms, except for nitrogen and oxygen. Accordingly, it has, in the past, often been viewed as enigmatic that such halogens can interact attractively with negatively charged (nucleophilic) sites such as the lone pairs of Lewis bases

36 P. Metrangolo, G. Resnati (eds.), *Halogen Bonding: fundamentals and applications*. Vol. 126 of *Structure and Bonding*, Springer, Berlin, **2008**.

37 H. Wang, W. Wang, W. J. Jin, *Chem. Rev*. **2016**, *116*, 5072–5104. P. Metrangolo, G. Resnati et al., *Chem. Rev*. **2016**, *116*, 2478–2601. P. Politzer, J. S. Murray, T. Clark, *Phys. Chem. Chem. Phys*. **2013**, *15*, 11178 and *ChemPhysChem* **2013**, *14*, 278.

B. Nevertheless, a halide R–X (X = halogen) will frequently form a weakly bonded complex R–X····:B with a negative site of B. This effect is called halogen bonding, and there are some structural similarities between halogen bonds R–X····:B and hydrogen bonds R–H····:B, but the latter are usually stronger.

An instructive example is the attractive interaction between a chlorine molecule and trimethyl phosphane along the threefold symmetry axis of the LEWIS base:

$$Cl - Cl\cdots{:}PMe_3$$

The bond energy of this complex in the gas phase has been calculated as 64 kJ mol^{-1}, and the Cl····P distance is predicted as 261.5 pm (sum of covalent radii: 209 pm, of VAN DER WAALS radii: 355 pm). The bond energy consists of an ionic and a covalent contribution. The ionic part is the result of the COULOMB attraction between the positive potential at the **σ hole** of Cl_2 and the negative electron cloud of the phosphorus lone pair. The σ hole results from the depletion of electron density at the side of an atom opposite to a σ bond (see Figure 4.12). The covalent bond, on the other hand, is established by electron density delocalization from the phosphorus lone pair into the antibonding σ* MO (LUMO) of the chlorine molecule. Using Br_2 or I_2 instead of Cl_2 the interaction energy is only slightly lower. Many similar complexes between diatomic halogen molecules with amines, phosphanes and other LEWIS bases have been studied computationally.[38]

Next, we analyze the attraction between two molecules of phosphoryl tribromide.[39] The oxygen atom of $POBr_3$ is slightly negatively charged and is attracted by the σ hole at the bromine atom of a neighboring molecule opposite to the PBr bond (Figure 4.12). Therefore, a nearly linear axis P–Br····$OPBr_3$ results between the two molecules. Previously, this had been unexpected since both oxygen and bromine carry negative partial charges. However, the electronic charge is not evenly distributed across the surface of an atom. Instead, there are often regions of positive and negative potential. Since the surface potential of the oxygen atom of $OPBr_3$ is negative (Figure 4.12) the atom is attracted by the σ hole of the bromine atoms.

The bond energy of the dimer $(POBr_3)_2$ has been calculated as 15 kJ mol^{-1} with an internuclear distance Br····O of 291 pm (VAN DER WAALS distance: 335 pm). The stability of the dimer depends on the temperature since the entropy change ΔS of the dimerization is negative and may dominate the GIBBS reaction energy ($\Delta G = \Delta H - T \cdot \Delta S$). But even if ΔG should be slightly positive and the complex thermodynamically unstable in the gas phase, this does not completely preclude the occurrence of the interaction. It simply means that the equilibrium constant for the formation of the complex is less than 1.

38 V. Oliveira, E. Kraka, D. Cremer, *Inorg. Chem.* **2017**, *56*, 488.
39 P. Politzer, J. S. Murray, *ChemPhysChem* **2013**, *14*, 278.

Such subtle intermolecular interactions are widespread in chemistry and are important to understand the structure of molecular crystals and of the interaction of drugs with corresponding receptors, for example. They may also serve as "pre-reactive complexes." In a similar fashion, *chalcogen bonding* has been proposed for interactions of the type $R_2E\cdots:B$ with E = S or Se and B a LEWIS base.[40] In these cases, the σ hole is located in the extension of one of the R–E bonds. For aromatic compounds, π holes have also been proposed and their interaction with LEWIS bases has been studied extensively.[40]

40 V. Oliviera, D. Cremer, E. Kraka, *J. Phys. Chem. A* **2017**, *121*, 6845.

Part II: **Chemistry of the Non-Metals**

The strictest *criterium to define nonmetals* in contrast to metals is the electric conductivity. Typically, metals show a finite conductivity at ambient conditions, whereas the conductivity of nonmetals is close to zero. With this definition, 23 of the known chemical elements are nonmetals, and these are the subject of this textbook, namely hydrogen, boron, carbon, silicon, germanium, nitrogen, phosphorus, arsenic, the chalcogens, that is, oxygen through tellurium, as well as halogens and noble gases.

All nonmetals, however, show more or less pronounced semiconducting properties at elevated temperatures (depending on the size of the band gap). While the conductivity of metals decreases with temperature as thermal motion impedes the mobility of the electrons, semiconductors conduct electrical currents with less resistance at higher temperatures, that is, their conductivity rises. Indeed, the temperature dependence of electrical conductivity provides a more precise definition of metals and nonmetals.

In addition, several nonmetallic elements exist as various *allotropes* of differing conductivity. For example, diamond is insulating while graphite shows metallic conductivity. Phosphorus exists as white, red, violet and black allotropes, the conductivity of which at normal conditions increases in this order. Similarly, yellow arsenic is insulating, but the gray metallic form of this element is conducting. The same holds for insulating red and semiconducting gray selenium.

Pressure has a profound effect on the conductivity of materials as well. For example, elemental sulfur is a thermal and electrical insulator at ambient pressure but turns into a viable semiconductor at higher pressures and is even superconducting at temperatures below 17 K and a pressure of 160 GPa. Similar observations have been made for other nonmetallic elements.[1] The most spectacular case is the superconductivity of solid hydrogen sulfide, discovered only in 2015 by DROZDOV, EREMETS et al.[2] The required pressure is 153 GPa, but the maximum critical temperature (T_c) is 203 K (at 200 GPa), which is above the boiling point (b.p.) of liquid nitrogen and is higher than for any other superconducting material. Silane (SiH_4) also turns into a metallic conductor at pressures above 50 GPa but requires pressures >95 GPa and very low temperatures (<17 K) to acquire superconducting properties.[2]

Despite these ambiguities, it is practical and theoretically justified to treat the nonmetals separately from the ambient pressure metals since many similarities exist among these 23 elements. This is a consequence of the *electronic configuration*

1 Oxygen exhibits metallic conductivity at pressures above 96 GPa (P. P. Edwards, F. Hensel, *ChemPhysChem*. **2002**, *3*, 53) while elemental hydrogen shows a conductivity comparable to those of alkali metals at 180 GPa and 4400 K (F. Hensel, P. P. Edwards, *Chem. Eur. J.* **1996**, *2*, 1201. G. J. Ackland, M. D. Knudson et al., *Science* **2015**, *348*, 1430, 1455).

2 Review: Y. Yao, J. S. Tse, *Chem. Eur. J.* **2018**, *24*, 1769. The metallization of H_2S at very high pressures is probably due to auto-dissociation to the ions $[H_3S]^+$ and $[SH]^-$; see E. E. Gordon et al., *Angew. Chem. Int. Ed.* **2016**, *57*, 3682).

https://doi.org/10.1515/9783110578065-005

of the valence shell, which is characterized by the (partial) occupation of *s* and *p* orbitals while the *d* orbitals are empty and can thus be neglected to a first approximation, resulting in a highly effective nuclear charge. Therefore, the ionization energies of nonmetal atoms are considerably larger (7.9–24.6 eV) than those of most metals (1 eV = 96.485 kJ mol^{-1}).

In general, conductivity is not a simple phenomenon to explain, and there may be several mechanisms impeding the motion of electrons in a solid or liquid material.[3] The overlap of many atomic orbitals in condensed phases creates numerous molecular orbitals with ever so slightly varying energy. This results in the loss of the discrete nature of the orbitals so that they are more adequately described as "bands" of densely spaced energy levels. The bonding MOs constitute the *valence band* and the antibonding MOs the *conduction band*. Depending on their occupation and on the energy gap between the two bands, the material is either insulating or conducting at room temperature. Increasing the pressure normally reduces the *band gap*, which is typically >3 eV for insulators, 0.5–3 eV for semiconductors and nonexistent or well below 0.5 eV for metals.[4] More details will be discussed in later chapters.

3 R. Hoffmann, *Angew. Chem. Int. Ed.* **1987**, *26*, 846–878.

4 Note that the definition of insulator and semiconductor according to band gaps is arbitrary, but still upheld for practical considerations.

5 Hydrogen

Hydrogen[5] is a record holder among the chemical elements.[6] It is the most abundant element in the universe including our solar system, which consists of 71 mass% or 91 atom% of hydrogen atoms. Conversely, on the surface of the Earth, that is atmosphere, lithosphere (crust), hydrosphere (oceans, lakes and rivers) and biosphere, the lightest of all elements has a mass fraction of less than 1%. The human body consists of about 10 wt% of H, mainly in the form of water.

Hydrogen forms compounds with almost every other element and their number (including organic compounds) is consequently larger than for any other element. Water is the most abundant hydrogen compound on the Earth, and it is the most important source for production of elemental hydrogen; it contains 11.2 wt% H. In addition, hydrocarbons (e.g., crude oil and natural gas) are important sources for the industrial production of H_2. In Europe, more than 80% of the produced hydrogen gas comes from water and fossil fuels (including coal), which necessarily entails the production of carbon dioxide as a side product. Therefore, the environmentally friendly and energetically efficient production of H_2 from renewable resources, for example, by photochemical water splitting (as in green plants) or from biomass is a hot research topic.[5,7] The standard enthalpy needed, however, to cleave liquid water at 25 °C into the elements is 286 kJ mol^{-1}.

5.1 Elemental Hydrogen

5.1.1 Production and Uses

In principle, elemental hydrogen can be produced from all energy sources (fossil fuel, biomass, solar, wind and nuclear energy), but at present H_2 is produced on a huge scale mainly by the following four processes:[8]

5 D. Stolten, B. Emonts (eds.), *Hydrogen Science and Engineering*, Vols. 1 and 2, Wiley-VCH, Weinheim, Germany, **2016**. M. Kakiuchi, *Encycl. Inorg. Chem.* **2005**, *3*, 1882.

6 H.-J. Quadbeck-Seeger, R. Faust, G. Knaus, U. Siemeling, *World Records in Chemistry*, Wiley-VCH, Weinheim, Germany, **1999**.

7 E. Reisner et al., *Chem Soc. Rev.* **2016**, *45*, 9–23. M. M. Najafpour et al., *Chem. Rev.* **2016**, *116*, 2886–2936. J. D. Blakemore, R. H. Crabtree, G. W. Brudvig, *Chem. Rev.* **2015**, *115*, 12974–13005. See also the special issues *Hydrogen* in: *Chem. Rev.* **2007**, *107*, issue 10, and *Eur. J. Inorg. Chem.* **2011**, pp. 919 and 1005.

8 K. H. Büchel, H.-H. Moretto, D. Werner, *Industrial Inorganic Chemistry*, 2nd ed., Wiley-VCH, Weinheim, Germany, **2008**. M. Bertau, A. Müller, P. Fröhlich, M. Katzberg, *Industrielle Anorganische Chemie*, 4th ed., Wiley-VCH, Weinheim, Germany, **2013**.

https://doi.org/10.1515/9783110578065-006

(a) Catalytic reduction of water vapor by methane (from natural gas) or other lower alkanes at 800–900 °C and 3–25 bar using a nickel-based catalyst contained in a tubular reactor (*steam reforming process*):

$$CH_4 + H_2O \longrightarrow 3\,H_2 + CO \qquad \Delta H^\circ_{298} = 207\ \text{kJ mol}^{-1}$$

Since this reaction is endothermic, it requires an exothermic supporting reaction. This is the combustion of methane in a furnace to heat the reactor from outside.

To remove carbon monoxide from the mixture of H_2, CO and H_2O an iron oxide catalyst is used at 300–400 °C in a second reactor followed by another reactor with a copper and zinc containing catalyst at 220 °C. This cascade of catalysts helps to shift the so-called *water gas shift equilibrium* to the right-hand side:

$$CO + H_2O \rightleftharpoons H_2 + CO_2$$
$$\Delta H^\circ_{298} = -41\ \text{kJ mol}^{-1},\ \Delta G^\circ_{298} = -28\ \text{kJ mol}^{-1}$$

Finally, the carbon dioxide is removed by scrubbing the gas mixture with either methanol, monoethanol amine or methyl diethanol amine. Alternatively, CO_2 may be adsorbed under pressure at a suitable solid phase (e.g., activated charcoal) resulting in very pure H_2. CO_2 is then recovered by heating in case of the amine solutions or by reducing the pressure at the charcoal absorber (*pressure swing adsorption*). The recovered CO_2 is mainly used to produce urea as a fertilizer (Section 9.4.2) but may be stored underground in the longer term.[9] Approximately 50% of the world production of hydrogen is based on this process.

(b) *Partial combustion of higher hydrocarbons* in the presence of water vapor without the need for a catalyst:

$$-CH_2- + \tfrac{1}{2}\,O_2 \longrightarrow CO + H_2 \qquad \Delta H^\circ_{298} = -92\ \text{kJ mol}^{-1}$$
$$-CH_2- + H_2O \longrightarrow CO + 2\,H_2 \qquad \Delta H^\circ_{298} = 150\ \text{kJ mol}^{-1}$$

Heavy crude oil and residues of the crude oil distillation in refineries are used for this process. The first exothermic reaction produces the energy needed for the second endothermic reaction; the carbon monoxide is subsequently turned into CO_2 by the water gas shift reaction and is removed as discussed earlier.

(c) Reduction of water vapor by finely divided coal or petroleum coke at temperatures above 1100 °C and pressures of up to 40 bar (*coal gasification*) according to the following equation; the 1:1 mixture of H_2 and CO is called *synthesis gas* or simply *syngas*:

9 CCS technology (carbon capture and storage).

$$H_2O + C_{s.} \longrightarrow H_2 + CO \quad \Delta H = 131\ \text{kJ mol}^{-1}$$

This reaction is endothermic. Therefore, oxygen from an air separation unit is added to the steam to generate the necessary reaction temperature by partial combustion of coal. To produce pure hydrogen, the reaction mixture is subjected to catalytic reduction of remaining H_2O by carbon monoxide according to the water gas shift reaction mentioned earlier.

Coal gasification is carried out in many countries, on a particularly large scale in China and by SASOL in South Africa, with subsequent production of about 100 organic compounds from the syngas using the FISCHER–TROPSCH technology.

(d) Electrolysis of aqueous solutions of salts, acids or alkalis produces hydrogen of high purity but requires valuable electric energy:

$$NaCl + H_2O \xrightarrow{\text{energy}} NaOH + \tfrac{1}{2} H_2 + \tfrac{1}{2} Cl_2$$

For example, hydrogen is obtained as a side product during chlorine production from aqueous solutions of NaCl (*chlorine-alkali electrolysis*; see Section 13.5.1). For each ton of Cl_2, approximately 0.0028 t of H_2 and 1.128 t of NaOH(aq) are produced. Electrolysis of alkaline solutions such as KOH (30%) is also performed on a relatively large scale, usually at temperatures between 80 and 100 °C using Raney nickel for the electrodes. This technology is being tested for temporary energy storage since hydrogen gas produced from wind power (*power-to-gas*) can be stored in underground caverns and later used to produce electric power by fuel cells (transmission grid stabilization in times of overproduction of wind power).[10] Hydrogen may also be admixed at a limited percentage to natural gas to avoid the drawbacks related to transport and storage of pure hydrogen; these mixtures are called *enriched methane* and can be transported in pipelines and used with the existing gas infrastructure.[11] However, it should be noted that the *fuel value*, that is, the enthalpy released on combustion, is much lower for hydrogen (–285.8 kJ mol^{-1}) than for methane (–890.5 kJ mol^{-1}; both values are for 25 °C with formation of liquid water).

Approximately 4% of the worldwide hydrogen production is based on electrolytic processes, which can also be carried out at pressures of up to 60 bar.

The annual production of elemental hydrogen in the 27 countries of the *European Union* is about $48 \cdot 10^6$ t, and about 50% of it is used to synthesize *ammonia* from the elements by the HABER–BOSCH process (Section 9.4.2). The remainder is

10 A. Züttel, A. Bergschulte, L. Schlapbach (eds.), *Hydrogen as a Future Energy Carrier*, Wiley-VCH, Weinheim, Germany, **2008**. D. Stolten (ed.), *Hydrogen and Fuel Cells*, Wiley-VCH, Weinheim, Germany, **2010**.

11 M. de Falco, A. Basile (eds.), *Enriched Methane*, Springer, Heidelberg, Germany, **2016**.

used to produce *methanol* from CO and 2 H_2,[12] to synthesize *higher alcohols* from alkenes with CO and H_2 (*oxosynthesis*), for the *hydrogenation* of benzene to produce cyclohexane which in turn is needed for the synthesis of caprolactam. Furthermore, nitrobenzene is industrially reduced to aniline by hydrogen.

In addition, large amount of H_2 are needed for *hydrocracking* and *hydrotreating* of refinery products using various catalysts. The large-scale desulfurization of crude oil by hydrogenation in refineries requires elemental hydrogen (*hydrodesulfurization*; Section 12.4.1). Also, vegetable oils are turned into solid fats by hydrogenation of the carbon–carbon double bonds (*fat hardening*). Other well-known applications for hydrogen are as fuel for rockets, spacecrafts, cars and busses, for cutting and welding of metals by a H_2/O_2 torch and the reduction of metal oxides to produce pure Ge, Mo, W and Co commercially.

In *nickel–hydrogen batteries*, H_2 plays a special role. These very reliable secondary batteries are used in many spacecrafts, including the *International Space Station* and the famous HUBBLE space telescope. They are based on highly reversible redox reactions:[10]

$$\text{Positive electrode:} \quad \mathrm{NiO(OH) + H_2O + e^- = Ni(OH)_2 + [OH]^-}$$

$$\text{Negative electrode:} \quad \mathrm{1/2\,H_2 + [OH]^- = H_2O + e^-}$$

$$\text{Overall reaction:} \quad \mathrm{NiO(OH) + 1/2H_2 = Ni(OH)_2}$$

The electrolyte is 31% aqueous KOH; the voltage on load is 1.20–1.27 V. The battery is in a hermetically sealed metal vessel since hydrogen pressures up to 55 bar are reached on charging.[13] The primary power is provided either by photovoltaic or nuclear devices, the latter based on radioisotopes (e.g., Pu) in combination with a thermoelectric generator. Ni–H_2 batteries are characterized by a particularly long cycle life, minimum self-discharge and high energy density. During the years 1990–2010, they have been the workhorse for commercial communication satellites but in the future, they may be gradually replaced by lithium-ion batteries.

Hydrogen gas for laboratories is available in red-painted stainless steel cylinders, usually under a pressure of 200 bar, but H_2 may also be delivered as a *liquid* (LH_2) in well-insulated tank cars at a temperature of –253 °C (b.p.). At this temperature, hydrogen is stored at rocket launching sites in big spherical tanks, well separated from the tanks containing liquid oxygen. Furthermore, long steel cylinders are used for stationary storage and for transport of compressed hydrogen (up to

12 M. Bertau et al. (eds.), *Methanol: The Basic Chemical and Energy Feedstock of the Future*, Springer, Heidelberg, Germany, **2014**.

13 Therefore, a H_2-absorbing metal is sometimes used to form an alloy-like hydride which reversibly delivers H_2 if the pressure is dropped or the temperature is raised on discharging the battery (see Section 5.7.5). Nickel-metal hydride (NiMH) batteries have been used in automobiles before lithium-ion batteries took over.

100 bar) on trucks, while big stationary tanks (water-sealed gas holders or gasometers) are used for H_2 on site storage at moderate pressures.[10]

In addition, industrialized countries operate an extensive net of pipelines to transport hydrogen gas under a pressure of 20–30 bar back and forth between producers and consumers to handle fluctuations in supply and demand (pipeline length in Europe: 1500 km, in the USA: >750 km). To ship hydrogen over large distances (between continents) hydrogen-rich compounds such as liquid ammonia or methyl cyclohexane (C_7H_{14}) may be used. At the destination ammonia can be catalytically decomposed into the elements while C_7H_{14} may be dehydrogenated to 3 mol H_2 and 1 mol toluene (C_7H_8); the latter is shipped back to the producer for regeneration.

In the laboratory, small quantities of H_2 may be produced either by electrolysis of 30% aqueous KOH using nickel electrodes or by reaction of metallic zinc or iron with dilute aqueous acids such as HCl or H_2SO_4:

$$2\,[H_3O]^+ + Zn \longrightarrow H_2 + Zn^{2+} + 2\,H_2O$$

The hydrogen produced electrolytically under strict air-free conditions is very pure. On the other hand, the purity of H_2 obtained by reduction of hydrogen ions by metals depends on the purity of both the metal and the acid. The acid may still contain dissolved air, and the H_2 gas may contain AsH_3, H_2S and even hydrocarbons from corresponding impurities of the metal (arsenides, sulfides and carbides).

There are several *methods to purify hydrogen*. For example, the diffusion of hydrogen through an electrically heated tube of palladium or nickel leaves the impurities behind. On the other hand, H_2 may be reacted with metal powders such as Pd, U, Ti or the alloy FeTi at room or elevated temperatures; the resulting hydrides are decomposed at a higher temperature to produce pure H_2. For example, 1 g Pd powder absorbs 100 mL H_2 at 25 °C and 0.1 MPa and releases it at 200 °C. In industry, hydrogen is purified either by adsorption of the impurities to molecular sieves (porous silicates of the zeolite type; see Section 8.8.2) or by diffusion through a polymeric, hydrogen-selective membrane (consisting of polysulfones or polyimides) impermeable for the impurities.[10] This technology is often applied in ammonia synthesis and is used to recover unreacted H_2 from the equilibrium product mixture containing NH_3, N_2 and Ar as major impurities (Section 9.4.2). Argon as a constituent of air is a side product of nitrogen produced in an air separation unit.

5.1.2 Isotopes of Hydrogen

Natural hydrogen is a mixture of three isotopes with different neutron numbers in the nuclei: ^1H (light hydrogen or protium), ^2H (heavy hydrogen or deuterium, D) and ^3H (tritium, T) in an atomic ratio of $1{:}1.56 \cdot 10^{-4}{:}10^{-18}$. Only tritium is radioactive with a half-life of 12.3 years; it decomposes by e^- emission (β radiation) to give ^3He. Therefore,

tritium is used as a *radio tracer* to mark molecules. In Nature, tritium is generated in Earth's atmosphere from nitrogen atoms by capturing neutrons from cosmic radiation:

$$^{14}_{7}\mathrm{N} + {}^{1}_{0}\mathrm{n} \longrightarrow {}^{3}_{1}\mathrm{H} + {}^{12}_{6}\mathrm{C}$$

The natural reservoir of tritium on Earth's surface has been estimated to 11 kg, but a much larger amount was released into the atmosphere during the years 1953–1963 by nuclear weapon's tests above ground. This tritium is to a large extent deposited in the oceans as isotopomer HTO (super-heavy water). Since no nuclear tests above ground took place after 1963, the tritium concentration in natural waters now approaches the value cited earlier, which represents the radioactive equilibrium between continuous formation and decay. Industrially, tritium is produced by neutron bombardment of ^{6}Li (Section 5.7.3). The wastewater from nuclear power plants also contains traces of tritium as HTO. Commercially, tritium is available as a gas and as hydride UT_3/UH_3 from which HT may be released by heating. The use of tritium is strictly controlled;[14] its use in fusion reactions is discussed below.

Deuterium nuclei (symbol in physics: *d*) were formed shortly after the *Big Bang* by fusion of protons with liberation of positrons and electron neutrinos ($2p \rightarrow d + e^{+} + \nu_e$). The isotopes ^{1}H and ^{2}H differ more in mass from each other than the isotopes of any other element. Therefore, the physical and chemical properties of H versus D containing compounds differ much more than in case of other elements (e.g., reaction rates and equilibrium constants). Reaction rates of deuterated molecules are usually smaller than those of ordinary hydrogen compounds due to the lower vibrational energy (see Section 4.4.3). Such *isotopic effects* are used for the enrichment and separation of isotopomers from natural isotopic mixtures. For example, during the electrolysis of water, oxonium ions $[H_3O]^+$ are reduced (discharged) slightly faster than the partially deuterated ions $[H_2DO]^+$, thus leading to a gradual enrichment of HDO. With decreasing concentration of H_2O in the aqueous phase, more D_2O is formed according to the following equilibrium (equilibrium constant at 400 K in the vapor phase: 0.25):

$$2\,\mathrm{HDO} \rightleftharpoons \mathrm{H_2O} + \mathrm{D_2O}$$

G. N. LEWIS produced almost pure *heavy water* (D_2O) in 1933 for the first time. Today, D_2O is used as a cooling and moderating liquid in certain nuclear reactors that use the fission of ^{235}U nuclei as energy source.[15]

---

14 M. B. Kalinowski, *International Control of Tritium for Nuclear Nonproliferation and Disarmament*, CRC Press, Boca Raton, **2004**. F. Mannone (ed.), *Safety in Tritium Handling Technology*, Springer, Dordrecht, **1993**.

15 HAROLD CLAYTON UREY received the NOBEL prize in chemistry in the year 1934 for the discovery of deuterium.

The slightly varying atomic ratio D:H of natural waters is used to determine their origin since some fractionation takes place by evaporation as well as by biological processes.[16] Reference sample is the *Vienna Standard Ocean Water* with D:H = $1.5576 \cdot 10^{-4}$.

The vapor pressure and diffusion rate of deuterated compounds are often lower than those of related ordinary hydrogen compounds, which allows for isotopic enrichment or even separation by either fractional distillation, countercurrent diffusion or H/D exchange between liquid and vapor phases. Deuterium contents of up to 99.9% have been achieved. The physical properties of H_2, D_2, H_2O and D_2O are compiled in Table 5.1.

Table 5.1: Physical properties of H_2, D_2, H_2O and D_2O.

	H_2	D_2	H_2O	D_2O
Melting point at 1.013 bar (°C)	−259.2	−254.4	0.00	3.81
Boiling point at 1.013 bar (°C)	−252.8	−249.5	100.0	101.4
Critical temperature (°C)	−240.0	−234.8	374.2	370.9
Critical pressure (MPa)	1.315	1.665	22.1	21.9
Maximum density (g cm^{-3})			1.00	1.11
Viscosity at 20 °C (mPa s)			1.00	1.25
Ion product at 25 °C (mol^2 L^{-2})			$1 \cdot 10^{-14}$	$0.3 \cdot 10^{-14}$

Elemental deuterium (D_2) is produced by electrolysis of D_2O or by its reaction with metallic sodium or magnesium. Many deuterated compounds can be obtained by *isotopic exchange* reactions. For example, H_2, CH_4, NH_3 and H_2O react with D_2 on platinum or nickel powder as a catalyst to the isotopically substituted derivatives HD, HDO, CH_3D and NH_2D, respectively. The degree of substitution mainly depends on the mixing ratio of the starting compounds. The deuteration reaction can be monitored by infrared (IR) spectroscopy or mass spectrometry (MS). Isotopic exchange can also be achieved using D_2O or CH_3OD by repeated dissolution of the corresponding compound containing labile hydrogen atoms followed by evaporation of the mixture to dryness. This works, for example, with ammonium salts and hydrogen salts of polyprotic oxoacids such as $[HSO_4]^-$ or $[H_2PO_4]^-$. In other cases, deuterolysis by D_2O is applied, as the following examples illustrate:

$$Li[AlH_4] + 4\,D_2O \longrightarrow LiOD + Al(OD)_3 + 4\,HD\uparrow$$

$$SiCl_4 + 2\,D_2O \longrightarrow SiO_2 + 4\,DCl\uparrow$$

$$Al_2S_3 + 6\,D_2O \longrightarrow 2\,Al(OD)_3 + 3\,D_2S\uparrow$$

16 L. Hallis et al., *Science* **2015**, *350*, 795.

In an analogous manner, ND_3 is obtained from Mg_3N_2, D_2SO_4 from SO_3 and D_3PO_4 from P_4O_{10} by reaction with D_2O.

The isotope ^1H (nuclear spin $I = 1/2$) is an important probe to characterize molecules by *nuclear magnetic resonance* (NMR) *spectroscopy*.[17] In H_2 molecules, the two nuclear spins can be either parallel (*ortho*-H_2) or antiparallel oriented (*para*-H_2); the equilibrium ratio between these two nuclear spin isomers is 3:1 in gaseous H_2 at 25 °C. Since the conversion of *o*-H_2 into *p*-H_2 is slightly exothermic, cooling of hydrogen gas (*n*-H_2) shifts the equilibrium to 1:1 at 77 K. The reaction is very slow unless catalyzed by W, Ni or charcoal. As the physical properties of the two spin isomers of hydrogen differ, this phenomenon needs to be taken into account during liquefaction of dihydrogen.

5.1.3 Properties of Hydrogen

Elemental hydrogen is a colorless, odorless and tasteless gas, which is hardly soluble in water. H_2 is the lightest of all gases: 1 L of H_2 at 25 °C and 1.013 bar has a mass of only approximately 90 mg. Therefore, H_2 had been used to lift balloons and airships in the past.[18] Today, the use of helium is mandatory for safety reasons. About 1 kg H_2 has a volume of 12 m^3 at standard conditions but only of 0.026 m^3 at 700 bar as applied in electric cars powered by fuel cells.

At 20 °C hydrogen is relatively unreactive. Due to its high dissociation enthalpy of 436 kJ mol^{-1}, cleavage of the H–H bond occurs only at very high temperatures. The dissociation constant $K_p = p^2(H)/p(H_2)$ amounts to only $3.14 \cdot 10^{-4}$ kPa at 2000 K but to 2.81 kPa at 3000 K (p represents partial pressures of the components). However, strong dissociation up to 90% can be achieved in a powerful microwave discharge at low pressures (0.5–5 hPa). Behind the discharge tube the atoms recombine as follows:

$$H + H + M \longrightarrow H_2 + M^*$$

where M is a collision partner, that is, an atom, a molecule or the vessel wall, which can absorb part of the recombination enthalpy (equals the negative dissociation enthalpy), insuring against renewed dissociation (M* is a thermally or electronically excited state of M). The half-life of the hydrogen atoms (ca. 0.1 s) is a function of experimental conditions such as pressure and dimensions of the vessel.

17 Deuterium ($I = 1$) can also be used for NMR spectroscopy but needs special conditions and therefore is of minor relevance.

18 The first flight of a German "Zeppelin" airship (LZ1) took place in 1900; LZ4 was destroyed by a spark, and on 6 May 1937 the airship "Hindenburg" burned out during landing at Lakehurst, New Jersey, USA, immediately after a thunderstorm.

However, hydrogen atoms have been detected several meters from the dissociation site since high flow rates can be achieved in vacuum lines.

Hydrogen atoms ($H^\bullet$) are extremely reactive and reduce oxides to elements even at room temperature (e.g., SO_2, CuO, PbO, Bi_2O_3 and SnO_2) or to lower oxides (e.g., NO_2 to NO). Many nonmetals form volatile hydrides on reaction with H atoms (O_2, S_8, P_4, As, Sb, Ge and halogens). Hydrogen atoms play an important role as intermediates in chain reactions; for example, the detonation of $H_2 + O_2$ (*oxyhydrogen*) and $H_2 + Cl_2$ mixtures, which proceed according to the following reaction mechanisms (only reactions with large rate constants are shown):[19]

	Oxyhydrogen reaction	**Chlorine-hydrogen reaction**
initiation reactions:	$H_2 \longrightarrow 2\,H^\bullet$	$Cl_2 \longrightarrow 2\,Cl^\bullet$
	$H_2 + O_2 \longrightarrow H^\bullet + HO_2^\bullet$	
chain reactions:	$H^\bullet + O_2 \longrightarrow O^{\bullet\bullet} + OH^\bullet$	$Cl^\bullet + H_2 \longrightarrow H^\bullet + HCl$
	$H^\bullet + O_2 + M \longrightarrow HO_2^\bullet + M^*$	$H^\bullet + Cl_2 \longrightarrow Cl^\bullet + HCl$
	$HO_2^\bullet + H^\bullet \longrightarrow 2\,OH^\bullet$	
	$O^{\bullet\bullet} + H_2 \longrightarrow H^\bullet + OH^\bullet$	
chain termination:	$H^\bullet + OH^\bullet + M \longrightarrow H_2O + M^*$	$Cl^\bullet + H^\bullet + M \longrightarrow HCl + M^*$
	$2\,OH^\bullet + M \longrightarrow H_2O_2 + M^*$	$2\,Cl^\bullet + M \longrightarrow Cl_2 + M^*$
	$O^{\bullet\bullet} + H_2 + M \longrightarrow H_2O + M^*$	$2\,H^\bullet + M \longrightarrow H_2 + M^*$
	$2\,H^\bullet + M \longrightarrow H_2 + M^*$	
	$2\,HO_2^\bullet \longrightarrow H_2O_2 + O_2$	
	$HO_2^\bullet + H^\bullet \longrightarrow H_2 + O_2$	

The strongly endothermic *initiation reactions* can be started thermally or, in the case of chlorine, also photochemically. The resulting free radicals then react exothermally with molecules or other radicals until the chains are terminated either by wall destruction reactions or by homogeneous chain terminating processes (*radical chain reactions*). In some cases, collision partners M are needed to absorb part of the reaction enthalpy either as kinetic or rovibrational energy. The excited species M* may then trigger other reactions by providing the necessary activation energy. Details of the reaction mechanisms depend on the pressure of the gas mixture and the reaction temperature; the concentrations of the radicals $H^\bullet$ and $OH^\bullet$ can be determined during the reaction by fluorescence spectroscopy.

5.2 Hydrogen Ions H^+

Hydrogen forms the ions H^+ and H^-. The hydride ion H^- is present in hydride salts like LiH and CaH_2 (Section 5.7.4). Hydrogen ions H^+ as free protons can be

19 W. Liang, C. K. Law, *Phys. Chem. Chem. Phys.* **2018**, *20*, 742.

generated from H_2 gas either in a glow discharge or in the ion source of a mass spectrometer. After dissociation of H_2, the ionization of hydrogen atoms occurs by collision with high energy electrons. The solar particle radiation that constantly hits the Earth's atmosphere (*solar wind*) consists of 95% of protons and 4% of α particles together with an equivalent amount of electrons so that the gas as a whole is electroneutral.

Unlike other ions, free protons H^+ cannot exist in condensed phases. Their small diameter results in such a strong electric field that they are immediately solvated, for example:

$$H^+ + H_2O \longrightarrow [H_3O]^+ \qquad H^+ + H_3PO_4 \longrightarrow [H_4PO_4]^+$$

$$H^+ + NH_3 \longrightarrow [NH_4]^+ \qquad H^+ + HF \longrightarrow [H_2F]^+$$

$$H^+ + R_2O \longrightarrow [R_2OH]^+ \qquad H^+ + H_2SO_4 \longrightarrow [H_3SO_4]^+$$

The protonated solvent molecules may be further solvated. Oxonium ions $[H_3O]^+$ produced by protonation of water are further solvated to a series of hydronium ions $[H_5O_2]^+$, $[H_7O_3]^+$ and $[H_9O_4]^+$ (see Sections 5.3 and 5.6). These ions are also termed diaqua-, triaqua- and tetraaqua-hydrogen ions. In honor of their discoverers, $[H_3O]^+$ is called EIGEN ion and $[H_5O_2]^+$ is referred to as ZUNDEL ion or complex.[20] The completely hydrated proton is called hydrogen ion and written as $H^+(aq)$.

The total hydration enthalpy ΔH of the proton,

$$H^+(g.) + H_2O(l.) \longrightarrow [H_3O]^+(aq) \qquad \Delta H^\circ_{298} = -1090 \text{ kJ mol}^{-1}$$

is (in absolute values) much larger than that of other singly charged cations (g. for gaseous, and l. for liquid). ΔH is the sum of the hydration enthalpies of the following two reactions:

$$H^+(g.) + H_2O(g.) \longrightarrow [H_3O]^+(g.) \qquad \Delta H^\circ_{298} = -690 \text{ kJ mol}^{-1}$$

$$[H_3O]^+(g.) + n\,H_2O(l.) \longrightarrow H^+(aq) \qquad \Delta H^\circ_{298} = -400 \text{ kJ mol}^{-1}$$

The half-life of $[H_3O]^+$ in water is extraordinarily small (ca. 10^{-13} s) because of the exchange equilibrium:

$$[H_3O]^+ + H_2O^* \rightleftharpoons H_2O + [H_3O^*]^+$$

Therefore, the excess proton is not localized at an individual oxygen atom but is continuously changing its place in a hydrogen bond (see Section 5.6.5):

20 MANFRED EIGEN (1927–2019), German physical chemist, NOBEL prize in chemistry of the year 1967. GEORG ZUNDEL (1931–2007), German physicist.

A similar rapid proton exchange is also observed (e.g., by NMR spectroscopy) in other compounds with labile hydrogen atoms (protons), for example, between NH_3 and $[NH_4]^+$.

Pure water dissociates only slightly:

$$2\ H_2O \rightleftharpoons [H_3O]^+ + [OH]^-$$

This equilibrium is strongly temperature dependent. The GIBBS energy of this reaction is 98 kJ mol^{-1} at 298 K. The molar ion product $k_w = c(H^+) \cdot c(OH^-)$ is $1.001 \cdot 10^{-14}$ $mol^2\ L^{-2}$ at 25 °C but $5.483 \cdot 10^{-13}$ $mol^2\ L^{-2}$ at 100 °C. The concentrations of H^+ and $[OH]^-$ are thus $1 \cdot 10^{-7}$ mol L^{-1} each at 25 °C but $7.4 \cdot 10^{-7}$ mol L^{-1} at 100 °C. The negative of the common logarithm of the hydrogen ion is the pH:[21]

$$pH = -{}^{10}\log\ c(H^+)$$

If the concentrations of H^+ and $[OH]^-$ are equal, the solution is neutral. For 25 °C, this is the case at pH = 7.00, but at 100 °C neutrality is reached at pH = 6.13. In alkaline solutions, $[OH]^-$ ions dominate ($c[H^+] < c[OH^-]$) and in acidic solutions H^+ ions: ($c[H^+] > c[OH^-]$). At pH = 1.0, there is approximately one $[H_3O]^+$ ion per 500 molecules of H_2O; conversely at pH = 13 one $[OH]^-$ anion for the same amount of water molecules. The surface water of oceans is presently at pH = 8.1, much lower than 200 years ago. For the year 2100, a pH of 7.8 is expected owing to the increasing CO_2 concentration of the atmosphere (presently ca. 410 ppm). The difference between the pH values of 8.1 and 7.7 corresponds to an increase in the acidity or hydrogen ion concentration by a factor of 2.5!

The aqueous ions H^+ and $[OH]^-$ have extremely high migration velocities in an electric field; despite pronounced solvation, both migrate orders of magnitude faster than other ions owing to a special mechanism for charge transport. As liquid water is strongly organized by hydrogen bonds (see Section 5.6), the transport of $[H_3O]^+$ can take place by simple positional exchange of protons within hydrogen bonds ("proton hopping" due to a double minimum potential):

Hydroxide ions can migrate likewise by a concerted "hopping" of protons from right to left:

21 The pH (*p*otentia *h*ydrogenii) was introduced in 1909 by S. P. L. SØRENSEN (Danish biochemist).

This mechanism of *protic conductance* was suggested by THEODOR GROTTHUSS (1785–1822) in 1806 and is therefore known under his name; it is also responsible for the extraordinary high reaction rate of the neutralization reaction:

$$[H_3O]^+ + [OH]^- \rightleftharpoons 2\,H_2O$$

Other pure (water-free) protic solvents are also weakly dissociated, for example, liquid ammonia, liquid hydrogen fluoride and anhydrous sulfuric acid:

$$2\,NH_3 \rightleftharpoons [NH_4]^+ + [NH_2]^-$$

$$3\,HF \rightleftharpoons [H_2F]^+ + [HF_2]^-$$

$$2\,H_2SO_4 \rightleftharpoons [H_3SO_4]^+ + [HSO_4]^-$$

The degree of dissociation can be determined by electric conductivity measurements. Because of their similarity with water such liquids are known as *water-like solvents* (also see Section 9.4.8).

5.3 Acids

The auto-dissociation of water and water-like solvents is of type:

$$HA \rightleftharpoons H^+ + A^-$$

where all reactants are solvated. Since SVANTE ARRHENIUS[22] published his theory of electrolytic dissociation in 1887, hydrogen ions, that is, solvated protons, are held responsible for the acidity of an aqueous solution. Consequently, a compound is an acid in water if $c(H^+) > c(OH^-)$. This definition may be generalized for all protic (nonaqueous) solvents HA with an acid defined as a substance, which increases the concentration of the solvated protons $[H_2A]^+$, for example, $[H_3SO_4]^+$ in sulfuric acid and $[H_4PO_4]^+$ in phosphoric acid. The latter two cations are termed sulfate acidium and phosphate acidium ion, respectively.

In aqueous systems, the molecules HCl, HBr, HI, H_2SO_4, HNO_3, $HClO_4$ and H_3PO_4 are well-known acids, which apparently dissociate but in fact rather protonate solvent molecules:

22 Swedish chemist and physicist (1959–1927); NOBEL prize in chemistry in 1903.

$$HCl + H_2O \longrightarrow [H_3O]^+ + Cl^-$$

$$H_2SO_4 + H_2O \longrightarrow [H_3O]^+ + [HSO_4]^-$$

$$H_2SO_4 + 2\,H_2O \longrightarrow 2\,[H_3O]^+ + [SO_4]^{2-}$$

Acids having one acidic hydrogen are monoprotic, H_2SO_4 is diprotic and H_3PO_4 is triprotic.

Nonprotic compounds can also increase the hydrogen ion concentration, for example, by reaction with the solvent:

$$Cl_2O_7 + 3\,H_2O \longrightarrow 2\,[H_3O]^+ + 2\,[ClO_4]^-$$

$$SO_3 + 2\,H_2O \longrightarrow [H_3O]^+ + [HSO_4]^-$$

These and other *acid anhydrides* such as CO_2, N_2O_5, P_4O_{10}, SO_2, SeO_2 and XeO_3 behave in water as acids although they do not contain the functional groups of the solvent. Therefore, they are termed as *ansolvo acids*, while protic acids are *solvo acids*.

5.3.1 Oxonium Salts

Strong protic acids HA and acid anhydrides react with water to crystalline hydrates $HA \cdot nH_2O$ (n = 1, 2, 3...), which are in fact oxonium or hydronium salts $[H_3O]^+A^-$, $[H_5O_2]^+A^-$ and others, as shown by structural investigations (X-ray or neutron diffraction on single crystals). Examples are given in Table 5.2.

Table 5.2: Oxonium salts of strong acids.

Composition	Structure	Melting point (°C)
$HX \cdot H_2O$ (X = F, Cl, Br, I)	$[H_3O]X$	−36 (X = F)
$HCl \cdot 2\,H_2O$	$[H_5O_2]Cl$	−18
$HCl \cdot 3\,H_2O$	$[H_5O_2]Cl \cdot H_2O$	−25
$HBr \cdot 4\,H_2O$	$[H_7O_3][H_9O_4]Br_2 \cdot H_2O$	−56
$HClO_4 \cdot H_2O$	$[H_3O][ClO_4]$	+50
$HClO_4 \cdot 2\,H_2O$	$[H_5O_2][ClO_4]$	−20.6
$HClO_4 \cdot 3\,H_2O$	$[H_7O_3][ClO_4]$	−47
$H_2SO_4 \cdot H_2O$	$[H_3O][HSO_4]$	+8.5
$H_2SO_4 \cdot 2\,H_2O$	$[H_3O]_2[SO_4]$	−38.9
$H_2SO_4 \cdot 4\,H_2O$	$[H_5O_2]_2[SO_4]$	−29.9
$H_2SeO_4 \cdot 4\,H_2O$	$[H_5O_2]_2[SeO_4]$	−52

On the other hand, the dihydrate of the weak oxalic acid, $(COOH)_2 \cdot 2H_2O$, is not an oxonium salt since its two acidic protons at the carboxyl groups are connected to the water molecules by hydrogen bonds only, yielding a true *hydrate*. Hydrates and oxonium salts can be distinguished by IR spectroscopy since H_2O, $[H_3O]^+$ and $[H_5O_2]^+$ have characteristic absorption bands. The trigonal-pyramidal oxonium ion is isoelectronic with the ammonia molecule and both are of C_{3v} symmetry. In different oxonium salts, the bond angles H–O–H are usually in the range 112–117°, but in the vapor phase $[H_3O]^+$ is almost planar. The basic geometries of $[H_3O]^+$, $[H_5O_2]^+$, $[H_7O_3]^+$ and $[H_9O_4]^+$ as determined by X-ray diffraction analysis of corresponding salts are shown in Figure 5.1.

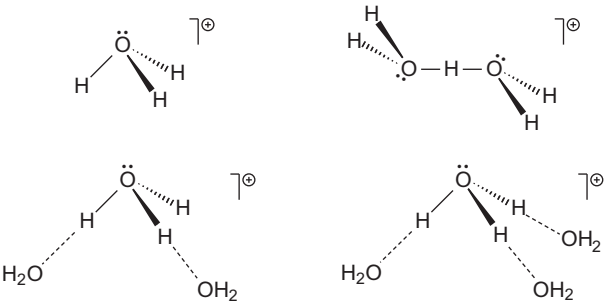

Figure 5.1: Structures of the ions $[H_3O]^+$, $[H_5O_2]^+$, $[H_7O_3]^+$ and $[H_9O_4]^+$ in salts with weakly coordinating (weakly basic) anions.

Discrete $[H_5O_2]^+$ ions as in Figure 5.1 (although connected to anions by hydrogen bonds) exist in the structure of $[H_5O_2][ClO_4]$. In general, the two water molecules of $[H_5O_2]^+$ are connected by a single proton, located centrally or occupying two closely neighboring positions separated by a small energy barrier, depending on the anion. The internuclear distance d_{OO} = 242 pm of this OHO bridge is small and argues for a symmetrical hydrogen position. The four outer H atoms are located pairwise above and below the paper plane of Figure 5.1. In the vapor phase, the cation $[H_5O_2]^+$ is of C_2 symmetry with d_{OO} = 239 pm and a bond angle O–H–O of 174°, while in $[H_5O_2][SbF_6]$ the cation symmetry is C_{2h} with a center of inversion. The structures of $[H_7O_3]^+$ and $[H_9O_4]^+$ are analogous with pyramidally coordinated oxygen atoms (Figure 5.1) and all hydrogen bonds asymmetrical.

The crystal structures of oxonium salts of strong mineral acids resemble those of the corresponding ammonium salts and the salts $[H_3O][ClO_4]$ and $[NH_4][ClO_4]$ are even *isomorphic*. Oxonium salts have markedly lower melting points (m.p.s) than the ammonium analogs and the m.p.s of the hydronium salts are lower still (Table 5.2). Oxonium and hydronium salts are acids in water, and completely ionized (at not too high concentrations). Alkyl and alkoxy derivatives of oxonium salts

such as $[ROH_2]X$ and $[R_2OH]X$ are formed from alcohols ROH and ethers R_2O with strong protic acids HX (e.g., HF/AsF_5, $HClO_4$ and H_2SO_4). "Dimers" with bridging protons as in $[(ROH)_2H]X$ and $[(R_2O)_2H]X$ are also known and are formally derivatives of the ZUNDEL complex $[H_5O_2]^+$.

How many water molecules are needed to initiate dissociation of HCl or HBr *in the gas phase* to form hydronium halides (ion pairs)? This problem has been studied by quantum-chemical calculations and spectroscopic methods. The minimal number of water molecules is four, resulting in a hydrogen bonded complex $[(H_3O)(H_2O)_3]X$ (X = Cl, Br), in which the cation $[H_3O]^+$ and the halide anion are separated by three bridging water molecules:

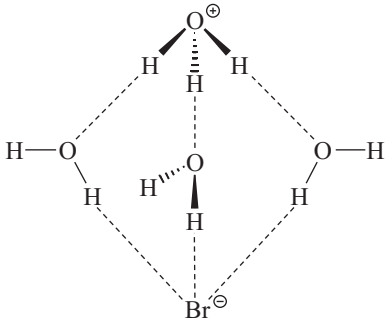

In an analogous manner, the aqueous ions $[H_3O]^+$ and $[OH]^-$ need to be separated by at least three bridging water molecules not to neutralize each other.

5.3.2 Liquid Ammonia

Liquid NH_3 is the most important water-like solvent since the *ammonia system* (Section 9.4.8) is very similar to the aqueous system and is therefore widely used in preparative chemistry and in industry. In the ammonia system, acids are substances that increase the concentration of $[NH_4]^+$, for example, ammonium salts. Obviously, in view of the stronger basicity of ammonia compared to water, protic acids HA known from the aqueous system also react as acids in liquid ammonia:

$$HCl + NH_3 \longrightarrow [NH_4]^+ + Cl^-$$

These solutions behave like aqueous acids, that is, they change indicator colors, react with active metals to evolve hydrogen and can be neutralized with bases. The auto-dissociation of liquid ammonia, however, is much weaker than that of water; the ion product $k_A = c[NH_4^+] \cdot c[NH_2^-]$ is only 10^{-29} mol^2 L^{-2}. Consequently, the neutrality point is at pH = 14.5.

5.3.3 Anhydrous Sulfuric Acid

Anhydrous sulfuric acid is a solvent of very low proton affinity. In most solvents, H_2SO_4 acts as a protonating agent. In order to protonate H_2SO_4, very strong protic acids are therefore needed, for example, anhydrous fluorosulfonic acid (HSO_3F), trifluoromethyl sulfonic acid (HSO_3CF_3, triflic acid), disulfuric acid ($H_2S_2O_7$) as well as mixtures of HSO_3F with SbF_5 and SO_3 (for more anhydrous acids, see Section 5.5.2). These so-called *super acids* can be used to protonate even very weak bases such as H_2SO_4, which function as acids for most intents and purposes:

$$H_2SO_4 + HSO_3F \longrightarrow [H_3SO_4]^+ + [SO_3F]^-$$

JOHANNES N. BRØNSTED[23] and independently THOMAS MARTIN LOWRY[24] defined acids in 1923 as proton donors, and bases as proton acceptors. In this sense, H_2SO_4 is a base toward HSO_3F, and H_3PO_4 is a base toward H_2SO_4:

$$H_3PO_4 + H_2SO_4 \longrightarrow [H_4PO_4]^+ + [HSO_4]^-$$

In other words, whether a compound functions as an acid or a base is determined by the chemical environment. Protonated acid molecules like $[H_3SO_4]^+$ (acidium ions) have been isolated as salts, for example, $[D_3SO_4][ClO_4]$ and $[P(OH)_4][ClO_4]$ (tetrahydroxo phosphonium perchlorate) which are readily soluble in nitromethane and ionize to give conducting solutions. The acid or base strength of a substance depends on the solvent and, therefore, no absolute definition can be made.

Other protic solvents are important in inorganic chemistry too,[25] and the concepts developed above can be applied analogously to alcohols ROH, glacial acetic acid CH_3COOH, liquid H_2S, HCN and HF as well as to HSO_3F.

5.4 Bases

According to Arrhenius, the hydroxide ion $[OH]^-$ is responsible for the basic properties in water, and therefore $c[OH^-] > c[H^+]$ holds in basic solutions. All chemicals that increase the hydroxide ion concentration in water are bases. Typical examples are the hydroxides of the alkali and alkaline earth metals, but there are also bases lacking $[OH]^-$ ions and yet producing alkaline solutions in water. This holds for the salt-like oxides and amides of the alkali and alkaline earth metals as well as for ammonia (NH_3), hydrazine (N_2H_4) and others, which all react with water to hydroxide ions:

23 Danish physical chemist (1879–1947).

24 British chemist (1874–1936).

25 J. Jander, Ch. Lafrenz, *Wasserähnliche Lösungsmittel*, VCH, Weinheim, **1968**. J. J. Lagowski (ed.), *The Chemistry of Non-Aqueous Solvents*, Vols. 1–3, Academic Press, New York, **1966–1970**.

$$O^{2-} + H_2O \longrightarrow 2\,[OH]^-$$
$$[NH_2]^- + H_2O \rightleftharpoons NH_3 + [OH]^-$$
$$NH_3 + H_2O \rightleftharpoons [NH_4]^+ + [OH]^-$$

In water, the ions $[OH]^-$ are solvated as $[HO(H_2O)_4]^-$ with four water molecules linked by one hydrogen bridge each to the oxygen atom of the hydroxide anion which thus reaches the coordination number of C.N. = 5.[26]

In the aqueous system, a base is defined by BRØNSTED and LOWRY as a proton acceptor, which applies to $[OH]^-$, O^{2-} and NH_3. Likewise, the solvent anions $[NH_2]^-$, $[HSO_4]^-$ and $[HF_2]^-$ are responsible for basic properties in corresponding protic solvents. For example, the salt-like amides ($M[NH_2]$) in liquid ammonia, the hydrogen sulfates ($M[HSO_4]$) in anhydrous sulfuric acid and the hydrogen difluorides ($M[HF_2]$) in liquid HF correspond to the salt-like hydroxides in the water system. All these salts increase the concentration of the solvent anions.

Above it was shown that phosphoric acid is protonated by anhydrous sulfuric acid, and hence acts as a base like ammonia in water. Protons are transferred to the species of highest proton affinity (basicity). The equation:

$$H_2SO_4 + H_2O \longrightarrow [H_3O]^+ + [HSO_4]^-$$

means either that H_2SO_4 in the solvent H_2O acts as an acid (proton donor), or that H_2O in the solvent H_2SO_4 acts as a base B (proton acceptor). Basicity is defined as the GIBBS energy ΔG^o of the following general reaction:

$$B + H^+ \longrightarrow [BH]^+$$

In Table 5.3 the calculated basicities of various small molecules and ions are listed, valid for aqueous solutions at 25 °C.

Table 5.3: Calculated basicities (ΔG^o_{298}; kJ mol^{-1}) of small molecules and ions in water at 25 °C (after M. Swart, E. Rösler, F. M. Bickelhaupt, *Eur. J. Inorg. Chem*. **2007**, 3646).

NH_3: −643	$[NH_2]^-$: −818	H_2O: −504	$[OH]^-$: −738	F^-: −638
PH_3: −571	$[PH_2]^-$: −743	H_2S: −515	$[SH]^-$: −663	Cl^-: −577
AsH_3: −521	$[AsH_2]^-$: −721	H_2Se: −511	$[SeH]^-$: −645	Br^-: −564
SbH_3: −506	$[SbH_2]^-$: −707	H_2Te: −530	$[TeH]^-$: −638	I^-: −568

The data in Table 5.2 show that the basicities of the isoelectronic anions $[NH_2]^-$, $[OH]^-$ and F^- decrease in this order due to the increasing nuclear charge (Z_{eff}) of the atom to be protonated. For this reason, the amide ion is unstable in water being

26 D. Marx, A. Chandra, M. E. Tuckerman, *Chem. Rev*. **2010**, *110*, 2174.

protonated to NH_3 ($\Delta G^\circ_{298} < 0$). The highest basicity in water is observed for the solvated electron e^-(aq); see Section 9.4.8.

5.5 The Relative Strength of Acids and Bases

5.5.1 Dilute Solutions

It was shown earlier that acid or base function depends on the chemical environment and the same holds for the strength of acids and bases. In dilute aqueous solutions to which the law of mass action can be applied, the acid strength is given by the following equilibrium constant K_a:

$$HA + n\,H_2O \rightleftharpoons H^+(aq) + A^-(aq) \qquad K_a = \frac{c\,(H^+) \cdot c\,(A^-)}{c\,(HA)}$$

Formally, this reaction describes the dissociation of acid HA in water; therefore, K_a is also termed as *dissociation constant* or *acid constant* (index "a" is derived from the Latin word "*acidum*" for acid). The larger the dissociation constant of HA, the more the above equilibrium is on the right-hand side and the stronger the acid. The strength of a base B is likewise given by a base constant K_b according to the following equilibrium reactions (M = metal):

$$NH_3 + H_2O \rightleftharpoons [NH_4]^+ + [OH]^-$$

$$MOH \rightleftharpoons M^+ + [OH]^-$$

In general:

$$B + H_2O \rightleftharpoons [BH]^+ + [OH]^- \qquad K_b = \frac{c\,(BH^+) \cdot c\,(OH^-)}{c\,(B)}$$

However, often the base strength is given by the dissociation constant of the *conjugate acid* $[BH]^+$ according to the equilibrium with related equilibrium constant $K_a\,(BH^+)$:

$$[BH]^+ + H_2O \rightleftharpoons B + [H_3O]^+$$

In water at 25 °C: $K_b = 10^{-14}/K_a(BH^+)$.

Polyprotic acids such as H_2SO_4 and H_3PO_4 have several dissociation constants since the deprotonation occurs in a stepwise manner:

$$H_2SO_4 + n\,H_2O \rightleftharpoons H^+(aq) + [HSO_4]^- \qquad K_{a1}$$

$$[HSO_4]^- + n\,H_2O \rightleftharpoons H^+(aq) + [SO_4]^{2-} \qquad K_{a2}$$

The values of K_a may differ by several orders of magnitude; therefore, it is more practical to use pK_a values defined as follows:

$$pK_a = -\log K_a$$

In the following sections, the relative strengths of aqueous acids will be discussed first for binary covalent hydrides such as HF and HCl, followed by oxoacids such as sulfuric acid $SO_2(OH)_2$ and nitric acid $NO_2(OH)$, which contain the acidic hydrogen atoms linked to oxygen.

5.5.1.1 Binary Covalent Hydrides

Covalent volatile hydrides are known for all nonmetals except the noble gases. These hydrides can be proton donors or acceptors in water. The best-known acids are the hydrogen halides, HX (X = F, Cl, Br, I) whose acid strengths vary considerably. It is instructive to investigate the factors influencing the acid strength of these relatively simple systems. The equilibrium constant K_a for the reaction:

$$HX(aq) \rightleftharpoons H^+(aq) + X^-(aq)$$

can be calculated from the GIBBS reaction energy $\Delta_r G°$:

$$\Delta_r G^\circ = -R\ T \ln K_a$$

where R represents the universal gas constant and T the temperature. $\Delta_r G°$ may be obtained from the reaction enthalpy $\Delta_r H°$ and the change of entropy $\Delta_r S°$ according to the *Second Law of Thermodynamics*:

$$\Delta_r G^\circ = \Delta_r H^\circ - T \cdot \Delta_r S^\circ$$

An energy cycle may be used to obtain the value of $\Delta_r G°$ which cannot be measured directly:

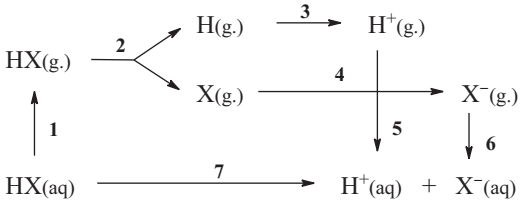

The sum of the $\Delta_r G°$ values for steps 1 through 6 must be equal to that of step 7 since $\Delta_r G°$ is independent on the route from start to goal (law of energy conservation). Estimated values of $\Delta_r G°$ from calculations and experiments are listed in Table 5.4.[27]

27 R. Schmid, A. M. Miah, *J. Chem. Educ.* **2001**, *78*, 116.

Table 5.4: GIBBS energies $\Delta G°_{298}$ (kJ mol^{-1}) of the hypothetical steps in the dissociation of hydrogen halides (HX) in water by an energy cycle (steps 1–7 after R. Schmid, A. M. Miah, *J. Chem. Educ.* **2001**, *78*, 116; pK_a data of HCl, HBr and HI after I. Leito et al., *J. Phys. Chem. A* **2016**, *120*, 3663).

	Reaction	HF	HCl	HBr	HI
1:	HX(aq) → HX(g.)	23.6	13.4	17.4	−6.1
2:	HX(g.) → H(g.) + X(g.)	540	404	339	272
3:	H(g.) → H^+(g.) + e^-	1314	1314	1314	1314
4:	X(g.) + e^- → X^-(g.)	−324	−345	−321	−292
5 + 6:	H^+(g.) + X^-(g.) → H^+(aq) + X^-(aq)	−1537	−1409	−1382	−1347
7:	HX(aq) → H^+(aq) + X^-(aq)	+17.5	−22.5	−33.1	−59.5
pK_a:		+3.1	−5.9	−8.8	−9.5
μ (D):		1.87	1.11	0.83	0.45

Molecular dipole moments μ(HX) are given for comparison (in Debye).

The pK_a values in Table 5.4 show that the acid strength of the hydrogen halides in water increases enormously from HF to HI. While aqueous HF is about as weak as acetic acid, aqueous HI is among the strongest acids. This is surprising, since the dipole moments of the gaseous molecules decrease in the same direction (Table 5.4). The proton donor ability is apparently not controlled by the polarity of the element-hydrogen bond. The same holds for water-like solvents. For example, HBr is a stronger acid than HCl also in glacial acetic acid. The main reason for this trend of acidities is the dissociation enthalpy of the gaseous HX molecules, which decreases sharply from HF to HI.

The same trend in dissociation constants is found in the chalcogen hydrides for which the pK_a data decrease in the order $H_2Te > H_2Se > H_2S > H_2O$; that is, aqueous H_2Te is a stronger acid than H_2S, which in turn is more acidic than H_2O (see Section 12.7.1).

5.5.1.2 Oxoacids

Oxoacids of nonmetals (E) are covalent hydroxides of general formula $EO_m(OH)_n$, which act as proton donors in water. The OH bonds are similar in all cases, yet there are large differences in thermodynamic parameters and acid strengths. The pK_a values for several oxoacids are given in Table 5.5.

The extremely strong acids $HClO_4$, HSO_3CF_3 (TfOH), HNO_3 and H_2SO_4 are virtually completely ionized in the first step in water; hence, pK_1 values are difficult to determine and different values have been reported in the literature. In contrast, H_3PO_4 and HNO_2 are only moderately strong acids and HOCl, H_3BO_3 as well as H_3AsO_3 are weak acids.

In polyprotic acids, $pK_{a1} < pK_{a2} < pK_{a3}$, as expected on electrostatic grounds since the removal of a proton from an anion requires more energy than from a neutral molecule.

Table 5.5: pK_a values of oxoacids of nonmetals and their anions in aqueous solution at 25 °C. Except NH_3SO_3, the hydrogen atom is linked to oxygen. The data for $HClO_4$ and H_2SO_4 are uncertain and a range is given (see I. Leito et al., *J. Phys. Chem. A* **2016**, *120*, 3663 and references cited therein).

	pK_a		pK_a		pK_a
HSO_3CF_3	−14.7	$HClO_2$	1.94	$[H_2PO_4]^-$	7.2
$HClO_4$	−10 ... −12	$[HSeO_4]^-$	2.05	$[HSO_3]^-$	7.2
H_2SO_4	−4 ... −8	H_3PO_4	2.15	HOCl	7.5
HNO_3	−1.3	H_3AsO_4	2.25	HOBr	8.69
H_2SeO_4	<0	H_2SeO_3	2.57	H_3BO_3	9.14
$H_2S_2O_3$	0.6	H_5IO_6	3.29	H_3AsO_3	9.22
NH_3SO_3	1.0	HNO_2	3.3	$[HPO_4]^{2-}$	12.37
H_3PO_3	1.8	$[HSeO_3]^-$	6.60		
$[HSO_4]^-$	1.92	$[H_2AsO_4]^-$	7		

For the acids H_2CO_3 and H_2SO_3, which are unknown in water, K_a and pK_a are determined by using the concentration of dissolved CO_2 and SO_2, respectively, in the law of mass action, that is, CO_2 and SO_2 are treated as anhydrides:

$$CO_2(aq) \rightleftharpoons H^+(aq) + [HCO_3]^-(aq) \qquad K_a = \frac{c(H^+) \cdot c(HCO_3^-)}{c(CO_2)}$$

The pK values thus obtained do not correspond to the true acid strength of the hypothetical acids H_2CO_3 and H_2SO_3 (for a detailed discussion of carbonic acid, see Section 7.7.3). In a similar fashion, the basicity of the hypothetical base $[NH_4][OH]$ is determined using the concentration of aqueous ammonia:

$$NH_3(aq) \rightleftharpoons [NH_4]^+(aq) + [OH]^-(aq)$$

These concepts can be extended to dilute *nonaqueous solutions* in which the dissociation constants may be determined from the pH value, the electrical conductivity or the m.p. depression.

5.5.2 Concentrated and Nonaqueous Acids

The acids HCl, $HClO_4$ and H_2SO_4 may be almost completely dissociated in dilute aqueous solution, yet these solutions are not the most acidic systems by far. In fact, as the acid concentration in the system H_2O/H_2SO_4 increases, the acidity, that is, the proton donor strength, increases as well although the degree of dissociation decreases. Pure anhydrous sulfuric acid is only weakly self-dissociated. The ion

product $c(H_3SO_4^+) \cdot c(HSO_4^-)$ is only about 10^{-4} mol^2 L^{-2} at 25 °C; still 100% sulfuric acid is a stronger proton donor than any aqueous acid.[28] The same holds for hydrogen fluoride, which dissociates into $[H_2F]^+$ and $[HF_2]^-$ ions (see Section 13.4.1).

In order to determine the proton donor strength of a concentrated aqueous solution or an anhydrous acid, the method proposed by LOUIS P. HAMMETT[29] may be used: a weak base B, for example, nitroaniline, is added which is partially protonated:

$$H^+ + B \rightleftharpoons [HB]^+ \qquad K_a(HB^+) = \frac{c(H^+) \cdot c(B)}{c(HB^+)}$$

The so-called HAMMETT acidity function H_0 is defined in analogy with pH:

$$H_0 = -\log c(H^+)$$

If H_0 is substituted for $c(H^+)$ in the equation for the equilibrium constant $K_a(HB)$, we obtain:

$$H_0 = pK_a(HB)^+ + \log \frac{c(B)}{c(HB^+)}$$

The ratio $c(B)/c(HB^+)$ can be determined photometrically if B has a different color in the free and the protonated form. For example, mono-, di- and trinitrotoluene are colorless but turn yellow upon protonation. The pK_a value of $[HB]^+$ can be determined in dilute solution, where it is identical with the easily accessible pH value.

For 100% sulfuric acid, the acidity function amounts to $H_0 = -11.9$, whereas in the 0.1 N acid (0.05 mol L^{-1}) pH = 1.0. Thus, the acidity of anhydrous H_2SO_4 is by 13 orders of magnitude higher than that of dilute sulfuric acid. Acids and mixtures of acidities higher than 100% sulfuric acid are called *super acids*. Examples are the anhydrous acids HSO_3Cl ($H_0 = -13.8$), HSO_3CF_3 (−14.3), HSO_3F (−15.1) and HF (−15.1). However, the HAMMETT acidity function H_0 can even have values near −26, for instance, in mixtures of strong LEWIS acids such as SO_3 with H_2SO_4 (i.e., $H_2S_2O_7$) or with $B(OSO_3H)_3$ as well as in mixtures of HSO_3F with SbF_5 and possibly even additional SO_3. The latter mixture is known as *magic acid* since it protonates even alkanes. The added LEWIS acids form complexes with the acid anions shifting the dissociation equilibrium to the right-hand side and thus increasing the acidity.

In Figure 5.2, the HAMMETT acidity function H_0 of various LEWIS acids in the anhydrous solvents HSO_3F (left) and HF (right) are shown. Even small concentrations of LEWIS acid sometimes increase the protic acidity dramatically.

The acidity H_0 of a 1:1 mixture of HSO_3F and SbF_5 is approximately −21 and for an analogous mixture of HF and SbF_5 it is approximately −25. In the latter solution,

28 R. J. Gillespie, *Acc. Chem. Res.* **1968**, *1*, 202. T. O'Donnell, *Superacids and Acidic Melts as Inorganic Chemical Reaction Media*, VCH, Weinheim, **1993**.

29 US American physicist (1894–1987).

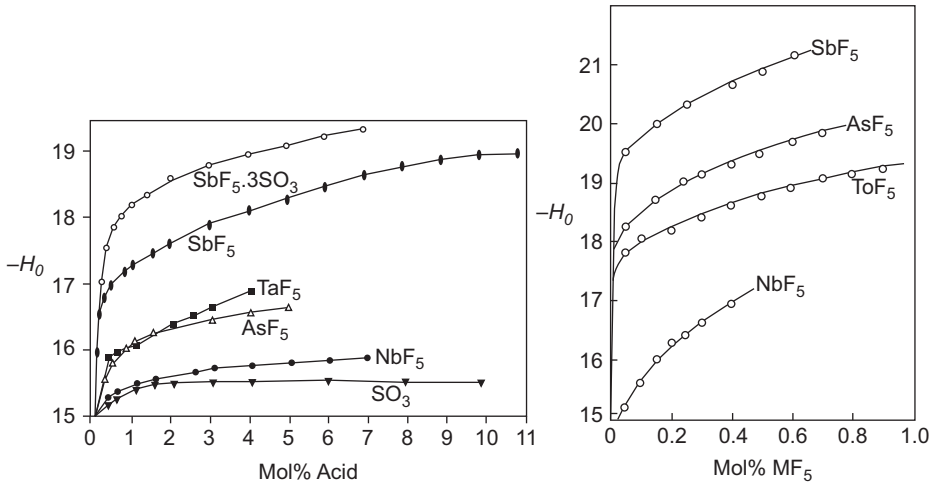

Figure 5.2: Hammett acidity function H_0 for solutions of Lewis acids in HSO_3F (left) and in anhydrous HF.

complex anions such as $[Sb_2F_{11}]^-$ as well as cations $[H_3F_2]^+$, $[H_2F]^+$ and $[H_4F_3]^+$ have been detected, at concentrations decreasing in this order.[30] These mixtures can protonate substances with small proton affinity, which do not react as bases in other media. For example, HNO_3 is protonated in anhydrous sulfuric acid to the acidium cation $[H_2NO_3]^+$, which decomposes into $[NO_2]^+$ and H_2O:

$$HNO_3 + 2\ H_2SO_4 \longrightarrow [NO_2]^+ + [H_3O]^+ + 2\ [HSO_4]^-$$

This mixture is called *nitrating acid*, and is used to prepare nitro derivatives of aromatic hydrocarbons:

$$R{-}H + [NO_2]^+ \longrightarrow R{-}NO_2 + H^+$$

The nitronium ion $[NO_2]^+$ is just an example for a substantial number of cations that are too electrophilic to exist in water:

$$[NO_2]^+ + 3\ H_2O \longrightarrow 2\ [H_3O]^+ + [NO_3]^-$$

Many novel compounds have been synthesized in mixtures of similarly high acidity using *weakly coordinating anions* to crystallize the cations.[31] Examples are the

30 P. M. Esteves, A. Ramirez-Solis, C. J. A. Mota, *J. Am. Chem. Soc.* **2002**, *124*, 2672.
31 T. A. Engesser, M. R. Lichtenthaler, M. Schleep, I. Krossing, *Chem. Soc. Rev.* **2016**, *45*, 789–899. G. A. Olah, G. S. Prakash, A. Molnár, J. Sommer, *Superacid Chemistry*, 2nd ed., Wiley, Hoboken, **2009**.

species $[H_2SO_3CF_3]^+$, $[H_2SO_3F]^+$, $[S_8]^{2+}$, $[Te_4]^{2+}$ and $[I_4]^{2+}$ which will be discussed in detail in later chapters. Among the strongest protic acids prepared so far are the halogenated carborane derivatives $H[HCB_{11}F_{11}]$ and $H[HCB_{11}Cl_{11}]$,[32] (carboranes are discussed in Section 6.7) as well as the systems $HBr/AlBr_3$ and $H[Al(OTeF_5)_4]$.[33] The latter two superacids are strong enough to protonate benzene to a salt with the benzenium cation $[C_6H_7]^+$ (Figure 5.3). The superacid $H[Al(OTeF_5)_4]$ is prepared from Et_3Al and $HOTeF_5$ in *ortho*-difluorobenzene solution by elimination of ethene; the acidic proton is linked to a solvent molecule.

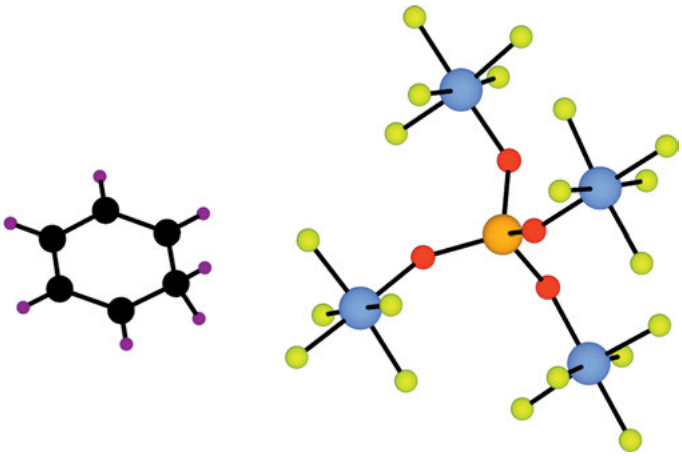

Figure 5.3: Molecular structure of $[C_6H_7][Al(OTeF_5)_4]$ in the solid state (yellow, fluorine; red, oxygen; blue, tellurium). The cation is of approximate C_s symmetry and the positive ionic charge is concentrated at the carbon atom opposite to the CH_2 group (after Wiesner, Riedel et al.[33b]).

Solid superacids are used as *catalysts*, for example, for the isomerization of hydrocarbons.[34] For the Brønsted acidity of metal-organic frameworks (MOFs), see Krossing et al. and Wiesner et al.[33].

32 C. A. Reed et al., *J. Am. Chem. Soc.* **2006**, *128*, 3160 and *Angew. Chem. Int. Ed.* **2016**, *55*, 1382. H. Willner et al., *Angew. Chem. Int. Ed.* **2007**, *33*, 6346.

33 (a) I. Krossing et al., *Angew. Chem. Int. Ed.* **2014**, *53*, 1689; (b) A. Wiesner, S. Riedel et al., *Angew. Chem. Int. Ed.* **2017**, *56*, 8263.

34 For solid superacids, see: K. Arata, *Adv. Catal.* **1990**, *37*, 165; W. G. Klemperer et al., *J. Am. Chem. Soc.* **2014**, *136*, 12844; J. C. Vedrine et al., *J. Catal.* **1993**, *143*, 616; Y. Tang et al., *Stud. Surf. Sci. Catal.* **1994**, *90*, 507.

5.6 Hydrogen Bonds (H-Bonds)

5.6.1 Introduction

The physical properties of covalent hydrides such as H_2O, NH_3 and HF exhibit intermolecular interactions much stronger than ordinary VAN DER WAALS forces (Chapter 3). Hydrogen atoms are specifically involved in this type of interaction, which is usually much weaker than typical covalent bonds but still can reach bond enthalpies of up to 140 kJ mol^{-1}, especially if ions are involved. This interaction is called hydrogen bonding[35] with characteristic bond enthalpies of 10–65 kJ mol^{-1}. If anions are involved, however, bond enthalpies of up to 140 kJ mol^{-1} have been determined. Hydrogen-bonding interactions are ubiquitous in chemical and biological systems and play fundamental roles in the structure, function and dynamics of many chemical and biological systems.

Hydrogen bonds are formed between molecules with partially positive hydrogen atoms and electronegative counteratoms possessing one or more lone electron pairs acting as proton acceptors, such as F, O and N, and to a lesser degree Cl, S and P. However, hydrogen bonds are also known with bonding electron pairs, such as π electrons in multiple bonds or aromatic systems, especially in organic and metal-organic compounds.[36] Intramolecular hydrogen bonds are also well known.

A simple electrostatic model illustrates how and why hydrogen bonds are formed:

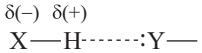

The positively charged hydrogen atom of the polar covalent XH bond (hydrogen bond donor) is attracted by the lone pair of electrons on atom Y (hydrogen bond acceptor). This attraction is stronger, the larger the difference of electronegativities and the smaller the size difference between atoms X and H. Together, these two factors define the polarity of the XH bond, which is ultimately the determining factor for the strength of the hydrogen bond donor ability of XH. Examples for polarized bonds with positively charged H atoms are FH, OH and NH, but normally not CH unless the electronegativity of carbon is enhanced by inductive effects as in $CHCl_3$ or by a low C.N. as in acetylene C_2H_2. In addition, the atom Y should be small

35 P. L. Huyskens, W. A. P. Luck, T. Zeegers-Huyskens (eds.), *Íntermolecular Forces*, Springer, Berlin, **1991**. S. Scheiner, *Hydrogen Bonding – A Theoretical Perspective*, Oxford Univ. Press, New York, **1997**. G. A. Jeffrey, *An Introduction to Hydrogen Bonding*, Oxford University Press, Oxford, **1997**. T. Steiner, *Angew. Chem. Int. Ed.* **2002**, *41*, 48–76. M. Meot-Ner, *Chem. Rev.* **2012**, *112*, PR22–PR103.

36 The bonding enthalpy of the benzene–water adduct $C_6H_6{\cdot}H_2O$ is approximately 13 kJ mol^{-1}; one of the OH groups points toward the center of the benzene ring while the other OH is freely rotating; see S. Tsuzuki, K. Honda, T. Uchimaru, M. Mikami, K. Tanabe, *J. Am. Chem. Soc.* **2000**, *122*, 11450.

and electronegative to ascertain a high electron density at the hydrogen bond acceptor site.

With decreasing distance between atoms H and Y there will be increasing overlap of the corresponding orbitals and a covalent bond is formed. The related orbitals are the σ* MO of the XH bond (LUMO) and the lone pair orbital on atom Y, which is usually the HOMO the molecule (see Figure 2.26). The resulting partial delocalization of the lone pair electrons into the σ* MO results in a lower energy of the system (see below).

This simple model explains why H_2O, NH_3 and HF form strong hydrogen bonds in the liquid and solid states while liquid H_2S, PH_3 and HCl are only weakly associated with VAN DER WAALS forces. In fact, the pK_a value of HX and the pK_b value of YR are correlated to the interaction enthalpy of the corresponding hydrogen bond XH····YR.

5.6.2 General Properties of Hydrogen Bonds

The following general properties of hydrogen bonds are important:[37]

(a) Most hydrogen bonds are *asymmetrical*, that is, the hydrogen atom is not at the midpoint between X and Y but much closer to X than to Y. Therefore, the XH bond is much stronger than the HY interaction. Only the strongest hydrogen bonds are symmetrical. This requires X and Y being identical and either oxygen or fluorine. In this case, a covalent 3-center 4-electron bond is formed (see Section 2.4.6).

(b) Most hydrogen bonds are linear or slightly bent. A linear geometry yields maximum attraction between H and Y at minimal repulsion between the negatively charged atoms X and Y, thus maximizing the bond enthalpy. The weaker the H bridge, the more strongly the valence angle XHY may deviate from the ideal value of 180°.

(c) The bond angle α(H····Y–R) is normally observed in the range 110–140°:

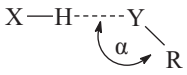

(d) In most hydrogen bonds, the C.N. of hydrogen is 2 but higher numbers are observed as well, for example in the crystal structure of nitramide $H_2N–NO_2$ (X = N, Y = O):

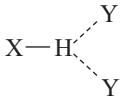

37 R. Desiraju, *Angew. Chem. Int. Ed.* **2011**, *50*, 52–59.

Such H bonds are called branched or bifurcated. In crystalline carbohydrates, about 25% of all H bridges are bifurcated and in solid amino acids their fraction is even higher.

(e) In most cases, only one hydrogen atom is directed toward each lone pair of Y. In crystalline ammonia at 160 K, however, three hydrogen bonds extend from each nitrogen atom, which can thus be considered as hypercoordinate (C.N. = 6 or 3 + 3).[38] The directionality is a defining characteristic of hydrogen bonds.

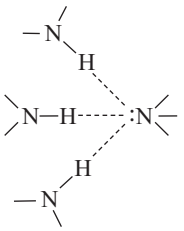

In liquid water, there are also hypercoordinate oxygen atoms (see below). If atom Y has several lone pairs as in the anions F^-, Cl^- and Br^- there may be up to six hydrogen atoms linked to one Y. For example, the anion $[H_4F_5]^-$ consists of a central fluoride ion, which is tetrahedrally coordinated by four HF molecules: $[F(HF)_4]^-$. The adduct between pyridine and hydrogen chloride of composition pyridine · 6HCl is in fact a pyridinium salt $[C_6H_5NH]Cl{\cdot}5HCl$ with a central chloride anion to which five HCl and one NH bonds are directed.

5.6.3 Experimental Detection of Hydrogen Bonds

5.6.3.1 Physical Constants

Intermolecular interactions in the liquid and the solid state strongly influence physical constants of compounds such as m.p. and b.p., enthalpies of fusion ($\Delta_{fus}H°$), vaporization ($\Delta_{vap}H°$) and sublimation ($\Delta_{sub}H°$), dipole moment (μ), dielectric constant (ε) and viscosity (η). These parameters increase upon hydrogen bond formation in comparison to nonassociated samples. But definite proof of H-bonds is only obtained by spectroscopic or structural investigations as well as by quantum-chemical calculations.

In Figure 5.4, the *boiling points* of binary hydrides, forming five homologous series, are shown. Normally, b.p.s increase with molecular mass as with the noble gases and the hydrides of Group 14 elements. The hydrides of the lightest elements of Groups 15, 16 and 17, however, show anomalously high b.p.s. As discussed in Chapter 3,

38 R. Boese et al., *J. Phys. Chem. B* **1997**, *101*, 5794.

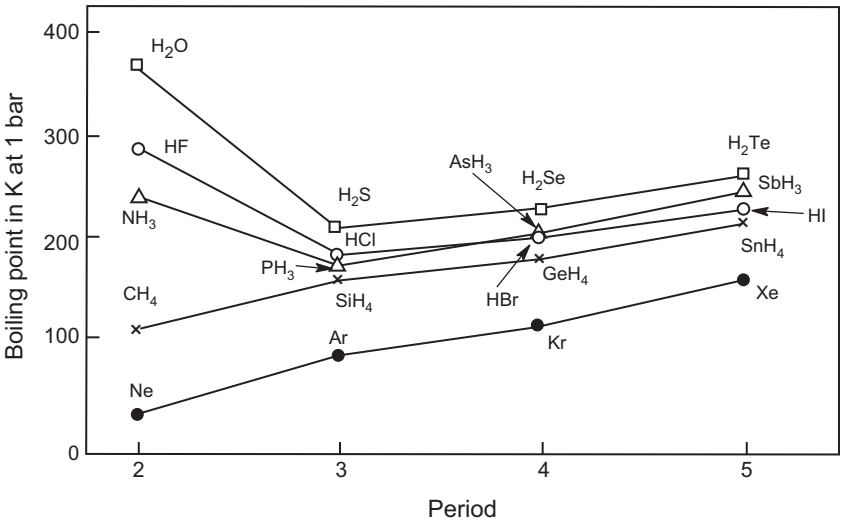

Figure 5.4: Boiling points at ambient pressure of binary hydrides of main group elements in comparison with the noble gases showing the influence of hydrogen bonding especially in liquid H_2O, HF and NH_3.

VAN DER WAALS forces alone cannot account for this effect, and therefore strong association by hydrogen bonds must be postulated in the liquid phase in contrast to the gas phase. Evidently, CH_4 does not form hydrogen bonds. Hence, in the series CH_4–NH_3–H_2O–HF–Ne, methane and neon have the lowest b.p.s and water has the highest. In case of dimethyl ether, however, without positively charged hydrogen atoms, there are also no H bonds and hence the b.p. of Me_2O (–25 °C) is much lower than that of water (+100 °C) and fits well in the series Me_2X (X = O, S, Se, Te).

Corresponding trends are also found for the enthalpies of vaporization of the binary hydrides. Since the intermolecular distances in the vapor phase are much larger than in condensed phases, vaporization is accompanied by the breaking of all or most hydrogen bonds, and the needed energy adds to that for the breaking of VAN DER WAALS interactions and for the volume expansion work. Therefore, in the series CH_4–NH_3–H_2O–HF–Ne water has the highest enthalpy of vaporization (see below for data).

The *dipole moments* and *dielectric constants* of water and water-like solvents are relevant for the solubility of salts. The larger the μ and ε, the more soluble are ionic compounds (Section 2.1.7). All strongly hydrogen bonded molecular liquids such as HF, NH_3, HCN and HSO_3F have large ε values.

The *viscosity* of water is much higher than that of its organic derivatives of type R_2O (ethers), which are unable to form hydrogen bonds. Particularly high viscosities are found in compounds with several OH groups such as glycerol and anhydrous sulfuric and phosphoric acids as these typically form three-dimensional hydrogen

bonded networks. Honey and syrup (essentially aqueous solution of sugars) provide other examples.

Extraordinarily high values of the property parameters discussed so far may indicate stronger than usual intermolecular interactions but not their nature. This also holds for the *molecular mass in solution* from which the degree of association of a solute in an inert solvent can be deduced. Specific methods to detect hydrogen bonds unequivocally are discussed in the following sections.

5.6.3.2 Structure Determination

X-ray and neutron diffraction on single crystals are employed to determine the structures of molecules in the solid state, that is, the atomic positions and internuclear distances, while electron diffraction is applied to investigate gaseous samples. By these techniques, hydrogen bonds can be unequivocally detected. If the internuclear distance d_{XY} of a group X–H···Y is smaller than the sum of van der Waals radii of atoms X and Y, hydrogen bonding can be presumed. In cases in which the hydrogen atom position can be determined accurately, the internuclear distance d_{HY} should be smaller than the sum of the van der Waals radii of atoms H and Y. For example, in crystalline hydrogen fluoride, the distance between two fluorine atoms of neighboring HF molecules in the infinite zig-zag chain is d_{FF} = 249 pm, which is 45 pm less than the sum of van der Waals radii (see Section 3.4; Table 3.3). The corresponding distance d_{FF} for the anion of $K[HF_2]$ is even smaller (226 pm). These data clearly indicate strong H-bonds (for more examples, see Section 5.6.4).

For hydrogen bonds between equal atoms as in O–H···O or almost equal atoms as in N–H···O and O–H···N, a unique nonlinear correlation exists between the distances of the two neighboring bonds in X–H···Y: the stronger the hydrogen bond, the shorter the distance H···Y but the longer the bond X–H.

5.6.3.3 Molecular Spectroscopy

The most sensitive method to detect hydrogen bonds is IR spectroscopy. The polar X–H bond in a bridge X–H···Y results in a strong absorption band in the IR spectrum. The frequency or wavenumber of the nonassociated X–H molecule can be determined in the vapor phase or at high dilution in an inert nonpolar solvent such as CS_2 or CCl_4. The ν(X–H) stretching mode usually shifts to lower wavenumbers ("redshift") on association and becomes markedly broader and more intense because the XH bond is weakened and even more polarized by H-bond formation.[39] The associated compound of interest can be investigated by either using a strongly polar solvent such as acetonitrile (MeCN) or dimethyl sulfoxide or by simply increasing the

39 In rare cases, a blue shift is observed for relatively weak H-bonds, mainly for X = C as in $F_3C–H···OH_2$; see Y. Mo et al., *Chem. Eur. J.* **2014**, *20*, 8444.

concentration of HX in an inert solvent. The following comparison of the stretching modes of the bonds in CH_4, HCl and H_2O illustrates the influence of hydrogen bonding (ν_3 is the asymmetric stretching vibration of CH_4 and H_2O, respectively):

	Gaseous	Liquid	Solid (at 90 or 10 K, respectively)
CH_4 (ν_3):	2914	2909	2906 cm^{-1} (no H-bonds)
HCl:	2886	2785	2768 cm^{-1} (weak H-bonds)
H_2O (ν_3):	3707	3400	3277 cm^{-1} (moderately strong H-bonds)

The X–H····Y hydrogen bond weakens the internal X–H bond since the σ* MO of X–H is populated by electron density from the lone pair of the acceptor atom Y (hyperconjugation). The result is an increase of the internuclear XH distance (d) and consequently of the *dipole moment* since $\mu = \delta e \cdot d$. In a diatomic molecule, the value of the dipole moment determines the IR absorption intensity. At the same time, the partial charges on the atoms X and H increase since the bonding electrons of X–H are repelled by the lone pair of the acceptor atom Y (mutual polarization).[40] This increases the dipole moment of bond X–H even further.

For O–H····O hydrogen bonds, an inverse correlation exists between the wavenumber of the OH stretching mode and the internuclear distance d_{OO}, which to some extent reflects the hydrogen bond strength. In addition, there is a positive correlation between d_{OO} and the chemical shift of the proton in the ^{1}H-NMR spectrum.

The IR spectrum of hydrogen bonded compounds shows not only the vibration of the X–H bond but also of the H····Y bond. The latter is usually termed XY vibration since the group XH vibrates as an entity against the atom Y (caused by the small mass of H and the strength of the XH bond). Such XY vibrations occur at very low wavenumbers and are not easy to detect since the corresponding spectral region is often obscured by bending vibrations. Fortunately, the stretching vibration ν(XY) can often be detected by Raman spectroscopy. For example, for liquid ethanol ν_{OO} was observed at 270 cm^{-1}. From the temperature dependence of the Raman scattering intensity at this wavenumber, the bond enthalpy of the H-bond in ethanol was calculated as 10.5 kJ mol^{-1}.[41]

Isotopic substitution of H by D also helps to identify H-bond-related signals in vibrational spectra. For small molecules such as the dimer $(H_2O)_2$ the dissociation energy D_0 of the hydrogen bond O–D····O is slightly higher (14.9 kJ mol^{-1}) than for the nondeuterated molecule [D_0(O–H····O) = 13.2 kJ mol^{-1})] due to the smaller zero-point vibrational energy of deuterium compounds owing to the larger mass of deuterium.

40 D. Feil, *J. Mol. Struct.* **1990**, *237*, 33. P. O. Astrand, K. Ruud, K. V. Mikkelsen, T. Helgaker, *J. Phys. Chem. A* **1998**, *102*, 7686.

41 H. G. M. Edwards, D. W. Farwell, A. Jones, *Spectrochim. Acta* **1989**, *45A*, 1165.

To a certain extent, hydrogen bonds can also be detected by ^{1}H-NMR spectroscopy since the electron density at the bridging hydrogen atom is reduced compared to the unassociated molecule. Consequently, the proton signals occur at lower field strength. For example, the triplet of the OH group of unassociated ethanol is observed at 5.2 ppm while a solution of ethanol in CCl_4 shows a singlet between 1 and 4 ppm, depending on the concentration and hence the degree of association. In some cases, even mass spectrometry can be used to detect H-bonds.[42]

5.6.4 Examples of Special Hydrogen Bonds

5.6.4.1 Hydrogen Fluoride

Solid hydrogen fluoride at −125 °C (m.p. −83.6 °C) consists of infinite planar zig-zag chains of HF molecules that are associated via linear, asymmetric hydrogen bonds:[43,44]

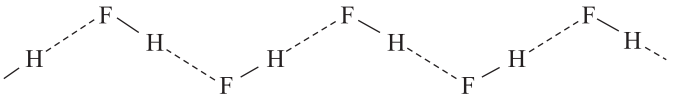

d(FF) = 249(1) pm, angle FFF = 116°

For liquid HF (b.p. 19.5 °C) similar but not planar chain-like molecules are assumed on the basis of neutron diffraction experiments performed at 23 °C/1.2 bar. The results are consistent with the presence of short, bent, strongly hydrogen-bonded chains, with strong interchain interactions and very little branching. Despite the strength of the hydrogen bond in the liquid, the chains appear to be curtailed in length at around an average of seven molecules per chain.[45] The saturated HF vapor at 20 °C consists of an equilibrium mixture of monomeric HF and oligomers $(HF)_n$ with n = 2–6, which can be detected by mass spectrometry. As usual, such gas phase equilibrium is strongly pressure and temperature dependent. Structures and bonding properties of the oligomers will be discussed below.

Salts of the acids $(HF)_n$ are synthesized from the fluorides MF and HF and contain hydrogen bonds too. The hydrogen difluoride anion $[HF_2]^-$ has even one of the strongest known hydrogen bonds (Section 2.4.6). In $K[HF_2]$ the anion is linear and symmetric ($D_{\infty h}$ symmetry):

---

42 N. Nishi et al., *J. Am. Chem. Soc.* **1988**, *110*, 5246.

43 The solid-state structure of HOF is analogous but with planar zig-zag chains of O–H···O bridges; the fluorine atoms are sticking out from these chains.

44 The other hydrogen halides HX (X = Cl, Br, I) form various solid phases with complex crystal structures and sometimes with disorder; see A. F. Wells, *Structural Inorganic Chemistry*, 5th ed., Clarendon, Oxford, **1986**, p. 362.

45 J. F. C. Turner et al., *Angew. Chem. Int. Ed.* **2004**, *43*, 1952.

$$[F-H-F]^-,\ d_{HF}=113\text{pm},\ d_{FF}=226\text{pm}$$

In $[NH_4][HF_2]$ symmetric $[HF_2]^-$ ions are connected to $[NH_4]^+$ cations via N–H····F hydrogen bonds. These *outer hydrogen bonds* between ions are formed at the expense of the internuclear distance d_{FF} in the anion, which increases to 232 pm but the interionic hydrogen bond enthalpy results in a higher lattice energy of the salt. Hydrogen fluoride, owing to the strong mutual interaction of HF molecules and fluoride anions, forms a whole series of *acid salts* MX·*n*HF (n = 1–4). For example, $K[H_2F_3]$ consists of bent anions of C_{2v} symmetry, while the anion $[H_3F_4]^-$ forms a trigonal pyramid (C_{3v}), and $[H_4F_5]^-$ is of T_d symmetry. In contrast to $[HF_2]^-$ ions, these larger anions show asymmetric hydrogen bonds between HF molecules and a central fluoride anion.

5.6.4.2 Ice and Water[46]

At least 12 crystalline phases of H_2O are known to be stable or metastable in certain temperature and pressure ranges; the phase diagram of H_2O is shown in Figure 5.5. The numbering of the solid phases reflects the historic order of discovery.

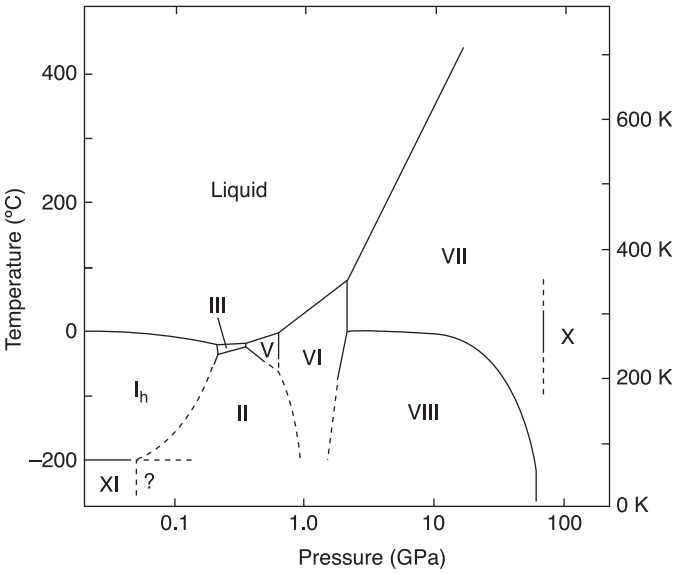

Figure 5.5: Phase diagram of the water system in semilogarithmic representation. The different polymorphic modifications are indicated by roman numerals; ice I_c, IV and IX are metastable (after V. E. Petrenko, R. W. Whitworth, *Physics of Ice*, Oxford Univ. Press, Oxford, **1999**).

46 R. Ludwig, *Angew. Chem. Int. Ed.* **2001**, *40*, 1808–1827. W. F. Kuhs (ed.), *The Physics and Chemistry of Ice*, Royal Society of Chemistry, Cambridge, **2007**.

At 0 °C (273.15 K) and a pressure of 1013 hPa, water normally solidifies in air to form **hexagonal ice I_h**, with a hexagonal packing of the oxygen atoms similar to the structure of wurtzite (ZnS).[47] Under its own vapor pressure, air-free water solidifies at 273.16 K. The ice I_h structure (Figure 5.6) apparently consists of cyclic arrangements of OH groups forming six-membered rings (consisting of six O and six H atoms); on average, each oxygen atom is surrounded tetrahedrally by four others. At higher pressures, water crystallizes at lower temperatures, for example, at −4.0 °C at a pressure of 50 MPa. At all temperatures above −100 °C water crystallizes as ice I_h (e.g., behind high-flying aircrafts forming condensation trails).

In ice I_h, the smallest internuclear d_{OO} is 276 pm at −50 °C, and the density at 0 °C is 0.917 g cm^{-3}; therefore, ice floats on water. The vapor pressure is 611.2 Pa = 6.1 mbar at 0 °C, and the enthalpy of sublimation has been determined as 47 kJ mol^{-1}. Since two H bonds per molecule are broken on vaporization, the enthalpy of these bonds can be estimated as approximately 18.5 kJ mol^{-1} per bond (see below). The hydrogen atoms are located either exactly on the oxygen–oxygen axes to give linear bridges or the bridges are slightly bent. Since the valence angle in the water molecule is 104.5° (in contrast to the tetrahedral angle of 109.5° between the oxygen atoms in ice), the hydrogen bonds are most likely slightly bent. The bond length d_{OH} = 98.5 pm is larger than that in gaseous H_2O (95.8 pm), which together with d_{OO} indicates asymmetric H-bonds.

Other crystalline modifications of H_2O are denser than ice I_h and exist only at higher pressures or lower temperatures. Most of them are metastable at liquid nitrogen temperature (−196 °C) and can then be investigated even at ambient pressure. Some of them contain rings of four or five rather than six OH groups. In addition, vitreous (amorphous) ice can be prepared by condensation of water vapor at low temperatures; on warming, this allotrope turns into cubic ice I_c with a diamond structure of the oxygen atoms, and finally into ice I_h.

At high pressures (60 GPa), ice X with symmetric hydrogen bridges has been prepared, where the intra- and intermolecular OH bonds are identical. In orthorhombic ice XI the hydrogen atoms have fixed positions in asymmetric H bonds (no disorder) and only under these circumstances the OH internuclear distances can be accurately determined (98.5 pm).

Near the m.p. the surface of supercooled ice I_h crystals is covered by a thin layer of liquid water the thickness of which varies between 10 and 100 nm with temperature. This water layer is important for crystal growth and determines the differing morphologies of *snow flakes*, for example, which are either plate-like or

47 However, very small, dust-free droplets of water as in clouds can be supercooled down to −38 °C without crystallizing. Several amorphous ice forms can be prepared by vapor condensation at temperatures near 100 K.

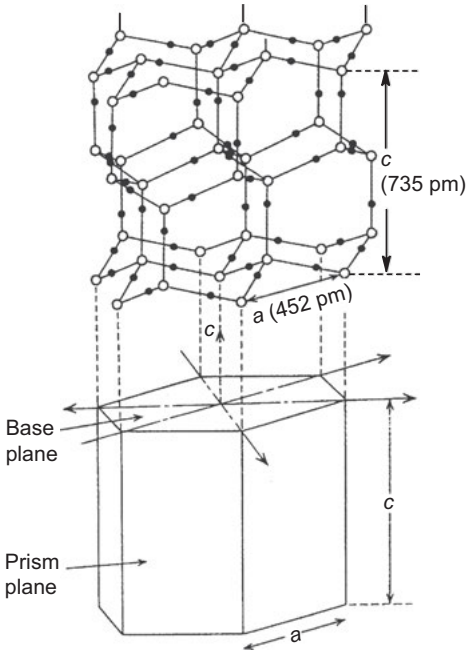

Figure 5.6: Crystal structure of hexagonal ice I_h. The oxygen positions are indicated by open circles and the hydrogen atoms by smaller full circles. However, the hydrogen atoms are disordered since two equivalent positions exist for each OHO unit (O—H····O and O····H—O; symmetric double minimum potential). The coordination of the oxygen atoms by neighboring O atoms is (on average) tetrahedral; the resulting hexagonal symmetry of the crystals is shown in the lower part of the figure.

prismatic but always with a hexagonal symmetry.[48] The good sticking properties of snow balls at not too low temperatures and the motion of glaciers are also a consequence of this water layer.

Water is the most abundant liquid on Earth. It exhibits the most anomalous behavior, and is a prerequisite for life. The structure of liquid water near the m.p. is rather complex.[49] Most probably, it is a mixture of numerous oligomers $(H_2O)_n$ and larger clusters of up to 100 molecules in which the molecules are interconnected by hydrogen bonds in a similar manner as in ice I_h. In other words, most molecules are engaged in four hydrogen bonds. Near the surface, however, there must be molecules with less than four H-bonds as shown in Figure 5.7. One of the most important arguments in favor of this model is the dielectric constant, which is 92.0 for ice at

48 Y. Furukawa, *Chem. unserer Zeit* **1997**, *31*, 58 (with numerous figures). W. J. Smit, H. J. Bakker, *Angew. Chem. Int. Ed.* **2017**, *56*, 15540.
49 Y. Marcus, *Chem. Rev.* **2009**, *109*, 1346. P. Gallo et al., *Chem. Rev.* **2016**, *116*, 7463–7500 (17 authors, 404 references).

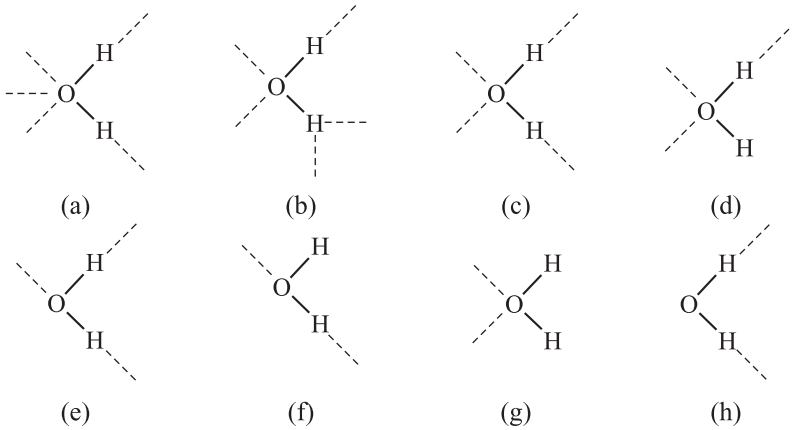

Figure 5.7: Eight possible bonding situations of the atoms in liquid water, ordered by decreasing number of hydrogen bonds. Hydrogen bonds indicated by broken lines are longer than regular covalent O–H bonds; these O–H–O units are not necessarily linear (see text). In structure (a) the oxygen atom is hypercoordinated while (b) shows a bifurcated hydrogen bond. The relative abundance of these bonding situations at room temperature is approximately c > d,e > f > a > b > g,h.

the m.p. and 88.5 for water at 0 °C. It decreases with temperature to 55.5 at 100 °C and to 34.5 at 200 °C. At the surface of the water clusters, however, there is a continuous "coming and going" due to the short half-life of the OHO hydrogen bridges of approximately 10^{-11} s. This short time is the consequence of the low bond enthalpy, which is only slightly larger than the thermal vibrational energy at 25 °C.

The mean internuclear distance between neighboring oxygen atoms in liquid water at 25 °C is 285 pm, slightly larger than in ice I_h (276 pm). The density of pure water reaches a maximum of 0.99997 g cm^{-3} at 4.0 °C, but for D_2O the density maximum is observed at 11.2 °C (Section 5.1; Table 5.1). The fact that the maximal density of water is larger than that of ice is explained by the presence of bifurcated hydrogen bonds shown in Figure 5.7, which leads to a better space filling and an increase of the mean C.N. of oxygen atoms from 4.0 in ice to 4.5–4.7 in water; at 0 °C/1.013 bar the density is 0.99984 g cm^{-3}.

Besides the mentioned high-molecular-weight clusters, smaller oligomers $(H_2O)_n$ with n = 2, 3, 4... are also present in liquid water at 25 °C, albeit in low concentrations. The structures of such species will be discussed below. Their presence can be detected by injecting water in a high vacuum followed by mass spectrometry of the resulting molecular beam.

The concentration of "free OH" groups not involved in hydrogen bonds was derived from IR and Raman spectra of liquid water as well as from X-ray diffraction as approximately 20% at 25 °C, and 70% at the critical point of 374 °C/22.1 MPa (computational simulations gave a value of 25% at 25 °C). At the critical point, the density ρ of water is only 0.322 g cm^{-3} and the dielectric constant ε is only 6 with

the consequence that ionic and polar substances are less soluble while nonpolar compounds are better soluble than at ambient conditions.[50] The enthalpy of vaporization of water at 25 °C/1 bar (44 kJ mol^{-1}) is only slightly smaller than that of ice (47 kJ $mol^{-1)}$, indicating similar structures. The mean hydrogen bond enthalpy of water can be derived from these data as approximately 17 kJ $mol^{-1.}$

On **dissolution of salts** in an excess of water, the ions are hydrated, that is, the electric field of the ions cleaves some of the hydrogen bonds of water and new structures are formed, characterized by a shell of well-ordered water molecules on the surface of the ions. This kind of interaction between the dipole moments of water molecules and the electric charge of ions is called *structure formation* and is typically observed for small ions with a high electric field strength such as H^+, Li^+, Na^+, Mg^{2+}, F^-, $[SO_4]^{2-}$. In this way, Li^+ coordinates four, Na^+ six and Ca^{2+} 12 water molecules in the first coordination shell. The orthophosphate ion $[PO_4]^{3-}$ binds 12 water molecules, which are linked with one H atom to the oxygen atoms of the anion by hydrogen bonds. The second H atom is connected to nearby water molecules in the bulk of the solution, which are less well ordered and able to move freely almost as in pure water due to the weaker field of the ion. Therefore, this second hydration sphere is called the region of *structure breaking*.

This kind of interaction is typical not only for the second hydration shell of small ions but also for the first hydration shell of larger ions with weaker electric fields such as K^+, Rb^+, Cs^+, Br^-, I^-, $[SCN]^-$, $[ClO_4]^-$. In other words, structure formation increases the number of hydrogen bonds compared to pure water while structure breakers cause the opposite.[51] These structural changes are responsible, for example, that dissolution of NaF in water increases the viscosity while CsI affects the opposite if the concentrations are low.

At higher concentrations the situation is different. In a concentrated aqueous solution of NaCl (e.g., 3 mol L^{-1}), the cations are only partially hydrated since there are simply not enough H_2O molecules available for a full hydration shell of sodium ions. At this and higher concentrations, the average distance between cations and anions is smaller than the diameter of a water molecule and consequently the formation of *ion pairs* is observed, as the following example shows (M: univalent ion):[52]

$$[M(H_2O)_4]^+ + Cl^- \rightleftharpoons [M(H_2O)_3Cl] + H_2O$$

A saturated aqueous solution of NaCl at –10 °C contains 69% of the salt as separated ions and 31% as ion pairs, as shown by the freezing point depression. Under these circumstances, the activity coefficients of the ions are much smaller than 1.

50 H. Weingärtner, E. U. Franck, *Angew. Chem. Int. Ed.* **2005**, *22*, 2672–2692.

51 For figures showing the hydration shells of alkali metal ions with up to 20 water molecules, see F. Schulz, B. Hartke, *ChemPhysChem*. **2002**, *3*, 98.

52 Y. Marcus, G. Hefter, *Chem. Rev*. **2006**, *106*, 4585. A. A. Zavitsas, *Chem. Eur. J*. **2010**, *16*, 5942.

The formation of ion pairs is a requirement for *seed formation*, which precedes crystallization. The fact that salts bind water by hydration is used for *salting-out* of proteins from aqueous solutions; $[NH_4]_2[SO_4]$ or $K_3[PO_4]$ may be used for this purpose.

Seawater freezes at the surface at approximately –1.9 °C due to the salt concentration of 3.5% on average, but at –2.5 °C at a depth of 1500 m owing to the higher pressure.[53] On formation of pure ice crystals, the salt concentration in the mother liquor increases and the freezing point decreases. On further cooling, ice and various salts crystallize from seawater in the following order: $Ca[CO_3] \cdot 6H_2O$, $Na_2[SO_4] \cdot 10H_2O$, $MgCl_2 \cdot 8H_2O$, $NaCl \cdot 2H_2O$, KCl and eventually $MgCl_2 \cdot 12H_2O$ at –43 °C. This order reflects increasing solubility. But even at –50 °C, a concentrated solution, called brine, is obtained. On the other hand, *evaporation* of seawater at +20 °C yields mainly anhydrous salts. In this manner, the huge salt deposits were formed in Northern Germany in the prehistoric past. Their thickness sometimes reaches more than 1000 m.

Water vapor at room temperature and <90% of the saturation pressure behaves nearly as an ideal gas and, therefore, must be monomeric H_2O. At higher temperatures near the saturation vapor pressure oligomers such as $(H_2O)_2$ are present. These oligomers have been trapped in a matrix of argon or nitrogen at 20 K and studied by IR spectroscopy. At the critical point, the concentration of monomeric H_2O is only 72%.

Water is only sparingly soluble in **nonpolar solvents** such as aliphatic and aromatic hydrocarbons, CCl_4 and CS_2, predominantly as the monomer. However, at low temperatures, oligomers $(H_2O)_n$ with $n = 2–6$ have been detected by IR spectroscopy in such solutions. In weakly polar solvents such as partially chlorinated hydrocarbons, water dissolves as both monomers and oligomers. In polar solvents such as alcohols, ethers, ketones, amines, nitriles, carboxylic acids and sulfoxides, which are suitable for participating in hydrogen bonding, solvent–water complexes are formed, whose composition is temperature- and concentration dependent.

Nonpolar (hydrophobic) solutes such as noble gases, H_2, N_2, O_2, CH_4, CF_4, C_2F_6 and SF_6 are only sparingly soluble in liquid water (molar fractions < $8 \cdot 10^{-5}$ at 25 °C).[54] For example, the saturation concentration of methane at 25 °C is only $2.5 \cdot 10^{-3}$ mol% due to the positive GIBBS energy of hydration ($\Delta G^o = \Delta H^o - T\Delta S^o = +8.4$ kJ mol^{-1}) that results from a small negative enthalpy of solution (ΔH^o) and a much larger negative entropy term ($T\Delta S^o$). The loss of entropy ($\Delta S^o < 0$) is caused by the cleavage of hydrogen bonds in the water phase to make room for the

53 The salt concentration of ocean water at the surface varies between 3.7% near the equator and 3.4% in Antarctica, where freshwater from melting glaciers dilutes the seawater.

54 T. M. Letcher, R. Battino, *J. Chem. Educ.* **2001**, *78*, 103.

methane molecule. At the surface of the hydrophobic solute molecule, a new order of water molecules is established, which is mainly responsible for the entropy decrease. This extremely important phenomenon is called *hydrophobic effect*.[55] It can be described as antipathy of liquid water for nonpolar molecules or surfaces. Since the origin of the hydrophobic effect is mainly entropic, it is strongly temperature dependent.

Gaseous *n*-alkanes C_nH_{2n+2} with carbon atoms between 2 and 7 are even more hydrophobic than methane since the entropy loss on dissolution in water is larger. In the case of *liquid n-alkanes*, however, the rather strong dispersion forces (Section 3.6.3) between these molecules in the liquid phase need to be overcome upon dissolution in water and are mainly responsible for their low solubility.[56] Therefore, mixtures of these compounds with water typically show phase separation.

Hydrophobic effects play a major role in many aqueous systems. For example, the stability of biological membranes and the tertiary structure of proteins are due to such effects. In addition, the flotation of minerals and the aggregation of surfactants in water are consequences of hydrophobic interactions.

5.6.4.3 Gas Hydrates and Clathrate Hydrates

Elemental chlorine reacts with water at 0 °C and 1013 hPa pressure to a crystalline *gas hydrate* of m.p. +10 °C and of approximate composition $Cl_2 \cdot 7H_2O$.[57] The cubic structure of this material consists of a host lattice of water molecules forming pentagon–dodecahedrons and similar cages in which the chlorine molecules are hosted as so-called "guests" (Figure 5.8).

The polyhedrons of water molecules are connected by hydrogen bonds forming a three-dimensional structure that exists only with small "guests" such as He, Ne, Ar, Kr, Xe, H_2, N_2, Cl_2, Br_2, CH_4, H_2S, AsH_3, SO_2, SF_6 or other small molecules. The symmetry of the host lattice depends on the composition of the gas hydrate (molar ratio), on pressure and temperature as well as on the nature of the mainly hydrophobic guest molecules. The composition can vary but there is a saturation value for the guest species.

Methane hydrate (MH)[58] forms enormous deposits on the seafloor near certain coasts. Therefore, MH is one of the largest energy reserves on Earth since its total

55 W. Blokzijl, J. B. F. N. Engberts, *Angew. Chem.* **1993**, *105*, 1611; M. E. Paulaitis, S. Garde, H. S. Ashbaugh, *Curr. Opin. Colloid Interf. Sci.* **1996**, *1*, 376. N. T. Southall, K. A. Dill, A. D. J. Haymet, *J. Phys. Chem. B* **2002**, *106*, 521.

56 V. Barone, M. Cossi, J. Tomasi, *J. Chem. Phys.* **1997**, *107*, 3210.

57 E. D. Sloan, *Clathrate Hydrates of Natural Gases*, 2nd ed., Dekker, New York, **1998**. J. S. Loveday, R. J. Nelmes, *Phys. Chem. Chem. Phys.* **2008**, *10*, 936.

58 J. M. Schicks, *Chem. unserer Zeit* **2008**, *42*, 310.

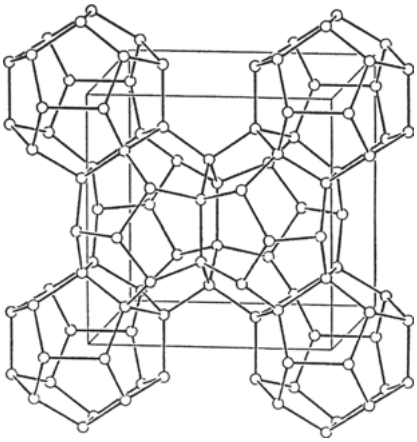

Figure 5.8: Cage structure of the water molecules in clathrates of cubic type I. Given are the positions of the oxygen atoms that form pentagonal–dodecahedral polyhedrons (symbol $[5^{12}]$) and less symmetrical polyhedrons of type $[5^{12}6^2]$. In these symbols, the number of edges of the cage-defining planes (e.g., 5) is given together with the number of such planes per cage as exponent.

combustion energy is said to be larger than those of all crude oil and natural gas reserves combined. The decomposition temperature of MH at ambient pressure (1013 hPa) is −79 °C but increases sharply with pressure to +47 °C at 0.5 GPa. MH is by far the best investigated gas hydrate because of its importance for future energy supply although mining is not trivial. In addition, MH is possibly present also on other planets and moons of the solar system. In this context, it is interesting to note that the air bubbles and the "air hydrate" deep in the ice shields of Greenland and Antarctica provide a possibility to reconstruct the composition and temperature of Earth's atmosphere in previous centuries. There is a strong correlation between the CO_2 content of these bubbles and the historic temperature, which can be derived from the $^{16}O/^{18}O$ isotopic ratio of the water molecules.

Some strong acids form similar *inclusion compounds* with water called *clathrate hydrates*. In this case, the water molecules together with the oxonium cations $[H_3O]^+$ form cages that are occupied by the acid anions.

5.6.4.4 Ammonia and Amines

Solid ammonia (m.p. = −77.7 °C, b.p. = −33.4 °C) forms a cubic structure with all hydrogen atoms engaged in identical hydrogen bonds in which case each nitrogen atom takes part in three H-bonds (for a figure, see Section 5.6.2). The internuclear distance $d_{N\cdots H}$ is 240 pm and the angle α(N–H···N) is 161°. Particularly strong N–H···N hydrogen bonds are observed in certain protonated diamines containing the nitrogen atoms in neighboring positions to allow the bridging proton to be linked to both N atoms. Examples are the following two bis-dimethylamines, which are derivatives of the aromatic hydrocarbons naphthalene and fluorene, respectively:

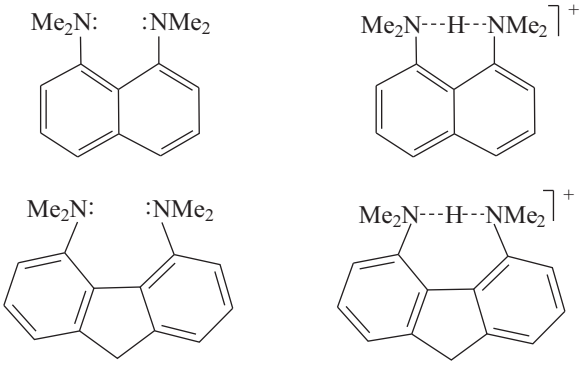

The pK_a(BH$^+$) values of these protonated diamines in water are between 12.1 and 12.8. In other words, the proton is tightly bonded. Such compounds are called ***proton sponges***[59] due to their pronounced ability to remove protons from solutions just like a sponge sucks up water. The very short hydrogen bond in protonated bis-dimethylamino fluorene is practically linear with d_{NN} = 263 pm. For other uncharged N-donor molecules, pK_a(BH$^+$) values of up to 17 have been determined.[60]

The following inclusion compound of an ammonium cation in the cage of a spherical *cryptand* molecule (**A**) with formation of four N–H····N hydrogen bonds (**B**) is particularly interesting:

A:

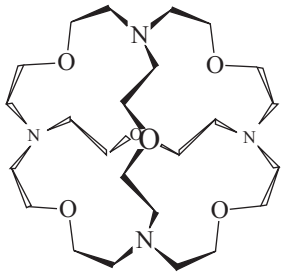

B:

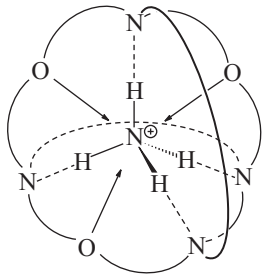

Supramolecular complexes[61] of this type are important models for the recognition of substrates (here [NH_4]$^+$) by a receptor (**A**). Hydrogen bonds of type N–H····N and N–H····O are also responsible for the double-helix structure of desoxyribonucleic acid (DNA), in which the nucleic bases thymine and adenine are connected by two and cytosine and guanine by three hydrogen bonds to each other.

Besides the hydrogen bonds of types

F – H····F O – H····O N – H····N

59 J.-C. Chambron, M. Meyer, *Chem. Soc. Rev.* **2009**, *38*, 1663.
60 R. Schwesinger, *Nachr. Chem. Techn. Lab.* **1990**, *38*, 1214.
61 J. M. Lehn, *Angew. Chem. Int. Ed.* **1988**, *27*, 89–112.

discussed so far, there are also H-bonds between other atoms X and Y. Table 5.6 contains well-known examples from inorganic chemistry.

Table 5.6: Types of hydrogen bonds in selected inorganic compounds (Me: methyl, Et: ethyl).

O–H····O $(H_2O)_n$ H_2SO_4 $B(OH)_3$ $K_2[HPO_4]$ $Na[HCO_3]$ AlO(OH) $Cu[SO_4] \cdot 5\ H_2O$ $Ca[SO_4] \cdot 2\ H_2O$ $K_2[XeO_4] \cdot 8\ H_2O$ $[H_3O][ClO_4]$ H_2O_2	**F–H····F** $(HF)_n$ $K[HF_2]$ $K[H_2F_3]$	**O–H····S** $Ba[S_2O_3] \cdot H_2O$	**N–H····Cl** $[NH_4]Cl$ $[N_2H_6]Cl_2$
	O–H····N NH_2OH $2NH_3 \cdot H_2O$	**N–H····F** $[NH_4][HF_2]$ $[NH_4]_2[SiF_6]$ $[NH_4][BF_4]$	**Cl–H····O** HCl in Et_2O
		N–H····O $H_2N–NO_2$ NH_2OH	**C–H····O** C_2H_2 in Me_2CO Me_2SO in $CHCl_3$
	O–H····Cl $MnCl_2 \cdot 2\ H_2O$ $[H_5O_2]Cl \cdot H_2O$	**N–H····N** NH_3 $[NH_4][N_3]$ N_2H_4	**C–H····N** $(HCN)_n$
			Cl–H····Cl $[NR_4][HCl_2]$

The planar anion $[(FH_2O)_2]^{2-}$ is a remarkable example for O–H····F hydrogen bonds: the salt $[Zn(en)_3][F(H_2O)_2F]$ is obtained on heating a suspension of ZnF_2 with ethylene diamine (en) in aqueous methanol [distances d(F····O) = 258.6 and 267.9 pm]:

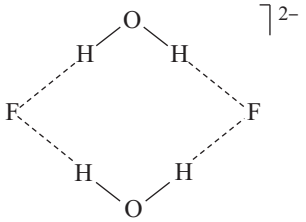

An interesting example of a C–H····N hydrogen bond is the recently prepared HCN adduct $(C_6F_5)_3B$····NCH····NCH, which crystallizes from a solution of the strongly LEWIS acidic borane in the presence of an excess of liquid HCN (b.p. 26 °C, m.p. –13 °C). The structural unit BNCH in the adduct is linear, while the hydrogen bridge is slightly bent. Strictly linear clusters of HCN molecules have been found in solid, liquid and gaseous hydrogen cyanide.[62]

The structures of many hydrogen compounds are influenced by the gain of energy from hydrogen bond formation, but there are also numerous substances that

62 A. Schulz et al., *Angew. Chem. Int. Ed.* **2018**, *57*, 9170.

do not show H-bonds although the conditions seem to be fulfilled. This holds true for the crystalline hydroxides NaOH, $Ca[OH]_2$, $Mg[OH]_2$ and $Fe[OH]_2$, for instance.

5.6.5 Theory of Hydrogen Bond Formation

Hydrogen bonds X–H···Y are mainly formed between small and highly electronegative atoms X and Y, and the strongest bonds are observed if X and/or Y are fluorine, oxygen or nitrogen atoms.[63] Only with these "bridge head atoms" symmetrical H-bonds are occasionally observed, especially within ions.[64] The energy of the hydrogen atom in an H-bond can be described by three potential energy curves, depending on the distance between X and Y; see Figure 5.9.

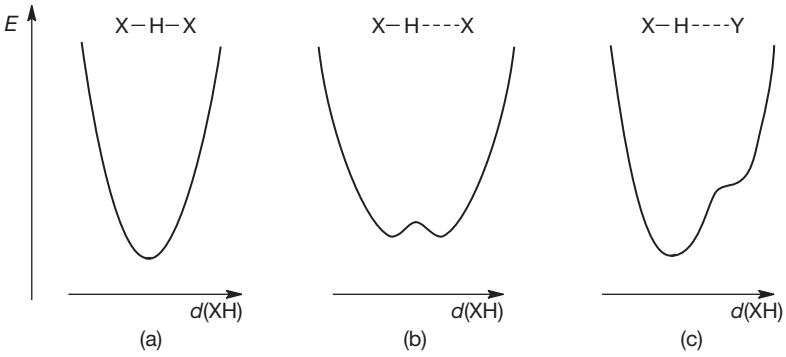

Figure 5.9: Energy of the hydrogen atom in various hydrogen bonds as a function of the internuclear distance d_{XH} at constant distances d_{XX}, respectively, d_{XY}: (a) symmetrical bond X–H–X as in $K[HF_2]$. (b) Two equivalent minima between two identical atoms X as in ice I_h and $K[H_2PO_4]$. (c) Asymmetric potential curve for differing atoms X and Y, which is the most common case of H-bonds.

The theoretical treatment of hydrogen bonds is easiest for the symmetrical bridge X–H–X with a center of symmetry. Such bonds are formed only at small distances d_{XX} resulting in considerable orbital overlap and partial covalent interaction. The resulting three-center four-electron bond as in $[HF_2]^-$ has already been discussed in Chapter 2 and illustrated in Figure 2.27. Only one electron pair is needed to bind the three atoms, but this kind of interaction is weaker than common two-center two-electron bonds. Further examples for symmetric hydrogen bonds are the anions

63 S. Scheiner, *Hydrogen Bonding – A Theoretical Perspective*, Oxford University Press, New York, **1997**. D. C. Clary, D. M. Benoit, T. Van Mourik, *Acc. Chem. Res*. **2000**, *33*, 441.
64 J. Emsley, *Chem. Soc. Rev*. **1980**, *9*, 91 (review on strong H bonds).

$[HO_2]^{3-}$ in $Cr[HO_2]$ as well as $[H(CO_3)_2]^{3-}$, $[H(NO_3)_2]^-$ and $[H(SO_4)_2]^{3-}$ in the corresponding acidic sodium salts. Furthermore, the cation $[H_5O_2]^+$ is of C_{2h} symmetry in $[H_5O_2][SbF_6]$.

While symmetric hydrogen bonds can be considered as mainly covalent, the asymmetric bonds are more difficult to explain. Calculations show that the energy of an H atom between two oxygen atoms corresponds to curve (a) in Figure 5.9 only for small OO distances (240–260 pm). For larger values of d_{OO}, the curve transforms into case (b) of Figure 5.9, first forming a small maximum between the minima resulting in two energetically equivalent positions for the hydrogen atom (*symmetrical double minimum potential*). With increasing values of d_{OO} the maximum grows, and it becomes increasingly difficult for the hydrogen atom to switch over to the neighboring position. The quantum-mechanical interaction between these two positions (*tunnel effect*) results in a splitting of the vibrational energy levels of those modes in which the hydrogen atom takes part.

In general, hydrogen bonds are formed by the combined forces from electrostatic interaction, mutual polarization of the reactants, VAN DER WAALS attraction and covalent interaction through charge transfer. The most frequent case is the asymmetric H-bond according to curve (c) in Figure 5.9. In this case, atom X has the higher *proton affinity* and the proton remains firmly attached to the hydrogen bond donor atom. Some data for proton affinities (E_{pa}) of small gaseous molecules and anions are given in Table 5.7 (for aqueous solutions, see Table 5.3).

Table 5.7: Proton affinities (kJ mol^{-1}) of gaseous molecules and ions.[a]

NH_3	854	H_2O	691	HF	484
$[NH_2]^-$	1690	$[OH]^-$	1635	$[F^-]$	1554
PH_3	785	H_2S	705	HCl	567
$[PH_2]^-$	1551	$[HS]^-$	1470	$[Cl^-]$	1395

[a]S. G. Lias, *J. Phys. Chem. Ref. Data* **1988**, *17*, 1–861 and **1984**, *13*, 695–808; NIST Standard Reference Database 69 – August **1997** (http://www.webbook.nist/gov).

For electrostatic reasons, the proton affinity of anions is larger than for comparable neutral molecules. The data for NH_3 and F^- show that the reaction of one molecule of the LEWIS base NH_3 with one molecule of the protic acid HF in the vapor phase will give a VAN DER WAALS molecule $H_3N\cdots H–F$ rather than an ion-pair $[H_3NH]^+\cdots F^-$. Only if many molecules of ammonia and hydrogen fluoride are combined, solid ammonium fluoride $[NH_4]F$ is formed since in this case lattice energy (Section 2.1.5) is gained and released. In solution, the solvation enthalpies need to be considered, which will typically favor ion formation in polar solvents such as water. Similar considerations hold for gaseous adducts $H_2O\cdots H–X$ between water and protic acids *versus* solid oxonium salts $[H_3O]X$.

The above-mentioned gaseous oligomers of water and hydrogen fluoride molecules have been studied extensively both by experiment and theory since they are also constituents of the corresponding liquids. The structure of the dimer $(HF)_2$ has been determined computationally as follows:[65]

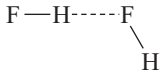

$d(FF) = 274(1)$ pm, $\text{angle}_{FFH} = 112(1)°$

If the two dipole molecules HF interacted only electrostatically, a linear or a parallel orientation should be most stable since this would maximize distances between equally charged atoms and minimize the separation of opposite charges. On the other hand, a mainly covalent interaction by overlap between one of the $2p_\pi$ lone pair orbitals of fluorine with the outer lobe of the σ* MO of a neighboring HF molecule (on the hydrogen side) should result in a bond angle of 90°.[66] Evidently, the calculated angle of 108° is a compromise between the two types of interaction maximizing the total interaction energy to 19 kJ mol^{-1} (dissociation enthalpy). The oligomers $(HF)_n$ with $n = 3–5$ are cyclic.[65]

The structure of $(HF)_2$ represents a section of the infinite chain structure of solid HF (see Section 5.6.4). It may serve as a model for other weak hydrogen bonds. The partial delocalization of electron density from the fluorine $2p_\pi$ HOMO into the antibonding molecular orbital of a neighboring HF molecule explains the weakening of its bond leading to a larger HF bond length. The bonding situation in the cyclic oligomers $(HF)_n$ with $n = 4–6$ can be explained similarly. It should be kept in mind, however, that the electrostatic interaction is the dominating contribution to weak hydrogen bonds.[67]

Oligomeric water clusters have been studied extensively in recent years.[68] The gaseous dimer $(H_2O)_2$ is of similar structure as $(HF)_2$ (C_s symmetry):

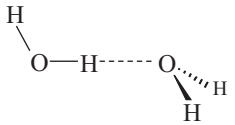

$d(OO) = 297.6$pm

The smallest angles between the oxygen–oxygen axis and the C_2 axis of the molecule on the right-hand side is 57° and the bridging hydrogen atom is located slightly above this axis with $d_{OH,bridge} = 96.5$, $d_{O\cdots H,bridge} = 194.9$ and $d_{OH,ext} = 95.8–96.0$ pm

65 W. Klopper, M. Quack, M. A. Suhm, *J. Chem. Phys.* **1998**, *108*, 10096, and *Mol. Phys.* **1998**, *94*, 105.
66 P. Schuster, *Z. Chem.* **1973**, *13*, 41; A. E. Reed, L. A. Curtiss, F. Weinhold, *Chem. Rev.* **1988**, *88*, 899.
67 A. C. Legon, *Chem. Soc. Rev.* **1987**, *16*, 467.
68 R. Ludwig, *Angew. Chem. Int. Ed.* **2001**, *40*, 1808–1827. W. F. Kuhs (ed.), *The Physics and Chemistry of Ice*, Royal Society of Chemistry, Cambridge, **2007**.

(at 0 K). The dissociation energy $(H_2O)_2$ has been determined experimentally and theoretically as 13.7 kJ mol^{-1} at 0 K (D_o) and as 15 kJ mol^{-1} at 25 °C (ΔH^o_{298}).[69] The partial charges of the atoms that form the H-bond are considerably enhanced compared to the monomeric water molecule resulting in a dipole moment of 2.70 D for the dimer. The structure of $(H_2O)_2$ can be understood in a similar fashion as the structure of $(HF)_2$ assuming electrostatic and covalent interactions together with mutual polarization and VAN DER WAALS attraction. However, the charge transfer is very small. In general, the stronger the O–H···O hydrogen bond and the smaller the OO distance, the larger the internuclear distance within the OH groups.

According to spectroscopic investigations and quantum-chemical calculations, the most stable oligomers $(H_2O)_3$, $(H_2O)_4$ and $(H_2O)_5$ are cyclic with shortest OO internuclear distances of 281, 275 and 274 pm, respectively;[70] see Figure 5.10.

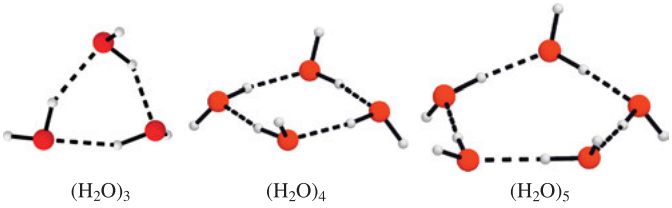

Figure 5.10: Calculated structures of the water oligomers $(H_2O)_n$ with n = 3–5.

Their dissociation energies per hydrogen bond slowly increase with number of molecules due to the cooperativity of the H-bonds, which is caused by mutual polarization. For example, for the trimer 15.9 kJ mol^{-1} at 0 K (D_0) has been determined while for liquid water 17 kJ mol^{-1} has been found (at 25 °C). Larger water clusters are cage-like to maximize the number of hydrogen bonds per oxygen atom. Oligomers of this type with up to eight monomers have been detected by X-ray crystallography in cavities of salts as *water of hydration*. Furthermore, rings of five water molecules have been observed in the structure of ice III and in some gas hydrates (Section 5.6.4). Some of the ammonia oligomers $(NH_3)_n$ with n = 3–6 have cyclic structures as well; the dissociation energy of the ammonia dimer is D_e = 13 kJ mol^{-1}.[71]

69 E. Dunn, E. K. Pokon, G. C. Shields, *J. Am. Chem. Soc.* **2004**, *126*, 2647; H. Reisler et al., *J. Am. Chem. Soc.* **2012**, *134*, 15430, and *Acc. Chem. Res.* **2014**, *47*, 2700.

70 M. B. Day, K. N. Kirschner, G. C. Shields, *J. Phys. Chem. A* **2005**, *109*, 6773. E. Miliordos, S. S. Xantheas, *J. Chem. Phys.* **2015**, *142*, 234303.

71 P. E. Janeiro-Barral, M. Mella, E. Curotto, *J. Phys. Chem. A* **2008**, *112*, 2888.

A characteristic feature of *weak hydrogen bonds* is their short half-life, which distinguishes them from shorter, partially covalent bonds. In the liquid and gaseous states, weak H-bonds are continuously broken and re-established, often between different bond partners because of fluctuations in the vibrational energy of the molecules, which is equipartitioned only on average. Instantaneously, it can surpass the bond energy, especially with smaller bond energies and at higher temperatures. The mean vibrational energy of 2.5 kJ mol^{-1} per degree of freedom determines a lifetime of fractions of a second (at 25 °C) for hydrogen bonds with a bond energy between 10 and 50 kJ mol^{-1}. An example of a very weakly hydrogen-bonded complex is the dimer $(H_2S)_2$ with a structure similar to the water dimer but a hydrogen bond energy of only 7 kJ mol^{-1} at 0 K (D_0).

It is a remarkable fact that only hydrogen is forming linear bridge bonds between highly electronegative partner atoms and no other small atoms such as lithium. This may be due to the absence of inner electrons at hydrogen, which would be repelled by the lone pair electrons of the acceptor atom Y. Lithium, on the other hand, prefers higher C.N.s. In Chapter 6, we will discuss intermolecular *dihydrogen bonds* in which positively and negatively charged H atoms attract each other as in the structure of $Na[BH_4] \cdot 2H_2O$.

5.7 Hydrogen Compounds (Hydrides)

5.7.1 Introduction

Hydrogen compounds may be classified into different groups based on their bonding and physical properties:

(a) Covalent hydrides of the nonmetals and related ions:
Bonding: from mainly covalent and nonpolar to strongly polar
Examples: B_2H_6, $[BH_4]^-$, SiH_4, $[NH_2]^-$, $[NH_4]^+$, P_2H_4, H_2O_2, H_2S_2, $[HF_2]^-$, HBr

(b) Complex ions of certain metals with hydrido ligands:
Bonding: from mainly covalent and nonpolar to strongly polar
Examples: $[AlH_4]^-$, $[AlH_6]^{3-}$, $[ReH_9]^{2-}$, $[Ni_4H_{12}]^{5-}$, $[FeH_6]^{4-}$, $[PtH_6]^{2-}$, $[Pt_2H_9]^{5-}$

(c) Salt-like hydrides of the alkali and alkaline earth metals:
Bonding: predominantly ionic
Examples: LiH, NaH, MgH_2, CaH_2

(d) Polymeric hydrides of the metals in Groups 11–13:
Bonding: from mainly covalent and nonpolar to strongly polar
Examples: $(BeH_2)_x$, $(AlH_3)_x$, $(CuH)_x$

(e) Metal-like hydrides of many transition metals:
Bonding: partly metallic, partly covalent or ionic
Examples: PdH_n, UH_3, $FeTiH_2$

There are no sharp boundaries between these groups, and some compounds are difficult to classify. After all, there is a continuous transition between the different bonding types. Coordination numbers of hydrogen atoms in hydrides range from 1 to 6. Most metals in Groups 6–9 of the Periodic Table as well as silver are reluctant to form hydrides.

5.7.2 Covalent Hydrides

All nonmetal hydrides and most organic compounds belong to this group. The nonmetals except the noble gases form volatile hydrides, as do some of the main group metals such as Sn, Sb, Bi and Po. The higher homologues of these hydrides are, however, liquids of low volatility or nonvolatile (e.g., polyboranes, polysilanes and polysulfanes). Certain derivatives of the covalent hydrides are ionic, for example, salts with the anions $[BH_4]^-$, $[NH_2]^-$ and $[OH]^-$ as well as cations $[NH_4]^+$, $[PH_4]^+$ and $[H_3O]^+$. These compounds will be discussed in chapters on the corresponding central atoms.

5.7.2.1 Activation of H_2 Molecules

The dihydrogen molecule has the strongest homonuclear single bond with a homolytic dissociation enthalpy of 432 kJ mol^{-1} at 25 °C (Section 2.4.2). Some reactions of H_2 have already been discussed in Section 5.1. The heterolytic cleavage of the H–H bond into H^+ and H^-, however, requires the much higher energy of 1696 kJ mol^{-1} since the ionization energy of H atoms (13.60 eV) is much higher than the electron affinity of H (0.755 eV; 1 eV = 96.5 kJ mol^{-1}). Nevertheless, there are special reagents that can initiate this cleavage, even at room temperature. Examples are the *frustrated LEWIS pairs* that have been discussed in Section 2.5. For instance, a 1:1 mixture of $^tBu_3P$ and $(C_6F_5)_3B$ reacts at 25 °C with H_2 to the salt-like phosphonium hydridoborate $[^tBu_3PH]^+[(C_6F_5)_3BH]^-$, which is stable in solution up to 150 °C. The phosphane and the borane cannot form an adduct directly because of their bulky substituents. The thus necessarily remaining cavity between them is well suited to polarize a H_2 molecule to such an extent that heterolysis takes place. The bond energies of the newly formed BH and PH bonds combined with the COULOMB energy of the salt evidently compensate the heterolytic dissociation energy of the H_2 molecule. In effect, a *metal-free activation of dihydrogen* is achieved.[72]

Covalent element–hydrogen bonds can also be found in certain **metal hydrides**. Examples are the binary hydrides of Be, Mg, Al and Ga, which are polymeric

72 D. W. Stephan, *Acc. Chem. Res.* **2015**, *48*, 306–316. D. W. Stephan, G. Erker, *Angew. Chem. Int. Ed.* **2015**, *54*, 6400–6441. G. Erker, D. W. Stephan (eds.), *Frustrated Lewis-Pairs I and II*, Springer, Berlin, **2013**.

and nonvolatile at ambient temperatures. On the other hand, complex hydrides of transition metals are known in large numbers.[73] Some of these are volatile such as $[MnH(CO)_5]$, others are salt-like (e.g., $K_2[ReH_9]$) and considered as coordination compounds with the monoatomic ligand H^-. This hydride ion can also serve as a bridging ligand connecting two or more metal atoms. An impressive example is the chromium hydride $[(Cp^*CrH)_4]$ with cubane structure and hydrogen of C.N. three within the cube-like core Cr_4H_4 (Cp^* = pentamethyl cyclopentadiene ligand).[74] In $[(Ph_3P)_2N][HCo_6(CO)_{15}]$, the hydrogen ligand is at the center of an octahedron of metal atoms and hence of C.N. = 6.[75] While these aspects are subject of the coordination chemistry of metal compounds and thus in principle beyond the scope of this book, the interaction of H_2 with single metal atoms and bulk metals is of utmost significance both for the understanding of reactivity of H_2 and the catalytic processes occurring at the surface of metals. The following section is therefore devoted to the ligand properties of dihydrogen.

5.7.3 H_2 as Ligand in Coordination Compounds

Most bulk metals and some metal complexes react with molecular hydrogen with cleavage of the H–H bond.[76] For example, VASKA's 16-electron complex adds dihydrogen to an octahedral *cis*-dihydrogen complex:

$$[IrCl(CO)(PPh_3)_2] + H_2 \longrightarrow [IrCl(H)_2(CO)(PPh_3)_2]$$

In this *oxidative addition reaction*, the molecular hydrogen formally oxidizes Ir(I) to Ir(III) and is in turn reduced to H(–I). Remarkably, the reaction is reversible and molecular hydrogen is released again by purging with argon or in a vacuum (*reductive elimination*). The internuclear HH distance in this complex (240 pm) is much larger than in molecular H_2 (74 pm); any bonding interaction between the two H atoms in the complex is certainly negligible.

However, in 1984 it was observed that $[W(CO)_3(cht)]$ with the cycloheptatriene ligand "cht" reacts with bulky phosphanes such as $(iPr)_3P$ by ligand exchange to the purple 16-electron complex $[W(CO)_3(PR_3)_2]$, which surprisingly adds H_2 as a molecular ligand by *side-on* coordination to the yellow $[W(H_2)(CO)_3(PR_3)_2]$:

---

73 R. H. Crabtree, *Encycl. Inorg. Chem.* **2005**, *3*, 1327 and 1805. K. Yvon, G. Renaudin, *Encycl. Inorg. Chem.* **2005**, *3*, 1814. W. Bronger, *Angew. Chem. Int. Ed.* **1991**, *30*, 759.

74 R. A. Heintz et al., *Angew. Chem. Int. Ed.* **1992**, *31*, 1077.

75 T. F. Koetzle et al., *Angew. Chem. Int. Ed.* **1979**, *18*, 80.

76 R. H. Crabtree, *Chem. Rev.* **2016**, *116*, 8750–8769. G. J. Kubas, *Proc. Natl. Acad. Sci. USA* **2007**, *104*, 6901, and *Chem. Rev.* **2007**, *107*, 4152. A. S. Weller, J. S. McIndoe, *Eur. J. Inorg. Chem.* **2007**, 4411. S. Sabo-Etienne, B. Chaudret, *Coord. Chem. Rev.* **1998**, *178–180*, 381. M. Gellier et al., *J. Am. Chem. Soc.* **2005**, *127*, 17592.

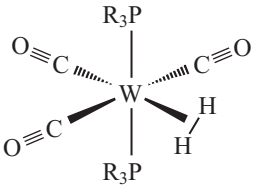

The internuclear HH distance in this compound was determined by neutron diffraction at 30 K as 84 pm, which is only 10 pm more than in free H_2. Evidently, the molecule H_2 still exists in this complex, which is further supported by the HH stretching frequency of 2695 cm^{-1} and the NMR coupling constant J_{HD} = 33.5 Hz determined for the partly deuterated complex (prepared from HD). For dihydrido complexes with separated H ligands, the coupling constant is typically much smaller (about 2 Hz). In fact, there is a linear relationship between the internuclear distance and this coupling constant:

$$d_{HH}(\text{pm}) = 143 - 1.68 \cdot {}^{1}J_{HD}$$

Compared to free H_2, the H–H bond in metal complexes is more or less weakened, that is, the hydrogen molecule is "activated." This can be rationalized by the bonding model shown in Figure 5.11. The occupied $1\sigma_g$ MO of H_2 overlaps with an empty atomic orbital of the metal atom establishing a σ bond with electron density transfer $H_2 \rightarrow M$. At the same time, an occupied atomic orbital of M overlaps with the antibonding $1\pi_u$ MO of H_2 forming a π bond. The latter is called *backbond* since electron density is flowing back to the H_2 ligand. Both bonds weaken the HH interaction since electron density is removed from a bonding MO, and at the same time the antibonding MO of H_2 is partially populated.

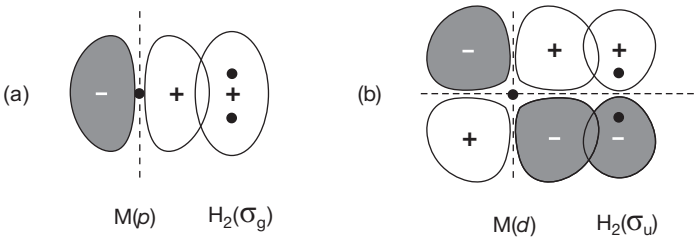

Figure 5.11: Orbital overlap between the metal atom M and the hydrogen molecule in dihydrogen complexes with *side-on* coordination: (a) σ bond by overlap of the occupied molecular orbital $1\sigma_g$ of H_2 with an unoccupied σ orbital of the metal atom (e.g., 3*p*) donating electron density to the metal atom; (b) π bond by overlap of the unoccupied molecular orbital $1\sigma_u$ of H_2 with an occupied π orbital of the metal atom (e.g., 3*d*).

More than 600 complexes with η^2-H_2 ligands have been prepared for almost all transition metals, mainly by adding H_2 to a 16-electron precursor complex or by protonation

of a hydrido complex. The stronger the donor strength of the metal atom, the more the HH bond is weakened. Ligands with particularly long HH bonds are called "stretched H_2 ligands." In other words, there is a continuous transition between dihydrogen and dihydrido complexes, the latter with $d_{HH} > 130$ pm. In addition, there are mixed hydrido dihydrogen complexes as well as *bis*-dihydrogen complexes, for example, $[RuH_2(H_2)_2(PR_3)_2]$ and $[Fe(H_2)(H)_2(PR_3)]$.

These results are of extraordinary importance for the understanding of catalytic reactions in industry and biology in which small molecules are activated either by metal complexes (*homogeneous catalysis*) or on the surface of powdered bulk metals (*heterogeneous catalysis*). The storage of dihydrogen by bulk metals discussed in Section 5.7.5 also starts with the coordination of the H_2 molecule, followed by dissociation.

5.7.4 Salt-Like Hydrides

Alkali metals and alkaline earth metals (Mg, Ca, Sr and Ba) react with hydrogen gas at high temperatures exothermally to form colorless, salt-like hydrides MH or MH_2:

$$2\,M(l.) + H_2(g.) \rightleftharpoons 2\,MH(s.)$$

In order to overcome the substantial activation energy of these equilibrium reactions, high temperatures are needed. But since the reactions are exothermic, the equilibrium shifts to the left-hand side with increasing temperature. Therefore, the preparation of pure compounds, with exception of LiH, is difficult. In certain temperature intervals, the dissociation pressure $p(H_2)$ obeys an ARRHENIUS equation ($\log p = -A/T + B$). To prepare pure hydrides the reaction mixture is equilibrated at high temperatures, for example, at 725 °C for Li and at 500 °C for Ca, and then slowly cooled in an atmosphere of hydrogen gas to maximize the yield of hydride. Alternatively, higher pressures of H_2 may be applied as in the case of Mg. Only LiH (m.p. 691 °C) melts without decomposition owing to the unfavorable position of the equilibrium and the relatively small enthalpies of formation of the other salt-like hydrides.

The alkali metal hydrides MH crystallize in cubic rock-salt structures while the alkaline earth hydrides MH_2 form tetragonal crystal structures (rutile type) with large lattice energies: MgH_2 2718 kJ mol^{-1} and CaH_2 2410 kJ mol^{-1}. These structures consist of metal cations and hydride anions H^-, isoelectronic with helium. Proof for the negative ionic charge comes from electrolysis of a eutectic hydride–chloride mixture such as LiH/LiCl which has a lower melting point than pure LiH and which evolves hydrogen gas at the anode (*anodic oxidation*):

$$2\,H^- \longrightarrow H_2 + 2\,e^-$$

This reaction is analogous to the generation of chlorine in the electrolysis of molten NaCl (Section 13.5.1).

Hydride anions react with proton donors instantaneously to elemental hydrogen:

$$H^+ + H^- \longrightarrow H_2$$

Therefore, salt-like hydrides are vigorously decomposed by water and acids. Calcium hydride is most easily handled as it is least reactive. It is used as a *drying agent* for inert organic solvents such as ethers and hydrocarbons. The insoluble side product $Ca[OH]_2$ can simply be filtered off.

Ternary compounds MHX are formed when CaH_2, SrH_2 or BaH_2 are fused with their respective metal halides MX_2 in a hydrogen atmosphere:

$$CaH_2 + CaCl_2 \longrightarrow 2\,CaHCl$$

These halido hydrides crystallize in the tetragonal system. The larger their anion, the deeper the color of the salt due to polarization of anions by cations: while CaHCl is colorless, crystals of BaHI are black.

The formation of salt-like hydrides with the anion H^- suggests that hydrogen should be considered as a halogen homologue and listed atop Group 17 of the Periodic Table. Thermodynamic considerations, however, indicate the purely formal character of these analogies. The enthalpy of the reaction

$$\frac{1}{2}X_2(g.) \longrightarrow X(g.) \xrightarrow{+e^-} X^-(g.)$$

to convert hydrogen or a halogen to the corresponding anion is given by:

$$\Delta H^\circ_{298} = \frac{1}{2}D\,(X_2) - E_{ea}(X)$$

From the dissociation energies D (Table 4.1) and the electron affinities E_{ea} (Figure 2.2), the reaction enthalpies ΔH°_{298} are obtained as follows:

X_2:	H_2	F_2	Cl_2	Br_2	I_2
ΔH°_{298}:	+151	−193	−126	− 155	−167 kJ mol^{-1}

Hydride formation, in contrast to halides, is endothermic owing to the large dissociation energy of the H_2 molecule and the small electron affinity of the hydrogen atom. Thus, only the most electropositive metals with smallest ionization energies are able to form salt-like hydrides; otherwise, the lattice energies of the salts (Chapter 2.1) would not compensate the energies for the endothermic evaporation and ionization of the metal.

Salt-like hydrides are used as *hydrogenation and reducing agents* and to prepare other hydrides. Lithium aluminum hydride or lithium tetrahydrido alanate $Li[AlH_4]$ is most important. It is prepared by hydrogenation of $AlCl_3$ or $AlBr_3$ with LiH:

$$4\,LiH + AlX_3 \longrightarrow Li[AlH_4] + 3\,LiX \qquad X=Cl, Br$$

$Li[AlH_4]$ (m.p. 150 °C) is a colorless, water-sensitive compound, which dissolves in dry ether as dietherate $Li[AlH_4] \cdot 2R_2O$. This solution is used to convert halides such as $BeCl_2$, BCl_3, $SiCl_4$, Si_2Cl_6 and $AsCl_3$ into the corresponding binary hydrides, for example:

$$2\ Si_2Cl_6 + 3\ Li[AlH_4] \longrightarrow 2\ Si_2H_6 + 3\ LiCl + 3\ AlCl_3$$

Lithium aluminum hydride contains the tetrahedral anion $[AlH_4]^-$ which is isoelectronic with silane SiH_4 and the phosphonium cation $[PH_4]^+$. With larger cations, higher coordination numbers of aluminum are possible as in $Ba[AlH_5]$ and $K_3[AlH_6]$.

Salt-like hydrides are also used to prepare transition metal hydrido complexes. For example, finely divided platinum metal reacts with KH in an atmosphere of hydrogen at 580–775 K depending on the pressure to $K_2[PtH_4]$ (at 0.1–1 MPa) or to $K_2[PtH_6]$ (at 1.5–1.8 GPa):[77]

$$2\ KH + Pt + \frac{x}{2}\ H_2 \longrightarrow K_2[PtH_{2+x}]$$

In these remarkable reactions, elemental hydrogen formally oxidizes platinum to the oxidation states +2 or +4, respectively. The planar anion $[PtH_4]^{2-}$ is of D_{4h} symmetry while $[PtH_6]^{2-}$ is of octahedral symmetry. The hydrido ferrate(II) complex $Mg_2[FeH_6]$ is particularly noteworthy for showing the highest known *hydrogen storage* volume efficiency (150 g H_2 L^{-1}) of all materials.

The hydride ^{6}LiD is used as thermonuclear fuel for the fusion reaction in *hydrogen bombs*.[78] By addition of some LiT, the following extremely exothermic nuclear reactions are triggered if the ignition temperature of 10^8 K is reached by a preceding nuclear fission. At this temperature, all atoms exist as ions forming a *plasma* (1 MeV = $96.485 \cdot 10^6$ kJ mol^{-1}):

$$^6Li + n \longrightarrow T + {}^4He + 4.8\ MeV$$

$$D + T \longrightarrow {}^4He + n + 17.6\ MeV$$

The fusion of deuterium and tritium nuclei is also expected to take place in the fusion reactor ITER, which is presently under construction in Cadarache (Southern France).[79] The liberated energy of 17.6 eV is released as kinetic energy of both the α particles (20%; heating the plasma) and the neutrons (80%; heating the walls of the reactor). These fast neutrons can in principle be used to generate more tritium from ^{7}Li (natural abundance 92.5%):

$$^7Li + n \longrightarrow T + {}^4He + n$$

---

77 W. Bronger, G. Auffermann, *Angew. Chem. Int. Ed.* **1994**, *33*, 1112.

78 The first hydrogen bomb was tested by the USA on 1 November 1952 on the Enewetak Atoll of the Marshall Islands.

79 ITER: International thermonuclear experimental reactor; see J. Ache, *Angew. Chem. Int. Ed.* **1989**, *28*, 1–20.

The slow neutrons released in this reaction will be used to split ^{7}Li (present as a blanket in the walls of the reactor) into He and T ("breeding" of T which is returned to the plasma). In the end, natural lithium and deuterium are turned into the extraordinarily stable helium atom. There are enough deuterium and lithium reserves on Earth to have this process running for hundreds if not thousands of years. However, the necessary fusion temperature is $2 \cdot 10^{8}$ K! Consequently, enormous technical problems need to be overcome. Many countries take part in this ambitious 15 billion Euro project, which is supposed to ignite its first plasma in 2025, to reach full performance in 2030 (delivering 10 times more energy than it uses) and to permanently produce electric energy by the year 2050.

In stars (including the Sun), the fusion reaction $4\ p \rightarrow 2\ \alpha + 2\ e^{+}$ or $4\ H^{+} \rightarrow {}^{4}He^{2+} + 2\ e^{+}$ (*hydrogen burning*) takes place at $1.5 \cdot 10^{7}$ K and a density of 100 g cm^{-3} with the liberation of an energy of 26 MeV. In addition, two electron neutrinos and two γ photons are emitted per α particle; $^{2}H^{+}$ as well as $^{3}He^{2+}$ are intermediates in this stepwise process.[80] Only after 99.99% of the hydrogen atoms originally formed in the "Big Bang" have been consumed, the fusion of α particles (*helium burning*) to carbon and oxygen nuclei starts, which requires a temperature of 10^{8} K at a density of 10^{3} g cm^{-3}. In the Sun, the mass ratio H:He in the photosphere is about 2.63, while heavier elements account for less than 2 wt%. In the atmosphere of the Earth, hydrogen and helium are rare (see Section 14.2) despite the permanent new supply because they escape to the space due to their low weight and the relatively low gravity of our planet as compared to the giant gas planet Jupiter, for example.

5.7.5 Metal- and Alloy-Like Hydrides (Insertion Hydrides)

Many transition metals react reversibly with molecular hydrogen to form nonstoichiometric hydrides, the composition of which depends on temperature and hydrogen pressure:

$$M + \frac{x}{2} H_2 \rightleftharpoons MH_x$$

The hydrogen content increases with decreasing temperature and increasing pressure. Suitable metals are Mg, Ti, Nb, Fe, U, Pd and Pt. The products are usually dark-colored powders, which retain metallic properties to some extent such as *electrical conductivity* and *paramagnetism*. In many cases, the hydrogen content is continuously variable, but stoichiometric or near-stoichiometric compositions are sometimes obtained, for example in TiH_2 and UH_3. Compounds of this type can be used as *hydrogen storage materials* as the molecular hydrogen can easily be recovered by heating

80 M. Binnewies, H. Willner, J. Woenckhaus, *Chem. unserer Zeit* **2015**, *49*, 164.

and lowering the pressure.[81] The uptake of H_2 by metals is exothermic in case of Ti, Zr, V, Nb, Ta, Pd and the alloy FeTi, but endothermic for Mg, Cr, Mo, Fe, Co, Ni, Pt, Cu, Ag and Au. There is always a considerable loss of entropy during absorption of H_2. Unfortunately, the reaction of H_2 with common metals can lead to *embrittlement of materials*, for example, steel pipelines and high-pressure reactors, due to the hydrogenation of the dissolved carbon (e.g., as cementite, Fe_3C) to methane.

The uptake of hydrogen by metallic palladium, which is an important mechanistic step of hydrogenation catalysis, is shown in Figure 5.12. Palladium at 25 °C and a hydrogen pressure of 1 bar absorbs 0.6 mol H per mol of metal ($PdH_{0.6}$). The maximum hydrogen content is obtained at −78 °C with the composition $PdH_{0.83}$ and an enthalpy of formation of −40 kJ $mol^{-1.}$ This hydride crystallizes in the cubic system with a defect NaCl structure.

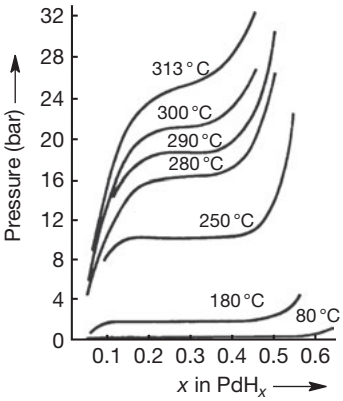

Figure 5.12: Isotherms of the dissociation pressure of the palladium–hydrogen system (1 bar = 0.1 MPa).

The distance between the layers of palladium atoms (lattice planes) increases considerably during hydrogen uptake, from 389 pm for the composition $PdH_{0.03}$ (α-phase) to 401.8 pm for $PdH_{0.6}$ (β-phase).[82] Simultaneously, the magnetic susceptibility χ of metallic palladium decreases linearly with increasing hydrogen content and disappears completely in the diamagnetic phase $PdH_{0.65}$. This effect is ascribed to the lattice expansion upon hydrogen absorption.

The paramagnetism of elemental palladium indicates that some of its 10 valence electrons occupy the conduction band, leaving holes in the valence band. The gap between these bands is apparently small but increases with the distance between the palladium atoms since orbital overlap is diminished, and an increasing

81 M. Sterner, J. Stadler, *Energiespeicher*, Springer, Berlin, **2012**. L. M. Kustov et al., *Mendeleev Commun.* **2014**, *24*, 1–8.

82 M. P. Pitt, E. MacA. Gray, *Europhys. Lett.* **2003**, *64*, 344.

proportion of electrons occupies the lower energy valence band until diamagnetic behavior is reached once all valence electrons are transferred.

Removal of hydrogen from $PdH_{0.65}$ in vacuo yields β-Pd in which the expanded crystal structure and the diamagnetism are preserved. At high temperatures, hydrides of palladium form only under high pressure (see Figure 5.12). At red heat, however, hydrogen diffuses unimpeded through a palladium foil, a phenomenon that can be utilized for hydrogen purification.

5.7.5.1 Bonding of Hydrogen in Alloy-Like Hydrides

When H_2 molecules approach the surface of a transition metal such as Ni or Pd, physisorption occurs through weak dispersion forces (Chapter 3). The molecular orbitals of H_2 then interact with the electronic band system of the metal. Bevor chemisorption of isolated H atoms can occur; an energy barrier must be overcome to achieve dissociation. For most transition metals, however, this barrier is small. While the $1\sigma_g$ MO of H_2 is well below the bottom of most metal *d* band orbitals, the $1\sigma_u$ level is above the FERMI energy of the metal (highest occupied level; E_F). This $1\sigma_u$ MO mixes with metal orbitals of the same symmetry resulting in novel bonding and antibonding MOs. Electron density is then delocalized into the σ* MO of H_2, thus weakening the HH bond and eventually leading to dissociation. Metals with partly occupied *d* bands can accept the 1*s* electron of the hydrogen atoms in which case the chemisorption is exothermic. Therefore, the electropositive metals are the most reactive toward hydrogen, namely the members of Groups 3–5 of the Periodic Table, as well as lanthanides and actinides. The same holds for intermetallic compounds such as $LaNi_5$, ZrV_2, $CeNi_3$, TiFe and Mg_2Ni.

There is experimental evidence that the hydrogen atoms occupy interlattice positions of an expanded metal structure, forming a quasi-alloy. Therefore, the name *insertion hydrides*. For instance, niobium metal crystallizes as a cubic body-centered structure which is known for its high capacity for hydrogen insertion. The hydrogen atoms occupy some of the six tetrahedral sites per metal atom (Figure 5.13). For electrostatic reasons, however, it is impossible to occupy all positions of this type. Since the hydrogen electrons are delocalized into the conduction band orbitals of the metal structure, the interstitial positions are formally occupied by protons, which repel each other. This model explains the high mobility of hydrogen in metals. For example, the diffusion coefficient of hydrogen in niobium at 25 °C is 10^{-5} cm^2 s^{-1}, which means that a metal sheet of 1 mm is penetrated by hydrogen gas in 100 s.

According to neutron diffraction studies, some stoichiometric polynuclear hydrido complexes of transition metals also show coordination numbers up to 6 for some of the hydrogen atoms. Most remarkable is the cluster-like yttrium compound $(Cp'Y)_4H_8$ [$Cp' = C_5Me_4(SiMe_3)$] with a hydrogen atom at the center of a tetrahedron of

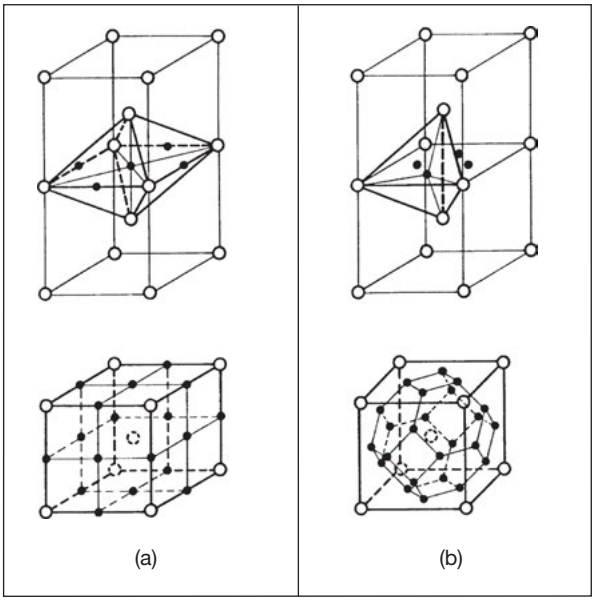

Figure 5.13: Possible interstitial positions for hydrogen atoms in the cubic body-centered crystal structure of a metal (open circles indicate metal atoms, full circles hydrogen atoms). (a) octahedral sites; (b) tetrahedral sites. In the lower diagrams all possible interstitial positions are shown.

four metal atoms, which are bridged by one three-coordinate and six two-coordinate hydrogen atoms.[83]

The alloy FeTi is utilized commercially as a *hydrogen storage material*.[84] Its characteristic properties are a relatively low density but high capacity for hydrogen dissolution with formation of $FeTiH_2$, a small exothermic reaction enthalpy, a low dissociation pressure of H_2 at 25 °C and its low costs. By gentle heating of the hydride, very pure hydrogen gas is liberated. Other hydrogen storage materials are the alloys $LaNi_5$ and $LaMg_2Ni$, although they are too heavy for application in cars.[85] Therefore, other light-weight materials such as graphene and carbon nanotubes,[86] MOFs[87] as

83 R. Bau et al., *J. Am. Chem. Soc.* **2008**, *130*, 3888 and references cited therein.
84 L. Schlapbach, *Top. Appl. Phys.* **1988**, *63*, 1 and **1992**, *67*, 1.
85 The very quiet electrically powered German submarines of classes 212A and 214 use SIEMENS fuel cells for power generation and a Ti-Zr-V-Mn-Fe alloy (*Hydralloy C*) for hydrogen storage; this material is kept in steel cylinders of 5 m length and 50 cm diameter and serves also as necessary ballast. The molecular oxygen is stored on board in liquid form (LOX).
86 V. Tozzini, V. Pellegrini, *Phys. Chem. Chem. Phys.* **2013**, *15*, 80.
87 L. J. Murray, M. Dinca, J. R. Long, *Chem. Soc. Rev.* **2009**, *38*, 1294 and *Angew. Chem. Int. Ed.* **2008**, *47*, 6766–6779.

well as hydrides of boron and magnesium are under investigation for reversible hydrogen storage. At present, however, hydrogen-powered cars, busses and regional trains store H_2 as a compressed gas at pressures up to 70 MPa (700 bar) in lightweight composite cylinders,[88] but the costs for compression of hydrogen to >100 bar are problematic. Nevertheless, Japan is developing a large-scale transportation, power production and heating technology based on molecular hydrogen and fuel cells (F cells) with high energy efficiency. The main concerns in this context are supply and storage of H_2 as well as safety issues. After all, hydrogen–air mixtures are explosive at 300 K and ambient pressure of 0.1 MPa with wide explosive limits at H_2 concentrations of 5 and 75 vol%.

88 U. Eberle, M. Felderhoff, F. Schüth, *Angew. Chem. Int. Ed.* **2009**, *48*, 6608–6630.

6 Boron

6.1 Introduction

Boron is the first element and the only nonmetal in Group 13 of the Periodic Table. The chemistry of boron[1] is unique and particularly fascinating in the sense that it is distinguished not only from its heavier homologues Al, Ga, In and Tl, but also from all other nonmetals. Similarities exist to some extent to *silicon (diagonal relationship* in the Periodic Table), but the pronounced preference of boron atoms to engage in cage-like structures of high stability is not encountered in any other nonmetal.

Although it is a rather rare component of the Earth's crust (ca. 0.001%), huge deposits of boron in enriched form are known, albeit exclusively in the form of oxo species such as borates. The most important *boron minerals* for mining are *borax* $Na_2[B_4O_5(OH)_4]\cdot 8H_2O$, *kernite* $Na_2[B_4O_6(OH)_2]\cdot 3H_2O$ and *colemanite* $Ca[B_3O_4(OH)_3]\cdot H_2O$. The countries with the largest production are Turkey, the USA (California) and Argentina. Traces of boron are encountered in natural waters. The oceans contain approximately 4.6 mg L^{-1} as boric acid $B(OH)_3$. Boron is an essential element for plants, animals and human beings, although the borate concentration in organisms is typically very low. For instance, human blood contains only about 0.01–0.17 mg(B) L^{-1}, while red wine boasts concentrations of up to 10 mg(B) L^{-1} in the form of boric acid.

Natural boron consists of two isotopes, ^{10}B (19.9%) and ^{11}B (80.1%).[2] The more abundant isotope ^{11}B is commercially available in isotopically enriched compounds for use in NMR spectroscopy. Despite its quadrupole moment (I = 3/2) and the resulting line broadening, ^{11}B is a popular NMR probe due to its rapid relaxation and consequently short acquisition times. The higher nuclear spin of ^{10}B (I = 3) with the resulting higher quadrupole moment, its lower sensitivity and lower natural abundance account for a less wide application for NMR purposes. Both isotopes give rise to coupling to other NMR active nuclei, for example, in the ^1H-NMR spectra of BH species. In general, NMR spectroscopy is the by far the most important technique for the structure elucidation of boron–hydrogen compounds.[3]

The numerous uses of boron and its compounds are discussed in the individual chapters.

1 D. M. Schubert, R. J. Brotherton, *Encycl. Inorg. Chem.* **2005**, *1*, 499. Topical Issue Boron Chemistry in *Inorg. Chim. Acta* **1999**, *289*, Issues 1–2. W. Siebert (ed.), *Advances in Boron Chemistry*, Royal Society, **1997**. J. F. Liebman, A. Greenberg, R. E. Williams (eds.), *Advances in Boron and the Boranes*, VCH, Weinheim, **1988**.

2 The isotopic ratio $^{11}B/^{10}B$ varies depending on the provenance of the minerals between roughly 3.92 and 4.14, corresponding to an ^{11}B content between 79.7 and 80.6%.

3 S. Hermánek, *Inorg. Chim. Acta* **1999**, *289*, 20.

https://doi.org/10.1515/9783110578065-007

6.2 Bonding Situation

6.2.1 LEWIS Acidity and Adduct Formation

The boron atom in the ground state has a valence electron configuration of $2s^2p^1$; in covalent species, it can therefore adopt all formal oxidation states between 0 and +3. Numerous compounds of BX_3 type exist, in which boron adopts a trigonal planar coordination, for example, BF_3, BCl_3, BMe_3 and $B(OH)_3$. This geometry follows from the VSEPR model (Section 2.2.2) and is confirmed by MO calculations as the energetically most favorable. The bonding situation in BF_3 was discussed earlier (Section 2.4.8). In trigonal-planar coordination environments, the p_z orbital of the central atom remains formally empty as in BH_3 and BMe_3. This orbital of relatively low energy is typically the LUMO and is thus available for coordinative binding of LEWIS bases. As a consequence, neutral species of the BX_3 type are LEWIS acids of often considerable strength.[4] Substituted silanes of the SiX_4 type similarly react as LEWIS acids – albeit in most cases are much weaker. The relative acidities of the LEWIS acids BX_3 can be determined through the enthalpy change ΔG^o during the reaction with a suitable LEWIS base. These measurements are carried out with bases such as Me_3N or pyridine. The higher the GIBBS energy ΔG^o of the reaction, the more stable is the acid–base pair and – per definition – the higher the *acidity* of BX_3:

$$Me_3N + BX_3 \rightleftharpoons Me_3\overset{\oplus}{N}-\overset{\ominus}{B}X_3$$

From such measurements the following order of acceptor strengths has been deduced:

$$BH_3 > BI_3 \approx BBr_3 > BCl_3 > BF_3 > BH_2Me > BHMe_2 > BMe_3$$

It should be noted though that the above sequence depends to some extent on the LEWIS base. Similarly, the acidity in the gas phase may be quite different from that in solution. Nonetheless, the above order is surprising insofar as that one might expect the highest acidity for BF_3. Due to the large electronegativity difference ($\Delta\chi_P$ = 2.1), this molecule contains extremely polar BF bonds that result in a highly positive partial charge at the boron atom and an increased acceptor strength.[5] On the other hand, the fluorine atoms have nonbonding electron pairs in $2p_\pi$ orbitals with the same symmetry as the vacant $2p_\pi$ orbital at boron (Figures 2.32 and 2.33). The overlap

4 The boron center in the yellow salt $K_2[B(CN)_3]$ is formally in the oxidation state +1 and thus behaves as a nucleophile; the anion is D_{3h} symmetric: E. Bernhardt, H. Willner, *Angew. Chem. Int Ed.* **2011**, *50*, 12085.

5 The reason for the covalent structure of BF_3 (in contrast to the ionic homologue AlF_3) is the extremely high ionization energy to form the cation B^{3+} (71.4 eV), which cannot be compensated by the sum of electron affinities of the three F atoms (together 10.2 eV) and the lattice energy of the hypothetical salt $B^{3+}3F^-$.

of these orbitals results in a four-center π bond, which is delocalized over the entire molecule and thereby reduces the partial charges on all atoms to some extent. Nonetheless, quantum-chemical calculations exhibit atomic charges of +1.41*e* at the boron center and −0.47*e* at each fluorine atom.[6] Due to the π bond the LUMO of the BF_3 molecule is higher in energy than in molecules such as BH_3 and BMe_3 and consequently BF_3 is a worse acceptor (the LUMO is the π* MO; compare Chapters 2.4.8 and 2.5). When BF_3 is combined with NH_3 to give the adduct $H_3N–BF_3$, the charge at boron is reduced to +1.26*e*, whereas the N atom's charge is lowered from −1.06*e* in the free NH_3 molecule to −0.91*e* in the adduct.[7]

For BCl_3, this intramolecular π backdonation is even slightly stronger than for BF_3. Due to this and the smaller difference in electronegativities, the charge at the boron atom amounts to just +0.28*e*. Because of the lower energy of the LUMO, however, the LEWIS acidity of BCl_3 is slightly larger than that of BF_3. Some perfluorinated trialkyl- and triphenylboranes are even stronger LEWIS acids that – just like BH_3 – form relatively stable adducts even with CO.[8]

Upon adduct formation with an amine a significant charge transfer occurs from the donor to the boron halide. The resulting coordinative σ bond increases in strength with the *charge capacity* of the acceptor to which the electron density is transferred. The *charge capacity* κ was defined by POLITZER as the reciprocal difference between ionization energy and electron affinity: $\kappa = 1/(E_i - E_{ea})$; see also Section 4.6.3. The experimentally determined electron affinities of BF_3, BCl_3 and BBr_3 increase in this sequence. Apparently, the larger the molecule, the more easily an additional electron can be accommodated. This contributes to the strength of the interaction of an amine with the boron halide, which increases from BF_3 via BCl_3 to BBr_3.

In case of BH_3, which is formed by dissociation of diborane(6) B_2H_6, π backdonation cannot occur. Therefore, the p_π AO at boron remains vacant and consequently BH_3 is the strongest LEWIS acid of the BX_3 type toward amines and phosphanes.[9] On the other hand, the lower acidity of alkyl-substituted boranes BR_3 can be attributed to steric hindrance of the reaction with the amine by the organic groups. With increasing size of the substituents at boron, the acceptor strength is diminished drastically.

The π backdonation in compounds of type BX_3 not only strengthens the BX bonds, but also leads to a considerable *barrier of rotation* about these bonds, for example, in alkoxy boranes $R_2B–OR$. For such molecules, the energetically most favorable conformation is achieved at a torsional angle of 0° at the B–O bond.

6 G. Frenking et al., *J. Am. Chem. Soc.* **1997**, *119*, 6648, and *Inorg. Chem.* **2003**, *42*, 7990.
7 D. Lentz et al., *J. Phys. Chem. A* **2010**, *114*, 10185.
8 H. Willner et al., *J. Am. Chem. Soc.* **2002**, *124*, 15385.
9 F. Bessac, G. Frenking, *Inorg. Chem.* **2006**, *45*, 6956. Towards fluoride, BH_3 is a weaker acid than the trihalides: I. Krossing et al., *Angew. Chem. Int. Ed.* **2003**, *42*, 1531.

Consequently, the $B(OH)_3$ molecule is perfectly planar; even the H atoms reside in the same plane (Figure 6.11). Due to similar π backdonation, the planar form of $H_2B–NH_2$ with a torsion angle of $\tau = 0°$ is by 136 kJ mol^{-1} more stable than the twisted form with $\tau = 90°$. In notable contrast to the isoelectronic twisted ethylene (a diradical with triplet ground state), the twisted form of $H_2B–NH_2$ is a closed shell species with a nonbonding electron pair at the nitrogen center. The twisting also changes the partial atomic charges at boron from +0.42*e* with $\tau = 0°$ to + 0.67*e* at $\tau = 90°$.

If a LEWIS acid BX_3 reacts intermolecularly with a LEWIS base, a coordinative or dative σ bond is formed. Concomitantly, the symmetry of the environment at the boron atom changes from (approximately) D_{3h} to (approximately) C_{3v}. Only if the four ligand atoms in the resulting complex are identical (as in $[BF_4]^-$), an ion of T_d symmetry is obtained. Nonequivalence of the substituents implies more or less pronounced deviations from tetrahedral symmetry. The energy required for the deformation of the LEWIS acid counteracts the adduct formation and is thus a decisive factor for its acidity.[10]

In summary, the following (to some extent interrelated) factors determine the *acidity of boranes* of type BX_3 toward a given LEWIS base:

a) The amount of positive partial charge at the boron atom
b) The charge capacity of the borane
c) The steric hindrance by the substituents X
d) The deformation energy of BX_3
e) The π backdonation by lone pairs at the substituents
f) The LUMO energy of BX_3

Depending on the ligands, the resulting adducts can be neutral or carry a negative or positive charge as the following examples illustrate (py = pyridine):[11]

$$[BH_4]^- \quad [Me_3NBH_3] \quad [py_2BH_2]^+ \quad [py_4B]^{3+}$$

Most compounds of type BX_3 are sensitive to hydrolysis to orthoboric acid. BBr_3 and BCl_3 react violently with water; BF_3, by contrast, much more slowly:

$$BX_3 + 3\,H_2O \longrightarrow B(OH)_3 + 3\,HX$$

$$X = F, Cl, I, Me, OMe, NMe_2, H(B_2H_6)$$

Conversely, the tetrahedral anions $[BX_4]^-$ are remarkably inert toward water. In that, they resemble the isoelectronic carbon halides CX_4. For instance, $Na[BF_4]$ dissolves in water without decomposition, $K[BH_4]$ can be stored in humid air at 25 °C

10 This deformation energy is larger for BF_3 than for BCl_3 and in case of the borane–amine complexes of the same order of magnitude as the dissociation energies: M. Yánez et al., *Chem. Eur. J.* **2010**, *16*, 11897.

11 Regarding the di- and trications compare A. L. Cowley et al., *Dalton Trans.* **2008**, 6421.

and the complex $Cl_3B{\leftarrow}NMe_3$ is even stable in boiling water! This shows that the hydrolysis of BX_3 species occurs via initial tetrahedral adducts with the H_2O molecule, which can only be formed from the BX_4 species through dissociation of one of the ligands as all valence orbitals at the boron atom are occupied.

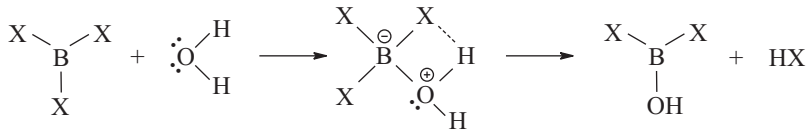

In case of BF_3 the intermediate of hydrolysis, $BF_3{\cdot}OH_2$, can even by isolated. The aminolysis of boron trihalides with secondary amines follows a similar mechanism. The intermediate products $BX_3{\cdot}NHR_2$, BX_2NR_2 and $BX(NR_2)_2$ are isolable on the way to the final product $B(NR_2)_3$.

6.2.2 Coordination Numbers and Multiple Bonds

The boron atom differs from the other nonmetals of the second row inasmuch as it has more valence orbitals than valence electrons. Nonetheless, boron can adopt all coordination numbers from 1 to 8 in its compounds. The following compounds serve as examples of this remarkable coordinative flexibility:

1	2	3	4	5 6 7 8
BF	HOBO	BF_3	$[BF_4]^-$	crystalline elemental boron, boranes, carboranes

The compounds of monovalent boron are called *borylenes*. The most prominent representative of these highly reactive species is the monofluoride BF, which is treated further in Section 13.4.6 as a subvalent species of the nonmetals. Borylenes are characterized by a nonbonding σ pair of electrons as well as by two vacant $2p_\pi$ AOs at the boron atom. Phenylborylene PhB can be generated at low temperatures by photolysis of the bis(azide) $PhB(N_3)_2$. Otherwise, borylenes are predominantly known as ligands in transition metal complexes.[12]

In sharp contrast to carbon and silicon, boron does rarely engage in two-center homonuclear single bonds; most reported cases comprise the >B–B< unit. A prominent example is B_2Cl_4, which is known since 1925 (Section 6.8.2).[13] More extended

12 C. A. Anderson, H. Braunschweig, R. D. Dewhurst, *Organometallics* **2008**, *27*, 6381.
13 Review: H. Braunschweig, R. D. Dewhurst, *Angew. Chem. Int Ed.* **2013**, *52*, 3574.

homoatomic chains and larger rings with electron-precise BB bonds are almost completely absent.[14] The anions of metal borides may contain chains, rings, ladders, layers and clusters, but even in these cases multicenter bonding is prevalent (Section 6.4.1). In elemental boron, in all boranes with more than two boron atoms (see, e.g., B_8F_{12}, Section 13.4.6), in carboranes and various other boron clusters, BB multicenter bonding is the key to structure and stability almost without exception.

Unlike carbon, nitrogen and oxygen atoms, the boron atom shows little inclination to engage in double bonds, although in more recent times species with such bonds are being prepared in increasing numbers. Terminal B=O bonds are only encountered in high temperature gas phase molecules such as H–O–B=O. Even sterically protected iminoboranes RB=NR oligomerize at 20 °C more or less rapidly. Ionic species such as $K_3[BN_2]$, $K_3[BP_2]$ and $K_3[BAs_2]$ are more stable; they contain the following anions of $D_{\infty h}$ symmetry, which are isolelectronic with CO_2, CS_2 and CSe_2, respectively:

$$[N{=}B{=}N]^{3-} \quad [P{=}B{=}P]^{3-} \quad [As{=}B{=}As]^{3-}$$

Covalent species with classical BB *double and triple bonds*, however, did not become accessible until recently.[13,15] An early example is the adduct L(H)B=B(H)L, in which two *N*-heterocyclic carbenes L act as neutral electron donors to the central diborene(2) moiety (Dip: 2,6-diisopropylphenyl):

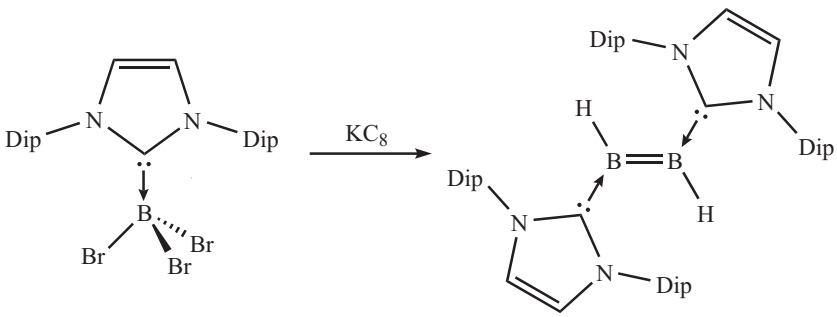

Adduct formation causes distortion of the otherwise linear arrangement of the diborene(2) to a *trans*-bent geometry.[16] Typical BB double bonds show lengths between 155 and 159 pm. The first stable species with BB triple bond was obtained by

14 An exception is *cyclo*-$B_6(NEt_2)_6$, which is formed on heating of the *hypercloso* isomer to 200 °C: A. Berndt et al., *Eur. J. Inorg. Chem.* **2009**, 5577.

15 Y. Wang, G. H. Robinson, *Chem. Commun.* **2009**, 5201.

16 This deformation also causes the lifting of the degeneracy of the acetylene-like frontier orbitals of diborene(2) changing the ground state from triplet to singlet.

dehalogenation of the corresponding brominated precursor in 2012 and structurally characterized (d_{BB} = 145 pm).[13] Despite the sterically demanding carbene ligands, the BB moiety is highly reactive and readily adds chalcogens or even relatively unreactive molecules such as CO:[13,17]

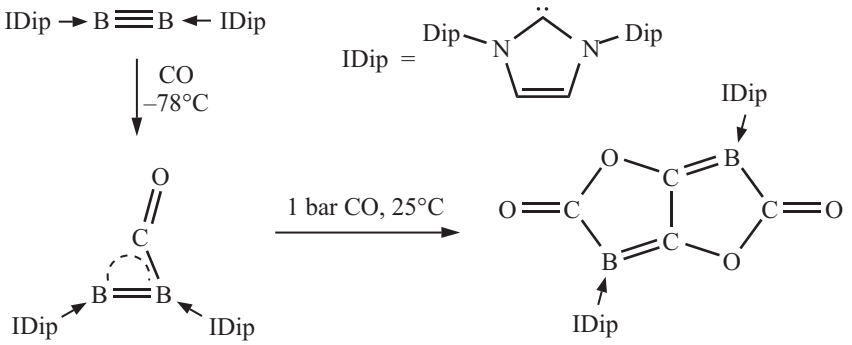

As expected on the basis of the VSEPR model, the central CBBC moiety is linear.

6.2.3 Similarities and Differences to Other Non-Metals

Because of the low electronegativity of the boron atom (2.0 on the ALLRED–ROCHOW scale) the bonds B–F, B–O, B–Cl and B–N are strongly polar and thus very stable (see Table 4.1).[18] The BH bond is also slightly polarized toward hydrogen, which carries a partial negative charge. Therefore, the reactivity of boranes resembles that of silanes ($H^{\delta-}$) more than that of alkanes. For instance, boranes are generally sensitive to hydrolysis and some ignite spontaneously when exposed to air. Their structures, however, are completely different from those of other nonmetal hydrides.

The negative partial charge at the H atoms of boranes leads to interesting effects. For example, in the solid ammonia–borane adduct $H_3B{\cdot}NH_3$ negatively and positively polarized H atoms of adjacent molecules occur in spatial proximity giving rise to weak intermolecular *dihydrogen bonds* of length d_{HH} = 202 pm (about double the VAN DER WAALS radius of hydrogen).[19] This interaction readily explains why the compound eliminates H_2 on heating. In solution, the H_2 elimination indeed occurs with second-order kinetics suggesting a bimolecular mechanism (Section 6.10). Even shorter dihydrogen bonds with d_{HH} = 177–195 pm are present in the dihydrate of sodium borohydride, $Na[BH_4]{\cdot}2H_2O$.

17 H. Braunschweig et al., *Angew. Chem. Int. Ed.* **2015**, *54*, 10271.
18 D. J. Grant, D. A. Dixon, *J. Phys. Chem. A* **2009**, *113*, 777.
19 C. A. Morrison, M. M. Siddick, *Angew. Chem. Int. Ed.* **2004**, *43*, 4780.

The closest similarities between boron and other nonmetals are those to silicon: just like the silanes, the boranes are molecular entities, and they are highly volatile and display a manifold of structures. The chlorides BCl_3 and $SiCl_4$ are both monomeric and sensitive to water. The most important oxide of boron is B_2O_3, which like SiO_2, but unlike CO_2, NO_2 and Cl_2O, forms a polymeric 3D network. B_2O_3 reacts with metal oxides and hydroxides to borates. As in the oxide itself, the borates contain the thermally and chemically very resistant BOB bridges, which are akin to the SiOSi bridges in silicates and similarly stabilized by π backdonation and strong polarity:

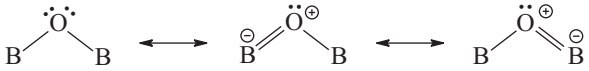

In contrast to silicic acid and carbonic acid,[20] a number of different boric acids can readily be isolated in pure, crystalline form.

6.3 Elemental Boron

Elemental boron crystallizes in about 16 modifications, some of which are only stable due to lattice defects or traces of impurities, while others just exist at high pressures or as metastable phases. A few pure boron phases have been characterized by X-ray diffraction. These consist of 3D infinite arrangements of boron atoms, with different structural subunits to the unit cell (Table 6.1). β-Rhombohedral boron is probably the stable modification at ambient pressure and crystallizes from the melt under these conditions. α-Rhombohedral and β-tetragonal boron are high-temperature and high-pressure modifications, although the energy differences to the β-rhombohedral form are very small according to quantum-chemical calculations. The reported α-tetragonal boron (T-50) had long been regarded as a boron-rich compound containing small amounts of carbon and sometimes nitrogen atoms intermittently, but – according to more recent work – is to be considered a metastable phase of pure boron with 50 atoms in the unit cell. Occasionally, β-tetragonal boron is put in doubt as a pure boron phase.[21a] Frequently, elemental boron is obtained as an amorphous solid of unknown structure.

20 Pure carbonic acid can only be isolated at cryogenic temperatures: T. Loerting et al., *J. Am. Chem. Soc.* **2013**, *135*, 7732; P. Schreiner et al., *Angew. Chem. Int. Ed.* **2014**, *53*, 11766.

21 a) B. Albert, H. Hillebrecht, *Angew. Chem. Int. Ed.* **2009**, *48*, 8640. b) T. Ogitsu, E. Schwegler, G. Galli, *Chem. Rev.* **2013**, *113*, 3425.

Table 6.1: Some modifications of elemental boron.

Name	Space group	Atoms per unit cell	Structures in unit cell
α-Rhombohedral boron	$R\bar{3}m$	12	One B_{12} icosahedron
β-Rhombohedral boron	$R\bar{3}m$	320[a]	B_{84}, B_{10} and B_1 units
β-Tetragonal boron (T-192)	$P4_1$ or 4_3	192[a]	B_{12} and other units

[a]Atoms in the unit cell. Note, however, that some positions are only partially occupied.

6.3.1 Preparation of Elemental Boron

Given the strong BO bonds in borates and in the oxide B_2O_3, the production of elemental boron is difficult and costly. For this reason, boron is only produced on a small scale commercially (about 100 t/a), predominantly by reduction of B_2O_3 with magnesium in an inert argon atmosphere. The product is washed with hydrochloric acid to remove the MgO. This process affords an amorphous product of limited purity (ca. 95%), which does also contain some MgB_2. Boron of higher purity is obtained by reduction of gaseous BCl_3 with H_2. On the laboratory scale, highly pure boron can be obtained by reaction of BBr_3 with H_2 or by pyrolysis of BI_3 or B_2H_6, provided the starting materials have been purified accordingly.

Upon pyrolysis of BI_3 at a hot tantalum wire (800–1100 °C) crystals of α-rhombohedral boron are formed, in particular if the employed BI_3 is very pure. B_2H_6 decomposes to boron and hydrogen already at 600–800 °C.

The reduction of BBr_3 (or BCl_3) by H_2 is conducted at 800–1600 °C on a hot substrate (*chemical vapor deposition*, CVD):

$$2\,BBr_3 + 3\,H_2 \rightleftharpoons 2\,B_{s.} + 6\,HBr$$

Wires of tantalum and tungsten are suitable substrates for boron deposition. Depending on the temperature and other reaction conditions, amorphous α-rhombohedral or β-rhombohedral boron is obtained. The latter crystallizes from a boron melt as well (m.p. about 2450 °C), for example, during the purification of boron by zone melting in vacuum. The boron wires growing on tungsten wires by CVD are employed industrially for the mechanical strengthening of plastic and metal (Al, Ti) components due to their extremely high strength and rigidity, resulting in *composite materials* for airplanes, space flight and sports equipment such as golf clubs, tennis rackets or fishing rods.

Depending on the modification, boron forms dark-red, brown or black shiny crystals that are extremely hard (harder than corundum Al_2O_3, lighter than aluminum, stronger than steel). The hardness of β-rhombohedral boron is 9.3 (according to

MOHS). Boron is a semiconductor in all of its modifications with bandgaps for α- and β-rhombohedral boron ranging from 1.6 to 2.0 eV.

The different allotropes of boron are monotropic and their relationship in the phase diagram is largely unclear, as all interconversions are kinetically hampered due to the unusually complicated structures. According to recent theoretical investigations, however, β-rhombohedral boron is the most stable phase up to the melting point (about 2450 °C).[21b] At high temperatures, boron is extraordinarily corrosive as it forms *borides* with many metals and thus acts as a strong reducing agent toward oxides, even such as CO or SiO_2! It is therefore very difficult to produce crystalline boron of high purity.[22] In contrast, boron is rather inert at low temperatures; it is neither attacked by hydrofluoric nor by hydrochloric acid, but is oxidized by hot strongly oxidizing acids such as nitric acid or its mixture with hydrochloric acid (*aqua regia*). Upon melting with alkali hydroxides, the corresponding borates are obtained with concomitant evolution of H_2.

6.3.2 Solid-State Structures of Elemental Boron

The simplest structure of all boron modifications belongs to α-*rhombohedral boron* (α-B; density 2.46 g cm^{-3}).[21] The unit cell contains just 12 atoms. These form a regular icosahedron (Figure 6.1) with 20 equilateral triangles constituting the surface.

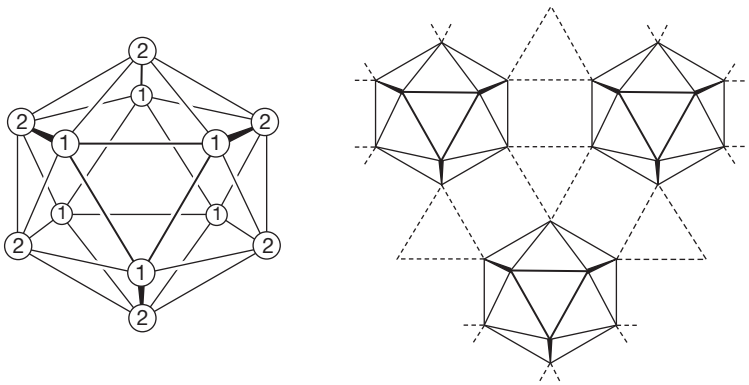

Figure 6.1: Structure of α-rhombohedral boron, consisting of B_{12} icosahedra (left). The connectivity of the B_{12} units is shown on the right-hand side. The atoms marked with "1" are six-coordinate, those with "2" seven-coordinate.

22 Due to the difficulties of producing high-purity boron, inconsistent values for melting points or other physical properties are found in the literature.

All vertices of an icosahedron are equivalent by symmetry. Each atom inside an icosahedral arrangement constitutes the apex of a pentagonal pyramid with its five nearest neighbors as the base. In a sense, the icosahedron is formed from two such pyramids that turn toward each other with their bases, but not as mirror images of one another, instead rather twisted by 36°. Each boron atom thus resides on a fivefold rotational axis of symmetry (C_5).

The shortest internuclear distances in the B_{12} icosahedron amounts to 177 pm on average. In α-boron these icosahedra are connected in the following manner: six of the 12 vertices (marked with "1" in Figure 6.1) are connected to an additional boron atom of one of six neighboring icosahedra at a distance of 170 pm. Each of these adjacent icosahedra is thus situated precisely on the C_5 axis of the original B_{12} unit. The six boron atoms designated as "2" have two additional contacts to vertices of two individual icosahedra, thus forming an equilateral triangle of 200 pm edge length with the atom in question. Around 50% of all atoms therefore exhibit a coordination number of seven, the other half is six-coordinate. In this manner, a face-centered cubic packing of icosahedra is obtained; the interior of the icosahedra forms an empty space. When heated to temperatures above 1000 °C, α-boron transforms irreversibly into β-boron via several intermediate phases.[21]

The structure of β-*rhombohedral boron* is much more complicated and can be described in various manners.[21] The hexagonal unit cell contains 320 atoms. The structure consists of icosahedral B_{12} units, which are surrounded by 12 B_6 units in such a way that a nearly spherical B_{84} building block results ("super-icosahedron"). These B_{84} units constitute a face-centered cubic packing, which are connected through the interstitial positions by single atoms and B_{10} units. Since the positions of the single atoms are only partially filled, the total number of atoms per unit cell is somewhat uncertain. The majority of atoms have a coordination number of six. The density amounts to 2.33 g cm^{-3}.

At a pressure of 20 GPa and a temperature of 2000 K, β-boron is transformed into a phase referred to as either γ-boron or γ-B_{28}, which consists of a face-centered cubic packing of B_{12} icosahedra with B_2 dumbbells in the octahedral interstitial spaces. γ-B_{28} occupies a significant part of the phase diagram and is metastable at normal pressure.[23] Finally, β-tetragonal boron (Table 6.1) is generated from BBr_3 and H_2 at 1500 K. It equally consists of B_{12} units but is cross-linked in a complicated manner with numerous defects inasmuch as certain positions of the unit cell are only partially occupied. In addition, it is still controversial whether some of these defects are not rather stabilized by the presence of either carbon or nitrogen heteroatoms.

23 A. R. Oganov et al., *Nature* **2009**, *457*, 863. U. Häussermann, A. S. Mikhaylushkin, *Inorg. Chem.* **2010**, *49*, 11270. J. Qin et al., *Phys. Rev. B* **2012**, 85, 014107.

6.3.3 Bonding in Elemental Boron

In crystalline modifications of boron, the coordination numbers are between four and eight. Given that boron only has three valence electrons at its disposal, all atoms necessarily engage in multicenter bonding. This bonding type has been discussed in detail for other compounds (Section 2.4). The number of bonding partners is not so much limited by the degree of orbital overlap, but rather by steric requirements. The orbital overlap thus follows as shown in Figure 6.2 in an exemplary manner: In case (a) the 2*p* atomic orbitals of three symmetrically arranged boron atoms overlap to give an equilateral triangle (symmetry D_{3h}), resulting in one bonding and two degenerate antibonding orbitals. Two electrons are sufficient for a stable bond since any additional electron would have to reside in a destabilizing antibonding orbital. In the less symmetrical case (b) one 2*p* orbital of the central atom overlaps with one orbital each of the two adjacent atoms (symmetry C_{2v}) resulting in one bonding, one nonbonding and one antibonding MO. Although in this case as well, two electrons suffice to form a stable bond, additional electrons occupy the nonbonding orbital and therefore do not weaken the bond as in (a). Case (a) is referred to as a closed three-center two-electron bond, while (b) is called an open three-center two-electron bond.

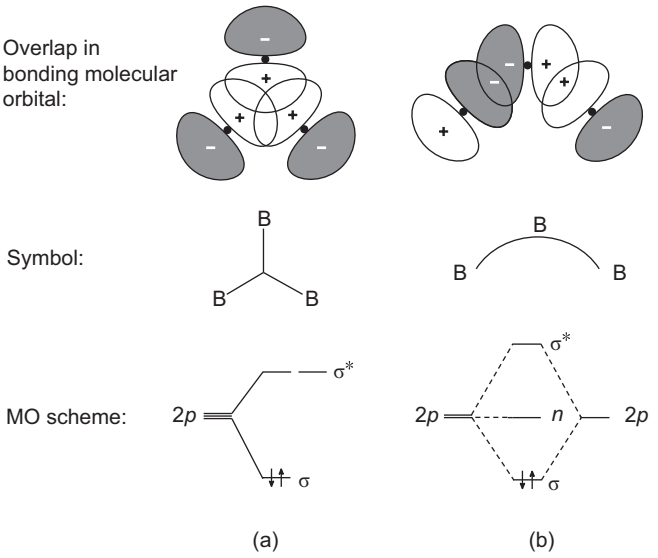

Figure 6.2: Two types of three-center two-electron bonds as occurring in boranes, carboranes and elemental boron. (a) Closed three-center two-electron bond (symmetry D_{3h}). (b) Open three-center two-electron bond (symmetry C_{2v}).

These two bonding types are also found in the higher boranes as well as in α-rhombohedral boron between the icosahedra. For the B_{12} building blocks

themselves, however, multicenter bonding of higher order has to be assumed in order to satisfyingly account for the high stability of the icosahedral motif. Each atom has four atomic orbitals, one of which needs to be retained for bonds to the outside of the icosahedron. Therefore, three orbitals are left for bonding inside the B_{12} scaffold. An MO analysis thus needs to consider 36 atomic orbitals in the icosahedron; the resulting MO diagram is shown in Figure 6.3. Apparently, 13 bonding and 23 more or less antibonding orbitals are obtained by linear combination of the atomic orbitals. This means that 26 valence electrons are necessary to attain the maximum stability of the icosahedron. Of the 36 electrons of the 12 boron atoms in total, 10 are left for so-called exohedral bonds to the exterior of the polyhedron.

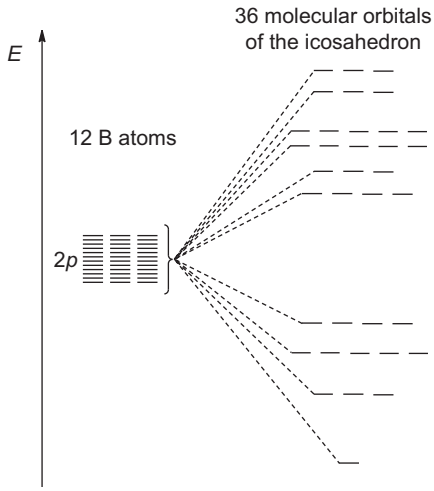

Figure 6.3: Energy level diagram for the molecular orbitals of a B_{12} icosahedron (symmetry I_h). At each boron atom three atomic orbitals have been considered for the bonding in the icosahedron; the fourth AO is reserved for bonds to the exterior. The result is 13 bonding MOs of variable symmetries.

This result corresponds exactly to experimental findings. For instance, the hypothetical borane $B_{12}H_{12}$ is unknown, because the 10 electrons available for exohedral bonds are insufficient to sustain 12 electron-precise two-center two-electron bonds to the terminal H atoms. In contrast, the very stable dianion $[B_{12}H_{12}]^{2-}$ with two additional electrons is well known and consists of a B_{12} icosahedron, in which each boron atom is bonded to one hydrogen atom.

Accordingly, only half of the bonds between the icosahedra of α-rhombohedral boron can consist of two-center two-electron bonds. For this purpose, six electrons per cluster are required (the bonds originate from the atoms designated as “1” in Figure 6.1). The remaining four electrons allow for the formation of six closed three-center bonds to two neighboring icosahedra (two three-center bonds per participating cluster).

6.4 Borides and Boron Carbides

6.4.1 Borides

Many metals, but also C, Si, Ge, N, P, As, O, S and Se, form binary species with elemental boron upon heating.[21a,24] In case of metals, their composition varies between M_5B and MB_{100}. Table 6.2 provides an overview about binary compounds of boron with selected main-group elements.

Table 6.2: Binary compounds of boron with selected main-group elements.

LiB_{1-x}	BeB_3	$B_{13}C_2$	BN	B_2O_3
Li_2B_6	BeB_{15}	$B_{50}C_2$	$B_{13}N_2$	B_6O
Li_3B_{14}	MgB_2	SiB_{36}	$B_{50}N_2$	B_2S_3
LiB_{10}	MgB_7	SiB_6	B_6P	B_8S_{16}
Na_2B_{29}	Mg_5B_{44}	SiB_3		$B_{12}S$
Na_3B_{20}	MgB_{12}	GeB_{90}	BAs	$B_{13}Se$
	$MgB_{17.9}$		B_6As	
	CaB_6			
	SrB_6			
	BaB_6			

Some of these borides find application as extremely hard, chemically inert and fireproof materials with varying degrees of electrical conductivity ranging from semiconductivity to metallic conductivity and even superconductivity (e.g., MgB_2 below 39 K). The production on a larger scale starts with B_2O_3, the corresponding metal oxide and an electropositive oxophilic metal such as Mg or Al; these components are reacted at temperatures of up to 2000 °C, for example:

$$CaO + 3\,B_2O_3 + 10\,Mg \longrightarrow CaB_6 + 10\,MgO$$

On a smaller scale and for the preparation of high purity borides, the corresponding elements are directly reacted, if needed under participation of a metal melt as a reaction medium. The simultaneous reduction of a metal halide and a boron halide with hydrogen at 1000–1400 °C is suitable for the production of pure borides, for instance, by CVD:

$$TiCl_4 + 2\,BCl_3 + 5\,H_2 \longrightarrow TiB_2 + 10\,HCl$$

24 T. Lundström, *Encycl. Inorg. Chem.* **2005**, *1*, 481.

While in metal-rich borides single interstitial boride ions are surrounded by between six and eight metal atoms, higher boron contents increasingly lead to the formation of BB bonds, which results in a broad variety of structural motifs: B_2 pairs, fragments of B_n chains, infinite single, double or triple chains ("ladders"), branched chains, layers and finally 3D networks of B_n clusters (such as icosahedra) with interstitial metal atoms (Figure 6.4).

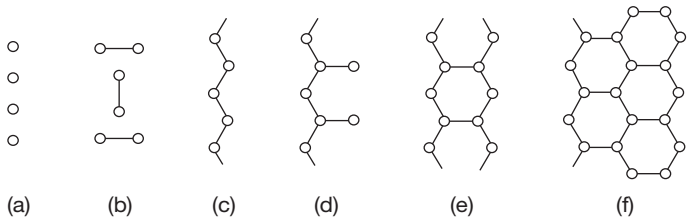

Figure 6.4: Structural motifs in metal borides. (a) Isolated boron atoms as in $Nb_2Fe_{14}B$; (b) B_2 dumbbells as in Cr_5B_3; (c) zig-zag chains as in FeB; (d) branched chain as in $Rb_{11}B_8$; (e) double chain or ladder as in Ta_3B_4 and (f) triple chain as in V_2B_3.

The hexagonal structure of the superconducting MgB_2 is particularly noteworthy. It consists of planar layers of fused B_6 rings in analogy to the layer-structure of graphite. The Mg^{2+} ions are intercalated between the layers in such a manner that the cations reside above and below the center of each B_6 ring. The resulting intercalated boron layers formally consist of B^- anions and are therefore isoelectronic to the graphene layers of graphite. MgB_2 is therefore similar to ionic graphite compounds (Section 7.4.2). The hexaborides MB_6 (M = Ca, Sr, Ba), on the other hand, consist of three-dimensionally corner-linked $[B_6]^{2-}$ octahedrons with intercalated M^{2+} cations.

Due to the high melting points (e.g., TiB_2: 3500 K) some metal borides are employed as *high-temperature materials* as some of them are inert toward air and metal melts even at temperatures above 1200 °C. TiB_2, for instance, is used for jacket pipes of thermocouples and the construction of containers for molten metals such as aluminum. CaB_6, on the other hand, serves as deoxygenating agent for copper melts, as boron is hardly soluble at all in copper. Ferroboron, an alloy of iron and boron, hardens steel. Several ternary metal borides find also applications, for example, Mo_2FeB_2, which is a representative of the so-called *cermets* (*ceramic metal*). The ternary alloy $AlMgB_{14}$ is almost as hard as diamond and thus suitable for cutting tools. Numerous amorphous multinary phases with boron show glass-like behavior at ambient temperatures and are therefore referred to as *bulk metallic glasses*. In many cases they show superior hardness and form stability to comparable crystalline metals.[25]

25 A. Inoue, *Engineering* **2015**, *1*, 185.

6.4.2 Boron Carbides

Boron carbide B_4C is an inexpensive, extremely hard, but light-weight material.[26] Due to its extraordinary mechanical properties, it is employed, for example, in bullet-proof body armor, and as abrasive or for cutting discs. By a large margin, it is the most important boron-rich boride. As the ^{10}B isotope has a large neutron capture cross section, B_4C rods are utilized for the regulation of the nuclear chain reaction in nuclear reactors by neutron absorption. For the same reasons, borax mineral is dissolved in the emergency cooling water to interrupt the chain reaction if necessary. Thermal (slow) neutrons react with ^{10}B under emission of an α particle to give stable ^{7}Li. This strongly exothermic nuclear reaction (2.4 MeV) is also used for the treatment of brain tumors: a ^{10}B-enriched nontoxic and water-soluble compound needs to accumulate as selectively as possible in the affected tissue prior to neutron irradiation. The tumor cells are then killed by the high kinetic energy of the generated Li atoms and the α radiation. Healthy tissue is much less affected as elements such as H, C, N, O, P and S only have neutron capture cross sections, which are smaller than that of ^{10}B by several orders of magnitude.[27]

Industrially, boron carbide is produced on a ton-scale in an electric arc furnace by reduction of liquid boron oxide with coke at 1400–2300 °C:

$$2\ B_2O_3\ +\ 7\ C_{s.}\ \longrightarrow\ B_4C\ +\ 6\ CO \qquad \Delta H^{\circ}_{298} = 1812\ \text{kJ mol}^{-1}$$

Boron carbide (m.p. 2470 °C) is chemically stable up to 600 °C and resists oxidation by air up to 1000 °C due to a protective layer of B_2O_3. At higher temperatures B_4C burns with a bright green flame, for example, in pyrotechnical mixtures. Boron carbide can be sintered into molds without additives at very high temperatures (2200–2250 °C) and various pressures. In this way, armor plates, mortars, sand blasting nozzles and so on are manufactured. The composition of boron carbide can vary within wide limits (C content 10–20 atom%), which is why the empirical formulae $B_{12}C_3$ or $B_{13}C_2$ are often encountered. The structure is based on α-rhombohedral boron. The phase $B_{12+x}C_{3-x}$, for instance, consists of B_{12} icosahedra that are connected either directly or through interstitial boron or carbon atoms. At higher carbon contents (such as B_4C) $B_{11}C$ icosahedra are present.

Structurally related to boron carbide, the silicide SiB_3 consists of a network of B_{12} icosahedra and Si_2 units and represents an air-stable high-temperature semiconductor. The hardest boride is B_6O, which is a frequent impurity in elemental boron

26 A. W. Weimer (ed.), *Carbide, Nitride and Boride Materials – Synthesis and Processing*, Chapman&Hall, London, **1997**.

27 D. Gabel, *Chemie unserer Zeit* **1997**, *31*, 235. M. F. Hawthorne, A. Maderna, *Chem. Rev.* **1999**, *99*, 3421. I. B. Sivaev, V. V. Bregadze, *Eur. J. Inorg. Chem.* **2009**, 1433.

and borides, probably due to boron's oxophilicity. The structure once again consists of B_{12} icosahedra, connected by interstitial oxygen atoms.

6.5 Boranes and Hydroborates

6.5.1 Introduction

Boron and hydrogen form numerous binary compounds of often unusual compositions that do not show any analogies to the hydrides of other nonmetals.[28] Most of the so-called *boranes* belong to either of two generic groups with the following empirical formulae:

$\mathbf{B}_n\mathbf{H}_{n+4}$: B_2H_6, B_4H_8, B_5H_9, B_6H_{10}, B_8H_{12}, $B_{10}H_{14}$, $B_{12}H_{16}$, $B_{14}H_{18}$, $B_{16}H_{20}$, $B_{18}H_{22}$*

$\mathbf{B}_n\mathbf{H}_{n+6}$: B_4H_{10}, B_5H_{11}, B_6H_{12}, B_9H_{15}*, $B_{10}H_{16}$, $B_{13}H_{19}$, $B_{14}H_{20}$

The species with an asterisk exist as two different isomers. Besides many other stable boranes have been reported (e.g., B_8H_{18}, $B_{15}H_{23}$, $B_{20}H_{16}$ and $B_{20}H_{26}$), as well as several unstable compounds. Notably, the simplest borane, BH_3, also belongs to the latter and thus only occurs as a transient intermediate. The by far most important boron hydride is *diborane* B_2H_6. Many boranes are highly toxic and highly flammable or even pyrophoric (they self-ignite on exposure to air). While the more volatile boranes form explosive mixtures with air or neat oxygen, others are air-stable solids. All boranes are endothermic species and their combustion to B_2O_3 and H_2O is therefore extraordinarily exothermic:

$$B_2H_6 + 3\,O_2 \longrightarrow B_2O_3 + 3\,H_2O \qquad \Delta H^\circ_{298} = -2138\ \text{kJ mol}^{-1}$$

The *nomenclature* of boranes will be illustrated by the following examples:

BH_3: (mono)borane(3) B_2H_6: diborane(6) B_4H_{10}: tetraborane(10)

A Greek prefix indicates the number of boron atoms and is followed by the root word, "borane." The number in brackets after the root denotes the number of hydrogen atoms or other residues (such as alkyl groups).

Hydroborates or *boranates*, also referred to as borohydrides, are salt-like compounds with B and H containing anions. The simplest of such anions is the tetrahydroborate $[BH_4]^-$ (*boranate anion*), which serves as starting material for the industrial scale production of diborane(6) and monoborane adducts. In addition,

28 N. S. Hosmane, J. A. Maguire, *Encycl. Inorg. Chem.* **2005**, *1*, 494; N. N. Geenwood, in H. W. Roesky (ed.), *Rings, Clusters and Polymers of Main Group and Transition Elements*, Elsevier, Amsterdam, **1989**, p. 49.

numerous larger anions exist, some of which feature complicated structures (Section 6.5.4).

6.5.2 Diborane(6)

B_2H_6 is a colorless gas (b.p. –92.5 °C), which can readily be prepared in the laboratory by treatment of boron halides of type BX_3 with hydride sources such as:

$$4\,BCl_3 + 3\,Li[AlH_4] \xrightarrow{Et_2O} 2\,B_2H_6\uparrow + 3\,LiCl + 3\,AlCl_3$$

$$4\,BF_3 + 3\,Na[BH_4] \xrightarrow[Et_2O]{25°C} 2\,B_2H_6\uparrow + 3\,Na[BF_4]$$

Under suitable conditions, LiH and NaH can also be employed. A convenient method is the decomposition of boranate with concentrate phosphoric acid (85%):

$$2\,Li[BH_4] + H_3PO_4 \longrightarrow B_2H_6 + 2\,H_2 + Li_2[HPO_4]$$

On an industrial scale, diborane(6) is produced by catalytic gas phase hydrogenation of BCl_3 with H_2 at 450 °C or by reaction of BF_3 with $Na[BH_4]$ in diglyme (see above equation).[29] In all these reactions, not the anticipated monoborane BH_3 is obtained, but rather its dimer B_2H_6. Both species, however, are related by a dynamic equilibrium:

$$B_2H_6 \rightleftharpoons 2\,BH_3$$

The corresponding dissociation enthalpy of B_2H_6 amounts to 172 kJ mol^{-1}, that is, the equilibrium at 25 °C is completely on the side of the dimer. The reason for this dimerization is the extremely strong LEWIS acidity of the BH_3 molecule, which – in the absence of suitable donors – reacts with itself in such a way that each boron atom formally acquires an octet of electrons. This is made possible through the formation of two three-center two-electron BHB bonds. The following molecular structure of gaseous B_2H_6 results:

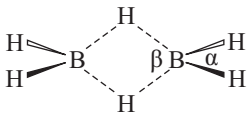

$\alpha_{HBH} = 121.7°$ $\quad d_{BH} = 119$ pm (terminal)

$\beta_{HBH} = 96.4°$ $\quad d_{BH} = 133$ pm (bridge)

$\gamma_{BHB} = 83.6°$ $\quad d_{BB} = 176$ pm

Although both boron atoms are coordinated in a distorted tetrahedral manner by four H atoms, there is a considerable bonding interaction between them as evidenced by

29 diglyme = bis(2-methoxyethyl)ether, $MeOC_2H_4OC_2H_4OMe$.

d_{BB} = 176 pm, which corresponds to the distance of boron nuclei in the icosahedra of elemental boron. The molecular symmetry is D_{2h}. According to quantum-chemical calculations the valence orbitals of the boron atoms are sp^2 hybridized.[30] Considering the smaller BH distance, the bonds to the terminal hydrogen atoms are regarded as two-center two-electron bonds between the sp^2 hybrids at boron and the 1*s* AOs of hydrogen. At each boron atom, two orbitals remain for the BHB bridges: (a) the sp^2 hybrids pointing toward each other along the BB bond account for σ interaction with the two 1s AOs of the bridging H atoms and (b) the orthogonal 2*p* orbitals overlap in π manner with the antibonding combination of the 1*s* orbitals of the H atoms (Figure 6.5).[31]

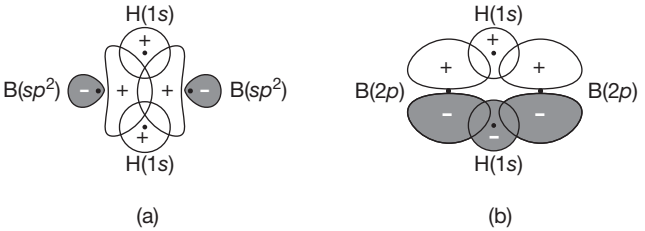

Figure 6.5: Overlap of the atomic orbitals to two molecular orbitals that roughly correspond to the notion of two three-center two-electron BHB bonds in diborane(6). (a) The sp^2 hybrid orbitals of the two boron atoms pointing toward each other are combined with the in-phase pair of the hydrogens' 1*s* orbitals. (b) The 2*p* orbitals orthogonal to the BB bond overlap with the out-of-phase pair of the 1*s* AOs of the hydrogen atoms. The terminal hydrogen atoms are omitted.

The resulting molecular orbitals are filled with the two remaining electrons of the boron atoms and the two electrons from the bridging hydrogens.[32] As additional electrons would have to occupy antibonding MOs, they should weaken the BB bond. Diborane(6) therefore cannot really be regarded as an *electron-deficient* molecule. While the atomic charges at the bridging hydrogen atoms are close to zero, the boron atoms carry approximately one positive charge (+1.20*e*) and the terminal H atoms about half a negative charge each (−0.62*e*).[30]

Treatment of B_2H_6 with strong LEWIS bases (or donors D) can cleave the two bridging bonds leading to *borane adducts* ($D{\cdot}BH_3$):

$$B_2H_6 + 2\,D \longrightarrow 2\,D{-}BH_3$$

$$D = CO, NR_3, PH_3, PF_3, PR_3, Me_2S$$

30 F. Wang, W. Pang, M. Huang, *J. Electron Spectr. Rel. Phenom.* **2006**, *151*, 215.

31 M. M. Balakrishnarajan, R. Hoffmann, *J. Am. Chem. Soc.* **2004**, *126*, 13119.

32 The interaction between the boron atoms is often neglected for simplicity, but the observation of bent BHB bridges such as the one in the $[B_2H_7]^-$ anion supports the importance of this interaction.

Examples: Borane carbonyl $H_3B{\cdot}CO$ is formed from diborane(6) and carbon monoxide in an equilibrium reaction and can be stabilized by a CO atmosphere. By reaction of $H_3B{\cdot}PH_3$ with $Li[BH_4]$ or B_2H_6/BuLi the salt $Li_3[P(BH_3)_4]$ has been produced, which can formally be regarded as four BH_3 molecules coordinated by one phosphide anion P^{3-}. The stable BH_3 adducts with R_3N, R_2NH and RNH_2 as well as with dimethyl sulfide Me_2S are commercially available. For example, borane–amine adducts are prepared from the amine hydrochlorides and boranates at 20–40 °C:

$$Na[BH_4] + [R_2NH_2]Cl \longrightarrow H_3B^{\ominus}-N^{\oplus}R_2H + NaCl + H_2$$

The liquid $H_3B{\cdot}SMe_2$ serves as selective reducing agent and for hydroboration reactions in organic chemistry (Section 6.6). The dimethyl sulfide (Me_2S) can easily be replaced by stronger LEWIS bases such as amines.

6.5.3 Higher Boranes

The higher boranes are colorless species of strongly variable thermal stability. Some are sensitive to hydrolysis and oxidation, often even pyrophoric in air, while others can be stored indefinitely at room temperature under air. For example, *iso*-B_9H_{15} is unstable even at −30 °C, while $B_{20}H_{16}$ is a solid that melts at 197 °C. B_4H_{10} is a gas at room temperature (b.p. 16 °C); the other boranes are liquids or even solids. The toxicity and the high price of these compounds prevented commercial applications of the higher boranes, although there have been large-scale attempts by the military to employ pentaborane(9) as rocket or jet propellant. The less toxic *closo*-hydroborate salts as well as the related carboranes, however, are subject to intense studies in the context of the above-mentioned cancer therapy by neutron capture (Section 6.4.2) and related medicinal applications.[33]

6.5.3.1 Preparation

The following methods are suitable for the synthesis of higher boranes. The resulting product mixtures are typically separated by fractioning distillation or condensation at reduced pressure or by preparative gas chromatography.

(a) Thermolysis of B_2H_6 or other boranes under precisely defined conditions:

$$2\,B_2H_6 \xrightarrow{120°C} B_4H_{10} + H_2$$

$$5\,B_2H_6 \xrightarrow{200–240°C} 2\,B_5H_9 + 6\,H_2$$

$$2\,\textit{iso}\text{-}B_9H_{15} \xrightarrow{>-30°C} B_8H_{12} + B_{10}H_{14} + 2\,H_2$$

33 I. B. Sivaev, V. V. Bregadze, *Eur. J. Inorg. Chem.* **2009**, 1433.

(b) LEWIS base catalyzed transformations:

$$4\,B_4H_{10} \xrightarrow{Me_3N} 3\,B_2H_6 + 2\,B_5H_9 + 2\,H_2$$
$$B_5H_{11} \xrightarrow{(CH_2)_6N_4} B_9H_{15}$$

(c) Acid treatment of magnesium boride Mg_3B_2 resulting in complex mixtures mainly composed of not only B_2H_6, but also B_4H_{10}, B_5H_9, B_5H_{11}, B_6H_{10} and $B_{10}H_{14}$.[34]

(d) Hydrogen cleavage through electrical discharge:

$$2\,B_5H_9 \longrightarrow B_{10}H_{16} + H_2$$
$$2\,B_{10}H_{14} \longrightarrow B_{20}H_{16} + 6\,H_2$$

(e) Protonation of hydroborate anions with the following rearrangement:

$$K[B_9H_{15}] + HCl \xrightarrow{-80°C} B_9H_{15} + KCl + \tfrac{1}{2}H_2$$
$$[B_{20}H_{18}]^{2-} \xrightarrow{+H^+(aq)} n\text{-}B_{18}H_{22} \text{ and } iso\text{-}B_{18}H_{22}$$

The processes (a) and (b) are by far the most universally applicable. During the thermolysis of B_2H_6 very short-lived BH_3 occurs as reactive intermediate, which combines with B_2H_6 to give the unstable B_3H_9. Spontaneous hydrogen evolution results in B_3H_7, which adds a further equivalent of BH_3 to give B_4H_{10}.

6.5.3.2 Structures

For his accomplishments regarding the elucidation of the diverse structures of boranes, WILLIAM N. LIPSCOMB was awarded the NOBEL prize in chemistry in 1976. With increasing number of boron atoms more complicated motifs arise, which are, however, occasionally simplified by high symmetry. They can be constructed from the following structural elements:

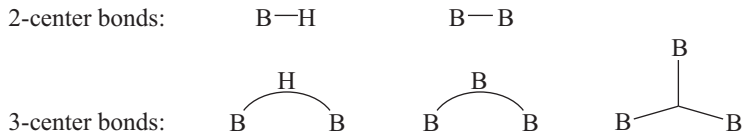

34 This reaction was employed by ALFRED STOCK and coworkers during the years of 1909–1916 for the synthesis of the first boranes (B_4H_{10}, B_2H_6 and $B_{10}H_{14}$). The numerous groundbreaking contributions of STOCK (1876–1946), mainly regarding laboratory instrumentation and fundamental chemistry of the elements boron and silicon, prompted the German Chemical Society (GDCh) in 1950 to establish the ALFRED-STOCK-Memorial Prize, which is to this day one of the most important awards for inorganic chemistry worldwide.

In Figure 6.6 the structures of B_4H_{10}, B_5H_9, B_6H_{10} and $B_{10}H_{14}$ are shown as examples. For the first three of these molecules, additional topological formulae are given using the above symbols for the different bonding modes. Besides these cluster-like species, the so-called macropolyhedral boranes are known: they typically consist of two or more B_xH_y clusters, connected by a BB bond (e.g., $B_{20}H_{26}$).

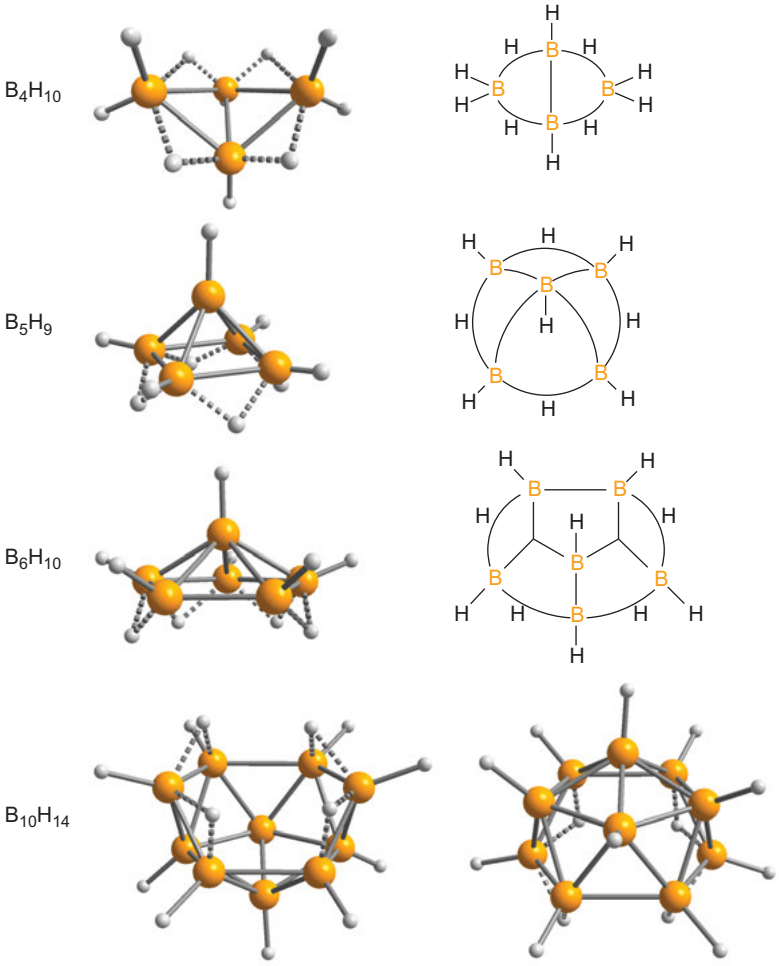

Figure 6.6: Geometry and topological formulae of boranes B_4H_{10} (C_{2v}), B_5H_9 (C_{4v}) and B_6H_{10} (C_{5v}), as well as two views of decaborane(14) $B_{10}H_{14}$. In the latter molecule, each boron atom carries a terminal hydrogen; in addition there are four bridging H atoms.

Numerous *substitution products* are derived from the higher boranes through replacement of terminal H atoms by monovalent residues (halogen atoms, organyl groups). The substructures of the B_n scaffolds of the boranes and hydroborate

anions are classified as *closo*, *nido*, *arachno* and *hypho* clusters, depending on whether they have a cage-like (*closo*), nest-like (*nido*, open on one side), spider web-like (*arachno*, open on two sides) or net-like (*hypho*, open on three sides) structures. $B_{20}H_{16}$ is a *closo*-borane of D_{2d} symmetry. The hydrides of the general formula B_nH_{n+4} such as B_5H_9, B_6H_{10} and $B_{10}H_{14}$ are *nido* clusters (Figure 6.6), whereas compounds of the formula B_nH_{n+6} exhibit *arachno* structures. An example is B_4H_{10} of C_{2v} symmetry, in which the boron atoms are hexacoordinate. Which structure such a cluster adopts strongly correlates to the number of valence electrons available for cluster bonding (*skeletal electrons*).

In order to determine that number, simple rules devised by K. WADE et al. and D. MINGOS are available. These rules are derived from MO considerations, similar to those in Section 6.3.3 regarding the number of bonding electrons in an icosahedron. It can be shown by group theory that a polyhedron of n vertices will always accommodate $(n + 1)$ electron pairs for cluster bonding ($2n + 2$ electrons). Therefore, any additional electron pair has to occupy an antibonding MO, adversely affecting the cluster's integrity. As a result, cluster bonds will be broken to show progressively more open faces. Each prefix thus corresponds to a defined number of skeletal electrons: $2n + 2$ (*closo*), $2n + 4$ (*nido*), $2n + 6$ (*arachno*) and $2n + 8$ (*hypho*).[35] As the open faces of the cluster can be closed by capping with a virtual additional atom, the structures of the *nido*-, *arachno*- and *hypho*-boranes are derived from a hypothetical polyhedron with one, two or three additional vertices, respectively. Unrelated to the above rules, certain higher boron hydrides are referred to as *conjuncto*-boranes to account for the fact that their structures can be derived by the formal assembly of smaller borane units.

6.5.4 Hydroborates

Of all hydroborates the aforementioned boranate anion $[BH_4]^-$ is by far the most important. This anion is isoelectronic with CH_4 and $[NH_4]^+$ and thus of T_d symmetry. It can be obtained by simple reaction of B_2H_6 with hydride anions in diethylether in analogy to the related donor–acceptor interaction with LEWIS bases:

$$B_2H_6 + 2\,MH \xrightarrow{Et_2O} 2\,M[BH_4] \qquad M = Li, Na, K$$

35 The number of skeletal electron available for cluster bonding can be calculated as follows: (1) each vertex contributes its valence electrons minus 2 (for exohedral bonding or nonbonding electron pairs); (2) each radical residue attached to the cluster brings in one electron, while each coordinating base adds both the electrons of its donated lone pair and (3) the charge of the cluster has to be considered by addition of its value for anions and subtraction for cations.

The technical syntheses of these three salts are based on the reaction with readily available inexpensive boron–oxygen precursors. The SCHLESINGER process (commonly used in the US) employs the methyl ester of boric acid (trimethylborate) in the reaction with excess sodium hydride at 260 °C:

$$B(OMe)_3 + 4\,NaH \longrightarrow Na[BH_4] + 3\,NaOMe$$

The hydrolysis of the reaction mixture affords methanol, which is distilled off and recycled, while NaOH is extracted with isopropylamine. The aqueous phase yields solid $Na[BH_4]$ after evaporation to dryness.

The *borosilicate process*, developed by the BAYER AG, proceeds according to the following equation:

$$Na_2[B_4O_7]\cdot 7SiO_2 + 16\,Na + 8\,H_2 \xrightarrow{400–500°C} 4\,Na[BH_4] + 7\,Na_2[SiO_3]$$

The borosilicate glass used as starting material is obtained from a melt of quartz and borax and is finely ground after cooling. After the reaction, $Na[BH_4]$ is extracted from the mixture with liquid NH_3 under pressure. By treatment of $Na[BH_4]$ with LiCl, $Li[BH_4]$ is obtained, which is more soluble in organic solvents; with KOH the thermally more robust $K[BH_4]$ is prepared. All three boranates serve as reducing agents.

While B_2H_6 is extremely sensitive toward O_2 and H_2O, sodium boranate $Na[BH_4]$ can be kept in dry air and $K[BH_4]$ even in humid air without decomposition. All alkali boranates are salts and thus readily dissolve in water. $Li[BH_4]$ can also be dissolved in tetrahydrofuran (THF) as solvated ions. In contrast, the aluminum boranate $Al(BH_4)_3$, accessible from $AlCl_3$ and $Ca[BH_4]_2$, is a covalent species with AlHB multicenter bonding and as such a relatively volatile liquid at 25 °C. The Al atom is octahedrally coordinated by H atoms in this compound.

$Na[BH_4]$ is an effective hydride transferring reagent. With B_2H_6 it reacts depending on the conditions to various different hydroborates:

$$2\,Na[BH_4] + B_2H_6 \xrightarrow{0°C} 2\,Na[B_2H_7]$$

$$Na[BH_4] + B_2H_6 \xrightarrow[0.2\ MPa]{25–35°C} Na[B_3H_8] + H_2$$

$$2\,Na[BH_4] + 5\,B_2H_6 \xrightarrow[Et_3N]{180°C} Na_2[B_{12}H_{12}] + 13\,H_2$$

The following syntheses are more selective and thus simpler:

$$3\,Na[BH_4] + I_2 \longrightarrow Na[B_3H_8] + 2\,NaI + 2\,H_2$$

$$5\,Na[B_3H_8] \longrightarrow Na_2[B_{12}H_{12}] + 3\,Na[BH_4] + 8\,H_2$$

In more recent times, perfluorinated alkyl borates $[B(R^F)_4]^-$ have been used successfully as weakly coordinating anions during the synthesis of novel species with strongly electrophilic cations.

The higher hydroborates show the same structural elements as boranes. An unambiguous *nomenclature* of these anions with charges varying between −1 and −4 is achieved as follows:

$$[B_2H_7]^-\text{: heptahydrodiborate}(1-), C_s \text{ symmetry}$$

$$[B_6H_6]^{2-}\text{: hexahydro-}\textit{closo}\text{-hexaborate}(2-), O_h \text{ symmetry}$$

The observation that the BHB bridge in the anion $[H_3B{-}H{-}BH_3]^-$ is bent supports the presence of a bond, albeit weak, between the boron atoms (Section 6.5.2). Of the plethora of hydroborates with more than one boron center, those of the general formula $[(BH)_n]^{2-}$ (n = 6–12) are particularly interesting as they show polyhedral *closo* structures in accordance with the WADE–MINGOS rules (Section 6.5.3).[36] Their extraordinary stability compared to the corresponding boranes has been associated with *spherical aromaticity*.[37] More recently, it was pointed out that spherically aromatic boron clusters and HÜCKEL-aromatic hydrocarbons are related by the total number of electrons and the number of π electrons, respectively.[38] Of the seven anions, $[B_{10}H_{10}]^{2-}$ and $[B_{12}H_{12}]^{2-}$ are the most stable ones, both thermally and against hydrolysis, and therefore also the most thoroughly studied. $Na_2[B_{12}H_{12}]$ readily dissolves in water and is practically nontoxic.

Salts with the anion $[B_{12}H_{12}]^{2-}$ are formed on heating of diborane(6)/boranate mixtures in the presence of LEWIS bases (see above), as well as through oxidation of $Na[BH_4]$ with elemental iodine by thermal disproportionation of the initially formed $Na[B_3H_8]$. Salts of $[B_{10}H_{10}]^{2-}$ are best obtained from $B_{10}H_{14}$ and a tertiary amine in refluxing xylene (R = Et).

$$B_{10}H_{14} + 2\,R_3N \xrightarrow{-H_2} B_{10}H_{12}(NR_3)_2 \longrightarrow [R_3NH]_2[B_{10}H_{10}]$$

An alternative method is the thermolysis of tetraethylammonium boranate:

$$10\,[R_4N][BH_4] \longrightarrow [R_4N]_2[B_{10}H_{10}] + 8\,R_3N + 11\,H_2 + 8\,C_2H_6$$

By heating of the reaction products with caustic soda $Na_2[B_{10}H_{10}]$ is obtained. The structures of the dianions $[B_{10}H_{10}]^{2-}$ and $[B_{12}H_{12}]^{2-}$ are shown in Figure 6.7. In $[B_{10}H_{10}]^{2-}$, the boron vertices constitute a polyhedron of a bicapped quadratic

36 F. Schlüter, E. Bernhardt, *Inorg. Chem.* **2011**, *50*, 2580 and cited literature.
37 Z. Chen, R. B. King, *Chem. Rev.* **2005**, *105*, 3613
38 J. Poater, M. Solà, C. Viñas, F. Teixidor, *Chem. Eur. J.* **2016**, *22*, 7437.

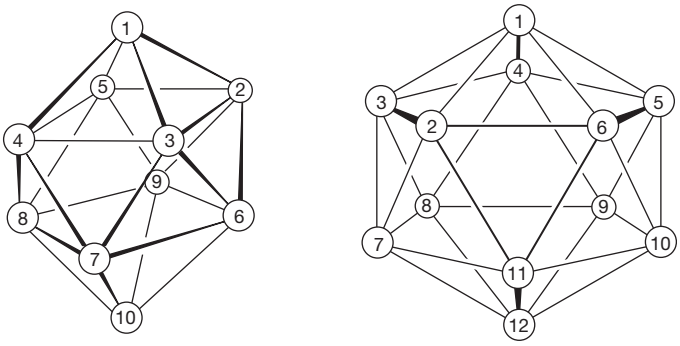

Figure 6.7: Structures of B_n scaffolds of the anions $[B_{10}H_{10}]^{2-}$ (left; D_{4d} symmetry) and $[B_{12}H_{12}]^{2-}$ (right; I_h symmetry). The numbering of boron atoms serves naming purposes in case of substitution.

antiprism, in the dianion $[B_{12}H_{12}]^{2-}$ the familiar B_{12} icosahedron. Each boron vertex carries a terminal hydrogen atom, bonded by an electron-precise two-center two-electron bond. In $[B_{12}H_{12}]^{2-}$ all 12 boron atoms (and the H atoms) are equivalent by symmetry. The ^{11}B-NMR spectrum of an isotopically pure sample therefore consists of just a single doublet due to the ^{1}J coupling to the adjacent protons. According to PAETZOLD, the formal replacement of one of the $[BH]^-$ units by $[NH]^+$ gives the neutral *heteroborane* $NB_{11}H_{12}$ (azadodecaborane), in which all vertices, including nitrogen(!), show a coordination number of 6.

In $[B_{10}H_{10}]^{2-}$ the two apical positions (the "poles") are equivalent to one another, as are the eight remaining ("equatorial") boron atoms. The ^{11}B-NMR spectrum therefore consists of two doublets in an intensity ratio of 1:4. The dianions $[B_{10}H_{10}]^{2-}$ and $[B_{12}H_{12}]^{2-}$ are chemically similar and of pronounced stability compared to all other hydroborates. The water-soluble alkali metal salts are stable up to at least 600 °C and 800 °C, respectively; even at 100 °C they are not attacked by aqueous bases, resist mild oxidizing agents and dilute hydrochloric acid does not react with $[B_{12}H_{12}]^{2-}$ at 100 °C and only slowly with $[B_{10}H_{10}]^{2-}$! This remarkable resistance against acids and bases is kinetic in nature as hydrolysis to boric acid and hydrogen should readily occur from a thermodynamic perspective.

The reason for this behavior is seen in the very pronounced (quasi-aromatic) spherical delocalization of electrons in the highly symmetric B_n scaffolds. This is why all reactions that remove a boron atom from the cage and thus reduce symmetry are associated with a high activation barrier. Indeed, those hydroborate anions are most stable that feature a closed and highly symmetric B_n core.

As in the case of other aromatic systems, the dianions $[B_{10}H_{10}]^{2-}$ and $[B_{12}H_{12}]^{2-}$ undergo numerous electrophilic and nucleophilic *substitution reactions* under

retention of the B_n cluster.[39] Both dianions thus react with F_2, Cl_2, Br_2 and I_2 to partially or totally halogenated derivatives such as $[B_{12}F_{12}]^{2-}$, $[B_{12}Cl_{12}]^{2-}$, $[B_{12}Br_{12}]^{2-}$ and $[B_{12}I_{12}]^{2-}$, depending on the reaction conditions. The icosahedral dianion $[B_{12}Cl_{12}]^{2-}$ can be oxidized by AsF_5 via the blue radical monoanion to the neutral $B_{12}Cl_{12}$ of D_{3d} symmetry, which was isolated in the form of equally blue crystals.[40] The monoanion $[B_{12}Cl_{12}]^{\bullet-}$ is extremely electrophilic as shown by binding of N_2 and even the noble gases krypton and xenon in the gas phase. Moreover, $[B_{12}Cl_{12}]^{2-}$ serves as a weakly coordinating anion for the isolation of reactive cations, for example, $[CPh_3]_2[B_{12}Cl_{12}]$. By reaction of $Cs_2[B_{12}H_{12}]$ with H_2O_2 (30%) at 105 °C, the hydroxyl derivative $Cs_2[B_{12}(OH)_{12}]$ is obtained. Furthermore, the diprotic super acid $H_2B_{12}Cl_{12}$ and the very strong methylating agent $Me_2B_{12}Cl_{12}$ were reported, in which the two hydrogen atoms or two methyl groups, respectively, are bound to opposing chloro substituents of the cluster.[40]

If $[B_{10}H_{10}]^{2-}$ is consecutively treated with nitric acid and $Na[BH_4]$, the diazonium salt $B_{10}H_8(N_2)_2$ is generated, which can be sublimed at 100 °C in vacuum. Two N_2 molecules are coordinatively bound to the apical B atoms. This colorless salt reacts with NH_3, pyridine, CO, H_2S and MeCN under replacement of both N_2 molecules by a new ligand.

6.6 Organoboranes

The partial or complete substitution of H atoms in boranes by alkyl or aryl groups (R) leads to organoboranes,[41] of which the derivatives of BH_3 are by far the most important. The most common synthetic routes to compounds of type RBH_2, R_2BH and R_3B are:

(a) *Hydroboration* of alkenes with diborane(6) or borane adducts:

$$BH_3{\cdot}D \underset{+D}{\overset{-D}{\rightleftharpoons}} BH_3 \xrightarrow{+\text{alkene}} RBH_2 \xrightarrow{+\text{alkene}} R_2BH \xrightarrow{+\text{alkene}} R_3B$$

The donor D is either THF or dimethyl sulfide (Me_2S) in these cases. The reaction temperature is typically between 0 °C and 20 °C. The alkene coordinates to the electron-deficient boron center with its π electrons, followed by the insertion into the BH bond. Mono- and diorganoboranes are dimers in most cases, in analogy to diborane(6) at 20 °C: $(RBH_2)_2$ and $(R_2BH)_2$. Only very bulky substituents shift the dimerization equilibrium to the side of the monomer. For

39 F. Teixidor et al., *Chem. Soc. Rev*. **2013**, *42*, 3318.

40 C. Knapp et al., *Angew. Chem.* **2010**, *122*, 3616 and **2011**, *123*, 572. J. Warneke et al., *Angew. Chem. Int. Ed.* **2017**, *56*, 7980. C. Jenne et al., *Chem. Eur. J.* **2016**, *22*, 16032.

41 F. Jäkle, J. A. Soderquist, *Encycl. Inorg. Chem.* **2005**, *1*, 560. M. Zaidlewicz, *Kirk-Othmer Encycl. Chem. Technol.* **2005**, *13*, 631.

example, the mesityl-substituted derivative $Mes_2B^H_HBMes_2$ is dimeric in the solid state, but in solution dimer and monomer can both be observed (dissociation enthalpy 70 kJ mol^{-1}).[42]

(b) Reaction of boron–halogen or boron–oxygen compounds with organometallic reagents:

$$BF_3 + 3\ RMgCl \longrightarrow R_3B + 3\ MgClF$$
$$BBr_3 + Ph_2Hg \longrightarrow Ph_2BBr + HgBr_2$$

Organoboranes are often sensitive to air and sometimes pyrophoric. They play an important role in organic synthesis. In contrast to the parent diborane B_2H_6 and to hexamethyl dialuminum Me_6Al_2, the compounds of type R_3B are without exception monomeric. The strong LEWIS acid trimethyl borane reacts with MeLi in Et_2O to the tetramethyl borate complex $Li[BMe_4]$. The solid-state structure of $Li[BMe_4]$ is dominated by intermolecular CH···Li interactions. The more bulkily substituted Ph_3B and $(C_6F_5)_3B$ are LEWIS acids as well; their acidity compared to BCl_3 ranks as follows: $(C_6F_5)_3B > BCl_3 > Ph_3B$. The complexes $K[BPh_4]$ and $Na[B(CN)_4]$ contain four BC bonds each.

The very strong LEWIS acid $B(C_6F_5)_3$ is a useful catalyst in organic synthesis as well as an important reagent in organometallic chemistry.[43] With certain chelating ligands, this species reacts to adducts with the coordination number 5 at boron.

The heterocyclic *boratabenzene anion* $[C_5H_5BR]^-$ is an aromatic organoboron species, which is isoelectronic to corresponding substituted benzene derivatives. It was isolated with a number of different substituents R in the form of alkali metal salts. Even the parent anion $[C_5H_5BH]^-$ is accessible as the lithium salt by treatment of the neutral PMe_3 adduct of borabenzene with $Li[AlH_4]$ as a hydride source.[44] Such anions coordinate to metal atoms in a similar sandwich mode as $[C_5H_5]^-$.[45] While borate anions are certainly more common, also a surprisingly high number of cationic boranes $[R_2B]^+$ are known: in borinium, borenium and boronium cations the boron center is additionally coordinated (and thus stabilized) by the lone pairs of 0, 1 and 2 donor ligands, respectively.[46] The only donor-free borinium cation so far, $[Mes_2B]^+$ (Mes = 2,4,6-trimethylphenyl), was obtained as a stable carborate salt (see Section 6.7) in a straightforward manner by fluoride abstraction from Mes_2BF.[47]

42 T. B. Marder et al., *J. Organomet. Chem.* **2003**, *680*, 165.
43 G. Erker, *Dalton Trans.* **2005**, 1883.
44 D. A. Hoic, W. M. Davis, G. Fu, *J. Am. Chem. Soc.* **1995**, *117*, 8480.
45 X. Zheng, G. E. Herberich, *Eur. J. Inorg. Chem.* **2003**, 2175.
46 W. E. Piers, S. C. Bourke, K. D. Conroy, *Angew. Chem. Int. Ed.* **2005**, *44*, 5016–5036. T. S. De Vries, A. Prokofjevs, E. Vedejs, *Chem. Rev.* **2012**, *112*, 4246.
47 Y. Shoji, N. Tanaka, K. Mikami, M. Uchiyama, T. Fukushima, *Nature Chem.* **2014**, *6*, 498.

6.7 Carboranes

The replacement of single boron atoms of the polyhedral scaffolds in boranes or hydroborates by other nonmetal atoms results in *heteroboranes*, which are referred to as carba-, aza-, phospha-, thiaboranes and so on depending on the hetero element.[48] The by far most important class are the carbaboranes (short: carboranes), mixed hydrides of boron and carbon.

The first carborane, $B_3C_2H_5$, was obtained in low yield from the reaction of the pentaborane B_5H_9 with acetylene in an electric discharge. During this remarkable reaction the triple bond of acetylene is cleaved. The 1,5-dicarba-*closo*-pentaborane(5) has the structure of a trigonal bipyramid with the C atoms in the apical positions:

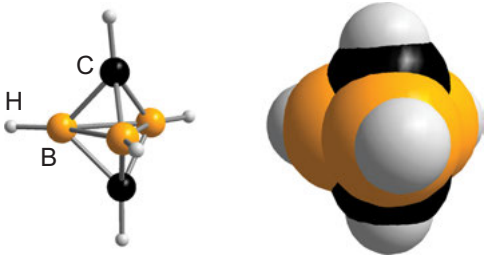

As a general rule, the isomers of dicarbaborane with the largest distance between the carbon atoms are the most stable.

The best investigated group of carboranes adheres to the generic formula $C_2B_{n-2}H_n$. These compounds are formally derived from the *closo*-hydroborate $[(BH)_n]^{2-}$ by replacement of two $[BH]^-$ units by isoelectronic CH moieties. In this manner, neutral molecules with likewise closed structures are obtained, which in contrast to the homonuclear species allow for different positional isomers. This will be exemplified on the dicarba-*closo*-decaboranes $C_2B_{10}H_{12}$, which are formally derived from the icosahedral dianion $[B_{12}H_{12}]^{2-}$ (Figure 6.8).[49]

The two carbon atoms can assume different positions in relation to each other: 1,2 (*ortho*), 1,7 (*meta*) or 1,12 (*para*). The numbering of positions starts at the apex of the icosahedron, continues clockwise in the pentagonal plane below, likewise in the next plane and ends at the position opposite to atom 1 (Figure 6.8).

48 R. N. Grimes, *Carboranes*, 2nd ed., Academic Press, Amsterdam, **2011**.

49 The monocarbaborane $[CB_{11}H_{12}]^-$ is an important weakly coordinating anion for the synthesis of particularly strong electrophiles and superacids; see C. A. Reed, *Acc. Chem. Res*. **1998**, *31*, 133 and **2010**, *43*, 121; S. Körbe, P. J. Schreiber, J. Michl, *Chem. Rev*. **2006**, *106*, 5208; C. Knapp, *Compr. Inorg. Chem*. II, Kap. 1.25, Elsevier, Amsterdam, **2013**.

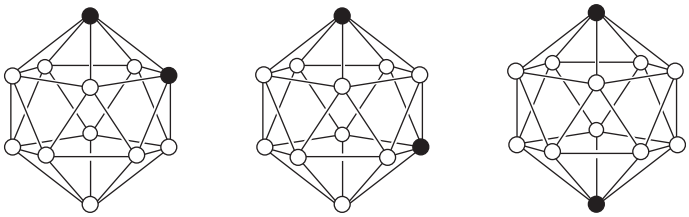

1,2-$C_2B_{10}H_{12}$ 1,7-$C_2B_{10}H_{12}$ 1,12-$C_2B_{10}H_{12}$

Figure 6.8: Icosahedral scaffolds of the three isomeric *closo*-carboranes of composition $C_2B_{10}H_{12}$. The numbering of atomic positions corresponds to that in Figure 6.7.

1,2-$C_2B_{10}H_{12}$ (m.p. 320 °C) is formed during the reaction of *nido*-$B_{10}H_{14}$ with acetylene in the presence of LEWIS bases (D) such as dialkylsulfides R_2S, nitriles RCN, phosphanes R_3P or tertiary amines R_3N:

$$B_{10}H_{14} + RC{\equiv}CR \xrightarrow{D} R{-}C\overset{B_{10}H_{10}}{\diagup\!\bigcirc\!\diagdown}C{-}R + 2\,H_2$$

Besides hydrogen, the groups R can also be alkyl, aryl or other residues, by virtue of which a large number of C-substituted carboranes is accessible. The *ortho*-isomer 1,2-$C_2B_{10}H_{12}$ is stable until about 470 °C. Above this temperature, it slowly isomerizes to the *meta*-isomer 1,7-$C_2B_{10}H_{12}$ in good yield (m.p. 265 °C), which finally can be transformed into the thermodynamically stable *para*-isomer 1,12-$C_2B_{10}H_{12}$ in low yield by further heating to above 615 °C (m.p. 261 °C). The C_2B_{10} scaffold starts to decompose at temperatures above 630 °C. During the isomerization, a nonicosahedral *closo*-structure occurs as an intermediate, which was isolated in the form of a derivative and characterized by X-ray diffraction on single crystals.[50]

The carboranes $C_2B_{10}H_{12}$ are chemically similarly resistant as *closo*-hydroborates. They are neither attacked by boiling water, nor by strong oxidizing or reducing agents. In contrast, nucleophilic reagents lead to the partial degradation of the C_2B_{10} cage, resulting in carboranes with between six and nine boron atoms. The formation of the *nido*-carborane $C_2B_9H_{13}$ from $C_2B_{10}H_{12}$ by treatment with alkoxides serves as an example:

$$C_2B_{10}H_{12} \xrightarrow{[MeO]^-} [C_2B_9H_{12}]^- \begin{cases} \xrightarrow{H^+} C_2B_9H_{13} \\ \xrightarrow{NaH} [C_2B_9H_{11}]^{2-} \end{cases}$$

50 A. J. Welch et al., *Angew. Chem. Int. Ed.* **1997**, *36*, 645.

The anion $[C_2B_9H_{12}]^-$ is derived from the C_2B_{10} icosahedron by loss of a boron atom, that is, the removal of one apex next to the two carbon atoms (Figure 6.8). By the action of NaH it can be deprotonated a second time to give $[C_2B_9H_{11}]^{2-}$. Application of the WADE–MINGOS rules (Section 6.5.3) gives a *nido*-structure for both species, $[C_2B_9H_{12}]^-$ with one bridging H atom, $[C_2B_9H_{11}]^{2-}$ with an open pentagonal face and only terminal hydrogen atoms. The vacant position is well suitable for the coordination to metals due to the five π orbitals, nearly perpendicular to the pentagonal plane. The carborate dianion $[C_2B_9H_{11}]^{2-}$ (colloquially referred to as "dicarbollide") is therefore a similarly good ligand as the cyclopentadienide anion $[C_5H_5]^-$. Consequently, a ferrocene-analogous anionic complex $[Fe(C_5H_5)(C_2B_9H_{11})]^-$, which is readily oxidized to the corresponding Fe(III) species, is obtained from $FeCl_2$, $Na_2[C_2B_9H_{11}]$ and $Na[C_5H_5]$. The structures of these and other *metallacarbaboranes*[51] of Fe, Co and Ni with two dicarbollide ligands are shown in Figure 6.9.

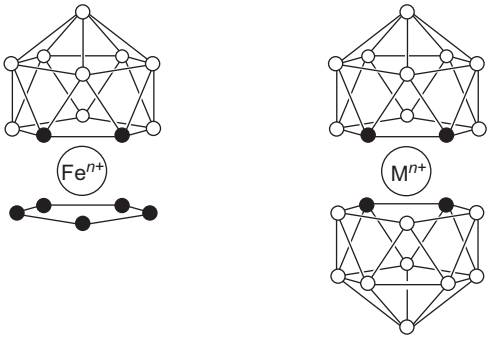

Figure 6.9: Metal complexes with the dianionic dicarbollide ligand $[1,2\text{-}C_2B_9H_{11}]^{2-}$. The black circles represent CH and the open circles BH moieties. The mixed-ligand complex (left) is known as diamagnetic anionic Fe(II) ($n = 2$; $x = 1$) and as paramagnetic neutral Fe(III) species ($n = 3$; $x = 0$). The charge of the bis(dicarbollide) complexes (right) depends on the oxidation state of the metal ($M^{n+} = Fe^{2+}$, Co^{3+}, Ni^{3+}, Ni^{4+}; $x = 4 - n$).

A huge number of carboranes and their substitution products have been synthesized, even those with a B:C ratio of near 1. The latter species constitute a transition from the spherically delocalized boranes to the electron-precise hydrocarbons. Potential applications are found inter alia in the pharmaceutical sciences.[52]

51 E. Housecroft, *Encycl. Inorg. Chem.* **2005**, *1*, 524.

52 M. Scholz, E. Hey-Hawkins, *Chem. Rev.* **2011**, *111*, 7035.

6.8 Boron Halides

The most important binary boron halides are of the type BX_3 (X = F, Cl, Br, I). They are also referred to as *trihaloboranes*. Besides, several subhalides with lower halogen content are known, for example, B_2X_4 and B_4X_4. In these subvalent species the oxidation states of the boron atoms are smaller than +3.

6.8.1 Trihalides (BX_3)

BF_3 (b.p. –100 °C) has the highest technological importance of all boron halides, followed by BCl_3 (b.p. 12.5 °C). The industrial preparation of both halides starts from borax, boric acid or boron carbide:

$$Na_2[B_4O_7] + 7\,SO_3 + 6\,CaF_2 \longrightarrow 4\,BF_3 + 6\,Ca[SO_4] + Na_2[SO_4]$$

$$B(OH)_3 + 3\,HF \xrightarrow{H_2SO_4} BF_3 + 3\,H_2O$$

$$2\,B(OH)_3 + 6\,HSO_3F \longrightarrow 2\,BF_3 + 6\,H_2SO_4$$

$$B_4C + 6\,Cl_2 \xrightarrow{700°C} 4\,BCl_3 + C_{s.}$$

BF_3 is commercially available compressed in stainless steel cylinders or as the liquid etherate $BF_3{\cdot}OEt_2$ (see below). The technologically less relevant BBr_3 (b.p. 91 °C) and BI_3 (b.p. 210 °C) are prepared as follows:

$$BF_3 + AlBr_3 \longrightarrow BBr_3 + AlF_3$$

$$K[BH_4] + 2\,I_2 \longrightarrow BI_3 + KI + 2\,H_2$$

All trihalides of boron are colorless and at 25 °C either gaseous (BF_3, BCl_3), liquid (BBr_3) or solid (BI_3). They consist of trigonal planar molecules of D_{3h} symmetry without permanent dipolar moment.

As LEWIS acids, all boron trihalides, particularly BF_3 and BCl_3, react with amines, ethers, nitriles, ketones, *N*-heterocyclic carbenes[53] and other LEWIS bases to adducts (Section 6.2). In a wider sense, the borate salts $Na[BF_4]$ and $Na_2[SO_4BF_3]$ can also be regarded as LEWIS acid–base adducts, in which the F^- or $[SO_4]^{2-}$ anions assume the role of the base. The tetrahaloborates $[BX_4]^-$, in particular $[BF_4]^-$, constitute very stable anions, analogous to perchlorate $[ClO_4]^-$. Tetrafluoroborates are prepared from BF_3 and ionic fluorides or chlorides:

53 D. P. Curran et al., *Angew. Chem. Int. Ed.* **2011**, *50*, 10257.

$$BF_3 + KF \longrightarrow K[BF_4]$$
$$4\,BF_3 + 3\,KCl \longrightarrow 3\,K[BF_4] + BCl_3$$

$BF_3{\cdot}OMe_2$ is a colorless liquid (b.p. 126 °C) and $BCl_3{\cdot}NMe_3$ forms colorless sublimable crystals (m.p. 243 °C). With small amounts of liquid water BF_3 reacts via an isolable adduct $BF_3{\cdot}OH_2$ to a solution of oxonium tetrafluoroborate:

$$4\,BF_3 + 4\,H_2O \longrightarrow 4\,BF_3{\cdot}OH_2 \xrightarrow{+2\,H_2O} 3\,[H_3O]^+ + 3\,[BF_4]^- + B(OH)_3$$

This solution also contains the anions $[BF_3(OH)]^-$, $[BF_2(OH)_2]^-$ and so on as intermediates to the concomitantly formed boric acid $B(OH)_3$.[54] In the literature the aqueous solution of $[H_3O][BF_4]$ is often referred to as tetrafluoro boric acid (HBF_4). This very strong acid ($pK_a = -4.9$) is commercially synthesized from 70% hydrofluoric acid and orthoboric acid:

$$B(OH)_3 + 4\,HF \longrightarrow [H_3O][BF_4] + 2\,H_2O$$

It is predominantly utilized for the production of tetrafluoroborates. The tetrafluoroborates of Cu, Zn, Cd, Ni and Pb are used in electroplating. The thermal stability of the haloborates increases with the size of the counter cation. While $Na[BF_4]$ decomposes at 384 °C, $Cs[BF_4]$ melts without decomposition at 550 °C. In contrast to $[BF_4]^-$, the anions $[BCl_4]^-$, $[BBr_4]^-$ and $[BI_4]^-$ are sensitive to hydrolysis and can only be isolated as stable salts with large counter cations. The dinuclear haloborate anions $[X_3B{-}X{-}BX_3]^-$ with a bridging halide anion were theoretically predicted[55] in analogy to the corresponding hydroborate salt $[H_3B{-}H{-}BH_3]^-$ (see Section 6.5.4.), but have not been isolated yet.

As *acid chlorides* of boric acid, the boron trihalides react with element–hydrogen bonds according to the following scheme:

$$\rangle B{-}X + H{-}E{-} \longrightarrow \rangle B{-}E + H{-}X{-} \qquad E = O, N, P, S$$

For instance, they are hydrolyzed with excess water giving boric acid $B(OH)_3$ and HX. With alcohols, BCl_3 and BBr_3 react to boric esters $B(OR)_3$, with secondary amines to the corresponding amides $B(NR_2)_3$. Methanethiol MeSH reacts with BCl_3 to $MeS{-}BCl_2$ and HCl.

54 In the solid state, the dihydrate $BF_3{\cdot}2H_2O$, a colorless viscous liquid, has the structure of a monohydrate of hydroxotrifluoro boric acid $H[BF_3(OH)]{\cdot}H_2O$.

55 T. T. Takaluoma et al., *Inorg. Chem.* **2016**, *55*, 3599.

Another characteristic reaction is the *substituent exchange*. In a liquid mixture of BCl_3 and BBr_3, equilibrium is established after a few hours at 25 °C, which can be monitored by ^{11}B-NMR or Raman spectroscopy:

$$BCl_3 + BBr_3 \rightleftharpoons BBrCl_2 + BBr_2Cl$$

BF_3 and BCl_3 react in a similar manner. Trialkylboranes can be converted to alkyldifluoroboranes with commercial BF_3 etherate:

$$R_3B + 2\,BF_3{\cdot}OEt_2 \longrightarrow 3\,RBF_2 + 2\,Et_2O$$

BF_3 and $B(OH)_3$ react in the gas phase to give a mixture of $BF_2(OH)$ and $BF(OH)_2$. Upon heating, boron oxide, B_2O_3, reacts with BF_3 and BCl_3 to trifluoro and trichloroboroxine $B_3O_3X_3$, respectively. These planar heterocycles contain six-membered B_3O_3 rings with alternating atom sequence (*pseudo heterocycles*).

BF_3 and, to some extent, BCl_3 are powerful *catalysts* for a number of organic syntheses. The LEWIS acidic properties are likely playing a decisive role. For instance, the nitration of arenes with N_2O_5 is catalyzed by BF_3, which is attributed to the formation of nitronium cations:

$$O_2N-O-NO_2 + BF_3 \longrightarrow [NO_2]^+ + [F_3B-ONO_2]^-$$

6.8.2 Subhalides[56]

The already mentioned diboron tetrahalides B_2X_4 contain a BB single bond. In the solid state, they consist of planar molecules of D_{2h} symmetry with all valence angles close to 120°. In solution or in the gas phase, however, B_2Cl_4 adopts the lower D_{2d} symmetry, as the two halves of the molecule are twisted by 90°. The energy barrier for this torsion about the BB axis is just 7.5 kJ mol^{-1}. Apparently, crystal packing forces are responsible for the slightly less favorable conformation in the solid state.

B_2F_4 is generated by cocondensation of BF_3 and copper atoms. To this end, metallic copper is evaporated by inductive heating in a graphite block and the monoatomic copper vapor is condensed with BF_3 at –196 °C:

$$2\,BF_3 + 2\,Cu \longrightarrow F_2B-BF_2 + 2\,CuF$$

B_2F_4 is a colorless gas at standard conditions. In the gas phase, it reacts with BF to further subfluorides such as B_3F_5, B_8F_{12} (Section 13.4.6) and $B_{10}F_{12}$.[57] B_2Cl_4 is

56 T. B. Marder et al., *Chem. Rev.* **2016**, *116*, 9091–9161.
57 P. L. Timms et al., *Dalton Trans.* **2005**, 607.

obtained as colorless liquid in low yield upon decomposition of BCl_3 in a high-frequency discharge in the presence of mercury vapor:

$$2\ BCl_3\ +\ 2\ Hg \longrightarrow Cl_2B-BCl_2\ +\ Hg_2Cl_2$$

Similarly, the reduction of BCl_3 to B_2Cl_4 occurs in an electrical discharge between copper electrodes or in the presence of copper coils. B_2F_4 can also be obtained by fluorination of B_2Cl_4 with SbF_3 (halogen exchange). In fact, all diboron tetrahalides B_2X_4 can conveniently be prepared starting from $B_2(OMe)_4$ in a series of exchange reactions.[58]

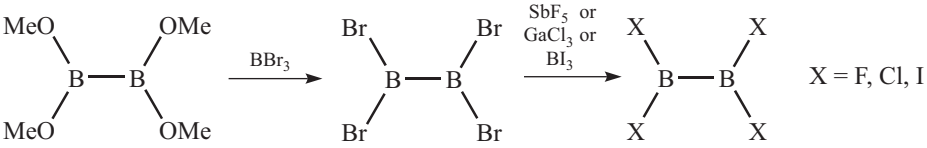

With alkenes and alkynes, the diboron tetrahalides react in a 1,2-addition in most cases:

$$X_2B-BX_2\ +\ H_2C=CH_2 \longrightarrow X_2B-CH_2-CH_2-BX_2$$

B_2Cl_4 behaves as acid halide of hypoboric acid $B_2(OH)_4$ and as a LEWIS acid. The most interesting reaction, however, is the disproportionation, which occurs slowly at room temperature but much faster on heating:

$$B_2Cl_4 \longrightarrow BCl_3\ +\ \tfrac{1}{n}(BCl)_n \qquad n = 8-12$$

In the end, B_8Cl_8, B_9Cl_9, $B_{10}Cl_{10}$, $B_{11}Cl_{11}$ and $B_{12}Cl_{12}$ are isolated as stable, sublimable products. These diamagnetic chlorides consist of closed polyhedral B_n clusters, not too dissimilar to the *closo*-hydroborate, although they have two skeletal electrons less according to WADE–MINGOS rules (also see $[B_{12}Cl_{12}]^{2-}$ in Section 6.5.4). Such a situation is referred to as *hypercloso*. The smallest such cluster is B_4Cl_4, which is obtained as a side product of the B_2Cl_4 synthesis during the electrical discharge in the presence of Hg. As most stable representatives of the $[BCl]_n$ species above, the structures of B_4Cl_4 and B_8Cl_8 are shown in Figure 6.10. In case of the B_4Cl_4 molecule, the boron atoms form a regular tetrahedron, for B_8Cl_8 a dodecahedron. Assuming electron-precise two-center two-electron bonds, four of the 12 valence electrons of B_4Cl_4 are required for the bonding to the terminal chloro substituents, that is, B_4Cl_4 possesses eight skeletal electrons for cluster bonding. Therefore, four closed three-center bonds can be formed, one for each face of the tetrahedron. The BB distances amount to 170 pm.

58 H. Braunschweig et al., *Chem. Commun.* **2017**, *53*, 8265.

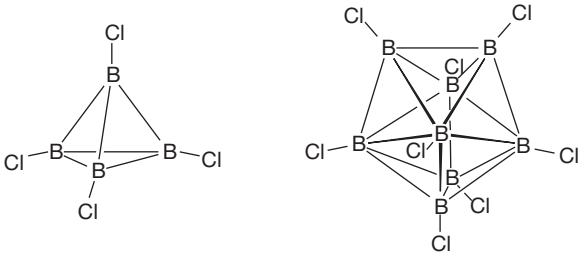

Figure 6.10: Structures of subchloride clusters B_4Cl_4 (tetrahedron) and B_8Cl_8 (dodecahedron).

Excessive chlorination of B_4Cl_4 leads to BCl_3 via B_2Cl_4. With lithium organic compounds (LiR), B_4Cl_4 reacts to the corresponding *tetrahedranes* $(BR)_4$, which can also be obtained in a more straightforward manner by reductive dehalogenation of RBF_2 with Na/K alloy (M) in pentane (R = ^{t}Bu):

$$4\,R{-}BF_2 \;+\; 8\,M \longrightarrow (RB)_4 \;+\; 8\,MF$$

Compounds with a B_4 scaffold can assume different structures depending on the substituents. Aside from tetrahedral, the B_4 unit can also be cyclic (R = NMe_2, NEt_2), open-chained or diamond-shaped (bicyclic).[59] The latter derivatives contain planar tetracoordinate B atoms and display aromatic character.

6.9 Boron–Oxygen Species

6.9.1 Introduction

Boron and oxygen form thermally and chemically extraordinarily stable compounds. The most important representatives are boron trioxide B_2O_3, orthoboric acid $B(OH)_3$ and various metaboric acids $(HBO_2)_n$ as well as numerous polymeric borates. *Borax* and *colemanite* are the most prominent *boron mineral*s (Section 6.1) from which practically all other boron compounds and elemental boron are produced. In industry, boron–oxygen species are predominantly used for the production of glass, ceramics, enamel and detergents as well as on a smaller scale as fluxes for soldering and welding or as flame-retardants and anticorrosives. Borates are also employed as a component of fertilizers in order to compensate for the boron deficit of agricultural soils.

More recently, with the acid $H_2B_{12}(OH)_{12}$ and its salts $M_2[B_{12}(OH)_{12}]$ icosahedral *closo*-borates with boron–oxygen bonds became available (Section 6.5.4).

59 A. Berndt et al., *Angew. Chem. Int. Ed.* **2002**, *41*, 1526. W. Siebert et al., *ibid* **2002**, *41*, 1529.

6.9.2 Boron Trioxide and Boric Acids

Orthoboric acid H_3BO_3 [or $B(OH)_3$] occurs in Nature as the mineral *sassoline*, but is produced nowadays exclusively and at a huge scale by hydrolysis of *borax* or *colemanite* with aqueous sulfuric acid:

$$Na_2[B_4O_5(OH)_4] + H_2SO_4 + 3\,H_2O \xrightarrow{25°C} 4\,H_3BO_3\downarrow + Na_2[SO_4]$$

$$Ca[B_3O_4(OH)_3] + H_2SO_4 + 2\,H_2O \xrightarrow{90°C} 3\,H_3BO_3 + Ca[SO_4]\downarrow$$

During the first reaction the poorly soluble boric acid precipitates directly, while sodium sulfate crystallizes only on cooling. Conversely, in the second case, *gypsum* $Ca[SO_4]\cdot 2H_2O$ precipitates from the hot solution and boric acid is obtained after filtration and cooling. Boric acid is a weak *ansolvo acid*, which is poorly soluble in water and remains in solution as the nearly completely undissociated monomer. The solubility increases strongly with temperature (positive solvation enthalpy) from 4.7 wt% at 20 °C to 27.5 wt% at 100 °C. The pK_a value of 9.14 refers to the following equation:

$$B(OH)_3 + 2\,H_2O \rightleftharpoons [H_3O]^+ + [B(OH)_4]^-$$

In the crystalline state, $B(OH)_3$ molecules are connected to two-dimensionally infinite layers by hydrogen bonds, while between individual layers only VAN DER WAALS forces are active (Figure 6.11), which is manifest in the scaly appearance of the colorless crystals (m.p. 171 °C). Boric acid is volatile in steam distillation.

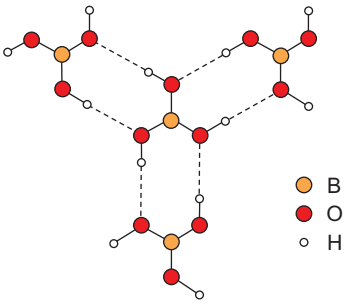

Figure 6.11: Excerpt from a layer of orthoboric acid. The planar $B(OH)_3$ molecules are connected by linear unsymmetrical hydrogen bonds to cyclic subunits.

Hypodiboric acid $(HO)_2B–B(OH)_2$ (also referred to as *diboronic acid*) adopts a similar layer structure with hydrogen bonds between the OH groups. It is obtained by hydrolysis of B_2Cl_4 or $B_2(OR)_4$.[60]

60 N. C. Norman et al., *New. J. Chem.* **2003**, *27*, 773.

As most oxoacids of nonmetals, boric acid condenses to boron trioxide upon heating through intermediate oligo- and polyboric acids:

$$3\ B(OH)_3 \xrightarrow[-3H_2O]{90\text{–}130^\circ C} B_3O_3(OH)_3 \xrightarrow{140\text{–}160^\circ C} (HBO_2)_n \xrightarrow[-H_2O]{400^\circ C} B_2O_3$$

The initially formed *cyclo*-triboric acid (α-*metaboric acid*) adopts the structure shown in Figure 6.12. It consists of planar boroxine cycles (B_3O_3), which is a frequently encountered structural element in boron chemistry. Here as well, the individual molecules are connected to layers by hydrogen bonds.

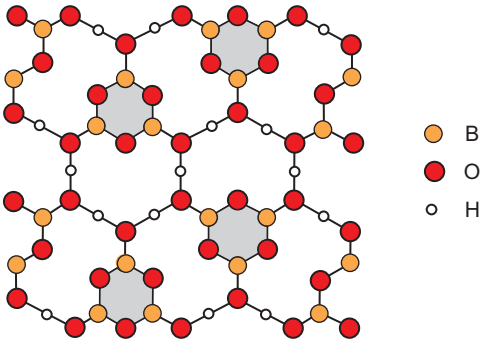

Figure 6.12: Excerpt from a layer of the solid-state structure of *cyclo*-triboric acid $B_3O_3(OH)_3$. All OH groups form hydrogen bonds to neighboring molecules. The six-membered rings of individual molecules of *cyclo*-triboric acid are shaded in gray.

Upon stronger heating two additional modifications of metaboric acid are obtained (β: monoclinic, γ: cubic), in which the boroxine rings are directly connected by bridging oxygen atoms. This requires that the boron atoms partially (β-HBO_2) or completely (γ-HBO_2) assume a coordination number of 4. From these modifications, the anhydride B_2O_3 is formed by slow dehydration at red heat; it is difficult to crystallize and thus mostly obtained in glassy form from the melt (see glasses, Section 8.9). Hexagonal B_2O_3 (m.p. 455–475 °C) consists of trigonal-planar BO_3 groups, which are linked by shared oxygen atoms to rings and ribbons in a three-dimensionally infinite network. On very strong heating, B_2O_3 evaporates as V-shaped molecules O=B–O–B=O of C_{2v} symmetry. Boron trioxide is also generated by burning (or oxidation) of amorphous boron in a very strongly exothermic reaction that can be utilized in rocket propellants. If B_2O_3 is reacted with elemental boron in a ball mill at temperatures of 1300–1700 °C, microcrystalline B_6O is obtained, which is almost as hard as diamond (see Section 6.4.1).[61]

61 X. Liu et al., *J. Solid State Chem.* **2010**, *183*, 1697.

Boron trioxide is hygroscopic and reacts with water back to $B(OH)_3$, with alcohols in the warmth to boric acid esters $B(OR)_3$. The technically important trimethyl ester is a colorless liquid (b.p. 68 °C), which is used for the synthesis of $Na[BH_4]$ (Section 6.5.2). In aqueous base, B_2O_3 dissolves to borates, with HF it forms BF_3. Boron trioxide is produced on a large industrial scale and mostly used in the ceramic and glass industries (borosilicate glass) as well as for the production of other boron species. For example, the glass Pyrex®, which is very resistant to corrosion and temperature changes, contains about 13 wt% of B_2O_3.

Aqueous solutions of borates contain the anion $[B(OH)_4]^-$ only a high pH values (pH > 11). At lower pH values, such solutions consist of $B(OH)_3$ and $[B(OH)_4]^-$ alongside each other and the following condensation reaction occurs at suitable concentrations:

$$2\ B(OH)_3 + [B(OH)_4]^- \rightleftharpoons [B_3O_3(OH)_4]^- + 3\ H_2O$$

The trimeric anion is derived from *cyclo*-triboric acid through addition of an $[OH]^-$ ion to one of the boron atoms. Although it is the dominating species in aqueous solution, $[B_3O_3(OH)_5]^{2-}$, $[B_4O_5(OH)_4]^{2-}$ and $[B_5O_6(OH)_4]^-$ are also present. In the neutral and acidic regions or upon strong dilution these *polyanions* hydrolyze to $B(OH)_3$. They also occur in several crystalline borates and show the following structures:

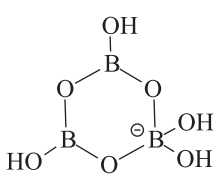

$[B_3O_3(OH)_4]^-$

$+ [OH]^- \longrightarrow [B_3O_3(OH)_5]^{2-}$

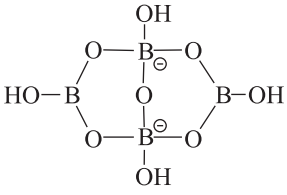

$[B_4O_5(OH)_4]^{2-}$

(in borax)

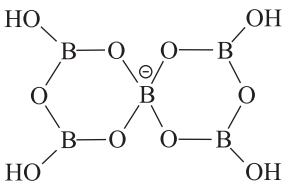

$[B_5O_6(OH)_4]^-$

In addition to $[B(OH)_4]^-$, $B(OH)_3$ condenses with other polyhydroxo species in aqueous solution, such as glycerol, catechol or the sugar alcohol mannitol. The oxonium ions $[H_3O]^+$ formed according to the scheme below can be titrated directly with a sodium hydroxide titer unlike the free boric acid:

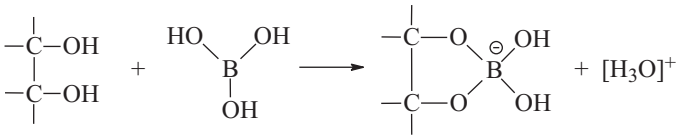

In organic chemistry, the organyl-substituted *boronic acids* $RB(OH)_2$ (with R = alkyl or aryl) are frequently employed reagents, which can be obtained by hydrolysis of

$RBCl_2$.[62] The parent species $HB(OH)_2$ was detected spectroscopically in the reaction mixture of diborane(6) and steam.

6.9.3 Borates

Borates[63] are known of almost all metals, but the sodium derivatives are the technologically most important. They are distinguished into monomeric borates, low-molecular di-, tri-, tetra- and pentaborates, as well as higher-molecular polyborates. All borate anions contain BO_3 triangles and/or BO_4 tetrahedrons as building blocks. In case of the polymeric borates, the BO_3 moieties are linked at the corners by shared oxygen atoms, while the BO_4 units are both corner- and edge-sharing. This linkage can also occur with other oxoanions, for example, as in the sulfatoborate $K_5[B(SO_4)_4]$, which contains five corner-sharing EO_4 tetrahedra with the boron atom at the center (E = B, S). Water-free borates are formed upon melting of $B(OH)_3$ with metal oxides, hydroxides or carbonates. The naturally occurring borates are hydrated almost without exception, that is, they contain chemically bound water (OH groups) or crystallization water (H_2O molecules).[64] This also applies to salts crystallized from aqueous solution.

Monoborates contain the following anions:

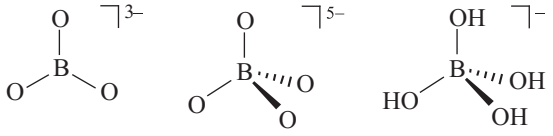

From these three motifs, the diborate anions $[B_2O_5]^{4-}$ and $[B_2O(OH)_6]^{2-}$ can be built by condensation. *Sodium tetraborate* $Na_2[B_4O_5(OH)_4]\cdot 3H_2O$, which is obtained by crystallization of borax at temperatures above 61 °C, is the boron compound traded in the largest quantities worldwide. *Sodium perborate* is utilized on a large scale as bleaching agent;[65] it is produced from alkaline sodium tetraborate solution and H_2O_2. The product precipitates at 25 °C in the composition of $Na_2[B_2(O_2)_2(OH)_4]\cdot 6H_2O$. The boron atoms in the anion of this salt are bridged by two peroxo moieties, that is, perborate is more precisely referred to as peroxodiborate:

---

62 T. Graening, *Nachr. Chemie* **2009**, *57*, 34. D. G. Hall, *Boronic Acids*, Wiley-VCH, Weinheim, **2005**.

63 D. M. Schubert, *Struct. Bonding* **2003**, *105*, 1. D. A. Keszler, *Encycl. Inorg. Chem.* **2005**, *1*, 472.

64 Regrettably, the formulae of borates are not displayed in a uniform manner in the literature. Occasionally, the chemically bonded water is summed up with the water of crystallization, for example, in the formula $Na_2[B_4O_7]\cdot 10H_2O$ for *borax* (*tincal*), instead of $Na_2[B_4O_5(OH)_4]\cdot 8H_2O$. Only the second formula correctly represents the structure.

65 As a component of laundry detergents. An aqueous solution of "sodium perborate-tetrahydrate" $Na[BO_3]\cdot 4H_2O$ [identical to $Na_2[B_2O_4(OH)_4]\cdot 6H_2O$] reacts like a alkaline H_2O_2 solution.

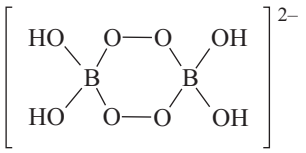

The B_2O_4 heterocycle shows a chair conformation.

All structurally characterized tri-, tetra- and pentaborates contain the boroxine ring B_3O_3, either isolated as in $Na_3[B_3O_6]$ (the sodium salt of *cyclo*-triboric acid), fused with a second ring as in borax, or spirocyclically connected with a second ring through a shared boron atom (Section 6.9.1). $Ba[B_2O_4]$, which is employed for optical frequency converters (just like $Li[B_3O_5]$),[66] also features boroxine rings and thus crystallizes in a layer structure: the *structural formula* is therefore $Ba_3[B_3O_6]_2$. The mineral *kernite* contains polymeric anions composed of spirocyclically linked B_3O_3 rings. Conversely, certain higher-molecular metaborates such as $Ca[BO_2]_2$ contain open-chain anions:

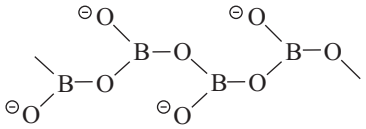

A related material is found in *tourmaline*, a complex borate-hexasilicate with a boron content of about 3%, which is the most abundant boron-containing mineral, but is only employed in jewelry due to its low boron concentration.[67] The general formula for tourmaline is not very helpful due to the strongly varying occupation of the cation positions with Li, Na, Mg, Ca, Fe, Al and others. For instance, the variety *dravite* has the composition of $NaMg_3Al_6[OH]_4[BO_3]_3[Si_6O_{18}]$. A similar empirical formula, but a completely different structure is found for the borosilicate glass Duran®, which is common in laboratory and industry (Section 8.9).

So far, most of the discussed BO compounds do not contain BB bonds. Oxidation of the very stable hydroborate dianion $[B_{12}H_{12}]^{2-}$ with H_2O_2 (30%), however, affords the *closo*-dianion $[B_{12}(OH)_{12}]^{2-}$. With concentrated sulfuric acid the free acid $H_2B_{12}(OH)_{12}$ can be obtained at 150 °C, which is stable up to 300 °C. This acid and its conjugate anion contain an icosahedral B_{12} unit, covered by a likewise icosahedral sphere of 12 oxygen atoms. The two OH_2 groups of the acid reside in positions 1 and 12 (compare Figure 6.8). All alkali metal salts of $[B_{12}(OH)_{12}]^{2-}$ as well as the free acid are poorly soluble in water.

66 For the generation of visible or ultraviolet light in pulsed high-energy lasers.

67 W. Schumann, *Gemstones of the World*, 5th ed., Sterling Publishing, New York, **2013**. P. Rustemeyer, *Faszination Turmalin*, Spektrum Verlag, Heidelberg, **2003**.

With *sulfur* and *selenium*, boron forms numerous heterocyclic systems, both as neutral molecules and thio- and seleno borate anions.[68] For instance, the binary chalcogenides B_2S_3, BS_2, BSe_2 and B_8S_{16} are all composed of trigonal-planar BX_3 groups, which are interconnected by four-, five- and six-membered planar rings. Heterocycles of the composition of B_2S_2, B_2S_3, B_3S_3, B_2S_4 and B_4S_2 are also known as the corresponding substituted species. As expected on the basis of the high degree of unsaturation, the latter species also contains BB bonds. At each boron atom either a monovalent residue R or an additional sulfur atom resides. As with oxo borates, the heavier thio borates contain boron atoms of coordination number 3 and 4. All boron–sulfur species are very sensitive to air and moisture.

6.10 Boron–Nitrogen Compounds

6.10.1 Bonding Situation

The aforementioned *ammonia–borane adduct* (Section 6.2.3) is obtained from diborane(6) and ammonia at low concentrations and in donor solvents (D). It is important that NH_3 be reacted with $D{\cdot}BH_3$ rather than with B_2H_6 as in the latter case the boronium boranate $[H_2B(NH_3)_2]^+[BH_4]^-$ is obtained as major product. This so-called diammoniate of diborane is an ionic isomer of ammonia–borane. It is also formed in a solid-state reaction by ball-milling of $Na[BH_4]$ with $[NH_4]F$ through $[NH_4][BH_4]$ as an unstable intermediate. $H_3B{\cdot}NH_3$ is isoelectronic and even isosteric with ethane C_2H_6. Both molecules show a staggered conformation with the H atoms avoiding each other:

$$\overset{\ominus}{H_3B}-\overset{\oplus}{N}H_3 \quad (d_{BN} = 167.2\ \text{pm}) \qquad\qquad H_3C-CH_3 \quad (d_{CC} = 154\ \text{pm})$$

The indicated distances are valid in the gas phase; in the solid state the bond length d_{BN} of $H_3B{\cdot}NH_3$ amounts to only 156.5 pm (at 220 K).[69] The analogy between BN and CC bonds leads to many structural similarities between saturated carbon and boron/nitrogen species. The strong polarization of the BN molecules, however, results in a completely different reactivity. The H atoms of the $H_3B{\cdot}NH_3$ molecule show protic character at the nitrogen atoms (+0.40*e* at N) and are mildly hydridic at the boron centers (–0.08*e* at B). The much higher electronegativity of nitrogen also accounts for the accumulation of negative charge at nitrogen (B: –0.13*e*; N: –0.83*e*). The resulting intramolecular interactions lead to the high melting point of $H_3B{\cdot}NH_3$ (m.p. 104 °C), while C_2H_6 (b.p. –89 °C) is a gas.

68 O. Conrad, C. Jansen, B. Krebs, *Angew. Chem. Int. Ed.* **1998**, *37*, 3208.
69 W. T. Klooster et al., *J. Am. Chem. Soc.* **1999**, *121*, 6337. N. J. Hess et al., *J. Phys. Chem. A* **2009**, *113*, 5723.

The covalent σ bond >B–N<, which is the basis for *aminoboranes*, connects a LEWIS acidic with a LEWIS basic center, directly adjacent to one another. The electron deficiency at the boron atom is thus alleviated by the formation of a dative π bond as shown in the following resonance structures:

(a) (b)

Due to the contribution of resonance form (b), aminoboranes are isosteric with the CC double bond of alkenes, which results in structural similarities between unsaturated carbon species and the corresponding BN compounds (H_2BNH_2 is planar just as ethylene). The analogy becomes particularly apparent, if the LEWIS acidity at the boron center is further increased, for example, as follows:

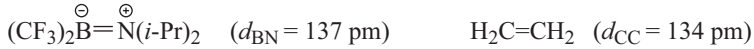

The π bond of aminoboranes, however, is much weaker than that of alkenes. This can be quantified by the torsion of the bond planes by 90° against each other rendering the former $2p_\pi$ AOs orthogonal. The energy required for this torsion is approximately twice as high for C_2H_4 than for H_2BNH_2. While C_2H_4 is transformed into a diradical with triplet configuration at a torsional angle of $\tau = 90°$, H_2BNH_2 remains in a singlet state with a lone pair of electrons at the nitrogen center. The partial charges change during this process from –1.00 at $\tau = 0°$ to –1.16 at $\tau = 90°$ at nitrogen and from +0.42 to +0.67 at boron.

Finally, *iminoboranes* are structurally related to alkynes:

These interrelationships are explained in the following on selected examples, although the total number of BN compounds known is much larger.[70] Analogous compounds are known for boron and phosphorus.[71] The π bonding component, however, is significantly weaker or even completely absent in BP bonds.

6.10.2 Ammonia–Borane

The crystalline ammonia–borane complex $H_3B{\cdot}NH_3$ mentioned above decomposes on heating to *aminoborane* H_2BNH_2 and H_2 in a mildly exothermic reaction. As aminoborane is rather unstable, it undergoes further transformations even at low temperatures,

70 Review: G. Bélanger-Chabot, H. Braunschweig, D. K. Roy, *Eur. J. Inorg. Chem.* **2017**, 4353.
71 I. Manners et al., *Chem. Rev.* **2010**, *110*, 4023. J. Li et al., *Eur. J. Inorg. Chem.* **2010**, 1763.

for example, to the heterocyclic borazine $(HBNH)_3$ and H_2. The hydrolysis of $H_3B{\cdot}NH_3$ liberates large quantities of H_2 as the hydrogen atoms originate both from H_2O and BH_3 molecules, while NH_3 is left behind together with $B(OH)_3$. Both the thermolysis and hydrolysis are catalyzed by transition metal complexes. Therefore, the adduct $H_3B{\cdot}NH_3$ is discussed as a viable *hydrogen storage material* (see below). The most facile synthesis of $H_3B{\cdot}NH_3$ is from $Na[BH_4]$ and $[NH_4]_2SO_4$ in THF at 40 °C:[72]

$$2\ Na[BH_4] + [NH_4]_2[SO_4] \longrightarrow 2\ H_3B{\cdot}NH_3 + Na_2[SO_4] + 2\ H_2$$

$H_3B{\cdot}NH_3$ is well soluble in water without decomposition.

Ammonia–borane and the related hydrazine–borane have attracted enormous attention in the last 15 years, because such species can in principle act as hydrogen storage.[73] The underlying assumption is that a large proportion of the contained hydrogen (19.6 wt% for $H_3B{\cdot}NH_3$) can be liberated under certain, preferably mild conditions and that the spent fuel can be fully rehydrogenated after usage one way or the other. The closest approach to an economically feasible cycle abstains from a complete thermal dehydrogenation of $H_3B{\cdot}NH_3$ to boron nitride[74] and stops instead at the so-called polyborazylene of composition $(HBN)_n$. The advantage of the liberation of only 2.5 equivalents of H_2 is that polyborazylene reacts readily with hydrazine H_2NNH_2 to regenerate $H_3B{\cdot}NH_3$ in a near quantitative manner.[75] In concert with industrially already established processes – such as the production of hydrazine from ammonia – proof of principle for the full recycling of the employed fuel is provided (Figure 6.13).

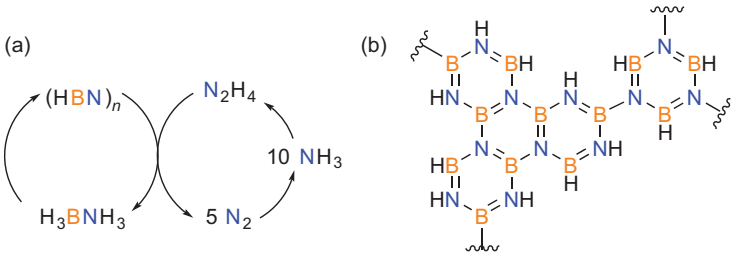

Figure 6.13: (a) Regeneration of polyborazylene $(HBN)_n$ to ammonia–borane $H_3B{\cdot}NH_3$ by treatment with hydrazine H_2NNH_2; (b) depiction of the amorphous polyborazylene structure (both adapted from Sutton et al.).[75]

72 P. V. Ramachandran, P. D. Gagare, *Inorg. Chem.* **2007**, *46*, 7810.
73 A. Staubitz, A. P. M. Robertson, I. Manners, *Chem. Rev.* **2010**, *110*, 4079. N. C. Smythe, J. C. Gordon, *Eur. J. Inorg. Chem.* **2010**, 509.
74 S. L. Suib et al., *Inorg. Chem.* **2011**, *50*, 783.
75 A. D. Sutton et al., *Science* **2011**, *331*, 1426.

When $H_3B{\cdot}NH_3$ is treated with the adduct $BH_3{\cdot}THF$, the liquid aminodiborane(6) $B_2H_5NH_2$ is formed under elimination of H_2. The amino group formally replaces a bridging hydrogen atom of the parent molecule B_2H_6. The aminodiborane(6) reacts with NH_3 in a straightforward manner to give $H_3NBH_2NH_2BH_3$ as colorless crystals (m.p. 62 °C).[76] Apparently, intermolecular dihydrogen bonds (as in $H_3B{\cdot}NH_3$), enabled by the considerable partial charges at H, B and N, account for a much lower vapor pressure than in the isolelectronic and isosteric butane molecule. With sodium in THF at 20 °C, ammonia–borane reacts under evolution of H_2 to give $Na[H_2N{-}BH_3]$, which eliminates $Na[NH_2]$ upon warming to give $Na[H_3B{-}NH_2{-}BH_3]$.[77]

6.10.3 Borazine

Alongside the above-mentioned BN species, a large number of substituted aminoboranes $R_2B{-}NR'_2$ (R = H, organyl, halogen, R′ = organyl) have been prepared. For the formation of the BN bonds, either the condensation of BCl and NH species is employed, or one resorts to a salt elimination reaction, for example, from a BCl species and a lithium amide:

$$R_2B{-}X + Li{-}NR'_2 \longrightarrow R_2B{-}NR'_2 + LiX$$

By this route, for example, 1,3,5-trichloroborazine (m.p. 84 °C) is obtained from BCl_3 and $[NH_4]Cl$ via the elimination of HCl (m.p. 84 °C) and can easily be reduced to the parent borazine by $Li[BH_4]$ or $Na[BH_4]$:[78]

$$3\,BCl_3 + 3\,[NH_4]Cl \xrightarrow[PhCl]{150°C} B_3N_3Cl_3H_3 + 9\,HCl\uparrow$$

$$B_3N_3Cl_3H_3 + 3\,Na[BH_4] \xrightarrow[n\text{-}Bu_2O]{25°C} B_3N_3H_6 + 3\,NaCl + \tfrac{3}{2}\,B_2H_6$$

Most conveniently, borazine is produced from $Na[BH_4]$ and $[NH_4]_2SO_4$ in tetraglyme at 45 °C in the presence of $AlCl_3$ as catalyst.[73] *N*-substituted borazines are obtained accordingly from the corresponding substituted amines or ammonium salts, *B*-substituted borazines as mentioned before by substitution of the chloro substituents of $B_3N_3H_3Cl_3$. Borazine itself is a colorless liquid of aromatic odor (b.p. 55 °C), which is reminiscent of the isosteric benzene (b.p. 80 °C) in several physical constants. The molecular structure is best described by the following resonance formulae:

76 X. Chen, J.-C. Zhao, S. G. Shore, *J. Am. Chem. Soc.* **2010**, *132*, 10658.

77 G. S. Girolami et al., *J. Am. Chem. Soc.* **2010**, *132*, 7254.

78 The crystalline adduct, $Cl_3B{\cdot}NH_3$, is obtained as primary product, which eliminates HCl upon heating to give 1,3,5-trichloro borazine presumably via $Cl_2B{-}NH_2$ and ClB=NH: A. G. Avent et al., *J. Chem. Soc. Chem. Commun.* **1995**, 855.

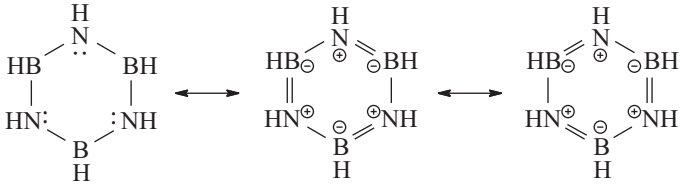

The molecule is perfectly planar in the solid state and the BN distances are near-identical (average 142.9 pm). The inside angles of the ring amount to 117° at the boron atoms and 123° at nitrogen (D_{3h} symmetry). The BN bonds, however, are *strongly polarized* and therefore drastically different from those of benzene in terms of reactivity. Irrespective of the negative formal charges at the B atoms (and positive at the N atoms), the electronegativity difference between B and N results in the accumulation σ electron density at nitrogen. Borazine is therefore much more reactive than benzene. It adds three equivalents of HX (X = Cl, OH or OCH_3) to give *cyclo*-$B_3N_3H_9X_3$, which in case of X = Cl can be converted to the cyclohexane analog *cyclo*-triborazane $B_3N_3H_{12}$ (m.p. 204 °C) by hydrogenation with $Na[BH_4]$. Through the thermolysis of borazine at 380 °C species corresponding to analogs of biphenyl and naphthalene are obtained:

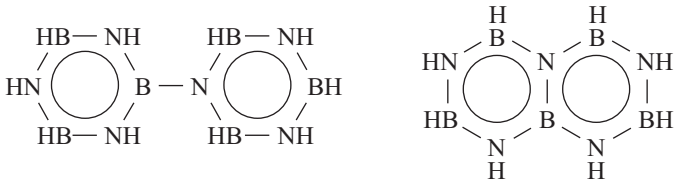

The π bonding in the BN analogs to aromatic hydrocarbons can be rationalized as follows. As in benzene (Figure 7.2), the six $2p_\pi$ AOs of borazine (perpendicular to the ring plane) overlap to a cyclic π system. The linear combination of these orbitals results in three bonding and three antibonding molecular orbitals (Figures 6.14 and 7.2).

In contrast to benzene, however, the π electrons are not equally contributed by all ring atoms, but rather by the N atoms alone. This not only explains a much lower energy gain from π bond formation, but also implies a higher electron density at the N orbitals (larger coefficients in the MO). The weak π bonds are thus polarized in exactly the same manner as the BN σ bonds: the nitrogen atoms carry a negative and the B atoms a positive partial charge, that is, the opposite of the formal charges. Borazine and related species are therefore considered to be significantly less aromatic than benzene.[79] Accordingly, borazine adds three equivalents of HCl in such a way that three new NH and three BCl bonds are formed. Complete hydrolysis with water consequently results in NH_3 and $B(OH)_3$.

79 B. Kiran, A. K. Phukan, E. D. Jemmis, *Inorg. Chem.* **2001**, *40*, 3615.

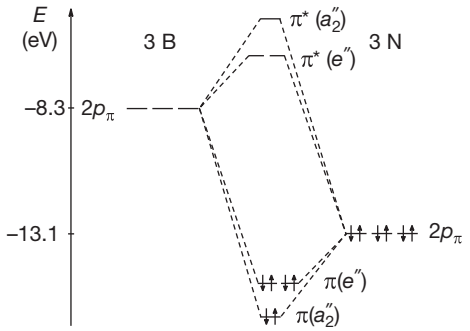

Figure 6.14: Energy terms for the π bonds in planar borazine $B_3N_3H_6$. The molecular orbitals are generated from the interaction of three boron and three nitrogen 2*p* atomic orbitals perpendicular to the ring plane, while all six electrons originate from the N atoms (dative bonding). The HOMO–LUMO energy difference amounts to 7.91 eV.

6.10.4 Boron Nitride

Just like elemental carbon, the isoelectronic boron nitride exists in several principal modifications, which formally correspond to graphite (α-BN) and diamond (β- and γ-BN).[26,80] Hexagonal α-BN (also referred to as h-BN) is formed as a powder on melting of orthoboric acid with urea in an NH_3 atmosphere at 500–950°C and subsequent annealing at 1800 °C:

$$2\ B(OH)_3 + (H_2N)_2CO \longrightarrow 2\ \text{h-BN} + CO_2 + 5\ H_2O$$

In industry, the conversions of B_2O_3 either with coke in a nitrogen atmosphere at temperatures above 1500 °C, with ammonia at 900 °C or with CaB_6 under nitrogen at 1500 °C are also employed for the production of h-BN. Microporous h-BN is generated by annealing of B_2O_3 with guanidine hydrochloride at 1100 °C in a N_2/H_2 atmosphere. Coatings of h-BN are produced by CVD of BCl_3 and NH_3 or through pyrolysis of borazine (pyrolytic BN, p-BN):

$$BCl_3 + NH_3 \xrightarrow{200–1300°C} \text{h-BN} + 3\ HCl$$

As graphite, h-BN consists of planar layers of fused six-membered rings, but the $(BN)_x$ layers are stacked in a different manner (Figure 6.15). Mainly VAN DER WAALS forces are active in keeping together the layers.

The covalent BN distance in h-BN is with 144.6 pm just slightly larger than in borazine. One can therefore equally assume weak coordinative π bonds, which add

80 Q. Weng, X. Wang, X. Wang, Y. Bando, D. Golberg, *Chem. Soc. Rev.* **2016**, *45*, 3989.

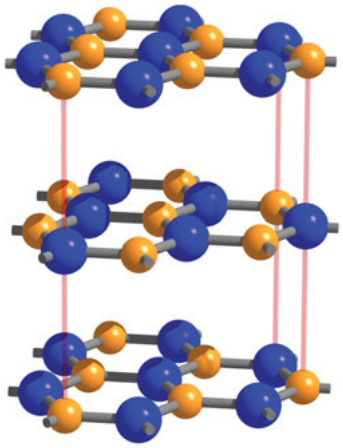

Figure 6.15: Excerpt of the solid-state structure of hexagonal α-boron nitride (h-BN). The planar layers consist of six-membered B_3N_3 heterocycles. The sequence of layers is such that B and N atoms of neighboring layers lie one above the other (ABAB . . .), thus maximizing the electrostatic attraction due to opposing partial atomic charges.

to the very strong σ bonds. This bonding situation leads to an extreme thermal robustness far above 2000 °C. The layer structure results in a mechanical softness of h-BN similar to graphite's; it is therefore employed as high-temperature lubricant.[81] The melting point is approximately 3200 °C. In contrast to graphite h-BN is colorless and an electrical *insulator* with a forbidden zone of about 500 kJ mol^{-1} (ca. 5.2 eV). These differences result from the clearly differing band structures of both materials. While in graphite the band of π orbitals consists of a quasi-continuous sequence of states of which the energetically lower half is filled with electrons (Figure 7.5), the π band of h-BN is split into two subordinate bands due to the differing electronegativities of the B and N atoms. Only the energetically lower band derived from the bonding π MOs (the valence band) is filled with electrons (cf. the energy level diagram of borazine).

By employing suitable micromechanic manipulations such as "peeling", ultrasound or by means of an electron beam, single BN layers can be exfoliated from h-BN, in complete analogy to the preparation of graphene from graphite (Section 7.3.1). By employing appropriate conditions during deposition, it is also possible to directly prepare such single layers or multilayer coatings from boric acid and urea or from ammonia–borane.[82]

As a powder, h-BN is utilized as filler for rubbers and plastics. By hot molding of the powder at 1700–1900 °C in inductively heated graphite molds under nitrogen, an endless variety of extremely heat-resistant workpieces such as crucibles, melting

81 Colorless h-BN is nontoxic and is used in cosmetics such as creams, eye shadow and lipsticks due to it silky gloss.

82 C. N. R. Rao, A. Nag, *Eur. J. Inorg. Chem.* **2010**, 4244. G. R. Whittell, I. Manners, *Angew. Chem. Int. Ed.* **2011**, *50*, 10288

pans, coatings for combustion chambers in rocketry and heat insulation for plasma ovens can be produced, taking advantage of the high tolerance of h-BN for changes in temperature. The material is air-stable up to 1000 °C and a good heat conductor. h-BN is not only thermally very stable, but also chemically rather inert. Nonetheless, various functionalized h-BN materials are accessible by partial cleavage of the polarized π bonds by reactive species such as radicals (e.g., from organic peroxides ROOR).[80] By F_2, h-BN is broken down completely to give BF_3 and N_2 as well as by HF to $[NH_4][BF_4]$. In boiling water, it slowly hydrolyzes to NH_3 and $B(OH)_3$.

As graphite is converted to diamond at high pressure (Section 7.3.2), hexagonal h-BN (maximal density 2.34 g cm^{-3}) can be turned into two modifications of higher density. These transformations are accompanied by a change in coordination number of all atoms from 3 to 4. The coordinative π bonds within the layers are formally replaced by coordinative σ bonds between the now corrugated layers:

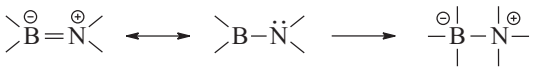

The thus obtained boron nitride either crystallizes as an AB compound in the cubic zinc blende (ZnS) structure (β-BN or c-BN) or in the hexagonal wurtzite structure (γ-BN or w-BN). The phase diagram of BN, however, differs significantly from that of carbon. Under standard conditions c-BN is thermodynamically stable according to more recent investigations. The conversion of h-BN to c-BN, however, is kinetically hindered. Therefore, c-BN is obtained from h-BN at about 1500 °C and 6 GPa pressure; at considerably higher pressures, γ-BN is formed instead. The BN distance of c-BN amounts to 156 pm. At temperatures above 1390 °C, the so-called *inorganic diamond* reconverts to the *inorganic graphite* (h-BN), which thus represents the high-temperature form.[83] Even BN nanotubes have been synthesized in analogy to the carbon nanotubes (Chapter 7.3.4).

Just as diamond (c-C), cubic c-BN (density 3.49 g cm^{-3}) is colorless, electrically insulating and extremely hard, but in addition also air-stable up to temperatures of 1400 °C. The material is therefore used as abrasive and for cutting and drilling equipment under the brand names *Borazon* and *Amborit*. Together with SiC, Si_3N_4 and B_4C, boron nitride belongs to the *nonoxidic ceramic materials*. The extremely good heat dissipation by c-BN and c-C is attributed to lattice vibrations. The high cost of c-BN, however, is limiting its applications to special situations in which thermal resistance is an issue.

Ternary ceramics of the approximate composition BCN and BC_2N have also been reported, which can formally be deduced from c-BN and h-BN by partial replacement of the atoms by C atoms, that is, these materials can be regarded as a solid solution of graphite in h-BN and of diamond in c-BN (with BN, BC, CC and CN

83 V. L. Solozhenko, V. Z. Turkevich, W. B. Holzapfel, *J. Phys. Chem. B* **1999**, *103*, 2903.

bonds).[84] For the preparation, mixtures of urea, boric acid and active charcoal are heated. Graphene-like BCN layers can also be prepared.[82]

6.10.5 Nitridoborates

Nitridoborates[85] contain planar anions of compositions $[BN]^{n-}$ (n = 2–4), $[BN_2]^{3-}$, $[BN_3]^{6-}$, $[B_2N_4]^{6-}$ and $[B_3N_6]^{9-}$, which adopt the following structures in corresponding compounds:

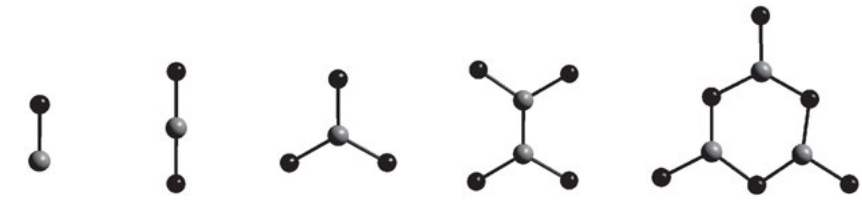

$[BN]^{n-}$ $[BN_2]^{3-}$ $[BN_3]^{6-}$ $[B_2N_4]^{6-}$ $[B_3N_6]^{9-}$

Nitridoborates are formed through strong heating of h-BN with nitrides, azides or amides of alkali and alkaline earth metals. Thermally these compounds are very stable, but under air rapid decomposition occurs. Alkali and alkaline earth metal cations give rise to salt-like species with the linear dinitridoborate anion, which is isoelectronic with the anions $[C_3]^{4-}$, $[CN_2]^{2-}$ and $[N_3]^-$ as well as with the CO_2 molecule. Two phases are known of $Li_3[BN_2]$, which differ by the relative arrangement of cations and anions. α-$Li_3[BN_2]$ is transformed into β-$Li_3[BN_2]$ at 862 °C, which in turn melts at 916 °C.

84 R. Riedel, J. Bill, A. Kienzle, *Appl. Organomet. Chem.* **1996**, *10*, 241.

85 H.-J. Meyer et al., *Z. Anorg. Allg. Chem.* **2000**, *626*, 625 and *Angew. Chem. Int. Ed.* **2002**, *41*, 3322.

7 Carbon

7.1 Introduction

Similar to the other elements of the second row of the Periodic Table, carbon differs in various ways from the heavier congeners in Group 14. The dominant reasons for these differences are the strong bonds with H atoms and the other nonmetals of the second row, that is, with B, C, N, O and F. Of particular importance is the competitive strength of double and triple bonds to carbon in comparison to the corresponding number of single bonds. The number of carbon compounds is consequently much higher than that of any other element except hydrogen. It is therefore justified to treat this class of compounds separately as *Organic Chemistry*. The special bonding situations possible at the C atom confer properties to most organic species that are distinctly different from those of other nonmetal compounds. This will be elaborated upon later on.

Traditionally, all carbon species without CH bonds belong to the realm of *Inorganic Chemistry*. This includes, for instance, the allotropic modifications and a few simple compounds of carbon such as halides, oxides, oxoacids and other chalcogenides as well as nitrides. Moreover, organic residues play an important role in the inorganic chemistry of nonmetals as substituents. Substances of that sort are referred to as *organoelement compounds* as a subgroup of the organometallic species. Once again, these classifications demonstrate that the division of molecular chemistry in inorganic and organic chemistry is arbitrary, but still upheld mainly due to historical reasons.

Naturally occurring carbon compounds are the carbonates (*limestone* and *dolomite*), graphite and diamond, coal and oil, natural gas, including shale gas and methane hydrate,[1] as well as numerous other organic species of biological origin (biomass). Biogas contains up to 70% of CH_4. This is complemented by CO_2 in the air (0.041% as of April 2018) and in water, especially the oceans. Despite the small CO_2 concentration of currently 410 ppm, the atmosphere contains about $0.79 \cdot 10^{12}$ t, the hydrosphere estimated $38 \cdot 10^{12}$ t and the lithosphere about $66 \cdot 10^{15}$ t of carbon. Notably, the CO_2 concentration in the atmosphere of 200 years ago was only 280 ppm. Limestone is the second most abundant mineral at the Earth's surface after quartz.

1 Natural gas extracted in Northern Germany, for example, near the town of Söhlingen, consists of >90% CH_4 alongside 1% CO_2, a few percent N_2, small concentrations of other hydrocarbons up to C_{23} and finally traces of Hg. In addition, natural gas is always saturated with water. Other Northern German sources provide a natural gas with an H_2S content of up to 35% ("sour gas"). After removal of H_2S, H_2O, higher hydrocarbons and Hg, natural gas is an important energy carrier. In Germany, the natural gas piping system has a total length of more than 320,000 km (200,000 miles).

https://doi.org/10.1515/9783110578065-008

Just like other nonmetals, carbon is a part of a global biogeochemical cycle, which has been heavily influenced by mankind in more recent history.[2] For instance, transport and logistics have used more than $4.4 \cdot 10^9$ t crude oil in 2008 alone. The by far largest part of crude oil is converted to other forms of energy by combustion (93% including transport, heating and electricity), only 7% are needed for chemical syntheses.

Natural carbon consists of 98.89% of the isotope ^{12}C with a nuclear spin of $I = 0$. For NMR spectroscopy, the small content of ^{13}C (1.11%; $I = ½$) is thus essential. The radioactive isotope ^{14}C occurs in traces and is a β-emitter with a half-life of 5570 years. The ^{14}C isotope is generated by cosmic radiation producing thermal neutrons in the atmosphere, which in turn collide with ^{14}N to give ^{14}C and ^{1}H. The thus formed carbon atoms are instantly oxidized to $^{14}CO_2$, which is assimilated by the photosynthesis of green plants. All living organisms therefore share a constant and defined concentration of ^{14}C until their death, from which moment on it declines by radioactive decay. This circumstance allows for the determination of the age of organic material (*carbon clock*). By means of carbon dating, the age of items can be determined up to 50000 years. In order to increase accuracy, a correction for the not quite constant solar activity during this period has to be applied. Practically, all biomass on the Earth as well as coal, oil and natural gas stem from the reduction of CO_2 to carbohydrates by photosynthesis under concomitant release of oxygen by cleavage of water (see Section 11.1.1). The oxygen ends up in the atmosphere and dissolved in ocean water, but also in the weathering products of original sulfide minerals that are turned into oxides and sulfates.

7.2 Bonding Situation in Group 14

Of the elements of Group 14, carbon, silicon and germanium are typical nonmetals. The latter two, however, already show semiconductor properties in the solid state and the higher homologues tin and lead are metals.[3] The electronic configuration of the carbon atom is $2s^2p_x^1p_y^1$ (^3P state). As the energy difference between the ground state and the excited ^5S state ($2s^1p_x^1p_y^1p_z^1$) is only about 4 eV (386 kJ mol^{-1}), all four valence orbitals engage in the covalent bonds in most carbon species. According to MO theory, however, it is unnecessary to promote valence electrons to an energetically higher state, let alone to hybridize atomic orbitals. Quite the contrary, the vast majority of stable molecules can be readily rationalized by analysis of the electronic ground state (Section 2.4).

2 H. Pütter, *Chem. unserer Zeit* **2013**, *47*, 184. A. Körtzinger, *Chem. unserer Zeit* **2010**, *44*, 118. F. J. Millero, *Chem. Rev.* **2007**, *107*, 308.

3 This distinction is – as noted before – mostly arbitrary: graphite does show many of the hallmarks of a metal (e.g., conductivity), while α-tin is nonmetallic in most regards.

The **coordination number** of carbon in its compounds adopts all values between 1 and 8, although 3 and 4 clearly dominate. Examples include:

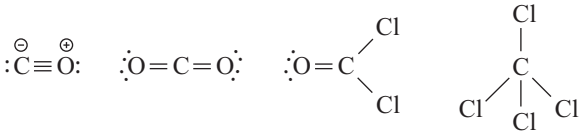

Coordination numbers higher than 4 are realized in carboranes and certain organometallic species such as hexamethyl dialuminum Me_6Al_2, in which the organic group assumes a bridging position:

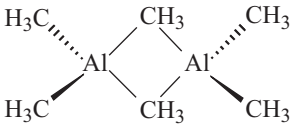

$\text{angle}_{CAlC} = 110°$ (in the ring)
$\text{angle}_{AlCAl} = 70°$

The coordination sphere of aluminum is distorted tetrahedral, while the bridging C atoms are pentacoordinate. Coordination numbers 5–8 are also encountered in certain transition metal clusters, in which a C atom is incorporated into a metallic cage. For instance, the ruthenium carbonyl complex $[Ru_6C(CO)_{17}]$ consists of an octahedral Ru_6 cluster with a carbon atom at the center. The cobaltate dianion $[Co_8C(CO)_{18}]^{2-}$ contains a square-antiprismatic metal cluster with an interstitial carbide ion. Charge and oxidation numbers of these *carbidic C atoms* are poorly defined and open to speculations.

According to the PAULING scale, the carbon atom is assigned an **electronegativity** of $\chi_P = 2.50$ (Table 4.8). In general, this value does not allow for the formation of ionic bonds even with strongly electronegative nonmetals, for instance, under formation of a hypothetical cation C^{4+}. Consequently, CF_4 and CO_2 are not ionic, but rather molecular gases with covalent bonds to carbon. Only the cations of type $[R_3C]^+$ with just one positive charge are isolable in the form of carbocation salts (*carbenium ions*).[4] Examples include protonated carbonic acid $[C(OH)_3]^+$, the trihalocarbenium ions $[CX_3]^+$ (X = Cl, Br, I) and the tris(azido)carbenium ion as the hexachlorostibate salt $[C(N_3)_3][SbCl_6]$.

On the other hand, the C atom does form negatively charged *carbides* with strongly electropositive metals, which *formally* contain anions such as C^{4-} (methanide, isoelectronic with N^{3-}, O^{2-}, F^- and Ne),[5] $[C_2]^{2-}$ (acetylide, isoelectronic with N_2 and CO)[6] or $[C_3]^{4-}$ (allenide, isoelectronic with CO_2):[7]

4 For his research on carbenium ions (carbocations), GEORGE A. OLAH (1927–2017) was awarded the NOBEL prize in chemistry in 1994.

5 A. Maercker, *Angew. Chem.* **1992**, *104*, 598, and cited literature.

6 S. Hemmersbach, B. Zibrowius, U. Ruschewitz, *Z. Anorg. Allg. Chem.* **1999**, *625*, 1440. In industry, $Ca[C_2]$ is produced from $Ca[CO_3]$ and coke in an electric arc furnace.

7 $Ca_3[C_3]Cl_2$ is generated at 900 °C from Ca, $CaCl_2$ and graphite: H.-J. Meyer, *Z. Anorg. Allg. Chem.* **1991**, *593*, 185.

C^{4-}: Li_4C, Be_2C, Al_4C_3 $[C_2]^{2-}$: $K_2[C_2]$, $Ca[C_2]$ $[C_3]^{4-}$: $Ca_3[C_3]Cl_2$

Calcium carbide $Ca[C_2]$ crystallizes in a tetragonally distorted NaCl structure with the $[C_2]^{2-}$ aligned in parallel on the anion positions. $Ca_3[C_3]Cl_2$ formally contains the nearly linear ion $[C_3]^{4-}$ surrounded by countercations next to two chloride anions. The bonds in the crystalline carbides Li_4C, Be_2C and Al_4C_3, as well as in numerous transition metal carbides[8] are strongly polar but predominantly covalent, as multiply charged anions such as C^{4-} would spontaneously loose electrons to monocharged species in order to reduce COULOMB repulsion (Section 2.1.3).

Negatively polarized C atoms are also present in certain *carbon complexes*, in which LEWIS bases are connected to an electron-deficient C atom as donating ligands. For example, the carbodiphosphorane $Ph_3P{=}C{=}PPh_3$, which is formally a diphosphaallene, is now regarded as bis-ylidic structure based on the PCP angle, which varies between 130° and 180° depending on the solvent from which it crystallized:[9]

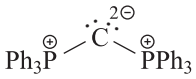

Analogous considerations apply to the complex $Ph_3PCCCPPh_3$.[10]

Ions of the type $[R_3C]^-$ are called *carbanions*. In general, however, it should be noted that the tendency of the C atom to engage in ionic bonding is not very pronounced. Quite the contrary, of particular importance are in fact the nonpolar to weakly polar CC and CH bonds, which form the backbone of most organic species. The CC σ bond shows the second highest bond enthalpy of all homonuclear single bonds between two nonmetals (after H_2; compare Figure 4.2). Instead of ionic bonds, C atoms readily form chains and rings and the corresponding compounds are typically chemically robust. Similarly, the CH bond is characterized by a high bond enthalpy and is only weakly polar. Due to these circumstances, alkanes and the derived alkyl residues (containing only CC and CH single bonds) are particularly inert. Alkanes are defined by the general formula C_nH_{2n+2}, (e.g., CH_4, C_2H_6) and alkyl groups by $-C_nH_{2n+1}$ with one hydrogen atom less. The bonding situation in CH_4 has been described in Section 2.4.10.

The tetracoordinate C atom is distinguished from most other nonmetals inasmuch as that it does neither feature energetically accessible vacant orbitals, nor nonbonding electron pairs (lone pairs). The attack of nucleophilic and electrophilic reagents is therefore equally difficult. In addition, the small C atom (e.g., in compounds such as

8 W. Lengauer, A. Eder, *Encycl. Inorg. Chem.* **2005**, *2*, 674; H. Tulhoff, *Ullmann's Encycl. Ind. Chem.* **1986**, *A5*, 61.

9 P. J. Quinlivan, G. Parkin, *Inorg. Chem.* **2017**, *56*, 5493.

10 H. Schmidbaur, A. Schier, *Angew. Chem. Int. Ed.* **2013**, *52*, 176.

CF_4) is perfectly shielded against the attack of any reagent, while larger Group 14 atoms (as in SiF_4) are far less shielded. This is one of the most pertinent reasons for the special properties of saturated carbon species. It readily explains, for instance, why SiF_4 and $SiCl_4$ are rapidly hydrolyzed at 20 °C according to

$$SiX_4 + 2\,H_2O \longrightarrow SiO_2 + 4\,HX$$

whereas CF_4 and CCl_4 are perfectly stable against H_2O at this temperature despite the fact that the analogous reactions to CO_2 and HF or HCl are thermodynamically viable ($\Delta G^o < 0$). Only at higher temperatures, CF_4 starts to react with water to COF_2 and HF.

The ability of the C atom to form thermodynamically competitive multiple bonds is generally known (see CO and CO_2; Chapter 4). In particular, the atoms C, N, O and S are suitable partners to form double and triple bonds with carbon, but given the right conditions also Si, Ge, P, As, Se and Te. With a larger covalent radius of the partner atom, the trend to trade the double bond for two single bonds by spontaneous oligo- or polymerization increases. Examples for compounds with p–p π bonds are:

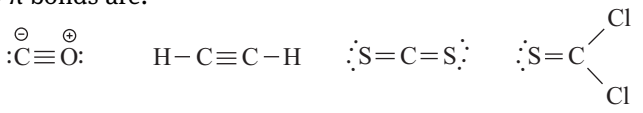

carbon-monoxide — ethyne — carbon-disulfide — thiophosgene

All four compounds shown are thermodynamically unstable but persist at standard conditions as the activation barrier for the transition to stable species is too high for a spontaneous reaction at 25 °C.[11] Please note, however, that graphite with its σ and π bonds is thermodynamically more stable than diamond, which only contains σ bonds (see below).

Another peculiarity of carbon chemistry is the far-reaching delocalization of π electrons in *aromatic systems* such as benzene (C_6H_6) or the *cyclo*-pentadienide anion $[C_5H_5]^-$ (Figure 7.1). These planar molecules are of high symmetry (D_{6h} and D_{5h}, respectively) as all CC bonds are equivalent. If the plane of the molecule is defined as the *xy*-plane in Cartesian coordinates, the σ bonds of the C atoms can be constructed with the atomic orbitals 2*s* and $2p_xp_y$ (cf. BF_3; Section 2.4.8).

11 The respective more stable products are graphite and CO_2, benzene, polymeric CS_2 and dimeric $CSCl_2$. Even ethylene C_2H_4 is thermodynamically unstable regarding its polymerization to polyethylene (PE).

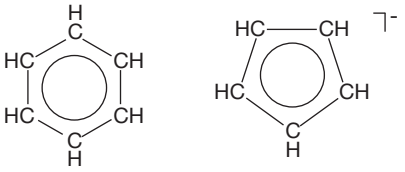

Figure 7.1: Benzene (left) and the *cyclo*-pentadienide anion (right) as examples for Hückel aromatic species with equivalent CC and CH bonds. Circles represent the delocalization of six π-electrons.

The p_z orbitals of the C atoms, perpendicular to the plane of the molecule, overlap with each other so that molecular orbitals of π symmetry result, which extend over the entire ring. The ring plane constitutes a nodal plane for these MOs. For the graphical representation of the in-phase or out-of-phase overlap, it is convenient to project the π orbitals into this plane, which depicts the *2p* orbitals as filled and empty circles rather than the three-dimensional dumbbells. In case of six C atoms, six singly occupied *2p* orbitals are to be combined, which gives a set of six π MOs (Figure 7.2). Symmetry considerations require that two doubly degenerate MOs are part of this set. The energy of the MOs increases with the number of nodal planes. Figure 7.3 shows the energy term diagram for the π MOs of benzene. The three bonding MOs are occupied by the six electrons, which results in unusually strong CC bonds (CC distance 140 pm).

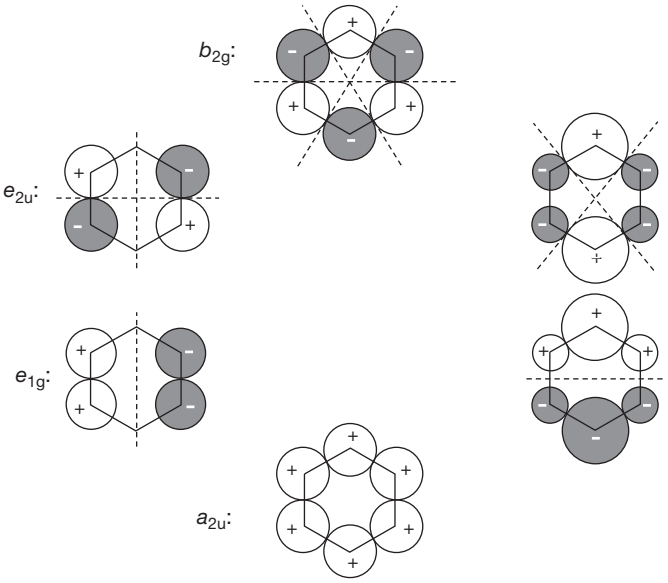

Figure 7.2: The six π molecular orbitals of benzene. The lobes above the plane of the $2p_\pi$ orbitals of the six C atoms are projected into the molecular plane along a perpendicular axis. Six orthogonal π MOs are generated by linear combination of the six AOs. The energy of the MOs increases with the number of nodal planes (shown as dashed lines). The a_{2u} and e_{1g} levels are filled with the six electrons (see Figure 7.3).

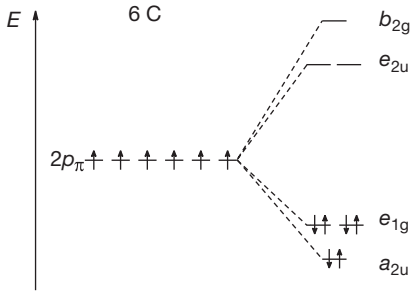

Fig. 7.3: Energy-level diagram of the π molecular orbitals of the benzene molecule. All π electrons reside in bonding MOs on two different energy levels (a_{2u} and e_{1g}).

As the energetic splitting of the π orbitals is smaller than that of the σ orbitals, the e_{1g} level constitutes the HOMO while the e_{2u} is the LUMO of the benzene molecule. The HOMO–LUMO energy difference amounts to 6.55 eV.

If a planar ring of *identical atoms* contains six or, more generally, $2n + 2$ (n = 0, 1, 2, ...) π electrons, it constitutes an aromatic system (HÜCKEL aromaticity). HÜCKEL aromatics are also known for other nonmetals than carbon. Simple examples include the square ions $[S_4]^{2+}$, $[Se_4]^{2+}$ and $[Te_4]^{2+}$ (Section 12.5). In structural formulae, the delocalization of π electrons is represented by a circle in which the number of π electrons can be indicated if desired. Heterocycles with aromatic character related to benzene are pyridine (C_5H_5N, azabenzene), silabenzene (C_5SiH_6) and phosphabenzene (C_5H_5P):

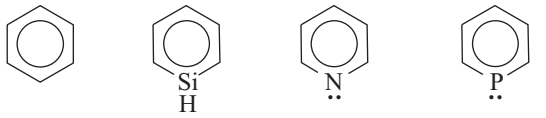

benzene — sila-benzene — pyridine — phospha-benzene

The π electrons of the three heterocyclic species are less perfectly delocalized across all ring atoms since the electronegativities of carbon, on the one hand, and silicon, nitrogen and phosphorus, on the other hand, differ substantially (Table 4.8). Moreover, due to the lower symmetry (C_{2v}) the degeneracy of the benzene MOs is lifted in the heterocyclic derivatives.

7.3 Carbon Allotropes

Under standard conditions, pure carbon exists as two well-investigated polymeric allotropes, namely *graphite* and *diamond*.[12] Both occur as minerals but can also be

12 A. Krueger, *Carbon Materials and Nanotechnology*, Wiley-VCH, Weinheim, **2010**. K. H. Büchel, H.-H. Moretto, D. Werner (eds.), *Industrial Inorganic Chemistry*, 2nd ed., Wiley-VCH, Weinheim, **2008**.

prepared synthetically. Of all solid elements these two materials constitute the softest and hardest. Further elemental modifications have been produced in the laboratory. The cage-like carbon molecules C_n ($n > 20$) are collectively referred to as *fullerenes*. Structurally related to graphite and the fullerenes are *graphene* and the carbon nanotubes (CNTs), which as novel materials with intriguing properties are produced on a 1000 t scale. The carbon-rich products *coal, coke, carbon fibers* and *carbon black* are of highest technological importance.

7.3.1 Graphite and Graphene

Graphite is the thermodynamically stable carbon modification under standard conditions (density 2.22 g cm^{-1}). The structure consists of planar layers of fused six-membered rings. A single layer is referred to as *graphene* in analogy to polycyclic aromatic species such as anthracene or phenanthrene. Within the layers the atoms are bonded by σ and π bonds, whereas in between layers only VAN DER WAALS dispersion forces are active (Figure 7.4).

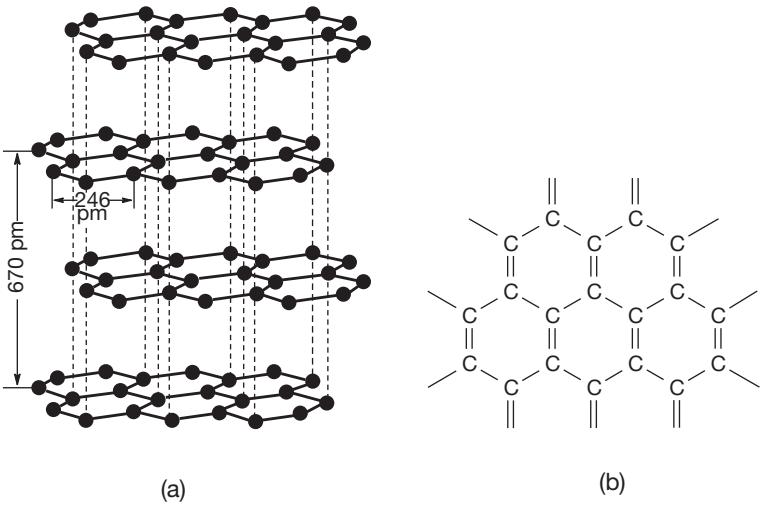

Figure 7.4: (a) Excerpt from the structure of hexagonal graphite; (b) bonding situation in individual planar layers depicted as one of several resonance structures of the delocalized π bonds. The shortest nuclear distances amount to 141.5 pm.

In the layers of graphite, each C atom is surrounded by three nearest neighbors in an equilateral triangle. The valence orbitals 2*s*, $2p_x$ and $2p_y$ containing three of the four valence electrons form the σ framework. Consequently, the angles between the bonds are 120°. The fourth electron resides in the $2p_z$ orbital, which is perpendicular

to the plane of the graphene layer and thus of π symmetry. These p_π orbitals overlap with one identical orbital at each of the three neighboring atoms.[13] In this way, molecular orbitals result that extend throughout the entire graphene layer. The resonance structure in Figure 7.4 illustrates that formally two π bonds are present per cyclic C_6 unit. In reality, however, all CC bonds are completely equivalent. The CC distance is with d_{CC} = 141.5 pm slightly larger than in benzene (d_{CC} = 140 pm). The edges of native graphene layers are highly reactive and rapidly saturated presumably by hydrogen atoms and OH groups.

Ordinary graphite crystallizes in a hexagonal structure with the layers stacked in the ABAB ... sequence shown in Figure 7.4a.[14] The black color of graphene and the good electrical conductivity within the layers are due to the easily excitable and very mobile (within their layer) π electrons, which form a *two-dimensional electron gas*. The overlap of a near infinite number of π orbitals results in what is called a valence band (bonding MOs) and a conductance band (antibonding MOs) which overlap slightly. Therefore, graphite is a pretty good *metallic conductor*, although the conductivity strongly depends on the lattice orientation: it is five orders of magnitude better along the graphene planes than perpendicular to them. In Figure 7.5, the *density of states* (DOS) of graphite is shown. Although there is a minimum at the FERMI level (highest occupied level at 0 K; dotted line), the DOS is continuous without band gap.

The distance between the graphene planes is 335 pm, which indicates VAN DER WAALS-type interaction (Chapter 3). The weak forces between the layers result in a facile fission of graphite crystals parallel to the hexagonal planes and allow for the application of graphite as a lubricant. In addition, graphite is used for the production of high-temperature bricks and for heat-resistant furnace and nozzle linings. Its high electrical conductivity is exploited in electrodes for arc furnaces and batteries. The best-known application of graphite is probably that as a component of pencil mines.

Natural *deposits* of graphite are found in China, Korea, Canada and Madagascar, but also in Germany and Austria. Synthetic graphite is produced according to the ACHESON process from pulverized petroleum coke (or anthracite), which is mixed with tar to a malleable doughy mass. The rods cast from this mass are initially burned at 800–1300 °C (coked) and then heated electrically to 3000 °C, which results in the crystallization of the previously amorphous carbon (*graphitization*). By thermal decomposition of hydrocarbons at 800 °C, pyrolytic graphite and glassy carbons are produced under H_2 elimination (HOPG, *highly oriented pyrolytic graphite*).

13 The bonding situation is similar to those in the molecules BF_3 (Section 2.4.8) and benzene (see above).

14 Rhombohedral graphite with the layers stacked in an ABC sequence is also known.

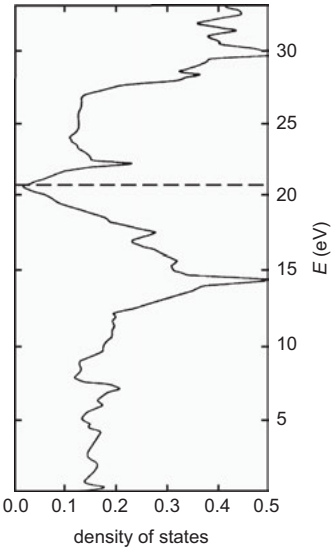

Figure 7.5: Density of states of graphite (horizontal axis: number of states per eV and C atom). The dashed line represents the FERMI level, that is, the highest occupied level at 0 K. Valence and conductance bands are not separated by a band gap.

7.3.1.1 Graphene

Through the effect of ultrasound or mechanically with an adhesive tape, single layers of graphite can be exfoliated.[15] Another method of production is the chemical vapor deposition (CVD) by pyrolysis of methane, ethylene, acetylene or benzene on a metal substrate. With these methods, high-purity graphene almost free of defects is accessible in minute amounts. Macroscopic quantities are obtained through the action of ultrasound on graphite oxide (Section 7.4.1) as exfoliation step and subsequent reduction with gaseous hydrazine N_2H_4 providing reduced graphene oxide (rGO). In this process, however, a product with numerous defects (e.g., pentagon–heptagon pairs or residual oxygen) is obtained. In any case, the depicted graphene structure in Figure 7.4b must be regarded as an idealized representation only.

It is differentiated between monolayers and multilayers (<10) of graphene. The dimensions of a single layer are typically within several microns (about 100,000 carbon atoms). For the rediscovery[16] and physical characterization of this "miracle material" during the first decade of the millennium, the NOBEL prize in physics was awarded in 2010 to ANDRE GEIM and KOSTYA NOVOSELOV.[17] Yearly, more than 10000

15 M. Sharon, M. Sharon (eds.), *Graphene – An Introduction to the Fundamentals and Industrial Applications*, Wiley, Hoboken, **2015**. Topical issue on graphene, *Acc. Chem. Res.* **2013**, 46, issue 1–3. S. Guo, S. Dong, *Chem. Soc. Rev.* **2011**, *40*, 2644. K. Balasubramanian, M. Burghard, *Chem. unserer Zeit* **2011**, *45*, 240. D. R. Dreyer, R. S. Ruoff, C. W. Bielawski, *Angew. Chem. Int. Ed.* **2010**, *49*, 9336.

16 The long history of graphene from a laboratory curiosity to a *high-tech* material is described by H.-P. Boehm, *Angew. Chem. Int. Ed.* **2010**, *49*, 9332.

17 A. K. Geim, *Angew. Chem. Int. Ed.* **2011**, *50*, 6966; K. S. Novoselov, *ibid.* 6986.

publications are published on this topic, and in 2013, the European Union issued a 10-billion-Euro research program on graphene for a duration of 10 years.

Graphene layers are of extraordinary mechanical stability, but at the same time flexible and highly electrically conductive. They are therefore suitable as electrode material for fuel cells, capacitors, batteries, solar cells, transistors and sensors. The chemical modification and functionalization of graphene is a "hot" topic of organic chemistry.[15,18] For instance, the reduction with lithium in water or liquid ammonia (BIRCH reduction) affords polyhydrogenated graphene, also referred to as *graphane*.

7.3.2 Diamond

Figure 7.6 shows the phase diagram of carbon: only at pressures above 10 GPa, diamond is the thermodynamically stable modification.[19] This can be attributed to the much higher density of diamond (3.51 g cm^{-1}) in comparison to that of graphite (2.22 g cm^{-1}). Gaseous carbon exists only at temperatures above 4000 K and very low pressures (not shown in Fig. 7.6).

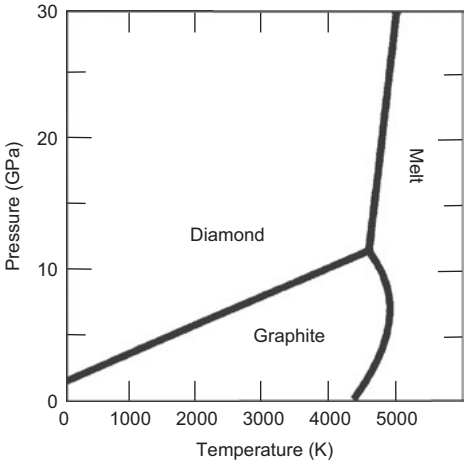

Figure 7.6: Schematic phase diagram of carbon.

For the transformation of graphite to diamond, it can either be exposed to high static pressures, to shockwaves or irradiated with high-energy electrons or ions.

18 K. S. Kim et al., *Chem. Rev.* **2012**, *112*, 6156.

19 U. Schwarz, *Chem. unserer Zeit* **2000**, *34*, 212 (richly illustrated).

The technical *synthesis of diamonds* is generally carried out in a melting process. In certain liquid metals and metal alloys, the solubility of graphite under pressure is higher than that of diamond, for example, in Fe, Co, Ni and mixtures of these metals. For instance, about 4.0 wt% of graphite, but only 3.6 wt% of diamond are soluble in liquid nickel at 1800 K and 9 GPa. From a saturated solution of graphite in the liquid metal, diamond therefore crystallizes preferentially. In this manner, crystals with edges of up to 1 mm are obtained, albeit with trace impurities of the employed metal. Through fractional crystallization from liquid Ni, water clear crystals with edges of up to 1 cm can be obtained.[20] For modern processes, a Fe–Co melt is employed, which contains some titanium and copper and allows for the fabrication of clear diamond crystals of up to 9 mm diameter.

Natural diamonds originated from crystallization of silicate melts at high pressures.[18] The necessary pressure requires that the formation of diamonds occurs at depths of more than 140 km. The diamonds thus formed are transported to the surface through volcanism, where they are liberated by the weathering of the surrounding rock and found inter alia in river sediments. Predominantly, however, diamond-containing rocks are mined over- and underground and processed accordingly. About 20 t of diamonds worldwide are extracted annually. Major locations include Southern Africa, Russia (Eastern Siberia) and Australia.

The production of synthetic diamonds exceeds the amount of extracted natural diamonds by far. The mass (the "weight") of diamonds used in jewelry is given in carat: 1 carat = 0.2 g. The decisive factors for the quality of so-called *brilliants* are the cut, the color, the weight and the purity regarding inclusions. About 98% of natural diamonds contain up to 0.2% of nitrogen, which results in strong absorptions in the UV and the IR. Very pure diamonds are transparent down to 225 nm. A rare variety in nature is boron-containing diamonds, which show a bluish color and are p-semiconducting. *Carbonados* are natural polycrystalline diamonds, which often contain graphite and other impurities and are thus black in color. About 80% of all natural and synthetic diamonds are used for production of tools.

The *diamond structure* consists of a three-dimensional network of carbon atoms (Figure 7.7).[21] Each atom is surrounded in a tetrahedral fashion by four nearest neighbors connected by σ bonds similar to those in the CH_4 molecule (Section 2.4.10). This perfectly cross-linked bonding mode leads to the circumstance that diamond is the hardest material known, in sharp contrast to the soft graphite. Pure diamond crystals are colorless and electrically insulating.

The *thermal conductivity* of diamond is much higher than that of copper or silver, in particular at low temperature! Heating of diamond in air at 600–800 °C

20 M. Takano, Y. Takeda, O. Ohtaka, *Encycl. Inorg. Chem.* **2005**, *3*, 1785.

21 Meteorites also contain hexagonal diamond crystals with a structure corresponding to wurtzite. The six-membered rings therein show both chair and boat-like conformations: J. Donohue, *The Structures of the Elements*, Wiley, New York, **1974**.

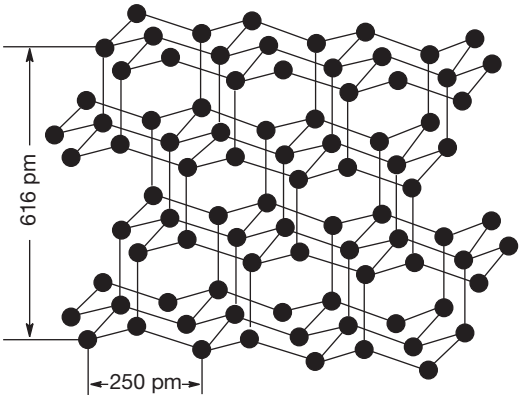

Figure 7.7: Excerpt from the structure of cubic diamond. Each atom is coordinated in a perfectly tetrahedral fashion. The structure formally consists of six-membered rings in a chair conformation. All internuclear distances are 154.5 pm.

leads to its combustion to CO and CO_2. On even stronger heating under exclusion of air it is transformed to graphite (at about 1500 °C). The high activation barrier of this reaction, however, impedes the spontaneous transformation of diamonds to the thermodynamically more stable graphite modification under standard conditions. Diamonds resist the attack of acids; bases react with diamond only above 500 °C. Nowadays, lasers are used for the cutting of diamonds although the more time-intensive traditional techniques with diamond dust or even softer abrasives are still employed in the jewel industry.

Cubic structures of the diamond-type are also found in the stable modifications (under standard conditions) of silicon, germanium and gray tin (α-Sn). In contrast to diamond, which is an insulator, Si and Ge are inherent semiconductors, when sufficiently purified by zone melting or other techniques. This means that they show a weak electrical conductivity strongly increasing with temperature. Diamond becomes a semiconductor only at very high temperatures, which is related to the size of the *forbidden zone* (band gap) between the valence and the conductance bands, which decreases from carbon to tin. From the overlap of the 2*s* and 2*p* orbitals of neighboring carbon atoms, bonding and antibonding molecular orbitals result. The bonding MOs of a diamond crystal constitute the valence band, and the antibonding MOs form the energetically much higher conductance band. As the valence band is completely filled with electrons, electrical conductivity is only possible when some of the electrons are excited to the otherwise empty conductance band. The necessary energies (in kJ mol^{-1}) are 530 for diamond, 108 for Si, 64 for Ge and only 8 for α-Sn. In case of diamond, this high energy can only be achieved by irradiation with X-rays. In contrast, for Si and Ge simple heating is sufficient to result in a substantial reduction of the electrical resistance. Through *doping*, for example, with boron, even diamonds can be rendered electrically conductive at 25 °C. The DOS of diamond is displayed in Figure 7.8.

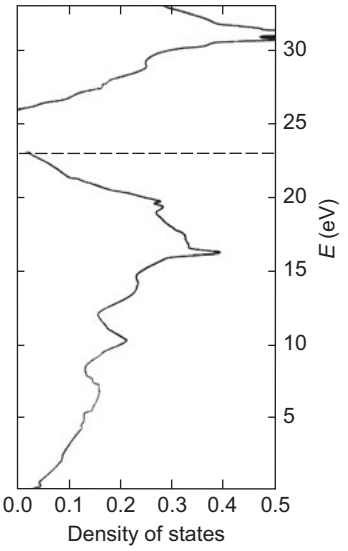

Figure 7.8: Density of states of diamond (horizontal axis: number of states per eV and C atom). The dashed line represents the Fermi level, that is, the highest occupied level at 0 K. Valence and conductance bands are now separated by a band gap of 5.5 eV, in contrast to graphite (Figure 7.5).

Diamond can also be deposited from the gas phase from a mixture of a few percent of hydrocarbons in dihydrogen, for example, thermally at 2000–2800 °C or by plasma treatment at a pressure of 1–10 kPa. The alkyl radicals generated through homolytic cleavage of CH bonds by collision with hydrogen atoms maintain their completely saturated nature due to the large excess of hydrogen. Under these conditions, the C-centered radicals react under formation of CC bonds, giving rise to the growing sp^3 network of diamond:[22]

$$CH_4 + H^\bullet \longrightarrow CH_3^\bullet + H_2$$

$$2\,CH_3^\bullet \longrightarrow C_2H_6$$

$$C_2H_6 + H^\bullet \longrightarrow C_2H_5^\bullet + H_2 \Longrightarrow \text{diamond}$$

A dense diamond coating is grown on a suitably heated substrate (500–1000 °C; e.g., Ti or W), thus modifying the chemical and physical properties of the surface to resemble that of diamond (CVD). In this manner, the coating of even very complex three-dimensional objects such as mechanical tools is possible.

Industrial diamonds are utilized for production of tools, for example, for turning, drilling, cutting of profiles, drawing of wires and as material for bearings.

22 B. Dischler, C. Wild (ed.), *Low-Pressure Synthetic Diamond*, Springer, Berlin, **1998**. K. Kohse-Höinghaus, *Chem. unserer Zeit* **1998**, *32*, 242.

7.3.3 Fullerenes

The fullerenes are a class of compounds consisting of molecules of the type C_n. For certain even values of $n \geq 20$ stable, spherical or elliptical cages are formed.[23] The best-known molecule of this sort is C_{60} or [60]fullerene which is structurally closely related to a classical football (soccer ball in the USA): 60 carbon atoms are located at the corners of 12 equilateral pentagons and 12 equilateral hexagons (Figure 7.9). In contrast to diamond and graphite, fullerenes are soluble in certain organic and inorganic solvents, which facilitate the chemical derivatization enormously. Alongside C_{60} ("Buckminster fullerene"), the most prominent species isolable in pure form are C_{70}, C_{76}, C_{80}, C_{82} and C_{84}.[24] Fullerenes consist of carbon atoms exclusively; they are carbon allotropes by definition.

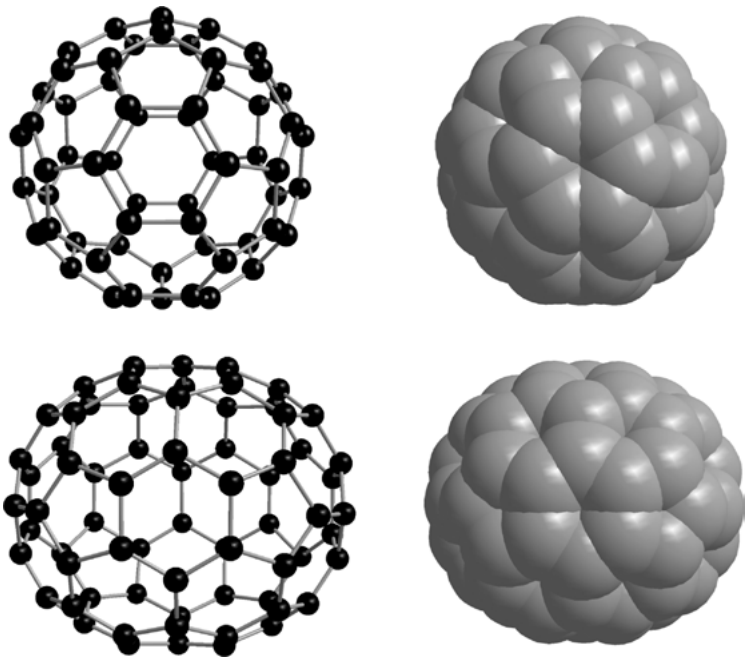

Figure 7.9: Molecular structure of fullerenes C_{60} (above; I_h symmetry) and C_{70} (below; D_{5h} symmetry) in the solid state.

23 A. Hirsch, M. Bettreich, *Fullerenes – Chemistry and Reactions*; Wiley-VCH, Weinheim, **2005**. F. Langa, J.-F. Nierengarten, *Fullerenes – Principles and Applications*, RSC, Cambridge, **2007**.

24 For the discovery of fullerenes, the NOBEL prize in Chemistry in 1996 was awarded to the following authors: R. F. Curl, *Angew. Chem. Int. Ed.* **1997**, *36*, 1566; H. W. Kroto, *ibid.* 1578; R. E. Smalley, *ibid.* 1594.

7.3.3.1 Preparation

Fullerenes of various sizes are contained in the soot-like product, which is formed on evaporation of graphite in an electric arc under helium and subsequent condensation of the vapors on a cold surface. Helium with its excellent heat dissipation properties is predominantly needed for cooling the vapor. Different heating sources such as through electrical resistance, laser irradiation or high-frequency plasma can also be applied for the evaporation of graphite. Graphite is transferred to the gas phase as small molecules such as C_2, which react with larger agglomerates upon cooling. The resulting mixture of carbon molecules condenses in the colder parts of the apparatus, extracted with suitable solvents such as toluene and finally fractioned by liquid chromatography.[25] By crystallization of the different fractions, the fullerenes (e.g., C_{60} and C_{70}) are obtained in purities above 98%. Even larger C_n clusters can be isolated from such mixtures, albeit in small yield (isolation by preparative reversed-phase HPLC). C_{60} and C_{70} are soluble in hexane, CH_2Cl_2, CS_2 and toluene.

Nowadays, fullerene mixtures are produced on a ton scale through incomplete combustion of hydrocarbons in a strongly soot forming flame at approximately 1500 °C and under reduced oxygen pressure (20 mbar). The ratio of C to O in the gas flow is about 1 and 10% argon is added for dilution. With this method, fullerenes have become relatively inexpensive commodities for research and applications.

7.3.3.2 Structures

As some fullerenes exist in several isomers, the symmetry of the cage is typically indicated for identification purposes: C_{60}-I_h is of I_h symmetry, that is, all C atoms are equivalent (one signal in the ^{13}C-NMR spectrum). All stable fullerene molecules contain 12 pentagons of carbon atoms, which are fused with five adjacent hexagons of carbon exclusively, almost never with an adjacent second pentagon (*isolated pentagon rule*, IPR). In case of C_{60}, this results in 20 hexagons, and for C_{70}–D_{5h} 25 (Figure 7.9). The five-membered rings account for the curvature of the surface. The internuclear distances in solid C_{60} are 135.5 and 146.7 pm, which is slightly below and above the value for graphite (141.5 pm; see Table 4.7). The isomer C_{76}–D_2 is a chiral molecule, which could be separated into the enantiomers. The *trigonal coordination* of the C atoms in fullerenes may resemble that of graphene at first sight. Their curvature, however, results in bond angles slightly below 120° and the spherical nature makes the termination of edges by heteroatoms unnecessary. The occupied 2*p* orbitals are perpendicular to the spherical plane and form a delocalized π electron system. As C_{60} has two triply degenerate unoccupied MOs of low energy, the compound is a potent electron acceptor. The band gap of crystalline C_{60} amounts to 1.9 eV, that is, the solid compound is a semiconductor.

25 A. D. Darwish et al., *J. Chem. Soc. Chem. Commun.* **1994**, 15.

7.3.3.3 Properties

Fullerenes are brown to black solids; in solution C_{60} exhibits a magenta color and C_{70} is described as port-wine red. Both compounds are stable for prolonged periods of time at 20 °C; some fullerenes, however, slowly decompose in the presence of air and water vapor. The formation enthalpy $\Delta_f H^o$ of crystalline C_{60} at 298 K amounts to 2282 kJ mol^{-1} (38 kJ mol^{-1} per C-atom referenced to graphite); the density is 1.78 g cm^{-3}.

7.3.3.4 Reactivity

With the exception of commercially available C_{60}, pure fullerenes are expensive and thus only available in small quantities.[26] Nonetheless, countless derivatives have been prepared, predominantly of C_{60}. Electrochemically and with alkaline metals, fullerenes can be reduced in a stepwise manner to different *fulleride anions*. The solid alkali metal salts $M[C_{60}]$, $M_2[C_{60}]$ and $M_3[C_{60}]$ correspond to the intercalation compounds of alkali metals with graphite (Section 7.5.2), that is, the cations are intercalated between the C_{60} anions. The monoanion $[C_{60}]^-$ dimerizes at low temperatures and in the presence of suitable cations to $[C_{120}]^{2-}$.[27] The trianion of $K_3[C_{60}]$ exists in a doublet ground state and is a metallic conductor that turns superconductive at 19 K. Salts with highly charged fulleride anions such as $[C_{70}]^{6-}$ have also been prepared. $K_6[C_{60}]$ has a cubic body-centered structure. As ionic compounds, alkali metal fullerides are soluble in THF and liquid ammonia. With MeI, they react to polymethylated C_{60}. A completely different structure is found in the salt $[Li@C_{60}][PF_6]$, in which a Li^+ cation is located at the interior of the C_{60} molecule; this remarkable compound crystallizes above 97 °C in a rock salt structure[28] (also see below: endohedral complexes).

With the halogens F_2, Cl_2 and Br_2, respectively, C_{60} reacts in a stepwise manner with numerous covalent halides such as $C_{60}F_{18}$, $C_{60}F_{20}$, $C_{60}F_{24}$, $C_{60}F_{48}$, $C_{60}Cl_6$, $C_{60}Cl_{24}$, $C_{60}Cl_{30}$, $C_{60}Br_6$, $C_{60}Br_8$ and $C_{60}Br_{24}$. An enormous number of additional halides, also derived from unstable fullerenes, were prepared and structurally characterized.[29] As in the case of graphite fluorides (Section 7.4.1), for every two new CX σ bonds one CC π bond needs to be broken so that C atoms with approximate tetrahedral coordination result. In an extreme scenario, a completely saturated derivative of type $C_{60}X_{60}$ would be generated, which, however, has not been realized experimentally so far. By hydrogenation or Zn/HCl reduction, fullerene hydrides

26 A. Hirsch, M. Bettreich, *Fullerenes – Chemistry and Reactions*, Wiley-VCH, Weinheim, **2005**.
27 M. Jansen et al., *Chem. Eur. J.* **2011**, *17*, 1798.
28 S. Aoyagi et al., *Angew. Chem. Int. Ed.* **2012**, *51*, 3377.
29 S. I. Troyanov et al., *Chem. Eur. J.* **2011**, *17*, 10662; *Inorg. Chem.* **2012**, *51*, 2719 and 11226; *Angew. Chem. Int. Ed.* **2012**, *51*, 8239.

(fulleranes) such as $C_{60}H_2$, $C_{60}H_4$, $C_{60}H_{18}$ and $C_{70}H_{38}$ are obtained.[30] At higher hydrogen contents, the fullerene scaffolds tend to become unstable.

The oxidation of fullerenes with peroxoacids or O_2 under irradiation leads to oxides or epoxides; ozonides have also been described.[31] In this manner, for example, $C_{60}O$, $C_{60}O_2$, $C_{120}O$ and $C_{70}O$ were obtained. The reaction of C_{60} with AsF_5 gives (aside from AsF_3) the polymeric salt $[C_{60}][AsF_6]_2$, which contains a zig-zag chain of $[C_{60}]^{2+}$ dications and shows semiconducting properties. With suitable (hydrophilic) functional groups, water-soluble fullerene derivatives were synthesized.[32] The numerous organic and organometallic derivatives of fullerenes are beyond the scope of this book.

Heterofullerenes are cages with some of their carbon atoms formally replaced by hetero elements such as boron or nitrogen. The *azafullerenes* are by far the best investigated, for example, $(C_{59}N)_2$, $C_{59}NH$ and $C_{59}NR$.[33] Fullerenes with encapsulated atoms or molecules are referred to as *endohedral complexes*, which are denoted by the symbol @. For instance, He@C_{60} (read: helium at C_{60}) is obtained by heating of C_{60} in the presence of KCN at 600 °C under a He pressure of 270 MPa.[34] By using the isotope ^{3}He with its nuclear spin of $I = ½$, the specific magnetic shielding inside of fullerene cages and their derivatives (including anions) can be studied by ^{3}He-NMR spectroscopy.[35] All other noble gases (except Rn) as well as H_2 and even large metal atoms have been caged at the interior of C_{60} with its accessible void of about 330 pm in diameter (distance between two opposing C atoms minus twice the VAN DER WAALS radius of the C atom). For the preparation of compounds such as La@C_{60}, La@C_{82} or U@C_{82}, graphite is evaporated together with the corresponding metal halide or oxide (*metallofullerenes*).[36] La@C_{82} is stable in air and soluble in toluene and CS_2. The incorporation of metal atoms or carbides and nitrides can stabilize even fullerene cages that violate the isolated pentagon rule: in C_{68} two pentagons are fused at the edges. Examples for the incorporation of carbides and nitrides include the species Sc_2C_2@C_{68} and Sc_3N@C_{70}.[37] Countless compounds of this sort, in part also with exohedral substituents, have been prepared and enrich contemporary materials sciences.

30 D. Johnels et al., *Angew. Chem. Int. Ed.* **2008**, *47*, 2796 and cited literature.
31 D. Heymann, R. B. Weisman, *Compt. Rend. Chim.* **2006**, *9*, 1107.
32 E. Nakamura, H. Isobe, *Acc. Chem. Res.* **2003**, *36*, 807.
33 O. Vostrowsky, A. Hirsch, *Chem. Rev.* **2006**, *106*, 5191.
34 R. J. Cross, A. Khong, M. Saunders, *J. Org. Chem.* **2003**, *68*, 8281.
35 F. Diederich et al., *Chem. Eur. J.* **1997**, *3*, 1071. M. Rabinovitz et al., *Angew. Chem. Int. Ed.* **2003**, *42*, 3136.
36 X. Lu, L. Feng, T. Akasaka, S. Nagase, *Chem. Soc. Rev.* **2012**, *41*, 7723. M. Yamada, T. Akasaka, S. Nagase, *Acc. Chem. Res.* **2010**, *43*, 92. L. Echegoyen et al., *Angew. Chem. Int. Ed.* **2009**, *48*, 7514.
37 L. Dunsch, *Nachr. Chemie* **2007**, *55*, 503. L. Dunsch, S. Yang, *Phys. Chem. Chem. Phys.* **2007**, *9*, 3067.

7.3.4 Carbon Nanotubes

Tubular arrangements of carbon atoms at the nanoscale (CNTs)[38] are important in materials science and electronics due to their extraordinary mechanical and electronic properties. The number of publications regarding this relatively recently discovered class of materials grows almost exponentially. CNTs are differentiated into *single-wall* and *multiwall nanotubes* (SWNTs and MWNTs) and into open and closed tubes. An idealized structure is shown in Figure 7.10, from which the fullerene-like topology of tricoordinate C atoms, albeit in a tubular instead of a spherical arrangement, becomes apparent. Formally, a graphene layer is rolled up into a tube. Therefore, the C atoms are predominantly arranged in hexagons (at the walls), although pentagons are required to create the necessary curvature of the half spheres at the end of the CNTs. The diameter of SWNTs is typically between 0.8 and 2.0 nm (1 nm = 10^{-9} m), and the length can range from 100 nm up to several centimeters.

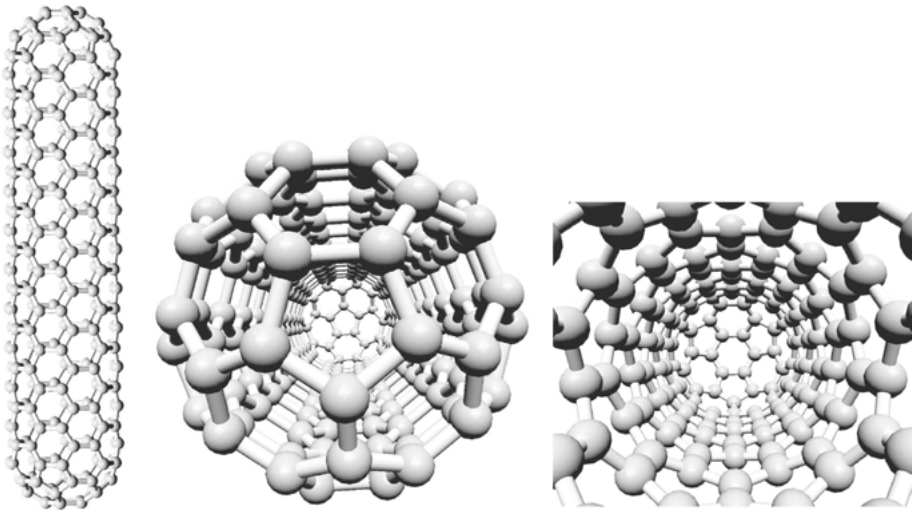

Figure 7.10: Structure of single-wall carbon nanotubes (SWNT). The ends can be closed in different manners (jcrystal.com/steffenweber/gallery/NanoTubes/NanoTubes.html).

The CNTs represent carbon fibers of highest tensile strength. They boast an extreme thermal conductivity and they have interesting electrical properties (semi- or

38 T. Akasaka, F. Wudl, S. Nagase (eds.), *Chemistry of Nanocarbons*, Wiley, Hoboken, **2010**. D. M. Guldi, N. Martin, *Carbon Nanotubes and Related Structures*, Wiley-VCH, Weinheim, **2010**. P. J. F. Harris, *Carbon Nanotube Science*, Cambridge Univ. Press, **2009**. H. Frauenrath et al., *Angew. Chem. Int. Ed.* **2010**, *49*, 6496. Also see topical issue of *Acc. Chem Res.* **2002**, issue 12.

metallic conductors, depending on their chirality). The exterior surface can be modified and functionalized in a similar manner as fullerenes (Section 7.3.3). At the interior, molecules such as sulfur or iodine can be hosted in the form of atomic chains or rods. Even fullerenes have been introduced to CNTs.

The synthesis of CNTs is preferably done by vapor deposition at about 1000 K (pyrolysis) from a hydrocarbon such as methane, ethane, acetylene, benzene or xylene in a fluidized bed reactor. Under these conditions, the added (organometallic) precursor is transformed to metallic nanoparticles, which readily dissolve carbon in the form of carbide and rapidly transport it predominantly via the surface to the growing CNTs at the other side of the particle (Figure 7.11).

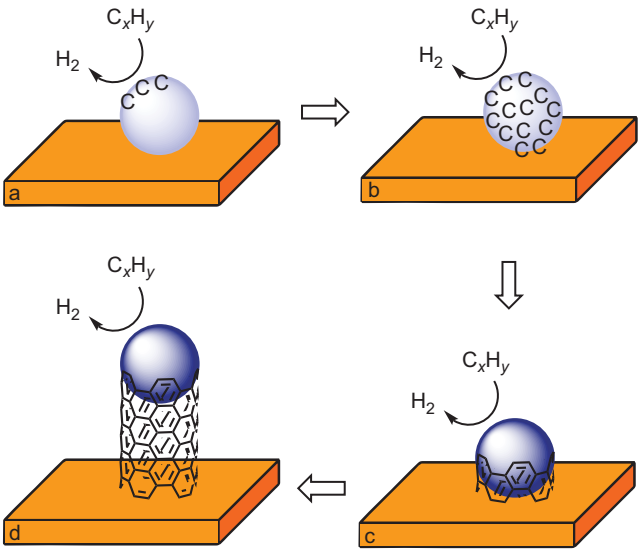

Figure 7.11: Schematic mechanism of metal-catalyzed growth of carbon nanotubes from a substrate catalyzed by a metal nanoparticle: (a) decomposition of hydrocarbon C_xH_y with liberation of H_2 starts; (b) diffusion of C atoms via the surface to backside of particle; (c) saturation of particle surface with C atoms initiates tube growth; (d) tube continues to grow as long as hydrocarbon supply not exhausted (adapted from: J.-P. Tessonnier, D. S. Su, *ChemSusChem* **2011**, *4*, 824).

Fe, Co and Ni are particularly suitableas metal nanoparticles; iron pentacarbonyl $Fe(CO)_5$ and ferrocene $(C_5H_5)_2Fe$ are typical precursors. As a complementary method, the growth of CNTs from a mixture of CH_4 and H_2 on a SiO_2 film at 900 °C was reported. The tubes often form bundles or are tangled in balls. Subsequent heating to 1800–2600 °C anneals structural defects and evaporates residual metal. The functionalization is achieved with common protocols of organic chemistry. The caps and open ends of the CNTs are particularly reactive as the ideally trigonal planar coordination of the C atoms is most strongly distorted in these regions.

The functionalization can dramatically improve the solubility of the otherwise insoluble and infusible CNTs in organic solvents. MWNTs consist of several, tightly fitting concentric tubes, which reach outer diameters of up to 250 nm. The diameter of CNTs corresponds to the size of the nanoparticle from which the tubes are growing. Depending on the orientation of the six-membered rings, the CNTs are chiral or achiral (helical chirality).

In 2011 already, several thousand tons of CNTs were produced worldwide, predominantly MWNTs. The largest producers are the U.S., Japan, China and Germany, where the Bayer AG had established a yearly production capacity of 200 tons per year in 2009. The most important application fields are composite materials with increased strength, electrically conducting coatings, electrodes for Li ion batteries, field emission displays and carriers for catalysts. Even fibers are spun from CNTs, which is possible due to their solubility in chlorosulfuric acid.[39]

7.4 Graphite Compounds

Derivatives of graphite cannot be considered as simple molecular carbon compounds due to their polymeric nature retaining the typical layered structure. This class of compounds is conveniently subdivided according to the nature of bonding to the newly introduced moiety. These bonds can be either predominantly covalent or ionic. Apart from natural graphite such materials can be prepared from highly oriented pyrolytic graphite (HOPG).

7.4.1 Covalent Graphite Compounds

Under suitable conditions, graphite reacts with fluorine at 350–650 °C in a strongly exothermic reaction, but without ignition to the stable, crystalline graphite fluorides $(C_2F)_n$ and $(CF)_n$.[40] At 350–400 °C the black $(C_2F)_n$, is obtained, in particular when natural graphite is used as starting material. At 600–640 °C grayish white $(CF)_n$, is formed from natural graphite or petroleum coke. Both species are electrical insulators with densities of about 3 g cm^{-1}. Intermediate compositions occur as mixtures of both compounds. These graphite fluorides show layered hexagonal structures. In case of $(CF)_n$, a fluorine atom is bonded to each carbon resulting in its tetrahedral coordination and thus in puckered planes of six-membered rings in either chair or boat conformation (Figure 7.12a).

39 M. Pasquali et al., *Science* **2013**, *339*, 182. A. J. Hart et al., *Science* **2013**, *339*, 535.
40 N. Watanabe, T. Nakajima, H. Touhara, *Graphite Fluorides*, Elsevier, Amsterdam, **1988**; R. Hagiwara, M. Lerner, N. Bartlett, *J. Chem. Soc., Chem. Commun*. **1989**, 573.

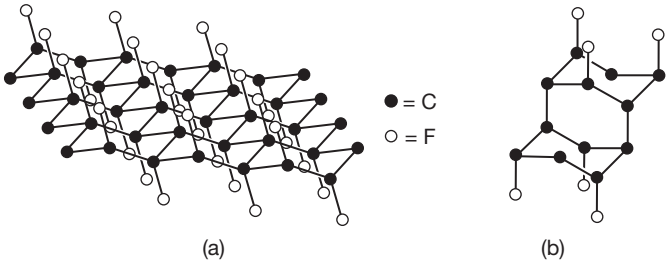

Figure 7.12: Excerpts from the structures of polymeric graphite fluorides $(CF)_n$ (left) and $(C_2F)_n$ (right).

The distance of individual planes amounts to about 600 pm and depends slightly on the quality of the used graphite starting material.

In the fluoride $(C_2F)_n$ as well, all carbon atoms are tetrahedrally coordinated, but rather in double layers, covalently connected by CC bonds on the facing sides and fully substituted with fluorine atoms on the opposing sides (Figure 7.12b). The CC distances (153 pm) correspond to those in diamond; the interlayer distance of two double layers is 809 pm. At the edges of the layers, CF_2 and CF_3 groups saturate otherwise free valencies. On heating, graphite fluorides disproportionate to volatile carbon fluorides (CF_4, C_2F_6, etc.) and amorphous carbon black.

The graphite fluorides are hydrophobic and chemically resistant. They are of importance as lubricants and water repellents. Moreover, they are responsible for the so-called *anode effect*, which is a strong increase of overpotential during the electrolysis of the fluoride containing melts in aluminum smelting and in the production of fluorine (Section 13.4.1). The anode effect can be avoided by using electrodes of amorphous carbon, rather than graphite.

Lithium-graphite fluoride batteries operate on the following exothermic reaction:

$$n\,\mathrm{Li} + (\mathrm{CF})_n \longrightarrow n\,\mathrm{LiF} + \mathrm{C}_n$$

As an electrolyte, a solution of $Li[PF_6]$ in propylene carbonate is most commonly used (see also Section 13.4.4). Such batteries are environmentally benign and can be stored or operated without significant loss in performance for more than 10 years. Recently, it was shown that fluorinated graphite can be exfoliated thermally to obtain fluorinated graphene sheets.[41]

7.4.1.1 Surface Compounds

The atoms at the surface and edges of atomic lattices such as those in diamond or graphite occur in a strongly distorted coordination environment as they do not

41 Z. Sofer et al., *Chem. Eur. J.* **2016**, *22*, 17696.

have a sufficient number of neighbors for the use of all their valence electrons in covalent bonds. The remaining unpaired electrons and thus free valencies (*dangling bonds*) confer an increased reactivity to these atoms. Therefore, atomic or molecular residues chemically bind to such surfaces (*chemisorption*). A chemisorbed species can be considered a surface compound if the bonds to the newly introduced moieties are of similar strength than in molecular compounds.

Diamond powder, which is normally hydrophobic, is turned hydrophilic by heating to 500 °C in an O_2 atmosphere or by treatment with oxidizing agents. Surface oxides of the following type are formed in this process:

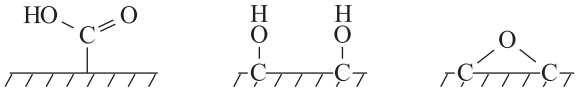

By heating of samples to 800 °C in high vacuum, these impurities can be removed, and a native surface be regenerated albeit with a potential loss of material (desorption as CO, CO_2, H_2O). The clean surface, however, once more rapidly reacts with air after cooling to room temperature. With Cl_2, F_2 and H_2, higher temperatures are required for the formation of surface compounds.

In the case of graphite or graphite-like microcrystalline carbon, surface compounds are preferably formed at the edges of the planar layers, as within the layers all valencies of the atoms are used in bonding to the three nearest neighbors. By oxidation of graphite with either (a) O_2 at 400 °C, (b) fuming nitric acid at 25 °C or (c) a mixture of concentrated sulfuric acid with $Na[NO_3]$ and $K[MnO_4]$, **graphite oxide** (GO) is obtained, which – after rinsing and freeze-drying – contains the functional groups depicted below:[42]

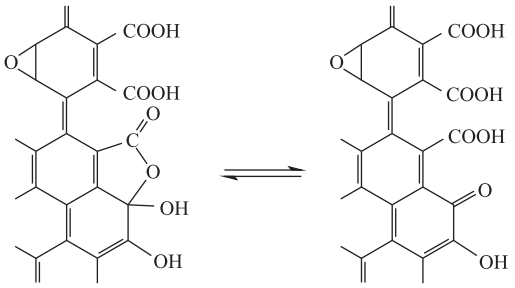

While the edges are mostly occupied by carboxyl groups, the surfaces contain epoxy and hydroxyl functionalities. The presence of these heteroatoms between the

42 D. Chen, H. Feng, J. Li, *Chem. Rev.* **2012**, *122*, 6027. A. Bonanni, A. Ambrosi, M. Pumera, *Chem. Eur. J.* **2012**, *18*, 4541. J.-M. Tour et al., *J. Am. Chem. Soc.* **2012**, *134*, 2815. J. Kim, L. J. Cote, J. Huang, *Acc. Chem. Res.* **2012**, *45*, 1356.

former graphene layers allows for their relatively facile separation. The carbon content is approximately 45–76% if the material is produced according to the HUMMERS method (c). On the other hand, such preparations also contain noticeable quantities of $-OSO_2OH$ groups, linked to the C atoms. On heating of the nearly colorless samples, H_2O, CO_2 and CO are eliminated consecutively.[43] The functional groups can be titrated with a sodium hydroxide titer as long as they contain acidic protons; keto groups are determined with a sodium methoxide titer. It is also possible to modify the graphite oxide samples by ion exchange reactions. Soot, that is, particularly finely divided carbon, can contain up to 15% of oxygen after oxidative treatment with NO_2, HNO_3 or O_3.

Surface compounds can be characterized by ^{13}C-NMR, IR and Raman spectroscopy, photoelectron spectroscopy with X-rays, extended X-ray absorption fine structure, thermogravimetric analysis and by chemical means (through titration). Surface species (also known for various other materials such as silicon, silicon dioxide and metals) are obviously of significant practical interest as they strongly influence the mechanical, electrical, optical and chemical properties of the bulk material. Surface oxides of carbon play a technologically eminently important role during the oxidation of carbon to CO and CO_2. In more recent times, graphite oxide has gathered enormous attention as precursor for production of graphene (Section 7.3.1).

7.4.2 Ionic Graphite Compounds

With certain reaction partners, graphite reacts either under electron uptake (a) or electron loss (b). During this process, ionic compounds of the following nature are obtained (M = metal):

$$\text{(a) } C_n + M \longrightarrow M^+C_n^- \qquad \text{(b) } C_n + A \longrightarrow C_n^+A^-$$

The strongly electropositive alkali metals K, Rb, Cs, as well as at higher temperatures Li and Na, react smoothly with graphite. The alkaline earth metals Ca, Sr, Ba and the lanthanides Sm, Eu, Yb and Tm also require increased reaction temperatures. The potassium compounds have been investigated the most thoroughly.[44]

Under exclusion of air, potassium reacts with thoroughly dried graphite at temperatures above 200 °C in an exothermic reaction and a stepwise manner to the composition KC_{60}, followed by KC_{48}, KC_{36} and KC_{24} and finally to KC_8. The exact

43 S. Eigler et al., *Carbon* **2012**, *50*, 3666 und *Chem. Eur. J.* **2013**, *19*, 9490.
44 A. Charlier, M. F. Charlier, D. Fristot, *J. Phys. Chem. Solids* **1989**, *50*, 987. M. S. Dresselhaus, G. Dresselhaus, *Adv. Phys.* **2002**, *51*, 1.

composition largely depends on the stoichiometry and the reaction temperature. These compounds are either bronze-colored (KC_8) or blue-gray and paramagnetic in contrast to the diamagnetic graphite. The structures of the different phases are displayed in Figure 7.13.

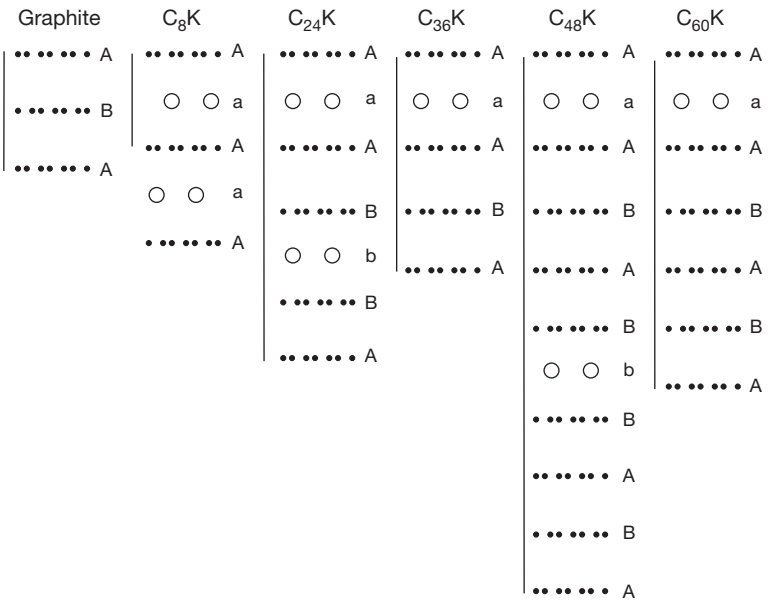

Figure 7.13: Schematic representation of the structures of potassium graphite compounds of different composition. The vertical lines indicate the identity period (*c*-axis of the unit cell).

The potassium atoms intercalate between the graphene planes of the graphite structure. In KC_8 – which may be formed last but is nonetheless referred to as "stage-1" – each interlayer is occupied. For the other phases, only every second, third, fourth and fifth interlayers contain potassium atoms (stage-2, stage-3, etc.). The 4*s* valence electrons of the K atoms are transferred into the conductance band of graphite so that mostly ionic bonding results. The CC distance in KC_8 is with 143.1 pm slightly larger than in graphite (141.5 pm), which is attributed to the partial filling of the antibonding π* levels. The *electrical conductivity* of KC_8 has a positive temperature coefficient; the compound thus displays metallic behavior. Along the graphene planes the conductivity is ten times higher, perpendicular to the planes a hundred times higher than in neat graphite. At 1.0 K, KC_8 turns into a superconductor in the direction of the planes. The analogous NaC_8 reacts with tetrabutylammonium bromide at 60 °C under ion exchange, that is, the cation $[Bu_4N]^+$ is incorporated between the layers instead of Na^+.

Upon heating in vacuum, potassium graphites decompose into the elements. In water, the intercalated potassium is hydrolyzed to KOH and H_2, liberating elemental graphite. By reaction with alkyl halides, potassium graphite can be transformed to substituted graphene derivatives. In organic and organometallic synthesis, KC_8 is employed as a reducing agent, for instance, in dehalogenation reactions. Rb and Cs also form phases of the net composition MC_8; with many other metals, however, the stoichiometry MC_6 is preferred in stage-1 (e.g., CaC_6). Graphite intercalation compounds with two different metals can be obtained by using binary alloys for the preparation.

The intercalation of Li^+ ions and electrons into a graphite anode also takes place in **lithium-ion batteries** during the charging process. Lithium ions migrate from the lithium cobaltate(III) cathode ($LiCoO_2$) to the anode. The cobaltate of the cathode is thus converted into a lithium-poor variety $Li_{1-x}CoO_2$. The electrolyte typically consists of a solution of $Li[PF_6]$ in a polar organic solvent. During discharge, the opposite process takes place. Such rechargeable batteries or *accumulators* have a nominal voltage of 3.6 V and a much higher storage capacity and longevity than more traditional accumulators such as the lead battery. Nowadays, they constitute the most important power source for portable electronic devices and electric cars.[45]

Graphite reacts with strong oxidants such as Cl_2, Br_2, N_2O_5, SO_3 as well as with the mixtures H_2SO_4/HNO_3 and F_2/HF according to the Scheme (b) on page 288. For example, C_8Cl, C_8Br, $C_{24}[HSO_4]\cdot 2H_2SO_4$ and $C_{24}[HF_2]\cdot 2HF$ are obtained as products. In many cases, these compounds are produced by anodic oxidation of graphite in the presence of a suitable reaction partner (e.g., $HClO_4$). As previously described for the reduction products of graphite (see above), some of the oxidation products display an enhanced electrical conductivity so that ionic bonding can be assumed (formation of positive holes in the valence band of graphite). In certain cases, conductivities equal to that of aluminum are achieved!

Many *metal halides*, in particular fluorides and chlorides, can be intercalated between the layers of graphite by sublimation. For instance, $FeCl_3$ reacts with graphite in the presence of Cl_2 below 300 °C to materials of compositions $C_nFeCl_4\cdot xFeCl_3$ with $n \approx 27$ and $x \approx 3$ (Figure 7.14). The interplane distance of the graphite structure is widened from 335 to 940 pm by the intercalation of $FeCl_3$ molecules and $[FeCl_4]^-$ anions.

The electrical conductivity of intercalation compounds with metal halides surpasses that of copper in certain cases (e.g., with AsF_5).

Ionic graphite compounds are characterized by a layer structure, the stepwise incorporation of the reaction partner between these layers and the sensitivity to water, which decomposes the species to elemental graphite plus the reaction product of water and the intercalated species itself. These properties of graphite are important for its application as electrode material in batteries and for electrolysis.

45 D. J. Sollmann, *Nachr. Chemie* **2007**, *55*, 979. Topical issue "Batteries" in *Chem. Rev.* **2004**, *104*, Issue 10.

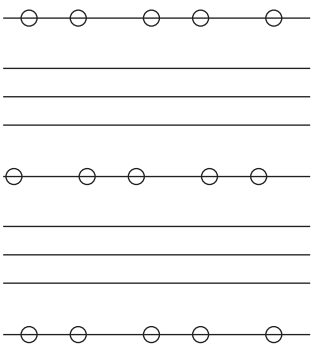

Figure 7.14: Schematic representation of the structure of the intercalation compound of $FeCl_3$ in graphite. The layers of iron and chlorine atoms are denoted by solid lines.

In addition, graphite compounds also show *catalytic properties*, for example, in the isomerization of hydrocarbons.[46] It should be noted that other species with a layer structure in the solid state also form intercalation compounds, for example, silicates, metal hydroxides and metal dichalcogenides.[47]

7.5 Carbon Black, Coal and Coke

A technologically very important form of carbon is *carbon black*.[48,49] It is not to be confused with *soot* (a mostly undesired product of incomplete combustion) as the latter often contains considerable quantities of residual hydrocarbons and other potentially hazardous components (see below). The better part of carbon black production is used as filler in rubbers (e.g., for tires), the rest is applied as black pigment for paints, inks, toner and plastics, on the one hand, and as a component of electrode materials, on the other hand. C*arbon black* is produced in huge quantities, predominantly from *anthracene oil* with its high content of aromatic hydrocarbons, obtained itself by distillation from coal, tar or mineral oil. The anthracene oil is burned with a lack of oxygen at 1200–1900 °C, according to the following idealized equation:

$$C_{18}H_{12} + 3\,O_2 \longrightarrow 18\,C_{s.} + 6\,H_2O$$

For this purpose, a horizontal reactor of 20 m length is employed into which the anthracene oil is injected through a nozzle together with natural gas and preheated air. As the rear part is cooled by injection of water, the undesired oxidation of

46 K. Arata, *Adv. Catal.* **1990**, *37*, 165.
47 A. J. Jacobson, *Encycl. Inorg. Chem.* **1994**, *3*, 1556.
48 O. Vohler et al., *Ullmann's Encycl. Ind. Chem.* **1986**, *A5*, 95.
49 J.-B. Donnet, R. C. Bansal, M.-J. Wang (eds.), *Carbon Black*, Dekker, New York, **1993**.

carbon black is suppressed (*furnace black process*). The combustion of methane results in very high temperatures, while the amount of air is insufficient for the complete oxidation of the anthracene oil. Its carbon content is therefore deposited as carbon black. The largest production site for carbon black with a yearly capacity of 160,000 t in 80 different varieties is located at Kalscheuren near Cologne. Unlike soot, carbon black consists of 99.5% carbon with only traces of H, O, N and S. It can either be produced as an amorphous solid or as microcrystalline graphite. The particle sizes range from 15 to 200 nm, and for pigment applications from 20 to 80 nm. The reaction mechanism for the formation of carbon black is complex and consists of a stepwise degradation of two-dimensional aggregates of fused aromatic carbacycles saturated by hydrogen atoms at the edges (polycyclic aromatic hydrocarbons). Fullerenes are side products in trace quantities (Section 7.3.3).[50]

Carbon fibers are obtained by pyrolysis of cotton or synthetic fibers. Depending on the temperature, the resulting fibers are either amorphous (500–1500 °C) or crystalline, that is, graphitized (2000–3000 °C).[51] They are light-weighed, strong and resistant to heat and corrosion. Carbon fibers are employed on a large scale for the reinforcement of composite materials for cars, airplanes and spacecraft, but also for sports equipment such as tennis rackets or golf clubs.

Activated Charcoal is a porous material, which is produced either by partial oxidation of carbon, for example by water vapor, or by carbonization of organic material. Typical starting materials are wood, sawdust, straw, nutshells, soft coal, peat and coke.[52] The large inner surface of activated carbons and the related *mesoporous carbon materials* accounts for their very good absorbent properties.

Coal[53] does actually not consist of carbon alone, but rather is a physical mixture of organic and inorganic species. The organic part originates from the lignin and cellulose of ancient wood. Apart from C, it also contains substantial quantities of H, O, N and S. The composition of the organic part of an American coal was determined as $C_{100}H_{87.9}O_{8.8}N_{1.5}S_{1.3}$. The oxygen content gives rise to phenolic OH groups, carbonyl and carboxyl functionalities, as well as ether bridges and furans. Alongside unsaturated C_6 and C_5 rings, saturated rings and alkyl chains are also present. The precise structure of the organic matrix is, however, unknown. The organic sulfur is present in the form of thiols, thioethers and thiophene units.[54] The inorganic components of coal are sand, clay, carbonates, shale and pyrite, which

50 K.-H. Homann, *Angew. Chem. Int. Ed.* **1998**, *37*, 2434.

51 I. N. Ermolenko, I. P. Lyubliner, N. V. Gulko, *Chemically Modified Carbon Fibers*, VCH, Weinheim, **1990**.

52 O. Vohler et al., *Ullmann's Encycl. Ind. Chem.* **1986**, *A5*, 95. C. Liang, Z. Li, S. Dai, *Angew. Chem. Int. Ed.* **2008**, *47*, 3696.

53 J. C. Crelling, *Ullmann's Encycl. Ind. Chem.* **1986**, *A7*, 153.

54 The sulfur content of German hard coal is equally distributed between the organic and inorganic parts.

account for the ashes left after combustion (SiO_2, Al_2O_3, CaO and Fe_2O_3). In addition, traces of Cu, Cr, Mn, Ni, P, Pb, Zn and radioactive nuclides are found. The carbon content by mass increases from wood (about 60%), via the intermediate products peat, soft and hard coal all the way to anthracite (>90%). Representative partial structures of anthracite and soft coal are shown in Figure 7.15. In Germany, as of April 2019, about 30% of the electricity was generated by the combustion of hard and soft coals.

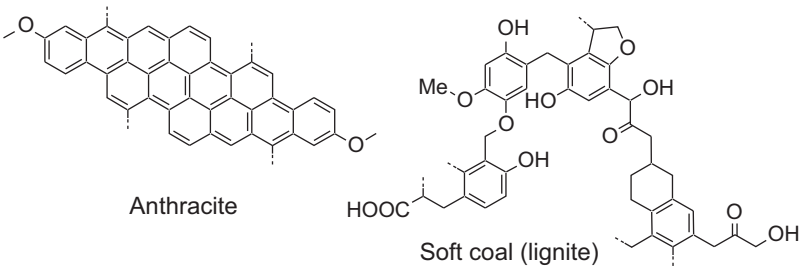

Figure 7.15: Representative partial structures of anthracite (left) and soft coal or lignite (right).

Coke is the residue of dry distillation of coals under exclusion of air, the so-called coking process during which species such as CH_4, C_2H_2, CO, H_2O, H_2S, NH_3 and other gases escape, and the carbon content rises. Coke is a porous but firm carbon, which, however, still contains the incombustible inorganic components of coal.

7.6 Carbon Halides

The simplest halides of carbon are those of the CX_4 type, known for all halogens X. The subhalide CF_2 (Section 13.4.6) and fluorinated (hydro)carbons (Section 13.4.4) as well as the graphite fluorides (Section 7.4.1) are discussed in the indicated sections.

Tetrafluoromethane (CF_4) is a rather inert gas (b.p. –128 °C), which is produced on an industrial scale by excessive fluorination of carbon.[55] It is used by the electronics industry for dry etching of silicon in the production of integrated circuits. During this process, CF_4 is partially decomposed to CF_3 radicals and F atoms by a high frequency discharge at a pressure of 0.1–1.0 hPa. The F atoms react with silicon to volatile SiF_4. Due to its inert nature, CF_4 accumulates in the atmosphere and acts as a greenhouse gas.

55 Regarding other CF species, see T. Liang, C. N. Neumann, T. Ritter, *Angew. Chem. Int. Ed.* **2013**, *52*, 8214.

Tetrachloromethane (b.p. 76 °C) is an important solvent and reagent, which is obtained by the chlorination of methane (Section 13.5.2) or, alternatively, CS_2:

$$CS_2 + 3\,Cl_2 \longrightarrow CCl_4 + S_2Cl_2$$

The once common use in the dry-cleaning of clothes is now prohibited due to its toxicity. The halides CBr_4 (pale-yellow crystals) and CI_4 (red crystals) are commercially less important but can be used as mild brominating or iodinating reagents in the presence of radical starters such as dibenzo peroxide. As a curious side-note, the substitution of all four hydrogens of methane to ClBrClF gives a molecule with five different atoms. It contains an *asymmetric center* and is therefore chiral.

At −78 °C, CCl_4, CBr_4 and CI_4 react with SbF_5 in SO_2ClF as a solvent to yield the corresponding trihalomethylcarbenium ions, which were characterized by ^{13}C-NMR spectroscopy as well as by trapping reactions:[56]

$$CX_4 + SbF_5 \longrightarrow [CX_3]^+ + [SbXF_5]^-$$

By reaction of CI_4 with the silver aluminate ($Ag[Al(OR)_4]$) the salt $[CI_3][Al(OR)_4]$ was prepared and characterized in the solid state by X-ray diffraction on single crystals [R = $C(CF_3)_3$].[57] The cation is isosteric and isoelectronic with BI_3 and therefore of the same D_{3h} symmetry.

7.7 Carbon Chalcogenides

7.7.1 Oxides

In times of changing climate, the combustion products of fossil fuels are in the news almost every day, in particular the greenhouse gas carbon dioxide. In 2017, through combustion of coal, oil, natural gas and biomass 36.2 gigatons ($36.2{\cdot}10^9$ t) of CO_2 were emitted into the atmosphere, 28% of the total amount in China, 15% in the USA, 10% in the EU and 7% in India. In Germany, the emission of CO_2 in 2016 was roughly at $8.0{\cdot}10^8$ t. It is assumed that the CO_2 content of the atmosphere will likely continue to rise from currently 410 ppm until the year 2200. Only after that date a slow decline is expected as the fossil fuel resources decrease until mostly consumed in the year 2400. As a countermeasure, it is planned to remove CO_2 from the exhaust stream of power and coal gasification plants and store it under pressure in depleted natural gas deposits (*carbon capture and storage*). Such facilities are already in place in Norway. For other greenhouse gases see Section 4.4.3.

56 G. A. Olah, L. Heiliger, G. K. S. Prakash, *J. Am. Chem. Soc.* **1989**, *111*, 8020.
57 I. Krossing et al., *Angew. Chem. Int. Ed.* **2003**, *42*, 1531.

In addition to CO_2, several other low molecular oxides of carbon are known in pure form:

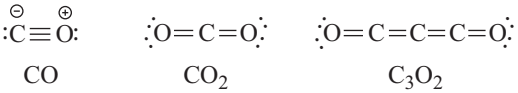

CO CO_2 C_3O_2

Furthermore, a few higher molecular cyclic oxides such as C_6O_6, $C_{12}O_6$, $C_{12}O_9$ and $C_{40}O_{10}$ have been prepared by purely organic methods, which are therefore beyond the scope of this book. Finally, several supra- to macromolecular fullerene and graphene/graphite oxides are known (Section 7.3.3).

7.7.1.1 Carbon Monoxide

CO as a toxic, colorless and odorless gas is always formed when coal or carbon compounds are burned with insufficient oxygen:

$$C(s.) + O_2(g.) \longrightarrow CO_2(g.) \qquad \Delta H^\circ_{298} = -394 \text{ kJ mol}^{-1}$$

$$CO_2(g.) + C(s.) \rightleftharpoons 2\,CO(g.) \qquad \Delta H^\circ_{298} = 173 \text{ kJ mol}^{-1}$$

The second reaction is called BOUDOUARD equilibrium. This endothermic reaction plays an important role in various technical processes. Following LE CHATELIER's principle, the equilibrium is shifted to the side of CO with increasing temperature. By the same reasoning, the relative proportions are strongly pressure dependent; an increase in pressure leads to the formation of CO_2 and solid carbon. Under standard conditions CO is thermodynamically unstable, but the disproportionation to carbon dioxide and carbon is kinetically hindered by a high activation barrier so that CO exists at 25 °C as a metastable compound. CO is hardly soluble in water and organic solvents; its boiling point is 82 K.[58]

In industry, large quantities of CO are produced in the *steam reforming* process for production of H_2 from CH_4 and H_2O, as well as during coal gasification (Section 5.1). It can also be obtained by partial oxidation of hydrocarbons, for example:

$$CH_4 + \tfrac{3}{2}O_2 \xrightarrow{1200\text{–}1500^\circ C} CO + 2\,H_2O$$

CO is the anhydride of formic acid, from which it can be liberated in the laboratory by dehydration with hot concentrated sulfuric acid:

$$HCOOH + H_2SO_4 \longrightarrow CO\uparrow + [H_3O][HSO_4]$$

Sulfuric acid acts as an acidic catalyst in this reaction and binds the liberated water due to its hygroscopic nature. Under pressure, CO reacts with NaOH in the reverse reaction under formation of sodium formate:

---

58 H. Ledon, *Ullmann's Encycl. Ind. Chem.* **1986**, *A5*, 203.

$$CO + NaOH \xrightarrow{160°C} HCOONa$$

With liquid sulfur, CO reacts to carbonyl sulfide COS or O=C=S (b.p. – 50 °C), which is used as a precursor for organosulfur compounds.

CO is a very important reducing agent, which burns with O_2 in a strongly exothermic reaction to CO_2 ($\Delta H°_{298} = -283$ kJ mol^{-1}). With transition metals, CO forms coordinate bonds. The resulting *carbonyl complexes* are known in large numbers. For instance, in the presence of nickel it reacts to the volatile $Ni(CO)_4$, with finely divided iron to $Fe(CO)_5$. The bonding of the CO ligands in the metal carbonyls is analogous to the N_2 ligands in dinitrogen complexes (Section 9.2). As CO and N_2 are *isoelectronic molecules*, the analogy is not ending there: both species show similar physical properties (b.p. of CO: –191°, of N_2: –196 °C). Despite the formal charges in the CO formula, the dipole moment of the molecule is very small (0.11 D) due to the compensation of formal charges by the inductive charge transfer caused by the electronegativity differences between C and O. The oxygen atom is nonetheless slightly positive, the C atom negatively charged by the same amount (Section 4.6.3). The enthalpy of dissociation of CO (1076 kJ mol^{-1}) is even larger than that of N_2 (942 kJ mol^{-1}). The CO triple bond is thus considered as the strongest of all covalent bonds in neutral molecules.

The *toxicity* of CO is mainly based on its fast reaction with the iron center of the red-colored blood pigment hemoglobin, upon which a carbonyl complex is formed that is unsuitable for O_2 transport. As CO binds about 200 times more strongly than O_2 it also displaces the latter from its hemoglobin complex. After respiration of air with a CO content of about 0.1% for 1 h, approximately half of the hemoglobin molecules are blocked by CO. The treatment of choice for CO poisoning is therefore the hyperbaric oxygen donation under several atmospheres of O_2 in order to reverse the equilibrium reaction.

In the presence of activated charcoal, CO is chlorinated by Cl_2 in an exothermic reaction to give the extremely toxic phosgene, the acid chloride of carbonic acid. Similarly, the hydrogenation of CO is of tremendous industrial importance. Depending on the catalyst, it proceeds to methanol, methane or lower hydrocarbons (gasoline). The latter reaction is the so-called FISCHER–TROPSCH process:

$$x\,CO + y\,H_2 \xrightarrow{\text{Cu/Cr/Zn-oxide}} CH_3OH$$
$$\xrightarrow[-H_2O]{\text{Fe/Co}} C_nH_{2n+m}$$
$$\xrightarrow{\text{Ni}} CH_4 + H_2O$$

7.7.1.2 Carbon Dioxide

CO_2 is formed on complete combustion of coal, wood, oil, gasoline, diesel fuel, natural and biogas (methane).[59] It is also liberated in large quantities during calcination of limestone and on decomposition of carbonates by acids. Animals and humans produce CO_2 during respiration; an adult person exhales about 1 kg of CO_2 per day. Thus, the world population of presently 7.7 billion people generates approximately 2.5 billion tons of CO_2 annually just by breathing.

In industry, CO_2 is mainly produced as a side product of the ammonia synthesis, more precisely the production of the required hydrogen from methane and coal.[60] It is mostly used for production of carbonates (such as baking soda), urea and soda water, in fire extinguishers and, in its solid form, as dry ice for cooling and cleaning purposes. Dry ice is commercially available as blocks or slates and sublimes under ambient pressure at −78 °C without melting.[61] The extraction of caffeine from green (unroasted) coffee beans is carried out with hypercritical CO_2 under high pressure (high-pressure extraction; 7.5–50 MPa). By expansion (lowering the pressure) of the separated CO_2 phase to about 5 MPa the temperature is reduced, and the caffeine crystallizes and can be collected. The CO_2 is recompressed again and recycled for further extraction. The vapor pressure of CO_2 amounts to 5.73 MPa at 20 °C; the critical temperature is 31 °C. CO_2 readily dissolves in many organic solvents, less so in H_2O.[62] The chemical behavior of carbon dioxide is dominated by its LEWIS acidity and the resulting electrophilicity. With the extremely acidic carborate acid $H(CHB_{11}F_{11})$, however, it can nonetheless be protonated at an oxygen atom as shown by the appearance of corresponding IR stretching bands.[63] According to theoretical calculations, the bridging proton in the resulting cation of $[(CO_2)_2H]^+[CHB_{11}F_{11}]^-$ shows a linear OHO coordination by two CO_2 molecules.

Under *very high pressure*, CO_2 polymerizes to a phase the structure of which corresponds to *tridymite* SiO_2 (Section 8.7) with tetrahedrally coordinated C atoms and CO single bonds; at extreme pressures (>50 GPa) this phase is transformed into a structure that is analogous to *stishovite* with six-coordinate carbon atoms and three-coordinate oxygen atoms. In addition, an ionic high-pressure phase $[CO]^{2+}[CO_3]^{2-}$ has also been observed.[64]

---

59 By extraction with organic amines, CO_2 can be removed from exhausts of combustion processes and then be liberated again in pure form by heating for subsequent use, for example, for the production of sodas.

60 CO_2 is washed from the $H_2/CO_2/N_2$ mixture by scrubbing with aqueous potassium carbonate (formation of $K[HCO_3]$) or with ethanolamine under pressure and recovered from the solution by heating.

61 The white pole caps of Mars probably consist of dry ice, as the atmosphere of the "red planet" consists of 96% CO_2 at a pressure of 6.1 hPa at the cold Martian surface.

62 S. Topham, *Ullmann's Encycl. Ind. Chem.* **1986**, *A5*, 165.

63 S. Cummings, H. P. Hratchian, C. A. Reed, *Angew. Chem. Int. Ed.* **2016**, *55*, 1382.

64 C.-S. Yoo, A. Sengupta, M. Kim, *Angew. Chem. Int. Ed.* **2011**, *50*, 11219.

Through **photosynthesis** of green plants as well as of certain algae (phytoplankton) the CO_2 of the atmosphere and the oceans is reduced to carbohydrates at a scale of 200 billion tons $(CH_2O)_n$ per year. The current combined anthropogenic and natural emission of CO_2 is significantly higher so that the CO_2 concentration in the atmosphere increases steadily. Since the year 1920, this leads to a gradual warming of the Earth's surface, including the atmosphere and the hydrosphere (Section 4.4.3). In addition, the higher CO_2 concentration also leads to an increasing acidification of the ocean waters due to the equilibrium formation of carbonic acid. Currently, the pH value of oceanic surface water is 8.1, gradually decreasing with depth where the CO_2 content rises because of the oxidation of organic material. From 1988 to 1998, the pH value has decreased by 0.04 units, which corresponds to an increase in oxonium ion concentration by 10%. The warming of the ocean waters together with the melting of glaciers and the land-based polar icecaps led to an increase in the sea levels by 1.7 mm per year on average between 1890 and 1992. In order to limit the increase in atmospheric CO_2 concentration, attempts are underway to use this gas as a C_1 synthetic building block. A promising approach is the catalytic hydrogenation of CO_2 to formic acid as developed by the company BASF.

Just like the isoelectronic azide anion $[N_3]^-$, the linear CO_2 molecule contains two orthogonal and degenerate 3-center 4-electron π bonds (see MO scheme in Section 2.4.6). CO_2 is the only thermodynamically stable carbon oxide. The unstable *peroxide* CO_3 is formed upon UV irradiation of a solution of O_3 in solid or liquid CO_2. At standard conditions, CO_3 is unstable in the gas phase and its structure is still a subject of intense investigation.[65]

7.7.1.3 Other Carbon Oxides

Tricarbon dioxide (C_3O_2) is formed as a colorless gas (b.p. 7 °C) upon dehydration of malonic acid to its anhydride with P_4O_{10} in vacuum at 150 °C:

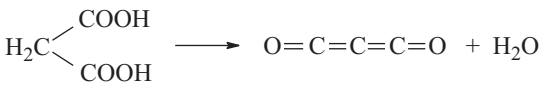

C_3O_2 is also obtained by UV irradiation of CO:

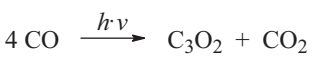

At 25 °C, C_3O_2 can be stored under reduced pressure. At ambient pressure, however, polymerization to a red solid of unknown structure occurs. With water, C_3O_2 reacts back to malonic acid.

65 W. T. Borden et al., *Chem. Sci.* **2016**, *7*, 1142.

The bonding in the C_3O_2 molecule can be described as follows: The CC distances of 128 pm are markedly larger than the CO distances (116 pm; for comparison 113 pm in free CO and 116 pm in CO_2). The bond angle at the central C atom is 156°. Apparently, the CC bonds can be regarded as coordinative in nature, rather than as two cumulated allene-type double bonds. This is rationalized by two CO molecules acting as donor ligands toward a central C atom with two nonbonding electron pairs:

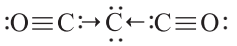

The energy required for the linearization of the molecule, however, is extremely small. In case of a linear scaffold of three C atoms and two terminal O atoms, two sets of perpendicular 2*p* orbitals extend over all five atoms. Their linear combination gives rise to two bonding, one nonbonding and two antibonding orbitals of π-symmetry for both sets.

Another interesting, albeit unstable carbon oxide is the formal CO_2 dimer 1,2-dioxetanedione

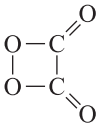

that is formed on decomposition of peroxy oxalate anions. It plays a pivotal role as an intermediate in the well-known luminescent glow sticks.

7.7.2 Sulfides, Selenides and Tellurides

CS_2 and CSe_2 are the heavier analogues of CO_2; CTe_2 has not been isolated yet. *Carbon disulfide* (CS_2) is a colorless, toxic and highly flammable liquid of b.p. 46 °C, which is industrially produced from methane and excess sulfur vapor:

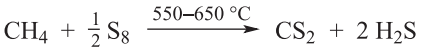

The concomitantly formed hydrogen sulfide is oxidized back to elemental sulfur according to the CLAUS process (Section 12.3.1). CS_2 is used as solvent as well as for the production of CCl_4, vulcanization chemicals, pharmaceutic products and synthetic fibers (*viscose*).[66] The primary raw material for the production of viscose is the pulp

66 A. D. Dunn, W.-D. Rudorf, *Carbon Disulphide in Organic Chemistry*, Wiley, New York, **1989**; M. D. S. Lay et al., *Ullmann's Encycl. Ind. Chem.* **1986**, *A5*, 185; G. Gattow, W. Behrendt, *Carbon Sulfides and Their Inorganic and Complex Chemistry, Top. Sulfur Chem.*, Vol. 2, Thieme, Stuttgart, **1977**.

from trees and other plants, which consists of cellulose to over 90%. The OH groups of the glucose units of cellulose are partially deprotonated by caustic soda, which leads to swelling. This product ("CellONa") is then reacted with CS_2 to give the xanthogenate [Cell-O–C(=S)–S]Na as a viscous, spinnable mass called viscose. Subsequently, the viscose is wet spun by pressing it through spinning nozzles into a sulfuric acid bath to give solid fibers (CellOH) and regenerating the employed CS_2.

In the presence of metal oxides as catalysts, CS_2 hydrolyzes with H_2O to CO_2 and H_2S via the mixed chalcogenide COS as intermediate. With aqueous bases or sulfides, trithiocarbonates are formed:

$$3\ CS_2 + 6\ NaOH \longrightarrow 2\ Na_2[CS_3] + Na_2[CO_3] + 3\ H_2O$$

$$CS_2 + K_2S \longrightarrow K_2[CS_3]$$

CS_2 also serves for the production of thiocyanates by reaction with NH_3:

$$CS_2 + 2\ NH_3 \longrightarrow NH_4[SCN] + H_2S$$

The thiocyanate Na[SCN] is obtained by treatment of the ammonium salt with NaOH.

Carbon diselenide (CSe_2), a yellow, lachrymatory liquid of b.p. 125 °C, is obtained by the introduction of gaseous CH_2Cl_2 into liquid selenium:

$$CH_2Cl_2 + 2\ Se(l.) \xrightarrow{600°C} CSe_2 + 2\ HCl$$

All mixed chalcogenides of carbon are known except for COTe.

CS_2 polymerizes under pressure (4 GPa) at 150 °C or on irradiation (λ = 313 nm), CSe_2 does so already at standard conditions and without external trigger. When gaseous CS_2 is led through an electric discharge at 10 Pa, carbon monosulfide can be detected and condensed ("frozen out") at –190 °C together with excess CS_2. CS is a carbene-analogous molecule and thus of similar reactivity as CF_2, SiF_2 and BF (Section 13.4.6). In the gas phase, CS decomposes within 1 min via the unstable transient C_2S_2 as follows[67]:

$$2\ CS \longrightarrow S{=}C{=}C{=}S$$

$$2\ C_2S_2 \longrightarrow C_3S_2 + CS_2$$

C_3S_2 is a brown-red liquid with an almost linear cumulene structure corresponding to that of C_3O_2: S=C=C=C=S. Analogous Se or Te compounds are unknown. In more

67 R. Steudel, *Z. Anorg. Allg. Chem.* **1968**, *361*, 180. E. K. Moltzen, K. J. Klabunde, A. Senning, *Chem. Rev.* **1988**, *88*, 391.

recent times, a number of cyclic carbon sulfides have been prepared, which are stable at 25 °C, for example, C_3S_8, C_4S_6, C_6S_8, C_6S_{10}, C_6S_{12} and C_9S_9.[68]

7.7.3 Carbonic Acid and Carbonates

This section deals with H_2CO_3, H_2CS_3 and H_2CSe_3 as well as derived species. If a bottle of champagne is opened without appropriate cooling, one immediately realizes how well CO_2 dissolves in water at higher pressures and how quickly it escapes upon a reduction in pressure. The CO_2 partial pressure in the bottle amounts to roughly 7 bar and the cork can reach speeds of up to 60 km h^{-1} if the pressure is rapidly released! Up to 5 L of gaseous CO_2 can be dissolved in 0.75 L of champagne; the pH value is therefore in the range of 3.0–3.2. The CO_2 concentration in the solution can be determined (together with other carbon species) by ^{13}C-NMR spectroscopy.[69] Although CO_2 is the anhydride of *carbonic acid* (H_2CO_3), it reacts only slowly with H_2O at pH = 7 and 25 °C in a weakly endothermic reaction of *pseudo*-first-order kinetics:

$$CO_2 + H_2O \rightleftharpoons H_2CO_3 \qquad K_c = \frac{c(H_2CO_3)}{c(CO_2)} = 1.5 \cdot 10^{-3}$$

$$K_c^* = \frac{c(H_2CO_3)}{c(CO_2) \cdot c(H_2O)} = 2.7 \cdot 10^{-5}\,\mathrm{L\,mol^{-1}}$$

In the equilibrium constant K_c, the concentration of water has been assumed constant in contrast to $K_c^\star$, as can readily be deduced from the units. In a solution of CO_2 in pure water, even after equilibration most carbon dioxide is physically dissolved as unreacted CO_2(aq) and only solvated by hydrogen bonding. Just about 0.15% is present as H_2CO_3, $[HCO_3]^-$ and $[CO_3]^{2-}$:

$$H_2CO_3 + H_2O \rightleftharpoons [H_3O]^+ + [HCO_3]^- \qquad K_1 = \frac{c(H_3O^+) \cdot c(HCO_3^-)}{c(H_2CO_3)} = 2.8 \cdot 10^{-4}\ \mathrm{mol L^{-1}}$$

$$K_1^* = \frac{c(H_3O^+) \cdot c(HCO_3^-)}{c(CO_2) \cdot c(H_2O)} = 3 \cdot 10^{-7} \qquad K_1^{**} = \frac{c(H_3O^+) \cdot c(HCO_3^-)}{c(H_2CO_3) \cdot c(H_2O)} = 3.6 \cdot 10^{-6}$$

If the entire CO_2 concentration is considered, an aqueous CO_2 solution ("carbonic acid") is a very weak acid: $pK_1^\star = 6.5 \pm 0.1$ at 25 °C; for the second dissociation step, one obtains $pK_2^\star = 10.3$:[70]

68 C. P. Galloway, T. B. Rauchfuss, X. Yang in R. Steudel (ed.), *The Chemistry of Inorganic Ring Systems*, Elsevier, Amsterdam, **1992**, S. 25. J. Beck et al., *J. Chem. Soc., Dalton Trans*. **2006**, 1174.

69 G. Liger-Belair, G. Polidori, P. Jeandet, *Chem. Soc. Rev*. **2008**, *37*, 2490. M. Vignes-Adler, *Angew. Chem. Int. Ed*. **2013**, *52*, 187.

70 J. C. Peiper, K. S. Pitzer, *J. Chem. Thermodyn*. **1982**, *14*, 613 (p*K* values also for seawater).

$$[HCO_3]^- + H_2O \rightleftharpoons [H_3O]^+ + [CO_3]^{2-} \qquad K_2^* = \frac{c(H_3O^+) \cdot c(CO_3^{2-})}{c(HCO_3^-) \cdot c(H_2O)} = 4.6 \cdot 10^{-11}$$

The hydration of CO_2 to hydrogen carbonate (also termed as bicarbonate) is of high physiologic importance as this reaction is responsible for the pH regulation in the blood of mammals and therefore also for the transport of CO_2, formed during respiration. The activation enthalpy of the reaction amounts to 62 kJ mol^{-1}, which would correspond to a rather slow equilibration at the body temperature of 37 °C and the blood pH value of 7.40. The zinc-containing enzyme *carboanhydrase* speeds up the reaction by a factor of 10^7.[71]

In weakly alkaline solutions, CO_2 directly dissolves to hydrogen carbonates ($\Delta H^o_{298} = -50$ kJ mol^{-1}):

$$CO_2 + [OH]^- \rightleftharpoons [HCO_3]^- \qquad K_c = 4 \cdot 10^7 \text{ mol}^{-1}\text{L}$$

This reaction is much faster than the above-mentioned hydration of CO_2 to H_2CO_3. In seawater with an average pH value of 8.1, most of the CO_2 is therefore present in the form of hydrogen carbonate.[72]

Due to its very small concentration in water, the true carbonic acid (H_2CO_3) is mostly dissociated into $[HCO_3]^-$ and $[H_3O]^+$. Neat H_2CO_3 can therefore not be isolated from aqueous solution as any dehydration attempt will lead to CO_2 evolution by complete decomposition of H_2CO_3.[73] In the gas phase, however, H_2CO_3 has been produced by pyrolysis of di-*tert*-butyl carbonate under elimination of isobutene.[74] Claims that solid H_2CO_3 can be sublimed in vacuum from acidified methanolic solutions of K[HCO_3] at temperatures as high as 200 K turned out to be erroneous; the species in question was later identified as monomethyl hydrogen carbonate, HCO_2OMe. According to ab initio and matrix isolation studies, the planar H_2CO_3 molecule forms centrosymmetric dimers in the solid state, which are connected by two bridging hydrogen bonds. The monomolecular decomposition of gaseous H_2CO_3 to CO_2 and H_2O is exothermic but kinetically hindered (activation energy, E_a = 184 kJ mol^{-1}), which means that single molecules are comparatively stable. In contrast, the inhibition is rather small in the presence of water (E_a = 70 kJ mol^{-1}) due to the formation of cyclic hydrates, which allow for a proton transfer similar to the GROTTHUSS mechanism (Section 5.2). If an aqueous bicarbonate solution is acidified very rapidly, the primary

71 W. Kaim, B. Schwederski, *Bioinorganic Chemistry – Inorganic Elements in the Chemistry of Life: An Introduction and Guide*, Wiley, Chichester, **2013**.

72 A. Körtzinger, *Chem. unserer Zeit* **2010**, *44*, 118.

73 In industry, gaseous CO_2 is nevertheless often referred to as carbonic acid.

74 J. A. Tossell, *Inorg. Chem.* **2006**, *45*, 5961. T. Loerting, J. Bernard, *ChemPhysChem* **2010**, *11*, 2305. X. Wang et al., *J. Phys. Chem. A* **2010**, *114*, 1734. P. Schreiner et al., *Angew. Chem. Int. Ed.* **2014**, *53*, 11766. S. K. Reddy, S. Balasubramanian, *Chem. Commun.* **2014**, *50*, 503.

product is H_2CO_3, but the acid quickly decomposes to CO_2 and water. The true carbonic acid is much more acidic ($pK_1 = 3.45$) than the above-mentioned hydrated CO_2.

A crystalline derivative of carbonic acid is the trihydroxo carbenium salt $[C(OH)_3][SbF_6]$, which is prepared as follows at −60 °C:

$$OC(OSiMe_3)_2 + 3\,HF + SbF_5 \longrightarrow [C(OH)_3][SbF_6] + 2\,Me_3SiF$$

The hexafluoroantimonate decomposes at −4 °C under CO_2 elimination. The planar carbenium cation (C_{3h} symmetry) is connected to the surrounding anions through hydrogen bonds.[75]

By feeding CO_2 into caustic soda (NaOH), the corresponding carbonate is obtained initially. Upon further CO_2 addition, this is converted to the hydrogen carbonate due to the progressively lowered pH value:

$$CO_2 + 2\,NaOH \longrightarrow Na_2[CO_3] + H_2O$$

$$Na_2[CO_3] + CO_2 + H_2O \longrightarrow 2\,Na[HCO_3]$$

Both salts are found in extensive deposits in the USA. In other parts of the world, soda is mostly produced according to the SOLVAY process from limestone and rock salt:

$$Ca[CO_3] \xrightarrow{\Delta T} CaO + CO_2\uparrow$$

$$NH_3 + CO_2 + H_2O \longrightarrow [NH_4][HCO_3]$$

$$[NH_4][HCO_3] + NaCl \longrightarrow Na[HCO_3]\downarrow + [NH_4]Cl$$

$$2\,Na[HCO_3] \xrightarrow{\Delta T} Na_2[CO_3] + H_2O + CO_2\uparrow$$

$$CaO + 2\,[NH_4]Cl \longrightarrow CaCl_2 + 2\,NH_3\uparrow + H_2O$$

These equilibrium reactions are driven by the evolution of gases or precipitation of solids. Summing up the above equations under consideration of the recycling of CO_2 and NH_3 gives:

$$Ca[CO_3] + 2\,NaCl \longrightarrow Na_2[CO_3] + CaCl_2$$

Huge amounts of soda are used in the production of glass, in particular for glass bottles. Furthermore, soda serves as a starting material for production of other sodium salts (phosphates, silicates, chromates and nitrates). In the structure of K $[HCO_3]$, dimeric anions are present, which contain two bridging hydrogen bonds.

With ionic fluorides of large cations, CO_2 reacts to *fluorocarbonates* at 25 °C:[76]

75 R. Minkwitz, S. Schneider, *Angew. Chem.* **1999**, *111*, 749.

76 X. Zhang, U. Groß, K. Seppelt, *Angew. Chem. Int. Ed.* **1995**, *34*, 1858.

$$[Pip]^+F^- + CO_2 \longrightarrow [Pip]^+[CO_2F]^- \quad [Pip]^+: \text{hexamethylpiperidinium}$$

The anion $[CO_2F]^-$ is isoelectronic to the nitrate anion, but is instantly decomposed by water to bicarbonate, HF and CO_2. Trithio- and triselenocarbonates are obtained from CS_2 and CSe_2, respectively, through the following reactions:

$$CS_2 + [SH]^- + [OH]^- \longrightarrow [CS_3]^{2-} + H_2O$$

$$CSe_2 + [SeH]^- + [OH]^- \longrightarrow [CSe_3]^{2-} + H_2O$$

Mixed chalcogenocarbonates can be synthesized in an analogous manner. In general, the anions of type $[CE_3]^{2-}$ (E = O, S, Se) are trigonal planar (D_{3h} symmetry). Just as in the isoelectronic BF_3 molecule, the six π-electrons are delocalized with just one pair in a bonding molecular orbital (Section 2.4.8). This delocalization can be described by the following resonance structures:

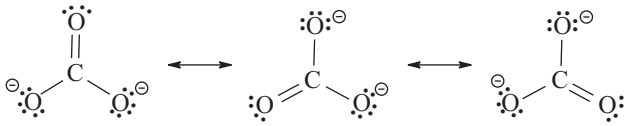

In contrast to carbonic acid, the free *trithiocarbonic acid* can be isolated from strongly acidic aqueous solution by adding a suspension of $Ba[CS_3]$ in H_2O to 10% hydrochloric acid at 0 °C. H_2CS_3 separates as red oil, which crystallizes from $CH_2Cl_2/CHCl_3$ with a lemon yellow color (m.p. −27 °C). The molecules of H_2CS_3 are perfectly planar. In water, H_2CS_3 is an acid of medium strength (K_1 = 1.2 at 0 °C). In a similar manner, albeit in diethylether as solvent, the acid H_2CSe_3 has been prepared from $Ba[CSe_3]$ as dark-red highly viscous oil (dec. > −10 °C). Both acids slowly decompose at 25 °C to CS_2/H_2S and CSe_2/H_2Se, respectively.

7.7.3.1 Carbonic Peracids

Peroxodicarbonate has been synthesized through anodic oxidation of carbonate at −20 °C and isolated as the potassium salt:

$$2\,[CO_3]^{2-} \longrightarrow [C_2O_6]^{2-} + 2\,e^-$$

The anion consists of two planar CO_3 units, connected by an OO bond of 147 pm with a COOC dihedral angle of 93°.[77] In addition, the peroxocarbonate salts $K[HCO_4]\cdot H_2O_2$ and $K_2[CO_4]\cdot 3.5H_2O_2$, prepared by reaction of $K[HCO_3]$ with H_2O_2 (30%) at −10 °C, contain a COO group and thus are derivatives of monoperoxocarbonic acid.[78] The corresponding

77 M. Jansen et al., *Angew. Chem. Int. Ed.* **2002**, *41*, 1922.

78 A. Adam, M. Mehta, *Angew. Chem. Int. Ed.* **1998**, *37*, 1387. D. E. Richardson et al., *Inorg. Chem.* **2010**, *49*, 11287. F. Hinrichs, A. Adam, *Z. Anorg. Allg. Chem.* **2011**, *637*, 426.

free acids H_2CO_4 and $H_2C_2O_6$, however, are unknown. In contrast to such true *peracids*, the so-called sodium percarbonate used as a bleaching agent in large amounts is an adduct of $Na_2[CO_3]$ and H_2O_2 (Section 11.3.3).

Aqueous trithiocarbonate solutions dissolve sulfur under formation of perthiocarbonate $[CS_4]^{2-}$. From the salt $[NH_4]_2[CS_4]$ and HCl gas at −78 °C in Me_2O, perthiocarbonic acid (H_2CS_4) has been obtained as yellow crystals, which slowly decompose at this temperature (more rapidly at the m.p. of −37 °C) to H_2S, CS_2 and sulfur. The connectivities of H_2CS_4 and $[CS_4]^{2-}$ are as follows:

7.8 Carbon Nitrides

Molecular carbon–nitrogen compounds are ubiquitous in organic chemistry in the form of amines, amino acids, imines, cyanates, isocyanates and various other nitrogen-containing functional groups. Conversely, CN species without CH bonds are relatively rare. The biomolecule guanidine $(H_2N)_2C{=}NH$ combines two amino groups and one imine functionality at a single carbon atom. Its deprotonated salts continue to attract attention due to their delocalized structure related to the carbonates discussed in the previous section. For instance, the reaction of strontium with guanidine in liquid ammonia gives the doubly deprotonated strontium salt, $Sr[C(NH)_3]$.[79]

7.8.1 Hydrogen Cyanide and Cyanides

Hydrogen cyanide (HCN) is a colorless, extremely toxic liquid (b.p. 25 °C) of high technological importance.[80] It is sometimes also referred to as *prussic acid* ("Blausäure" in German) due to its use in the production of Prussian blue, $Fe_4[Fe(CN)_6]_3$. Several processes are used for the production of HCN, which all start with methane and ammonia (BMA process: "Blausäure aus Methan und Ammoniak," in English "prussic acid from methane and ammonia"). The ANDRUSSOW process relies on the partial oxidation of a mixture of methane and ammonia above 1000 °C on a Pt/Rh or Pt/Ir catalyst:

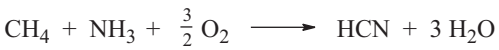

79 R. Dronskowski et al., *Angew. Chem. Int. Ed.* **2015**, *54*, 12171.
80 H. Klenk et al., *Ullmann's Encycl. Ind. Chem.* **1987**, *A8*, 159.

While the above reaction is strongly exothermic, the methane-ammonia process of the company EVONIK requires external heating and the gas mixture is dehydrogenated at 1200–1250 °C on a Pt/Al catalyst:

$$CH_4 + NH_3 \longrightarrow HCN + 3H_2 \qquad \Delta H^\circ_{298} = 256 \text{ kJ mol}^{-1}$$

Neat liquid HCN tends to polymerize exothermically to a brown to black solid. It can be stabilized by cooling to 5 °C and addition of some orthophosphoric acid (H_3PO_4) or formic acid (HCOOH). The cyanides NaCN and KCN are produced by reaction of the concentrated aqueous hydroxides with HCN. Metal cyanides are employed in electroplating and for the hardening of steel. As salts of a weak acid, alkali metal cyanides undergo hydrolysis in aqueous solutions liberating free HCN. Similarly, CO_2 (e.g., from air) liberates HCN from cyanides in the presence of H_2O:

$$NaCN + CO_2 + H_2O \longrightarrow Na_2[CO_3] + HCN$$

The toxic gas cyanogen $(CN)_2$ (b.p. –21 °C) is obtained by oxidation of cyanide anions with mild oxidizing agents:[81]

$$2\,KCN + Cu[SO_4] \longrightarrow \tfrac{1}{2}\,(CN)_2\uparrow + CuCN + K_2[SO_4]$$

Copper(I) is reoxidized to Cu(II) by H_2O_2 so that as a net outcome HCN reacts with H_2O_2 to $(CN)_2$ and H_2O. Industrially, cyanogen is produced through catalytic oxidation of HCN with Cl_2 or NO_2. The reaction of NaCN with elemental chlorine affords chlorocyan (b.p. 13 °C), which is extremely toxic as well:

$$NaCN + Cl_2 \longrightarrow ClCN + NaCl$$

The covalent cyanides HCN, ClCN and – in lesser quantities – $(CN)_2$ serve for the industrial synthesis of numerous organic nitrogen compounds including herbicides and amino acids. Together with acetone and methanol, HCN is also the starting point for the production of *acrylic glass* (polymethyl methacrylate). With $Ca[CO_3]$ at 800 °C, HCN reacts to *calcium cyanamide* that contains the carbodiimide anion $[CN_2]^{2-}$, which is isoelectronic to CO_2 ($D_{\infty h}$ symmetry):

$$2\,HCN + Ca[CO_3] \longrightarrow Ca[CN_2] + CO + CO_2 + H_2$$

The industrial production of the cyanamide, however, uses the nitridation of calcium carbide by elemental nitrogen at high temperatures. The extreme *toxicity* of cyanides (and thus prussic acid) is due to their irreversible coordination to the metal cations

81 A better method on the laboratory scale is the pyrolysis of diacetylglyoxime: D. J. Park, A. G. Stern, R. L. Willer, *Synth. Commun.* **1990**, *20*, 2901.

(Fe, Cu) of the enzyme *cytochrome c oxidase*, which is responsible for the reduction of O_2 to H_2O during the mitochondrial respiratory chain.

When graphite is evaporated in the presence of $(CN)_2$, α,ω-dicyano polyynes are obtained, that is, rod-shaped molecules with cyano groups at both ends. Compounds of type NC–C_{2n}–CN have been isolated with n = 3–8, for example, $C_{18}N_2$:[82]

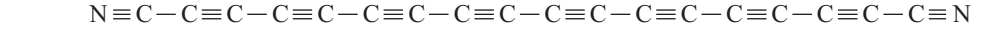

These remarkable substances form colorless crystals that decompose to a black polymer at 20 °C. Apparently, graphite evaporates as small C_n molecules (as also shown by the formation of fullerenes), which react with the CN radicals generated from $(CN)_2$ at high temperatures.

7.8.2 Binary Carbon–Nitrogen Species

Binary carbon nitrides are obtained as polymeric substances of varying composition from the pyrolysis of organic nitrogen compounds such as guanidine or by CVD methods. The structures of the idealized empirical formula C_3N_4 are probably related to that of graphite.[83] Such materials have attracted a lot of interest due to their use as photocatalysts for water splitting,[84] more recently also for their semiconducting properties and immense thermal stability.[85] Through application of high pressures and high temperatures (30 GPa/3000 K), a diamond-like product of the approximate composition C_2N_2 has been produced, which is at least as hard as diamond itself.[86]

An example for a molecular binary CN species is provided by tetraazidomethane $C(N_3)_4$ with a nitrogen content of more than 93%. The compound is formed by nucleophilic attack of azide anions at trichloro acetonitrile at 50 °C and can be isolated as colorless explosive liquid:

Expectedly, $C(N_3)_4$ is highly reactive and readily adds, for instance, to CC double and triple bonds. With water, the azide of carbonic acid $(N_3)_2CO$ is formed.[87]

82 A. Hirsch et al., *Chem. Eur. J.* **1997**, *3*, 1105.
83 J. Xu et al., *Phys. Chem. Chem. Phys.* **2013**, *15*, 4510.
84 L. Qu et al., *Angew. Chem. Int. Ed.* **2015**, *54*, 11433.
85 Review: M. Antonietti et al., *Chem. Soc. Rev.* **2016**, *45*, 2308.
86 T. Komatsu, *Phys. Chem. Chem. Phys.* **2004**, *6*, 878. See also: R. Riedel et al., *Angew. Chem. Int. Ed.* **2007**, *46*, 1476.
87 K. Banert et al., *Angew. Chem. Int. Ed.* **2007**, *46*, 1168.

8 Silicon and Germanium

8.1 Introduction

Silicon and germanium, together with carbon, tin and lead, constitute Group 14 of the Periodic Table. In this group, the transition from nonmetallic to metallic behavior occurs between Ge and Sn. Considering its chemistry, carbon is classified as a nonmetal, despite the existence of an allotrope with metallic conductivity. Silicon and germanium are semiconductors in the elemental state, but – just as carbon – are considered nonmetals based on their reactivity.

Elemental silicon as well as various silicon compounds are of highest technological importance. It is the basis of microelectronics and photovoltaics and therefore pivotal for modern society, if not the future of mankind. Silicates have been known since antiquity as materials such as clay, porcelain, glass, ceramics and enamel. As zeolites, they are important heterogeneous catalysts for various processes. Polysiloxanes ("silicones") are indispensable polymers in daily life, but also for less common high-tech applications. Silica, finally, is used in various areas, for example, as absorbent (and drying agent), as filler for polymers such as rubber and as solid platform for catalysts.[1]

After oxygen, silicon[2] is the second most abundant element in the Earth's crust, making up for about 27.7 wt%. In contrast to carbon, Si does not occur in elemental form, but rather almost without exception as oxygen compounds (SiO_2 and silicates).[3] The two elements form very strong bonds with each other, which explains the high affinity of silicon to oxygen; together, both elements account for three quarters of the mass of the Earth's crust. The natural isotopic mixture consists of ^{28}Si (92.2%), ^{29}Si (4.7%) and ^{30}Si (3.1%). ^{29}Si with its nuclear spin of $I = ½$ is well suitable for NMR spectroscopic investigations.

Germanium[4] is quite similar to silicon in its chemical behavior, although there are a number of important differences, predominantly in reaction kinetics. For example, unlike SiH_4, which is extremely pyrophoric in the presence of oxygen and sensitive to hydrolysis at slightly raised pH, GeH_4 turns out to be almost inert toward air and even concentrated aqueous solutions of NaOH. In disagreement to the PAULING scale, this suggests substantially differing electronegativities

1 B. Friede, E. Gaillou, *Chem. unserer Zeit* **2018**, *52*, 84.

2 P. D. Lickiss, *Encycl. Inorg. Chem.* **2005**, *8*, 5109. Also see topical issue: *Chem. Rev.* **2005**, *105*, No. 5. P. Jutzi, U. Schubert (eds.), *Silicon Chemistry*, Wiley-VCH, Weinheim, **2003**.

3 The very rare mineral *moissanite* (SiC) is a notable exception. Moreover, inclusions of other oxygen-free silicon species such as silicides have been found in some minerals: L. Dobrzhinetskaya et al., *Lithos* **2018**, *310–311*, 355 and cited literature.

4 C. Qin, L. Gao, E. Wang, *Encycl. Inorg. Chem.* **2005**, *3*, 1630.

https://doi.org/10.1515/9783110578065-009

χ for Si and Ge and thus prompted ALLRED and ROCHOW to develop a new scale to better reflect the differences in chemical behavior (Si: χ_P = 1.90, χ_{AR} = 1.74; Ge: χ_P = 2.01, χ_{AR} = 2.02; also see Section 4.6.2). Nonetheless, in general germanium strongly resembles silicon in its chemical behavior and the chemistry described herein for silicon species is in many cases representative for the corresponding germanium compounds. Important differences will be highlighted where appropriate.

Although Ge is widely distributed as companion of numerous minerals, for example, of Zn and Cu, it is a comparatively rare element ($7{\cdot}10^{-4}$ wt% of the Earth's crust). In concentrated form it is mainly encountered as sulfur compounds (thiogermanates). In the mineral $4Ag_2S{\cdot}GeS_2$, CLEMENS WINKLER discovered the element germanium in 1886 in Freiberg/Germany. This discovery was one of the early triumphs of the Periodic Table of Elements, which had predicted the existence of an element below silicon, referred to as "eka-silicon." Of the five natural isotopes ^{70}Ge (20.5 %), ^{72}Ge (27.4 %), ^{73}Ge (7.8 %), ^{74}Ge (36.5 %) and ^{76}Ge (7.7 %), only ^{73}Ge ($I = {}^9/_2$) is suitable for NMR spectroscopy; all others have a nuclear spin of 0. The high quadrupole momentum of ^{73}Ge, however, leads to extreme broadening of lines and renders the practical use for routine NMR spectroscopy impossible at present, excepting the most symmetrical of cases such as GeH_4.

8.2 Bonding Situation

Like all other elements of Group 14, Si and Ge have four electrons in the valence shell with an $s^2p_x^1p_y^1$ configuration (^{3}P ground state). Consequently, the most important oxidation states of silicon and germanium are +2 and +4. Small molecules (i.e., without sterically very demanding substituents and/or electronically stabilizing moieties) of divalent silicon cannot be isolated at room temperature. Nevertheless, they can be generated in equilibrium with other species at elevated temperature as well as under nonequilibrium conditions, for example, in a microwave plasma or in flow reactors. In addition, such molecules have been obtained in an inert, frozen and thus rigid matrix by photolysis of suitable precursors at low temperatures.[5] Under such conditions, reactive species can be readily studied spectroscopically (matrix isolation). Examples include the following *silylenes* SiX_2 and diatomic species of a transient nature:

$$SiH_2 \quad SiF_2 \quad SiCl_2 \quad Si_2 \quad SiO \quad SiS$$

5 For thermodynamically disfavored species, the activation barriers of all possible decomposition pathways have to be at least 60–80 kJ mol^{-1} for survival for about one day under standard conditions (25 °C/1 bar).

The three silylenes form angular singlet molecules of C_{2v} symmetry that closely correspond to carbenes of type CX_2 (*carbene-analogous species*). The bonding situation resembles that of the H_2O molecule (Section 2.4.7), only that there are two electrons less at the central atom, that is, the *p* orbital perpendicular to the plane of the molecule is unoccupied (LUMO). Silylenes tend to dimerization and oligomerization. SiH_2 is an important transient intermediate of the CVD of highly pure silicon by thermolysis of SiH_4 (see Section 8.3).

Silicon monoxide SiO is the analog of CO and plays a decisive role as an intermediate of technical high-temperature processes (see SiC and Si_3N_4). In addition to the σ bond, SiO has two orthogonal π bonds, although much weaker than those of carbon monoxide. This relative weakness has been attributed to the much less pronounced overlap of the $2p_\pi$ orbitals of oxygen with the $3p_\pi$ orbitals of silicon than with the $2p_\pi$ orbitals of carbon (Section 4.2.2). A more elaborate theoretical analysis, however, suggests that relative instability of π bonds is mostly an effect of the highly effective overlap of $3p_\sigma$ orbitals and the thus increased stability of σ bonds. Similar considerations apply to Si_2 (corresponding to C_2) and SiS as well as to a whole variety of thermodynamically viable diatomic molecules involving silicon (and the other heavier Group 14 elements).

By using *bulky* and/or *electronically stabilizing substituents*, it has nonetheless been possible to isolate numerous silylenes at room temperature,[6] for example, the following species [Ar: (2,6-Mes)$_2$C$_6$H$_3$)]:

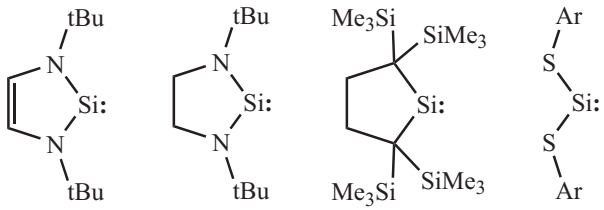

Analogous species of germanium have also been reported, in part prior to the silicon examples.[6] The nitrogen donor ligands result in the partial delocalization of the nonbonding electron pair at nitrogen into the vacant $3p_\pi$ AO of the silicon atom, which stabilizes the molecule. Silylenes and germylenes are also employed as ligands in transition metal complexes, occasionally with remarkable performance in homogeneous catalysis.[7]

6 Y. Mizuhata, T. Sasamori, N. Tokitoh, *Chem. Rev.* **2009**, *109*, 3479.

7 M. Driess et al., *J. Am. Chem. Soc.* **2017**, *139*, 13499.

The following species is formally referred to as a *trisilaallene*, which is best described as a hybrid of several resonance structures. The neutral structure is akin to the *trans*-bent structures of *disilenes* with just one Si=Si double bond (see Section 8.11.2) and can be rationalized by assuming contributions of the two mono(ylidic) forms. The bis(ylidic) resonance structure – supported by more recent theoretical investigations[8] – can alternatively be written as a complex of Si(0) with two silylene ligands and two lone pairs at the central silicon atom. The SiSiSi angle in the trisilaallene amounts to 137° in line with dominating contributions of the mono and bis(ylidic) resonance forms:

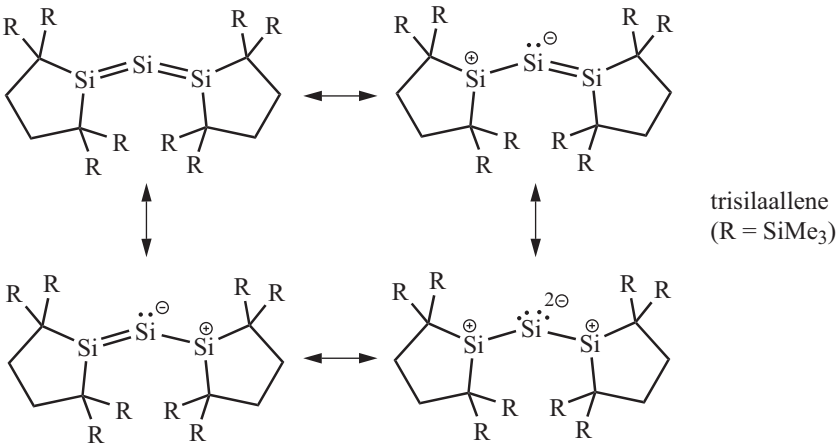

The by far most frequent and hence most important bonding situation of silicon (similarly germanium) is tetravalent as in SiH_4 and its countless derivatives. In analogy to the alkanes C_nH_{2n+2}, silicon and germanium form hydrides of the general formulae Si_nH_{2n+2} (*silanes*) and Ge_nH_{2n+2} (*germanes*). SiH_4 and GeH_4 are tetrahedral molecules just like CH_4. The higher silanes and germanes contain homonuclear SiSi and GeGe bonds, respectively, as do the corresponding halides Si_nX_{2n+2} and Ge_nX_{2n+2} (X=F, Cl, Br, I).

The bonding in SiH_4 can be understood in strict analogy to molecular orbital treatment of the CH_4 molecule (Section 2.4.10): the valence orbitals of the central atom ($3sp_xp_yp_z$) combine with the four 1*s* AOs of the hydrogen atoms to four bonding and four antibonding MOs (four five-center bonds). The eight valence electrons occupy the totally symmetric and the three degenerate bonding MOs. This bonding pattern is also present in organosilanes, in the tetravalent silicon halides as well as in tetrahedral oxoanions derived from $[SiO_4]^{4-}$. The high average bond energies of SiH,

8 N. Takagi, T. Shimizu, G. Frenking, *Chem. Eur. J.* **2009**, *15*, 3448.

SiC, SiF, SiCl and SiO bonds (300–580 kJ mol^{-1}) are responsible for the considerable thermal stability of many silicon compounds (see Table 4.1).

Silicon (less so germanium) is distinguished from carbon by its lower electronegativity resulting from the much larger atomic radius. The ALLRED–ROCHOW scale lists the following values for the electronegativities (χ_{AR}):

C: 2.5 Si: 1.7 Ge: 2.0

As the electronegativity of hydrogen (χ_{AR}=2.2) is in between these values, the EH bonds are polarized differently in the corresponding hydrogen species. For all saturated species of type SiX_4 and GeX_4, the central atoms are positively charged, turning these compounds into LEWIS acids. This is particularly true for the Si derivatives, as the electronegativity of Si is considerably smaller than that of Ge. The LEWIS acidity has far reaching consequences for the structural chemistry of silicon. If no LEWIS base is at hand, an intramolecular backdonation from lone pairs at the ligands can slightly alleviate the electron deficiency at the silicon center. Examples are known for species with bonds between silicon and N, O and F, and – to a lesser extent – their heavier congeners. In these bonds, a partial delocalization of the formally nonbonding electrons at the N, O or F atoms occurs into the vacant σ* MOs of t_2 symmetry at the central atom. Such π back-bonding is relatively weak; it can also be described as a *hyperconjugation* effect, as described before for other molecules. These concepts are the result of extensive *ab initio* MO calculations; they rationalize the structural peculiarities summarized in Table 8.1.

Table 8.1: Comparison of bond angles C–E–C, Si–E–Si and Ge–E–Ge in homologous species (E=N or O).

$H_3C–O–CH_3$:	111.5°	$(H_3C)_3N$:	110.6°
$H_3Si–O–SiH_3$:	144.1°	$(H_3Si)_3N$:	119.7°
$H_3Ge–O–GeH_3$:	126.5°	$(H_3Ge)_3N$:	120°

While dimethyl ether $(H_3C)_2O$ shows a regular bond angle of 111.5° at the central oxygen atom, $(H_3Ge)_2O$ has a widened angle of 126.5° and $(H_3Si)_2O$ even of 144.1°. According to the VSEPR model, the withdrawal of electron density from the oxygen atom with the concomitant formation of dative π bonds leads to a widening of the angle. In case of the nitrogen species, the effect is even stronger: for trimethylamine Me_3N the bond angles at the N atom amount to 110.6°, but for trisilylamine and trigermylamine to 120°, that is, in both cases the N atom is coordinated in a perfectly trigonal planar manner! In this geometry, the p_π AO at nitrogen can overlap with 3*p* orbitals at each of the neighboring Si and Ge atoms, which contribute significantly to the bonding $e_{2''}$ MOs of the molecule. In addition to the influence on the bond angles, this partial π character leads to a strengthening of the SiN, SiO and SiF

bonds, respectively. Therefore, the average bond energy in SiF_4 is much larger than in CF_4 and GeF_4, while normally the bond energies steadily decrease going down in any particular group of the Periodic Table (see Table 8.2). Similar considerations apply to $SiCl_4$, although the high polarity of the bonds certainly exerts an influence as well. The extraordinarily thermal stability of SiO_2 can also be attributed to the unusually high bond energy. The bond angles at the bridging O atoms of the different SiO_2 modifications cover the range from 144° to 147°; in the disiloxane $[^tBu(OH)_2Si]_2O$ even 180° are reached.

Table 8.2: Average bond enthalpies of selected element combinations at 25 °C (kJ mol^{-1}).

	–H	–F	–Cl	–O–
C	411	485	327	358
Si	326	582	391	452
Ge	289	452	349	–

Alongside these direct backbonding interactions, other dative bonds occur in some silicon compounds, for example, in the structural motif SiON. In molecules such as $(CF_3)F_2Si–O–NMe_2$ unusually small bond angles are observed at the oxygen atom (in the gas phase: 84°), which can be attributed to a dative bond from nitrogen to silicon or – alternatively – to electrostatic interaction between these two atoms with opposite partial charges. This Si···N attraction also exists in species with several methylene spacers between the silicon atom and the nitrogen donor, which may result in ring closure, in particular at lower temperatures.[9]

As LEWIS acids, the tetrahalides SiX_4 and GeX_4 form adducts with donors (LEWIS bases) such as fluoride ions or tertiary amines and phosphanes, for example:

$$SiF_4 + F^- \longrightarrow [SiF_5]^- \xrightarrow{F^-} [SiF_6]^{2-}$$

$$GeF_4 + F^- \longrightarrow [GeF_5]^-$$

$$SiCl_4 + bipy \longrightarrow [(bipy)SiCl_4]$$

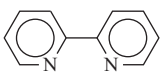

bipy = 2,2'-bipyridine

The resulting compounds are formally hypervalent. The pentacoordinate derivatives have a trigonal bipyramidal structure. Just like the analogous phosphoranes, they suffer rapid intramolecular ligand exchange in solution at room temperature (BERRY *pseudo-rotation*), as long as they conform to the general rule that the most

9 N. M. Mitzel et al., *J. Am. Chem. Soc.* **2005**, *127*, 13705 and *Inorg. Chem.* **2008**, *47*, 10554.

electronegative substituents are located in the axial positions. The octahedral hexafluorosilicate dianion $[SiF_6]^{2-}$ is isoelectronic to the neutral SF_6. The six identical mostly covalent bonds can be explained by the concept of multicenter bonding (Section 2.6): only the silicon orbitals 3*s*, p_x, p_y and p_z (not the *d* orbitals!) are combined with the $2p_\sigma$ orbitals of the fluorine atoms. According to this approach, only eight valence electrons are present at the Si atom and the species is therefore not really hypervalent. Consequently, the more appropriate term *hypercoordinate* should be used. Hypercoordinate silicon compounds with coordination numbers of 5 and 6 are known in great numbers.[10] They play an important role as reaction intermediates in nucleophilic substitution reactions, for instance, during the hydrolysis of silicon halides:

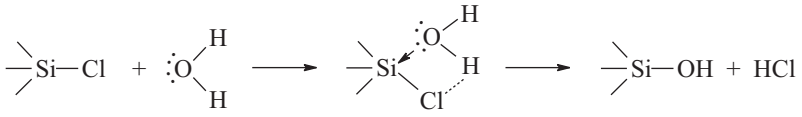

The primary product of this reaction is a pentacoordinate adduct that subsequently eliminates one equivalent of HCl to give a silanol. The assumption of this intermediate is supported by the isolation of the above mentioned $SiCl_4$-base adducts. By repetition of this nucleophilic substitution, all four Cl atoms are finally replaced by OH groups, that is, orthosilicic acid $Si(OH)_4$ is formed. In the case of CCl_4, the analogous reaction is thermodynamically viable ($\Delta G^o < 0$), but kinetically hindered as the considerably smaller C atom is efficiently shielded by the large chlorine atoms against nucleophilic attack. The increased steric strain raises the energy of the pentacoordinate species to such an extent that it is turned from an intermediate (Si) into a transition state (C). Therefore, CCl_4 hydrolyzes very slowly even when heated with water; CF_4 and CCl_4 do not show LEWIS acidic behavior. These examples illustrate that many analogies between the chemistry of carbon and that of silicon only refer to composition and structures of compounds, while their reactivity can be drastically different due to differing atomic radii.

The *coordination number* of silicon in its compounds can adopt values between 1 and 10. It is defined as the number of nearest neighboring atoms of the central atom in a distance equal or at least similar to the sum of covalent radii. The by far most frequent coordination number of silicon is 4 (quartz, silicates, silanes, halo- and organosilanes), followed by 6 as in $[SiF_6]^{2-}$. Examples for the coordination number 10 are given by the following two sandwich complexes of Si(II) and Si(IV), in which the pentamethylcyclopentadienide anions $[Me_5C_5]^-$ (left) and carbollide dianions $[C_2B_9H_{11}]^{2-}$ (right) act as ligands (C atoms in black; H atoms not drawn):

10 C. Chuit et al., *Chem. Rev*. **1993**, *93*, 1371. R. R. Holmes, *Chem. Rev*. **1996**, *96*, 927. R. Tacke et al., *Inorg. Chem*. **2007**, *46*, 5419. D. Kost, I. Kalikhman, *Acc. Chem. Res*. **2009**, *42*, 303.

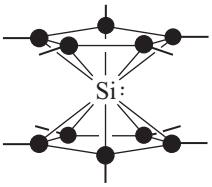

$[(Me_5C_5)_2Si]$

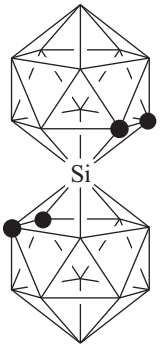

$[(C_2B_9H_{11})_2Si]$

Trigonal planar coordination of silicon atoms is typically found in silylium cations, but only with weakly coordinating counter-anions and sterically demanding substituents. Even very weakly coordinating carborate anions show substantial interaction with the cationic silicon center as in the silyl cation of the salt $[Me_3Si][HCB_{11}F_{11}]$, which deviates significantly from planarity.[11]

Just like carbon, silicon forms a number of unsaturated species with p–p π bonds. Examples are:[12]

>Si=C<	>Si=N–	>Si=O	–Si≡C–
Silene	Silazene	Silanone	Silyne
(silaethene)	(silanimine)	(silaketone)	(silaethine)
>Si=Si<	>Si=P–	>Si=S	–Si≡Si–
Disilene	Silaphosphene	Silanthione	Disilyne

Under standard conditions, however, species of these types are only stable and hence isolable in pure form if the multiple bonds are either shielded by large substituents or stabilized by electronic effects.[13] Several bulky substituents have been developed to this end. They *kinetically hinder* intermolecular reactions and thus prevent *oligomerization*. The relevant thermodynamic relationships shall be explained in more detail on the pertinent case of disilenes. The parent species $H_2Si{=}SiH_2$ cannot be isolated in pure form. For this, the same reasons apply as in the cases of the diatomic molecules disulfur S=S (Section 4.2.3) and diphosphorus

11 H. Willner et al., *Angew. Chem. Int. Ed.* **2007**, *46*, 6346.

12 R. C. Fischer, P. P. Power, *Chem. Rev.* **2010**, *110*, 3877.

13 For example, >Si=O, >Ge=O, >Si=S, >Si=Se and >Si=Te: M. Driess et al., *J. Am. Chem. Soc.* **2010**, *132*, 3038 and 6912 as well as *Angew. Chem. Int. Ed.* **2013**, *52*, 4302. R. Tacke et al., *Chem. Eur. J.* **2012**, *18*, 16288.

P_2 (Section 10.2), which are unstable at room temperature as well. The conversion of the SiSi double bond into two single bonds is exergonic under these conditions, that is, the GIBBS energy of the reaction is negative. Therefore, intermediately formed Si_2H_4 almost instantly oligomerizes to higher *cyclo*-silanes or polymeric $(SiH_2)_{2n}$:

$$n\,H_2Si{=}SiH_2 \longrightarrow -(SiH_2)_{2n}- \qquad \Delta G^\circ < 0$$

In case of the homologous ethene $H_2C{=}CH_2$, the corresponding polymerization to the thermodynamically more stable polyethylene is also exergonic but associated with a higher activation barrier. For this reason, it happens spontaneously only at higher temperatures or in the presence of a catalyst. In a first approximation, the π bond of disilenes is largely analogous to that of alkenes (see Section 8.11.2 for a more detailed discussion). The overlap integral and thus the splitting between the π and the π* orbital is generally smaller for larger orbitals (Figure 8.1). As a consequence, disilenes are far more reactive than alkenes.

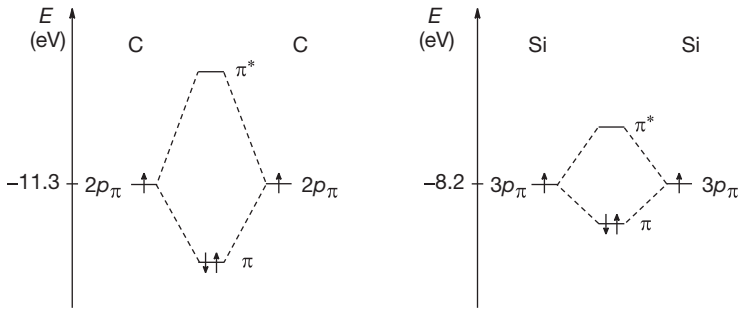

Figure 8.1: Energy term diagrams for the π bonds of alkenes (left) and disilenes (right). The splitting between the π and π* molecular orbitals is about twice as high for alkenes than for disilenes.

Irradiation of such unsaturated molecules can excite a bonding π electron into the π* MO. The energy required for the excitation (HOMO–LUMO gap) can be measured by UV–Vis spectroscopy. For alkenes, this energy typically corresponds to a wavelength of 200 nm (6.2 eV), while the longest wavelength absorption of disilenes is observed in the range from 390 to 480 nm in most cases (2.5–3.1 eV). Accordingly, disilenes absorb light in the purple to blue region and show an intense yellow to orange color.

The double bond between the two Si atoms leads to a rotational barrier of more than 100 kJ mol^{-1} for the torsion about the SiSi axis. The corresponding energy profile is shown in Figure 8.2 (*torsion potential*).

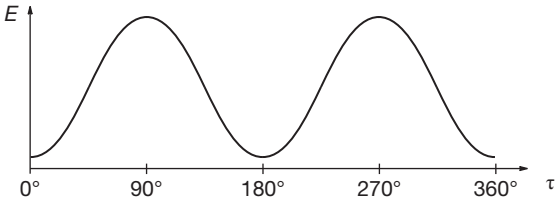

Figure 8.2: Energy *E* as a function of the torsion angle τ at the SiSi double bond of disilenes $R_2Si{=}SiR_2$.

At torsional angles (τ) of 90° and 270°, the energy of the molecule reaches a maximum, because the zero net overlap of the then orthogonal *p* orbitals completely prevents a π bonding interaction: the molecule has a triplet state in this case. The energy difference between the minima and maxima corresponds to the activation energy for the rotation about the SiSi axis and thus for the *E-Z* isomerization of unsymmetrically substituted disilenes. Saturated silanes show a much smaller barrier of rotation about the SiSi single bond (5 kJ mol^{-1} for Si_2H_6).

For *germanium*, similar considerations apply.[12] As for disilenes, the barrier ($\Delta H°_{298}$) for the rotation about the double bond of digermenes $R_2Ge{=}GeR_2$ is within the same order of magnitude at 1 eV (Si=Si: 1.1 eV, Ge=Ge: 0.9 eV).

8.3 The Elements Silicon and Germanium

Under standard conditions, silicon and germanium crystallize in the cubic *diamond structure* with internuclear distances of 235.2 pm (SiSi) and 245.0 pm (GeGe). By application of high pressure, other modifications with higher densities have been obtained.[14] Graphene- or fullerene-like modifications, however, are unknown for both elements, which is another manifestation of the relative weakness of the heavier multiple bonds.

Elemental silicon (m.p. 1414 °C) is industrially produced from SiO_2 by reduction of purified quartz with coke and charcoal in an electric arc furnace at ca. 2000 °C (electric arc- or carbothermal process):

$$SiO_2 + 2\,C(s.) \longrightarrow Si(l.) + 2\,CO\uparrow \qquad \Delta H^{\circ}_{2100} = 695\ kJ\ mol^{-1}\ (Si)$$

14 U. Schwarz et al., *Inorg. Chem.* **2012**, *51*, 8686. J. Donohue, *The Structures of the Elements*, Wiley, New York, **1974**.

This reaction is endothermic and results in molten so-called metallurgic silicon, which still contains the minor components of quartz and coke as impurities (particularly Fe, Al, Ca and Ti as silicides). This crude silicon (purity > 98 %) serves as component of alloys with aluminum and magnesium and as starting material for the production of organosilanes, polysiloxanes (silicones), silicon nitride and electronic grade silicon. The world production of silicon in 2017 was higher than $7{\cdot}10^6$ t, more than half of it in China.

For the production of silicon on a small scale, SiO_2 is reduced with Mg or Al in exothermic reactions, although depending on the stoichiometry substantial amounts of silicides are formed as by-products:

$$3\ SiO_2 + 4\ Al \longrightarrow 3\ Si + 2\ Al_2O_3$$

Very pure silicon as required for *microelectronics* or *photovoltaics*[15] is obtained by the thermal decomposition of volatile Si compounds, which in turn are produced from metallurgic silicon. The most important process uses trichlorosilane as the volatile intermediate. For its production, finely ground metallurgic silicon is converted to a mixture of chlorosilanes by treatment with gaseous hydrogen chloride in a fluidized bed reactor at 330 °C:

$$Si(s.) + 3\ HCl \longrightarrow SiHCl_3 + H_2 \qquad \Delta H^\circ_{298} = -218\ kJ\ mol^{-1}$$

$SiHCl_3$ (b.p. 32 °C) is separated from impurities and side-products such as BCl_3, SiH_2Cl_2, $SiCl_4$ and metal chlorides ($AlCl_3$, $FeCl_2$) by fractional condensation and repeated distillation and thus highly purified. During the reduction of $SiHCl_3$ with H_2, electronic grade silicon is deposited in polycrystalline, compact form on an initially thin silicon rod, which is electrically heated to above 1100 °C:

$$4\ SiHCl_3 + 2\ H_2 \longrightarrow 3\ Si(s.) + SiCl_4 + 8\ HCl \qquad \Delta H^\circ_{1400} = 964\ kJ\ mol^{-1}$$

Ultrapure silicon in granular form is also produced by pyrolysis of highly purified silane at 600 °C (also see Section 8.5.1):

15 Photovoltaics are concerned with the direct conversion of light into electrical energy with the help of semiconducting materials. In Germany the installed capacity in the year 1997 amounted to 45 MW but had increased by almost three orders of magnitude to 41000 MW by 2017. For the production of solar-grade silicon and photovoltaic cells see: G. Bye, B. Ceccaroli, *Sol. Energ. Mat. Sol. Cells* **2014**, *130*, 634.

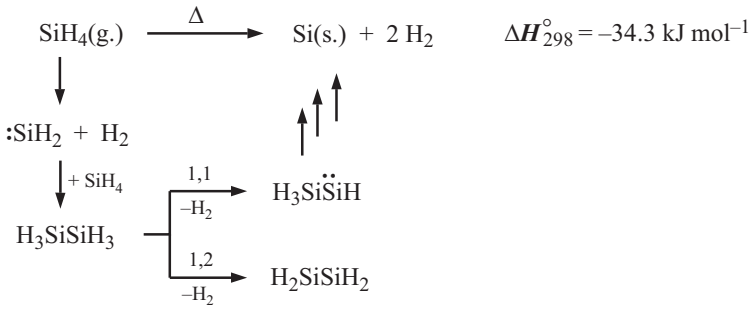

As primary product, the silylene SiH_2 occurs, which inserts into the SiH bond of a second silane molecule to give disilane Si_2H_6 as an intermediate.[16] The disilane then undergoes further elimination of H_2 to produce disilene $H_2Si{=}SiH_2$ and the isomeric silyl silylene $H(H_3Si)Si$:. The latter 1,1-elimination reaction is kinetically more favorable, but both species are capable of proceeding to silanes of higher molecularity by SiH insertion reactions. Which size of silane molecules is required for the onset of nucleation of elemental silicon remains an open question. Without doubt, however, the conditions of silane pyrolysis (pressure, temperature, etc.) are of tremendous importance to determine the dominant mechanistic scenario and with that the quality of the produced silicon.

An alternative decomposition pathway is the homolysis of the disilane intermediate to two SiH_3 radicals, suitable to initiate radical chain reactions to Si and H_2.[17] In a microwave plasma, this reaction leads to the deposition of amorphous silicon (a-Si) on nonconducting surfaces, for example, for solar cells and LCDs (*liquid crystal displays*). The resulting a-Si contains considerable amounts of residual hydrogen (a-Si:H), which is a desired side-effect that saturates the free valences at the surface (*dangling bonds*). The so-called chemical vapor deposition (CVD) is of high importance for various compound classes. In general, during such processes, a reactive gas stream (occasionally diluted by an inert carrier gas such as H_2 or N_2) is injected into a reactor containing a hot substrate on which the film is deposited by thermal decomposition of the reactive gas.

Another example is the reaction of SiH_4 with $SiBr_4$ or SiI_4, which is conducted at 450–800 °C and serves for the deposition of polycrystalline layers of silicon, for instance, on glass or other silicate surfaces:

$$SiH_4 + SiX_4 \longrightarrow 2\,Si(s.) + 4\,HX$$

For the production of monocrystalline Si, the element is molten in a quartz crucible under an atmosphere of argon and at a temperature just above the melting point.

16 B. L. Slakman, H. Simka, H. Reddy, R. H. West, *Ind. Eng. Chem. Res.* **2016**, *55*, 12507.
17 W. A. Eger, A. Genest, N. Rösch, *Chem. Eur. J.* **2012**, *18*, 9106.

A thin monocrystalline rod of silicon is lowered below the surface of the melt, which serves as a seed for further crystallization. The seed crystal is slowly removed from the melt under rotation at a rate corresponding to its growth. A rod-shaped single crystal (*ingot*) of up to 30 cm of diameter and 2 m of length can be obtained with a weight of 265 kg (CZOCHRALSKI process). As an interesting side note, CZOCHRALSKI discovered this method by accidently tipping the steel tip of his quill into a tin melt rather than into the ink.[18] About 95% of the world production of silicon monocrystals is produced according to this process, which are then sawn into wafer-thin silicon slices (actually called *wafers*), subsequently polished, etched and coated for further elaboration as integrated circuits.[19]

For the ultrapurification of polycrystalline Si and Ge (depletion of impurities to less than 10^{-9} atom%), the above ingots are treated by the *zone melting process*, which is based on the superior solubility of impurities in the melt compared to the solid state. The melt zone is generated by inductive heating and migrates through the rod-shaped ingots, which are thus recrystallized, without contact to any substance other than the protective gas argon. For the *doping* of silicon with boron or phosphorus in order to increase the electrical conductivity, traces of B_2H_6 and PH_3, respectively, are added to the protective gas and decompose under liberation of H_2 in the hot zone of the melt.

Silicon crystallizes in octahedral, hard and brittle crystals of dark-gray color (density 2.33 g cm^{-3}). This material is a *semiconductor* with a bandgap of 1.12 eV (108 kJ mol^{-1}) that only weakly conducts electrical currents at 25 °C. On heating or in the presence of impurities, however, the *conductivity* strongly increases. For example, the doping with 1 ppm of boron causes a rise in conductivity by the factor 10^5. The boron atoms are incorporated into the diamond-like structure instead of Si atoms. As boron possesses one valence electron less than silicon, not all electronic states are occupied in the valence band of the doped material (p-doping). Conversely, the doping with phosphorus atoms leads to a surplus of one electron per P atom, which has to occupy states in the conductance band (n-doping). In both cases, the partially occupied bands result in increased electrical conductivity.

With water, silicon reacts at the surface according to the equation:

$$Si + 2\,H_2O \longrightarrow SiO_2 + 2\,H_2$$

The formed SiO_2 protects deeper layers from further reaction. In aqueous bases, however, silicon dissolves completely under H_2 evolution:[20]

18 J. Evers et al., *Angew. Chem. Int. Ed.* **2003**, *42*, 5684.

19 Review on chemical processing of Si wafers: N. Marchak, J. P. Chang, *Annu. Rev. Chem. Biomol. Eng.* **2012**, *3*, 235.

20 The surface oxidation of silicon with hydroxides is of tremendous importance for the production of integrated circuits. The thus produced SiO_2 serves as dielectric (insulating) barrier between

$$Si + 4\,NaOH \longrightarrow Na_4[SiO_4] + 2\,H_2$$

Silicon resists the attack of most acids with the exception of a mixture of HNO_3 and HF. In air, particularly upon shredding, Si is rapidly covered by surface oxides, which enormously reduce its reactivity (*passivation*). In contrast, nonpassivated, finely divided silicon is pyrophoric.

Germanium is predominantly obtained from Ge-containing zinc ores such as ZnS and $Zn[CO_3]$, which generate GeO_2-containing fly ash upon roasting (burning in an air stream). In contrast to silicon, the crude dioxide can be directly converted to volatile $GeCl_4$ (b.p. 85 °C) by treatment with concentrated hydrochloric acid. The $GeCl_4$ is purified by fractional distillation and then hydrolyzed to very pure GeO_2, used for the reduction to the element:

$$GeO_2 + 2\,H_2 \longrightarrow Ge_{l.} + 2\,H_2O$$

Further purification is achieved by zone melting as in the case of silicon. Germanium crystallizes in grayish-white, brittle octahedrons (m.p. 938 °C, b.p. 2830 °C; density 5.32 g cm^{-3}). It is resistant to nonoxidizing acids but reacts with oxidizing acids to GeO_2. In molten alkaline hydroxides, it dissolves with evolution of hydrogen as germanates. In contrast to glass, elemental germanium is transparent to infrared radiation in a wide range (5000–600 cm^{-1}) and it is therefore used in lenses and mirrors of night vision gear that registers the heat signature of objects and creatures (thermal cameras). In semiconductor technology, germanium (bandgap 0.66 eV) has been replaced almost completely by the much less expensive silicon.

8.4 Silicides and Germanides

Many metals react with *silicon* upon heating to stoichiometric binary compounds, which are referred to as *silicides* and are related to similar species of other main-group elements (borides, carbides, nitrides, etc.). With strongly electropositive metals their valence electrons are more or less completely transferred to silicon resulting in negatively charged silicide ions of various sizes in a predominantly ionic bonding situation with the metal cations. The resulting materials are representatives of the so-called ZINTL phases. A few examples with silicon are listed in Table 8.3.

The efficient transfer of the electrons from metal to silicon in ZINTL phases is manifest in the structures of the anions; in most cases they arrange in a manner as if they consisted of the corresponding isoelectronic element. The most prominent

---

the semiconducting (electronically active) zones. Regarding the surface chemistry of silicon see: H. N. Waltenburg, J. T. Yates, *Chem. Rev.* **1995**, *95*, 1589.

Table 8.3: Silicides of electropositive metals (ZINTL phases) with constitution and symmetry of the anions.

Composition	Anions
Ca_2Si	Si^{4-}
Li_7Si_2	Si^{4-} and $[Si_2]^{6-}$ ("dumbbells")
Ba_3Si_4	$[Si_4]^{6-}$ ("butterfly"; C_{2v})
NaSi	$[Si_4]^{4-}$ (T_d; as P_4)
SrSi	$[Si_n]^{2n-}$ (helical chains as in sulfur)
$M_{12}Si_{17}$ (M: Na–Cs)	$2[Si_4]^{4-}$ (T_d) and $[Si_9]^{4-}$
$CaSi_2$	Puckered layers of fused $[Si_6]^{6-}$ rings

silicides are Mg_2Si and Ca_2Si, which formally contain Si^{4-} anions (isoelectronic to an argon atom and thus isolated). NaSi is a salt with tetrahedral anions $[Si_4]^{4-}$, isoelectronic and isostructural to the P_4 molecule of white phosphorus (Figure 8.3). Therefore, the compound is also referred to as $Na_4[Si_4]$ in the literature. It is produced from the elements at 650 °C. While NaSi is insoluble, $K_6Rb_6Si_{17}$ (more precisely $K_6Rb_6[Si_4]_2[Si_9]$) can be dissolved in liquid ammonia; $[Si_4]^{4-}$ can then be detected in the resulting solution by ^{29}Si-NMR spectroscopy.[21] The silicides CaSi and SrSi formally contain Ca^{2+} or Sr^{2+} ions and planar zig-zag chains of $[Si_n]^{2n-}$, isoelectronic with chains of polymeric sulfur. In contrast, the anions in $CaSi_2$ show a layer structure. The puckered layers consist of fused Si_6 rings, very similar to those of the isoelectronic black phosphorus or gray arsenic (Figure 10.2). The Ca^{2+} ions are intercalated between the layers. Many metals of higher electronegativity form *alloys* of varying composition with silicon (e.g., ferrosilicon, see Section 8.6.2).

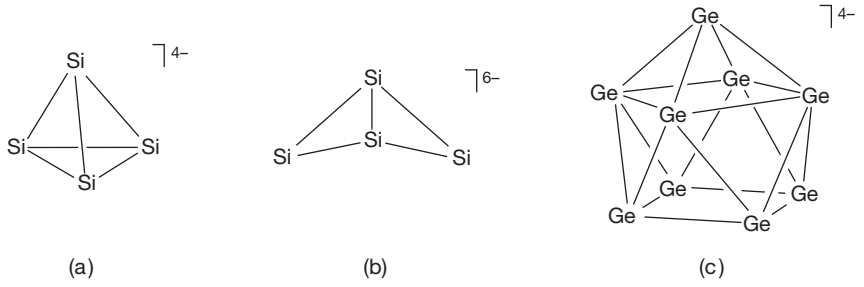

Figure 8.3: Structures of tetrelide anions: (a) $[Si_4]^{4-}$ (Td), (b) $[Si_4]^{6-}$ (C_{2v}) and (c) $[Ge_9]^{4-}$ (C_{4v}).

Under exclusion of oxygen, $CaSi_2$ quantitatively reacts with Cl_2 according to the following equation:

21 N. Korber, R. M. Gschwind et al., *Angew. Chem. Int. Ed.* **2013**, *52*, 4483.

$$CaSi_2 + Cl_2 \longrightarrow 2\,Si(s.) + CaCl_2$$

The resulting finely divided silicon is highly reactive: it ignites spontaneously even in water and burns to SiO_2 and H_2 in the process! With excess Cl_2 it reacts via $(SiCl)_n$ to chlorosilanes of the types Si_nCl_{2n+2} (chains), Si_nCl_{2n} (rings) and Si_nCl_{2n-2} (bicyclic, e.g., $Si_{10}Cl_{18}$). With methanol, this activated silicon reacts violently to $Si(OMe)_4$ and H_2 at 20–60 °C. If $CaSi_2$ is treated with concentrated hydrochloric acid at −30 °C, layered $(SiH)_n$ is formed. Silicon monochloride $(SiCl)_n$, which has a similar layer structure as graphite fluoride, is obtained from $CaSi_2$ and ICl. It can be fluorinated to $(SiF)_n$ with SbF_3 and hydrogenated to $(SiH)_n$ with $Li[AlH_4]$. On exposure to acids, amorphous, brown hydrides of composition $SiH_{0.7-0.9}$ are formed from CaSi, while Ca_2Si is converted to SiH_4.

Both silicon and germanium react with alkaline metals to alloys that readily dissolve in liquid ammonia to polyatomic anions, the so-called solvated **Zintl ions**.[22] These deeply colored species can be isolated from solution in crystalline form as solvent-separated ion pairs if the cations are spatially separated by coordination with cryptands such as 2,2,2-crypt. Ions such as $[Si_5]^{2-}$, $[Si_9]^{2-}$, $[Si_9]^{3-}$, $[Ge_4]^{2-}$, $[Ge_5]^{2-}$, $[Ge_9]^{2-}$ and $[Ge_9]^{4-}$ are obtained according to the following exemplary equations:

$$2\,Na + 4\,Ge + 2\,crypt \longrightarrow [Na(crypt)]_2^+[Ge_4]^{2-}$$
$$6\,K + 18\,Ge + 6\,crypt \longrightarrow [K(crypt)]_6^+[Ge_9]^{2-}[Ge_9]^{4-}$$

Polyhedral Zintl anions typically adhere to the Wade–Mingos rules (Section 6.5.3). Depending on the electron count, they form clusters of different symmetry. The nine-atom clusters are by far the most important: *nido*-$[Ge_9]^{4-}$ is a tricapped square antiprism with C_{4v} symmetry (Figure 8.3), while *closo*-$[Ge_9]^{2-}$ is a tricapped trigonal prism of D_{3h} symmetry. These homoatomic anions are competent ligands in transition metal complexes with coordination modes ranging from η^1 to η^6. Alkali metal germanides such as $M_4[Ge_9]$ can be prepared directly from the elements by heating under exclusion of air.

The Zintl anions of germanium are related to neutral, partially substituted clusters such as $Ge_8[N(SiMe_3)_2]_6$ and $Ge_8[C_6H_3(O^tBu)_2]_6$, which are synthesized from a solution of $(GeBr)_n$ and the corresponding alkali metal salts of the ligands. Numerous representatives of this class of compounds as well as analogous heteroatomic clusters have been reported.[23] The anionic cluster $\{Ge_9[Si(SiMe_3)_3]_3\}^-$ can either be obtained from

22 Solvated Zintl ions are known for Si, Ge, Sn, Pb, As, Sb, and Bi: S. C. Sevov, J. M. Goicoechea, *Organometallics* **2006**, *25*, 5678. T. F. Fässler et al., *Coord. Chem. Rev.* **2001**, *215*, 347 and *Angew. Chem. Int. Ed.* **2011**, *50*, 3630. N. Korber et al., *Angew. Chem. Int. Ed.* **2009**, *48*, 8770 and *Z. Naturforsch. Part B* **2010**, *65*, 1059.

23 A. Schnepf, *Eur. J. Inorg. Chem.* **2008**, 1007.

$(GeBr)_n$ in low yield or by treatment of $K_4[Ge_9]$ with $ClSi(SiMe_3)_3$ in approximately 80% yield. In case of silicon, the number of partially substituted ZINTL anions is as limited as that of neutral metalloid clusters.[24] The reductive functionalization of unsaturated silicon clusters $Si_6[C_6H_2(^iPr)_3]_6$ with lithium/naphthalene yields anionic Si_6 clusters $\{Si_6[C_6H_2(^iPr)_3]_5\}^-$ with three unsubstituted vertices as rare examples.[24,25] These regioisomeric nucleophilic reagents allow for the facile introduction of various functional groups in two distinct positions of the Si_6 scaffold by treatment with suitable electrophiles such as R'_2PCl, R′C(O)Cl or R'_3SiCl.

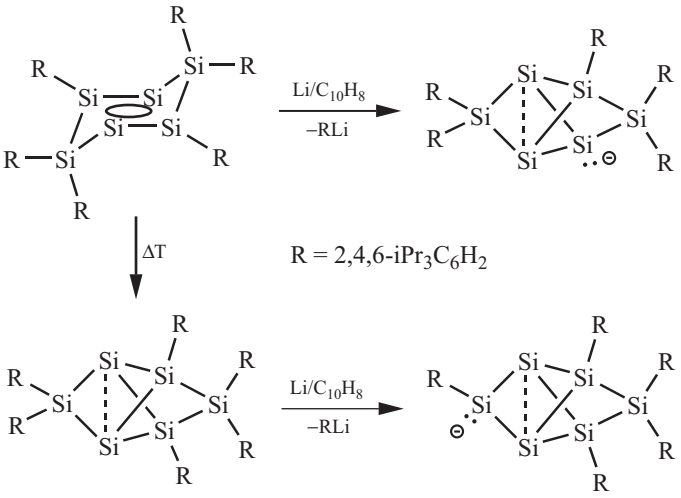

8.5 Hydrides of Silicon and Germanium

Silicon forms a large number of linear and branched *silanes* of the general formula Si_nH_{2n+2}. Formally, they correspond to the alkanes, but are much more reactive. Cyclic silanes Si_nH_{2n} and polymeric hydrides of composition $SiH_{0.7–0.9}$ are also known (Section 8.4). Of the open-chain silanes, all representatives up to $n = 15$ ($Si_{15}H_{32}$) have been isolated or at least confirmed experimentally. Silanes are colorless without exception and in part gaseous ($n = 1, 2$), in part liquid ($n > 2$). SiH_4 condenses at b.p. –112° and freezes at m.p. –185 °C. The SiH bond of silanes is about 90 kJ mol^{-1} weaker than the CH bond of alkanes. Therefore, the activation barriers of analogous reactions are much smaller for silicon than for carbon. Silanes are thermally stable at 25 °C, albeit under exclusion of O_2 and H_2O. In contrast to hydrocarbons (which require ignition

24 Review: Y. Heider, D. Scheschkewitz, *Dalton Trans.* **2018**, *47*, 7104.
25 D. Scheschkewitz et al., *Chem. Sci.* **2019**, *10*, 4523.

to burn), silanes are often pyrophoric and burn to SiO_2 and H_2O. Silanes and substituted derivatives such as Et_3SiH and particularly $(Me_3Si)_3SiH$ are strong *reducing agents* for application predominantly in organic synthesis,[26] which underscores the pronounced oxophilicity of silicon.

The corresponding *germanes* Ge_nH_{2n+2} are known up to Ge_9H_{20}. The higher hydrides of germanium are air sensitive, whereas GeH_4 and Ge_2H_6 are practically inert toward oxygen. Germanium hydrides with $n > 2$ are therefore handled in glass or steel apparatus under vacuum or inert gases. GeH_4 is a gas (b.p. −88 °C); the higher germanes are liquids or solids at 25 °C. The GeGe internuclear distance amounts to 240.3 pm in Ge_2H_6 and 241.7 pm in Me_6Ge_2. As in case of silicon, substances of formal composition GeH and GeH_2 are polymeric and contain GeGe bonds. Cyclic binary hydrides of germanium are unknown so far despite the fact that numerous substituted species *cyclo*-Ge_nR_{2n} have been reported even with small substituents as R = Me. Unsurprisingly, unsaturated hydrides tend to oligomerize or polymerize very rapidly under standard conditions and have only been characterized in ultracold matrices.[27]

8.5.1 Preparation of Hydrides

Silanes: SiH_4, Si_2H_6 and Si_3H_8 are best prepared by reaction of the corresponding chlorides with $Li[AlH_4]$ or LiH in diethylether:

$$SiCl_4 + Li[AlH_4] \longrightarrow SiH_4\uparrow + LiCl + AlCl_3$$
$$Si_2Cl_6 + 6\,LiH \longrightarrow Si_2H_6\uparrow + 6\,LiCl$$

A silane mixture (crude silane) is formed on hydrolysis of Mg_2Si with 20% phosphoric acid at 50–60 °C. As early as 1916, the analogous reaction with hydrochloric acid had been carried out by ALFRED STOCK and coworkers.

$$Mg_2Si + 4\,H^+ \longrightarrow SiH_4 + 2\,Mg^{2+}$$

The required magnesium silicide is obtained in an exothermic reaction by heating the thoroughly ground elements to 650 °C under argon. The crude silane contains all linear silanes up to $n = 15$, although the relative concentrations decrease substantially with the molecular mass. The separation of the mixture is possible by

26 C. Chatgilialoglu, *Chem. Eur. J.* **2008**, *14*, 2310.
27 X. Wang, L. Andrews, G. P. Kushto, *J. Phys. Chem. A* **2002**, *106*, 5809.

fractional vacuum distillation or preparative gas chromatography. The higher silanes ($n > 3$) consist of *isomeric mixtures* of branched and unbranched molecules. For instance, *n*-tetrasilane $H_3Si(SiH_2)_2SiH_3$ and *iso*-tetrasilane $(H_3Si)_3SiH$ have been isolated and identified by ^{1}H- and ^{29}Si-NMR spectroscopy. So far, the mechanism of formation of these silanes remains obscure. *cyclo*-Si_6H_{12} is best prepared by reduction of $[NR_4]_2[Si_6Cl_{14}]$ with $Li[AlH_4]$.[28]

Neat SiH_4 on a 50 mg scale is formed on dry heating of $Li[AlH_4]$ with excess SiO_2 to 170 °C. On an industrial scale, pure SiH_4 is obtained from $SiCl_4$ and LiH in an LiCl–KCl melt. Higher silanes can be generated from SiH_4 by the effect of silent electric discharges just as those used for the production of ozone:

$$SiH_4 \longrightarrow SiH_2 + H_2$$
$$SiH_2 + SiH_4 \longrightarrow Si_2H_6$$
$$SiH_2 + Si_2H_6 \longrightarrow Si_3H_8$$

In this manner, mixed Si–Ge hydrides are also preparatively accessible by starting from an SiH_4/GeH_4 mixture. The intermediate silylene SiH_2 is a highly reactive carbene analog of C_{2v} symmetry, which has also been detected spectroscopically during the UV photolysis of phenylsilane.[29] Furthermore, it is produced during the thermolysis of disilanes such as methyldisilane by *dismutation* (also referred to as *disproportionation*) of Si(III) to Si(II) and Si(IV):

$$MeH_2Si{-}SiH_3 \longrightarrow MeSiH_3 + SiH_2$$

The dismutation reaction can be understood as an extrusion of silylene from an SiH bond. The insertion into covalent bonds (i.e., the reverse) is a characteristic reaction of silylenes (see Section 8.3, formation of Si_2H_6) as well as the addition to unsaturated compounds such as dienes.

Germanes: Monogermane GeH_4, a colorless and air-stable gas, is best prepared by reduction of GeO_2 with $Na[BH_4]$ in dilute aqueous acetic acid. Ge_2H_6 is formed as a side product of this reaction. The hydrolysis of Mg_2Ge with aqueous hydrochloric acid or with $[NH_4]Br$ in liquid ammonia predominantly leads to GeH_4, alongside small quantities of Ge_2H_6 and traces of higher germanes with up to 9 Ge atoms. The latter, however, can be obtained more conveniently by the decomposition of GeH_4 in a silent electric discharge.

28 P. Boudjouk et al., *J. Am. Chem. Soc.* **2001**, *123*, 8117. H.-W. Lerner et al., *Inorg. Chem.* **2012**, *51*, 8599.

29 M. J. Almond, S. L. Jenkins, *Encycl. Inorg. Chem.* **2005**, *8*, 5080. J. M. Jasinski, R. Becerra, R. Walsh, *Chem. Rev.* **1995**, *95*, 1203.

8.5.2 Reactions of Silanes and Germanes

Upon heating, silanes decompose to the elements (Section 8.3). In this way, high-purity silicon is industrially produced from SiH_4 at 570–670 °C (although the decomposition of $HSiCl_3$ is employed on a much larger scale). As intermediates, higher silanes occur, which can be isolated under suitable reaction conditions. In contrast to alkanes, the silanes contain negatively polarized hydrogen and consequently a positively charged Si atom [$Si^{\delta+}$–$H^{\delta-}$], which favors the reaction with hydroxide ions and thus the hydrolysis under basic conditions:

$$SiH_4 + 2\,KOH + H_2O \longrightarrow K_2[SiO_3] + 4\,H_2$$
$$Si_2H_6 + 4\,KOH + 2\,H_2O \longrightarrow 2\,K_2[SiO_3] + 7\,H_2$$

Conversely, hydrolysis does not take place in neutral water or slightly acidic aqueous solutions.

The polarity of the SiR linkage (R=Ph, MeS, ^{i}PrS) is also responsible for the thermodynamically favorable formation of silyl cations (also referred to as *silylium cations*):

$$R_4Si + [Ph_3C][ClO_4] \xrightarrow{CH_2Cl_2} [R_3Si][ClO_4] + Ph_3CR$$

Various halides such as HCl, BCl_3 and PCl_3 react with silanes under hydrogen–halogen exchange:

$$SiH_4 + HX \xrightarrow{AlX_3} SiH_3X + H_2 \qquad X= Cl, Br, I$$
$$3\,Si_2H_6 + BCl_3 \longrightarrow 3\,Si_2H_5Cl + \tfrac{1}{2}\,B_2H_6$$

The partially halogenated silanes are suitable for condensation reactions:

$$2\,H_3SiCl + H_2O \longrightarrow (H_3Si)_2O + 2\,HCl$$
$$3\,H_3SiI + 4\,NH_3 \longrightarrow (H_3Si)_3N + 3\,[NH_4]I$$
$$4\,H_3SiI + 3\,N_2H_4 \longrightarrow (H_3Si)_2N{-}N(SiH_3)_2 + 2\,[N_2H_6]I_2$$
$$3\,H_3SiBr + 3\,K[PH_2] \xrightarrow{-100°C} (H_3Si)_3P + 2\,PH_3 + 3\,KBr$$

The salts of silanes, the silanides, are produced either by reduction under hydrogen evolution or by cleavage of the comparatively weak SiSi bond of disilane, for example, with potassium hydride:

$$SiH_4 + K \longrightarrow K[SiH_3] + \tfrac{1}{2} H_2$$
$$Si_2H_6 + KH \longrightarrow K[SiH_3] + SiH_4$$

Both reactions occur at 25 °C in 1,2-dimethoxyethane (monoglyme, $H_3COCH_2CH_2OCH_3$). $K[SiH_3]$ crystallizes at 25 °C in a NaCl structure. The anion is pyramidal just as the isoelectronic PH_3. With various element halides, $K[SiH_3]$ reacts under nucleophilic substitution:

$$Me_2AsCl + K[SiH_3] \longrightarrow H_3Si{-}AsMe_2 + KCl$$
$$MeI + K[SiH_3] \longrightarrow MeSiH_3 + KI$$
$$PhGeBr_3 + 3\,K[SiH_3] \longrightarrow PhGe(SiH_3)_3 + 3\,KBr$$

GeH_4 and Ge_2H_6 react in a similar manner as SiH_4 and Si_2H_6. On heating, the germanes decompose into the elements. By employing gold nanoparticles as catalysts, germanium can also be obtained in the form of nanowires. GeH_4 is attacked by oxygen only when heated and then oxidized to GeO_2 and H_2O. It even resists an attack by 30% aqueous sodium hydroxide. In analogy to SiH_4, it forms germyl halides GeH_3X and metal germanides, for example, $K[GeH_3]$, which is obtained from K and GeH_4 in liquid NH_3 or in hexamethylphosphortriamide (HMPA, carcinogenic) and serves as precursor for the synthesis of organic derivatives.

8.6 Halides of Silicon and Germanium

The most important binary halides of *silicon* are of the type Si_nX_{2n+2}, that is, they are formally derived from the silanes by replacement of H atoms by X=F, Cl, Br and I (*perhalosilanes*). SiF_4 and above all $SiCl_4$ are industrially produced on a very large scale. Moreover, less well-characterized halides of higher molecularity of types $(SiX_2)_n$ and $(SiX)_n$ have been reported (see Section 8.4) as well as the unstable monomeric subhalides SiF_2 and $SiCl_2$. In addition, all mixed tetrahalides of type SiX_nY_{4-n} have been prepared. The ternary halides with residual hydrogen SiH_nX_{4-n} are also important.

Germanium forms binary halides of the types GeX_4, Ge_2X_6, GeX_2 and $(GeX)_n$ (X=F, Cl, Br, I) as well as the hydride halides GeH_nX_{4-n}.

8.6.1 Fluorides

Silicon tetrafluoride SiF_4 (tetrafluorosilane) is a colorless gas, which can be produced by fluorination of Si or SiO_2,[30] but is more conveniently prepared as follows:

$$2\,CaF_2 + 2\,H_2SO_4 + SiO_2 \longrightarrow SiF_4\uparrow + 2\,Ca[SO_4] + 2\,H_2O$$

To bind the generated water and thus to avoid the hydrolysis of SiF_4, concentrated sulfuric acid is employed. Very pure SiF_4 can be made on a laboratory scale by pyrolysis of barium hexafluorosilicate $Ba[SiF_6]$:

$$Ba[SiF_6] \xrightarrow[\text{vacuum}]{300\text{–}350\,^\circ C} BaF_2 + SiF_4\uparrow$$

On an industrial scale, SiF_4 is obtained as a side product of the production of phosphoric acid from apatite (Section 10.12.1).

The hydrolysis of SiF_4, which leads to SiO_2 and HF with an excess of water, is an equilibrium reaction:

$$SiF_4 + 2\,H_2O \rightleftharpoons SiO_2 + 4\,HF$$

In the gas phase, hexafluorodisiloxane $F_3Si{-}O{-}SiF_3$, a colorless gas, is obtained as main product at an excess of SiF_4. With small amounts of liquid water, however, SiF_4 reacts according to:

$$3\,SiF_4 + 6\,H_2O \longrightarrow 2\,[H_3O]_2[SiF_6] + SiO_2$$

The oxonium salt of hexafluoro silicic acid is a strong acid, which reacts with hydroxides and carbonates to the corresponding hexafluorosilicates. $Na_2[SiF_6]$ is used in some regions alongside NaF for the fluoridation of drinking water for the purpose of caries prophylaxis; $Mg[SiF_6]$ serves as an insecticidal wood protection agent in building construction.

GeF_4 (b.p. –37 °C) is produced by heating $Ba[GeF_6]$ to 600 °C, which in turn is obtained from BaF_2, GeO_2 and hydrofluoric acid. GeF_4 is a colorless gas, strongly fuming in air, which reacts with water to GeO_2 and oxonium hexafluorogermanate $[H_3O]_2[GeF_6]$. SiF_4 and GeF_4 are strong LEWIS acids, which form 1:1 and 1:2 *adducts* with LEWIS bases such as ammonia, amines, ethers, ketones, amine oxides, dimethylsulfoxide, hydrogen sulfide and acetonitrile. Some examples are:

30 The reaction of F atoms with Si to SiF_4 and SiF_2 plays a role in the etching process of Si wafers through electric discharge in a CF_4 atmosphere (plasma etching at 1–150 Pa): D. L. Flamm in J. Y. Corey, E. R. Corey, P. P. Gaspar (eds.), *Silicon Chemistry*, Horwood Publ., Chichester **1988**, p. 391.

$$SiF_4(NH_3)_2 \quad SiF_4[OS(CH_3)_2]_2 \quad GeF_4(SH_2)_2 \quad GeF_4(NCCH_3)$$

The complex anions $[SiF_6]^{2-}$, $[GeF_5]^-$ and $[GeF_6]^{2-}$ also belong to this class of compounds.

The monomeric gaseous difluoride SiF_2 is also known, the synthesis and reactivity of which will be discussed in the chapter on fluorine (Section 13.4.6). Si_2F_6 can be obtained through halogen exchange from Si_2Cl_6 with ZnF_2.

The difluoride GeF_2 is a solid, which is far more robust than the gaseous SiF_2. In general, one can conclude that the stability of the oxidation number +2 in Group 14 increases significantly from carbon to lead. GeF_2 forms colorless crystals, in which the GeF_2 units are connected in chains such that each germanium atom shows trigonal pyramidal coordination by three fluorine atoms with FGeF angles around 90° (the lone pair occupies the fourth position of a pseudo tetrahedron; additional weak inter-chain contacts have only a mild distortive effect). GeF_2 is formed by reduction of GeF_4 with Ge at 150–300 °C or from Ge and HF at 225 °C:

$$Ge(s.) + GeF_4 \rightleftharpoons 2\,GeF_2$$
$$Ge(s.) + 2\,HF \longrightarrow GeF_2 + H_2$$

8.6.2 Chlorides

Silicon tetrachloride $SiCl_4$ is by far the most important binary halide of silicon. It is formed in countless reactions by chlorination of elemental Si or its compounds. On an industrial scale, silicon-rich *ferrosilicon* is chlorinated, which is an Fe–Si alloy with a silicon content of more than 90%:

$$Fe/Si + \frac{7}{2}Cl_2 \xrightarrow{>400°C} SiCl_4 + FeCl_3$$

Ferrosilicon (Fe/Si) is produced by reduction of quartz with coke in the presence of iron scraps or iron oxides, which requires a slightly lower temperature than for the reduction of quartz alone. Fe/Si reacts more rapidly with chlorine than pure silicon; the reaction is strongly exothermic. $SiCl_4$ is a colorless liquid (b.p. 58 °C), which is purified by fractional distillation and then serves for production of very pure silicon (via SiH_4). The best understood reaction of $SiCl_4$ is its hydrolysis, leading to silica and hydrochloric acid via intermediate products:

$$\underset{\text{tetra-chlorosilane}}{SiCl_4} \xrightarrow{+H_2O} \underset{\text{trichloro-silanol}}{SiCl_3OH} \xrightarrow{+SiCl_4} \underset{\text{hexachloro-disiloxane}}{Cl_3Si-O-SiCl_3} \xrightarrow{+3H_2O} \underset{\text{silica gel}}{2\,SiO_2(aq)} + 6\,HCl$$

Said intermediates can be isolated by careful hydrolysis with substoichiometric amounts of water under cooling. With alcohols, the corresponding *silicic esters* $Si(OR)_4$ result.

Although various stable donor–acceptor complexes with tertiary amines and phosphanes exist, $SiCl_4$ is considered to be a weaker LEWIS acid than SiF_4 because of the nonexistence of certain adducts such as the $[SiCl_6]^{2-}$ ion. Besides water, $SiCl_4$ reacts with alcohols and with NH_3 by elimination of HCl. For instance, hexachlorodisilazane is formed at −60 °C in ether and in 40% yield:

$$2\ SiCl_4 + 3\ NH_3 \longrightarrow Cl_3Si-NH-SiCl_3 + 2\ NH_4Cl$$

As side product, *cyclo*-hexachlorotrisilazane $(SiCl_2NH)_3$ can be isolated. With GRIGNARD reagents such as RMgBr or with organolithium compounds, SiCl species react to organosilicon derivatives (Section 8.11).

Si_2Cl_6 and higher chlorosilanes Si_nX_{2n+2} (up to $n = 6$) are formed during the chlorination of $CaSi_2$ at 140 °C (Section 8.4) and on the electrochemical decomposition of $SiCl_4$ at a Si electrode. An interesting synthesis of higher chlorosilanes is the catalytic disproportionation of lower homologues by reaction with trimethylamine (Me_3N) or tetramethylethylendiamine (TMEDA):

$$4\ Si_2Cl_6 \longrightarrow Si_5Cl_{12} + 3\ SiCl_4$$

For example, if an excess of Me_3N is allowed to react with Si_2Cl_6, *neo*-pentasilane $Si(SiCl_3)_4$ is obtained.[31] During this reaction the cleavage of $SiCl_2$ from hexachlorodisilane is promoted by adduct formation with the amine. The $SiCl_2$ then inserts into the SiCl bonds of an additional Si_2Cl_6 molecule. *N*-heterocyclic carbenes can also be used for the trapping of $SiCl_2$, which crystallizes as a stable adduct.[32]

When $SiCl_4$ vapor is conducted over Si above 1000 °C, gaseous $SiCl_2$ (dichlorosilylene) is formed in equilibrium, but disproportionates again upon slow cooling:

$$Si(s.) + SiCl_4 \rightleftharpoons 2\ SiCl_2 \qquad K_p = 1\ \text{bar (at 1615 K)}$$

In contrast, when rapidly quenched to low temperatures, $SiCl_2$ polymerizes to perchloropolysilane $(SiCl_2)_n$ with a linear chain structure. Low molecular perchlorosilanes up to Si_6Cl_{14} are obtained as side products. If BCl_3, CCl_4 or PCl_3 are added prior to condensation, the carbene-analogous $SiCl_2$ inserts into the ECl bonds to yield $Cl_2B–SiCl_3$, $Cl_3C–SiCl_3$ and $Cl_2P–SiCl_3$, respectively.

31 M. Holthausen, H.-W. Lerner et al., *Chem. Eur. J.* **2011**, *17*, 4715 and *Inorg. Chem.* **2012**, *51*, 8599.
32 H. Roesky, D. Stalke et al., *Angew. Chem. Int. Ed.* **2009**, *48*, 5683.

Germanium tetrachloride $GeCl_4$ (tetrachlorogermane) is either prepared from the elements or from GeO_2 and concentrated hydrochloric acid. The colorless, in air just slightly fuming liquid (b.p. 83 °C) is rapidly hydrolyzed by water. In marked contrast to $SiCl_4$, however, this reaction to GeO_2 as the final product is not irreversible and several products may exist in equilibrium depending on the conditions. Nonetheless, the hydrolysis of $GeCl_4$ under nonequilibrium conditions is important for the production optical fibers (see Section 8.9). In a microwave discharge, $GeCl_4$ can be converted to Ge_2Cl_6 and Cl_2. Monomeric dichlorogermylene $GeCl_2$ is generated by reduction of $GeCl_4$ with Ge at temperatures above 680 °C as well as during the thermal decomposition of trichlorogermane:

$$GeHCl_3 \rightleftharpoons GeCl_2 + HCl$$

$GeCl_2$ forms colorless crystals at 25 °C, which are rapidly hydrolyzed to $Ge(OH)_2$ and slowly oxidized in air to GeO_2 and $GeCl_4$. In solid $GeCl_2$ and even in the adduct $GeCl_2$•1,4-dioxane the molecules are associated through Cl bridges. A salt with the trichlorogermanate(II) anion $[GeCl_3]^-$ is obtained from CsCl, $GeCl_4$ and a reducing agent such as phosphinic acid H_3PO_2.

8.6.3 Other Silicon Halides

$SiBr_4$ (b.p. 153 °C) and SiI_4 (b.p. 121 °C) can be synthesized from the elements at elevated temperatures. Both compounds are colorless, moisture-sensitive and thermally less stable than SiF_4 and $SiCl_4$. In addition, all permutations of the mixed halides of type $SiX_{(4-n)}Y_n$ are known.

The *ternary chlorosilanes* SiH_3Cl, SiH_2Cl_2 and $SiHCl_3$ are obtained as follows:

$$Si + 3\,HCl \xrightarrow[300°C]{CuCl_2} SiHCl_3 + H_2$$

$$SiCl_4 + H_2 \longrightarrow SiHCl_3 + HCl$$

$$2\,SiHCl_3 \xrightarrow[300°C]{AlCl_3} SiCl_4 + SiH_2Cl_2$$

$$SiH_4 + HCl \longrightarrow SiH_3Cl + H_2$$

The reaction products are separated by fractional distillation. Trichlorosilane is an industrial product, which is needed not only in the ultrapurification of silicon (Section 8.3), but also for the synthesis of organosilanes. With H_2O, $SiHCl_3$ reacts to SiO_2, HCl and H_2; in an oxygen atmosphere it burns to SiO_2, HCl and water. SiH_2Cl_2 and $SiHCl_3$ form adducts with amines.

Certain alkenes add partially chlorinated silanes under *hydrosilylation*[33] to yield organochlorosilanes:

$$RHC{=}CH_2 + H{-}SiCl_3 \longrightarrow RH_2C{=}CH_2{-}SiCl_3$$

Such reactions proceed by a radical mechanism unless they are catalyzed by transition metal complexes or bases. The radical reactions are initiated by organic peroxides. Hexachloroplatinic acid $[H_3O]_2[PtCl_6]$ is an efficient catalyst[34] for the hydrosilylation of cyclic and open-chain alkenes. Besides $SiHCl_3$, the silanes SiH_2Cl_2, $MeSiHCl_2$, $EtSiHCl_2$, Et_3SiH and $(EtO)_3SiH$ are employed. In this manner, numerous organosilicon species are produced industrially (Section 8.11.1). The hydrosilylation reaction is of particular importance for the *cross-linking of polysiloxanes*.

8.7 Oxides of Silicon and Germanium

With oxygen, silicon and germanium form the following binary species, which are polymeric under standard conditions without exception:

$$SiO \quad SiO_2 \quad GeO \quad GeO_2$$

The dioxides exist in several crystalline and amorphous *modifications*. In contrast, the thermodynamically unstable monoxides are amorphous and thus despite their technological importance as materials poorly characterized so far. Both monoxides and dioxides evaporate on strong heating as monomers.

8.7.1 Silicon Dioxide

The by far most important oxide of silicon is SiO_2, which occurs in nature in countless crystalline and amorphous forms and is technologically employed on a large scale. More than 30 allotropic forms of SiO_2 are known. *Quartz* (Bergkristall, Amethyst), *tridymite*, *cristobalite* and the high-pressure modifications *coesite* and *stishovite* are crystalline; *opal* (*chalcedony*, *agate*, *flintstone*) and diatomaceous earths are amorphous or microcrystalline, mostly with certain water content. The latter are obtained from fossil deposits of the so-called diatoms, a class of microalgae with silica scaffolds. Mighty deposits of diatom shells of up 100 m are being exploited, for instance, in Russia, Great Britain, North Africa and California (see Section 8.8.1). This highly

33 C. Marschner, *Encycl. Inorg. Chem.* **2005**, *3*, 1926.

34 It is assumed that the alkene coordinates to the metal center first. Then the silane would oxidatively add to the transition metal. The subsequent shift of the metal-bound hydrogen to the alkene is followed by reductive elimination of the organosilicon product.

porous material is employed for filters in brewing and drinking water conditioning, as thermal insulation and as cleaning agent in toothpastes. If the diatomaceous silica is reduced with magnesium vapors at 650 °C, highly porous elemental silicon is formed from which the MgO is removed with hydrochloric acid. This nanocrystalline Si has more or less the same structure as the silica starting material. Its treatment with methane at 950 °C results in SiC, from which the Si component can be removed as volatile $SiCl_4$ with Cl_2 at 950 °C. The remaining amorphous carbon still contains the pore structure of the diatomaceous earth as well as additional nanopores (ø < 2 nm) due to the contraction caused by the smaller atomic radius of carbon compared to silicon.[35]

The following temperature-dependent equilibria exist between the SiO_2 modifications thermodynamically stable at ambient pressure:

$$\underset{\text{(trigonal)}}{\alpha\text{-quartz}} \overset{575°C}{\rightleftharpoons} \underset{\text{(hexagonal)}}{\beta\text{-quartz}} \overset{867°C}{\rightleftharpoons} \underset{\text{(hexagonal)}}{\beta\text{-tridymite}} \overset{1470°C}{\rightleftharpoons} \underset{\text{(cubic)}}{\beta\text{-cristobalite}} \overset{1713°C}{\rightleftharpoons} \text{melt}$$

α-Tridymite and α-cristobalite are thermodynamically unstable at all temperatures but turn out to be metastable forms in practice. All SiO_2 modifications stable below pressures of 9 GPa contain *tetrahedrally* coordinated Si atoms, which are connected to a three-dimensional network by two-coordinate O atoms. The SiO bonds are strongly polar and very stable. In the high-pressure modification *stishovite*, which crystallizes above 1300 °C and at a pressure of 12 GPa in the rutile structure, the Si atoms are octahedrally coordinated by O atoms leading to a coordination number of 3 at oxygen.

Because of the complicated three-dimensional interconnections of the atoms in the SiO_2 modifications, phase transitions are slow unless the crystal symmetry is maintained (e.g., α→β and vice versa). For this reason, only very slow cooling of SiO_2 melts gives crystalline phases such as cristobalite. More rapid cooling typically results in glasses. The glass obtained from super-cooled melts of quartz (therefore often referred to as fused quartz or fused silica) is metastable at 25 °C but slowly crystallizes on annealing at 1000 °C.

Crystalline and glassy SiO_2 are resistant to most acids (except for hydrofluoric acid) and dilute bases; upon melting with alkali metal oxides (as hydroxides or carbonates), however, metasilicates are formed:

$$SiO_2 + 2\,NaOH \longrightarrow Na_2[SiO_3] + H_2O$$

35 K. H. Sandhage et al., *Energy Environ. Sci.* **2011**, *4*, 3980.

Finely divided silica, in particular when freshly prepared by hydrolysis of $SiCl_4$, is much more reactive as such preparations still contain numerous silanol functionalities (SiOH), which are transformed in the chemically much more resistant siloxane groups (SiOSi) by elimination of H_2O on storage or heating. Particularly fine silica with low water content is industrially produced on a large scale by *flame hydrolysis* of $SiCl_4$ (*pyrogenic* or *fumed silica*) according to the equation:

$$SiCl_4 + 2\,H_2 + O_2 \longrightarrow SiO_2 + 4\,HCl$$

At the very high temperatures of oxyhydrogen flames, spherical amorphous SiO_2 particles of about 10 nm diameter are formed, which are also known under the tradename *aerosil*. The required $SiCl_4$ can be produced at 900 °C from ferrosilicon and HCl gas:

$$Fe/Si + 6\,HCl \longrightarrow SiCl_4 + FeCl_2 + 3\,H_2$$

HCl and H_2 are recycled during this two-step process. Silica is used as filler in white silicone sealants as white pigment alongside TiO_2, and is employed in cosmetics and pills due to its purity. All tires of more recent European cars contain silica, which replaces part of the carbon black and allows for a higher abrasion resistance and thus longer service life. Moreover, silica influences the flow behavior of paints and varnishes and is used in the polishing of silicon wafers during their processing to microchips. Silica can also be obtained by precipitation from solution (see Section 8.8.2).

8.7.2 Silicon Monoxide

When SiO_2 is heated with silicon in a molar ratio of 3:1 to 1250–1400 °C in high vacuum, SiO escapes into the gas phase:

$$Si(s.) + SiO_2(s.) \rightleftharpoons 2\,SiO\uparrow$$

While SiO is stable in the gas phase, its structure in the condensed phase is still contended due to its amorphous nature and the relative lack of analytical data. Recent high-energy electron beam diffraction data, however, suggest that "SiO" consist of nano-sized clusters of elemental silicon and SiO_2, which result from the disproportionation of SiO on cooling.[36] Depending on the annealing conditions,

36 A. Hirata, M. Chen et al., *Nature Comm.* **2016**, *7*, 11591.

these are separated by very thin residual interfaces of SiO (down to atomic dimensions).

SiO_2 can be reduced to SiO by coke as well. As a consequence, the monoxide is formed as a by-product during the carbothermal production of elemental silicon (Section 8.3) and evaporates from the reaction zone. It is reoxidized to SiO_2 in the upper part of the furnace and condenses as so-called microsilica. For each ton of silicon, 200–400 kg of microsilica are obtained, which happens to be a valuable material for the production of concrete. This form of SiO_2 consists of isolated spherical particles of 0.02–1.0 μm diameter.[37]

By matrix techniques at low temperature, monomeric SiO has been isolated together with the heterocycles $(SiO)_2$ and $(SiO)_3$ in solid Ar or N_2. The dissociation enthalpy of SiO (715 kJ mol^{-1}) is less than double the value for the SiO single bond. Upon polymerization of these small $(SiO)_n$ species, new SiO and SiSi single bonds are formed.

8.7.3 Germanium Oxides

Unlike in the case of silicon, there are no natural sources of germanium dioxide worth exploiting. Therefore, the entire demand of GeO_2 is produced by hydrolysis of $GeCl_4$ with aqueous NH_3. This procedure results in the hexagonal modification of GeO_2, which is sparingly soluble in water under acidic condition; its structure corresponds to that of β-quartz (tetrahedral coordination of Ge). In aqueous bases, GeO_2 dissolves to germanates. On heating to 380 °C, hexagonal GeO_2 transforms into the tetragonal form, which is almost completely insoluble in water and crystallizes in a rutile structure (octahedral coordination of Ge).

GeO_2 can be reduced to monomeric GeO by heating with elemental germanium. Polymeric GeO is conveniently obtained by reduction of GeO_2 with H_3PO_2 in HCl-acidic solution to yield $Ge[OH]_2$ initially, which is subsequently dehydrated to $(GeO)_n$ at 650°C. $(GeO)_n$ reacts with HCl to $GeHCl_3$ and H_2O at 175°C. Based on the observations for $(SiO)_n$, it is reasonable to assume the presence of nano-sized domains of Ge and GeO_2 in the native $(GeO)_n$ as well, although definite proof is lacking due to the amorphous nature of $(GeO)_n$. On annealing at higher temperatures, however, Ge nanocrystals are obtained, the size of which can be controlled by the annealing conditions.[38]

37 During the construction of the Burj Khalifa in Dubai (828 m) about 20000 t of micro-silica were used: P. Sharma, *Int. J. Res.* **2015**, *2*, 596 and B. Friede, E. Gaillou, *Chem. unserer Zeit* **2018**, 52, 84.
38 A. S. Helmy, G. A. Ozin et al., *Angew. Chem. Int. Ed.* **2017**, *56*, 6329.

8.8 Oxoacids, Silicates and Germanates

8.8.1 Silicic Acid and Siloxanes

In analogy to the oxoacids of the neighboring nonmetals in the Periodic Table, the simplest oxoacid of silicon should be of empirical formula H_4SiO_4:

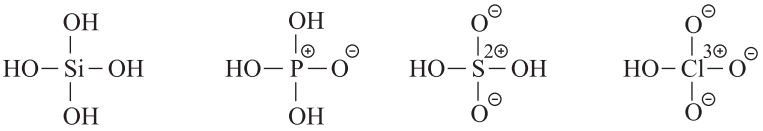

Orthosilicic acid $Si(OH)_4$, in contrast to the three other acids above, cannot be isolated in pure form. By using favorable interactions with hydrogen-bond donor solvents such as *N,N*-dimethylacetamide, however, $Si(OH)_4$ has been isolated from the hydrogenolysis reaction of tetrakis(benzyloxy)silane $Si(OCH_2C_6H_5)_4$ as an adduct to two chloride ions in up to 96% yield (Figure 8.4). The chloride ions stem from added $[R_4N]Cl$ and the product molecule $Si(OH)_4$ is embedded in a matrix of the organic ammonium counter ions and solvent molecules and has been characterized by diffraction methods in the solid state.[39]

Hydrolysis of $SiCl_4$ with a large excess of water at a constant pH of 3.2 results in a dilute solution of $Si(OH)_4$. This weak acid, however, is unstable and condenses spontaneously with elimination of H_2O in an exothermic reaction even in the presence of water. The resulting mixture contains various oligo- and poly(silicic) acids, some of which can be isolated and characterized employing the same methodology as in case of $Si(OH)_4$.

The degree of condensation depends on the pH value; the dimerisation rate is highest at pH ≈ 9 involving the anions $[H_3SiO_4]^-$ and $[H_5Si_2O_7]^-$. The pK_a values amount to 9.85 for H_4SiO_4 and 9.0 for $H_6Si_2O_7$. Apparently, under basic conditions, the anion $[H_3SiO_4]^-$ attacks a nearby conjugate acid molecule H_4SiO_4 in a nucleophilic manner and under the expulsion of a hydroxide ion. As to be expected, the backward reaction, that is, the dissolution of SiO_2, is also fastest at pH ≈ 9.[40] As H_4SiO_4 contains four OH groups, the condensation can initially proceed one-dimensionally under formation of chains and rings, then two-dimensionally to sheets and finally three-dimensionally to insoluble water-containing silica gel:

39 K. Sao, S. Shimada et al., *Nature Comm.* **2017**, *8*, 140.
40 G. J. McIntosh, *Phys. Chem. Chem. Phys.* **2012**, *14*, 996. P. J. Jansen et al., *J. Am. Chem. Soc.* **2012**, *133*, 6613.

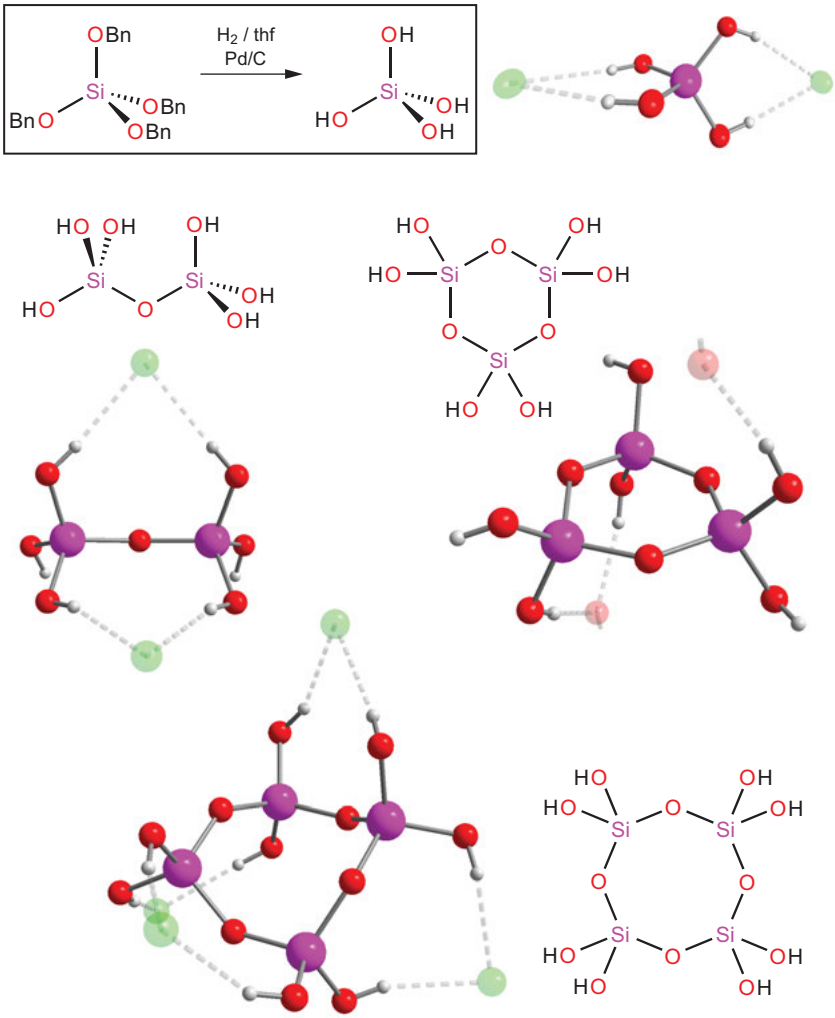

Figure 8.4: Silicic acid and partially condensed derivatives obtained by hydrogenolysis of suitable benzyloxyderivatives.[39] The structural models shown are excerpts from extensive H-bonding networks involving chloride ions (green), ammonium ions and cocrystallized solvent molecules (not shown).

$$n\,\mathrm{Si(OH)_4} \rightleftharpoons (\mathrm{SiO_2})_n\downarrow + 2n\,\mathrm{H_2O}$$

The natural formation of silicates with their various counter cations can be imagined as an intercepted condensation to silica by the blockage of one or more of the four OH groups by deprotonation.

In pure water, SiO_2 dissolves exclusively as undissociated $Si(OH)_4$. The concentration at saturation over a quartz solid phase is just $7{\cdot}10^{-5}$ mol L^{-1} (20 °C/0.1 MPa). Nevertheless, organisms such as diatoms, radiolarians, sponges and some plants

accumulate silicon for the mechanical stabilization of their body through silica scaffolds $SiO_2 \cdot nH_2O$ (*biomineralization*).[41] The solubility of amorphous, precipitated SiO_2 is $2 \cdot 10^{-3}$ mol L^{-1} (at pH ≈ 7), considerably higher than that of quartz. The differing solubilities of amorphous and crystalline SiO_2 in aqueous solution are exploited for the industrial production of large quartz crystals. The so-called hydrothermal synthesis uses water just below the critical temperature (374 °C/22.1 MPa). Under these high pressure conditions SiO_2 is relatively soluble at pH values above 7. A vertically positioned tubular steel autoclave filled with alkaline water (0.5–1.0 M NaOH or $Na_2[CO_3]$) is heated to 340 °C in the bottom zone with amorphous SiO_2 or powdered quartz, while the growing zone with seed crystals is kept at 330 °C. After 20–100 days, crystals of α-quartz have grown to lengths of several decimeters and diameters of a few centimeters. Presumably, natural quartz crystals formed in a similar way. α-Quartz is an important material, which combines optical transparency over a wide spectral window (IR to UV) with high chemical and thermal resistance. Quartz crystals are also employed for their piezoelectric effect.[42]

On hydrolysis of monochlorosilane, a silanol is formed initially (hydroxosilane), which spontaneously condenses to disiloxane:

$$H_3Si{-}Cl + H_2O \longrightarrow H_3Si{-}OH + HCl$$

$$2\ H_3Si{-}OH \longrightarrow H_3Si{-}O{-}SiH_3 + H_2O$$

With aliphatic alcohols, chlorosilanes react to alkoxysilanes.

Cautious hydrolysis of $SiHCl_3$ leads to the unstable silanetriol $SiH(OH)_3$ and then – under polycondensation – to oligomers of composition $(HSiO_{1.5})_{2n}$ with n = 4–7. This class of compounds can be stabilized by methylation with methylnitrite (MeONO) and show cage-like structures such as the following:

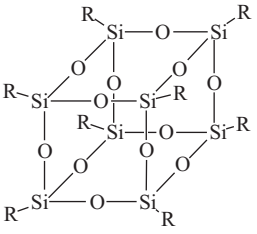

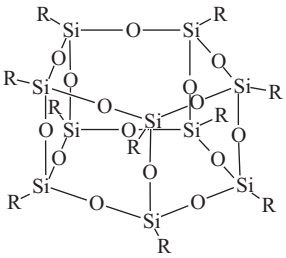

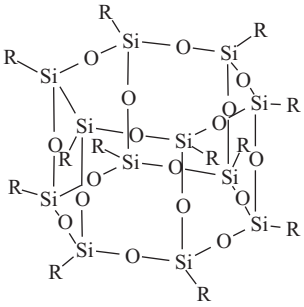

In analogy to silicone nomenclature, the octamer is often referred to as T_8H_8 ("T" for trifunctional precursor, see Section 8.11.3). The bond angles at the oxygen atoms

41 D. Volkmer, *Chem. unserer Zeit* **1999**, *33*, 6. R. Tacke, *Angew. Chem. Int. Ed.* **1999**, *38*, 3015. N. Kröger, *Nachr. Chemie* **2013**, *61*, 514.

42 Piezoelectric effect: The length change of a crystal as a reaction to an applied voltage; leads to oscillations with alternating currents (quartz crystal oscillators in electric clocks).

strongly depend on the substituents R but are closer to 180° (linear angle) than to 109.5° (tetrahedral angle). The most convenient synthesis of the octamers is the hydrolysis of $RSi(OEt)_3$ in the presence of $[^tBu_4N]F$ (R=cyclopentyl, phenyl, etc.):

$$8\ RSi(OEt)_3 + 12\ H_2O \longrightarrow R_8Si_8O_{12} + 24\ EtOH$$

This reaction is catalyzed by LEWIS bases such as NH_3.[43] Such supramolecular species are globally referred to as *silsesquioxanes* (lat. *sesqui* = one and a half), and more particularly the octameric representative as polyhedral octasilsesquioxane. The general formula is $(RSiO_{1.5})_{2n}$. They can also be synthesized by kinetically controlled hydrolysis of organotrichlorosilanes as well as through oxidation of the corresponding polysilanes (Section 8.11.1) with *meta*-chloroperbenzoic acid.[44] Variation of the organic residue R allows for the tuning of particular properties such as amphiphilic or liquid-crystalline behavior as well as the catalytic activity.[45] Silsesquioxanes are also considered as molecular models for the structures of silica and condensed silicates. In *heterosilsesquioxanes* either selected O atoms or RSi units are replaced by another atom with or without pending ligands (e.g., NR, TiOR, VO, CrO_2) taking into consideration possible differences in the valence electron count.

During the hydrolysis of tetraethoxysilane $(EtO)_4Si$ (also referred to as tetraethylorthosilicate (TEOS) or silicic acid tetraethylester), related mesoporous SiO_2 materials with pore sizes of 2–30 nm are formed, which are most conveniently characterized by ^{29}Si-MAS-NMR spectroscopy in the solid state.[46]

8.8.2 Silicates

Silicates are formed by melting SiO_2 (quartz sand) with oxides, hydroxides or carbonates. Depending on the ratio of reactants a certain part of the *siloxane bridges* is cleaved leading initially to high-molecular and subsequently to low-molecular anions:

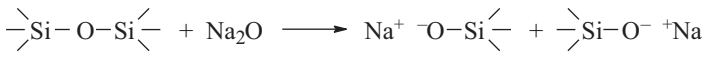

Sodium and potassium silicates are commercially available as aqueous solutions referred to as *water glass*. They are produced from melts of quartz powder and alkali carbonate at 1600 °C:

43 L. Gonzales et al., *ChemPhysChem* **2009**, *10*, 940.
44 H. Matsumoto et al., *Organometallics* **2005**, *24*, 765.
45 K. Kuroda et al., *Chem. Eur. J.* **2008**, *14*, 8500. I. Nishang, O. Brüggemann, I. Teasdale, *Angew. Chem. Int. Ed.* **2011**, *50*, 4592. H. Liu, M. Puchberger, U. Schubert, *Chem. Eur. J.* **2011**, *17*, 5019.
46 S. Haffer, M. Tiemann, M. Fröba, *Chem. Eur. J.* **2010**, *16*, 10447. T. Lebold, J. Michaelis, C. Bräuchle, *Phys.Chem.Chem.Phys.* **2011**, *13*, 5017.

$$SiO_2 + 2\,Na_2[CO_3] \longrightarrow Na_4[SiO_4] + 2\,CO_2\uparrow$$

Alternatively, they are accessible by hydrothermal digestion from quartz and NaOH at 200 °C in an autoclave. Depending on the molar ratio, a mixture of ortho-, oligo- and meta-silicates is obtained. After dissolution in water, predominantly *hydrogen silicates* such as $M[H_3SiO_4]$ and $M_2[H_2SiO_4]$ are present due to hydrolysis; the solutions are therefore strongly alkaline:

$$Na_4[SiO_4] + 3\,H_2O \rightleftharpoons 4\,Na^+ + 3\,[OH]^- + [H_3SiO_4]^-$$

Hydrogen silicate anions condense to various linear, cyclic and cage-like oligomers depending on concentration, pH value and temperature. Of these oligomers, 48 defined structures with up to nine Si atoms have been detected in solution by ^{29}Si-NMR.[47] Examples include a prismatic hexamer and a cubic octamer, which structurally corresponds to the cubic silsesquioxane shown in Section 8.8.1 (polyhedral silsesquioxanes with $R = O^-$ are also referred to as *spherosilicates*).

Acidifying aqueous silicate solutions affords free silicic acids initially, which then spontaneously condense and precipitate to silica gel (SiO_2·aq) still containing numerous silanol groups as well as a substantial amount of water immobilized by H-bonds. Such products are technically referred to as *precipitated silica*; their solid residue upon baking is up to 25% of the wet mass. Silica gel is obviously very hydrophilic. For some applications, however, hydrophobicity is required, which is achieved by treatment of silica gel with organochlorosilanes (R_3SiCl or R_2SiCl_2) and thus conversion of silanol end groups into the corresponding disiloxane (SiOSi) moieties.[48] For example, the hydrophobic C18 stationary phase for high-performance liquid chromatography (HPLC) is produced in this manner by reaction of SiO_2·aq with $C_{18}H_{37}SiMe_2Cl$ (dimethyl octadecyl chlorosilane).

Some anions of low molecularity found in **silicate minerals** are displayed in Figure 8.5. More than 1000 naturally occurring silicates have been characterized and hundreds of synthetic silicates are known. Apart from X-ray diffraction, ^{17}O- and ^{29}Si-NMR spectroscopy can be employed for the analysis of solid silicates.

Orthosilicates (or *nesosilicates*[49]) contain the tetrahedral anion $[SiO_4]^{4-}$, which is isoelectronic to the sulfate anion. Examples include *olivine* $Mg_2[SiO_4]$ and *garnet* $Ca_3Al_2[SiO_4]_3$. Natural *sorosilicates* are *thortveitite* $Sc_2[Si_2O_7]$ and *barysilite* $Pb_3[Si_2O_7]$. The anions of thortveitite contain linear siloxane bridges. $Ca_2[SiO_4]$ and $Ca_3[SiO_5]$

47 C. T. G. Knight, R. J. Balec, S. D. Kinrade, *Angew. Chem. Int. Ed.* **2007**, *46*, 8148.

48 P. M. Price, J. H. Clark, D. J. Macquarrie, *Dalton Trans.* **2000**, 101.

49 The nomenclature is derived from the Greek words for island (nesos), heap (soros), cyclos (circle), fibre (inos), leaf (phyllon), builder (tecton). Square brackets are used in this book to indicate anions of a definite size while elemental compositions as for *wollastonite* $CaSiO_3$ with a polymeric anion are given without brackets.

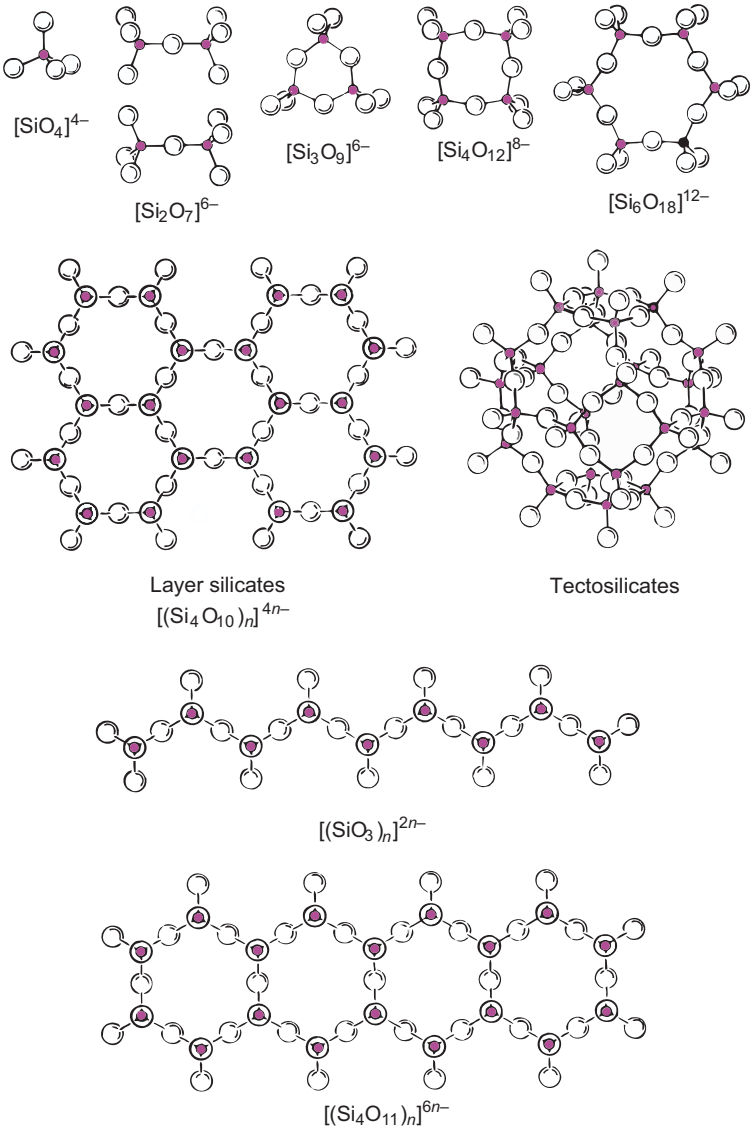

Figure 8.5: Structures of selected silicate anions.

(alongside $Ca_3[Al_2O_6]$) are main components of **Portland cement**, which is obtained by strong heating of limestone $Ca[CO_3]$ with sand (SiO_2) and clay $NaMgAl_5[(Si_4O_{10})_3]$.

In the different *cyclosilicates*, the SiO_4 tetrahedra are connected by shared O atoms in such a way that heterocycles with alternating atom sequence SiOSiO . . . . result (the SiO units being regarded as discrete ring members). These silicates of general formula $[(SiO_3)_n]^{2n-}$ are also called *metasilicates*. Natural examples are

α-*wollastonite* $Ca_3[Si_3O_9]$ and *beryl* $Be_3Al_2[Si_6O_{18}]$. Representatives with n = 3, 4, 6, 8, 9, 12 and 18 have been structurally characterized. In addition, bicyclic and dimeric anions are known.

The disilicate anion is the starting structure for a large number of chain-like anions as contained in the *inosilicates*; at very large chain lengths they correspond to the idealized formula $[(SiO_3)_n]^{2n-}$ (Figure 8.5). Natural silicates of that sort are, for instance, β-*wollastonite* $CaSiO_3$ and *enstatite* $MgSiO_3$.[49] In crystals of these minerals, negatively charged chains are arranged in a parallel fashion with intercalated cations, for example, $Ca_n[(SiO_3)_n]$. Electrostatic forces account for the integrity of the crystal. As size and charge of the cations is obviously of secondary importance in such structures, metasilicates with variable cations are also known, for example, *diopside* $CaMgSi_2O_6$ and *spodumen* $LiAlSi_2O_6$.

When several $(SiO_3)_n$ chains are connected via shared oxygen atoms, double-chain and band structures are formed in a first instance and finally two-dimensional indefinite layers (*phyllosilicates*). Possible connectivities are shown in Figure 8.5. The *amphiboles* belong to the class of band silicates, while *clays* and *mica* are layer silicates. The different forms of *asbestos* also consist of band or layer silicates.[50] A well-known layer silicate is *bentonite*, which consists of a mixture of various clay minerals with *montmorillonite* $NaMgAl_5[(Si_4O_{10})_3]\cdot 12H_2O$ as main component. Bentonite is mined in large amounts. Due to its large inner surface, it is used as absorbent for the purification of nutritional oils, wines and juices or as drying agent.

In case of a three-dimensional connection of SiO_4 tetrahedra via shared corners, the structures of *quartz*, *tridymite* and *cristobalite* result. In these cases, all oxygen atoms are engaged in siloxane bridges; the silicate framework is overall neutral and thus no counter cations are required. Nonetheless, ionic silicates, namely the framework or *tectosilicates*, are derived from these SiO_2 structures and contain three-dimensionally indefinitely extended anions. These are formally obtained by replacing up to 50% of the Si atoms of the $(SiO_2)_n$ structure by the isoelectronic Al^-. For electroneutrality, an appropriate number of cations is necessary. Examples for such **alumosilicates** are *orthoclase* (potassium feldspar) $KAlSi_3O_8$ and *anorthite* (calcium feldspar) $CaAl_2Si_2O_8$. The cations are located in the empty spaces of the framework consisting of SiO_4 and AlO_4 tetrahedra. The *ultramarines* also belong to the alumosilicates; their blue or green color is due to the encapsulated polysulfide radical anions (yellow $[S_2]^{\bullet-}$ and blue $[S_3]^{\bullet-}$), which have been detected by Raman and ESR spectroscopy. The blue form has been traded since antiquity as *lapislazuli*, a valuable while light-fast blue pigment and semiprecious stone. It is mainly found in Afghanistan and Chile. Since about 200 years, however, this silicate is also produced synthetically.[51]

50 A highly recommendable review on structure, properties and health issues associated to asbestos: C. Röhr, *Chem. unserer Zeit* **1998**, *32*, 64 (in German).

51 T. Chivers, P. Elder, *Chem. Soc. Rev*. **2013**, *42*, 5996. Picture gallery: www.holliday-pigments.com

The widespread occurrence of alumosilicates makes aluminum the third most abundant element in the Earth's crust after O and Si; with 8.2 % it is the most frequently occurring metal. It should be noted in passing that alumosilicates can also be derived from the oligo- and polysilicate anions discussed above. As most other alkaline polysilicate anions, the alumosilicates constitute important geological sinks for carbon dioxide: erosion by carbonic acid from rain generates $Ca[CO_3]$, thus irreversibly binding CO_2.

A particularly interesting and technically tremendously important group of alumosilicates are the **zeolites**.[52] The structures of these microporous crystalline solids are characterized by large empty spaces. The structure of the mineral *faujasite* $[Na_2,Ca,Mg]_{29}[Al_{58}Si_{134}O_{384}]\cdot 240\,H_2O$, for instance, consists of basket-like building blocks as shown in Figure 8.6. They are connected in such a manner that numerous empty spaces and channels are created, which contain the counter-cations and the better part of water indicated in the above formula, while the minor part is chemisorbed to the inner surface as silanol groups. As the bonding of the counter-cations is electrostatic, they can easily be replaced, which allows

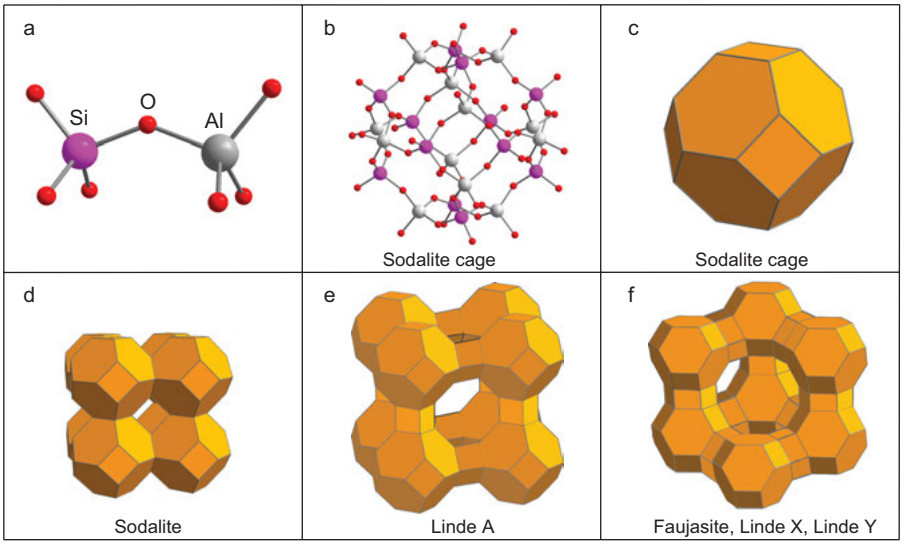

Figure 8.6: Schematic structures of zeolites of different kinds: (a) dinuclear building block in alumosilicates (two corner-sharing tetrahedra); (b) sodalite cage of 24 tetrahedra; (c) sodalite cage, schematic (Al and Si atoms connected to form edges of polyhedron, O atoms omitted); (d) structure of sodalite; (e) structure of zeolite A (e.g., Linde A) and (f) structure of the zeolites *faujasite*, Linde X and Linde Y.

52 C. D. Williams, *Encycl. Inorg. Chem.* **2005**, *8*, 5831. J. Cejka et al. (eds.): *Introduction to Zeolite Science and Practice*, 3rd ed., Elsevier, New York, **2007**.

for the use of *zeolites* as *cation exchange materials*. The empty spaces of the *faujasite* structure are only accessible through windows of a defined size (Figure 8.6). The inner diameter of the cages amounts to 660 and 1160 pm, respectively, while the corresponding windows are just 250 and 740 pm wide. This structural peculiarity of many natural and synthetic zeolites is exploited by using these materials as water insoluble absorbents and *molecular sieves*. If the water bound in the empty cages by hydrogen bridges is removed by heating the zeolite in vacuum to about 350 °C, a strongly hygroscopic material is obtained which is suitable for drying gases and solvents. After application as a drying agent, it can be regenerated by repeating the heating process. The drying effect is based on the strong hydrogen bonds of the water molecules to the anionic oxygen atoms of the silicate framework, which cannot be formed by ethers, esters, hydrocarbons and so on and are considerably weaker for alcohols and amines. For similar reasons, water vapor can be removed by zeolites from gas streams of O_2, N_2, Cl_2 and noble gases. In addition, a sieve effect is active: smaller molecules can enter the inner cage through the pores, while larger ones cannot. For example, this effect allows for the removal of O_2 from argon and the separation of gas mixtures such as the nitrogen and oxygen of air.[53]

Zeolites are employed as absorbent/stationary phase in gas *chromatography*, for example, for the separation of *ortho*- and *para*-H_2[54] and of H_2, HD and D_2.

Nowadays, zeolites are predominantly synthetic. They are produced, for instance, by dissolving the mineral *boehmite* (AlOOH) in aqueous sodium hydroxide to yield sodium aluminate $Na[Al(OH)_4]$, which is then converted with water glass (Na_2SiO_3) to gel-like alumosilicates. By treatment with water vapor, crystallization of the gel is induced. The properties of the thus prepared zeolites can be adjusted to the intended use by variation of the size of cages and windows. The most important synthetic zeolite is "Linde A" with the idealized composition of $Na_{12}[Al_{12}Si_{12}O_{48}]\cdot 27\,H_2O$, which is mainly used in detergents as water softening agent (Zeolite A, $NaAlSiO_4$).[55] *Faujasite* is industrially produced as well. Furthermore, zeolites serve as *catalysts* in the petrochemical industries (e.g., the silicon-rich zeolite ZSM 5). In order to obtain zeolites with tailor-made pore and channel sizes, bulky amines are employed during synthesis as structure-directing agents.

53 M. Yu, R. D. Noble, J. L. Falconer, *Acc. Chem. Res.* **2011**, *44*, 1196.

54 The nuclear spin isomerism of hydrogen was discovered in 1925 by PAUL HARTECK and K. F. BONHOEFFER in Berlin-Dahlem. In *o*-H_2 the nuclear spins of the H atoms are aligned in parallel fashion, in *p*-H_2 antiparallel. *o*-H_2 is about 80 J mol^{-1} higher in energy than *p*-H_2. At 25 °C hydrogen gas consists of about 75% *o*-H_2 and 25% *p*-H_2; near 0 K the equilibrium is completely shifted to *p*-H_2.

55 Modern washing detergents consist of about 40% so-called builder (e.g., Zeolite A), 35% bleaching agent (e.g., perborate), 20% surfactants, 1% each enzymes and graying inhibitors, 0.3% optical whiteners and 2% additional components.

The actual templating moieties are the cations, the size of which is varied by the coordinating amines. The amines are burned off at the end of the production process by heating the product to 500 °C in the presence of oxygen (*calcination*). Particularly large pores of 15–100 Å diameter and thus an extremely large inner surface (>1000 $m^2\ g^{-1}$) are obtained by the addition of cationic surfactants that organize into micelles in solution and form complexes with the alumosilicate anions to determine the structure of the mesoporous final product.[56] More than 190 different zeolite structures have been synthesized so far.

The major application of zeolites in the petrochemical industry is the cracking of higher hydrocarbons to smaller molecules. The acidic SiOH groups at the zeolite (inner) surface assume a pivotal catalytic role. Their BRØNSTED acidity depends on the environment of the silicon atom in question, for which the following NMR spectroscopically proven possibilities exist:[57]

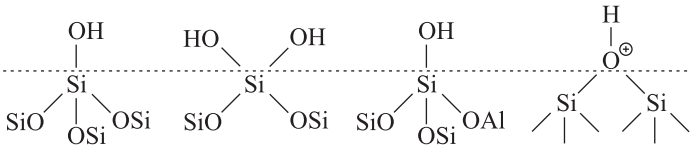

The acidity in this row increases from left to right.

Another notable aspect is the synthesis of *titanosilicates*, that is, zeolites with part of the Si atoms replaced by Ti, which are of interest for catalytic applications in particular. Just like Si and Al, Ti is coordinated tetrahedrally by O atoms in these materials, but unlike silicon can also undergo redox reactions (Ti^{III}/Ti^{IV}).

8.8.3 Germanates

In analogy to silicon, germanium does not form room temperature-stable oxoacids without additional measures. In contrast, a large number of the corresponding salts is known, namely germanates and polygermanates. These salts are obtained by dissolution of GeO_2 in aqueous bases or by melting of GeO_2 with metal oxides. Depending on the stoichiometric ratio and the reaction conditions, ortho-germanates $[GeO_4]^{4-}$ or open-chain meta-germanates $[(GeO_3)_n]^{2n-}$ as well as different oligogermanates with anions such as $[Ge_2O_7]^{6-}$, $[Ge_5O_{11}]^{2-}$, $[Ge_5O_{12}]^{4-}$ and $[Ge_9O_{20}]^{4-}$ are obtained.

56 J. Y. Ying, C. P. Mehnert, M. S. Wong, *Angew. Chem. Int. Ed.* **1999**, *38*, 56.
57 A. Baiker et al., *Angew. Chem. Int. Ed.* **2010**, *49*, 7776. C. P. Grey et al., *J. Am. Chem. Soc.* **2012**, *134*, 9708.

8.9 Glasses

When silicon dioxide or certain silicates are molten and then cooled down in a sufficiently rapid manner, glass-like products are typically obtained instead of crystalline materials. These silicate glasses are of tremendous practical importance. Therefore, the glassy state and its difference to the crystalline state shall be put to closer scrutiny.[58]

A glass is a solid material with a dense packing of atoms, which may show partially ordered areas across a few molecular units but lacks the long-range periodical order of crystalline structures. In case of silica glass ("quartz glass"), according to scanning electron microscopic measurements the arrangement of SiO_2 units can be imagined as in Figure 8.7.[59]

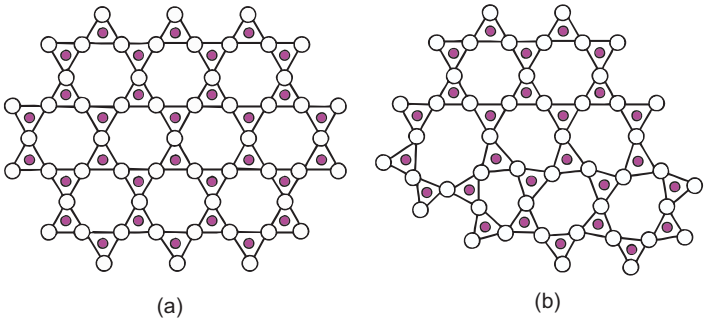

Figure 8.7: Schematic two-dimensional image of the connectivity of SiO_4 tetrahedra (a) in crystalline and (b) glassy SiO_2. The coordination number of Si atoms (in magenta) is 4 in both cases (the fourth O atom is situated above and below the paper plane). The "ring sizes" (number of tetrahedra) varies between 4 and 9 in the glassy state in contrast to crystalline quartz where it is 6.

Glass formation is a consequence of kinetically hindered crystallization, that is, the glass has not reached thermodynamic equilibrium. It is in a metastable amorphous state, which is of higher energy than the corresponding crystal. The vast majority of glasses are obtained by cooling the corresponding melts, less frequently by condensation of vapors or according to the sol-gel process (see below). The reason for the kinetic hindrance of the crystallization process is the high viscosity of the melt in the case of silicates. Even in the absence of long-range order, the three-dimensional network of the strong SiOSi bridges is largely preserved. Moreover, the SiO_2 melt has a complicated composition with molecular clusters of

58 J.-L. Adam, J. Lucas, *Encycl. Inorg. Chem.* **2005**, *6*, 3670. C. Rüssel, D. Ehrt, *Chem. unserer Zeit* **1998**, *32*, 126.

59 M. Heyde et al., *Angew. Chem. Int. Ed.* **2012**, *51*, 405.

various sizes. This particularly applies to silicates with polymeric anions; anions of different sizes exist in equilibrium.

Besides those of SiO_2 and silicates, glasses with three-dimensional (unordered) network structures are also known for other oxides such as B_2O_3, GeO_2, P_2O_5, As_2O_5, Sb_2O_5, TeO_2 and their oxosalts with polymeric anions (*oxide glasses*). Most of the commonly used glasses, however, are multicomponent systems, which are molten from 7 to 10 different oxides. Said oxides are referred to as *network builders*, in contrast to *network modifiers* (predominantly the oxides of alkali and alkaline earth metals), which diminish the three-dimensional connections through formation of terminal O atoms (see Figure 8.5).

In addition, the large group of *chalcogen glasses* is similarly characterized by polymeric structures with covalent bonds. Elemental selenium belongs to this class of compounds as well as the binary systems SiS_2, $GeSe_2$, As_2S_3 and As_2Se_3 and ternary and quaternary mixtures such as $As_{12}Ge_{33}Se_{55}$. The latter is commercially produced for it is transparent in the infrared. Such chalcogenide glasses are semiconductors without exception with bandgaps between 1 and 3 eV. They are typically produced from the melts by cooling.

In contrast to crystalline materials, glasses do not show a sharp melting point, but become gradually softer on heating. At the so-called glass transition temperature T_g, they start to behave as a real, albeit highly viscous liquid that flows when an external force is applied (e.g., gravitation). If the volume expansion (or length extension) of a piece of glass is measured as a function of temperature, T_g is the temperature at which the linear expansion coefficient increases abruptly. The viscosity at T_g is typically within the range 10^{12}–10^{13} Pa s. By slow thermal annealing (*tempering*) at temperatures above T_g, tensions in the glass can be reduced (relaxation). On the other hand, at such temperatures, there is the danger of crystallization onset or phase segregation. Only well above the *softening temperature* T_s (viscosity of about 10^6 Pa s) glasses can be processed by deformation (*glass blowing*).

Silica glass (also "quartz glass") shows a particularly high glass transition temperature of about 1200 °C. In this case, for glass blowing or the production of optical components such as lenses, prisms or windows, temperatures above 1800 °C are required. Transparent silica glass is obtained by melting pure quartz crystals in the oxyhydrogen flame or electrically. For *fused silica*, which is only translucent, pure sand is incompletely molten at ca. 1800 °C. Some crystalline phase boundaries and gas bubbles remain and give the final product a milky appearance. *Glass fibers* for optical conductors are produced in a complicated manner by gas phase deposition of SiO_2. These fibers can conduct light without significant losses over hundreds of miles when ultrapure SiO_2 is used,[60] which in turn is obtained by gas phase

60 For his contributions to this technology, CHARLES KUEN KAO (1933–2018) was awarded the NOBEL Prize in physics of the year 2009.

oxidation of electronic grade $SiCl_4$ in a high-frequency plasma or in an oxyhydrogen flame:

$$SiCl_4 + O_2 \xrightarrow{1200–1800°C} SiO_2 + 2\,Cl_2$$

The inside of a silica glass tube is coated with ultrapure SiO_2 by injection of an $SiCl_4/O_2$ mixture on one side and pumping off Cl_2 on the other side at an overall pressure of 2 kPa, while it is heated to 1200 °C from the outside or brought to reaction by a microwave gas discharge. In the latter case, the discharge zone is slowly moved through the tube so that a thick layer of ultrapure SiO_2 is deposited, which can be doped with small amounts of germanium by addition of $GeCl_4$ in order to increase the refractive index. Subsequently, the tube is heated to higher temperatures until it collapses and then drawn into the optical fiber. World-wide, more than 10^9 km of optical fiber cables are installed.

For the chemical laboratory, the **borosilicate glasses** Jenaer Geräteglas 20, Duran, Rasotherm and Pyrex are particularly suitable (trade names). Their anions are related to alumosilicates, only that Al is mostly replaced by B. The frequently employed *Duran glass* consists of SiO_2 (74%), B_2O_3 (14%), Al_2O_3 (3.5%), Na_2O (4.5%), BaO (3%) and traces of K_2O and CaO. Alkali silicate glasses show much lower glass transition and softening temperatures than silica glass (Duran: T_g = 534 °C). On the other hand, such glasses are typically somewhat less resistant to hydrolytic and thermal wear. *Window glass* consists of SiO_2 (72%), Al_2O_3 (1.5%), Na_2O (14.5%), CaO (8.5%) and MgO (3.5%). Technically produced glass fibers (*glass wool*) have a similar composition as Duran; they are produced by melting of quartz sand, soda $Na_2[CO_3]$, pottash $K_2[CO_3]$, borax, feldspar, dolomite $MgCa[CO_3]_2$ and recycled glass and are predominantly employed for heat insulation in buildings.[61]

A particularly heat-resistant glass is produced from the *nesosilicate* $LiAlSiO_4$ with certain additives and is used for ceramic stove tops under the trade name CERAN. More recently, so-called bioactive (bio-compatible) glass is being employed for special implants: it consists of Na_2O (24.5%), CaO (24.5%), P_2O_5 (6.0%) and SiO_2 (45.0%) and is not repelled by the human body, but metabolized instead with time.[62] During this process, a silicon-rich layer of calcium apatite is formed on the surface of the implant, which resembles the mineral component of bone. In an ideal case, the glass is slowly dissolved in the body fluids and replaced by natural bone tissue.

61 Other inorganic fibers are stone fibers (rock wool), carbon and graphite fibers as well as fibers from silicon carbide or Al_2O_3.

62 H. O. Ylänen (ed.), *Bioactive glasses*, Woodhead Publ., Philadelphia, **2011**. J. R. Jones, A. G. Clare (eds.), *Bio-Glasses*, Wiley, Chichester, **2011**. Apatite: $Ca_5[PO_4]_3[OH]$.

Another option for producing glass is given by the so-called **sol-gel process**,[63] which does not require melting of materials. An alkoxide such as $Si(OEt)_4$ (silicic ester, often referred to as TEOS) serves as precursor, which is dissolved in ethanol and then hydrolyzed by slow addition of water under base or acid catalysis. The rate of replacement of OEt by OH groups limits the spontaneous polycondensation of the latter. Via a transparent *sol* (a dispersion of colloidal particles) a solid gel of SiO_2(aq) is formed, subsequently dehydrated at 120 °C to a so-called xerogel and finally transformed into a glass at 600–1200 °C under considerable shrinkage. The glass formation occur above the glass transition temperature, but below the melting temperature. Through the addition of alkoxides of other elements, glasses of various compositions are produced by the sol-gel process. If the gel described above is dried under conditions that it retains its volume, a very loose *aerogel* is formed with a density of typically only 0.1 g cm^{-3}, which thus floats on water. These gels are excellent heat insulators, as highly porous materials they are also suitable for the immobilization of catalysts.[64]

Glassy freezing is also observed for many other systems that may even consist of small molecules or ions in the melt. For instance, a melt of $K[NO_3]$ with between 30 and 47 mol% $Ca[NO_3]_2$ freezes as a glass, because the differing cationic charges and sizes make crystallization more difficult.

Another frequent case is the glassy freezing of compounds, which are associated by *hydrogen bonds* such as concentrated sulfuric or phosphoric acid, glycerol and other alcohols. The movement of the molecules is restricted by this association and crystal growth thus hindered.

In general, glasses are higher in energy than the corresponding crystalline species as they still contain a part of the melting enthalpy set free on crystallization.

The ceramic materials porcelain, earthen and stoneware are closely related to glass, but normally contain a crystalline component of at least 30%. Similarly, *glass ceramics* also have considerable crystalline components, which are deliberately introduced by the controlled tempering of a glass. Normally, the tiny crystallites are statistically distributed in the amorphous glass matrix so that no anisotropic properties result.

8.10 Silicon–Nitrogen Compounds

Silicon forms a large number of compounds with SiN bonds. These bonds can most easily be constructed by the condensation of silicon halides with ammonia or primary and secondary amines:

63 J. D. Wright, N. A. J. M. Sommerdijk, *Sol-Gel Materials, Chemistry and Applications*, Gordon and Breach, Amsterdam, **2001**. Topical issue *Sol-Gel Chemistry and Materials*, in *Acc. Chem Res*. **2007**, *40*, No. 9. M. Pagliaro, *Silica-Based Materials for Advanced Chemical Applications*, RSC, Cambridge, **2009**.
64 N. Hüsing, U. Schubert, *Angew. Chem. Int. Ed.* **1998**, *37*, 22. A. C. Pierre, G. M. Pajonk, *Chem. Rev*. **2002**, *102*, 4243. K. Kanamori, K. Nakanishi, *Chem. Soc. Rev*. **2011**, *40*, 754.

$$3\ H_3Si{-}Cl\ +\ 4\ NH_3 \longrightarrow (H_3Si)_3N\ +\ 3\ [NH_4]Cl$$

Like the analogous trimethylamine, trisilylamine is a colorless liquid, but it is a much weaker LEWIS base. With Me_2NH, H_3SiBr formally reacts to Me_2NSiH_3, which, however, does not exist as a monomer, but rather as cyclic pentamer (m.p. 3 °C):

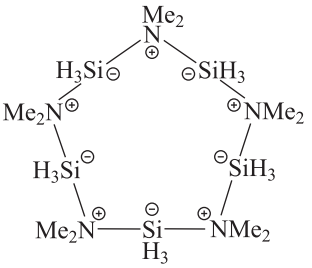

$d_{SiN} = 198$ ppm
$\text{angle}_{NSiN} = 178°$
$\text{angle}_{SiNSi} = 110°$

The pentamer contains coordinate σ bonds between the N atoms of one molecule and the Si atoms of another. The coordination number at nitrogen is raised to 4 and that of silicon to 5. Silylamines are hydrolyzed by water.

With ammonia, $SiCl_4$ reacts at 25 °C in CH_2Cl_2 via intermediates to polymeric silicon diimide if the primary product mixture is finally heated to 600 °C for the completion of the reaction and the removal of the side product by sublimation:

$$SiCl_4\ +\ 6\ NH_3 \longrightarrow Si(NH)_2\ +\ 4\ [NH_4]Cl$$

$Si(NH)_2$ is technically produced, but extremely sensitive to hydrolysis. According to the *hydride displacement law*[65] it formally corresponds to the equally polymeric SiO_2. Just as countless silicates (oxosilicates) can be derived from the latter, many *nitridosilicates* can be obtained from $Si(NH)_2$, which contain tetrahedral SiN_4 units.[66] The simplest anion of that sort is encountered in $Ba_5[Si_2N_6]$, which consists of two edge-sharing SiN_4 tetrahedra resulting in discrete $[Si_2N_6]^{10-}$ ions with formally 10 negative charges. In more strongly networked nitridosilicates, the SiN_4 units can also be linked three-dimensionally, for example, in $MgSiN_2$. In addition, a growing number of synthetic oxonitridosilicates with ternary anions is known. For silicon nitride see Section 8.12.2.

When $SiCl_4$ is heated in refluxing benzene with an excess of $Na[N_3]$, colorless silicon tetraazide $Si(N_3)_4$ is formed, while the same reaction in MeCN at 25 °C gives the colorless salt $Na_2[Si(N_3)_6]$.[67] In contrast to the initiating explosive $Pb[N_3]_2$, the sodium salt can be handled safely and $Si(N_3)_4$ is persistent in solution.

---

65 According to this law, the groups CH_2, NH and O are comparable in terms of their bonding situation, that is, they are isoelectronic and isolobal; similarly, the groups CH_3, NH_2, OH and F.

66 W. Schnick, H. Huppertz, *Chem. Eur. J.* **1997**, *3*, 249 and 679. F. Liebau, *Angew. Chem. Int. Ed.* **1999**, *38*, 1733.

67 P. Portius et al, *Angew. Chem. Int. Ed.* **2010**, *49*, 8013.

8.11 Organosilicon Compounds

A virtually unlimited number of organic silicon compounds are known.[68] For example, the organosilanes and the organosiloxanes (*silicones*) belong to this class of compounds. Functionalized derivatives of both are of tremendous technological importance. With few exceptions, the organic chemistry of *germanium*[69] is analogous to that of silicon, although of much less practical importance.

8.11.1 Organosilanes

The most important *laboratory methods* for the construction of SiC bonds are the alkylation and arylation of chlorosilanes such as $SiCl_4$ with Li-, Zn-, Hg- or Al-organyls or with GRIGNARD compounds:

$$SiCl_4 + 4\,RMgX \longrightarrow R_4Si + 2\,MgX_2 + 2\,MgCl_2 \qquad X = Cl, Br$$

With $SiHCl_3$, the corresponding triorganylsilanes R_3SiH are obtained, for example:

$$SiHCl_3 + 3\,i\text{PrLi} \longrightarrow i\text{Pr}_3SiH + 3\,LiCl$$

Starting from Si_2Cl_6, hexamethyldisilane Me_6Si_2 can be produced, which reacts with MeLi or Na[OMe] to trimethylsilyl salts M[Me_3Si] (M=Li, Na) that in turn can be employed for the synthesis of unsymmetrically substituted organosilanes:

$$Me_6Si_2 + MeLi \longrightarrow Me_3SiLi + Me_4Si$$

$$Me_3SiLi + R{-}X \longrightarrow Me_3Si{-}R + LiX \qquad X = Cl, Br$$

$$Me_3SiLi + Ph_3SiCl \longrightarrow Me_3Si{-}SiPh_3 + LiCl$$

Another important procedure for the synthesis of organosilicon compounds is the *hydrosilylation* discussed in Section 8.6.3.

The method of highest technical significance is the so-called direct process according to MÜLLER and ROCHOW,[70] in which alkyl or aryl chlorides are reacted in a fluidized bed reactor with finely ground silicon at 270–320 °C in the presence of a copper catalyst. The most important application of this process is the exothermic reaction of CH_3Cl with Si predominantly yielding Me_2SiCl_2, which is the main component in the production of many polysiloxanes (*silicones*, Section 8.11.3):

---

68 H. Sakurai, *Encycl. Inorg. Chem.* **2005**, *8*, 5159; R. West et al., *ibid.* **2005**, *6*, 3389. M. Weidenbruch, *Chem. Rev.* **1995**, *95*, 1479; E. Hengge, R. Janoschek, *ibid.* 1495; M. K. Steinmetz, *ibid.* 1527.

69 M. B. Holl, D. R. Peck, *Encycl. Inorg. Chem.* **2005**, *3*, 1650.

70 Developed by the German RICHARD MÜLLER and the US-American EUGENE ROCHOW independently in 1941; see D. Seyferth, *Organometallics* **2001**, *20*, 4978.

$$Si(s.) + 2\ MeCl \xrightarrow{Cu} Me_2SiCl_2$$

During the reaction, the copper additive (Cu, CuO, Cu_2O, CuCl, etc.) is reduced to elemental copper if not already added as such. Cu atoms diffuse into the silicon grains to give catalytically active copper silicide compartments Cu_xSi near the surface.[71] The electron surplus at the silicon surface is likely needed to facilitate the oxidative addition of MeCl to elemental silicon to give a surface-bonded silylene MeSiCl. The insertion of this silylene into the CCl bond of a second equivalent of MeCl yields the desired main product Me_2SiCl_2. Competing pathways (e.g., the insertion into the SiCl bond of Me_2SiCl_2) in concert with the reversibility of all relevant processes under the applied conditions result in the formation of side products via other silylene species such as $SiCl_2$ and Me_2Si. The product mixture thus typically contains all monosilanes of the Me_nSiCl_{4-n} type (n = 0, 1, 3, 4) as well as disilanes; it is separated by distillation. Me_2SiCl_2 has the highest boiling point of the Si_1 derivatives (b.p. 70 °C). By dehalogenation of diorganodichlorosilanes with Li, Na or KC_8 various organopolysilanes can be prepared (see below).

The SiC bond is thermally very stable and chemically not particularly reactive. For example, tetramethyl silane Me_4Si (TMS; b.p. 27 °C) only decomposes above 650 °C. The mean SiC bond enthalpy amounts to 318 kJ mol^{-1} (Table 4.1), but the first SiC dissociation enthalpy of TMS of 387 kJ mol^{-1} is even higher. TMS cannot be hydrolyzed by dilute sodium hydroxide, although the reaction to SiO_2 and CH_4 is exergonic, that is, thermodynamically feasible.

A pecularity of peralkylated oligosilanes R–$(R_2Si)_n$–R is the σ *hyperconjugation* or σ *delocalization*, which leads to a red-shift of the longest wavelength absorption in the near UV with increasing $n > 3$. This effect is based on secondary orbital interactions that affect the energy of the σ and σ* orbitals between the Si atoms of the chain in the HOMO–LUMO region.[72] The following scheme shows the relevant interactions for *anti*- and *syn*-conformations of an oligosilane chain:

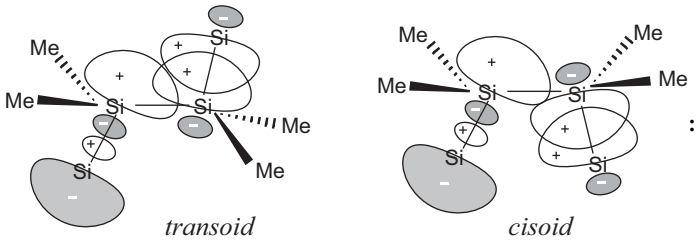

71 Y. Ji, F. Su et al., *J. Catal.* **2017**, *348*, 110 and literature cited therein.

72 A. Bande, J. Michl, *Chem. Eur. J.* **2009**, *15*, 8504.

While the primary and geminal interactions are conformation independent, the overlap of vicinal orbitals in the HOMO is bonding in case of *syn*-conformations (SiSiSiSi torsion angles of about 0°) and antibonding for the *anti*-conformations (SiSiSiSi torsion angles of about 180°). In the LUMO the situation is exactly the opposite. Overall, the HOMO–LUMO gap is lowered for *anti*- and raised for *syn*-conformations. With increasing chain length, the σ→σ* excitation effected by a photon therefore results in a red-shifted absorption for polysilanes in a predominantly *anti*- or *transoid*-conformation, while (enforced) *syn*- or *cisoid*-conformations give rise to a blue-shift.[73] Ultimately, the excitation of an electron into the antibonding LUMO can lead to the homolytic cleavage of SiSi bonds under formation of silyl radicals.

Functionalized organosilanes either carry a functional group at the Si atom (H, Na, OH, OMe) or the organic residue (R) contains one of the functional groups known from organic chemistry. Tris(trimethylsilyl)silane $(Me_3Si)_3SiH$ is a reducing agent in organic synthesis, which is concomitantly converted into a silyl radical. If there are four different groups linked to the tetrahedrally coordinated Si atom, *chirality* occurs just as in the case of the corresponding carbon compounds. An example is methylnaphthylphenylsilane $(CH_3)(C_{10}H_7)(C_6H_5)SiH$, the racemic mixture of which has been separated into the enantiomers.

The bis(triethoxypropyl)tetrasulfane $(EtO)_3Si–(CH_2)_3–S_4–(CH_2)_3–Si(OEt)_3$ (Si 69®) is used on a large scale for the vulcanization of rubber for tires in concert with silica (SiO_2) as a filler.[74] While the tetrasulfane moiety crosslinks the organic polymer under formation of covalent SC bonds, the ethoxy groups react with surface silanol moieties of the fumed silica resulting in very strong SiOSi linkages. In this way the filler is intimately connected with the organic matrix, leading to lower abrasion during use and thus an extended service life of the tires.

A plethora of large rings, long chains and polyhedral clusters can formally be constructed from the organosilane building blocks R_2Si and RSi, and many of these compounds have been synthesized. Clusters such as tetrasilatetrahedrane, hexasilaprismane and octasilacubane shown below can be obtained by reductive dehalogenation of the corresponding trichlorosilanes $RSiCl_3$:

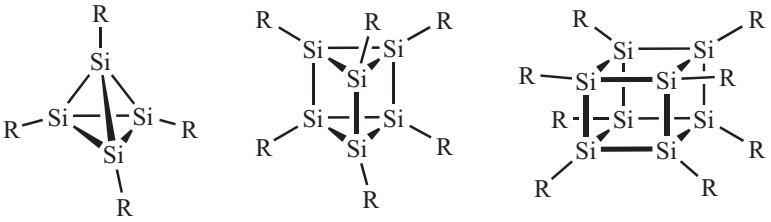

73 K. Tamao et al., *J. Am. Chem. Soc.* **2003**, *125*, 7486.

74 Bis(triethoxysilylpropyl)tetrasulfane (TESPT) is made from sodium tetrasulfide and the corresponding substituted propylchloride.

The smaller the targeted cluster, the larger the substituents R need to be to stabilize the clusters kinetically, for example, by 2,6-diisopropylphenyl in case of hexasilaprismane. Dehalogenation of trichlorosilanes with smaller organic residues R typically gives mixtures of polymers and unstrained clusters. If two bulky groups are present in the halosilane precursor, small rings (e.g., *cyclo*-trisilane for R = ^{t}Bu) or even species with a SiSi double bond result (see Section 8.11.2), thus minimizing the steric interactions between the two substituents due to the decreasing inner bond angles. Conversely, the reduction of R_2SiCl_2 bearing smaller organic substituents R such as methyl, for example, with liquid sodium in refluxing toluene, results in *organopolysilanes*:[75]

$$n\ R_2SiCl_2 + 2n\ Na \longrightarrow (R_2Si)_n + 2n\ NaCl$$

During this process, which proceeds in a radical chain reaction, larger cyclic oligomers occur as side products. Numerous substituted *cyclo*-silanes of the types $R_{10}Si_5$ and $R_{12}Si_6$ are known. They correspond to the analogous *cyclo*-alkanes. When R_2SiCl_2 (R = Mes = 2,4,6-trimethylphenyl) and Si_2Cl_6 are employed during dehalogenation in the appropriate stoichiometric ratio, pentasilapropellane R_6Si_5 with two unsubstituted vertices is formed. The isomeric species R_6Si_5 as well as two isomers of a hypothetical hexasilabenzene R_6Si_6 are accessible by reduction of an unsymmetrical 1,1,2-trichloro-*cyclo*-trisilane. Such clusters are referred to as *siliconoids* due to their alleged role in the *gas phase deposition* of silicon from molecular precursors.[24]

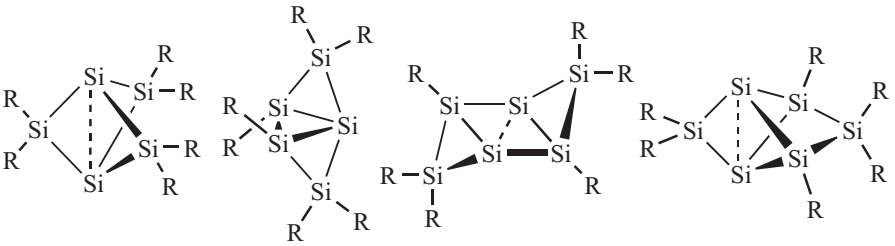

Saturated polysilanes show unusual properties leading to a number of (potential) applications:[75] they are light-sensitive (photo-sensitive) and with aromatic substituents they can be melted without decomposition and thus be spun into fibers. The pyrolysis of $(Me_2Si)_n$ under inert gas leads to a carbosilane polymer, which can be cast into molds. Subsequent controlled oxidation of the carbosilane gives β-siliconcarbide (Section 8.12.1), which retains the original shape of the workpiece.

75 M. Valant et al., *Sci. Rep.* **2016**, *6*, 35450 and literature cited therein.

By treatment of methylchlorosilanes with aqueous hydrofluoric acid, the corresponding methylfluorosilanes are obtained via the silanols as intermediates:

$$MeSiCl_3 + 3\,HF \xrightarrow{H_2O} MeSiF_3 + 3\,HCl$$

$MeSiF_3$ is a gas, which reacts to methylpentafluorosilicate with aqueous KF solution, but is stable toward hydrolysis itself:

$$MeSiF_3 + 2\,KF \xrightarrow{H_2O} K_2[MeSiF_5]$$

On the other hand, phenylpolysilanes such as *cyclo*-$(Ph_2Si)_5$ react with strong acids HX (X=Cl, Br, OTf, etc.) under elimination of benzene to *cyclo*-$(SiX_2)_5$, which in turn can be reduced with $Li[AlH_4]$ to *cyclo*-$(SiH_2)_5$.

8.11.2 Unsaturated Organosilicon and Organogermanium Compounds

The formal dimerization of the carbene analogues discussed in Section 8.2 results in SiSi double bonds.[12,76] Indeed, silicon and germanium form stable species that correspond to alkenes, and even alkynes and aromatics of carbon chemistry. Given that the parent species such as disilene $H_2Si{=}SiH_2$ and digermene $H_2Ge{=}GeH_2$ (in analogy to ethene $H_2C{=}CH_2$) are unstable toward oligomerization to cyclic silanes and germanes, bulky substituents are necessary to suppress this reaction kinetically and allow for the isolation of such species in pure form. In addition, the *sterically demanding substituents* reduce the stability of the cyclic oligomers and thus also provide thermodynamic stabilization to the unsaturated compounds.

Besides the *t*-butyl group the following substituents are commonly applied for the introduction of steric bulk:

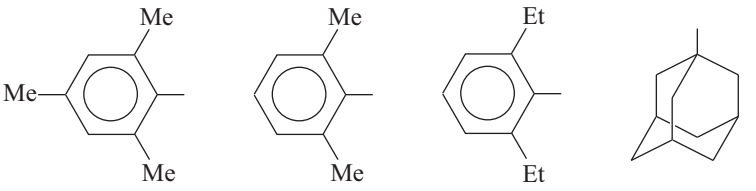

mesityl (Mes) | xylyl (Xyl) | 2,6-diethylphenyl | 1-adamantyl (Ad)

76 V. Y. Lee, A. Sekiguchi, *Organometallics* **2004**, *23*, 2822 and *Angew. Chem. Int. Ed.* **2007**, *46*, 6596. A. Sekiguchi, *Pure Appl. Chem.* **2008**, *80*, 447. R. West, *Polyhedron* **2002**, *21*, 467. M. Weidenbruch, *Eur. J. Inorg. Chem.* **1999**, 373.

Even considerably larger substituents such as R = 2,4,6-triisopropylphenyl or $SiMe(^tBu)_2$ are being employed to protect extremely sensitive structures. Organodisilenes R_4Si_2 are thus prepared by reductive dehalogenation of certain diorganyldihalosilanes (a), through photolysis of *cyclo*-trisilanes (b) as well as by the dimerization of more or less stable silylenes R_2Si (c):

$$\text{(a)}\quad 2\ R_2SiBr_2 + 4\ Li \xrightarrow{-78°C} R_2Si{=}SiR_2 + 4\ LiBr$$

$$\text{(b)}\quad 3\ R_2SiCl_2 + 6\ Li \longrightarrow \textit{cyclo}\text{-}R_6Si_3 + 6\ LiCl$$

$$\textit{cyclo}\text{-}R_6Si_3 \xrightarrow{h\cdot\nu} R_2Si{=}SiR_2 + R_2Si:$$

$$\text{(c)}\quad 2\ R_2Si: \longrightarrow R_2Si{=}SiR_2$$

The UV photolysis of *cyclo*-R_6Si_3 (prepared as shown above) in cyclohexane at 25 °C affords the corresponding disilene in almost quantitative yield, as the initially formed silylene dimerizes instantly according to equation (c). The product is obtained as yellow air-sensitive crystals (R = 2,6-dimethylphenyl). The UV photolysis of acyclic trisilanes also affords disilenes:

$$Mes_2Si(SiMe_3)_2 \xrightarrow[-50°C]{h.\nu} Mes_2Si: + Mes_3Si{-}SiMes_3$$

$$2\ Mes_2Si: \longrightarrow Mes_2Si{=}SiMes_2$$

The Si=Si bonds of disilenes are generally characterized by more or less pronounced deviations from the usual planar coordination environment of the CC double bond of alkenes. Two principle structural peculiarities are observed: the so-called *trans*-bending of the double bond (quantified by the *trans*-bent angle θ) and its torsion (also referred to as twisting, measured as the twist angle τ; see Figure 8.8). The former is a consequence of the strong preference of silylenes for an electronic singlet state (the two nonbonding electrons are paired). According to a model developed by CARTER, GODDARD, MALRIEU and TRINQUIER (*CGMT model*), dimers of singlet carbene analogues $R_2Si:$ cannot form through a head-on approach of the two fragments due to PAULI repulsion. This is avoided by canting the two fragments in such a manner that each σ lone pair of electrons interacts with the vacant p_z orbital of the other fragment. The strength of this interaction is always weaker than in classical planar double bonds, which is manifest in the smaller HOMO–LUMO gap.

Nonetheless, the significantly shorter SiSi distance of about 214–225 pm, the often substantial rotational barrier for the torsion about the SiSi bond vector (Section 8.2) and the increased wavenumber of the SiSi stretching vibration strongly support the presence of SiSi double bonds. As a consequence, *E*/*Z* isomerism is observed in case of asymmetrical substitution (RR′Si=SiRR′). The *E*-isomer is generally more stable but can be transformed into the *Z*-isomer by UV irradiation. By ^{29}Si-NMR spectroscopy the spontaneous *Z*→*E* isomerization can be monitored. From the

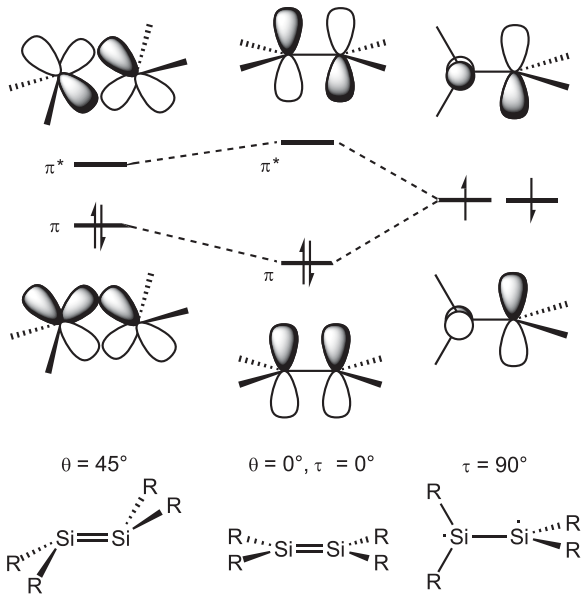

Figure 8.8: Distortions of SiSi double bonds and their consequences for the frontier orbitals: *trans*-bending (left) and twisting (right). The *trans*-bent angle θ is defined as the deviation from 90° of the angle between the Si–Si bond vector and the normal of the plane through the silicon atom and the pending substituent atoms. The twisting angle τ is the angle between the normals of the two planes thus defined.

temperature dependency of its kinetics, activation enthalpies between 105 and 130 kJ mol^{-1} have been deduced for several disilenes. For the related stilbene (PhHC=CHPh), this enthalpy amounts to 179 kJ mol^{-1}. Despite the steric protection, disilenes readily engage in addition reactions with various reagents such as oxygen and other chalcogens, water, alkynes, alkenes, nitriles and isonitriles. Less reactive, air-stable disilenes are accessible with very bulky indacenyl-based substituents and have been used as emissive layers in organic LEDs.[77]

Digermenes are synthesized in a similar manner as disilenes. As the thermodynamic stability of the divalent germylenes is higher than that of silylenes, the GeGe double bond is typically considerably weaker. The double bonds of digermenes therefore deviate even more from planarity than in disilenes with an often much larger degree of *trans*-bending. Furthermore, many digermenes readily dissociate to the constituting fragments in solution.

Despite the high reactivity of disilenes, functionalized derivatives are readily accessible for many silicon-containing double bonds.[78] Metalated disilenes (so-called

77 K. Tamao, T. Matsuo et al., *Chem. Commun.* **2012**, *48*, 1030.
78 C. Präsang, D. Scheschkewitz, *Chem. Soc. Rev.* **2016**, *45*, 900.

disilenides) are typically synthesized by reductive cleavage of one of the bulky substituents of the appropriate precursor by an alkali metal. These analogues of vinyl anions can be employed for the nucleophilic transfer of the Si=Si moiety to various electrophiles. In the case of R = 2,4,6-$^{i}Pr_3C_6H_2$, the reaction with aryl (di)halides uniformly yields the corresponding aryldisilenes or arylene-bridged tetrasilabutadienes. Tetrasilabutadienes without bridge between the Si=Si units are generally accessible by mild oxidation of disilenides (R = aryl, silyl, alkyl):

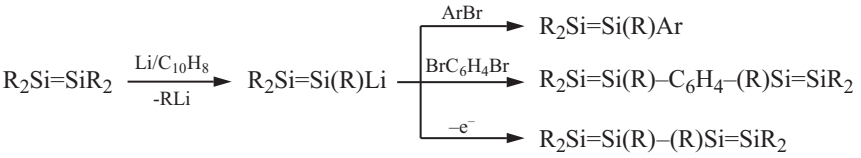

Of the corresponding *digermenides* so far only a single example has been fully characterized (R = 2,4,6-*i*$Pr_3C_6H_2$).[79] It is considerably more sensitive toward oxidation to the butadiene than the corresponding disilenide.

Further examples for unsaturated Si and Ge compounds that have been isolated in pure form are the following cyclic molecules:

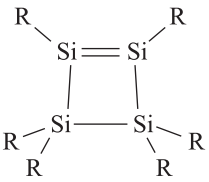

cyclo-tetrasilene
(R = $SiMe_2$*t*-Bu)

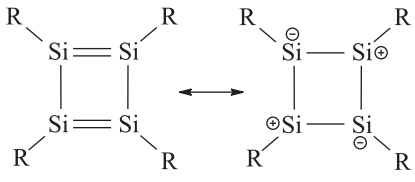

tetrasilacyclobutadiene
(R = octamethylhydrindacenyl)

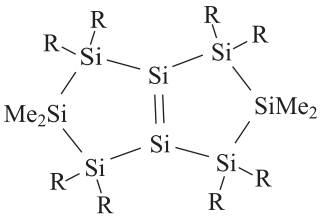

octasilapentalene (R = $SiMe_3$)

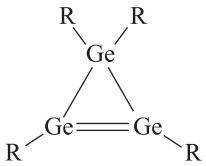

cyclo-trigermene

The *cyclo*-tetrasilene isomerizes photochemically (λ > 420 nm) to the corresponding saturated bicyclo[1.1.0]tetrasilane, which in the dark rearranges back to the

79 D. Scheschkewitz et al., *Organometallics* **2018**, *37*, 632.

unsaturated species. The tetrasilacyclobutadiene is rhombic and avoids the unfavorable (antiaromatic) cyclic delocalization of four π electrons through a pronounced charge polarization of the Si=Si double bonds as shown by the pyramidalization of the two silicon centers with formal negative charges.[80]

The synthesis of compounds with **SiSi triple bond** proved to be a particular preparative challenge.[12,76] According to quantum chemical calculations, the parent disilyne (HSi≡SiH) does not show the linear geometry of acetylene, but rather forms a bicyclic molecule with an SiSi single bond bridged by two H atoms (C_{2v} symmetry). More recently, however, compounds with a true SiSi triple bond of type RSi≡SiR have been prepared using very bulky aryl or silyl substituents.[81] In contrast to alkynes the bond angles at the dicoordinate Si atoms are not 180°, but rather about 137° in an *E*-conformation. The reduced symmetry ($D_{\infty h} \rightarrow C_{2h}$) allows for a stabilizing interaction of bonding π electrons with antibonding σ* MOs of the adjacent bonds to the substituents (hyperconjugation). The central SiSi distance of about 206 pm is considerably smaller than the single bond distance in elemental silicon (235 pm) and the shortest observed SiSi double bond distance (214 pm). With particularly bulky organic substituents the corresponding digermynes R–Ge≡Ge–R have also been prepared.[82]

Silabenzene C_5SiH_6 and *germabenzene* C_5GeH_6 are unstable, but derivatives with the bulky substituent Tbt at the heteroatom have been isolated as persistent species at 25 °C (Tbt: 2,4,6-tris[bis(trimethylsilyl)methyl]phenyl). All properties of these compounds support their aromatic character.[83] The corresponding derivatives of naphthalene and anthracene have also been synthesized. In contrast, substituted hexasilabenzenes are unknown and quantum-chemical calculations predict that the lowest energy structure for Si_6H_6 is not the structure analogous to benzene, but rather a siliconoid cluster with two unsubstituted vertices as shown in Section 8.11.1.[84] In general, compared to more compact cluster-like motifs, the relative stability of classical unsaturated carbon structures decreases with increasing content of silicon.[85] For further examples of aromatic silicon and germanium compounds the interested reader is referred to the original literature.[76]

80 K. Tamao et al., *Science* **2011**, *331*, 1306.

81 N. Wiberg et al., *Z. Anorg. Allg. Chem.* **2004**, *630*, 1823. A. Sekiguchi, M. Ichinohe, R. Kinjo, *Bull. Chem. Soc. Japan* **2006**, *79*, 825. N. Tokitoh et al., *J. Am. Chem. Soc.* **2008**, *130*, 13856. Review: D. Scheschkewitz, *Z. Anorg. Allg. Chem.* **2012**, 2381.

82 P. P. Power et al., *Angew. Chem. Int. Ed.* **2002**, *41*, 1785 and *Chem. Commun.* **2003**, 2091 and *J. Am. Chem. Soc.* **2003**, *125*, 11626. N. Tokitoh et al., *J. Am. Chem. Soc.* **2006**, *128*, 1023.

83 N. Tokitoh at al., *J. Am. Chem. Soc.* **2008**, *130*, 13856 and *Acc. Chem. Res.* **2004**, *37*, 86.

84 D. Scheschkewitz et al., *Angew. Chem. Int. Ed.* **2011**, *50*, 7936.

85 A. S. Ivanov, A. I. Boldyrev, *J. Phys. Chem. A* **2012**, *116*, 9591.

8.11.3 Organosiloxanes

The chemical resistance of the CSi bond and the high bond energy of SiO bonds are of enormous practical importance for the properties and the resulting applications of **silicones**, which are polymeric diorganosiloxanes of the following schematic composition:

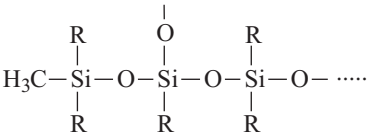

Starting materials for the production of silicones are mostly methylchlorosilanes, which are produced according to the MÜLLER–ROCHOW process (Direct Process, Section 8.11.1). Their hydrolysis or methanolysis leads to the corresponding oligomeric products with chemically and thermally very stable siloxane bridges:[86]

$$n\,Me_2SiCl_2 + n\,H_2O \longrightarrow (Me_2SiO)_n + 2n\,HCl$$

$$n\,Me_2SiCl_2 + 2n\,MeOH \longrightarrow (Me_2SiO)_n + 2n\,MeCl + n\,H_2O$$

The HCl generated during the hydrolysis is separated and used in the conversion of methanol to MeCl, which is recycled into the MÜLLER–ROCHOW process as is the MeCl obtained from the methanolysis reaction. During such a polycondensation the monofunctional Me_3SiCl results in chain termination (M), difunctional Me_2SiCl_2 propagates the chain (D) and the trifunctional $MeSiCl_3$ acts as crosslinking or branching unit (T). If $SiCl_4$ is added further branching to more extended networks occurs by introduction of quaternary silicon centers (Q). These groups can be detected by ^{29}Si-NMR spectroscopy. By appropriate adjustment of mixing ratio and conditions, the average degree of polymerization and the three-dimensional structure of the polymers can be predetermined and liquid, oily, waxy or solid substances produced. Initially, the polycondensation of Me_2SiCl_2 affords a mixture of cyclic and linear oligomers. The latter are converted to cyclic oligomers by heating with KOH. The main product is the tetramer $(Me_2SiO)_4$ alongside smaller amounts of pentamer. These rings are separated by distillation and then subjected to an anionic *ring opening polymerization* (ROP) at 140 °C. In the presence of an anionic initiator (alkali metal oxide or hydroxide or other LEWIS bases) the higher molecular weight polysiloxanes are produced. Cationic ROP is carried out with perfluorinated

86 This hydrolysis with subsequent polycondensation was discovered in 1904 by the British chemist FREDERIC STANLEY KIPPING, who also introduced the term *silicone*. The important Kipping Award for merits in silicon chemistry was named after him.

sulfonic acids or H_2SO_4 as catalysts. The valence angles SiOSi in organopolysiloxanes are typically between 130° and 140°, the internuclear distances d_{SiO} on average at 164 pm. The mechanical elasticity of silicones is due to the nearly unhindered rotation about the SiO bonds.

By variation of the organic substituents and the end groups a broad variety of *properties* can be adjusted. The classical polydimethylsiloxanes are transparent, colorless, chemically and thermally resistant, hydrophobic and nonflammable. In addition, the viscosity does not change very much with temperature. Practical *applications* of silicones are as heat-transfer fluids for high temperatures in thermostats and heat exchangers, as coolants in transformers, as hydraulic oils, as lubricants and insulation material, for seals, foils, membranes, varnishes as well as in cosmetics and in medicine for implants. Silicon oils typically have a linear structure MD_nM. In addition, silicone rubber contains fillers (e.g., silica). Low-molecular (cyclic) diorganylsiloxanes show insecticide properties as they tend to suffocate insects by clogging their respiratory systems; for mammals these substances are considered as nontoxic. Another advantage of silicones over purely organic polymers is their high ignition temperature (450 °C) and that – once ignited – they burn to nontoxic substances such as H_2O, CO_2 and SiO_2. The world production of silicones and siloxanes has been estimated to $4.8{\cdot}10^6$ t in 2017.

From organotrichlorosilanes $RSiCl_3$, the corresponding trialkoxides can be produced by alcoholysis, which form the basis for organosilicon *brick and stone protection agents*. The compounds are used for the impregnation of porous and corrosion-susceptible sandstones and related materials of buildings and monuments. With air humidity, hydrolysis of the alkoxy groups followed by polycondensation leads to (presumably surface-bonded) silsesquioxane moieties (see Section 8.8.1). In this way, the pores of the stones are covered with a hydrophobic protective layer, which prevents liquid water entering the pores, but still retains considerable gas permeability.

8.12 Other Silicon Compounds

8.12.1 Silicon Carbide

Silicon carbide is one of the most important nonoxidic ceramic materials.[87] The reduction of SiO_2 (e.g., high-purity sand) with coke (petroleum coke) in a stoichiometric ratio of 1:3 at temperatures above 2000 °C in an electric furnace yields silicon carbide SiC instead of elemental silicon:

$$SiO_2 + 3\,C(s.) \longrightarrow SiC(s.) + 2\,CO \qquad \Delta H^\circ_{298} = 619\ kJ\ mol^{-1}$$

87 G. Roewer et al., *Struct. Bond.* **2002**, *101*, 59.

The ACHESON process employs an electric arc between carbon electrodes for heating, while the ESK process uses electrical resistance heating.[88] Such batch-wise large-scale production results in a technical-grade product, which is green or black due to the presence of impurities. Pure SiC crystallizes either in the hexagonal wurtzite structure (α-SiC) or in the cubic zincblende structure (β-SiC) and is a colorless semiconductor (bandgap 1.9 eV). α-SiC is the high-temperature (stable above ca. 2100 K), β-SiC the low-temperature modification. The conversion of the two phases, however, is kinetically hindered and the commercially available SiC is therefore mostly α-SiC. Both modifications are thermally and chemically (e.g., against acids) extremely resistant and of similar hardness as diamond. Under the name *carborundum*, SiC is used as abrasive and under the name *silit* for the production of heating resistors in electrical furnaces for very high temperatures. Due to its very good heat conductivity, high-temperature heat exchangers are manufactured from silicon-infiltrated SiC. In the steel industries, SiC serves to increase the silicon content of the steel melt (alloying) as well as for deoxygenation of liquid cast iron (formation of SiO_2). It is also suitable for fire-resistant crucibles, muffle furnaces and other furnace linings. The SiC bricks used for the latter purpose are produced from powdery SiC together with a binder. SiC is rapidly covered with a protective SiO_2 layer upon exposure to air, which prevents further oxidation even at high temperatures.

SiC is considered as modern high-performance ceramic (just like Si_3N_4; see following section). It can also be produced as fibers by pyrolysis of polymeric carbosilane fibers.[89,90a]

8.12.2 Silicon Nitride

Si_3N_4 is an important ceramic material[90], which is valued for its stability against oxidation, its hardness and wear-resistance, its breaking strength and small thermal expansion coefficient. Silicon nitride crystallizes in two hexagonal modifications. In both, the Si atoms are tetrahedrally coordinated by nitrogen, while the N atoms are connected to three Si atoms with strong covalent bonds in trigonal-planar fashion. The structures formally consist of layers, which are stacked in an ABAB sequence in the high-temperature modification (β-Si_3N_4) and in an ABCDABCD sequence in the low-temperature form (α-Si_3N_4). The high-pressure phase γ-Si_3N_4 crystallizes in the spinel structure-type.

---

88 The ESK process was named after the *Elektroschmelzwerk Kempten* in Allgäu, Germany, now a subsidiary of 3M.

89 M. Birot, J.-P. Pillot, J. Dunoguès, *Chem. Rev*. **1995**, *95*, 1443.

90 (a) A. W. Weimer (ed.), *Carbide, Nitride and Boride Materials – Synthesis and Processing*, Chapman&Hall, London, **1997**. (b) H. Lange, G. Wötting, G. Winter, *Angew. Chem. Int. Ed. Engl.* **1991**, *30*, 1579.

The most important industrial synthesis of silicon nitride is the direct *nitriding* of ground Si at 1100–1400 °C:

$$Si_3(s.) + 2\,N_2 \longrightarrow Si_3N_4 \qquad \Delta H^{\circ}_{298} = -755\ \text{kJ mol}^{-1}$$

During his process, α-Si_3N_4 is formed as a colorless, electrically insulating powder. The formation of β-Si_3N_4 takes place in a noticeable manner above 1500 °C. The relative content of α- and β-form as well as amorphous product can be determined either by powder X-ray diffraction or by solid state ^{29}Si-NMR spectroscopy.

Of practical relevance is also the *carbothermal reduction* of SiO_2 in a stream of N_2 or NH_3. The primary product in this case is SiO:

$$3\,SiO_2 + 2\,N_2 + 6\,C \xrightarrow{1450°C} Si_3N_4 + 6\,CO$$

Furthermore, powdery α-Si_3N_4 is obtained by annealing silicon diimide (Section 8.10) at 900–1500 °C:

$$3\,Si(NH)_2 \longrightarrow Si_3N_4 + 2\,NH_3$$

Finally, Si_3N_4 can also be produced by gas phase deposition either as powder or as film:

$$3\,SiCl_4 + 4\,NH_3 \longrightarrow Si_3N_4 + 12\,HCl$$

Si_3N_4 powder is formed into workpieces by sintering at very high temperatures and pressures, for example, at 1800 °C and 10–80 bar under addition of binders such as MgO, Y_2O_3 or Al_2O_3. For example, valves for combustion engines are produced in this manner. The higher thermal resilience compared to metals allows for higher combustion temperatures and thus a higher efficiency of the engine. At the same time, the lower density of 3.2 g cm^{-3} reduces the engine weight. For similar reasons, Si_3N_4 is also employed for the rotors of turbochargers.

8.12.3 Silicon Sulfides

In analogy to the oxides SiO and SiO_2, polymeric SiS and SiS_2 as well as the corresponding selenides and tellurides are known. SiS_2 is formed on heating of the elements at 800–1400 °C or through conversion of SiO_2 with Al_2S_3 at 1100 °C. In contrast to SiO_2 with its 3D network structure, SiS_2 consists of chains, which contain Si atoms in a distorted tetrahedral environment in a spirocyclic arrangement (edge-sharing SiS_4 tetrahedra):

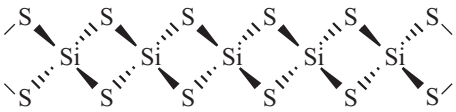

The chain-like structure is reflected in a fibrous habitus of the colorless SiS_2 crystals. SiS_2 is more reactive than SiO_2 and hydrolyses, for instance, to SiO_2(aq) and H_2S. If SiS_2 is heated with Si in vacuum to about 850 °C or if CS_2 vapors are conducted over solid Si at 2 hPa and 1000 °C, monomeric SiS is formed, which condenses on cold surfaces as red, glassy $(SiS)_n$.

Another interesting silicon–sulfur species is the silanethione $H_2Si{=}S$, which has been generated by electric discharge from a mixture of SiH_4 and H_2S and was detected by microwave spectroscopy (C_{2v} symmetry). The internuclear distance d_{SiS} of 193.6 pm corresponds to a double bond.[91a] The analogous difluorosilanethione $F_2Si{=}S$ is formed during reaction of SiS with F_2 or by pyrolysis of $(F_3Si)_2S$ at temperatures above 500 °C alongside SiF_4. It was identified spectroscopically at low temperatures in a solid argon matrix (together with other products). The quantum-chemically calculated d_{SiS} in this species is 191.1 pm.[91b] Related small molecules were detected in gas phase mixtures, for example, Si=S, O=Si=S, S=Si=S and *cyclo*-Si_2S.[91a,c]

91 (a) J. Gauss et al., *J. Chem. Phys.* **2011**, *134*, 034306. (b) H. Bürger et al., *Eur. J. Inorg. Chem.* **1999**, 2013. (c) J. Gauss et al., *Phys. Chem. Lett.* **2011**, *2*, 1228.

9 Nitrogen

Nitrogen is an essential element of life, which occurs in amino acids, purine bases and many other heterocycles and thus determines the structure and function of important components of living organisms such as proteins, nucleic acids and countless enzymes and hormones. The human body contains only 3% of nitrogen, although this amount makes it the fourth most abundant element following O, C and H. The chemical industry therefore produces large amounts of nitrogen-based fertilizers in order to meet the nutritional requirements of a growing world population.[1] In addition to N_2, natural nitrogen species occurring in larger quantities are saltpeter ($K[NO_3]$) (mainly from India) and the so-called Chile saltpeter ($Na[NO_3]$), both of which, however, are practically not employed anymore in Europe. As in the case of other nonmetals, a complex geobiochemical nitrogen cycle exists on the Earth involving almost all oxidation states of the element.[2]

Together with phosphorus, arsenic, antimony and bismuth, the element nitrogen[3] constitutes Group 15 of the Periodic Table. All of these elements have five electrons in their valence shell. The chemistry of nitrogen differs from that of the higher homologues at least as much as the chemistry of carbon does from that of silicon, and the chemistry of oxygen from that of sulfur. The reasons are the same: a rapid increase in the atomic radius from N to P and a considerably higher electronegativity of N versus the other elements of the group. The lack of *d* orbitals in the valence shell of nitrogen, however, *does not* play a role in the observed differences.

For these reasons, the chemistry of nitrogen is treated separately in this chapter; in Chapter 10 the elements phosphorus and arsenic will be covered. Natural nitrogen is almost isotopically pure, consisting of 99.64% ^{14}N and only of 0.36% ^{15}N. The latter is used in enriched form for NMR spectroscopic studies and in mass spectrometry for the isotopic labeling of nitrogen species.

9.1 Elemental Nitrogen

Dinitrogen (N_2) is the main component of dry air with 78.09 vol% (Section 14.2). In addition, considerable amounts of N_2 are dissolved in the oceans. The majority of nitrogen compounds is produced from nitrogen of the air.

1 In Germany, the introduction of the systematic use of mineral fertilizers in 1880 led to a doubling of yields of potatoes and rye within 10 years. Today, approximately 40% of the worldwide agricultural production depends on nitrogen-based fertilizers.

2 D. E. Canfield, A. N. Glazer, P. G. Falkowski, *Science* **2010**, *330*, 192.

3 A. Hammerl, T. M. Klapötke, *Encycl. Inorg. Chem.* **2005**, *6*, 3531 and online edition.

https://doi.org/10.1515/9783110578065-010

Elemental nitrogen is one of the most important *industrial gases*. In general, six out of 10 of the main starting materials of chemical industries are gases: N_2, O_2, Cl_2, NH_3, C_2H_4 (ethylene) and C_3H_6 (propylene). N_2 is obtained on a very large scale from the condensation of cooled air and subsequent fractional distillation. Nitrogen isolated in this manner still contains a part of the noble gases, particularly argon with a boiling point just 10 K higher than that of N_2. By membrane separation, nitrogen of 95% purity is obtained from air on a similarly large scale. Here, advantage is taken of the differing solubility and diffusion rates in organic plastics of N_2 and Ar, on the one hand, and of O_2, H_2O and CO_2, on the other hand.[4] Chemically pure nitrogen can be obtained on a laboratory scale by thermal decomposition of ultrapure sodium azide at 275 °C:

$$2\ NaN_3 \longrightarrow 2\ Na + 3\ N_2$$

Almost the entire amount of nitrogen gathered from air is reduced to ammonia with hydrogen according to the HABER–BOSCH process. In turn, a considerable portion of the ammonia is catalytically oxidized to NO (OSTWALD process), which is further converted to NO_2 by O_2. The dissolution of NO_2 in water followed by further oxidation with air yields nitric acid:

$$N_2 \xrightarrow[Fe]{H_2} NH_3 \xrightarrow[Pt/Rh]{O_2} NO \xrightarrow{O_2} NO_2 \xrightarrow{H_2O,\ O_2} HNO_3$$

Practically, all other nonmetallic nitrogen species are produced starting from NH_3 or HNO_3 (or both).

Molecular nitrogen is a rather inert gas (m.p. 63.3 K; b.p. 77.4 K), which for this reason is employed as an inexpensive protecting gas during certain chemical syntheses and in food industry (in the latter case, often as a mixture with CO_2) in order to extend the durability of packaged fruit, meat, vegetables, spices, cheese, juice, beer and dairy products. Liquid nitrogen is an inexpensive and thus popular cooling agent, not only in chemistry and physics, but also in biology, medicine, food technology, technical applications and last but not least during the Christmas lectures at universities.

For the chemical activation of the N_2 molecule, high temperature or a catalyst is needed in general. This applies to almost all reactions, which cleave the NN triple bond. For instance, the synthesis of ammonia is conducted at 380–550 °C and at a pressure of 40–50 MPa and still requires an iron-based catalyst. As the sole element, lithium reacts with N_2 to (in pure form) ruby-red Li_3N even at room temperature although preparatively useful conversion rates require heating at 150–500 °C.

The reason for the inertness of nitrogen is the extremely high dissociation enthalpy of the N_2 molecule with its triple bond (Section 2.4.3):

$$:N{\equiv}N: \longrightarrow :\dot{N}\cdot + \cdot\dot{N}: \qquad \Delta H^\circ_{298} = 942\ kJ\ mol^{-1}$$

4 G. Maier, *Angew. Chem. Int. Ed.* **1998**, *37*, 2960.

Therefore, most of the reactions of N_2 are endothermic. The dissociation can also be achieved by electric discharges, which result in a plasma of extremely reactive N atoms. For example, N_2 reacts in such plasmas with metallic sodium to dark-blue crystals of sodium nitride (Na_3N).

Irrespective of the low reactivity of the dinitrogen molecule, certain microorganisms can assimilate nitrogen from air at ambient conditions and use it for the synthesis of amino acids (via NH_3 as an intermediate). This remarkable process is of tremendous importance for animal and plant life, as the soluble nitrogen species in soil typically do not suffice to meet the nitrogen demand of plants, in particular in an agricultural setting. From a chemical perspective, this enzymatic N_2 activation (*nitrogen fixation*) is only partially understood. As a first step, coordination of the N_2 molecule to several adjacent heavy metal ions occurs, which are contained within the protein matrices of the so-called *nitrogenase* enzymes (one Mo, seven Fe and one carbon atom form an $MoCFe_7$ cluster).[5] The net reaction equation of the enzymatic nitrogen fixation is:

$$N_2 + 8\,e^- + 16\,ATP + 8\,H^+ \longrightarrow 2\,NH_3 + H_2 + 16\,ADP + 16\,P_i$$

ATP (see Section 10.12.1) acts as an energy carrier and is cleaved under release of energy into the corresponding diphosphate (ADP) and the ionic monophosphate (P_i), while N_2 is undergoing a stepwise 6-electron reduction and simultaneous protonation to two molecules of ammonia. The complexed nitrogen hydrides diazene (N_2H_2) and hydrazine (N_2H_4) occur as intermediates.[6]

In 1964, the first purely inorganic complexes with N_2 as a ligand have been prepared. These simple complexes serve as model species to study the activation of N_2 through complex formation. In the meantime, this topic has been researched intensively so that hundreds of dinitrogen complexes are known.

9.2 N_2 as Complex Ligand

The nitrogen molecule is isosteric to CO and isoelectronic to $[NO]^+$ and $[CN]^-$ of which numerous transition complexes are known:

5 Nitrogenases are a class of enzymes, which catalyzes the reduction of N_2 to NH_3. They typically contain clustered reaction centers of sulfide-bridged Fe and Mo atoms (FeMo cofactor, FeMoco), in turn bonded to the protein matrix; see Y. Hu, B. Schmid, M. W. Ribbe, *Encycl. Inorg. Chem.* **2005**, *6*, 3621. F. Barriere, ibid. **2005**, *6*, 3637. B. M. Barney et al., *Dalton Trans*. **2006**, 2277.

6 D. Sellmann et al., *Chem. Eur. J*. **2004**, *10*, 819.

It was therefore to be anticipated on simple grounds of analogy that N_2 should also coordinate to transition metal centers to form stable complexes. Indeed, more than 250 dinitrogen complexes have been prepared with almost all transition metals including lanthanides.[7] Various structural motifs are observed with between one and three molecules of N_2 per central atom as well as multinuclear complexes in which the nitrogen molecule adopts a bridging position. Although the HOMO of N_2 is mainly nonbonding with considerable electron density at the ends of the molecule, the energy difference to the two degenerate π bonding orbitals is relatively small (Section 2.4.3), which allows for the variable coordination modes:

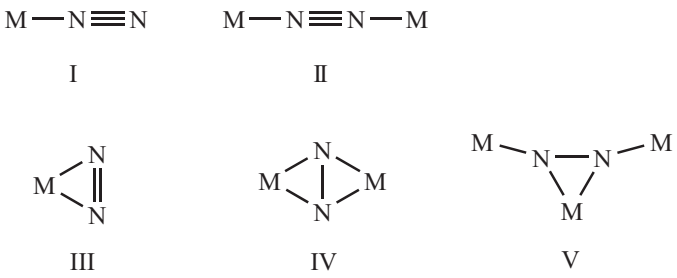

The most common coordination mode for both mononuclear and bridging N_2 ligands is *end-on* as in I and II, but numerous *side-on complexes* have been prepared as well (III and IV). Mixed bridging coordination modes as in V are observed less frequently. The syntheses of the N_2 complexes will be explained on a few examples:

(a) Addition of N_2 to a complex with or without ligand exchange:

$$[Ru(H_2O)(NH_3)_5]Cl_2 + N_2 \longrightarrow [Ru(N_2)(NH_3)_5]Cl_2 + H_2O$$

In many cases, a precursor complex is reduced in an N_2 atmosphere. This method has the largest scope as it also comprises the use of the many examples of dihydrido and dihydrogen complexes, which typically liberate H_2 to be replaced by N_2 reversibly.[8]

(b) Oxidation of hydrazido complexes with H_2O_2:

$$[CpMn(CO)_2(N_2H_4)] + 2\,H_2O_2 \xrightarrow[Cu^{2+}]{-40^\circ C} [CpMn(CO)_2(N_2)] + 4\,H_2O$$

(c) Reduction of metal salts with hydrazine, which itself is oxidized to N_2:

$$2\,[NH_4]_2[OsCl_6] + 3\,N_2H_4 + 14\,NH_3 \xrightarrow[H_2O]{100^\circ C} 2\,[Os(N_2)(NH_3)_5]Cl + 10\,[NH_4]Cl$$

---

7 M. Hidai, Y. Mizobe, *Chem. Rev.* **1995**, *95*, 1115. H.-J. Himmel, M. Reiher, *Angew. Chem. Int. Ed.* **2006**, *45*, 6264. Y. Ohki, M. D. Fryzuk, *Angew. Chem. Int. Ed.* **2007**, *46*, 3180. P. J. Chirik et al., *Organometallics* **2007**, *26*, 2431.

8 J. Ballmann, R. F. Munhá, M. D. Fryzuk, *Chem. Commun.* **2010**, *46*, 1013.

(d) Thermolysis of azido complexes:

$$[Ru(H_2O)(NH_3)_5]^{2+} \xrightarrow[-H_2O]{+\,[N_3]^-} [Ru(N_3)(NH_3)_5]^{+} \xrightarrow[-\,½\,N_2]{\Delta T} [Ru(N_2)(NH_3)_5]^{2+}$$

(e) Azotation of an ammine complex with nitrous acid:

$$[Os(N_2)(NH_3)_5]Cl_2 + HNO_2 \longrightarrow [Os(N_2)_2(NH_3)_4]Cl_2 + 2\,H_2O$$

The bonding situation in N_2 complexes has been clarified by structure analyses, spectroscopic observations (infrared and RAMAN spectra[9]) and theoretical studies on model compounds.

In the mononuclear *end-on* complexes the bonding of the N_2 ligands to the metal center largely corresponds to that of CO in carbonyl complexes. The M=N=N moiety is essentially linear. In contrast to CO, however, bridging between two metal atoms typically involves the coordination of both atoms of the N_2 molecule.

The M–N interaction formally consists of one dative σ bond by the nitrogen lone pair to the metal center and one or even two dative bonds of π symmetry from metal to antibonding acceptor orbitals at nitrogen (*backdonation*); see Figure 9.1.

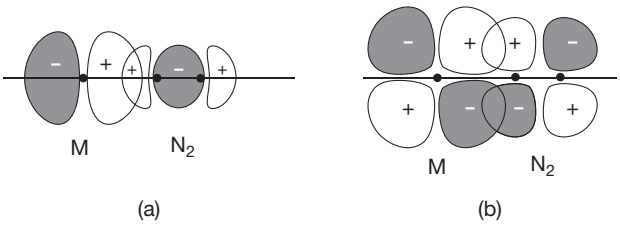

Figure 9.1: The covalent bond between a metal atom (M) and an N_2 molecule in dinitrogen complexes with *end-on* coordination. (a) σ bond through overlap of the HOMO of N_2 ($3\sigma_g$–$\lambda 2\sigma_g$) with a σ atomic orbital of M; (b) π backbonding through overlap of an occupied *d* AO of M with the LUMO of N_2 ($1\pi_g$).

The σ bond is formed by overlap of the highest occupied σ MO ($3\sigma_g$) of the N_2 molecule and an unoccupied σ orbital of the central atom (Figure 9.1a). Through this bond, electron density is transferred from the ligand to the metal center. In order to partially compensate for this additional charge, electron density is "returned" to the ligand through other orbitals, namely the occupied *d* orbitals at the metal of π

9 While the NN stretching vibration of N_2 is IR-inactive in the gas phase, it is active in terminal *end-on* bonded N_2 ligands as the bonding to the metal induces a dipole moment. In symmetrically bridging *end-on* coordination modes it is therefore once more inactive, but observable in the RAMAN spectrum, which is a manifestation of the complementariness of IR and RAMAN methods.

symmetry with the lowest unoccupied orbitals of the N_2 ligand, the two antibonding $\pi^\star$ orbitals (Figure 9.1b). Due to the rotational symmetry of the M=N=N unit, π bonding can occur in two perpendicular planes if sufficient *d* electrons are available at the metal, and the nature of the remaining ligands is compatible with it. While this π backbonding strengthens the metal–ligand interaction, it also weakens the NN bond due to the antibonding nature of the accepting orbitals at the ligand. This is clearly manifest in the internuclear distances d_{NN}, which are larger than in case of free N_2 in most complexes (up to 155 pm vs. 110 pm in N_2). Consequently, the excitation of the NN stretching requires less energy (lower force constants) and the corresponding vibrations occur at higher wavenumbers.

The backbonding is of decisive importance for the stability and reactivity of N_2 complexes of transition metals. Its occurrence necessarily requires that the metal be in a low oxidation state so that its *d* orbitals are occupied by electrons. Upon oxidation of the metal, the N_2 ligand is eliminated. Similarly, some N_2 complexes liberate nitrogen when treated with CO (irreversible ligand displacement). This indicates a higher stability of carbonyl complexes and explains why so far no room temperature-stable binary complexes of the type $M(N_2)_n$ could be obtained that would correspond to the homoleptic metal carbonyls such as $Ni(CO)_4$ and $Fe(CO)_5$. Only at low temperatures such complexes have been detected spectroscopically.

The thermal stability of N_2 complexes varies significantly. Some decompose only at temperatures higher than 300 °C. As the weakening of the NN bond necessarily entails its activation for reactions, the reactivity of these complexes is subject to extensive studies, but so far has not led to any applications in practice. The protonation of coordinated N_2 to NH_3 succeeds in selected cases only. Through other approaches, however, complexes have been prepared with N_2H_2 and N_2H_4 ligands, which are plausible intermediates during the enzymatic reduction of N_2 to NH_3.

Spectroscopic investigations show that bulk metals can also bind N_2 at their surfaces and it has been proven that formation of a bond between metallic iron and molecular N_2 is the initial step of the industrial NH_3 synthesis (Section 9.4.2).

9.3 Bonding in Nitrogen Compounds

The lightest element of Group 15, nitrogen has five valence electrons of $2s^2p_x^1p_y^1p_z^1$ configuration at its disposal (^4S ground state). The valence shell does not contain *d* orbitals and ab initio calculations show that the next unoccupied levels 3*s* and 3*p* are much higher in energy and therefore do not contribute to any significant extent to the covalent bonds in nitrogen species.[10]

10 Note that analogous conclusions also apply to elements of the higher rows of the Periodic Table, that is, phosphorus, arsenic, antimony and bismuth.

As all other nonmetals of the second row, the N atom formally seeks to acquire the electronic configuration of neon. This is achieved through formation of three covalent bonds or the corresponding ions as the following examples illustrate:

Covalent: NH_3, NF_3, NCl_3
Mixed: $[NH_2]^-$ in KNH_2, $[NH]^{2-}$ in Li_2NH, $[N_2]^{2-}$ in SrN_2
Ionic: N^{3-} in Li_3N and in Ba_3N_2

The coordination number of the N atom in its compounds can vary between one (N_2) and eight (Li_3N).

Similar to its neighbors in the Periodic Table (carbon and oxygen), nitrogen shows a pronounced tendency to engage in multiple bonding. Suitable partners for strong π bonds are predominantly the atoms C, N and O, as well as to a lesser extent Si, P and S:

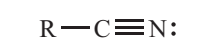
covalent cyanides and cyano complexes


dinitrogen


nitrosyl cation


sulfur nitride trifluoride

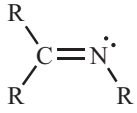
covalent imides

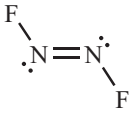
difluorodiazene


nitronium cation

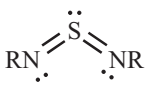
sulfur dimides

A more detailed analysis of the bonding in the two sulfur species can be found in Section 12.13. Apart from the three unpaired 2*p* electrons, the nonbonding electron pair at nitrogen can also be recruited for covalent bonding.[11] Formally, such bonds are coordinative (dative) in nature as, for example, in the ions $[NH_4]^+$, $[NF_4]^+$ and $[N_2H_6]^{2+}$ as well as in the following species:

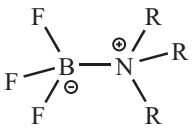
boron trifluoride-trialkylamine

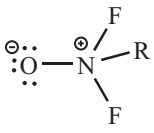
trifluoro-aminoxide

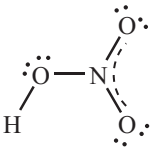
nitric acid


tetramminecopper ion

11 Many nitrogen species, inorganic and organic, are suitable N-donor ligands toward transition metals due to the nonbonding electrons at the N atom; see D. A. House, *Encycl. Inorg. Chem.* **2005**, *1*, 210.

Compounds of the type R_3N (R: any residue) typically show a pyramidal coordination at the nitrogen center and usually act as LEWIS bases. The interaction energy toward LEWIS acids strongly depends on the substituents R. For example, in case of NH_3, it amounts to 82.0 kJ mol^{-1} for coordination to SO_3. Due to inductive electron donation of methyl groups, the value is almost doubled to 151.9 kJ mol^{-1} for NMe_3 and with 25.5 kJ mol^{-1} much smaller for the electron-poor nitrogen atom of pyridine. These energies correlate with the energy difference between the donor orbital of the base and the virtual acceptor orbital (LUMO) of SO_3 (see Section 2.5). Unsurprisingly, trimethylamine is a stronger base than ammonia toward BCl_3 and to $AlCl_3$ as well.

Typically, the bond angles of amines NR_3 are close to the tetrahedral angle (see Table 2.5). Molecules of this sort can undergo *pyramidal inversion*, which is an intramolecular rearrangement leading to an equivalent (and energetically degenerate) conformation with the N atom on the other side of the plane defined by the three nearest substituent atoms as exemplified by the case of NH_3 in the following:

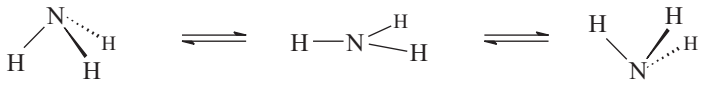

This reaction is characterized by a symmetrical double minimum potential: the planar transition state is of D_{3h} symmetry.[12] The planarization is the continuation of the symmetric deformation vibration of the NH_3 molecule. In case of NH_3 and the methylamines Me_xNH_{3-x} (x = 0–3), the energy barriers (E_a) between the two conformations have the following values: 24 kJ mol^{-1} (NH_3), 20 kJ mol^{-1} ($MeNH_2$) and 31 kJ mol^{-1} (Me_3N). Therefore, even at room temperature, rapid inversion is observed. In case of NH_3, inversion occurs even at 0 K due to a *tunnel effect* of the hydrogen atoms, that is, the molecule is dynamic at all temperatures.[13] The height of the barrier for derivatives of ammonia depends on the nature of the substituents R. Electronegative groups lead to an increase in E_a (e.g., NF_3: about 300 kJ mol^{-1}). Amines with three different substituents ($R^1R^2R^3N$) are chiral so that the above-mentioned conformers are image and mirror image (*enantiomers*). The separation of the enantiomers, however, is impossible unless the rapid racemization at nitrogen is prevented, for instance, by connecting all three substituents.

12 A planar transition state is also involved in the inversion of PH_3, AsH_3, NF_3 and NCl_3. In contrast, PF_3, PCl_3, PBr_3 and the other halides of heavier pnictogens invert through a T-shaped transition of C_{2v} symmetry (cf. the structure of ClF_3); P. Schwerdtfeger, P. Hunt, *Adv. Mol. Struct. Res.* **1999**, *5*, 223.

13 In crystalline NH_3, however, all hydrogen atoms are engaged in hydrogen bonds to adjacent molecules; see Section 5.6.2.

Some derivatives of ammonia are planar at the N atom instead of pyramidal. An example is trisilylamine $N(SiH_3)_3$ with a planar NSi_3 scaffold:

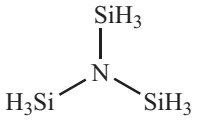

$d_{NSi} = 173.4$ pm
$\text{angle}_{SiNSi} = 119.7°$

The planar geometry at nitrogen can be explained by partial delocalization of the nonbonding electron pair into vacant orbitals at the silyl groups (dative π bond). In principle, the *3d* orbitals at the silicon atoms have the appropriate π symmetry, but the antibonding σ* MOs of identical symmetry are much lower in energy and can accept electron density in the sense of a so-called *negative hyperconjugation*. This backdonation entails the following consequences:

(a) Increase of the bond angles at nitrogen,
(b) strengthening of the SiN bonds,
(c) decrease of the LEWIS basicity of the N atoms and
(d) weakening of the SiH bonds.

π-Bonds such as these always occur if an electron acceptor is directly adjacent to the donor and the energy difference between the HOMO of the donor fragment and the LUMO of the acceptor fragment is not too large (Section 2.5). The delocalization of the nitrogen electrons into the acceptor orbitals does not need to be very pronounced; it is more important that nonbonding electron density from the nitrogen atom be employed in π symmetric interactions. Simple inductive withdrawal of electrons by strongly electronegative substituents alone does not lead to a planar geometry. In line with that, the radical cation $[NH_3]^{\bullet+}$ is planar, while the molecule NF_3 is not (angle FNF = 102.2°).

Further examples of compounds with such dative π bonds are:

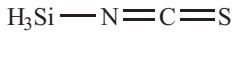

$\text{angle}_{SiNC} = 180°$

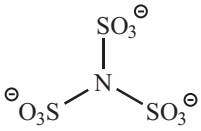

$\text{angle}_{SNS} = 120°$

In the hydrazine derivatives $(H_3Si)_2N–N(SiH_3)_2$, $(Me_3Si)_2N–N(SiMe_3)_2$ and $(Cl_3Si)_2N–N(SiCl_3)_2$, the geometry at the N atoms is likewise planar. The steric repulsion of large substituents can also result in planar geometries at the nitrogen center. For example, this is the case for the perfluorinated amines $(C_2F_5)_3N$ and $(C_3F_7)_3N$.

In this context, it should be noted that similar backdonation effects are also known for oxygen (Section 11.2) and fluorine atoms (Section 13.4.5) so that nitrogen does not stand out in this regard. For the higher homologues of nitrogen, however, these π bonds are fairly weak (see Section 10.2), which disfavors planarization

and thus substantially increases the barrier of inversion. Therefore, the molecules $P(SiH_3)_3$ and $As(SiH_3)_3$ have pyramidal scaffolds at the pnictogen center. In the same vein, inversion barriers at phosphanes and arsanes are sufficiently high for the isolation of enantiomers of type $R^1R^2R^3E$.

The following nitrogen compounds show that the N atom can adopt all nine oxidation states between −3 and +5:

−3	−2	−1	0	+1	+2	+3	+4	+5
NH_3	N_2H_4	N_2H_2	N_2	N_2F_2	NO	NF_3	NO_2	N_2O_5

Mixed-valent compounds with N atoms in different oxidation states are, for example, the oxide N_2O_3 and nitramide $H_2N{-}NO_2$.

9.3.1 Bond Enthalpies and Formation Enthalpies

Due to the exceptionally large dissociation enthalpy of the N_2 molecule, the preparation of nitrogen compounds from the elements often requires considerable reaction enthalpies. Even the oxidation with dioxygen, which is exothermic for most other elements, is endothermic in this case:

$$\tfrac{1}{2}\,N_2 \;+\; \tfrac{1}{2}\,O_2 \;\rightleftharpoons\; NO \qquad \Delta H^\circ_{298} = 90.3\ \text{kJ mol}^{-1}\ (\text{NO})$$

Compounds with a positive standard formation enthalpy are referred to as endothermic, for example, the gaseous nitrogen oxides, the azides, hydrazine, S_4N_4 and NCl_3. These species are metastable at room temperature and tend to decompose spontaneously if the activation energies of decay reactions are sufficiently small (e.g., for AgN_3 and NCl_3) or if they are decreased by a catalyst (e.g., for N_2H_4 by Cu^{2+} ions). One of the reaction products of these decompositions is typically N_2. Exothermic nitrogen compounds are: NH_3, Li_3N, NF_3 and N_2F_4.

From these considerations follows that the reaction of two endothermic nitrogen compounds under formation of N_2 will liberate unusually large amounts of enthalpic energy. Therefore, such reactions are suitable for running rocket propulsion engines. For instance, the third stage of the European rocket “Ariane” uses unsymmetrical dimethyl hydrazine ($Me_2N{-}NH_2$) with liquid N_2O_4 as an oxidizing agent. Upon mixing of the two components, a spontaneous cold reaction occurs and – after ignition – combustion with a red flame to three extremely stable products:

$$Me_2N{-}NH_2\ (\text{l.}) \;+\; 2\ N_2O_4\ (\text{l.}) \longrightarrow 3\ N_2 \;+\; 2\ CO_2 + \;4\ H_2O$$

During this reaction, −1667 kJ are liberated per mol of dimethylhydrazine under standard conditions! This huge amount of energy leads to tremendous heating of the gas mixture and thus to the strong propulsion of the rocket.

Single bonds between two nitrogen atoms as in hydrazine are weak in most cases. The weakness of these bonds is inter alia due to the repulsion between the nonbonding electron pairs in the structural motif >N–N< (see Section 4.2.2 for more details). The same effect occurs in bonds of types >N–O– and –O–O–. As a consequence of this bond weakening, hydrazine N_2H_4 and hydroxylamine NH_2OH are thermally much less stable than, for instance, ethane C_2H_6. Higher homologues of these compounds such as triazane ($H_2N–NH–NH_{2)}$ and hydroxyl hydrazine ($H_2N–NH–OH$) could so far not be isolated in pure form. These compounds can be expected to be of similar low stability as observed for H_2O_3 and H_2O_4, the higher homologues of hydrogen peroxide (Section 11.3.4). The lower NN single bonding enthalpy is also responsible for the occurrence of nitrogen as triply bonded N_2 rather than tetrahedral N_4 (as in P_4) or polymeric N_x in analogy to red or black phosphorus (P_x). Only at very high pressures, N_2 is transformed into a polymeric structure corresponding to black phosphorus.[14]

The salts of N_2H_4 with the dication $[N_2H_6]^{2+}$ are considerably more stable than hydrazine. Due to protonation, the NN bond in these salts does not suffer from the repulsion of the lone electron pairs anymore. The two positive charges are delocalized over the six H atoms, because their electronegativity is smaller than that of nitrogen. For the same reason, triazanium salts with the cation $[H_2N–NH_2–NH_2]^+$ can be prepared, while triazane N_3H_5 itself is unknown. Triazanium salts that are doubly organosubstituted at the central nitrogen atom are even rather stable. Stabilization of NN single bonds by inductive substituent effects is also possible as it accounts for partial positive charge at the nitrogen centers through hyperconjugation and thus a reduction of lone pair repulsion (Figure 9.2).

An example for negative hyperconjugation is provided by hexakis(trifluoromethyl)tetrazane, $R_2N–NR–NR–NR_2$ (R = CF_3), a colorless liquid of considerable thermal stability. The N_4 chain of the compound is helical in the gas phase with a torsion angle of 95° at the central NN bond; the coordination at the N atoms is planar, which can be explained by the delocalization of the nonbonding electron pairs into the σ* MOs of the CF bonds.[15] Another possibility for stabilizing longer nitrogen chains is the use of aromatic substituents in conjunction with the presence of one or more N=N *double bonds*. In this regard, a few chain-like compounds are known, namely triazene ($PhN=N–NMe_2$), pentadiazene (PhN=N–NMe–N=NPh), hexadiazene (PhN=N–NPh–NPh–N=NPh) and octatriazene (PhN=N–NPh–N=N–NPh–N=NPh) as well as the cyclic phenylpentazole, which contains an almost planar, aromatic pentacycle:[16]

14 M. I. Eremets et al., *Nature Mater.* **2004**, *3*, 558.

15 J. M. Shreeve, H. Oberhammer et al., *Angew. Chem. Int. Ed.* **1995**, *34*, 586.

16 Solid state structure by X-ray diffraction: J. D. Wallis, J. D. Dunitz, *J. Chem. Soc. Chem. Commun.* **1983**, 910. The NN internuclear distances are in the range of 130–135 pm.

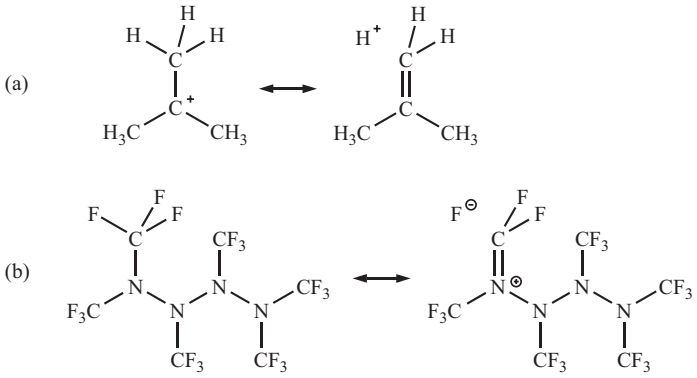

Figure 9.2: (a) Hyperconjugative stabilization of the *t*-butyl cation; (b) negative hyperconjugation in $(F_3C)_2N\text{-}N(CF_3)\text{-}N(CF_3)\text{-}N(CF_3)_2$.

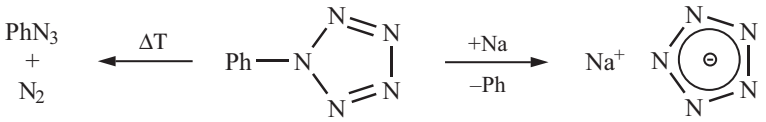

The thermal decomposition of phenyl pentazole leads to the formation of phenyl azide and N_2. Reduction of the same pentazole with sodium metal cleaves the phenyl group as a neutral radical leaving behind the cyclic planar pentazolate anion *cyclo*-$[N_5]^-$, which was detected by negative-ion mass spectrometry of a tetrahydrofurane solution after HPLC separation.[17] The treatment of a modified phenyl pentazole derivative with *meta*-chlorobenzoic acid in the presence of the iron(II) salt of the amino acid glycine yields the stable salt $[H_3O]_3[NH_4]_4Cl[N_5]_6$, the solid state structure of which was determined by single-crystal X-ray diffraction.[18] In this salt, *cyclo*-$[N_5]^-$ derives its stability from an extensive network of hydrogen bonds to the $[NH_4]^+$ and $[H_3O]^+$ counterions and the co-crystallized chloride. In addition, *cyclo*-$[N_5]^-$ has been described as the anion of the binary high-pressure phase $Li[N_5]$.[19]

In general, nitrogen-rich highly energetic molecules and salts are a cutting-edge research topic.[20] An example is the following salt, which contains a remarkable cation consisting of 11 N atoms in a chain:

17 Y. Haas et al., *Angew. Chem. Int. Ed.* **2016**, *55*, 13233.

18 B. Hu, M. Lu et al., *Science* **2017**, *355*, 374; see also B. Hu, C. Sun et al., *Angew. Chem. Int. Ed.* **2017**, *56*, 4512.

19 D. Laniel et al., *Inorg. Chem.* **2018**, *57*, 10685.

20 J. M. Shreeve et al., *Angew. Chem. Int. Ed.* **2006**, *45*, 3584. T. M. Klapötke et al., *Eur. J. Inorg. Chem.* **2015**, 2794. T. M. Klapötke, *Chemistry of High-Energy Materials*, 4th ed., de Gruyter, Berlin, **2017**.

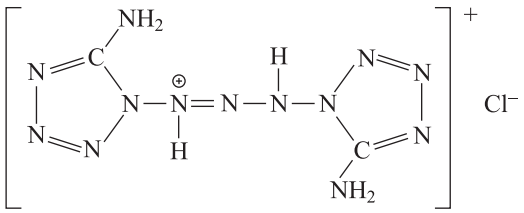

The compound is prepared in a multistep synthesis from diamino tetrazole by azotation with $Na[NO_2]$. It is stable up to approximately 100 °C; its explosive force corresponds to that of trinitrotoluene![21]

Some nitrogen species exist as stable *free radicals* at room temperature. Representatives of this class of compounds are the oxides NO and NO_2, the fluoride NF_2 and the dipotassium nitrogen oxide bis(sulfonate) (FREMY's salt) $K_2[ON(SO_3)_2]$, which is obtained from the reaction of NO with $K_2[SO_3]$. These compounds are *open-shell molecules* as their electronic configuration remains incomplete. The unpaired electrons are usually delocalized. All these radicals exist in equilibrium with the corresponding dimers, which are diamagnetic (*closed shell*) and dominate at lower temperatures and higher pressures (LE CHATELIER'S principle). The dissociation enthalpies determined from these equilibria vary significantly, but are without exception very small compared to the usual single bond enthalpies:

$$N_2O_2 \rightleftharpoons 2\ NO \qquad \Delta H^\circ_{298}: 8.7\ kJ\ mol^{-1}$$

$$N_2O_4 \rightleftharpoons 2\ NO_2 \qquad 57\ kJ\ mol^{-1}$$

$$N_2O_3 \rightleftharpoons NO + NO_2 \qquad 40.5\ kJ\ mol^{-1}$$

$$N_2F_4 \rightleftharpoons 2\ NF_2 \qquad 87\ kJ\ mol^{-1}$$

The lowest energy isomers of N_2O_2, N_2O_4, N_2O_3 and N_2F_4 contain NN bonds, which are relatively weak due to the delocalization of nonbonding electron density of the O and F atoms into the antibonding σ* MO of the NN bond (*negative hyperconjugation*). A list of NO internuclear distances is given in Section 4.3 (Table 4.4).

9.4 Nitrogen Hydrides

9.4.1 Introduction

Four volatile hydrides of nitrogen are known in pure form: ammonia (NH_3), hydrazine ($H_2N–NH_2$), hydrogen azide (HN_3) and tetrazene ($H_2N–N=N–NH_2$). In addition,

21 G. Cheng et al., *Angew. Chem. Int. Ed.* **2013**, *52*, 4875.

the salts ammonium azide $[NH_4][N_3]$ and hydrazinium azide $[N_2H_5][N_3]$ are stable binary NH compounds. The unstable diazene (HN=NH) occurs as transient intermediate.

Ammonia with its world production of about $1.5 \cdot 10^8$ t or 10^{13} mol per year is the by far most important nitrogen hydride, which is further processed to fertilizers to approximately 87%. Starting from NH_3, a whole variety of other nitrogen species is prepared. In its liquid state, NH_3 is a water-like solvent (Section 9.4.8), which is also used as a cooling medium for chilling purposes due to its large evaporation enthalpy.

9.4.2 Ammonia (NH_3)

Ammonia is produced in an exothermic reaction from the elements, which requires high temperatures (400–500 °C) and a catalyst for the activation of both the N_2 and H_2 molecules in order to achieve sufficiently high reaction rates (HABER–BOSCH process):

$$N_2 + 3\,H_2 \rightleftharpoons 2\,NH_3 \qquad \Delta H^\circ_{298} = -91.8\ \text{kJ mol}^{-1}(N_2)$$

Metallic α-iron, which is finely distributed on Al_2O_3, acts as a catalyst. The promoters CaO and K_2O increase the stability of the catalyst by inhibiting agglomeration (and thus deactivation) of the small iron particles.[22] Because of the volume reduction (negative reaction volume), the equilibrium can be shifted toward the formation of NH_3 by applying high pressures (20–40 MPa). Figure 9.3 shows the NH_3 equilibrium concentration as a function of pressure and temperature.

The separation of NH_3 from the unconverted H_2/N_2 mixture is achieved by condensation. In this manner, NH_3 is technically produced on a huge scale from synthesis gas and nitrogen from air. It is mostly employed for the production of fertilizers such as $[NH_4]_2[SO_4]$, $[NH_4][NO_3]$ and $(H_2N)_2CO$ (urea) as well as for the conversion to nitric acid. The first ammonia production plant based on the HABER–BOSCH process started operations at the BASF in Ludwigshafen-Oppau in 1913; in 1917 a second plant in Leuna near Merseburg (Germany) became operational.[23]

Today, the reaction mechanism of the ammonia synthesis is mostly understood.[24] Initially, both N_2 and H_2 molecules are adsorbed to the surface of the iron crystals, then chemically activated through electron transfer from the bulk metal to the ligands (see molecular complexes with H_2 and N_2 ligands: Sections 5.7.3 and 9.2) and cleaved to chemisorbed N and H atoms so that a mixed iron hydride and nitride is

22 K. H. Büchel, H.-H. Moretto, P. Woditsch, *Industrial Inorganic Chemistry*, Wiley-VCH, Weinheim, **2000**. Winnacker-Küchler, *Chemische Technik: Anorganische Grundstoffe*, Vol. 3, 5th ed., Wiley-VCH, Weinheim, **2005.**

23 FRITZ HABER was awarded the NOBEL Prize in chemistry in 1918, CARL BOSCH in 1931.

24 For his contributions to the understanding of the elementary steps during heterogeneous catalysis, GERHARD ERTL was awarded the NOBEL Prize in chemistry in 2007 (NOBEL lecture: *Angew. Chem. Int. Ed.* **2008**, *47*, 3524).

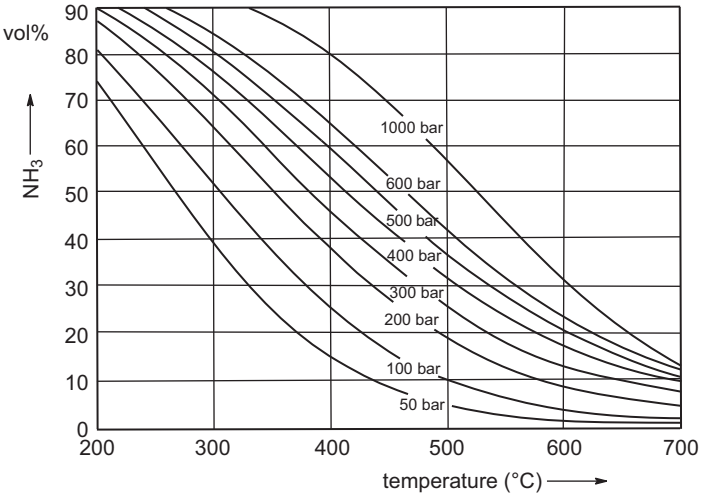

Figure 9.3: HABER–BOSCH process: equilibrium concentration of NH_3 in a mixture with H_2 and N_2 as a function of temperature and pressure with an initial molar ratio of H_2:N_2 = 3:1.

formed. Remarkably, the reactions of N_2 and H_2 with metallic iron to FeH and FeN groups are *exothermic* despite the very high dissociation enthalpies! The chemisorbed atoms then react with each other via surface-adsorbed NH and NH_2 radicals to NH_3 which is finally desorbed from the surface.

NH_3 is commercially available in liquid form in stainless steel cylinders (b.p. −33.4 °C). In the laboratory, it can also be produced from ammonium salts and strong bases:

$$[NH_4]Cl + NaOH \longrightarrow NH_3 + NaCl + H_2O$$

Concentrations of NH_3 in the air as little as 100 ppm cause eye irritations.

Upon heating, NH_3 partially decomposes into the elements. It is therefore also employed as hydrogenation and nitridation reagent as well as a hydrogen storage material. In the presence of air or O_2, ammonia is oxidized to N_2 and H_2O on heating. If a NH_3–air mixture is reacted at a Pt/Rh catalyst with very short contact times, however, the following reaction occurs preferentially:

$$2\,NH_3 + \tfrac{5}{2}\,O_2 \longrightarrow 2\,NO + 3\,H_2O \qquad \Delta H^\circ_{298} = -453\ \text{kJ mol}^{-1}$$

The indicated enthalpy refers to the net conversion according to the reaction equation; per mol NO, only 227 kJ is liberated. Industrially, NO is produced at a temperature of 800–940 °C and a pressure of 0.1–0.5 MPa in high yields. Upon cooling, it reacts with further O_2 to NO_2, which is hydrolyzed in the presence of air to give *nitric acid*:

$$2\,NO_2 + \tfrac{1}{2}\,O_2 + H_2O \longrightarrow 2\,HNO_3$$

The industrial production of nitric acid by the OSTWALD process[25] was introduced in Germany in 1915 at BASF. It made the import of Chile saltpeter redundant in the following years. Another industrial synthesis with NH_3 is the production of hydrogen cyanide, which requires very high temperatures:

$$CH_4 + NH_3 \longrightarrow HCN + 3\,H_2 \qquad \Delta H^\circ_{298} = 256\ \text{kJ mol}^{-1}$$

Through neutralization with sodium and potassium hydroxide, respectively, KCN and NaCN are produced from HCN (Section 7.8). All three compounds are extremely toxic.

Ammonia is a gas with a stinging smell and a very high exothermic solubility in water. Concentrated aqueous solutions contain up to 35 wt% of NH_3. The high solubility is due to the structural relationship between H_2O and NH_3 and their ability to form intermolecular hydrogen bonds (Section 5.6). These solutions mostly contain molecular NH_3 albeit in a solvated form. The electrical conductivity and the reaction of solutions as bases, however, indicate the following equilibrium:

$$NH_3 + H_2O \rightleftharpoons [NH_4]^+ + [OH]^-$$

The equilibrium is almost completely on the left-hand side. The base constant $K_b = c[NH_4]^+ \cdot c[OH]^- / c[NH_3]$ at 25 °C amounts only to $1.8 \cdot 10^{-5}$ mol L^{-1}. Therefore, even a relatively diluted 0.1 molar NH_3 solution is dissociated to just 1% at 25 °C; aqueous ammonia is a weak base.[26] $[NH_4][OH]$ does not exist as a stable compound, although at low temperature the crystalline hydrates $NH_3 \cdot {}^1\!/_2 H_2O$, $NH_3 \cdot H_2O$ and $NH_3 \cdot 2H_2O$ have been prepared, which do not contain ammonium cations but a network of hydrogen bonds.

Strong BRØNSTED acids such as HCl, H_2SO_4 or HNO_3 react with ammonia almost quantitatively to the corresponding ammonium salts, which are known in large numbers. The similar cationic radii of $[NH_4]^+$ and K^+ often lead to a similar solubility as the corresponding potassium salts. Ammonium salts contain the tetrahedral $[NH_4]^+$ ion, which is isoelectronic to $[BH_4]^-$ and CH_4, and dissociate completely in aqueous solution. As the conjugated acid of a weak base, the $[NH_4]^+$ ion is a weak BRØNSTED acid. Solutions of ammonium salts with neutral counteranions of strong acids are thus acidic:

$$[NH_4]^+ + H_2O \rightleftharpoons NH_3 + [H_3O]^+ \qquad pK_a(NH_4^+) = 9.26$$

$[NH_4]Cl$ is a side product of the SOLVAY process for the production of sodium carbonate (Section 7.7). The salts $[NH_4]_2[SO_4]$ and $[NH_4][NO_3]$ are employed as nitrogen

25 WILHELM OSTWALD (1853–1932), German researcher in catalysis, NOBEL prize in chemistry in 1909.
26 For strong nitrogen bases compare Section 5.6.4.

fertilizers[27] on a very large scale, while $[NH_4]Cl$ is inter alia used as electrolyte for dry batteries. Another very important nitrogen fertilizer is **urea**, which is industrially produced from NH_3 and CO_2 in a two-step process:

$$2\,NH_3 + CO_2 \longrightarrow [NH_4][NH_2COO] \qquad \Delta H^\circ_{298} = -117\ \text{kJ mol}^{-1}$$

$$[NH_4][NH_2COO] \longrightarrow (NH_2)_2CO + H_2O \qquad \Delta H^\circ_{298} = 16\ \text{kJ mol}^{-1}$$

During the first step at 170–190 °C and 13–20 MPa, ammonium carbamate is obtained from liquid ammonia and CO_2, which subsequently decomposes more slowly to urea and water. Urea is a colorless and odorless solid, which readily dissolves in water and is thus also employed as a de-icing agent for roads and runways of airports. The enzyme *urease* catalyzes the hydrolysis of urea to NH_3 and CO_2. With acids such as HNO_3 and oxalic acid, urea acts as a nitrogen base ($pK_b = 13.9$) forming insoluble 1:1 salts.

Depending on the conditions, ammonium nitrate decomposes on heating to H_2O, N_2, N_2O and NO_2. This decomposition can occur in an explosive manner. Catastrophic events with exploding fertilizer warehouses have occurred repeatedly: in 1921 in Ludwigshafen (Germany), in 2001 in Toulouse (France) and in 2013 in Texas. Therefore, the transport and application of $[NH_4][NO_3]$ is only allowed in diluted form. As a mixture with 6% of diesel fuel, $[NH_4][NO_3]$ is used in quarries as inexpensive explosive (tradename ANFO).

Under anhydrous conditions, the H atoms of the NH_3 molecule can be replaced by strongly electropositive metals. For example, gaseous NH_3 reacts with alkali metals to salt-like amides:

$$Li + NH_3 \xrightarrow{400^\circ C} Li[NH_2] + \frac{1}{2}\,H_2$$

On stronger heating, some amides are converted to imides initially and subsequently to nitrides with elimination of NH_3.

$$2\,M[NH_2] \longrightarrow M_2[NH] + NH_3$$

$$3\,M_2[NH] \longrightarrow 2\,M_3N + NH_3$$

In case of alkali and alkaline earth metals, these salts formally contain the ions $[NH_2]^-$, $[NH]^{2-}$ and N^{3-}. At contact with water, they are instantly hydrolyzed to NH_3 and metal hydroxides.

All nonmetals except most noble gases can form covalent element–nitrogen bonds. The number of corresponding compounds is far too large for a detailed discussion. The two most important reactions for the formation of covalent element–nitrogen bonds, however, are as follows:

27 Ammonium sulfate is a side product of the caprolactam synthesis (nylon) in large quantities.

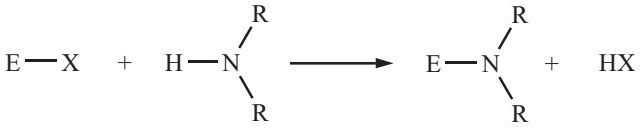

E = BR_2, CR_3, SiR_3, NR_2, PR_2, AsR_2, SR, SeR, Cl
X = F, Cl, Br, I

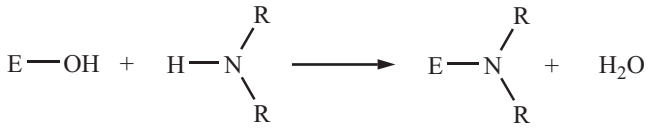

E = BR_2, NR_2, PR_2, SR, Cl

In this manner, many important compounds are produced from ammonia, amides or imides, which are described in the section concerning the respective element.

9.4.3 Hydrazine (N_2H_4)

Hydrazine[28] is one of the rare species with an NN single bond. Due to the reasons discussed in Section 4.1, this bond has a rather low dissociation enthalpy of 286 kJ mol^{-1}. Therefore, hydrazine is an endothermic compound (enthalpy of formation at 298 K: 95.4 kJ mol^{-1}), and its production and handling require certain precautions. In most cases, aqueous solutions with a maximum hydrazine content of 64 wt% are employed, the so-called *hydrazine hydrate*, which is an azeotropic mixture of composition $N_2H_4 \cdot H_2O$ and can be handled without the danger of explosion. In Germany and the USA, hydrazine is predominantly produced according to the BAYER process, which is a modification of the older RASCHIG process. Concentrated NH_3(aq) is mixed with dilute hypochlorite solution and acetone at 35 °C, whereupon a ketazine is formed:

$$NH_3 + Na[ClO] \longrightarrow NH_2Cl + NaOH$$

$$NH_2Cl + NH_3 + NaOH + 2\,Me_2CO \longrightarrow Me_2C{=}N{-}N{=}CMe_2 + NaCl + 3\,H_2O$$

Excess ammonia is distilled from the mixture followed by an acetone–water azeotrope at 95 °C. Subsequently, the ketazine is hydrolyzed with water under pressure at 180 °C:

$$Me_2C{=}N{-}N{=}CMe_2 + 2\,H_2O \longrightarrow N_2H_4 + 2\,Me_2CO$$

28 E. W. Schmidt, *Hydrazine and Its Derivatives*, 2nd ed., Vol. 2, Wiley, Chichester, **2001**.

The liberated acetone is separated by distillation and recycled, while the remaining N_2H_4 solution is concentrated to about the azeotropic mixture by evaporation. A higher N_2H_4 content of approximately 95% can be achieved by distillation from solid NaOH. Completely anhydrous hydrazine is produced by drying the concentrate with BaO, which reacts with water to $Ba[OH]_2$, or with $Ba[N_2]$ (barium pernitride), which is quantitatively converted to $Ba[OH]_2$, N_2H_4 and N_2 with water. The formation of hydrazine hydrate from the elements is exothermic:

$$N_2 + 2\,H_2 \xrightarrow{H_2O} N_2H_4(aq) \qquad \Delta_f G^\circ = -128\ \text{kJ mol}^{-1}$$

Pure N_2H_4 is a colorless, oily liquid (m.p. 2 °C; b.p. 114 °C), which strongly fumes in air. Upon heating or initiation by ignition, N_2H_4 explodes with tremendous force to yield N_2 and NH_3. The gaseous molecule N_2H_4 is similarly twisted as H_2O_2 with a torsion angle of $\tau = 91°$ between the C_2 axes of the two NH_2 groups (*gauche* conformation; molecular symmetry C_2). The molecule thus has a dipole moment of 1.84 D. The NN internuclear distance amounts to $d_{NN} = 144.7$ pm. During rotation about the NN bond, two energetic maxima have to be overcome: the *anti* and the *syn* conformations that correspond to barriers of 12.8 kJ mol^{-1} ($\tau = 180°$) and 41.8 kJ mol^{-1} ($\tau = 0°$), respectively.[29]

Hydrazine is miscible with water in any ratio. Both neat N_2H_4 and the aqueous solution are strongly toxic. In aqueous solution, N_2H_4 reacts as a reducing agent, as a weak base and as a complex ligand. Halogens are reduced to halides, Cu(II) salts to metallic copper via copper(I)oxide, silver and mercury salts directly to the metals. In air, N_2H_4 is slowly autoxidized. Characteristic reactions of N_2H_4 include the reduction of selenite and tellurite to elemental Se and Te. More recently, it has been shown that N_2H_4 is also capable of hydrogenating $(BNH)_n$ (borazylene), the residue of ammonia-borane dehydrogenation, back to H_3NBH_3 (see Section 6.10.2). In all these cases, N_2H_4 is oxidized to N_2. Finely divided metals decompose hydrazine hydrate catalytically, typically to mixtures of H_2, N_2 and NH_3. Rh/Ni nanoparticles (4:1) lead to the more selective formation of H_2 and N_2.

In water, N_2H_4 is a *bifunctional base*, from which two series of salts with the cations $[N_2H_5]^+$ and $[N_2H_6]^{2+}$ are derived ($pK_{b1} = 6.1$; $pK_{b2} = 15$). These ions are isoelectronic to the molecules CH_3NH_2 and C_2H_6, respectively. Salts containing $[N_2H_5]^+$ ions dissolve in water under simple dissociation, while those with $[N_2H_6]^{2+}$ suffer hydrolysis according to

$$[N_2H_6]^{2+} + H_2O \rightleftharpoons [N_2H_5]^+ + [H_3O]^+$$

The most important salts are hydrazinium sulfate $[N_2H_6][SO_4]$ and the hydrogen sulfate $[N_2H_5][HSO_4]$. The first protonation already transforms hydrazine into a weaker

29 J.-W. Son, H.-J. Lee, Y.-S. Choi, C.-J. Yoon, *J. Phys. Chem. A* **2006**, *110*, 2065.

base than NH_3 in water (pK_a: 7.94 vs. 9.26 for NH_3). Just like NH_3, it readily forms complexes with many metal ions, in which N_2H_4 acts as a bidentate N-donor ligand, for example, in $[M(N_2H_4)_2]Cl_2$ with M = Mn, Fe, Co, Ni, Cu or Zn.

Hydrazine hydrate is used for corrosion suppression in steam production plants and as a reducing agent. It also serves as a starting material for organic hydrazides, which are applied as insecticides, herbicides and pharmaceuticals.[30] The classical tuberculosis medication *Neoteben* is a hydrazine derivative:

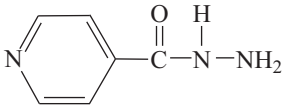

Anhydrous dimethylhydrazine is used as a rocket propellant with N_2O_4 as an oxidizing agent, for instance, in the European satellite launch vehicle Ariane 5 (Section 9.3). Since recently, hydrazine has also been discussed as a hydrogen storage medium.

A spectacular hydrazine derivative, which has been structurally characterized recently, is the bis(triphenylphosphane)azine:

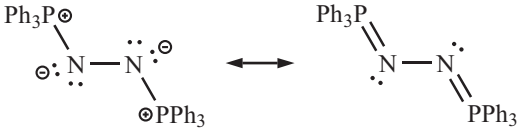

It forms garnet-red crystals, which decompose exothermically at the melting point of 184 °C into N_2 and Ph_3P. The NN internuclear distance of d_{NN} = 149.7 pm is slightly larger than in hydrazine (144.7 pm); the central PNNP unit is planar. The compound is formed by twofold deprotonation of the bis(phosphonium) salt $[Ph_3P(H)NN(H)PPh_3]Cl_2$ with $K[^tBuO]$.[31]

9.4.4 Diazene (Diimine), N_2H_2

The molecule HN=NH[32] is the parent compound of organic azo compounds, for example, of azobenzene (PhN=NPh). The diimine is extremely unstable (endothermic) and has only been detected in the gas phase at low partial pressures, in solutions as an intermediate and in solid matrices at temperatures below −165 °C. Metal complexes with N_2H_2 as a ligand have also been characterized. At standard conditions, N_2H_2 disproportionates to N_2H_4 and N_2 or decomposes to N_2 and H_2. Of the three planar isomers

30 *Chem. unserer Zeit* **2003**, *37*, 88–127 (three reviews).

31 C. Jones, G. Frenking et al., *Angew. Chem. Int. Ed.* **2013**, *52*, 3004.

32 D. Sellmann, A. Hennige, *Angew. Chem. Int. Ed.* **1997**, *36*, 276 and references cited therein.

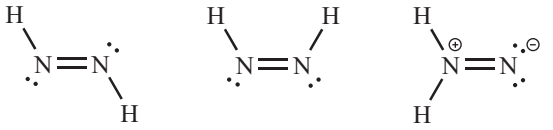

the *trans*-species is the most stable, the *cis*-isomer is by 22 kJ mol^{-1} higher in energy and the *iso*-species is the least stable. *trans*-N_2H_2 is generated by thermolysis of phenylsulfonyl hydrazide Ph–SO_2–NH–NH_2 at about 120 °C with subsequent condensation of the product at −196 °C. In contrast, the derivative methyldiazene (MeNNH) can be isolated in pure form.

The stable salts of diazene, the *diazenides* or *pernitrides*, for example, $Li_2[N_2]$, $Sr[N_2]$ and $Ba[N_2]$ with the anion $[N_2]^{2-}$ (d_{NN} in $Sr[N_2]$: 122.5 pm) are prepared from the elements at high pressure. In these reactions, nitrogen oxidizes the metal (and the metal reduces the N_2 molecule).[33] In contrast, the compounds $Os[N_2]$, $Ir[N_2]$ and $Pt[N_2]$ of identical stoichiometry are better described as *ionic hydrazides* than as diazenides as they formally contain the anion $[N_2]^{4-}$ with much longer internuclear NN distances almost corresponding to NN single bonds (d_{NN} in $Pt[N_2]$: 141 pm).[34]

Within the framework of highly energetic species, the heterocyclic compound 3,3′-azo-bis(6-amino-1,2,4,5-tetrazine) ($C_4N_{12}H_4$) has been prepared, which can formally be considered as a derivative of ammonia, hydrazine and diazene:

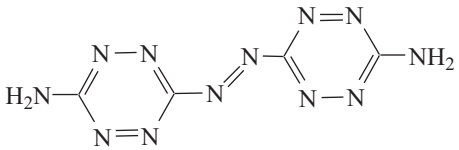

The C and N atoms of this molecule all reside in the same plane. The compound is thermally stable up to 250 °C and shows an extremely high formation enthalpy of 862 kJ mol^{-1}. In similar species, even chains of 8, 10 and 11 N atoms have been realized without interruption by C atoms (see also Section 9.3).[35]

9.4.5 Hydrogen Azide (HN_3) and Azides

Hydrogen azide is the parent compound of a large number of covalent and ionic azides. In contrast to the basic hydrides NH_3 and N_2H_4, HN_3 is a weak acid in water

33 R. Kniep et al., *Angew. Chem. Int. Ed.* **2001**, *40*, 547 and *Inorg. Chem.* **2001**, *40*, 4866 as well as *Angew. Chem.* **2002**, *41*, 2288. W. Schnick et al., *Angew. Chem. Int. Ed.* **2012**, *51*, 1873.
34 M. Wessel, R. Dronskowski, *J. Am. Chem. Soc.* **2010**, *132*, 2421.
35 S.-P. Pang et al., *J. Am. Chem. Soc.* **2010**, *132*, 12172. T. M. Klapötke, D. G. Piercey, *Inorg. Chem.* **2011**, *50*, 2732.

(pK_a = 4.64) and is thus also referred to as *hydrazoic acid*. In strongly acidic media, however, HN_3 is protonated to the cation $[H_2NNN]^+$.

Sodium azide is industrially produced by passing N_2O into a sodium amide melt at 190 °C:

$$2\ Na[NH_2] + N_2O \longrightarrow Na[N_3] + NaOH + NH_3$$

Another possibility is the oxidation of amide with molten nitrate in a ratio of 3:1 at 180 °C:

$$3\ Na[NH_2] + Na[NO_3] \longrightarrow Na[N_3] + 3\ NaOH + NH_3$$

The reaction mixture is separated into pure components by fractionate crystallization from water.

Aqueous HN_3 can be obtained from $Na[N_3]$ by ion exchange or by reaction with dilute H_2SO_4 and subsequent distillation. Both compounds are extraordinarily toxic. Water-free HN_3 is a clear, hygroscopic liquid of low viscosity (m.p. −80 °C, b.p. 36 °C), which readily decomposes into elements under explosion (endothermic formation enthalpy).[36] As in case of the covalent azides, the single bond HN–NN is cleaved in an endothermic reaction with liberation of dinitrogen. The carbene-analogous intermediate NH (*nitrene*) is in fact formed during the thermal decomposition of gaseous HN_3. Despite the thermodynamic preference for the triplet state (^{3}NH), its formation is spin-forbidden, which effectively shuts down this reaction channel kinetically.[37] In condensed phases, the predominantly formed high-energy singlet nitrene (^{1}NH) can be transformed with comparative ease into the lower energy triplet state by *spin crossover*. The nitrenes NR with R = H, alkyl or aryl are highly reactive and insert readily into element–hydrogen bonds. Photolysis of aqueous HN_3, for instance, yields hydroxylamine (H_2NOH) through insertion of nitrene NH into an OH bond of a H_2O molecule:

$$HN_3 \xrightarrow{h\cdot\nu} N_2 + NH$$
$$NH + H{-}OH \longrightarrow H_2N{-}OH$$

Aqueous solutions of up to 20 wt% HN_3 can be handled without the risk of explosion. They dissolve Zn, Fe, Mn and Cu with N_2 evolution, that is, HN_3 formally reacts as an oxidizing agent, which itself is reduced to NH_3 (and N_2) in the process. Ionic azides produced by salt metathesis reaction from $Na[N_3]$ often resemble the corresponding chlorides in appearance and solubility. Therefore, the anion $[N_3]^-$ is an example of a pseudohalide ion (Section 13.6).

---

36 In contrast, the salt $[H_2N_3][SbF_6]$ is not explosive and stable at 25 °C. It is prepared from HN_3, HF and SbF_5.

37 V. D. Knyazev, O. P. Korobeinichev, *J. Phys. Chem. A* **2010**, *114*, 839.

In contrast to the bent molecule HN_3 (C_s symmetry), the linear azide ion ($D_{\infty h}$ symmetry) contains two identical NN bonds:

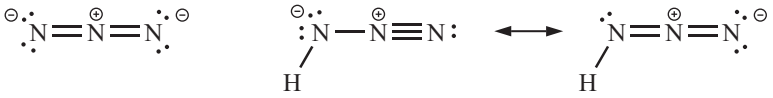

d_{NN} = 116 pm
angle$_{NNN}$ = 180°

d_{NN} = 124 and 113 pm
angle$_{NNN}$ = 171°
angle$_{HNN}$ = 109°

The ion $[N_3]^-$ is isoelectronic to CO_2, N_2O, $[NO_2]^+$ and $[OCN]^-$, and hence the description of the bonding situation in CO_2 (Section 2.4.6) can be adopted to the azide ion in principle. In the crystalline state, HN_3 forms a planar network of NH···N hydrogen bonds with two N atoms connected to each H atom. Only the central N atoms do not directly participate in this network. The reaction of fluorophosgene F–CO–Cl with $Na[N_3]$ yields $CO(N_3)_2$, which upon pyrolysis at low pressure decomposes to the purple, gaseous diazirinone of C_{2v} symmetry by elimination of N_2:[38]

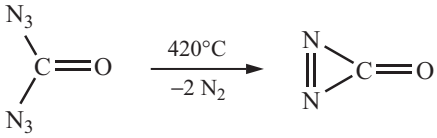

At 20 °C, N_2CO persists for several hours at reduced pressure but decomposes to N_2 and CO eventually.

While purely ionic azides decompose in a controlled manner to N_2 and the metal on heating, covalent azides as well as azides of the heavy metals often explode already on impact. Lead azide $Pb[N_3]_2$ is an important *explosive initiator*.

Azide ions are excellent ligands in metal and nonmetal complexes, which allows for the synthesis of extremely nitrogen-rich molecules and ions. Examples are the anions $[Te(N_3)_6]^{2-}$ and $[Nb(N_3)_7]^{2-}$. With large counterions such as $[PPh_4]^+$, the corresponding salts are relatively stable. Such compounds are also of interest within the context of high-energy fuels, because the decomposition to N_2 liberates large amounts of energy. This also applies to a series of other rather exotic materials with several NN bonds. For instance, HN_3 reacts with $[N_2F][SbF_6]$ (Section 9.5.1) at low temperatures and in the presence of HF to yield the salt $[N_5][SbF_6]$ containing the spectacular bent cation $[N_5]^+$ (C_{2v} symmetry):

38 X. Zeng et al., *Eur. J. Inorg. Chem.* **2012**, 3403.

$$HN_3 + [N_2F][SbF_6] \longrightarrow [N_5][SbF_6] + HF$$

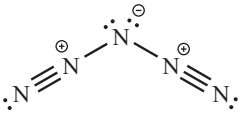

d_{NN} = 110 and 130 pm; angle$_{NNN}$ = 116° and 168°

This compound decomposes only when heated above 70 °C.[39] Numerous other salts with the pentanitrogen cation have been prepared through salt metathesis albeit many are unstable at 25 °C and extraordinarily sensitive to impact.

Of particular interest despite their facile decomposition are also the halogen azides X–N_3 (X = F, Cl, Br, I) that have been structurally characterized in recent times. Several synthetic approaches exist as shown by the following examples:[40]

$$[N_3]^- + [ClO]^- + 2\,H^+ \xrightarrow{-195 \text{ bis } -5\,^\circ C} Cl{-}N_3 + H_2O$$

$$Ag[N_3] + I_2 \xrightarrow{-5\,^\circ C} I{-}N_3 + AgI$$

These planar molecules form chained polymers in the crystal with the halogen atoms in bridging positions either interacting by halogen bonds (Cl···Cl) as in ClN_3 or through (almost) linear NXN units as in BrN_3 and IN_3. The NN internuclear distances are similar to those in HN_3.

9.4.6 Tetrazene(2) (N_4H_4)

The thermolysis of bis(trimethylsilyl)diazene yields – presumably via a *nitrene* intermediate – the dimer tetrakis(trimethylsilyl)tetrazene. By protic cleavage of the $SiMe_3$ substituents with trifluoroacetic acid at −78 °C, the parent tetrazene is obtained, which is stable only below −30 °C:[41]

$$(Me_3Si)_2N{-}N{=}N{-}N(SiMe_3)_2 + 4\,CF_3COOH \longrightarrow N_4H_4 + 4\,CF_3COOSiMe_3$$

N_4H_4 forms colorless subliming crystals with the molecules in the more favorable *trans*-conformation (C_{2h} symmetry):

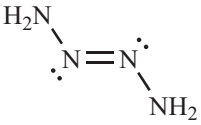

39 K. O. Christe et al., *Inorg. Chem.* **2001**, *123*, 6308.

40 S. Schulz, G. Jansen et al., *Angew. Chem. Int. Ed.* **2012**, *51*, 12850.

41 N. Wiberg, H. Bayer, H. Bachuber, *Angew. Chem. Int. Ed.* **1975**, *14*, 177; M. Veith, G. Schlemmer, *Z. Anorg. Allg. Chem.* **1982**, *494*, 7.

At 0 °C, N_4H_4 decomposes lively to N_2, $[NH_4][N_3]$ and $[N_2H_5][N_3]$.

9.4.7 Hydroxylamine (NH_2OH)

Hydroxylamine ($H_2N–OH$) is formally a derivative of ammonia, which, however, can also be regarded as a hybrid between hydrazine ($H_2N–NH_2$) and hydrogen peroxide (HO–OH). Hydroxylamine is technically prepared according to the following processes:

(a) Reduction of nitrite with sulfite at 0 °C followed by hydrolysis of the hydroxylamine disulfonate at 100 °C (modified RASCHIG process):

$$[NH_4][NO_2] + 2\,SO_2 + NH_3 + H_2O \longrightarrow [NH_4]_2[HON(SO_3)_2]$$

$$2\,[NH_4]_2[HON(SO_3)_2] + 4\,H_2O + 2\,NH_3 \longrightarrow [NH_3OH]_2[SO_4] + 3\,[NH_4]_2[SO_4]$$

The byproduct ammonium sulfate is used as a nitrogen fertilizer.

(b) Catalytic hydrogenation of NO in a sulfuric acid medium at 40–60 °C with a platinum or palladium catalyst (BASF process):

$$2\,NO + 3\,H_2 + 2\,H^+ \xrightarrow{Pt} 2\,[NH_3OH]^+$$

NH_2OH is a very weak base in water (pK_b = 8.2 at 25 °C), weaker than ammonia. With acids, it forms stable and highly water-soluble hydroxylammonium salts $[NH_3OH]X$, from which it can be recovered by reaction with NaOH or sodium methylate:

$$[NH_3OH]X + CH_3ONa \longrightarrow NH_2OH + CH_3OH + NaX$$

Neat hydroxylamine forms colorless, hygroscopic crystals of m.p. 32 °C, which slowly decompose even at room temperature; above 100 °C the reaction to NH_3, N_2 and H_2O proceeds in an explosive manner, N-oxides and H_2 are formed in traces. As an intermediate of the decomposition, ammonia oxide (H_3NO) is suspected, which appears to be preferentially formed in a bimolecular mechanism rather than the anticipated 1,2-hydrogen shift. The NO bond dissociation energy of H_3NO at 0 K was calculated as 250 kJ mol^{-1}.[42]

Hydroxylamine is commercially available as aqueous solution (50%). High-purity samples persist for as long as 1 year at 25 °C but suffer slow autoxidation. Aqueous hydroxylamine is employed in pharmaceutical industry and for the purification of silicon wafer surfaces.

42 M. S. Mannan et al., *J. Phys. Chem. A* **2010**, *114*, 9262. Amine oxides R_3NO are known with R = F and organic residues.

Hydroxylamine is a reducing agent, for example, toward Cu^{2+}, $[Hg_2]^{2+}$ and Ag^+; it is oxidized to N_2 in the process. With other (stronger) oxidizing agents, N_2O, NO, $[NO_2]^-$ or $[NO_3]^-$ can also be formed. Only very strong reducing agents such as Sn^{2+}, V^{2+} and Cr^{2+} reduce NH_2OH all the way to NH_3. The most important use of $[NH_3OH]^+$ salts is the synthesis of caprolactam by oxiamation of cyclohexanone and subsequent BECKMANN rearrangement in the presence of fuming sulfuric acid:

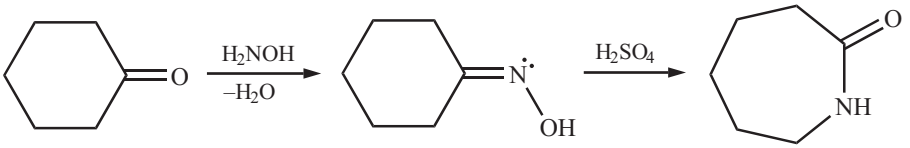

Caprolactam is ring-opened by the addition of sub-stoichiometric amounts of water. The resulting capronic acid polycondensates to chains of 6-polyamide (trade names: Perlon and Nylon). The initiation of the ring opening is also possible with anionic nucleophiles, which allows for the preparation of monodisperse 6-polyamide by *living ring-opening polymerization*.[43]

9.4.8 Water-Like Solvents

Water-like solvents are such liquids, which are similar to water in their solubilizing properties toward many polar inorganic and organic compounds. Moreover, they should be liquid in a broad temperature range and have a low viscosity in order to be useful as solvents in practice. The following compounds are thus considered as water-like solvents in their anhydrous and liquid state:

(a) Protic solvents:
NH_3, HF, H_2SO_4, HSO_3F, CH_3COOH, HCl, HCN
(b) Aprotic solvents:
SO_2, N_2O_4, BrF_3, $SeOCl_2$, $POCl_3$, NOCl as well as certain halides of As, Sb, Bi and Hg

Pure water-like solvents often show a certain low electrical conductivity. In contrast, solutions of various substances (mainly salts) in these solvents conduct electricity much more efficiently, which proved the presence of ions and led to the coinage of the term *ionizing solvent*. This term is even applied to those solvents in the list that do not show any autodissociation (e.g., liquid SO_2). Due to the preferred formation of ions in water-like systems, many reactions can be followed by conductometric or potentiometric measurements.

43 Review: J. Karger-Kocsis et al., *Polymers* **2018**, *10*, 357.

In the following, *liquid ammonia* as the most important and representative example will be discussed in detail. Under ambient pressure, ammonia melts at −77.7 °C (triple point) and boils at −33.4 °C.

9.4.8.1 Solubilities in Liquid Ammonia

The solubility of a salt in any solvent depends on the ratio of the lattice enthalpy to the sum of solvation enthalpies of the ions (Section 2.1.7). The solvation is strongly influenced by the relative permittivity or dielectric constant (ε) of the solvent, which is significantly differing between water (78.3) and liquid ammonia (16.9, both values at 25 °C). Therefore, the solubility of a given substance in water and ammonia can be very different.

For instance, the solubility of the potassium halides in NH_3 increases with the size of the anions in the series KF – KCl – KBr – KI, which corresponds to the situation in water. On the other hand, the solubility of silver halides in NH_3 changes in the same manner according to:

$$AgF < AgCl < AgBr < AgI,$$

which is precisely the opposite behavior as in water. At 25 °C, about 207 g of AgI dissolves in 100 mL of liquid NH_3 (molar ratio ca. 1:5)! This high solubility is due to the high solvation enthalpy of the cation Ag^+, which can be attributed to the pronounced stability of the ammine complex $[Ag(NH_3)_2]^+$. For the same reason, the addition of ammonia dissolves the otherwise insoluble AgCl (and at higher concentrations also AgBr) even in water.

The peculiar solubilities in ammonia allow for reactions that would otherwise not occur, for example, the following *metathesis*:

$$2\,AgCl + Ba[NO_3]_2 \underset{H_2O}{\overset{NH_3}{\rightleftharpoons}} 2\,Ag[NO_3] + BaCl_2$$

In this equilibrium reaction, $BaCl_2$ is the component with the lowest solubility in NH_3 and precipitates from solution. As a consequence, the reaction proceeds from left to right in NH_3 while the low solubility of AgCl in H_2O shifts the reaction the other way round. Salts of polyvalent anions such as sulfates, sulfites, carbonates, phosphates, oxides and sulfides are hardly soluble or even insoluble in liquid NH_3.

9.4.8.2 Autodissociation of Liquid Ammonia

Liquid ammonia is only marginally dissociated even at its boiling point:

$$2\,NH_3 \rightleftharpoons [NH_4]^+ + [NH_2]^- \qquad c\,(NH_4^+) \cdot c\,(NH_2^-) = 10^{-29}\ (-33°C)$$

The ion product is even smaller than that of ethanol (ca. 10^{-20})! Nonetheless, all substances that increase the concentration of ammonium ions in liquid ammonia are

acids, for example, all soluble $[NH_4]^+$ salts with highly solvated anions I^-, $[CN]^-$, $[SCN]^-$, $[NO_3]^-$, $[NO_2]^-$, $[N_3]^-$ and $[BF_4]^-$. These compounds correspond to the oxonium salts in water.

The acidic solutions of the ammonium salts share the property to dissolve base metals such as Mg or Al with evolution of hydrogen:

$$Mg + 2\,[NH_4]^+ \longrightarrow Mg^{2+} + 2\,NH_3 + H_2\uparrow$$

Just as in aqueous acids, magnesium silicide decomposes in NH_3 with formation of silane:

$$Mg_2Si + 4\,[NH_4]^+ \longrightarrow 2\,Mg^{2+} + 4\,NH_3 + SiH_4\uparrow$$

Compounds that increase the concentration of amide anions in ammonia behave as bases. For this purpose, $K[NH_2]$ and $Ba[NH_2]_2$ are particularly suitable as $Na[NH_2]$ is insoluble and $Li[NH_2]$ and $Ca[NH_2]_2$ are only sparingly soluble in ammonia. These ionic amides correspond to the hydroxides in water.

Neutralization reactions occur between acids and bases, which – as in water – can be followed either by colored indicators or electrometrically. For example, the titration of the strong base $K[NH_2]$ with a $[NH_4]Cl$ solution yields the insoluble salt KCl:

$$[NH_4]^+ + Cl^- + K^+ + [NH_2]^- \longrightarrow KCl\downarrow + 2\,NH_3$$

The equivalence point is characterized by a minimum in electrical conductivity.

9.4.8.3 Ammonolysis

Many nonmetal halides react with dry ammonia under condensation. This applies even to liquid ammonia. For instance, BCl_3 reacts at temperatures well below 0 °C according to:

$$BCl_3 + 6\,NH_3 \longrightarrow B(NH_2)_3 + 3\,[NH_4]Cl$$

Boron triamide is a weak, that is, hardly dissociated base in the ammonia system. It is the analogue of orthoboric acid in the aquosystem, which in turn is formed during the hydrolysis of BCl_3. Under suitable conditions, sulfur (S_8) reacts with liquid NH_3 in a preparatively useful manner to heptasulfur imide:

$$S_8 + NH_3 \longrightarrow S_7NH + H_2S$$

9.4.8.4 Solvated Electrons in Liquid Ammonia

The most remarkable property of dry, liquid ammonia is without doubt its ability to dissolve certain metals to give blue (in higher concentrations bronze-colored)

solutions.[44] This particularly concerns the alkali and alkaline earth metals with their good (Li, Na, K, Ca) to very good (Cs) solubility. At −50 °C, between 0.19 and 0.43 mol, alkali metals are dissolved in 1 mol of NH_3. Upon evaporation of ammonia, the alkali metals are mostly recovered unchanged, while alkaline earth metals crystallize as hexammine complexes, for example, $Ca(NH_3)_6$.

At very low temperatures, also $Li(NH_3)_4$ has been prepared and structurally characterized. This bronze-colored and electrically conducting material (m.p. −184 °C) consists of nearly tetrahedral molecules in which a central Li^+ cation is coordinated by the N atoms of the four ammonia ligands. The unpaired electron resides in an *s*-type orbital (SOMO) that consists predominantly of the 2*s* and 3*s* AOs of lithium and the a_1-symmetric orbitals of the NH_3 ligands (see Figure 2.34). In other words, the spin density is delocalized over the entire molecule. Therefore, weak H···H bonds occur between the four NH_3 ligands of one molecule as well as between neighboring molecules, initiated by the unpaired electrons. As the distance between the lithium centers is larger than in bulk lithium metal, such compounds are sometimes referred to as *expanded metals*.[45] $Li(NH_3)_4$ can also be regarded as an *electride*, a term that will be explained later.

Apart from the dissolution of alkali and alkaline earth metals in liquid ammonia, other methods for the preparation of "solvated electrons" are the pulse radiolysis of neat liquid ammonia and the electrolysis of ammonia solutions of metal salts. In the latter case, the blue color is developed at the cathode. The metal solutions show a number of *common properties*, which are approximately independent of the employed metal. Both the blue and the bronze-colored solutions exhibit very good electrical conductivity and the charge carrier mobility is very high, that is, the solutions must contain ions, electrons or both. The conductivity of concentrated solutions is equal to that of neat metals such as sodium or mercury. Magnetic susceptibility measurements have revealed that the blue solutions are paramagnetic at low concentrations with one unpaired electron per dissolved metal atom. At increasing concentrations, the susceptibility decreases until diamagnetic behavior is reached (and a minimum in electrical conductivity). Upon further increasing metal concentration, paramagnetic behavior is observed once again. The explanation of these and other experimental findings discussed in the following assumes the *reversible ionization of the metal atoms*:

$$M + x\,NH_3 \rightleftharpoons M^+_{am} + e^-_{am}$$

On the one hand, this reaction is favored by the low lattice enthalpy and the relatively small ionization energy of the alkali and alkaline earth metals; on the other

44 J. L. Dye, *Progr. Inorg. Chem.* **1984**, *32*, 327; P. P. Edwards, *Adv. Inorg. Chem. Radiochem.* **1982**, *25*, 135.

45 R. M. Ibberson et al., *Angew. Chem. Int. Ed.* **2009**, *48*, 1435. E. Zurek, X.-D. Wen, R. Hoffmann, *J. Am. Chem. Soc.* **2011**, *133*, 3535.

hand, it benefits from the high solvation enthalpy of the cations. The common properties of the blue metal solutions are primarily attributed to "free" electrons solvated by ammonia [e^-_{am} or $e^-@(NH_3)_n$]. With rising concentration, however, ion pairs $[M_{am}]^+[e_{am}]^-$ are formed initially, followed by antiferromagnetic interactions between neighboring electrons resulting in so-called *bipolarones* ($e^-_{am} \cdot e^-_{am}$) with antiparallel spins and thus diamagnetism. In addition, solvated metal anions (*alkalide ions*) are formed, which are diamagnetic as well:

$$M_{am} + e^-_{am} \rightleftharpoons M^-_{am}$$

These reactions also account for the reduced electrical conductivity [at molar fractions of lithium <0.01 mol Li/mol(Li + NH_3)]. Above this concentration and up to 0.08 mol Li/mol (Li + NH_3), however, the conductivity rises by a factor of 10^4. While diluted Li/NH_3 solutions show properties of electrolyte solutions, the more concentrated solutions discussed below are more akin to liquid metals.

Information on the structure of solvated electrons (e^-_{am}) is obtained from measurements of the density and UV-Vis spectra of the solutions as well as from theoretical model calculations. The system Li/NH_3 is the easiest to model and thus the most thoroughly investigated.[46] The density of liquid NH_3 amounts to 0.68 g cm^{-3} at the boiling point; in contrast, the density of the metal solutions is considerably *lower*. For example, the density of a Li solution saturated at 19 °C is 0.477 g m^{-3}, which is the lowest density of all known liquids at that temperature! As the metal cations behave normally in these solutions, the reduction in density (in other words, the increase in volume) must be attributed to the solvated electrons. From precise measurements of the density the space requirement of solvated electrons was estimated to be 94 mL mol^{-1}. This is a much larger value than determined, for instance, for the large iodide ion in liquid ammonia.

This remarkable finding is interpreted as a sign for the presence of large cavities around the solvated electrons, which are formed as a consequence of the COULOMB repulsion with the valence electrons of the NH_3 molecules. The best agreement with experiments is achieved if five to eight NH_3 molecules are attributed to each electron. The inner surface of the cavities is formed by hydrogen atoms of ammonia carrying a partial positive charge; the NH bonds point toward the inside of the cavity. The radius of the cavity can be estimated to 300–340 pm on the basis of the density of the metal solutions and the absorption spectra (Figure 9.4). Notably, the solvated electron does not seem to occupy the center of this cavity, but a SOMO of the tetraammine lithium complex $Li(NH_3)_4$ instead, which is derived from the antibonding MOs of the NH bonds of the cluster (the LUMOs of individual NH_3 molecules). The delocalized electron thus connects the four NH_3 molecules by many but weak H···H interactions. This novel type of HH bonds is formed at the expense of the otherwise present NHN

46 E. Zurek, P. P. Edwards, R. Hoffmann, *Angew. Chem. Int. Ed.* **2009**, *48*, 8198.

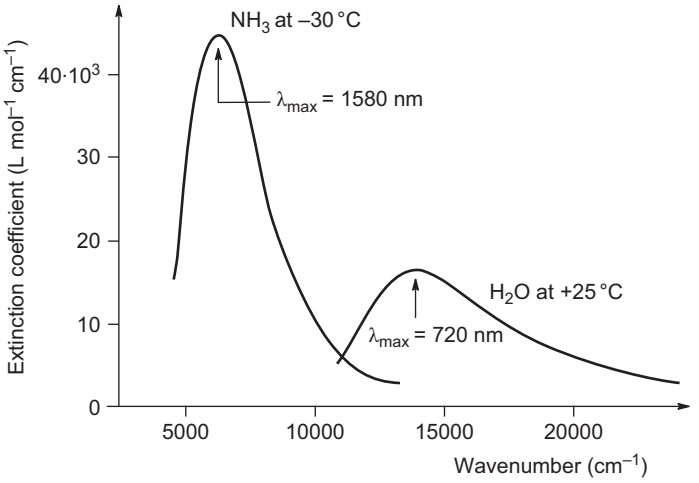

Figure 9.4: Absorption spectra of solvated electrons in liquid ammonia (left) and in water (right).

hydrogen bonds between the ammonia molecules; both types of bonds show comparable strength. The calculated absorption spectrum of $Li(NH_3)_4$ together with that of (e^-_{am}) reproduces the experimentally determined spectrum (Figure 9.4).

The absorption spectrum of potassium in liquid NH_3 consists of a single broad band at 1580 nm, which tails into the visible region with the flank at shorter wavelengths and thus accounts for the blue color. The idea of cavities in the liquid phase gains support from the solid-state structure of the similarly blue *electrides* in which the "free" electrons are apparently hosted in cavities of the crystal structure (see below).

The concentrated metal solutions exhibit a high reflectivity and therefore metallic luster. At molar fractions of >0.10 mol Li/mol(Li + NH_3) the solvated electrons indeed behave just like a free electron gas. Such concentrated solutions are obtained from the more dilute solutions by solvent evaporation or by cooling. In the latter case, phase separation occurs into a more concentrated (but specifically lighter!) phase and a more dilute (but heavier) blue solution. Saturation is reached at about 0.2 mol Li/mol(Li + NH_3), which roughly corresponds to the formula $Li(NH_3)_4$. The radicals couple their spin antiferromagnetically at high concentrations so that only weak if any paramagnetism is detected.

Solvated electrons and alkalide ions were also isolated as crystalline compounds, which are stable at low temperatures.[47] For example, metallic sodium reacts with a solution of the cryptand 2,2,2-crypt[48] in $EtNH_2$ to golden-yellow crystals

47 J. L. Dye et al., *J. Am. Chem. Soc.* **1999**, *121*, 10666 and cited literature.

48 In the cryptand 2,2,2-crypt (or C222) two nitrogen atoms are connected by three identical oligoether bridges to $N(CH_2CH_2OCH_2CH_2OCH_2CH_2)_3N$. The crown ether 18-crown-6 consists of an 18-membered ring of six $–CH_2–CH_2–O–$ units.

of $[Na(2,2,2\text{-crypt})]^+Na^-$, in which the complexed cation does not have a very pronounced polarizing effect due to its size and therefore allows for the formation of *natride ions* (Na^-). The ^{23}Na-NMR spectra of such compounds show clearly separated signals for the ions Na^+ and Na^-! While alkalides are also known in case of K, Rb and Cs, the lightest alkali metal, lithium, does not form such anions. At least 40 crystalline alkalides have been structurally characterized, most of them with sodium.

If Cs metal is dissolved in a solution of a crown ether such as 18-crown-6 in dimethylether below −40 °C, the salt $[Cs(18\text{-crown-}6)_2]^+e^-$ is obtained upon concentrating the solution. Its crystal structure as well as optical and magnetic properties have been interpreted in the sense that the free electrons occupy cavities with a diameter of about 240 pm. Solid compounds with electrons as anions are called *electrides*.[49] In order for the alkalides and electrides to be persistent, the complex cations need to be as large as possible and in any case nonreducible. It is particularly remarkable that the crystal structures of $[Cs(18\text{-crown-}6)_2]^+Na^-$ and $[Cs(18\text{-crown-}6)_2]^+e^-$ are very similar. The lattice positions of the natride ions in the former are empty in the latter and provide the cavities for the electride anions e^-. In all likelihood, however, the electrons are delocalized about the H atoms of the crown ether that form the walls of the cavity.

9.4.8.5 Reactions of Solvated Electrons in Liquid Ammonia

The most important reaction of solvated electrons e^-_{am} is the so-called *amide reaction*, that is, the decomposition of metal ammonia solutions under formation of metal amide:

$$NH_3 + e^-_{am} \rightleftharpoons [NH_2]^- + \tfrac{1}{2}\,H_2 \qquad K_c = \frac{c\,(NH_2^-)\cdot p_{H_2}^{1/2}}{c\,(e^-_{am})}$$

This reaction is kinetically hindered, and the metal solutions are metastable. Upon longer standing or addition of a catalyst (Ni, Fe_3O_4, Pt), however, they decompose spontaneously with discoloration and hydrogen evolution.

The amide reaction is *reversible*: a $K[NH_2]$ solution in ammonia partially reacts with hydrogen at increased pressure (10 MPa) to e^-_{am} and NH_3, which is readily detected and quantitatively monitored by the intensity of the appearing blue color. By variation of pressure and temperature, the equilibrium constant $K_c = 5{\cdot}10^5$ kPa$^{1/2}$ (25 °C) and the reaction enthalpy $\Delta_r H°_{298} = -67$ kJ mol^{-1} of the amide reaction have been determined.

Solvated electrons are strongly reducing agents, which turn most nonmetals into monoatomic or polyatomic anions depending on the stoichiometry[50] (Table 9.1). Through evaporation of the solvent NH_3, the resulting salts can be isolated in pure

49 Review: J. L. Dye, *Acc. Chem. Res.* **2009**, *42*, 1564.

50 The polyatomic anions of Groups 14 and 15 are called ZINTL ions (see Section 8.4).

Table 9.1: Reactions of nonmetals with alkali metals in liquid ammonia.

Nonmetal	Metal	Reaction products
C_{60}	K, Rb	$M_3[C_{60}]$
P_4	Li–Cs	M_3P, $M_3[P_7]$, $M_3[P_{11}]$
	K	$K_3[P_3H_2]$
As	Na	$[Na(NH_3)_5]_2[As_4]$
	Cs	$Cs_3[As_7]$
O_2	Li	Li_2O, $Li_2[O_2]$, $Li[O_2]$
	Na	Na_2O, $Na_2[O_2]$
	K	$K[O_2]$, $K_2[O_2]$
	Rb	$Rb_2[O_2]$, $Rb[O_2]$
O_3	Li	$Li[O_3]\cdot 4\ NH_3$
S_8	K	K_2S, $K_2[S_2]$, $K_2[S_4]$
Se	K	K_2Se, $K_2[Se_2]$, $K_2[Se_3]$, $K_2[Se_4]$
Te	K	K_2Te, $K_2[Te_2]$

form or as the ammoniate in many cases. In organic synthesis, the reduction of benzene to 1,4-cyclohexadiene is achieved by alkali metals in liquid ammonia (BIRCH reduction).

On addition of water to the blue solutions of e^-_{am}, the reaction to H atoms occurs, which is described in the following section.

9.4.8.6 Solvated Electrons in Water

Solvated electrons can also be generated and detected in water, ice and many other media.[51] In liquid water, however, solvated electrons react much faster with the solvent than in ammonia, namely to hydroxide ions and hydrogen atoms:

$$e^-_{aq} + H_2O \longrightarrow [OH]^- + H$$

The half-life of this reaction is only $0.8\cdot10^{-3}$ s. It follows that electrons in water can only be observed for about 1 ms; the corresponding experiments thus require elaborate measuring technology. Hydrated electrons are formed on α-, β- or γ-irradiation of water according to the equation

$$H_2O \longrightarrow [H_2O]^+ + e^-_{aq}$$

51 (a) D. M. Bartels et al., *J. Phys. Chem. A* **2015**, *119*, 9148. B. Abel et al., *Phys. Chem. Chem. Phys.* **2012**, *14*, 22 and *Angew. Chem. Int. Ed.* **2011**, *50*, 5264. L. Turi, P. J. Rossky, *Chem. Rev.* **2012**, *112*, 5641. F. A. Gianturco et al., *Phys. Rep.* **2011**, *508*, 1. (b) S. Bauerecker, P. Jungwirth et al., *Angew. Chem. Int. Ed.* **2016**, *55*, 13019.

or by photochemical ionization of dissolved large anions such as iodide or hexacyanoferrate(II):

$$I^-_{aq} \xrightarrow{h\cdot\nu} I + e^-_{aq}$$

Due to the required very high irradiation intensity, pulsed methods are generally preferred (*pulse radiolysis*), either with beams of accelerated electrons or with a pulsed laser of 218 nm wavelength. Most electrons liberated from H_2O show energies below 10 eV and exist in a highly reactive, "pre-solvated" state for a very short time (<1 ps) before transforming into a more stable, tightly bonded and less reactive hydrate. The cation radical $[H_2O]^{\cdot+}$ reacts with another H_2O molecule to $[H_3O]^+$ and a hydroxyl radical $OH^{\cdot}$.

Hydrated electrons also occur as intermediates during chemical reactions. Examples for such reactions are the conversion of H atoms with alkaline solutions according to

$$H + [OH]^- \longrightarrow H_2O + e^-_{aq}$$

or the decomposition of sodium amalgam in water:

$$Na(Hg) \xrightarrow{H_2O} Na^+_{aq} + e^-_{aq}$$

If a drop of liquid sodium–potassium alloy is carefully placed from a syringe on the surface of liquid water in an inert atmosphere a similar reaction takes place and formation of hydrated electrons has been observed by their blue color originating at the interface between metal and water; the hydrogen gas produced simultaneously slows the reaction down and no explosion occurs. The reflection spectrum of the reaction mixture shows a minimum near 720 nm in accordance with Figure 9.4.[51b]

Evidence for the hydrated electrons e^-_{aq} can also be obtained by trapping with N_2O, which is reduced to N_2 in a characteristic manner:

$$N_2O + 2e^-_{aq} + H_2O \longrightarrow N_2 + 2\,[OH]^-$$

The absorption spectrum of electrons in water differs from that of the blue metal solutions in NH_3 mostly in the position of the longest wavelength absorption at 720 nm at 25 °C (see Figure 9.4). This absorption led to the discovery of hydrated electrons in 1962. The excitation energy for this optical transition amounts to 167 kJ mol^{-1} in H_2O versus 84 kJ mol^{-1} in liquid NH_3. With rising temperature, the maximum is shifted to the infrared region (1200 nm at 300 °C). The best agreement with experimental findings and theoretical calculations is achieved if a cage model is assumed of consisting between 4 and 6 water molecules forming the walls of the cage for the hydrated electron. In analogy to the situation in NH_3, the electron formally resides in a spherical orbital, which is formed from the antibonding MOs of

the adjacent OH bonds. Consequently, these bonds are weakened as manifest in the redshift of the OH stretching vibration by about 200 cm^{-1}. The effective ionic radius of hydrated electrons has been estimated to approximately 240 pm. The vertical ionization energy[52] of the electron was determined by photoelectron spectroscopy to 3.4 eV. In case of dilute alkali metal–ammonia solutions this energy is only 1.27 eV.

The redox potential of hydrated electrons against the standard hydrogen electrode is –2.87 V. Therefore, they are *very strong reducing agents*, which reduce almost all inorganic compounds except for the alkali and alkaline earth metal cations and the halide anions. Selected examples are shown in Table 9.2. One can distinguish between simple or dissociative electron capture. All reactions proceed extremely rapidly. For example, the rate constants for the bimolecular reactions of e^-_{aq} with O_2, CO_2 or N_2O are within the order of 10^{10} L mol^{-1} s^{-1}. Therefore, even traces of these species diminish the lifetime of e^-_{aq} considerably. In strongly acidic solutions, e^-_{aq} is protonated to H atoms, which can be generated and studied in this manner.

Table 9.2: Reactions of hydrated electrons with selected compounds.

Starting material	Primary reaction product	Secondary products
H	H^-	$H_2 + [OH]^-$
CO_2	$[CO_2]^-$	$[C_2O_4]^{2-}$
N_2O	$[N_2O]^-$	$N_2 + O^-$
$[NH_4]^+$	NH_4	$NH_3 + H$
$[NO_3]^-$	$[NO_3]^{2-}$	NO_2
Cu^{2+}	Cu^+	Cu^+
Zn^{2+}	Zn^+	$Zn + Zn^{2+}$
$[MnO_4]^-$	$[MnO_4]^{2-}$	$[MnO_4]^{2-}$

The prehydrated electrons are of particular importance in context of biological radiation damage, which is inter alia occurring during the radiation therapy of cancers with short-wave (“hard”) X-rays. For example, the DNA can be damaged when the electron enters a strongly antibonding MO, which may result in the cleavage of the corresponding bond. This effect is desired in order to induce apoptosis (“cell death”) of malignant cells but is obviously detrimental for healthy tissue. Presolvated electrons are particularly effective due to their lower bond energy.

52 The vertical excitation energy is the energy necessary for the removal of the electron from the water phase without relaxation of the microstructure of the then empty cavity.

9.5 Halides and Oxohalides of Nitrogen

9.5.1 Halides

All halides of nitrogen can be formally derived from the hydrides by substitution of H by X (X = F, Cl, Br, I):

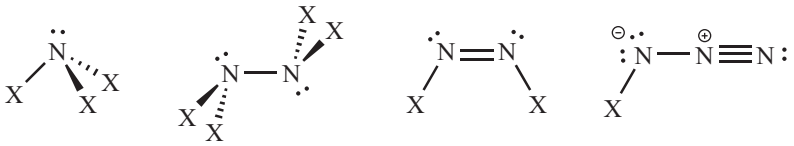

nitrogen trihalide | dinitrogen tetrahalide (*trans* and *gauche*) | dinitrogen dihalide (*cis* and *trans*) | halogen azide

In case of the NH_3 derivatives, partially halogenated compounds (haloamines NH_2X and dihaloamines NHX_2) as well as mixed halides are known. Their stability decreases with increasing atomic mass of the halogen so that only in case of fluorine (X = F) all possible permutations have been prepared.[53] Compounds with NCl, NBr and NI bonds are thermodynamically unstable (endothermic) and in many cases also kinetically labile even at 25 °C. Only NF_3 and NH_2Cl are of practical importance.

The *trihalides* (NX_3) are obtained by complete halogenation of NH_3 or $[NH_4]^+$ salts with the corresponding elemental halogen:

$$NH_3 + 3\,X_2 \longrightarrow NX_3 + 3\,HX$$

NF_3 is formed as a colorless gas (b.p. –129 °C) by reaction of NH_3 with dilute fluorine in the presence of copper or by *electrofluorination* of urea or $[NH_4]F$ in liquid hydrogen fluoride at a nickel anode (Section 13.4.3). NF_3 is unreactive at room temperature and a very weak LEWIS base (in contrast to NH_3) so that it only forms coordinate bonds with extremely strong LEWIS acids. This reduced basicity is due to the inductive effect of the three fluorine atoms, which leads to a partial positive charge at the N atom (Section 4.6.3). At higher temperatures (>200 °C), NF_3 is very reactive and a strong oxidizing agent due to the beginning dissociation into NF_2 radicals and fluorine atoms. Therefore, NF_3 is employed on a large scale in semiconductor industries for the cleaning of reactors used in chemical vapor deposition for dry etching of silicon wafers as well as in the production of *liquid crystal displays*.[54]

Derivatives of NF_3 are the tetrafluoroammonium salts $[NF_4][BF_4]$ and $[NF_4][SbF_6]$ with tetrahedral cations and nitrogen in the +5 oxidation state. These and

53 H. J. Emeléus, J. M. Shreeve, R. D. Verma, *Adv. Inorg. Chem.* **1989**, *33*, 139.
54 A. Tasaka, *J. Fluorine Chem.* **2007**, *128*, 296.

analogous salts are produced from the corresponding components by photolysis at low temperatures or in a gas discharge:[55]

$$NF_3 + F_2 + BF_3 \longrightarrow [NF_4][BF_4]$$

With O_2, trifluoroamine reacts in a glow discharge to give trifluoroamine oxide (ONF_3), a colorless, very toxic gas (b.p. –85 °C) which is isoelectronic to the $[NF_4]^+$ ion. Alternatively, ONF_3 can be prepared in high yield from NOF and F_2 under UV irradiation. The principally plausible pentafluoride NF_5, which would be the lighter homologue of the well-known PF_5, does not exist, which is due to the much smaller covalent radius of nitrogen compared to phosphorus. Five fluorine atoms at nitrogen would have to approach each other too closely. Therefore, the hypothetical equilibrium $NF_5 \rightleftharpoons NF_3 + F_2$ is completely on the product side. Nonetheless, the calculated D_{3h} structure of NF_5 corresponds to a minimum on the potential energy surface.

Nitrogen trichloride is an extremely endothermic compound (in contrast to exothermic NF_3). NCl_3 is formed on bubbling of Cl_2 into an acidic aqueous solution of $[NH_4]Cl$. Neat NCl_3 is a yellow, highly explosive oil, which dissolves in organic solvents, but has not been extensively studied due to the associated dangers. It slowly reacts with water to give NH_3 and HOCl.

The chlorination of NH_3 in the gas phase with insufficient amounts of chlorine (diluted with N_2) yields chloroamine, which tends to decompose spontaneously in pure form:

$$2\,NH_3 + Cl_2 \longrightarrow NH_2Cl + [NH_4]Cl$$

$$3\,NH_2Cl \longrightarrow N_2 + [NH_4]Cl + 2\,HCl$$

In analogous manner, bromoamine can be produced. NH_2Cl readily dissolves in water and diethylether. It is an important intermediate during the synthesis of hydrazine derivatives and other nitrogen compounds. For example, it reacts with dimethylamine to 1,1-dimethylhydrazine, which is used as a rocket propellant:

$$2\,Me_2NH + NH_2Cl \longrightarrow Me_2NNH_2 + [Me_2NH_2]Cl$$

Nitrogen tribromide (NBr_3) is generated by the reaction of bromine with acidic solutions of ammonium salts. By reaction of iodine with concentrated aqueous ammonia solution, $NI_3{\cdot}NH_3$ is obtained as black and – just like NBr_3 – highly explosive solid.

The halides of type N_2X_4 are derived from hydrazine but only *tetrafluorohydrazine* is known. It is a colorless gas, which is either prepared by reduction of NF_3 with copper at 375 °C or with mercury vapor in a glow discharge:

55 K. O. Christe et al., *Inorg. Chem.* **2006**, *45*, 7981.

$$2\ NF_3 + M \longrightarrow N_2F_4 + MF_x \qquad M: Cu, As, Sb, Bi, Hg$$

N_2F_4 (b.p. −73 °C) is an exothermic compound. The connectivity corresponds to that in hydrazine although the *trans*- and *gauche*-conformers are in equilibrium at 25 °C in the gas phase. In the *trans*-species the NF_2 groups are twisted against each other by 180°, resulting in inversion symmetry (C_{2h} symmetry). In case of the slightly less stable (by 1 kJ mol^{-1}) *gauche*-conformer the twist angle is only 67°.[56] In contrast to NF_3, tetrafluorohydrazine is extraordinarily reactive and thus a strong fluorinating agent even at 25 °C. This is explained by the unusually low dissociation enthalpy of the NN bond, which causes N_2F_4 to exist in equilibrium with the radical NF_2 at reduced pressures:

$$N_2F_4 \rightleftharpoons 2\ NF_2^{\bullet} \qquad \Delta H^{\circ}_{298} = 87\ \text{kJ mol}^{-1}(N_2F_4)$$

At ambient pressure, the dissociation is detectable at higher temperatures. Therefore, N_2F_4 typically reacts with many substrates to products containing the NF_2 moiety, for example, with Cl_2 under UV irradiation to $NClF_2$, with S_2F_{10} to $F_2N–SF_5$ or with NO to $F_2N–NO$. The deep-blue nitrogen difluoride radical is isoelectronic to the ozonide ion and shows a bent structure just as the latter.

Dinitrogen difluoride N_2F_2 (difluorodiazene)[57] is best prepared through the reduction of N_2F_4 with the graphite intercalation compound $C_x{\cdot}AsF_5$ (x = 10–12):

$$2\ C_x{\cdot}AsF_5 + 3\ N_2F_4 \xrightarrow{6\ d} 2\ [C_xF_2]^+[AsF_6]^- + 3\ \textit{trans}\text{-}N_2F_2$$

Difluorodiazene exists in two stereoisomeric planar modifications: the *cis*- or *Z*-form is by 6 kJ mol^{-1} more stable than the *trans*- or *E*-form. Despite this small difference, equilibrium between the two is only reached at higher temperature due to a rotational barrier of 250 kJ mol^{-1}. Mixtures of both stereoisomers can therefore be separated into the components at room temperature or below by distillation in high vacuum or by gas chromatography. On the other hand, N_2F_2 decomposes to NF_3, N_2 and F_2 above 250 °C. The isomerization can be achieved within a few days by addition of catalytic amounts of a strong LEWIS acid such as AlF_3 or SbF_5:

$$2\ \textit{trans}\text{-}N_2F_2 + SbF_5 \longrightarrow [N_2F][SbF_6] + \textit{cis}\text{-}N_2F_2$$

trans-N_2F_2 is stable toward O_2 and H_2O, and it decomposes into the elements at 300 °C. *cis*-N_2F_2 reacts with AsF_5 at 25 °C to the salt $[N_2F][AsF_6]$, which contains the linear cation $[N_2F]^+$ (d_{NN} = 109 pm; isoelectronic to CO_2, N_2O and $[NO_2]^+$).

Haloazides are formed by reaction of halogens with azides:

56 J. R. Durig, Z. Shen, *J. Phys. Chem. A* **1997**, *101*, 5010.

57 K. O. Christe et al., *J. Am. Chem. Soc.* **1991**, *113*, 3795 and *Inorg. Chem.* **2010**, *49*, 6823.

$$F_2 + HN_3 \longrightarrow FN_3 + HF$$

$$Cl_2 + NaN_3 \xrightarrow{H_2O} ClN_3\uparrow + NaCl$$

$$I_2 + AgN_3 \xrightarrow[0°C]{Et_2O} IN_3 + AgI$$

Fluoroazide (or trinitrogen fluoride) is a yellow-green gas, which slowly decomposes at 25 °C to N_2F_2 and N_2. The other haloazides are explosive in neat form and extremely dangerous substances (see Section 9.4.5).

9.5.2 Oxohalides of Nitrogen

Two series of oxohalides with nitrogen–halogen bonds are known:

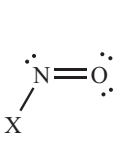

nitrosyl halide
(X = F, Cl, Br)

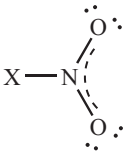

nitryl halide
(X = F, Cl, Br)

The already mentioned species NOF_3 and $ONNF_2$ are also to be counted among the oxohalides of nitrogen as is ONOF. Analogues of these with halogens other than fluorine are not known.

The *nitrosyl halides* represent the acid halides of nitrous acid (HONO), formally derived through replacement of an OH group by a halogen atom. In an analogous manner, the *nitryl halides* are related to nitric acid ($HONO_2$). If just the hydrogen atom of nitric acid is replaced by a halogen atom, the *halonitrates* ($XONO_2$) with X in the oxidation state +1 result (X = Cl, Br, I; Section 13.5.6). In case of fluorine, the difference in polarization suggests that the corresponding species is better referred to as pernitryl fluoride or nitryl hypofluoride $FONO_2$.[58]

Nitrosyl halides are formed by the reaction of NO with the corresponding halogen:

$$X_2 + 2\,NO \rightleftharpoons 2\,XNO$$

While FNO is stable, ClNO and particularly BrNO dissociate already at 25 °C into the starting materials. INO is completely unstable at this temperature. All three nitrosyl halides are strongly oxidizing. FNO (b.p. −60 °C) is colorless, ClNO (b.p. −5 °C) is

58 On the structure of crystalline ClNO, $ClNO_2$ and $ClONO_2$: A. Obermeyer, H. Borrmann, A. Simon, *J. Am. Chem. Soc.* **1995**, *117*, 7887.

orange-yellow and BrNO (b.p. 24 °C) is red. All three molecules are bent resulting in C_s symmetry. Nitrosyl chloride is also formed during the reaction of HCl gas with N_2O_3 in the presence of P_4O_{10}, by the reaction of hydrochloric acid with $Na[NO_2]$ and on mixing the concentrated acids HCl and HNO_3. The latter mixture is known as *aqua regia* and used as a strongly oxidizing reagent, for example, for the cleaning of glassware from organic residues.

As derivatives of nitrous acid, the nitrosyl halides primarily hydrolyze to HNO_2 and HX, subsequently also HNO_3 and NO are formed by disproportionation of HNO_2:

$$XNO + H_2O \longrightarrow HNO_2 + HX$$
$$3\,HNO_2 \longrightarrow HNO_3 + 2\,NO + H_2O$$

Certain metal halides (LEWIS acids) react with ClNO to nitrosyl salts such as $[NO][SbCl_6]$ and $[NO]_2[PtCl_6]$, which are also referred to as nitrosonium salts.

Both *nitryl halides* FNO_2 and $ClNO_2$ are colorless gases consisting of planar molecules of C_{2v} symmetry. The bonding situation is similar to that in nitric acid. FNO_2 (b.p. –72 °C) can be produced by fluorination of NO_2 or by halogen exchange from $ClNO_2$:

$$NO_2 + CoF_3 \xrightarrow{300°C} FNO_2 + CoF_2$$
$$2\,NO_2 + F_2 \xrightarrow{25°C} 2\,FNO_2$$
$$ClNO_2 + HF \xrightarrow{25°C} FNO_2 + HCl$$

Nitryl chloride (b.p. –15 °C) is obtained by oxidation of ClNO with Cl_2O, N_2O_5 or O_3, by chlorination of N_2O_5 with PCl_5, or most conveniently by treatment of anhydrous nitric acid with chlorosulfuric acid:

$$HNO_3 + HSO_3Cl \longrightarrow ClNO_2\uparrow + H_2SO_4$$

$ClNO_2$ is toxic and corrosive; it decomposes to Cl_2 and NO_2 at 100 °C. The alkaline hydrolysis yields nitrite and hypochlorite. Both isomeric bromides, $BrNO_2$ and BrONO, are unstable at 25 °C.

9.6 Oxides of Nitrogen

9.6.1 Introduction

Nitrogen oxides are of tremendous importance, for instance, as intermediate products for manufacture of nitric acid, as air pollutants from combustion engines, and within the context of the depletion of atmospheric ozone (Section 11.1.3). They occur in the global nitrogen cycle and act as regulators of body function in mammals and humans

(NO). The nitrogen oxides in Table 9.3 are known in pure form; several of these oxides exist as isomers of variable connectivity.

Table 9.3: Oxides of nitrogen isolated in pure form (in brackets: formation enthalpies of the gaseous compounds at 298 K in kJ mol^{-1})[a].

Oxidation state of nitrogen:	+1	+2	+3	+4	+5
	N_2O (82.1)	NO (90.3) N_2O_2 (81.6)	N_2O_3 (82.8)	NO_2 (33.1) N_2O_4 (9.1)	N_2O_5 (11.3)

[a]According to the database: webbook.nist.gov/chemistry

In the gas phase, all nitrogen oxides are *endothermic* compounds, which decompose into the elements on heating. They contain NO and, in some cases, NN bonds. Only NO and NO_2 are radicals (*open-shell molecules*).

9.6.2 Dinitrogen Oxide (N_2O)

N_2O is a colorless, unreactive gas (b.p. −89 °C), which is produced in both laboratory and industry by decomposition of ammonium nitrate:

$$[NH_4][NO_3] \xrightarrow{180–250°C} N_2O + 2\,H_2O$$

This reaction is catalyzed by chloride ions. At temperatures above 300 °C, it can take an explosive course. Therefore, the technical process employs an 80–85% aqueous solution of $[NH_4][NO_3]$, which is introduced into a melt of $Na[NO_3]/K[NO_3]$ at 260 °C. Another laboratory method makes use of the condensation of amidosulfuric acid with concentrated nitric acid at 50–80 °C:

$$H_3\overset{\oplus}{N}–\overset{\ominus}{S}O_3 + HNO_3 \longrightarrow N_2O + [H_3O][HSO_4]$$

The N_2O molecule is linear ($C_{\infty v}$ symmetry). The internuclear distances of d_{NN} = 112.9 pm and d_{NO} = 118.8 pm approximately correspond to those in the azide ion (116 pm) and in the $[NO_2]^+$ cation (106.6 pm). In fact, dinitrogen oxide is isosteric with CO_2 and isoelectronic to the ions $[NO_2]^+$ and $[N_3]^-$.

N_2O dissolves only sparingly in water and without any reaction. When breathed in, it exhibits a pleasant odor and a narcotic effect. It is therefore commercially available as *laughing gas* in steel cylinders for anesthetic purposes. Moreover, it is also used as propellant in spray cans (e.g., for whipped cream). In organic

chemistry, N_2O is employed as a mild oxidant. It is a byproduct of the commercial synthesis of adipic acid and released into the environment. In addition, biogenic N_2O is formed through the reduction of nitrates by microorganisms. In the atmosphere, N_2O acts as significant *greenhouse gas* due to its persistence (Section 4.4.3). A certain proportion even reaches stratospheric heights and participates indirectly in ozone depletion after oxidation to NO_x. After the production of chlorinated fluorocarbons has been discontinued, N_2O is regarded as the dominating ozone-depleting stratospheric gas of the current century.[59] It is also formed during thunderstorms by electric discharges in the upper atmosphere.

9.6.3 Nitrogen Monoxide (NO) and Dinitrogen Dioxide (N_2O_2)

The monoxide NO is produced on a huge industrial scale by catalytic oxidation of NH_3, predominantly for the production of nitric acid (Section 9.4.2). A much smaller part serves as a starting material for the synthesis of hydroxylamine (Section 9.4.7). In the laboratory, KIPP's gas evolution apparatus is most conveniently used for the preparation of NO from sodium nitrite and 3 molar sulfuric acid:

$$3\ Na[NO_2] + 3\ H_2SO_4 \longrightarrow 2\ NO\uparrow + HNO_3 + H_2O + 3\ Na[HSO_4]$$

Initially, unstable nitrous acid is formed which subsequently disproportionates to NO and HNO_3. Another method yielding relatively pure NO is the reduction of nitrites by iodide or iron(II) ions.

NO is a colorless, toxic gas, which – in contrast to N_2O – is rather reactive (b.p. –152 °C, m.p. –164 °C). The NO molecule has an uneven number of electrons and is therefore a radical and as such paramagnetic. The dimerization equilibrium

$$2\ NO \rightleftharpoons N_2O_2 \qquad \Delta H^\circ_{298} = -8.7\ kJ\ mol^{-1}$$

at standard conditions is almost completely on the left-hand side. In the liquid and the solid state, however, nitrogen(II) oxide is completely dimerized. Dinitrogen dioxide is likewise colorless and consists of planar molecules of *cis*-N_2O_2 in all phases (C_{2v} symmetry):[60]

59 A. R. Ravishankara, J. S. Daniel, R. W. Portmann, *Science* **2009**, *326*, 123.

60 S. G. Kukolich, *J. Am. Chem. Soc.* **1982**, *104*, 4715. The structure of *cis*-N_2O_2 in the gas phase has been determined by microwave spectroscopy, which requires a permanent dipolar moment in the molecule. *trans*-N_2O_2 is not a permanent dipole.

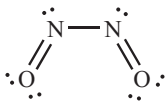

$d_{NN} = 227.7$ pm
$d_{NO} = 115.5$ pm
$\text{angle}_{ONN} = 97.9°$

The bond in the molecule NO can be understood according to MO theory with the help of the diagram developed for N_2 in Section 2.4.3. With 11 valence electrons, the π* level is occupied with one electron (SOMO, *singly occupied molecular orbital*). A π*–π* bond is thus responsible for the very weak NN bond in N_2O_2 according to the following scheme:

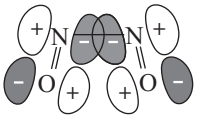

The π* electron of NO is relatively easy to detach; hence, the molecule is a reducing agent. In the process, it is oxidized to the nitrosyl cation $[NO]^+$ which is isoelectronic to the N_2 molecule. With O_2, NO undergoes an exhermic equilibrium reaction to NO_2 and N_2O_4 (reaction enthalpy –140 kJ mol^{-1} for 2 NO → 2 NO_2). It has long been assumed that this reaction proceeds via the weakly bound dimer N_2O_2 as intermediate:

$$N_2O_2 + O_2 \rightleftharpoons N_2O_4 \rightleftharpoons 2\,NO_2$$

At very low concentrations, for example, in air, the oxidation would proceed very slowly (if at all) in this mechanistic scenario, as the postulated pre-equilibrium 2 NO ⇌ N_2O_2 would lie almost completely on the side of monomeric NO owing to the low partial pressures. Although the reaction rate indeed strongly depends on the partial pressure of NO, some theoretical and experimental studies concluded that the initial product is not N_2O_2, but rather that NO and O_2 combine to the radical O=NOO·, which subsequently would react with further NO to a dinitroso peroxide ONOONO.[61a] The homolytic cleavage of its central OO bond would finally result in two molecules of NO_2, which in turn exist in equilibrium with the NN bonded dimer N_2O_4.

However, according to more recent high-level ab initio calculations and more sophisticated experimental work the proposed pre-equilibrium NO + O_2 ⇌ ONOO is completely on the left side and the doublet-state radical ONOO does not exist except as a VAN DER WAALS molecule with an interaction enthalpy of just –2 kJ mol^{-1}.[61b] Also, there is no experimental evidence for the proposed peroxide ONOONO. Therefore, the original assumption of N_2O_2 as the primary intermediate seems to be the only correct

61 (a) L. F. Olson et al., *J. Am. Chem. Soc.* **2002**, *124*, 9469. W. H. Koppenol et al., *Chem. Eur. J.* **2009**, *15*, 6161. (b) W. Eisfeld, K. Morokuma, *J. Chem. Phys.* **2003**, *119*, 4682. H. Beckers, X. Zeng, H. Willner, *Chem. Eur. J.* **2010**, 16, 1506.

one. A multistep reaction sequence such as this one is seemingly characterized by a *negative activation energy*, that is, the reaction is slowed down by higher temperatures, as the slightly exothermic NO dimerization is then shifted more and more to the left-hand side, mainly for entropic reasons.

Under high pressures, NO slowly decomposes at 30–50 °C according to:

$$3\ NO \longrightarrow N_2O + NO_2$$

With the halogens F_2, Cl_2 and Br_2, nitrogen monoxide reacts to the corresponding nitrosylhalides XNO. These react with LEWIS acids such as BF_3 and $SbCl_5$ to the nitrosyl salts $[NO][BF_4]$ and $[NO][SbCl_6]$, respectively. As the N atom of the nitrosyl cation $[NO]^+$ is in the oxidation state +3, these salts can also be accessed starting from N_2O_3. Nitrosyl hydrogensulfate (*lead chamber crystals*) is formed in such a manner from N_2O_3 and concentrated sulfuric acid:

$$N_2O_3 + 3\ H_2SO_4 \longrightarrow 2\ [NO][HSO_4] + [H_3O][HSO_4]$$

Other examples for $[NO]^+$ salts are $[NO][ClO_4]$, $[NO]_2[PtCl_6]$ and $[NO][AsF_6]$. The stronger bond of the cation $[NO]^+$ in comparison with that of NO is manifest in the smaller internuclear distance d_{NO} and the larger valence force constant f_r of the gaseous ion:

$$\begin{array}{lll} \text{NO(g.):} & d = 115.1\,\text{pm} & [\text{NO}]^+\text{(g.):} \quad d = 106.3\,\text{pm} \\ & f_r = 15.9\ \text{Ncm}^{-1} & f_r = 24.8\ \text{Ncm}^{-1} \end{array}$$

All nitrosyl salts react with water to nitrite ions or nitrous acid depending on the pH:

$$[NO]^+ + 2\ H_2O \longrightarrow HNO_2 + [H_3O]^+$$

In transition metal complexes, NO can act as π acceptor ligand, similarly as CO, $[CN]^-$ and N_2. Typical examples are the tetrahedral nitrosyl complexes $[Cr(NO)_4]$ and $[Co(CO)_3NO]$ as well as the octahedral anion $[Fe(CN)_5NO]^-$. The bonding situation between NO and the central metal atom corresponds to those with the ligand N_2 (Section 9.2), only that NO is just a 3-electron ligand, which formally donates its unpaired electron to the metal center and receives electron density from the metal through backdonation. The three mentioned complexes thus fulfill the *18-electron rule* (noble gas shell at the central atom). NO can also function as a bridging ligand between two metal centers.

Nitrogen monoxide is formed in undesirably large quantities in power, heating and waste burning plants as well as in combustion engines of cars, trucks, airplanes, ships and some trains according to the following equation:

$$N_2 + O_2 \rightleftharpoons 2\ NO \qquad \Delta H^\circ_{298} = 180.6\ \text{kJ mol}^{-1}(N_2)$$

In this manner, NO is released into the atmosphere either directly or after oxidation to NO_2. This NO formation reaction requires very high temperature or a catalyst in both directions, because a bimolecular reaction with a four-center transition state is *symmetry-forbidden*. Indeed, the uncatalyzed reaction proceeds via atomic oxygen instead (*thermal NO*).[62] Highly heated air therefore already contains 1 vol% NO at 2000 K in equilibrium, at 3000 K as much as 5 vol%. In a similar manner, NO is formed in large quantities in the atmosphere by lightning during thunderstorms. Approximately $7 \cdot 10^6$ t N per year is converted in this manner to NO_x, which is finally washed out in the form of nitric acid with rain and thus made available as natural nitrogen fertilizer.

For the *purification of exhaust gases* from automotive vehicles with combustion engines, these are equipped with a catalyst in the exhaust stream, which promotes the reduction of NO and NO_2 by CO and hydrocarbons. At the same time residual hydrocarbons and CO are oxidized to CO_2 und H_2O. The catalyst consists of a ceramic support of a honeycomb structure with an Al_2O_3 coating and approximately 2 g of platinum group metals (Pt, Rh and/or Pd).

In modern power plants, NO is reduced catalytically by an exactly defined amount of NH_3 according to the equation

$$4\,NO + 4\,NH_3 + O_2 \xrightarrow{350°C} 4\,N_2 + 6\,H_2O$$

and is thus removed from the exhaust (deNO_x process).[63] The employed catalyst typically consists of V_2O_5 and WO_3 on a TiO_2 carrier. A similar process is used for the denitrification of the exhaust of Diesel engines of trucks, busses and cars: in this case, a solution of urea ("AdBlue") is sprayed into the hot exhaust stream. A more recent process for the denitrification of exhausts from power plants and sulfuric acid production plants uses ozone for the oxidation of all nitrogen oxides to N_2O_5, which is then washed out with water as HNO_3 (see Section 11.1.3).

Nitrogen monoxide is one of the most intensively investigated molecules in biomedical research[64] as it occurs in traces in animals and humans, where it acts as a *neurotransmitter* for the regulation of blood pressure, blood coagulation and the immune response. For this discovery, the NOBEL Prize in medicine and physiology was awarded in 1998. The biosynthesis of NO proceeds in a complex 5-electron reaction through enzymatic oxidation and deamination of the nitrogen-rich amino acid arginine to citrulline and NO (=NH → =N–OH → =O + NO).[65] After having executed its

62 The NO formed during combustion from nitrogen species in the fuel is distinguished as *fuel NO*. Of all fossil fuels, only natural gas does not contain nitrogen compounds.

63 R.-M. Yuan, G. Fu, X. Xu, H.-L. Wan, *Phys. Chem. Chem. Phys.* **2011**, *13*, 453. There are also other procedures for removal of NO_x from the exhaust; see H.-G. Schäfer, F. N. Riedel, *Chemiker-Ztg.* **1989**, *113*, 65.

64 A. Daiber, V. Ullrich, *Chem. unserer Zeit* **2002**, *36*, 366.

65 S. Pfeiffer, B. Mayer, B. Hemmens, *Angew. Chem. Int. Ed.* **1999**, *38*, 1714.

task, NO is oxidized in the body to nitrite and nitrate (also see Section 9.7.1). Due to the small physiological concentrations of NO, this oxidation is relatively slow; the lifetime of NO in human blood amounts to approximately 2 min. Certain organic NO species such as nitroglycerin as well as the N-heterocyclic pharmaceutically active ingredients of the commercial *impotency medications* Viagra and Cialis liberate NO under physiological conditions and are therefore employed for the treatment of diseases associated with NO regulation issues.

9.6.4 Dinitrogen Trioxide (N_2O_3)

N_2O_3 is the anhydride of nitrous acid. It is obtained by saturating liquid N_2O_4 with gaseous NO at −80 °C:

$$NO + NO_2 \rightleftharpoons N_2O_3 \qquad \Delta H^\circ_{298} = -40.5 \text{ kJ mol}^{-1}$$

In the gas phase, N_2O_3 is mostly, although not completely, dissociated into NO and NO_2 at 25 °C and ambient pressure. According to LE CHATELIER's principle the equilibrium can be shifted to the right-hand side by lowering the temperature or increasing the pressure. The molecule N_2O_3 is planar in all phases and contains a weak NN bond with a large internuclear distance just like N_2O_4:[66]

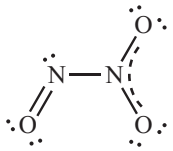

d_{NN} = 189 pm (−160°C)

Liquid N_2O_3 is dark-blue and solidifies as blue crystals at −100 °C. In organic solvents as well, it dissolves with a blue color. In contrast to NO and NO_2, N_2O_3 is diamagnetic.

With bases, N_2O_3 reacts to nitrite ions and with water accordingly to HNO_2:

$$N_2O_3 + 2\,[OH]^- \longrightarrow 2\,[NO_2]^- + H_2O$$

In practice, an equilibrium mixture of N_2O_3, NO and NO_2 (and minor quantities of the symmetrical dimers) is introduced into water to yield HNO_2 (see Section 9.7.4). With strong acids, nitrosyl salts such as $[NO][ClO_4]$ are formed with elimination of water. With alcohols, esters of nitrous acid are obtained, e.g. ethylnitrite C_2H_5ONO.

66 J. Horakh, H. Borrmann, A. Simon, *Chem. Eur. J.* **1995**, *1*, 389.

9.6.5 Nitrogen Dioxide (NO_2) and Dinitrogen Tetroxide (N_2O_4)

The dioxide NO_2 is an industrial intermediate of the production of nitric acid. In the laboratory, it is prepared by mixing stoichiometric amounts of NO and O_2 or by thermal decomposition of dry heavy metal nitrates in an O_2 stream:

$$Pb[NO_3]_2 \xrightarrow{400°C} PbO + 2\,NO_2 + \frac{1}{2}O_2$$

NO_2 is a brown, paramagnetic gas which contains variable equilibrium concentrations of colorless, diamagnetic N_2O_4 as a function of pressure and temperature:

$$2\,NO_2 \rightleftharpoons N_2O_4 \qquad \Delta H^\circ_{298} = -57\ \text{kJ mol}^{-1}(N_2O_4)$$

The position of the equilibrium ($\Delta G^\circ_{298} = -5.0$ kJ mol^{-1}) can be determined by measuring the volume (pressure), the magnetic susceptibility or the light absorption. Gaseous nitrogen(IV) oxide is dissociated to about 90% at 100 °C/0.1 MPa ($K_p = 6.50$ bar^{-1} at 298 K). Even the liquid is still brown due to the presence of NO_2 at temperatures near the boiling point (21 °C). With decreasing temperature, the color becomes progressively less intense and colorless crystals of N_2O_4 are obtained at −11 °C. Nitrogen dioxide is a toxic and extremely corrosive gas, which starts to decompose to NO and O_2 in an endothermic reaction above 150 °C; complete decay is reached above 800 °C.

NO_2 is an oxidizing agent and can be reduced relatively easily to the nitrite anion $[NO_2]^-$ but can also be oxidized further to the nitronium cation $[NO_2]^+$. It is instructive to compare the properties of these three redox-related species:

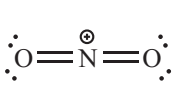

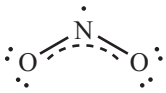

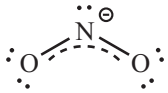

angle:	180°	134°	115°
f_r(NO):	17.2	10.4	7.7 N cm^{-1}

The bonding in the nitrite ion is similar to that in the isoelectronic ozone molecule. Accordingly, the N atom forms two σ bonds to the O atoms. The electronic structure of the NO_2 radical is largely analogous. According to EPR spectroscopic measurements, the unpaired electron is localized in a σ orbital at the N atom. The repulsion between the nonbonding electrons is smaller than in case of $[NO_2]^-$, which results in a strengthening of the bonds as indicated by the larger valence force constant f_r. The three *p* orbitals orthogonal to the molecular plane contain four electrons in total. One of the resulting π MOs is bonding while another is mostly nonbonding, and its electrons are thus typically attributed to a lone pair at the negatively charged oxygen atoms in the LEWIS resonance structures. In case of $[NO_2]^+$, the bonding situation is analogous to that in CO_2 (Section 2.4.6).

In the gas phase, N_2O_4 consists of planar molecules of D_{2h} symmetry:

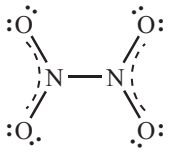

$d_{NN} = 175.6$ pm

The unusually long NN bond correlates with the low dissociation enthalpy of 54 kJ mol^{-1} and the partial charges at the N atoms of +0.46 atomic units. N_2O_4 isomers of lower stability have been detected by vibrational spectroscopy at low temperatures: one features two perpendicular NO_2 groups, another is of C_s symmetry with $ONONO_2$ connectivity, which is about 44 kJ mol^{-1} higher in energy than the global minimum structure. In liquid IF_5 or anhydrous acids such as HNO_3 and H_2SO_4, dinitrogen tetroxide N_2O_4 dissolves as salt-like nitrosyl nitrate $[NO][NO_3]$, which – in case of IF_5 – crystallizes on cooling. In neat form, however, it does hardly dissociate at all as shown by its low electrical conductivity.

Alkaline hydrolysis of NO_2 and N_2O_4 leads to nitrite and nitrate ions:

$$N_2O_4 + 2\,[OH]^- \longrightarrow [NO_2]^- + [NO_3]^- + H_2O$$

N_2O_4 is therefore a mixed anhydride of the two acids HNO_2 and HNO_3.

NO_2 and N_2O_4 are strong oxidizing agents, which convert even relatively noble metals into nitrates. In this manner, metal nitrates can easily be prepared in anhydrous form. N_2O_4 is used as oxidizing agent in rocket engines (for the oxidation of N_2H_4, $MeHNNH_2$ or Me_2NNH_2; see Section 9.3).

As a consequence of combustion processes, NO_2 is released into the atmosphere together with NO, where both persist for about 6–48 h and are ultimately washed out as nitric acid (contributing to the so-called *acid rain*). Upon irradiation with sunlight, however, NO_2 is also cleaved into NO and electronically excited O atoms in the ^{1}D state. From these and dioxygen, toxic ozone is formed near the Earth's surface $[O_2 + O(^1D) \rightarrow O_3]$ contributing to what is called *summer smog* or photochemical smog. As NO is subsequently reoxidized by O_2 to NO_2, up to 10 O_3 molecules can be formed from one NO_2 molecule on hot summer days posing a significant health risk. O_3 and NO_2 also react to the unstable radical $NO_3^\bullet$, which like $OH^\bullet$ is a strong oxidizing agent and participates in the nitrogen cycle in the troposphere. Another important nitro species in the atmosphere is the peroxoacetyl nitrate [PAN, $MeC(O)OONO_2$], which is formed by addition of NO_2 to acetyl radicals $CH_3CO^\bullet$.[67]

9.6.6 Dinitrogen Pentoxide (N_2O_5)

N_2O_5 is the anhydride of nitric acid and can be obtained from it by careful dehydration with P_2O_5:

67 G. Lammel, P. Wiesen, *Nachr. Chem. Tech. Lab.* **1996**, *44*, 477.

$$2\,HNO_3 + P_2O_5 \xrightarrow{0°C} N_2O_5 + \frac{2}{n}(HPO_3)_n$$

N_2O_5 is also produced by oxidation of N_2O_4 with O_3 as well as by anodic oxidation of HNO_3 in the presence of N_2O_4. It forms colorless, subliming crystals, which slowly decompose to NO_2 and O_2 at room temperature and violently react with water to HNO_3. Gaseous N_2O_5 consists of molecules with the following geometry (C_2 symmetry):

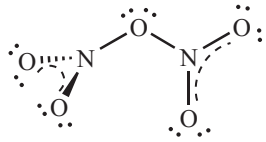

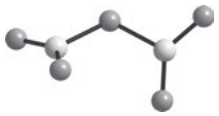

d_{NO} = 118.8 pm (terminal)
d_{NO} = 149.8 pm (bridging)
angle$_{NON}$ = 111.8°

The two planar NO_3 units share one oxygen atom and are twisted by about 133° against each other. On heating of the gas, partial dissociation occurs to NO_2 and unstable NO_3. In solvents such as CCl_4 and $CHCl_3$, N_2O_5 dissolves as molecules. In the solid state, however, it exists as nitronium nitrate $[NO_2]^+[NO_3]^-$. Salts with the cation $[NO_2]^+$ are also formed when N_2O_5 is dissolved in strong mineral acids:

$$N_2O_5 + HClO_4 \longrightarrow [NO_2][ClO_4] + HNO_3$$
$$N_2O_5 + HSO_3F \longrightarrow [NO_2][SO_3F] + HNO_3$$

Alternatively, nitronium salts can be produced from nitrogen(V) compounds, for example:

$$HNO_3 + 2\,SO_3 \longrightarrow [NO_2][HS_2O_7]$$
$$ClNO_2 + SbCl_5 \longrightarrow [NO_2][SbCl_6]$$

All these species are colorless salts, which are decomposed by water. The cation $[NO_2]^+$ is a major component of the so-called *nitrating acid*, a mixture of the anhydrous acids HNO_3 (98%) and concentrated H_2SO_4, which is used on a large industrial scale for the conversion of aromatic hydrocarbons into the corresponding nitro derivatives:

$$[NO_2]^+ + Aryl{-}H \longrightarrow Aryl{-}NO_2 + H^+$$

During this reaction, $[NO_2]^+$ is formed by protonation of $HONO_2$ at the OH group followed by the elimination of water. N_2O_5 itself, dissolved in CH_2Cl_2 or HNO_3, is also suitable for the nitration of arenes at room temperature.

9.7 Oxoacids of Nitrogen

9.7.1 Introduction

The two most important oxoacids of nitrogen are nitric acid (HNO_3) and nitrous acid (HNO_2). In addition, the following oxoacids are known: hyponitrous acid (HON–NOH),

peroxonitrous acid (HOONO) and peroxonitric acid ($HOONO_2$) (Table 9.4). The latter two species are unstable in general but persist for some time in dissociated form in aqueous solutions. Peroxonitrite $[O{=}N{-}O{-}O]^-$, however, is of considerable physiological importance.[65] Orthonitric acid H_3NO_4 (the analogue of phosphoric acid, see Section 10.12) is unknown, but a few orthonitrates with the tetrahedral anion $[NO_4]^{3-}$ have been prepared. The acid strength of above oxoacids rises strongly with increasing oxidation state of the nitrogen atom(s) and hydrogen is always linked to oxygen even if formulae such as HNO_2 and HNO_3 are used for convenience.

Table 9.4: Oxoacids of nitrogen.

Oxidation state of nitrogen:	**+1**	**+3**	**+5**
	HONNOH	(HONO) (HOONO)	$HONO_2$ $HOONO_2$

The compounds in brackets have not been isolated in pure form.

Of the derived salts, nitrates are of highest importance, predominantly as nitrogen fertilizers for agriculture. The nitrate content in drinking water in the EU should not exceed 50 mg L^{-1} (44 mg L^{-1} in the USA) and the upper limit for nitrite is 0.1 mg L^{-1}. In some countries in Northern Europe, however, groundwater already contains up to 100 mg L^{-1} nitrate from wastewater contamination from cities, industry and agriculture. In such cases, the nitrate content needs to be reduced by dilution with uncontaminated water prior to distribution and nutritional uses. The acute toxic effect of $[NO_3]^-$ is actually negligible, although it is somewhat increased through reduction to $[NO_2]^-$ by gastrointestinal bacteria. The nitrite anion is the true course of concern as it is oxidizing the hemoglobin of blood to methemoglobin. The Fe(III) center of the latter is much less efficient as an oxygen carrier leading to methemoglobinemia, a disease that results in blue-colored skin and ultimately may lead to internal suffocation. Due to the much lower activity of the enzyme responsible for the reconversion to hemoglobin (cytochrome b_5 reductase) directly after birth, this condition is particularly threatening to infants.[68] In addition, $[NO_2]^-$ reacts with amines to carcinogenic nitrosamines under acidic conditions or at elevated temperatures.

Since recently, however, also beneficial effects of nitrite and nitrate anions have come into focus as they seem to act as a reservoir for NO,[69] which is an important neurotransmitter (see Section 9.6.3).

68 M. P. Sherman et al., *Nitric Oxide* **2000**, *4*, 35.

69 N. S. Bryan, J. L. Ivy, *Nutr. Res.* **2015**, *35*, 643. N. S. Bryan, *Funct. Foods Health Dis.* **2016**, *6*, 691.

9.7.2 Nitric Acid (HNO_3 or $HONO_2$)

Nitric acid and its salts, the nitrates, are of great importance for producing fertilizers (e.g., ammonium nitrate), explosives and other organic nitro compounds. Chile saltpeter $Na[NO_3]$ is a natural source of nitrate, albeit of continuously decreasing importance. Aqueous nitric acid is produced on an industrial scale by absorption of NO_2/N_2O_4 from the catalytic oxidation of NH_3 in water under pressure:

$$N_2O_4 + H_2O \longrightarrow HNO_3 + HNO_2$$
$$3\,HNO_2 \longrightarrow HNO_3 + 2\,NO + H_2O$$

The NO formed during the disproportionation of HNO_2 is returned into the production cycle and oxidized once more to NO_2. The aqueous acid can be concentrated by evaporation up to 68 wt% HNO_3. This solution is referred to as *concentrated nitric acid*, which boils at 122 °C as *azeotropic mixture* (molar ratio HNO_3:H_2O = 1:1.65).[70] Such a mixture can only be concentrated further by vacuum distillation in the presence of sulfuric acid as a dehydrating agent. In industry, concentrated nitric acid is treated with N_2O_4 and O_2 under elevated pressure to yield essentially anhydrous HNO_3 (98–99%). In the laboratory, anhydrous nitric acid is obtained by reaction of $K[NO_3]$ with concentrated sulfuric acid, followed by distillation of neat HNO_3 (b.p. 84 °C/1013 hPa) under vacuum. Concentrated nitric acid containing excess NO_2 is of brown color and referred to as *fuming nitric acid*. During distillation at ambient pressure and on prolonged exposure to light, HNO_3 partially decomposes back to NO_2, O_2 and H_2O:

$$2\,HNO_3 \longrightarrow 2\,NO_2 + \tfrac{1}{2}O_2 + H_2O$$

Therefore, HNO_3 is stored in brown bottles in the laboratory. Anhydrous nitric acid is a colorless liquid, which is partially autodissociated into $[NO_2]^+$, $[NO_3]^-$ and H_2O leading to a considerable electrical conductivity:

$$3\,HNO_3 \rightleftharpoons [H_3O]^+ + [NO_2]^+ + 2\,[NO_3]^-$$

Equilibrium is reached very rapidly, which leads to the detection of just one collapsed signal in the ^{15}N-NMR spectrum under standard operating conditions. The nitrate anion is of trigonal-planar geometry (D_{3h} symmetry), and nitric acid is a planar molecule of C_s symmetry in the gas phase (HON angle 102°):

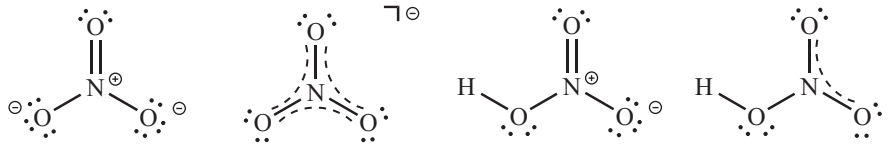

70 A mixture with identical compositions in both liquid and gas phases thus cannot be separated by distillation unless the pressure is changed.

The σ bond scaffold of the nitrate ion is superimposed by a delocalized π bond (dotted lines), which is formed by the overlap of the four 2*p* orbitals perpendicular to the molecular plane. The linear combination of these AOs results in one bonding (a_2''), two nonbonding (e'') and one antibonding MO (a_2''; compare the isoelectronic BF_3 in Section 2.4.8). All three NO internuclear distances are therefore equal. The valence force constant of 8.0 N cm^{-1} corresponds to a certain multiple bond character (bond order ca. 1.3). In the HNO_3 molecule, however, the π bond is only delocalized across the nitro group, while the OH group is connected to the N atom through a simple σ bond. This follows from the different NO internuclear distances, which amount to 121 pm (2x) and 141 pm; the ONO angle in the nitro group is 130°.

Anhydrous nitic acid is a strong oxidizing agent and the aqueous solution is a strong BRØNSTED acid. The concentrated acid dissolves copper, silver and mercury, but not gold or platinum.[71] Depending on the concentration, HNO_3 is reduced to NO_2 (concentrated acid) or NO (dilute acid):

$$[NO_3]^- + 4\,H^+ + 3\,e^- \longrightarrow NO + 2\,H_2O$$

$$[NO_3]^- + 2\,H^+ + e^- \longrightarrow NO_2 + H_2O$$

On the other hand, certain base metals in pure form (Al, Fe, Cr) are not dissolved by concentrated nitric acid due to formation of a thin but dense and strongly adhering oxide layer, which prevents the further attack of the acid. This process is called *passivation*.

Concentrated nitric acid of the composition $H_2O{\cdot}HNO_3$ freezes at −38 °C to crystals of oxonium nitrate $[H_3O][NO_3]$. By reaction of HNO_3 with NH_3 and with metal hydroxides or carbonates, the corresponding *nitrates* can be obtained, which readily dissolve in water without exception. Alkali metal nitrates decompose to nitrites on heating, while the thermolysis of heavy metal nitrates affords NO_2 and metal oxides:

$$K[NO_3] \longrightarrow K[NO_2] + \tfrac{1}{2}O_2$$

$$Cu[NO_3]_2 \longrightarrow CuO + 2\,NO_2 + \tfrac{1}{2}O_2$$

In particular at higher temperatures, nitrates are therefore strong oxidizing agents. $K[NO_3]$ is produced from KCl and HNO_3 and is the main component of *gun powder*. $Na[NO_3]$ is an important fertilizer and also a component of many explosives. By

71 Gold and platinum metals are dissolved by *aqua regia*, a 3:1 mixture of conc. HCl and conc. HNO_3, which contains very strong oxidants such as Cl_2 and NOCl. Moreover, the generated metal cations are bonded as ate-complexes due to the presence of chloride ions in high concentrations (as $[AuCl_4]^-$ and $[PtCl_6]^{2-}$), thus reducing the noble character of these metals according to the NERNST equation.

nascent hydrogen (e.g., from Zn and aqueous HCl), the nitrate ion is reduced to NH_3 even at room temperature. On melting of $Na[NO_3]$ with Na_2O at 300 °C, colorless sodium orthonitrate $Na_3[NO_4]$ is obtained with a tetrahedral anion that is isoelectronic to CF_4. The corresponding acid H_3NO_4, however, is unknown (in contrast to the heavier homologue, phosphoric acid H_3PO_4; see Section 10.12).

Toward transition metal ions, the nitrate ion usually acts as a bidentate *complex ligand*. For instance, the anhydrous nitrates of Ti^{4+}, Co^{3+} and Cu^{2+} contain coordinatively (not ionically) bonded nitrato groups. These nitrates are therefore volatile without decomposition even at mildly elevated temperature.

Concentrated aqueous nitric acid (50–70%) is employed for manufacture of nitrogen fertilizers such as ammonium nitrate and for the conversion of insoluble phosphate ore ($Ca_3[PO_4]_2$) into water-soluble hydrogen phosphate (Section 10.12.1). The anhydrous acid is used for nitration of organic compounds.

9.7.3 Peroxonitric Acid (HNO_4 or $HOONO_2$)

Peroxonitric acid is unknown in pure form, but can be prepared as dilute aqueous solution by reaction of concentrated hydrogen peroxide with aqueous nitric acid or with the salt $[NO_2][BF_4]$, in each case at temperatures below 0 °C:

$$HOOH + [NO_2][BF_4] + H_2O \longrightarrow HOONO_2 + [H_3O][BF_4]$$
$$HOOH + HONO_2 \longrightarrow HOONO_2 + H_2O$$

The species $HOONO_2$, however, is also formed in the upper atmosphere in a reversible reaction of the radicals $HO_2^{\bullet}$ and $NO_2^{\bullet}$. The molecule consists of a planar $OONO_2$ unit and an approximately perpendicular OH group. As both the OO and the NO single bonds are readily cleaved homolytically, the high reactivity of HNO_4 is no surprise. In acidic solution the half-life is about 30 min, in alkaline solution rapid decomposition to nitrite and O_2 occurs (salts of peroxonitric acids are therefore unknown). Aqueous HNO_4 is a strong oxidant, which oxidizes chloride ions to Cl_2.[72]

9.7.4 Nitrous Acid (HNO_2 or HONO)

Nitrous acid is unstable and cannot be isolated in pure form. Only in the gas phase and in dilute aqueous solution, HONO persists for limited periods of time. In

72 E. H. Appelman, D. J. Gosztola, *Inorg. Chem.* **1995**, *34*, 787. A. R. Ravishankara et al., *J. Phys. Chem. A* **2005**, *109*, 586.

contrast, its salts, the nitrites, are stable in both the solid state and in solution. They are prepared in the following manner:

$$NO + NO_2 + 2\,NaOH \longrightarrow 2\,Na[NO_2] + H_2O$$

$$Na[NO_3] + Fe \xrightarrow{\Delta T} Na[NO_2] + FeO$$

Sodium nitrite is used in food industries for preservation purposes, mainly against *clostridium* bacteria on meat, which cause *food poisoning* (botulism) through their toxins. In nitrate-fertilized soils, nitrite is produced by reducing bacteria, which in turn is converted to volatile HNO_2 (at acidic pH values) that can even end-up in the atmosphere. Through salt metathesis $Na[NO_2]$ is readily converted to $Ba[NO_2]_2$, which yields a pure, dilute solution of HNO_2 upon treatment with sulfuric acid and subsequent separation of precipitated insoluble $Ba[SO_4]$. Such aqueous solutions disproportionate slowly (more rapidly on heating) according to:

$$3\,HNO_2 \longrightarrow [H_3O]^+ + [NO_3]^- + 2\,NO$$

Conversely, in the gas phase HNO_2 is in equilibrium with its decomposition products in an endothermic reaction:

$$2\,HNO_2 \rightleftharpoons NO_2 + NO + H_2O$$

Gaseous nitrous acid exists as two different planar conformers, namely *cis*- and *trans*-HNO_2:

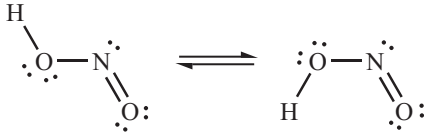

trans *cis*

The *trans*-isomer is by 2 kJ mol^{-1} more stable than the *cis*-form. The isomerization via rotation about the central bond requires an activation enthalpy of 45 kJ mol^{-1}. This value can be taken as a reasonable approximation of the π bond energy as the π bond has to be broken to allow free rotation, whereas the σ component persists. Aqueous HNO_2 (pK_a = 3.35 at 18 °C) is only slightly stronger than acetic acid and reacts either as reductant (e.g., with permanganate $[MnO_4]^-$) or as oxidant (e.g., with H_2S, I^- and Fe^{2+}).

The *nitrites* of the alkali metals and of barium and thallium as well as ammonium nitrite are ionic salts, that is, there is little covalent interaction. Nonetheless, organic nitro compounds R–NO_2 as well as esters of nitrous acid R–O–NO with mainly covalent bonds to the organic residue are formally related to the nitrites. In organic chemistry $Na[NO_2]$ is employed in the synthesis of nitroso and diazo compounds. Just like

nitrate, the nitrite ion can act as a *complex ligand* toward metal ions (M), either as nitro group M–NO_2 or as nitrito group M–ONO. Related covalent structures are also encountered in transition metal nitrites. One of the best-known nitro complexes is sodium hexanitrocobaltate $Na_3[Co(NO_2)_6]$.

$Na[NO_2]$ reacts with H_2O_2 to the yellow *peroxonitrite ion* $[ONOO]^-$, a strong oxidizing agent, which is fairly stable in alkaline solution but slowly isomerizes to nitrate and can thus not be isolated in pure form (also see Section 9.7.5).[73]

Aqueous HNO_2 reacts with excess H_2O_2 at 0 °C to *peroxonitric acid* ($HOONO_2$), which has been obtained in at most 1.5-molar concentration but decomposes at 22 °C in acidic solution with a half-life of 30 min (Section 9.7.3). In alkaline solution, rapid decomposition occurs to nitrite and O_2. As to be expected, $HOONO_2$ is a powerful oxidizing agent.[74]

9.7.5 Peroxonitrous Acid (HOONO)

Nitrogen monoxide and tetramethylammonium superoxide react in liquid ammonia to the corresponding peroxonitrite, which was isolated as yellow, microcrystalline and hygroscopic powder:

$$[Me_4N][O_2] + NO \longrightarrow [Me_4N][OONO]$$

This reaction is important for two reasons: (1) There are indications that the superoxide anions formed during the respiratory chain of mammals similarly react with NO to toxic peroxonitrite,[75] and (2) peroxonitrous acid is assumed to be a product of the reaction of $OH^\bullet$ radicals with NO_2 in the stratosphere and thus may act as resting state for radicals in the ozone depletion reaction. Gaseous HOONO molecules are planar and of *cis–cis* conformation, probably due to an intramolecular O···H hydrogen bond. The aqueous acid HOONO is rather weak ($pK_a = 6.5 \pm 0.1$) and only stable for about 1 s under physiological conditions (pH = 7.4); homolysis of the OO bond and recombination of the two resulting radicals leads to isomerization to nitric acid $HONO_2$. In contrast, in strongly alkaline solution the peroxonitrite anion decomposes in a bimolecular reaction to nitrite and O_2. The equilibrium constant of the reaction

$$HOONO + H_2O \rightleftharpoons HONO + H_2O_2$$

73 S. Goldstein, G. Czapski, *Inorg. Chem.* **1995**, *34*, 4041; J. R. Leis, M. E. Pena, A. Ríos, *J. Chem. Soc. Chem. Commun.* **1993**, 1298.

74 E. H. Appelman, D. J. Gosztola, *Inorg. Chem.* **1995**, *34*, 787; Z. Chen, T. P. Hamilton, *J. Phys. Chem.* **1996**, *100*, 15731.

75 A. Daiber, V. Ullrich, *Chemie unserer Zeit* **2002**, *36*, 366.

has been determined to be $7.5 \cdot 10^{-4}$ mol L^{-1}.

The above-mentioned salt $[Me_4N][OONO]$ contains a planar anion of *cis*-conformation. Under dry conditions, it is persistent at room temperature; on heating to 110 °C, it isomerizes to nitrate without weight loss in an exothermic reaction. Conversely, nitrate ions are prompted to rearrange to peroxonitrite by UV irradiation (200 nm, π–π^* excitation). Peroxonitrites are strong 2-electron oxidants.

9.7.6 Hyponitrous Acid $(HON)_2$ and Nitramide (H_2NNO_2)

The acid $(HON)_2$ is known both in pure form and as its salts, the hyponitrites. If $Na[NO_2]$ is reduced with sodium amalgam at 0 °C in water, a solution of $Na_2[N_2O_2]$ is obtained from which the yellow, sparingly soluble $Ag_2[N_2O_2]$ can be precipitated with $Ag[NO_3]$:

$$2\ Na[NO_3] + 4\ Na + 2\ H_2O \longrightarrow \textit{trans}\text{-}Na_2[N_2O_2] + 4\ NaOH$$

Adding the silver salt to ethereal HCl solution yields the free acid, which crystallizes in colorless, explosive sheet-like crystals upon concentration of the filtered solution. The very weak acid $(HON)_2$ ($pK_1 = 7.2$) slowly and irreversibly decomposes even in the cold according to the following equation:

$$(HON)_2 \longrightarrow N_2O + H_2O$$

The O atoms of $(HON)_2$ as well as of the corresponding anion are in *trans* position to each other:

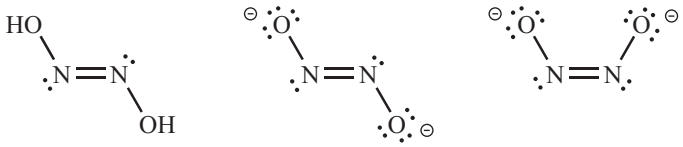

trans-$(NOH)_2$ *trans*-$[N_2O_2]^{2-}$ *cis*-$[N_2O_2]^{2-}$

The *rotation* about the NN bond – like in the case of other azene derivatives – is only possible if a relatively high barrier is overcome. The necessary activation enthalpy is not available at room temperature so that isomerization cannot occur through this pathway. Instead, inversion at one of the nitrogen atoms happens with a much lower barrier. With nitrogen bases $(HON)_2$ reacts to the corresponding *trans*-hyponitrites, several of which have been characterized structurally.[76]

76 D. S. Bohle et al., *Inorg. Chem.* **1999**, *38*, 2716.

Colorless *cis*-$Na_2[N_2O_2]$ is formed during the reaction of NO with Na in liquid ammonia at −50 °C as an amorphous powder as well as in crystalline form by heating Na_2O with N_2O at 360 °C.[77] With water, the compound reverts to N_2O and NaOH.

Hyponitrites are reductants, which are oxidized to nitrites by I_2 and to nitrates by Br_2 and Fe^{3+}. The anion $[N_2O_2]^{2-}$ is also known as a ligand in transition metal complexes.

The isomeric nitramide H_2NNO_2 is a subliming white solid (m.p. 81–84 °C), which is obtained by nitration of sodium amidosulfate $Na[SO_3NH_2]$. Nitramide crystallizes in stacked two-dimensional layers. Within the layers, individual molecules are connected by hydrogen bonds, but no stronger than VAN DER WAALS forces keep the layers together in the crystal structure.[78] H_2NNO_2 is the parent compound for many explosives and indeed highly explosive itself upon shock or contact with acids.[79]

77 C. Feldmann, M. Jansen, *Z. Anorg. Allg. Chem.* **1997**, *623*, 1803.

78 A. Häußler, T. M. Klapötke, H. Piotrowski, *Z. Naturforsch.* **2002**, *57b*, 151.

79 Cyclotrimethylenetrinitramine $[O_2NNCH_2]_3$ is a widely employed explosive, which is formally derived from nitramide, but is actually prepared from hexamethylenetetramine (urotropine) in nitric acid. It is also known as hexogen or RDX.

10 Phosphorus and Arsenic

10.1 Introduction

In Group 15 of the Periodic Table, as in both neighboring groups, the metallic character increases when going down. More specifically, there is a transition from a purely nonmetallic element (N) via elements with nonmetallic and metallic modifications to purely metallic elements (Sb, Bi). This chapter addresses the two elements besides nitrogen, which are clearly nonmetallic under standard conditions: phosphorus[1] and arsenic.[2] The chemistry of arsenic, however, is only briefly described as many of the arsenic compounds resemble the corresponding phosphorus species. Phosphorus can thus be considered as a *representative element* and is discussed in more detail. This also reflects the extraordinarily important role of phosphorus compounds in industry and for the physiology of living organisms. Collectively, the elements of Group 15 are often referred to as *pnictogens*.

The importance of phosphorus and its compounds can hardly be overestimated. It suffices to recall that the human body consists of 1.1% of phosphorus, predominantly in the bones and teeth, but also in the form of adenosine triphosphate (ATP), the energy carrier of life, as well as in the scaffolds of DNA and RNA and finally in the phospholipids of cell walls. Therefore, most foods naturally contain phosphate, and huge quantities of P-containing fertilizers are produced annually in order to supply the essential minerals for life processes to crops and indirectly also to livestock. Phosphorus and arsenic, however, are also important for modern technology, for instance, for production of semiconductors such as AlP and GaAs as well as for the n-doping of silicon and other semiconductors. Phosphorus-containing ligands, on the other hand, are indispensable components of transition metal catalysts for important industrial processes in organic chemistry.

10.2 Bonding Situation in P and As Compounds

The valence electron configuration of the phosphorus atom in its ground state is $3s^2 3p_x^1 p_y^1 p_z^1$. With the three half-filled orbitals, the P atom can support three covalent

1 D. E. C. Corbridge, *Phosphorus – Chemistry, Biochemistry and Technology*, 6th ed., Elsevier, Amsterdam, **2013**. M. E. Schlesinger, *Chem. Rev.* **2002**, *102*, 4267 (thermodynamics). P. F. Kelly, *Encycl. Inorg. Chem.* **2005**, *7*, 4308. New Aspects of Phosphorus Chemistry, Parts I–V, *Top. Curr. Chem.*, Vols. *220, 223, 229, 232* and *250* (**2000**–**2005**). M. Regitz, O. J. Scherer (eds.), *Multiple Bonds and Low Coordination in Phosphorus Chemistry*, Thieme, Stuttgart, **1990**.

2 M.-A. Munoz-Hernández, *Encycl. Inorg. Chem.* **2005**, *1*, 268.

https://doi.org/10.1515/9783110578065-011

bonds or form a threefold negative phosphide anion P^{3-}.[3] Between these two extremes, intermediate stages are possible as the following examples demonstrate:

Three covalent bonds: PH_3, PCl_3, PMe_3, P_4
Covalent and ionic bonding: $[PH_2]^-$ and Na^+ in $Na[PH_2]$
Ionic bonding: P^{3-} and Na^+ in Na_3P

Analogous species are known for arsenic. All of them feature an octet of electrons at the central atom. According to the rules of the VSEPR model (Section 2.2.2), phosphanes (PX_3) and arsanes (AsX_3) are of trigonal-pyramidal geometry without exception with valence angles usually in the range of 90–102° (Table 2.5). The smaller angles are readily rationalized if the three covalent σ bonds are constructed from the three *p* orbitals of the central atom. The valence angle α should thus be close to 90°, which is approximately realized in PH_3 (α = 93.5°). Conversely, in PF_3 (α = 97.7°) there is a certain amount of π backdonation (*hyperconjugation*) from the fluorine ligands due to the high positive partial charge at the phosphorus center induced by the electronegativity difference between P and F. The formally nonbonding $2p_\pi$ orbitals of the fluorine atoms donate electron density into the lowest unoccupied orbitals of *e* symmetry at the P atom, which have dominant 3*p* components and are weakly antibonding regarding the PF bonds (Section 2.4.9). As a consequence of this interaction, the PF bonds acquire a certain multiple bond character, which together with a considerable ionic contribution explains their high bond enthalpy (490 kJ mol^{-1}).[4] Alternatively, the relatively large valence angle can be explained by the electrostatic repulsion of the partial negative charges at the substituents. Due to the increasing spatial demand of the heavier halogen atoms, the angle increases in the row PF_3–PCl_3–PBr_3–PI_3 (Table 2.5).

In compounds of the type PX_3 and AsX_3 (X = univalent group), the nonbonding electron pair at the central atom can engage in an additional σ bond, which is formally to be considered as a dative bond. For example, such a bond can be generated by protonation of EH_3 to the cation $[EH_4]^+$. The four covalent bonds of such tetrahedral cations are identical, however, resembling those of the valence isoelectronic CH_4 (Section 2.4.10; valence angle 109.5°). Examples of such phosphonium and arsonium cations are (R: organic residue):

$$[PH_4]^+ \quad [PCl_4]^+ \quad [R_4P]^+ \quad [AsH_4]^+ \quad [AsCl_4]^+ \quad [R_4As]^+$$

The LEWIS basicity of the pnictogen centers in compounds of type EX_3, however, is strongly diminished with increasing atomic radius. This is manifest in the following values for *proton affinities* in the gas phase (values in kJ mol^{-1}):

3 Regarding the existence of small, multiply charged anions compare Section 2.1.3.
4 A. E. Reed, P. von R. Schleyer, *J. Am. Chem. Soc.* **1987**, *109*, 7362.

NH_3: 854 PH_3: 785 AsH_3: 748

NMe_3: 949 PMe_3: 959 $AsMe_3$: 897

Dative bonds are also present in numerous transition metal complexes with ligands of the type EX_3 such as PF_3 or Ph_3P. In these complexes, the molecule EX_3 is not only a σ donor, but also a π acceptor due to the relatively low energy of the two lowest unoccupied molecular orbitals, which can accept electron density from the metal center. These LUMOs are not *d* orbitals, which are too high in energy, but rather antibonding σ* orbitals with a predominant 3*p* character at the P atom.

The decisive difference in the chemistry of nitrogen, on the one hand, and the chemistry of phosphorus and arsenic, on the other hand, results from the much larger *atomic radii* of the heavier pnictogens (Table 4.3) as well as from their lower *electronegativity* (Table 4.8). The larger radii allow for higher coordination numbers and thus for the formation of *hypercoordinate compounds* (Section 2.6). Examples are given by the following pentacoordinate species of trigonal-bipyramidal geometry:

PF_5 PCl_5 Ph_5P AsF_5 $AsCl_5$ Me_5As

as well as by the octahedral ions:

$[PF_6]^-$ $[PCl_4]^-$ $[PCl_6]^-$ $[AsF_6]^-$ $[AsCl_6]^-$

The bonding situation in these ions corresponds to that in the isoelectronic sulfur species SF_4 and SF_6. In all cases of hypercoordinate species, the σ bonds can be described as multicenter bonds. For PF_5, for instance, the σ interactions of the four valence orbitals at phosphorus with the 2*p* orbitals of the five F atoms result in four bonding, one nonbonding and four antibonding molecular orbitals.[5] The 10 valence electrons occupy the five lowest energy terms, which results in a closed shell electronic configuration (four bonding and one nonbonding electron pair). The nonbonding pair is delocalized across the five F atoms so that only eight valence electrons are present at the P center and the octet rule is not violated.[6] The equatorial bonds are formed by the 3*s*, $3p_x$ and $3p_y$ atomic orbital of phosphorus, while the axial bonds consist of the 3*s* and $3p_z$ orbitals. The former bonds are slightly shorter which is mostly a consequence of increased steric strain in the axial positions with *three* nearest neighbors at 220 pm *versus two* near neighbors each at 220 and at 266 pm in the equatorial positions. But since the repulsive Coulomb interaction decreases with the square of the distance, the long-range interaction across 266 pm

5 T. A. Albright, J. K. Burdett, M.-H. Whangbo, *Orbital Interactions in Chemistry*, Wiley, New York, **2013**. The *d* orbitals in the compounds discussed here are mostly relevant as polarizing functions as their electron population is very small; see D. L. Cooper et al., *J. Am. Chem. Soc*. **1994**, *116,* 4414.
6 Obviously, there is additional π backdonation of nonbonding electrons of the fluorine ligands into σ* MOs at the central atom, which, however, is counterbalanced by the inductive electron withdrawal by the electronegative ligands.

can be neglected to a first approximation. Therefore, the PF internuclear distances in gaseous PF_5 amount to 153 pm for the equatorial and 158 pm for the axial positions.

To certain atoms, phosphorus and arsenic can also form regular π bonds in addition to the σ framework. The strongest, hence most important π bonds are those of the p_π–p_π type. Bonding partners suitable for π bonding to phosphorus are predominantly the lighter nonmetals B, C, N and O, but also a variety of heavier main group elements such as P, S, Si and As. Two types of π interactions can be thus distinguished:

(a) If the considered P atom is trivalent as in phosphaalkenes R–P=CR_2, the phosphazenes R–P=N–R or the diphosphenes R–P=P–R, the π bond is formed through the overlap of two p_π orbitals just as in the corresponding diazenes R–N=N–R. This situation can be regarded as a classical π bond. Similar considerations apply to the phospha-alkynes R–C≡P, which contain a triple bond that resembles the one in nitriles R–C≡N and in molecules such as N_2 and P_2. Classical π bonds are also present in phosphinines (phosphabenzenes)[7] and arsinines, which are planar molecules with cyclic aromatic systems including the p_π orbital of the respective heteroatom:

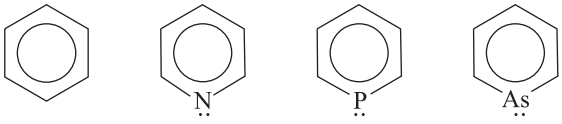

benzene pyridine phosphinine arsinine

Besides, a large number of aromatic heterocycles with two or more phosphorus atoms in the ring is known, for example, the diphosphatriazolate anion *cyclo*-[1,2-P_2N_3]$^-$, which is prepared in quantitative yield by the thermal transfer of a P_2 unit from an organic diphosphane to sodium or ammonium azide.[8] Just like benzene itself, hexaphosphabenzene is a competent ligand in transition metal complexes with a perfectly planar P_6 ring that coordinates in η^6 fashion, for example, to molybdenum centers. The residual lone pairs at the P atoms can be employed for coordination of additional metal centers.[9]

(b) If the considered Group 15 atom is pentavalent as in the phosphane oxides (R_3P=O) or the phospha-ylides (R_3P=CH_2), the π interaction is more akin to the π backdonation in hypercoordinate species. It occurs between the p_π orbitals at the substituent and the unoccupied σ* MOs at the P atom (*hyperconjugation*). The PO internuclear distance in Ph_3PO is d_{PO} = 149 pm and thus much smaller than in the bridging POP bonds of P_4O_{10} (160 pm). Since the valence orbitals 3*s*

7 Review: A. J. Ashe III, *Eur. J. Inorg. Chem.* **2016**, 572.
8 C. Hering-Junghans, E. Rivard, *Angew. Chem. Int. Ed.* **2015**, *54*, 10077.
9 M. Scheer et al., *Angew. Chem. Int. Ed.* **2015**, *54*, 13110.

and $3p_xp_yp_z$ of the P atom have been used for the σ framework and the 3*d* orbitals are energetically inaccessible, the π interaction of the two 2*p* AOs of the terminal O atom has to employ the two lowest lying antibonding σ* MOs at phosphorus. The doubly degenerate MOs show predominant 3*p* character. Two weak π bonds result; the consequences for the PO bond are approximately described by the following resonance structures with a dominating contribution by structure (b):[10]

(a) (b)

As this π backdonation is considerably weaker than the σ bonds, a definitive bond order cannot be given. Additionally, the strengthening of the bond by ionic contributions due to the difference in electronegativity is difficult to quantify. The π bonds to the terminal O atoms of phosphate ions and phosphorus oxides are to be described in an analogous manner, as well as to the terminal S atoms in thiophosphate ions and phosphorus sulfides. The phosphazenes of pentavalent phosphorus do not contain any classical π bonds either. Nonetheless, the chemical literature (and this book) often describes these bonds by a double line as in P=O and P=N for convenience. The reader is encouraged to recall on these occasions that the thus depicted "double" bond is very close in strength to a strongly polarized single bond (covalent bond plus electrostatic attraction and a small contribution of hyperconjugation).

In summary, it should be noted that the P atom can engage in various strongly differing bonding situations, which entails an extraordinarily manifold of compounds. The coordination numbers vary between 1 and 6; the by far most frequently occurring compounds show coordination numbers of 3 and 4. The formal oxidation numbers vary between −3 and +5. Examples are given with the following compounds:

−3	−2	−1	0	+1	+2	+3	+4	+5
Li_3P	$Ca_2[P_2]$	LiP	P_4	H_3PO_2	P_2F_4	P_4O_6	$H_4P_2O_6$	P_4O_{10}

Analogous considerations apply to arsenic.

10.3 Phosphorus and Arsenic as Elements

Phosphorus and arsenic are monoisotopic elements, of which just a single stable isotope is known, namely ^{31}P with the nuclear spin $I = ½$ and ^{75}As with $I = 3/2$. Both

10 D. G. Gilheany, *Chem. Rev.* **1994**, *94*, 1339. B. Gamoke, D. Neff, J. Simons, *J. Phys. Chem. A* **2009**, *113*, 5677.

nuclei are well suited for NMR spectroscopy. Of the 16 radioactive phosphorus isotopes, ^{32}P is the by far most important; it is produced by neutron irradiation from $^{32}S(n,p)$ or $^{31}P(n,\gamma)$ and decays as a β emitter with a half-life of 14.28 days. Neutron activation analysis is also used for the determination of arsenic in all sorts of samples.

10.3.1 Production of the Elements

Phosphorus as a highly reactive and particularly oxophilic element is encountered in the Earth's crust almost exclusively in the form of orthophosphates of which the apatites are most important, namely *fluorapatite* ($Ca_5[(PO_4)_3F]$), *chlorapatite* ($Ca_5[(PO_4)_3Cl]$) and *hydroxyapatite* ($Ca_5[(PO_4)_3(OH)]$). Besides, there are enormous deposits of amorphous *phosphorite* with a composition approximately corresponding to fluorapatite. In the year 2000, about $133 \cdot 10^6$ t of phosphate has been extracted. The bones of vertebrates consist of about 30% of collagen (a chained protein) and 70% of minerals, 87% of which is $Ca_5[(PO_4)_3(OH)]$ and 12% $Ca[CO_3]$. In the Earth's crust phosphorus is the 11th most abundant element.

Elemental phosphorus is produced from phosphorite by reduction with coke. Quartz is added in order to form a liquid slag of calcium silicate and fluoride or fluorosilicate that can flow freely from the furnace:

$$2\ Ca_5[(PO_4)_3F] + 15\ C + 9\ SiO_2 \longrightarrow 3\ P_2 + 15\ CO + 9\ Ca[SiO_3] + CaF_2$$

The very high temperature of 1400–1500 °C necessary for this reduction is reached in an electric arc furnace.[11] At this temperature, the phosphorus vapor exiting the furnace together with the carbon monoxide predominantly consists of P_2 molecules.[12] On cooling of the gas mixture rid of dust components, phosphorus is condensed by spraying of water into the gas stream. P_2 dimerizes to P_4 and is obtained as liquid white phosphorus (m.p. 44 °C, b.p. 280 °C; annual world production of about $0.9 \cdot 10^6$ t). Due to the high energy cost and environmental issues, P_4 production has been relocated predominantly to China, where approximately 70% of white phosphorus is produced.[13]

---

11 A modern furnace has a diameter of 12 m and produces 4 t P_4 per hour. To produce 1 t P_4, about 8 t of phosphorite, 2.8 t of quartz pebbles (SiO_2), 1.25 t of coke, 0.05 t of electrode mass (carbon) and 13 MWh of energy are needed. Side products are 7.7 t slags, 0.15 t ferrophosphorus (Fe_2P) and 2500 m^3 exhaust gas with about 85% CO content. The fluoride contained in the phosphorite ends up in the slag as CaF_2 or $Ca_4[Si_2O_7F_2]$.

12 The equilibrium $P_4 \rightleftharpoons 2\ P_2$ ($\Delta H^\circ_{298} = 240.6$ and $\Delta G^\circ_{298} = 193.7$ kJ mol^{-1}) lies on the right-hand side at temperatures above 1200 °C due to the positive reaction entropy; this is in analogy to the equilibrium $S_8 \rightleftharpoons 4S_2$; see Section 4.2.3. At 800 °C and ambient pressure less than 1%, P_4 is dissociated to P_2.

13 From a less regional point of view, this is a considerable problem and a prime example of economic considerations still being more important than the environmental impact.

All other phosphorus allotropes are produced from white phosphorus. About 70% of white phosphorus serves for the production of very pure *thermic phosphoric acid*, the remainder is converted to red phosphorus, phosphorus sulfides, chlorides and oxychlorides as well as to organic phosphorus compounds.

Arsenic mostly occurs in Nature in cationic forms (arsenic sulfides) and as anions (arsenides). Important minerals are the red *realgar* As_4S_4 and the yellow *auripigment* As_2S_3, both of which have been used in antiquity already and are converted to volatile arsenic trioxide (As_2O_3, "white arsenic") by roasting. *Arsenopyrite* (FeAsS) is a companion of iron ores. Due to the wide occurrence of metal arsenides, arsenic ores do not have to be mined. Instead, the element is obtained as a side product of the copper, tin, silver and gold purification. The technical As_2O_3 obtained upon roasting of the ores is either purified by sublimation or directly converted to $AsCl_3$ with HCl. The latter is fractionally distilled (b.p. 130 °C) and reduced as a vapor with H_2 at approximately 620 °C to metallic *gray arsenic*. Ultrapure arsenic (purified by sublimation) is employed for the synthesis of the semiconductor gallium arsenide (GaAs), which serves for the production of high-performance microprocessors in mobile phones, satellites and traffic control systems.

While the human body contains less than 0.3 ppm As, the concentration in some sea animals is as high as 3–30 ppm (Section 10.10.3).

10.3.2 Modifications of Phosphorus and Arsenic

White phosphorus is a colorless to yellowish, at room temperature waxy substance, which does not conduct electricity and consists of tetrahedral P_4 molecules in all phases.[14] This allotrope of phosphorus is toxic, extremely reactive and in finely divided form pyrophoric (self-igniting) in air. P_4 dissolves in organic solvents, particularly well in CS_2, but not in water and it is thus stored under water and kept wet to avoid oxidation or even self-ignition. The bonding in P_4 has been discussed previously (Section 2.4.9).

If white phosphorus is heated to 180–350 °C, particularly in the presence of catalytic quantities of iodine, it is converted in an exothermic reaction into polymeric, amorphous *red phosphorus*,[15] which crystallizes upon further heating to 450–550 °C under intensification of the color and is then referred to as violet phosphorus or HITTORF's *phosphorus*. Furthermore, by choosing suitable reaction conditions (about 580 °C) a fibrous modification of phosphorus has been prepared that is structurally

14 A. Simon, H. Borrmann, J. Horakh, *Chem. Ber*. **1997**, *130*, 1235; H. Okudera, R. E. Dinnebier, A. Simon, *Z. Kristallogr*. **2005**, *220*, 259.

15 In the technical process, red phosphorus is produced in large ball mills at a temperature slowly rising from 270 to 350 °C. Subsequently, it is washed with hot aqueous NaOH to remove residual P_4, dried under N_2 and stabilized against autoxidation by addition of $Mg[OH]_2$ or $Al[OH]_3$ if needed.

related to HITTORF's phosphorus.[16] These red modifications are specifically denser and significantly less reactive than white phosphorus and thus nontoxic. In addition, they are insoluble in CS_2 and with that identified as polymeric, which is also manifest in the much higher melting point of 610 °C. This "melting point" is really a decomposition temperature as these polymeric networks melt (and evaporate) under depolymerization resulting in P_4 molecules under ambient pressure. At temperatures above 800 °C, P_4 dissociates reversibly into two P_2 molecules with a formation enthalpy of 144 kJ mol^{-1} at 298 K.[11] The bond situation in P_2 corresponds to that in N_2 (Figure 2.23).

When white or red phosphorus are heated under high pressure (1.2 GPa at 200 °C), both are transformed into orthorhombic *black phosphorus*, which constitutes the thermodynamically most stable form under standard conditions. This reaction can be carried out in a high-energy ball mill, in which the steel balls locally generate the required temperature and pressure when hitting the walls and simultaneously the phosphorus. Larger crystals of P_{black} are obtained by prolonged heating of P_{red} in an evacuated ampoule to 600 °C in the presence of Au, Sn and SnI_4.[17] Black phosphorus crystallizes depending on the (increasing) pressure either in orthorhombic (semiconducting), rhombohedral (semimetallic) or cubic (metallic) structures. The density of these materials surpasses that of violet phosphorus; the cubic form is a superconductor at low temperature. Black phosphorus is insoluble and unreactive, but nonetheless slowly converts to phosphoric acid in humid air. At temperatures above of 550 °C it transforms into violet phosphorus, which then is the thermodynamically most stable form until the melting point (610 °C).

10.3.2.1 Structures of P and As Modifications

Phosphorus: *White phosphorus* forms several phases, the structures of which were difficult to determine as the near-spherical shape of the P_4 molecule experiences strong librations (pendulum motions) even at low temperature.[13] The α-phase, which is encountered at room temperature, is theoretically transformed into a β-phase at −76 °C, while below about −113 °C a cubic γ-phase is stable. All phases consist of P_4 molecules; the phase transitions are kinetically hindered.

The crystal structure of *HITTORF's phosphorus* is complicated and consists of tubular strands of P_2, P_8 and P_9 units, which are connected to neighboring perpendicular strands to form double layers (Figure 10.1b). The structural principle of fibrous phosphorus is very similar: it only differs inasmuch as that the interconnections of the above-described strands happen at the end of the P_9 unit and in parallel to the first strand (Figure 10.1a).[16] Both modifications contain only tricoordinate P atoms, which are interconnected by single bonds of 217–230 pm length.

16 M. Ruck et al., *Angew. Chem. Int. Ed.* **2005**, *44*, 7616.

17 S. Lange, P. Schmidt, T. Nilges, *Inorg. Chem.* **2007**, *46*, 4028.

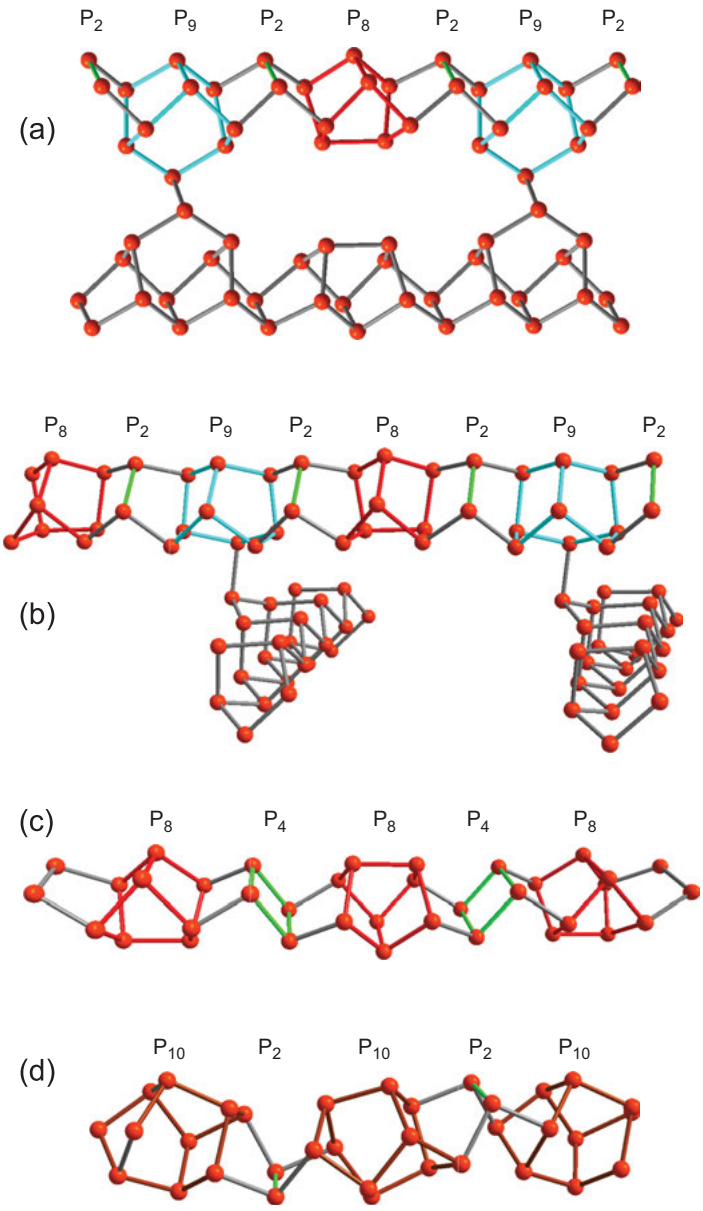

Figure 10.1: Connectivity of tubular phosphorus strands in fibrous phosphorus (a), in violet or HITTORF's phosphorus (b) and in two CuI–P_n phases (c, d; see text); adapted from M. Scheer, G. Balázs, A. Seitz, Chem. Rev. **2010**, *110*, 4236.

For *red phosphorus*, a structure of helical chains of P_2 and P_{10} units is assumed,[18] similar to the phosphorus substructure in $(CuI)_3P_{12}$, which has been determined by X-ray diffraction (Figure 10.1d). A related *phosphorus nanotube* with the motif P_4/P_8 is present in the adduct $(CuI)_8P_{12}$ (Figure 10.1c). These adducts are formed, when CuI is heated with red phosphorus to temperatures of 400–500 °C for several days. The phosphorus polymers can be isolated from these phases by extraction of the CuI with aqueous KCN solution.[19]

The crystals of orthorhombic black phosphorus consist of parallel stacked double layers of P atoms in six-membered rings in a chair conformation. In these layers, the rings are axially interconnected (Figure 10.2, right). The building principle of the structure results in a pronounced puckering of the layers. The forces between the layers are weak at standard pressure but increase significantly at pressures of about 10 GPa during the transition to a simple cubic phase.[20] Conversely, the interconnection of P_6 rings in *rhombohedral phosphorus* and the As_6 rings in the isostructural *gray arsenic* is equatorial (Figure 10.2, left).

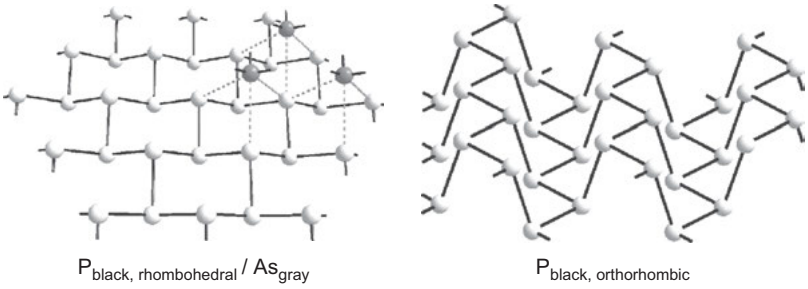

Figure 10.2: Structures of *orthorhombic black phosphorus* (right) and of *rhombohedral phosphorus* and *gray arsenic*, respectively (left).

In both halves of the double layer, the P atoms form zig-zag chains with valence angles of 97° and single bonds of 222.4 pm length.[17] Each P atom of the chain is additionally connected with an atom in the other half of the double layer (internuclear distance d_{PP} = 224.5 pm, angle 102°) so that a system of condensed six-membered rings is obtained. Remarkably, the smallest distance between two not directly connected atoms of a double layer (d'_{PP} = 331 pm) is considerably shorter than the VAN DER WAALS distance of 380 pm. This suggests the presence of weak dative bonds. The ratio d'/d is approximately 1.49 and corresponds to that in gray selenium (Table 12.3),

18 H. Hartl, *Angew. Chem. Int. Ed. Engl.* **1995**, *34*, 2637; S. Böcker, M. Häser, *Z. Anorg. Allg. Chem.* **1995**, *621*, 258.
19 M. H. Möller, W. J. Jeitschko, *J. Solid State Chem.* **1986**, *65*, 178. A. Pfitzner, E. Freudenthaler, *Angew. Chem. Int. Ed.* **1995**, *34*, 1647. A. Pfitzner et al., *Angew. Chem. Int. Ed.* **2004**, *43*, 4228.
20 M. Ceppatelli et al., *Angew. Chem. Int. Ed.* **2017**, *56*, 14135

which also shows semiconducting properties. The smallest distance between the double layers of black phosphorus is with 359 pm still significantly smaller than the VAN DER WAALS distance. Nonetheless, the bonds between the double layers are weak and cause a similarly facile cleavage along the layers as in graphite.[19]

The band gap of orthorhombic black phosphorus is 0.33 eV. In analogy to graphene (Section 7.3.1), single double layers of black phosphorus are sometimes called *phosphorene*, but since this material only contains single bonds (and no double bonds as the suffix -ene would suggest) it is also referred to as 2D-phosphane or simply as black phosphorus single sheets.[21] Such single sheets are either prepared micromechanically in case of small samples or by ultrasonication of the bulk on a larger scale. The semiconducting properties of black phosphorus are retained in the 2D material (in contrast to the metallic graphene), which creates various opportunities for application, for example, as field effect transistors in microelectronics. In the form of isolated double layers, the otherwise unreactive black phosphorus degrades within hours in humid air. The stability can be increased considerably by coverage with a protective layer of Al_2O_3, graphene or boron nitride. The sensitivity of phosphorene toward moisture has been exploited in humidity sensors.

The density of phosphorus modifications rises steadily from white (1.82 g cm^{-3}) and red (~2.16), via violet (2.35) and orthorhombic (2.70) to rhombohedral (3.56) and cubic phosphorus (3.88 g cm^{-3}). Red phosphorus is employed for production of matches and in pyrotechnics.

Due to the low reactivity of red and black phosphorus modifications, white phosphorus is used preferentially in synthesis. Its reactivity at low temperature can be enhanced by activation, whereupon products are obtained that contain residual PP bonds or even extended P_n scaffolds. The activation can be effected by main group elements and their compounds[22] or by transition metal complexes.[23] Just three particularly fascinating new and strictly inorganic reaction products will be presented here together with the synthetic procedures.[24] The cation $[NO]^+$ inserts into one of the PP bonds of P_4, when the salt $[NO][Al\{OC(CF_3)_3\}_4]$ is reacted with white phosphorus in CH_2Cl_2 at room temperature. The product contains the C_{2v}-symmetric cation $[P_4NO]^+$ with the above-mentioned weakly coordinating aluminate cation derived from perfluoro-*tert*-butanol. If an excess of P_4 is employed, the salt $[P_9][Al\{OC(CF_3)_3\}_4]$ is obtained, which features the first homoatomic *polyphosphorus cation* (D_{2d} symmetry):

21 Reviews: H. Wang, M. Dresselhaus et al., *Proc. Natl. Acad. Sci. U. S. A.* **2015**, *112*, 4523. M. Pumera et al., *Angew. Chem. Int. Ed.* **2017**, *56*, 8052.

22 M. Scheer, G. Balázs, A. Seitz, *Chem. Rev.* **2010**, *110*, 4236. M. Scheer et al., *Angew. Chem. Int. Ed.* **2010**, *49*, 6860.

23 B. M. Cossairt, N. A. Piro, C. C. Cummins, *Chem. Rev.* **2010**, *110*, 4164. M. Caporali et al., *Chem. Rev.* **2010**. *110*, 4178. S. Dürr, D. Ertler, U. Radius, *Inorg. Chem.* **2012**, *51*, 3904.

24 I. Krossing et al., *Angew. Chem. Int. Ed.* **2010**, *49*, 8139 and **2012**, *51*, 6529.

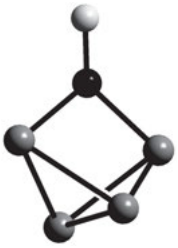

$[P_4NO]^+$

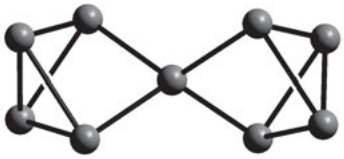

$[P_9]^+$

Considering the central P atom of $[P_9]^+$ as P^+ (isoelectronic with Si), the tetrahedral coordination becomes plausible. In $[P_4NO]^+$, the positive charge is largely localized at the two P atoms connected to the nitrogen atom (depicted in black). Similarly, the protonation of P_4 with the BRØNSTED superacid $H[Al(OTeF_5)_4]$ exclusively yields the edge-protonated $[P_4H]^+$ according to ^{31}P-NMR data (see Fig. 2.35).[25]

Arsenic: Three crystalline modifications are known of *arsenic*, which are very similar to the analogous phosphorus allotropes. The thermodynamically stable form at ambient conditions is the *rhombohedral gray arsenic*. It conducts electricity and shows metallic luster (density 5.78 g cm^{-3}). Its crystals consist of puckered layers of As atoms, which are connected to six-membered rings within the layers. Each atom has three nearest neighbors in its own layer at a distance of 252 pm as well as three next but one neighbors in the adjacent layer at 312 pm. These secondary contacts are shown in Figure 10.2 (left) with dashed bonds to the three darkened atoms of the next layer. The local coordination of the As atoms is therefore 3 + 3 and distorted octahedral. The VAN DER WAALS distance is 400 pm in this case.

On heating, gray arsenic sublimes at about 610 °C without prior melting. During this process, *depolymerization* occurs in a similar manner as for red and black phosphorus; the vapor consists of tetrahedral As_4 molecules (d_{AsAs} = 244 pm). If this vapor is introduced into ice-cold CS_2, a solution of As_4 is obtained, from which *yellow arsenic*, consisting of As_4 molecules, crystallizes upon concentrating and cooling. This modification corresponds to white phosphorus and is an electrical insulator. At room temperature, yellow arsenic is rapidly converted to gray arsenic, in particular when exposed to light. Polymerization of yellow arsenic to 1D chains has been achieved at the interior of carbon nanotubes.[26]

In gaseous mixtures of P_4 and As_4 at temperatures around 1000 °C, the mixed tetrahedral molecules AsP_3, As_2P_2 and As_3P have been detected spectroscopically, but only AsP_3 was isolated in pure form. This was achieved by taking advantage of ligand transfer from an anionic niobium complex with a P_3 ligand (L = 2,6-diisopropylphenyl):

25 C. Müller, S. Riedel et al., *Chem. Sci.* **2018**, *9*, 7169

26 C. G. Salzmann et al., *Angew. Chem. Int. Ed.* **2018**, *57*, 11649.

$$Na[L_3NbP_3] + AsCl_3 \xrightarrow[THF]{22°C} AsP_3 + L_3NbCl_2 + NaCl$$

AsP_3 melts without decomposition at 72 °C but decomposes slowly at 300 °C to red phosphorus and gray arsenic. In a similar fashion as P_4, the mixed AsP_3 exhibits so-called *spherical aromaticity*, which is characterized by a diamagnetic cluster current. Numerous transition metal complexes are known with As_4, As_3P and AsP_3 as ligands.[27]

Metallic arsenic is considerably less toxic than As_2O_3; in low concentration it is employed as a hardening component of lead, bronze and copper alloys as well as for production of certain glasses.

10.4 Hydrides of Phosphorus and Arsenic

The most important hydrides of phosphorus and arsenic are:

PH_3	$H_2P–PH_2$	AsH_3
Phosphane	Diphosphane	Arsane
(phosphine)		(arsine)

Only two further hydrides are known of arsenic. Diarsane (As_2H_4) is formed during the decomposition of AsH_3 in a glow discharge and is only persistent at temperatures below –100 °C. Triarsane (As_3H_5) is formed in traces upon acidic hydrolysis of MgPAs alloy. In contrast, a large number of hydrides are known in the case of phosphorus. As described in Section 4.2, the average bond enthalpy of the PP single bond is considerably larger than that of NN or AsAs single bonds. Just like sulfur and silicon, phosphorus shows a pronounced tendency to form chains, rings and cages, which are not observed to any comparable extent for either nitrogen or arsenic.[28] Apart from PH_3 and P_2H_4, however, only P_3H_5, P_5H_5 and P_7H_3 have been isolated in pure form showing the following structures:

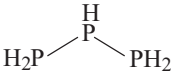

Chain

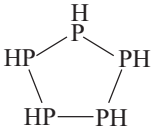

Ring

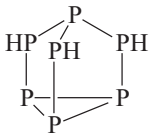

Cage

PH_3, P_2H_4 and P_3H_5 are the starting members of the homologous series of *chain-like phosphanes* with the general formula P_nH_{n+2}. Conversely, P_5H_5 is a representative

27 C. Schwarzmeier, M. Sierka, M. Scheer, *Angew. Chem. Int. Ed.* **2013**, *52*, 858. B. M. Cossairt, C. C. Cummins, *J. Am. Chem. Soc.* **2009**, *131*, 15501.

28 M. Baudler, K. Glinka, *Chem. Rev.* **1993**, *93*, 1623.

of the *monocyclic phosphanes* of the general formula P_nH_n, while P_7H_3 is a typical *polycyclic phosphane*. Apart from these compounds, numerous phosphorus-rich hydrides have been identified by NMR spectroscopy. These phosphanes are unstable and can be enriched to some extent but cannot be obtained in pure form. Many substituted derivatives (organophosphanes), however, as well as salts (polyphosphides) have been isolated (see Sections 10.5 and 10.6).

10.4.1 Phosphane and Arsane

PH_3 is a colorless, extremely toxic gas (b.p. –88 °C) with the characteristic odor of garlic or rotten fish, which is best produced in the lab by hydrolysis of calcium phosphide:

$$Ca_3P_2 + 6\,H_2O \longrightarrow 2\,PH_3\uparrow + 3\,Ca[OH]_2$$

As side product, diphosphane is formed, which can be separated by fractionate condensation and distillation. For the technical PH_3 synthesis, white phosphorus is disproportionated in hot aqueous sodium hydroxide solution:

$$P_4 + 3\,NaOH + 3\,H_2O \longrightarrow PH_3\uparrow + 3\,Na[H_2PO_2]$$

The phosphinate (obsolete name: hypophosphite) formed as a side product serves as a technical reductant. In an alcoholic medium, the reaction can also be conducted in such a manner that phosphonate is formed, whereupon the yield in PH_3 is doubled:

$$P_4 + 4\,NaOH + 2\,H_2O \longrightarrow 2\,PH_3\uparrow + 2\,Na_2[HPO_3]$$

AsH_3 (b.p. –62 °C) is a similarly toxic gas, which is generated by the hydrogenation of arsenic compounds:

$$AsCl_3 + 3\,Li[AlH_4] \xrightarrow{-90\,^\circ C} AsH_3\uparrow + 3\,LiCl + 3\,AlH_3$$

$$[HAsO_4]^{2-} + [BH_4]^- + 2\,H^+ \longrightarrow AsH_3\uparrow + [B(OH)_4]^-$$

Arsane (AsH_3) is also generated by the reaction of nascent hydrogen (from zinc and dilute sulfuric acid) with water-soluble arsenic compounds. This reaction is employed for the detection of arsenic by the MARSH test for which the gas mixture of H_2 and AsH_3 is ignited after exiting a nozzle and the flame directed to a cold surface where a black arsenic mirror is deposited.

PH_3 and AsH_3 are sensitive to oxidation and burn in air to H_3PO_4 and As_2O_3, respectively, together with H_2O. Upon heating, PH_3 decomposes partially, and AsH_3 completely into the elements. Both hydrides show positive formation enthalpies [$\Delta_f H°_{298}(PH_3)$: +5.5 kJ mol^{-1}; AsH_3: +66.4 kJ mol^{-1}]. The molecules PH_3 and AsH_3 are of trigonal-pyramidal geometry just like NH_3 but the valence angles strongly decrease from NH_3 to SbH_3:

NH_3: 107.3° PH_3: 93.8° AsH_3: 91.8° SbH_3: 91.7°

The nonbonding electron pairs of PH_3 and AsH_3 are much less directional than in NH_3 as they occupy orbitals of almost pure *s* character. Therefore, the LEWIS basicity of the hydrides decreases strongly from NH_3 to AsH_3. The less pronounced tendency toward hybridization is also responsible for the much higher barrier of *pyramidal inversion* (Section 9.3) in comparison to NH_3 and the amines (NH_3: 24, PH_3: 156 kJ mol^{-1}). Therefore, chiral substituted phosphanes[29] and arsanes can be separated into *enantiomers* at 25 °C.

Reactions: On protonation of the hydrides PH_3 and AsH_3, the tetrahedral phosphonium and arsonium ions $[PH_4]^+$ and $[AsH_4]^+$ are formed. Salts with these cations dissociate much more readily into PH_3 and AsH_3 and the corresponding acids than it is the case for the analogous ammonium salts. $[PH_4]I$, which is obtained under anhydrous conditions from PH_3 and HI, sublimes under dissociation at 80 °C, $[PH_4]Cl$ even at −28 °C. In aqueous solution, $[PH_4]I$ hydrolyzes to PH_3, $[H_3O]^+$ and I^-. Consequently, pure PH_3 can conveniently be produced from $[PH_4]I$ and a base:

$$[PH_4]I + KOH \longrightarrow PH_3\uparrow + KI + H_2O$$

$[AsH_4]Br$ and $[AsH_4]I$ are formed when AsH_3 and HBr or HI are co-condensed at −160 °C. At room temperature, the parent arsonium salts with just hydrogen substituents are unstable.

If PH_3 is introduced into a solution of sodium in liquid ammonia, colorless crystals of the salt $Na[PH_2]$ are obtained:

$$PH_3 + Na \xrightarrow{NH_3\ (l.)} Na[PH_2] + \tfrac{1}{2} H_2$$

Arsane (AsH_3) reacts in an analogous manner. The organic derivatives of dihydrogenphosphides, $Li[PR_2]$ and $K[PR_2]$, are accessible from R_2PCl and the corresponding alkali metal and are immensely valuable in synthesis, for example, in the formation of PP bonds:

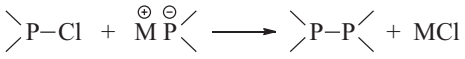

Industrially, PH_3 and AsH_3 are employed for the incorporation of traces of phosphorus and arsenic into semiconductor silicon (*n-doping*). The semiconductor gallium arsenide can be produced from AsH_3 and Me_3Ga by elimination of methane. In addition, PH_3 serves for the epitaxial growth of InP and GaInAsP layers as well as for the *hydrophosphination* of formaldehyde in hydrochloric acid solution:

$$PH_3 + 4\,HCHO + HCl \longrightarrow [P(CH_2OH)_4]Cl$$

29 K. M. Pietrusiewicz, M. Zablocka, *Chem. Rev*. **1994**, *94*, 1375.

Phosphonium chloride $[PH_4]Cl$ is applied to cellulose textile (cotton) and artificial fibers in order to convey flame-retardant properties.

10.4.2 Diphosphane(4)

As in the case of oligoboranes, the names of the higher phosphanes indicate the number of P atoms and – in brackets – the number of H atoms. Diphosphane(4) P_2H_4,[30] the analogue of hydrazine N_2H_4, is formed as a side product during the hydrolytic decomposition of Ca_3P_2 as this phosphide is produced from calcium and excess phosphorus and therefore not only contains P^{3-} ions, but also the diphosphide $Ca_2[P–P]$:

$$Ca_2[P_2] + 4\,H_2O \longrightarrow P_2H_4 + 2\,Ca[OH]_2$$

$Ca_2[P_2]$ contains dumbbells of $[P_2]^{4-}$ ions, which are isoelectronic with the disulfide anion $[S_2]^{2-}$. Due to its lower volatility, P_2H_4 can be separated from PH_3 by distillation and be isolated as a colorless liquid. The decomposition of PH_3 in an electric discharge also yields P_2H_4 (and H_2). In the gas phase, just as in the case of the analogous N_2H_4, P_2H_4 molecules exist predominantly in the *gauche* conformation with d_{PP} = 222 pm. P_2H_4 is pyrophoric in air and decomposes slowly to PH_3 and higher phosphorus hydrides with less hydrogen content. Triphosphane (P_3H_5) has been isolated in pure form while the higher homologues (P_4H_6 to P_9H_{11}) have been detected only spectroscopically (MS, NMR):

$$2\,P_2H_4 \longrightarrow PH_3 + P_3H_5$$

A mixture of P_3H_5 and P_4H_6 decomposes above –20 °C as follows:

$$P_3H_5 + P_4H_6 \longrightarrow \textit{cyclo}\text{-}P_5H_5 + 2\,PH_3$$

An interesting salt of triphosphane(5) is formed during the reduction of P_4 with potassium in liquid ammonia at –40 °C; it was isolated in crystalline form as the ammoniate $K_3[P_3H_2]\cdot 2.3NH_3$. The H atoms of the anion are located at the terminal P atoms.[31]

Pentaphosphane(5) is the thermally and thermodynamically most stable *cyclo*-polyphosphane. The tricyclic P_7H_3 (structure, see above) is obtained in the following manner:

$$Li_3[P_7] + 3\,Me_3SiCl \longrightarrow (Me_3Si)_3P_7 + 3\,LiCl$$

$$(Me_3Si)_3P_7 + 3\,MeOH \xrightarrow{-40\,^\circ C} P_7H_3 + 3\,Me_3SiOMe$$

30 M. Baudler, K. Glinka, *Chem. Rev*. **1993**, *93*, 1623 and **1994**, *94*, 1273.
31 N. Korber et al., *Inorg. Chem*. **2009**, *48*, 1911.

10.5 Phosphides

Phosphorus forms binary compounds with almost all elements; in most cases, several stoichiometric ratios are possible.[32] Therefore, a very large number of binary phosphides and polyphosphides are known. Representative examples are the following structurally characterized phases produced from lithium and phosphorus:

Li_3P	LiP	Li_3P_7	$Li_3P_{8.33}$	LiP_5	LiP_7	LiP_{15}
(P^{3-})	$^1_\infty(P^-)$	$([P_7]^{3-})$	$([P_7]^{3-})([P_{11}]^{3-})$	$^3_\infty([P_5]^-)$	$^1_\infty([P_7]^-)$	$^1_\infty([P_{15}]^-)$

The composition of the respective anions is indicated below the empirical formula: the structures variously comprise monoatomic trianions, polycyclic cage anions and one-, two- and three-dimensionally connected polyanions, represented by $^x_\infty$ with x indicating the dimensionality. For example, $^1_\infty([P_7]^-)$ is a one-dimensionally connected indefinite chain of P_7 cages, each cage carrying one negative charge. The frequently observed cage ions $[P_7]^{3-}$ and $[P_{11}]^{3-}$ show the following structures:

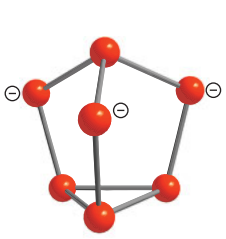

$[P_7]^{3-}$

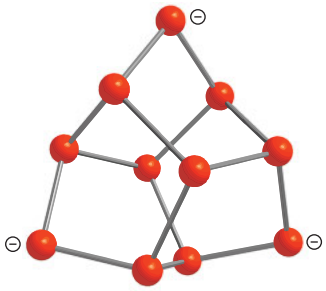

$[P_{11}]^{3-}$

The binary systems Na/P and K/P comprise a similarly large number of compounds.[33] Most of these phosphides are electron-precise and thus only contain 2-center 2-electron (2c,2e) bonds; the two-coordinate P atoms formally carry the negative charges. In addition, molecular polyphosphide anions are known that exclusively consist of two-coordinate P atoms (see below).

Many metal phosphides are produced by cautious heating of phosphorus with the corresponding metal under exclusion of air, for example, Na_3P, Ca_3P_2, CaP and $Li_3[P_7]$. Another suitable method is the reduction of phosphorus with alkali and alkaline earth metals in liquid ammonia (Section 9.4.8). If red phosphorus is digested with $K[PH_2]$ in dimethylformamide, $K[P_5]$ and $K_2[HP_7]$ are formed from which $K_2[HP_7]$

32 R. Pöttgen, W. Hönle, H. G. v. Schnering, *Encycl. Inorg. Chem.* **2005**, *7*, 4255 and *Chem. Rev.* **1988**, *88*, 243.

33 J. M. Sangster *J. Phase Equil. Diffus.* **2010**, *31*, 62 and 68.

can be separated by crystallization; K[P_5] remains in solution. It contains the cyclic anion $[P_5]^-$ shown below, which is just one of many examples of nonmetallic anions and cations with planar rings of between four and ten atoms. The bonding in such planar species can formally be dissected into σ framework and π system. Further representatives of this compound class are $[P_4]^{2-}$, $[As_4]^{2-}$, $[S_4]^{2+}$, $[P_6]^{4-}$ and $[S_5N_5]^+$. The number of available electrons (6, 10 or 14) in the π orbitals of these species adheres to the $4n + 2$ rule derived from HÜCKEL MO theory of aromatic species. The cyclic delocalization of the π electrons leads to particularly stable compounds. For instance, the square-planar $[P_4]^{2-}$ constitutes the anion of the salt $Cs_2[P_4]{\cdot}2NH_3$[34] and the hexagonal-planar $[P_6]^{4-}$ that of $K_4[P_6]$:[35]

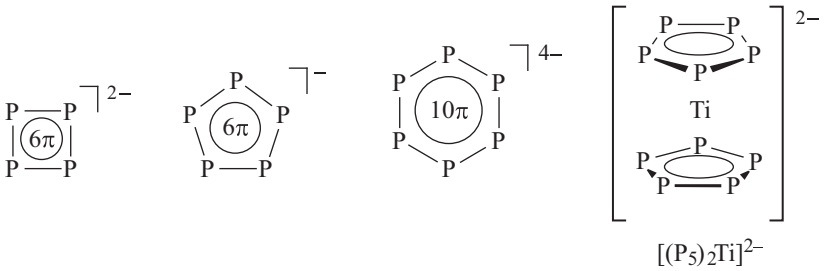

$[(P_5)_2Ti]^{2-}$

The $[E_4]^{2+}$ cations (E = S, Se, Te), which are valence isoelectronic to $[P_4]^{2-}$, are also 6π-electron HÜCKEL aromatics (Section 12.5). The π MOs of the four- and five-membered ring systems are shown in Figure 10.3. The aromatic character of $[P_4]^{2-}$, $[P_5]^-$ and $[P_6]^{4-}$ also becomes apparent in their ability to function as ligands toward transition metals.[36] A particularly beautiful example for such a metallocene-like sandwich complex is the dianion $[(\eta^5\text{-}P_5)_2Ti]^{2-}$ containing Ti(0) and shown above.[37]

Alongside the ionic phosphides, covalent (e.g., BP, SiP) and metal-like (e.g., ferrophosphorus, Fe_2P) examples exist. Accordingly, the *electrical conductivity* of phosphides ranges from those of insulators, semi-conductors and metallic conductors to low-temperature superconductors. AlP and Zn_3P_2 serve as a source of toxic PH_3 in pest control. They are produced from red phosphorus and the corresponding metal powder.

Gallium phosphide obtained from the ultrapure elements is used for the production of green light emitting diodes. The analogous *gallium arsenide* (GaAs) is an important semiconducting material (m.p. 1240 °C; zinc blende structure), which is prepared by melting together the elements under an H_2 atmosphere and purified by growing single crystals according to the methods of BRIDGMAN or CZOCHRALSKI.[38] The band gap of

34 N. Korber et al., *Angew. Chem. Int. Ed.* **2003**, *42*, 4029 and *Inorg. Chem.* **2006**, *45*, 1117.
35 H. P. Abicht, W. Hönle, H. G. V. Schnering, *Z. Anorg. Allg. Chem.* **1984**, *519*, 7.
36 Complexes with P_n and As_n ligands: O. J. Scherer, *Acc. Chem. Res.* **1999**, *32*, 751. M. Peruzzini, L. Gonsalvia, A. Romerosa, *Chem. Soc. Rev.* **2005**, *34*, 1038.
37 E. Urnezius et al., *Science* **2002**, *295*, 832.
38 J. F. Janik, *Powder Techn.* **2005**, *152*, 118.

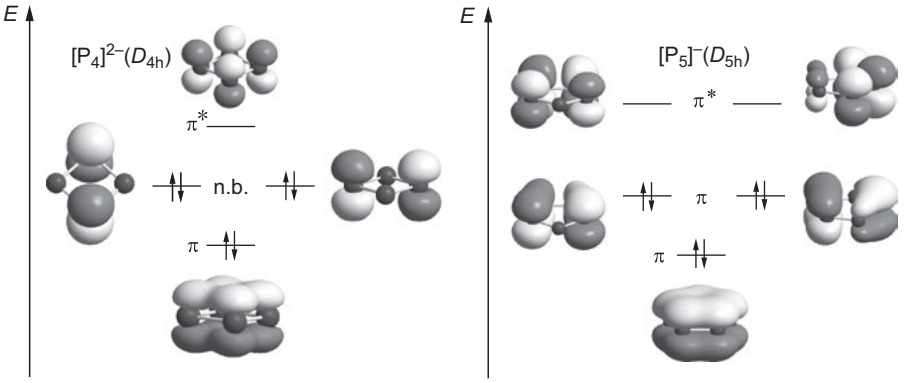

Figure 10.3: The π molecular orbitals of the Hückel aromatics $[P_4]^{2-}$ and $[P_5]^-$. Analogous MOs in adapted form are encountered in the ions $[E_4]^{2+}$ (E = S, Se, Te).

1.42 eV can be tuned into the visible region by addition of Al, which allows for the production of alloys of the composition $Al_nGa_{1-n}As$ suitable for LEDs and lasers.

10.6 Organophosphanes

The H atoms of the hydrides of phosphorus can formally be replaced by alkyl, aryl (R) or silyl groups (SiR_3).[39] Numerous such derivatives of acyclic, monocyclic and polycyclic phosphanes are known.[40] The most important organophosphanes are the monophosphorus species of type PR_3 and the monocyclic derivatives $(PR)_n$ with $n = 3–6$.

The PR_3 synthesis is typically achieved from PCl_3 and organometallic compounds RM (M = Li, MgX). In these reactions, the chlorine atoms are substituted by R in a stepwise manner, although the relative reaction rates of first, second and third substitution may not always allow for the isolation of the partially substituted intermediates. For example, triphenylphosphane is accessible from PCl_3 and either PhMgBr or PhLi. Occasionally, the reductive dehalogenation of PCl_3 and RCl with sodium can be employed. Industrially, numerous phosphanes are produced from PH_3 by *hydrophosphination*, i.e. the addition of PH bonds to olefins.

39 R. Engel, J. I. Cohen, *Encycl. Inorg. Chem.* **2005**, *7*, 4355. K. B. Dillon, F. Mathey, J. F. Nixon, *Phosphorus – The Carbon Copy: From Organophosphorus to Phosphaorganic Chemistry*, Wiley, **1998**.
40 Organo derivatives: M. Baudler, K. Glinka, *Chem. Rev.* **1993**, *93*, 1623. Silyl derivatives: G. Fritz, P. Scheer, *Chem Rev.* **2000**, *100*, 3341.

Organically substituted phosphanes and arsanes are stronger LEWIS bases than the corresponding hydrides. For example, Ph_3P reacts with phenyl iodide to the salt-like tetraphenylphosphonium iodide:

$$PCl_3 + 3\ PhLi \xrightarrow{-3LiCl} Ph_3P \xrightarrow{+PhI} [Ph_4P]I$$

Analogous considerations apply to Ph_3As, which is produced from $AsCl_3$. Organophosphanes and -arsanes serve as *ligands* in transition metal complexes. The size (cone angle) and donor properties (HOMO energy) can be tuned by variation of R.[41] In many cases, bidentate bis(phosphane) ligands such as $R_2P–(CH_2)_n–PR_2$ are preferred due to the increased stability of the corresponding complexes based on the *chelate effect*. In case of R = Ph the following abbreviations are common: dppm (n = 1), dppe (n = 2) and dppp (n = 3). The corresponding metal complexes are industrial *catalysts* of tremendous importance.

Typically, during dehalogenation of diorganylchlorophosphanes (R_2PCl), the corresponding diphosphanes (R_4P_2) are formed. If the P atom is shielded by sterically demanding substituents, however, a room-temperature persistent dialkylphosphanyl radical is obtained, which exists in monomeric form even in the solid state (yellow crystals):[42]

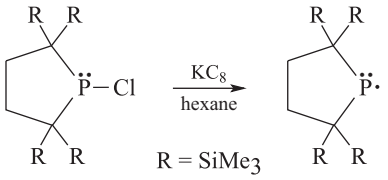

Potassium graphite is employed as a reducing agent (Section 7.5.2).

In the series of *cyclic phosphanes* R_nP_n, for example, the phenyl compounds with n = 3–6 are known showing the following structures:

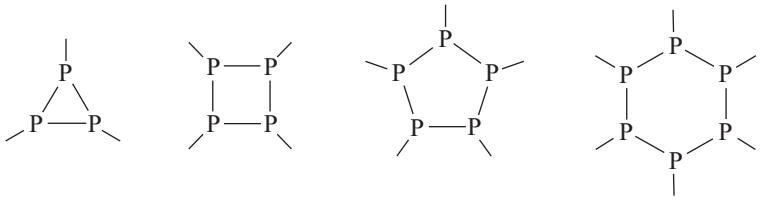

Only the P_3 ring is planar, all other cycles are puckered. The relative stability of ring sizes varies with the size of the substituents; small rings are stabilized by large

41 P ligands: A. Schier, H. Schmidbaur, *Encycl. Inorg. Chem.* **2005**, *7*, 4101. Chiral phosphanes: D. S. Glueck, *Chem. Eur. J.* **2008**, *14*, 7108. Cone angle: K. A. Bunten et al., *Coord. Chem. Rev.* **2002**, *233–234*, 41.

42 S. Ishida, F. Hirakawa, T. Iwamoto, *J. Am. Chem. Soc.* **2011**, *133*, 12968.

substituents as the steric strain on the outer angles favors smaller inner angles within the ring. The following synthetic pathways provide access to *cyclo*-phosphanes:

$$RPH_2 + Cl_2PR \longrightarrow \frac{2}{n}(RP)_n + 2\,HCl$$

$$RPX_2 + 2\,M \longrightarrow \frac{1}{n}(RP)_n + 2\,MX \qquad M: Li, Na, Mg; X: Cl, Br$$

$$P_4 + 2\,RMgBr + 2\,RBr \longrightarrow \frac{4}{n}(RP)_n + 2\,MgBr_2$$

All monocyclic phosphanes as well as the ionic polyphosphides are based on rings with sizes between 3 and 6. From the polyphosphides, the corresponding organopolyphosphanes can be obtained by alkylation with MeBr:

$$Li_3[P_7] + 3\,MeBr \longrightarrow Me_3P_7 + 3\,LiBr$$

By chlorination, the oligophosphanes can be cleaved to smaller organylchlorophosphanes, although salts with phosphinochlorophosphonium cations can also be obtained under certain conditions, for example:

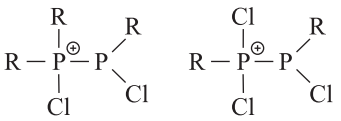

R = Ph, Et

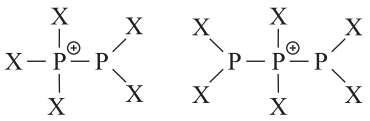

X = Br, I

To this end, it is necessary to add a suitable chloride ion acceptor such as $AlCl_3$ or $GaCl_3$ that binds the liberated halide ions.[43]

Arsenic: Besides the numerous polyphosphanes, many analogous compounds with AsAs single bonds have been prepared, for example, As_2I_4, Me_4As_2, As_4S_3 as well as *cyclo*-arsanes $(RAs)_n$ such as $(CF_3As)_4$, $(MeAs)_5$ and $(PhAs)_6$.[44]

10.7 Diphosphenes and Phosphaalkynes

Diphosphenes are the phosphorus homologues of diazenes RN=NR:

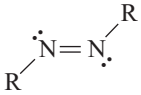

E-diazene

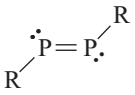

E-diphosphene

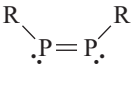

Z-diphosphene

43 J. J. Weigand, N. Burford et al., *J. Am. Chem. Soc.* **2009**, *131*, 17943. N. Burford et al., *Inorg. Chem.* **2011**, *50*, 3342 and *Chem. Asian J.* **2008**, *3*, 28.

44 I. Haiduc, D. B. Sowerby (eds.), *The Chemistry of Inorganic Homo- and Heterocycles*, Vol. 2, Academic Press, London, **1987**.

Both compound classes typically show planar scaffolds CNNC and CPPC, which leads to the existence of *cis*- and *trans*-isomers. They are also referred to as *Z* and *E* isomers; this nomenclature is derived from the German words "zusammen" (together) and "entgegen" (opposing), which identifies the relative positions of the residues R. Diphosphenes stable under standard conditions have only been obtained after the realization that bulky substituents were required to suppress the dimerization to *cyclo*-tetraphosphanes. The synthesis finally succeeded with the reductive dehalogenation of organyldichlorophosphanes with magnesium:

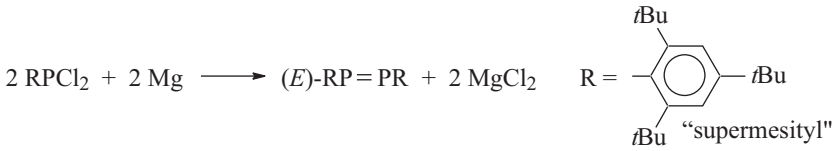

During this synthesis, the *E* isomer is obtained, which is air-stable. The PP internuclear distance of 203 pm as determined in the solid state by X-ray diffraction is significantly smaller than that in black phosphorus (222 pm). This shortening is due to a $(p–p)\pi$ bond in addition to the σ bond; this bonding situation is similar to that of alkenes and diazenes. The isomerization to the *Z* isomer is achieved by laser irradiation: a π electron is excited from the HOMO to the LUMO(π^*), which results in a practically vanishing rotational barrier of the PP bond. The rotational barrier for the parent compound HP=PH amounts to 132 kJ mol^{-1} and the *E* isomer is by 13 kJ mol^{-1} more stable than the Z isomer.[45] Numerous analogous species R–E=E–R with P=P, P=As, P=Sb and As=As multiple bonds have been prepared.[46] Even molecular compounds with Sb=Sb and Bi=Bi double bonds are known.[47] In contrast to disilenes and their heavier homologues, E=E double bonds of Group 15 show a remarkably "classical" behavior.[48]

Further species with classical double bonds involving phosphorus are known in the form of phosphoryl compounds such as Cl–P=O[49] and the related phosphazenes of three-valent phosphorus (–P=N–) as well as in phosphaalkenes (–P=C<) and the phosphasilenes (–P=Si<).[50] Conversely, triple bonds to phosphorus have rarely been realized. Examples are the *phosphaalkynes* R–C≡P, which correspond to the nitriles R–C≡N. A phosphaalkyne, stable at 20 °C, can be prepared as follows:[51]

45 W. W. Schoeller et al., *J. Chem. Soc. Faraday Trans.* **1997**, *93*, 2957. H. F. Schäfer III et al., *J. Phys. Chem. A* **2009**, *113*, 13227.

46 E. Niecke, O. Altmeyer, M. Nieger, *Angew. Chem. Int. Ed. Engl.* **1991**, *30*, 1136. M. Yoshifuji, K. Toyota, *Chem. Org. Silicon Comp.* **2001**, *3*, 491 and *Pure Appl. Chem.* **2005**, *77*, 2011.

47 N. Tokitoh, Y. Arai, R. Okazaki, S. Nagase, *Science* **1999**, *120*, 433.

48 P.P. Power, *Chem. Rev.* **1999**, *99*, 3463.

49 M. Binnewies, H. Schnöckel, *Chem. Rev.* **1990**, *90*, 321.

50 Compounds with C=P bonds: J. I. Bates, J. Dugal-Tessier, D. P. Gates, *Dalton Trans.* **2010**, *39*, 3151. Compounds with Si=P bonds: V. Nesterov, N. C. Breit, S. Inoue, *Chem. Eur. J.* **2017**, *23*, 12014.

51 F. Mathey, *Angew. Chem. Int. Ed.* **2003**, *42*, 1578.

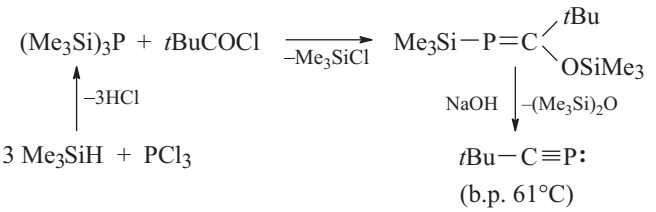

The CP internuclear distance of 153.6 pm is considerably smaller than CP single bonds (187 pm) and thus corresponds to a triple bond. On heating to 130 °C in a sealed tube, the compound tetramerizes to tetraphosphacubane $(RCP)_4$, which only contains single bonds.[52] The arsa- and phosphaalkynes Mes*C≡E (E = P, As; Mes* = 2,4,6-*tert*-$Bu_3C_6H_2$) can be converted to the corresponding five-membered 1,2,3-triazoles by "clicking" with organic azides in a [2 + 3] HUISGEN cycloaddition.[53]

A spectacular mixed phosphaalkene and diphosphene is obtained from the reaction of a bulky N-stabilized carbene with P_4: $R_2C{=}P{-}P{=}P{-}P{=}CR_2$ (CR_2 denotes the carbene moieties). The CP_4C chain is planar and exists as a mixture of *Z* and *E* isomers. The latter is dark-blue and melts at 184 °C.[54]

From organophosphorus compounds, which occasionally feature phosphorus atoms in unusual bonding situations, π conjugated polymers with unique properties have been prepared.[55] Structural building blocks of such materials are:

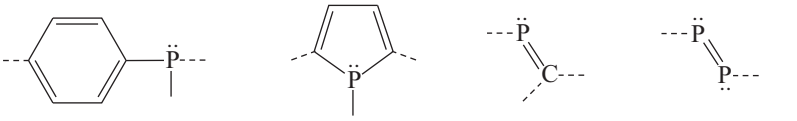

Dashed bonds indicate all positions, where phosphorus can be incorporated into the polymer as a structural element. As the electronic properties of the phosphorus centers can readily be modified by oxidation or adduct formation with LEWIS acids or metals, these materials are promising for the application in optoelectronics.

10.8 Halides of Phosphorus and Arsenic

Elemental phosphorus reacts with all halogens under formation of phosphorus halides and halide ions. The following molecules and ions (with exception of P_2X_{10}) have been structurally characterized:

52 A. Mack, M. Regitz, *Chem. Ber.* **1997**, *130*, 823.
53 C. Müller et al., *Angew. Chem. Int. Ed.* **2016**, *55*, 11760.
54 G. Bertrand et al., *Angew. Chem. Int. Ed.* **2007**, *46*, 7052.
55 T. Baumgartner, R. Reau, *Chem. Rev.* **2006**, *106*, 4681.

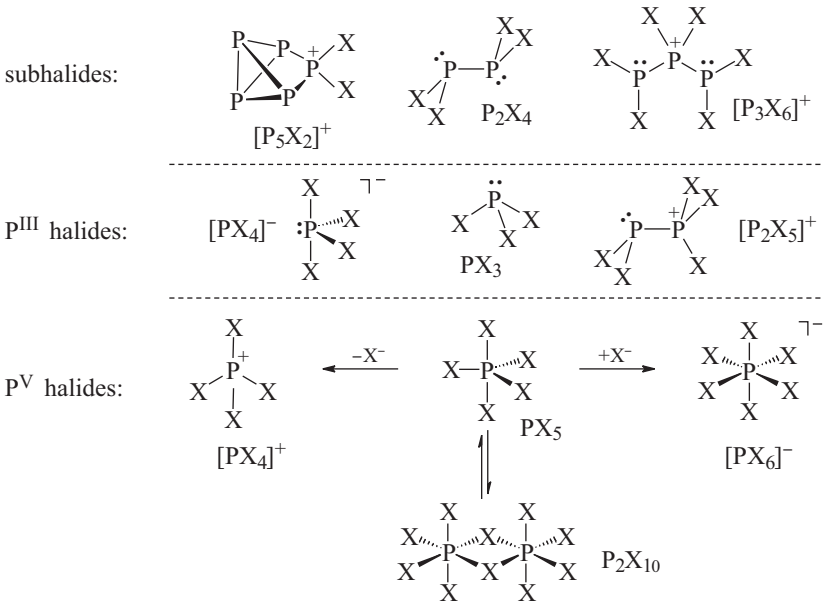

The by far most important are the neutral halides PX_3 and PX_5. Their thermal stability decreases with rising atomic mass of the halogen to such an extent that PI_5 is unknown; only salts with the cation $[PI_4]^+$ are available. PCl_3 and PCl_5 are of high technological significance. Besides the binary compounds, numerous mixed halides as well as oxo- and thiohalides exist, of which $POCl_3$ and $PSCl_3$ are the most prominent.

Arsenic also forms halides of the types AsX_3, As_2X_4 and AsX_5 as well as the ions $[AsX_2]^+$, $[AsX_4]^-$, $[AsX_4]^+$ and $[AsX_6]^-$. In addition, numerous multinuclear, halogen-bridged anions exist, such as $[As_2Br_8]^{2-}$, $[As_3I_{12}]^{3-}$ as well as the subvalent $[As_6X_8]^{2-}$ with local D_{3d} symmetry.[56]

10.8.1 Trihalides (EX_3; E = P, As)

All binary phosphorus trihalides of type PX_3 are known. PF_3 is obtained from PCl_3 and fluorination agents such as CaF_2, AsF_3 or ZnF_2; AsF_3 is produced from As_2O_3 by reaction with hydrogen fluoride:

$$2\ PCl_3 + 3\ CaF_2 \longrightarrow 2\ PF_3 + 3\ CaCl_2$$
$$As_2O_3 + 6\ HF \longrightarrow 2\ AsF_3 + 3\ H_2O$$

56 G. A. Fisher, N. C. Norman, *Adv. Inorg. Chem.* **1994**, *41*, 233. U. Müller, H. Sinning, *Angew. Chem. Int. Ed.* **1989**, *28*, 185. C. A. Ghilardi et al., *Chem. Commun.* **1988**, 1241.

Phosphorus trifluoride is a colorless gas (b.p. –102 °C), and AsF_3 is a colorless liquid (b.p. 63 °C). The by far highest importance of all phosphorus trihalides is due to PCl_3 (m.p. –94 °C, b.p. 76 °C), which is produced technically on a large scale from P_4 and Cl_2 in boiling PCl_3 or in the gas phase. It is the starting material for the manufacture of PCl_5, $POCl_3$, $PSCl_3$, phosphonic acids and its derivatives. PCl_3 and PBr_3 are colorless liquids, PI_3 forms red crystals. All of them are formed from the elements in exothermic reactions; the same applies to $AsCl_3$ (m.p. –16°, b.p. 130 °C), $AsBr_3$ (m.p. 31°, b.p. 221 °C) and AsI_3 (m.p. 140 °C).

All trihalides of phosphorus and arsenic are toxic and sensitive to hydrolysis. Except for AsI_3, which crystallizes in a layered structure, they form molecular crystals and can thus be distilled or sublimed. With element–hydrogen bonds of nonmetal hydrides, they react characteristically under elimination of HX:

$$PCl_3 + 3\,H_2O \longrightarrow H_3PO_3 + 3\,HCl$$

$$PCl_3 + 6\,NH_3 \longrightarrow P(NH_2)_3 + 3\,NH_4Cl$$

In an analogous manner, phosphonic acid esters are produced from PCl_3 and alcohols; with amines such as Me_2NH, the important intermediates R_2NPCl_2 and $(R_2N)_2PCl$ are obtained. PN bonds can also be formed using trimethylsilyl reagents:

$$RPCl_2 + Me_2N{-}SiMe_3 \longrightarrow RClP{-}NMe_2 + Me_3SiCl$$

The substituted phosphanes $RPCl_2$, R_2PCl and R_3P are typically produced from PCl_3 and organolithium or GRIGNARD compounds (Section 10.6). Triphenylphosphane, however, is synthesized in a WURTZ-type reaction with chlorobenzene:

$$PCl_3 + 3\,PhCl + 6\,Na \longrightarrow Ph_3P + 6\,NaCl$$

All trihalides of P and As can react either as LEWIS acids or as LEWIS bases. Therefore, PF_3 and PCl_3 are suitable ligands in transition metal complexes. For instance, PCl_3 reacts with $[Ni(CO)_4]$ to $[Ni(PCl_3)_4]$; PF_3 forms complexes such as $[Fe(CO)_n(PF_3)_{5-n}]$ with $n = 0$–4. Toward Me_3N, however, PCl_3 and $AsCl_3$ behave as LEWIS acids:

$$Me_3N + PCl_3\,(AsCl_3) \longrightarrow Me_3\overset{\oplus}{N}{-}\overset{\ominus}{P}Cl_3\,(-\overset{\ominus}{A}sCl_3)$$

Also, with halide ions, PX_3 molecules (X = F, Cl, Br) react as LEWIS acids and form *phosphanides*:[57]

$$PCl_3 + [Et_4N]Cl \longrightarrow [Et_4N][PCl_4]$$

Liquid AsF_3 is partially dissociated into ions and hence conducts electrical currents:

$$2\,AsF_3 \rightleftharpoons [AsF_2]^+ + [AsF_4]^-$$

57 Phosphanides are covalent derivatives of the hypothetical anion $[PH_4]^-$: K. B. Dillon, *Chem. Rev.* **1994**, *94*, 1441. $[PCl_4]^-$ is of C_{2v} symmetry.

These ions, which are isoelectronic to GeF_2 and SeF_4, respectively, can be isolated in the form of crystalline salts:

$$AsF_3 + SbF_5 \longrightarrow [AsF_2][SbF_6]$$
$$AsF_3 + KF \longrightarrow K[AsF_4]$$
$$AsCl_3 + [Me_4N]Cl \longrightarrow [Me_4N][AsCl_4]$$

The structure of $[AsF_2][SbF_6]$ is best described as a species in between an ionic salt and an adduct of the molecules AsF_3 and SbF_5.

With O_2 and other oxidizing agents, PCl_3 reacts to $POCl_3$; with sulfur, $PSCl_3$ is formed on heating. Both compounds are also produced technically in this manner. Phosphoryl chloride ($POCl_3$, also referred to as phosphorus oxychloride) is used in the production of hexamethylphosphoric triamide (HMPT, HMPA), which is an important highly polar, but aprotic solvent:

$$POCl_3 + 6\ Me_2NH \longrightarrow PO(NMe_2)_3 + 3\ [Me_2NH]Cl$$

The molecules $POCl_3$ and $PSCl_3$ exhibit a distorted tetrahedral structure and the PO and PS bonds can be assigned a certain double bond character. This also applies to the PS bond in PSF_3 as the following comparison of the PS stretching force constants with that of the PS single bond in $P(SMe)_3$ shows:

	$P(SMe)_3$	$PSCl_3$	PSF_3
f_{PS}(N cm^{-1}):	2.56	4.89	5.21

The strength of the PO and PS bonds in phosphoryl and thiophosphoryl species strongly depends on the electronegativity of the substituents X (just as in case of the SO bond of thionyl compounds $X_2S{=}O$; see Section 4.4.2). The largest force constants are reached with X = F. In case of arsenic, only a monomeric oxofluoride is known, namely $AsOF_3$, which is produced from $AsCl_3$, As_2O_3 and F_2.

10.8.2 Tetrahalides (E_2X_4; E = P, As)

The two iodides P_2I_4 and As_2I_4 are the most stable tetrahalides of phosphorus and arsenic, respectively. They are produced from the elements with an excess of element E so that part of the PP bonds of P_4 and the AsAs bonds of gray arsenic are retained:

$$P_4 + 4\ I_2 \xrightarrow{CS_2} 2\ P_2I_4 \quad \text{(red crystals, m.p. 126°C)}$$

In crystalline diphosphorus tetraiodide the molecules show a *trans*-structure of C_{2h} symmetry. P_2Cl_4, P_2F_4 and H_2PPF_2 have also been synthesized.

10.8.3 Pentahalides (EX_5; E = P, As)

With excess Cl_2 and Br_2, respectively, the phosphorus trihalides PCl_3 and PBr_3 react to PCl_5 and PBr_5. This reversible reaction is an *oxidative addition*, while the backreaction is a *reductive elimination*:

$$PCl_3 + Cl_2 \rightleftharpoons PCl_5$$

From PCl_5 and fluorinating agents such as AsF_3 or HF the pentafluoride (PF_5) is obtained. Molecular PI_5, however, is unknown. In case of arsenic, AsF_5, which is synthesized from the elements, is the only pentahalide stable at 25 °C. The by far highest importance is due to PCl_5, which forms yellowish crystals (m.p. 167 °C). It is industrially produced from PCl_3 and Cl_2 in batch reactors or lead-cladded towers. In the gas phase (during sublimation) PCl_5 is partially dissociated into the components.

Structures: The molecules PF_5 and AsF_5 have a trigonal-bipyramidal structure. This is also true for gaseous PCl_5 with internuclear distances d_{PCl} = 202 pm (equatorial) and 213 pm (axial). In contrast, solid PCl_5 exists as a salt $[PCl_4]^+[PCl_6]^-$. Such kind of isomerism between molecules and a salt is referred to as *bond isomerism*. In the gas phase, PBr_5 is completely dissociated into PBr_3 and Br_2. In the solid state, is consists of tetrabromophosphonium and bromide ions: $[PBr_4]^+Br^-$. Cations of the type $[PX_4]^+$ are isoelectronic to the corresponding silicon tetrahalides and thus of tetrahedral structure. The anions $[PX_6]^-$ from regular octahedra.

In the trigonal-bipyramidal PF_5, the three equatorial and the two axial fluorine atoms are nonequivalent. Two different internuclear distances (d_{PF} = 153 and 158 pm) and valence force constants f_{PF} are observed (see Section 10.2). The *^{19}F nuclear magnetic resonance spectrum* of PF_5 should therefore consist of two signals in the intensity ration of 3:2, which should both be split into a doublet due to the ^1J coupling of the ^{19}F atoms (I = ½) to the ^{31}P nuclei (I = ½). Furthermore, the ^2J coupling between the two different sorts of fluorine should be observed. In reality, however, only one doublet is found, that is, all F atoms are magnetically equivalent. This seeming contradiction is resolved by the assumption of so-called *pseudorotation*, which allows for a rapid interchange of the positions of the equatorial and axial F atoms so that they appear to be equivalent on the NMR timescale (Figure 10.4). During this intramolecular rearrangement[58] the internuclear distances and valence angles change only slightly, which is why only a small energy barrier has to be surmounted. The pseudorotation of PF_5 can therefore not be frozen out even at –150 °C. Analogous considerations apply to AsF_5.

58 P. Wang et al., *J. Chem. Soc. Chem. Commun.* **1990**, 201. The pseudorotation according to BERRY applies to acyclic phosphanes. For cyclic derivatives the alternative "turnstile" mechanism can also be considered; W. S. Sheldrick, *Top. Curr. Chem.* **1978**, *73*, 1.

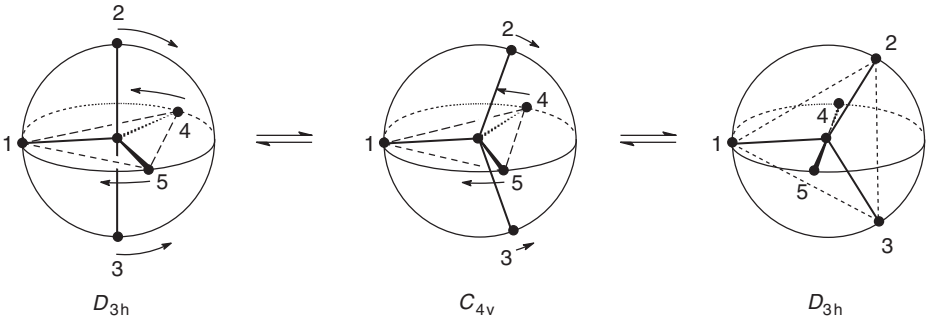

Figure 10.4: Pseudorotation of a trigonal-bipyramidal molecule. The D_{3h} structure at the left-hand side is converted via a C_{4v} transition state to the new D_{3h} geometry on the right. Through this the two former axial substituents (2, 3) assume an equatorial position.

Pseudorotation can be expected for all trigonal-bipyramidal molecules and derived structures in general, thus also for SF_4 and ClF_3. For compounds with mixed substitution pattern such as Me_2PF_3, however, it turned out that of the theoretically imaginable isomers I, II and III only the one with the more electronegative atoms in axial positions can be detected, let alone isolated (isomer I):

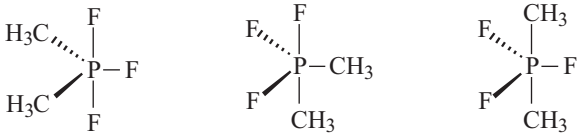

Due to the unequal substituents no pseudorotation occurs in such molecules, which can be explained with varying degrees of spatial demand exerted by the bonding electrons (Section 2.2.2).

Reactivity: PF_5 and AsF_5 are colorless gases, which are immediately decomposed by water and therefore strongly fume in humid air. They are strong LEWIS acids and thus also excellent fluoride ion acceptors:

$$PF_5 + LiF \longrightarrow Li[PF_6]$$

$$PF_5 + Me_3N \longrightarrow Me_3\overset{\oplus}{N}-\overset{\ominus}{P}F_5$$

$$PF_5 + Me_3P \longrightarrow Me_3\overset{\oplus}{P}-\overset{\ominus}{P}F_5$$

$$2\,AsF_5 + 2\,HF \rightleftharpoons [H_2F]^+ + [As_2F_{11}]^- \quad \text{(in liquid HF)}$$

$Li[PF_6]$ dissolved in organic solvents is employed as electrolyte in lithium-ion batteries. PCl_5 reacts with chloride anions to $[PCl_6]^-$. Water reacts with PCl_5 violently to $POCl_3$ initially and finally to H_3PO_4:

$$PCl_5 \xrightarrow[-2HCl]{+H_2O} POCl_3 \xrightarrow[-3HCl]{+3H_2O} PO(OH)_3$$

With ammonia and amines, the corresponding PN species are formed (see below).

On heating PCl_5 dissociates reversibly to PCl_3 and Cl_2 (see above). It can therefore act as a chlorination agent:

$$P_4O_{10} + 6\,PCl_5 \longrightarrow 10\,POCl_3$$
$$SO_2 + PCl_5 \longrightarrow SOCl_2 + POCl_3$$
$$ROH + PCl_5 \longrightarrow RCl + POCl_3 + HCl$$

PCl_5 dissolves in unpolar solvents such as CCl_4 or benzene as monomer or dimer. P_2Cl_{10}, which has also been detected in PCl_5 vapor, probably shows a structure of two PCl_6 octahedra sharing one edge and thus two chlorine atoms. Conversely, PCl_5 dissolves ionically as $[PCl_4][PCl_6]$ in acetonitrile (MeCN) and nitrobenzene ($PhNO_2$). With chloride ion acceptors such as BCl_3 and $SbCl_5$, PCl_5 reacts to salts with the tetrachlorophosphonium cation $[PCl_4]^+$.

Arsenic pentachloride is only stable below –50 °C; it is formed during the irradiation of an $AsCl_3/Cl_2$ mixture. The molecules in the crystalline state are trigonal-pyramidal.[59] $AsBr_5$ is unknown; but salts with the ions $[AsX_4]^+$ (X = Cl, Br) and $[AsCl_6]^-$ are stable at 25 °C:

$$AsCl_3 + Cl_2 + PCl_5 \longrightarrow [AsCl_4][PCl_6]$$
$$[Et_4N]Cl + AsCl_3 + Cl_2 \longrightarrow [Et_4N][AsCl_6]$$
$$AsBr_3 + Br_2 + Ag^+ \longrightarrow [AsBr_4]^+ + AgBr$$

Besides PF_5 and PCl_5, also mixed derivatives PCl_nF_{5-n} have been characterized by electron diffraction in the gas phase.[60] Further mixed pentahalides of phosphorus have been reported.

10.8.4 Strong LEWIS Acids

The molecule PF_5 and even more so its homologues AsF_5 and SbF_5 are strong LEWIS acids. In general, SbF_5 is employed in technical processes as the strongest binary LEWIS acid stable under standard conditions. As such compounds have a tremendous potential in both application and basic research, their *acid strength* will be briefly explained here. In principle, this value can be determined by the reaction with a donor in which the reaction enthalpy ΔH°_{298} can be taken as a measure of acid strength (see Section 6.2). The use of variable donors, however, has demonstrated that the thus defined acid strength is not a generally applicable quantity,

59 S. Haupt, K. Seppelt, *Z. Anorg. Allg. Chem.* **2002**, *628*, 729.
60 H. Oberhammer et al., *Inorg. Chem.* **1986**, *25*, 2828.

but depends instead on the donor employed for comparison. To minimize steric factors by using a particularly small donor, the *fluoride ion affinity (FIA)* is commonly applied for the quantification of acid strength of compounds such as AsF_5 and SbF_5. It is typically determined by monitoring of equilibrium fluoride ion transfer reactions by ^{19}F-NMR spectroscopy (for other methods see: L. Greb, *Chem. Eur. J.* **2018**, *24*, 17881–17896).

Various metal and nonmetal fluorides are capable to form complex anions (*ate complexes*) with fluoride ions. Particularly strong F^- acceptors are BF_3, AsF_5, SbF_5 and PtF_5, as well as AlF_3, SiF_4 and PF_5. Treatment of the latter with suitable fluoride sources yields the following ate-complexes, which are isoelectronic with SF_6:

$$[AlF_6]^{3-} \qquad [SiF_6]^{2-} \qquad [PF_6]^-$$

The central atoms of these ions are octahedrally coordinated and thus relatively well shielded against the attack of nucleophiles such as water due to steric and electronic reasons. Whereas SiF_4 and PF_5 hydrolyze immediately with water, the hexafluoride ions readily dissolve in water without decomposition. Apart from solutions, also ionic crystals and melts of the corresponding salts are known. The conjugated acids H_3AlF_6, H_2SiF_6 and HPF_6, however, cannot be prepared in anhydrous form, but decompose immediately under liberation of HF to the corresponding element fluoride. In aqueous solution the oxonium salts are present and $[H_3O]_2[SiF_6]$ crystallizes on cooling of "H_2SiF_6 solutions" in water.

Through reaction of covalent fluorides with F^- acceptors, salt-like species can be obtained, which do not show analogies in case of the other halogens:

$$IF_7 + AsF_5 \longrightarrow [IF_6][AsF_6]$$

$$2\,XeF_2 + PtF_5 \longrightarrow [Xe_2F_3][PtF_6]$$

$$\left\{\begin{array}{l} 3\,ONF + 2\,IrF_6 \longrightarrow 2\,[NO][IrF_6] + ONF_3 \\ ONF_3 + AsF_5 \longrightarrow [ONF_2][AsF_6] \end{array}\right\}$$

$$NF_3 + F_2 + SbF_5 \xrightarrow[18.5\ MPa]{200^\circ C} [NF_4][SbF_6]$$

This behavior is based on the pronounced electron deficiency (high positive charge) at the central atom due to the inductive effect of the fluorine atoms. In the absence of LEWIS bases, some of these species reduce the electron deficiency by either intramolecular π backdonation or intermolecular coordination of lone pairs at the fluorine ligands of a second molecule. Intramolecular π backdonation is active in BF_3, SiF_4 and PF_3 (Section 2.4.8). In case of liquid SbF_5, however, an intermolecular coordination with bridging fluorine atoms is observed. While SbF_5 molecules in the gas phase show the geometry of a trigonal bipyramid at high temperature, for the liquid phase the following *cis*-connection of SbF_6 octahedra has been observed below 15 °C (m.p. 7 °C), which leads to chain-like and cyclic oligomers:

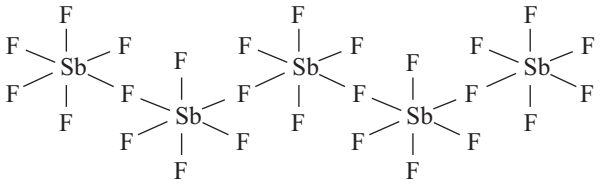

This structure follows from the ^{19}F-NMR spectrum: in case of SbF_5 oligomers, each SbF_5 unit contains three different sorts of nonequivalent F atoms with differing coordination environment:

(a) The F atoms of the upper and lower apex of the octahedra,
(b) the mono-coordinate F atoms of the equatorial planes and
(c) the bridging F atoms, which are shared by two octahedra.

As the intensity of the resonance signal is proportional to the number of involved fluorine atoms, a three-line spectrum is thus expected with relative intensities of 2:2:1, which corresponds exactly to the experimental finding. If the SbF_6 octahedra were *trans*-connected, only two lines in the intensity ratio of 4:1 would be observed. In the crystalline state, SbF_5 is tetrameric with the $(SbF_5)_4$ molecules consisting of mildly distorted *cis*-connected SbF_6 octahedra. The structures of the gaseous oligomers Sb_2F_{10} and Sb_3F_{15}, which are formed at moderate temperatures, are to be considered in an analogous manner. In ^{19}F-NMR spectroscopy, CCl_3F is used as a reference compound; the chemical shifts vary across the very large range of 900 ppm (for comparison: in ^{1}H-NMR spectroscopy, about 20 ppm).

The strength of common LEWIS acids defined by their *FIA* is given in Table 10.1. EX_n is the LEWIS acid under standard conditions (Index "ss" for *standard state*). The larger the *FIA*, the stronger the LEWIS acid EX_n.

$$EX_n + F^-(g.) \xrightarrow{-\Delta_r H = FIA} [X_nE{-}F]^-(g.)$$

From Table 10.1, it is known that the *FIA* values depend on the physical state of the acid. This is particularly obvious in case of SbF_5, which is liquid under standard conditions and forms the ions $[SbF_6]^-$, $[Sb_2F_{11}]^-$, $[Sb_3F_{16}]^-$ and $[Sb_4F_{21}]^-$ with fluoride ions. From polymeric SbF_5, the corresponding oligomers need to be formed first, which requires a certain amount of enthalpy. Therefore, the FIA of *n* equivalents of liquid SbF_5 is by about 43–55 kJ mol^{-1} lower than that of gaseous Sb_nF_{5n}.

10.9 Phosphoranes and Arsoranes

The substitution products of the hypothetical hydride PH_5 (which according to ab initio calculations is trigonal-pyramidal) are called *phosphoranes*. Either some or all H atoms can be substituted. Strictly speaking, PF_5 (pentafluorophosphorane) and gaseous PCl_5 (pentachlorophosphorane) also belong to this class of compounds,

Table 10.1: Strength of *Lewis* acids defined by the *fluoride ion affinity* (*FIA*).

LEWIS acid/anion	FIA (kJ mol^{-1})	LEWIS acid/anion	FIA (kJ mol^{-1})
$As(OTeF_5)_5/[FAs(OTeF_5)_5]^-$	593	$BI_{3\ (g)}/[FBI_3]^-$	448
$Sb_4F_{20\ (g)}/[Sb_4F_{21}]^-$	584	$B(C_6F_5)_3/[FB(C_6F_5)_3]^-$	444
$Sb_3F_{15\ (g)}/[Sb_3F_{16}]^-$	582	$GaBr_{3\ (g)}/[FGaBr_3]^-$	436
$AuF_5/[AuF_6]^-$	556	$SbF_{5\ (l)}/[SbF_6]^-$	[434]
$B(OTeF_5)_3/[FB(OTeF_5)_3]^-$	550	$BBr_{3\ (g)}/[FBBr_3]^-$	433
$Sb_2F_{10\ (g)}/[Sb_2F_{11}]^-$	549	$GaCl_{3\ (g)}/[FGaCl_3]^-$	432
$4\ SbF_{5\ (l)}/\ [Sb_4F_{21}]^-$	[534]	$GaF_{3\ (g)}/[FGaF_3]^-$	431
$3\ SbF_{5\ (l)}/\ [Sb_3F_{16}]^-$	[528]	$AsF_{5\ (g)}/[AsF_6]^-$	426
$2\ SbF_{5\ (l)}/[Sb_2F_{11}]^-$	[506]	$BCl_{3\ (g)}/[FBCl_3]^-$	405
$AlI_{3\ (g)}/[FAlI_3]^-$	499	$PF_{5\ (g)}/[PF_6]^-$	394
$AlBr_{3\ (g)}/[FAlBr_3]^-$	494	$AlI_{3\ (s)}/[FAlI_3]^-$	[393]
$SbF_{5\ (g)}/[SbF_6]^-$	489	$AlBr_{3\ (s)}/[FAlBr_3]^-$	[393]
$AlF_{3\ (g)}/[FAlF_3]^-$	467	$BF_{3\ (g)}/[BF_4]^-$	338
$AlCl_{3\ (g)}/[FAlCl_3]^-$	457	$AlCl_{3\ (s)}/[FAlCl_3]^-$	[332]
$GaI_{3\ (g)}/[FGaI_3]^-$	454		

Unless otherwise stated, the values refer to LEWIS acids in the gas phase. Values in square brackets indicate the FIA for the standard state of the corresponding LEWIS acid (g: gaseous; l: liquid; s: solid).

but not solid PCl_5 or PBr_5, which are salt-like containing tetrahedral cations and the corresponding anions (Section 10.8.3).

PH_5 has not been observed so far, presumably because the elimination of H_2 would form the very strong HH bond rendering the reaction overall exothermic and exergonic ($\Delta G^\circ_{298} < 0$). However, the following types of covalently bonded phosphoranes are known (R = organyl):

PF_5, RPF_4, R_2PF_3, R_3PF_2	$P(OR)_5$	R_5P	PCl_5, $RPCl_4$, R_2PCl_3
Fluorophosphoranes	Oxophosphoranes	Organophosphoranes	Chlorophosphoranes

Amino groups R_2N– serve as substituents to the pentavalent P atom as well and a large number of mixed derivatives are known. The possibly simplest derivatives are the three fluorophosphoranes HPF_4, H_2PF_3 and H_3PF_2. These colorless, gaseous compounds are prepared from anhydrous hydrogen fluoride and a PH species:[61]

61 R. Minkwitz et al., *Inorg. Chem.* **1989**, *28*, 4238 and **1998**, *37*, 4662 as well as *J. Phys. Chem.* **1989**, *93*, 6672.

$$HPO(OH)_2 + 4\,HF \longrightarrow HPF_4 + 3\,H_2O$$
phosphonic acid

$$H_2PO(OH) + 3\,HF \longrightarrow H_2PF_3 + 2\,H_2O$$
phosphinic acid

$$H_2P{-}PH_2 + 4\,HF \longrightarrow H_3PF_2 + [PH_4][HF_2]$$
diphosphane

HPF_4 has also been obtained from PF_5 and Me_3SiH through H/F exchange; H_2PF_3 is formed from the reaction of $Na[H_2PO_2]$ with HSO_3F:[62]

$$Na[H_2PO_2] + 3\,HSO_3F \xrightarrow{-25°C} H_2PF_3 + Na[HSO_4] + H_2S_2O_7$$

During the alkaline hydrolysis of HPF_4 and H_2PF_3 the starting materials are formed again as the corresponding anions. HPF_4 decomposes at 25 °C in a slow irreversible reaction to PF_3 and HF while H_2PF_3 is stable even at 100 °C. In contrast, H_3PF_2 keeps only for about 1 h at 25 °C.

The halides of phosphorus serve for the synthesis of organically substituted phosphoranes, as the following reactions show:

$$PCl_3 \xrightarrow{PhMgBr} Ph_3P \xrightarrow{+PhI} [Ph_4P]I \xrightarrow[-LiI]{+PhLi} Ph_5P$$

$$PCl_3 + RCl + AlCl_3 \longrightarrow [RPCl_3][AlCl_4] \xrightarrow[AsF_3]{HF\ or} RPF_4$$

$$2\,R_3P + SF_4 \longrightarrow 2\,R_3PF_2 + \tfrac{1}{8}\,S_8$$

$$2\,PF_5 + Ph_4Sn \longrightarrow PhPF_4 + [Ph_3Sn][PF_6]$$

Phosphoranes are strong LEWIS acids that react with donors such as tertiary amines or fluoride ions to 1:1 adducts in which the P atom is octahedrally coordinated and anions of the types $[PR_6]^-$ and $[P(OR)_6]^-$ have also been prepared.

The above mentioned tetracoordinate phosphane oxides, sulfides and selenides also belong to the class of phosphoranes as well as the imines $R_3P{=}NR$ (iminophosphoranes), which are accessible from primary amines and PCl_5. In order to avoid confusion with the pentacoordinate phosphoranes, the coordination number can be indicated as superscript in combination with the Greek letter σ before the compound name: σ^4- versus σ^5-phosphoranes while the letter λ is used to indicate the valence of the central atom. Thus, $R_3P{=}NR$ is a σ^4,λ^5-phosphorane.

Compounds of **arsenic** corresponding to the phosphoranes are known as *arsoranes* albeit in much smaller numbers.[63] They contain bonds between arsenic, on the one hand, and C, N, O, S and/or halogens, on the other hand. Well-known examples are AsF_5, pentaphenylarsenic (Ph_5As) and the methylester of orthoarsenic

62 D. Mootz et al., *Z. Naturforsch. B* **1997**, *52*, 1051.

63 R. Bohra, H. W. Roesky, *Adv. Inorg. Chem.* **1984**, *28*, 203.

acid $As(OMe)_5$. The coordination number 5, however, cannot always be directly concluded from the empirical formula alone. For instance, Me_3AsBr_2 exists as the salt $[Me_3AsBr]^+Br^-$, while Me_3AsCl_2 is a covalent species with pentacoordinate arsenic.

All σ^5-phosphoranes and σ^5-arsoranes structurally or spectroscopically characterized so far contain trigonal-bipyramidal coordinated central atoms, although the geometry occasionally approaches that of a square pyramid.[64] The most electronegative substituents are typically located at the apexes of the bipyramid. The *pseudorotation* described for PF_5 in Section 10.8.3 has also been observed for other phosphoranes, for example, diethylaminotetrafluorophosphorane Et_2NPF_4, which contains two F atoms each in axial and equatorial positions. Although the F atoms are NMR spectroscopically equivalent at room temperature, the pseudorotation can be sufficiently slowed down by cooling to −85 °C so that two signals are observed. Generally, no pseudorotation occurs if it would force the more electronegative substituents into the equatorial positions as in the cases of H_3PF_2 or Me_3PF_2.

10.10 Oxides of Phosphorus and Arsenic

As very oxophilic elements, phosphorus and arsenic form a considerable number of binary oxides.[65] In a stream of air, phosphorus burns to P_4O_6 at reduced O_2 partial pressure and to P_4O_{10} with an excess of O_2. The latter is the by far most important oxide of phosphorus. Several intermediate oxides, namely P_4O_7, P_4O_8 and P_4O_9, have been prepared as well as polymeric P_2O_5 and the ozonide P_4O_{18}. Analogous oxides of arsenic are also known, of which As_2O_3 and As_2O_5 are the most important. In contrast to the nitrogen oxides, which are endothermic without exception, the phosphorus and arsenic oxides are *exothermic compounds*, that is, their enthalpies of formation are negative.

10.10.1 Phosphorus(III) Oxides

P_4O_6 is produced through burning of P_4 in a stream of air in a flow apparatus; it is mandatory that this be done with a shortage of oxygen. The product can be purified from the concomitantly formed higher oxides including P_4O_{10} and the evaporated P_4 by sublimation after the volatile P_4 has been transformed into nonvolatile red phosphorus by UV irradiation. P_4O_6 is a colorless, waxy solid at room temperature (m.p. 24 °C). It consists of cage-like P_4O_6 molecules in all phases and in solution.

64 Regarding the stereochemistry at penta- or hexacoordinate phosphorus, see W. S. Sheldrick, *Top. Curr. Chem.* **1978**, *73*, 1.

65 J. Clade, F. Frick, M. Jansen, *Adv. Inorg. Chem.* **1994**, *41*, 327. B. T. Sterenberg, L. Scoles, A. J. Carty, *Coord. Chem. Rev.* **2002**, *231*, 183.

These cages are formally derived from the P_4 tetrahedron by replacement of all six PP bonds by bent POP units:

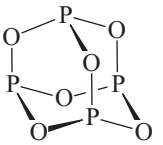

d_{PO} = 164 pm (g.)
angle_{POP} = 126.4°
angle_{OPO} = 99.8°

Although not directly bonded anymore, the four P atoms still form an expanded tetrahedron (T_d symmetry). P_4O_6 is stable in air at 25 °C. It reacts with excess cold water to phosphonic acid (H_3PO_3) with the connectivity $HPO(OH)_2$ (phosphorous acid):

$$P_4O_6 + 6\,H_2O \longrightarrow 4\,H_3PO_3$$

Evidently, P_4O_6 is the anhydride of phosphonic acid. With hot water, however, disproportionation occurs leading among other species to PH_3, H_3PO_4 and elemental phosphorus. More recently, the synthesis and complete characterization of the ozonide P_4O_{18} has been achieved by reaction of P_4O_6 with O_3 in a [1 + 3] cycloaddition:[66]

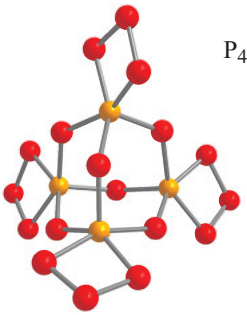

P_4O_{18}

In the ozonide, each of the four phosphorus atoms of P_4O_6 carries an O_3 unit and is thus part of a four-membered PO_3 ring. P_4O_{18} is therefore a P(V) oxide; it decomposes slowly to P_4O_{10} and O_2 even at −35 °C.

10.10.2 Phosphorus(V) Oxides

In excess oxygen, phosphorus burns under development of extraordinary amounts of heat to so-called phosphorus pentoxide (P_2O_5, or more correctly P_4O_{10}). Even on an industrial scale, this oxide is produced by burning of P_4:

66 A. Dimitrov, B. Ziemer, W. D. Hunnius, M. Meisel, *Angew. Chem. Int. Ed.* **2003**, *42*, 2484.

$$P_4(g.) + 5\ O_2 \longrightarrow P_4O_{10}(g.) \qquad \Delta_f H^\circ_{298} = -2904\ \text{kJ mol}^{-1}\ (P_4O_{10})$$

In order to remove incompletely oxidized species, P_4O_{10} is sublimed in vacuum at red heat and in an O_2 flow. This way, colorless hexagonal crystals are obtained, which consist of P_4O_{10} molecules. These are formally derived from P_4O_6 by the addition of an exohedral O atom to each P atom. By electron diffraction, the following parameters have been determined for the molecule in the gas phase:

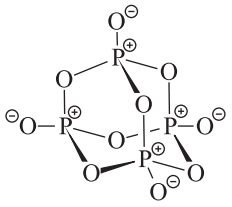

(a)

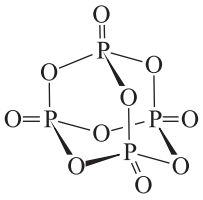

(b)

$d_{P=O}$ = 143 pm
$d_{P\text{-}O}$ = 160 pm
$\text{angle}_{P\text{-}O\text{-}P}$ = 123.5°
$\text{angle}_{O=P\text{-}O}$ = 116.5°
$\text{angle}_{O\text{-}P\text{-}O}$ = 101.6°

The terminal PO bonds are considerably shorter than those of the cage. Therefore, they are often drawn as double bonds as in (b) although the true bonding situation is better described by structure (a) with strongly polar single bonds.

The most characteristic property of P_4O_{10} is its violent reaction with water, similar to that of SO_3. The hydrolysis takes place via the intermediates tetrametaphosphoric acid ($H_4P_4O_{12}$) and diphosphoric acid ($H_4P_2O_7$) to finally give orthophosphoric acid (H_3PO_4):

$$P_4O_{10} \xrightarrow{+2\ H_2O} H_4P_4O_{12} \xrightarrow{+2\ H_2O} 2\ H_4P_2O_7 \xrightarrow{+2\ H_2O} 4\ H_3PO_4$$

During the first step, two of the six POP bridges of P_4O_{10} are hydrolyzed resulting in the cyclic metaphosphoric acid $(HPO_3)_4$:

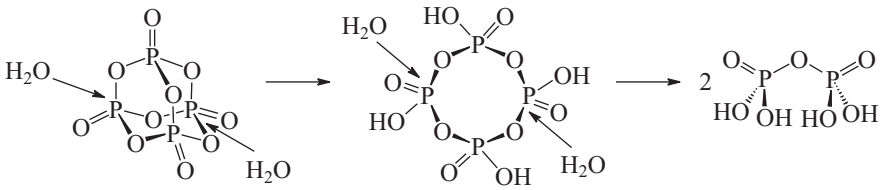

With liquid water P_4O_{10} reacts almost explosively to H_3PO_4 due to the large reaction enthalpy of −377 kJ mol^{-1}. With little water, for example, with water vapors or slightly wet solvents, which themselves are inert toward P_4O_{10}, it melts away to a syrupy mixture of polyphosphoric acids. P_4O_{10} is therefore one of the most effective drying agents for gases and solvents. Moreover, it can be employed for the elimination of water from compounds. In this manner, the anhydride N_2O_5 is obtained from HNO_3 and correspondingly Cl_2O_7 from $HClO_4$, SO_3 from H_2SO_4, and C_3O_2 (tricarbon dioxide) from malonic acid.

If P_4O_{10} is heated at 450 °C in a sealed ampoule for extended periods of time, the thermodynamically stable orthorhombic modification is formed, which

consists of layers of P_6O_6 rings with the PO_4 tetrahedra connected with each other at three corners. This structure resembles that in the isoelectronic phyllosilicates (Section 8.8.2).[67]

Industrially, P_4O_{10} is used to produce the very pure thermic phosphoric acid, and serves as water desiccating agent as well as for the synthesis of phosphoric acid esters by reaction of the oxide with either ethers or alcohols:

$$P_4O_{10} + 6\ Et_2O \longrightarrow 4\ PO(OEt)_3$$

$$P_4O_{10} + 6\ ROH \longrightarrow 2\ ROPO(OH)_2 + 2\ (RO)_2PO(OH)$$

Phosphoric acid triesters are used as flame retardants,[68] hydraulic liquids and PVC softeners, as additives for lubricants and as extracting agents for metal ions. From P_4O_{10}, HF and H_2O, fluorophosphoric acid (H_2PO_3F) is obtained; its salts are needed for special applications, for example, as corrosion inhibitors.

10.10.3 Phosphorus(III,V) Oxides

The two oxides, P_4O_6 and P_4O_{10}, are the end links of a series that is formally created by the stepwise addition of terminal O atoms to the P_4O_6 molecule:

$$P_4O_6(T_d) \quad P_4O_7(C_{3v}) \quad P_4O_8(C_{2v}) \quad P_4O_9(C_{3v}) \quad P_4O_{10}(T_d)$$

The three mixed phosphorus(III,V) oxides are obtained either by thermal disproportionation or stoichiometric oxidation of P_4O_6. The reduction of P_4O_{10} with red phosphorus also leads to the formation of mixed-valent oxides:

$$2\ P_4O_6 + O_2 \xrightarrow{+\ CCl_4} 2\ P_4O_7$$

$$P_4O_{10} + P_{red} \xrightarrow{150\text{–}450\,^\circ C} P_4O_8, P_4O_9$$

The last mentioned reaction is carried out under N_2 in a bomb tube. Depending on the reaction conditions, mixtures or co-crystals of different oxides are obtained, which can be separated by sublimation. Structure determinations by X-ray diffraction on single crystals have shown that P_4O_9, P_4O_8 and P_4O_7 have molecular structures analogous to P_4O_{10} with one, two or three of the terminal O atoms missing.[69] The oxides can be readily identified from their ^{31}P-NMR spectra.

67 D. Stachel, I. Svoboda, H. Fuess, *Acta Cryst. C* **1995**, *51*, 1049.
68 Review: F. R. Wurm et al., *Angew. Chem. Int. Ed.* **2018**, *57*, 10450.
69 S. Strojek, M. Jansen, *Z. Naturforsch. B* **1997**, *52*, 906.

10.10.4 Arsenic Oxides

Arsenic burns in air or neat O_2 to arsenic(III) oxide, which can also be produced by the hydrolysis of $AsCl_3$ with small amounts of water:

$$2\,As + \frac{3}{2}\,O_2 \longrightarrow As_2O_3$$

$$2\,AsCl_3 + 3\,H_2O \longrightarrow As_2O_3 + 6\,HCl$$

Arsenic trioxide is the most important compound of arsenic as it the starting material for the synthesis of many other derivatives. As_2O_3 dissolves in hot water as *arsenious acid* H_3AsO_3 or $As(OH)_3$ but mostly crystallizes on cooling as cubic As_4O_6 crystals (solubility at 25 °C: 21.6 g L^{-1}). In nitrobenzene and in the gas phase (during sublimation) as well, P_4O_6 analogous molecules are present (T_d symmetry). As_2O_3 is a strong poison with a lethal dose of only 1.5 mg per kg body weight.[70] For this reason, drinking water may not contain more than 0.01 mg As per liter (0.01 ppm). In the European Union the allowed daily intake of arsenic [As(III) and As(V)] is 0.3 µg/kg body mass.

On the other hand, arsenic(III) oxide is used in the treatment of leukemia. Sea water contains on average only 0.024 ppm As, but the element is enriched in algae, fish and crustaceans by up to a factor of 10^5! More than 100 naturally occurring organoarsenic compounds have been identified in these species. Groundwater in some countries (e.g., in India, Bangladesh and Thailand) contains considerably higher concentrations of arsenic than seawater and therefore needs to be detoxified prior to consumption.

If As_4O_6 is heated to temperatures above 200 °C, it is converted to polymeric As_2O_3, which crystallizes in a monoclinic structure. Above 260 °C and under increased O_2 pressure, the mixed-valent, polymeric AsO_2 is formed. The natural product *Arsenicin A*, which has been isolated from a sponge, is formally a derivative of As_4O_6, in which three O atoms have been replaced by isolobal CH_2 groups resulting in a molecule of C_2 symmetry.

On dissolving elemental arsenic or As_2O_3 in concentrated nitric acid, a solution of *arsenic acid* (H_3AsO_4) is obtained, which can be isolated as the hydrate $2H_3AsO_4{\cdot}H_2O$ by cautious evaporation and dehydration, but is readily converted to arsenic(V) oxide on warming:

$$2\,H_3AsO_4 \xrightarrow{300°C} As_2O_5 + 3\,H_2O$$

As_2O_5, which eliminates oxygen on further heating, only slowly dissolves in water resulting once again in H_3AsO_4. The polymeric structure of this oxide consists of AsO_4 tetrahedra and AsO_6 octahedra connected to ribbons through shared corner atoms. As_2O_5 and P_2O_5 form co-crystals with each other.

---

70 An entertaining account on historic murder with arsenic trioxide (historically and misleadingly referred to as "white arsenic") in German language can be found at G. Süss-Fink, *Chem. unserer Zeit* **2012**, *46*, 100.

10.11 Sulfides of Phosphorus and Arsenic

On heating under equilibrium conditions, red and white phosphorus react with sulfur to give the sulfides P_4S_3, P_4S_4 (α and β), P_4S_5 (α and β), P_4S_6 (α to ε), P_4S_7, P_4S_9 and P_4S_{10} depending on the molar ratio. Besides, there are numerous other phosphorus sulfides prepared by special protocols.[71] These compounds form yellow to pale-yellow molecular crystals, which are more or less well soluble in CS_2 depending on the polarity. P_4S_{10} is technically produced on a 100 kt scale from the liquid elements at temperatures above 300 °C. The structure of P_4S_{10} corresponds to that of P_4O_{10}, that is, there are bridging and terminal S atoms. In P_4S_9, one of the terminal S atoms is missing (compare P_4O_9). The structures of the most important phosphorus sulfides are shown in Figure 10.5.

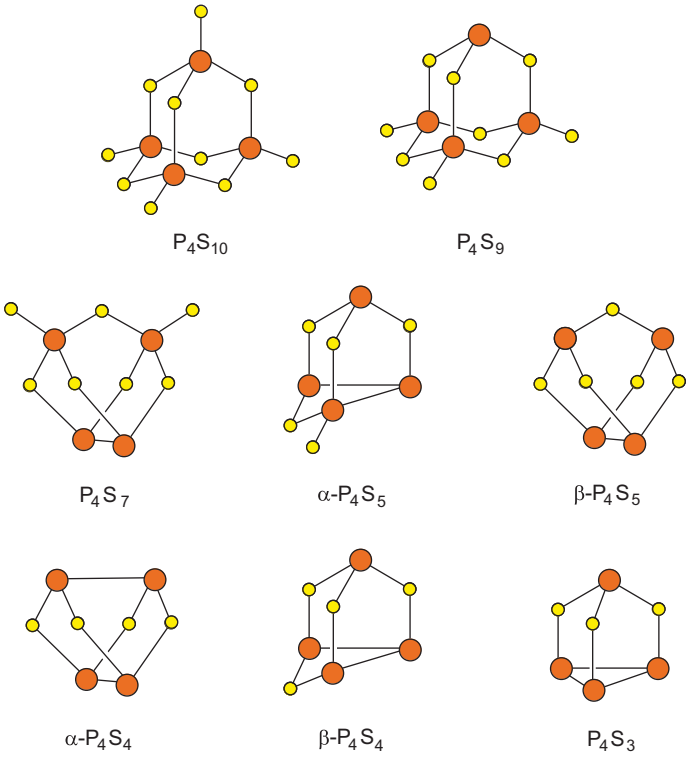

Figure 10.5: Molecular structures of the most important binary phosphorus sulfides (large orange circles: phosphorus; small yellow circles: sulfur).

71 T. Rödl, A. Pfitzner, *Z. Anorg. Allg. Chem.* **2012**, *637*, 1507. A. Pfitzner et al., *Angew. Chem. Int. Ed.* **2011**, *50*, 10996. M. E. Jason, T. Ngo, S. Rahman, *Inorg. Chem.* **1997**, *36*, 2633 and 2641. R. Blachnik et al., *Z. Anorg. Allg. Chem.* **1995**, *621*, 1637 and **1999**, *625*, 1966. T. Bjorholm, H. J. Jakobsen, *J. Am. Chem. Soc.* **1991**, *113*, 27.

As in case of the phosphorus oxides, the sulfides also contain thermally very stable heterocyclic structures. This even applies to the homocyclic P_3 ring in P_4S_3, which corresponds to the three-membered rings in the P_4 molecule. P_4S_3 can be distilled without decomposition (m.p. 174 °C; b.p. 408 °C). The ion $[P_7]^{3-}$ in the salt $Sr_3[P_7]_2$ is isoelectronic and isostructural with P_4S_3. In contrast, P_4S_5 disproportionates on heating to P_4S_3 and P_4S_7 (m.p. 308 °C) and P_4S_{10} (m.p. 288 °C) decomposes partly on melting to give P_4S_9 and elemental sulfur. Alternatively, P_4S_{10} can be desulfurized to P_4S_9 with PCl_3 (in turn converted to $PSCl_3$). Also, in case of other phosphorus sulfides, equilibrium between different molecular species is established that can be monitored by ^{31}P-NMR spectroscopy. In total, 19 binary phosphorus sulfides are known. Sulfur-rich P_xS_y melts tend to form glasses on cooling.[72]

Phosphorus sulfides are highly flammable and have thus to be handled under an inert gas at elevated temperatures. P_4S_{10} reacts with water to H_3PO_4 and H_2S, with alcohols to H_2S and esters of dithiophosphoric acid $HS–PS(OR)_2$, which is produced industrially in this manner:

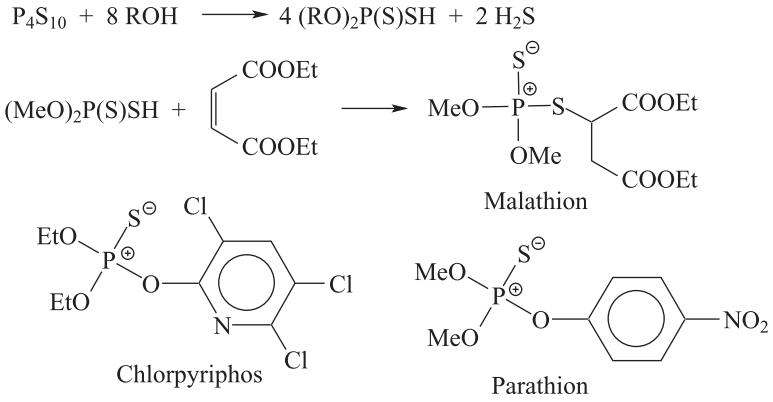

The esters of dithiophosphoric acid serve for the production of *insecticides* such as Malathion, as flotation aid for the separation of ores, and as additive for lubricant oils. Malathion (also Carbafos, Maldison, Mercaptothion) is the most frequently employed insecticide in the USA; closely related with these compounds are the thiophosphates Parathion and Chlorpyriphos shown above. These species irreversibly bind to the enzyme cholinesterase.

P_4S_{10} is also an important *sulfurization reagent* in organic synthesis for the conversion of carbonyl to thiocarbonyl compounds.[73] The extreme oxophilicity of P(V) plays its part in this procedure, which results in an S/O exchange. To the same end, one can also employ LAWESSON's reagent $(MeO–C_6H_4–PS_2)_2$, which is produced by

72 M. Tullius, D. Lathrop, H. Eckert, *J. Phys. Chem.* **1990**, *94*, 2145.
73 T. Ozturk, E. Ertas, O. Mert, *Chem. Rev.* **2010**, *110*, 3419.

reaction of P_4S_{10} with anisole and contains a four-membered P_2S_2 ring as central structural unit.[74]

Treatment of P_4S_3 with I_2 in CS_2 at 20 °C leads to cleavage of a PP bond and formation of the halide β-$P_4S_3I_2$, which rearranges at 125 °C to the isomeric α-$P_4S_3I_2$. These diiodides react with $(Me_3Sn)_2S$ to α- and β-P_4S_4, respectively, and Me_3SnI. On treatment of P_4S_3 with the Ag^+/PX_3 reagent (X = F to I), the cations $[P_5S_3X_2]^+$ are obtained, which structurally resemble α-P_4S_5 inasmuch as the P=S group is replaced by $P^+–X$ and the sulfur atom of the four-membered ring by P–X.[75]

If P_4O_6 is heated with S_8 or P_4O_{10} with P_4S_{10}, various oxosulfides of phosphorus are obtained with structures corresponding to those of the binary oxides in which the terminal or bridging O atoms are partially replaced by sulfur.[76]

Elemental **arsenic** reacts with sulfur to the compounds As_4S_3, As_4S_4, As_2S_3 and As_2S_5. The sulfides As_4S_4 (*realgar*) and As_2S_3 (*auripigment*) occur as minerals. The mineral *alacranite* (As_8S_9), however, consists of a 1:1 mixture of As_4S_4 and As_4S_5.

As_2S_3 and As_2S_5 are formed on precipitation with H_2S from aqueous hydrochloric As(III)- or As(V) solutions. Monoclinic As_2S_3 crystallizes as a polymer, just as monoclinic As_2O_3. As_4S_3 consists of P_4S_3-analogous molecules (Figure 10.5). As_4S_4 also contains cage-like molecules, which are structurally related to the S_4N_4 molecule (Section 12.13) although the N atoms of S_4N_4 are replaced by S atoms and the S atoms of S_4N_4 by As. The arsenic sulfides As_4S_4 and As_2S_3 dissolve in anhydrous amines and liquid ammonia.

10.12 Oxoacids of Phosphorus and Arsenic and Their Derivatives

The oxoacids of phosphorus and their salts, esters and other derivatives are the most important phosphorus compounds. Due to large variety of this class of compounds, it is useful to initially consider the structural elements from which the individual oxo-, thio- and halogenoacids are derived and subsequently discuss their properties and reactivity of the corresponding compounds.

10.12.1 Oxoacids with One P Atom

All oxoacids contain the P–OH group which is responsible for the acidic properties according to the following reaction with water:

74 T. Ozturk, E. Ertas, O. Mert, *Chem. Rev.* **2007**, *107*, 5210.
75 M. Gonsior, I. Krossing, E. Matern, *Chem. Eur. J.* **2006**, *12*, 1703.
76 J. Clade, F. Frick, M. Jansen, *Adv. Inorg. Chem.* **1994**, *41*, 327.

$$>P-OH + H_2O \longrightarrow >P-O^- + [H_3O]^+$$

In addition, all oxoacids contain terminal O atoms and occasionally PH groups. The three most important monophosphoric acids may illustrate this as examples:

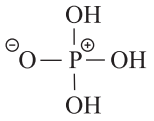

orthophosphoric acid
H_3PO_4

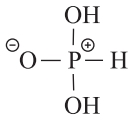

phosphonic acid
H_3PO_3

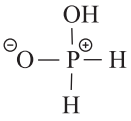

phosphinic acid
H_3PO_2

In contrast to POH groups, the PH bond does not protonate water to oxonium ions. The P-bonded hydrogen atoms are rather hydridic than protic and can thus not be titrated in water. H_3PO_3 is a diprotic and H_3PO_2 a monoprotic acid, which can be expressed by formulae such as $HPO(OH)_2$ for phosphonic acid and $H_2PO(OH)$ for phosphinic acid.

The unstable molecule H_2POH is the parent species of the well-known substituted phosphinous acids R_2POH (R = perfluoralkyl; see below).

These acids can be produced in the following manner:

(a) Protonation of anions, for example:

$$Ca_3[PO_4]_2 + 3\ H_2SO_4 \longrightarrow 2\ H_3PO_4 + 3\ Ca[SO_4]$$

(b) Hydrolysis of covalent halides:

$$POCl_3 + 3\ H_2O \longrightarrow H_3PO_4 + 3\ HCl\uparrow$$

$$PCl_3 + 3\ H_2O \longrightarrow H_3PO_3 + 3\ HCl\uparrow$$

(c) Hydrolysis of phosphorus oxides:

$$P_4O_{10} + 6\ H_2O \longrightarrow 4\ H_3PO_4$$

$$P_4O_6 + 6\ H_2O \longrightarrow 4\ H_3PO_3$$

If a lone pair of electrons is located at the P atom (as in PCl_3 and P_4O_6), the POH group formed by hydrolysis isomerizes as follows to the phosphane oxide:

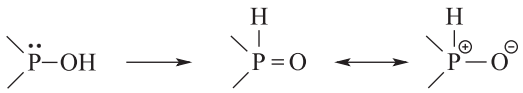

This rearrangement is akin to the well-known keto-enol tautomerism. In fact, it is an equilibrium reaction, albeit almost completely on the right-hand side. Therefore, the product of PCl_3 hydrolysis is not the expected phosphorus hydroxide $P(OH)_3$, but rather $H–PO(OH)_2$. The readily detectable PH group of phosphonic acid (IR and NMR spectroscopy) is also formed during the disproportionation of white phosphorus in aqueous alkaline solution according to the scheme:

$$>P{-}P< + H_2O \xrightarrow{[OH]^-} >P{-}H + O{=}\overset{H}{\overset{|}{P}}<$$

$$\text{e.g.}\quad P_4 + 3\,[OH]^- + 3\,H_2O \longrightarrow PH_3\uparrow + 3\,[H_2PO_2]^-$$

This reaction corresponds to the disproportionation of Cl_2 to HCl and HOCl and of S_8 to H_2S and thiosulfate in alkaline solution. In all three cases, a nucleophilic attack by hydroxide ions occurs at the element–element bonds. If P_4 is incorporated in a complex as in $[\{CpRuL_2\}_2P_4][CF_3SO_3]_2$, serving as a bridging ligand (L = Ph_3P), hydrolysis with excess water at 20 °C gives a series of complexes with the P-donor ligands PH_3, $PH(OH)_2$, P_2H_4, $H_2P{-}PH{-}PH(OH)$ and $(HO)_2P{-}PH{-}PH{-}PH(OH)$ alongside H_3PO_3; four of these PH species possibly also occur as reactive intermediates during the alkaline hydrolysis of neat P_4.[77]

10.12.1.1 Orthophosphoric Acid and Orthophosphates

Phosphoric acid, the by far most important phosphorus compound, is produced in huge quantities, of all mineral acids only surpassed by sulfuric acid. H_3PO_4 is technically prepared from the minerals *fluorapatite* and *phosphorite* of composition $Ca_5[(PO_4)_3F]$. The phosphate is either digested with sulfuric acid (production of *wet phosphoric acid*) or reduced to white phosphorus with coke, which in turn is burned to P_4O_{10} with excess air and hydrolyzed to H_3PO_4 (*thermic phosphoric acid*; see Section 10.10). Only thermic phosphoric acid is of food quality and is therefore used as an acidifier for sodas and other food products.

By far more important, however, is the wet phosphoric acid, which is prepared as follows:

$$Ca_5[(PO_4)_3F] + 5\,H_2SO_4 + 2\,H_2O \longrightarrow 3\,H_3PO_4 + 5\,Ca[SO_4]\cdot 2\,H_2O + HF\uparrow$$

The side product gypsum is filtered off. On evaporation of the initially dilute acid, HF partially reacts with SiO_2 contained in the mineral to SiF_4, which escapes together with HF and is then converted to various fluorine compounds. In this manner, an H_3PO_4 solution of about 85–90% is obtained, which is further purified by precipitation of unwanted cations and multistage liquid–liquid countercurrent extraction. Anhydrous H_3PO_4 can be obtained by evaporation of aqueous solutions in vacuum at 80 °C. It forms colorless crystals (m.p. 42 °C), which consist of H_3PO_4 molecules connected to layers by hydrogen bridges. Hydrogen bonds are also present in concentrated aqueous H_3PO_4 solutions, which cause their syrupy viscosity.

H_3PO_4 is a triprotic *acid of medium strength* (see Table 5.5). Its salts are of the empirical formulae $M[H_2PO_4]$ (dihydrogen phosphates), $M_2[HPO_4]$ (hydrogen

77 P. Stoppioni et al., *Inorg. Chem.* **2009**, *48*, 1091.

phosphates) and $M_3[PO_4]$ (orthophosphates). At physiological pH, phosphate ions exist predominantly as $[HPO_4]^{2-}$. Orthophosphates are known for almost all metallic elements. They contain the tetrahedral ion $[PO_4]^{3-}$ with an electronic structure corresponding to that of the isoelectronic anions $[SiO_4]^{4-}$, $[SO_4]^{2-}$ and $[ClO_4]^-$ (Section 2.6).

The technically most important phosphate is $Ca[H_2PO_4]_2$, which unlike calcium orthophosphate is soluble in water and therefore used as **fertilizer** and as nutritional supplement for animals under the trade name "superphosphate." Just like H_3PO_4, it is produced by digestion of apatite or phosphorite with H_2SO_4, although in a molar ratio of mineral to acid of 2:7. In this case, the resulting gypsum remains in the product. If H_3PO_4 is employed in the process instead of H_2SO_4, a gypsum-free product can be obtained (*triple phosphate*), that is, a fertilizer with particularly high P content. If nitric acid is used for the digestion, a combined P-N fertilizer is produced. In the same vein, $[NH_4]_2[HPO_4]$ is made from NH_3 and H_3PO_4, as an important component of fertilizers. An undeniable problem with all these processes is the natural uranium content of phosphate minerals, which results in up to 2 g uranium per kg of phosphorus in said fertilizers. Even more of an issue for humankind, however, are the limited natural deposits of phosphate minerals. Major producers of phosphate minerals are China, Morocco, Tunisia, Russia, Brazil and USA.

As a consequence, the recovery of phosphorus from various forms of waste is actively being pursued already.[78] The precipitation of orthophosphate from communal wastewater is an important process in order to avoid the *eutrophication of surface waters* and to recover valuable phosphate ions. For this purpose, iron(III) salts are added to form the particularly insoluble $Fe[PO_4]$ at a pH of 6.0, which is filtered off and employed in agriculture as phosphorus fertilizer. In a similar fashion, $[NH_4]Mg[PO_4]$ can be precipitated after microbiological wastewater treatment by addition of $MgCl_2$; the ammonium magnesium phosphate is filtered off and used as a long-time fertilizer.[78]

Esters of orthophosphoric acid are either produced by reaction of P_4O_{10} with alcohols or phenols or by condensation of alcohols with $POCl_3$ followed by hydrolysis:

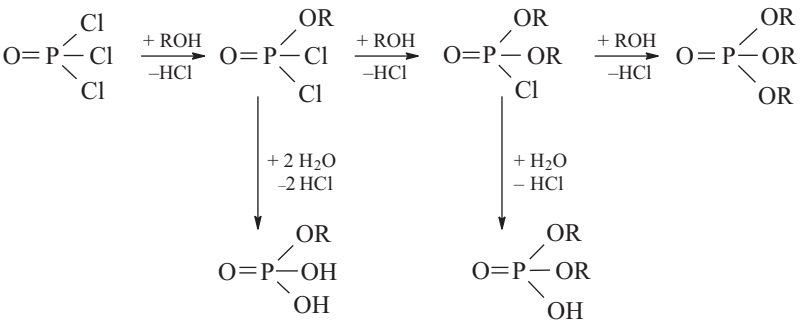

78 J. C. Slootweg et al., *Sustainability* **2018**, *10*, 1790.

The direct conversion of white phosphorus with phenols in the presence of air and catalytic quantities of iodine also gives triaryl phosphates.[79] Such compounds are added to plastics as softeners and flame retardants.

Phosphoric acid esters play a prominent role in biological processes, for instance, ATP as "energy storage":[80]

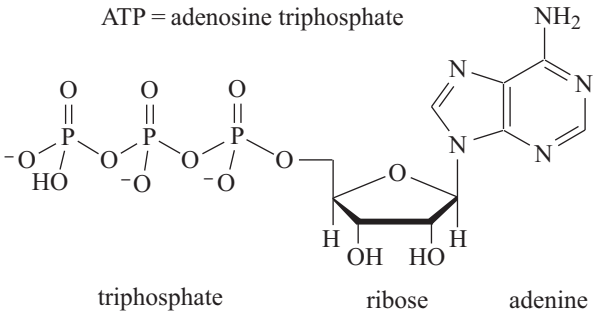

During the enzymatic hydrolysis of ATP to monophosphate ions and adenosine diphosphate under physiological conditions (pH = 6.4–8.8) a standard enthalpy of –20.5 kJ mol^{-1} is released at 25 °C but this value also depends on the ion strength. The nucleic acids DNA and RNA are diesters of phosphoric acid.

10.12.1.2 Phosphonic Acid (H_3PO_3 or $HPO(OH)_2$)

Phosphonic acid is prepared by cautious hydrolysis of PCl_3 with concentrated hydrochloric acid and can then be obtained in crystalline form by evaporation of the solution (m.p. 70 °C). Industrially, PCl_3 is hydrolyzed with steam at 190 °C. The crystal structure is characterized by strong intermolecular OH···O hydrogen bonds. H_3PO_3 is readily soluble in water and dissociates in two steps to give hydrogen phosphite $[HPO_2(OH)]^-$ and phosphite $[HPO_3]^{2-}$ ions, which can both be isolated as metal salts. As all compounds with PH bonds or with phosphorus in the oxidation state +3, H_3PO_3 and its anions are strong *reducing agents*. On heating, the acid decomposes according to

$$4\ H_3PO_3 \longrightarrow PH_3\uparrow + 3\ H_3PO_4$$

This reaction is suitable for the production of phosphane (PH_3).

79 K. M. Armstrong, P. Kilian, *Eur. J. Inorg. Chem.* **2011**, 2138.

80 Regarding the discovery of ATP by KARL LOHMANN in Berlin in 1929, see P. Langen, F. Hucho, *Angew. Chem. Int. Ed.* **2008**, *47*, 1824.

10.12.1.3 Phosphinic or Hypophosphorous Acid (H_3PO_2)

White phosphorus disproportionates in warm $Ba[OH]_2$ solution according to the equation:

$$2\ P_4 + 3\ Ba[OH]_2 + 6\ H_2O \longrightarrow 3\ Ba[H_2PO_2]_2 + 2\ PH_3\uparrow$$

From barium phosphinate $Ba[H_2PO_2]_2$, the free acid can be liberated with H_2SO_4 or by cation exchange. H_3PO_2 has been isolated in crystalline form by evaporation from aqueous solutions (m.p. 26 °C). Phosphinic acid $H_2PO(OH)$ is a monoprotic acid of medium strength and a strong reductant since phosphorus is in the formal oxidation state +1. The anhydrous acid disproportionates at 140 °C to give PH_3 and H_3PO_3, which in turn decomposes to PH_3 and H_3PO_4. These disproportionation reactions correspond to those of the lower chlorine and bromine oxoacids and their salts. Sodium phosphinate $Na[H_2PO_2]$, previously referred to as hypophosphite, is used as a *reducing agent* in electroplating.

10.12.1.4 Phosphinous Acid (H_3PO) and Hydroxophosphane (H_2POH)

Substituted phosphane oxides of type $R_2HP{=}O$ with R = alkyl have been known for a long time. The more recently prepared perfluorinated compounds $(CF_3)_2POH$ and $(C_2F_5)_2POH$, however, rather exist as hydroxoacids than as phosphane oxides, both in the gas phase and the solid state, which has been ascertained by electron diffraction and X-ray structural analysis, respectively.[81] In contrast, liquid $(C_2F_5)_2POH$ is an equilibrium mixture of both tautomers, probably due to strong association through hydrogen bonds. $(CF_3)_2POH$, a colorless liquid, is prepared by reaction of $(CF_3)_2PNEt_2$ with three equivalents of *p*-tolylsulfonic acid.

10.12.2 Condensed Phosphoric Acids

Condensed phosphoric acids and phosphates[82] contain the structural motif P–O–P, which is formed during condensation reactions of two POH fragments under elimination of water:

$$P{-}OH + HO{-}P \longrightarrow P{-}O{-}P + H_2O$$
$$P{-}OH + Cl{-}P \longrightarrow P{-}O{-}P + HCl$$

The catalytic oxidation of phosphonic acids and their esters with oxygen from the air also leads to condensation:[83]

81 J. Bader, B. Hoge et al., *Chem. Eur. J.* **2011**, *17*, 13420 and **2009**, *15*, 3567.
82 J. P. Attfield, *Encycl. Inorg. Chem.* **2005**, *7*, 4240.
83 L.-B. Han et al., *Angew. Chem. Int. Ed.* **2010**, *49*, 6852. M. A. Pasek et al., *Angew. Chem. Int. Ed.* **2008**, *47*, 7918.

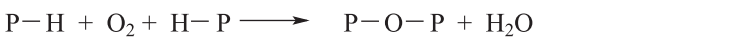

The condensed phosphates correspond to the polysulfates (S–O–S) and polysilicates (Si–O–Si). As in these cases, the condensation can result in either chain-like or cyclic structures.

In the following, only condensed phosphoric acids and their derivatives with phosphorus(V) will be considered. The parent species is diphosphoric acid $H_4P_2O_7$, which is formed on heating of H_3PO_4 to temperatures above 200 °C or through condensation of H_3PO_4 with $POCl_3$:

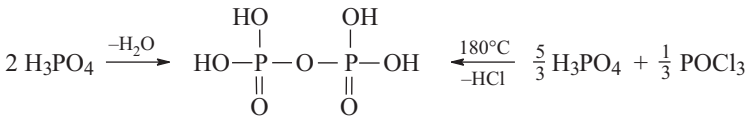

Diphosphates are obtained by thermal water elimination from two hydrogen phosphate anions:

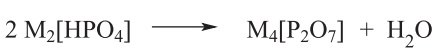

Higher condensed phosphates are generated by dehydration of mixtures of hydrogen phosphate and dihydrogen phosphate or of neat dihydrogen phosphates:

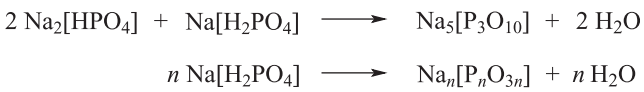

The end groups are formed from $[HPO_4]^{2-}$ ions, the chain-propagating units from $[H_2PO_4]^-$ ions, and cross-linking moieties are introduced by addition of H_3PO_4:

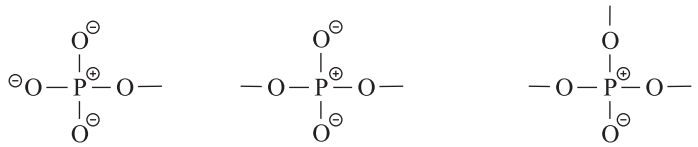

end group (I) repeat unit (II) branching unit (III)

If a condensed phosphate contains only moieties of types I and II, it must consist of chain-like anions and is referred to as a *polyphosphate*, for example, sodium triphosphate $Na_5[P_3O_{10}]$. The general formula of polyphosphates is $M_{n+2}[P_nO_{3n+1}]$ (M = monovalent cation). In contrast, anions consisting of chain-propagating units II exclusively such as $Na_3[P_3O_9]$ are necessarily cyclic and are called *metaphosphates* with a general formula of $M_n[P_nO_{3n}]$. Anions of condensed phosphates that contain a certain proportion of cross-linking units III are called *ultraphosphates*. The building blocks I–III can be distinguished by their characteristic chemical shifts in the ^{31}P-NMR spectrum.

The POP bridges are hydrolyzed to POH groups by water; condensed phosphates are therefore slowly converted to orthophosphoric acid in aqueous solution. By cautious hydrolysis, however, intermediate products can be isolated. For instance, from the hydrolysis of P_4O_{10} with ice-cold water the cyclic tetrametaphosphoric acid ($H_4P_4O_{12}$) is obtained in 70% yield (Section 10.10.2), which has been isolated as the sodium salt.

Metaphosphates are the salts of the polymeric acids $(HPO_3)_n$, with n adopting values from 3 upward. The above-mentioned sodium trimetaphosphate $Na_3[P_3O_9]$ contains the cyclic anion $[P_3O_9]^{3-}$ in a chair conformation, which is isoelectronic with trimeric sulfur trioxide S_3O_9:

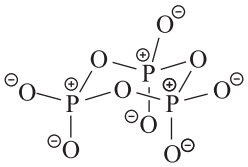

The valence angles at the bridging O atoms shared by two PO_4 tetrahedra are about 127° in $[P_3O_9]^{3-}$. In general, they can adopt values between 120° and 180° in polyphosphates.

Polyphosphates of low molecularity had been employed on a large scale as water softeners in the past as the anions form soluble *chelate complexes* with divalent metal ions such as Ca^{2+} and Mg^{2+}. In the meantime, polyphosphates in detergents were largely replaced by zeolites. Polyphosphates are also employed for preservation purposes in food technology (additives to meats, condensed milk and cheese spread), in the leather, textile and paper industries and as a component of toothpaste.

10.12.3 Peroxophosphoric Acids

If one or two OH groups of orthophosphoric acid are formally replaced by OOH groups, monoperoxophosphoric acid (H_3PO_5) and diperoxophosphoric acid (H_3PO_6) are obtained, respectively. Both compounds can be prepared by perhydrolysis of P_4O_{10}, that is, by reaction with H_2O_2/H_2O mixtures:

$$P-O-P \; + \; H_2O_2 \xrightarrow{-20°C} P-OOH \; + \; HO-P$$

Peroxodiphosphates with the anion $[P_2O_8]^{4-}$ are prepared in analogy to the synthesis of peroxodisulfates $[S_2O_8]^{2-}$ by anodic oxidation of phosphate ions:

$$2\,[PO_4]^{3-} \longrightarrow [P_2O_8]^{4-} + 2\,e^-$$

The anion, which can be isolated as $K_4[P_2O_8]$, contains a POOP bridge.

10.12.4 Thiophosphoric Acids

If the O atoms of oxoacids are formally replaced by sulfur atoms, the corresponding thioacids are obtained. While the free thioacids are unstable, their salts with the corresponding trianions can be isolated in pure form:

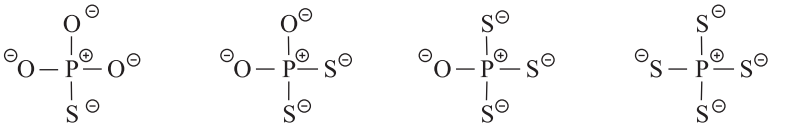

monothiophosphate dithiophosphate trithiophosphate tetrathiophosphate

Salts of all four anions can be prepared by alkaline hydrolysis or thiolysis of P_4S_{10}:

$$P_4S_{10} + 6\,Na_2S \xrightarrow{H_2O} 4\,Na_3[PS_4]$$

$$P_4S_{10} + 12\,NaOH \longrightarrow 2\,Na_3[PO_2S_2] + 2\,Na_3[POS_3] + 6\,H_2O$$

Thioacids and their salts are also derived from phosphonic acid (H_3PO_3), for example, with the anion $[HPOS_2]^{2-}$.

Numerous condensed thiophosphates are known. For example, P_4S_{10} reacts with liquid ammonia to $[NH_4]_3[P_3S_9]$, a *cyclo*-nonathiotriphosphate with a P_3S_3 pseudoheterocycle. Selenophosphates with and without PP bonds in the anions have also been synthesized.[84] If P_4 is treated with triethylammonium sulfide, however, the salt of the hypothetic thiophosphoric acid $(HPS_2)_4$ is formed, which contains a square homocyclic P_4 scaffold of D_{4h} symmetry:[85]

$$P_4 + 2\,[Et_3NH]_2[S_4] \xrightarrow{CHCl_3} [Et_3NH]_4[P_4S_8]$$

10.12.5 Halogeno- and Amidophosphoric Acids

Further variations of phosphoric acids are derived by formal replacement of one or more OH groups by other monovalent substituents such as F, Cl, Br, NH_2, CN or N_3. Finally, it should be briefly mentioned that several phosphoric acids with PP bond are known (lower phosphoric acids).

10.12.6 Oxo- and Thioacids of Arsenic and Their Salts

Important representatives of this class of compounds are:

84 M. G. Kanatzidis et al., *Inorg. Chem.* **2010**, *49*, 3092.

85 H. Falius, W. Krause, W. S. Sheldrick, *Angew. Chem. Int. Ed.* **1981**, *20*, 103.

Arsenites $MAsO_2$ and $M_3[AsO_3]$; salts of the unstable arsenious acid H_3AsO_3 or $As(OH)_3$
Arsenates $M[H_2AsO_4]$, $M_2[HAsO_4]$ and $M_3[AsO_4]$; salts of arsenic acid H_3AsO_4
Thioarsenites $M_3[AsS_3]$; salts of trithioarsenious acid $As(SH)_3$
Thioarsenates $M_3[AsS_4]$; salts of tetrathioarsenic acid H_3AsS_4

As the only stable acid of these salts, the arsenic acid $H_3AsO_4 \cdot H_2O$ can be prepared as the hydrate, namely by oxidation of As_2O_3 with concentrated nitric acid and evaporation of the solution below 30 °C. This acid is approximately as strong as phosphoric acid (Table 5.5) and a medium-strength oxidizing agent. Conversely, the very weak arsenious acid H_3AsO_3 ($pK_a = 9.2$) is only known as aqueous solution of As_2O_3, in which the species is predominantly present as $As(OH)_3$. Orthoarsenites such as $Ag_3[AsO_3]$ are derived from it as well as the polymeric metaarsenites $M_n[As_nO_{2n}]$ with As–O–As bridges, for example, in the potassium salt of composition $KAsO_2$. Organic arsonic acids are of connectivity $R–AsO(OH)_2$.

Thioarsenites and -arsenates are obtained by dissolution of As_2S_3 and As_2S_5 in aqueous sulfide solution, for example, of Na_2S. The free acids of these salts can be prepared by acidification with HCl but decompose to H_2S and the corresponding arsenic sulfide at low temperatures already. Numerous seleno- and telluroarsenites are known, many of which are semiconductors.[2,86]

10.13 Phosphorus(V) Nitrides and Nitridophosphates

Phosphorus–nitrogen species form a particularly interesting class of compounds as the PN unit is isoelectronic and even isosteric with the SiO moiety; similar structures and properties can thus be expected. For instance, the polymeric nitrides of composition PN(NH) and PNO are isoelectronic with SiO_2 and therefore crystallize in a network structure related to that of β-cristobalite (Section 8.7), which consists of corner-connected tetrahedra. The unstable monomeric molecule $O=P^+=N^-$ and the isomeric $O=N^+=P^-$ have been generated by photolysis of phosphoryl triazide $PO(N_3)_3$ in an argon matrix at 16 K and detected spectroscopically. The two molecules can be interconverted by irradiation with light of suitable wavelength.[87a] At similar conditions, $F_2P{\equiv}N$ has been obtained by photolysis of the azide $F_2P–N_3$ and identified by IR spectroscopy together with isomeric *cis*-FP=NF. Both molecules are planar.[87b]

86 A. Fromm, W. S. Sheldrick, *Z. Anorg. Allg. Chem.* **2008**, *634*, 225. M. Kanatzidis et al., *J. Am. Chem. Soc.* **2010**, *132*, 3484. Telluroarsenite: B. Eisenmann, H. Schäfer, *Z. Anorg. Allg. Chem.* **1979**, *456*, 87.

87 (a) X. Zeng, H. Beckers, H. Willner, *J. Am. Chem. Soc.* **2011**, *133*, 20696 and (b) *Angew. Chem. Int. Ed.* **2009**, *48*, 4828.

At standard conditions, *phosphinonitriles* with the formal $R_2P{\equiv}N$ unit are only stable if the multiple bond is stabilized by bulky and highly electronegative substituents R. For instance, the following derivative has been prepared by photolysis of the corresponding azide and isolated as yellow crystals and characterized by X-ray crystallography (Dip = diisopropylphenyl):[88]

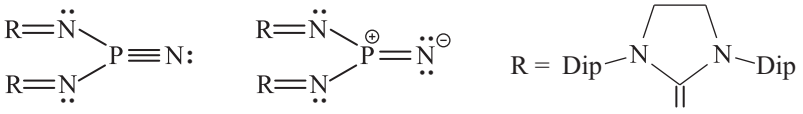

(a) (b)

The central PN_3 moiety is planar with internuclear PN distances of 162 pm (2×) and 146 pm as well as calculated atomic charges of +1.92 (P), −0.96 (2N) and −1.22 (N). Accordingly, the bonding situation is best represented by formula (b). In the literature, such species are either referred to as *nitridophosphanes* (more appropriately in view of the electronic structure) or as phosphinonitrenes or phosphinonitriles.

Phosphorus(V) nitride is formed on ammonolysis of PCl_5 or $(PCl_2N)_3$ at 780 °C as a colorless mixture of α- and β-P_3N_5:

$$3\ PCl_5 + 5\ [NH_4]Cl \longrightarrow P_3N_5 + 20\ HCl$$

Phase-pure P_3N_5 is obtained by pyrolysis of phosphonium salt $[P(NH_2)_4]I$:

$$3\ [P(NH_2)_4]I \xrightarrow{825°C} \alpha\text{-}P_3N_5 + 3\ [NH_4]I + 4\ NH_3$$

α-P_3N_5 is a beige-colored powder, which is insoluble in common solvents and even in hot acids or bases. The structure of α-P_3N_5 consists of corner-connected PN_4 tetrahedra. At high pressure (11 GPa) and high temperature (1500 °C), α-P_3N_5 is converted to γ-P_3N_5, which is built from PN_4 tetrahedra and PN_5 square pyramids.[89] With Li_3N (in turn accessible from the elements), P_3N_5 reacts depending on the stoichiometric ratio and the temperature to different salt-like nitridophosphates such as $Li_7[PN_4]$, $Li_{12}[P_3N_9]$ and $Li_{10}[P_4N_{10}]$. While the former two anions consist of (corner-connected) PN_4 tetrahedra, $[P_4N_{10}]^{10-}$ exhibits a structure that corresponds to that of the isoelectronic P_4O_{10} (T_d symmetry). Further nitridophosphates such as $M[P_4N_7]$ with M = Na–Cs, $M_3[P_6N_{11}]$ with M = K–Cs and $M[P_2N_4]$ with M = Ca, Sr have been prepared by reaction of the corresponding metal azides with P_3N_5.[90]

88 G. Bertrand et al., *Science* **2012**, *337*, 1526. A. Schulz, A. Villinger, *Angew. Chem. Int. Ed.* **2013**, *52*, 3068.

89 S. Horstmann, E. Irran, W. Schnick, *Angew. Chem. Int. Ed. Engl.* **1997**, *36*, 1873. W. Schnick et al., *Angew. Chem. Int. Ed.* **2001**, *40*, 2643 and *Chem. Eur. J.* **2002**, *8*, 3530.

90 W. Schnick et al., *Chem Eur. J.* **1999**, *5*, 2548; *J. Solid State Chem.* **2001**, *156*, 390; *Z. Anorg. Allg. Chem.* **2001**, *627*, 2469; *Chem. Eur. J.* **2007**, *13*, 6841.

10.14 Phosphazenes

Phosphazenes are mostly oligomeric species with the structural motif –P=N–. Due to their various commercial applications, they constitute the most important class of phosphorus–nitrogen compounds. The following convenient classification is applied (regarding the depiction with PN double bonds see below):

cyclo-phosphazenes

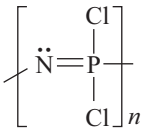

n= 3, 4, 5...

open-chain phosphazenes

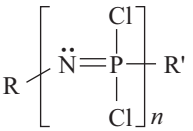

n = 1, 2, 3...

R: e.g. Cl
R': e.g. PCl_4

Phosphazenes are obtained in the complex reaction of PCl_5 with $[NH_4]Cl$ at 120 °C in an autoclave or at 135 °C and ambient pressure in tetrachloroethane or dichlorobenzene. The formation of cyclic phosphazenes is based on the following net equation:

$$n\,PCl_5 + n\,[NH_4]Cl \longrightarrow -[PCl_2{=}N-]_n + 4n\,HCl$$

For the individual steps of this reaction, which is also carried out on an industrial scale, the following mechanism is assumed. It is supported by the isolation of the intermediates except for those in round brackets, which are only hypothetical:

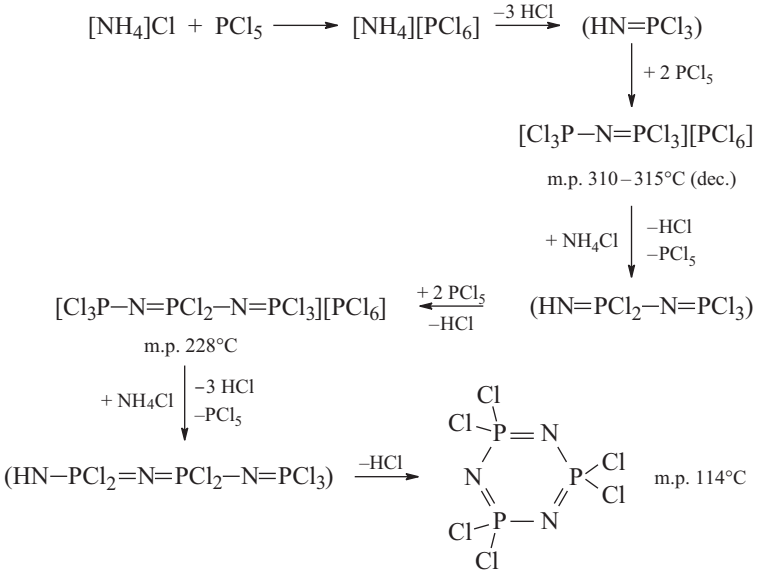

Colorless, crystalline hexachloro-*cyclo*-triphosphazatriene $(NPCl_2)_3$ is the main product of this reaction. In addition, the higher homologues $(NPCl_2)_n$ with n = 4–7 are obtained in yields decreasing with size. They can be separated by distillation in vacuum. *Cyclo*-phosphazenes are the starting material for a large number of

derivatives, which are produced by nucleophilic substitution of the chloro-substituents without compromising the integrity of the ring. In this manner, the Cl atoms are replaced partially or completely by F, Br, alkyl, aryl, O-alkyl, S-alkyl, NH_2, N_3 and other groups. Suitable reagents are $K[SO_2F]$ (halogen exchange), GRIGNARD reagents (alkylation), alcoholates, thiolates, ammonia, amines or Me_3SiN_3. FRIEDEL–CRAFTS reactions are also possible. The bromo derivatives are accessible by treatment with PBr_3/Br_2. Alternatively, the partly or completely organo-substituted phosphazenes can also be prepared by reacting $[NH_4]Cl$ with $RPCl_4$ or R_2PCl_3. With potent protonation, methylation and silylation reagents, the cationic derivatives with the corresponding substituent attached to one of the N atoms can be prepared.[91]

The molecular structures of various cyclic phosphazenes have been determined by X-ray diffraction on single crystals (Figure 10.6).

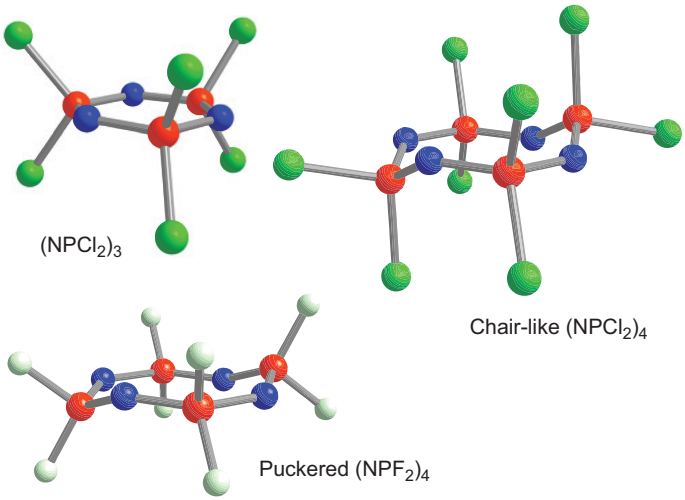

Figure 10.6: Molecular structures of cyclic phosphazenes: planar $(NPCl_2)_3$, chair-like $(NPCl_2)_4$ and slightly less puckered $(NPF_2)_4$.

The six-membered ring of $(NPCl_2)_3$ is planar; the six inner valence angles are 120° (D_{3h} symmetry). All internuclear distances d_{PN} are identical (158 pm) and considerably shorter than the sum of single bond covalent radii (177 pm). A certain PN multiple bond character gains further support from the relatively large valence force constants f_{PN}. $(NPCl_2)_4$ crystallizes either in the chair- or the boat-conformation (C_{2h} and S_4 symmetry, respectively) and the chair-like $(NPF_2)_4$ ring is slightly less puckered.

91 Y. Zhang, F. S. Tham, C. A. Reed, *Inorg. Chem.* **2006**, *45*, 10446.

10.14.1 Bonding Situation

In contrast to benzene and despite its high symmetry, $(NPCl_2)_3$ does not feature an aromatic π electron system.[92] As previously discussed (Section 10.2), a singly bonded representation of phosphazenes with positive formal charges at phosphorus and negative at nitrogen atoms may be more appropriate on grounds of the pronounced difference in electronegativity between P and N. The UV spectra and other properties of cyclic phosphazenes can be explained by a certain multiple bond character conveyed by three-center bonds extending throughout each PNP moiety in addition to the strongly polar PN σ bonds. Considering the threefold rotational axis (C_3) of the ring as the *z*-axis of the coordinate system, the "π bonds" can thus be formed by partial delocalization of the nonbonding electrons from the p_z orbitals of the nitrogen atoms into unoccupied antibonding σ* MOs of the PCl bonds at the adjacent positively charged phosphorus atoms (*hyperconjugation*).[93] This bonding situation is analogous to that in the sulfate ion (Section 2.6). Therefore, just as the cyclic metasilicates and the cyclic sulfur trioxide trimer (S_3O_9), the cyclic phosphazenes can be considered as systems of corner-connected tetrahedra.

This model explains numerous experimental observations: the identical internuclear distances in $(NPCl_2)_3$, the stability of the rings and the similar chemical behavior of $(NPCl_2)_3$ and $(NPCl_2)_4$. The number of PN units can be increased at will without significant changes in properties to be expected for an aromatic system. The nonplanarity of larger rings is also in line with this model considering the minimization of ring strain.

With asymmetric substitution of some Cl atoms of $(NPCl_2)_3$, the valence angles and internuclear distances in the ring change and it becomes nonplanar. This nonplanarity offers numerous possibilities of isomerism: the ring can adopt different conformations (chair and boat), the position of substituents can vary (regioisomerism) and equal substituents can reside on the same or on different sides of the ring.

The cyclic phosphazenes are the historically earliest examples of inorganic heterocycles. Similar *ring systems* are formed by all nonmetals except for the noble gases. Particularly common are heterocycles with two elements in alternating sequence (*pseudoheterocycles*). Besides the simple rings, condensed, poly- and spirocyclic ring systems frequently occur in inorganic chemistry.[94]

---

92 V. Jancik, F. Cortés-Guzmán, R. Herbst-Irmer, D. Matínez-Otero, *Chem. Eur. J.* **2017**, *23*, 6964.
93 A. B. Chaplin, J. A. Harrison, P. J. Dyson, *Inorg. Chem.* **2005**, *44*, 8407.
94 T. Chivers, I. Manners, *Inorganic Rings and Polymers of the p-Block Elements*, RSC, Cambridge, **2009**. R. Steudel (ed.), *The Chemistry of Inorganic Ring Systems*, Elsevier, Amsterdam, **1992**. I. Haiduc, D. B. Sowerby (eds.), *The Chemistry of Inorganic Homo- and Heterocycles*, Vols. 1 and 2, Academic Press, London, **1987**. I. Haiduc, *Encycl. Inorg. Chem.* **2005**, *7*, 4329.

10.14.2 Polyphosphazenes

If $(NPCl_2)_3$ is heated to 250 °C for longer periods of time, a rubber-like polymer of identical composition is formed, a polyphosphazene, which is insoluble in all solvents and hence apparently consists of cross-linked chains.[95] The material is hydrolyzed by water. Shorter heating to 230–250 °C results in a chain-like polymer $(NPCl_2)_n$ with n = 10000–15000, soluble in organic solvents and still amenable to nucleophilic substitution reactions, for example, with LiR, RMgX, RNH_2, R_2NH or RONa (R = organic residue). The Cl atoms are replaced in a stepwise manner during this process, which can be monitored by ^{31}P-NMR spectroscopy allowing for the sequential introduction of different substituents.

The polymerization of $(NPCl_2)_3$ probably occurs according to an ionic mechanism (Figure 10.7a) via the heterolysis of a PCl bond and electrophilic attack of a cationic phosphenium center at a nitrogen atom of a second molecule (*ring-opening polymerization*). The addition of catalytic quantities of LEWIS acids facilitates chloride abstraction and thus allows for lower reaction temperatures of about 200 °C significantly reducing the amount of undesired cross-linking. A "living" version of polyphospazene polymerization is possible with trichlorophosphoraneimine ($Cl_3P{=}NSiMe_3$) as monomeric precursor (Figure 10.7b): the process is initiated by the addition of PCl_5 as a LEWIS acid, which yields a cationic azonium diphosphorane with a $[PCl_6]^-$ counteranion by cleavage of Me_3SiCl. The polymeric chain can then be extended virtually at will by the addition of further monomer to the "living" polymer, which results in very narrow molecular weight distributions. The use of $Cl_3P{=}NSiMe_3$ in the initiating step suppresses chain growth in one of the two possible directions, which has been exploited for the preparation of block-copolymers.[96]

The polyphosphazenes constitute the largest group of inorganic polymers.[94,97] They exhibit valuable physical and chemical properties and are therefore considered for various applications. For instance, a heat and sound-insulating foam has been produced with R = –OAr, inflammable fibers are obtained with R = $-OCH_2CF_3$ and hydrocarbon-resistant materials suitable for fuel lines, seals and O-rings are prepared with R^1 = $-OCH_2CF_3$ and R^2 = $-OCH_2(CF_2)_nCHF_2$. Further variation of the substituents can either result in water-soluble or hydrophobic, in hydrolyzable or nonhydrolyzable polymers with many potential applications.[98]

95 Review: S. Rothemund, I. Teasdale, *Chem. Soc. Rev.* **2016**, *45*, 5200.

96 A. Presa Soto, I. Manners, *Macromolecules* **2009**, *42*,40; I. Teasdale et al., *Macromol. Rapid Commun.* **2014**, *35*, 1135.

97 Reviews on inorganic polymers: H. R. Allcock, *Chemistry and Applications of Polyphosphazenes*, Wiley, Hoboken, N. J., **2003**. V. Blackstone, A. P. Soto, I. Manners, *Dalton Trans.* **2008**, 4363.

98 M. Gleria, R. De Jaeger (eds.), *Phosphazenes: A Worldwide Insight*, Nova Sci. Publ., Hauppauge, N. Y., **2004**. P. H. R. Allcock, *Encycl. Inorg. Chem.* **2005**, *7*, 4586.

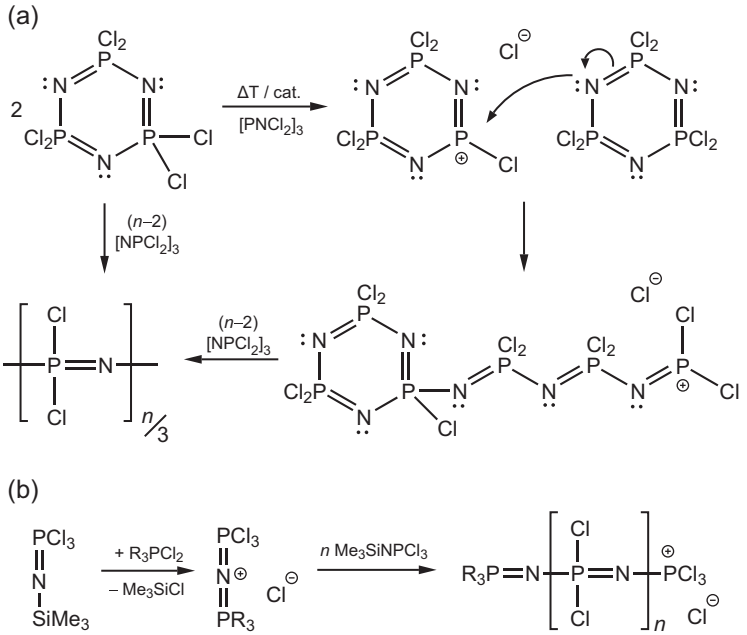

Figure 10.7: (a) Probable mechanism for the thermally or catalytically induced ring-opening polymerization of $(NPCl_2)_3$. (b) "Living polymerization" of trichlorophosphorane imine $Cl_3P{=}NSiMe_3$. Adapted from S. Rothemund and I. Teasdale.[95]

The chain-like $(PN)_n$ backbone of polyphosphazenes shows a *cis–trans* planar conformation (dihedral angle alternately 0° and 180°). They stand out with their high mechanical flexibility (low glass transition temperature), thermal stability, oxidation resistance and optical transparency above 220 nm, that is, polyphosphazenes are positively distinguished from many organic polymers. To a certain extent, they resemble the polysiloxanes (silicones) with the isoelectronic $(SiO)_n$ backbone. The very strong PN and SiO bonds are responsible for the high thermal resilience of such polymers. Only the high cost of synthesis has so far prevented a more widespread application of polyphosphazenes.

11 Oxygen

Oxygen[1] is the *most abundant element* on the accessible surface of the Earth to which it contributes 47.4 mass% (including oceans and atmosphere). Besides the molecular oxygen O_2 in the atmosphere ("dioxygen") the element occurs in ocean waters, rivers, lakes and atmospheric humidity, as well as in numerous minerals such as oxides and oxosalts of metals and nonmetals (borates, carbonates, silicates, nitrates, phosphates, sulfates, etc.). In addition, oxygen, together with H, C, N, S and P, is an essential constituent of all living organisms to which it contributes more than 50 wt%. Thus, oxygen may be considered by far the most important element.

Natural oxygen is a mixture of three *isotopes* with the following mass contributions: ^{16}O (99.76%), ^{17}O (0.05%) and ^{18}O (0.20%). The isotope ^{18}O is used for isotopic labeling of molecules for elucidating reaction mechanism. It can be prepared from $H_2{}^{18}O$, which in turn is isolated by fractional distillation of natural water. The isotope ^{17}O with a nuclear spin $I = {}^5/_2$ is used in nuclear magnetic resonance (NMR) spectroscopy.

11.1 Elemental Oxygen

11.1.1 Molecular Oxygen, O_2

Pure oxygen (O_2) is industrially produced by fractional distillation ("rectification") of liquid air using the higher vapor pressure of liquid N_2 compared to O_2. Dry air consists of 20.95 vol% (23.16 wt%) O_2, 78.08 vol% N_2, 0.93% noble gases (mainly argon; Chapter 14) and 0.04% CO_2.[2] These components can be separated by fractional condensation followed by fractional distillation due to differences in the boiling points. However, since distillation has a high energy demand almost pure oxygen is produced for some industrial consumers by separating gaseous air using membranes or molecular sieves (e.g., zeolites; Section 8.2.2).[3] Main producers of industrial gases are the companies Linde plc, Messer Group and Air Liquide (France).

Large amounts of oxygen are required by the steel industry for the reduction of the carbon content of pit iron (4% C) to values typical for steel (0.5–1.5%). Production of 1 t of steel requires about 100 kg O_2 (combustion of carbon using an oxygen lance). The chemical industry needs oxygen for a large number of oxidation reactions, often requiring a catalyst. Most often air or oxygen-enriched air is applied

1 D. T. Sawyer et al., *Encycl. Inorg. Chem.* **2005**, *6*, 4054.

2 In addition, there are traces of CH_4 (1.73 ppm), N_2O (0.3 ppm), NO (0.2 ppm), H_2 (0.5 ppm) and CO (1 ppm). The water content of air can go up to 4%; see D. Möller, *Luft: Chemie, Physik, Biologie, Reinhaltung, Recht*, de Gruyter, Berlin, Germany, **2003**.

3 H.-W. Häring (ed.), *Industrial Gases Processing*, Wiley-VCH, Weinheim, Germany, **2008**.

https://doi.org/10.1515/9783110578065-012

unless pure oxygen is needed. Examples are the CLAUS process (oxidation of H_2S to sulfur; see Section 12.3.1), the WACKER process (oxidation of ethene to acetaldehyde), the production of formaldehyde from methanol, of ethylene oxide from ethylene and of terephthalic acid from *p*-xylol, all on a million tons per year scale. Furthermore, the production of several types of soot from mineral oil (Section 7.4) uses large amounts of O_2. To enrich process air by dioxygen usually results in a higher productivity (*process intensifying*). Welding and cutting with acetylene burners also involve oxygen as does artificial respiration with pure oxygen. The explosive *Oxyliquit* is obtained if liquid oxygen is sucked into charcoal.

The oxygen of air is produced by *photosynthesis* by green plants which started approximately $3 \cdot 10^9$ years ago by a common ancestor of extant *cyanobacteria* as part of the biological evolution. It is estimated that today's oxygen concentration of Earth's atmosphere was reached about $0.65 \cdot 10^9$ years ago, but during the following 400 million years the oxygen content of the atmosphere varied between approximately 13 and 35 vol%. Photosynthesis comprises the photochemical *oxidation of water* catalyzed by the manganese containing enzyme *water oxidase*:

$$2\ H_2O \xrightarrow{h \cdot \nu} O_2 + 4\ H^+ + 4\ e^-$$

The enzymatic oxidation of water takes place at a cluster of four oxygen-bridged manganese atoms and one Ca^{2+} ion ($CaMn_4O_5$ cluster), which is embedded in a protein. In 1941 already it has been shown by ^{18}O-labeling that the liberated oxygen originates only from water molecules rather than from assimilated carbon dioxide. Production of one molecule O_2 by photosystem II requires the absorption of four photons of wavelength <680 nm. Four more photons are needed by photosystem I to produce ATP as an energy-rich molecule for the reduction of CO_2 to the carbohydrate hexose (ATP; Section 10.12.1). Photosynthesis turns approximately 10^{10} t of carbon annually from CO_2 into carbohydrates.

At present there are tremendous research activities underway to scale up the photochemical water oxidation for industrial application turning solar energy into chemical energy in the form of elemental hydrogen. One of the problems to be overcome is to develop a catalyst which is not destroyed by the molecular oxygen side product.

In laboratories, very pure oxygen can be prepared by electrolysis of 30% aqueous potassium hydroxide using nickel electrodes. On a small scale, the catalytic decomposition of 30% aqueous hydrogen peroxide at a platinized nickel foil may also be used; the metal foil is lowered into the aqueous phase as oxygen is demanded. Quantitative decomposition of 1 kg H_2O_2 (29.4 mol) yields up to 300 L molecular oxygen at standard conditions since the solubility of O_2 in water is only 44 mg L^{-1} (20 °C, 1.013 bar). However, for most purposes the commercial pressurized oxygen gas in steel cylinders is suitable; the gas pressure may be as high as 300 bar.

Gaseous oxygen is odor- and colorless, but liquid O_2 is pale blue colored (m.p. −218 °C, b.p. −183 °C). The bonding situation in the O_2 molecule has been discussed

in Section 2.4.3. In its triplet ground state ($^3O_2$) the molecule has two unpaired electrons of equal spin. Therefore, gaseous and liquid dioxygen are *paramagnetic*, a circumstance utilized for quantitative O_2 determination in gas mixtures. In the solid state, O_2 is either paramagnetic (γ-phase) or diamagnetic (α- and β-phases). In 2006, it was discovered that solid O_2 oligomerizes at very high pressures to dark-red rhombic O_8 molecules (ε-phase) with four $\pi^\star$–$\pi^\star$ bonds between the four aligned molecules forming a cube-like cluster.[4]

Diamagnetic dioxygen in the excited singlet state ($^1O_2$) is generated in a variety of chemical reactions, which are discussed in the following section.

11.1.1.1 Singlet Dioxygen ($^1O_2$)

Two singlet states of dioxygen[5] have been predicted independently by ROBERT S. MULLIKEN in the USA and by ERICH HÜCKEL in Germany during the years 1928–1930. These two singlet states differ from the triplet ground state ($^3\Sigma_g$) only by the electron configuration at the $1\pi_g$ level:

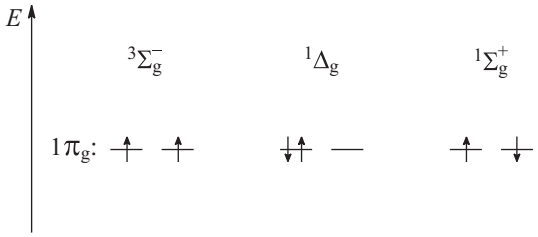

The bond properties of O_2 in its different electronic states are given in Table 11.1.[6]

Table 11.1: Bond properties of gaseous dioxygen ($^{16}O_2$) in the triplet ground state and two electronically excited singlet states (*d*: internuclear distance, *D:* bond energy at 0 K).[a]

	$^3\Sigma_g^-$	$^1\Delta_g$	$^1\Sigma_g^+$
d_{OO} (pm):	120.75	121.56	122.69
D (kJ mol^{-1}):	491	396	333
Relative energy (kJ mol^{-1}):	0	95	158

[a]K. P. Huber, G. Herzberg, *Constants of Diatomic Molecules*, van Nostrand-Rheinhold, New York, **1979**.

4 R. Steudel, M. W. Wong, *Angew. Chem. Int. Ed.* **2007**, *46*, 1768. Y. Meng et al., *PNAS* **2008**, *105*, 11640.

5 A. A. Gorman, *Chem. Soc. Rev.* **1991**, *10*, 205. V. Nerdello et al., *Chem. Commun.* **1998**, 599.

6 Accurate calculations of the energy differences between $^1O_2$ and $^3O_2$ show that correct values are obtained only if the partial occupation of higher molecular orbitals are taken into account (*complete active space* calculations). For $^3O_2$ the population $(1\pi_u)^{3.92}(1\pi_g)^{2.07}(2\pi_u)^{0.01}$ is obtained and for $^1O_2$: $(1\pi_u)^{3.87}(1\pi_g)^{2.12}(2\pi_u)^{0.01}$. The $2\pi_u$ MO results from the linear combination of the four $3p_\pi$ AOs.

The short-lived state $^1\Sigma_g^+$ is relatively unimportant since it rapidly converts to O_2 ($^1\Delta_g$), which plays a major role in certain oxidation reactions. Molecules in these excited states are generated in electrical discharges in pure oxygen gas and have also been detected in the Earth's atmosphere due to excitation by the Sun's radiation. At reduced pressure, gaseous $O_2(^1\Delta_g)$ has a lifetime of approximately 45 min since a unimolecular reaction to the ground state $^3\Sigma_g^-$ is forbidden by the *law of spin conservation*. Therefore, the deactivation proceeds by a bimolecular reaction and with emission of the excess energy in the form of red light of wavelengths 633 and 703 nm. Two emission lines are observed since $^3O_2$ can be produced either in its vibrational ground state (633 nm) or in its first vibrationally excited state (703 nm):

$$2\ O_2(^1\Delta_g) \longrightarrow 2\ O_2(^3\Sigma_g^-)$$

The reverse reaction, that is, the absorption of red light, is responsible for the blue color of liquid and solid O_2.

In solution $^1O_2$ is formed by *thermal decomposition of peroxides*. For example, if chlorine gas is bubbled into ice-cold hydrogen peroxide solution a very attractive red glow is observed from the deactivation of $^1O_2$ formed by decomposition of the intermediate chlorine peroxide:[7]

$$H_2O_2 + Cl_2 + 2\ [OH]^- \longrightarrow [ClOO]^- + Cl^- + 2\ H_2O$$
$$[ClOO]^- \longrightarrow {}^1O_2 + Cl^-$$

For reasons of spin conservation $^3O_2$ cannot be a product in this reaction since the number of unpaired electrons (or total spin quantum numbers) would be different on both sides of the equation. The *law of spin conservation* requires that the sum of spin quantum numbers on both sides of an equation should be identical if the reaction is expected to proceed at low or moderate temperatures, that is, with a small activation energy. Therefore, the reactions of $^3O_2$ with diamagnetic molecules such as H_2 or organic compounds are kinetically hindered at 25 °C due to a high activation energy. This is very fortunate since otherwise all organic matter on the Earth would easily ignite and spontaneously combust in air.

Electronically excited dioxygen molecules are also formed during the decomposition of hydrogen peroxide catalyzed by molybdate $[MoO_4]^{2-}$ ions:

$$2\ H_2O_2 \longrightarrow {}^1O_2 + 2\ H_2O$$

At pH values between 8 and 13, the first product is the bis-peroxo anion $[Mo(O)_2(O_2)_2]^{2-}$, which in turn decomposes in a rate-determining reaction of first order to $[MoO_4]^{2-}$ and $^1O_2$.

---

7 *N*-Bromsuccinimide may be used instead of chlorine; see S. Albrecht, H. Brandl, T. Zimmermann, *Chem. unserer Zeit* **1998**, *32*, 251 (with impressive color photos).

Phosphonic esters $(RO)_3P$ are known to add ozone at low temperatures with formation of *covalent ozonides* by [1 + 3] cycloaddition followed by [2 + 2] cycloreversion to $^1O_2$ and phosphoric esters at higher temperatures:[8]

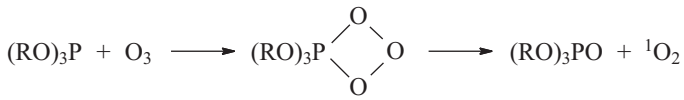

The lifetime of $^1O_2$ in solution is in the range 4–600 μs, depending on the solvent. Suitable solvents are $CFCl_3$, CF_2Cl_2 and deuterated compounds such as CD_3CN (long half-life of $^1O_2$). The deactivation of $^1O_2$ occurs in a first-order reaction by energy transfer by vibrational excitation of the solvent molecules. Alternatively, the excess energy of $^1O_2$ can be emitted as radiation of wavelength 1250 nm (*phosphorescence*) since the interaction with the solvent molecules slightly reduces the symmetry of $^1O_2$ and partially lifts the selection rules.[9]

In contrast to $^3O_2$, the energy-rich $^1O_2$ reacts with many organic compounds at room temperature already. For instance, peroxides are formed with 1,3-dienes by [4 + 2] cycloaddition, and [2 + 2] cycloaddition occurs with alkenes, alkynes, ketenes, allenes, sulfines and oximes. Certain alkenes react with $^1O_2$ to hydroperoxides ROOH (*en*-reaction). Therefore, singlet dioxygen plays an important role also in living organisms where it may be formed either by decomposition of peroxides or by photochemical excitation of $^3O_2$ to $^1O_2$ catalyzed by certain pigments in the skin. In the latter case, the pigments function as *sensitizers* by absorbing the photons followed by energy transfer to O_2. The singlet dioxygen produced in this way can kill living cells. On the one hand, irradiation has an antibacterial effect; on the other hand, negative effects may occur by such *reactive oxygen species* (ROS).[10]

11.1.1.2 Complexes with O_2 as a Ligand

Molecular oxygen is needed by almost all organisms for *respiration* in order to sustain the *metabolism* to oxidize fats, carbohydrates and proteins to water, carbon dioxide and urea. The energy gained is used to synthesize ATP as an internal energy storage compound. Adults take up approximately 800 L O_2 per day of which approximately 5% (50 g) is turned into ROS such as $[O_2]^{\bullet -}$, $[HO_2]^{\bullet}$, $[OH]^{\bullet}$, H_2O_2 and $[ONOO]^-$ (peroxonitrite). All ROS are extremely toxic triggering cancer and premature aging; therefore, these species need to be removed from the organism, for example by antioxidants.[11]

8 A. Dimitrov, K. Seppelt, *Eur. J. Inorg. Chem.* **2001**, 1929.
9 P. R. Ogilby et al., *J. Am. Chem. Soc.* **2010**, *132*, 8098.
10 P. R. Ogilby, *Chem. Soc. Rev.* **2010**, *39*, 3181.
11 M. Battran, *Naturwiss. Rundschau* **2002**, *55*, 513.

Since the solubility of O_2 in water at 20 °C and a partial pressure of 1.013 bar is only 44 mg L^{-1} many organisms use metal complexes to fix O_2 as a ligand for storage, activation and transportation within their bodies. Almost all transition metals form O_2 complexes. The formal oxidation number of the coordinated oxygen atoms varies between 0, –½ and –1 as in O_2, $[O_2]^{\bullet-}$ (superoxide) and $[O_2]^{2-}$ (peroxide), respectively. In Figure 11.1, the various atomic arrangements observed in metal complexes with O_2 ligands are shown.

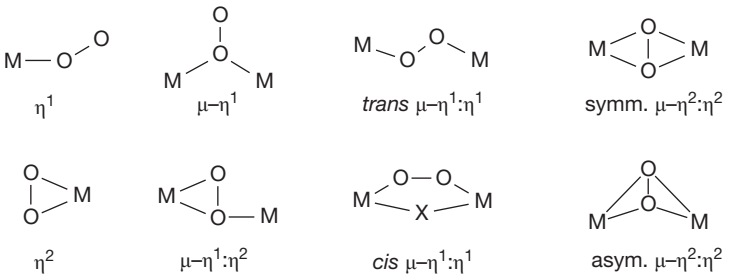

Figure 11.1: Arrangements of the O_2 unit observed in metal complexes with the dioxygen ligand as determined by X-ray structure analyses.

The oxidation number of oxygen atoms in dioxygen complexes can sometimes be determined by magnetic susceptibility measurements or electron spin resonance (ESR) spectroscopy. In addition, determination of the wavenumber of the OO stretching vibration by RAMAN spectroscopy can help to acquire information about the OO bond strength (see Section 11.2.6). However, in other cases, the oxidation states of the metal and oxygen atoms remain a matter of dispute. The position of the metal in the Periodic Table as well as other ligands eventually determine the bonding situation of the O_2 unit.

Let us consider some real examples of dioxygen complexes. Certain transition metals react with O_2 at room temperature in solution either by a simple addition of the new η^2 ligand or by ligand displacement:

$$[RuCl_2(AsPh_3)_3] + O_2 \longrightarrow [RuCl_2(O_2)(AsPh_3)_3]\downarrow$$

$$[Pt(PPh_3)_4] + O_2 \longrightarrow [Pt(O_2)(PPh_3)_2]\downarrow + 2\ PPh_3$$

Such reactions are typical for electron-rich transition metals (Mn, Co, Ni, Ru, Ir, Rh, Pd and Pt) in low oxidation states. Some of these complexes are in equilibrium with the free O_2 ligand, which can be liberated by heating or purging with an inert gas:

$$[Rh(O)_2(diphos)_2]PF_6 \underset{}{\overset{MeOH}{\rightleftharpoons}} [Rh(diphos)_2]PF_6 + O_2$$

diphos: $Ph_2P-(CH_2)_2-PPh_2$

In some cases, the O_2 ligand can be removed chemically by flushing with H_2 resulting in a dihydrido complex, which in turn reacts with O_2 back to the dioxygen complex.

Electron-poor transition metals such as Ti, V, Cr, Mo and W in high oxidation states also form complexes with a η^2-O_2 ligand, but as a peroxo group with the oxidation state –1 for the O-atoms, for example:

$$2\,[CrO_4]^{2-} + 9\,H_2\mathbf{O}_2 + 2\,[OH]^- \longrightarrow 2\,[Cr(O_2)_4]^{3-} + 10\,H_2O + O_2$$

During this reaction the Cr(VI) atom in the yellow chromate $K_2[CrO_4]$ is reduced by hydrogen peroxide (!) to Cr(V); the resulting brown tetraperoxo chromate $K_3[CrO_8]$ is *paramagnetic* (d^1 complex). The coordination geometry at the central atom of the anion is quasi-tetrahedral:

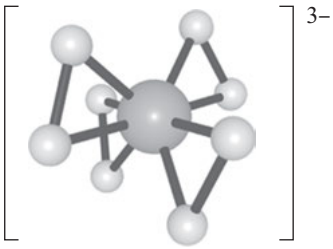

The internuclear distances d_{OO} of 146.6 pm are close to the OO bond lengths in ionic peroxides such as $Na_2[O_2]$ and $Ba[O_2]$ (149 pm).

In acidic solution, hydrogen chromate ($[HCrO_4]^-$) reacts with H_2O_2 to a blue species, which is sometimes referred to as "CrO_5" in textbooks but exists in water as a neutral complex $[(H_2O)CrO(O_2)_2]$ containing Cr(VI). This compound can be extracted from the aqueous phase by a strong donor solvent **D** such as pyridine or diethylether as blue solvate $[\mathbf{D}CrO(O_2)_2]$ with two η^2-peroxo ligands. This reaction is used in analytical chemistry as a test for chromate ions.

In the complexes mentioned so far, the O_2 ligand forms a triangle with the metal atom (local symmetry either C_{2v} or C_s) and functions as a π and π* donor and π* acceptor. If the $D_{\infty h}$ symmetry of O_2 is reduced to C_{2v} in the complex, the antibonding π* level splits into two sublevels resulting in pairing of the two single electrons in the lower of the two antibonding MOs. The interaction of these ligand MOs with the empty *d* orbitals of a metal atom M is shown in Figure 11.2. The two strongest interactions are between the occupied $1\pi_u$ MO of O_2 and the d_z^2 AO of M establishing a σ donor bond if the metal orbital is empty (coordinate bond). The

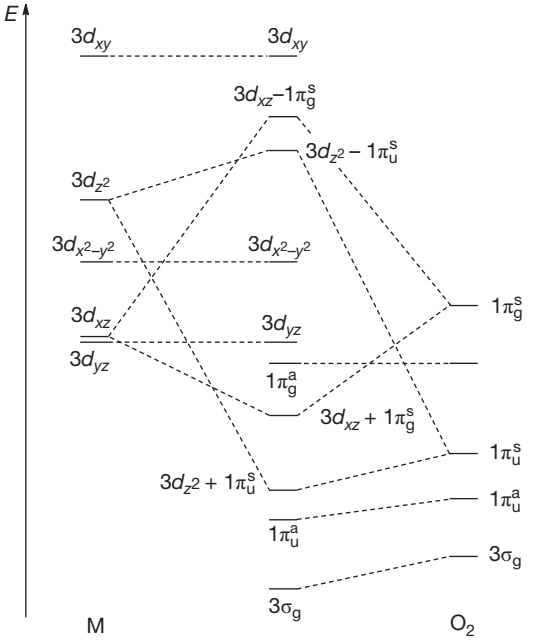

Figure 11.2: Schematic energy-level diagram for the molecular orbitals of η^2-dioxygen complexes with *side-on* coordination of the ligand to a metal atom M of the first transition metal row. The five originally degenerate *d* orbitals of M split into four separate levels due to the (asymmetric) field of the ligands. Similarly, the reduction of symmetry of O_2 from $D_{\infty h}$ for the free molecule to C_{2v} as a η^2-ligand causes the formerly degenerate orbitals of π symmetry to split into four single levels (the symmetry labels g and u apply to the ligand only).

combination of the empty $1\pi_g$ MO of O_2 with the d_{xz} AO of M establishes a π bond if this *d* orbital is occupied (coordinate backbonding). The overlap of these orbitals is shown in Figure 11.3.

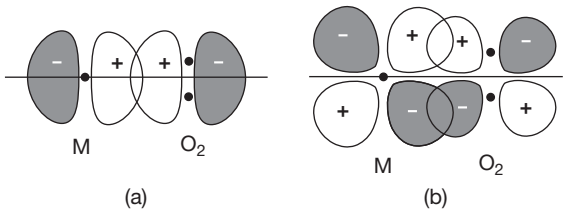

Figure 11.3: Schematic representation of the overlap between two metal orbitals and two ligand orbitals in O_2 complexes with side-on coordination. (a) σ bond between an empty *p* or *d* orbital of the metal atom M and the occupied $1\pi_u$ MO of the ligand O_2. (b) π bond (back bonding) between an occupied *d* orbital of M and the empty $1\pi_g$ MO of O_2.

The coordinate backbonding ($1\pi_g \leftarrow d_{xz}$) is all the stronger the higher the electron density at the metal atom, which depends on the type of metal and on the other ligands. Especially the electronegativity χ of the ligands has a major impact. The larger the χ, the more electron density is withdrawn from the metal and the weaker is the backbonding to O_2. Since the delocalization of electron density from the metal into the antibonding ligand MO weakens the OO bond, the length *d* of this bond varies with the electronegativity of the other ligands as the OO bond lengths of the following iridium complexes illustrate (χ_{AR}: ALLRED–ROCHOW electronegativity):

$$[Ir(O_2)Cl(CO)(PPh_3)_3]: \; d_{OO} = 130\text{pm} \qquad \chi_{AR}(Cl) = 2.8$$

$$[Ir(O_2)I(CO)(PPh_3)_3]: \; d_{OO} = 151\text{pm} \qquad \chi_{AR}(I) = 2.2$$

Similar bond lengths d_{OO} have been observed in other mononuclear dioxygen complexes (range 130–152 pm). Compounds that lose the O_2 ligand relatively easily show OO bond lengths close to that of gaseous O_2 (121 pm), for example, in the cation of $[Ir(O_2)(diphos)_2][PF_6]$, d_{OO} = 152 pm (diphos = a chelating bisphosphane). The weakening of the OO bond is also manifest in the Raman spectrum by the OO stretching vibration. Wavenumbers ν_{OO} down to 800 cm^{-1} have been determined compared to 1556 cm^{-1} in free O_2.

In complexes with the peroxido ligand $[O_2]^{2-}$, electron density is transferred from the ligand to the metal atom both from the π and the π* level, provided the metal has no or only a few *d* electrons (Figure 11.2).

Dioxygen complexes serve as model compounds to study the mechanisms of oxygen transfer reactions in living organisms.[12] Many organisms contain proteins with metal complexes as *prosthetic groups* (reaction centers), which serve as storage, carrier and transfer reagents for oxygen atoms, for example, in respiration processes. Quite often these are iron complexes with the O_2 unit in η^1 coordination (Figure 11.1).[13]

Dioxygen complexes also serve as models for inorganic oxidation reactions catalyzed by transition metals.[14] Usually, the O_2 ligand is more reactive than free O_2 molecules at the same temperature. For example, $[RuCl_2(O_2)(AsPh_3)_3]$ reacts at room temperature with Ph_3P to Ph_3PO and with SO_2 to a sulfato complex. Therefore, O_2 ligands are considered as *activated dioxygen*. If such complexes are diamagnetic the *law of spin conservation* is easily obeyed, in contrast to reactions with paramagnetic O_2 gas. There are also numerous complexes with the isoelectronic S_2 molecule as a ligand.

12 R. J. Jones, D. A. Summerville, F. Basolo, *Chem. Rev*. **1979**, *79*, 139.

13 See the special issue on *Metal-Dioxygen Complexes* in *Chem. Rev*. **1994**, *94*, 567–856.

14 L. I. Simandi, *Catalytic Activation of Dioxygen by Metal Complexes*, 2nd ed., Kluwer Acad. Publ., 2014. D. H. R. Barton, A. E. Martell, D. T. Sawyer (eds.), *The Activation of Dioxygen and Homonuclear Organic Oxidations*, Plenum, New York, **1993**.

11.1.2 Atomic Oxygen

Free oxygen atoms can be generated by homolytic dissociation of O_2 in a high-frequency or microwave gas discharge (*plasmalysis*). The degree of dissociation depends on the intensity of the discharge, the gas pressure and the geometry of the vessel since recombination of atoms to O_2 at low pressure occurs mainly at the walls. Certain compounds, however, when applied to the walls can serve as *negative catalysts* (poisoning of the catalyst). Besides recombination in the gas phase by a three-body collision, the recombination at the walls occurs between adsorbed oxygen atoms and the released reaction enthalpy is absorbed by the glass surface in the form of heat (vibrational energy):

$$O + O \longrightarrow O_2 \qquad \Delta H^\circ_{298} = -499 \text{ kJ mol}^{-1}$$

The given recombination enthalpy is valid for oxygen atoms in the ^3P ground state with two unpaired electrons and for O_2 in its triplet ground state. The term symbol ^3P indicates the spin multiplicity $2S + 1$ and the orbital momentum L (symbol P for $L = 1$). Since $S = \Sigma s$ and $s = ½$ the multiplicity is 3 or triplet. Oxygen atoms in the electronically excited singlet state ^1D are by 201 kJ mol^{-1} higher in energy and have all electrons paired.

Ground state oxygen atoms react at room temperature and pressures of a few hundred Pascal with gaseous O_2 in a three-body collision to give ozone:

$$O + O_2 + M \longrightarrow O_3 + M^* \qquad \Delta H^\circ_{298} = -107 \text{ kJ mol}^{-1}$$

The collision partner M is expected to absorb part of the released enthalpy as vibrational or electronic excitation energy (M*) to avoid the immediate back reaction. M can be any inert atom or molecule or even the wall of the vessel. The stationary ozone concentration obtained in O–O_2 mixtures, however, is rather small because of a rapid degradation reaction between O_3 and oxygen atoms:

$$O + O_3 \longrightarrow 2\,O_2 \qquad \Delta H^\circ_{298} = -393 \text{ kJ mol}^{-1}\ (O_3)$$

This reaction is fast since at low pressures the probability for a two-body collision is much higher than for a three-body collision such as the ozone formation or the recombination of atoms according to $O + O + M \rightarrow O_2 + M^*$. Therefore, to prepare O_3 the gaseous O–O_2 mixture behind the electrical discharge is cooled by a *cold finger* filled with liquid nitrogen. On this cold surface, ozone formation takes place with high yield and the dark-blue product will immediately be frozen and in this way protected from decomposition by secondary reactions.

In low-temperature experiments, oxygen atoms can be prepared by photolysis of O_3 or NO_2, applying the matrix isolation technique:

$$O_3 \xrightarrow{h\cdot\nu} O_2 + O$$
$$NO_2 \xrightarrow{h\cdot\nu} NO + O$$

These reactions will be discussed further in Section 11.3.5.

Oxygen atoms are extremely strong oxidants reacting with many substances even at low temperatures. The concentration of O atoms in a gas stream can be determined by *titration* with continuously added known amounts of NO_2 which are initially reduced to NO:

$$NO_2 + O \longrightarrow NO + O_2$$

In a secondary reaction, NO is rapidly re-oxidized to electronically excited NO_2 molecules, which spontaneously lose their excess energy as photons in the form of a yellow-greenish emission:

$$NO + O \longrightarrow NO_2^* \xrightarrow{-h\cdot\nu} NO_2$$

For the continuous titration of oxygen atoms in a gas stream the concentration of the added NO_2 is slowly increased until the greenish emission disappears, that is, until all oxygen atoms are consumed by NO_2 and the secondary reaction with NO cannot longer take place. NO is hence both the indicator and the titrant for oxygen atoms in this process.

When platinum crystals or foils are exposed to molecular oxygen, the O_2 molecule dissociates spontaneously even at 165 K since electron density is transferred from the electron-rich metal to the antibonding MOs of O_2 weakening the OO bond. The strongly exothermic adsorption of the formed oxygen atoms provides part of the dissociation enthalpy since each O atom is linked to several metal atoms with formation of PtO bonds. Such reactions are of enormous importance in *heterogeneous catalysis*, for example, the oxidation of ammonia to NO for the large-scale manufacture of nitric acid; see Section 9.4.2.

11.1.3 Ozone, O_3

Besides O_2, ozone or *trioxygen* is the only molecule consisting entirely of oxygen atoms, which can be prepared in pure form at room temperature and ambient pressure. However, O_3 is an endothermic compound and therefore thermodynamically unstable:

$$\frac{3}{2}\,O_2 \longrightarrow O_3 \qquad \Delta_f H^\circ_{298} = 143\ \text{kJ mol}^{-1}$$

Pure ozone, especially in liquid and solid form, is explosive and should be handled with great care. Its exothermic decomposition to O_2 is accompanied by

volume expansion, which is utilized to determine the ozone concentration in mixtures with O_2.

To prepare a continuous stream of ozone-containing oxygen an apparatus invented by WERNER VON SIEMENS in 1888 is used (*ozone generator*). Dry and pure oxygen gas of 25 °C and 0.1 MPa is led through the slit between two concentric metallized glass tubes, in which O_2 is exposed to a high-voltage silent discharge. If the glass tubes are cooled to room temperature (they warm by dielectric loss) and the flow rate is not too small, ozone concentrations of up to 10% are obtained. The formation of O_3 occurs both via excited O_2 molecules and oxygen atoms as well as by dissociative ion recombination reactions:

$$O_2^* + O_2 \longrightarrow O + O_3$$
$$O + O_2 + M \longrightarrow O_3 + M^* \quad (M: \text{e.g. } N_2)$$
$$[O_2]^+ + [O_2]^- \longrightarrow O + O_3$$

The collision partner M absorbs some of the energy released during exothermic ozone formation. Pure ozone is obtained by fractional condensation as its boiling and melting points (m.p. –193 °C, b.p. –112 °C) are considerably higher than those of O_2. Ozone is diamagnetic, deep blue, very toxic and has a characteristic smell which can be recognized in air at a concentration as low as 200 μg m^{-3}. O_3 is a strong, clean and environmentally friendly oxidant and is therefore used instead of chlorine to treat drinking water and water in swimming pools. In addition, organic compounds in wastewater are oxidized by ozone. A modern application of O_3 is the treatment of flue gas of power stations and sulfuric acid plants to turn nitrogen oxides into nitric acid (HNO_3), which can be washed out by scrubbing the gas with water (LoTOx process).

For quantitative analysis of O_3, the gas mixture is bubbled into an aqueous solution of potassium iodide in the presence of boric acid as a buffer. One mol of elemental iodine is formed for each mol of O_3 consumed:

$$O_3 + 2\,I^- + H_2O \longrightarrow O_2 + I_2 + 2\,[OH]^-$$
$$B(OH)_3 + [OH]^- \longrightarrow [B(OH)_4]^-$$

The initial reaction is the attack of the nucleophile I^- at the ozone molecule with release of O_2 followed by protonation of the hypoiodite ion $[IO]^-$, which is then attacked by another iodide ion to give I_2:

$$I^- + O_3 \longrightarrow [I{-}O{-}O{-}O]^- \longrightarrow [IO]^- + O_2$$
$$[IO]^- + H_2O \longrightarrow IOH + [OH]^-$$
$$IOH + I^- \longrightarrow I_2 + [OH]^-$$

Such reactions are called *nucleophilic displacements*.

In the absence of reducing agents, ozone reacts with hydroxide ions of water via short-lived $[HO_4]^-$ ions to H_2O_2 or its anion $[HO_2]^-$:

$$O_3 + [HO]^- \longrightarrow [HO_4]^-$$

$$[HO_4]^- \rightleftharpoons HO_2^\bullet + [O_2]^{\bullet -} \longrightarrow [HO_2]^- + {}^3O_2$$

The molecule O_3 is of C_{2v} symmetry with bond lengths of 127.2 pm, a bond angle of 117.8° and a dipole moment of 0.53 D in the gas phase. In the solid state, the bond lengths are 125.7 pm and there is a weak intermolecular interaction between terminal atoms. The ionization energy of O_3 is 12.5 eV. The experimental dissociation enthalpy $O_3 \rightarrow O_2(^3\Sigma_g) + O(^3P)$ is 109.2 kJ mol^{-1}. Besides two σ bonds ozone has a 3-center-4-electron π bond which can be symbolized by the following canonical structures:

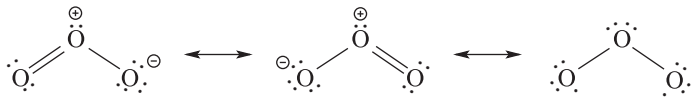

(a) (b) (c)

In Table 11.2 the bond properties of O_3 are compared with those of O_2 and its anions superoxide and peroxide.

Table 11.2: Experimental bond properties of compounds with oxygen-oxygen bonds at 298 K without correction for anharmonicity (g.: gaseous).

	O_2 (g.)	O_3 (g.)	$[O_2]^-$ (g.)	$[O_2]^{2-}$ (in Na_2O_2)
OO bond length (pm)	121	127.2	135	149
Stretching force constant f_r (N cm^{-1})	11.4	5.7	5.4	2.8
Mean bond enthalpy (kJ mol^{-1})	495	300	395	–

The data in Table 11.2 show that there is a correlation between bond lengths and stretching force constants and this also holds for the mean bond energies of O_2 and $[O_2]^-$ in the gas phase. However, the mean bond energy of O_3 is unusually small indicating weak bonds.

The 3-center π bond of O_3 results from the overlap of the three atomic 2*p* orbitals, which are oriented perpendicularly to the molecular plane. By suitable linear combinations, three MOs are obtained (one bonding, one weakly antibonding and one strongly antibonding) as shown in the following diagram:

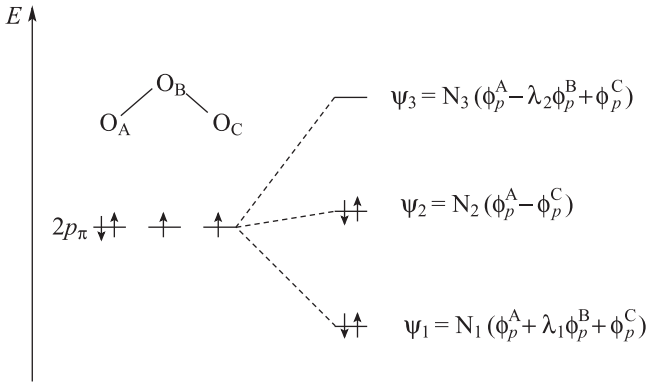

Since the 2*p* orbitals are occupied by four electrons, the strongly antibonding MO remains unoccupied.[15] Quantum-chemical calculations have revealed that the partial charges at the terminal atoms of O_3 are only −0.14 *e* and that the molecule has a *partial diradical character* since the spin densities at the terminal atoms are ±0.52 (α/β).[16] This can be symbolized by the canonical structure (c) for O_3 with uncharged atoms and two *unpaired electrons of opposite spins* at the terminal atoms (singlet ground state).[17] According to these calculations, structure (c) contributes as much to the energy of the molecule as structures (a) and (b) combined. The internuclear distance between the equally charged terminal atoms is only 218 pm, much less than the VAN DER WAALS distance of 280 pm. This may be the reason for the relatively small mean bond energy of O_3. A hypothetical cyclic O_3 molecule of D_{3h} symmetry is predicted to be 130 kJ mol^{-1} less stable than the C_{2v} structure. The rather unusual bonding situation of ozone may explain its high reactivity, e.g. in dipolar cycloadditions with alkenes and alkynes.

Ozone is a trace component in **Earth's atmosphere** from the surface up to at least 100 km. In the upper atmosphere (*stratosphere*: altitude 12–50 km) ozone is formed by UV photolysis of O_2 by radiation of wavelength ≤250 nm followed by reaction of oxygen atoms with O_2. This process is most important above the Equator where the Sun's intensity is at maximum. The highest ozone concentrations of ca. $5 \cdot 10^{12}$ molecules per cm^3 (4 mg m^{-3}) are observed at an altitude of 15–30 km where

15 The isoelectronic nitrite anion $[NO_2]^-$ has a similar bonding situation with a 3-center 4-electron π bond, and the same holds for SO_2; see Y. Lan, S. E. Wheeler, K. N. Houk, *J. Chem. Theor. Comput.* **2011**, *7*, 2104.

16 F. Weinhold, C. R. Landis, *Discovering Chemistry with Natural Bond Orbitals*, Wiley, Hoboken, **2012**, S. 47–48. E. Miliordos, S. S. Xantheas, *J. Am. Chem. Soc.* **2014**, *136*, 2808.

17 This is no contradiction to the MO energy-level diagram but describes the delocalization of the electrons in the weakly antibonding molecular orbital ψ_2. An "electron pair" is defined as two electrons of opposite spin in one orbital but not necessarily in the same space section. This holds for all electrons in molecules. If the separation of these two electrons is large (e.g., in an extended molecular orbital) a singlet diradical results.

the temperatures are in the range 210–250 K. This so-called *ozone layer* contains 90% of all atmospheric O_3 and absorbs 99% of the Sun's hard UV radiation of wavelengths ≤320 nm. The absorption maximum of O_3 is at 260 nm. UV photolysis of O_3 produces oxygen atoms both in the ^3P ground state as well as in the ^1D excited state. It is this process that made the *evolution of life* on land outside the oceans, lakes and rivers possible.

The *troposphere* (altitude 0–12 km) contains approximately 10% of the atmospheric ozone, but in very low concentrations. The total amount of ozone in a vertical column in the atmosphere above ground can be determined from the absorption of sunlight as well as by straylight of laser radiation sent vertically into the sky. The O_3 concentration in air is given in DOBSON units (DU); 100 DU are equivalent to a 1 mm layer of pure gaseous O_3 of 1.013 bar and at 273.2 K. Typical extreme values in Germany are 350 DU in the spring and 280 DU in December.

Several natural and anthropogenic trace gases decompose O_3 in the stratosphere. Most important are nitrogen oxides which turn O_3 into O_2 by a catalytic cycle:[18,19]

$$NO + O_3 \longrightarrow NO_2 + O_2$$
$$NO_2 + O \longrightarrow NO + O_2$$

NO is produced in the stratosphere from laughing gas (N_2O) of bio- and anthropogenic origin. Due to its low reactivity, N_2O is transported to higher altitudes by convection where it reacts with excited oxygen atoms $O(^1D)$ to two NO molecules. The net reaction of the above catalytic cycle is therefore $2\ O_3 \rightarrow 3\ O_2$. Nowadays, N_2O emission is the *most important anthropogenic source of ozone-destroying compounds*. The concentration of N_2O in the atmosphere is steadily rising and is probably responsible for permanent ozone depletion (*ozone hole*).

Water molecules react with oxygen atoms to $OH^\bullet$ radicals, which decompose O_3 to O_2 and $HO_2^\bullet$ radicals. The latter is attacked by oxygen atoms with formation of $OH^\bullet$ and O_2. By these *natural production and destruction processes* a stationary ozone concentration is normally achieved in the stratosphere (*dynamic equilibrium*).

Chlorine and bromine atoms, however, are even more catalytically active than NO and $OH^\bullet$ radicals. These atoms are generated in the stratosphere by UV photolysis of halogenated hydrocarbons and destroy ozone according to the following scheme (M: inert collision partner):

18 PAUL CRUTZEN, MARIO MOLINA and FRANK ROWLAND jointly received the Nobel prize in chemistry for the year 1995 for discovering the ozone depletion mechanisms in Earth's atmosphere.

19 P. J. Crutzen, *Angew. Chem. Int. Ed.* **1996**, *35*, 1758; M. J. Molina, *Angew. Chem. Int. Ed.* **1996**, *35*, 1758; F. S. Rowland, *Angew. Chem. Int. Ed.* **1996**, *35*, 1786; see also the special issue of *Chem. unserer Zeit* **2007**, *41*, issue 4; M. Dameris, *Angew. Chem. Int. Ed.* **2010**, *49*, 489 and 8092.

$$Cl^{\bullet} + O_3 \longrightarrow ClO^{\bullet} + O_2$$
$$2\,ClO^{\bullet} + M \longrightarrow Cl_2O_2 + M^*$$
$$Cl_2O_2 \xrightarrow{h\cdot\nu} Cl^{\bullet} + OOCl^{\bullet}$$
$$OOCl^{\bullet} + M \longrightarrow O_2 + Cl^{\bullet} + M^*$$

An inverse correlation between the concentrations of $ClO^{\bullet}$ and O_3 exists as a consequence of this very efficient cycle. Each chlorine (bromine) atom triggers several hundred thousand cycles. This leads to large seasonable variations of the stratospheric ozone concentration in some regions on Earth resulting in a higher UV radiation levels on the ground and consequently a higher risk of skin cancer.[20] Natural processes such as photosynthesis are also negatively affected by UV radiation. The infamous ozone hole in Antarctica is defined as a region in which the total ozone concentration in the atmosphere is below 220 DU, that is, 70% of its normal level although there has been some recovery in recent years (except for those with strong volcanic eruptions).[21]

Many countries have phased out the production of such halogenated hydrocarbons (Montreal Protocol), which are long-lived in the atmosphere and can be transported by convection into the stratosphere where they are decomposed with formation of halogen atoms.[22] This holds especially for the halogenated hydrocarbons CF_2Cl_2, $CFCl_3$ and $CFCl_2CClF_2$ as well as the corresponding bromine derivatives (halones; Section 13.4.4). The chlorine peroxide Cl_2O_2 mentioned above is a derivative of hydrogen peroxide; both molecules are of C_2 symmetry. Other chlorine compounds also play a role in ozone depletion such as HCl, HOCl and $ClONO_2$ (chlorine nitrate, Section 13.5.6). These species are formed during the reaction of chlorine atoms with methane and by recombination of the radicals Cl + OH and ClO + NO_2. From these compounds, novel chlorine atoms are produced by photolysis of Cl_2 molecules as follows:[23]

$$ClONO_2 + H_2O \longrightarrow HOCl + HONO_2$$
$$HCl + HOCl \longrightarrow Cl_2 + H_2O$$
$$HCl + ClONO_2 \longrightarrow Cl_2 + HONO_2$$

20 Between two and three million cases of skin cancer occur worldwide per year, about 5% of which are melanoma.

21 S. Solomon et al., *Science* **2016**, *353*, 269.

22 A natural precursor of chlorine atoms in the stratosphere is chloromethane (CH_3Cl) produced by fungi and oceanic microorganisms at a scale of approximately $5{\cdot}10^6$ t/a.

23 J. G. Anderson et al., *Science* **2012**, *337*, 835.

Bromine nitrate $BrONO_2$ is the most abundant bromine compound in the atmosphere; it reacts in an analogous manner as chlorine nitrate.

Atmospheric ozone concentrations near the ground are normally in the range 40–80 μg m^{-3}, but certain pollutants such as NO_2 in connection with intense sunlight raise the concentration to levels of up to 200 μg m^{-3}. Photons of wavelengths <430 nm decompose NO_2 (from automobile exhaust gases) to NO and $O(^3P)$ followed by reaction of the oxygen atoms with O_2 to O_3. Ozone in concentrations as high as this level are toxic to many plants including conifers. The *photochemical summer smog* in big cities around the world is formed by reaction of O_3 with unsaturated organic compounds.[24] The reaction with aqueous iodide may be used to determine local O_3 concentrations (see above).

11.2 Ionic and Covalent Oxygen Compounds

Stepwise *reduction* of O_2 (e.g., by highly electropositive metals) yields a series of anionic species: superoxide $[O_2]^{\bullet -}$, peroxide $[O_2]^{2-}$ and finally oxides with the anions $O^{\bullet -}$ or O^{2-}. In the presence of proton donors such as water, the anions $[HO_2]^-$ and $[OH]^-$, respectively, are formed. Reduction processes like these are of enormous importance both in chemistry and biology including medicine since they are the basis of respiration of animals and (at night) plants by which organic compounds are oxidized exothermically to CO_2 and H_2O accompanied by reduction of O_2 to H_2O.[25] On the other hand, the O_2 molecule can also be *oxidized* using very strong oxidants (or electrical discharges) affording the dioxygenyl cation $[O_2]^{\bullet +}$. Corresponding compounds with reduced and oxidized oxygen species will be discussed in the following sections.

11.2.1 Oxides

Oxides are compounds with negatively polarized or charged oxygen atoms but without oxygen-oxygen bonds. The oxidation number of the oxygen atoms is usually −2. There are ionic oxides such as MgO, and covalent oxides such as CO_2 as well as polymeric compounds like SiO_2. Nonmetal oxides form *molecular crystals* dominated by covalent interactions rather than ionic structures.

11.2.1.1 Ionic Oxides

The most electropositive metals (e.g., alkali and alkaline earth metals) reduce O_2 in strongly exothermic reactions to ionic oxides such as Na_2O, CaO and Al_2O_3. Their

24 D. Johnson, G. Marston, *Chem. Soc. Rev*. **2008**, *37*, 699.
25 See the topical issue of *Chem. Rev*. **2018**, *118*, issue 5.

crystal structures contain the oxide ion O^{2-} which is isoelectronic with the Ne atom. The hypothetical formation of this anion from gaseous O_2 is strongly *endothermic*:

$$\frac{1}{2}O_2(g.) + 2\,e^- \longrightarrow O^{2-}(g.) \qquad \Delta_r H° = 904 \text{ kJ mol}^{-1}$$

Even the formation of O^{2-} from *oxygen atoms* by formal addition of two electrons would still be endothermic by +634 kJ mol^{-1}. Therefore, free (gaseous) oxide ions do not exist since they would immediately eliminate an electron with formation of $O^{\bullet-}$ (electron autodetachment) The latter ion is formed by exothermic addition of one electron to an oxygen atom as has been discussed in Section 2.1.3 (electron affinity of the elements).

In ionic oxides the anions O^{2-} are stabilized by the electric field of the surrounding cations through the transfer of electron density from the anions to the cations (Section 2.1). The coordination numbers (C.N.) of the anions in metal oxides are between 4 and 8 as the following examples illustrate: ZnO (wurtzite structure, C.N. = 4), MgO (rock salt structure, C.N. = 6), Li_2O as well as Na_2O (antifluorite structures, C.N. = 8). These oxides are colorless. Coordination numbers in salts depend mainly on the stoichiometry as well as on the ratio of the corresponding ionic radii.

If highly electropositive metals like Rb and Cs are treated with the correct amount of molecular oxygen at ambient temperature the deeply colored metal-rich ionic *suboxides* Rb_6O, Rb_9O_2, Cs_4O, Cs_7O and $Cs_{11}O_3$ are obtained. The three cesium suboxides contain the trigonal unit O_3Cs_{11} formed by three octahedral OCs_6 groups each sharing two adjacent faces; this unit is surrounded by neutral cesium atoms resulting in the formula $Cs_{10}[Cs_{11}O_3]$ for the composition Cs_7O.

The oxide ion O^{2-} is a very strong *proton acceptor*. Therefore, ionic oxides which are soluble in proton donor solvents like water or alcohols are immediately protonated with formation of hydroxides. In water, the equilibrium

$$O^{2-} + H_2O \rightleftharpoons 2\,[OH]^-$$

is completely on the right-hand side. Metal hydroxides $M^+[OH]^-$ and their organic derivatives $M^+[OR]^-$ (alkoxides) contain oxygen atoms linked to the neighboring atoms partly by ionic and partly by covalent bonds.

11.2.1.2 Covalent Oxides

All nonmetal oxides contain oxygen atoms in mainly covalent bonds which may, however, be strongly polarized. The following bonding situations are most important:

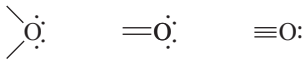

The coordination numbers of oxygen in covalent oxides vary between 1 and 3. The **coordination number 1** is realized in the examples:

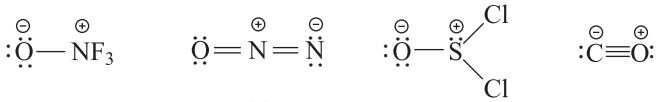

(1) (2) (3) (4)

These bond types are quite frequent and observed also in all mononuclear *oxoanions* such as $[CO_3]^{2-}$, $[SO_4]^{2-}$, $[ClO_4]^-$ as well as in numerous *molecular oxides* like SiO, NO_2, XeO_3 and the terminal atoms in P_4O_{10} and Cl_2O_7.

The **coordination number 2** is found in water and its many formal derivatives such as OF_2, Cl_2O, HOCl, and the bridging atoms in N_2O_5, P_4O_{10} and Cl_2O_7. The bonding situation in H_2O has been discussed in Section 2.4.3. The bond angles at oxygen in these derivatives are usually close to 105° but in some cases much larger angles are observed, even 180° as in some silicate anions.[26] A condition for larger bond angles EOE is that the elements E are strong electron acceptors (LEWIS acids) withdrawing electron density from the oxygen atom.[27] With suitable elements E formation of coordinate π bonds is assumed by overlap of an occupied 2*p* AO at oxygen with an unoccupied antibonding σ* orbital of one of the EX bonds (X: substituent atom). If the geometry at oxygen is linear, even two such coordinate bonds can theoretically be formed:

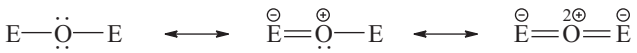

Bonding situations of this type are observed with E = Si, P and S, but also with metals such as Ru in compounds with low-lying acceptor orbitals at E. The bond angle α at oxygen in disiloxane $(H_3Si)_2O$ is 144° in contrast to 112° in the analogous dimethyl ether $(H_3C)_2O$. Similarly, α_{SiOSi} is 144° in α-quartz and 147° in α-cristobalite, both crystalline modifications of silicon dioxide (Section 8.7). Quite similar bond angles have been determined for certain metasilicates. In the phosphorus oxides P_4O_6 and P_4O_{10} and in metaphosphates POP bond angles of between 121° and 134° have been observed while the SOS angle in the disulfate anion $[S_2O_7]^{2-}$ is 124°. The largest angle EOE of 180° was found for the anion $[O_3P{-}O{-}PO_3]^{4-}$ in $Zr[P_2O_7]$. These examples demonstrate that two-coordinate oxygen atoms can form intramolecular coordinate π bonds if the LEWIS base oxygen is linked to a suitable LEWIS acidic center. The high positive partial charges at Si, P and S in the above examples are

26 A. F. Wells, *Structural Inorganic Chemistry*, 5th ed., Clarendon, Oxford, **1984** (standard reference for structural information).

27 This view is supported by the bond angle in the cation $[H_2O]^+$ (110°) which is larger than the angle in the neutral water molecule (104.5°). This finding is in line with the prediction by the VSEPR model (Section 2.2.2).

responsible for the LEWIS acidity of the central atoms in polynuclear silicates, phosphates and sulfates.

However, larger than expected bond angles are not always an indication of coordinate π bonds since steric effects may also play a role. In bent groups E–X–E the internuclear distance d_{EE} will always be smaller than the VAN DER WAALS distance between two E atoms (Chapter 3), especially if X is smaller than E. If E bears a negative partial charge, repulsion between the atoms E results in widening the bond angle compared to reference molecules.

The **coordination number 3** is also frequently observed in oxygen compounds, for example, the oxonium ion $[H_3O]^+$ as well as donor-acceptor complexes between ethers (as LEWIS bases) with boron trifluoride (as LEWIS acid):

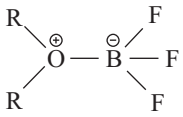

The geometry at the three-coordinate oxygen atom is usually trigonal-pyramidal. Since the oxygen atom has still one lone pair left its geometry can also be referred to as *pseudo-tetrahedral* (see VSEPR model; Section 2.2.2). In rare cases these lone pair electrons are also engaged in bonding, provided a neighboring atom has a suitable acceptor orbital available to establish a coordinate π bond.

11.2.2 Peroxides

Peroxides contain oxygen of oxidation number –1 in the form of ions $[O_2]^{2-}$ and $[RO_2]^-$ or in covalent molecules of type ROOR (R: organic or inorganic atom or group). All these species contain weak OO single bonds, which are quite reactive owing to the low dissociation energy (Section 4.2.2). Industrially *important peroxides* are hydrogen peroxide H_2O_2 and its salts $Na_2[O_2]$ and $Ba[O_2]$, as well as sodium perborate (Section 6.9.3), ammonium peroxodisulfate $[NH_4]_2[S_2O_8]$ (Section 12.12.6), and sodium percarbonate used in large quantities as a bleaching agent in detergents.

11.2.2.1 Ionic Peroxides

Salt-like peroxides are known with the alkali and alkaline earth metals Ca, Sr and Ba.[28] Most important are $Na_2[O_2]$ and $Ba[O_2]$. Sodium peroxide is produced by combustion of sodium metal in CO_2-free air at 350–400 °C in a rotary kiln; the oxide Na_2O is an intermediate in this reaction:

28 W. Hesse, M. Jansen, W. Schnick, *Progr. Solid State Chem.* **1989**, *19*, 47.

$$2\,Na + O_2 \longrightarrow Na_2[O_2] \qquad \Delta H^\circ_{298} = -512\ kJ\ mol^{-1}$$

$Na_2[O_2]$ is a yellow hygroscopic salt of m.p. 675 °C which forms hydrates with 2 and 8 H_2O. It is a strong oxidant reacting violently with organic compounds as well as with powdered sulfur, charcoal and aluminum. On reaction with CO_2, all alkali peroxides release oxygen:

$$Na_2[O_2] + CO_2 \longrightarrow Na_2[CO_3] + \tfrac{1}{2}O_2$$

In the paper and textile industries $Na_2[O_2]$ is used as a bleaching agent (e.g., for waste-paper). Barium peroxide is produced by heating BaO powder in air to 500–600 °C (at a pressure of 0.2 MPa):

$$BaO + \tfrac{1}{2}O_2 \rightleftharpoons Ba[O_2] \qquad \Delta H^\circ_{298} = -71\ kJ\ mol^{-1}$$

$Na_2[O_2]$ and $Ba[O_2]$ decompose on heating to the corresponding oxides with liberation of dioxygen. Therefore, $Ba[O_2]$ is used in pyrotechnical mixtures to achieve green flame colors. Careful *hydrolysis* of ionic peroxides produces H_2O_2 and its anion $[HO_2]^-$ since $[O_2]^{2-}$ is a strong proton acceptor. In other words, ionic peroxides are the salts of a strong base (e.g., NaOH) and a weak two-protic acid (H_2O_2):

$$[O_2]^{2-} + H_2O \longrightarrow [HO_2]^- + [OH]^-$$

Hydroxide ions catalyze the decomposition of H_2O_2 to H_2O and O_2; therefore, in order to produce hydrogen peroxide the peroxide needs to be added to cold and dilute acid.

11.2.2.2 Covalent Peroxides

Hydrogen peroxide is the most important covalent representative of this class of compounds and other covalent peroxides may be considered as derivatives of H_2O_2. For details, see Section 11.3.2 below.

The reaction of alkenes with ozone produces instable peroxides first postulated by RUDOLF CRIEGEE. The smallest so-called Criegee intermediate is *formaldehyde oxide* $H_2C{=}O{-}O$, the infrared spectrum of which has been reported.[29] This molecule is of C_s symmetry and is formed by reaction of O_2 with $CH_2I^\bullet$ radicals, which in turn are produced by photolysis of methylene diiodide CH_2I_2.

29 Y.-P. Lee et al., *Science* **2013**, *340*, 174.

11.2.3 Superoxides

Combustion of Rb or Cs metal in an atmosphere of oxygen at 0.1 MPa does not produce oxides or peroxides but superoxides of composition $M[O_2]$ instead, which contain the radical anion $[O_2]^{\bullet-}$. An older name for superoxides is hyperoxides. The salts $Na[O_2]$ and $K[O_2]$ are obtained from the corresponding peroxides by reaction with dioxygen at high pressure (30 MPa) and at elevated temperatures (500 °C). $Li[O_2]$, on the other hand, can only be prepared from lithium atoms and O_2 at low temperatures or from $Li_2[O_2]$ and O_3. It has only been observed spectroscopically and is unknown in pure form. Evidently, the stability of ionic superoxides increases with the size of the cation.

Formally the superoxide anion[30] is formed by addition of an electron to a O_2 molecule, which has a positive electron affinity. The following reaction is therefore exothermic:

$$O_2(g.) + e^- \longrightarrow [O_2]^-(g.) \qquad \Delta H^\circ_{298} = -E_{ea}(O_2) = -42\ \text{kJ mol}^{-1}$$

In fact, electroreduction of O_2 in a nonaqueous electrolyte produces $[O_2]^{\bullet-}$ as a stable intermediate.[31]

Important superoxides are $Ba[O_2]_2$, $Sr[O_2]_2$, $[Me_4N][O_2]$ as well as complex salts with very large cations.[32] $Na[O_2]$, $K[O_2]$, $Rb[O_2]$ and $Cs[O_2]$ crystallize at room or elevated temperature in a rock-salt structure with disordered anions due to their almost free rotation (high-temperature phases). At lower temperatures several phase changes are observed with frozen rotation, and tetragonal, orthorhombic and monoclinic phases are obtained. $K[O_2]$ is soluble in acetonitrile and dimethyl formamide (DMF). It is used in organic synthesis as oxidizing agent, especially for organosulfur compounds. While $[O_2]^{\bullet-}$ is a relatively stable species in aprotic solvents, it rapidly disproportionates in aqueous solution. For its detection the UV absorption band near 250 nm as well as its RAMAN spectrum are used.

Superoxides are yellow to orange-colored solids and strong oxidants. $K[O_2]$ is produced industrially by oxidation of suspended liquid potassium with oxygen-enriched air. It is used for regeneration of used air, for example, in submarines and spacecrafts, since it absorbs both CO_2 and H_2O and concomitantly liberates O_2:

$$4\ K[O_2] + 4\ CO_2 + 2\ H_2O \longrightarrow 4\ K[HCO_3] + 3\ O_2$$

Superoxides are paramagnetic with one unpaired electron that can be detected by ESR spectroscopy. A convenient preparation in DMSO solution is the electrochemical

30 M. Hayyan, M. A. Hashim, I. M. AlNashef, *Chem. Rev.* **2016**, *116*, 3029–3085.
31 Z. Peng et al., *Angew. Chem. Int. Ed. Engl.* **2015**, *54*, 8165.
32 H. Seyeda, M. Jansen, *J. Chem. Soc., Dalton Trans.* **1998**, 875.

reduction of O_2. $[O_2]^{\bullet-}$ is a strong BRØNSTED base (proton acceptor) and a mild 1-electron reductant (it is turned into O_2 in the process). On hydrolysis of pure superoxides H_2O_2, $[HOO]^-$, O_2 and $[OH]^-$ are formed in vigorous reactions:

$$[O_2]^{\bullet-} + H_2O \longrightarrow HO_2^{\bullet} + [OH]^-$$

$$2\,HO_2^{\bullet} \longrightarrow H_2O_2 + O_2$$

$$H_2O_2 \longrightarrow H_2O + \tfrac{1}{2}\,O_2$$

The reaction intermediate $HO_2^{\bullet}$ is a weak acid in water ($pK_a = 4.8$). This radical can also be generated by photolysis of hydrogen iodide in a matrix of solid dioxygen at 4 K as observed by IR spectroscopy (*matrix isolation* of reactive species):

$$HI \xrightarrow{h\cdot\nu} H^{\bullet} + I^{\bullet}$$

$$H^{\bullet} + O_2 \longrightarrow HO_2^{\bullet}$$

Decomposition of H_2O_2 vapor in electrical discharges produces $HO_2^{\bullet}$ also; its bonding is discussed in Section 11.5.

One-electron reduction of O_2 with formation of $[O_2]^{\bullet-}$ occurs in all biological respiration processes by mitochondria as an unwanted side reaction. At physiological pH values $[O_2]^{\bullet-}$ is immediately protonated to $HO_2^{\bullet}$ which is a powerful oxidant for membrane lipids as well as DNA resulting in mutagenic damages. Therefore, during the biological evolution, an antidote had to be developed. This is the enzyme *superoxide dismutase*, which catalyzes the rapid disproportionation of $HO_2^{\bullet}$ to H_2O_2 and O_2.

11.2.4 Ozonides

As mentioned earlier, the tendency to form higher (oxygen-rich) oxides increases with cation radius. With the relative large cations Na^+, K^+, Rb^+, Cs^+ and $[Me_4N]^+$, ozonides of composition $M[O_3]$ have been synthesized[33] containing the bent, paramagnetic anion $[O_3]^{\bullet-}$ with an unpaired electron in a strongly antibonding π^* MO (see the energy-level diagram of O_3 in Section 11.1.3).[34] The OO bond lengths of alkali ozonides are in the range 133.3–135.3 pm compared to crystalline ozone with 125.7 pm; the OOO bond angles are in the range 113.0–114.6°.

Ozonides are formed in the reaction of ozone with solid hydroxides of potassium, rubidium or cesium if the reaction enthalpy is neutralized by cooling:

33 M. Jansen, H. Nuss, *Z. Anorg. Allg. Chem.* **2007**, *633*, 1307.

34 The electron affinity of O_3 is 2.1 eV or 202 kJ mol^{-1}.

$$K[O_2] + O_3 \longrightarrow K[O_3] + O_2$$

The ozonides are separated from insoluble hydroxides by extraction with liquid ammonia. Evaporation of the ammonia solution affords crystalline products. The alkali ozonides (Na to Cs) slowly decompose at room temperature, more rapidly at 35–50 °C with formation of superoxides and O_2. Tetramethylammonium ozonide $[Me_4N][O_3]$ is thermally slightly more stable. More than 40 ionic ozonides with large cations have been prepared. For covalent ozonides with cyclic structures formed on addition of O_3 to phosphonic acid esters $(RO)_3P$, see Section 11.1.1.

11.2.5 Dioxygenyl Compounds

Salts with the dioxygenyl cation $[O_2]^{\bullet+}$ contain oxygen atoms with the oxidation number +½. Formally, this dioxygen(+1) ion is obtained on ionization of O_2 by removal of an electron from one of the degenerate antibonding π* MOs:

$$O_2(g.) \longrightarrow [O_2]^+(g.) + e^- \qquad \Delta H^\circ_{298} = E_i(O_2) = 1168 \text{ kJ mol}^{-1}$$

Owing to the high ionization energy, this process can only be realized chemically by reaction with species of very high electron affinity. Platinum hexafluoride reacts at 25 °C with oxygen gas to the volatile orange-colored salt $[O_2][PtF_6]$, which is isomorphous with $K[PtF_6]$:

$$\begin{aligned} O_2 + PtF_6 &\xrightarrow{25^\circ C} \\ & \qquad [O_2][PtF_6] \\ O_2 + Pt + 3\,F_2 &\xrightarrow{450^\circ C} \end{aligned}$$

In this reaction, Pt(VI) oxidizes O_2 to $[O_2]^+$ and is reduced to Pt(V). At 450 °C, $[O_2]$ $[PtF_6]$ can be obtained directly from the elements.

Another route to dioxygenyl salts employs dioxygen difluoride (O_2F_2), which reacts with fluoride acceptors to liberate elemental fluorine:

$$O_2F_2 + BF_3 \longrightarrow [O_2][BF_4] + \frac{1}{2}F_2$$

The LEWIS acids PF_5, AsF_5 and SbF_5 react analogously; $[O_2][AsF_6]$ and $[O_2][SbF_6]$ can also be obtained from mixtures of F_2, O_2 and AsF_5 or SbF_5 on irradiation. Orthorhombic $[O_2][BF_4]$ is isomorphous with nitrosyl tetrafluoroborate $[NO][BF_4]$. The structural similarities between $[O_2]^+$ and $[NO]^+$ salts are based on similar spatial demands and identical charges of the two cations.

The paramagnetic $[O_2]^+$ ion contains one unpaired electron in the antibonding $1\pi_g$ MO (Section 2.4.3). The *magnetic moment* of dioxygenyl salts is therefore the

composite of the individual cation and anion moments in case the latter is also paramagnetic as in $[O_2][PtF_6]$.

One of the most interesting reaction of $[O_2]^+$ is the reversible addition of chlorine to form the planar trapezoidal cation $[Cl_2O_2]^+$, which has been isolated as the black paramagnetic salts $[Cl_2O_2][SbF_6]$ and $[Cl_2O_2][Sb_2F_{11}]$.[35] The two components of the $[Cl_2O_2]^+$ ion are connected by a rare π^*-π^* bond as in the high-pressure molecule O_8 (Section 11.1.1) and in the rectangular ion $[I_4]^{2+}$ (Section 13.5.4).

Covalent dioxygenyl compounds of type $O_2R^\bullet$ contain groups R with electronegativities greater than that of oxygen to generate a positive partial charge on the O_2 unit. Otherwise derivatives of the hydroperoxy radical $HO_2^\bullet$ with negative oxygen atoms would result. Hence, only fluorine and perfluorinated substituents such as CF_3 and SF_5 qualify for R. The radical $[O_2F]^\bullet$ is formed by the reaction of photochemically generated fluorine atoms (from F_2) with O_2 at very low temperatures (matrix isolation):

$$2\,O_2 + 2\,F^\bullet \longrightarrow 2\,O_2F^\bullet \rightleftharpoons O_4F_2$$
$$2\,O_2F^\bullet \longrightarrow O_2 + O_2F_2$$

Dioxygenyl fluoride $O_2F^\bullet$ has been detected by IR and ESR spectroscopy. On warming the solid O_2 matrix to temperatures that allow diffusion, $O_2F^\bullet$ dimerizes reversibly to the chain-like tetraoxygen difluoride (O_4F_2) which decomposes to O_2 and O_2F_2 on further warming. For details on the bonding in dioxygenyl compounds, see Section 11.4.

11.2.6 Bond Properties of the Ions $[O_2]^{\bullet+}$, $[O_2]^{\bullet-}$ and $[O_2]^{2-}$

It is very instructive to analyze the bond properties of the molecules and ions $[O_2]^+$, O_2, $[O_2]^-$ and $[O_2]^{2-}$ on the basis of simple MO theory. Table 11.3 lists the experimental

Table 11.3: Properties of the oxygen-oxygen bonds in the gaseous species $[O_2]^+$, O_2 and $[O_2]^-$ as well as of the peroxide dianion $[O_2]^{2-}$ in solid Na_2O_2. The covalent bond strength decreases with increasing number of electrons in the antibonding $1\pi_g$ MO.

	Number of π* electrons	Bond length (pm)	Force constant (N cm^{-1})	Dissociation energy, D_0^0 (kJ mol^{-1})
$[O_2]^+$ (g.)	1	111.6	16.5	643
O_2 (g.)	2	120.7	11.4	495
$[O_2]^-$ (g.)	3	135	5.4	395
$[O_2]^{2-}$ (Na_2O_2)	4	149	2.8	204

35 T. Drews, W. Koch, K. Seppelt, *J. Am. Chem. Soc.* **1999**, *121*, 4379.

internuclear distances, force constants and dissociation enthalpies of these species, which indicate that the OO bond weakens in the series from $[O_2]^+$ to $[O_2]^{2-}$, that is, with increasing occupation of the antibonding $1\pi_g$ molecular orbital shown in Figure 2.21 (Section 2.4.3).

The four species differ mainly in the number of $\pi^\star$ electrons that increases stepwise from $[O_2]^+$ to $[O_2]^{2-}$. The occupancy of the inner MOs remains unchanged, but the splitting of AOs into MOs is a function of the degree of overlap and, therefore, depends on the internuclear distance and ionic charge. Consequently, it is not reasonable to compare the bond strengths using "π bond orders." It also should be noticed that an isolated ion $[O_2]^{2-}$ does not exist since electron autodetachment with formation of $[O_2]^-$ would occur spontaneously. Consequently, the bond properties of $[O_2]^{2-}$ can only be derived from solid or dissolved peroxides in which the true number of electrons on the $[O_2]^{2-}$ unit is uncertain because of the interaction with surrounding cations.

11.3 Hydrides of Oxygen and Peroxo Compounds

11.3.1 Introduction

Water is probably the most important compound on the Earth.[36] Life has originated in aqueous systems and the human body contains 65–70% of water, depending on the age. Food often consists mainly of water too, as the following examples show: lean meat 76%, fish 81%, tomatoes 94%, other vegetables and fruits contain 80–90% H_2O (see http://dietgrail.com/water/). The physical properties of water have been discussed in Chapter 5 (hydrogen) and the bond properties of the water molecule in Section 2.4.7.

Hydrogen peroxide (H_2O_2) is another important hydride of oxygen which is produced in large quantities. H_2O and H_2O_2 are the only binary oxygen hydrides, which can be prepared in pure form. The oxygen-rich hydrides H_2O_n with $n = 3$ and 4 have been detected in the vapor phase and in dilute solutions by IR, MW and ^{1}H-NMR spectroscopy. They are formed on decomposition of H_2O_2 vapor in a microwave discharge by a sequence of radical recombination reactions:

$$H_2O_2 \rightarrow H^\bullet + HO_2^\bullet;\ 2\ HO_2^\bullet \rightarrow H_2O_4;\ H_2O_2 \rightarrow 2\ OH^\bullet;\ OH^\bullet + HO_2^\bullet \rightarrow H_2O_3$$

Solutions of **hydrogen trioxide** (H_2O_3) have been prepared from ozone and anthrahydroquinone (and other reducing agents) in analogy to the industrial synthesis of H_2O_2 (see below). The low thermal stability of H_2O_3 and H_2O_4 at room temperature results from the low mean bond enthalpy and the even lower dissociation enthalpy

36 Karl Höll, *Wasser* (A. Grohmann, ed.), 8th ed., de Gruyter, Berlin, **2002**.

of OO single bonds, as discussed in Section 4.2.3. Hydrogen peroxide is also a metastable compound, which slowly decomposes at room temperature to water and O_2; many catalysts are known to accelerate this exothermic decomposition. Slightly more stable are covalent derivatives of H_2O_2 and H_2O_3, namely di- and trioxides $R–O_n–R$ (n = 2 or 3) with R = F, CF_3, SF_5 and others.

The radicals $HO_n^{\bullet}$ with n = 1 and 2 are intermediates in important chemical reactions, for example, in the violent reaction of H_2 with O_2 and in processes occurring in the upper atmosphere. Both radicals have been isolated in low-temperature inert matrices and were characterized by IR, ESR and UV spectroscopy. The hydroperoxyl radical $HO_2^{\bullet}$ is an intermediate in the hydrolysis of superoxides (Section 11.2.3) but rapidly decomposes in water in a bimolecular reaction to H_2O_2 and O_2.

11.3.2 Water

Water is available on the Earth in unlimited amounts, but 97% of it is saltwater in the oceans.[36] The remaining 3% are mostly stored as ice in Antarctica, Greenland, at the North Pole and in glaciers. The water in rivers, lakes and in the underground water table (fresh water) can be used as drinking water or for industrial applications only after purification. Ammonium, nitrite and nitrate ions are anthropogenic (manmade) impurities that are tolerated only to certain upper limits. In addition, brackish and ocean waters are used after *desalination* either by evaporation and condensation or by *inverse osmosis*.[37] The latter process is applied on a large scale in the USA, China, Israel and on the Arabic peninsula. Worldwide 19000 desalination plants are in operation.

The first step in the *purification of freshwater* is the oxidation of organic impurities, including bacteria (sterilization) by treatment with strong oxidants such as Cl_2, O_3 or ClO_2. UV irradiation to generate hydroxyl radicals is also applied. During these procedures, Fe(II) and Mn(II) ions are turned into higher oxidation states leading to precipitation as insoluble hydroxides. Chlorination by Cl_2, however, produces unwanted chlorinated organic compounds. Therefore, ozone and chlorine dioxide are preferred. After oxidation the water is treated by physical measures such as flocculation, sedimentation, filtration and absorption (e.g., at charcoal).[36] If the concentration of hydrogen carbonate is too high (*hard water*) treatment with a slurry of $Ca[OH]_2$ (lime milk) leads to precipitation as $Ca[CO_3]$ resulting in *soft water* after filtration:

$$Ca[HCO_3]_2 + Ca[OH]_2 \longrightarrow 2\,Ca[CO_3]\downarrow + 2\,H_2O$$

37 K. H. Büchel, H.-H. Moretto, D. Werner, *Industrial Inorganic Chemistry*, 2nd ed., Wiley-VCH, Weinheim, Germany, **2008**, Chapt. 1.1.

Demineralized water is obtained from fresh water by ion exchange at an insoluble organic polymer (e.g., polystyrene) containing suitable functional groups at its surface. The water passes through a cation exchanger followed by an anion exchanger removing, for instance, sodium and chloride ions in the process in exchange for the constituents of water:

$$\text{cation exchange: } [H_3O]^+[PS-SO_3]^- + Na^+ \longrightarrow Na^+[PS-SO_3]^- + [H_3O]^+$$

$$\text{anion exchange: } [PS-NMe_3]^+[OH]^- + Cl^- \longrightarrow [PS-NMe_3]^+Cl^- + [OH]^-$$

$$\text{net reaction: } [H_3O]^+ + [OH]^- \longrightarrow 2\,H_2O$$

The remaining salt concentration is determined by electric conductivity measurements and residual concentrations of down to 0.02 g L^{-1} can be obtained. The cation exchanger is regenerated by rinsing with dilute hydrochloric acid and the anion exchanger by aqueous sodium hydroxide:

$$Na^+[PS-SO_3]^- + HCl(aq) \longrightarrow [H_3O]^+[PS-SO_3]^- + NaCl$$

$$[PS-NMe_3]^+Cl^- + NaOH \longrightarrow [PS-NMe_3]^+[OH]^- + NaCl$$

Very pure and air-free water is produced in laboratories by repeated distillation in a quartz apparatus.

A person of 70 kg contains about 45 L of water, 17 L extracellularly and 28 L intracellularly. The recommended daily water intake is approximately 1.25 L by drinking, 1.0 L in the form of food and 0.25 L is generated by oxidation of food components such as fat and protein within the body. On the loss side, 1.5 L H_2O is excreted as urine and 0.15 L with the feces while 0.85 L is lost by evaporation from skin and lungs. In this way, uptake and loss are in balance with 2.5 L each.

The molecular structures of ice, liquid and gaseous water as well as the solvent properties of water have been discussed in Section 5.6.4 in context with hydrogen bonding. Very important is the strong solvation of ions in liquid water due to the large dipole moment of the small H_2O molecules. Furthermore, H_2O molecules are thermally very robust owing to their high OH bond energies. The high polarity of OH bonds makes water an important reagent in hydrolytic reactions.

At temperatures above 374 °C and pressures >22 MPa (critical point), the solvent properties of this *hypercritical water* are very different from those at normal conditions. The density of this fluid is lower than 0.322 g cm^{-3} and the polarity is much smaller than at standard conditions. Therefore, the solubility of polar and ionic substances is much lower while the solubility of nonpolar compounds is much higher in hypercritical water.[38]

38 H. Weingärtner, E. U. Franck, *Angew. Chem. Int. Ed.* **2005**, *44*, 2672–2692. D. Bröll, H. Vogel, et al., *Angew. Chem. Int. Ed.* **1999**, *38*, 2998–3014.

11.3.3 Hydrogen Peroxide, H_2O_2

11.3.3.1 Preparation

Hydrogen peroxide is one of the most important products of the chemical industry and comes as either 35% or 85% aqueous solution. The worldwide annual production capacity exceeds $2.2 \cdot 10^6$ t H_2O_2. The dominating synthetic route is called *anthraquinone process* by which molecular oxygen is reduced to H_2O_2 by anthrahydroquinone (AO-process; R: ethyl, *t*-butyl or *t*-amyl):[39]

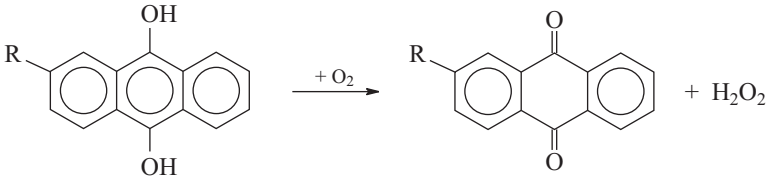

This multistep reduction proceeds by a radical-chain mechanism and is carried out in an organic solvent mixture immiscible with water. H_2O_2 is extracted from the solvent by water using the countercurrent distribution method. Subsequently, the quinone is reduced back to hydroquinone by hydrogenation with H_2 at 40 °C and a pressure of 4 bar on a Ni- or Pd-based catalyst. Since the aromatic diol/quinone mixture is not consumed the net reaction is the production of aqueous H_2O_2 from the gaseous elements:

$$H_2\,(g.) + O_2\,(g.) \longrightarrow H_2O_2\,(aq.) \qquad \Delta G^\circ_{298} = -134\ \text{kJ mol}^{-1}$$

Industrially produced hydrogen peroxide is stabilized by traces of sodium diphosphate, sodium stannate or organic chelating ligands (100–1000 ppm) to bind transition metal ions, which would catalyze the otherwise spin-forbidden decomposition of H_2O_2 to H_2O and O_2.

Hydrogen peroxide is used in almost all branches of the chemical industry,[39] mainly for bleaching of cellulose, textiles, straw, feathers, hair and waste paper as well as for lightening of wood for veneers. Furthermore, freshwater and wastewater treatment is done with H_2O_2 and oxidative removal of industrial waste is another important application. H_2O_2 is also employed for the synthesis of perborates, percarbonates and organic peroxides as well as the industrial oxidation of organic compounds, for example, propylene is oxidized to propylene oxide.[40]

---

39 J. M. Campos-Martin, G. Blanco-Brieva, J. L. G. Fierro, *Angew. Chem. Int. Ed.* **2006**, *45*, 6962–6984. H. Offermanns, G. Dittrich, N. Steiner, *Chem. unserer Zeit* **2000**, *34*, 150.

40 G. Strukul (ed.), *Catalytic Oxidations with Hydrogen Peroxide as Oxidant*, Kluwer, Dordrecht, **1992**. R. Noyori, M. Aoki, K. Sato, *Chem. Commun.* **2003**, 1977.

Sodium percarbonate used as a bleaching agent in detergents is an adduct of composition $Na_2[CO_3]\cdot 1.5\ H_2O_2$ rather than a salt of percarbonic acid (H_2CO_4); it is prepared from soda and hydrogen peroxide. In slightly alkaline solutions, the peroxide exists as the anion $[HOO]^-$, which reacts with tetra-acetyl derivative of ethylene diamine $Ac_2N–CH_2–CH_2–NAc_2$ (EDTA) as a component of most detergents and washing powders to *peracetic acid* $CH_3C(=O)OOH$. The peracetic acid in turn oxidizes organic dyestuffs and dirt even at temperatures as low as 40 °C, resulting in the desired cleaning and bleaching effects.[41]

11.3.3.2 Properties and Structure of H_2O_2

Anhydrous H_2O_2 is prepared as colorless needle-like crystals of m.p. −0.9 °C by fractional crystallization from concentrated aqueous solutions. Liquid H_2O_2 is almost colorless but light blue in thick layers. Due to strong association by hydrogen bonds, it is a viscous, syrupy liquid of b.p. 150 °C. Anhydrous H_2O_2 is stored in polyethylene bottles with cooling. The decomposition to H_2O and O_2 is catalyzed even by traces of transition metal ions[42] as well as by Pt, MnO_2 and alkali ions:

$$H_2O_2 \longrightarrow H_2O + \tfrac{1}{2}\,O_2 \qquad \Delta H^\circ_{298} = -100.4\ \text{kJ mol}^{-1}$$

The radicals $HO^\bullet$ and $HO_2^\bullet$ are intermediates in this reaction, which starts by homolytic cleavage of the OO bond.

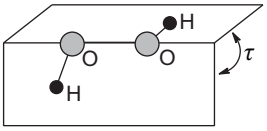

d(OO) = 149 pm
d(OH) = 96.5 pm
Angle OOH = 99.4°
τ = 112°

Figure 11.4: Structure of the H_2O_2 molecule in the gas phase (symmetry C_2). In the solid state the molecular parameters are slightly different due to intermolecular hydrogen bonds.

The molecule H_2O_2 is of C_2 symmetry and therefore chiral (see Figure 11.4). In the two enantiomers, the dihedral angle τ is either +112° or −112°.[43] The value of 112° is a compromise between 90° and 180° due to two effects. On the one hand, the

41 S. Glathe, D. Schermer, *Chem. unserer Zeit* **2003**, *37*, 336.

42 For example, in the so-called FENTON reaction, the ubiquitous Fe^{2+} ion reduces H_2O_2 to $[OH]^-$ and $HO^\bullet$ with formation of Fe^{3+}. The hydroxyl radical then reacts with H_2O_2 to H_2O and $HO_2^\bullet$ and the latter radical reduces Fe^{3+} back to Fe^{2+} with formation of O_2 and H^+. In the presence of certain chelating ligands, even the formation of hydroxo and oxocomplexes of Fe^{4+} has been observed; D. Meyerstein et al., *Chem. Eur. J.* **2009**, *15*, 8303.

43 J. A. Dobado, J. M. Molina, D. P. Olea, *J. Mol. Struct.* (*Theochem.*) **1998**, *433*, 181. L. Margules, J. Domaison, J. E. Boggs, *J. Mol. Struct.* (*Theochem.*) **2000**, *500*, 245.

two lone pairs in the 2*p* orbitals at oxygen repel each other and this repulsion would be at a maximum at τ = 0° (*cis*-planar structure of C_{2v} symmetry) as well as at τ = 180° (*trans*-planar conformation of C_{2h} symmetry) but at a minimum at τ = 90° (helical structure with orthogonal 2*p* AOs). On the other hand, the two hydrogen atoms repel each other due to their positive partial charges and are therefore trying to enforce a dihedral angle of 180°. Consequently, the minimum energy of the molecule is obtained at τ = 112°. Similar torsion angles have been determined for gaseous substituted peroxides, depending on the size of the substituents: MeOOMe 119°, F_5SOOSF_5 129°, $Me_3SiOOSiMe_3$ 143°. The torsion angle is defined as positive if *clockwise* rotation about the OO bond brings the OH bond closest to the observer into the same plane with the other OH bond; otherwise, τ is negative (τ = +112° is equivalent to τ = −248°). Enantiomers have identical enthalpies of formation.

The barrier for rotation about the OO bond of H_2O_2 is only 4.6 kJ mol^{-1} at τ = 180° (*trans*-barrier) but 30.7 kJ mol^{-1} at τ = 0° (*cis*-barrier); the latter barrier is higher because of the repulsive H···H interaction, which can be estimated as 30.7–4.6 = 26.1 kJ mol^{-1} at τ = 0°. Because of the low *trans*-barrier, the enantiomers cannot be separated. In solid H_2O_2 the torsion angle is ±120.5° (at 110 K) since the molecules are associated by hydrogen bonds.

The low OO bond enthalpy of H_2O_2 resulting from the high electron density at the oxygen atoms is responsible for the high reactivity and the facile formation of free $OH^{\bullet}$ radicals, which can also be produced by photolysis of H_2O_2 (Section 11.3.4). On the other hand, H_2O_2 also reacts as a nucleophile forming adducts with LEWIS acids such as Fe^{2+} ions.

11.3.3.3 Reactions of H_2O_2

H_2O_2 dissociates in dilute aqueous solutions by proton transfer:[44]

$$H_2O_2 + H_2O \rightleftharpoons [H_3O]^+ + [HO_2]^- \qquad K_c = 2\cdot10^{-12}\ \text{mol L}^{-1}(20°C)$$

Hence, H_2O_2 is a weak acid in water (pK_a = 11.7) since the dissociation constant of water is much smaller ($1.8\cdot10^{-16}$ mol L^{-1}). Alkaline solutions of hydrogen peroxide contain the anions $[OH]^-$ and $[HO_2]^-$. Such solutions can be obtained on hydrolysis of $Na_2[O_2]$ or $K[O_2]$ (Section 11.2), but readily decompose. The anion $[HO_2]^-$ is a strong nucleophile, which, for instance, attacks SO_2 with oxidation to hydrogen sulfate:

$$[HOO]^- + SO_2 \longrightarrow [HOOS(O)O]^- \longrightarrow [HSO_4]^-$$

44 D. T. Sawyer, *Encycl. Inorg. Chem.* **1994**, *6*, 2947.

Aqueous hydrogen peroxide is most stable at pH < 4, but both in acid and alkaline solutions it is a strong oxidant and the oxygen atoms are reduced to the oxidation state –2:

$$H_2O_2 + 2\,e^- \longrightarrow 2\,[OH]^-$$

For example, H_2O_2 oxidizes iodide to I_2, H_2S to elemental sulfur, SO_2 to $[SO_4]^{2-}$, $[NO_2]^-$ to $[NO_3]^-$, As_2O_3 to $[AsO_4]^{3-}$, Cr(III) salts to chromate(VI) and Fe(II) to Fe(III). The oxidation of nonmetallic substrates is accelerated by 1-electron catalysts such as iron and copper ions, which are ubiquitous impurities.

Toward stronger oxidants H_2O_2 acts as a reducing agent:

$$H_2O_2 \longrightarrow O_2 + 2\,H^+ + 2\,e^-$$

This is the case with $[MnO_4]^-$, Cl_2, Ce(IV) salts and O_3. Permanganate is reduced in acid solution to Mn^{2+} which is utilized in the volumetric determination of H_2O_2. From the absence of isotopic exchange with the water solvent when using $H_2{}^{18}O_2$, it has been concluded that the oxygen liberated originates from H_2O_2 exclusively and that the OO bond remains intact during oxidation. Similarly, no isotopic exchange occurs in the decomposition of H_2O_2 catalyzed by $FeCl_3$ supporting the following reaction mechanism:

$$H_2O_2 + FeCl_3 \longrightarrow [FeCl_3(OH)_2]$$

$$[FeCl_3(OH)_2] + H_2O_2 \longrightarrow FeCl_3 + 2\,H_2O + O_2$$

The second step involves the concerted transfer of the two hydrogen atoms of H_2O_2 to the "adduct" of H_2O_2 and $FeCl_3$ which is a bis-hydroxo complex of Fe(V). The reaction is exothermic, and the mixture gets hot, which may result in an *explosive decomposition*, especially with concentrated H_2O_2. Therefore, mixtures of this type are used to propel torpedoes and small rockets using the considerable volume increase by evaporating water and the liberated O_2. The iron-containing enzyme *catalase* present in nearly all living organisms exposed to oxygen (such as bacteria, plants and animals) decomposes hydrogen peroxide in a controlled manner with formation of water and less harmful O_2 (Section 11.1.1). Catalase has one of the highest turnover numbers of all enzymes; one catalase molecule can convert millions of hydrogen peroxide molecules. In addition, there are a several types of *peroxidases* in organisms to destroy peroxides by reduction. Glutathione peroxidases use glutathione as an electron donor and are active with both hydrogen peroxide and organic hydroperoxide substrates.

Inhibitors such as phosphate ions and a variety of organic carbonic acids act as "negative catalysts" that stabilize hydrogen peroxide by complex formation with the catalyzing transition metal ions. Therefore, commercial hydrogen peroxide contains such reagents in low concentrations.

Peroxoborates contain the cyclic anion

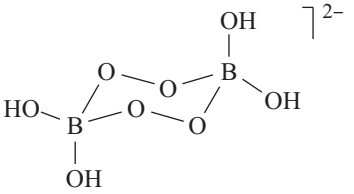

as sodium salt, which is produced in enormous amounts and used as a bleaching agent in detergents. Alternatively, *percarbonate* $Na_2[CO_3]\cdot 1.5\ H_2O_2$ can be used for this purpose. Sodium perborate is manufactured from sodium tetraborate (e.g., kernite) and H_2O_2 at 20–30 °C resulting in the crystallization of $Na_2[B_2(O_2)_2(OH)_4]$.

Other commercial oxidants are the triple salts *caroate* and *oxone* of composition $2K[HSO_5]\cdot K[HSO_4]\cdot K_2[SO_4]$ formed on mixing H_2O_2 (85%) with oleum containing 57–74% free SO_3 at 8 °C followed by neutralization by K[OH] or $K_2[CO_3]$. Oxone is an important reagent in organic synthesis[45]; it contains the anion $[HOOSO_3]^-$ of peroxomonosulfuric acid H_2SO_5. The corresponding monoperoxo phosphoric acid H_3PO_5 is prepared from concentrated H_2O_2 and P_4O_{10} by "perhydrolysis."

Hydrogen peroxide is the starting material for the preparation of many organic peroxides used as initiators for polymerization reactions. Peroxocarbonic acids are industrial intermediates, for example, in large-scale epoxidation reactions. Propylene epoxide is produced on a huge scale from propylene and hydrogen peroxide using a Ti-containing zeolite catalyst. Naturally, the reactivity of H_2O_2 in anhydrous solvents is very different from that in water.[44]

11.3.4 Hydrogen Trioxide, H_2O_3

Hydrogen trioxide (or trioxidane by IUPAC nomenclature) is a labile but important oxidant in low-temperature oxidations, in atmospheric and environmental chemistry, in chemistry of combustion and flames, in radiation chemistry of aqueous media, as well as in biochemical oxidations.[46] H_2O_3 can be generated by reduction of ozone with a variety of hydrogen compounds in polar solvents, preferentially with 1,2-diphenylhydrazine at −78 °C:

$$O_3 + PhHN - NHPh \rightarrow HOOOH + PhN = NPh$$

Concentrations of up to 0.1 mol(H_2O_3) L^{-1} have been obtained. H_2O_3 is also formed on reaction of O_3 with H_2O_2 in nonaqueous solvents, and especially in the catalyzed low-temperature hydrolysis of hydrotrioxides such as $Ph_3Si–OOOH$ in polar

45 V. Jadhav, M. Y. Park, Y. H. Kim, *Chem. Peroxides* **2006**, *2*, 1001.
46 J. Cerkovnik, B. Plesnicar, *Chem. Rev.* **2013**, *113*, 7930–7951.

solvents. The half-life of aqueous H_2O_3 is only a few milliseconds at 20 °C, but in polar solvents such as deuterated acetone or *tert*-butyl methyl ether the estimated half-life is 16 min due to strong hydrogen bonding to the solvent molecules. The short lifetime in water is explained by concerted proton shifts in a cyclic hydrogen-bonded adduct between H_2O_3 and two water molecules (water-assisted decomposition). The decomposition products are $^1O_2$ and H_2O_2. The experimental pK_1 value of H_2O_3 in water has been estimated as 9.5 ± 0.5 compared to 11.7 for H_2O_2 and it has been characterized by ^{1}H- and ^{17}O-NMR spectra.

In the gas phase, the helical H_2O_3 molecule is of C_2 symmetry with the two hydrogen atoms on opposing sides of the O_3 plane and with molecular parameters d_{OH} = 96.3 pm, d_{OO} = 142.8 pm, α_{HOO} = 101.1° and τ(HOOO) = 81.8°. The barrier for rotation about the OO bonds is very low and rapid internal rotation occurs at room temperature. The OO bond dissociation enthalpy of H_2O_3 at 298 K has been calculated as 139 kJ mol^{-1} compared to 209 kJ mol^{-1} for H_2O_2. For other covalent trioxides, see Section 11.5.

11.3.5 Hydroxyl Radical, OH$^\bullet$

The hydroxyl radical is a *strong oxidant* and a reaction intermediate in many important oxidation processes including the combustion of organic and inorganic hydrogen compounds. In Earth's troposphere OH$^\bullet$ oxidizes trace compounds such as CO and CH_4 to water-soluble products, which are then washed out by rain. During respiration of mammals, low concentrations of OH$^\bullet$ are formed by stepwise reduction of O_2. By reaction with DNA, undesired products are formed some of which are mutagenic. Therefore, food should contain radical scavengers such as glutathione, carotenoids, polyphenols and the vitamins A, C and E (antioxidants).[47] By far the largest amount of O_2 used in respiration processes, however, is directly reduced to water in a 4-electron reduction process catalyzed by enzymes containing iron or copper ions and without radical intermediates.[48]

The homolytic dissociation of an OH bond of water molecules requires 498 kJ mol^{-1} and, therefore, is not a suitable route to generate OH$^\bullet$ radicals. Photochemical dissociation of H_2O_2 at the OO bond requires much less energy than the photolysis of water and radiation from a mercury medium-pressure lamp of wavelength <300 nm is suitable. This process is used in the *industrial purification of wastewater* from organic impurities (*advanced oxidation process*, AOP).[49]

47 M. Battran, *Naturwiss. Rundschau* **2002**, *55*, 513.
48 J. P. Klinman, *Acc. Chem. Res.* **2007**, *40*, 325.
49 T. Oppenländer, *Photochemical Purification of Water and Air. Advanced Oxidation Processes (AOPs): Principles, Reaction Mechanisms, Reactor Concepts*, Wiley-VCH, Weinheim, **2003**.

In the upper atmosphere, $OH^\bullet$ radicals are generated by photolysis of ozone, which produces oxygen atoms either in the ground state (^3P) or in the excited ^1D-state, depending on the wavelength:

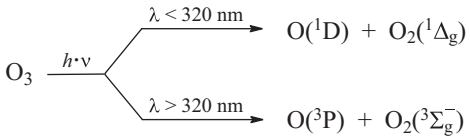

The excited O atoms have a lifetime of ca. 150 s and react with water vapor:

$$O(^1D) + H_2O \longrightarrow 2\ OH^\bullet$$

Relatively high radical concentrations of several 10^7 molecules cm^{-3} are obtained in those parts of the troposphere exposed to sunlight.[50] Another source of $OH^\bullet$ in the lower atmosphere is the photolysis of HNO_2 which is emanated from nitrate-containing soil where bacteria reduce nitrate ions to nitrous acid at acidic pH values.[51] In typical urban environments, $OH^\bullet$ concentrations of approximately 10^6 molecules cm^{-3} have been measured, even indoors.

The most important reaction partner of $OH^\bullet$ radicals in the troposphere is CO, which is emitted in huge quantities into the atmosphere where it is oxidized to CO_2 with formation of hydrogen atoms. The latter reduce O_2 to $HO_2^\bullet$ radicals:

$$H^\bullet + O_2 + M \longrightarrow HO_2^\bullet + M^*$$

The $HO_2^\bullet$ radicals oxidize NO to NO_2 regenerating the $OH^\bullet$ radicals in the process. In fact, most reactions of $OH^\bullet$ are radical-chain reactions that *regenerate* the $OH^\bullet$ radicals. This does not hold for the reactions with NO_2 yielding HNO_3, with SO_2 producing sulfuric acid via the intermediate $HOSO_2^\bullet$, and with H_2S which initially gives $HS^\bullet$ radicals and SO_2. These reactions therefore *remove* $OH^\bullet$ from the atmosphere. Methane reacts with $OH^\bullet$ by hydrogen abstraction to methyl radicals (and water), which are then oxidized to formaldehyde (HCHO) by O_2 via several intermediates.

As the mentioned oxidation products of CO, NO, SO_2, H_2S and CH_4 are soluble in water, they are washed out of the atmosphere by rain. It has been estimated that $3{\cdot}10^9$ t CO, $0.5{\cdot}10^9$ t CH_4 and a similar amount of isoprene (from trees) are oxidized annually in the atmosphere. In other words, $OH^\bullet$ radicals are responsible for the *self-cleansing of Earth's atmosphere* at altitudes of up to 12 km (troposphere), especially in the regions near the Equator where the intensity of Sun's radiation and

50 D. Möller, *Luft: Chemie, Physik, Biologie, Reinhaltung, Recht*, de Gruyter, Berlin, **2003**, pp. 286–324.

51 H. Su et al., *Science* **2011**, *333*, 1616.

consequently the radical concentration are highest.[52] The atmospheric lifetime of $OH^{\bullet}$ varies between 0.01 and 1 s, depending on the concentration of volatile organic compounds (VOC).

In the absence of reducing agents the hydroperoxyl radical $HO_2^{\bullet}$ disproportionates in a spin-allowed bimolecular self-reaction to H_2O_2 and $^3O_2$.

Photolysis of water by γ-rays[53] in the presence of N_2O as well as sonolysis of water by high-frequency ultrasound produces $OH^{\bullet}$ in concentrations suitable for kinetic experiments:

$$H_2O \xrightarrow{h\cdot\nu} H^{\bullet} + OH^{\bullet}$$

$$H^{\bullet} + N_2O \longrightarrow N_2 + OH^{\bullet}$$

The same happens during the photolysis of aqueous anions such as nitrite, nitrate, sulfate, peroxodisulfate and dithionate yielding $O^{\bullet-}$ radical ions which are protonated to $OH^{\bullet}$ by $[H_3O]^+$.[54] Some of these reactions occur in ocean water under the influence of the Sun's radiation. The lifetime of $OH^{\bullet}$ in pure water is in the range of microseconds.

11.4 Fluorides of Oxygen

11.4.1 Introduction

In analogy to the hydrides $HO_n^{\bullet}$ and H_2O_n discussed in Section 11.3, oxygen forms fluorides of compositions $O_nF^{\bullet}$ and O_nF_2 with positively polarized oxygen atoms.[55] Since the oxidation numbers of oxygen are positive, these compounds should not be termed fluorine oxides. The mixed species hydroxyl fluoride (HOF, hydrogen hypofluorite) is also known. A comparison of the bonding situations in oxygen hydrides and fluorine oxides demonstrates the formal character of this analogy.

Radicals of type $O_nF^{\bullet}$ are known with n = 1 and 2 only. Both species are unstable and although they have not been prepared as pure compounds, they could still be detected by IR and ESR spectroscopy. Fluorides of type O_nF_2 have been isolated with n = 1, 2 and 4; O_3F_2 reported in the older literature has turned out as a mixture of O_2F_2 and O_4F_2, but the trioxide $(CF_3)_2O_3$ is known as a pure compound. With exception of OF_2 all oxygen fluorides are thermodynamically unstable with respect to decomposition to the elements.

---

52 See the topical issue *Chem. Rev*. **2003**, *103*, issue 12. A. Wahner, G. K. Moortgat, *Chem. unserer Zeit* **2007**, *41*, 192. D. Vione et al., *Chem. Rev*. **2015**, *115*, 13051–13092.

53 High-energy photons of very short wavelengths produced by radioactive nuclides or in a cyclotron (pulse radiolysis).

54 H. Herrmann, *Phys. Chem. Chem. Phys*. **2007**, *9*, 3935.

55 R. Marx, K. Seppelt, *Dalton Trans*. **2015**, *44*, 19659 and references cited therein.

11.4.2 Oxygen Difluoride, OF_2

Oxygen difluoride is prepared by bubbling fluorine gas into 2% aqueous NaOH (0.5 M) at 25 °C:

$$2\,F_2 + 2\,NaOH \longrightarrow OF_2 + H_2O + 2\,NaF$$

The maximum yield of OF_2 is 80% since a fraction is systematically lost by hydrolysis:

$$OF_2 + 2\,[OH]^- \longrightarrow O_2 + 2\,F^- + H_2O$$

Similar yields are obtained in the reaction of fluorine gas with moistened potassium or cesium fluoride. Oxygen difluoride is also prepared by electrolysis of aqueous $K[HF_2]$. All reactions proceed through HOF as intermediate, which can be prepared from F_2 and ice water and isolated in milligram amounts as colorless crystals (m.p. –117 °C). HOF contains an oxygen center of formal zero oxidation state. Hydroxyl fluoride is unstable at 25 °C and is often erroneously termed as hypofluorous acid in analogy to HOCl, which, however, contains oxygen of oxidation state –2. HOF reacts with F_2 to OF_2 and HF and with H_2O to H_2O_2 and HF; aqueous iodide is oxidized to $[I_3]^-$, $[OH]^-$ and F^-. More stable than HOF is the derivative CF_3OF obtained by reaction of COF_2 with F_2.

OF_2 is a colorless toxic gas (m.p. –223 °C, b.p. –145 °C) with a standard enthalpy of formation of –17 kJ mol^{-1}. The molecular symmetry is C_{2v} with a bond angle of 103.3°. OF_2 is a much stronger oxidant than F_2 but less reactive. Aqueous hydrogen halides are oxidized by OF_2 to the corresponding halogens:

$$OF_2 + 4\,HX \longrightarrow H_2O + 2\,HF + 2\,X_2 \qquad X = Cl, Br, I$$

Many nonmetals are oxidized or fluorinated by OF_2. Upon ignition, steam reacts explosively with OF_2 to form oxygen and HF, and H_2S reacts explosively even at room temperature. Krypton and xenon are fluorinated by OF_2 in sunlight at 25 °C to the difluorides.

Pure OF_2 is not explosive but decomposes on heating to 220–250 °C or on irradiation to O_2 and F_2. UV photolysis at 4 K in a matrix of N_2 produces $OF^\bullet$ radicals that have been detected by IR spectroscopy:

$$OF_2 \xrightarrow{h.v} OF^\bullet + F^\bullet$$

The radical $OF^\bullet$ is also obtained during irradiation of a N_2O/OF_2 mixture in a matrix of N_2 by reaction of fluorine atoms with N_2O:

$$F^\bullet + N_2O \longrightarrow [OF]^\bullet + N_2$$

On warming to room temperature, the matrix-isolated $OF^{\bullet}$ radicals recombine mainly to O_2F_2, which is discussed in the following Section.

11.4.3 Dioxygen Difluoride, O_2F_2

Dioxygen difluoride is most easily prepared by UV irradiation of liquid oxygen–fluorine mixtures at –196 °C. The compound is also formed in a high-voltage glow discharge of the gaseous elements at low temperatures (77–90 K) and pressures (10–20 hPa). Alternatively, the flowing gas mixture may be heated in a nickel tube to 600–800 °C. Furthermore, UV photolysis of O_3/F_2 mixtures at 120–195 K produces O_2F_2 together with OF_2:

$$F^{\bullet} + O_3 \longrightarrow O_2 + OF^{\bullet}$$
$$2\,OF^{\bullet} \longrightarrow O_2F_2$$
$$OF^{\bullet} + F_2 \longrightarrow OF_2 + F^{\bullet}$$

Yellow to brownish O_2F_2 (m.p. –164 °C) is soluble in $CClF_3$ with yellow color. The solid compound decomposes already at –78 °C to the elements in a slightly exothermic reaction with $O_2F^{\bullet}$ radicals as intermediates. Its gas phase structure from microwave studies corresponds to that of H_2O_2 (Figure 11.4) with C_2 symmetry, bond angles OOF of 109.2° and a torsion angle τ = 88.1°. The dissociation enthalpy of the unusually short OO bond (122 pm) has been calculated as 193 kJ mol^{-1} although only 81 kJ mol^{-1} is required to dissociate one of the rather weak OF bonds of length d_{OF} = 158 pm homolytically. The *trans*-barrier for rotation about the OO bond (81 kJ mol^{-1}) is relatively high, which is explained by hyperconjugation between the oxygen 2*p* lone-pairs and the σ^* MOs of the OF bonds (see the following section). In the solid state, the OO bond of O_2F_2 (d_{OO} = 118 pm)[55] is shorter than that of O_2.

O_2F_2 is a strong oxidizing and fluorinating agent, converting Cl_2 to ClF and ClF_3, while H_2S is turned into SF_6. With elemental sulfur, O_2F_2 explodes already at –180 °C. Fluoride ion acceptors form dioxygenyl salts from O_2F_2 (see Section 11.2.5).

11.5 Bonding Situation in Oxygen Hydrides and Fluorides

In Table 11.4, some bond properties of the oxygen hydrides and fluorides are compared. The OH bonds are normal single bonds with nearly identical internuclear distances, but their *dissociation enthalpies* differ considerably as the following data show (in kJ mol^{-1} at 25 °C):

$OH^{\bullet}$: 429 H_2O: 497 H_2O_2: 363

Table 11.4: Bond lengths d (pm) and valence force constants f_r (N cm^{-1}) of the covalent bonds in the gaseous hydrides and fluorides of oxygen including some radicals (data of O_2 are given for comparison).

Molecule	d_{OH}	d_{OO}	f_r(OH)	f_r(OO)	Molecule	d_{OF}	d_{OO}	f_r(OF)	f_r(OO)
$HO^\bullet$	97	–	7.1	–	$OF^\bullet$	132	–	5.42	–
H_2O	96	–	7.7	–	OF_2	141	–	3.95	–
HOF	96	–	6.9	–	HOF	144	–	4.0	–
$HO_2^\bullet$	97	133	6.5	5.9	$O_2F^\bullet$	–	–	1.43	10.5
H_2O_2	95	149	7.4	4.6	O_2F_2	158	122	1.50	10.3
O_2	–	121	–	11.4	O_2	–	121	–	11.4

The low value for H_2O_2 is the result of a stabilization of the formed $HO_2^\bullet$ radical by a 3-electron π bond between the oxygen atoms as indicated by the short OO bond length of 133 pm, which is intermediate between those of O_2 (121 pm) and H_2O_2 (149 pm). The valence force constants f_r(OO) support this interpretation (Table 11.4).

The oxygen fluorides show interesting structural anomalies. The OF bond of the $OF^\bullet$ radical can be regarded as a regular single bond (2-electron bond) with its length of 132 pm close to the sum of the covalent single bond radii (Table 4.3). However, in all other oxygen fluorides the OF bond is longer, especially in $O_2F^\bullet$ and O_2F_2. At the same time, the OO bond properties of the latter two species hardly differ from those of the O_2 molecule with its double bond. Evidently, the high electronegativity of fluorine stabilizes the σ* orbitals of the OF bonds making them suitable acceptors for the 2*p* lone-pair electrons at the oxygen atoms. In effect, two dative π bonds are formed along the OO axis in addition to the σ bond (Figure 11.5). This type of *hyperconjugation* is also called *anomeric effect*.

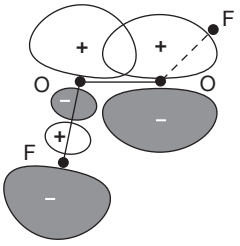

Figure 11.5: Hyperconjugation between the 2*p* lone-pair orbital at one of the oxygen atoms of O_2F_2 by overlap with the empty σ* MO of one of the OF bonds, which is located approximately within the same plane. While the strength of the OO bond increases, the OF bond is weakened. The same coordinate π bond can be assumed for the other side of the molecule.

The weak OF bonds of O_2F_2 are responsible both for its thermal instability and high reactivity even at low temperatures. The dissociation enthalpy of O_2F_2 to give $O_2F^\bullet$ and $F^\bullet$ has been calculated as 81 kJ mol^{-1}, which is 78 kJ mol^{-1} less than the

dissociation enthalpy of F_2.[56] In case of the oxygen hydrides any hyperconjugation can be neglected considering the low electronegativity of hydrogen (i.e., the orbital energy of the σ* AOs of the OH bonds is too high).

Molecules with longer *chains of oxygen atoms* are CF_3OOOCF_3 and $CF_3OC(O)OOOC(O)OCF_3$, which have been prepared at low temperatures and are formal derivatives of H_2O_3 with a helical COOOC backbone.[57] Traces of the hydrogen peroxide homologues H_2O_3 and H_2O_4 are formed together with H_2O_2 when a mixture of H_2 and O_2 is subjected to a microwave discharge at reduced pressure and the products are immediately frozen with liquid nitrogen. The RAMAN spectrum of this product mixture shows signals for all three oxygen hydrides. On warming to room temperature, H_2O_3 and H_2O_4 decompose to H_2O_2 and O_2.[58] H_2O_3 can better be prepared by reduction of ozone as described in Section 11.3.4.

56 E. Kraka, Y. He, D. Cremer, *J. Phys. Chem. A* **2001**, *105*, 3269.
57 K. Suma, Y. Sumiyoshi, Y. Endo, *J. Am. Chem. Soc.* **2005**, *127*, 14998.
58 A. V. Levanov et al., *Eur. J. Inorg. Chem.* **2011**, 5144.

12 Sulfur, Selenium and Tellurium

12.1 Introduction

Sulfur is one of the most important elements both for life as well as for the chemical and pharmaceutical industries. Even in extraterrestrial space sulfur compounds are abundant albeit in low concentrations.[1] Sulfur contributes 0.07 wt% to the crust of Earth, while selenium and tellurium are much less abundant. However, elemental sulfur and sulfur-containing minerals occur in substantial *deposits*. Important sulfur minerals are: *pyrite* FeS_2, *galena* PbS, *zinc-blende* (*sphalerite*) ZnS, *cinnabar* HgS, *chalcopyrite* $CuFeS_2$ and *chalcocite* Cu_2S as well as several sulfates such as *gypsum* $Ca[SO_4]\cdot 2H_2O$,[2] *bassanite* $Ca[SO_4]\cdot 0.5H_2O$, *anhydrite* $Ca[SO_4]$ and *baryte* $Ba[SO_4]$. Gypsum is the most abundant sulfate mineral (by volume). Ocean water contains 2.7 g L^{-1} sulfate, and river waters only ca. 0.01 g L^{-1}. Elemental sulfur is mainly produced from fossil fuels such as crude oil and coal as well as from sour natural gas containing H_2S.

All organisms contain inorganic and organic sulfur compounds. Therefore, sulfur is an important component of fertilizers for plants, together with nitrogen, phosphorus and potassium. A human of 70 kg contains about 170 g S, mainly in the form of the amino acids cysteine, cystine and methionine, but only 0.02 g Se, for example, as selenocysteine. Important Se containing enzymes are glutathione peroxidase and glycerol reductase.[3] Therefore, sulfur and selenium are *essential elements* for mammals. Tellurium compounds, on the other hand, are toxic. Vegetarian food contains selenium mainly as selenomethionine, while meat contains traces of selenocysteine. The selenium content of food depends on the Se concentration of the soil on which the plants grow and the animals graze. Relatively high Se concentrations are found in Brazil nuts and in whole-meal bread as well as in liver, poultry and fish.

The *atomic weights* of most elements vary slightly owing to natural variations in the relative abundances of the isotopes. This variation is used to determine the *origin* of a particular sample (a mineral or biological material). In case of sulfur, the variation may be ±0.01 units, while individual samples can be determined at an accuracy of ±0.00015 (mainly by mass spectrometry). Due to the historic developments in analytical methods, published atomic weights have also changed with

1 A. Müller, B. Krebs (eds.), *Sulfur – Its Significance for Chemistry, for the Geo-, Bio- and Cosmosphere and Technology*, Elsevier, Amsterdam, **1984**. R. Steudel (ed.), *Elemental Sulfur and Sulfur-Rich Compounds, Parts I and II*, Springer, Heidelberg, **2003** (*Top. Curr. Chem.*, Vols. 230 und 231). F. A. Devillanova (ed.), *Handbook of Chalcogen Chemistry*, Royal Society of Chemistry, London, **2006**.

2 In the year 2000, a cave was discovered during mining operations near Naica in Northern Mexico at a depth of 290 m containing huge single crystals of selenite, a modification of $Ca[SO_4]\cdot 2H_2O$, some of which are 13 m long.

3 A. Böck, *Encycl. Inorg. Chem.* **2005**, *8*, 4970.

https://doi.org/10.1515/9783110578065-013

time. For example, when the first international Table of Atomic Weights was published in 1905 the mean relative atomic mass of selenium was given as 79.2, while todays accepted value is 78.96 (see Table 12.1).

Table 12.1: Properties of the heavier chalcogens.

Element	Valence electron configuration	Color of the most stable allotrope	m.p. (°C)	b.p. (°C)	Natural abundance of isotopes in mol%
S	$3s^2p^2p^1p^1$	yellow	115[a]	445	^{32}S: 95.0, ^{33}S: 0.76, ^{34}S: 4.22, ^{36}S: 0.02
Se	$4s^2p^2p^1p^1$	gray to black	221	685	^{74}Se: 0.9, ^{76}Se: 9.2, ^{77}Se: 7.6, ^{78}Se: 23.7, ^{80}Se: 49.8, ^{82}Se: 8.8
Te	$5s^2p^2p^1p^1$	metallic, brass-colored	450	990	^{120}Te: 0.01, ^{122}Te: 2.57, ^{123}Te: 0.89, ^{124}Te: 4.76, ^{125}Te: 7.10, ^{126}Te: 18.89, ^{128}Te: 31.73, ^{130}Te: 33.97
Po	$6s^2p^2p^1p^1$	–	254	962	all isotopes radioactive

[a]Triple point

Selenium and tellurium have stable and relatively abundant isotopes suitable for nuclear magnetic resonance (NMR) spectroscopy. For example, the nuclides ^{77}Se (natural abundance 7.6%), ^{123}Te (0.89%) and ^{125}Te (7.1%) have nuclear spins I = ½. Me_2Te is used as a reference for chemical shifts, which cover a range from –1800 to +3100 ppm. ^{125}Te is also used for MÖSSBAUER spectroscopy. In case of sulfur, only ^{33}S (I = 3/2) is suitable for NMR spectroscopy, but due to its low abundance (0.75%) and its quadrupole moment the signals are weak and broad. Polonium exists only as radioactive nuclides.

12.2 Bonding Situations and Tendencies in Group 16

The elements sulfur, selenium[4] and tellurium[5] resemble each other in their *chemical properties* much more than their lightest homolog oxygen. This is partially due to their relatively similar covalent single bond radii r_1, which also determine the electronegativities χ. As the following data illustrate, r_1 and χ change much more from oxygen to sulfur than from sulfur to selenium to tellurium:

4 B. Krebs, S. Bonmann, I. Eidenschink, *Encycl. Inorg. Chem.* **2005**, *8*, 4931.

5 T. Chivers, R. S. Laitinen, *Chem. Soc. Rev.* **2015**, *44*, 1717–1739. D. J. Woollins, R. S. Laitinen (eds.), *Selenium and Tellurium Chemistry*, Springer, Berlin, **2011**. R. S. Laitinen, R. Oilunkaniemi, *Encycl. Inorg. Chem.* **2005**, *9*, 5516.

	O	S	Se	Te
Covalence radius r_1 (pm):	66	105	120	138
χ(Allred–Rochow):	3.5	2.4	2.5	2.0

Therefore, sulfur and selenium should have similar chemistries. In other words, the chemistry of sulfur is be taken as representative for that of selenium. Similar relationships apply to the element pairs Si/Ge, P/As and Cl/Br.

All chalcogen atoms E have the valence electron configuration $s^2p_x^2p_y^1p_z^1$ with two unpaired electrons of parallel spins (^{3}P ground state; Table 8.1). The octet configuration of the following noble gas can be reached by either two covalent single bonds as in H_2S or by uptake of two electrons as in chalcogenide ions E^{2-}, for example, Na_2S. Additional substituents can be accommodated either by coordinate bonds as in the sulfonium cation $[SCl_3]^+$ or by multicenter bonds as in the molecules SF_4, Me_4Te and TeF_6. These hypercoordinate species have been discussed in Section 2.6 and more examples are given in Table 2.11.

In general, chalcogens occur in their compounds in nine oxidation states from −2 to +6, as in the following examples:

−2	−1	0	+1	+2	+3	+4	+5	+6
H_2S	H_2S_2	S_8	S_2Cl_2	SCl_2	$[S_2O_4]^{2-}$	SO_2	S_2F_{10}	SO_3

The *coordination numbers* (C.N.) of S, Se and Te in their covalent compounds typically vary between 1 and 6 (e.g., SF_6, SeF_6, Me_6Te), but in addition there are tellurium anions with C.N. = 8, for example, $[TeF_8]^{2-}$.

Group 16 of the Periodic Table descends from pure nonmetals (O, S) via elements with semiconductor properties (Se, Te) to a metal (Po) that has a specific resistance of $43{\cdot}10^{-3}$ Ω cm and, unlike other chalcogens, the positive temperature coefficient of the electrical resistance characteristic of metals. The lighter chalcogens O and S are nonconductors at ambient pressure, but specific resistances decrease markedly from sulfur to tellurium. This can be explained by the differing crystal structures of the thermodynamically stable allotropes at standard conditions. The *coordination numbers in the solid phases* at ambient pressure increase from 1 for O_2 via 2 for *cyclo*-S_8 to 2 + 4 for polymeric selenium and tellurium and reaching eventually 6 at polonium. Higher coordination numbers favor a higher electric conductivity.

Application of very high pressures enforces higher coordination numbers and consequently higher electric conductivities. For example, elemental sulfur changes from a molecular crystal to a layer structure with C.N. = 4 and metallic conductivity at 83 GPa. At 162 GPa, this phase is transformed into the rhombohedral structure of

β-Po with C.N. = 6 and a density of 6.5 g cm^{-3}. The latter two phases even become superconducting at temperatures of 10 and 17 K, respectively.[6]

All chalcogens E (excepting Po) form homoatomic chains and rings with single bonds at ambient conditions. The relatively low mean bond enthalpy of the bonds OO and TeTe has already been discussed in Section 4.4.4 (see also Figure 4.2). On the other hand, sulfur with its strong SS single bonds shows the highest tendency of ring and chain formation in Group 16, similar to phosphorus and silicon, and is only surpassed by carbon. Therefore, sulfur has the largest number of crystalline allotropes of all elements. In addition, many polychalcogen cations $[E_n]^{x+}$ are known both for sulfur, selenium and tellurium as well as mixed species.

The *tendency to form double bonds* in molecules stable at ambient temperature decreases in Group 16 from oxygen to tellurium. Examples are:

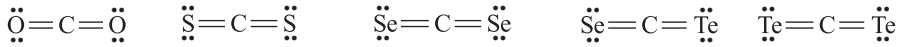

colorless gas | colorless liquid | yellow liquid | red-brown | unknown

The dioxides, however, show rather different structures with a stepwise increase of the coordination number of the chalcogen from S to Te:

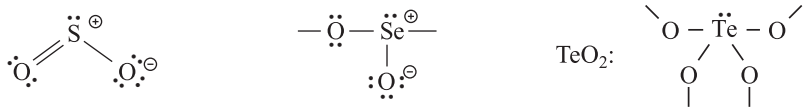

molecular gas | chain-like polymer | polymeric

A detailed discussion of the bonding situation in SO_2, SO_3 and the sulfate ion is given in Section 2.6. In general, multiple bonds are more easily formed the smaller the electronegativity difference of the participating atoms, and the greater the sum of their electronegativities. This holds for the following compounds partly prepared already in the 1960s proving that the heavier nonmetal atoms are also capable of forming *double bonds in compounds stable at 25 °C*:

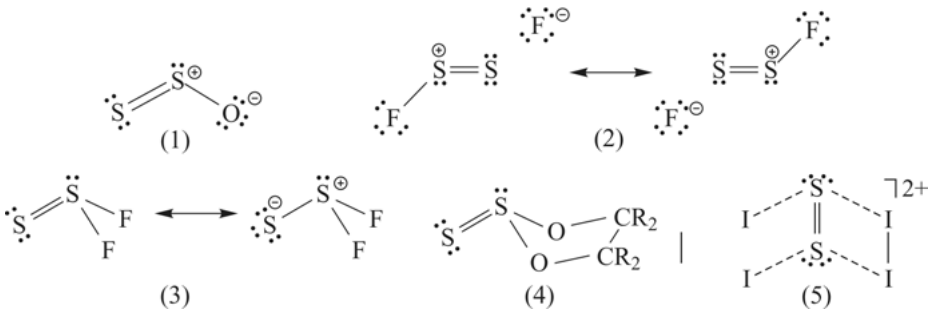

6 V. V. Struzhkin et al., *Nature* **1997**, *390*, 382, and references cited therein.

The molecules and ions above are given in the order they were prepared. Most spectacular is the cation $[S_2I_4]^{2+}$ with its extremely short SS bond of 184 pm, isolated with the weakly coordinating anions $[AsF_6]^-$ and $[SbF_6]^-$.[7] More details on these species are given in Sections 12.10 and 12.12. Only much later than examples (1) and (2), thermally stable compounds with SiSi and PP double bonds have been prepared; see Sections 8.11.2 and 10.7, respectively.

The stability of chalcogen–oxygen compounds with *high oxidation numbers* decreases in Group 16 from S to Te. Therefore, TeO_3 and SeO_3 are stronger oxidants than SO_3, and Se(IV) is reduced to Se(0) by S(IV). For instance, the selenite anion $[SeO_3]^{2-}$ is reduced to elemental selenium by the disulfite ion $[S_2O_5]^{2-}$, which is converted to sulfate.

12.3 Preparation of the Elements

12.3.1 Production of Sulfur

Large natural underground deposits of sulfur exist in the USA, Mexico and Poland, but elemental sulfur is mainly produced by the desulfurization of crude oil, of sour natural gas and of coal. Only on a very small scale, sulfur is still mined in volcanic areas as in Indonesia. Historically, Southern Italy (Sicily) has been the main origin of elemental sulfur during the industrialization of Western Europe in the early nineteenth century. In 1900, Sicily produced 500,000 t of elemental sulfur.[8] Another source of sulfur for the production of sulfuric acid is the mineral pyrite (FeS_2), with large deposits in many countries.

Natural sulfur melts at 120 °C. Therefore, in the historic FRASCH process of sulfur mining, the element was liquified in its underground deposits by superheated water (ca. 150 °C) under pressure and in this way separated from accompanying sand and limestone. The liquid sulfur was pumped to the surface and purified by vacuum distillation.[9] During the twentieth century this process had been carried out on a large scale in the Southern United States, both onshore and offshore. The sulfur deposits of diameters between 0.5 and 6 km are at depths of 200–500 m. Owing to the high energy costs and for environmental reasons, the FRASCH process became unprofitable and was replaced by the CLAUS process for sulfur production (see below).

---

7 J. Passmore et al., *Inorg. Chem.* **2005**, *44*, 1660.

8 This business was so profitable that it attracted the attention of criminals and is considered the economic origin of the Italian mafia; see P. Buonanno, R. Durante, G. Prarolo, P. Vanin, *The Economic Journal* **2015**, *125*, F175-F202.

9 HERMANN FRASCH (1851–1914) emigrated at age 16 from Germany to the USA and introduced this intelligent process in Louisiana where the first FRASCH sulfur was produced in 1895; see W. Botsch, *Chem. unserer Zeit* **2001**, *35*, 324 (with many color pictures).

Nowadays most of the elemental sulfur needed for sulfuric acid production and other purposes comes from desulfurization processes of which the *hydrodesulfurization of crude oil* in refineries around the world (HDS process) is most important.[10,11] Crude oil and its distillation products such as heating oil, gas oil, gasoline, kerosene (jet fuel) and so on contain organic sulfides, disulfides, thiophene derivatives and thiols, which have to be removed or their concentration considerably reduced for environmental reasons. Combustion of these sulfur compounds produces SO_2, which yields sulfuric acid in the atmosphere and gives rise to health problems, corrosion of buildings, monuments and other structures as well as to acid rain. Varying sulfur contents are allowed in these petrochemical products in different countries.

In the **HDS process,** catalytic hydration of organosulfur compounds with H_2 produces H_2S and sulfur-free hydrocarbons according to the following scheme:

The reaction is carried out at 300–400 °C and 2–6 MPa H_2 pressure on a Mo/Ni or Mo/Co catalyst. In order to reach low residual sulfur contents, a two-stage process is employed. During the first stage (desulfurization to ca. 350 ppm S), the more reactive thiols, sulfides and disulfides are desulfurized. In the second stage at higher temperatures and pressures, the less reactive thiophene derivatives are converted. The lower the desired sulfur content, the longer the reaction time and the higher the costs.

The hydrogen sulfide produced by the HDS process is further treated in the same manner as H_2S from *natural sour gas*, which is produced, for example, in Alberta (Canada), the USA, Northern Germany, Southern France and elsewhere. The gas contains a few percent H_2S, but in some cases up to 50%. The corrosive and highly toxic hydrogen sulfide is removed in *gas sweetening plants* by scrubbing with an aqueous solution of an amino alcohol such as methyl diethanol amine [MDEA, $CH_3N(C_2H_4OH)_2$] from which the dissolved H_2S together with some CO_2 is set free by heating. This enriched acid gas mixture is then sent to a CLAUS plant for oxidation of H_2S to elemental sulfur of high purity (Figure 12.1).[12] This seemingly simple reaction proceeds in several steps. First, about one third of the H_2S is burned in the CLAUS furnace at 950–1200 °C with O_2-enriched process air to H_2O and SO_2, but the latter reacts immediately with remaining H_2S to S_2 and H_2O according to equation (2):

10 R. J. Angelici, *Encycl. Inorg. Chem.* **2005**, *3*, 1860; Special issue of *Polyhedron* **1997**, *16*, issue 18 (11 contributions).

11 Most of the world's largest oilfields are in the Middle East, but there are also supergiant oilfields (>10 billion barrels) in India, Brazil, Mexico, Venezuela, Kazakhstan and Russia.

12 The original process has been patented to CARL FRIEDRICH CLAUS (1827-1900) in 1883 both in Berlin and London. Today only the modified CLAUS process invented by I.G. Farben in Germany is applied; see B. Schreiner, *Chem. unserer Zeit* **2008**, *42*, 378.

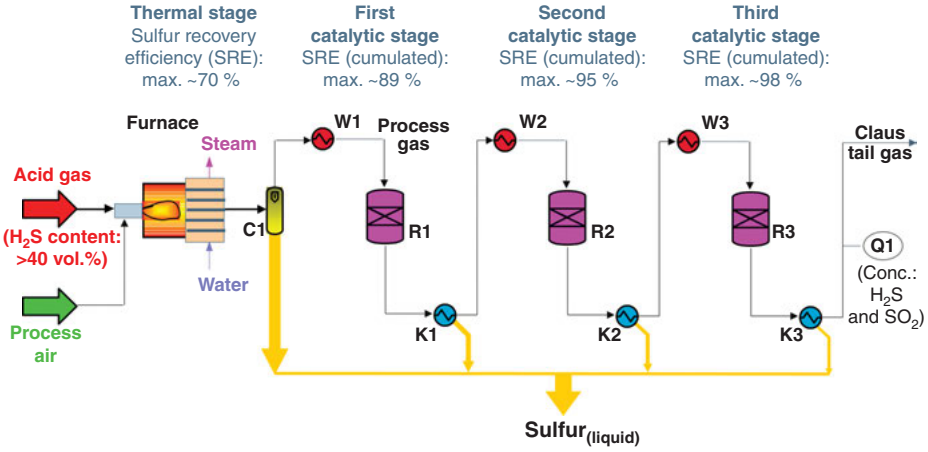

Figure 12.1: Flowchart for the different stages of the CLAUS process for oxidation of H_2S to liquid sulfur and water (C: cooler, W: heat exchangers, R: reactors with catalyst, K: sulfur condensers; at Q1 the composition of the tail gas is measured).

$$H_2S + \frac{3}{2}O_2 \longrightarrow SO_2 + H_2O \qquad \Delta H = -518.0\ \text{kJ mol}^{-1}$$

$$SO_2 + 2\,H_2S \rightleftharpoons \frac{3}{2}S_2 + 2\,H_2O \qquad \Delta H = +47.3\ \text{kJ mol}^{-1}$$

$$3H_2S + \frac{3}{2}O_2 \longrightarrow \frac{3}{8}S_8 + 3\,H_2O \qquad \Delta H^\circ_{298} = -664\ \text{kJ mol}^{-1}$$

For completion of the slightly endothermic equilibrium reaction (2), the hot gas mixture is cooled in a heat exchanger **C** to 200–300 °C to condense liquid sulfur according to reaction (3) with simultaneous production of steam. The remaining gas is reheated in heat exchanger **W1** to 350 °C before it enters the first reactor **R1** containing a Al_2O_3 or TiO_2 based catalyst. Behind the first catalytic stage the gas is cooled again to condense sulfur in **K1** and reheated before it enters the next reactor. The catalyst temperatures decrease from stage to stage to shift the endothermic equilibrium (2) more and more to the right; in the last reactor **R3** the catalyst temperature is about 180 °C.[13] By the intermediate removal of one of the products (sulfur) very high yields (sulfur recovery efficiencies, SRE) are obtained. The tail gas contains still traces of H_2S and SO_2 besides H_2O. It is reduced with H_2 to H_2S which is returned to the feed gas of the CLAUS furnace.

In 2012, the worldwide production of CLAUS and FRASCH sulfur was ca. $45{\cdot}10^6$ t. While in the past this production was somewhat higher than the global sulfur demand and huge blocks of elemental sulfur have been built for storage, at present (2018) the demand is slightly higher than the production and consequently sulfur prices rise and stockpiles shrink.

13 Sometimes only two and sometimes four catalytic stages are used in CLAUS plants.

Desulfurization of *industrial waste gases* of power plants and refineries containing SO_2 or mercaptans is also important. These processes will be discussed in the sections on sulfur–oxygen compounds (Section 12.10.1). Furthermore, biogas and off-gas from sewage plants usually contain H_2S, which must be removed before the gas can be used as "biomethane" or being fed into pipelines.

To transport elemental sulfur produced by the CLAUS or FRASCH processes in the liquid state either steam-heated pipelines, railroad tank cars as well as tank ships are used. In the solid form sulfur is transported in a "formed" state to avoid sulfur dust that can be explosive in mixtures with air.[14] About 85% of the elemental sulfur is used for the production of H_2SO_4, the rest for rubber vulcanization and the production of sulfur halides, carbon disulfide, thiosulfate, sulfur dyes, lubricants and pharmaceuticals. Sulfur is also used as a depot fertilizer, which is slowly oxidized to sulfate in soil. Furthermore, elemental sulfur is applied in vineyards to control fungi such as *erysiphales*, which is the most harmful pest in the wine growing business. Most probably, sulfur oxides and lower oxoacids are the active fungicides generated by slow oxidation of S_8 in air.

12.3.2 Production and Uses of Selenium and Tellurium

Selenium and tellurium are less widely distributed in Earth's crust than sulfur. They occur as selenides and tellurides, traces of which are also present in sulfidic ores. On roasting (burning) of these ores to metal oxides and SO_2, solid SeO_2 and TeO_2 are formed and are contained in the fly ash from which they are isolated by extraction with water. The aqueous solutions are then reduced by SO_2:

$$H_2SeO_3 + 2\,SO_2 + H_2O \longrightarrow Se\downarrow + 2\,H_2SO_4$$

However, the main resource of Se and Te is the anode sludge of electrolytic copper and nickel refining. Crude copper contains Te as Cu_2Te, Ag_2Te and $(Ag,Au)_2Te$.[15] The latter two compounds are also found in silver and gold ores.

The global annual production of Se is more than 2500 t and of Te about 140 t. Selenium is used in glass manufacturing to decolorize the green tint caused by iron impurities in glass containers and other soda-lime silica glass. It is also used in art glass and other glasses, such as that used in traffic lights, to produce a ruby red color and in architectural plate glass to reduce solar heat transmission through the glass. Glass manufacturing accounted for about 35% of the selenium market in

14 R. Steudel, *Chem. unserer Zeit* **1996**, *30*, 226 (with color pictures).

15 G. Knockaert, *Ullmann's Encycl. Ind. Chem.*, 6th ed., electronic release, **1998**. Main supplier for selenium in Europe is Aurubis AG in Hamburg with its daughter company RETORTE GmbH near Nürnberg.

2002. An estimated 24% of the selenium market involves metallurgical uses, and more than one-half of the metallurgical selenium is used as an additive to cast iron, copper, lead and steel alloys. In these applications, it improves machinability as well as casting and forming properties.

Elemental selenium is also used as *photoconductor* in radiography with X-rays, in high-throughput copying machines, in rectifiers and in photocells. The selenide $CuInSe_2$ is employed in thin film solar cells. Furthermore, selenium compounds are added to fertilizers. Selenium is also applied as alloy. The same holds for tellurium in alloys with copper, iron and lead. Numerous applications are known for Te in the electronic industry and in metallurgy. High-purity tellurium is used in electronics applications, such as thermoelectric and photoelectric devices. Thermal imaging devices use mercury–cadmium telluride as a sensing material. Semiconducting materials containing bismuth telluride are employed in electronics and consumer products as thermoelectric cooling devices. These devices consist of a series of couples of semiconducting materials, which, when connected to a direct current, cause one side of the thermoelement to cool, while the other side generates heat. These thermoelectric coolers are most commonly used in military and electronics applications, such as the cooling of infrared detectors, integrated circuits, medical instrumentation and laser diodes.

Finally, selenium and tellurium compounds are useful reagents and catalysts in organic synthesis.[16]

12.4 Allotropes of the Chalcogens

12.4.1 Sulfur

All native deposits of elemental sulfur contain S_8 molecules and all industrial processes to produce elemental sulfur also yield mainly S_8 molecules, which are thermodynamically more stable at 25 °C/0.1 MPa than other ring sizes or chain-like molecules. However, by smart synthetic routes it has been possible to prepare many other sulfur allotropes, which are metastable at room temperature but slowly convert to S_8 in most cases.[17] Consequently, sulfur is the element with the largest number of crystalline allotropes, most of which consist of cyclic molecules. There are *monotropic and enantiotropic modifications*. Only the latter convert in a *reversible* manner to the stable form and therefore show up in the phase diagram of the element. Monotropic allotropes must be synthesized under conditions that avoid conversion to S_8, that is, at low temperatures and in the absence of catalysts and intense light.

16 R. S. Laitinen, R. Oilunkaniemi (eds.), *Selenium and Tellurium Reagents in Chemistry and Materials Science*, de Gruyter, Berlin, 2018.

17 R. Steudel, B. Eckert, *Top. Curr. Chem.* **2003**, *230*, 1–79.

The **phase diagram** of elemental sulfur near ambient pressure is shown in Figure 12.2.

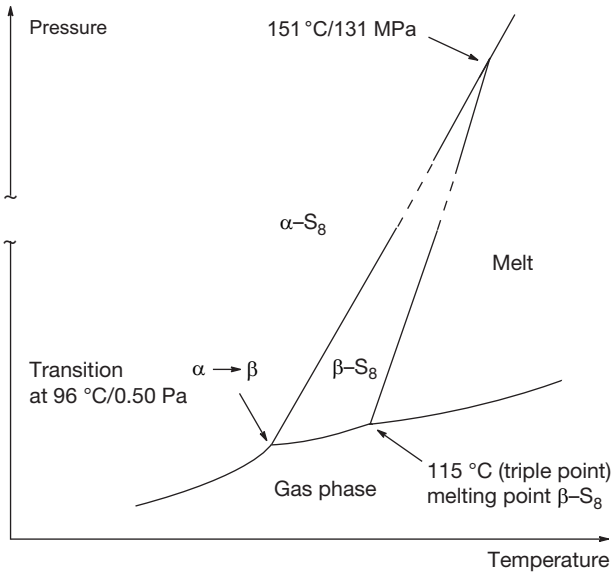

Figure 12.2: Schematic phase diagram of elemental sulfur (not to scale). At standard conditions orthorhombic α-S_8 is thermodynamically stable; monoclinic β-S_8 is of lower density and therefore exists only up to pressures of 131 MPa.

Cyclo-octasulfur crystallizes from solvents as orthorhombic crystals with 16 molecules per unit cell at standard conditions (α-S_8; Figure 12.3). In α-S_8 the atoms lie in two parallel planes giving the ring a *crown shape* (symmetry D_{4d}). The mean internuclear distance is 204.8 pm, the bond angles are 108° and the torsion angles ±98°. Since S_8 is more stable than other ring sizes, these angles may be considered as optimum values for sulfur–sulfur single bonds. The yellow crystals of α-S_8 are very brittle, highly soluble in CS_2 and moderately soluble in $CHBr_3$, 1,4-$C_6H_4Cl_2$ and toluene. The solubility in water at 25 °C is only ca. 7 μg L^{-1}.

12.4.1.1 Thermal Behavior of Sulfur

At 96 °C (vapor pressure 0.4 Pa; first triple point) the thermodynamically stable α-modification rearranges into monoclinic β-sulfur, which is by $\Delta H° = 32$ kJ mol^{-1} less stable but still consists of S_8 molecules. This phase change is slow in single crystals but faster in powdered sulfur. The vapor pressure of β-S_8 at 100 °C is high enough that it can be sublimed in vacuo for purification. β-S_8 melts at 120 °C, but this so-called ideal melting point is not identical with the *triple point* at which solid, liquid and gaseous phases are in equilibrium; the *equilibrium melting point*

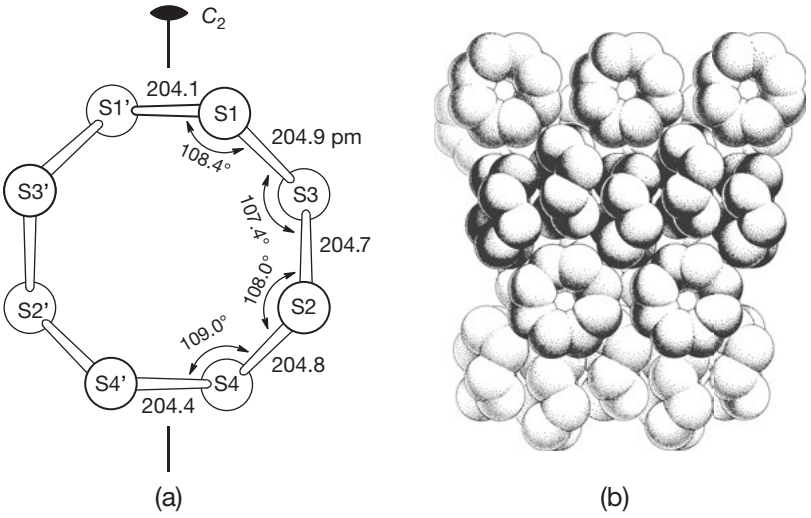

Figure 12.3: (a) Molecular structure of S_8 in orthorhombic α-sulfur at 25 °C. The twofold rotation axis C_2 exchanges the positions of atoms S(*n*) and S(*n'*). The site symmetry C_2 is the result of interactions with neighboring molecules. Isolated S_8 molecules are of D_{4d} symmetry. (b) The packing of S_8 rings in orthorhombic α-sulfur.

is at 115 °C ("natural melting point" of sulfur). The melting point depression of 5 K from the ideal to the natural melting point arises from the slow attainment of a chemical equilibrium between smaller and larger sulfur molecules formed from S_8 in the liquid phase.

Liquid sulfur consists solely of S_8 molecules only immediately after melting of β-S_8. Such a freshly prepared melt crystallizes in fact at 120 °C with formation of β-S_8. At the melt temperature, S_8 molecules slowly convert to a complex mixture of rings and chains of differing sizes that have been identified both by RAMAN spectroscopy and, after quenching the melt and extraction by CS_2, by *high-pressure liquid chromatography* (HPLC). In addition, the vapor above the melt contains sulfur molecules of between 2 and 8 atoms. In the melt the molecules S_n ($n \neq 8$) act as "impurities" causing a melting point depression of 5 K from which their total concentration has been calculated as ca. 5.5 mol% at 115 °C. As will be shown below, sulfur melts after thermal equilibration consist of all homocycles from S_6 on upward to at least S_{26} and of polymeric sulfur (S_∞ or S_μ), which is insoluble in CS_2 at 25 °C.[18] It takes about 12 h to fully establish the equilibration at 120 °C.[19]

18 R. Steudel, *Top. Curr. Chem.* **2003**, *230*, 81–116.

19 In the older literature, the soluble part of quenched sulfur melts was divided into the so-called λ-sulfur (S_8 rings) and π-sulfur (non-S_8 ring molecules).

The position of the chemical equilibrium

$$x\,S_8 \rightleftharpoons y\,S_n \quad (n \neq 8)$$

in liquid sulfur strongly depends on the temperature with the concentrations of the less stable ring molecules increasing with temperature up to 159 °C (Table 12.2).[20] Near the triple point between solid, liquid and gaseous sulfur, the melt is yellow and of low viscosity. But above 159 °C the viscosity increases sharply by five orders of magnitude and reaches a maximum near 178 °C. At 200 °C, the melt is red-brown and resin-like; free radicals have been detected by ESR spectroscopy, although in low concentrations. The high viscosity indicates the formation of polymeric sulfur molecules, which are thermally degraded on further heating resulting in a decrease of the viscosity above 200 °C while the radical concentration increases. At the *boiling point* (445 °C) sulfur melts are dark red-brown and of low viscosity.

Table 12.2: Molecular composition of liquid sulfur after equilibration at the given temperatures and followed by quenching in liquid nitrogen, extraction with CS_2 and quantitative HPLC analysis (values in mass-%). The cumulated concentrations of the large rings S_x (x = 11, 13, 14 . . .) has been calculated as difference to 100%. S_μ symbolizes insoluble polymeric sulfur. After R. Steudel, R. Strauss, L. Koch, *Angew. Chem. Int. Ed.* **1985**, *24*, 59.

Species	Temperature			
	116 °C	122 °C	159 °C	220 °C
S_8	93.6	93.1	83.4	54.3
S_7	3.1	3.3	5.2	4.6
S_6	0.5	0.6	0.9	0.9
S_9	0.3	0.4	0.6	0.6
S_{10}	0.1	0.1	0.2	0.2
S_{12}	0.4	0.4	0.5	0.4
ΣS_x	1.8	1.9	6.2	4.8
S_μ	0.2	0.2	3.0	34.2

These phenomena reflect the changing composition of the melt. The viscosity and other physical properties show a discontinuity at 159 °C where high-molecular weight ring and chain molecules are spontaneously formed. Their concentrations increase with temperature in the region 159 °C to 200 °C, and the chain length grows to probably 10^5 atoms. Catenane-like species (intertwined rings) may also be formed to account for the extreme viscosity near 178 °C. The contribution of

20 To be more correct, the concentration ratios c_i/c_8 increase with temperature up to the boiling point.

polymeric sulfur to the total sulfur content at 220 °C is 34%, while smaller (soluble) ring molecules S_n ($n \neq 8$) account for only 11.5% at this temperature. Increasing temperature thermally cracks the polymers and the molecular sizes decrease as does viscosity. At the same time, the increasing concentration of diradical chain molecules darkens the color. Among these fragments, the highly colored species S_2, S_3, S_4 and S_5 have been proposed as constituents of hot sulfur melts since they definitely exist in sulfur vapor above the melt (see below).

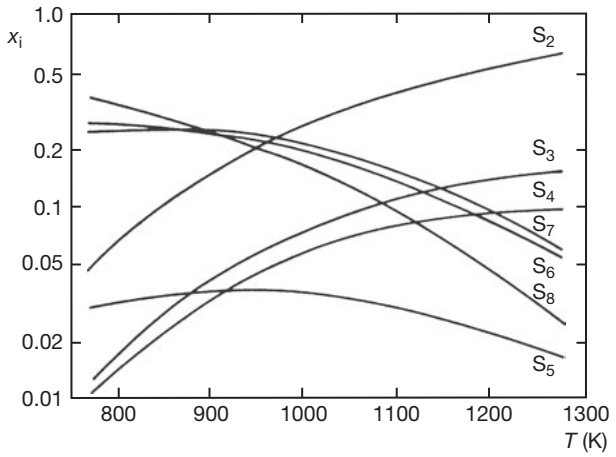

Figure 12.4: Molecular composition of saturated sulfur vapor (in equilibrium with the melt) as a function of the absolute temperature *T*. The mol fractions $x_i = c_i/\Sigma c_i$ of the species S_2 till S_8 are shown in semilogarithmic manner at the ordinate (c_i: molar concentration of species i). Disulfur S_2 dominates above 1000 K.

Sulfur Vapor

The molecular composition of sulfur vapor is almost as complex as that of the liquid phase but easier to study by spectroscopic techniques.[21] By mass spectrometry the species S_n with n = 2–8 have been detected and shown to exist in temperature- and pressure-dependent equilibria (Figure 12.4). *Saturated vapor* at temperatures above 1000 K consists mainly of S_2, which is probably the cause of the violet color. At the critical point (1313 K), the average molecular size is $S_{2.78}$. Sulfur atoms are formed only above 2500 °C and at very low pressures (1 mPa) since the double bond in S_2 is quite strong. All molecules S_n with $n > 4$ are cyclic and yellow or orange-yellow. The red S_4 molecule is chain-like, planar and of C_{2v} symmetry (*cis*-conformation); its C_{2h} isomer (*trans*-conformation) is less stable but has nonetheless been detected in sulfur

21 R. Steudel, Y. Steudel, M. W. Wong, *Top. Curr. Chem.* **2003**, *230*, 117–134.

vapor by resonance RAMAN spectroscopy at high temperatures. There are no oxygen analogues of these tetrasulfur isomers. On the other hand, the yellow S_3 molecule (thio-ozone) is bent as are O_3, SO_2 and S_2O.

Disulfur S_2 has a $^3\Sigma_g$ triplet ground state as does O_2, that is, both molecules are paramagnetic and contain double bonds. In unsaturated sulfur vapor at a pressure of 0.1 Pa, S_2 is the main constituent already at 600 K and can be isolated by rapid quenching the vapor together with a noble gas to 4 K. The matrix-isolated S_2 can then be studied spectroscopically and chemically. On warming the matrix it forms S_4.[22] Quenching of saturated sulfur vapor in a solvent is used for the manufacture of polymeric sulfur (Crystex®), which is used for large-scale rubber vulcanization (tire production). In this process the highly reactive constituents of the sulfur vapor polymerize together with most of the S_8 and the polymer precipitates from the solvent while remaining S_8 stays dissolved. The world production of polymeric sulfur is 450,000 t per year.

If high-temperature sulfur vapor is reacted with a hot, dehydrated **zeolite crystal** it penetrates the porous structure of the aluminosilicate and forms exotic ions by disproportionation, which are trapped in the cavities of the zeolite structure. In the case of the cadmium containing Zeolite X, $Cd_{48}[Si_{100}Al_{92}O_{384}]$, the formerly unknown ions $[S_4]^{4+}$ (tetrahedral) and $[S_4]^{2+}$ (chain-like) have been identified besides sulfide anions by X-ray structural analysis. Bent $[S_3]^{2+}$ and pyramidal $[S_4]^{2-}$ ions have been trapped in cavities of $Na_{12}[Si_{12}Al_{12}O_{48}]$. All these homoatomic sulfur ions are said to be stabilized by strong electrostatic interactions with the surrounding sodium ions or oxygen atoms, respectively.[23]

12.4.1.2 Monotropic Sulfur Allotropes

Only α- und β-S_8 are enantiotropic sulfur modifications since they can reversibly be transformed into each other (provided the temperature changes very slowly). All other sulfur modifications can only be prepared from liquid sulfur, by application of a very high pressure or by chemical reactions in solution from which the target species can be crystallized.[24] The homocycles S_n (n = 6–20) are of special interest since they are components of liquid sulfur (see above) and their molecular structures provide information about the factors responsible for the differing thermal stabilities and chemical reactivities.

It has been known for more than 100 years that acidification of aqueous sodium thiosulfate results in precipitation of elemental sulfur. In this case, it mainly consists of S_6 molecules that can be extracted in toluene and isolated in 12% yield as egg-yellow rhombohedral light-sensitive crystals:

---

22 In a similar manner, S_3 and S_4 have been studied spectroscopically by matrix isolation experiments; see ref. 21.

23 K. Seff et al., *J. Phys. Chem. C* **2018**, *122*, 21833 and *J. Phys. Chem. B* **2003**, *107*, 3117.

24 R. Steudel, B. Eckert, *Top. Curr. Chem.* **2003**, *230*, 1–79.

$$Na_2S_2O_3 + 2\,HCl \longrightarrow \tfrac{1}{n}\,S_n + SO_2 + 2\,NaCl + H_2O$$

S_7, S_8 and polymeric sulfur are side-products of this reaction. The formation of S_6 proceeds through the following equilibria of chain-growth reactions between sulfane mono- and di-sulfonic acids and their anions:

$$[S_2O_3]^{2-} + [HS_2O_3]^- \rightleftharpoons [S_3O_3]^{2-} + [HSO_3]^-$$
$$[S_3O_3]^{2-} + [HS_2O_3]^- \rightleftharpoons [S_4O_3]^{2-} + [HSO_3]^-$$

and finally:

$$[S_7O_3]^{2-} \rightleftharpoons S_6 + [SO_3]^{2-}$$

In a similar manner, other ring sizes are split off from the long-chain sulfane monosulfonate anions but S_6 is the main product. Although S_6 has also been prepared from S_8 at a very high pressure of 7.2 GPa and a temperature of 700 °C, it is not an enantiotropic allotrope since the conversion of S_8 into S_6 occurs via a trigonal polymeric phase and is irreversible.[25] The higher stability of S_6 compared to S_8 at high pressures follows from its higher density (LE CHATELIER's principle to reduce the external pressure).[26] In fact, S_6 has the highest density of all cyclic sulfur allotropes.

All cyclic sulfur molecules can be synthesized in good yields from a complex precursor molecule by ligand transfer reactions. For example, the π complex $[Cp_2TiS_5]$ (Cp = $[\eta^5\text{-}C_5H_5]^-$, cyclopentadienide anion) contains the six-membered metallacycle TiS_5, which can be prepared from Cp_2TiCl_2 and ionic polysulfides such as $[NH_4]_2[S_5]$. The titanocene pentasulfide forms violet air-stable crystals of m.p. 211 °C and reacts with sulfur chlorides S_nCl_2 (n = 1–8) in organic solvents at 0 °C or with SO_2Cl_2 as follows:

$$[Cp_2TiS_5] + S_nCl_2 \longrightarrow S_{5+n} + [Cp_2TiCl_2] \quad (1)$$
$$x\,[Cp_2TiS_5] + x\,SO_2Cl_2 \longrightarrow S_{5x} + x\,SO_2 + x\,[Cp_2TiCl_2] \quad (2)$$

According to equation (1), the homocycles with 6, 7, 9, 11, 12 and 13 atoms have been prepared while reaction (2) provides access to the rings with 10, 15 and 20 sulfur atoms (x = 2–4), which can be separated by fractional crystallization. A similar synthetic route uses a zinc hexasulfido complex with a TMEDA ligand (tetramethyldiamino ethene) for the synthesis of S_{14}:

$$(TMEDA)ZnS_6 + S_8Cl_2 \rightarrow S_{14} + (TMEDA)ZnCl_2$$

25 L. Crapanzano et al., *Nature Mat.* **2005**, *4*, 550.

26 When any system at equilibrium is subjected to change in concentration, temperature, volume or pressure, the system readjusts itself to partly *counteract the effect of the applied force* and equilibrium is shifted.

The allotropes S_7, S_{18} and S_{20} have also been prepared from quenched sulfur melts by fractional crystallization.

The structures of most sulfur allotropes have been determined by X-ray crystallography, partly at low temperatures (Figure 12.5). The *average bond lengths* in the homocycles S_8 (205 pm), S_6 (206 pm) and S_{12} (205 pm) are almost identical but not in S_7 (209 pm). However, the lengths of individual bonds may deviate considerably from these average values as can be seen in the structure of S_7 shown in Figure 12.6.

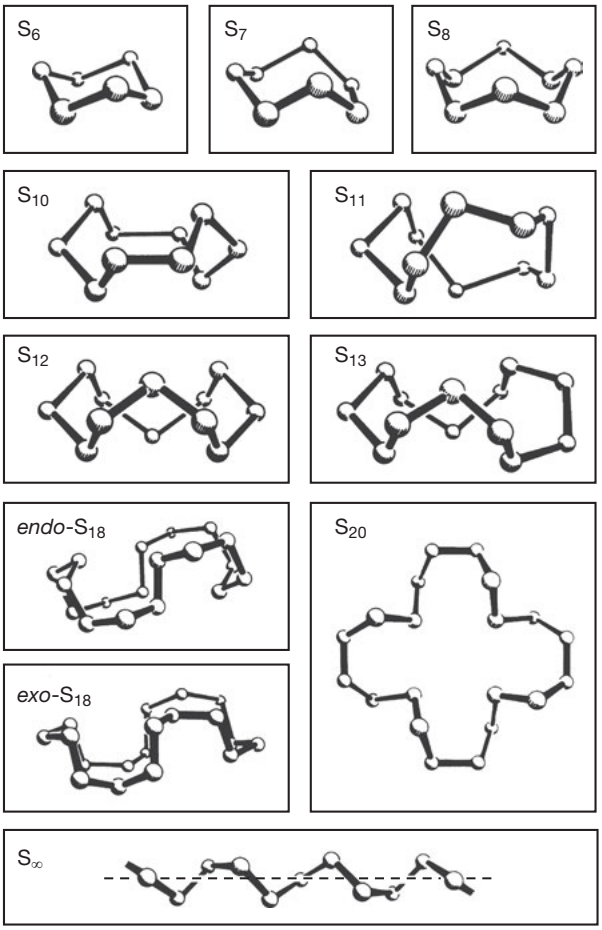

Figure 12.5: Molecular structures of the homocycles S_6, S_7, S_8, S_{10}, S_{11}, S_{12}, S_{13}, endo-S_{18}, exo-S_{18}, S_{20} and of polymeric S_∞, all determined by X-ray diffraction on single crystals. The molecular symmetries are: S_6 (D_{3d}), S_7 (C_s), S_8 (D_{4d}), S_{10} (D_2), S_{12} (D_{3d}), S_{13} (C_2), *endo*-S_{18} (C_{2h}), *exo*-S_{18} (C_i), S_{20} (D_2), S_∞ (S_3).

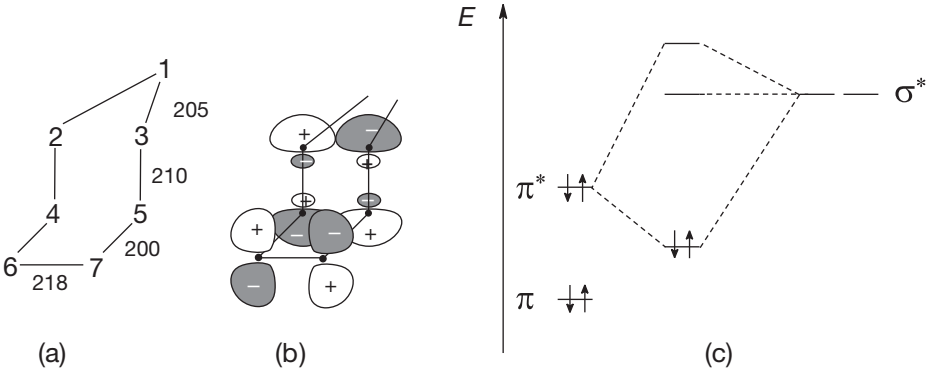

Figure 12.6: Structure and bonding situation of *cyclo*-heptasulfur S_7 (C_s symmetry). (a) Conformation, numbering of atoms and bond lengths (in pm). (b) Schematic representation of the hyperconjugation between the occupied π* molecular orbital at bond S(6)–S(7) and the empty σ* MOs at bonds S(3)–S(5) and S(2)–S(4), respectively (shown is the possible orbital overlap). (c) Energy level diagram showing the stabilization of the electrons in the π* HOMO at bond S(6)–S(7) by its interaction with the two empty σ* MOs at bonds S(2)–S(4) and S(3)–S(5) resulting in short bonds S(4)–S(6) and S(5)–S(7) by π bonding while the bonds S(2)–S(4) and S(3)–S(5) expand due to delocalization of electron density into an antibonding MO.

The *structure of the S_7 molecule* is most unusual and can possibly explain why this allotrope is the least stable at room temperature in the solid state. The individual bond lengths vary between 200 and 218 pm with an alternating pattern from bond to bond (Figure 12.6a). The single bond distance of 205 pm as in S_8 is observed only for the two bonds at the apex of the S_7 molecule where one atom (no. 1) is located within the mirror plane of the molecule. The long bond between atoms (6) and (7) results from the torsion angle of 0° at this bond. As in H_2O_2 (Section 11.3.3) and in H_2S_2, the optimum torsion angle τ between two-coordinate chalcogen atoms of Me_2S_2 and polysulfide anions such as $[S_4]^{2-}$ is close to 90° since the repulsion between the lone-pair electrons in the nonbonding *p* AOs is minimal at this value. At τ = 0° the 3*p* AOs at atoms (6) and (7) are no longer nonbonding but overlap and split into a bonding π MO and an antibonding π* MO that are both occupied. The π* MO is the HOMO of the molecule (Figure 12.6b). In order to reduce the electrostatic repulsion, electron density is delocalized from the π* MO into the two σ* MOs at bonds S(3)–S(5) and S(2)–S(4) as shown in Figure 12.6c. This interaction creates two π bonds between atoms S(4)–S(6) and S(5)–S(7), which contract (200 pm) at the expense of the bonds S(3)–S(5) and S(2)–S(4), which are weakened (210 pm) compared to the bonds in S_8.

The long bond S(6)–S(7) of 218 pm is probably responsible for S_7 to be such an unstable and highly reactive allotrope. In contrast, the strain-free ring of S_{12} is almost as stable as *cyclo*-S_8 and decomposes only near the melting point of 148 °C. All other

sulfur allotropes decompose already below 70 °C and this decomposition is accelerated by visible light.[27] Decomposition products are S_8 and polymeric sulfur, which can be separated by extraction with CS_2. Industrially *polymeric sulfur for rubber vulcanization* is produced by quenching of sulfur vapor in CS_2, which results in a polymerization of all the less stable components of the vapor:

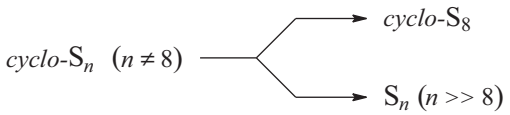

The varying stability of S_n rings may arise through deviations from ideal valence and torsion angles. Thermodynamically, however, the *mean bond enthalpies* of the rings with $n \neq 8$ are at most by 4 kJ mol^{-1} or 1.5% lower than that of S_8. The facile conversion of these species into S_8 is caused by the relatively low dissociation enthalpy of the first SS bond (ring opening reaction) as discussed in Section 4.2.3 where it is explained why elemental sulfur is a solid and not a gas like oxygen.

Sulfur homocycles are weak S-donor ligands forming a variety of metal complexes, for example, $[Cu(S_8)(S_{12})]^+$ and $[Cu(S_{12})(CH_2Cl_2)]^+$, which have been isolated with large complex anions.[28]

Inorganic homocycles are known also from other nonmetals such as B, Si, N, P, As, Se and Te with ring sizes of between 3 and 8.[29]

12.4.2 Allotropes of Selenium and Tellurium

In contrast to elemental sulfur, the thermodynamically stable allotropes of selenium and tellurium at standard conditions are polymeric. The crystal structures of gray hexagonal selenium (m.p. 221 °C) and of hexagonal tellurium (m.p. 450 °C) consist of helical chains of threefold symmetry (Figure 12.7). The coordination numbers 2 + 4 mean that all atoms have a distorted octahedral environment with two closest neighbors within the chain and four more distant neighbors in three adjacent chains. Single bonds are formed within the chains, but the more distant neighbors are closer than the VAN DER WAALS distance of 380 pm for Se and 412 pm for Te, respectively. Only polonium, the heaviest element of Group 16, crystallizes in a regular cubic structure with coordination number 6; see Table 12.3.

27 R. Steudel, B. Eckert, *Top. Curr. Chem.* **2003**, *230*, 1–79.

28 I. Krossing et al., *Angew. Chem. Int. Ed.* **2009**, *48*, 1133; see also: Y. Steudel, M. W. Wong, R. Steudel, *Eur. J. Inorg. Chem.* **2005**, 2514.

29 R. Steudel (ed.), *The Chemistry of Inorganic Ring Systems*, Elsevier, Amsterdam, **1992**; C. E. Housecroft, *Clusterverbindungen von Hauptgruppenelementen*, VCH, Weinheim, **1996**. I. Haiduc, *Encycl. Inorg. Chem.* **2005**, *4*, 2028. H. W. Roesky (ed.), *Rings, Clusters and Polymers of Main Group and Transition Elements,* Elsevier, Amsterdam, **1989**.

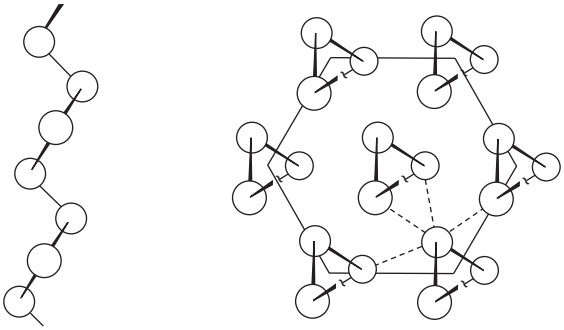

Figure 12.7: Schematic view of the crystal structures of hexagonal selenium and tellurium. Left: The polymeric molecules are of helical structure. Right: View along the hexagonal symmetry axis of the unit cell. The chains are oriented in parallel and of same sense of rotation within the crystal. The interchain interaction is indicated for one individual atom by four dotted lines (2 + 4 coordination). For internuclear distances see Table 12.3.

Table 12.3: Internuclear distances d between closest neighbors and between the next but one neighbors d' in the crystal structures of the stable allotropes of selenium, tellurium and polonium at 25 °C/1.013 MPa.

	d (pm)	d' (pm)	d'/d
Se (hexagonal)	237.4	342.6	1.44
Te (hexagonal)	283.5	349.4	1.23
Po (cubic)	335.9	335.9	1.00

At 25 °C gray selenium is a poor *p*-type semiconductor (band gap 1.85 eV at 4 K and 1.74 eV at 300 K), but the conductivity increases sharply on irradiation. The conductivity of metallic tellurium is much higher (band gap 0.33 eV) but highly anisotropic and does not change much on irradiation. Both elements form a continuous series of mixed crystals (solid solutions). Polonium metal crystallizes in the rock-salt structure. From the data in Table 12.3 it is obvious that the electric conductivity of the chalcogens increases with the coordination number of the atoms in the crystal structures since more orbitals overlap, leading to a band structure characteristic of metals. Therefore, the conductivity of sulfur, selenium and tellurium also increases with pressure, which reduces the ratio d'/d and increases the average coordination number.

Several other allotropes are known for selenium.[30] Quenching of liquid selenium provides glassy black selenium used as a semiconductor. The precipitation of selenium

30 R. Steudel, E.-M. Strauss, *Adv. Inorg. Chem. Radiochem.* **1984**, *28*, 135–166.

from aqueous solutions of $[HSeO_3]^-$ by reduction with SO_2 yields a red amorphous material which on refluxing in CS_2 slowly dissolves by depolymerization:

$$[HSeO_3]^- + 2\ SO_2 + H_2O \rightarrow\ Se \downarrow\ +\ 2\ [HSO_4]^- + H^+$$

The resulting CS_2 solution contains the homocycles Se_8, Se_7 and Se_6, with concentrations decreasing in this order. These species exist in *dynamic equilibrium* as demonstrated by HPLC analysis:

$$Se_8 \leftrightarrows {}^{8}\!/_{7}\ Se_7 \leftrightarrows {}^{4}\!/_{3}\ Se_6$$

On evaporation of the solution, red crystals of α-Se_8 and dark-red prismatic crystals of β-Se_8 (both monoclinic) have been obtained together with a few crystals each of Se_6 and Se_7. However, Se_7 is best prepared from $[Cp_2TiSe_5]$ and Se_2Cl_2 by ligand transfer in CS_2:

$$[Cp_2TiSe_5]\ +\ Se_2Cl_2\ \longrightarrow\ Se_7\ +\ [Cp_2TiCl_2]$$

In solution Se_7 slowly converts to Se_6 and Se_8 until the mentioned equilibrium has been established.

Heating to 130 °C converts all metastable Se allotropes into gray hexagonal selenium. The largest selenium homocycle ever (Se_{19}) has been prepared as part of a complex cation of composition $[Cu_2Se_{19}]^{2+}$ combined with a large weakly coordinating anion.

Many binary selenium sulfide heterocycles S_xSe_y have been prepared by ligand transfer reactions from mixed sulfur–selenium melts, for example, S_7Se, 1,2-S_6Se_2 and 1,2,3-Se_3S_5.[31] They have been characterized by X-ray crystallography, HPLC and ^{77}Se-NMR spectroscopy.[32] The conformations of these cyclic compounds are equivalent to those of the corresponding sulfur homocycles.

Metallic tellurium is insoluble in most organic solvents, but dissolves in strong N-donor solvents, obviously with depolymerization and reversible complex formation. Several high-pressure allotropes as well as two-dimensional preparations ("tellurene") are also known for tellurium. The vapors above liquid selenium and tellurium (E) consist of all homoatomic molecules from E_2 to E_6 but with E_7 and E_8 only in low concentrations. The chair-like Te_6 molecule has been isolated as ligand in a matrix of silver iodide as crystalline phase $[(AgI)_2Te_6]$.

31 From the precursors $[Cp_2TiS_5]$ and $[Cp_2TiSe_5]$ more than 20 heterocycles Se_xS_y are accessible by reactions with some of the sulfur and selenium halides discussed in Sections 12.12.2 and 12.12.4.

32 R. S. Laitinen, P. Pekonen, *Coord. Chem. Rev.* **1994**, *130*, 1.

12.5 Homoatomic Chalcogen Cations

Chalcogen cations isolated in salts with large anions are closely related chemically and structurally to elemental sulfur, selenium and tellurium:[33]

$[S_4]^{2+}$	$[S_8]^{2+}$	$[S_8]^{+}$	$[S_{19}]^{2+}$		
$[Se_4]^{2+}$	$[Se_8]^{2+}$	$[Se_{10}]^{2+}$	$[Se_{17}]^{2+}$		
$[Te_4]^{2+}$	$[Te_6]^{2+}$	$[Te_6]^{4+}$	$[Te_7]^{2+}$	$[Te_8]^{2+}$	$[Te_8]^{4+}$

These species are prepared by oxidation of the respective chalcogens at low or moderate temperatures with strong oxidants such as SO_3, AsF_5, WCl_6, $S_2O_6F_2$ and others in a weakly nucleophilic solvent (HF, SO_2, HSO_3F, H_2SO_4) or in a salt melt. The ratio chalcogen/oxidizing agent determines the product composition as demonstrated by the following examples:

$$S_8 + 2\,S_2O_6F_2 \longrightarrow 2\,[S_4]^{2+} + 4\,[SO_3F]^-$$

$$S_8 + S_2O_6F_2 \longrightarrow [S_8]^{2+} + 2\,[SO_3F]^-$$

$$17\,Se_{s.} + 2\,WCl_6 \xrightarrow{350°C} [Se_{17}]^{2+} + 2\,[WCl_6]^-$$

$$4\,Te_{s.} + 2\,WCl_6 \longrightarrow [Te_4]^{2+} + 2\,[WCl_6]^-$$

$$15\,Te_{s.} + TeCl_4 + 2\,ReCl_4 \longrightarrow 2\,[Te_8]^{2+} + 2\,[ReCl_6]^{2-}$$

In addition, polymeric cations as well as mixed chalcogenium ions of the element combinations S/Se, S/Te and Se/Te have been isolated. The ions $[Se_8]^{2+}$ (bottle-green) and $[Te_4]^{2+}$ (carmine-red) are formed on boiling the elements in concentrated sulfur acid, which is utilized for the qualitative detection of elemental selenium and tellurium, respectively. No heating is necessary if peroxodisulfate $K_2[S_2O_8]$ is added to the reaction mixtures. Therefore, the chalcogens dissolve in fuming sulfuric acid with characteristic colors (sulfur: blue; selenium: green; tellurium: red).[34]

Chalcogen cations are reduced to the elements by hydrazinium sulfate $[N_2H_6][SO_4]$:

33 J. Beck, *Coord. Chem. Rev*. **1997**, *163*, 55. I. Krossing, *Handbook of Chalcogen Chemistry*, Chapt. 7.1, Royal Society of Chemistry, London, **2006**.

34 The intense blue color is probably caused by the by-product $[S_6]^{2+}$ while the cation $[S_8]^{2+}$ is red-brown; see I. Krossing, J. Passmore, *Inorg. Chem*. **2004**, *43*, 1000.

$$\underset{\text{gray}}{Se_{s.}} \xrightleftharpoons{[S_2O_8]^{2-}} \underset{\text{green}}{[Se_8]^{2+}} \xrightleftharpoons[N_2H_4]{[S_2O_8]^{2-}} \underset{\text{yellow}}{2[Se_4]^{2+}} \xrightleftharpoons[N_2H_4]{[S_2O_8]^{2-}} \underset{\text{colorless}}{8\ SeO_2}$$

In water chalcogen cations hydrolyze with disproportionation into the element and the corresponding dioxide:

$$2\ [Se_4]^{2+} + 6\ H_2O \longrightarrow 7\ Se_{s.} + SeO_2 + 4\ [H_3O]^+$$

Several crystalline polychalcogenium salts have been prepared with large and weakly coordinating anions such as $[AsF_6]^-$, $[SO_3F]^-$, $[HS_2O_7]^-$, $[Sb_2F_{11}]^-$, $[AlCl_4]^-$ and $[WCl_6]^-$. The solids "S_2O_3" (blue), "$SeSO_3$" (yellow) and „$TeSO_3$" (carmine), prepared from the elements in liquid SO_3 as described in the older literature, are also chalcogenium salts with polysulfate anions, for example, "$TeSO_3$" ≡ $[Te_4][S_4O_{13}]$, rather than oxides.

Spectroscopic, magnetic and chemical properties indicate that all polychalcogen cations are cyclic or polycyclic. Crystal structure determinations have revealed interesting and partly unexpected structures, as in $[Te_4][AlCl_4]_2$ and $[Se_8][AlCl_4]_2$:

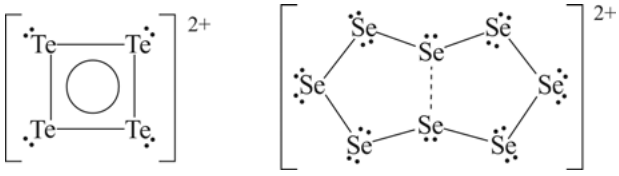

The three simplest cations $[S_4]^{2+}$ (colorless), $[Se_4]^{2+}$ (yellow) and $[Te_4]^{2+}$ (carmine) are square-planar and of D_{4h} symmetry with six π electrons. Therefore, they may be considered as aromatic rings according to the HÜCKEL rule.[35] Their σ bonds are constructed from *s*, p_x and p_y orbitals as in H_2O (Section 2.4.7) using four electrons per atom. This leaves two electrons per neutral atom occupying the p_π orbital yielding six π electrons for the cation. Linear combination of the four p_π orbitals produces four MOs as shown in Figure 12.8. The electron pair occupying the π_u MO contributes to the bonding interaction resulting in a slightly shorter S–S bond (200 pm) than in S_8 (205 pm) despite the torsion angles of 0°. However, the positive ion charge also results in some contraction of the covalent bonds.

The cations $[S_8]^+$, $[S_8]^{2+}$, $[Se_8]^{2+}$ and $[Te_8]^{2+}$ are bicyclic with an *endo–exo* conformation resulting in C_s symmetry. Consequently, the ^{77}Se-NMR spectrum of $[Se_8]^{2+}$ consists of five lines in the intensity ratio 1:2:2:2:1. Two atoms are three-coordinate since a chalcogen cation E^+ is isoelectronic with a pnictogen atom such as phosphorus, arsenic or antimony, which are three-coordinate usually. However, the weak transannular

35 According to ERICH HÜCKEL (1896–1980) a planar ring of like atoms is "aromatic" if the number of π electrons is $4n + 2$ (n = 0, 1, 2, 3 . . .).

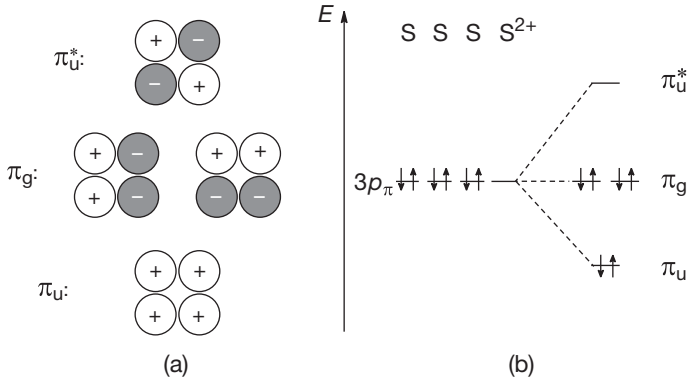

Figure 12.8: Construction of the four π MOs for the square-planar cation $[S_4]^{2+}$. (a) Linear combination of the four $3p_\pi$ AOs yielding four MOs shown as projections into the molecular plane. (b) Energy level diagram for the atomic and molecular orbitals. The six π electrons are evenly delocalized over the four atoms but only two contribute to the bonding interaction (four-center bond).

bond of $[Se_8]^{2+}$ is considerably longer (283 pm) than the other bonds (232 pm) and the same holds for the other eight-atomic cations. In the salt $[Te_8][WCl_6]_2$ the bicyclic cation is of lower symmetry.

The ions $[Te_7]^{2+}$ and $[Se_{10}]^{2+}$ are also bicyclic, while $[Te_6]^{2+}$ is boat-shaped and $[Te_6]^{4+}$ has the form of a prism. The structure of $[Te_8]^{4+}$ can be derived from a cube with two opposite corners missing. The larger ions $[Se_{17}]^{2+}$ and $[S_{19}]^{2+}$ consist of two seven-membered rings connected by a chain of three respective five atoms. In other words, they also contain two three-coordinate atoms each. Since the length of this connecting chain can vary one can imagine many more polychalcogen cations of this type.

12.6 Chain Growth and Degradation Reactions

The *formation of homoatomic chains and rings* is a characteristic property of the chalcogens S, Se and Te, although catenation is also observed with other main group elements.[36] The following synthetic procedures are most useful, explained with sulfur as a representative element:

(a) Condensation of hydrides with halides:

$$-S-H + Cl-S- \longrightarrow -S-S- + HCl$$

36 J. Reedijk, K. Poeppelmeier (eds.), *Comprehensive Inorganic Chemistry II*, Vol. 1, Elsevier, Amsterdam, **2013**.

(b) Reaction of metal sulfides (or polysulfides) with halides:

$$-S^- M^+ + Cl-S- \longrightarrow -S-S- + MCl$$

(c) Oxidation of hydrides, for example, by iodine:

$$-S-H + I_2 + H-S- \longrightarrow -S-S- + 2\,HI$$

(d) Condensation of a hydride or chloride with a hydroxo group, for example, an oxoacid:

$$-S-H + HO-S- \longrightarrow -S-S- + H_2O$$

(e) Sulfurization of covalent or ionic sulfides by S_8 on heating in the presence of a nucleophile (LEWIS base):

$$xS_8 + R-S_2-R \longrightarrow R-S_n-R$$

$n = 3, 4, ...;$ R = H, Cl, organyl or metal

For the *degradation of homoatomic chains or rings* several possibilities exist. Compounds with at least two neighboring SS bonds lose most easily one or more sulfur atoms, for example, on heating. The final (most stable) products are usually mixtures of disulfides and S_8 but sulfur oligomers may also be formed. A controlled degradation can be achieved by *nucleophilic attack* at the central sulfur atom in groups of type S–S–S. Suitable nucleophiles are organic phosphanes R_3P, which are turned into phosphane sulfides R_3PS, cyanide ions that give thiocyanate $[SCN]^-$, ionic sulfides including HS^- and $[S_n]^{2-}$ as well as hydrogen sulfite ions $[SO_3H]^-$ resulting in thiosulfate $[S_2O_3]^{2-}$. The mentioned reagents turn S_8 quantitatively into the mentioned products at 20–80 °C and suitable pH values.

Such degradation reactions proceed stepwise by an S_N2 mechanism.[37] For example, the attack of cyanide ions on the S_8 homocycle leads to ring opening, which is usually the slowest and therefore rate determining step:

$$S_8 + [CN]^- \longrightarrow [NC-S-S-S-S-S-S-S-S]^-$$

The reaction product is rapidly degraded with the hypothetical intermediates $[S_7CN]^-$, $[S_6CN]^-$ and so on until all SS bonds have been cleaved:

$$S_8 + 8\,[CN]^- \longrightarrow 8\,[SCN]^-$$

37 S_N2: Nucleophilic (N) substitution (S) of 2nd order.

Reaction of the formed thiocyanate with Fe^{3+} ions to the red complex $[Fe(SCN)_3]$ is used to determine the original amount of sulfur photometrically. Organic polysulfanes containing adjacent SS bonds react analogously (R: alkyl or aryl group):

$$R{-}S{-}S{-}S{-}R \; + \; [CN]^- \longrightarrow \; R{-}S{-}S{-}R \; + \; [SCN]^-$$

Compounds with sulfur chains or rings are thus sensitive toward nucleophilic agents like alkali, sulfite, cyanide, hydrogen sulfide ions as well as ammonia and amines. S_8 is even attacked by superheated water at temperatures above 150 °C under pressure resulting in exothermic disproportionation in analogy to the corresponding reactions of white phosphorus and of elemental halogens in alkaline solutions:

$$1/2\ S_8 + 4\ H_2O \rightarrow 3\ H_2S + H_2SO_4$$

Polythionates are intermediates in this reaction. It is worth noting here that the hydroxide ion concentration in water increases with temperature accelerating this disproportionation.

12.7 Chalcogen Hydrides

Volatile covalent hydrides H_2E are known for E = S, Se and Te. Sulfur also forms long-chain sulfanes H–S_n–H (n = 1, 2, 3 . . .). Many derivatives thereof (RS_nH and R_2S_n) bear organic and inorganic end-capping groups such as alkyl, aryl, halogens, sulfonic acid and so on. The sulfur chain-lengths may reach 35 atoms and beyond. Similar derivatives R_2E_n are known for E = Se and Te but only with rather short chains.

12.7.1 Hydrides H_2E (E = S, Se, Te)

The hydrides H_2S (b.p. −60 °C), H_2Se (b.p. −42 °C) and H_2Te (b.p. −4 °C) are colorless, poisonous, noxious gases, which are heavier than air. H_2S ignites spontaneously in air at 260 °C and forms explosive mixtures with air when the hydrogen sulfide content is between 4 and 44 vol%. The maximum allowed concentration of H_2S at a workplace is only 10 ppmv![38] Suitable preparative methods are as follows:

(a) From the elements after the equilibrium has been established, for example, on heated pumice chips:

$$H_2 \; + \; S(g.) \; \underset{}{\overset{600°C}{\rightleftharpoons}} \; H_2S$$

$$H_2 \; + \; Se(g.) \; \overset{350\text{-}400°C}{\rightleftharpoons} \; H_2Se$$

38 For an exposure of 8 h (in parts per million volume).

The preparation of H_2Te from the elements requires electrolysis of sulfuric acid (50%) between a tellurium cathode and a platinum anode with cooling to 0 °C and exclusion of light.

(b) Most conveniently from ionic metal chalcogenides by protonation of the anions with dilute acids under anoxic conditions:

$$Na[HS] + H_3PO_4 \xrightarrow{H_2O} H_2S + Na[H_2PO_4]$$

$$Al_2S_3 + 6\,H_2O \longrightarrow 3\,H_2S + 2\,Al(OH)_3 \qquad \text{analogous: } D_2S,\ H_2Se$$

$$Al_2Se_3 + 6\,HCl \xrightarrow{H_2O} 3\,H_2Se + 2\,AlCl_3 \qquad \text{analogous: } H_2Te$$

H_2S, H_2Se and H_2Te are subject to *autoxidation* both in air and in air-containing aqueous solution yielding water and the respective element; therefore, their preparation requires exclusion of oxygen especially in the case of H_2Se and H_2Te. The sulfur deposits in volcanic areas originate mainly from the autoxidation of H_2S as a component of the volcanic exhalations. The hydrides H_2O and H_2S are exothermic, while H_2Se and H_2Te are endothermic compounds. Hydrogen sulfide is of enormous industrial importance in the context of the desulfurization of crude oil, sour natural gas and coal and the production of elemental sulfur (Section 12.3.1). As a reagent H_2S is used for the large-scale synthesis of the amino acid methionine, which is used as additive for animal feed.

Aqueous solutions of H_2S, H_2Se and H_2Te are slightly acidic, and the acid strength increases in this order as manifest in the first dissociation constants K_a (at 25 °C):

		H_2S	H_2Se	H_2Te
$H_2E \rightleftharpoons H^+ + [HE]^-$	K_1:	$1.0\cdot10^{-7}$	$1.9\cdot10^{-4}$	$2.3\cdot10^{-3}$
$[HE]^- \rightleftharpoons H^+ + E^{2-}$	K_2:	10^{-14} to 10^{-18}	$8.8\cdot10^{-16}$	$\sim1.6\cdot10^{-11}$

This unexpected sequence in dissociation constants results from the decrease in mean EH bond energy from sulfur to tellurium (Table 4.1). The extremely small second dissociation constant of H_2S is difficult to determine and depends on the ion strength of the solution. $K_2(H_2S)$ is the smaller, the higher the ion strength since ion pairs such as $[NaS]^-$ are formed between sulfide and sodium cations at high concentrations.[39] The average value of $K_2(H_2S) = 10^{-16}$ mol L^{-1} means that sulfide ions S^{2-} do virtually not exist in solutions of pH < 12, and the more realistic value of 10^{-17} mol L^{-1} indicates that many solubility products of insoluble metal sulfides reported in the literature may be in error.

39 D. Rickard, G. W. Luther, *Chem. Rev.* **2007**, *107*, 514; V. S. Vorobets, S. K. Kovach, G. Ya. Kolbasov, *Russ J. Appl. Chem.* **2002**, *75*, 229. D. J. Phillips, S. L. Phillips, *J. Chem. Eng. Data* **2000**, *45*, 981.

Nevertheless, certain transition metal sulfides such as CuS, HgS and Ag_2S can be precipitated by H_2S even from strongly acidic solutions of the metal ions. Most probably the hydrated metal ions (e.g., $[Cu(H_2O)_6]^{2+}$) react with hydrogensulfide ions $[HS]^-$ by ligand exchange to the corresponding complexes (e.g., $[Cu(SH)(H_2O)_5]^+$) from which the solid sulfide (e.g., CuS) precipitates in a series of deprotonation, aggregation and elimination reactions. The value of $K_1(H_2S)$ also depends on the salt concentration or ion strength. For instance, in seawater at 25 °C: $pK_1 = 6.51$ and $K_1 = 3.24 \cdot 10^{-7}$.[39] With rising temperatures up to 120 °C, $K_1(H_2S)$ increases, followed by a decrease at higher temperatures, which is explained by a change in hydration of the anion.

Hydrogen sulfide is an important signaling molecule (gasotransmitter) in mammals and partly responsible for blood pressure and other parameters. At physiological pH value of 7.4 and a body temperature of 37 °C, H_2S dissolved in blood consists of 81% $[HS]^-$ and 19% H_2S, while the concentration of S^{2-} is negligible.[40]

Ionic metal chalcogenides M[HE] and M_2E, if soluble in water, hydrolyze due to the small values of the dissociation constants of H_2E (see above). This reaction is used to prepare the hydrides H_2E by adding little water to suitable barium or aluminum chalcogenides (BaE or Al_2E_3). Only metal chalcogenides with a very small solubility product c = (cation)·c(anion) can coexist with water. Obviously, the solubility of sulfides, selenides and tellurides is strongly pH dependent. Consequently, metal chalcogenides can be prepared from aqueous solutions only if they are insoluble. The soluble sulfides, selenides and tellurides of the alkali and alkaline earth metals as well as aluminum are prepared from the elements either in a dry process or in a solvent of low proton donor strength such as ethanol or liquid ammonia (Section 9.4.8 and Table 9.1).

The hydrides H_2E (E = S, Se, Te) react both as weak reducing agents and in condensation reactions with the halides of boron, silicon germanium, phosphorus, sulfur and selenium (Section 12.6). Important *organic derivatives* of H_2S and H_2Se are the amino acids cysteine $HS–CH_2–CH(NH_2)–COOH$ and selenocysteine $HSe–CH_2–CH(NH_2)–COOH$, which occur in many proteins and enzymes and are responsible for the redox balance in mammals. By enzymatic hydrolysis of cysteine, traces of H_2S are produced.[40]

12.7.2 Polysulfanes, H_2S_n ($n > 1$)

Hydrogen sulfide dissolves in liquid sulfur with sulfurization in an equilibrium reaction:

$$H_2S + S_n(l.) \rightleftharpoons H_2S_{n+1}$$

40 M. R. Filipovic et al., *Chem. Rev*. **2018**, *118*, 1253-1337. C. Szabó, *Nature Rev*. **2007**, *6*, 917.

The solubility of H_2S in the temperature range 200°–400 °C is ca. 0.2 g/100 g of sulfur but decreases both at higher and lower temperatures. This dissolution reaction is important in the CLAUS process for the production of elemental sulfur from H_2S (Section 12.3.1) as the produced sulfur has to be free of H_2S for safety reasons. The sulfanes H_2S_n are chain-like molecules[41] in analogy to the *n*-alkanes C_nH_{2n+2} and the linear phosphanes P_nH_{n+2}. They can be detected and determined by ^{1}H-NMR spectroscopy: the chemical shifts of the members with up to 35 sulfur atoms are sufficiently different to identify individual species in mixtures.[42]

The sulfanes H_2S_n are thermodynamically unstable; the hypothetical reaction of H_2S with solid α-S_8 at 25 °C is endothermic ($\Delta H°_{298} > 0$) and endergonic ($\Delta G°_{298} > 0$). The decomposition of sulfanes is catalyzed even by traces of ammonia or hydroxides as well as by quartz powder. The composition of the polysulfanes or mixtures thereof can thus conveniently be determined from the evolved H_2S and the mass of the remaining S_8.

12.7.2.1 Synthesis of Polysulfanes

Well-defined polysulfanes can be prepared as follows:

(a) Addition of aqueous sodium polysulfide (Na_2S_n) at –10 °C to dilute HCl whereupon a mixture of H_2S_n molecules precipitates as a heavy yellow oil. This "crude sulfane" is cracked and fractionated by distillation to give the sulfanes H_2S_2 and H_2S_3 together with S_8. The higher sulfane members up to $n = 6$ are prepared by vacuum distillation of the crude oil or by selective extraction.

(b) Condensation of lower sulfanes ($n = 1, 2$) with dichlorosulfanes S_nCl_2 ($n = 1$–4) at –50 °C yields higher sulfanes with up to eight sulfur atoms:

$$2\,H_2S + SCl_2 \longrightarrow H_2S_3 + 2\,HCl$$

$$2\,H_2S + S_2Cl_2 \longrightarrow H_2S_4 + 2\,HCl$$

$$2\,H_2S_2 + SCl_2 \longrightarrow H_2S_5 + 2\,HCl$$

A large excess of the starting sulfane suppresses the formation of longer chains. The reaction mixture is separated by vacuum distillation.

Polysulfanes are liquids whose yellow color intensifies with molecular mass while the viscosity increases and the vapor pressure decreases. The higher members ($n > 6$) cannot be separated from each other or from S_8 by distillation. Polysulfanes are soluble in CS_2. The structure of gaseous H_2S_2 is analogous to that of H_2O_2 (Figure 11.4) except for the torsion angle of 90°. A derivative of disulfane

41 Review: R. Steudel, *Top. Curr. Chem.* **2003**, *231*, 99-125.

42 The corresponding selenium compounds are unstable but numerous organic selanes R_2Se_n and species with mixed S/Se chains (thiaselanes) have been identified by NMR spectroscopy.

is the hydroxodisulfane HSSOH that has been prepared in the gas phase by pyrolysis of tBu$_2$S$_2$O with elimination of two mol *iso*-butene C_4H_8. Since HSSOH is formally an oxoacid it will be discussed together with other hydroxosulfanes in Section 12.11.1. Trisulfane H_2S_3 exists in the gas phase as *cis*- and *trans*-forms which are in equilibrium (see the structure of the pentasulfide ion in Figure 12.9). The rotational *trans*-barrier at the SS bonds of H_2S_3 is ca. 26 kJ mol^{-1}.

The pK_a values for the first/second dissociation reaction of sulfanes in water (deprotonation) have been estimated as follows: 5.11/10.03, 4.31/7.83, 3.91/6.63, 3.61/6.03, 3.58/5.51, 3.48/5.18 and 3.40/4.94 for H_2S_2 to H_2S_8. In other words, the aqueous sulfanes are much stronger acids than H_2S and the hydrogendisulfide ion $[HS_2]^-$ is the dominating S_2 ion at pH < 9.5. The gas phase acidities of the oligosulfanes calculated by quantum-chemical methods also increase with increasing sulfur chain-length.

Polysulfanes are used for condensation reactions (Section 12.6). For example, H_2S_7 as a component of crude sulfane oil reacts with thionyl chloride at –40 °C in CS_2/Me_2O to *cyclo*-octasulfur oxide:[43]

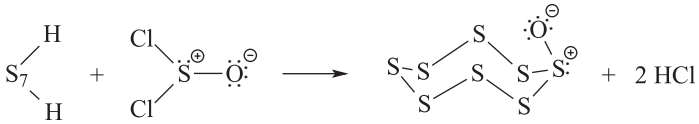

S_8O crystallizes from CS_2 in intensely yellow needles which slowly decompose at 25 °C, more vividly at 78 °C, to SO_2 and polymeric sulfur. The eight-membered ring is a puckered crown such as that in orthorhombic α-S_8 but of C_s symmetry (for details see Section 12.10.3).

12.8 Metal Chalcogenides

Formally, metal chalcogenides are salts of the weak acids H_2E_n (E = S, Se, Te; n = 1, 2, ...). Nearly all metals form sulfides, selenides and tellurides, either as binary, ternary (e.g., *chalcopyrite* $CuFeS_2$) or even more complex phases. Sometimes several phases exist in a metal–chalcogen system. Metal chalcogenides, especially sulfides, occur in Nature as numerous minerals and ores, which are mined for their metal content (e.g., zinc blende ZnS, galena PbS, argentite Ag_2S, stibnite Sb_2S_3). Only iron pyrite [iron(II) disulfide FeS_2] is mined for its sulfur content.[44] Many transition metal selenides and tellurides are semiconductors: $CuInSe_2$ and CdTe are used for

43 R. Steudel, *Top. Curr. Chem.* **2003**, *131*, 203-230.

44 FeS_2 is the most abundant sulfidic mineral on Earth and may have played a decisive role in the early phase of biological evolution; G. Wächtershäuser, *Microbiol. Rev.* **1988**, *52*, 452. FeS_2 is formed exothermally from FeS and H_2S with evolution of H_2.

solar cells and $Cd_xHg_{1-x}Te$ with $x = 0–1$ is applied in optoelectronic equipment such as night vision devices.

The structures and chemical properties of metal oxides versus metal sulfides, selenides and tellurides are quite different owing to the lower electronegativities and higher polarizabilities of the heavier chalcogen atoms and their tendency to form stable chains and rings. Examples are the *metallacycles* $[Cp_2TiS_5]$ and $[NH_4]_2[Pt(S_5)_3]$. The latter compound exhibits three such rings with octahedrally coordinate platinum common to all three.[45] Analogous five- and seven-membered rings are also known.

Only the ionic chalcogenides of the alkali metals[46] will be discussed here while the chalcogenides of the nonmetals are covered in the corresponding chapters regarding these elements.

12.8.1 Chalcogenides of Alkali Metals

When aqueous sodium or potassium hydroxide is saturated with H_2S, solutions of the hydrogen sulfides Na[HS] and K[HS] are formed. From such solutions, hydrated sulfides crystallize upon addition of equivalent amounts of base and cooling:

$$Na[OH] + H_2S \rightleftharpoons Na[SH] + H_2O$$
$$Na[SH] + Na[OH] \rightleftharpoons Na_2S + H_2O$$

The salts $Na_2S{\cdot}9H_2O$ and $K_2S{\cdot}5H_2O$ are manufactured in this way. In air, slow autoxidation takes place with yellow discoloration resulting in polysulfides and thiosulfate. Dehydration is also accompanied by partial decomposition. Therefore, the anhydrous sulfides are produced by nonaqueous routes. Na_2S, for instance, is made by reduction of $Na_2[SO_4]$ by low-ash coal such as anthracite at 700–1100 °C:

$$Na_2[SO_4] + C_{s.} \longrightarrow Na_2S + 4\,CO$$

Na_2S is mainly used in tanning for depilation of hides as well as for synthesis of sulfur dyes. On a small scale, sodium and potassium sulfides, selenides and tellurides are made by reduction of the corresponding chalcogens with equivalent amounts of alkali metal in liquid ammonia (Table 9.1):

$$16\,K + S_8 \xrightarrow{NH_3} 8\,K_2S\downarrow$$

---

45 Many metal complexes with the S-donor ligands H_2S, $[HS]^-$, S^{2-}, $[RS]^-$ and $[S_n]^{2-}$ have been prepared; see S. R. Collinson, M. Schröder, *Encycl. Inorg. Chem.* **2005**, *8*, 4811. N. Takeda, N. Tokitoh, R. Okazaki, *Top. Curr. Chem.* **2003**, *231*, 153.

46 For other metals, see: M. G. Kanatzidis, *Encycl. Inorg. Chem.* **2005**, *2*, 825. W. S. Sheldrick, in: *Handbook of Chalcogen Chemistry*, 2nd ed., RSC Publ., **2013**, 514.

Na_2Se, Na_2Te, K_2Se and K_2Te are prepared in an analogous manner. Solvated electrons are the active reducing agent (Section 9.4.8), and the equilibrium is shifted to the right by precipitation of the insoluble colorless chalcogenides, which crystallize in the *antifluorite structure* (CaF_2) where calcium positions are occupied by chalcogenide ions and fluoride positions by the metal ions.

12.8.2 Polychalogenides

Heating of sodium or potassium chalcogenides with elemental chalcogen at 500–600 °C and in the absence of air (e.g., in an ampoule) produces salt-like polychalcogenides:[47]

$$Na_2S + \frac{1}{8}S_8 \xrightarrow{500°C} Na_2S_2$$

$$K_2S + \frac{3}{8}S_8 \xrightarrow{500°C} K_2S_4$$

$Na_2[S_2]$ (light yellow), $K_2[S_{2-6}]$ (yellow to red), $Na_2[Se_2]$ (gray) und $Na_2[Te_2]$ (gray-black, glossy metallic) have been prepared in this way. Heating of aqueous alkaline sulfide solutions with sulfur and in the absence of air produces polysulfide solutions in a series of degradation reactions by nucleophilic attack:

$$[HS]^- + S_8 \rightleftharpoons [S_9]^{2-} + H^+$$

$$[S_9]^{2-} + [HS]^- \rightleftharpoons 2\,[S_5]^{2-} + H^+$$

These solutions contain polysulfide anions with up to at least 13 sulfur atoms, which exist in dynamic and rapidly established equilibrium:

$$2\,[S_n]^{2-} \rightleftharpoons [S_{n-x}]^{2-} + [S_{n+x}]^{2-}\ (n > x)$$

The exact mechanism of these interconversion reactions is unknown; most probably radical anions $[S_n]^-$ and ion pairs such as $[NaS_n]^-$ play a role as intermediates.[48a] Polysulfides are rapidly oxidized in air with formation of thiosulfate and elemental sulfur, especially in solution.

For determination of individual polysulfide anions in solutions, the equilibrium needs to be quenched abruptly. This can be achieved by *derivatization* either by protonation in concentrated hydrochloric acid or, more conveniently, by methylation with methyl triflate $CH_3SO_2CF_3$. The resulting mixture of dimethyl polysulfanes

47 (a) R. Steudel, *Top. Curr. Chem.* **2003**, *231*, 127–152. (b) R. Steudel, T. Chivers, *Chem. Soc. Rev.* **2019**, *48*, 3279.

48 (a) R. Steudel, Y. Steudel, *Chem. Eur. J.*, **2013**, *19*, 3167. (b) Z. Wen et al., *Adv. Funct. Mater.* **2013**, *23*, 1005.

Me_2S_n is subsequently analyzed by ^{1}H-NMR spectroscopy or HPLC.[49] The methylation is often used in microbiologic and environmental studies.

Stoichiometric polychalcogenides of alkali metals are prepared from the elements in liquid ammonia. In some cases, the reaction of carbonate with the corresponding chalcogen in methanol is successful, for example, for the synthesis of $Cs_4[Se_{16}]$ at 160 °C/1.3 MPa (see below).

The reaction between liquid sodium and liquid sulfur to sodium polysulfides is used in **sodium–sulfur batteries** at ca. 320 °C to produce and reversibly store electric energy. The two electrodes are contained in a steel cylinder and separated by a ceramic diaphragm of sodium polyaluminate $Na[Al_{11}O_{17}]$ ("β-aluminum oxide"), which is a conductor for sodium ions at high temperatures. The sulfur is sucked into a net of carbon fibers for better electric conductivity. On discharging, sodium is oxidized to Na^+ that migrates through the diaphragm where the sulfur is mainly reduced to the tetrasulfide $Na_2[S_4]$ (m.p. 295 °C). The formation of $Na_2[S_4]$ from the elements is exothermic by –412 kJ mol^{-1} (at 298 K) and most of this energy can be recovered as electric power. The maximum voltage is 2.08 V and the energy density of 790 W h kg^{-1} is five times as high as for the common lead-acid battery. The reverse reactions take place during the charging of the battery.

Another promising development is the **lithium–sulfur battery**, which operates at room temperature with a polar solvent to allow the lithium cations migrating back and forth between the lithium metal anode and the sulfur cathode.[47b,50] In principle, the reactions taking place are the same as in the chemical syntheses of alkali polysulfides discussed above but ion pairs play a major role.

12.8.3 Structures of Polychalcogenide Anions[47]

The anions $[S_n]^{2-}$ of alkali and alkaline earth polysulfides are isoelectronic with the corresponding dichlorosulfanes $S_{n-2}Cl_2$. Such chain-like molecules can adopt different conformations. While $Na_2[S_2]$ contains dumbbell-shaped anions in analogy to $Na_2[O_2]$, the trisulfide anion $[S_3]^{2-}$ is bent and isoelectronic to SCl_2. The chiral tetrasulfide anion has a *gauche*-conformation in analogy to H_2O_2 and H_2S_2. In crystals of $Na_2[S_4]$ and $K_2[S_4]$, the two enantiomers are present in a 1:1 ratio, with the torsion angle either positive or negative (Figure 12.9). In the pentasulfide anion the torsion angles at the two central bonds are either + + or – – (enantiomers) but can also be + – (identical to – +). In other words, there are three isomers, the first two of which are optical isomers.

49 J. Hahn, *Z. Naturforsch. Part B* **1985**, *40*, 263 (protonation). A. Kamyshny, O. Lev et al., *Environm. Sci. Technol.* **2007**, *41*, 2395 (methylation).

50 Y.-X. Yin, S. Xin, Y.-G. Guo, L.-J. Wan, *Angew. Chem. Int. Ed.* **2013**, *52*, 13186 – 13200.

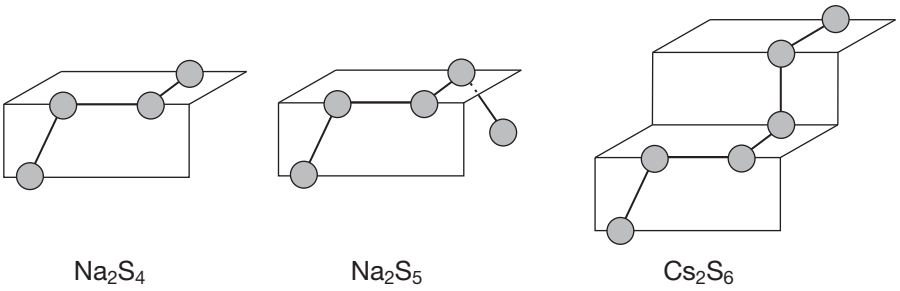

Figure 12.9: Structures of the anions in the salts $Na_2[S_4]$, $Na_2[S_5]$ and $Cs_2[S_6]$ as determined by X-ray crystallography. Symmetries of the anions: $[S_4]^{2-}$ and $[S_6]^{2-}$: C_2; $[S_5]^{2-}$: C_s. In $Na_2[S_4]$ and $Cs_2[S_6]$ the S–S–S–S torsion angles are all positive, in $Na_2[S_5]$ the motif of the anion is + –.

The signs of the torsion angles S–S–S–S are called the *motif* of the structure. In $Na_2[S_5]$ the motif is + – (symmetry C_s), while in $K_2[S_5]$, $Rb_2[S_5]$ and $Cs_2[S_5]$ the anions are helical with the motifs + + and – – (symmetry C_2) in a 1:1 ratio in the single crystals. Theoretically there are 2^n motifs possible for n torsion angles. For the hexasulfide anion (n = 3) there are already 2^3 = 8 torsion angle combinations of which four are pairwise identical resulting in a total of six isomers (rotamers). The crystal structure of $Cs_2[S_6]$ contains helical anions with all torsion angles of same sign.

The anions of alkali *polyselenides* are usually analogous to those of the polysulfides, but certain selenium-rich salts have either spirocyclic anions as in $Cs_2[Se_{11}]$ (Figure 12.10a) or the structures contain additional elemental selenium in the form of the homocycles Se_6 or Se_7. The bonding situation of the square-planar coordinate atom in the anion of $Cs_2[Se_{11}]$ corresponds to that of tetrachloroiodate $[ICl_4]^-$ (see Section 13.5.5).

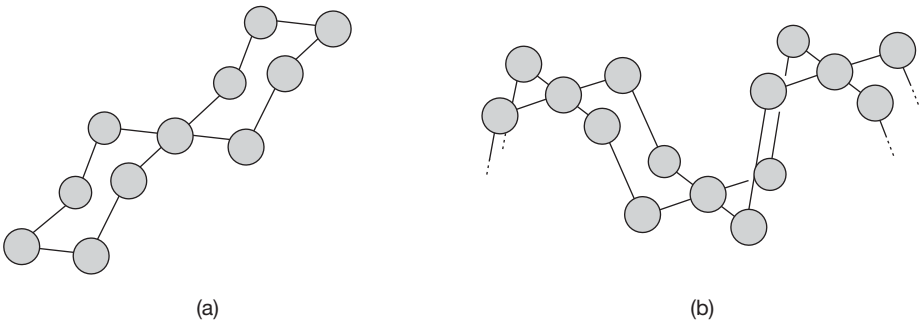

Figure 12.10: Anion structures of the salts $Cs_2[Se_{11}]$ (a) and $Cs_2[Te_5]$ (b). The spirocyclic $[Se_{11}]^{2-}$ is monomeric while anions of composition $[Te_5]^{2-}$ are polymeric. Characteristic features are the square-planar coordination of single atoms and the formation of chair-like six-membered rings.

Polytellurides of the alkali metals[51] show unique structures quite different from polysulfides since tellurium atoms prefer higher coordination numbers than 2, which are achieved by additional dative $np^2 \rightarrow n\sigma^\star$ bonds. The root cause for this behavior is the decreasing HOMO–LUMO energy difference in Group 16 from sulfur to tellurium. While the structures of $[Te_2]^{2-}$, $[Te_3]^{2-}$ and $[Te_4]^{2-}$ resemble those of the corresponding polysulfides, the more tellurium-rich anions show cyclic, polycyclic or infinite anion structures with two-, three- and four-coordinate atoms (Figure 12.10b). For example, the crystal structure of $Cs_3[Te_{22}]$ consists of polymeric $[Te_6]^{3-}$ ions together with crown-shaped neutral Te_8 molecules (unknown as neat compound). On the other hand, $Cs_2[Te_{13}]$ contains chain-like ions $[Te_{13}]^{2-}$ of C_s symmetry. The type of product obtained depends on the stoichiometry, on the reaction conditions and on the size of the cation. In mixed polychalcogen (S/Se/Te) anions tellurium prefers the positions with the highest coordination number.

Solutions of polychalcogenides in polar solvents have been studied by UV-Vis, Raman, NMR (^{77}Se, ^{125}Te), ESR and electrospray mass spectroscopy, which revealed that some of the solutions also contain the radicals $[S_3]^{\bullet-}$ and $[Se_2]^{\bullet-}$ in equilibrium with the corresponding dimers $[S_6]^{2-}$ and $[Se_4]^{2-}$. The same holds for melts of alkali polysulfides. The ubiquitous radical $[S_3]^{\bullet-}$ is responsible for the brilliant blue color of the mineral *lapis lazuli*,[47,52] which has been used by artists as an air-stable pigment for thousands of years (see silicates in Section 8.8.2).

12.9 Organo Polysulfanes R_2S_n

The hydrogen atoms in sulfanes H_2S_n can be replaced by alkyl and aryl groups R as in diorganopolysulfanes $R–S_n–R$, which often are called organic polysulfides despite the covalent bonds between R and the sulfur chain. They are thermally more stable than the sulfanes H_2S_n and therefore much more important both in Nature and in chemistry. The chain-length seems to be unlimited and species with up to 35 sulfur atoms have been detected but only species with up to 13 sulfur atoms have been isolated in pure form. In addition, there are numerous cyclic organosulfanes.[53] Sulfur-rich members are synthesized using *sulfur transfer reagents* such as $[Cp_2TiS_5]$:

51 W. S. Sheldrick, *Z. Anorg. Allg. Chem.* **2012**, *638*, 2401–2424. D. M. Smith, J. A. Ibers, *Coord. Chem. Rev.* **2000**, *200-202*, 187–205.

52 T. Chivers, P. Elder, *Chem. Soc. Rev.* **2013**, *42*, 5996.

53 R. Steudel, *Chem. Rev.* **2002**, *102*, 3905. R. Steudel, M. Kustos, *Encycl. Inorg. Chem.* **2007**, Vol. 8, online edition.

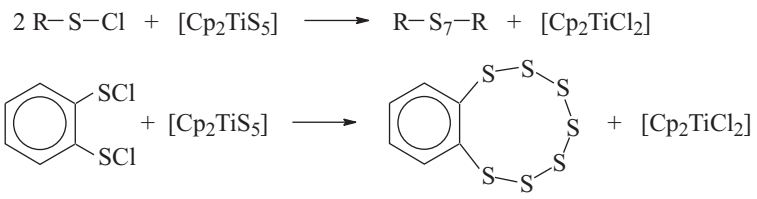

These reactions proceed quantitatively. At the melting point most acyclic organopolysulfanes equilibrate with homologues of shorter and longer chains. Disulfanes R_2S_2 together with S_8 are the final and most stable decomposition products.

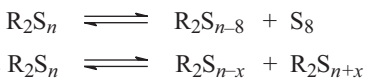

The most important application of organosulfanes is the vulcanization of rubber by sulfur, which is to connect neighboring chains of the organic polymer (e.g., polyisoprene) mainly by disulfane groups. Since modern tires also contain SiO_2 as a filler to reduce gasoline consumption, the following silyl derivative is applied to interconnect the organic polymer with the silica particles by covalent bonds: $(EtO)_3Si–C_3H_6–S_4–C_3H_6–Si(OEt)_3$ (triethylsilyl propyl tetrasulfane, abbreviated as TESPT). On heating for vulcanization, the ethoxy groups react with OH groups on the surface of silica to form covalent siloxane brides (Si–O–Si) with liberation of EtOH. At the same time the polysulfane group reacts with the vinylic hydrogen atoms of polyisoprene to form the required CS bonds.[54]

In organisms, organic disulfanes are widespread. Peptides contain S_2 groups between chains of amino acids, for example, in insulin in the form of cystine. Many sulfur-rich organopolysulfanes have been isolated from a variety of lower organisms, for example, algae, onions, garlic, ascidiacea and mushrooms.[53]

12.10 Chalcogen Oxides

The chalcogens S, Se and Te can easily be oxidized and all three burn in air if ignited. Enormous amounts of SO_2 are ejected into Earth's atmosphere each year by volcanoes[55] and flows of burning liquid sulfur can be observed

54 A. Travert et al., J. *Phys. Chem. C* **2014**, *118*, 4056.

55 For example, it has been estimated that during the eruption of El Chichón (Mexico) in the spring of 1982 ca. $13{\cdot}10^{12}$ g (13 Megatons) of SO_2 have been released into the atmosphere resulting in ca. $20{\cdot}10^{12}$ g sulfate, which circulated up to 3 years around the globe in the stratosphere causing global cooling as well as "romantic sunsets"; H.-U. Schmincke, *Volcanoes and Climate*, in *Volcanoes*, Springer, Berlin, **2004**, p. 261.

on the slopes of volcanoes in Italy and Indonesia.[56] Since ancient times the oxidation of sulfur has been used in *gun powder* (black powder), which is a mixture of 75% $K[NO_3]$, 13% charcoal and 12% sulfur. On ignition it produces mainly CO_2, N_2, $K_2[SO_4]$ and $K_2[CO_3]$ with violent deflagration.

The following chalcogen dioxides and trioxides are most important; they are partly monomeric and partly polymeric at 25 °C:

$$SO_2 \quad SeO_2 \quad TeO_2 \quad SO_3 \quad SeO_3 \quad TeO_3$$

The bonding situation in SO_2 and SO_3 has been discussed in Section 2.6. Sulfur also forms the so-called *lower oxides*, most of which consist of homocyclic molecules with the oxidation number of sulfur lower than in SO_2:

$$S_2O \quad S_2O_2 \quad S_6O \quad S_6O_2 \quad S_7O \quad S_7O_2 \quad S_8O \quad S_9O \quad S_{10}O$$

The monoxides SO, SeO and TeO are highly reactive high-temperature species, which only exist in equilibrium with the dioxides and the elements as well as in electric gas discharges. They have been studied by UV spectroscopy in the gas phase and using matrix-isolation techniques at low temperatures, which allows vibrational spectra to be recorded.

In addition, polymeric sulfur oxides with high sulfur content and polymeric sulfur peroxides are known. The species Se_2O_5, Te_4O_9, Te_2O_5 and TeO_3 are likewise polymeric with selenium and tellurium atoms in oxidation states of +4 and +6. Furthermore, numerous ternary chalcogen oxides have been prepared.[57]

12.10.1 Dioxides

Sulfur dioxide is one of the most important chemicals in industry as an intermediate in the large-scale production of sulfuric acid. It is mainly produced by combustion of liquid sulfur but also by the oxidative roasting process of sulfidic minerals such as *pyrite* FeS_2, *zincblende* (*sphalerite*) ZnS, *galena* PbS, *chalcopyrite* $CuFeS_2$ and many other minerals for metal production. Another source of SO_2 is $Ca[SO_4]$, which is reduced by coke in the presence of SiO_2. Finally the waste products $Fe[SO_4]$ (from TiO_2 production) and spent sulfuric acid are decomposed thermally to recover the sulfur as SO_2.

Combustion of coal, crude oil, diesel oil, heating oil, gasoline and wood generates SO_2 since all solid and liquid fossil fuels contain sulfur compounds.[58] In this

56 A. J. L. Harris, S. B. Sherman, R. Wright, *Geology* **2000**, *28*, 415. https://www.youtube.com/watch?v=qmkmStZc240

57 M. S. Wickleder, *in: Handbook of Chalcogen Chem*istry, Royal Society of Chemistry, London **2006**, 344.

58 Crude oil and its derivatives contain sulfur in the form of organic sulfides (thioethers, R_2S), disulfanes (R_2S_2), thiols (RSH) and thiophene derivatives. Coal contains also inorganic sulfur, e.g.

way human-made SO_2 is injected into the atmosphere.[59] Therefore, power plants must have a flue gas desulfurization unit based on one of the following methods:

(a) In the gypsum process the flue gas is treated with an aqueous slurry of $Ca[OH]_2$ or $Ca[CO_3]$:

$$Ca[OH]_2 + SO_2 + \tfrac{1}{2}O_2 \longrightarrow Ca[SO_4] + H_2O$$

$$Ca[CO_3] + SO_2 + \tfrac{1}{2}O_2 \longrightarrow Ca[SO_4] + CO_2$$

In many power plants gypsum $Ca[SO_4]\cdot 2H_2O$ is produced this way for use in the construction industry. Traces of iron and manganese ions present in chalk catalyze the oxidation of SO_2 to the oxidation state +6.

(b) In the WELLMAN–LORD process the flue gas is treated with aqueous $Na_2[SO_3]$, which is basic due to hydrolysis:

$$Na_2[SO_3] + SO_2 + H_2O \rightleftharpoons 2\,Na[HSO_3]$$

Since this reaction is reversible SO_2 can subsequently be isolated by heating the solution, which is then recycled to the absorber. The SO_2 is reduced to elemental sulfur either by natural gas (CH_4) or by H_2S according to the CLAUS process (Section 12.3.1).

In Europe and North America, the phenomenon of *acid rain* has basically been overcome by modern desulfurization units in power plants, while in Asia it is still a considerable environmental problem. On the downside, many agricultural farms in Europe now suffer from a *sulfur deficit in soil*, which needs to be compensated by sulfate containing fertilizers (together with N, P and K, sulfur is an essential element to plants). This is despite the fact that enormous amounts of sulfur compounds are constantly emitted into the atmosphere from natural sources, mainly dimethyl sulfide Me_2S (DMS, ca. $4\cdot 10^7$ t/a) from oceans. DMS is produced by phytoplankton (floating microorganisms)[60] and is oxidized in air to SO_2 and methane sulfonic acid $MeSO_3H$. This strong acid is one of the main constituents of acid rain besides H_2SO_4 and HNO_3.

SO_2 is a colorless, poisonous[61] and corrosive gas (m.p. –75.5°, b.p. –10 °C), which is monomeric in all phases. Its gas phase molecular parameters are:

---

pyrite FeS_2; see W. L. Orr, C. M. White (eds.), *Geochemistry of Sulfur in Fossil Fuels, ACS Symp. Ser.* Nr.429, Washington, **1990**.

59 For a review on anthropogenic SO_x and NO_x emissions, see C. Brandt, R. van Eldik, *Chem. Rev.* **1995**, *95*, 119.

60 A. Vardi et al., *Science* **2015**, *348*, 1466.

61 Agricultural plants suffer already at SO_2 concentrations of >30 µg/m^3 air. In European cities up to 0.1 ppm SO_2 had been measured at times when acid rain was still a problem.

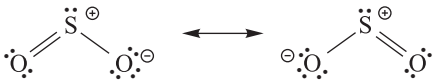

d (SO) = 143 pm, angle 119°

$f_r = 10$ N cm^{-1}, $\mu = 1.63$ D

The bonds in SO_2 resemble those of SO_3 (Section 2.6) with nearly identical bond lengths and stretching force constants. Aqueous SO_2 is a weak reducing agent, turning selenites and tellurites into the respective elements and chlorites to ClO_2, itself being oxidized to H_2SO_4 in the process. With fluorine and chlorine gas, SO_2 forms the corresponding sulfuryl halides SO_2X_2. Certain nonmetal chlorides exchange oxygen for chlorine to form thionyl chloride:

$$PCl_5 + SO_2 \longrightarrow POCl_3 + SOCl_2$$

$$COCl_2 + SO_2 \longrightarrow CO_2 + SOCl_2$$

Toward LEWIS acids and bases SO_2 is amphoteric, forming crystalline complexes both with tertiary amines as in $Me_3N{\rightarrow}SO_2$, and with transition metal compounds, for example, in the dinuclear iron carbonyl $[Fe_2(CO)_8SO_2]$. SO_2 also adds reversibly to oxoanions such as sulfate at 20 °C forming the mixed S(IV)S(VI) anion $[O_3S{-}O{-}SO_2]^{2-}$, which has been isolated as $[Me_4N]_2[S_2O_6]$. This anion is an isomer of dithionate and adds another SO_2 molecule forming a rather asymmetrical $[O_2S{-}O{-}S(O)_2{-}O{-}SO_2]^{2-}$ ion in which the central sulfate anion serves as a LEWIS base and the two SO_2 molecules as LEWIS acids.[62]

Liquid sulfur dioxide is a water-like solvent albeit without autodissociation. It nevertheless dissolves salts by solvation and is used as reaction medium for redox and complexation reactions, especially for double decompositions where oxygen transfer plays a role as in the formal "neutralization" of sulfites with thionyl chloride:

$$SOCl_2 + M_2[SO_3] \longrightarrow 2\,MCl + 2\,SO_2$$

The ions $[SOCl]^+$ and $[SO_3]^{2-}$ are intermediates in this reaction:

$$SOCl_2 \rightleftharpoons [SOCl]^+ + Cl^-$$

$$M_2[SO_3] \rightleftharpoons 2\,M^+ + [SO_3]^{2-}$$

$$[SOCl]^+ + [SO_3]^{2-} \longrightarrow 2\,SO_2 + Cl^-$$

12.10.1.1 Selenium and Tellurium Oxides

SeO_2 and TeO_2 are formed by burning the elements or by oxidation with concentrated nitric acid followed by evaporation of the solution and heating the residue to 300 °C (SeO_2) or 400 °C (TeO_2). **SeO_2** forms colorless crystals, soluble in water,

62 J. Passmore et al., *Inorg. Chem.* **2013**, *52*, 7193.

benzene and glacial acid; it sublimes at 315 °C. The vapor consists of bent molecules SeO_2 of C_{2v} symmetry (d_{SeO} = 174 pm, angle 101°). In the solid state, however, selenium dioxide forms nonplanar polymeric chains of corner-sharing SeO_3 pyramids:

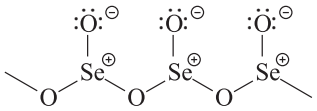

d(SeO) = 178 pm (within chain)
d(SeO) = 173 pm (seleninyl groups)

Due to the difference in electronegativities between oxygen (3.50) and selenium (2.48), the bonds in $(SeO_2)_n$ are partially ionic, partly covalent; the covalent single bond SeO distance is 183 pm.

SeO_2 dissolves in water as selenous acid H_2SeO_3. Vacuum evaporation of the solution gives colorless crystals of H_2SeO_3 which effloresce in air to give SeO_2.

SeO_2 is a selective oxidizing agent being easily reduced to elemental selenium and used in organic synthesis (RILEY oxidation). With HCl it forms the addition compound $SeO_2 \cdot 2HCl$, which can be dehydrated to seleninyl chloride by concentrated sulfuric acid:

$$SeO_2 \cdot 2\,HCl + H_2SO_4 \longrightarrow SeOCl_2 + [H_3O][HSO_4]$$

Colorless **α-TeO_2** (m.p. 733 °C) is formed on combustion of Te in O_2, on oxidation of Te by concentrated nitric acid and on thermal decomposition of telluric acid $Te(OH)_6$. The tetragonal structure of α-TeO_2 consists of pseudo-trigonal bipyramidal coordinate Te atoms of coordination number 4 (type AX_4E) and with two different Te–O distances (equatorial 190 pm, axial 208 pm). Yellow orthorhombic **β-TeO_2** occurs as the mineral tellurite with a layered structure. α-TeO_2 is sparingly soluble in water, but is more soluble in $SeOCl_2$. In hydrochloric acid, it is converted to hexachlorotellurate ions $[TeCl_6]^{2-}$. With sodium hydroxide, it reacts to tellurites or oxotellurates(IV). TeO_2 can be reduced to elemental tellurium by coal, aluminum or zinc.

12.10.2 Trioxides

Sulfur trioxide is produced on a very large scale by catalytic oxidation of SO_2 by air in the *Contact Process* developed by BASF in Germany around the year 1901:

$$SO_2 + \tfrac{1}{2}\,O_2 \rightleftharpoons SO_3 \qquad \Delta H^\circ_{700} = -97.4\ \text{kJ mol}^{-1};\ K_p(700\text{K}) = 240\ \text{bar}^{-0.5}$$

This equilibrium is frozen at room temperature but shifts to the left-hand side on heating due to the negative reaction enthalpy. Thus, a catalyst containing vanadium(V)

oxoanions on a silicate support activated by $K_2[SO_4]$ is used to increase the reaction rate at moderate temperatures. In the modern *Double Contact Process* developed by Bayer AG, the first catalyst is heated to 600 °C for a rapid reaction despite a poor SO_3 yield. The formed SO_3 is then selectively absorbed by scrubbing the gas stream with H_2SO_4 at a lower temperature, and the remaining gas is sent to another catalyst bed heated to 420 °C for maximum yield, which in total approaches 99.5%. The true nature of the polynuclear vanadium sulfato compound from which the oxygen transfer to SO_2 takes place is complex,[63] but schematically the oxidation of SO_2 can be described by the following equations:

$$\begin{aligned} SO_2 + 2\,V^{5+} + O^{2-} &\longrightarrow SO_3 + 2\,V^{4+} \\ 2\,V^{4+} + \tfrac{1}{2}\,O_2 &\longrightarrow 2\,V^{5+} + O^{2-} \\ \hline SO_2 + V_2O_5 &\longrightarrow SO_3 + V_2O_4 \end{aligned}$$

Since SO_3 cannot be efficiently absorbed from the reaction mixture by water (due to the absence of a permanent dipole moment the dissolution process in water is kinetically hindered), it is washed out selectively by sulfuric acid resulting in oleum, which is subsequently diluted by water to give H_2SO_4:

$$(n-1)\,SO_3 + H_2SO_4 \longrightarrow H_2S_nO_{3n+1} \xrightarrow{+(n-1)\,H_2O} n\,H_2SO_4$$

Polysulfuric acids $H_2S_nO_{3n-1}$ with differing SO_3 contents are commercially available as *oleum* or *fuming sulfuric acid* that releases the excess SO_3 on distillation, a process employed to prepare sulfur trioxide on a laboratory scale.

12.10.2.1 Allotropes of SO_3

Gaseous sulfur trioxide consists of SO_3 and S_3O_9 molecules in pressure- and temperature-dependent equilibrium:

$$3\,SO_3 \rightleftharpoons S_3O_9 \qquad \Delta H^\circ_\circ = -126\ \text{kJ mol}^{-1}\ (S_3O_9)$$

The molecule SO_3 is trigonal-planar (D_{3h} symmetry) with d_{SO} = 141.7 pm. Condensation at the boiling point of 44.5 °C (1013 Pa) yields a colorless liquid of low viscosity consisting predominantly of S_3O_9 molecules and little SO_3. Ice-like orthorhombic crystals of **γ-SO_3** form at the melting point of 17 °C consisting entirely of S_3O_9. The heterocyclic structure of this trimeric sulfur trioxide is characterized by a chair-like S_3O_3 ring with three bridging and six terminal oxygen atoms:

63 I. E. Wachs et al., *Appl. Catal. B* **1998**, *19*, 103.

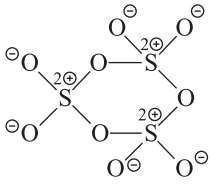

$d(SO) = 163$ pm
angle (OSO) = 99°
angle (SOS) = 121°
} within ring

$d(SO) = 137$ pm (axial)
$d(SO) = 143$ pm (equat.)
} terminal atoms

This structure can be thought of as consisting of three distorted SO_4 tetrahedra joined by shared corner atoms. Similar structures are encountered in two other allotropes of SO_3 and in polysulfates as well as in polysulfuric acids. At temperatures below 30 °C, especially below 20 °C and in the presence of traces of water, S_3O_9 polymerizes slowly to monoclinic **β-SO_3**, which consists of chain-like molecules probably end-capped by OH groups:

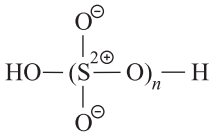

$d(S{-}OH) = 161$ pm, $d(S^{\oplus}{-}O^{\ominus}) = 141$ pm

Depolymerization of β-SO_3 to a mixture of SO_3 and S_3O_9 occurs at 32–45 °C with melting. To protect the commercial liquid sulfur trioxide from spontaneous polymerization, small amounts of stabilizers are added, mainly to bind traces of water.

The thermodynamically stable **α-SO_3** is formed by condensation of SO_3 on cold surfaces (−80 °C) and subsequent warming to 25 °C followed by irradiation with X-rays for several hours. The structure of α-SO_3 is not known but thought to be similar to that of β-SO_3; depolymerization of α-SO_3 occurs only at 62 °C, indicating a higher degree of polymerization.

12.10.2.2 Reactions of Sulfur Trioxide

Sulfur trioxide is extremely reactive, behaving as a strong oxidant, a LEWIS acid and more rarely as a LEWIS base. SO_3 oxidizes S_8 on warming to SO_2; SCl_2 is turned into a mixture of $SOCl_2$ and SO_2Cl_2, and PCl_3 into $POCl_3$. White phosphorus (P_4) burns in SO_3 to give P_4O_{10}. With LEWIS bases stable donor–acceptor complexes are formed, for example, the crystalline 1-pyridinyl sulfur trioxide ($C_5H_5N{\rightarrow}SO_3$). A similar adduct formation can be expected with water, but the primary product $H_2O{\rightarrow}SO_3$ rearranges intramolecularly to sulfuric acid with the catalytic assistance of a second water molecule allowing a cyclic transition state of lower activation energy:[64]

64 R. Steudel, *Angew. Chem. Int. Ed.* **1995**, *34*, 1313 and references cited therein. M. Torrent-Sucarrat, J. S. Francisco, J. M. Anglada, *J. Am. Chem. Soc.* **2012**, *134*, 20632.

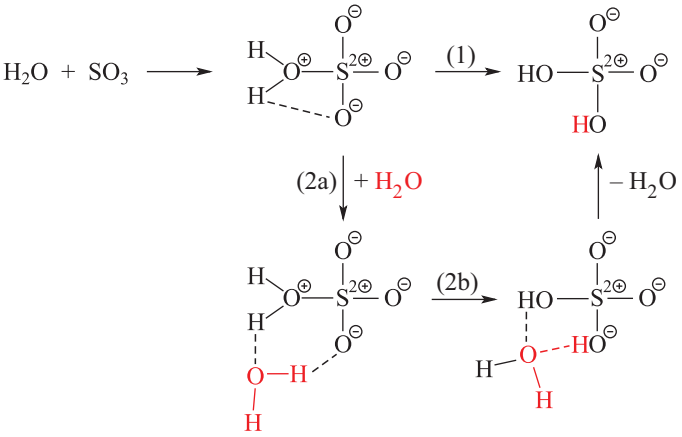

The direct intramolecular reaction from $H_2O{\rightarrow}SO_3$ to H_2SO_4 by a seemingly simple proton shift is hindered by a high activation energy.

Sulfur trioxide reacts with HCl to chlorosulfuric acid HSO_3Cl, and with NH_3 to the ammonium salt of amidosulfuric acid. In this reaction, SO_3 inserts into one of the NH bonds as the $-O-SO_2-$ group. The free amidosulfuric acid can be obtained by reaction with 60% nitric acid during which the anion is protonated:

$$2\ NH_3 + SO_3 \longrightarrow [NH_4][SO_3NH_2] \xrightarrow{+\ HNO_3} H_3\overset{\oplus}{N}{-}\overset{\ominus}{S}O_3\downarrow + [NH_4][NO_3]$$

While the name *amidosulfuric acid* suggests the molecular structure $H_2N{-}SO_3H$, the compound is in fact a *zwitterion* with a covalent SN bond and NH rather than OH acidity. The compound is also known as sulfamic acid; the SN bond length is 176 pm in the acid and 167 pm in the anion. Sulfamic acid forms salts such as $Li[SO_3NH_2]$, but under anhydrous conditions $Li_3[SO_3N]$ has been prepared, which is isoelectronic with $Li_3[PO_4]$.

With salts of inorganic acids SO_3 reacts with addition to the anions:

$$KF + n\ SO_3 \longrightarrow K[S_nO_{3n}F]$$

$$Na_2[SO_4] + (n-1)\ SO_3 \longrightarrow Na_2[S_nO_{3n+1}]$$

Sometimes SO_3 reacts with displacement of the anhydride:

$$K_2[SeO_4] + n\ SO_3 \longrightarrow K_2[S_nO_{3n+1}] + SeO_3$$

$$2\ K[ClO_4] + 3\ SO_3 \longrightarrow K_2[S_3O_{10}] + Cl_2O_7$$

$$K_2[CO_3] + 3\ SO_3 \longrightarrow K_2[S_3O_{10}] + CO_2$$

12.10.2.3 Selenium Trioxide

Selenium trioxide, prepared as shown above from $K_2[SeO_4]$ and liquid SO_3, forms colorless hygroscopic crystals (m.p. 118 °C) consisting of eight-membered Se_4O_{12} rings, which are in equilibrium with monomeric SeO_3 in the gas phase (D_{3h} symmetry; d_{SeO} = 169 pm). Decomposition to Se_2O_5 and O_2 occurs at temperatures above 160 °C. Se_2O_5 contains Se(IV) and Se(VI) atoms and reacts with water to a 1:1 mixture of H_2SeO_3 and H_2SeO_4. SeO_3 is a stronger oxidant than SO_3 and acts as LEWIS acid or base.

12.10.2.4 Tellurium Trioxide

Tellurium trioxide, a strong oxidizing agent, is obtained by dehydration of orthotelluric acid at 300–320 °C:

$$Te(OH)_6 \longrightarrow TeO_3 + 3\,H_2O$$

Depending on the reaction conditions either α-TeO_3 or β-TeO_3 is formed.[65] While α-TeO_3 reacts with water partly back to $Te(OH)_6$, β-TeO_3 is insoluble in water, in concentrated hydrochloric acid and even in concentrated KOH(aq). Above 400 °C, TeO_3 decomposes to Te_2O_5 und O_2. All tellurium oxides are polymeric with Te(IV) atoms trigonal-prismatically coordinated and Te(VI) atoms at the center of oxygen octahedrons.

12.10.3 Lower Sulfur Oxides

In all lower sulfur oxides,[66] the oxidation numbers of the sulfur atoms are +2 or zero. Disulfur monoxide S_2O is the most important; it is formed together with SO_2 and traces of SO_3 on combustion of elemental sulfur in pure oxygen at reduced pressure. Pure S_2O is obtained by passing $SOCl_2$ vapor at low pressure (10–50 Pa) over powdered Ag_2S at 160 °C:

$$OSCl_2 + Ag_2S \longrightarrow S_2O + 2\,AgCl$$

All members of the isoelectronic series O_3 – SO_2 – S_2O – S_3 are bent; the bonding situation in S_2O is analogous to that of SO_2:

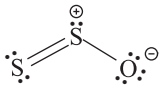

angle (SSO) = 118.0°
d(SO) = 145.7 pm
d(SS) = 188.7 pm

65 M. A. K. Ahmed, H. Fjellvag, A. Kjekshus, *J. Chem. Soc. Dalton Trans.* **2000**, 4542.
66 R. Steudel, *Top. Curr. Chem.* **2003**, *231*, 203-230. R. Steudel, Y. Steudel, *Eur. J. Inorg. Chem.* **2004**, 3513.

The SS bond is as short as in other compounds with SS double bonds. Nevertheless, S_2O can be kept only for a few days at pressures below 1 hPa and in the absence of moisture. It can be stabilized at temperatures below –30 °C as adduct with trimethylamine: $Me_3N{\rightarrow}S_2O$. At higher pressures and on condensation with liquid nitrogen followed by warming to 25 °C, it polymerizes in a radical-chain reaction with partial disproportionation and S_3 as an intermediate:

$$2\,S_2O \longrightarrow SO_2 + S_3$$

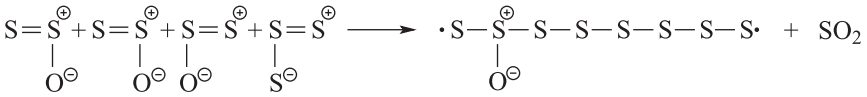

The resulting long-chain polysulfur oxides S_xO are insoluble in organic solvents and decompose at 100 °C to SO_2 and S_8. Cyclic sulfur-rich oxides are obtained on oxidation of sulfur rings by trifluoro peracetic acid in methylene chloride at 0 °C:

$$S_n + CF_3CO_3H \longrightarrow S_nO + CF_3CO_2H \qquad n = 6-10$$

All members of the series S_6O to $S_{10}O$ have been prepared as yellow to orange crystals. They decompose at room temperature slowly to SO_2 and sulfur. S_7O_2 is the only homocyclic dioxide isolated so far; it is even more labile than the monoxides. The molecular structures of S_7O (C_1 symmetry) and S_8O (C_s symmetry) as determined by X-ray crystallography are characterized by very different SS bond lengths (values in pm):[66]

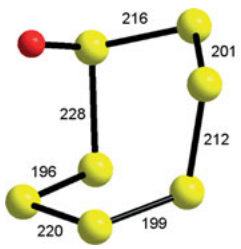

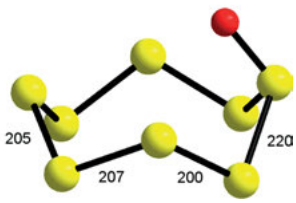

12.11 Oxo-, Thio- and Halo-Acids of the Chalcogens

12.11.1 Introduction

Sulfur forms a large number of oxoacids, from the highly reactive hydroxosulfanes HSOH, HOSOH, HSSOH and HOSSOH via sulfinic acid HS(O)OH and sulfurous acid H_2SO_3 up to sulfuric acid H_2SO_4 and its many derivatives (Table 12.4). Many of these compounds are important both in industry, in the natural sulfur cycle, in the chemistry of the atmosphere and accordingly also in environmental chemistry.

Table 12.4: Composition of the simplest sulfur oxoacids with oxidation numbers from 0 to +6. In most cases, several tautomers exist with differing names. Some acids are known only as anions in salts or in solution.

0	+1	+2	+3	+4	+5	+6
H_2SO	$H_2S_2O_2$	H_2SO_2	$H_2S_2O_4$	H_2SO_3	$H_2S_2O_6$	H_2SO_4, $H_2S_2O_7$, $H_2S_3O_{10}$ H_2SO_5, $H_2S_2O_8$ $H_2S_2O_3$, HSO_3F, HSO_3Cl

Replacement of oxygen in these acids by sulfur gives *thioacids*, for example, thiosulfuric acid:

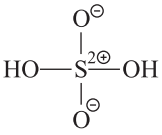

sulfuric acid

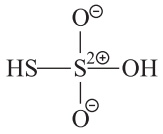

thiosulfuric acid

For a discussion of the sulfur oxidation states in thiosulfates, see Section 5.5.1. Substitution of an OH group by a halogen atom leads to the corresponding *haloacids*:

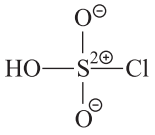

chlorosulfuric acid

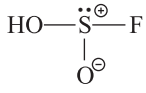

fluorosulfurous acid

The most important **oxoacids of selenium and tellurium** are selenous acid H_2SeO_3, selenic acid H_2SeO_4, the polymeric telluric acid H_2TeO_4 and the monomeric orthotelluric acid $Te(OH)_6$.

Some chalcogen oxoacids cannot be prepared as pure compounds at ambient conditions and are known only as anions in salts, in aqueous solutions or as reactive species in the vapor phase. This applies to all sulfur oxoacids with sulfur oxidation numbers smaller than +6. For example, the chain-like hydroxosulfanes HSOH, HOSOH, HSSOH and HOSSOH have been prepared by gas phase flash pyrolysis of the corresponding *iso*-propyl or *tert*-butyl precursors with elimination of propene or *iso*-butene,[67] for example:

$$C_4H_9\text{–}O\text{–}S_x\text{–}O\text{–}C_4H_9 \;\rightarrow\; H\text{–}O\text{–}S_x\text{–}O\text{–}H \;+\; 2\;C_4H_8 \;\; (x = 1,\; 2)$$

67 J. Gauss et al., *Inorg. Chem.* **2009**, *48*, 2269. G. Winnewisser et al., *Chem. Eur. J.* **2003**, *9*, 5501. R. Steudel et al., *Inorg. Chem.* **1992**, *31*, 941.

The molecular structures of the hydroxosulfanes as determined by microwave spectroscopy or quantum-chemical calculations are analogous to those of the sulfanes and peroxides with torsional angles near ±90° at the SO and SS bonds (*cis*- and *trans*-conformers). Some of these compounds are intermediates during the oxidation of H_2S but neither of them nor their anions are known in condensed phases except for samples obtained by matrix isolation at very low temperatures. Numerous organic derivatives of hydroxosulfanes are known and referred to as bis-alkoxysulfanes.

The *acidities* of chalcogen oxoacids[68] increase with the oxidation number of the central atom (Table 5.5).

Most chalcogen acids and their anions have individual trivial names (sulfate, sulfite, dithionate, etc.), but by a rational *nomenclature* the salts of all sulfur–oxygen ions are termed sulfates with the oxidation number of the sulfur atom(s) given in brackets. Sulfite ions are then sulfate(IV) ions.

The LEWIS structures used in this chapter are based on the results of recent quantum-chemical calculations and experimental charge distributions. The central sulfur atoms always have an octet configuration, accompanied by sometimes high positive atomic charges.[69] For a detailed discussion of the bonding situations, see Section 2.6.

12.11.2 Sulfurous Acid, H_2SO_3

Sulfur dioxide is highly soluble in water (ca. 45 vol SO_2/vol H_2O at 15 °C) to give a solution of sulfurous acid H_2SO_3 with reducing properties. However, this acid cannot be isolated by cooling or evaporation of solvent since evaporation yields SO_2 and H_2O, and on cooling the gas-hydrate $SO_2 \cdot 6H_2O$ crystallizes.[70] According to RAMAN spectra the solution contains SO_2 as well as the ions $[H_3O]^+$, $[SO_3H]^-$, $[HSO_3]^-$ and, at higher concentrations, disulfite ions $[S_2O_5]^{2-}$:

$$SO_2\,(aq) + 2\,H_2O \rightleftharpoons [H_3O]^+ + [SO_3H]^- \qquad pK_a = 1.86\ (25°C)$$

$$2\,[SO_3H]^- \rightleftharpoons H_2O + [S_2O_5]^{2-} \qquad K_c = 0.045\ L\ mol^{-1}\ (25°C)$$

$$[SO_3H]^- + H_2O \rightleftharpoons [H_3O]^+ + [SO_3]^{2-} \qquad K_a = 0.63 \cdot 10^{-7};\ pK = 7.2$$

68 A. H. Otto, R. Steudel, *Eur. J. Inorg. Chem.* **2000**, 617 and 2379.

69 C. Gatti et al., *Inorg. Chem.* **2012**, *51*, 8607. S. Grabowski et al., *Angew. Chem. Int. Ed.* **2012**, *52*, 6776.

70 In the vapor phase H_2SO_3 molecules have been detected by mass spectrometry albeit with a short lifetime, especially in the presence of water that catalyzes the decomposition.

The anion structures are as follows (shown is just one resonance structure each):

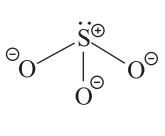

sulfite (C_{3v})
d (SO) = 153 pm
angle (OSO) = 107.4°

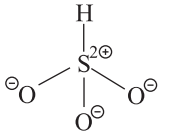

sulfonate (C_{3v})

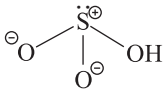

hydrogen sulfite
(C_s)

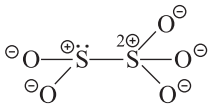

disulfite
d (SS) = 220.9 pm

The coordination geometry at the sulfur atom is distorted pyramidal and tetrahedral, respectively. Anions of composition $[HSO_3]^-$ exist in water as two tautomers with either OH or SH bonds. The relative concentrations of hydrogen sulfite ($[HO–SO_2]^-$ or $[SO_3H]^-$) and sulfonate ions ($[H–SO_3]^-$) have been determined by ^{17}O-NMR, RAMAN and XANES[71] spectroscopy. At room temperature hydrogen sulfite dominates but at higher temperatures sulfonate ions are increasingly formed by tautomerization.[72] Heating of aqueous SO_2 solutions to 200 °C results in exothermic disproportionation to H_2SO_4 and S_8.

With large cations such as $[NH_4]^+$, Rb^+ and Cs^+, crystalline sulfonates $M[HSO_3]$ have been prepared while solid hydrogen sulfites $M[SO_3H]$ are unknown. Organic derivatives of the two tautomeric anions are termed *sulfonates* (a) and *sulfurous acid half-esters* (b):

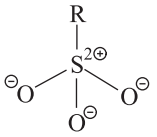

(a)

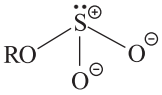

(b)

Saturation of aqueous NaOH with SO_2 gives a solution of sodium hydrogen sulfite, which reacts to sodium sulfite $Na_2[SO_3]$ with more NaOH or on boiling with $Na_2[CO_3]$:

$$Na[OH] + SO_2 \longrightarrow Na[SO_3H] \xrightarrow{+Na[OH]} Na_2[SO_3] + H_2O$$

$Na_2[SO_3]$ is a commercial reducing agent and antioxidant used, for example, in wine.

Sodium disulfite is formed if a solution of composition $Na[SO_3H]$ is evaporated or if aqueous $Na_2[SO_3]$ is saturated with SO_2:

$$2\ Na[SO_3H] \longrightarrow Na_2[S_2O_5] + H_2O$$

$$Na_2[SO_3] + SO_2 \rightleftharpoons Na_2[S_2O_5]$$

71 XANES: X-ray absorption near edge spectroscopy.

72 R. Steudel, Y. Steudel, *Eur. J. Inorg. Chem.* **2009**, 1393 and references cited therein.

The long and obviously weak SS bond in the disulfite anion (221 pm; see above) is probably responsible for the decomposition of $Na_2[S_2O_5]$ at 400 °C to give $Na_2[SO_3]$ and SO_2.[73]

Salt-like sulfites, hydrogen sulfites, sulfonates and disulfites behave similarly in redox reactions: all of them are easily oxidized to sulfate, for example, by air, iodine or iron(III) ions. In contrast, dithionate is formed with MnO_2. Dithionite is obtained on reduction of sulfite with sodium or zinc metal as well as by cathodic reduction (see below). Another important reducing agent, especially in the textile industry, is sodium hydroxymethane sulfinate (*Rongalit®*), which is prepared by reduction of hydrogen sulfite with zinc powder in the presence of formaldehyde in alkaline solution:

$$Na[SO_3H] + CH_2O + Zn + H_2O \rightarrow Na[HO{-}CH_2{-}SO_2] + Zn(OH)_2$$

An alternative route to Rongalit is the addition of formaldehyde to the dithionite anion:

$$Na_2[S_2O_4] + 2CH_2O + H_2O \rightarrow Na[HO{-}CH_2{-}SO_2] + Na[HO{-}CH_2{-}SO_3]$$

The sulfinate is the salt of *sulfinic acid* $R{-}SO_2H$ and contains sulfur of oxidation number +2.

Boiling of aqueous sulfite with elemental sulfur leads to *thiosulfate* by a series of nucleophilic degradation reactions with many highly reactive intermediates:

$$8\ Na_2[SO_3] + S_8 \longrightarrow 8\ Na_2[S_2O_3]$$

The sulfurous acid derivatives, fluorosulfurous acid HSO_2F, chlorosulfurous acid HSO_2Cl, thiosulfurous acid $H_2S_2O_2$ and dithiosulfurous acid H_2S_3O are unstable but some are known as salts or organic derivatives, for example:

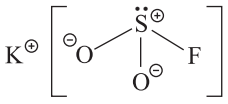

potassium fluorosulfite

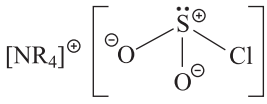

ammonium chlorosulfite

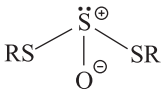

organyltrisulfane oxide

Potassium fluorosulfite $K[SO_2F]$ is prepared by reaction of KF with SO_2 at 25 °C; it serves as fluorinating agent but reversibly dissociates on heating to 70 °C. The SF bond length of 159.1 pm is similar to the corresponding values in SOF_2 (158.3 pm). Chlorosulfites are made in an analogous manner, for example, from $[^tBu_4N]Cl$ and SO_2.[74] Trisulfane 2-oxides R_2S_3O (dithiosulfites) are made by condensation of bulky

73 In industry hydrogen sulfite is usually termed as bisulfite, and disulfite is termed either as pyrosulfite or as metabisulfite.

74 J. Passmore, F. Grein et al., *Z. Anorg. Allg. Chem.* **2012**, *638*, 744 and references cited therein.

thiols RSH with thionylchloride $SOCl_2$ with elimination of HCl.[75] The bulky substituent R suppresses the bimolecular decomposition with formation of SO_2 and R_2S_3.

12.11.3 Selenous Acid (H_2SeO_3) and Tellurous Acid (H_2TeO_3)

Despite its polymeric nature selenium dioxide dissolves in water to give the weak acid H_2SeO_3, which can be isolated by evaporation of the solvent as colorless crystals that decompose to SeO_2 and water on warming. The orthorhombic crystal structure of H_2SeO_3 consists of layers of SeO_3 pyramids interconnected within the layers by OH···O hydrogen bonds. Selenous acid is a fairly strong oxidizing agent that is reduced by N_2H_4, SO_2, H_2S or HI to yield red selenium, for example:

$$H_2SeO_3 + N_2H_4 \longrightarrow Se\downarrow + N_2\uparrow + 3\,H_2O$$

Reaction of selenous acid with bases yields hydrogen selenites $M[HSeO_3]$ or selenites $M_2[SeO_3]$, depending on the stoichiometry. Sodium selenite $Na_2[SeO_3]$ is an animal feed additive to compensate the selenium deficit of agricultural soils in certain regions. $Na_2[SeO_3]$, $Ba[SeO_3]$ and $Zn[SeO_3]$ are used for coloration of glass and ceramics. Concentrated solutions of hydrogen selenites contain additional diselenite ions $[Se_2O_5]^{2-}$, which do not contain an Se–Se bond but a central Se–O–Se bridge, for example, in $[NH_4]_2[Se_2O_5]$ and $Zn[Se_2O_5]$.

Strong oxidizing agents such as F_2, O_3, $[MnO_4]^-$ or H_2O_2 convert H_2SeO_3 and selenites into selenic acid H_2SeO_4 and selenates, respectively.

Owing to its polymeric structure and high lattice energy, **TeO_2** is practically insoluble in water, unlike SO_2 and SeO_2. Attempts to prepare tellurous acid H_2TeO_3 by hydrolysis of $TeCl_4$ or by acidification of aqueous solutions of tellurites failed. Instead, products are obtained that spontaneously decompose to TeO_2 and H_2O. Tellurites, also known as tellurates(IV), are prepared by dissolution of TeO_2 in strongly alkaline aqueous solutions. They contain the anion $[TeO_3]^{2-}$ but polytellurites of composition $M_2[Te_nO_{2n+1}]$ have also been prepared, for example, $[NH_4]_2[Te_2O_5]$ containing the polymeric chain-like anion $[Te_2O_5]^{2-}$ with four-coordinate Te atoms.

12.11.4 Sulfuric Acid (H_2SO_4) and Polysulfuric Acids ($H_2S_nO_{3n+1}$)

Sulfuric acid is the most important sulfur compound. The world production exceeded $260{\cdot}10^6$ t in 2018 with China contributing the largest share to this enormous amount.[76] H_2SO_4 is almost exclusively produced by the *contact process*

75 See for example: R. Steudel et al., *Organometallics* **1999**, *18*, 2910, and *Z. Anorg. Allg. Chem.* **1995**, *621*, 1672.

76 Winnacker-Küchler, *Chemische Technik: Anorganische Grundstoffe*, Vol. 3, 5th ed., Wiley-VCH, Weinheim, **2005**. http://www.essentialchemicalindustry.org/chemicals/sulfuric-acid.html.

(Section 12.10.2) and used in the synthesis of fertilizers, plastics, dyes, titanium dioxide pigment, hydrogen fluoride and other chemicals, but it is needed also for lead-acid batteries and in metallurgy.

Pure sulfuric acid (100%) is a colorless oily liquid (m.p. 10.4 °C), which boils at 290–317 °C with partial decomposition to H_2O and SO_3. Solid and liquid H_2SO_4 are strongly associated by hydrogen bonds that cause the high melting temperature and the high viscosity. The liquid contains various ions and molecules in equilibrium concentrations:

$$2\,H_2SO_4 \rightleftharpoons [H_3SO_4]^+ + [HSO_4]^- \qquad \text{Ion product } 2.7\cdot10^{-4}\ \text{mol}^{-2}\,\text{L}^{-2}\ (25°\text{C})$$

$$2\,H_2SO_4 \rightleftharpoons [H_3O]^+ + [HS_2O_7]^-$$

$$2\,[HS_2O_7]^- \rightleftharpoons [HSO_4]^- + [HS_3O_{10}]^-$$

Dissolution of SO_3 in H_2SO_4 yields disulfuric acid $H_2S_2O_7$ and higher polysulfuric acids $H_2S_nO_{3n+1}$ (n = 3, 4) in reversible reactions:

$$2\,H_2SO_4 + 2\,SO_3 \rightleftharpoons 2\,H_2S_2O_7 \rightleftharpoons H_2SO_4 + H_2S_3O_{10}$$

Mixtures containing 20% or 65% of additional SO_3 (beyond the formula H_2SO_4) have melting point minima and are known as *fuming sulfuric acid* or *oleum*, while mixtures with different SO_3 concentrations are solids near 25 °C. The acidity of polysulfuric acids according to HAMMETT (Section 5.5.2) increases with the number of sulfur atoms.

Water reacts with H_2SO_4 to oxonium salts and hydrates thereof (Table 5.2). In dilute aqueous solution H_2SO_4 acts as a strong diprotic acid which is completely dissociated into $[H_3O]^+$ and $[HSO_4]^-$ while the acidity constant of the second step is only ca. 10^{-2} mol L^{-1}. Therefore, sulfates as well as hydrogen sulfates of most electropositive metals have been isolated.

These acids and their anions have the following structures with tetrahedral or nearly tetrahedral coordination of the sulfur atoms:

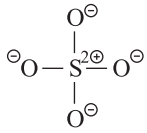

sulfate

d(SO) = 151 pm (4x)

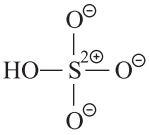

hydrogen sulfate

d(S—OH) = 156 pm (1x)
d(S—O) = 147 pm (3x)

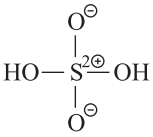

sulfuric acid

d(S—OH) = 153.5 pm (2x)
d(S—O) = 142.6 pm (2x)

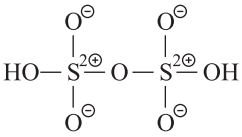

disulfuric acid

The bonding situation in the sulfate anion has already been discussed in Section 2.6. Polysulfates are prepared as follows:

$$2\ K[HSO_4] \xrightarrow{\Delta T} K_2[S_2O_7] + H_2O$$

$$K_2[SO_4] + (n-1)\ SO_3\ (g.) \longrightarrow K_2[S_nO_{3n+1}]$$

Tri-, tetra- and hexasulfates have been structurally characterized revealing anions of chains of corner-sharing SO_4 tetrahedra linked via common oxygen atoms.[77] All polysulfates are rapidly hydrolyzed by water to sulfate; on strong heating they liberate SO_3 and turn into sulfates as well.

Commercial *concentrated sulfuric acid* (98%) is weakly oxidizing but can be reduced by electropositive metals, on heating even by copper, to give SO_2. The acid is strongly dehydrating and carbonizes most carbohydrates. Anhydrous sulfuric acid is a water-like but strongly protonating solvent dissolving many salts due to its high dielectric constant (ε = 100 at 25 °C), but nonpolar compounds are generally dissolved only if they can be turned into ions by protonation.

Most anthropogenic sulfur emissions into the atmosphere will ultimately be oxidized to H_2SO_4, which reacts with traces of NaCl (from ocean spray) and ammonia to so-called sulfate aerosol. The colorless sulfate particles of this sol are hygroscopic and attract water molecules; they reflect sunlight in the upper atmosphere and counteract the well-known global warming. Since volcanic gases contain considerable concentrations of H_2S and SO_2, the concentration of sulfate aerosol increases significantly after strong volcanic eruptions and the average temperature on Earth's surface may drop by several degrees centigrade for several months or even years. For example, on 13 June 2011 the layer volcano Nabro in Eritrea ejected ca. $1.3{\cdot}10^6$ t of SO_2 into the atmosphere to a height of 9–14 km resulting in formation of sulfate aerosol within a few days. This stratospheric sol then spread over the whole Northern Hemisphere.[78]

12.11.5 Selenic Acid (H_2SeO_4) and Telluric Acids [H_2TeO_4 and $Te(OH)_6$]

Selenic acid forms colorless hygroscopic crystals of m.p. 58 °C, which are prepared by oxidation of SeO_2 with H_2O_2 (30%), bromine or chlorine in H_2O followed by evaporation of H_2O at 160 °C/2 hPa. Above 260 °C, H_2SeO_4 decomposes into SeO_2, H_2O and O_2. Selenates $M_2[SeO_4]$ are prepared by neutralization of the acid

77 M. S. Wickleder et al., *Z. Anorg. Allg. Chem.* **2012**, *638*, 758, and *Angew. Chem. Int. Ed.* **2012**, *51*, 4997 as well as *Angew. Chem. Int. Ed.* **2016**, *55*, 16165.

78 A. E. Bourassa et al., *Science* **2012**, *337*, 78.

with carbonate or by oxidation of selenites. Salts with the *orthoselenate anions* $[SeO_5]^{4-}$ and $[SeO_6]^{6-}$ are obtained by fusing selenates with oxides such as Li_2O or Na_2O at elevated O_2 pressure. Depending on the cation, the anion $[SeO_5]^{4-}$ forms a trigonal bipyramid (with Li^+) or a square-pyramid (with Na^+); $[SeO_6]^{6-}$ forms a regular octahedron.

H_2SeO_4 is as strong an acid as H_2SO_4 (Table 5.5) but a stronger oxidizing agent. Most selenates and hydrogen selenates are isomorphous with the corresponding sulfates and hydrogen sulfates. In addition, there are diselenates with the anion $[Se_2O_7]^{2-}$ as well as fluoro-, chloro-, amido- and peroxoselenates. $Na_2[SeO_4]$ is added to fertilizers in low concentrations to ensure the selenium needs of plants growing on selenium-deficient soil, and in this way the selenium requirements of animals and humans are also satisfied (see Section 12.1).

Orthotelluric acid $Te(OH)_6$ forms colorless crystals in which the central Te atom is octahedrally coordinated by OH groups (d_{TeO} = 191 pm). Therefore, it differs considerably from sulfuric and selenic acids. $Te(OH)_6$ is obtained by oxidation of Te or TeO_2 by $HClO_3$(aq), H_2O_2(30%) or a $K[MnO_4]/HNO_3$ mixture. The compound crystallizes from water on addition of ethanol. Similar highly hydrated compounds with octahedral coordination of the central atoms are known from elements in neighboring groups of the Periodic Table:

$[Sn(OH)_6]^{2-}$	**$[Sb(OH)_6]^-$**	**$Te(OH)_6$**	**$IO(OH)_5$**
hydroxostannate	hydroxoantimonate	orthotelluric acid	orthoperiodic acid

It is the larger size of the central atom, which allows for the higher coordination numbers than with the lighter homologs of these elements.

Orthotelluric acid is a medium strong and slowly acting oxidant and a weak diprotic acid in water (pK_1 = 7.70, pK_2 = 11.0) but it forms salts of the compositions $Li_6[TeO_6]$ and $Ag_6[TeO_6]$. However, most tellurates(VI) are prepared by solid-state reactions. Fusion of $Te(OH)_6$ with NaOH yields $Na_6[TeO_6]$. Reaction of $[Et_3N][OH]$ with aqueous $Te(OH)_6$ gives $[Et_3N]_2[TeO_4]$ as the only known salt that contains the tetrahedral ion $[TeO_4]^{2-}$ both in the solid state and in nonaqueous solution. Other tellurate(VI) salts contain octahedrally coordinate Te atoms.

The structures of $Li_6[TeO_6]$, $Li_4[TeO_5]$, $Li_2[TeO_4]$ and TeO_3 illustrate the sharing of 0, 2, 4 and 6 oxygen atoms between adjacent TeO_6 groups forming discrete $[TeO_6]^{2-}$ ions in $Li_6[TeO_6]$, dimeric ions $[Te_2O_{10}]^{8-}$ in $Li_4[TeO_5]$, chains in $Li_2[TeO_4]$ and a three-dimensional framework in TeO_3.[79]

Heating of $Te(OH)_6$ to 100–200 °C yields metatelluric acid H_2TeO_4 of which salts of compositions $Na_2[TeO_4]$ and $[NH_4][HTeO_4]$ with octahedrally coordinate Te atoms

79 A. F. Wells, *Structural Inorganic Chemistry*, 5th ed., Oxford Sci. Publ., Oxford, **1995**, p. 737.

are known. These octahedra are linked by shared oxygen atoms at the vertices resulting in an overall composition of $[TeO_4]^{2-}$. At temperatures above 220 °C, H_2TeO_4 is dehydrated to TeO_3 that is converted to Te_2O_5 at 400 °C and on further heating to TeO_2 and O_2. The dinuclear acid $H_2Te_2O_6$ is a polymeric mixed-valence compound with octahedrally coordinate Te(IV) and Te(VI) atoms.

12.11.6 Peroxosulfuric Acids (H_2SO_5, $H_2S_2O_8$)

The two peroxo acids

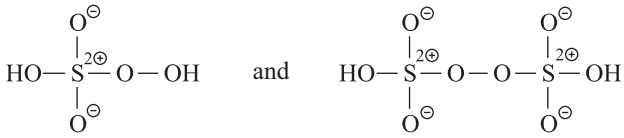

peroxomonosulfuric acid peroxodisulfuric acid

have been prepared in crystalline form by reacting H_2O_2 (100%) with chlorosulfuric acid with strong cooling; the molar ratio determines the reaction product:

$$HSO_3Cl + HOOH \xrightarrow{-HCl} HSO_3OOH \xrightarrow[-HCl]{+HSO_3Cl} HSO_3OOSO_3H$$

H_2SO_5 (CARO's acid; m.p. 47 °C) is hygroscopic and hydrolyzes in cold water slowly to H_2SO_4 and H_2O_2. The crystalline compound is strongly associated by hydrogen bonds; the OO distance is 146.4 pm and the torsion angle τ(SOOH) is 104°. These data are quite similar to those of H_2O_2. $H_2S_2O_8$ (m.p. 65 °C) is also hygroscopic and as strong an oxidizing agent as H_2SO_5; its hydrolysis to H_2SO_4 is highly exothermic.

Peroxodisulfates, are prepared by anodic oxidation of sulfates: $2\ [SO_4]^{2-} \rightarrow [S_2O_8]^{2-} + 2e^-$. They are strong oxidizing agents that convert Mn^{2+} ions into $[MnO_4]^-$ and Cr^{3+} ions into $[CrO_4]^{2-}$ in the presence of catalytic Ag^+ ions. $H_2S_2O_8$ can also be prepared from its salts, which are commercial products. The triple salt $2K[HSO_5]{\cdot}K[HSO_4]{\cdot}K_2[SO_4]$ is an industrial bleaching agent with the trade names Caroate and Oxone; it is thermally more stable than pure $K[HSO_5]$ and is produced from oleum and H_2O_2 followed by reacting the peroxomonosulfuric acid with KOH. The proton of $K[HSO_5]$ is linked to the peroxo group.

12.11.7 Halosulfuric Acids, $HS_nO_{3n}X$

Sulfur trioxide reacts with anhydrous HF, HCl and HBr to form the corresponding halosulfuric acids while HI is oxidized by SO_3 to iodine and water even at low temperatures:

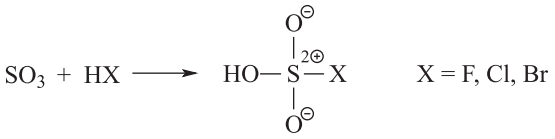

HSO_3F and HSO_3Cl are colorless liquids fuming in air due to hydrolysis of the vapors. HSO_3Br, prepared at −35 °C in liquid SO_2, decomposes slowly at its melting point of 8 °C to Br_2, SO_2 and H_2SO_4. The analogous decomposition is observed for HSO_3Cl on heating.

Fluoro- and chlorosulfates are readily prepared from the corresponding halides and SO_3:

$$CaF_2 + 2\ SO_3\ (g.) \longrightarrow Ca[SO_3F]_2$$

HSO_3F vigorously reacts with water to oxonium fluorosulfate $[H_3O][SO_3F]$ the anion of which hydrolyzes only slowly. Anhydrous HSO_3F (m.p. −89 °C, b.p. 163 °C) is a *fluorinating agent* as well as a highly acidic solvent of dielectric constant ε = 120 at 25 °C. The anions $[SO_3F]^-$ and $[ClO_4]^-$ are isosteric and about of equal size. Therefore, fluorosulfates and perchlorates form solid solutions (mixed crystals) and have similar solubilities.

Chlorosulfuric acid (m.p. −80 °C; b.p. 152 °C, dec.), also known as *chlorosulfonic acid*, reacts with water explosively;[80] it is an important *sulfonating agent* for organic compounds:

$$RH + HSO_3Cl \longrightarrow RSO_3H + HCl$$

12.11.8 Thiosulfuric Acid ($H_2S_2O_3$) and Sulfane Disulfonic Acids ($H_2S_nO_6$)

Thiosulfuric acid is unstable at ambient conditions but has been prepared at −60 °C in anhydrous hydrogen fluoride:[81]

$$Na_2S_2O_3 + 2\,HF \longrightarrow H_2S_2O_3 + 2\,NaF$$

The two products are separated by dissolution of the acid in cold acetonitrile, filtration and evaporation of the solvent below −30 °C. $H_2S_2O_3$ melts at −30 °C to give an oily liquid, followed by decomposition to sulfur, SO_2 and H_2O. According to quantum-chemical calculations, gaseous and nonaqueous thiosulfuric acid is of connectivity $HS–SO_2(OH)$, but in the presence of water the tautomer $SSO(OH)_2$

80 Solutions of SO_3 in HSO_3Cl have been used during World Wars I and II to produce *smoke screens* of HCl and H_2SO_4 by hydrolysis in humid air to mask the location or movement of military units such as infantry, tanks, aircrafts and ships.

81 M. Hopfinger, M. Seifert, A. J. Kornath, *Z. Anorg. Allg. Chem.* **2018**, *644*, 534.

with a sulfur–sulfur double bond is more stable due to strong OH····OH_2 hydrogen bonds.[82]

Acidification of *aqueous thiosulfate* by concentrated hydrochloric acid initially gives a clear solution of $H_2S_2O_3$ but elemental sulfur is precipitated in the form of milky droplets after a few minutes:

$$H_2S_2O_3 \longrightarrow H_2O + SO_2 + \tfrac{1}{n} S_n \quad (n = 6, 7, 8...)$$

The mechanism of this redox reaction has been discussed in Section 12.4 in the context of the preparation of S_6.

Thiosulfates are prepared by boiling aqueous sulfite with sulfur. Most important is the pentahydrate $Na_2[S_2O_3]{\cdot}5H_2O$, which has been used in photography as a fixer to dissolve unexposed AgBr as $[Ag(S_2O_3)_2]^{3-}$ from the photographic emulsion. Nowadays, $[NH_4]_2[S_2O_3]$ is used instead, which is obtained by dissolution of S_8 in aqueous $[NH_4]_2[SO_3]$ at 80–100 °C. Reaction of $[NH_4]_2[S_2O_3]$ with sulfuric acid in anhydrous methanol at low temperatures yields solid $[NH_4][HS_2O_3]$ containing an SH bond; it is the only hydrogen thiosulfate described so far, but decomposes at 25 °C already. The pentahydrate $Na_2[S_2O_3]{\cdot}5H_2O$ is used for *storage of solar heat* in buildings since it melts at 48.5 °C, while the melting enthalpy of 210 MJ/t can be recovered at night by crystallization of the salt.

The anion of anhydrous $Na_2[S_2O_3]$ is of C_{3v} symmetry (d_{SS} = 200.7 pm) and analogous to the sulfate ion; the oxidation numbers of the two sulfur atoms are –2 and +6:

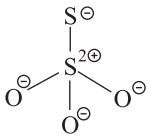

A highly characteristic and important reaction of thiosulfate is the oxidation by iodine to tetrathionate, which is used in *iodometry* for quantitative determination of either one:

$$2\,[S_2O_3]^{2-} + I_2 \longrightarrow [S_4O_6]^{2-} + 2\,I^-$$

The nucleophilic attack of the thiosulfate anion at I_2 yields the reaction intermediate $[I{-}S{-}SO_3]^-$, which is attacked by a second thiosulfate ion to give tetrathionate and iodide ions. Tetrathionates are the salts of the disulfane disulfonic acid $HO_3S{-}S{-}S{-}SO_3H$ which is unstable just like other *polythionic acids*, although polythionate salts can be prepared as follows:

Trithionate (n = 1): Condensation of SCl_2 with $[HSO_3]^-$ ions

$$SCl_2 + 2\,[HSO_3]^- \xrightarrow{H_2O} [S_3O_6]^{2-} + 2\,HCl$$

82 R. Steudel, Y. Steudel, *J. Phys. Chem. A* **2009**, *113*, 9920 and 11096.

Tetrathionate ($n = 2$): Oxidation of $[S_2O_3]^{2-}$ by I_2 (see above)

Pentathionate ($n = 3$): Condensation of SCl_2 with $[HS_2O_3]^-$ ions

$$SCl_2 + 2\,[HS_2O_3]^- \xrightarrow{H_2O} [S_5O_6]^{2-} + 2\,HCl$$

Hexathionate ($n = 4$): Condensation of S_2Cl_2 with $[HS_2O_3]^-$ ions

$$S_2Cl_2 + 2\,[HS_2O_3]^- \xrightarrow{H_2O} [S_6O_6]^{2-} + 2\,HCl$$

Polythionates have been isolated as colorless salts of alkali and alkaline earth metals. They occur in crater lakes of volcanoes in concentrations of up to 4 g L^{-1} and with n = 4–6. They play a role in the geobiochemical sulfur cycle since certain sulfur bacteria oxidize polythionates to sulfate. Formal derivatives of the pentathionate ion are the anions $[Se(SSO_3)_2]^{2-}$ and $[Te(SSO_3)_2]^{2-}$ in which the central sulfur atom has been replaced by Se or Te. Aqueous polythionates can be separated and determined by ion chromatography.

Sulfane monosulfonic acids $HS–S_n–SO_3H$ ($n \geq 1$) are intermediates in many reactions of thiosulfate and of polythionates but are unstable and can neither be prepared in pure form nor in the form of salts. Only the hydrogen thiosulfate anion in $[NH_4][HS_2O_3]$ is known as crystalline material (see above).

12.11.9 Dithionic Acid, $H_2S_2O_6$

Dithionic acid is known only in aqueous solution, but salts have been prepared by oxidation of hydrogen sulfite, for example with manganese(IV) oxide MnO_2:

$$2\,[HSO_3]^- \longrightarrow [S_2O_6]^{2-} + 2\,H^+ + 2\,e^-$$

$$2\,MnO_2 + 3\,SO_2 \longrightarrow Mn[S_2O_6] + Mn[SO_4]$$

In this one-electron oxidation reaction, the radical $[HSO_3]^\bullet$ is an intermediate, which dimerizes to the centrosymmetric dithionate anion:

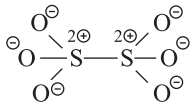

The oxidation of sulfite to dithionate by iron and manganese ions is an unwanted side-reaction during wet flue-gas desulfurization using the gypsum process described in Section 12.10.1.

Reaction of $Ba[S_2O_6]$ with dilute sulfuric acid yields aqueous $H_2S_2O_6$ as the by-product $Ba[SO_4]$ is insoluble and can thus be filtered off. Dithionic acid is a medium strong diprotic acid that disproportionates in solution at temperatures above 50 °C:

$$H_2S_2O_6 \longrightarrow H_2SO_4 + SO_2$$

Dithionates decompose in an analogous manner to sulfates and SO_2 on heating to temperatures above 200 °C.

12.11.10 Dithionous Acid, $H_2S_2O_4$

Dithionites are important industrial reducing and bleaching agents. The sodium salt is produced commercially by reduction of aqueous hydrogen sulfite by sodium amalgam, sodium formate, sodium boranate, zinc dust or electrochemically:

$$2\,[HSO_3]^- + 2\,e^- \longrightarrow [S_2O_4]^{2-} + 2\,[OH]^-$$

$$2\,SO_2 + Na[HCOO] + NaOH \longrightarrow Na_2[S_2O_4] + CO_2 + H_2O$$

The product (used in the textile and paper industries) crystallizes from the solution as $Na_2[S_2O_4]\cdot 2H_2O$, which can be dehydrated in vacuo or by recrystallization from anhydrous methanol. Dithionous acid[83] cannot be isolated under ambient conditions since dithionite solutions decompose when acidified:

$$2\,[S_2O_4]^{2-} + H_2O \xrightarrow{H^+} 2\,[HSO_3]^- + [S_2O_3]^{2-}$$

The anion of anhydrous $Na_2[S_2O_4]$ has a *cis*-configuration (a) due to interaction with the cations, while the dihydrate $Na_2[S_2O_4]\cdot 2H_2O$ contains the anion in a *gauche*-conformation (b):

(a) 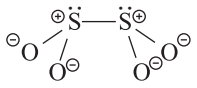

(b) 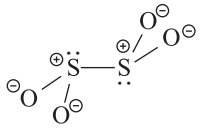

In solution the energetically more favorable *trans*-conformation of C_{2h} symmetry has been observed spectroscopically. In all crystalline dithionites, the SS bond is extremely long (239 pm in $Na_2[S_2O_4]$) and therefore easy to cleave homolytically. In fact, in solutions the dianion is in equilibrium with two radical monoanions:

$$[S_2O_4]^{2-} \rightleftharpoons 2\,[SO_2]^{\bullet -}$$

The $[SO_2]^{\bullet -}$ radical is of C_{2v} symmetry and isoelectronic with the ClO_2 molecule. The unpaired electron occupies an antibonding MO mainly located at the sulfur (chlorine) atom. Therefore, the central SS bond in dithionites is rather weak and long.

83 For the calculated gas phase structure, see: Y. Drozdova et al., *J. Chem. Phys. A* **1998**, *106*, 990.

The concentration of $[SO_2]^{\bullet-}$ in solution has been determined by ESR spectroscopy. The dissociation constant of $[S_2O_4]^{2-}$ in water at 25 °C is $1.4{\cdot}10^{-6}$ mol L^{-1}, and a 1 M sodium dithionite solution contains $1.2{\cdot}10^{-3}$ mol L^{-1} radical anions. In polar organic solvents such as DMF, DMSO and MeCN[84] the above equilibrium is even on the right-hand side. Therefore, dithionite solutions are very sensitive to O_2 since the law of spin conservation is obeyed if the radicals react primarily with triplet O_2 molecules rather than the dianion:

$$[S_2O_4]^{2-} + O_2 + H_2O \rightarrow [HSO_3]^- + [HSO_4]^-$$

12.11.11 Disulfane Dithionous Acid, $H_2S_4O_4$

The *polythionite* anion $[O_2S{-}S{-}S{-}SO_2]^{2-}$ is the only known example of this class of compounds; it has been prepared with $[TDAE]^{2+}$ as a counter ion by reduction of gaseous SO_2 with the electron donor tetrakis(dimethylamino)ethylene (TDAE) in acetonitrile.[85] The primary product is the purple dithionite $[TDAE][S_2O_4]$, which partly disproportionates in solution to the orange tetrathionite $[TDAE][S_4O_4]$ and the colorless disulfite $[TDAE][S_2O_5]$. In the nearly cubic crystal structure of $[TDAE][S_4O_4]$ the chain-like anions are partially disordered with three very different SS bond lengths: a short central bond of 200.3 pm is flanked by substantially longer neighboring bonds of 233.7 pm and – at the disordered side – 225.4 pm. The SSSS torsion angle is 87.4°. This structure can be regarded as composed of a central triplet-state S_2 molecule and two $[SO_2]^{\bullet-}$ radical anions, which share their unpaired electrons in π^* orbitals to form two weak σ bonds $S{-}SO_2$. As a result, the central bond increases in length from 189.2 pm in S_2 to 200.3 pm in the tetrathionite anion.

Thermodynamic calculations show that the ion $[S_4O_4]^{2-}$ is stable at 25 °C toward loss of sulfur and formation of dithionite only with large cations, and it has been suggested that the preparation of more polythionites can be expected in the future.[5] The free acid $H_2S_4O_4$ is unknown.

12.12 Halides and Oxohalides of the Chalcogens

12.12.1 Introduction

Important halides of the chalcogens are listed in Table 12.5. All chalcogens (E) form binary halides EX_2 due to their valence electron shell configuration of $s^2p_x^2p_y^1p_z^1$.

84 DMF: dimethyl formamide, DMSO: dimethyl sulfoxide, MeCN: acetonitrile.

85 J. Passmore et al., *Inorg. Chem.* **2013**, *52*, 13651.

Table 12.5: Important halides of the chalcogens. Compounds in parentheses are known in the gas phase or in solution only. Tellurium halides of oxidation number <+2 are partly polymeric.

Oxidation number:	**< +2**	**+2**	**+4**	**+5**	**+6**
Sulfur:	S_2F_2	(SF_2)	SF_4	S_2F_{10}	SF_6
	S_2Cl_2	SSF_2	SCl_4		$SClF_5$
	S_2Br_2	SCl_2			$SBrF_5$
	(S_2I_2)				
	S_nCl_2				
Selenium:	Se_2Cl_2	($SeCl_2$)	SeF_4		SeF_6
	Se_2Br_2	($SeBr_2$)	$SeCl_4$		$SeClF_5$
	(Se_2I_2)		$SeBr_4$		
Tellurium:	Te_3Cl_2	($TeCl_2$)	TeF_4		TeF_6
	(Te_2Cl_2)	($TeBr_2$)	$TeCl_4$		$TeClF_5$
	Te_2Cl	(TeI_2)	$TeBr_4$		$TeBrF_5$
	Te_2Br		TeI_4		
	Te_2I				
	TeI				

However, by multiple-center bonds tetra- and hexahalides can be obtained (see Section 2.6). In addition, halides with E–E bonds are known too, for example, S_2F_{10}, Se_2Br_2 and the polymeric TeI.

The molecular structures of the compounds listed in Table 12.5 cannot always be derived from the stoichiometric composition since seemingly analogous species may have quite different structures. For example, SF_4 is a gas consisting of molecules of C_{2v} symmetry, SCl_4 exists only below –30 °C as ionic crystal $[SCl_3]^+Cl^-$ and monoclinic $TeCl_4$ consists of Te_4Cl_{16} units in which four $[TeCl_3]^+$ cations are connected by four bridging tri-coordinate chloride anions resulting in a coordination number 3 + 3 for the tellurium atoms.

From Table 12.5 it follows that stable chalcogen halides are mainly formed with fluorine and chlorine while iodides of sulfur and selenium[86] exist only in rare cases. The tellurium-rich lower halides of compositions Te_2X (X = Cl, Br, I) and TeI are polymeric.[87] Te_2Cl_2 und Te_2Br_2 are instable and have been detected spectroscopically in solutions only. Most binary chalcogen halides are synthesized directly from the elements.

86 T. Klapoetke, J. Passmore, *Acc. Chem. Res.*, **1989**, *22*, 234–240.

87 Z. Xu, *in: Handbook of Chalcogen Chemistry*, Chapter 8.1, Royal Society of Chemistry, London, **2006**, 457.

12.12.2 Sulfur Halides

12.12.2.1 Fluorides

Sulfur burns in fluorine gas in an extremely exothermic reaction to hexafluoro-λ^6-sulfane or simply sulfur hexafluoride SF_6, which is industrially produced in this way on a large scale:

$$\frac{1}{8}S_8 + 3\,F_2 \longrightarrow SF_6 \qquad \Delta H^\circ_{298} = -1220\ \text{kJ mol}^{-1}$$

Even fluorination of SO_2 with F_2 yields SF_6:

$$SO_2 + 3\,F_2 \longrightarrow SF_6 + O_2$$

The strong bonds of the two molecules on the right-hand side of this equation compared to the weak bond in the fluorine molecule (155 kJ mol^{-1}) accounts for the exothermic and exergonic nature of this reaction. The mean bond enthalpy of SF_6 is 328 kJ mol^{-1}, but for the homolytic cleavage of the first S–F bond even 396 kJ mol^{-1} are required.

Sulfur hexafluoride is a colorless, odorless, nontoxic gas (b.p. –64 °C). Because of its low dielectric constant and high chemical inertness, it is used as an electrical insulator in high-voltage switches and transformators as well as a protecting gas in metallurgy, especially with molten magnesium (world production of SF_6 ca. 10000 t/a). In the past SF_6 also served for thermal insulation in double and triple glass windows. Unfortunately, SF_6 is a very efficient and long-lived *greenhouse gas*, which should not be released to the atmosphere where its exclusively human-made concentration increased already from 1 ppt in 1975 to 8 ppt in 2008. The radiative forcing of SF_6 is 23500 times that of CO_2!

SF_6 is resistant to molten KOH (m.p. 410 °C), to steam at 500 °C and to O_2 even in electric discharges. This behavior is astonishing since the hydrolysis of SF_6 is strongly exergonic ($\Delta G° < 0$):

$$SF_6 + 4\,H_2O \longrightarrow H_2SO_4 + 6\,HF$$

The resistance of SF_6 toward nucleophilic reagents is explained by the steric and electrostatic shielding of the sulfur atom by the negatively charged fluorine atoms. They impede the approach of a negatively charged atom of a LEWIS base resulting in kinetic hindrance as expressed by the high activation energy. In contrast, SF_4 reacts readily with water. SF_6 can be reduced by certain metals (Na in liquid NH_3) and reacts with some metal compounds such as $AlCl_3$ at moderate conditions and can be completely destroyed at 80 °C by a phosphane(R_3P)/silane($HSiR_3$) mixture yielding R_3PS and $FSiR_3$ in the presence of the rhodium complex $(Et_3P)_3RhH$ as a catalyst.[88]

88 T. Braun, B. Braun, *Angew. Chem. Int. Ed.* **2014**, *53*, 2745.

Derivatives of sulfur hexafluoride of type RSF_5 cannot be produced from SF_6 but are obtained from SF_4 or $SClF_5$, which are both much more reactive (see below).

Sulfur tetrafluoride SF_4 is a colorless, highly reactive gas prepared by fluorination reactions of commercial sulfur compounds:

$$\frac{1}{8}S_8 + 4\,CoF_3 \xrightarrow{130°C} SF_4 + 4\,CoF_2$$

$$3\,SCl_2 + 4\,NaF \xrightarrow[75°C]{MeCN} SF_4 + S_2Cl_2 + 4\,NaCl$$

The molecule SF_4 constitutes a trigonal bipyramid of C_{2v} symmetry with a lone pair in an equatorial position. Therefore, the low-temperature ^{19}F-NMR spectrum (–98 °C) of SF_4 consists of two signals for the two pairs of nonequivalent F atoms. At 25 °C only one signal is observed, which indicates rapid *pseudorotation* as in the case of PF_5 (Section 10.8.3); the activation energy for this intramolecular process is 25 kJ mol^{-1}.

The tetrafluoride reacts rapidly with water to SO_2 and HF via SOF_2 as an intermediate. With fluorides having large cations pentafluorosulfates(IV) are formed:

$$CsF + SF_4 \longrightarrow Cs[SF_5]$$

The $[SF_5]^-$ ion is a pseudo-octahedron with one corner occupied by a lone pair of electrons. On the other hand, strong fluoride ion acceptors abstract a fluoride ion from SF_4 yielding trifluorosulfonium salts:

$$SF_4 + BF_3 \longrightarrow [SF_3][BF_4]$$

The trigonal-pyramidal $[SF_3]^+$ cation is isoelectronic with PF_3. In the presence of NO_2, SF_4 reacts with O_2 to thionyl tetrafluoride SOF_4. For reasons of *spin conservation*, the uncatalyzed reaction is extremely slow. NO_2 serves as an oxygen transfer reagent, which is reduced by SF_4 to NO; the latter is in turn re-oxidized to NO_2 by O_2.

SF_4 is a strong and selectively reacting fluorinating agent, specifically for carbonyl and thiocarbonyl compounds:

$$R_2C{=}O + SF_4 \longrightarrow R_2CF_2 + SOF_2$$

This important reaction is used to introduce fluorine atoms into organic molecules. Inorganic oxides and sulfides can likewise be turned into fluorides:

$$I_2O_5 + 5\,SF_4 \longrightarrow 2\,IF_5 + 5\,SOF_2$$

SF_4 adds to many reactive compounds, sometimes with insertion into weak bonds:

$$R{-}C{\equiv}N + SF_4 \longrightarrow R{-}CF_2{-}N{=}SF_2$$

$$F_5S{-}O{-}O{-}SF_5 + SF_4 \longrightarrow F_5S{-}O{-}SF_4{-}O{-}SF_5$$

The iminium salt $[R_2N{=}SF_2][BF_4]$ is a commercial fluorinating agent.

Fluorination of SF_4 yields SF_6, and chlorofluorination by ClF in the presence of CsF results in $SClF_5$; these reactions are examples for *oxidative additions*:

$$SF_4 + ClF \xrightarrow{380°C} SClF_5$$

$$SF_4 + Cl_2 + CsF \xrightarrow{110°C} SClF_5 + CsCl$$

Sulfur chloride pentafluoride (b.p. –21 °C) is much more reactive than SF_6 due to the much lower bond enthalpy of the SCl bond in comparison to SF bonds. Therefore, $SClF_5$ undergoes radical reactions and it is hydrolyzed much more rapidly, that is, attacked by nucleophiles. In addition, $SClF_5$ is a strong oxidizing agent. At 400 °C, $SClF_5$ decomposes via SF_5 radicals to SF_4, SF_6 and Cl_2; the same reaction occurs on UV irradiation:

$$2\ SClF_5 \longrightarrow SF_4 + SF_6 + Cl_2$$

$SClF_5$ and $SBrF_5$ are used to incorporate SF_5 groups into unsaturated molecules by addition reactions:[89]

$$SClF_5 + C_2F_4 \longrightarrow F_5S{-}CF_2{-}CF_2{-}Cl$$

$$2\ SClF_5 + O_2 \xrightarrow{h\cdot\nu} F_5S{-}O{-}O{-}SF_5 + Cl_2$$

Hydrogen reduces $SClF_5$ as well as $SBrF_5$ on irradiation in a quartz vessel to the extremely toxic disulfurdecafluoride:

$$2\ SClF_5 + H_2 \longrightarrow F_5S{-}SF_5 + 2\ HCl$$

On heating, S_2F_{10} (b.p. 30 °C) dissociates homolytically at the SS bond, which is much longer (227 pm) than ordinary single SS bonds as in S_8 (205 pm). Reaction of S_2F_{10} with Cl_2 or Br_2 yields $SClF_5$ and $SBrF_5$, respectively. S_2F_{10} decomposes at 150–200 °C to SF_4 and SF_6.

12.12.2.2 Lower Sulfur Fluorides

The isomeric fluorides FSSF and SSF_2 are most interesting since they both contain SS double bonds. They are conveniently prepared by fluorination of either S_8 by AgF or of S_2Cl_2 by $K[SO_2F]$, respectively:

89 P. R. Savoie, J. T. Welch, *Chem. Rev*. **2015**, *115*, 1130-1190.

$$\frac{3}{8}\,S_8 + 2\,AgF \xrightarrow{125°C} FSSF + Ag_2S$$

$$S_2Cl_2 + 2\,K[SO_2F] \longrightarrow SSF_2 + 2\,KCl + 2\,SO_2$$

The chain-like difluorodisulfane FSSF (C_2 symmetry) is a colorless gas (b.p. 15 °C) that isomerizes to thiothionylfluoride SSF_2 (b.p. –11 °C; C_s symmetry) on contact with alkali fluorides. The latter compound disproportionates on warming to S_8 and SF_4. The short SS bonds of these fluorides (186–189 pm) can be explained by the following LEWIS structures:

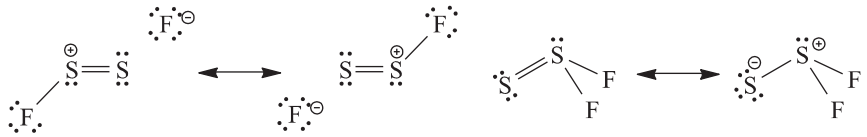

The SS double bonds are stabilized by the high positive charges at the central sulfur atoms, but in FSSF also by the (negative) *hyperconjugation* between the sulfur 3*p* lone pair and the empty σ* MOs at the nonadjacent SF bonds. Therefore, the SF bonds of FSSF are unusually long. In analogy to FOOF (Section 11.4.3), there are two coordinate π bonds at the SS axis.[90]

The two fluorides FSSF and SSF_2, the oxide S_2O and organic thionosulfites $(RO)_2S{=}S$[91] have all been prepared in the 1960s and have been the first examples of compounds with *multiple bonds between heavier nonmetallic elements* and reasonable thermal stability at 25 °C.

12.12.2.3 Chlorides, Bromides and Iodides[92]

Chlorination of elemental sulfur by Cl_2 at 25 °C yields mixtures of chain-like dichlorosulfanes by stepwise cleavage of the bonds of S_8:

$$-S-S- + Cl_2 \longrightarrow -S-Cl + Cl-S-$$

The products formed depend on the molar ratio. Primary product is Cl–S_8–Cl, obtained by ring opening, but with enough chlorine the final product is S_2Cl_2, which can be further chlorinated by an excess of Cl_2 in the presence of $FeCl_3$ as catalyst to give SCl_2 (b.p. 60 °C). SCl_2 is a red-brown liquid, which fumes in moist air, and can

90 R. Steudel et al., *J. Am. Chem. Soc.* **1997**, *119*, 1990.

91 D. N. Harpp et al., *J. Am. Chem. Soc.* **2006**, *128*, 291, and references cited therein.

92 H.-D. Lauss, W. Steffens, in *Ullmann's Encycl. Ind. Chem.*, online edition, Wiley, Weinheim, **2000**.

be purified by distillation. At 25 °C, it slowly equilibrates with the two starting compounds:

$$2\ SCl_2 \rightleftharpoons S_2Cl_2 + Cl_2$$

Therefore, the commercial product "SCl_2" contains considerable concentrations of S_2Cl_2 and Cl_2 and needs to be distilled directly prior to use (with addition of little PCl_3 to suppress new equilibration).

Dichlorodisulfane S_2Cl_2 is a straw-yellow liquid of pungent odor (b.p. 138 °C), which just like other sulfur chlorides hydrolyzes with water in a complex reaction to HCl, H_2S, S_8, SO_2 and sulfur oxoacids. S_2Cl_2 reacts with many elements, oxides and sulfides under formation of the corresponding chlorides but heating is required in most cases. Reaction of S_2Cl_2 with organic compounds results in sulfurization or chlorination or both.

Sulfur-rich chlorides S_nCl_2 (n = 3–8) can also be prepared by condensation of SCl_2 or S_2Cl_2 with hydrogen sulfide or higher sulfanes:

$$Cl{-}S_2{-}Cl + H{-}S_n{-}H + Cl{-}S_2{-}Cl \longrightarrow Cl{-}S_{n+4}{-}Cl + 2\ HCl$$

On the other hand, careful chlorination of the homocycles S_6, S_7 and S_8 at low temperatures in solution produces almost pure dichlorosulfanes $S_{6-8}Cl_2$, which after evaporation of the solvent are obtained as yellow to orange oily liquids.

SCl_2 and S_2Cl_2 are important industrial products. SCl_2 is oxidized by O_2 or SO_3 to $SOCl_2$ and SO_2Cl_2. All chlorosulfanes react with nonmetal hydrides with liberation of HCl and formation of novel element–sulfur bonds. Reaction with HBr yields *dibromosulfanes*:

$$S_nCl_2 + 2\ HBr \longrightarrow S_nBr_2 + 2\ HCl$$

The molecule SCl_2 is bent (C_{2v} symmetry), while S_2Cl_2 is of C_2 symmetry like H_2O_2. The sulfur-rich dichlorosulfanes are probably of similar structures as the isoelectronic polysulfide anions (Figure 12.9). Crystal structures of S_nCl_2 (n = 3–8) are not known since these species tend to solidify as glasses rather than single crystals, probably due to different conformations present in the liquid phase.

At −78 °C, SCl_2 reacts with liquid chlorine to colorless crystals of SCl_4, which decomposes back to the starting materials at −30 °C. SCl_6 in analogy to SF_6 is not known. SCl_4 does not consist of molecules like SF_4 but of trichlorosulfonium cations bridged by chloride anions, $[SCl_3]^+Cl^-$. Other salts with the pyramidal cation $[SCl_3]^+$ are: $[SCl_3][AlCl_4]$ and $[SCl_3][AsF_6]$. Organic sulfenyl trichlorides $RSCl_3$ obtained from disulfanes and an excess of Cl_2 via sulfenylchloride (RSCl) intermediates are related compounds. Thermally more stable than these trichlorides are the corresponding fluorides RSF_3.

Binary **sulfur iodides** exist only in solution since they tend to liberate I_2 with concomitant formation of elemental sulfur. Thus, S_2Cl_2 dissolved in CS_2 reacts with aqueous potassium iodide primarily in a halogen exchange reaction to S_2I_2 followed by spontaneous formation of mainly even-membered sulfur rings with S_6 as the main product, which has been isolated in 36% yield. Evidently a stepwise build-up of sulfur chains occurs until the chains are sufficiently long for ring closure:

$$S_2Cl_2 + 2\,KI \longrightarrow S_2I_2 + 2\,KCl$$
$$2\,S_2I_2 \longrightarrow S_4I_2 + I_2$$
$$S_2I_2 + S_4I_2 \longrightarrow S_6I_2 + I_2$$
$$S_6I_2 \longrightarrow \textit{cyclo}\text{-}S_6 + I_2$$

12.12.3 Sulfur Oxohalides

In thionyl halides SOX_2 (X = F, Cl, Br), the oxidation number of sulfur is +4. Formally, they are acid halides of sulfurous acid and of pyramidal geometry (C_s symmetry). Thionyl chloride $SOCl_2$ is the most important and is produced industrially by oxidation of SCl_2 with either SO_3 or SO_2Cl_2. In the laboratory, it may be synthesized by chlorination of SO_2 by PCl_5 with simultaneous oxygen transfer followed by fractionating distillation:

$$SO_2 + PCl_5 \longrightarrow SOCl_2 + POCl_3$$

$SOCl_2$ (b.p. 76 °C) is a colorless liquid that reacts rapidly with water to SO_2 and HCl, and with other compounds containing OH, NH or SH groups with elimination of HCl. In organic chemistry $SOCl_2$ is one of the most important *chlorination agents*. Other thionyl halides are obtained by halogen exchange reactions:

$$SOCl_2 \xrightarrow[MeCN]{+\,NaF,\,-\,NaCl} SOClF \xrightarrow[MeCN]{+\,NaF,\,-\,NaCl} SOF_2$$

$$SOCl_2 \xrightarrow[\text{liquid } SO_2]{+\,KBr,\,-\,KCl} SOBrCl \xrightarrow[\text{liquid } SO_2]{+\,KBr,\,-\,KCl} SOBr_2$$

Sulfuryl halides SO_2X_2, disulfuryl halides $S_2O_5X_2$, thionyl tetrafluoride SOF_4 and some other derivatives of SF_6 contain sulfur in the oxidation state +6. Sulfuryl fluoride SO_2F_2, the difluoride of sulfuric acid, is prepared by heating solid $Ba[SO_3F]_2$ prepared from $BaCl_2$ and HSO_3F:

$$Ba[SO_3F]_2 \xrightarrow{\Delta T} Ba[SO_4] + SO_2F_2$$

Sulfuryl difluoride (b.p. –55 °C) can also be obtained from SO_2Cl_2 by halogen exchange with NaF. SO_2Cl_2 is a colorless liquid (b.p. 69 °C) prepared industrially by addition of Cl_2 to SO_2 using activated carbon as a catalyst. SO_2Cl_2 is used to introduce the groups –Cl and $-SO_2Cl$ into organic molecules (*sulfochlorination*). Water decomposes sulfuryl halides to sulfuric acid and HX, and with ammonia sulfuryl diamide $SO_2(NH_2)_2$ (*sulfamide*; m.p. 92 °C) is formed; this diamide of sulfuric acid can be protonated by anhydrous superacids such as $HF{\cdot}BF_3$ and $HF{\cdot}SbF_5$ to yield the salts $[H_2N\text{-}SO_2\text{-}NH_3][BF_4]$ and $[H_3N\text{-}SO_2\text{-}NH_3][SbF_6]_2$, respectively.

Peroxodisulfurylfluorid $S_2O_6F_2$, the fluoride of peroxomonosulfuric acid, is a formal derivative of $S_2O_5F_2$ in which the bridging oxygen atom is replaced by a peroxo group. $S_2O_6F_2$ (b.p. 67 °C) is prepared by addition of F_2 to SO_3 in the presence of AgF_2:

$$SO_3 + F_2 \longrightarrow F{-}SO_2{-}O{-}F \xrightarrow{+\,SO_3} F{-}SO_2{-}O{-}O{-}SO_2{-}F$$

In this remarkable reaction, elemental fluorine oxidizes the two bridging oxygen atoms from oxidation number –2 in SO_3 to –1 in the peroxide. The intermediate product SO_3F_2 (b.p. –31 °C) is a hypofluorite but is usually termed as *fluorine fluorosulfate* although it does *not* contain positively polarized F atoms. Fluorosulfates of the other halogens are prepared from peroxodisulfuryl fluoride:

$$Cl_2 + S_2O_6F_2 \longrightarrow 2\,Cl(OSO_2F)$$

$$Br_2 + 2\,S_2O_6F_2 \longrightarrow Br(OSO_2F) + Br(OSO_2F)_3$$

$$I_2 + S_2O_6F_2 \longrightarrow I(OSO_2F),\ I_3(OSO_2F),\ I(OSO_2F)_3$$

In these compounds the heavier halogen atoms are in oxidation states +1 or +3, respectively, since they are linked to a more electronegative oxygen atom.

Fluorination of SOF_2 at 150 °C in the presence of Pt yields thionyl tetrafluoride, which can be further fluorinated in the presence of CsF to pentafluoro sulfur hypofluorite:

$$\overset{\ominus}{O}{-}\overset{\oplus}{S}F_2 + F_2 \xrightarrow{Pt} \overset{\ominus}{O}{-}\overset{\oplus}{S}F_4 \xrightarrow{+\,CsF,\,+\,F_2} FO{-}SF_5$$

Both fluorides are very reactive colorless gases; $FOSF_5$ has been used for the preparation of numerous derivatives.

12.12.4 Selenium and Tellurium Halides

12.12.4.1 Fluorides[87,93]

The fluorides of selenium and tellurium (Table 12.5) are analogous to those of sulfur as far as compositions are concerned, but structures and reactivities may be quite different. For example, the colorless toxic gaseous hexafluorides, formed on burning of the elements in fluorine, are more reactive than SF_6. Tellurium hexafluoride hydrolyzes slowly with liquid water already at 25 °C. Due to the larger radius of the Te atom, the attack of nucleophiles is less hindered than in SF_6. Therefore, TeF_6 is a weak LEWIS acid reacting with two equivalents of $[Me_4N]F$ at 0 °C to $[Me_4N]_2[TeF_8]$ and with amines to donor–acceptor complexes of type $[R_3N]_2TeF_6$, containing eight-coordinate Te atoms.

SeF_4 is a colorless liquid (m.p. –10 °C, b.p. 106 °C) formed by fluorination of elemental selenium in an F_2/N_2 mixture or with ClF_3. In organic chemistry, SeF_4 is used as a fluorinating agent that is easier to handle than gaseous SF_4. Gaseous SeF_4 has a structure analogous to SF_4. In the solid state, the Se atom exhibits in principle also *pseudo*-trigonal bipyramidal coordination but with bridging F atoms to neighboring molecules. However, these intermolecular interactions are weak and the Se···F bridges are long. In other words, SeF_4 is approximately monomeric in all phases. Solid TeF_4 (m.p. 130 °C) contains square-pyramidal TeF_5 units interconnected by two *cis*-bridging F atoms forming infinite chains through corner sharing. The geometry of the TeF_5 group is consistent with steric activity of the lone electron pair, and the arrangement can be described as a distorted octahedral coordination of the tellurium atom by five fluorine ligands and the lone pair.

The lower fluorides SeF_2, FSeSeF and $Se{=}SeF_2$ have been prepared in minute amounts and studied spectroscopically but they are too unstable to be of any practical importance.

12.12.4.2 Selenium Chlorides and Bromides[87]

The less stable chalcogen halides given in parentheses in Table 12.5 can often be prepared in solution as stable adducts with LEWIS bases and are then available for chemical reactions. In this way, the unstable selenium dichloride $SeCl_2$ has become a useful reagent for synthesis of organoselenium compounds and nitrogen–selenium heterocycles. It is prepared by treating elemental selenium with an equimolar amount of SO_2Cl_2 in THF or dioxane. In this solution $SeCl_2$ is stable for 1 day at 23 °C but has been stabilized as crystalline *bis*-adduct with THF that can be stored at –20 °C for weeks without decomposition. There is also a 1:2 adduct with tetrahydrothiophene.[94]

93 R. Kniep, A. Rabenau, *Top. Curr. Chem.* **1983**, *111*, 145. A. Engelbrecht, F. Sladky, *Adv. Inorg. Chem. Radiochem.* **1981**, *24*, 189.

94 A. Maaninen et al., *Inorg. Chem.* **1999**, *38*, 4093.

Selenium chlorides and bromides of type Se_2X_2 (X = Cl, Br) are well-characterized useful reagents for many synthetic applications. The molecules are of C_2 symmetry with torsion angles near 85°. In the liquid state, Se_2Cl_2 equilibrates with minor concentrations of $SeCl_2$ on the one hand and higher dichloroselanes Se_nCl_2 (n = 3, 4) on the other hand. Se_2Cl_2 is prepared as a dark-red oily liquid by comproportionation of Se with SeO_2 in concentrated HCl:

$$SeO_2 + 3\,Se + 4\,HCl \xrightarrow{-2H_2O} 2\,Se_2Cl_2 \rightleftharpoons SeCl_2 + Se_3Cl_2$$

Chlorination of elemental selenium by Cl_2 at 25 °C yields $SeCl_4$, which forms pale-yellow crystals consisting of cubane-like Se_4Cl_{16} clusters that can be sublimed at about 195 °C. The molecular structure consists of pyramidal $[SeCl_3]^+$ ions bridged by four chloride anions each. The coordination numbers are 3 + 3 for Se and 3 for the bridging Cl atoms. In the vapor phase $SeCl_4$ is almost completely dissociated into $SeCl_2$ and Cl_2. $SeCl_4$ is both a donor and an acceptor for chloride ions. In aqueous solution, it reacts with $[NH_4]Cl$ to the intense yellow hexachloroselenate(IV) $[NH_4]_2[SeCl_6]$, which crystallizes upon acidification by HCl gas:

$$SeO_2 + 4\,HCl \xrightarrow{-2\,H_2O} SeCl_4 \xrightarrow{+2\,[NH_4]Cl} [NH_4]_2[SeCl_6]$$

On the other hand, $SeCl_4$ reacts with $AlCl_3$ at reflux in SO_2Cl_2 to yellow crystals of $[SeCl_3][AlCl_4]$ in which each Se atom is coordinated by three closest Cl neighbors at a distance of 211 pm and three anionic chloride ions at a distance of 304 pm (distorted octahedron). In other words, cations and anions are linked both by ionic and covalent interactions. Selenenyl dichloride $SeOCl_2$ is another important Se(IV) halide obtained from SeO_2 and refluxing thionyl chloride:

$$SeO_2 + SOCl_2 \rightarrow SeOCl_2 + SO_2$$

$SeCl_4$ occurs as an intermediate in this reaction. $SeOCl_2$ can be turned into $SeOF_2$ by halogen exchange with KF.

12.12.4.3 Tellurium Chlorides and Bromides[87,93]

Tellurium halides of type Te_2X_2 (X = Cl, Br) are prepared by reducing elemental tellurium with superhydride $Li[BHEt_3]$ to lithium telluride followed by comproportionation with the corresponding tellurium tetrahalide. The dichloride Te_2Cl_2 is a yellow liquid, and the dibromide Te_2Br_2 an orange-red liquid; both have been characterized by ^{125}Te-NMR spectroscopy (just one signal each) and by derivatization reactions, but the exact molecular structures are unknown.

The crystal structure of $TeCl_4$ consists of cubane-like molecules Te_4Cl_{16} in which pyramidal $[TeCl_3]^+$ ions are bridged by chloride anions resulting in a distorted octahedral coordination just as in $SeCl_4$. $TeCl_4$ (m.p. 223 °C) is prepared from

the elements. $TeCl_6$ is unknown and $TeCl_2$ exists only in the vapor phase: if $TeCl_4$ or mixtures of Te and $TeCl_4$ are heated the bent molecule $TeCl_2$ can be detected spectroscopically in the gas phase (the same holds for $TeBr_2$):

$$TeCl_4 \rightleftharpoons TeCl_2 + Cl_2 \qquad \Delta H^\circ = 119\ \text{kJ mol}^{-1}$$

$$Te + TeCl_4 \rightleftharpoons 2\ TeCl_2$$

$TeCl_4$ has been used to synthesize *hypercoordinate organotellurium compounds*:[95]

$$TeCl_4 + 4\ MeLi \xrightarrow{-78^\circ C,\ Et_2O} Me_4Te + 4\ LiCl$$

$$Me_4Te + XeF_2 \xrightarrow{-30^\circ C} Me_4TeF_2 + Xe$$

$$Me_4TeF_2 + Me_2Zn \xrightarrow{0^\circ C,\ Et_2O} Me_6Te + ZnF_2$$

Hexamethyltellurium Me_6Te forms colorless crystals the bonding situation and stability of which have been discussed in Section 2.6. The thermally particularly stable derivative $(CF_3C_6H_4)_6Te$ is prepared by condensation of 4-$CF_3C_6H_4Li$ with $TeCl_4$;[96] it contains octahedrally coordinated Te atoms as in TeF_6.

12.12.4.4 Polymeric Tellurium Halides with Te–Te Bonds

The solid halides of composition TeX, Te_2X and Te_3Cl_2 (X = Cl, Br, I) are potential materials for electronic applications. These stable crystalline compounds benefit from intermolecular interactions resulting in higher coordination numbers of both the Te atoms and partly also of the bridging halogen atoms.[87,93] The crystal structure of Te_3Cl_2 consists of helical Te_n chains (as in elemental tellurium) but every third atom is linked to two chlorine atoms in a *pseudo*-trigonal bipyramidal coordination (taking the lone pair at Te into account). Thus, the representative structural unit is: $(–Te–Te–TeCl_2–)_n$; see Figure 12.11.

The solid halides of composition Te_2X consist of infinite chains of tellurium atoms with bridging and terminal halogen atoms and tellurium coordination numbers of 3 and 4 (Figure 12.11). In contrast, α-TeI consists of Te_4I_4 molecules forming a puckered four-membered Te_4 ring with four terminal iodine atoms that have relatively short Te···I contacts of 335–340 pm to neighboring molecules (Figure 12.11). Thus, it may be written as $(TeI)_4$. The band gaps of Te_3Cl_2 (1.52 eV) and α-TeI (1.32 eV) at 300 K are in the range of semiconductors but are larger than the band gap of elemental tellurium (0.34 eV).

95 W. R. McWhinnie, *Encycl. Inorg. Chem.* **1994**, *8*, 4117. M. Minoura et al., *Angew. Chem. Int Ed.* **1996**, *35*, 2660.

96 M. Minoura et al., *Tetrahedron* **1997**, *53*, 12195.

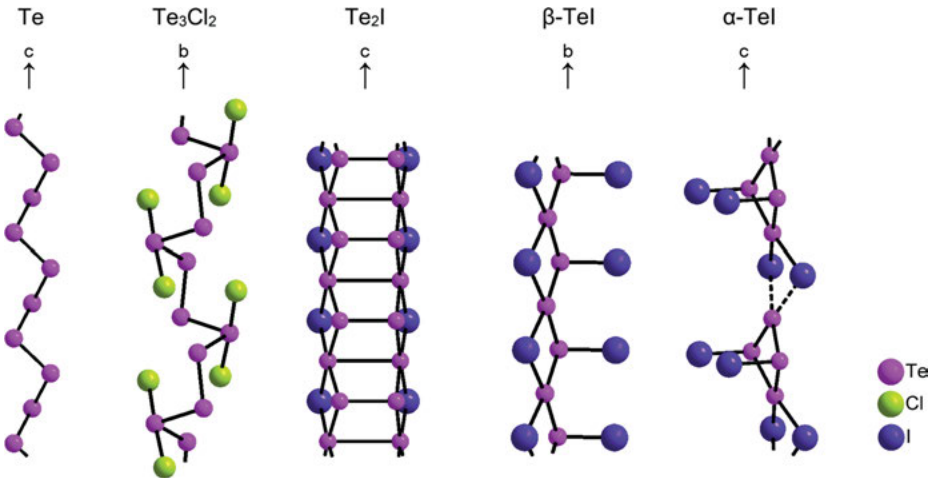

Figure 12.11: Structural units of the tellurium subhalides Te_3Cl_2, Te_2X, β-TeI and α-TeI (X = Cl, Br, I).

12.12.4.5 Halochalcogenate Anions

Formation of anions such as $[SeCl_6]^{2-}$, $[SeBr_6]^{2-}$, $[TeCl_6]^{2-}$, $[TeBr_6]^{2-}$ and $[TeI_6]^{2-}$ is a characteristic property of the heavier chalcogens, unlike sulfur.[97] They are prepared from the corresponding tetrahalides by addition of halide ions. In addition, there are numerous polynuclear chalcogenate(IV) anions, especially with tellurium. Examples are shown in Figure 12.12. Their structures can be derived from the tellurium tetrachloride structure by stepwise disintegration of the tetramer Te_4Cl_{16} through nucleophilic attack of the incoming chloride anions.

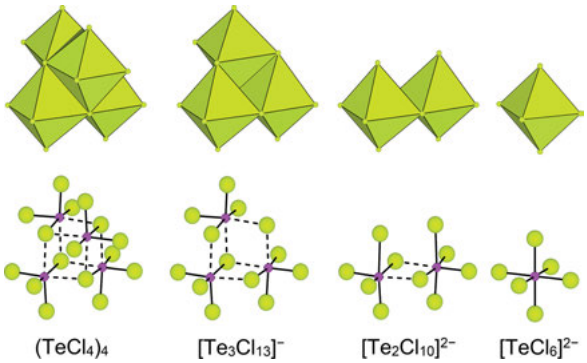

Figure 12.12: Molecular structures of polynuclear tellurium chloride species $(TeCl)_4$, $[Te_3Cl_{13}]^-$, $[Te_2Cl_{10}]^{2-}$ and $[TeCl_6]^{2-}$. Bottom: anion structures with covalent Te–Cl bonds and the longer bridging Te····Cl····Te bonds. Above: edge-sharing $TeCl_6$ octahedra.

97 B. Krebs, F. P. Ahlers, *Adv. Inorg. Chem.* **1990**, *35*, 235-317.

12.12.4.6 Bonding in Selenium and Tellurium Halides

The cations $[SeCl_3]^+$ and $[TeCl_3]^+$ are isoelectronic with the neutral chlorides $AsCl_3$ and $SbCl_3$ and all are of C_{3v} symmetry. The bridging of $[TeCl_3]^+$ ions in Te_4Cl_{16} by chloride ions can be explained by ionic interaction as well as by coordinate bonding between a LEWIS acid and a LEWIS base.

The strongly polarized covalent bonds in the octahedral molecules SeF_6 und TeF_6 are analogous to those in SF_6 since the electronegativities of S, Se and Te are not too different. The multicenter bonds in SF_6 have been discussed in Section 2.6 (see Figure 2.39). With increasing size of the central atom, the maximum possible coordination number increases as in $[TeF_7]^-$ (pentagonal bipyramid of symmetry D_{5h}) and in $[TeF_8]^{2-}$ (square antiprism of symmetry D_{4d}).

The ions $[SeX_6]^{2-}$ and $[TeX_6]^{2-}$ form regular octahedra although they are of type AX_6E and should be of lower symmetry than O_h according to the VSEPR model (Section 2.2). Evidently the lone pair (E) is stereochemically inactive and resides in a spherical *s*-type AO. The six bonds can be constructed from the three perpendicular *p* AOs by three-center four-electron σ type interactions as in SF_6 (Figure 2.41). On the other hand, the octahedral geometry is also enforced by the repulsion between the electron-rich and negatively charged substituents.

12.13 Sulfur–Nitrogen Compounds

Sulfur–nitrogen compounds contain the two elements in the following bonding situations, ordered by increasing coordination numbers of the sulfur atom:

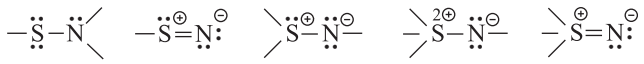

(a) (b) (c) (d) (e)

In addition, there are structures that are intermediates between some of these types, and it is not always trivial to draw a LEWIS type structures with an electron octet at sulfur; instead, "resonance structures" are sometimes needed to visualize the bonding situation. The oxidation numbers of sulfur range from 0 to +6 and the coordination numbers from 1 to 4. There are saturated and unsaturated sulfur–nitrogen compounds, and in addition to the covalent interaction there may be Coulomb attraction as evident from the formal charges shown above. Thus, "single" and "double" SN bonds are possible, but bond orders are questionable concepts as discussed in Chapter 4. The SN "double" bonds are characterized by shorter internuclear distances and higher stretching frequencies. To avoid the formal charges, bonding type (c) is sometimes written as >S=N–, and types (b) and (e) are simplified to a triple bond S≡N.

Numerous SN compounds are known; they are chain-like, cyclic or polycyclic species.[98] The majority consists of neutral molecules but both cationic and anionic species are also known. Only a few representative and interesting examples are mentioned here. Industrial applications of SN compounds have not been reported.

The best-known binary sulfur–nitrogen compound is the cage-like *tetrasulfur tetranitride*, which is formed in many reactions between sulfur halides and ammonia. In the laboratory, it is best prepared by passing gaseous ammonia into a cold solution of either SCl_2 or S_2Cl_2 in Cl_2-saturated CCl_4:

$$S_2Cl_2 + Cl_2 + NH_3 \longrightarrow S_4N_4, S_8, [NH_4]Cl$$

During this rather complex and exothermic redox reaction, some sulfur atoms are oxidized to the oxidation state +3, while others are reduced to elemental sulfur. The product mixture is washed with water to remove salts, and S_4N_4 is extracted from the residue by dioxane from which it is obtained as orange-yellow crystals (m.p. 178–187 °C, with decomposition). S_4N_4 is an *endothermic compound* ($\Delta_f H^o$ = 460 kJ mol^{-1}) that detonates on heavy impact, on strong heating and on grinding in a mortar.

In Figure 12.13 the molecular structure of S_4N_4 is shown, which contains a system of delocalized π electrons in three-center bonds. The SN bonds of 162 pm are much shorter than single bonds (176 pm; see Table 4.3). The closed-cage structure of the S_4N_4 molecule results from the two very long SS bonds of 258 pm that are much longer than the single bonds in S_8 (205 pm) but much shorter than the VAN DER WAALS distance (350 pm). No simple LEWIS structures can be drawn for molecules of this type.

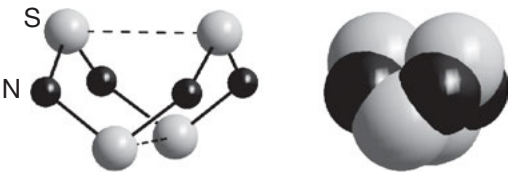

Figure 12.13: Molecular structure of tetrasulfur tetranitride S_4N_4 as ball-and-stick model and as space-filling model (D_{2d} symmetry). The sulfur atoms form a tetrahedron and the nitrogen atoms a square. All eight SN bonds are multiple bonds of identical length (162 pm), while the two very long SS bonds (258 pm) are partial bonds.

98 T. Chivers (ed.), *A Guide to Chalcogen-Nitrogen-Chemistry*, World Scientific, Singapore, **2004**. T. Chivers, *Encycl. Inorg. Chem.* **2005**, *8*, 5378.

S_4N_4 is a *highly reactive compound* and can thus be turned into numerous derivatives as shown in Figure 12.14. The simplest reaction is the thermal dissociation into two S_2N_2 molecules, catalyzed by elemental silver in the gas phase. Disulfur dinitride forms colorless crystals consisting of planar heterocycles of D_{2h} symmetry, which are valence-isoelectronic with the HÜCKEL-aromatic cation $[S_4]^{2+}$ (Figure 12.7). Reduction of S_4N_4 by tin(II) chloride yields colorless $S_4(NH)_4$ with a puckered crown-shaped ring structure similar to S_8. The SN bonds of $S_4(NH)_4$ (d_{SN} = 167 pm) are slightly shorter than single bonds; the coordination geometry at the nitrogen atoms is planar, in contrast to the pyramidal structure of ammonia. This indicates a partial delocalization of the nitrogen lone pairs into antibonding MOs of neighboring SN bonds (hyperconjugation).

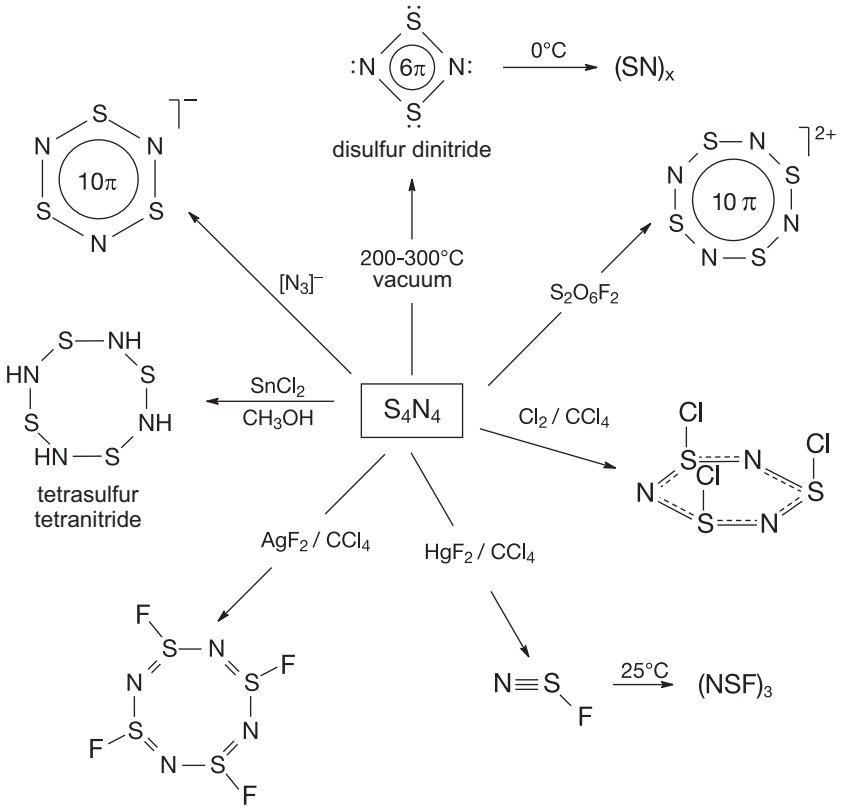

Figure 12.14: Representative reactions of tetrasulfur tetranitride S_4N_4.

Fluorination of S_4N_4 yields either crystalline $(NSF)_4$ or gaseous NSF, depending on the fluorinating agent employed (Figure 12.14). Further fluorination of NSF by AgF_2 gives NSF_3. The latter two fluorides have extremely short SN bonds corresponding

to the bonding situations (b) and (e) shown on page 591. NSF polymerizes at 25 °C within a few days to the heterocyclic $(NSF)_3$. The F atoms of $(NSF)_4$ are exocyclic and linked to sulfur atoms; consequently, there is no similarity to $S_4(NH)_4$. The nonplanar ring of $(NSF)_4$ has alternating bond lengths with d_{SN} = 154 and 166 pm.

Chlorination of S_4N_4 by Cl_2 yields primarily 1,5-$S_4N_4Cl_2$ (cleavage of one SS bond) and subsequently $(NSCl)_3$ by ring contraction (Figure 12.14). Reaction of $(NSCl)_3$ with the LEWIS acid $AlCl_3$ at 50 °C in CH_2Cl_2 results in thiazyl tetrachloroaluminate [SN][$AlCl_4$], a yellow salt the cation of which is valence-isoelectronic with the nitrosyl ion $[NO]^+$. The planar *cyclo*-tetrathiazyl cation $[S_4N_4]^{2+}$ of D_{4h} symmetry is obtained on oxidation of S_4N_4 with an excess of $S_2O_6F_2$ or $SbCl_5$. The cation $[S_4N_4]^{2+}$ is a HÜCKEL-aromatic system with 10 π electrons, six of which in bonding and four in antibonding MOs (d_{SN} = 155 pm). The *cyclo*-trithiazyl anion $[S_3N_3]^-$ is a similar 10 π electron system but of D_{3h} symmetry; it is prepared by reaction of S_4N_4 with ionic azides in the presence of a large cation (Figure 12.14).

The small aromatic heterocycle S_2N_2 polymerizes at 0 °C within several days in a solid-state reaction to brass-colored sulfur nitride $(SN)_x$ which has also been prepared in high yield from $(NSCl)_3$ and trimethyl silyl azide.[99] $(SN)_x$ forms fibrous crystals consisting of planar, parallel oriented zig-zag chains with slightly alternating bond lengths of 159 and 163 pm:

The one-dimensional infinite π electron system of $(SN)_x$ results in electrical conductivity, albeit highly anisotropic and thus at 25 °C approximately 50 times larger along the fibers than perpendicular to them. Depending on the purity of the material the conductivity at 25 °C is 4000 Ω^{-1} cm^{-1} and increases by a factor of 1000 on cooling to 4 K. Below 0.26 K $(SN)_x$ is even superconducting.[100] Thus, $(SN)_x$ is a *one-dimensional metal*.

The above examples show that the reactivity of S_4N_4 is unpredictable, which makes sulfur–nitrogen chemistry a fascinating research area. But there are also strategies for the *planned synthesis of SN compounds* as the following condensation reactions between NH and SX reagents show (X = F, Cl):

99 M. M. Labes, P. Love, L. F. Nichols, *Chem. Rev*. **1979**, *79*, 1.

100 A. J. HEEGER, A. G. MACDIARMID and H. SHIRAKAWA received the NOBEL prize in chemistry of the year 2000 for the characterization of electrically conducting polymers consisting of nonmetallic elements.

$$4\ Me_2NH + Cl_2SO \longrightarrow Me_2N{-}SO{-}NMe_2 + 2\ [Me_2NH_2]Cl$$

$$3\ Ph{-}NH_2 + Cl_2SO \longrightarrow Ph{-}N{=}S^{\oplus}{-}O^{\ominus} + 2\ [PhNH_3]Cl$$

$$3\ R{-}NH_2 + SF_4 \longrightarrow R{-}N{=}SF_2 + 2\ [RNH_3]F$$

$$R{-}N{=}SF_2 + 3\ H_2N{-}R \longrightarrow R{-}N{=}S{=}N{-}R + 2\ [RNH_3]F$$

Sulfur diimides have also been prepared from *N*-sulfinyl compounds by elimination of SO_2:

$$2\ R{-}N{=}S^{\oplus}{-}O^{\ominus} \longrightarrow R{-}N{=}S{=}N{-}R + SO_2$$

The parent unsubstituted thionyl imide HNSO is obtained as a colorless gas from thionyl chloride vapor and exactly stochiometric amounts of ammonia provided the reaction is carried out at low pressure and ambient temperature:

$$3\ NH_3 + SOCl_2 \longrightarrow HN{=}S^{\oplus}{-}O^{\ominus} + 2\ [NH_4]Cl$$

Gaseous HNSO forms planar molecules that exist as *cis* and *trans* isomers with the former being lower in energy. HNSO (m.p. –85 °C) polymerizes in condensed phases at temperatures above –70 °C. The LEWIS acid–base adduct $(C_6F_5)_3B{\leftarrow}N(H){=}S{=}O$ is stable at 25 °C but extremely moisture sensitive. The thionyl imide anion $[NSO]^-$ has been isolated as potassium salt from which HNSO can also be prepared by heating with stearic acid under vacuum.[101]

The isomeric molecule HSNO is referred to in the literature as either thionitrous acid or as S-nitroso thiol. It is thermodynamically less stable than HNSO, but salts with the thionitrite anion $[SNO]^-$ have been prepared with large cations such as $[Ph_4As]^+$. Organic nitroso thiols RSNO are accessible from nitrosyl chloride and a thiol RSH at 0 °C, for example:

$$Me_3C{-}SH + Cl{-}NO \longrightarrow Me_3C{-}S{-}N{=}O + HCl$$

Me_3CSNO is a green liquid that exists as *syn*- and *anti*-isomers due to the planar CSNO unit. The *anti*-conformer is dominating (ca. 80%) both in the gas phase and in solution at 25 °C.

The thionitrite anion $[SNO]^-$ has recently been recognized as a *bioactive species* with a biochemistry similar to that of NO and H_2S.[102] In fact, HSNO has been generated from gaseous NO and H_2S in a mass spectrometer. Disproportionation of NO on the metal surface is assumed as a preceding reaction:[103]

101 A. Schulz et al., *Angew. Chem. Int. Ed.* **2016**, *55*, 7680.
102 Review: M. Feelisch et al., *Dalton Trans.* **2016**, 5908–5919.
103 M. C. McCarthy et al., *J. Am. Chem. Soc.* **2016**, 138, 11441.

$$3\ NO \rightarrow N_2O + NO_2$$

$$NO + NO_2 \rightarrow N_2O_3$$

$$H_2S + N_2O_3 \rightarrow HSNO + HNO_2$$

HSNO is a highly reactive planar molecule with d_{SN} = 183.4 pm (*cis*-conformer) and 185.2 pm (*trans*-form); it reacts with excess H_2S to HNO and H_2S_2. Substituted nitrosothiols RSNO (e.g., S-nitrosoglutathione) occur naturally in bacteria, plants and mammals.

Nitrosating agents such as NO and nitrite ions react in water with polysulfide anions to the perthionitrite or nitrosodisulfide ion $[SSNO]^-$. This *cis*-planar ion has been isolated with the large bis(triphenylphosphane)iminium cation $[(Ph_3P)_2N]^+$ (abbreviated as PNP^+), which is isoelectronic with the carbobis(triphenylphosphine) molecule $(Ph_3P)_2C$ discussed in Section 7.2. In aqueous solution the orange-red, light-sensitive and thermally unstable though bioactive $[SSNO]^-$ ion is in equilibrium with NO and the yellow radical anion $[SS]^{\bullet-}$. The characteristic absorption band of $[SSNO]^-$ depends on the solvent and has been observed near 450 nm in organic solvents (THF, acetonitrile, acetone, DMF) but near 410 nm in water.

The reactions of *sulfur halides in liquid ammonia* (ammonolysis) usually yield a complex product mixture due to redox reactions occurring in parallel. For example, the reaction of S_2Cl_2 with NH_3, aside from S_8, yields the eight-membered heterocyclic sulfur imides S_7NH, $S_6(NH)_2$ and $S_5(NH)_3$. These compounds are formally derivatives of S_8 in which single S atoms have been replaced by divalent NH groups. $S_6(NH)_2$ and $S_5(NH)_3$ exist as three resp. two isomers since there is always at least one sulfur atom between the imido groups as is also the case in the 1,3,5,7-tetraimide $S_4(NH)_4$ (Figure 12.14). These sulfur imides have been separated chromatographically and isolated as colorless crystals. The best preparative access to heptasulfurimide S_7NH, however, is from S_8 and sodium azide in a two-step synthesis:

$$\frac{7}{8}\,S_8 + Na[N_3] + H_2O \longrightarrow S_7NH + Na[OH] + N_2$$

Nucleophilic attack of the azide ion on S_8 dissolved in hexamethyl phosphoric triamide $(Me_2N)_3PO$ (HMPA) yields a solution containing the deep-blue chain-like anion $[SSNSS]^-$, which on hydrolysis by water gives S_7NH. Salts with the planar $[S_4N]^-$ ion are known with several large cations; this bis(perthio)nitrite anion adopts an *E,Z*-conformation.

Sulfur–nitrogen compounds with sulfur in the oxidation state +6 are, for example, amidosulfuric acid H_3NSO_3 (Section 12.10.2) and other sulfonic acids of ammonia and hydroxylamine such as imidodisulfuric acid $HN(SO_3H)_2$ and hydroxylamine *N,N*-disulfuric acid $HON(SO_3H)_2$. These compounds are formed as unwanted side-products during flue gas desulfurization with an aqueous suspension of lime by reaction of SO_2 with NO_2, which exist as hydrogen sulfite and nitrite anions at pH = 5 of the scrubbing solution:

$$[NO_2]^- + 2\,[HSO_3]^- + H^+ \longrightarrow [HON(SO_3)_2]^{2-} + H_2O$$

$$[HON(SO_3)_2]^{2-} + [HSO_3]^- \longrightarrow [HN(SO_3)_2]^{2-} + [HSO_4]^-$$

The sulfimido group S=NR is formally isoelectronic with an S=O group and in this sense the sulfurimides $S(NR)_2$ are analogues of SO_2 (R: univalent organic or inorganic group such as $-SiMe_3$). In a similar manner, the following polyimido sulfur compounds can be structurally related to well-known sulfur oxides or oxoanions:

sulfur triimides $S(NR)_3$ are analogous to SO_3 (local D_{3h} symmetry at the central atom);

triimidosulfites $[S(NR)_3]^{2-}$ are analogous to $[SO_3]^{2-}$ (local C_{3v} symmetry at the central atom);

tetraimidosulfates $[S(NR)_4]^{2-}$ are analogous to $[SO_4]^{2-}$ (local T_d symmetry at the central atom).

Synthetic access to these imides is provided by the following reactions:[104]

$$NSF_3 + 2\,Li[N(SiMe_3)R] \longrightarrow S(NR)_2 + FSiMe_3 + 2\,LiF \quad (R = t\text{Bu})$$

$$OSF_4 + 3Li[N(SiMe_3)_2] \longrightarrow S(NSiMe_3)_3 + O(SiMe_3)_2 + FSiMe_3 + 3\,LiF$$

$$S(NR)_2 + 2\,Li[NHR] \longrightarrow Li_2[S(NR)_3] + RNH_2$$

$$S(NR)_3 + 2\,Li[NHR] \longrightarrow Li_2[S(NR)_4] + RNH_2$$

104 D. Stalke, *Chem. Commun.* **2012**, *48*, 9559.

13 The Halogens

13.1 Introduction

Of the six elements in Group 17 only the first four, namely, fluorine, chlorine, bromine and iodine, are of interest for most chemists. All known isotopes of astatine – discovered as late as 1940 – are radioactive and even the most stable ($^{210}_{85}$At) has a half-life of only 8.3 h. The element is thus of little importance. A few atoms of the element number 117 have been generated in 2010[1] and after independent confirmation recently been named tennessine (Ts) in allusion to the Oak Ridge Laboratory in Tennessee.

Selected properties of halogens are compiled in Table 13.1. From the perspective of produced amount, chlorine is by far the most important halogen for modern society; ca. 60% of all products of the chemical industry are prepared with the help of chlorine. Considering the impact of halogens on modern medicine, on agricultural chemistry and novel materials of high technology, however, fluorine is also extraordinarily important. One hundred and fifty medical drugs presently on the market contain fluorine atoms. Currently, about 30% of the newly approved drugs and about 40% of the active substances in an agricultural context (mostly pesticides) contain fluorine. Many high-performance polymers for semiconductor technology, fuel cells and other applications are likewise highly fluorinated. Liquid crystal displays of the newest generation contain fluorinated liquid crystals. Several processes for the edging of conductor paths for integrated circuits (microchips) on silicon wafers employ purely inorganic fluorine chemistry.[2] For the successful synthesis and the optimal application of such materials, a solid knowledge of structure and properties of the often reactive, hence difficult to handle, element fluorides is indispensable.

Fluorine and iodine are single-isotope elements, while chlorine and bromine consist of two natural isotopes each. The nuclide ^{19}F with a nuclear spin $I = ½$ is particularly well suited for nuclear magnetic resonance spectroscopy; all other naturally occurring halogen isotopes have a nuclear spin of $I > 1$. Artificially produced radioactive halogen isotopes are used for the investigation of reaction mechanisms by *isotopic labeling* and in medical diagnostics. For instance, the radioactive ^{18}F is produced from the stable oxygen isotope ^{18}O by the reaction with protons from a particle accelerator ($^{18}O + p \rightarrow {}^{18}F + n$) under liberation of a neutron. It is employed in *positron emission tomography* (PET) for the diagnosis of tumors, as it decays with a half-life of 1.83 h under emission of positrons to give back ^{18}O. The positrons almost instantly react with the surrounding electrons to yield two photons, which are

1 E. Williams, *Nature Chem.* **2018**, *10*, 1172.

2 For a highly readable introduction into the topic see: P. Kirsch, *Modern Fluoroorganic Chemistry*, 2nd ed., Wiley-VCH, Weinheim, **2013**.

https://doi.org/10.1515/9783110578065-014

Table 13.1: Properties of the halogens (the dissociation enthalpies *D* at 25 °C and the internuclear distances *d* apply to the gaseous species).

Element X_2	Valence electron configuration of X	m.p. (°C)	b.p. (°C)	*D* (kJ mol^{-1})	*d* (pm)	Isotopes (mol%)
F_2	$2s^2p^5$	−220	−188	155	141.2	^{19}F: 100
Cl_2	$3s^2p^5$	−101	−34	240	198.8	^{35}Cl: 75.8 ^{37}Cl: 24.2
Br_2	$4s^2p^5$	−7	+59	190	228.1	^{79}Br: 50.7 ^{81}Br: 49.3
I_2	$5s^2p^5$	114	184	151	266.6	^{127}I: 100

then registered by a suitable detector. Due to the short half-life of ^{18}F, the administration of ^{18}F-labeled radiodiagnostic drugs to patients must be done within a few hours of the ^{18}F production (from $H_2{}^{18}O$). Therefore, it needs to be incorporated into a suitable organic molecule by fast, reliable and high-yielding synthetic procedures before being administered by injection or inhalation. The by far most important PET tracer is ^{18}F-labeled 2-fluoro-2-desoxyglucose, which is metabolized by cells (and in increased quantities by tumor cells) just like natural glucose and is thus useful for the early-state localization of tumors. The search for novel radiodiagnostics is an ongoing field of research.[3]

13.2 Elemental Fluorine, Chlorine, Bromine and Iodine

13.2.1 Halogen Molecules

Owing to their valence configuration $s^2p_x{}^2p_y{}^2p_z{}^1$, the halogens exist as diatomic molecules in all physical states. These assemble to molecular crystals at moderate or low temperatures; the lattice enthalpy is provided by the weak VAN DER WAALS interactions between neighboring molecules. Therefore, the melting and boiling points of halogens are relatively low. Fluorine is a colorless gas with a yellowish tint at high pressures, while chlorine gas is yellow-green even at lower pressures. Bromine is a rusty red-brown liquid and iodine forms gray-black crystals with metallic luster, which readily sublime on heating producing a violet vapor.

The pronounced increase of the melting and boiling temperatures from fluorine to iodine has various reasons. As the halogen molecules do not have a dipole moment, the VAN DER WAALS forces are exclusively due to dispersion effects, which in turn depend on the *polarizability* of the atoms and thus molecules (Section 3.3).

3 V. Gouverneur, *Angew. Chem. Int. Ed.* **2015**, *54*, 9991.

Since the polarizability strongly increases with the atomic radius, the intermolecular interactions become stronger from fluorine to iodine. Cl_2, Br_2 and I_2 each crystallize in structures with planar layers. The layers are stacked in such a manner that the dihalogen molecules are located in the gaps between molecules of the above and below layers. Only VAN DER WAALS forces are active between these layers as indicated by the relatively large interatomic distances (for I_2: 425–433 pm). These weak forces manifest in the facile splitting of the crystals along the plane of the layers (space group *Cmca*). Within the layers, however, there are also intermolecular distances much smaller than the VAN DER WAALS distances so that weak covalent interactions can be assumed. This effect increases strongly from Cl_2 to I_2. The smallest distances between the atoms of two individual molecules in the case of iodine are 349 pm (single bond distance in gaseous iodine: 267 pm, VAN DER WAALS distance: 440 pm). At this internuclear distance, a considerable orbital overlap can be expected. Apparently, *intermolecular multicenter bonds* exist in crystalline iodine that extend throughout the layer and lead to the delocalization of electrons akin to that in metals. This explains certain physical properties of iodine: the dark color, the luster and a weak electric conductivity, which is 3400 times stronger within the layers then perpendicular to them. Crystalline iodine is thus a two-dimensional *semiconductor*. These multicenter bonds are formed through the partial delocalization of antibonding electrons from the occupied π* MOs of one molecule into the unoccupied σ* MOs of an adjacent molecule as indicated by the widening of the intramolecular iodine–iodine bond from 267 pm in the gas phase to 272 pm in the crystal.[4] The shown excerpt of a layer of the iodine structure determined at 4 K elucidates the possibilities of orbital overlap in between molecules of the planar network:

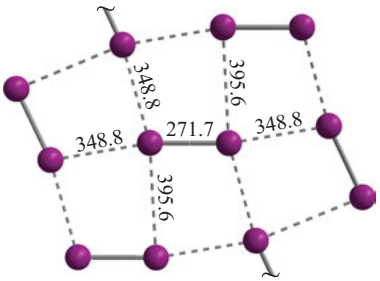

It is instructive to compare the strength of the intermolecular with the intramolecular bonds in the elemental halogens. From the sublimation enthalpy of iodine

4 In contrast, the internuclear distance d_{FF} of the F_2 molecule is almost the same for gas phase and solid state. As expected, the low polarizability of fluorine effectively prevents appreciable donation by nonbonding electron pairs into antibonding σ* levels: F. Kraus et al., *Chem. Eur. J.* **2019**, *25*, 3310 and C. Müller et al., *Chem. Eur. J.* **2019**, *25*, 3318.

(64.2 kJ mol^{-1}) and the data in Table 13.1, it can be deduced that the intermolecular interactions in solid iodine amount to remarkable 42% of the dissociation enthalpy of the I_2 molecule. In case of bromine, the enthalpy of evaporation is only 30.9 kJ mol^{-1}, that is, 22% of the Br_2 dissociation enthalpy. A certain stabilization by intermolecular electron delocalization is still active in the liquid and even the vapor, where the dimers $(Br_2)_2$ and $(I_2)_2$ can be detected spectroscopically. The equilibrium constant for the dimerization of gaseous Br_2 was determined to 2.5 ± 0.4 L mol^{-1} at 22 °C. A detailed description of the so-called halogen bonds, which play a significant role in molecular chemistry, will be given in Sections 13.3 and 13.5.3.

13.2.2 Halogen Atoms

All diatomic halogen molecules X_2 dissociate into atoms at elevated temperatures. The degree of thermal dissociation depends on pressure, temperature and of course the enthalpy of dissociation (Table 13.1). These bond enthalpies do not change in a uniform manner from F_2 to I_2; they rather reach a maximum at Cl_2. The relatively small value for F_2 is due to the repulsion of the nonbonding electron pairs of both atoms as well as the small atomic radius and the resulting high electron density (Section 4.2.2). As a consequence, the thermal degree of dissociation α is much higher for F_2 than for the other halogens under identical conditions. At 1000 K and 0.1 MPa, α is about 4% for F_2, 0.03% for Cl_2, 0.2% for Br_2 and about 3% for I_2. Alternatively, the dissociation of the halogen molecules can be achieved by irradiation or by a microwave discharge. For recombination of two halogen atoms in the gas phase, an additional collision partner M is required in order to at least partially dispense the liberated bond enthalpy (as kinetic energy of M). In the case of iodine atoms, an adduct IM is formed initially, which reacts with a further iodine atom to I_2 and M. Under such circumstances, the *activation energy* of the reaction is *negative* (the reaction is slowed down with rising temperature) as the adduct IM increasingly dissociates on warming. Moreover, the rate of reaction strongly depends on the nature of M.

13.2.3 Reactivity

Fluorine is the most reactive element of all. It reacts at room or elevated temperature with all other elements (except for the lighter noble gases) as well as with many inorganic and most organic compounds. Often these reactions proceed with tremendous violence, some as explosions. The reactivity and oxidative power of F_2 can be further increased by mixing it with a strong LEWIS acid such as AsF_5. Chlorine, bromine and iodine are much less reactive. On the one hand, the extreme

reactivity of fluorine is due to the smaller dissociation enthalpy; on the other hand, most bonds between an element E and fluorine are much stronger than in case of the other halogens. The corresponding reactions are very exothermic, which further increases the reaction rates. This will be illustrated by the *mean bond enthalpies* of CX bonds in the carbon tetrahalides CX_4. In brackets the typical range of the mean CX bond enthalpy in various bonding situations is given (kJ mol^{-1}):

$F_3C–F$	$Cl_3C–Cl$	$Br_3C–Br$	$I_3C–I$
485	327	285	213
(460 ··· 535)	(300 ··· 360)	(260 ··· 330)	(200 ··· 260)

The strong CF bonds are the basis for the numerous applications of fluorine-containing organic compounds (see Section 13.4.4).[1,5]

13.3 Bonding Situations

13.3.1 Halide Ions

All halogens form negative halide ions X^- as encountered in many common salts such as NaCl. The ability of halogens to form salts with most metals has been the namesake for this group of the Periodic Table (halogen = salt producing). The *electron affinity*, that is, the enthalpy liberated upon the attachment of an electron to the gaseous atom, is larger for halogens than for all other elements (Section 2.1.3).

The tendency of halogen molecules to be converted into the corresponding halide ions in aqueous solution according to

$$X_2 + 2\,e^- \rightleftharpoons 2\,X^- \qquad (1)$$

strongly decreases from F_2 to I_2. The more electronegative the halogen, the more the above equilibrium is shifted to the right hand side, that is, the GIBBS energy $\Delta G°(1)$ decreases from F_2 to I_2. This is also manifest in the corresponding *reduction potentials E°*, which are defined as follows:

$$E° = \frac{-\Delta G°}{n \cdot F}$$

n number of electrons (here: 2)

F Faraday constant (96 487 C mol^{-1})

5 D. O'Hagan, *Chem. Soc. Rev.* **2008**, *37*, 308.

The E° values under standard conditions are:

F_2	Cl_2	Br_2	I_2	At_2
+2.89	+1.36	+1.08	+0.62	+0.2 V

The reasons for this trend are, on the one hand, the different hydration enthalpies of the anions as well as on the other hand the dissociation enthalpies of the molecules (Table 13.1) and the electron affinities of the atoms (Figure 2.2). Because of these thermodynamic circumstances, each halogen expels its higher homologues from their halide salts. For the same reason, the reducing strength of the hydrogen halides increases from HF to HI. While HF and F^- can only be oxidized to F_2 electrochemically, relatively mild oxidizing agents are sufficient to oxidize HI or iodides to I_2.

13.3.2 Covalent Compounds

In covalent species, univalent halogens occur in oxidation states between −1 and +1. Examples are given by the compounds Cl_2, ClF, BrF and ICl. The oxidation state of the fluorine atom, however, is negative in all compounds (except for F_2) as fluorine is the most electronegative element and thus always the negatively polarized bonding partner.

As LEWIS bases, halogen atoms with a single covalent bond can engage in additional coordinative bonds and reach coordination numbers of 2 and 3 in this manner. This case is encountered, for instance, in halogen compounds with hydrogen bonds such as $(HF)_2$ as well as in numerous element halides in which halogen atoms adopt bridging positions. The example of fluoride-bridged anions $[F_5E{-}F{-}EF_5]^-$ (E = As, Sb) illustrates this bonding mode:

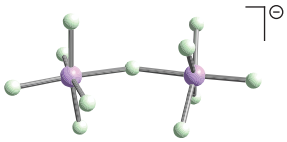

The geometry at the central fluorine atom of these anions is bent (C_{2v}). Compounds with higher coordinate fluorine atoms are known, but although MgF_2 crystallizes in the rutile structure with C.N.(F) = 3, it should rather be considered as an example for ionic bonding. Examples for bridging chlorine atoms are $(AlCl_3)_2$ and $(ICl_3)_2$ as well as the tetrachlorides of selenium and tellurium (Sections 12.12.4 and 13.5.5).

Due to the high ionization energy of the fluorine atom, compounds with fluorine cations F^+ or even with positively polarized F atoms cannot be prepared as pure compounds. (The molecular ion $[F_2]^+$ has been observed spectroscopically in

the gas phase.) In contrast, due to their strongly decreasing ionization energy and increasing atomic radii, this bonding situation is well known for the other halogens. The bonding partner must have a higher electronegativity than the halogen atom X. This is the case in the bonds XF and XO; fluorine and oxygen are most suitable for the formation of compounds with positively polarized Cl, Br and I atoms. Besides the already mentioned interhalogen species, bromine nitrate $BrONO_2$, chlorine hydroxide ClOH and iodine tris(fluorosulfate) $I(SO_3F)_3$ belong to this class of compounds. Bromine nitrate is the dominant reservoir for bromine in the stratosphere; it catalyzes ozone depletion under irradiation of light.

The heavier halogens Cl, Br and I also allow for considerably higher coordination numbers than fluorine. Suitable bonding partners are predominantly F and O, but also Cl to some extent. With these partners, chlorine and bromine achieve coordination numbers of up to 6 as in $[ClF_6]^+$, while iodine even reaches the coordination number 8, for example, in the anion $[IF_8]^-$. These and the analogous interhalogens belong to the class of "hypervalent" or more appropriately hypercoordinate species, which contain multicenter bonds according to MO theory (Section 2.6). In oxoacids and their anions, halogens also reach high coordination numbers in some cases, for example, in periodic acid $IO(OH)_5$. PhIO with a dicoordinate iodine center is an important oxidant.

13.3.3 Halonium Ions

The cations F^+, Cl^+, Br^+ and I^+ are such strong LEWIS acids, that is, strong electrophiles, that they cannot exist in condensed phases except in coordinate form, as, for example, in the following salts where pyridine ligands (C_5H_5N) transfer electron density to the halogen atoms:

$$[F(py)]F \qquad [Cl(py)_2][NO_3] \qquad [Br(py)_2][NO_3] \qquad [I(py)_2][NO_3]$$

Halogen cations X^+ are isoelectronic with the corresponding chalcogen atoms, for which the coordination number 2 is characteristic. The disilylhalonium ions of the salts $[Me_3Si–X–SiMe_3][B(C_6F_5)_4]$ (X = F, Cl, Br, I)[6] and the dialkylchloronium ions $[R–Cl–R]^+$ (R = Me, Et)[7] provide examples. The geometry at these formal halogen cations is bent. Quantum-chemical calculations have shown, however, that all halogen atoms of the latter cations except for iodine carry a partial negative charge, because the electronegativity of Si is considerably smaller than that of F, Cl and Br (Table 4.8). Halogen atoms with positive partial charges occur in the homoatomic cations $[X_3]^+$ (X = Cl, Br, I), the

6 M. Lehmann, A. Schulz, A. Villinger, *Angew. Chem. Int. Ed.* **2009**, *48*, 7444.

7 E. S. Stoyanov, I. V. Stoyanova, F. S. Tham, C. A. Reed, *J. Am. Chem. Soc.* **2010**, *132*, 4062.

salts of which are described in Section 13.5.4. Diaryliodonium salts have been employed in cross-coupling reactions as arylation reagents toward nucleophiles.[8]

13.3.4 Halogen Bonds

In the molecules CF_3X (X = Cl, Br, I) the CX bonds are strongly polarized with a positive partial charge at the X atoms due to the high electronegativity of the CF_3 moiety. At the same time, the density distribution of the nonbonding electrons is anisotropic in the sense that a positive pole is generated at the extension of the C–X vector, while a small excess of negative charge is present in the equatorial zone (p_π electron pairs). This effect increases with the difference in electronegativity between X and the CF_3 group, that is, it is strongest with X = I. The positive pole is referred to as *σ-hole* and exerts an attractive force toward the negatively polarized zone of a second molecule. Such an attractive X···X interaction is called *halogen bond*.[9] The atom with the positive pole is referred to as acceptor (A), the other is the electron density donor (D). The C–A···D–C moiety shows a valence angle of about 180° at the acceptor atom and of about 90° at the donor.[10] The transfer of nonbonding electron density into the σ* MO of the CX bond of the acceptor is comparable to that of strong hydrogen bonds (Section 5.6.5). The donor does not have to be a halogen atom; it can be any LEWIS-basic atom with nonbonding electron density such as N, O, S or Se. Conversely, the acceptor A is almost without exception either Cl, Br or I. This interaction is not to be confused with the halide bridges (see above). Halogen bonds are observed in many organohalogen compounds; even entire supramolecular architectures are based on this predominantly electrostatic interaction,[11] resembling the case of hydrogen bonds. If the donor is sufficiently strong, the acceptor atom does not necessarily have to carry a positive charge. For instance, Cl_2 forms adducts with H_2O and H_2S with the connectivity $ClCl\cdots OH_2$ and $ClCl\cdots SH_2$, respectively. Here, the nonbonding p_π electron pair at the chalcogen atom donates electron density into the σ* MO of the ClCl bond. Finally, the intermolecular interactions in solid iodine described above as well as those in polyhalides (Section 13.5.3) are effectively halogen bonds. The interaction of halide ions with suitable acceptor groups A has been employed for selective anion recognition.[12]

8 E. A. Merritt, B. Olofsson, *Angew. Chem. Int. Ed.* **2009**, *48*, 9052.

9 It may surprise that two equally charged atoms mutually attract each other, but they only do this if a particular geometry is present bringing the negative zone of one atom into the vicinity of the σ hole of another. Also see Section 4.7 and P. Metrangolo, G. Resnati et al., *Chem. Rev.* **2016**, *116*, 2478 as well as A. Varadwaj, H. M. Marques, P. R. Varadwaj, *Molecules* **2019**, *24*, 379.

10 E. Espinosa et al., *Angew. Chem. Int. Ed.* **2009**, *48*, 3838.

11 S.-Q. Zang, L.-Y. Wang et al., *Coord. Chem. Rev.* **2016**, *308*, 1.

12 A. Brown, P. D. Beer, *Chem. Commun.* **2016**, *52*, 8645.

From all the above considerations, it can be concluded that the element fluorine adopts a similar special position as oxygen in the group of the chalcogens. Therefore, fluorine will be treated separately before the other elements.

13.4 Fluorine

13.4.1 Preparation of Fluorine

In Nature, the element fluorine[13] predominantly occurs in the crystalline minerals *fluorspar* CaF_2 (*fluorite*), *cryolite* $Na_3[AlF_6]$ and *fluorapatite* $Ca_5[(PO_4)_3F]$.[14] The mineral *phosphorite* has the same composition as fluorapatite, only in amorphous form. A fluorspar occurring together with uranium minerals is partially decomposed by the radiation of the actinide over long periods of time resulting in its purple-black color (CaF_2 itself is colorless). Due to its penetrant odor, this mineral is referred to as "stinkspar." According to recent ^{19}F-NMR studies in the solid state, elemental fluorine is present, which is plausibly generated by the radiation-related electron detachment from F^-. When exposed to air (by crushing of the mineral), F_2 reacts with water vapor to ozone and HF; the characteristic odor is thus caused by these three gases. The dark color of the mineral is attributed to clusters of calcium atoms formed during radiolysis. When the mineral is heated to 300 °C, Ca and F_2 react with each other and the dark color disappears. More recently, elemental fluorine has also been detected in the NaF mineral *villiaumite*.[15]

The natural abundance of fluorine in the Earth's crust is only ca. 0.063%, which is, however, still larger than that of chlorine (ca. 0.013%). A high fluoride content of drinking water (which should not exceed 1 mg L^{-1}) is a considerable issue in many countries. Continued ingestion of fluoride ions above this threshold leads to the fluorosis of teeth and bones.[16] Certain regions of China, India, Sri Lanka and the African countries in the Rift Valley with altogether 260 million people are most strongly affected.

Elemental fluorine and most fluorides are produced from anhydrous HF (aHF). For the technical production of HF, dried fluorspar is heated with 100% sulfuric

13 D. D. DesMarteau et al., *Encycl. Inorg. Chem.* **2005**, *3*, 1561. Also see topical issue of *Chemical Reviews*: V. Gouverneur, K. Seppelt, *Chem. Rev.* **2015**, *115*, 563.

14 $Ca_5[(PO_4)_3F]$ is also an essential part of the teeth of vertebrae in the enamel. It is much more resistant to acids than hydroxyapatite $Ca_5[(PO_4)_3(OH)]$. Therefore, toothpastes typically contain amine fluoride for the replenishment of fluoride ions in the enamel, which helps protecting the teeth against caries.

15 J. Schmedt auf der Günne, F. Kraus et al., *Angew. Chem. Int. Ed.* **2012**, *51*, 7847 and *Chem. Eur. J.* **2016**, *22*, 18388. F. Kraus, *Nachr. Chem.* **2019**, *67*, 54.

16 S. Rayalu et al., *Chem. Rev.* **2012**, *112*, 2454.

acid to ca. 300 °C in a rotating tube furnace (kiln) which is heated from outside by a flame of natural gas:

$$CaF_2 + H_2SO_4 \longrightarrow 2\,HF + CaSO_4$$

This reaction is endothermic by +59 kJ mol^{-1} and therefore needs to be conducted at elevated temperature. The gaseous crude HF is washed with H_2SO_4 and then further purified by fractional condensation and subsequent distillation. For each ton of HF 3.5 t of $Ca[SO_4]$ are produced from which gypsum and cement are manufactured. The side product SiF_4 is used to produce hexafluoro silicic acid $[H_3O][SiF_6]$.

Considerable amounts of HF and SiF_4 are also gained from the conversion process of phosphorite to phosphoric acid (Section 10.12) and used in the synthesis of AlF_3 and $Na_3[AlF_6]$ for *aluminum production* by fused-salt electrolysis. The worldwide production capacity of HF amounts to about $1.6{\cdot}10^6$ t/a.

Hydrogen fluoride (m.p. −84 °C, b.p. 20 °C) is an excellent polar solvent for organic and inorganic compounds, although many metals, glass and other materials are corroded by HF. Some plastics, however, in particular fluorinated organic polymers (Teflon, KEL-F, PFA; see below), are inert against HF. Stainless steel can be used at standard temperatures and slightly above, while at higher temperatures copper, nickel and the Cu–Ni alloy Monel have proven useful. Hydrogen fluoride is extremely toxic; exposure of the skin to HF causes severe and slowly healing wounds (threshold limit value is 2 ppm for short time exposure, corresponding to 1.66 mg m^{-3}; the odor detection threshold is 0.1 to 0.2 mg m^{-3}).

Due to its high standard potential, chemical syntheses of *elemental fluorine* are rare.[17] Industrially, it is exclusively produced by anodic oxidation of fluoride ions. The electrolyte must not contain any other anions (e.g., $[OH]^-$). Anhydrous HF itself dissociates only weakly into ions:

$$3\,HF \rightleftharpoons [H_2F]^+ + [HF_2]^- \qquad c(H_2F^+){\cdot}c(HF_2^-) \approx 10^{-10}$$

Therefore, melts of composition KF·*x*HF with *x* varying between 2 and 13 are used for electrolysis.[18] The melting points of these electrolytes are between −100° and +72 °C and decrease with rising HF content. The electrolysis is typically carried out at about 95 °C. The fluoride ions in the electrolyte are strongly solvated as $[H_nF_{n+1}]^-$ resp. $[F^-{\cdot}n\mathrm{HF}]$. The first synthesis of fluorine had been carried out in 1886 in this manner by Henri Moissan who was awarded the Nobel prize in chemistry for this discovery in 1906.

17 A chemical synthesis of fluorine has been reported, namely, the thermal decomposition of potassium hexafluoro manganate with antimony pentafluoride: $K_2[MnF_6] + 2\,SbF_5 \rightarrow 2\,KSbF_6 + MnF_3 + 0.5\,F_2$. This method, however, has so far only been applied on a laboratory scale: K. O. Christe, *Inorg. Chem.* **1986**, *25*, 3722.

18 H. Groult et al., *J. Fluorine Chem.* **2007**, *128*, 285.

The cells for electrolysis as well as the cathodes are made of steel, while the anodes consist of graphite-free carbon. The composition of the electrolyte is held constant throughout electrolysis by introduction of fresh HF. The fluorine gas evolved at a bath voltage between 8.5 and 10 V contains HF and CF_4 and is therefore purified by cooling to −140 °C leading to the condensation of impurities. Hydrogen evolves at the cathode. The estimated global production in 2013 was about 28000 t.[19] About 60% of the thus produced elemental fluorine are used for the production of UF_6 for the nuclear industry, and the remainder is used in the synthesis of compounds such as NF_3, SF_6, ClF_3, C_3F_8, WF_6 and fluorographite (Section 7.5.1). F_2 is sold in stainless steel cylinders under a pressure of 28 bar.

13.4.2 Properties of Fluorine

Fluorine is a colorless, very toxic gas (see Table 13.1), which causes difficultly healing wounds on skin. Liquid F_2 is yellow. F_2 can be recognized even at very low concentrations of about 0.01 ppm by its pungent odor, which resembles that of a mixture of O_3 and Cl_2. Just as fluorine, many covalent fluorides such as S_2F_{10} and PF_3 are extremely toxic.

As fluorine reacts with nearly all other elements and many inorganic and organic compounds, only a few materials are suitable for the construction of apparatuses for experiments with F_2. On exposure with F_2, some metals and alloys are rapidly covered with a thin impenetrable and firmly adherent film of metal fluoride, which prevents the further attack by F_2 (*passivation*) and thus renders the material resistant against the element at 25 °C. Cu, Ni, steel, brass (Cu-Zn alloy), bronze (Cu–Sn alloy) and Monel (Ni–Cu alloy) are examples for such metals. Only in special cases, glass or ceramic components can be used (with N_2-diluted fluorine), because SiO_2 is fluorinated to gaseous SiF_4 if even traces of HF are present:

$$SiO_2 + 4\,HF \longrightarrow SiF_4 + 2\,H_2O$$
$$H_2O + F_2 \longrightarrow 2\,HF + \tfrac{1}{2}\,O_2$$

Alongside metallic materials, polymers such as polytetrafluoroethylene (PTFE, Teflon) and a perfluoroalkoxy copolymer (PFA) play a role, predominantly for joints, cold traps and flexible tubing.

For the disposal of small quantities of F_2, the gas is conducted over $CaCl_2$, Al_2O_3 or into 30% aqueous KOH solution:

$$2\,Al_2O_3 + 6\,F_2 \longrightarrow 4\,AlF_3 + 3\,O_2$$
$$2\,KOH + F_2 \longrightarrow 2\,KF + H_2O + O_2$$

19 A. Dreveton, *Procedia Eng.* **2016**, *138*, 240.

With water, F_2 reacts to HOF, which forms the adduct $CH_3CN{\cdot}HOF$ with acetonitrile. This mixture is an excellent *oxygen transfer reagent* for organic oxidations.[20] Toward very strong LEWIS acids F_2 reacts as a LEWIS base (ligand) forming complexes with either *side-on* or *end-on* coordination.

13.4.3 Preparation of Fluorides

All fluorides are ultimately produced from HF, either through the detour via elemental fluorine of by direct conversion with hydrogen fluoride or hydrofluoric acid (HF_{aq}). Hydrogen fluoride, which is strongly associated with hydrogen bonds in all states, is a water-like solvent. Its salts contain the anions F^-, $[HF_2]^-$, $[H_2F_3]^-$ and $[H_3F_4]^-$. The thermal decomposition of $K[HF_2]$ can be employed for the preparation of pure HF on the laboratory scale. Fluoride ion acceptors such as SbF_5 behave as *ansolvo acids* in liquid HF:

$$2\,HF + SbF_5 \rightleftharpoons [H_2F]^+ + [SbF_6]^-$$

The thus generated fluoronium cation $[H_2F]^+$ contains fluorine of coordination number 2 with a positive formal charge; the true charge at the F atom, however, is negative with the H atoms carrying partial positive charges. Soluble ionic fluorides react as bases in HF. In water, HF is only a weak BRØNSTED acid (Section 5.5), but the solution is highly corrosive and attacks glass under fluorination so that hydrofluoric acid is stored and handled in vessels made of polyethylene, platinum or lead.

For the preparation of covalent and ionic fluorides, the following procedures are applied:

(a) Reaction of HF or HF_{aq} with an oxide, hydroxide or carbonate; suitable for the synthesis of KF, $K[HF_2]$, $[NH_4]F$, $[NH_4][HF_2]$, BaF_2, AlF_3, $Na_3[AlF_6]$, BF_3, $K[BF_4]$, SiF_4.

(b) Halogen exchange by means of HF, NaF or KF (particularly suitable for the halides of Groups 14–16 of the Periodic Table):

$$PCl_3 + 3\,HF \xrightarrow{50°C} PF_3 + 3\,HCl$$

$$SbCl_5 + 5\,HF \longrightarrow SbF_5 + 5\,HCl$$

$$SPCl_3 + 3\,HF \xrightarrow[\text{sulfolane}]{150°C} SPF_3 + 3\,HCl$$

(c) Direct fluorination with F_2 (typically, the highest oxidation states are attained):

20 S. Rozen, M. Carmeli, *J. Am. Chem. Soc.* **2003**, *125*, 8118.

$$\tfrac{1}{8}S_8 + 3\,F_2 \longrightarrow SF_6$$
$$I_2 + 5\,F_2 \longrightarrow 2\,IF_5$$
$$AgCl + F_2 \longrightarrow AgF_2 + \tfrac{1}{2}Cl_2$$

Many elements and compounds react with F_2 under spontaneous ignition and pronounced heat development. For instance, solid F_2 and liquid H_2 still violently react at temperatures as low as 20 K! Therefore, rocket engines have been experimentally run with F_2 as an oxidant on the one hand and compounds such as H_2, B_2H_6, N_2H_4, C_2H_5OH, Li, LiH and BeH_2 as fuel on the other hand. In these trials, combustion temperatures of 4000–5600 K were achieved.

(d) Fluorination with metallic or nonmetallic fluorination agents such as AgF, AgF_2, CoF_3, MnF_3, ZnF_2, ClF_3, BrF_3, IF_5, AsF_5, SbF_3, SF_4, $K[SO_2F]$:

$$3\,PCl_5 + 5\,AsF_3 \xrightarrow{25°C} 3\,PF_5 + 5\,AsCl_3$$
$$OPCl_3 + ZnF_2 \xrightarrow{40°C} OPClF_2 + ZnCl_2$$
$$3\,COCl_2 + 2\,SbF_3 \xrightarrow{130°C} 3\,COF_2 + 2\,SbCl_3$$

(e) The *electrofluorination* is a particularly elegant approach (SIMONS process). For this process, the starting material is dissolved in anhydrous HF. If the solution is insufficiently conductive, some KF is added. The electrolysis is carried out at temperatures of 20 °C or lower with very large electrodes, typically with a nickel anode. The bath voltage (5–6 V) is adjusted so that F_2 evolution does not occur. Nonetheless, a variety of compounds is anodically fluorinated under these conditions, even alkyl groups. The reaction conditions exert a considerable influence on the nature and yield of the products. The process is mostly applied for the production of organic fluorine compounds:

$$CS_2 \longrightarrow CF_3SF_5$$
$$(n\text{-}C_4H_9)_3N \longrightarrow (n\text{-}C_4F_9)_3N$$
$$CH_3SO_2F \longrightarrow CF_3SO_2F$$
$$C_8H_{17}SO_2F \longrightarrow C_8F_{17}SO_2F$$
$$C_4H_8SO_2 \longrightarrow C_4F_9SO_2F$$

sulfolane

Sulfolane is the common name for cyclic tetrahydrothiophensulfone.

(f) Commercially available fluorination agents important for organic chemistry are the salts $[R_2NSF_2][BF_4]$ as well as the so-called Selectfluor:

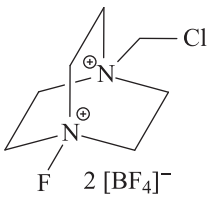

In addition, the amine–HF adducts $[Et_3NH][F(HF)_2]$ and py·9HF (OLAH's reagent; py = pyridine) are used in organic synthesis.

13.4.4 Applications of Fluorine Compounds

13.4.4.1 Liquid Hydrogen Fluoride[21]

In neat form, liquid HF (Section 13.4.1) is the preferred catalyst for the production of so-called alkylate from light olefins and branched isoalkanes, which is used as an antiknocking additive for gasoline. A related process with benzene instead of isoalkanes is employed for the synthesis of linear alkylbenzenes as precursors for the corresponding sulfonates (biodegradable surfactants). The considerable risks presented by the use of liquid HF, however, move alternatives such as $AlCl_3$ increasingly into focus. Hydrogen fluoride in neat and diluted form is also applied in the glass and ceramics industries to remove thin layers of glass or glassy components for the purification or conditioning of surfaces.

13.4.4.2 Uranium Hexafluoride

UF_6 is one of the oldest and at the same time most important molecular fluorine species. It was first synthesized by OTTO RUFF and ALFRED HEINZELMANN in Danzig (now Gdansk). RUFF alongside HENRI MOISSAN was one of the pioneers of fluorine chemistry. These days, UF_6 is prepared from the oxide U_3O_8 (isolated from uranium ores) in the following five-step synthesis:[22]

$$U_3O_8 \xrightarrow{HNO_3} UO_2(NO_3)_2 \xrightarrow{\Delta T} UO_3 \xrightarrow{H_2} UO_2 \xrightarrow{HF} UF_4 \xrightarrow{F_2} UF_6$$

Above 64 °C, UF_6 is a colorless gas, which is employed for the separation of the uranium isotopes ^{235}U and ^{238}U in gas centrifuges. In contrast, UF_4 is a green solid ("green salt," m.p. 1036 °C; b.p. 1417 °C).

13.4.4.3 Fluoride Ate-Complexes

Potassium tetra- and pentafluorido aluminates $K[AlF_4]$ and $K_2[AlF_5]$ are the main components of the commercial product *Nocolok*®, which is used on a large scale as a flux for blazing of aluminum components in modern car production, especially for radiators and air-conditioning systems. Nocolok is produced from $Al(OH)_3$, KOH and aHF. Its purpose is to dissolve the oxide layer on aluminum metal at a temperature

21 J. F. C. Turner, *Angew. Chem. Int. Ed.* **2004**, *43*, 1952.

22 F. Kraus, *Nachr. Chemie* **2008**, *56*, 1236. H. Groult et al., *J. Fluorine Chem.* **2007**, *128*, 285.

of ca. 560 °C and in a nitrogen atmosphere, just below the melting point of the solder and well below the melting point of Al (660 °C).

13.4.4.4 Fluorinated Hydro- and Chlorocarbons

For a long time, the hydrogen fluoride gained from fluorspar had mostly been used for the production of C–Cl–F compounds,[23] in essence the following derivatives of methane and ethane:

CCl_3F	$CHCl_2F$	$CCl_2F–CCl_2F$	$CCl_2F–CClF_2$
CCl_2F_2	$CHClF_2$	$CClF_2–CClF_2$	$CClF_2–CF_3$

These compounds are colorless and nontoxic. They are produced from the corresponding C–Cl and C–Cl–H species through partial halogen exchange by HF in the presence of SbF_5 as a catalyst and are distinguished by low boiling points and high chemical stability, nonflammability and good properties as solvents. Therefore, fluorinated hydro- and chlorocarbons have been applied as coolants in refrigeration systems, as solvents, as propellant in spray cans as well as blowing agents to produce foams. In the lab, they are suitable for the preparation of cold baths and as solvents for aggressive substances such as SO_3. Due to the harmful effects of these compounds on the stratospheric ozone layer (Section 11.1.3), the production of those species exclusively consisting of C, Cl and F (CFCs) was either limited or altogether discontinued (**Kyoto protocol** of 1997, extended until 2020 in Doha in December 2012). In Germany, the production of CFCs was discontinued as early as 1994, and since 2006 they are not even employed in medicinal applications anymore. Nonetheless, CCl_2F_2 (CFC-12) is still the most abundant CFC in the atmosphere as the lifetime of this molecule is very long (100 years). Compounds that contain residual hydrogen are less harmful as they readily decompose in the troposphere and thus do not reach the stratosphere. Examples of employed CFC replacements are $CH_2F–CF_3$, $CH_2=CF–CF_3$, hydrocarbons and CO_2.[24]

13.4.4.5 Fluorinated Polymers

Chlorodifluoromethane also serves as precursor for tetrafluoroethene and thus, ultimately, polytetrafluoroethylene (PTFE):

23 CFC: chlorofluorocarbons. For the disposal of CFCs, they are incinerated with H_2 and O_2, which results in HCl, HF, Cl_2 and CO_2.

24 In industry the cooling agents bear codes such as "R12" for CCl_2F_2, "R134a" for CH_2FCF_3, "HFO-1234yf" for CH_2CFCF_3 and "R744" for CO_2.

$$CHCl_3 + 2\,HF \xrightarrow{\text{cat.}} CHClF_2 + 2\,HCl$$

$$5\,CHClF_2 \xrightarrow[-\,5\,HCl]{750°C} F_2C{=}CF_2 + F_2C{=}CF{-}CF_3$$

Radical polymerization of tetrafluoroethene C_2F_4 at 20° to 100 °C and reduced pressure yields the material *polytetrafluoroethylene* $(-CF_2-CF_2-)_n$, abbreviated PTFE (trademarks: Hostaflon TF, Teflon). The polymerization reaction is strongly exothermic. PTFE is of extraordinary chemical robustness and can be used without decomposition in the temperature interval from −270° to +260 °C. It is inflammable, physiologically inert and is only attacked by molten alkali metals and – at higher temperatures/higher pressures – by F_2, ClF_3 and other strong fluorinating agents.[25] Similarly robust materials are polychlorotrifluoroethylene $(-CF_2-CFCl-)_n$, abbreviated PCTFE (trademarks: Hostaflon C2, KEL-F), as well as Viton $(-CHF-CF_2-CF_2-)_n$ and Teflon FEP $(-CF_2-CF_2-CF(CF_3)-)_n$. PCTFE can be obtained as oil, grease, wax or solid materials, depending on the degree of polymerization and is used as highly resistant vacuum grease and sealing material.

13.4.4.6 Fluorine Compounds for Energy Storage and Conversion

Lithium ion batteries mostly contain electrolytes consisting of $Li[PF_6]$ dissolved in a solvent such as ethylene carbonate, propylene carbonate or dimethyl carbonate. In order to increase the oxidation resistance and reduce the flammability, fluorinated carbonates are employed since recently, for example, monofluoroethylene carbonate. The proton conducting polymer *Nafion*, a sulfonated and fluorinated polymer, is used as membrane in *fuel cells* and can be obtained by one of the fluorination methods described above:

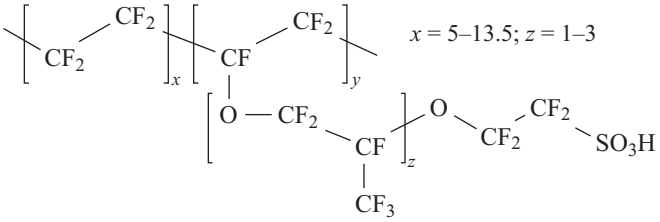

13.4.4.7 Fluorinated Compounds in Semiconductor Industry

NF_3, CF_4, C_2F_6 and SF_6 are used in the electronics industry for plasma etching of silicon. A microwave discharge generates fluorine atoms from these gases, which remove elemental silicon as SiF_4. In an analogous manner, fuel tanks of automobiles (these days made from organic polymers) are fluorinated at the surface, which

25 PTFE vessels are therefore employed in the production of ultrapure chemical for electronics as well as in trace analytics (ppb analytics), where even the tiniest impurities need to be avoided.

improves impermeability and chemical resistance. One of the classical *etching processes* of silicon wafers is based on the effect of hydrofluoric acid. Interestingly, the Si surface is terminated with SiH functions in the process. Since more recently, however, the gas ClF_3 is also employed in wafer etching. Conversely, NF_3 has been recently included into the amended Kyoto protocol as a long-lived substance harmful to the climate.

13.4.4.8 Liquid Crystals

All liquid-crystalline dyes used in the active-matrix displays of modern TFT screens (TFT: *thin film transistor*) are fluorinated. In this application, the large dipole moments of CF and SF bonds allow for highly reliable switching of the TFTs. Examples for such fluorinated materials are:

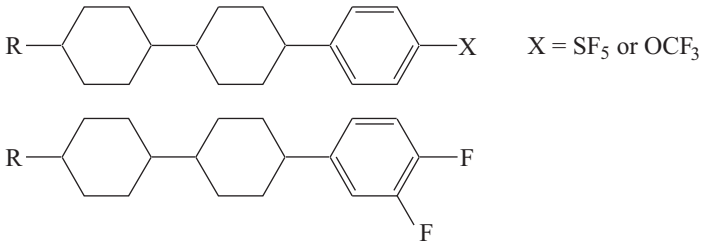

The use of the strongly polar and hydrolytically stable SF_5 group, which is generated by the fluorination of the corresponding disulfane RSSR with an F_2/N_2 mixture (1:9), improves material properties. The increasing effect on the dipole moment becomes apparent by comparison of the value for $PhCF_3$ (2.6 D) with that of $PhSF_5$ (3.4 D).

13.4.4.9 Fluorinated Pharmacologically and Agrochemically Active Substances

Fluorinated compounds are of enormous interest as pharmaceutics.[26] Fluorine and hydrogen have similar VAN DER WAALS radii (135 vs 120 pm), but in contrast to hydrogen, fluorine shows strong inductive and mesomeric effects. The high chemical stability of the CF bonds slows down the metabolism of fluorinated medications and hence increases the residence time in the body and with that the *bioavailability*. In addition, the replacement of CH by CF groups and of CH_3 by CF_3 groups increases the *lipophilicity*. This often completely alters the reactivity, an effect that is referred to as orthogonal reactivity of H and F. Due to these reasons, the selective substitution of H

26 V. Gouverneur et al., *Chem. Soc. Rev.* **2008**, *37*, 320. J.-P. Bégué, D. Bonnet-Delpon, *Bioinorganic and Medicinal Chemistry of Fluorine*, Wiley, Hoboken, **2008**. I. Ojima (ed.), *Fluorine in Medicinal Chemistry and Chemical Biology*, Wiley, Chichester, **2009**. D. O'Hagan, *J. Fluorine Chem.* **2010**, *131*, 1071. V. Gouverneur, K. Müller (eds.), *Fluorine in Pharmaceutical and Medicinal Chemistry*, World Sci. Publ. Co., **2012.**

by F frequently results in pharmaceutics that are up to 1000 times more active than the parent species! Examples are set by the cytostatic Fluoruracil, the anti-inflammatory Paramethason and the malaria drug Mefloquin:

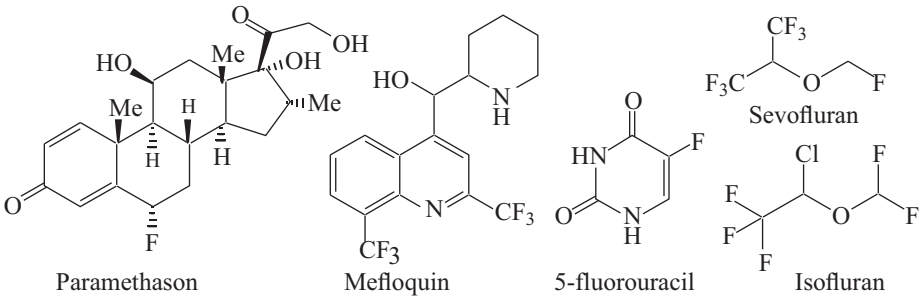

The narcotics Sevofluran, Isofluran and Halothan (CF_3–CHClBr) need also to be mentioned in this context. The narcotic effect of anesthetic substances increases with the ratio of solubility in lipids over the solubility in water. Therefore, the fluoro-substituted substances are far superior to the still employed laughing gas N_2O or the historically used narcotics diethylether and chloroform. Ultimately, however, these gases will end up in the atmosphere where their unreactive nature and resulting persistence is harmful to the climate.[27]

13.4.5 Bonding Situation in Fluorides

Individual nonmetal fluorides are covered in the chapters on the corresponding elements. Here, general and comparative considerations will be summarized that apply to all molecular fluorides collectively.

In some regard, fluorine is more related to the neighboring oxygen than to the other halogens. For instance, this is manifest in a comparison of the *electronegativities* χ, which are essential for the value of the bond enthalpies:

	F	O	Cl	Br	I
χ (Allred–Rochow):	4.10	3.50	2.83	2.74	2.21
χ (Pauling):	3.98	3.44	3.16	2.96	2.66

This difference becomes more obvious from the values for χ_{AR} than from those of χ_P. The *covalent and ionic radii* (*r*) of O and F are also closer to one another than to fluorine's heavier group homologues (in brackets the corresponding coordination numbers are given; the three covalent radii are for single bonds):

27 M. P. S. Andersen et al., *J. Phys. Chem. A* **2012**, *116*, 5806.

	O	F	Cl	O^{2-}	F^-	Cl^-
r (pm):	66	57	102	124(4) 126(6)	117(4) 119(6)	167(6)

Certain analogies between the solid-state chemistry of fluorides[28] and oxides result from these similarities. Also, the ability of fluorine to oxidize various elements to their highest oxidation states resembles that of oxygen. Corresponding compounds are, for example, AgF_2, $K_2[NiF_6]$ and SF_6. On the other hand, there are elements, which do not reach the highest oxidation state as binary fluorides, but only as oxyfluorides (or as oxides or oxoanions), for example, NOF_3, ClO_2F_3 and XeO_3F_2; the theoretically feasible molecules NF_5, ClF_7 and XeF_8 are unknown so far.

The *coordination numbers* attainable with fluorine substituents are mostly higher than those realized with the other halogens. For the following fluorides

$$[NF_4]^+ \quad SF_6 \quad XeF_6 \quad [PF_6]^- \quad IF_7 \quad ReF_7 \quad [SbF_7]^{2-} \quad [TeF_8]^{2-} \quad [XeF_8]^{2-}$$

no corresponding chlorides exist, let alone bromides or iodides. In addition to the much higher bond enthalpies of the fluorides, steric repulsion may also be a factor.

Despite its high electronegativity, fluorine forms molecular rather than salt-like fluorides with all nonmetals, albeit the bonds in these fluorides are obviously strongly polar. Due to their pronounced electronegativity, fluorine atoms exert a strong *inductive effect* in covalent bonds as the following examples illustrate:

(a) In SOF_2 the SO bond is considerably shorter than in any other thionyl species. Corresponding observations have been made for sulfuryl-, seleninyl-, selenyl- and phosphoryl compounds.
(b) $(CF_3)_3N$ is a much weaker LEWIS base than $(CH_3)_3N$. The group electronegativity of the CF_3 group is approximately 3.5 that of the CH_3 group about 2.4.
(c) CF_3COOH is a much stronger BRØNSTED acid than CH_3COOH.
(d) NF_3 is a much weaker LEWIS base than NH_3 and thus only forms ammonium salts such as $[NF_4]^+$ with extremely strong LEWIS acids. In contrast, protonation of NF_3 does not result in the corresponding ammonium, but rather the fluoronium salt with the cation $[H–F–NF_2]^+$.

13.4.6 Stabilization of Low Oxidation States

Relatively stable compounds are known in which a nonmetal adopts an unusually low oxidation state. Such *subvalent species* are preferentially formed with fluorine and oxygen, whereas they are much less stable with other bonding partners.

28 W. Massa, *Encycl. Inorg. Chem.* **2005**, *3*, 1535.

The best-known suboxide is carbon monoxide CO. Although CO is thermodynamically unstable regarding the disproportionation into CO_2 and graphite, the large activation enthalpy and entropy of this reaction leads to its metastability (i.e., persistency) at room temperature. In a similar manner, the stability of all other subvalent species is kinetic rather than thermodynamic in nature.

Boron monofluoride BF is isosteric to CO. It can be produced by reduction of BF_3 with crystalline boron in an equilibrium reaction:

$$BF_3(g.) + 2\,B(s.) \xrightarrow[1\ hPa]{2000°C} 3\,BF(g.) \xrightarrow{+BF_3} F_2B{-}BF_2 + F_2B{-}BF{-}BF_2$$

BF subsequently inserts into a bond of BF_3 to yield B_2F_4 and then B_3F_5. The latter is unstable and disproportionates to B_2F_4 and $B(BF_2)_3$, which in turn dimerizes to B_8F_{12}. This molecule contains a unique B_8 scaffold with a central bicyclobutane-like motif:

B_8F_{12} :

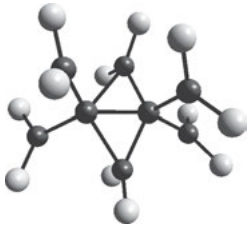

With CO, $B(BF_2)_3$ reacts to the adduct $(F_2B)_3BCO$ and with PF_3 to the crystalline $(F_2B)_3BPF_3$. Such reactions are carried out so that the reaction partner is added to the BF/BF_3 mixture after the hot zone followed by immediate condensation of the resulting mixture with liquid nitrogen.

In contrast to CO (d_{CO} = 113 pm), an approximate single bond is present in BF (d_{BF} = 126 pm). This follows not only from the internuclear distance but also from the valence force constant. The nonbonding electron pair and the vacant *p* orbitals at the boron atom confer carbene-like properties to the molecule: it preferably reacts in addition and insertion reactions under formation of two new single bonds. In the absence of suitable reaction partners, BF rapidly disproportionates to elemental boron and BF_3 at elevated temperatures; at low temperatures it oligo- or polymerizes instead.

Carbene-analogous compounds are also the fluorides CF_2 and SiF_2, which are both slightly more stable than BF. Difluorocarbene is formed in the following thermolysis and photolysis reactions:[29]

29 D. L. S. Brahms, W. P. Dailey, *Chem. Rev.* **1996**, *96*, 1585.

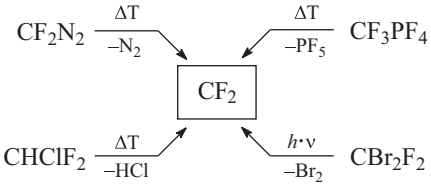

The half-life of dimerization from CF_2 to C_2F_4 at the pressures of pyrolysis amounts to about 1 s. C_2F_4 immediately reacts with further CF_2 to *cyclo*-C_3F_6, *cyclo*-C_4F_8 and to polymeric $(CF_2)_n$. Presumably, CF_2 also occurs as an intermediate during the synthesis of C_2F_4 and the thermal depolymerization of polytetrafluoroethylene (cf. Section 13.4.4).

The molecules CF_2 (α = 105°) and SiF_2 (α = 100°) are bent and diamagnetic with a *singlet ground state* and contain single bonds: d_{EF} = 130 (E = C) und 160 pm (E = Si). Difluorosilylene SiF_2 has a half-life of 150 s in the gas phase (25 °C; 20 Pa); it is prepared in high yield by reduction of SiF_4 with solid silicon as well as by thermal disproportionation of hexafluorodisilane Si_2F_6:[30]

$$\frac{1}{2}\,SiF_4(g.) + \frac{1}{2}\,Si(s.) \xrightarrow[20\ Pa]{1150°C} SiF_2(g.) \xleftarrow[-SiF_4]{700°C} Si_2F_6(g.)$$

In the absence of other reaction partners, SiF_2 reacts with SiF_4 to perfluorinated polysilanes Si_nF_{2n+2} (n = 1–14), on the one hand, and to diradical chain-like polymers $(SiF_2)_n$, on the other hand, which are found as structural motifs of the products of quenching reactions. With BF_3, SiF_2 reacts in a similar manner as with SiF_4, namely to $F_2B–(SiF_2)_n–F$ (n = 1–3: colorless liquids). From hexafluorobenzene and SiF_2, perfluorinated silylbenzenes $C_6F_5SiF_3$ and $C_6F_4(SiF_3)_2$ are obtained. Numerous other reactions with unsaturated organic species have been reported.

These examples illustrate the importance of subvalent species as *reaction intermediates* and for preparative purposes. Other surprisingly stable subfluorides of nonmetals are represented by the radicals $[NF_2]^\bullet$ and $[O_2F]^\bullet$, which exist in temperature and pressure-dependent equilibrium with their dimers N_2F_4 and O_4F_2, respectively (see Sections 9.5.1 and 11.4).

13.4.7 Stabilization of High Oxidation States

The most electronegative element, fluorine – unlike the other halogens – is capable of withdrawing sufficient electron density from nonmetallic atoms to allow for the isolation of compounds with the highest possible oxidation states. Representative

30 C.-S. Liu, T.-L. Wang, *Adv. Inorg. Chem. Radiochem.* **1985**, *29*, 1.

examples are $[NF_4]^+$, AsF_5, TeF_6, IF_7 and, to some degree, XeF_6. Hypervalency of some of these species, however, is still subject to intense debate, although calculated electron densities at the central atoms typically amount to values approximately equivalent to $8e^-$, in agreement with the classical octet rule.[31]

The realization of the highest oxidation states of transition metals normally also require the presence of fluorido (and occasionally oxido) ligands.[32] Examples include extremely strong oxidants such as MnF_4, NiF_4, AuF_5 and PtF_6, which are all prone to the elimination of F_2 even at relatively low temperatures (see Section 13.4.1).

13.5 Chlorine, Bromine and Iodine

13.5.1 Preparation and Properties of the Elements

13.5.1.1 Chlorine

In Nature, the element chlorine only occurs in bonded form due its high reactivity, predominantly as the chlorides of sodium, potassium and magnesium, but also in many organic compounds.[33,34] The most important resource for chlorine production is NaCl, which is found in seawater, in some saltwater lakes and as huge rock salt deposits formed by the drying-up of salty waters. Extended deposits exist all over the world; the largest underground salt mine is operated by Compass Minerals in Goderich (Ontario, Canada). In some warmer countries, NaCl is still produced by the evaporation of seawater in shallow saline ponds. In seawater the halogens F, Cl, Br and I are present in a ratio of 0.7 : 1000 : 35 : 0.03. The natural abundance of Cl in the Earth's crust amounts to 0.013%; the oceans contain about $5{\cdot}10^{16}$ t NaCl.

Elemental chlorine is one of the most important resources of the chemical industry, which is needed for the manufacture of numerous products such as pharmaceutical drugs, fertilizers, pesticides, plastics (e.g., PVC), textile fibers, dyes and new materials. Chlorine is therefore produced in enormous amounts by electrolysis of saturated aqueous NaCl solutions (brine) or hydrochloric acid. The worldwide production amounted to approximately $65{\cdot}10^6$ t per year in 2016; the majority of it in China (45%), the USA (20%) and Europe (15%). The following net equation describes the process during NaCl electrolysis, which accounts for 95% of chlorine production:

$$2\,NaCl + 2\,H_2O \xrightarrow{\text{energy}} 2\,NaOH + H_2\uparrow + Cl_2\uparrow$$

31 For a recent contribution on hypervalency see: A. Stirling, *Chem. Eur. J.* **2018**, *24*, 1709.

32 S. Riedel, M. Kaupp, *Coord. Chem. Rev.* **2009**, *253*, 606.

33 J.-P. Lang, *Encycl. Inorg. Chem.* **2005**, *2*, 866.

34 About 3500 naturally occurring organic compounds of chlorine, bromine and iodine are known, but only 12 of fluorine.

The key reaction is the anodic oxidation of the chloride ions. The cathode reaction depends on the procedure. There are three major variations of the so-called chloralkali process.[35] The *mercury cell process* employs liquid mercury as cathode material on which sodium ions are discharged rather than protons due to the very large overpotential of the latter. In this way, a diluted liquid sodium amalgam is obtained, which continuously flows out of the slightly inclined electrolysis cell. Subsequently, the amalgam is decomposed in a bed of graphite particles with water in counterflow. Catalyzed by graphite, the amalgam is hydrolyzed to caustic soda NaOH and hydrogen; the mercury is liberated and recycled into the electrolysis cell:

$$2\,Na + 2\,H_2O \longrightarrow 2\,NaOH + H_2\uparrow$$

The up to 200 anodes consist of graphite; the typical cell voltage is about 4.5 V.

In case of the *diaphragm cell process* and the nowadays preferred *membrane cell process*, anode and cathode compartments of the electrolysis cell are separated in order to avoid the mixing and thus the reaction of the products. While the ion-permeable diaphragm consists of either mineralic or PVC-based weaves coated with fluoro-organic resin, the impermeable membrane is made from a cation exchanger, which allows for the transport of Na^+ ions only. To avoid the destruction of the membrane by hot chlorine and sodium hydroxide solution, a PTFE copolymer is employed, which contains functional groups suitable for ion exchange (e.g., Nafion, Section 13.4.4). At the cathode, the following reaction takes place:

$$2\,H_2O + 2\,e^- \longrightarrow H_2 + 2\,[OH]^-$$

For every ton of chlorine produced by the chloralkali process, 1.1 t of NaOH are obtained. In 1997, about 64% of chlorine were produced in mercury cells, 24% in diaphragm cells and 11% in membrane cells (the remainder was obtained from other processes, for example, fused-salt electrolysis of NaCl for production of elemental sodium). As the membrane cell process uses about 30% less electric energy (2.5 MWh/t Cl_2) and is more environmentally benign (no mercury), new plants are built according to this method. In Europe, the last mercury cell-based chlorine production line was either shut-down or reconstructed according to the membrane cell process by the year 2018.[36] According to the *Minamata protocol* (named after the Minamata disease, which is caused by chronic exposure to methyl mercury species), the mercury cell process should be phased-out worldwide by 2025.

During the chlorination of organic compounds large amounts of hydrochloric acid accrue, which are electrolytically recycled to chlorine by a membrane cell

35 Winnacker-Küchler, *Chemische Technik: Anorganische Grundstoffe*, 5th ed., Volume 3, Wiley-VCH, Weinheim, **2005**, p. 427.

36 Except for smaller plants devoted to the production of alkoxides, for which viable alternatives are not available: M. Buhlman, *Nachr. Chem.* **2017**, *65*, 1210.

process, for example, at the company COVESTRO. Since 2003, an *oxygen-depolarized cathode* (ODC) is used, which allows for a lower cell-voltage and saves approximately 30% of electrical energy compared to the conventional membrane cell (1.8 MWh/t Cl_2).[37] The net reaction in this case is:

$$4\,HCl + O_2 \longrightarrow 2\,Cl_2 + 2\,H_2O$$

and for NaCl electrolysis:

$$2\,NaCl + H_2O + \tfrac{1}{2}O_2 \longrightarrow Cl_2 + 2\,NaOH$$

Elemental chlorine is also obtained from fused-salt electrolysis of NaCl and $MgCl_2$ for the production of metallic sodium and magnesium.

In the lab, Cl_2 is either taken from a steel cylinder or prepared by oxidation of chloride ions with strong oxidants under acidic conditions, for instance, through the reaction of concentrated hydrochloric acid with manganese(IV) oxide (MnO_2) or with $K[MnO_4]$:

$$4\,HCl + MnO_2 \longrightarrow Cl_2 + MnCl_2 + 2\,H_2O$$

This reaction corresponds to the classic DEACON process for chlorine production from HCl gas, which nowadays is carried out with a ruthenium oxide catalyst.

Chlorine is a green-yellow, toxic gas with a pungent smell that strongly attacks mucosal tissue. Gaseous Cl_2 is heavier than air and readily condenses to green-yellow liquid of b.p. −34 °C (vapor pressure at 20 °C: 65 kPa). It reacts with almost any metal (and many nonmetals), on warming often under ignition, for example, with alkali and alkaline earth metals, with Cu, Fe, As, Sb and Bi. Of the nonmetals, H_2 reacts in a particularly violent manner in an explosion-like chain reaction after ignition (Section 5.1). Also, many hydrogen compounds react lively with chlorine:

$$C_2H_2 + Cl_2 \longrightarrow 2\,C(s.) + 2\,HCl$$
$$NH_3 + 3\,Cl_2 \longrightarrow NCl_3 + 3\,HCl$$

Cl_2 is only sparingly soluble in water (6.5 g L^{-1} corresponding to 0.18 mol L^{-1} at 25 °C); in solution the following concentration-dependent equilibrium is established:

$$Cl_2 + H_2O \rightleftharpoons HOCl + HCl$$

Chlorine is employed in the synthesis of numerous inorganic and most of all organic compounds, which, however, are often just intermediates during the production of chlorine-free substances that are otherwise not accessible in an economic manner.[38]

37 J. Jörissen, T. Turek, R. Weber, *Chem. unserer Zeit* **2011**, *45*, 172 (with color pictures).
38 V. Hopp, *Chemiker-Ztg.* **1991**, *115*, 341.

In industry about one third of the produced chlorine is recycled. Examples for the application of *elemental chlorine* are the synthesis of chlorinated hydrocarbons, the production of many metal and nonmetal chlorides such as phosgene $COCl_2$ (from CO and Cl_2), PCl_3, SCl_2, S_2Cl_2 and $FeCl_3$ (each from the elements) as well as $SiCl_4$ and $TiCl_4$ from the dioxides by reduction with coke in the presence of Cl_2. Sodium hypochlorite (bleach, Na[ClO]) is obtained from caustic soda NaOH and Cl_2. The disinfection of drinking and bathing water as well as the bleaching of cellulose and paper with chlorine are decreasing in importance as hydrogen peroxide or ozone are used more and more frequently for this purpose (see Sections 11.3.3 and 11.1.3, respectively).

13.5.1.2 Bromine

Bromine[39] occurs in Nature only in bonded form, mostly associated with chlorine in analogous compounds. It is liberated in elemental form by introduction of Cl_2 into a slightly acidic aqueous solution of the bromides, which are contained in seawater, on the one hand, and are enriched during the production of potassium chloride, on the other hand; Br_2 is then chased from solution by an air stream:

$$2\,Br^- + Cl_2 \longrightarrow Br_2 + 2\,Cl^-$$

Subsequently, it can be dried with conc. H_2SO_4 and purified by distillation. A particularly high content of bromide ions is found in the Dead Sea (Israel/Jordan), from which more than half of the bromine traded worldwide is obtained. On a laboratory scale, Br_2 is prepared from KBr by oxidation in an acidic medium, for example, with MnO_2 and H_2SO_4.

Bromine is liquid at room temperature and of a deep red-brown color. It is more soluble in water than Cl_2 (34 g L^{-1} corresponding to 0.425 mol L^{-1} at 25 °C) and completely miscible with many nonpolar solvents (e.g., CCl_4). Although the reactivity of Br_2 is lower than that of Cl_2, both elements react in an analogous manner in general. Bromine is needed (about 20000 t per year) for the synthesis of organic pesticides and flame retardants such as 1,2,5,6,9,10-hexabromocyclododecane (HBCD). HBCD has been used as an additive for polystyrene foams in order to reduce the flammability (e.g., when employed as insulating material in construction) but was banned in the European Union in 2018. As HBCD is simply mixed into the polymer and is thus not chemically bonded, it escapes into the environment (surface waters) with time. It has been detected, for instance, in the eggs of seagulls and in shellfish.

Bromides are also used to produce AgBr, which is the light-sensitive material of many photographic films; some special films employ AgI instead. Since the advent of digital photography, however, the need for photographic films has reduced significantly.

---

39 D. Price, B. Iddon, B. J. Wakefield (eds.), *Bromine Compounds*, Elsevier, Amsterdam, **1988**.

13.5.1.3 Iodine

Iodine is found in Nature not only in the form of inorganic iodides and iodates, but also as organic compounds. The combustion of seaweed, which enriches iodine from seawater, together with $K_2[CO_3]$ yields iodide-containing ashes. This "biogenic" enrichment probably also explains the high iodide content of certain *fossil brines*, which are found underground in Japan, the USA and elsewhere. These brines are highly concentrated salt solutions (formed by the evaporation of ancient surface waters) from which iodine can be obtained by introducing a stream of Cl_2 and subsequent blowing-out with air – similarly as described for bromine:

$$2\,I^- + Cl_2 \longrightarrow I_2 + 2\,Cl^-$$

Chile is the world's largest producer of iodine and iodide. The *Chile saltpeter* $Na[NO_3]$ contains iodine in the form of $Ca[IO_3]_2$, which is accrued in the mother liquors as $Na[IO_3]$ during the purification of saltpetre by recrystallization. By reduction of $Na[IO_3]$ with SO_2 or $Na_2[SO_3]$ elemental iodine or iodide are prepared. Large amounts of iodine are also obtained in Japan from brines used in the extraction of natural gas. Iodides can be reduced to I_2 electrolytically or even by relatively mild oxidants.

Elemental iodine forms grayish black, scaly crystals with metallic luster, which readily sublime and can thus be purified this way. The sublimation enthalpy amounts to 62.4 kJ mol^{-1}. The vapor and certain *iodine solutions* (in CCl_4, $CHCl_3$, CS_2) are of violet color. In other solvents such as H_2O, ethers or dioxane iodine dissolves with brown color, in aromatic hydrocarbons with red color. The solubility in water at 25 °C is only 0.3 g or $2{\cdot}10^{-3}$ mol L^{-1}. The differences in color are due to intermolecular interactions: while the violet color is attributed to the unperturbed I_2 molecule, the brown and red colors originate from *charge transfer complexes*, which result from a partial electron donation from the solvent molecules (donor) to iodine (acceptor). Such *CT complexes* (also known for Br_2 and Cl_2) are mostly characterized by intense absorptions of visible light.

With triphenylphosphane, I_2 forms a yellow 1:1 adduct with a linear P–I–I unit, which is a donor–acceptor complex with partial delocalization of the nonbonding 3*s* electrons of phosphorus into the σ* LUMO of I_2, hence the comparatively large d_{I-I} of 316 pm.[40] This kind of charge transfer can happen to such an extent that the I–I bond is broken. For example, the analogous tBu$_3$P·I$_2$ in fact exists as the salt $[t\text{Bu}_3\text{PI}]^+I^-$ and the species of composition py·I_2 stoichiometry is better represented by the ionic formula $[I(py)_2]^+[I_3]^-$ (py = pyridine). A well-known CT complex of iodine is the blue *intercalation compound* of polyiodide ions in the central cylindrical open space of the helical structure of amylose, a component of starch. This iodine-starch complex ($\lambda_{max} \approx 600$ nm) is taken as analytical proof for iodine (polyiodide ions are covered in Section 13.5.3).

40 C. A. McAuliffe et al., *J. Chem. Soc. Chem. Commun.* **1991**, 1163.

Diiodine molecules can also act as electron donors and hence as ligands in transition metal complexes. For instance, $Ag[AsF_6]$ reacts with I_2 in liquid SO_2 to give the crimson-red polymeric complex $[AgI_2][AsF_6]$ in which the cation consists of a planar zigzag chain of the connectivity –Ag–I–I–Ag–I–I–. Each silver ion is coordinated by four additional fluorine atoms of the anions.[41] The I–Ag–I angle amounts to 99°. The Ag–I bonds can be understood as electron density from the π* MO (HOMO) of the iodine being delocalized into the empty 5*s* AO of the silver cation. Concomitantly, a certain back donation through charge transfer from the Ag (4*d*)-AO into the σ* MO of the ligand must be taken into account. Consequently, the I–I internuclear distance in the complex is only by 1 pm smaller than in the free I_2 molecule.

13.5.2 Halides

Almost all elements form halides, that is, binary element–halogen species in which the halogen typically represents the more electronegative bonding partner. These compounds either crystallize in ionic structures (KCl, AlF_3), form polymers (graphite fluoride) or exist as small molecules (SCl_2, PF_5). In addition to the binary halides, however, a large number of more complicated compounds are known, for example, the oxohalides (e.g., SOF_4), hydroxohalides (e.g., HSO_3Cl), complex anions (e.g., $[SiF_6]^{2-}$) and cations (e.g., $[PCl_4]^+$).

The fluorides of hydrogen and of selected nonmetals have been treated in Section 13.4. Further fluorides and the chlorides, bromides and iodides of most nonmetals are described in the sections of the respective elements. Here, only the hydrogen halides HCl, HBr and HI will be covered. In Sections 13.5.3–13.5.5, the binary compounds of two different halogens, the so-called interhalogens, will be discussed.

13.5.2.1 Hydrogen Halides HCl, HBr and HI

The hydrogen compounds of the halogens can be synthesized from the elements. As the GIBBS energy $\Delta G°$ of the reaction

$$H_2 + X_2 \rightleftharpoons 2\,HX \qquad X = \text{halogen}$$

strongly increases from fluorine to iodine,[42] the equilibrium is shifted further to the left with increasing weight of the halogen. While fluorine and chlorine quantitatively

41 T. S. Cameron, J. Passmore, X. Wang, *Angew. Chem. Int. Ed.* **2004**, *43*, 1995.

42 $\Delta G_{f,298}°$ is −273 (HF), −92 (HCl), −36 (HBr) and +26 (HI) kJ mol^{-1}, referring to the halogens in their standard states.

burn to HX in a hydrogen atmosphere, HBr can only be produced from the elements in good yields if the reaction temperature is held at 150–300 °C. This comparatively low temperature necessitates a catalyst to reach satisfying reaction rates (active charcoal or platinum). In case of hydrogen iodide (with a GIBBS formation enthalpy of only –5 kJ mol^{-1} with reference to the gaseous elements), the reaction has to be carried out in the same manner. HI decomposes into the elements even on gentle warming. The homogenous gas phase reaction of HX formation follows a radical chain mechanism in all four cases (Section 5.1).

Hydrogen chloride (b.p. –84 °C) is industrially produced through the protonation of chloride ions, which is achieved in practice by the reaction of KCl with concentrated sulfuric acid leading to HCl and $K_2[SO_4]$ on heating. HCl is also formed in huge amounts as necessary by-product of the technologically important chlorination of organic compounds[43] according to:

In this manner, methane is converted to the derivatives CH_3Cl, CH_2Cl_2, $CHCl_3$ and CCl_4 as well as benzene to chlorobenzene C_6H_5Cl. Furthermore, HCl is generated during the synthesis of isocyanates, produced on very large scale as precursors of polyurethanes:

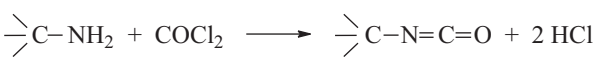

Hydrogen chloride is removed from the gaseous exhaust of the reaction by absorption with water and is either commercially sold as concentrated (30–32 wt%) or fuming hydrochloric acid (38 wt%) or is reconverted to Cl_2 electrolytically by the membrane cell process. Hydrochloric acid forms an azeotrope with water (b.p. 110 °C) at an HCl content of 20.2 wt%.[44]

HBr can also be produced by treatment of KBr with a strong nonvolatile mineral acid provided a nonoxidizing acid such as H_3PO_4 is used. A much more convenient method, in any case on a laboratory scale, is the hydrolysis of a nonmetal bromide such as PBr_3:

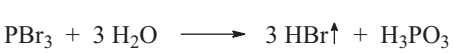

In an analogous manner, hydrogen iodide is obtained from PI_3.

All hydrogen halides are colorless gases under standard conditions (25 °C/1013 hPa), which can be liquefied with comparative ease. In the solid state, they form molecular crystals. HF is associated by strong hydrogen bonds in all phases

43 Vinyl chloride (and thus polyvinyl chloride, PVC) is produced from ethylene, O_2 and HCl.

44 An azeotropic mixture shows the same composition in gas and liquid phase. It boils at a constant temperature and cannot be separated by fractional distillation unless the pressure is changed.

(Section 5.6.4). For all other HX species, only the liquid state shows considerable dipole association. The dipole moments strongly decrease from HF (1.8 D) to HI (0.4 D; Table 5.4).

With small amounts of water, all hydrogen halides react to oxonium salts, which are only stable at low temperatures (Section 5.6.4). HF, HCl, HBr and HI are exceedingly well soluble in water. The acid strength of the solution increases remarkably from HF to HI (Table 5.4). While the degree of dissociation typically decreases with higher concentrations, precisely the opposite is observed for hydrofluoric acid. This is attributed to the equilibrium reaction

$$HF + H_2O \rightleftharpoons [H_3O]^+ + F^-$$

which is shifted to the right-hand side due to complexation of F^- ions by HF under formation of $[HF_2]^-$, $[H_2F_3]^-$, $[H_3F_4]^-$ and $[H_4F_5]^-$ with rising HF content. The salts $[H_3O]F$, $[H_3O][HF_2]$ and $[H_3O][H_3F_4]$ have been isolated in pure form.

Although it is generally assumed that dilute hydrochloric acid is completely dissociated, at a molar HCl : H_2O ratio of 0.28 : 1 (corresponding to near-concentrated hydrochloric acid of about 36 wt%) a nonnegligible fraction of $[HCl_2]^-$ anions is present. An aqueous HCl solution saturated at 20 °C has a concentration of 40.4 wt%.[45] Due to the formation of hydrogen bonds, HCl dissolves similarly well in alcohols and ethers.

A characteristic property of HBr and HI and their anions Br^- and I^- is the facile oxidation to Br_2 and I_2, respectively, which follows from the values of the redox potentials. HI is even oxidized by the oxygen of air so that acidic aqueous solutions of iodide slowly turn brown on exposure to air (autoxidation with formation of $[I_3]^-$).

13.5.3 Polyhalide Ions

In this section the so-called nonclassical polyhalide ions[46] are discussed, while the classical interhalogen anions such as $[ClF_4]^-$ are described in Section 13.5.5.

Elemental iodine dissolves much better in aqueous potassium iodide solutions than in pure water. The reason for this is the formation of complexes between I_2 molecules and iodide ions according to below equilibrium:

$$I^- + I_2 \rightleftharpoons [I_3]^- \qquad K_c = \frac{c(I_3^-)}{c(I^-) \cdot c(I_2)}$$

45 The gastric juice of humans and higher animals contains HCl in a concentration of 0.1–0.5% (pH value 2.3–0.9).

46 H. Haller, S. Riedel, *Z. Anorg. Allg. Chem.* **2014**, *640*, 1281.

The reaction enthalpy in water amounts to only –17 kJ mol^{-1}. From the red-brown solution, the black salt $K[I_3]\cdot H_2O$ crystallizes on evaporation or cooling. Water-free triiodide can be obtained with larger cations: $Rb[I_3]$, $Cs[I_3]$ and $[Co(NH_3)_6][I_3]_3$ have been isolated in crystalline, anhydrous form.

For the lighter homologues of iodine, the trend to polyhalide formation is somewhat less pronounced. Nonetheless, numerous crystalline polychlorides and -bromides are known, for example, $[Me_4N][Cl_3]$ and $[NH_4][Br_3]$ (see below). Moreover, a considerable number of *mixed polyhalide* ions have been prepared, which can contain two or more different halogens including fluorine. $[ICl_2]^-$, $[I_2Br]^-$, $[IBrF]^-$ and $[BrCl_2]^-$ serve as examples. Such anions are generated from a halide ion (or a suitable X^- donor) and a halogen molecule or an interhalogen compound

$$KI + Cl_2 \longrightarrow K[ICl_2]$$

$$PCl_5 + ICl \longrightarrow [PCl_4][ICl_2]$$

Large univalent cations are particularly suitable for the isolation of such salts; the reasons for this are described in Section 2.1.7.

The above-defined equilibrium constant K_c has the following values at 25 °C for the different trihalide ions: $[I_3]^-$: 725; $[ICl_2]^-$: 167; $[Br_3]^-$: 18; $[Cl_3]^-$: 0.01.[47] The triiodide is by far the most stable. This also applies to the anhydrous salts, which dissociate according to above equilibrium on heating. For $Cs[I_3]$, the equilibrium vapor pressure of I_2 reaches atmospheric pressure (0.1 MPa) at 250 °C.

All known trihalide ions are linear or quasi-linear (valence angles 170°–180°). In solution, the ions $[I_3]^-$, $[Br_3]^-$ and $[ICl_2]^-$ are centrosymmetric ($D_{\infty h}$ symmetry), that is, the internuclear distances are equal. In the crystalline state, however, a descent in symmetry frequently occurs due to an asymmetric interaction with the surrounding cations. The two I–I internuclear distances in the anion of $[NH_4][I_3]$ are thus 279 and 311 pm ($C_{\infty v}$ symmetry). In case of the mixed ions, the halogen of lowest electronegativity always occupies the central position.

Prior to the discussion of the *bonding situation*, it is useful to compare the bond properties of trihalide ions with that of dihalogen molecules. Not only the internuclear distance, but also the valence force constants show that the bonds in these ions are weaker than in the neutral molecules X_2 (Table 13.2).

MO theory allows for an elegant interpretation of the experimental findings.[48] If the z axis is defined as the principal molecular axis C_∞ of the linear $[I_3]^-$ ion, the three $5p_z$ orbitals of the iodine atoms overlap. As in the case of the linear $[HF_2]^-$ ion,

47 The trifluoride anion was detected by IR and Raman spectroscopy at low temperatures after co-condensation of gaseous KF, RbF or CsF with F_2 and excess argon at 15 K; $[F_3]^-$ is valence isoelectronic with KrF_2; its dissociation into F_2 and F^- is endothermic by about 100 kJ mol^{-1} in the gas phase: S. Riedel et al, *Inorg. Chem.* **2010**, *49*, 7156.

48 G. A. Landrum, N. Goldberg, R. Hoffmann, *J. Chem. Soc. Dalton Trans.* **1997**, 3605.

Table 13.2: Valence force constants of trihalide ions in comparison to those of dihalogen molecules (f_r in N cm^{-1}; after W. Gabes, R. Elst, *J. Mol. Struct.* **1974**, *21*, 1).

Br_2: 2.46	BrCl: 2.67	I_2: 1.72	ICl: 2.38	IBr: 2.07
$[Br_3]^-$: 0.94	$[BrCl_2]^-$: 1.08	$[I_3]^-$: 0.70	$[ICl_2]^-$: 1.06	$[IBr_2]^-$: 0.94

the interaction of these three orbitals results in three σ MOs of which one each is bonding, nonbonding and antibonding (Figure 13.1).

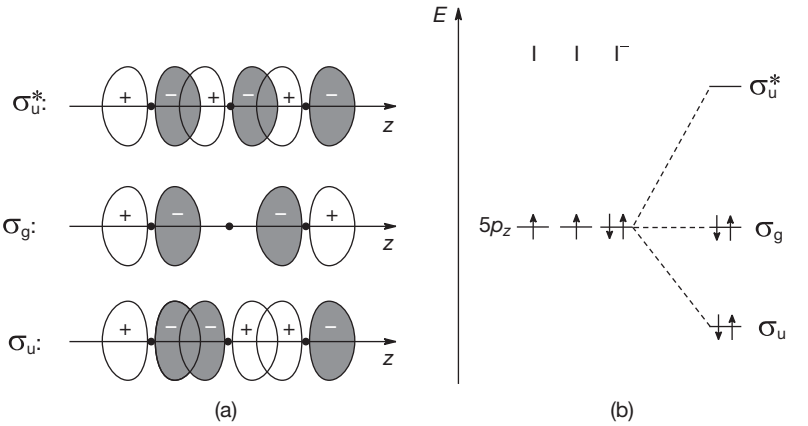

Figure 13.1: The three-center four-electron bond in the linear triiodide anion $[I_3]^-$. (a) Linear combinations of the three 5*p* atomic orbitals to three σ molecular orbitals (depicted without inner nodal planes for simplicity). (b) Energy diagram of the three σ MOs. While the bonding electron pair is delocalized across all three atoms, the nonbonding electron density is localized at the terminal atoms.

The three MOs are occupied with four electrons. Since only two of these are bonding, a relatively weak covalent bond results. The valence angle of 180° is a consequence of such a three-center four-electron σ bond since the orbital overlap would be reduced upon bending.[49] The negative charge of the ion is mostly located at the terminal atoms.

Elemental iodine shows a strong tendency toward the formation of *multicenter bonding*. This becomes apparent not only in the structure of crystalline iodine itself (Section 13.2), but also in the existence of numerous polyiodide anions such as $[I_5]^-$, $[I_7]^-$, $[I_9]^-$, $[I_8]^{2-}$, $[I_{10}]^{2-}$, $[I_{11}]^-$, $[I_{12}]^{2-}$, $[I_{13}]^{3-}$, $[I_{16}]^{2-}$ and $[I_{29}]^{2-}$, which have all been

49 The π orbitals of the three atoms overlap as well and are thus energetically split into bonding, nonbonding and antibonding MOs. As they are completely filled with electrons, they do, however, not contribute to the overall bond strength.

isolated in the form of defined salts and can be regarded as adducts of I_2 molecules to one or more anions I^-.[50] The anion of $[Me_4N][I_5]$ is bent with C_{2v} symmetry:

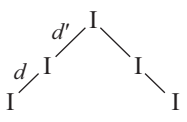

$d' = 317$ pm

$d = 281$ pm

$[I_5]^-$ (C_{2v})

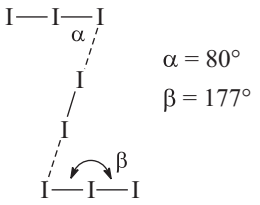

$[I_8]^{2-}$

This ion is nearly planar and consists of a central iodide ion to which two I_2 molecules are connected through two of its 5*p* orbitals. Similarly, the association of two and three molecules of I_2 to an $[I_3]^-$ ion becomes apparent from the internuclear distances of the ions $[I_7]^-$ and $[I_9]^-$, respectively. The diamagnetic salt $Cs_2[I_8]$ contains the Z-shaped anion $[I_8]^{2-}$ (see above), which formally consists of two unsymmetrical $[I_3]^-$ ions and a central I_2 molecule.

Polyhalide ions of chlorine and bromine with more than three atoms are known as well.[51] The pentabromide ion $[Br_5]^-$ and the corresponding pentachloride have been structurally characterized; $[Cl_7]^-$ and $[Cl_9]^-$ were detected by Raman spectroscopy as the $[NR_4]^+$ salts (R = alkyl group). The same applies to the corresponding polybromides. The dianions $[X_8]^{2-}$ adopt zigzag chains, which vary from a pronounced Z-shape for X = Br to a quasilinear arrangement for X = Cl.[52a] A $[Br_6]^{2-}$ salt has been isolated, although its dianion is probably better described as weakly bonded dimer of two $[Br_3]^-$ units.[52b] The relatively large polychlorides $[Cl_{11}]^-$, $[Cl_{12}]^{2-}$ and $[Cl_{13}]^-$ were isolated with suitable ammonium, phosphonium, arsonium and iminium counteractions.[52c] While $[Cl_{12}]^{2-}$ shows an analogous structure to the corresponding polyiodide, $[Cl_{11}]^-$ and $[Cl_{13}]^-$ exhibit central chloride ions, which are coordinated by five and six end-on bonded Cl_2 molecules, respectively, in square pyramidal and octahedral coordination spheres.

In case of bromine, salts with the anions $[Br_{10}]^{2-}$, $[Br_{11}]^-$ and $[Br_{20}]^{2-}$ have been prepared. $[Br_{10}]^{2-}$ consists of two Br_2 molecules and two $[Br_3]^-$ anions. In fact, all polyhalides can be understood by invoking halogen bonds between negatively charged donor ions and neutral acceptor molecules X_2 (see Section 13.3).

50 P. H. Svensson, L. Kloo, *Chem. Rev.* **2003**, *103*, 1649. C. Walbaum, I. Pantenburg, G. Meyer, *Z. Naturforsch.* **2010**, *65b*, 1077.

51 S. Riedel et al., *Chem. Eur. J.* **2012**, *18*, 5741 and *Angew. Chem. Int. Ed.* **2011**, *50*, 11528. C. Feldmann et al., *Inorg. Chem.* **2011**, *50*, 11683. M. Wolf, J. Meyer, C. Feldmann, *Angew. Chem. Int. Ed.* **2011**, *50*, 4970. X. Chen et al., *Inorg. Chem.* **2010**, *49*, 8684.

52 (a) S. Riedel et al., *Angew. Chem. Int. Ed.* **2016**, *55*, 10904. (b) S. Riedel et al., *Chem. Eur. J.* **2018**, *24*, 1072. (c) S. Riedel et al., *Angew. Chem. Int. Ed.* **2018**, *57*, 9136.

13.5.4 Positive Halogen Ions

Positive element ions have first been introduced in the context of chalcogens, for example, $[O_2]^+$, $[S_8]^{2+}$ and $[Se_4]^{2+}$. The less electronegative the corresponding element, the more readily they form.[53] Nonetheless, even for the heavier (and thus more electropositive) nonmetals, strong oxidants are usually required in order to oxidize the element to a positively charged ion. Owing to the strongly electrophilic character of such ions, they can only be prepared in the presence of weakly nucleophilic anions and solvents; in water, for instance, rapid disproportionation occurs.

It is to be expected that I_2 is the easiest of all halogens to be oxidized to a cation. Indeed, even molten iodine shows a significant electrical conductivity, which is attributed to the following auto-dissociation:

$$3\ I_2 \rightleftharpoons [I_3]^+ + [I_3]^-$$

The ion $[I_3]^+$ and analogous halogen cations of chlorine and bromine are prepared by oxidation of the elements, by comproportionation of the elements with suitable interhalogen species or by special custom-designed reactions in particular cases. The following salts are only stable at low temperature:

$$Cl_2 + ClF + AsF_5 \xrightarrow{-78°} [Cl_3][AsF_6] \quad \text{yellow crystals}$$

$$2\ Cl_2 + IrF_6 \longrightarrow [Cl_4][IrF_6] \quad \text{blue crystals}$$

So far, $[Cl_2]^+$ has only been detected in the gas phase. $[Cl_3]^+$ is isoelectronic with SCl_2 (C_{2v} symmetry) and $[Cl_4]^+$ forms a rectangle (D_{2h}) as a consequence of a π^*–π^* interaction between the formal components Cl_2 and $[Cl_2]^+$ (see below). Salts with the cations $[Br_2]^+$ and $[Br_3]^+$ are thermally more stable; they are obtained by oxidation of Br_2 with peroxodisulfuryl fluoride or BrF_5:

$$\text{(a)}\quad Br_2 + S_2O_6F_2 \longrightarrow 2\ BrSO_3F$$

$$Br_2 + 2\ BrSO_3F + 10\ SbF_5 \longrightarrow 2\ [Br_2][Sb_3F_{16}] + 2\ Sb_2F_9SO_3F$$

$$\text{(b)}\quad 7\ Br_2 + BrF_5 + 5\ AsF_5 \longrightarrow 5\ [Br_3][AsF_6]$$

The bromonium salt $[Br_2][Sb_3F_{16}]$ forms red paramagnetic crystals (m.p. 86 °C), whereas brown $[Br_3][AsF_6]$ is diamagnetic. This salt reversibly reacts with Br_2 to yield $[Br_5][AsF_6]$;[54] the planar cation $[Br_5]^+$ exhibits C_{2h} symmetry just like $[I_5]^+$:

53 N. Burford, J. Passmore, J. S. P. Sanders in: *From Atoms to Polymers*, J. F. Liebmann, A. Greenberg, eds., VCH, Weinheim, **1989**, p. 53.

54 H. Hartl, J. Nowicki, R. Minkwitz, *Angew. Chem. Int. Ed.* **1991**, *30*, 328.

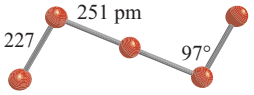

Concerning iodine, the ions $[I_2]^+$, $[I_3]^+$, $[I_5]^+$, $[I_4]^{2+}$ and $[I_{15}]^{3+}$ as well as mixed cations such as $[I_2Cl]^+$, $[I_2Br]^+$, $[I_3Cl_2]^+$ and $[I_3Br_2]^+$ have been isolated as salts. The light blue paramagnetic $[I_2]^+$, which had been mistakenly regarded as I^+ in the past, is formed when I_2 is dissolved in fuming sulfuric acid (65% SO_3 in H_2SO_4), whereupon SO_3 acts as an oxidizing agent, itself being reduced to SO_2 in the process. If neat sulfuric acid is employed as a solvent, I_2 can also be oxidized to $[I_2]^+$ using $S_2O_6F_2$. On cooling of the solutions, $[I_2]^+$ dimerizes to red diamagnetic $[I_4]^{2+}$. Dissolution of I_2 in oleum with only 25% of SO_3 or oxidation of an I_2/H_2SO_4 mixture by iodic acid HIO_3 both result in the brown $[I_3]^+$ ion, which continues to react with further I_2 to the likewise brown $[I_5]^+$. All polyiodine cations can alternatively be prepared by oxidation of I_2 with AsF_5 or SbF_5 in liquid SO_2:

$$2\ I_2 + 5\ SbF_5 \longrightarrow 2\ [I_2][Sb_2F_{11}] + SbF_3$$
$$3\ I_2 + 3\ AsF_5 \longrightarrow 2\ [I_3][AsF_6] + AsF_3$$
$$2\ I_2 + 4\ SbF_5 \longrightarrow [I_4][SbF_6][Sb_3F_{14}]$$

As mentioned above, $[I_3]^+$ reacts to $[I_5]^+$ with excess iodine and shows a structure analogous to $[Br_5]^+$. The chain-like cation $[I_{15}]^{3+}$ consists of three loosely bonded $[I_5]^+$ units with a center of inversion (*i*) at the central atom:

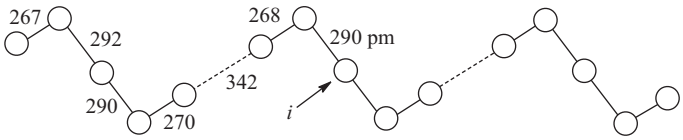

The covalent bond in the cations $[Cl_2]^+$, $[Br_2]^+$ and $[I_2]^+$ is expectedly stronger than that in the corresponding halogen molecules, which is manifest in the smaller internuclear distances as well as in the larger force constants (Table 13.3).

Table 13.3: Harmonic force constants f_r and bond lengths d of Cl_2, $[Cl_2]^+$, Br_2, $[Br_2]^+$, I_2 and $[I_2]^+$.

	$^{35}Cl_2$	$[^{35}Cl_2]^+$	$^{79}Br_2$	$[^{79}Br_2]^+$	$^{127}I_2$	$[^{127}I_2]^+$
f_r (N cm^{-1})	3.23	4.40	2.46	3.29	1.72	2.15
d (pm)	199	189	228	215	267	

This strengthening of the bonds can be easily explained with the previously discussed MO diagrams of the dihalogen (Section 2.4.3). The highest occupied levels are the antibonding π* orbitals. During the oxidation of X_2 to $[X_2]^+$ an antibonding

electron is thus removed. The resulting radical cation only tends to dimerize in case of $[I_2]^+$ and even there only at low temperatures. The $[I_4]^{2+}$ dimer as in the salt $[I_4][SbF_6][Sb_2F_{14}]$ is a planar rectangle (D_{2h} symmetry), which implies a bonding interaction between the two $[I_2]^+$ units mediated by π^* MOs in the plane of the molecule:

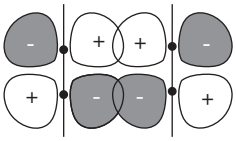

The cations of type $[X_3]^+$ are bent (C_{2v} symmetry).[55] $[Cl_3]^+$ is isoelectronic with SCl_2. The ion $[Cl_2F]^+$ is of C_s symmetry with the connectivity ClClF. The analogous cations $[ClF_2]^+$, $[BrF_2]^+$ and $[ICl_2]^+$ are treated in Section 13.5.5.

The planar ion $[I_5]^+$ can formally be regarded as a complex of a central iodine cation I^+ (iodonium ion) and two I_2 ligands. The iodonium ion also exists as a differently coordinated variety, namely as $[I(pyridine)_2]^+$. Salts of this cation are formed by disproportionation of I_2:

$$I_2 + 2\,py + AgNO_3 \xrightarrow{CHCl_3} [I(Py)_2]NO_3 + AgI$$

This iodine salt can be precipitated from solution with hydrocarbons and dissolves in $CHCl_3$ and acetone to give electrically highly conducting solutions. Electrolysis of such solutions expectedly yields elemental iodine at the cathode. Analogous complexes, albeit less stable, have also been prepared in case of chlorine and bromine.

13.5.5 Interhalogen Compounds

Compounds of the type XY_n with X and Y representing different halogens and n being an uneven number between 1 and 7 are referred to as interhalogen compounds. Besides binary species, a few ternary examples are known.

The simplest representatives of this class are the compounds XY that correspond to the elemental halogens X_2 and Y_2:

ClF	BrF	BrCl	IF	ICl	IBr
colorless gas	yellow solid at −100 °C	yellow solid at −100 °C	detected in noble gas matrix	red crystals	black crystals

55 K. O. Christe, R. Bau, D. Zhao, *Z. Anorg. Allg. Chem.* **1991**, *593*, 46; J. Li, S. Irle, W. H. E. Schwarz, *Inorg. Chem.* **1996**, *35*, 100.

These and other interhalogen compounds can be synthesized directly from the elements. The reaction conditions (temperature, reaction time, solvent or no solvent, ratio of reactants) determine which product is predominantly formed. The reaction mixtures are separated by sublimation or fractional distillation/condensation. With excess halogen Y_2 (mostly F_2) compounds of type XY_3, XY_5 and XY_7 are obtained:

$$\tfrac{1}{2}X_2 + \tfrac{1}{2}Y_2 \longrightarrow XY \xrightarrow{+Y_2} XY_3 \xrightarrow{+Y_2} XY_5 \xrightarrow{+Y_2} XY_7$$

The following species have been prepared (λ^3-, λ^5- and λ^7-chloranes, -bromanes and -iodanes):

ClF_3	BrF_3	IF_3	I_2Cl_6	ClF_5	BrF_5	IF_5	IF_7
colorless gas	yellow liquid	yellow solid (dec. > −30°)	yellow crystals	colorless gas	colorless liquid	colorless liquid	colorless gas

Excepting the dimeric iodine trichloride, all of these are fluorides of chlorine, bromine and iodine. Neither do any fluorine halides FY_n exist, nor bromides or iodides of type XBr_n and XI_n, which shows that for $n > 1$ only fluorine and in a single case also chlorine are suitable as substituents. Only the heavier halogens can adopt the role of the central atom. The trihalides XY_3 are T-shaped (C_{2v} symmetry), the pentahalides show a square-pyramidal geometry (C_{4v}) and IF_7 forms a slightly distorted pentagonal bipyramid. These structures correspond to predictions according to the electron pair repulsion model (Section 2.2.2), although they apply only to the gas phase. In condensed phases, *association* via bridging halogen atoms is frequently observed. For example, ClF_3, BrF_3 and ICl_3 are dimeric in the liquid and solid state. The molecule I_2Cl_6 is planar and shows the following centrosymmetric geometry:

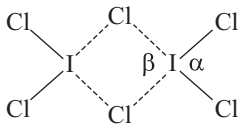

$d_{ICl} = 240$ pm $\quad \alpha = 94°$
$d_{I\text{--}Cl} = 270$ pm $\quad \beta = 84°$

An organic derivative of ICl_3 is phenyliodo dichloride $C_6H_5ICl_2$, which is prepared from phenyl iodide and chlorine as yellow, needle-shaped crystals. The structure is characterized by intermolecular ICl bridges in a zigzag chain so that an approximate square-planar coordination environment results for the iodine atoms akin to that in I_2Cl_6.

All halogen fluorides are very reactive, particularly those with central atoms in higher oxidation states. ClF_3 and BrF_3 are produced on a technical scale from the elements and used as strong fluorinating agents.[56]

56 S. Rozen, *Acc. Chem. Res.* **2005**, *38*, 803.

Various interhalogen species such as ICl, I_2Cl_6, BrF_3 and IF_5 show a considerable electrical conductivity as liquids (BrF_3: $8.0 \cdot 10^3\ \Omega^{-1}\ cm^{-1}$), which is attributed to autodissociation. Considering the association of the molecules in condensed phases, the dissociation requires just a slight shift of a bridging halogen atom:

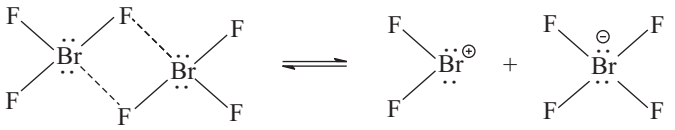

The assumption of such dissociation equilibria, which resemble the behavior of other solvents such as H_2O, NH_3, HF or H_2SO_4, is supported by the isolation of the corresponding complex ions as salt-like compounds. The cations are prepared by reactions with strong LEWIS acids, which function as halide acceptors:

$$BrF_3 + SbF_5 \longrightarrow [BrF_2][SbF_6] \qquad IF_5 + SO_3 \longrightarrow [IF_4][SO_3F]$$
$$ICl_3 + AlCl_3 \longrightarrow [ICl_2][AlCl_4] \qquad IF_7 + AsF_5 \longrightarrow [IF_6][AsF_6]$$

The anions are obtained from the reaction with an ionic halide:

$$NaF + BrF_3 \longrightarrow Na[BrF_4] \qquad KF + IF_5 \longrightarrow K[IF_6]$$
$$KF + ICl_3 \longrightarrow K[ICl_3F] \qquad [Me_4N]F + IF_7 \longrightarrow [Me_4N][IF_8]$$

Besides, halide ions and complex halide ions can be halogenated directly to further increase the number of halogen atoms:

$$KCl + 2\,F_2 \longrightarrow K[ClF_4]$$
$$[ICl_2]^- + Cl_2 \longrightarrow [ICl_4]^-$$

The mostly ionic structure of such compounds follows from structural analyses and from the fact that salts such as $[BrF_2][SbF_6]$ dissolve in liquid BrF_3 to yield solutions, which conduct electricity very well. The ion $[BrF_2]^+$ behaves as a solvoacid in those solutions and can be neutralized with the solvobase $[BrF_4]^-$. Neutralization reactions of this sort can be conveniently monitored conductometrically with the end of the reaction such as

$$[BrF_2][SbF_6] + Ag[BrF_4] \longrightarrow Ag[SbF_6] + 2\,BrF_3$$

being characterized by a minimum in conductivity. Analogous considerations apply to other ionogenic solvents.

The structures of the ions $[XY_{n-1}]^+$ and $[XY_{n+1}]^-$ mostly (yet not always) conform with expectations according to the VSEPR model (Section 2.2.2) as the following examples show:

$[BrF_2]^+$	$[BrF_4]^-$	$[IF_4]^+$	$[IF_6]^+$	$[IF_6]^-$
bent (C_{2v})	square-planar (D_{4h})	seesaw (C_{2v})	octahedral (O_h)	distorted octahedral

$[IF_2]^-$ is isoelectronic to XeF_2 and likewise shows a linear structure. $[IF_6]^-$ is isoelectronic to XeF_6 and both form distorted octahedra. In contrast, $[BrF_6]^-$ represents a regular octahedron and thus an exception of the VSEPR model.

The trend of heavier halogen atoms to higher coordination numbers, which becomes apparent in the formation of the halogen fluorides and especially in their association in condensed phases, gains further support from the presence of fluorine bridges between cations and anions of salts such as $[BrF_2][SbF_6]$ or $[ClF_2][AsF_6]$. For instance, the LEWIS acid $[BrF_2]^+$ in the former salt is connected to the octahedral anions $[SbF_6]^-$ by weak coordinative bonds to two F atoms:

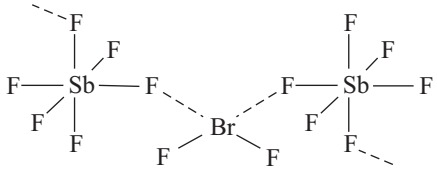

$d_{BrF} = 169$ pm
$d_{Br\cdots F} = 229$ pm
angle$_{FBrF} = 93.5°$ (in the cation)

The four fluorine neighbors are located within one plane with the central bromine atom. The internuclear distances $d_{Br\cdots F}$ are much smaller than the VAN DER WAALS distance of 325 pm. This cation–anion interaction is partially ionic and in part covalent and leads to distortion of the $[SbF_6]^-$ octahedron toward the cation. If BrF_3 is added to $[BrF_2][SbF_6]$ as fluoride ion donor, $[SbF_6]^-$ salts of the cations $[F_2BrFBrF_2]^+$ and $[F_2BrFBr(F_2)FBrF_2]^+$ are obtained.[57]

13.5.6 Oxygen Compounds of Chlorine, Bromine and Iodine

This group of compounds comprises the oxides, the oxoacids and their salts, the acid halides, the nitrates, fluorosulfates and perchlorates of chlorine, bromine and iodine as well as reagents such as iodosobenzene Ph–IO, which is employed as an oxidant in organic chemistry.

13.5.6.1 Oxides

More than 25 oxides of chlorine, bromine and iodine are known,[58] although only 11 have been prepared in pure form. The most important compounds are compiled in

57 F. Kraus et al., *Angew. Chem. Int. Ed.* **2018**, *57*, 14640.
58 M. Jansen, T. Kraft, *Chem. Ber.* **1997**, *130*, 307. H. S. P. Müller, E. A. Cohen, *J. Phys. Chem. A* **1997**, *101*, 3049. H. Oberhammer et al., *J. Phys. Chem.* **1994**, *98*, 8339.

Table 13.4. The halogens in these compounds adopt positive oxidation states without exception as oxygen is always the more electronegative bonding partner. Conversely, the binary fluorine–oxygen compounds OF, OF_2 and O_2F_2 must be regarded as oxygen fluorides and not as halogen oxides and have therefore been discussed in the oxygen chapter (Section 11.4).

Table 13.4: Important halogen oxides ordered by increasing oxygen content. Only the compounds in bold have been prepared as pure materials at 25 °C.

Chlorine	Bromine	Iodine
Cl_2O: Cl–O–Cl	**Br_2O:** Br–O–Br	
Cl_2O_2: Cl–O–O–Cl and Cl–ClO_2		
	Br_2O_3: Br–O–BrO_2	
ClO_2: O=Cl=O	BrO_2: O=Br=O	
Cl_2O_4: Cl–O–ClO_3		**I_2O_4**: $([IO_2]^+[IO_2]^-)_n$
		I_4O_9:
	Br_2O_5: O_2Br–O–BrO_2	**I_2O_5**: O_2I–O–IO_2
Cl_2O_6: $[ClO_2]^+[ClO_4]^-$ and O_2Cl–O–ClO_3		**I_4O_{12}**: $(IO_3)_4$
Cl_2O_7: O_3Cl–O–ClO_3		

Except for I_2O_5, all halogen oxides are endothermic species. Almost all are very reactive and strongly oxidizing. On heating, they decompose into the elements (explosively in case of the chlorine oxides). Therefore, their handling and characterization is difficult and their importance in terms of applications limited. The technically most important halogen oxide is ClO_2, which is widely used for *water disinfection*.

The diatomic monoxides are known for all halogens. They are generated, for instance, by oxidation of the halogen atoms by ozone.[59] These radicals play an infamous role in atmospheric chemistry during the depletion of stratospheric ozone[60] (Section 11.1.3).

13.5.6.2 Chlorine Oxides

Dichlorine oxide Cl_2O is formed as a yellow-red gas during the reaction of Cl_2 with HgO:

$$2\,Cl_2 + 2\,HgO \longrightarrow Cl_2O + HgO{\cdot}HgCl_2$$

A stream of chlorine, diluted with air, is led over dry mercury(II) oxide at 20 °C. Cl_2O (m.p. 2 °C) explodes on warming or when brought in contact with oxidizable

59 I. V. Nikitin, *Russ. Chem. Rev.* **2008**, *77*, 739.
60 A. Saiz-Lopez, R. von Glasow, *Chem. Soc. Rev.* **2012**, *41*, 6448. A. Saiz-Lopez et al., *Chem. Rev.* **2012**, *112*, 1773.

substances. With liquid water, Cl_2O reacts in an equilibrium reaction to hypochlorous acid, thus constituting the anhydride of this acid:

$$Cl_2O + H_2O \rightleftharpoons 2\,HOCl$$

The molecule is bent as to be expected given the relationship to H_2O (C_{2v} symmetry).

Dichlorine dioxide Cl_2O_2 exists in two isomeric forms as peroxide ClOOCl and as the thermodynamically more stable chlorine chlorite Cl–ClO_2. As the related oxide ClO_2, the peroxide is important for the chemistry of the upper atmosphere where it takes part in the depletion of ozone (see Section 11.1.3)

Chlorine dioxide ClO_2 is by far the most important chlorine oxide. It is a yellow gas (b.p. 10 °C), which is produced according to various procedures from chlorates. On the laboratory scale, concentrated sulfuric acid is added to $K[ClO_3]$ at 0 °C:

$$3\,K[ClO_3] + 3\,H_2SO_4 \longrightarrow 3\,HClO_3 + 3\,K[HSO_4]$$

$$3\,HClO_3 \longrightarrow 2\,ClO_2 + [H_3O][ClO_4]$$

For the technical synthesis, $Na[ClO_3]$ is reduced by SO_2 in aqueous sulfuric acid:

$$2\,Na[ClO_3] + SO_2 + H_2SO_4 \longrightarrow 2\,ClO_2 + 2\,Na[HSO_4]$$

ClO_2 is extremely explosive and decomposes when moderately heated, on contact with oxidizable substances or even without apparent cause in an exothermic reaction. When strongly diluted with CO_2, N_2 or simply air or after adduct formation with pyridine, however, ClO_2 can be handled safely. The oxide is moderately soluble in water and is employed in this form on a large scale for the oxidative disinfection and purification of drinking water.[61] Another important application is the bleaching of pulp during paper production (for which elemental chlorine had been used previously). In alkaline solution, ClO_2 disproportionates to chlorite and chlorate:

$$2\,ClO_2 + 2\,[OH]^- \longrightarrow [ClO_2]^- + [ClO_3]^- + H_2O$$

The molecule ClO_2 is bent and contains an unpaired electron. The valence angle in the gas phase amounts to 117.4°; resonance structure (a):

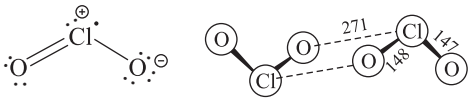

(a) (b)

61 For the generation of a dilute aqueous solution of ClO_2 in waterworks, a $Na[ClO_2]$ solution is either oxidized with Cl_2 or mixed with dilute hydrochloric acid (disproportionation of $HClO_2$).

$ClO_2^{\bullet}$ is isoelectronic with the radical anion $[SO_2]^{\bullet-}$, but unlike the latter it does not show any tendency to dimerize at room temperature.[62] In the solid state (at –150 °C), however, ClO_2 is dimeric and diamagnetic [see structure (b), distances in pm, C_i symmetry]. By reaction of ClO with ClO_2, the unstable oxide Cl_2O_3 is formed, which exhibits the connectivity Cl–O–ClO_2 (chlorine chlorate).

Oxidation of ClO_2 at 0 °C with ozone affords *dichlorine hexoxide* Cl_2O_6:

$$2\ ClO_2\ +\ 2\ O_3\ \longrightarrow\ Cl_2O_6\ +\ 2\ O_2$$

Another method for the synthesis of Cl_2O_6 is provided by the following reaction:

$$ClO_2F\ +\ HClO_4\ \longrightarrow\ Cl_2O_6\ +\ HF$$

Cl_2O_6 is a deep-red liquid at 20 °C, which solidifies at 3 °C. Below –30 °C, Cl_2O_6 can be stored without decomposition. In the gas phase and as a liquid, Cl_2O_6 consists of unsymmetrical molecules $O_2Cl–O–ClO_3$ with chlorine in the oxidation states +5 and +7. In the solid state, however, the compound exists as the ionic chloryl perchlorate $[ClO_2]^+[ClO_4]^-$. Accordingly, Cl_2O_6 reacts with water to chlorate and perchlorate ions. It thus constitutes the mixed anhydride of chloric acid and perchloric acid:

$$Cl_2O_6\ +\ 3\ H_2O\ \longrightarrow\ 2\ [H_3O]^+\ +\ [ClO_3]^-\ +\ [ClO_4]^-$$

The most persistent chlorine oxide is *dichlorine heptoxide* Cl_2O_7, which is isoelectronic with the disulfate ion $[S_2O_7]^{2-}$ and built in an analogous manner (two corner-sharing ClO_4 tetrahedra). Cl_2O_7 is formed upon cautious dehydration of perchloric acid with P_2O_5 at temperatures between –70° and 0 °C:

$$2\ HClO_4\ +\ P_2O_5\ \longrightarrow\ Cl_2O_7\ +\ 2\ HPO_3$$

The oxide Cl_2O_7 is distilled in vacuum from the concomitantly formed polymeric metaphosphoric acid HPO_3 as a colorless liquid (m.p. –92 °C). With water, Cl_2O_7 reacts back to $HClO_4$.

Chlorine perchlorate $ClClO_4$ (Cl_2O_4) is obtained as pale-yellow liquid (b.p. 45 °C) by treatment of perchlorates with chlorine fluorosulfate at –45 °C:

$$ClSO_3F\ +\ Cs[ClO_4]\ \longrightarrow\ ClClO_4\ +\ Cs[SO_3F]$$

Cl_2O_4 is a mixed-valent chlorine oxide with the connectivity Cl–O–ClO_3; with HCl, it reacts to Cl_2 and $HClO_4$.

---

62 Other relatively stable free radicals with 19 valence electrons are the ozonide ion $[O_3]^{\bullet-}$ (see Section 11.1.3) and $NF_2^{\bullet}$ (see Section 9.5.1).

13.5.6.3 Bromine Oxides

Three bromine oxides have been prepared in pure form and characterized by structural analyses.[63] Less stable compounds such as BrO and BrBrO may be involved in stratospheric ozone depletion.

Dibromine oxide Br_2O is formed during the reaction of Br_2 with HgO (in analogy to Cl_2O), but is best prepared by hydrolysis of $BrOTeF_5$:

$$2\ BrOTeF_5 + H_2O \longrightarrow Br_2O + 2\ HOTeF_5$$

Br_2O is a yellow gas that condenses to yellow (in a thick layer brown) crystals on cooling. The molecular symmetry is C_{2v} (valence angle in the gas phase: 112°, in the crystal: 114°).

From the reaction of Br_2 with O_3 in inert solvents such as CCl_3F, a mixture of Br_2O_3 and Br_2O_5 is obtained at −55 °C, which can be separated into the pure components through extraction with CH_2Cl_2 and EtCN and subsequent crystallization. The orange-yellow Br_2O_3 decomposes above −40 °C. In view of the connectivity, it should be referred to as mixed-valent bromine bromate $BrOBrO_2$ (C_1 symmetry) with bromine in the oxidation states +1 and +5. The colorless Br_2O_5 is only stable below −20 °C and has a structure analogous to I_2O_5 (see below).

13.5.6.4 Iodine Oxides

The most important binary I-O species is diiodine pentoxide I_2O_5, the anhydride of iodic acid, which is indeed prepared by thermal dehydration of the latter at about 250 °C:

$$2\ HIO_3 \longrightarrow I_2O_5 + H_2O$$

I_2O_5 is a colorless crystalline powder, which is stable against decomposition into the elements up to 300 °C. The crystals consist of I_2O_5 molecules with weak coordinative interactions between individual molecules

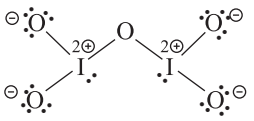

d_{IO} = 193 pm (bridging O)
d'_{IO} = 179 pm (terminal O).
angle $_{IOI}$ = 139°

I_2O_5 reacts with water to iodic acid. With CO, it quantitatively forms I_2 and CO_2 at 170 °C, which is taken advantage of for the iodometric quantification of CO.

Heating of HIO_3 in oleum (20% SO_3) to 195 °C followed by cooling to 25 °C produces colorless crystals of bis-iodyl disulfate $[I_2O_4][S_2O_7]$, which contains the

63 K. Seppelt, *Acc. Chem. Res.* **1997**, *30*, 111.

dimeric iodyl cation as a four-membered I_2O_2 ring with two exocyclic oxygen atoms on the same side of the ring (approximate C_2 symmetry).

The dehydration of H_5IO_6 with conc. H_2SO_4 leads to yellow tetrameric iodine trioxide I_4O_{12} containing two distinct sorts of iodine atoms with the coordination numbers 3 and 6 and the oxidation states +5 and +7. I_2O_4 is also a mixed-valent oxide and formally consists of the ions $[IO_2]^+$ and $[IO_2]^-$.

13.5.6.5 Oxoacids of the Halogens

The known oxoacids of chlorine, bromine and iodine are compiled in Table 13.5. Only a few of these compounds have been isolated in pure, anhydrous form, namely, perchloric acid $HClO_4$, iodic acid HIO_3, metaperiodic acid HIO_4 and orthoperiodic acid H_5IO_6. The other oxoacids are only stable in aqueous solution or in the gas phase. In contrast, the corresponding salts of all acids exist in pure form.

Table 13.5: Mononuclear oxoacids of the halogens (only compounds in bold are known as pure anhydrous acids). In all acids, hydrogen is exclusively linked to oxygen.

Oxidation state	Cl	Br	I
+1	HClO	HBrO	HIO
+3	$HClO_2$	$HBrO_2$	
+5	$HClO_3$	$HBrO_3$	**HIO_3**
+7	**$HClO_4$**	$HBrO_4$	**HIO_4, H_5IO_6**

Note that the empirical formulae in Table 13.5 do not represent the molecular structures. The hydrogen atom is always linked to an oxygen atom, not to the halogen center (i.e., as OH groups). The atom connectivity and the nomenclature are thus as follows: HOCl hypochlorous acid, HOClO chlorous acid, $HOClO_2$ chloric acid, $HOClO_3$ perchloric acid. The designation of bromine and iodine oxoacids is done in an analogous manner.

Multinuclear acids, as they frequently occur for other nonmetals, are unknown for chlorine and bromine. In case of iodine, however, salts exist with the anions $[I_3O_8]^-$, $[I_2O_9]^{4-}$, $[I_2O_{10}]^{6-}$ and $[I_3O_{14}]^{7-}$, which contain I(V) and I(VII) centers.

13.5.6.6 Oxoacids of Chlorine

Hypochlorous acid HOCl (chlorine hydroxide) is formed during the reaction of Cl_2 with gaseous or liquid water:

$$Cl_2 + H_2O \rightleftharpoons HOCl + HCl$$

In liquid water, the equilibrium is completely on the left-hand side as HOCl oxidizes the Cl^- ions of the completely dissociated hydrogen chloride to Cl_2 ($K_c = 3.35 \cdot 10^{-4}$ mol^2 L^{-2}). Only if the chloride ions are trapped, for example, with suspended HgO as insoluble $HgO \cdot HgCl_2$, relatively concentrated HOCl solutions can be obtained, although decomposition to hydrochloric acid and O_2 sets in at 0 °C already. From the concentrated solutions, dichlorine oxide as anhydride of hypochlorous acid can be extracted with CCl_4. The solutions thus contain Cl_2, HOCl and Cl_2O as equilibrium mixture and therefore their yellow color cannot be attributed to HOCl with confidence. HOCl is a very weak acid in water ($pK_a = 7.50$), but a strong oxidant. The HOCl molecule is bent with a valence angle in the gas phase of 102°. The disproportionation of chlorine in strongly alkaline solutions at temperatures below 35 °C yields *bleach*, which contains chloride and hypochlorite ions:

$$Cl_2 + 2\,NaOH \longrightarrow Na[ClO] + NaCl + H_2O \qquad \Delta H = -104\ \text{kJ mol}^{-1}$$

The very unstable *chlorous acid* $HClO_2$[64] is generated through the reversible disproportionation of ClO_2 in water. The salts are more stable than the free acid. They are produced on an industrial scale and used as bleaching agent for textiles. Sodium chlorite is formed by passing ClO_2 into solutions of $Na_2[O_2]$ or $NaOH/H_2O_2$:

$$2\,ClO_2 + H_2O_2 + 2\,NaOH \longrightarrow 2\,Na[ClO_2] + O_2 + 2\,H_2O$$

H_2O_2 acts as reducing agent in this reaction! Furthermore, $Na[ClO_2]$ can be prepared by reduction of $Na[ClO_3]$ with oxalic acid. In aqueous solution, $Na[ClO_2]$ is a strong oxidant. Structurally resembling the isoelectronic cation $[ClF_2]^+$, the anion $[ClO_2]^-$ is of C_{2v} symmetry. In the presence of certain metal complexes at pH = 7.1, $[ClO_2]^-$ decomposes to O_2 and Cl^-; anhydrous $Na[ClO_2]$ gives explosive mixtures with oxidizable substances.

Chloric acid $HClO_3$ can only be prepared in aqueous solution up to a concentration of 40% due to its facile decomposition. Such solutions are obtained according to the equation:

$$Ba[ClO_3]_2 + H_2SO_4(aq) \longrightarrow 2\,HClO_3(aq) + Ba[SO_4]\downarrow$$

The salts of chloric acid are called *chlorates*; they are exclusively obtained by disproportionation of hypochlorites through heating in aqueous solution:

$$3\,[ClO]^- \longrightarrow [ClO_3]^- + 2\,Cl^-$$

64 According to ab initio calculations, the most stable isomer of composition $HClO_2$ is the peroxide HOOCl followed by HOClO. Both molecules are not planar (torsion angle 80 ± 6°): J. S. Francisco et al., *J. Phys. Chem.* **1994**, *98*, 5644.

Presumably, the anion $[ClO]^-$ is oxidized by the free acid HOCl in the process. In practice, a hot NaCl solution (50–90 °C) is electrolyzed without separating cathode and anode compartments so that the anodically generated chlorine can react with the sodium hydroxide formed at the cathode (after the separation of the concomitantly formed hydrogen):

$$Cl_2 + [OH]^- \longrightarrow [ClO]^- + Cl^- + H^+$$

$$6\,[ClO]^- + 3\,H_2O \longrightarrow 2\,[ClO_3]^- + 4\,Cl^- + 3\,H_2 + \tfrac{3}{2}\,O_2$$

The worldwide capacity for this process was about $3.8 \cdot 10^6$ t $Na[ClO_3]$ in 2016, more than half of it in North America. Aqueous chloric acid and solid chlorates are very strong oxidants. $K[ClO_3]$ is used in large quantities to produce matches, fireworks and explosives. The most important application, however, is once more in the pulp and paper industry for bleaching purposes.

The chlorate anion $[ClO_3]^-$ is isoelectronic to the sulfite ion; both are trigonal pyramidal (C_{3v} symmetry). The free acid $HClO_3$ is C_s symmetric:

Perchloric acid $HClO_4$ is the most stable oxoacid of chlorine; it can be distilled as colorless liquid from a mixture of $K[ClO_4]$ and H_2SO_4 in vacuum:

$$K[ClO_4] + H_2SO_4 \longrightarrow HClO_4 + K[HSO_4]$$

Anhydrous $HClO_4$ can nonetheless violently decompose with explosion when heated or brought into contact with combustible substances. Therefore, experiments with $HClO_4$ require appropriate precautions. In aqueous solution, however, $HClO_4$ is perfectly stable and – as a very strong BRØNSTED acid – completely dissociated at sufficient dilution (Table 5.5). Perchlorates are produced by anodic oxidation of chlorates and thus ultimately from chlorine:

$$\tfrac{1}{2}\,Cl_2 + 4\,H_2O \longrightarrow [ClO_4]^- + 8\,H^+ + 7\,e^-$$

From an aqueous solution of $Na[ClO_4]$ and $[NH_4]Cl$, the sparingly soluble salt $[NH_4][ClO_4]$ is obtained, which is the most important propellant of solid rockets. For this purpose, it is mixed with aluminum powder in a polybutadiene matrix. Besides solid Al_2O_3, the strongly exothermic combustion reaction results in the gaseous products CO_2, N_2, Cl_2 and H_2O.[65] For instance, the two boosters of the Ariane 5

65 R. J. Seltzer, *Chem. Eng. News* **1988**, August 8, p. 7.

rocket contain 240 t of a mixture of $[NH_4][ClO_4]$ (68%), Al powder (18%) and polybutadiene (14 %), which burns off within 140 s after ignition! In addition to ammonium perchlorate, the potassium salt is frequently employed in pyrotechnics.[66]

The thermal disproportionation of certain chlorates such as $K[ClO_3]$ also yields perchlorates:

$$4\ K[ClO_3] \longrightarrow 3\ K[ClO_4] + KCl$$

When heated too strongly, however, $K[ClO_4]$ decomposes to KCl and O_2. The tetrahedral perchlorate ion is isoelectronic to the ions $[SO_4]^{2-}$, $[PO_4]^{3-}$ and $[SiO_4]^{4-}$; the corresponding acid $HClO_4$ shows the following structure in the gas phase:

In the series of chlorine oxoacids and their anions, the ClO bond strength increases with the oxidation state of the chlorine center. This is readily seen from the values of the valence force constants f_r (in N cm^{-1}):

$$[ClO]^-: 3.3 \qquad [ClO_2]^-: 4.2 \qquad [ClO_3]^-: 5.6 \qquad [ClO_4]^-: 7.2$$

As a consequence, numerous disproportionation reactions are observed, which typically result in oxygen-richer anions under concomitant formation of chloride ions. $HClO_4$ and $[ClO_4]^-$ are expectedly the most stable. Analogous situations are encountered with other nonmetals (e.g. S, Se, Br, I).

The dissociation constants of chlorine oxoacids in aqueous solution (K_a) also strongly increase with the oxidation state of the central atom and thus with the stability of the anion. The increase in bond enthalpy from $[ClO]^-$ to $[ClO_4]^-$ stabilizes the anion; the reduced negative charge at the oxygen atoms facilitates the heterolytic cleavage of the OH bond for electrostatic reasons:

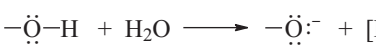

In an analogous manner, the rise of the first dissociation constant in the series

$$H_4SiO_4 < H_3PO_4 < H_2SO_4 < HClO_4$$

can be explained (Table 5.5).

66 F. Keller, *Chem. unserer Zeit* **2012**, *46*, 248 (with attractive illustrations).

13.5.6.7 Oxoacids of Bromine

The four oxoacids of bromine resemble the corresponding chlorine species. All four can only be prepared in aqueous solution, but their salts have been isolated in pure form. Hypobromites, bromites and bromates are formed depending on the temperature during the disproportionation of bromine in alkaline solution:

$$Br_2 + 2\,[OH]^- \longrightarrow [BrO]^- + Br^- + H_2O$$

$$2\,[BrO]^- \longrightarrow [BrO_2]^- + Br^-$$

$$[BrO]^- + [BrO_2]^- \longrightarrow [BrO_3]^- + Br^-$$

Conversely, perbromates cannot be obtained by disproportionation and their existence was therefore doubted for a long time. Perbromate ions do, however, form through oxidation of bromate ions by very strong oxidizing agents such as F_2 or XeF_2 as well as by anodic oxidation in aqueous solution:

$$[BrO_3]^- + F_2 + 2\,[OH]^- \longrightarrow [BrO_4]^- + 2\,F^- + H_2O$$

$$[BrO_3]^- + XeF_2 + H_2O \longrightarrow [BrO_4]^- + Xe + 2\,HF$$

From these solutions, the salt $Rb[BrO_4]$ has been crystallized by addition of RbF and converted to aqueous perbromic acid by ion exchange. The anions $[BrO]^-$, $[BrO_2]^-$, $[BrO_3]^-$ and $[BrO_4]^-$ have been characterized by ^{17}O- and ^{81}Br-NMR spectroscopy among other techniques; the BrO internuclear distances decrease with rising oxidation state of bromine.[67]

13.5.6.8 Oxoacids of Iodine

On dissolution of elemental iodine in aqueous NaOH, hypoiodite ions $[IO]^-$ are formed initially, which are converted to iodate and iodide with time by a further disproportionation:

$$I_2 + 2\,NaOH \longrightarrow Na[IO] + NaI + H_2O$$

$$3\,Na[IO] \longrightarrow Na[IO_3] + 2\,NaI$$

The acid HOI is even less stable than the hypoiodites. It is generated as an intermediate during the reaction of aqueous iodine solution with HgO. The acid HIO_2 and their salts (iodites) are unknown.

Iodic acid HIO_3 is prepared by oxidation of I_2 with either HNO_3, Cl_2, H_2O_2 or $HClO_3$ in aqueous solution and can be isolated as colorless crystals. HIO_3 is a strong oxidant. Its condensation under elimination of water results in I_2O_5.

---

67 W. Levason et al., *J. Chem. Soc. Dalton Trans.* **1990**, 349.

Iodates contain the pyramidal ion $[IO_3]^-$. In some salts of composition $M[IO_3]\cdot HIO_3$ and $M[IO_3]\cdot 2HIO_3$ one or two iodic acid molecules are connected to the iodate ions by OH···O hydrogen bonds. Such *acidic salts* are also known for other oxoacids, for example, $Na[NO_3]\cdot HNO_3$ in case of nitric acid. Traces of sodium iodate $Na[IO_3]$ are added to table salt in order to avoid nutritional iodine deficiency; the recommended daily intake for humans is 150 mg iodine.[68] If $Na[IO_3]$ is dissolved in 7 M HNO_3 and evaporated to dryness at 60 °C, crystals of $Na[I_3O_8]$ are formed; the chain-like polyiodate anion $[O_2IOI(O)_2OIO_2]^-$ is C_{2v} symmetric.

During the oxidation of I_2 or iodates with very strong oxidizing agents such as Na[ClO] (Cl_2 in NaOH) periodates are formed:

$$[IO_3]^- + [ClO]^- \xrightarrow[100°C]{[OH]^-} [IO_4]^- + Cl^-$$

Industrially, iodate is also anodically oxidized to periodate. Cooling of the aqueous solution gives the salt $Na_3[H_2IO_6]$, which is derived from orthoperiodic acid [hexaoxoiodine(VII) acid H_5IO_6], in turn prepared by treatment of the barium salt with concentrated sulfuric acid. Only upon crystallization of the sodium salt from dilute nitric acid $Na[IO_4]$ is formed. Periodates are strong oxidizing agents, which, for example, oxidize Mn^{2+} ions to permanganate and are also frequently employed in organic chemistry.

In the orthoperiodic acid H_5IO_6 and its anions $[H_4IO_6]^-$, $[H_3IO_6]^{2-}$, $[H_2IO_6]^{3-}$ and $[IO_6]^{5-}$, the central atom is coordinated octahedrally. The iodine atom thus behaves similar to its neighbors in the Periodic Table of which analogous species are known, while no such similarities exist for the lighter halogens. On heating to 130 °C, H_5IO_6 decomposes to I_2O_5, H_2O and O_2. By cautious dehydration of H_5IO_6 with $H_2S_2O_7$ at 50 °C, metaperiodic acid HIO_4 is obtained, which consists of one-dimensionally infinite chains of *cis*-edge connected IO_6 octahedra in the solid state. Each of the polymeric chains is additionally connected to four neighboring chains through hydrogen bonds.[69]

13.5.6.9 Acid Halides

Various acid chlorides are derived from the halogen oxoacids by formal replacement of an OH group by a halogen atom. As this halogen atom has to be more electronegative than the rest of the molecule, only fluorine and chlorine can adopt this role. The most important representatives are the halogenyl fluorides FXO_2 (X = Cl, Br, I) and $ClClO_2$, the perhalogenyl fluorides FXO_3 as well as iodine(VII) oxide pentafluoride IOF_5, which is formally a derivative of orthoperiodic acid $IO(OH)_5$. The only oxohalide that cannot

68 Chronic iodine deficiency results in a thyroid gland, which cannot produce hormones as needed by the human body anymore; H. Wagner, K. Franke, A. Röttger, *Nachr. Chemie* **2009**, *57*, 1192.
69 T. Kraft, M. Jansen, *Angew. Chem. Int. Ed.* **1997**, *36*, 1753.

be derived from an acid is chlorine(V) oxotrifluoride $ClOF_3$, which formally results from ClF_5 through substitution of two fluorine atoms by one oxygen atom.

Halogenyl fluorides $FClO_2$, $FBrO_2$, FIO_2 are derivatives of the acids $HClO_3$, $HBrO_3$ and HIO_3 (C_s symmetry):

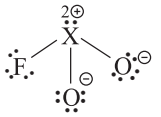

X = Cl, Br, I

$FClO_2$ is formed as a colorless gas by fluorination of ClO_2 with elemental fluorine or preferably with a milder fluorinating agent:

$$ClO_2 + AgF_2 \ (CoF_3, BrF_3) \xrightarrow{25°C} FClO_2 + AgF$$

The characteristic reactions of chloryl fluoride are the hydrolyis

$$FClO_2 + H_2O \longrightarrow HClO_3 + HF$$

and the formation of chloryl salts:

$$FClO_2 + AsF_5 \longrightarrow [ClO_2][AsF_6]$$
$$2\,FClO_2 + SnF_4 \longrightarrow [ClO_2]_2[SnF_6]$$

These salts consist of isolated ions, which can be confirmed by vibrational spectroscopy. The chloryl cation is isolelectronic to the SO_2 molecule and thus bent.

Toward fluoride ions, $FClO_2$ behaves as a LEWIS acid. From KF and $FClO_2$, the difluorochlorate $K[ClO_2F_2]$ is thus obtained, which is also accessible from $K[ClO_3]$ and HF by exchange of an O atom by two F atoms. Bromyl fluoride is prepared by fluorination of BrO_2 with BrF_5 in the form of colorless crystals (m.p. –9 °C). Colorless crystals of iodyl fluoride grow from a solution of I_2O_5 in anhydrous hydrogen fluoride:

$$I_2O_5 + HF \longrightarrow FIO_2 + HIO_3$$

Chlorine(V) oxotrifluoride $ClOF_3$ is obtained as colorless liquid from the reaction of F_2 with Cl_2O, $Na[ClO_2]$ or $ClNO_3$. The molecule has a seesaw structure in accordance with the VSEPR model. With BF_3, AsF_5 and SbF_5, it reacts to salts with the pyramidal cation $[ClOF_2]^+$.

Perhalogenyl fluorides $FClO_3$, $FBrO_3$, FIO_3 are derivatives of the perhalogen oxoacids $HOXO_3$ in which the OH group was replaced by fluorine. $FClO_3$ is isoelectronic with the perchlorate ion and has a distorted tetrahedral structure (C_{3v} symmetry). It is formed by fluorination of $K[ClO_3]$

$$K[ClO_3] + F_2 \longrightarrow FClO_3\uparrow + KF$$

and during the reaction of $K[ClO_4]$ with fluorosulfuric acid at 50–85 °C:

$$K[ClO_4] + HSO_3F \longrightarrow FClO_3\uparrow + K[HSO_4]$$

Perchloryl fluoride is a colorless gas (b.p. −47 °C), which is similarly resistant to hydrolysis as SF_6. This is due to the kinetic hindrance of nucleophilic attacks so that with concentrated sodium hydroxide solution, for instance, a reaction occurs only at temperatures of 200–300 °C despite the fact that thermodynamically the following equilibrium is completely on the right-hand side:

$$FClO_3 + 2\,[OH]^- \rightleftharpoons F^- + [ClO_4]^- + H_2O$$

$FClO_3$ does not react to perchloryl salts with fluoride ion acceptors.

In contrast, perbromyl fluoride (prepared from $K[BrO_4]$ and SbF_5 in liquid HF) is readily hydrolyzed by bases to perbromate and fluoride even at 25 °C. With fluoride ion acceptors such as SbF_5, $FBrO_3$ does not react to a perchloryl salt with the cation $[BrO_3]^+$, but rather under elimination of O_2 to $[BrO_2][SbF_6]$. Periodyl fluoride is prepared by the fluorination of periodates with F_2 in HF:

$$[IO_4]^- + F_2 \longrightarrow FIO_3 + F^- + \tfrac{1}{2}\,O_2$$

The oxide fluorides IO_2F_3, $HOIOF_4$ and IOF_5 are also derived from the various iodine (VII) oxoacids. They contain a central iodine atom of coordination number 5 or 6. IOF_5 is formed on treatment of IF_7 with POF_3 at 20 °C as a colorless liquid and consists of near-octahedral molecules of C_{4v} symmetry.

13.5.6.10 Halogen Derivatives of Oxoacids of Other Nonmetals

In certain oxoacids of the nonmetals hydrogen can be formally replaced by either Cl, Br or I. In this manner, chlorine nitrate Cl–O–NO_2 is formed by substitution of the hydrogen atom of nitric acid by Cl. Bromine and iodine are even capable of replacing the H atoms of several equivalents of an oxoacid, which results in oxidation states at the halogen atom higher than +1, for example, in iodine(III) nitrate $I(NO_3)_3$, in iodine (III) phosphate IPO_4 as well as in the frequently employed oxidant (in organic chemistry) phenyliodine bis(trifluoroacetate) $PhI(O_2CCF_3)_2$. These and analogous species contain positively polarized halogen atoms, albeit always covalently bonded to one or more oxygen atoms. In the case of iodine, however, there are also sulfonylimido compounds of the type $ArINSO_2Ar$ (Ar = aryl group) with a formal double bond between iodine and nitrogen (alternatively described by ylidic structures). These IN and IO bonds are predominantly covalent, but strongly polar. HNO_3, H_3PO_4, H_2SO_4, HSO_3F, $HBrO_3$, $HClO_4$ and CH_3COOH are examples of suitable oxoacids. The properties of such compounds will be discussed on a few selected examples.

Acetates: Iodobenzene is oxidized to dichloroiodobenzene $PhICl_2$ by Cl_2, which in turn can be converted to iodosylbenzene (or iodosobenzene) PhIO by alkaline hydrolysis. PhIO is a yellow polymeric and explosive solid of m.p. 210 °C. The structure of PhIO is characterized by an I-O zigzag chain with phenyl side groups. With

methanol, PhIO reacts under depolymerization to yield $PhI(OMe)_2$. The reactions of $PhICl_2$ or PhIO with glacial acetic acid gives the oxidant $PhI(O_2CCH_3)_2$, which reacts with CF_3COOH to $PhI(O_2CCF_3)_2$. By oxidation of PhIO with hypochlorite, periodate or ozone, iodyl benzene $PhIO_2$ is obtained, which is equally polymeric and an important oxidizing agent. These and analogous polyvalent organoiodine compounds have experienced an exponential development in organic syntheses since the early 1990s.[70]

Nitrates: Chlorine nitrate is formed as a pale-yellow liquid (colorless in the gas phase; m.p. –107 °C, b.p. 18 °C) by reaction of dichlorine oxide with dinitrogen pentoxide at –20 °C:

$$Cl_2O + N_2O_5 \xrightarrow{-20°C} 2\ ClONO_2$$

$ClONO_2$ is the mixed anhydride of the acids HOCl and HNO_3. It differs from nitrosyl chloride ClNO and from nitryl chloride $ClNO_2$ inasmuch as that a ClO bond is present. During the alkaline hydrolysis, $[ClO]^-$ and $[NO_3]^-$ are formed as expected.

$$ClONO_2 + 2\ [OH]^- \longrightarrow [ClO]^- + [NO_3]^- + H_2O$$

The positively polarized Cl atom of $ClONO_2$ reacts with negatively charged Cl atoms to Cl_2. This tendency can be used for the synthesis of other halogen nitrates:

$$BrCl + ClONO_2 \longrightarrow BrONO_2 + Cl_2$$
$$ICl_3 + 3\ ClONO_2 \longrightarrow I(ONO_2)_3 + 3\ Cl_2$$

ICl, HCl, $TiCl_4$ and CrO_2Cl_2 react in an analogous manner. All halogen nitrate molecules are planar and of C_s symmetry. Their thermal stability decreases from fluorine to iodine. Chlorine nitrate occurs in the stratosphere through the combination of the radicals ClO and NO_2. Together with HCl, $ClONO_2$ is among the most frequent chlorine compounds in the higher atmosphere (see Section 11.1.3); analogous considerations apply to $BrONO_2$.

Fluorosulfates: Chlorine fluorosulfate $ClOSO_2F$ is a yellow liquid, which is obtained in nearly quantitative yield from ClF and SO_3 at 25 °C:

$$ClF + SO_3 \longrightarrow ClOSO_2F$$

Iodine tris(fluorosulfate) $I(OSO_2F)_3$ is a yellow, polymeric solid, which is formed by the oxidation of I_2 with peroxodisulfuryl fluoride. With H_2O, $I(OSO_2F)_3$ reacts to $IO(OSO_2F)$ and HSO_3F. If $I(OSO_2F)_3$ is treated with $K[SO_3F]$ in liquid disulfuryl fluoride, the complex tetrakis(fluorosulfato)iodate(III) results:

$$K[SO_3F] + I(OSO_2F)_3 \xrightarrow{S_2O_5F_2} K[I(OSO_2F)_4]$$

70 V. V. Zhdankin, P. J. Stang, *Chem. Rev.* **2008**, *108*, 5299.

The colorless crystals of this salt, which can also be obtained from the reaction of $K[ICl_4]$ and $S_2O_6F_2$, contain square-planar coordinate iodine atoms, similar to those contained in the anion $[ICl_4]^-$. The analogous bromine compound is accessible from $K[BrO_3]$ and $S_2O_6F_2$ under O_2 evolution. In case of bromine, a bis(fluorosulfato)bromate(I) is also known and can be prepared as follows:

$$CsBr + S_2O_6F_2 \xrightarrow{Br_2} Cs[Br(OSO_2F)_2]$$

Perchlorates: Fluorine perchlorate $FOClO_3$ is prepared by passing dilute F_2 into 78% perchloric acid; it is transferred to the gas phase by heating of the mixture and then purified by fractional condensation:

$$F_2 + HOClO_3 \longrightarrow HF + FOClO_3$$

$ClOSO_2F$ reacts with $Cs[ClO_4]$ to chlorine perchlorate $ClOClO_3$ (see chlorine oxides). From Br_2 and $ClOClO_3$, bromine perchlorate is obtained at −45 °C:

$$Br_2 + 2\ ClOClO_3 \longrightarrow Cl_2 + 2\ BrOClO_3$$

$BrOClO_3$ is a red liquid, which decomposes above −20 °C. The gaseous molecules $FOClO_3$, $ClOClO_3$ and $BrOClO_3$ have the same symmetry as the parent species $HOClO_3$ (C_s).[71]

13.6 Pseudohalogens

Many univalent residues show a chemical behavior that strongly resembles that of the halogens. Such groups are referred to as *pseudohalogens*.[72] The following are classical examples:

–CN	**–N_3**	**–OCN**	**–CNO**	**–SCN**
cyanide	azide	cyanate	isocyanate	thiocyanate

These groups X form hydrogen species HX, which dissociate in water to give the ions $[H_3O]^+$ and X^- and thus resemble the hydrogen halides. From the acids HX, the corresponding salts MX can be derived. The silver salts AgX are hardly soluble in water (like silver halides). In some cases, the ions X^- can be oxidized to the free dimeric pseudohalogens X_2 such as dicyan $(CN)_2$ or so-called dirhodane $(SCN)_2$ [possibly better described as $S_2(CN)_2$, dicyanodisulfane]. Mixed species between

71 H. Oberhammer et al., *J. Phys. Chem.* **1994**, *98*, 8339.

72 H. Brand, A. Schulz, A. Villinger, *Z. Anorg. Allg. Chem.* **2007**, *633*, 22. For an overview of early results see: *Chemistry of the Pseudohalogens* (A. M. Golub, H. Köhler and V. V. Skopenko, eds.), Elsevier, Amsterdam, **1986**.

halogens and pseudohalogens such as cyanogen chloride ClCN and fluorine azide FN_3 are also known.

In contrast, oxidation reactions of cyanate $[OCN]^-$ and isocyanate $[CNO]^-$ produce unstable dimers OCN–NCO and ONC–CNO, respectively, which have been characterized at low temperature only.[73] The surprisingly stable phosphorus version of the cyanate ion $[PCO]^-$ is typically referred to as *phosphaethynolate* in order to account for the dominating contribution of $[P{\equiv}C{-}O]^-$ to the electronic structure.[74] The synthesis of the sodium salt Na[OCP] from cyclic ethylene carbonate and $Na[PH_2]$ is particularly convenient.[75] Even heavier analogues of the cyanate ion $[E{=}C{=}E']^-$ (derived by formal replacement of O or N atoms of the $[OCN]^-$ moiety by their heavier congeners) are accessible in a strictly analogous manner, namely, by reaction of thio- or seleno carbonates $(EtO)_2C{=}E$ (E = S, Se) with the sodium pnictide salts $Na[E'H_2]$ (E′ = P, As).[76]

Some of the mentioned pseudohalogens can replace halogens in covalent, ionic and complex compounds, for example, as in $PCl_3/P(CN)_3$ and $[AgCl_2]^-/[Ag(CN)_2]^-$. Their group electronegativity is similar to that of iodine.

Recently, more complex groups and ions have been synthesized, which can also be regarded as pseudohalogens,[72] for example, the planar methanide groups $-C(CN)_3$, $-C(CN)_2NO$ and $-C(CN)_2NO_2$.

73 T. Pasinszki, *Phys. Chem. Chem. Phys.* **2008**, *10*, 1411 and cited literature.

74 G. Becker et al., *Z. Anorg. Allg. Chem.* **1992**, *612*, 72. H.-F. Grützmacher, H. Grützmacher, *Angew. Chem. Int. Ed.* **2011**, *50*, 8420. A. R. Jupp, J. M. Goicoechea, *Angew. Chem. Int. Ed.* **2013**, *52*, 10064.

75 H. Grützmacher et al., *Angew. Chem. Int. Ed.* **2014**, *53*, 1641.

76 J. M. Goicoechea et al., *Angew. Chem. Int. Ed.* **2018**, *57*, 8230.

14 The Noble Gases

14.1 Introduction

The elements He, Ne, Ar, Kr, Xe and Rn form Group 18 of the Periodic Table. The pronounced chemical inertness, which has led to the group name "noble gases," is due to the particular electronic configuration. It distinguishes noble gases from all other nonmetals. In view of the hundreds of noble gas compounds prepared in the last approximately 60 years in particular for xenon,[1] however, inertness cannot be taken as a synonym for nobility anymore.

Apart from helium, the valence shell of which is fully occupied by two electrons, the noble gases have a valence electron configuration of s^2p^6, that is, complete *octets* without unpaired electrons. The special stability of this configuration shows in the *ionization energies* (Figure 2.1) and *effective nuclear charges* Z_{eff}, which are both larger than those of all other elements in the same row. Therefore, the noble gas atoms are smaller than the nonmetal atoms to their left in the Periodic Table. The *electron affinities* of the noble gases are zero, that is, these elements do not show any tendency toward the formation of negative ions. The noble gases are the only elements that exist as atoms under standard conditions. The interaction of noble gas atoms is restricted to weak VAN DER WAALS forces, hence the low boiling points (Table 3.2). Helium is an extreme case in this regard, as it condenses to liquid helium I at 4.2 K but cannot be solidified at normal pressures. Instead, it converts to a so-called superfluid state (He II) at 2.2 K, which is distinguished by a vanishing viscosity and an extremely high thermal conductivity.

Noble gas atoms are isoelectronic with the corresponding halide ions. There are, however, only very few chemical similarities between these anions of identical electron configuration and the noble gases, for example, when F^- is compared to Ne. For instance, Ne does not form stable complexes with strong LEWIS acids (e.g., BF_3) as F^- does, neither is it protonated in acidic solutions. More recently, coordination compounds of the heavier noble gases Ar, Kr and Xe have been detected spectroscopically in which the atoms are bonded as ligands to a metal atom in a similar manner as halide ions, for example, ArAuF, KrCuF and KrAgF. Only of xenon, however, isolable complexes of this sort have been reported, for example, the square-planar cation $[AuXe_4]^{2+}$ of the salt $[AuXe_4][Sb_2F_{11}]_2$. The noble gas atoms of oxidation state ±0 are coordinatively bonded to the extremely LEWIS acidic noble metal center in the oxidation state +2.[2]

1 W. Grochala, *Chem. Soc. Rev.* **2007**, *36*, 1533 (highly readable review). D. A. Atwood, B. Zemva, *Encycl. Inorg. Chem.* **2005**, *6*, 3651. J. H. Holloway, E. G. Hope, *Adv. Inorg. Chem.* **1998**, *46*, 51.
2 K. Seppelt, *Z. Anorg. Allg. Chem.* **2003**, *629*, 2427.

https://doi.org/10.1515/9783110578065-015

If n is the principal quantum number, the lowest unoccupied atomic orbitals of the noble gases is the s orbital of the $n + 1$ shell. The promotion energies for an np electron to the $(n + 1)s$ level have the following values (in eV):

Ne: 16.6 Ar: 11.5 Kr: 9.9 Xe: 8.3 Rn: 6.8

These energies are much higher than the bond energies of covalent bonds (1–5 eV); the promotion of valence electrons during the formation of noble gas compounds can therefore be excluded. Instead, the covalent bonds of noble gas atoms in neutral molecules are *multicenter bonds* without exception, which are not associated with the presence of unpaired electrons. Conversely, the spectroscopically detected gaseous ions such as $[He_2]^+$, $[HeF]^+$, $[ArF]^+$ and $[Ar_2]^+$ as well as the cations of stable salts such as $[XeF]^+$, $[Xe_2]^+$ and $[AuXe_4]^{2+}$ contain two-center bonds with two or three electrons. The preparation of a mixture of $[XeF][PtF_6]$ and other fluoroxenon salts by NEIL BARTLETT in 1962 provided the first evidence for the existence of stable xenon compounds, although the product was initially misassigned as $[Xe][PtF_6]$. The bonding situations in noble gas compounds are discussed in more detail in Section 14.6.

So far, room-temperature-isolable species have only been obtained for Kr, Xe and Rn. A rare case of a neutral argon species is HArF,[3] which has been generated by photolysis of HF in a solid argon matrix. Similar matrix studies have been reported even for neon,[4] and most recently the solid-state structure of Na_2He has been determined at extremely high pressures (>113 GPa) in a diamond anvil cell.[5] As the first chemically bonded neutral helium species so far, Na_2He crystallizes in a fluorite-type structure under these conditions. While only relatively few compounds have been prepared of krypton, which moreover are thermodynamically unstable at 25 °C, much more than 100 compounds of xenon have been isolated in pure form. The first binary xenon species were synthesized in 1962. In case of radon, its radioactivity is detrimental to experimental investigations to such an extent that only qualitative information is available regarding its compounds. The chemistry of noble gases is therefore mostly the chemistry of xenon and krypton.

14.2 Occurrence, Recovery and Applications

Dry air consists of 78.082 vol% N_2, 20.946% O_2 and 0.041% CO_2 as well as 0.934% noble gases. The latter volume fraction consists almost exclusively of argon as the following data show (vol%):

3 M. Räsänen et al., *Nature* **2000**, *406*, 874.
4 e.g. L. Andrews, S. Riedel et al., *Chem. Eur. J.* **2013**, *19*, 1397.
5 A. R. Oganov, X.-F. Zhou, H.-T. Wang, *Nat. Chem.* **2017**, *9*, 440.

He: 0.0005 (5.24 ppm)
Ne: 0.0018 (18.18 ppm)
Ar: 0.932
Kr: 0.0001 (1.14 ppm)
Xe: $8 \cdot 10^{-6}$ (0.087 ppm)
Rn: $6 \cdot 10^{-18}$

All six elements are isotopic mixtures. The isotopes ^{4}He (99.99986%), ^{3}He (0.00014%, nuclear spin $I = ½$), ^{20}Ne (90.5%), ^{40}Ar (99.6%) and ^{129}Xe (26.4%, $I = ½$) are of particular importance. The high proportion of ^{40}Ar in air is due to its constant formation from radioactive β^- decay of the nuclide ^{40}K, which has a very long half-life of 1.25 billion years and is therefore still present even 4.5 billion years after the formation of planet Earth, albeit in the very low abundance of 0.0117%.

The industrial recovery of noble gases (except for helium and radon) is based on the condensation and fractional distillation of air (*cryogenic rectification*). Argon can also be recovered from the residual gases of ammonia synthesis. The better part of helium is obtained from natural gases, which contain several percent of the lightest noble gas. Main producers are the USA, Qatar and Algeria, but massive helium fields have been discovered in Tanzania. The yearly world production of He amounts to about 5000 t. The enrichment of helium in natural gas is due to the circumstance that He is a product of the radioactive α decay of certain minerals (uranium and thorium ores as well as *monazite*), from which it can actually be isolated by crushing and heating in small quantities. The isotope ^{3}He is formed by the β decay of tritium (Section 5.1).

For the production of radon, a solution of a radium salt is left in a closed vessel for some time and then the produced noble gas is pumped off. The half-life of the most stable isotope of radon ^{222}Rn is 8.3 d. Sources of radon-containing mineral waters with an activity of up to 180,000 Bq L^{-1} are found in various regions worldwide and are employed in the heavily controversial radon spa therapies. This radon originates from subterranean uranium-containing minerals, which always contain radium as a part of the ^{238}U decay series.

The lighter noble gases He, Ne and Ar are commercially available in steel cylinders. He is used as a filling gas for balloons and airships, and in the laboratory it serves as carrier gas for gas chromatography. Liquid helium is an important coolant (b.p. 4.2 K), among other things for superconducting magnets of modern nuclear resonance spectrometers and for the 9300 magnets of the *Large Hadron Collider* at CERN near Geneva, which are cooled by 130 t of superfluid helium at 1.9 K. In addition, satellites in Earth's orbit are cooled with liquid helium.[6] As the helium resources on

6 For instance, the IR telescope "Herschel" was transported into orbit in 2009 with 2400 L of liquid helium onboard. The useful lifetime of the telescope depends essentially on the reach of this helium stock.

Earth are limited, the element needs to be used with care and evaporating gas should be recycled wherever possible.

Helium is also employed for studies of atoms and molecules at ultracold temperatures: nanodroplets of superfluid helium are generated by adiabatic expansion of ultracold helium gas into high vacuum. The subject of investigation is dissolved in these droplets as a few atoms or molecules.[7] With spectroscopic methods, new insights are gained, for example, on the stepwise assembly of NH_3 clusters, which is monitored by IR spectroscopy. Neon is used as a filling gas for electric discharge tubes (neon signs) and argon as protective gas for welding and conventional incandescent light bulbs. In the laboratory, ultrapure Ar is employed as protective gas for the handling of highly reactive substances with SCHLENK techniques or in a glovebox. Krypton and xenon are also used as filling gases for special lamps. Xenon is additionally employed as an anesthetic.

14.3 Xenon Compounds

A neutral xenon atom only engages in strong bonds with nonmetallic atoms or groups of high electronegativity. According to the current state of knowledge, these include only fluorine, oxygen, nitrogen and chlorine as well as strongly electron-withdrawing carbon substituents such as the C_6F_5 group. When at least one fluorine atom is present, however, other atoms can bind to xenon as well. The thermodynamically most stable noble gas compounds are the xenon fluorides and some derived fluoroxenates. The binary fluorides show negative formation enthalpies and can be prepared directly from the elements. Conversely, xenon–oxygen species are thermodynamically unstable (endothermic) and thus more or less labile, in part even explosive (e.g., xenon oxides). Almost all compounds known in crystalline form with xenon in a positive oxidation state are prepared from the xenon fluorides. XeF_2 is the only commercially available xenon compound; it is employed not only in organic chemistry as fluorination agent, but also during the manufacture of microelectronic systems as gaseous etching reagent for crystalline surfaces of Si, Mo and Ge.

Toward metal atoms in positive oxidation states, xenon can act as LEWIS base and ligand. To this interesting class of compounds belong, for instance, the cations $[AuXe_4]^{2+}$, $[HgXe]^{2+}$ and $[F_3AsAuXe]^{+}$, which have been isolated in crystalline form with the counter-ions $[SbF_6]^{-}$ or $[Sb_2F_{11}]^{-}$.[2]

7 S. Yang, A. M. Ellis, *Chem. Soc. Rev.* **2013**, *42*, 472.

14.3.1 Xenon Fluorides

In 1962, it was discovered that xenon reacts with elemental fluorine upon suitable activation by heating, irradiation or in an electric discharge to give the fluorides XeF_2, XeF_4 and XeF_6. With these results, the decade-old dogma that noble gases do not form covalent bonds in neutral molecules was finally made obsolete. The synthesis of these fluorides occurs via the following equilibrium reactions:

$$Xe + F_2 \rightleftharpoons XeF_2 \qquad \Delta H_o^\circ = -105.9 \text{ kJ mol}^{-1}$$

$$XeF_2 + F_2 \rightleftharpoons XeF_4 \qquad \Delta H_o^\circ = -104.1 \text{ kJ mol}^{-1}$$

$$XeF_4 + F_2 \rightleftharpoons XeF_6 \qquad \Delta H_o^\circ = -74.9 \text{ kJ mol}^{-1}$$

The indicated reaction enthalpies are valid for 0 K.[8] The higher the fluorine concentration in the reaction mixture, the larger the yield of higher fluorides. Small amounts of XeF_2 are obtained by irradiation of a mixture of Xe and F_2 in a 1:1 ratio; larger quantities are best prepared by UV irradiation in the presence of 1% of HF as a catalyst (often formed from residual water and F_2). XeF_6 is prepared in a heterogeneous reaction by heating a 1:5 Xe/F_2 mixture to 120 °C in the presence of NiF_2. In an analogous manner, XeF_4 is obtained by heating the same mixture to 300 °C at 0.6 MPa in a nickel container. As the similarity of reaction conditions suggests, XeF_4 is difficult to prepare in pure form so that it is typically purified chemically by taking advantage of its lower propensity to act as fluoride donor toward strong acids. Treatment of a mixture of the three different xenon fluorides with AsF_5 as a fluoride ion acceptor converts XeF_2 and XeF_6 to the corresponding nonvolatile cations so that pure XeF_4 can be recovered by sublimation. Attempts to prepare XeF_8 failed so far, although xenon does reach its highest oxidation state +8 in some oxygen species.

Some properties of xenon fluorides are compiled in Table 14.1. All three compounds form colorless crystals at room temperature, which sublime in vacuum and are built of isolated molecules in case of XeF_2 and XeF_4. The linear XeF_2 molecules ($D_{\infty h}$ symmetry) assume a parallel position in the tetragonal crystal structure with the Xe atoms forming a body-centered lattice. In this way, each xenon atom is coordinated by eight second-nearest fluorine neighbors (at a distance of 342 pm) in addition to the two directly bonded F atoms (see Figure 3.1). Xenon tetrafluoride consists of square-planar molecules of D_{4h} symmetry and crystallizes in a monoclinic structure. Depending on the temperature, XeF_6 crystallizes in six different modifications, which consist of tetrameric and/or hexameric cyclic aggregates with unsymmetrical F bridges between XeF_5 units. At room temperature, a cubic phase built from both tetrameric and hexameric units is most stable. A similar association was found in liquid SbF_5 (Section 10.8.3). In the gas phase, XeF_6 is a fluxional

8 D. A. Dixon et al. *Inorg. Chem.* **2010**, *49*, 261 and references therein.

Table 14.1: Properties of xenon fluorides (with symmetry in the gas phase and internuclear distances in the crystal).

	XeF_2 ($D_{\infty h}$)	XeF_4 (D_{4h})	XeF_6 (C_{3v})
Triple point (°C)	129	117	49
Average bond enthalpy (298 K; kJ mol^{-1})	128	124	124
XeF distance (pm)	200	195	185/194
Density (g cm^{-1})	4.32	4.04	3.73

molecule, which oscillates between C_{3v} and O_h symmetric structures of very similar energy (the C_{3v} structure is by about 7 kJ mol^{-1} more stable).[9]

In contrast, XeF_2 and XeF_4 are monomeric in all phases. The structures determined by electron diffraction in the gas phase and X-ray diffraction in the solid state confirm expectations according to the electron pair repulsion model (Section 2.2.2).

14.3.2 Reactivity of Xenon Fluorides

The three xenon fluorides are stable at 25 °C but decompose into the elements on heating. XeF_2 dissolves in water moderately well (ca. 25 g L^{-1} at 0 °C).[10] This solution decomposes just slowly, namely to HF, Xe and O_2 (see Section 14.3.3). Conversely, XeF_4 can only be stored in meticulously dried glass or quartz vessels (better in KEL-F, nickel or Monel containers).[11] XeF_6 reacts with glass and quartz to $XeOF_4$ and O_2. As expected, all xenon fluorides are very strong oxidants and fluorinating agents; the reactivity increases with the oxidation state of xenon. In general, xenon is instantly reduced to the oxidation state ±0 in redox reactions. XeF_2, however, is kinetically rather stable.

XeF_2 can be coordinated as a ligand to various metal cations as in $[Ba(XeF_2)_5][AsF_6]_2$.[12] In this complex, four of the five XeF_2 molecules are connected to the cation through the fluorine atoms in a bridging manner between two neighboring cations. The fifth XeF_2 molecule coordinates to the xenon atoms of adjacent ligands by weaker donor–acceptor interactions, just like in the solid-state structure of XeF_2 (Figure 3.1). In addition, the barium atoms are each coordinated by four fluorine atoms of the anions so that a coordination number of 12 is attained.

9 K. A. Peterson, D. A. Dixon, H. Stoll, *J. Phys. Chem. A* **2012**, *116*, 9777.

10 For a recent overview on Xe(IV) chemistry see: J. Haner, G. Schrobilgen, *Chem. Rev.* **2015**, *115*, 1255–1295.

11 KEL-F is the trade name for poly(fluorotrichloroethylene), Monel is a Cu/Ni alloy.

12 M. Gerken et al., *Inorg. Chem.* **2007**, *46*, 6069.

With certain hydroxo compounds, xenon fluorides react under condensation according to the following scheme:

$$-\mathrm{Xe}-\mathrm{F} + \mathrm{H}-\mathrm{O}- \longrightarrow -\mathrm{Xe}-\mathrm{O}- + \mathrm{HF}$$

This protocol allows for the syntheses of many compounds with XeO bonds. These reactions are described in Sections 14.3.3–14.3.5. Moreover, XeF_2, XeF_4 and XeF_6 can exchange fluoride ions under suitable conditions, behaving as F^- donors in some cases and as F^- acceptors in others. In this manner, salts with $[XeF_n]$-cations or -anions are obtained in analogy to the corresponding behavior of interhalogen compounds.

14.3.2.1 Redox Reactions

XeF_2 and XeF_4 react with H_2 at 300–400 °C, XeF_6 already at 25 °C, to HF and Xe:

$$XeF_2 + H_2 \longrightarrow Xe + 2\,HF$$

On agitation of a biphasic mixture with mercury, Xe and HgF_2 or Hg_2F_2 are obtained in quantitative reactions. These reactions are used for the analysis of xenon fluorides (determination of Xe by weighing and F^- by titration). Aqueous iodide solution is oxidized to I_2 by all xenon fluorides.

The reactivity toward oxidizable substances strongly increases from XeF_2 to XeF_6. Therefore, only XeF_2 dissolves in various liquids in molecular form and without reaction (HF, SO_2, CH_3NO_2, CH_3CN, CCl_4, dioxane). XeF_4 and XeF_6 readily dissolve in liquid HF.

14.3.2.2 Fluoride Transfer Reactions

XeF_2 behaves as F^- donor toward strong LEWIS acids. Depending on the stoichiometric ratio, it reacts with the pentafluorides of As, Sb, Bi, Ru, Ir and Pt to the following compounds:

$$XeF_2 + MF_5 \xrightarrow{2:1} [Xe_2F_3][MF_6]$$
$$XeF_2 + MF_5 \xrightarrow{1:1} [XeF][MF_6]$$
$$XeF_2 + MF_5 \xrightarrow{1:2} [XeF][M_2F_{11}]$$

These species are mostly colored and show melting points between 50° and 150 °C. According to X-ray structure analyses and vibrational spectra they are predominantly salt-like. The compounds of the first type contain the planar, V-shaped cation $[Xe_2F_3]^+$, with the following geometry in the hexafluoroarsenate:

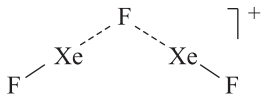

d_{XeF} = 190 pm angle$_{XeFXe}$ = 151°
$d_{Xe\cdots F}$ = 214 pm angle$_{FXeF}$ = 178°

The salts of the third type contain dinuclear complex anions with fluorine bridges like those in liquid SbF_5. For $[XeF][Sb_2F_{11}]$ the following structure has been determined:[13]

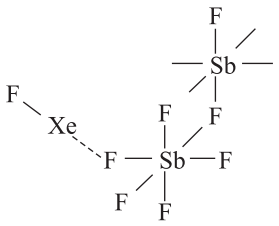

d_{XeF} = 188.8 pm
$d_{Xe\cdots F}$ = 234.3 pm
angle$_{XeFSb}$ = 148.1°
angle$_{FXeF}$ = 179.3°

The relatively small distance of the cation $[XeF]^+$ to one of the fluorine atoms of the anion is interpreted as a bond with partially covalent, partially ionic character. Analogous considerations apply to salts of the type $[XeF][MF_6]$ in general, given the high LEWIS acidity of $[XeF]^+$. Corresponding derivatives of XeF_4 are found in the salts $[XeF_3][SbF_6]$ and $[XeF_3][Sb_2F_{11}]$.

In the presence of the *magic acid* HF/SbF_5 (Section 5.5.2), $[XeF][Sb_2F_{11}]$ reacts with xenon to $[Xe_2]^+[Sb_4F_{21}]^-$, which – according to X-ray structure analysis – contains a weak Xe–Xe bond of 309 pm length; the anion consists of four corner-sharing SbF_6 octahedra:[14]

$$[XeF]^+ + 3\,Xe + H^+ \longrightarrow 2\,[Xe_2]^+ + HF$$

The bonding situation in such *xenonium cations* is discussed in Section 14.6.

Xenon hexafluoride can both accept and donate fluoride ions. It is a stronger F^- donor than the other two xenon fluorides. With AsF_5, SbF_5 and PtF_5, it reacts to salts of the type $[XeF_5][MF_6]$. In the arsenic species, the $[XeF_5]^+$ cations show an approximate square-pyramidal arrangement of the F atoms. The cations are connected by three unsymmetrical fluorine bridges between two octahedral $[AsF_6]^-$ anions so that the xenon atom is surrounded by one lone pair of electrons as well as by five nearest and three second-nearest F atoms. With AuF_5, XeF_6 reacts in a 1:2 ratio to the salt $[Xe_2F_{11}][AuF_6]$, the cation of which has the atom connectivity of $[F_5Xe–F–XeF_5]^+$.

Similarly high coordination numbers as in the $[XeF_5]^+$ salts occur in the anionic fluoroxenates, which are formed during the reaction of XeF_6 with alkali metal fluorides (apart from LiF). In this manner, the yellow salt $Cs[XeF_7]$ is obtained from CsF and liquid XeF_6 at 50 °C. At higher temperatures, this salt decomposes to $Cs_2[XeF_8]$ and XeF_6:

13 G. J. Schrobilgen et al, *Inorg. Chem.* **2010**, *49*, 8504.
14 T. Drews, K. Seppelt, *Angew. Chem. Int. Ed.* **1997**, *36*, 273.

$$2\,CsF + 2\,XeF_6 \xrightarrow{50°C} 2\,Cs[XeF_7] \xrightarrow[-XeF_6]{>50°C} Cs_2[XeF_8] \xrightarrow{400°C} 2\,CsF + Xe + 4\,F_2$$

The likewise yellow octafluoroxenate(VI) is one of the thermally most stable noble gas compounds; the anion has the structure of a square-antiprism. The anion of $Cs[XeF_7]$ forms a monocapped octahedron. The stability of both fluoroxenates demonstrates the considerable LEWIS acidity of XeF_6. Indeed, adducts with neutral donors have been reported, for example, with either one or two acetonitrile ligands depending on the stoichiometric ratio.[15] The products $[XeF_6(NCMe)_n]$ (n = 1, 2) are colorless solids that start to lose acetonitrile under dynamic vacuum at temperatures above −40 °C. Even at −78 °C, they detonate upon mechanical shock. The solid-state structure of the monoadduct exhibits local C_{3v} symmetry in the XeF_6 moiety. The acetonitrile ligand caps one surface of the heavily distorted octahedron with an internuclear distance of d_{XeN} = 276.2 pm, which is much shorter than the sum of van der Waals radii of 371 pm.

Besides the above-described salt-like compounds and donor–acceptor complexes, a series of stoichiometric cocrystals such as $XeF_2{\cdot}IF_5$, $XeF_2{\cdot}XeF_4$ and $XeF_2{\cdot}XeOF_4$ are known, which contain the nearly unperturbed individual molecules next to each other.

14.3.3 Oxides and Oxosalts of Xenon

The colorless XeF_2 dissolves in water as molecules without any visible sign of reaction, but with yellow color. Only after some time, more rapidly on heating or addition of bases, hydrolysis sets in. Instead of leading to XeO, however, oxidation of the oxygen atom of water is observed:

$$XeF_2 + H_2O \longrightarrow Xe + 2\,HF + \tfrac{1}{2}\,O_2$$

Presumably, FXeOH occurs as intermediate of this reaction, because in the presence of $[Xe_2F_3][AsF_6]$ (see Section 14.3.2) the spectacular orange-red cation $[Xe_3OF_3]^+$ is formed by condensation under concomitant HF elimination. It was isolated as the hexafluoroarsenate and characterized by X-ray diffraction. The angles at the Xe atoms of the FXeOXeFXeF chain are close to 180°, at the F bridge 150° and at the O-atom 120°.[16]

XeF_4 instantly reacts with water at 20 °C. Xe, O_2, HF and xenon trioxide XeO_3 are formed in a confusingly complex reaction. If hydrolysis is cautiously carried out at 0 °C or in dilute sulfuric acid, however, a polymeric yellow Xe(IV) oxide is

15 G. J. Schrobilgen et al., *Angew. Chem. Int. Ed.* **2015**, *54*, 14169.

16 G. J. Schrobilgen et al, *J. Am. Chem. Soc.* **2009**, *131*, 13474 and **2010**, *132*, 13823.

obtained, which is insoluble in water. The coordination of the Xe atom in this oxide is square-planar as in XeF_4.[17]

XeO_3 is best prepared by cautious hydrolysis of XeF_6 with excess H_2O at 20 °C and in the presence of MgO for trapping the concomitantly formed hydrofluoric acid. It can be isolated as colorless, extremely explosive crystals from aqueous solution by evaporation. Three different crystalline phases of XeO_3 are known, all of which contain hexacoordinate xenon centers with three covalent and three coordinating XeO interactions (distances XeO: 175.6–178.0 pm; Xe···O: 267.8–284.0 pm).[18] XeO_3 is hygroscopic and a strong oxidant. It dissolves in water mostly as molecules; the resulting solution is stable, extremely oxidizing and weakly acidic due to the following equilibrium with trace amounts of xenic acid H_2XeO_4:

$$2\,H_2O + XeO_3 \rightleftharpoons [H_3O]^+ + [HXeO_4]^-$$

Apparently, XeO_3 is not a proton acceptor but rather a LEWIS acid similarly to SO_3. As XeF_6 discussed above, it forms mono- and bis(acetonitrile) adducts.[19] While $[O_3Xe(NCMe)]$ is just as shock-sensitive as XeO_3 itself, $[O_3Xe(NCMe)_2]$ seems to be kinetically stable even at room temperature as it does not detonate when struck with a hammer. In the crystalline state, both species show a distorted octahedral coordination sphere, which is completed by one or two intermolecular contacts with the O atoms of a neighboring molecule.

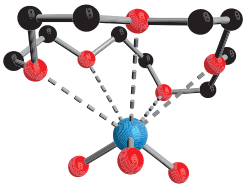

d_{XeO} = 175.6 to 178.0 pm
$d_{Xe\cdots O}$ = 289.5 to 312.4 pm

From an aesthetic point of view, the 15-crown-5 adduct of XeO_3 is particularly appealing: in the solid-state structure (see above), the Xe center at the apex of the XeO_3 pyramid is surrounded by the five oxygen atoms of the crown ether with three short (between 289.5 and 290.7 pm) and two longer (311.4 and 312.4 pm) XeO internuclear distances (the three covalent XeO bonds are between 175.6 and 178.0 pm long).[20] As in case of the bis(acetonitrile) adduct, no shock-sensitivity was observed. It is particularly noteworthy that XeO_3 can be dissolved in acetone without explosion, for example, during the synthesis of the crown ether adduct.

The pronounced tendency of XeO_3 to expand its coordination sphere also becomes apparent in the reaction with fluoride ions:

17 D. S. Brock, G. J. Schrobilgen, *J. Am. Chem. Soc.* **2011**, *133*, 6265.
18 J. T. Goettel, G. J. Schrobilgen, *Inorg. Chem.* **2016**, *55*, 12975.
19 G. J. Schrobilgen et al., *Angew. Chem. Int. Ed.* **2016**, *55*, 13780.
20 G. J. Schrobilgen et al., *Angew. Chem. Int. Ed.* **2018**, *57*, 12448

$$MF + XeO_3 \xrightarrow[0°C]{H_2O} M[XeO_3F] \qquad M: K, Rb, Cs$$

The fluoroxenates(VI) can be isolated in pure form from solution. They contain polymeric, chain-like anions consisting of XeO_3 pyramids connected by fluorine bridges.

Salts of the nonisolable xenic acid H_2XeO_4 can be obtained by mixing of XeO_3 and NaOH solutions in a stoichiometric ratio of 1:1 and subsequent freezing and evaporation of excess water by sublimation in vacuum (*freeze drying*). In this manner, $Na[HXeO_4]\cdot 1.5H_2O$ and $Cs[HXeO_4]\cdot 1.5H_2O$ have been prepared as colorless crystals.

If the XeO_3 solutions are too alkaline or when either XeO_3 or XeF_6 are directly dissolved in strong aqueous bases, disproportionation of Xe(VI) to Xe(0) and Xe (VIII) occurs:

$$2\,[HXeO_4]^- + 4\,Na^+ + 2\,[OH]^- \longrightarrow Na_4[XeO_6] + Xe + O_2 + 2\,H_2O$$

Perxenates such as $Na_4[XeO_6]\cdot nH_2O$ (n = 2, 6, 8) and $Ba_2[XeO_6]$ can also be obtained through *ozonization* of a XeO_3 solution under addition of the corresponding metal hydroxide. In contrast to the xenates(VI), the perxenates are thermally extraordinarily stable. The sodium salts are colorless and can be dehydrated by drying in vacuum at 100 °C. $Na_4[XeO_6]$ contains nearly octahedral $[XeO_6]^{4-}$ ions. On dissolution in water complete hydrolysis occurs according to the equation:

$$[XeO_6]^{4-} + H_2O \rightleftharpoons [HXeO_6]^{3-} + [OH]^-$$

Free perxenic acid is unknown. Acidification of $Ba_2[XeO_6]$ with concentrated sulfuric acid leads to the evolution of gaseous XeO_4:

$$Ba_2[XeO_6] + 4\,H_2SO_4 \longrightarrow 2\,Ba[SO_4]\downarrow + XeO_4\uparrow + 2\,[H_3O][HSO_4]$$

XeO_4 (m.p. −36 °C) is yellow at −196 °C and explosive even at −40 °C. In the gas phase, XeO_4 consists of molecules of T_d symmetry (isoelectronic with $[IO_4]^-$). It decomposes to the elements above 0 °C, often explosively. According to quantum-chemical calculations, a planar isomer of D_{2h} symmetry with OO bonds (a bis-peroxide) occurs as an intermediate; its activation energy for the decomposition into Xe and 2 O_2 is very small.[21]

14.3.4 Xenon Oxyfluorides

If two fluorine atoms of XeF_4 or XeF_6 are formally replaced by an oxygen atom, oxyfluorides are obtained. Almost all the theoretically feasible oxyfluorides of Xe(IV),

21 V. Slepkov, S. Kozlova, S. Gabuda, *J. Phys. Chem. A* **2011**, *115*, 7811.

Xe(VI) and Xe(VIII) are known. Upon cautious hydrolysis in acetonitrile at –45 °C, XeF_4 is transformed into the adduct $MeCN{\cdot}XeOF_2$, which can be rid of the coordinating solvent in vacuum to give monomeric $XeOF_2$ of C_{2v} symmetry. Just like in case of the corresponding adducts of xenon oxides (Section 14.3.3), the nitrile coordinates to the xenon center with the N atom.[22] XeF_6 reacts with small amounts of water and with certain oxides to $XeOF_4$, XeO_2F_2 and XeO_3F_2 in a stepwise manner:

$$2\ XeF_6 + SiO_2 \xrightarrow{50°C} 2\ XeOF_4 + SiF_4\uparrow$$

$$XeF_6 + H_2O \xrightarrow{20°C} XeOF_4 + 2\ HF\uparrow$$

$XeOF_4$ (m.p. –46 °C) is a colorless liquid consisting of molecules of C_{4v} symmetry (square-pyramidal), which is transformed into XeO_3 on complete hydrolysis. $XeOF_4$ only decomposes at temperatures as high as 300 °C.

The other oxyfluorides are formed in O/F exchange reactions from XeF_6 and XeO_3 or XeO_4:

$$XeF_6 + 2\ XeO_3 \xrightarrow{25°C} 3\ XeO_2F_2$$

$$XeF_6 + XeO_4 \longrightarrow XeO_3F_2 + XeOF_4$$

$$XeF_6 + XeO_3F_2 \longrightarrow XeO_2F_4 + XeOF_4$$

XeO_2F_4 was identified spectroscopically. The vibrational spectrum of XeO_3F_2 (m.p. –54 °C) is consistent with D_{3h} symmetry of the molecule. XeO_2F_2 (m.p. 31 °C) is C_{2v} symmetric.

14.3.5 Other Xenon Compounds

In a similar manner as with water, the xenon fluorides also react with other hydroxo compounds (E–OH) under elimination of HF. While with alcohols deflagration or even explosion occurs, various oxoacids are suitable for targeted condensation reactions:[23]

$$XeF_2 + HO{-}E \xrightarrow{-HF} F{-}Xe{-}O{-}E \xrightarrow[-HF]{+EOH} E{-}O{-}Xe{-}O{-}E$$

22 G. J. Schrobilgen et al., *J. Am. Chem. Soc.* **2007**, *129*, 3598.

23 K. Seppelt, *Acc. Chem. Res.* **1979**, *12*, 211; D. Lentz, L. Turowsky, K. Seppelt, *Z. Anorg. Allg. Chem.* **1992**, *609*, 153.

Fluorosulfuric acid HSO_3F and pentafluoroorthotelluric acid $HOTeF_5$[24] react with XeF_2 to the following compounds:

$XeF(OSO_2F)$	$Xe(OSO_2F)_2$	$XeF(OTeF_5)$	$Xe(OTeF_5)_2$
colorless	yellow	yellow liquid	colorless
m.p. 37°C	m.p. 44°C		m.p. 36°C

The driving force of these reactions is the large bond enthalpy of hydrogen fluoride. While both tellurium species are stable up to 130 °C, the fluorosulfates decompose slowly already at 25 °C to Xe and $S_2O_6F_2$ (and possibly XeF_2).

According to an X-ray diffraction study, the crystals of $XeF(SO_3F)$ consist of the following molecules:

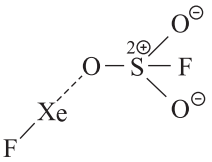

$d_{XeF} = 194$ pm angle$_{XeOS} = 124°$

$d_{Xe\cdots O} = 216$ pm angle$_{FXeO} = 177°$

The XeO bond is predominantly ionic. The other compounds show an analogous structure. $Xe(OTeF_5)_2$ contains a planar TeOXeOTe scaffold with the TeF_5 substituents in a *trans* arrangement.

At low temperatures, XeF_4 and XeF_6 react with HSO_3F in a similar manner as XeF_2. In the former case, $XeF_2(SO_3F)_2$ was isolated as a yellow-green liquid, which slowly decomposes at 25 °C to Xe, XeF_4 and $S_2O_6F_2$. In the latter case, $XeF_4(SO_3F)_2$ is formed, which is also a liquid and decomposes to XeF_4 and $S_2O_6F_2$ at room temperature. As in the case of xenon(II), the pentafluorooxotellurates are more stable. The colorless $Xe(OTeF_5)_4$ and the red-violet $Xe(OTeF_5)_6$ are obtained by reaction of XeF_4 and XeF_6, respectively, with $B(OTeF_5)_3$, in turn prepared from $HOTeF_5$ and BCl_3. In analogy to XeF_4, the central XeO_4 group of $Xe(OTeF_5)_4$ is planar.

The reaction of $HN(OSO_2F)_2$, with XeF_2 at 0 °C, affords HF and $F–Xe–N(OSO_2F)_2$, which contains a linear FXeN unit with strongly different internuclear distances XeF (197 pm) and XeN (220 pm). Treatment of $[XeF][AsF_6]$ with F_3SN at −20 °C yields $[F_3SNXeF][AsF_6]$ with a XeN bond of 223.6 pm length. The up–to-date shortest XeN bond with an internuclear distance of 208.4 pm was observed in the cation $[F_4SNXe]^+$.[25]

If XeF_2 is treated with $B(C_6F_5)_3$ at −50 °C in dichloromethane, an aryl transfer from boron to xenon occurs and the salt $[C_6F_5Xe]^+[(C_6F_5)_2BF_2]^-$ is obtained, a colorless compound with a XeC bond that is only stable below −30 °C and reacts with

24 $HOTeF_5$ is prepared according to $Te(OH)_6 + 5\ HSO_3F \rightarrow HOTeF_5 + 5\ H_2SO_4$; it is a very stable compound and a strong acid in water.

25 G. J. Schrobilgen et al., *J. Am. Chem. Soc.* **2009**, *131*, 7272.

AsF_5 under anion exchange to $[C_6F_5Xe]^+[AsF_6]^-$. This arylxenonium salt (m.p. 102 °C) can also be prepared from XeF_2, $(C_6F_5)_3B$ and AsF_5 in anhydrous HF and is stable up to 125 °C. A neutral molecule with a XeC bond is obtained as follows:[26]

$$[C_6F_5Xe][AsF_6] + Cs[OOCC_6F_5] \xrightarrow[25°C]{H_2O} C_6F_5{-}Xe{-}OC(O)C_6F_5 + Cs[AsF_6]$$

The xenon compound precipitates from aqueous solution; it decomposes at 85 °C in a strongly exothermic reaction to Xe and $C_6F_5C(O)OC_6F_5$. The central group C–Xe–O is linear (d_{XeC} = 212 pm, d_{XeO} = 237 pm). Other compounds with a XeC bond, albeit less stable, are C_6F_5XeF, C_6F_5XeCl, $(C_6F_5)_2Xe$ and $[C_6F_5XeF_2][BF_4]$.[12] For the characterization of such compounds ^{129}Xe-NMR spectroscopy is particularly valuable.[27] In Figure 14.1 the chemical shifts of selected xenon compounds are compiled. Apparently, elemental Xe is the most shielded and the resonance frequency correlates to the oxidation state of the xenon atom. $XeOF_4$ at 24 °C is used as standard reference.

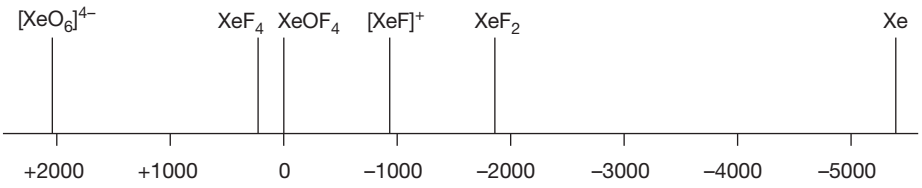

Figure 14.1: Chemical shifts of simple xenon compounds in ^{129}Xe-NMR spectroscopy. The deshielding increases with the oxidation state, although a few irregularities occur.

14.4 Compounds of Other Noble Gases

14.4.1 Argon

Traces of the molecule HArF are formed on UV irradiation of HF in an argon matrix at 7.5 K with subsequent tempering at 18 K. HArF was spectroscopically and computationally characterized as a linear molecule. On annealing of the matrix, exothermic decomposition to the starting materials HF and Ar occurs, which is associated with an activation barrier of about 96 kJ mol^{-1}. Analogous compounds HEX of krypton and xenon with covalent HE bonds, and various electronegative groups X were also generated in matrix isolation experiments and identified spectroscopically.[28]

26 H. J. Frohn, V. V. Bardin, *Organometallics* **2001**, *37*, 4750.
27 D. Raftery, *Ann. Rep. NMR Spectrosc.* **2006**, *57*, 205. M. Gerken, G. J. Schrobilgen, *Coord. Chem. Rev.* **2000**, *197*, 335.
28 M. Räsänen et al., *Phys. Chem. Low Temp.* **2011**, 419.

14.4.2 Krypton

Of krypton only compounds in the oxidation states 0 and +2 exist.[29] The only binary krypton species that has been isolated in pure form is the difluoride KrF_2. It is prepared by UV irradiation of a liquid mixture of Kr and F_2 in a molar ratio of 4:1 at −196 °C. KrF_2 can be purified by sublimation below −10 °C; at higher temperatures it decomposes into the elements. KrF_2 forms colorless crystals (with one high and one low temperature modification), which consist of linear molecules of $D_{\infty h}$ symmetry and dissolve in hydrogen fluoride. Unlike xenon fluorides, the compound is *endothermic* and decomposes above −20 °C. Its chemical reactivity, however, is analogous to that of XeF_2 as far as known. The average KrF bond enthalpy is only 48 kJ mol^{-1} and the enthalpy of formation has been determined by calorimetry to +60 kJ mol^{-1}. From the internuclear distance d_{KrF} = 189 pm, the covalent radius of the krypton atom can be estimated to 125 pm. With Hg, KrF_2 reacts to HgF_2 and Kr; with water or dilute aqueous NaOH it is instantly converted to O_2, Kr and HF or NaF. With strong LEWIS acids such as AsF_5, SbF_5, BiF_5 and AuF_5, krypton fluoride forms salts with the cations $[KrF]^+$ and $[Kr_2F_3]^+$. For example, SbF_5 reacts with KrF_2 at −20 °C to colorless crystals of $[KrF][Sb_2F_{11}]$, which decompose to Kr, F_2 and SbF_5 at the melting point of about 50 °C. Krypton–oxygen bonds are present in the relatively unstable $Kr(OTeF_5)_2$. Most likely, all krypton species are endothermic.

Krypton difluoride like XeF_2 can function as a ligand in metal complexes, for example, in $Mg(KrF_2)_4(AsF_6)_2$ and $[Hg(KrF_2)_8][AsF_6]_2 \cdot 2HF$.[29]

14.4.3 Radon

Investigations regarding the chemistry of *radon* are hampered by its α radiation and the short half-life. So far, no pure compounds have been isolated. With Cl, ClF_3 and other halogen fluorides, however, Rn reacts to RnF_2 at 25 °C. Other halides or oxides have not been reported yet.

14.5 Electronegativities of Noble Gases

In case of xenon and krypton, the electronegativities (χ) can be calculated according to the method by ALLRED and ROCHOW (Section 4.6.2) by the determination of the effective nuclear charge Z_{eff} with the SLATER rules:

29 G. J. Schrobilgen et al., *Inorg. Chem.* **2001**, *40*, 300; *Coord. Chem. Rev.* **2002**, *233–234*, 1; *Angew. Chem. Int. Ed.* **2017**, *56*, 6251 and *Angew. Chem. Int. Ed.* **2018**, *57*, 13167.

$$\chi = 3.59 \cdot 10^{3} \cdot \frac{Z_{\text{eff}}}{r^2} + 0.744$$

A 5*p* electron of xenon experiences the effective nuclear charge of Z_{eff} = 8.25. The same value is obtained for a 4*p* electron of krypton. The single bond covalent radii (r_1) of Xe and Kr can be estimated as follows: in gaseous XeF_2 the XeF internuclear distance is d_{XeF} = 200 pm, in KrF_2 it is with d_{KrF} = 189 pm slightly shorter. By subtraction of the covalent radius of the fluorine atom (57 pm), the following values are obtained for divalent krypton and xenon (in comparison with the values for the neighboring halogens):

r_1 (Kr): 132 pm	r_1 (Br): 114 pm
r_1 (Xe): 143 pm	r_1 (I): 133 pm

As expected, these radii are slightly larger than those of the corresponding halogen atoms, as the latter have been derived from species with two-center bonds. In an analogous manner, covalent radii of 138 pm are determined for xenon(IV) and 133 pm for xenon(VI). On this basis, the following χ_{AR} values are obtained for krypton and xenon:

Kr(II): 2.44 Xe(II): 2.19 Xe(IV): 2.30 Xe(VI): 2.42

According to these calculations, the electronegativities of krypton(II) and xenon (II) are smaller than those of the adjacent halogens bromine (2.74) and iodine (2.21). The reason is probably the large atomic radii of the noble gas atoms, derived from compounds with three-center bonds. When the internuclear distance of the cations $[FKr]^+$ (177 pm) and $[FXe]^+$ (189 pm) are used instead (which do contain electron-precise two-center bonds), atomic radii of r_1(Kr) = 120 and r_1 (Xe) = 132 pm are obtained and thus the following χ_{AR} values: Kr(II) = 2.80 and Xe (II) = 2.44.

On the other hand, according to the method of ALLEN, spectroscopic electronegativities can be calculated directly from the ionization energies of the isolated atoms (Section 4.6.2). With this method the following χ_{spec} values are determined for the noble gases (Table 4.8):

Ne: 4.79 Ar: 3.24 Kr: 2.97 Xe: 2.58

These values are to be preferred as they correspond well with the above ALLRED-ROCHOW values and, by the way, also with the expectation that noble gases should be slightly *more electronegative than the halogens* to their left in the Periodic Table.

14.6 Bonding Situation in Noble Gas Compounds

For a more detailed analysis of the bonding situations, the noble gas compounds are best treated separately as diatomic and multiatomic representatives.

14.6.1 Diatomic Molecules and Ions

As shown in Section 3.3, the diatomic neutral molecules He_2, Ne_2, Ar_2, Kr_2 and Xe_2 only exist as VAN DER WAALS complexes with very small bond enthalpies and at the same time very large internuclear distances compared to covalent bonds. For the diatomic cations, the situation is completely different. The first ever observed molecule with a covalent bond to a noble gas atom was the cation $[HHe]^+$, which was discovered by mass spectrometry in 1925. It corresponds to the isoelectronic H_2 molecule and features a regular two-electron σ bond just like the latter. The bond in $[HHe]^+$, however, is polar as the 1*s* orbital energies of H (–13.6 eV) and He (–24.6 eV) differ extremely. Moreover, all homonuclear and heteronuclear diatomic noble gas cations from $[He_2]^+$ to $[Xe_2]^+$ and from $[HeNe]^+$ to $[KrXe]^+$ have been detected in the gas phase. They all contain 2-center 3-electron bonds since the antibonding σ* MO is occupied by one electron less than the bonding σ orbital (Section 2.4.3). As expected, the dissociation enthalpy (D_o) of the homonuclear cations decreases with increasing atom size.[30] For the gaseous ion $[Xe_2]^+$ mentioned in Section 14.3.5, D_o was determined to 99 kJ mol^{-1}.

The dissociation enthalpies of the noble gas hydride cations $[HE]^+$ are identical with the proton affinities of the neutral noble gas atoms, which show the following values (kJ mol^{-1}):

He: 193 Ne: 218 Ar: 402 Kr: 444 Xe: 559

This trend corresponds to the strongly increasing polarizability α of the noble gas atoms (E) from He to Xe (Section 3.3). Salts with the cations $[HE]^+$ have not been isolated so far, but the formally derived cations $[XeF]^+$, $[XeCl]^+$ and $[Xe_2]^+$ can be prepared as salts, for example, $[XeF][SO_3F]$ and $[XeCl][Sb_2F_{11}]$. These cations contain covalent two-electron σ bonds.

14.6.2 Polyatomic Molecules and Ions

These compounds can be best understood with MO theory under the assumption of multicenter bonding.

30 G. Frenking, D. Cremer, *Structure Bonding (Berlin)* **1991**, *73*, 17.

The MO description of the XeF_2 molecule corresponds to that of the isoelectronic triiodide ion $[I_3]^-$, which is also linear (Section 13.5.3). If just the σ interactions between the central atom and the two ligand atoms are considered, only the 5*s* and $5p_z$ orbitals of the central atom and the $2p_z$ orbitals of both fluorine atoms are relevant due to the very low energy of the 2*s* orbital at fluorine. Both the 5*s* and the $5p_z$ orbitals of xenon overlap with the corresponding fluorine orbitals and two bonding and two antibonding MOs result (Figure 14.2). With six valence electrons in the original AOs, both bonding (σ_g and σ_u) and the lower antibonding ($\sigma_g^\star$) are occupied. The net result is a three-center σ bond, and the stabilization of the molecule is essentially due to the energetic lowering of the $5p_z$ electrons at xenon to the σ_u level.

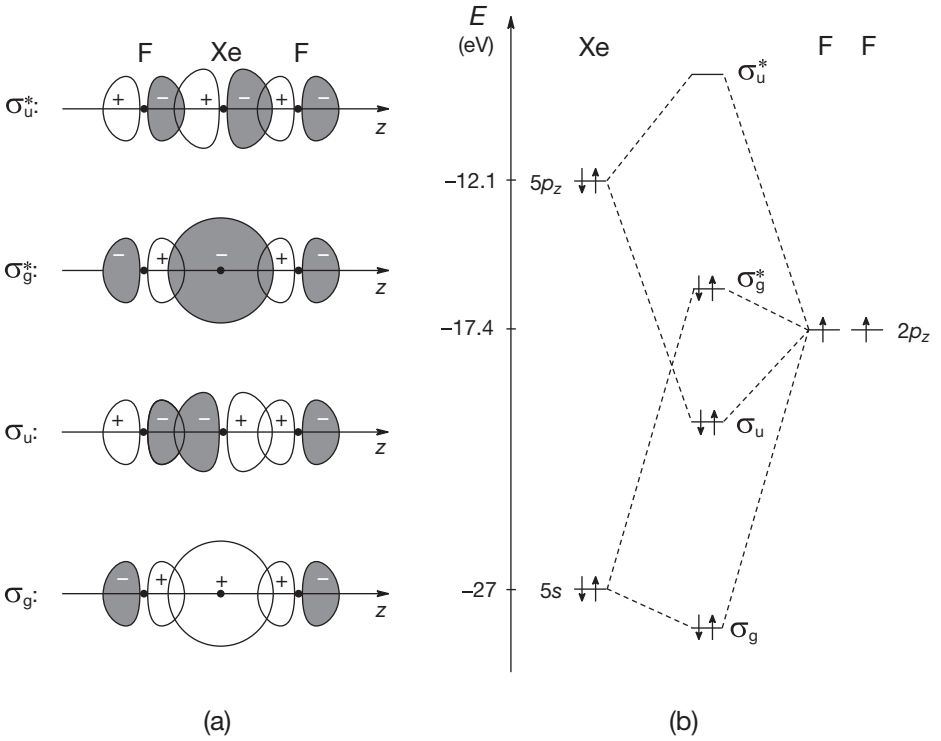

Figure 14.2: The covalent bond in xenon difluoride. (a) Linear combinations for the four σ molecular orbitals. (b) Schematic energy diagram for the σ molecular orbitals (the 2*s* AO of fluorine has an energy of –46.4 eV and can thus be disregarded here).

In a similar manner, the bonds in XeF_4 and in XeF_6 can be treated by considering the other 5*p* orbitals of the xenon atom as well for binding of two fluorine ligands each. With that, the square-planar XeF_4 and the octahedral XeF_6 are constructed. The observation that the molecule XeF_6 is not octahedral, but rather of C_{3v}

symmetry is due to several competing factors,[31] which will not be discussed in detail here. According to ab initio MO calculations the energy difference between the O_h and the C_{3v} structure is only ca. 7 kJ mol^{-1}. In neon and argon matrices at 5K, XeF_6 exhibits the C_{3v} structure.[31b] For the octahedral geometry, the MO diagram of the analogous SF_6 molecule can be applied in principle (Figure 2.39).

The considerable difference in electronegativities between xenon and fluorine accounts for the strongly polar bonds in xenon fluorides and the positive charge at the central atom. This positive charge increases from XeF_2 to XeF_6 and was experimentally proven by photoelectron spectroscopy. To this end the gaseous compounds are ionized by X-rays and the energies required for the detachment of electrons from the inner electron shells that do not contribute to bonding are determined (XPS or ESCA method: *electron spectroscopy for chemical analysis*). These energies have characteristic values for every element in the charge-neutral state. The higher the positive charge at the corresponding atom in a molecule, the higher the ionization energy E_i (Figure 14.3). Conversely, a negative partial charge leads to a lowering of the ionization energy, for example, at the fluorine atoms. In case of xenon in the present case, an electron is removed from the degenerate 3*d* level, which leads to the lifting of the degeneracy (JAHN–TELLER effect) in the resulting cation and a splitting into two discrete levels ($3d_{5/2}$ and $3d_{3/2}$).[32]

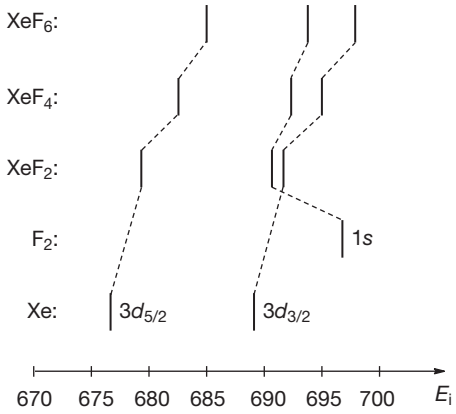

Figure 14.3: Schematic representation of the ionization energies of xenon and fluorine in the elemental state and in xenon fluorides determined by ESCA. The bars correspond to an ionization from the 1*s* level in case of fluorine and from the 3*d* level in case of xenon. The rising ionization energy demonstrates an increasingly positive charge at the corresponding atom and vice versa.

31 (a) M. Kaupp et al., *J. Am. Chem. Soc*. **1996**, *118*, 11939. (b) M. Gawrilow, H. Beckers, S. Riedel, L. Cheng, *J. Phys. Chem. A* **2018**, *122*, 119.

32 N. Bartlett et al., *J. Am. Chem. Soc*. **1974**, *96*, 1989; G. M. Bancroft et al., ibid. **1991**, *113*, 9125.

The high positive charge at the central atom of XeF_6 results in an attraction and thus partial backdonation of the seemingly nonbonding electron density in the $2p_\pi$ orbitals of the fluorine ligands into orbitals predominantly located at the central atom. These orbitals are to some extent the vacant 5*d* orbitals of xenon, but mostly the antibonding σ* MOs of those XeF bonds approximately perpendicular to the one in question. The latter effect is called *negative hyperconjugation*. By this backdonation the charges at the involved atoms are somewhat reduced and the bond energy slightly increased. Compared to the σ bonds, however, these weak dative π bonds are much less important.

The bonds in the oxides XeO_3 and XeO_4 correspond to those in the valence-isoelectronic oxoanions $[ClO_3]^-$ and $[ClO_4]^-$ as well as $[SO_4]^{2-}$. In these cases as well, the σ components are much stronger than the π components of the XeO bond (Section 2.6). They are therefore best represented by the following structural formulae with single rather than double bonds as well as the corresponding formal charges:

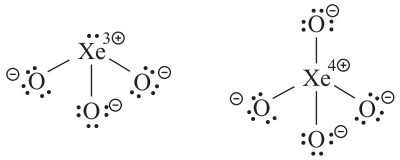

14.6.3 Existence and Nonexistence of Noble Gas Compounds

The question arises, why in analogy to XeF_2 the compounds H_2Xe, $XeCl_2$, $XeBr_2$ or Me_2Xe cannot be prepared as persistent species at 25 °C. The molecules H_2Xe, HXeCl and $XeCl_2$ have been detected in noble gas matrices at low temperature,[33] but such compounds are unstable under standard conditions. While the reaction

$$Xe + E{-}E \longrightarrow E{-}Xe{-}E$$

is exothermic for E = F, the formation of H_2Xe and $XeCl_2$ from the elements is strongly endothermic. This is mostly due to the much higher dissociation enthalpies (D^0_{298}) of H_2 (436 kJ mol^{-1}) and Cl_2 (244 kJ mol^{-1}) compared to that of F_2 (158 kJ mol^{-1}). Moreover, the noble gas compounds isolated so far clearly demonstrate that the substituents E need to be strongly electronegative in order to result in stable and isolable compounds. All compounds of Kr, Xe and Rn discussed in the preceding sections carry substituents with electronegativities larger than 3 and thus larger than that of

33 XeH_2: M. Pettersson, J. Lundell, M. Räsänen, *J. Chem. Phys*. **1995**, *103*, 205; N. Runeberg, M. Seth, P. Pyykkö, *Chem. Phys. Lett*. **1995**, *246*, 239. HXeCl, HXeBr, HXeI, HKrCl: M. Pettersson, J. Lundell, M. Räsänen, *J. Chem. Phys*. **1995**, *102*, 6423. HXeSH and HXeOH: M. Petterson et al., *J. Am. Chem. Soc*. **1999**, *121*, 11904 and *Inorg. Chem*. **1998**, *37*, 4884.

the central noble gas atom. This obviously applies not only to F and O, but also to the groups $-OTeF_5$, $-OSO_2F$, $-N(OSO_2F)_2$ and $-C_6F_5$, which show group electronegativities significantly larger than 3 due to the inductive effect of the pending F and O atoms. In contrast, the atoms H, Br and I as well as the groups CH_3 and C_6H_5 are not sufficiently electronegative to allow for isolable xenon compounds. If the electronegativity of E is low, the highest occupied valence orbitals at the substituents lie at higher energy than those at the noble gas center (Figure 14.2) and thus the stabilization of the central atom's electrons is considerably weaker. This does by no means exclude that single molecules with such substituents can be generated and detected for short periods of time in the gas phase or in cold and inert solid matrices (e.g., HXeF). *The stability of single molecules is strictly to be distinguished from the stability of a compound, that is, the collective bulk of molecules, as decomposition processes often occur intermolecularly*. Species such as HArF, HNeF and HXeF are best described as ion pairs $[HE]^+F^-$.[34]

The reason for the endothermic nature of the oxides of xenon despite oxygen's electronegativity of 3.4 is also the high dissociation enthalpy of the O_2 molecule (498 kJ mol^{-1}), which renders the formation reaction overall endothermic:

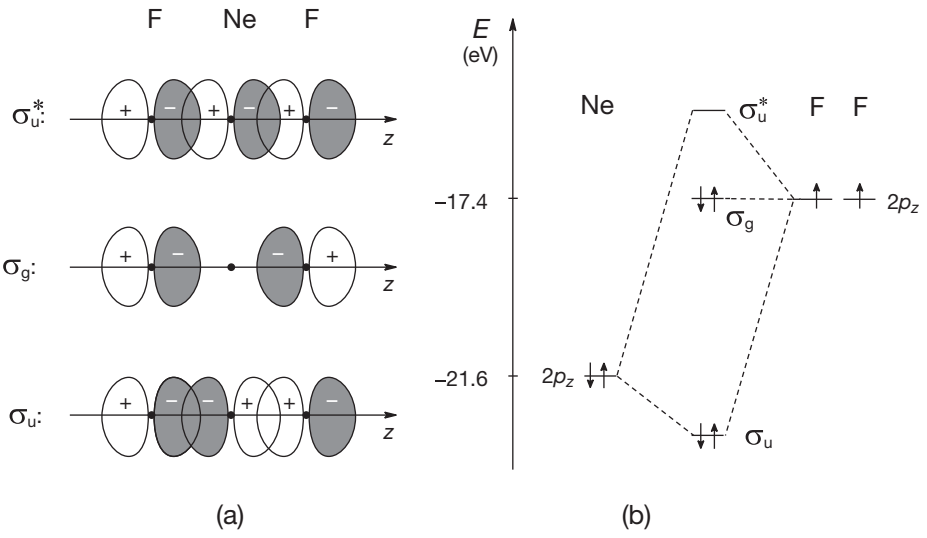

Figure 14.4: Theoretical bonding situation in the hypothetical molecule NeF_2. (a) Linear combination of the three atomic orbitals. (b) Energy term diagram of the σ molecular orbitals. The occupied 2*s* atomic orbitals of Ne and F are too low in energy for an interaction with the 2*p* AOs; they are practically to be regarded as core orbitals. Their interaction with each other leads to three doubly occupied MOs that do not contribute to bonding and were therefore omitted.

34 G. Merino et al., *J. Phys. Chem. A* **2009**, *113*, 9700.

$$Xe + 2\,O_2 \longrightarrow XeO_4$$

Why are there no fluorides in analogy to XeF_2 and KrF_2 known for argon, neon and helium? This question can be answered with a similar reasoning invoking electronegativities. As shown in the MO diagram in Figure 14.4, the potential central atoms are too electronegative in these cases, i.e. their highest occupied valence orbitals are too low in energy compared to the HOMOs at the substituents. The stabilization conferred to the electrons of the noble gas by these interactions is too small to overcome the repulsion of the nuclei. It is fairly apparent that argon is likely the best candidate for future synthesis of neutral and stable compounds. Until then the clathrates and other inclusion compounds (Section 5.6.4) are the only isolable "compounds" of the lighter noble gases.

Index

https://doi.org/10.1515/9783110578065-016